NAS1.9/4:33/12

RED SEAL

TECHNOLOGY & SCIENCE
DETROIT PUBLIC LIBRARY

Aerospace Reports

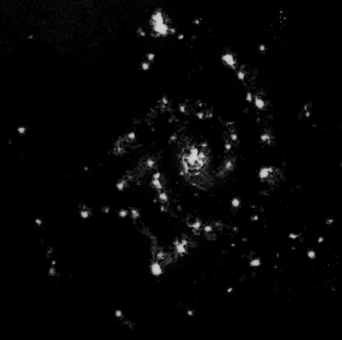

An Abstract Journal

NASA

Volume 33, Number 12
December 1995
N95-32373 to N95-34822

The NASA STI Office... in Profile

Since its founding, NASA has been dedicated to the advancement of aeronautics and space science. The NASA Scientific and Technical Information (STI) Office plays a key part in helping NASA maintain this important role.

The NASA STI Office provides access to the NASA STI Database, the largest collection of aeronautical and space science STI in the world. The Office is also NASA's institutional mechanism for disseminating the results of its research and development activities.

Specialized services that help round out the STI Office's diverse offerings include creating custom thesauri, building customized databases, organizing and publishing research results ... even providing videos.

For more information about the NASA STI Office, you can:

- **Phone** the NASA Access Help Desk at (301) 621-0390
- **Fax** your question to the NASA Access Help Desk at (301) 621-0134
- **E-mail** your question via the **Internet** to help@sti.nasa.gov
- **Write** to:

  NASA Access Help Desk
  NASA Center for AeroSpace Information
  800 Elkridge Landing Road
  Linthicum Heights, MD 21090-2934

DETROIT PUBLIC LIBRARY
3 5674 02477632 1

Scientific and Technical Aerospace Reports

Scientific and Technical Aerospace Reports (STAR), is published each month as a major product of the NASA Scientific and Technical Information (STI) Office.

Inside this issue you will find:

- **Front Matter** containing a typical citation and abstract sample explaining the standard format, including codes for ordering reports
- **An Abstract Section** containing citations and abstracts of reports and publications that provide comprehensive coverage of worldwide aerospace-related topics including aeronautics and space science technology. *STAR* lists published and publicly available reports entered into the NASA STI Database during the four weeks preceding publication of this issue. These citations and abstracts are listed by subject categories.
- **An Index Section**
  - Subject
  - Personal author
  - Corporate source
  - Contract number
  - Report number
- **An Appendix** containing a guide for ordering cited reports, registering with the NASA STI Office, and using the available products and services. Additionally, price schedules, phone numbers, and addresses are included in this information packed section.

NASA also sponsors the companion journal, *NASA Open Volumes on Aerospace (NOVA)*, which lists abstracts of the open literature on aerospace subjects available worldwide. *NOVA* is for internal NASA use only, available from the NASA Center for AeroSpace Information (CASI).

Entries found in *STAR* are available through the NASA online retrieval service, RECON.

The NASA STI Office gathers information through national and international agreements and exchanges and makes this information available to the NASA community and to the public in many forms through various outlets.

For additional information on the NASA STI Office, call the NASA Access Help Desk at (301) 621-0390, or write to:

NASA Center for AeroSpace Information
800 Elkridge Landing Road
Linthicum Heights, Maryland 21090-2934

US ISSN 0036-8741

DETROIT PUBLIC LIBRARY
DEC 12 1995
DEPOSITORY DOCUMENT

The New NASA Video Catalog is Here

Free!

To order your free copy call
the NASA Access Help desk at
(301) 621-0390,
fax to (301) 621-0134,
e-mail to help@sti.nasa.gov,
or via the Internet at
http://www.sti.nasa.gov/STI-homepage.html

EXPLORE THE UNIVERSE

This publication was prepared by the NASA Center for AeroSpace Information,
800 Elkridge Landing Road, Linthicum Heights, MD 21090-2934, (301) 621-0390.

Volume 33 Number 12 / December 1995

TABLE OF CONTENTS

AERONAUTICS For related information see also *Astronautics.*

01 AERONAUTICS (GENERAL) **3033**

02 AERODYNAMICS **3033**
Includes aerodynamics of bodies, combinations, wings, rotors, and control surfaces; and internal flow in ducts and turbomachinery. For related information see also *34 Fluid Mechanics and Heat Transfer.*

03 AIR TRANSPORTATION AND SAFETY **3042**
Includes passenger and cargo air transport operations; and aircraft accidents. For related information see also *16 Space Transportation* and *85 Urban Technology and Transportation.*

04 AIRCRAFT COMMUNICATIONS AND NAVIGATION **3047**
Includes digital and voice communication with aircraft; air navigation systems (satellite and ground based); and air traffic control. For related information see also *17 Space Communications, Spacecraft Communications, Command and Tracking* and *32 Communications and Radar.*

05 AIRCRAFT DESIGN, TESTING AND PERFORMANCE **3048**
Includes aircraft simulation technology. For related information see also *18 Spacecraft Design, Testing and Performance* and *39 Structural Mechanics.* For land transportation vehicles see *85 Urban Technology and Transportation.*

06 AIRCRAFT INSTRUMENTATION ..... **N.A.**
Includes cockpit and cabin display devices; and flight instruments. For related information see also *19 Spacecraft Instrumentation* and *35 Instrumentation and Photography.*

07 AIRCRAFT PROPULSION AND POWER **3050**
Includes prime propulsion systems and systems components, e.g., gas turbine engines and compressors; and onboard auxiliary power plants for aircraft. For related information see also *20 Spacecraft Propulsion and Power, 28 Propellants and Fuels,* and *44 Energy Production and Conversion.*

08 AIRCRAFT STABILITY AND CONTROL **3055**
Includes aircraft handling qualities; piloting; flight controls; and autopilots. For related information see also *05 Aircraft Design, Testing and Performance.*

09 RESEARCH AND SUPPORT FACILITIES (AIR) **3055**
Includes airports, hangars and runways; aircraft repair and overhaul facilities; wind tunnels; shock tubes; and aircraft engine test stands. For related information see also *14 Ground Support Systems and Facilities (Space).*

ASTRONAUTICS For related information see also *Aeronautics.*

12 ASTRONAUTICS (GENERAL) **3056**
For extraterrestrial exploration see *91 Lunar and Planetary Exploration.*

13 ASTRODYNAMICS ..... **N.A.**
Includes powered and free-flight trajectories; and orbital and launching dynamics.

14 GROUND SUPPORT SYSTEMS AND FACILITIES (SPACE) **3057**
Includes launch complexes, research and production facilities; ground support equipment, e.g., mobile transporters; and simulators. For related information see also *09 Research and Support Facilities (Air).*

15 LAUNCH VEHICLES AND SPACE VEHICLES **3057**
Includes boosters; operating problems of launch/space vehicle systems; and reusable vehicles. For related information see also *20 Spacecraft Propulsion and Power.*

16 SPACE TRANSPORTATION **3057**
Includes passenger and cargo space transportation, e.g., shuttle operations; and space rescue techniques. For related information see also *03 Air Transportation and Safety* and *18 Spacecraft Design, Testing and Performance.* For space suits see *54 Man/System Technology and Life Support.*

17 SPACE COMMUNICATIONS, SPACECRAFT COMMUNICATIONS, COMMAND AND TRACKING **3058**
Includes telemetry; space communications networks; astronavigation and guidance; and radio blackout. For related information see also *04 Aircraft Communications and Navigation* and *32 Communications and Radar.*

N.A.—No abstracts were assigned to this category for this issue.

18 SPACECRAFT DESIGN, TESTING AND PERFORMANCE **3058**
Includes satellites; space platforms; space stations; spacecraft systems and components such as thermal and environmental controls; and attitude controls. For life support systems see *54 Man/System Technology and Life Support.* For related information see also *05 Aircraft Design, Testing and Performance, 39 Structural Mechanics,* and *16 Space Transportation.*

19 SPACECRAFT INSTRUMENTATION **3059**
For related information see also *06 Aircraft Instrumentation* and *35 Instrumentation and Photography.*

20 SPACECRAFT PROPULSION AND POWER **3060**
Includes main propulsion systems and components, e.g., rocket engines; and spacecraft auxiliary power sources. For related information see also *07 Aircraft Propulsion and Power, 28 Propellants and Fuels, 44 Energy Production and Conversion,* and *15 Launch Vehicles and Space Vehicles.*

CHEMISTRY AND MATERIALS

23 CHEMISTRY AND MATERIALS (GENERAL) **3062**

24 COMPOSITE MATERIALS **3062**
Includes physical, chemical, and mechanical properties of laminates and other composite materials. For ceramic materials see *27 Nonmetallic Materials.*

25 INORGANIC AND PHYSICAL CHEMISTRY **3066**
Includes chemical analysis, e.g., chromatography; combustion theory; electrochemistry; and photochemistry. For related information see also *77 Thermodynamics and Statistical Physics.*

26 METALLIC MATERIALS **3077**
Includes physical, chemical, and mechanical properties of metals, e.g., corrosion; and metallurgy.

27 NONMETALLIC MATERIALS **3082**
Includes physical, chemical, and mechanical properties of plastics, elastomers, lubricants, polymers, textiles, adhesives, and ceramic materials. For composite materials see *24 Composite Materials.*

28 PROPELLANTS AND FUELS **3087**
Includes rocket propellants, igniters and oxidizers; their storage and handling procedures; and aircraft fuels. For related information see also *07 Aircraft Propulsion and Power, 20 Spacecraft Propulsion and Power,* and *44 Energy Production and Conversion.*

29 MATERIALS PROCESSING **3089**
Includes space-based development of products and processes for commercial application. For biological materials see *55 Space Biology:*

ENGINEERING For related information see also *Physics.*

31 ENGINEERING (GENERAL) **3089**
Includes vacuum technology; control engineering; display engineering; cryogenics; and fire prevention.

32 COMMUNICATIONS AND RADAR **3095**
Includes radar; land and global communications; communications theory; and optical communications. For related information see also *04 Aircraft Communications and Navigation* and *17 Space Communications, Spacecraft Communications, Command and Tracking.* For search and rescue see *03 Air Transportation and Safety,* and *16 Space Transportation.*

33 ELECTRONICS AND ELECTRICAL ENGINEERING **3101**
Includes test equipment and maintainability; components, e.g., tunnel diodes and transistors; microminiaturization; and integrated circuitry. For related information see also *60 Computer Operations and Hardware* and *76 Solid-State Physics.*

34 FLUID MECHANICS AND HEAT TRANSFER **3106**
Includes boundary layers; hydrodynamics; fluidics; mass transfer and ablation cooling. For related information see also *02 Aerodynamics* and *77 Thermodynamics and Statistical Physics.*

35 INSTRUMENTATION AND PHOTOGRAPHY **3115**
Includes remote sensors; measuring instruments and gauges; detectors; cameras and photographic supplies; and holography. For aerial photography see *43 Earth Resources and Remote Sensing.* For related information see also *06 Aircraft Instrumentation* and *19 Spacecraft Instrumentation.*

36 LASERS AND MASERS **3117**
Includes parametric amplifiers. For related information see also *76 Solid-State Physics.*

37 MECHANICAL ENGINEERING 3121
Includes auxiliary systems (nonpower); machine elements and processes; and mechanical equipment.

38 QUALITY ASSURANCE AND RELIABILITY 3125
Includes product sampling procedures and techniques; and quality control.

39 STRUCTURAL MECHANICS 3125
Includes structural element design and weight analysis; fatigue; and thermal stress. For applications see *05 Aircraft Design, Testing and Performance* and *18 Spacecraft Design, Testing and Performance.*

GEOSCIENCES For related information see also *Space Sciences.*

42 GEOSCIENCES (GENERAL) 3128

43 EARTH RESOURCES AND REMOTE SENSING 3142
Includes remote sensing of earth resources by aircraft and spacecraft; photogrammetry; and aerial photography. For instrumentation see *35 Instrumentation and Photography.*

44 ENERGY PRODUCTION AND CONVERSION 3148
Includes specific energy conversion systems, e.g., fuel cells; global sources of energy; geophysical conversion; and windpower. For related information see also *07 Aircraft Propulsion and Power, 20 Spacecraft Propulsion and Power,* and *28 Propellants and Fuels.*

45 ENVIRONMENT POLLUTION 3151
Includes atmospheric, noise, thermal, and water pollution.

46 GEOPHYSICS 3155
Includes aeronomy; upper and lower atmosphere studies; ionospheric and magnetospheric physics; and geomagnetism. For space radiation see *93 Space Radiation.*

47 METEOROLOGY AND CLIMATOLOGY 3157
Includes weather forecasting and modification.

48 OCEANOGRAPHY 3158
Includes biological, dynamic, and physical oceanography; and marine resources. For related information see also *43 Earth Resources and Remote Sensing.*

LIFE SCIENCES

51 LIFE SCIENCES (GENERAL) 3161

52 AEROSPACE MEDICINE 3164
Includes physiological factors; biological effects of radiation; and effects of weightlessness on man and animals.

53 BEHAVIORAL SCIENCES 3166
Includes psychological factors; individual and group behavior; crew training and evaluation; and psychiatric research.

54 MAN/SYSTEM TECHNOLOGY AND LIFE SUPPORT 3167
Includes human engineering; biotechnology; and space suits and protective clothing. For related information see also *16 Space Transportation.*

55 SPACE BIOLOGY ..... N.A.
Includes exobiology; planetary biology; and extraterrestrial life.

MATHEMATICAL AND COMPUTER SCIENCES

59 MATHEMATICAL AND COMPUTER SCIENCES (GENERAL) ..... N.A.

60 COMPUTER OPERATIONS AND HARDWARE 3177
Includes hardware for computer graphics, firmware, and data processing. For components see *33 Electronics and Electrical Engineering.*

61 COMPUTER PROGRAMMING AND SOFTWARE 3178
Includes computer programs, routines, algorithms, and specific applications, e.g., CAD/CAM.

62 COMPUTER SYSTEMS 3184
Includes computer networks and special application computer systems.

63 CYBERNETICS **3187**
Includes feedback and control theory, artificial intelligence, robotics and expert systems. For related information see also *54 Man/System Technology and Life Support.*

64 NUMERICAL ANALYSIS **3194**
Includes iteration, difference equations, and numerical approximation.

65 STATISTICS AND PROBABILITY **3197**
Includes data sampling and smoothing; Monte Carlo method; and stochastic processes.

66 SYSTEMS ANALYSIS **3197**
Includes mathematical modeling; network analysis; and operations research.

67 THEORETICAL MATHEMATICS ..... **N.A.**
Includes topology and number theory.

PHYSICS For related information see also *Engineering.*

70 PHYSICS (GENERAL) **3198**
For precision time and time interval (PTTI) see *35 Instrumentation and Photography*; for geophysics, astrophysics or solar physics see *46 Geophysics*, *90 Astrophysics*, or *92 Solar Physics.*

71 ACOUSTICS **3200**
Includes sound generation, transmission, and attenuation. For noise pollution see *45 Environment Pollution.*

72 ATOMIC AND MOLECULAR PHYSICS **3201**
Includes atomic structure, electron properties, and molecular spectra.

73 NUCLEAR AND HIGH-ENERGY PHYSICS **3210**
Includes elementary and nuclear particles; and reactor theory. For space radiation see *93 Space Radiation.*

74 OPTICS **3215**
Includes light phenomena and optical devices. For lasers see *36 Lasers and Masers.*

75 PLASMA PHYSICS **3219**
Includes magnetohydrodynamics and plasma fusion. For ionospheric plasmas see *46 Geophysics.* For space plasmas see *90 Astrophysics.*

76 SOLID-STATE PHYSICS **3225**
Includes superconductivity. For related information see also *33 Electronics and Electrical Engineering* and *36 Lasers and Masers.*

77 THERMODYNAMICS AND STATISTICAL PHYSICS **3233**
Includes quantum mechanics; theoretical physics; and Bose and Fermi statistics. For related information see also *25 Inorganic and Physical Chemistry* and *34 Fluid Mechanics and Heat Transfer.*

SOCIAL SCIENCES

80 SOCIAL SCIENCES (GENERAL) **3235**
Includes educational matters.

81 ADMINISTRATION AND MANAGEMENT **3235**
Includes management planning and research.

82 DOCUMENTATION AND INFORMATION SCIENCE **3236**
Includes information management; information storage and retrieval technology; technical writing; graphic arts; and micrography. For computer documentation see *61 Computer Programming and Software.*

83 ECONOMICS AND COST ANALYSIS **3244**
Includes cost effectiveness studies.

84 LAW, POLITICAL SCIENCE AND SPACE POLICY ..... **N.A.**
Includes NASA appropriation hearings; aviation law; space law and policy; international law; international cooperation; and patent policy.

85 URBAN TECHNOLOGY AND TRANSPORTATION **3245**
Includes applications of space technology to urban problems; technology transfer; technology assessment; and surface and mass transportation. For related information see *03 Air Transportation and Safety*, *16 Space Transportation*, and *44 Energy Production and Conversion.*

SPACE SCIENCES For related information see also *Geosciences.*

88 SPACE SCIENCES (GENERAL) ..... **N.A.**

89 ASTRONOMY **3245**
Includes radio, gamma-ray, and infrared astronomy; and astrometry.

90 ASTROPHYSICS **3246**
Includes cosmology; celestial mechanics; space plasmas; and interstellar and interplanetary gases and dust. For related information see also *75 Plasma Physics.*

91 LUNAR AND PLANETARY EXPLORATION **3247**
Includes planetology; and manned and unmanned flights. For spacecraft design or space stations see *18 Spacecraft Design, Testing and Performance.*

92 SOLAR PHYSICS **3248**
Includes solar activity, solar flares, solar radiation and sunspots. For related information see also *93 Space Radiation.*

93 SPACE RADIATION **3248**
Includes cosmic radiation; and inner and outer earth's radiation belts. For biological effects of radiation see *52 Aerospace Medicine.* For theory see *73 Nuclear and High-Energy Physics.*

GENERAL

Includes aeronautical, astronautical, and space science related histories, biographies, and pertinent reports too broad for categorization; histories or broad overviews of NASA programs.

99 GENERAL **3248**

SUBJECT INDEX **I-1**

PERSONAL AUTHOR INDEX **I-97**

CORPORATE SOURCE INDEX **I-109**

CONTRACT NUMBER INDEX **I-125**

REPORT NUMBER INDEX **I-129**

APPENDIX **A-1**

TYPICAL CITATION AND ABSTRACT

NASA SPONSORED — ON MICROFICHE

ACCESSION NUMBER → **N95-10148*#** National Aeronautics and Space Administration. Lewis Research Center, Cleveland, OH. ← CORPORATE SOURCE

TITLE → **EFFECTS OF A FORWARD-SWEPT FRONT ROTOR ON THE FLOWFIELD OF A COUNTERROTATION PROPELLER**

AUTHORS → M. Nallasamy (NYMA, Inc., Brook Park, OH.) and Gary G. Podboy Aug. 1994 19 p Presented at the 30th Joint Propulsion Conference, Indianapolis, IN, 27-29 Jun. 1994; sponsored by AIAA, ASME, SAE, and ASEE ← PUBLICATION DATE

CONTRACT OR GRANT → (Contract NAS3-27186; RTOP 538-03-11)

REPORT NUMBERS → (NASA-TM-106671; E-8994; NAS 1.15:106671; AIAA Paper 94-2694) Avail: CASI HC A03/MF A01; 6 functional color pages ← AVAILABILITY SOURCE AND PRICE CODE

The effects of a forward-swept front rotor on the flowfield of a counterrotation model propeller at takeoff conditions at zero degree angle of attack are studied by solving the unsteady three-dimensional Euler equations. The configuration considered is an uneven blade count counterrotation model with twelve forward-swept blades on the fore rotor and ten aft-swept blades on the aft rotor. The flowfield is compared with that of a reference aft-swept counterrotation geometry and Laser Doppler Velocimeter (LDV) measurements. At the operating conditions considered, the forward-swept blade experiences a higher tip loading and produces a stronger tip vortex compared to the aft-swept blade, consistent with the LDV and acoustic measurements. Neither the solution nor the LDV data indicated the formation of a leading edge vortex. The predicted radial distribution of the circumferentially averaged axial velocity at the measurement station agreed very closely with LDV data, while crossflow velocities showed poor agreement. The discrepancy between prediction and LDV data of tangential and radial velocities is due in part to the insufficient mesh resolution in the region between the rotors and in the tip region to track the tip vortex. The vortex is diffused by the time it arrives at the measurement station. The uneven blade count configuration requires the solution to be carried out for six blade passages of the fore rotor and five passages of the aft rotor, thus making grid refinement prohibitive.

Author

VOLUME 33 NUMBER 12 / December 1995

Scientific and Technical Aerospace Reports

A Monthly Publication of the National Aeronautics and Space Administration

01 AERONAUTICS (GENERAL)

N95-32782# General Accounting Office, Washington, DC. National Security and International Affairs Div.

REPORT TO CONGRESSIONAL COMMITTEES. B-2 BOMBER: COST TO COMPLETE 20 AIRCRAFT IS UNCERTAIN

8 Sep. 1994 20 p

(GAO/NSIAD-94-217; B-257642) Avail: CASI HC A03/MF A01; GAO, PO Box 6015, Gaithersburg, MD 20877 HC

Risks that remain in the B-2 program and issues that could affect the Air Force's ability to complete the acquisition of 20 operational aircraft within the cost limitation of the National Defense Authorization Act for fiscal year 1994 are identified. Significant development, testing, production, and modification efforts are required before the 20 operational aircraft meet their final performance configuration. Through fiscal year 1994, the Congress has appropriated $39,639.7 million, about 89 percent of the $44,656.0 million cost limitation established. We believe there is uncertainty about whether the Air Force will be able to complete B-2 acquisition within the cost limitation. About 57 percent of the planned flight test hours are not yet completed and testing to date has identified problems that are yet to be corrected. Much of the funding remaining to be appropriated is expected to pay for such things as B-2 support, including support equipment, spares, technical data, and interim contractor support. However, making an accurate estimate of these costs requires that DOD decide on the specific support approach for the B-2. CASI

N95-32783# General Accounting Office, Washington, DC. National Security and International Affairs Div.

ARMY AVIATION: MODERNIZATION STRATEGY NEEDS TO BE REASSESSED. REPORT TO CONGRESSIONAL REQUESTORS

21 Nov. 1994 54 p

(GAO/NSIAD-95-9; B-257915) Avail: CASI HC A04/MF A01; GAO, PO Box 6015, Gaithersburg, MD 20877 HC

The validity of the Army's plan for modernizing its aviation fleet is discussed and alternatives to the strategy's proposed armed reconnaissance and light attack helicopter are described. Funding issues surrounding the Army's decisions to acquire its aviation fleet are identified. Because the Bottom-Up Review used different total force structure and unit composition data than the Army to determine the size of the Army's attack and reconnaissance fleet, the validity of the Army's aviation modernization strategy is now questionable. In addition, the Army overstated the expected benefits and understated technical risks associated with the major systems that comprise its modernization strategy. Some field commanders and pilots are concerned that implementation of the current procurement plan could result in an inappropriate mix and quantity of helicopters and, therefore, adversely impact their operational effectiveness. Additionally, DOD and Army studies have not fully considered alternative helicopters and weapon systems that could accomplish many of the planned roles and missions of the strategy's centerpiece - the Comanche. For its aviation modernization strategy, the Army has chosen to use most of its available resources to procure Comanche helicopters and upgrade Apache helicopters while deferring or canceling funding of other Army helicopter modernization programs, such as medical evacuation and cargo helicopters, that the Army believes are important to the performance of its aviation missions. CASI

02 AERODYNAMICS

Includes aerodynamics of bodies, combinations, wings, rotors, and control surfaces; and internal flow in ducts and turbomachinery.

For related information see also *34 Fluid Mechanics and Heat Transfer.*

N95-32548# National Renewable Energy Lab., Golden, CO.

WIND TURBINE TRAILING EDGE AERODYNAMIC BRAKES

P. G. Migliore, L. Scott Miller (Wichita State Univ., Wichita, KS.), and Gene A. Quandt (Quandt, Gene A., Pocatello, ID.) Apr. 1995 10 p Presented at the 25th Annual Conference and Exhibition on Wind Power, Washington, DC, 26-30 Mar. 1995

(Contract DE-AC36-83CH-10093)

(DE95-004061; NREL/TP-441-7805; CONF-950309-2) Avail: CASI HC A02/MF A01

Five trailing-edge devices were investigated to determine their potential as wind-turbine aerodynamic brakes, and for power modulation and load alleviation. Several promising configurations were identified. A new device, called the spoiler-flap, appears to be the best alternative. It is a simple device that is effective at all angles of attack. It is not structurally intrusive, and it has the potential for small actuating loads. It is shown that simultaneous achievement of a low lift/drag ratio and high drag is the determinant of device effectiveness, and that these attributes must persist up to an angle of attack of 45 deg. It is also argued that aerodynamic brakes must be designed for a wind speed of at least 45 m/s (100 mph). DOE

N95-32682*# National Aeronautics and Space Administration. Ames Research Center, Moffett Field, CA.

SOFIA: AFT CAVITIES WIND TUNNEL TEST Final Report

31 Dec. 1994 70 p Prepared in cooperation with Rose Engineering and Research, Inc., Incline Village, NV.

(Proj. SOFIA)

(NASA-TM-110673; NAS 1.15:110673) Avail: CASI HC A04/MF A01

This appendix to the final report of SOFIA 2 is a collection of configuration photos of the wind tunnel test and a brief description of each for the Stratospheric Observatory for Infrared Astronomy (SOFIA). CASI

N95-32764*# National Aeronautics and Space Administration. Ames Research Center, Moffett Field, CA.

SOFIA 2 MODEL TELESCOPE WIND TUNNEL TEST REPORT

Paul Keas 12 Jan. 1995 190 p

(Proj. SOFIA)

(NASA-TM-110668; SER-PK-001; NAS 1.15:110668) Avail: CASI HC A09/MF A02

This document outlines the tests performed to make aerodynamic force and torque measurements on the SOFIA wind tunnel model telescope. These tests were performed during the SOFIA 2 wind tunnel test in the 14 ft wind tunnel during the months of June through August 1994. The test was designed to measure the dynamic cross elevation moment acting on the SOFIA model telescope due to aerodynamic loading. The measurements were taken with the telescope mounted in an open cavity in the tail section of the SOFIA model 747. The purpose of the test was to obtain an estimate of the full scale aerodynamic disturbance spectrum, by scaling up the wind tunnel results (taking into account differences in sail area, air density, cavity dimension, etc.). An estimate of the full scale cross elevation moment spectrum was needed to help determine the impact this disturbance would have on the telescope positioning system

requirements. A model of the telescope structure, made of a light weight composite material, was mounted in the open cavity of the SOFIA wind tunnel model. This model was mounted via a force balance to the cavity bulkhead. Despite efforts to use a 'stiff' balance, and a lightweight model, the balance/telescope system had a very low resonant frequency (37 Hz) compared to the desired measurement bandwidth (1000 Hz). Due to this mechanical resonance of the balance/telescope system, the balance alone could not provide an accurate measure of applied aerodynamic force at the high frequencies desired. A method of measurement was developed that incorporated accelerometers in addition to the balance signal, to calculate the aerodynamic force. Author

N95-32769*# National Aeronautics and Space Administration. Lewis Research Center, Cleveland, OH.

INVESTIGATION OF WATER DROPLET TRAJECTORIES WITHIN THE NASA ICING RESEARCH TUNNEL

Andrew Reehorst and Mounir Ibrahim (Cleveland State Univ., OH.) Aug. 1995 11 p Presented at the International Icing Symposium 1995, Montreal, Canada, 18-21 Sep. 1995; sponsored by the American Helicopter Society and SAE

(RTOP 508-68-10)

(NASA-TM-107023; E-9828; NAS 1.15:107023) Avail: CASI HC A03/MF A01

Water droplet trajectories within the NASA Lewis Research Center's Icing Research Tunnel (IRT) were studied through computer analysis. Of interest was the influence of the wind tunnel contraction and wind tunnel model blockage on the water droplet trajectories. The computer analysis was carried out with a program package consisting of a three-dimensional potential panel code and a three-dimensional droplet trajectory code. The wind tunnel contraction was found to influence the droplet size distribution and liquid water content distribution across the test section from that at the inlet. The wind tunnel walls were found to have negligible influence upon the impingement of water droplets upon a wing model. Author

N95-32821*# National Aeronautics and Space Administration. Langley Research Center, Hampton, VA.

DRAG MEASUREMENTS OF AN AXISYMMETRIC NACELLE MOUNTED ON A FLAT PLATE AT SUPERSONIC SPEEDS

Jeffrey D. Flamm and Floyd J. Wilcox, Jr. Jun. 1995 35 p

(RTOP 505-59-20-01)

(NASA-TM-4660; L-17416; NAS 1.15:4660) Avail: CASI HC A03/MF A01

An experimental investigation was conducted to determine the effect of diverter wedge half-angle and nacelle lip height on the drag characteristics of an assembly consisting of a nacelle fore cowl from a typical high-speed civil transport (HSCT) and a diverter mounted on a flat plate. Data were obtained for diverter wedge half-angles of 4.0 deg, 6.0 deg, and 8.0 deg and ratios of the nacelle lip height above a flat plate to the boundary-layer thickness (h(sub n)/delta) of approximately 0.87 to 2.45. Limited drag data were also obtained on a complete nacelle/diverter configuration that included fore and aft cowls. Although the nacelle/diverter drag data were not corrected for base pressures or internal flow drag, the data are useful for comparing the relative drag of the configuration tested. The tests were conducted in the Langley Unitary Plan Wind Tunnel at Mach numbers of 1.50, 1.80, 2.10, and 2.40 and Reynolds numbers ranging from 2.00 x 10(exp 6) to 5.00 x 10(exp 6) per foot. The results of this investigation showed that the nacelle/diverter drag essentially increased linearly with increasing h(sub n)/delta except near 1.0 where the data showed a nonlinear behavior. This nonlinear behavior was probably caused by the interaction of the shock waves from the nacelle/diverter configuration with the flat-plate boundary layer. At the lowest h(sub n)/delta tested, the diverter wedge half-angle had virtually no effect on the nacelle/diverter drag. However, as h(sub n)/delta increased, the nacelle/diverter drag increased as diverter wedge half-angle increased. Author

N95-34505# National Aerospace Lab., Tokyo (Japan).

SPECIAL PUBLICATION OF NATIONAL AEROSPACE LABORATORY

16 Jun. 1994 380 p IN ENGLISH and JAPANESE Presented at the 12th NAL Symposium on Aircraft Computational Aerodynamics, Tokyo, Japan, 14-16 Jun. 1994

(ISSN 0289-260X)

(NAL-SP-27) Avail: CASI HC A17/MF A03

The proceedings of the 12th NAL (National Aerospace Laboratory) Symposium on Aircraft Computational Aerodynamics are presented. Technological areas discussed include: computational aerodynamics as a tool for aircraft design, euler code, numerical study on stabilization flame over a flat plate, a variation of the Riemann problem solution and its application to implicit Godunov's scheme, multigris imcompressible NS solver, a flux splitting scheme, hypersonic CFD analysis for aerothermodynamic design of HOPE, numerical solution of inviscid and viscous flows about airfoils bt TVD method, solitary wave solution for mixing-layer turbulence, and direct numerical simulation of compressible isotropic turbulence. For individual titles, see N95-34506 through N95-34560.

N95-34506# Princeton Univ., NJ. Dept. of Mechanical and Aerospace Engineering.

REQUIREMENTS AND TRENDS OF COMPUTATIONAL AERODYNAMICS AS A TOOL FOR AIRCRAFT DESIGN **c05**

Antony Jameson *In* National Aerospace Lab., Special Publication of National Aerospace Laboratory 16 Jun. 1994 p 1-49 (For primary document see N95-34505 12-02)

Avail: CASI HC A03/MF A03

This paper discusses steps needed for the implementation of computational simulation techniques which could meet industrial needs. A critical issue examined in Section 3 is the choice of mathematical models: what level of complexity is needed to provide sufficient accuracy for aerodynamic design, and what is the impact on cost and turn-around. Section 4 addresses issues in the formulation of numerical algorithms which provide the fundamental building blocks for a numerical wind tunnel. Section 5 presents the results of some numerical calculations which require moderate computer resources and could be completed with the fast turn around needed for effective industrial use. Section 6 discusses automatic design procedures which can be used to produce optimum aerodynamic designs. Finally, Section 7 discusses the outlook for achieving the goal of a numerical wind tunnel. Author

N95-34507# Ishikawajima-Harima Heavy Industries Co. Ltd., Tokyo (Japan).

DESIGN OF SECONDARY FLOW CONTROL CASCADE USING NUMERICAL SIMULATION Abstract Only **c07**

Y. Ohkita, H. Kodama, K. Kikuchi (National Aerospace Lab., Tokyo, Japan.), C. Nozaki (National Aerospace Lab., Tokyo, Japan.), and A. Tamura (National Aerospace Lab., Tokyo, Japan.) *In* National Aerospace Lab., Special Publication of National Aerospace Laboratory 16 Jun. 1994 p 51-55 In JAPANESE (For primary document see N95-34505 12-02)

Avail: CASI HC A01/MF A03

The trend of axial turbomachine design is toward higher blade loadings which places more emphasis on secondary flow effects and the associated losses. Measurements of these complex three-dimensional flows in high speed compressor cascades has proven to be very difficult. On the other hand, a sophisticated numerical simulation can predict these flows and the losses successfully. This paper presents the results of a design which aims to reduce secondary flow and the losses at endwall regions of compressor stators, using numerical simulations. a comparison with the results obtained in rig tests will be also presented. Author

N95-34508# Tokyo Univ. (Japan). Graduate School.

A STUDY ON THE CONVERGENCE OF A 3-D EULER CODE FOR CASCADE FLOW CALCULATIONS Abstract Only **c34**

Daisaku Masaki and Shojiro Kaji *In* National Aerospace Lab., Special Publication of National Aerospace Laboratory 16 Jun. 1994 p 57-62 In JAPANESE (For primary document see N95-34505 12-02)

Avail: CASI HC A02/MF A03

A three-dimensional Euler code for cascade flow calculation has been developed to investigate unsteady flow phenomena such as rotating stall or surge. The time-dependent Euler solvers provide a single approach for subsonic, transonic and supersonic flows, and have inherent shock capturing capability. So they can provide important information of flow field such as shock location and pressure distribution. Moreover, they form a very essential part of N-S solvers, so it is important to develop a robust, accurate, and convergent Euler code. During this development, an insight which is thought to be important is obtained. There exists ambiguity about 'Roe's averaging' on density, and it was found that if this density average is used in appropriate ways, it is not only analytically incorrect, but can have detrimental effects

on numerical simulations. The example for such a case is shown. also, the result for a transonic compressor rotor cascade at its design point is presented. Author

N95-34509# Tokyo Univ. (Japan).
DSMC METHOD APPLIED FOR REACTING GAS FLOWS Abstract Only **c25**
Shigeo Obata and Toshio Nagashima *In* National Aerospace Lab., Special Publication of National Aerospace Laboratory 16 Jun. 1994 p 63-68 In JAPANESE (For primary document see N95-34505 12-02)
Avail: CASI HC A02/MF A03

A new reaction molecule model has been proposed for analyzing ignition process in supersonic shear flows. This model called Internal energy (IE) Model takes into account the effects of internal (rotational) energy upon the reaction occurrence and treats it in the same way as the translation energy in reaction collision process. IE model can simulate reaction process precisely by many elementary reactions and is successful in clarifying the details of weak combustion in two dimensional parallel shear flows between supersonic air and sonic hydrogen. The influence of modified plasma (atomic oxygen) flow upon ignition in the supersonic shear flows has been also discussed. Author

N95-34510# Saitama Univ., Urawa (Japan). Dept. of Mechanical Engineering.
NUMERICAL STUDY ON STABILIZATION OF A DIFFUSION FLAME OVER A FLAT PLATE **c25**
Xiao Wang, Shigeharu Ohyagi, and Tri Agung Rohmat *In* National Aerospace Lab., Special Publication of National Aerospace Laboratory 16 Jun. 1994 p 69-73 (For primary document see N95-34505 12-02)
Avail: CASI HC A01/MF A03

A numerical study is performed on the effects of stabilization of a diffusion flame in a flat plate boundary layer, into which fuel gas is injected vertically from the surface of the wall with a uniform velocity. A theoretical model is presented to couple fluid dynamics, chemistry and heat transfer on the surface of the flat plate. Governing equations of two-dimensional, compressible Navier-Stokes momentum, energy and chemical species are used and are numerically integrated by means of a finite difference method. Chemical reaction model is one-step, overall irreversible one with second-order, finite rate Arrhenius kinetics. Lots of computations are performed and five cases are discussed on understanding effects of Nusselt number, Damkohler numbers and free stream Reynolds number. By varying the Nusselt number, multiregion structures of mixing only, premixing-controlled reaction, fuel lean and rich reactions can be found. As the flow velocity decreases, the flame tends to have a large stand-off distance and more fuel mass of the burner is transferred upstream to enforce the local reaction and to improve the stabilization of the flame. Author

N95-34511# Mitsubishi Heavy Industries Ltd., Tokyo (Japan).
VERIFICATION OF TURBINE CASCADE FLOW WITH TIP CLEARANCE Abstract Only **c07**
Kunihiro Shimizu, Yoshiaki Miyake, Osamu Nozaki (National Aerospace Lab., Tokyo, Japan.), Kazuo Kikuchi (National Aerospace Lab., Tokyo, Japan.), and Atsuhiro Tamura (National Aerospace Lab., Tokyo, Japan.) *In* National Aerospace Lab., Special Publication of National Aerospace Laboratory 16 Jun. 1994 p 75-80 In JAPANESE (For primary document see N95-34505 12-02)
Avail: CASI HC A02/MF A03

This paper presents verification results of a single stage turbine cascade with lip clearance. The Flow through turbine cascades is calculated by using stage analysis code (CAS3DM) based on Chakravarthy-Osher's TVD scheme developed by National Aerospace Laboratory. The results show good agreements with the experimental data on the total pressure loss of the stator and the total pressure and total temperature distributions of the rotor, indicating the effectiveness of the code as a design tool for estimating loss of the cascade. Author

N95-34512# Ishikawajima-Harima Heavy Industries Co. Ltd., Tokyo (Japan).
A STUDY OF SUPERSONIC MIXING FLOW FIELD WITH RAMP INJECTOR Abstract Only **c34**
Yoshiyuki Yamane, Seiichi Sawaguchi, Yasunori Ando, Shigeru Aso (Kyushu Univ., Kasuga, Japan), and Masahiro Fukuda (National Aerospace Lab., Tokyo, Japan.) *In* National Aerospace Lab., Special Publication of National Aerospace Laboratory 16 Jun. 1994 p 81-86 In JAPANESE (For primary document see N95-34505 12-02)
Avail: CASI HC A02/MF A03

The purposes of the present paper are to investigate the structure of supersonic mixing flow field in ram/scramjet combustor and to develop the CFD code which will be used for the design of the combustor. One type of parallel injection method with ramp injector has been studied numerically and experimentally. The patterns of shock waves obtained by numerical simulations agreed with experimental results in schlieren photograph. Comparisons of static pressure distributions on the wall surface showed good agreement qualitatively. Numerical results captured the structures of flow field clearly, which were generating process of a pair of streamwise vortices and vortical roll-up of the jet. Oblique shocks made injectant gas lift off from wall surface, as found in calculations and experiments. According to these results, it could be said that the CFD code used in this study was useful for investigation of fuel-air mixing in supersonic flow field with parallel injection. From the numerical results, it was confirmed that the streamwise vortices generated by ramp injector and interaction between mixing field and oblique shocks were key factors for enhancement of fuel-air mixing in ram/scramjet combustor. Author

N95-34513# Mitsubishi Heavy Industries Ltd., Tokyo (Japan).
CALCULATION OF SUPERSONIC COMBUSTION IN SCRAMJET ENGINES Abstract Only **c07**
Hideyuki Taguchi and Yoshihiro Kawamata (Touhoku Univ., Japan.) *In* National Aerospace Lab., Special Publication of National Aerospace Laboratory 16 Jun. 1994 p 87-92 In JAPANESE (For primary document see N95-34505 12-02)
Avail: CASI HC A02/MF A03

A numerical simulation code has been carried out to predict flow fields in supersonic combustion ramjet (SCRAMJET) engines. In order to solve supersonic combustion flow fields in the engine, a chemical model was implemented to a 2D/3D supersonic flow simulation code. The purpose of this study was to make a fast and easy code for estimation of sub-scale engine tests. In this study, the Reynolds averaged compressible Navier-Stokes equations and the chemical species continuity equations were solved. The FDS method with the MUSCL approach and the diagonalized IAF method were used to solve the N-S equations. Chemical reactions of hydrogen-air mixture were calculated by the Rogers mode (5-species and 2-equations). Turbulent viscosity was calculated by the Baldwin-Lomax model. Calculations of supersonic combustion were conducted for a simplified model of the SCRAMJET engine. The results showed reasonable phenomena of the supersonic combustion. Author

N95-34514# National Aerospace Lab., Tokyo (Japan).
NUMERICAL SIMULATION OF HIGH ENTHALPY SHOCK TUNNEL Abstract Only **c09**
Katsuhiro Itoh and Masahiro Takahashi (Queensland Univ., Brisbane, Australia.) *In its* Special Publication of National Aerospace Laboratory 16 Jun. 1994 p 93-98 In JAPANESE (For primary document see N95-34505 12-02)
Avail: CASI HC A02/MF A03

One of the most important problems on a development of a reentry vehicle is the prediction of real gas effect. In order to obtain the real gas data of reentry by ground test, the hypervelocity wind tunnel having extremely high reservoir condition, in which temperature and pressure are up to 10,000K and 1,500atm, is required. A free piston shock tunnel is the most useful facility which can produce such hypervelocity flow. The National Aerospace Laboratory is planning to develop the large free piston shock tunnel which can simulate the reentry of HOPE. In the present paper, CFD applications to the design and operation of the free piston shock tunnel are studied. The two topics are presented. One is the quasi-1D simulation to predict actual performances of free piston shock tunnels. Other is the axisymmetric 2D simulation of the reflected shock-boundary layer interactions to clarify the mechanism of the driver gas contamination. Author

N95-34515# Kyoto Univ. (Japan). Graduate School.
ADAPTIVE GRID METHOD USING ELLIPTIC EQUATION FOR COMPRESSIBLE FLOWS Abstract Only **c34**
Masashi Yamakawa, Kenichi Matsuno, and Nobuyuki Satofuka *In* National

Aerospace Lab., Special Publication of National Aerospace Laboratory 16 Jun. 1994 p 99-104 In JAPANESE (For primary document see N95-34505 12-02)
Avail: CASI HC A02/MF A03

An adaptive grid generation method using elliptic equations is developed for compressible flows. In the present adaptive method, a control function is connected with a weight function, which controls the grid density. Thus, the weight function is important to generate the adaptive grid of high quality. A new approach for making the weight function is tried in this paper. To construct the weight function, a combination of the actual distribution of a flow property with a fictitious distribution of an artificial property is used. The adaptive method is applied to many shocked-flow problems of one and two dimensions. It is shown that the new weight function works well and the present adaptive method is promising for compressible flows, especially, shocked flows. Author

N95-34516# Nagoya Univ., Nagoya (Japan). Dept. of Aeronautical Engineering.
A VARIATION OF THE RIEMANN PROBLEM SOLUTION AND ITS APPLICATION TO IMPLICIT GODUNOV'S SCHEME c34
Igor Men'shov and Yoshiaki Nakamura *In* National Aerospace Lab., Special Publication of National Aerospace Laboratory 16 Jun. 1994 p 105-110 (For primary document see N95-34505 12-02)
Avail: CASI HC A02/MF A03

The present paper is devoted to investigate a variation of the exact Riemann problem (RP) solution with respect to a variation of the initial data. This variation may be written in the linear form by introducing variation matrices (VM) coupled with the corresponding side of initial discontinuity. It is shown that VM for the exact RP solution can be obtained in the explicit form for any initial data. Its application to the implicit Godunov scheme leads to the linear system of equations in Delta - from which is solved in two relaxation sweeps, backward and forward ones, by implementing LU approximate factorization. The advantage of the scheme obtained in such a way is large CFL number in calculating of super- and hypersonic-flows around blunt body. Author

N95-34517# Ship Research Inst., Tokyo (Japan).
A MULTIGRID INCOMPRESSIBLE NS SOLVER c34
Takanori Hino *In* National Aerospace Lab., Special Publication of National Aerospace Laboratory 16 Jun. 1994 p 111-116 (For primary document see N95-34505 12-02)
Avail: CASI HC A02/MF A03

A multigrid incompressible NS solver is developed. The solver employs artificial compressibility approach to obtain a steady state solution of the incompressible Navier-Stokes equations. The spatial discretization is based on the finite-volume method. The convection terms are evaluated by the third order upwind scheme with the flux-difference splitting. Time integration is made by the Runge-Kutta method. The algebraic turbulence model by Baldwin and Lomax is used. Nonlinear free surface conditions are implemented in local time stepping, residual smoothing and a multigrid method are used. Brief description of the numerical procedure is given together with the computational results for ship flows. Author

N95-34518*# National Aeronautics and Space Administration. Lewis Research Center, Cleveland, OH.
A FLUX SPLITTING SCHEME WITH HIGH-RESOLUTION AND ROBUSTNESS FOR DISCONTINUITIES c34
Yasuhiro Wada (National Aerospace Lab., Tokyo, Japan.) and Meng-Sing Liou *In* National Aerospace Lab., Special Publication of National Aerospace Laboratory 16 Jun. 1994 p 117-122 (For primary document see N95-34505 12-02)
Avail: CASI HC A02/MF A03

A flux splitting scheme is presented for the general non-equilibrium flow equations with an aim at removing numerical dissipation of Van-Leer-type flux-vector splittings on a contact discontinuity. The scheme is also recognized as an improved Advection Upwind Splitting Method (AUSM) where a slight numerical overshoot immediately behind the shock is eliminated. The proposed scheme has favorable properties: high-resolution for contact discontinuities; conservation of enthalpy for steady flows; numerical efficiency; applicability to chemically reacting flows. In fact, for a single contact discontinuity, even if it is moving, this scheme gives the numerical flux of the exact solution of the Riemann problem. Numerical experiments indicate no oscillation and robustness of the scheme for strong shock/expansion waves. Higher-order extension is also discussed. Author

N95-34519# National Aerospace Lab., Tokyo (Japan). Computational Sciences Div.
CONSTRUCTION AND ANALYSIS OF DIFFERENCE APPROXIMATION FOR SCALAR CONSERVATION LAWS AND ITS CONSISTENCY WITH ENTROPY CONDITION USING BOLTZMANN-LIKE APPROACH c34
Hideaki Aiso and Toshiyuki Iwamiya *In its* Special Publication of National Aerospace Laboratory 16 Jun. 1994 p 123-128 (For primary document see N95-34505 12-02)
Avail: CASI HC A02/MF A03

We are concerned with difference approximation for scalar conservation laws and the convergence. The problem is important not only from the theoretical viewpoint but also from the viewpoint of practical CFD (Computational Fluid Dynamics), because the results give some guidelines as to how to construct difference schemes for systems of conservation laws including the Euler equations even though their theoretical extension can not always be proved. Based on Godunov's difference approximation, we construct a difference approximation which has the accuracy of second order except around discontinuity. Here we rearrange the initial value used in each time advancement procedure of godunov's difference approximation. Then we prove that the difference approximation converges to the entropy solution. In the proof the Boltzmann-like approach is used as well as modified flux functions. Author

N95-34520# National Aerospace Lab., Tokyo (Japan).
HYPERSONIC CFD ANALYSIS FOR THE AEROTHERMODYNAMIC DESIGN OF HOPE
Yukimitsu Yamamoto, Yasuhiro Wada, and Minako Yoshioka (Fujitsu Ltd., Tokyo, Japan.) *In its* Special Publication of National Aerospace Laboratory 16 Jun. 1994 p 129-134 (For primary document see N95-34505 12-02)
Avail: CASI HC A02/MF A03

Numerical study of hypersonic flow around HOPE (H - II Orbiting Plane) is performed, using upwind TVD Navier-Stokes CFD code. Parametric computations are made to investigate the aerodynamic and aerothermodynamic characteristics of HOPE. In our calculations, NWT (Numerical Wind Tunnel) at NAL (National Aerospace Laboratory) is used. NWT is the parallel vector super computer system, which enlarges the applicability and data productivity of CFD in practical aerodynamic design. Numerical results are compared with the experimental data obtained at Calspan's shock tunnel. These works have been done as the joint research of NAL and NASDA. Author

N95-34521# Tokai Univ., Tokyo (Japan). Dept. of Aerospace.
NUMERICAL SOLUTIONS OF INVISCID AND VISCOUS FLOWS ABOUT AIRFOILS BY TVD METHOD
Hamid Reza Kheirandish, Goro Beppu, and Jiro Nakamichi (National Aerospace Lab., Tokyo, Japan.) *In* National Aerospace Lab., Special Publication of National Aerospace Laboratory 16 Jun. 1994 p 135-140 (For primary document see N95-34505 12-02)
Avail: CASI HC A02/MF A03

The need to properly compute steady and unsteady viscous flows surrounding airfoils at transonic speeds remains an outstanding problem in fluid dynamics. In transonic flow where viscous effects such as shock-boundary interactions and separation are dominant, methods based on the Navier-Stokes equations are needed. Calculations of unsteady transonic flow about oscillating airfoils where flutter, dynamic stall, buffet and moving shock waves on these surfaces change the entire flow fields and aerodynamic characteristics, are still stiff problems that stimulate more work and studies to be done. To simulate these problems correctly a robust computer program is needed. This report shows the works have been done up to now, i.e., developing a computer program and verifying it by applying to steady viscous and inviscid flow calculations and inviscid flow about an oscillating airfoil. Author

N95-34522# Tsukuba Univ. (Japan). Inst. of Engineering Mechanics.
SOLITARY WAVE SOLUTION FOR MIXING-LAYER TURBULENCE c34
Shunichi Tsuge and Satoru Ogawa (National Aerospace Lab., Tokyo, Japan.) *In* National Aerospace Lab., Special Publication of National

Aerospace Laboratory 16 Jun. 1994 p 141-146 (For primary document see N95-34505 12-02)
Avail: CASI HC A02/MF A03

A neoclassical statistical theory made applicable to wider classes of turbulence is proposed by separating independent variables into each space point of correlations. The separated dependent variables are shown to obey the Navier-Stokes equation in 6-D space (x,s) where s is the coordinate designated the eddy size. A solitary wave solution is obtained for a mixing layer. The integral of a bilinear product of this solution over the whole s-space gives Reynolds' stress that is free from empirical parameters.
Author

N95-34523# National Aerospace Lab., Tokyo (Japan).
DIRECT NUMERICAL SIMULATION OF COMPRESSIBLE ISOTROPIC TURBULENCE **c34**
Yuichi Matsuo and Kiyoshi Yamamoto *In its* Special Publication of National Aerospace Laboratory 16 Jun. 1994 p 147-152 (For primary document see N95-34505 12-02)
Avail: CASI HC A02/MF A03

Direct Numerical Simulations of compressible, homogeneous, decaying isotropic turbulence are conducted using a Fourier pseudo-spectral method in order to deepen our understanding of physics and mechanics of compressible turbulence and to generate statistical data bases useful for turbulence modeling. The simulations are carried out on a vector-parallel supercomputer NWT at NAL for a 128(exp 3) grid. The existence of eddy shocklets is confirmed at high turbulent Mach numbers. The time evolutions of turbulence statistics are also analyzed, indicating that the compressibility effects on turbulence is significant at higher fluctuating Mach numbers.
Author

N95-34524# Science Univ. of Tokyo (Japan).
CALCULATION FOR AERODYNAMIC CHARACTERISTICS ON DELTA WING WITH LEADING-EDGE SEPARATED VORTEX EFFECT USING BOUNDARY ELEMENT METHOD Abstract Only
Katsuhiro Kikuchi, Akihiro Kikuchi, and Mitsunori Yanagizawa *In* National Aerospace Lab., Special Publication of National Aerospace Laboratory 16 Jun. 1994 p 153-158 In JAPANESE (For primary document see N95-34505 12-02)
Avail: CASI HC A02/MF A03

In this paper, the method which allows the calculation of the characteristics for flow around a delta wing is described. Flow separations are certain to occur from the leading-edge on highly swept wings at moderate-to-high angles of attack. Since delta wing is considered as slender body, slender body theory is reported. So first, two-dimensional cross sections are generated by slicing three-dimensional model and the position and strength of leading-edge separation vortices is determined using vortex tracking method. In order to include the effect of leading-edge separation vortex a model is proposed. Some aerodynamic coefficients of delta wing are obtained from the present method and comparisons between numerical and experimental results show good agreement.
Author

N95-34525# Tokyo Univ. (Japan). Graduate School.
SIDEWALL-EFFECT OF THE WIND TUNNEL ON THE ESTIMATION OF THE AERODYNAMIC CHARACTERISTICS OF A DELTA WING Abstract Only
Koji Miyaji, Kozo Fujii, and Keiichi Karashima (National Aerospace Lab., Tokyo, Japan.) *In* National Aerospace Lab., Special Publication of National Aerospace Laboratory 16 Jun. 1994 p 159-164 In JAPANESE (For primary document see N95-34505 12-02)
Avail: CASI HC A02/MF A03

The effect of the sidewall of a wind tunnel on the flow over a delta wing is investigated numerically. The simulated results show the sidewall changes the flowfield remarkably. Boundary layers on the sidewall separate ahead of the wing and forms a horse-shoe vortex and this vortex changes the direction of the main flow and works for increasing the effective leading-edge sweep angle. As a result, aerodynamic characteristics of the delta wing change.
Author

N95-34526# Mitsubishi Electric Corp., Tokyo (Japan).
NUMERICAL SIMULATION OF FILM COOLING EFFECT AROUND AXISYMMETRIC BODY IN HYPERSONIC FLOW FIELD Abstract Only **c34**
Takuji Kurotaki, Yoshiko Nakamura, Ryujiro Kurosaki, Masayuki Katayama, and Shigeru Aso, (Kyushu Univ., Kasuga, Japan) *In* National Aerospace Lab., Special Publication of National Aerospace Laboratory 16 Jun. 1994 p 165-170 In JAPANESE (For primary document see N95-34505 12-02)
Avail: CASI HC A02/MF A03

Film cooling effects due to mass addition on axisymmetric body in hypersonic flow field are numerically investigated and results of numerical simulation are compared with experimental data. Experiments are conducted by using a conventional shock tunnel. Free stream Mach number is 4.25 and cooling gas (N2) is supplied through the slot located at the nose of a hemisphere model. The direction of mass addition is tangential from the model surface and heat flux around the body is measured. In numerical analysis, axisymmetric full Navier-Stokes equations are solved by an implicit finite difference method. LU-SGS scheme are used for the time integration and convective terms are evaluated by the MUSCL-type TVD scheme based on Roe-type flux splitting. Numerical results show significant decreases of surface heat flux which are also obtained in experiments and agreement of numerical and experimental results is qualitatively good. More detailed investigation of the flow inside the boundary layer indicates that the boundary layer consists of two sub layers and that the inner layer plays a role of adiabatic wall structure on the surface. These characteristics are considered most essential in the determination of film cooling effects in this type of hypersonic flow.
Author

N95-34527# Kyoto Univ. (Japan). Dept. of Aeronautical Engineering.
STRUCTURE OF WEAK SHOCK WAVES IN BUBBLY LIQUID **c34**
Ryuji Ishii and Takeshi Hashimoto (Toyota Motor Co., Tokyo, Japan.) *In* National Aerospace Lab., Special Publication of National Aerospace Laboratory 16 Jun. 1994 p 171-176 (For primary document see N95-34505 12-02)
Avail: CASI HC A02/MF A03

In this paper, steady and unsteady weak shock waves in a bubbly liquid are treated numerically. A new system of model equations describing the bubbly flow is applied and the flow structure behind a shock front is investigated in detail. It is shown that the heat conduction between the liquid and the gas phases through the bubble surface affects significantly the wave profile near the shock front. It is, however, shown that the velocity difference between the liquid and the gas phases affects the wave profile remarkably for weak shock waves. Radial oscillation of bubbles tends to produce oscillatory profile of the mixture pressure especially near the wave fronts. Numerical simulation shows that the weak shock consists of a precursor near the shock front and a main shock downstream of it. It is confirmed that the stationary shock wave for a constant polytropic-exponent model is realized as an asymptotic solution for a shock tube problem with uniform conditions in the low pressure and high pressure chambers.
Author

N95-34528# National Aerospace Lab., Tokyo (Japan).
THE EFFECT OF BUOYANCY ON FLOW AND HEAT TRANSFER IN CURVED PIPES Abstract Only **c34**
Munekazu Mochizuki and Hiroshi Ishigaki *In its* Special Publication of National Aerospace Laboratory 16 Jun. 1994 p 177-181 In JAPANESE (For primary document see N95-34505 12-02)
Avail: CASI HC A01/MF A03

Fully developed laminar flow in a heated horizontal curved pipe is studied numerically. The thermal boundary conditions at the wall are uniform wall heat flux axially and uniform wall temperature peripherally. Flow and heat transfer are governed by Dean number, Prandtl number and buoyancy number. Detailed prediction of the friction factor, average heat, transfer rate, velocity profile, temperature profile and secondary-flow streamlines are given.
Author

N95-34529# Kyoto Univ. (Japan).
DIRECT NUMERICAL SIMULATION OF INCOMPRESSIBLE HOMOGENEOUS ISOTROPIC TURBULENCE USING COMPRESSIBLE NAVIER-STOKES EQUATIONS Abstract Only **c34**
Hidetoshi Nishida, Makoto Kawamoto, and Yoshimi Torao (Shin-Meiwa Industry Co. Ltd., Japan.) *In* National Aerospace Lab., Special Publication of National Aerospace Laboratory 16 Jun. 1994 p 189-194 In JAPANESE (For primary document see N95-34505 12-02)
Avail: CASI HC A09/MF A03

In this paper, the incompressible homogeneous isotropic turbulence is simulated by using the compressible Navier-Stokes equations. The compressible Navier-Stokes equations are solved by the higher order method of lines. The spatial derivatives of the governing equations are discretized by the modified differential quadrature (MDQ) method, and the resulting system of the ordinary differential equations in time is integrated by the low-storage Runge-Kutta scheme. The direct numerical simulation is carried out with Re = 50 radical 2, Ma = 0.03. The present 10th order solutions are in good agreement with the incompressible solutions with 10th order of spatial accuracy obtained by the vorticity-streamfunction formulation. Author

N95-34530# National Aerospace Lab., Tokyo (Japan).
DIRECT NUMERICAL SIMULATION OF INCOMPRESSIBLE HOMOGENEOUS ISOTROPIC TURBULENCE USING NWT Abstract Only **c34**
Kiyoshi Yamamoto, Iwao Hosokawa (University of Electro-Communications, Tokyo, Japan.), and Shin-Ichi Oide (University of Electro-Communications, Tokyo, Japan.) *In its* Special Publication of National Aerospace Laboratory 16 Jun. 1994 p 195-200 In JAPANESE (For primary document see N95-34505 12-02)
Avail: CASI HC A02/MF A03

Direct numerical simulation (DNS) of incompressible homogeneous isotropic turbulence is conducted by the use of the Numerical Wind Tunnel (NWT), a parallel computer introduced to NAL last year. The DNS with 512 mesh points in space can be calculated by the NWT with 128 processor elements. The fully developed turbulent fields, velocity and temperature, are obtained by the DNS which used the Fourier spectral method for calculation of the Navier-stokes equation and the diffusion equation. The energy spectrum obtained takes the K (exp -5/3) power law in the inertial subrange. The probability distribution function has the Gaussian distribution for the velocity, but exponential function for the various velocity derivatives. The intense vorticity concentrates into short tube-like regions in space, but the temperature gradient into sheet-like regions. Author

N95-34531# Tokyo Noko Univ. (Japan).
EFFECT OF SCHEMES ON NUMERICAL SIMULATIONS OF SHOCK WAVE REFLECTION Abstract Only **c34**
Fumio Higashino, Yoko Takakura, Masahiro Yoshida (National Aerospace Lab., Tokyo, Japan.), and Satoru Ogawa (National Aerospace Lab., Tokyo, Japan.) *In* National Aerospace Lab., Special Publication of National Aerospace Laboratory 16 Jun. 1994 p 201-206 In JAPANESE (For primary document see N95-34505 12-02)
Avail: CASI HC A02/MF A03

The full Navier-Stokes equations were solved numerically by using a parallel computer at NAL to simulate oblique reflection of plane shock waves over a rigid wall. The dependent hyperbolic conservation forms for finite volume cells were integrated by applying a second order TVD scheme. The three stage Runge-Kutta method was used for time integration. Various types of Riemann solvers of both the Euler and the Navier-Stokes were tested to compare the accuracy of the results. The present numerical simulations show that the results computed by the Euler code showed good reflection patterns of the shock waves but the complicated flowfields behind the Mach stem were not well computed. The lambda shock wave created in front of the corner of a wedge was not simulated by the Euler code. The present scheme based on the Harten-Yee type TVD scheme coupled with Roe's approximate solver gave fairly good results in predicting various types of shock reflection. In the present computation the use of a 2-4 parallel processor was effective. Author

N95-34532# National Aerospace Lab., Tokyo (Japan).
ELEMENTARY BENCHMARKS OF THE NWT COMPUTER SYSTEM AND PROGRAM PERFORMANCE **c62**
Shigeki Hatayama *In its* Special Publication of National Aerospace Laboratory 16 Jun. 1994 p 207-212 (For primary document see N95-34505 12-02)
Avail: CASI HC A02/MF A03

The NWT computer system of the NAL comprises two system administrators, 140 processing elements and a crossbar network, which operates as a distributed-memory message-passing MIMD computer. Each processing element itself is a vector computer. This paper presents measurements of the elementary characteristic parameters of the NWT with SIMD computing and with MIMD computing in the local and global memory access, and measurements of the maximum actual performance obtained when we execute programs for computation of the incompressible viscous flow in two- and three-dimensional lid-driven cavities in parallel on the 128-processing element system. Author

N95-34533# National Aerospace Lab., Tokyo (Japan).
PERFORMANCE EVALUATION OF THE NWT WITH INCOMPRESSIBLE NS CODE Abstract Only **c34**
Takashi Nakamura and Masahiro Yoshida *In its* Special Publication of National Aerospace Laboratory 16 Jun. 1994 p 213-218 In JAPANESE (For primary document see N95-34505 12-02)
Avail: CASI HC A02/MF A03

We parallelized an incompressible CFD code to evaluate the effectiveness of the Numerical Wind Tunnel (NWT) for a code with small operations per grid point. The original CFD code is based on the MAC method and solved by the SOR method. Since the SOR iterative algorithm is not suitable for vector computers nor parallel computers, various methods to vectorize have been proposed. We chose the red and black method, a modified version. This method imposes smaller operations per grid point and less time of data transfer per iteration than compressible CFD codes with IAF methods. This study shows the parallelization performance on the NWT with the code. Author

N95-34534# Fujitsu Ltd., Tokyo (Japan). Parallel Computing Research Center.
HIGHLY PARALLEL COMPUTER AP1000: ARCHITECTURE AND BASIC SOFTWARE Abstract Only **c62**
Hiroyuki Sato *In* National Aerospace Lab., Special Publication of National Aerospace Laboratory 16 Jun. 1994 p 219-224 In JAPANESE (For primary document see N95-34505 12-02)
Avail: CASI HC A03/MF A03

Massively parallel computer, such as the AP1000 can be used for speeding up visualization of simulation results. To use the AP1000 highly parallel computer in visual computing, we developed: (1) video hardware having a 400 MB/s peak transfer rate, able to display HDTV images generated by processor at 30 frames/s, and (2) parallel disk hardware that uses a 3.5-inch disk drive for each cell, providing a large capacity and high aggregate transfer speed. We also developed parallel visualization software CaVis, implementing it with a pipeline of task programs, each of which represents a visualization phase. Author

N95-34535# Cray Research Japan, Tokyo (Japan).
PROGRAM DEVELOPING ENVIRONMENT AND A CFD APPLICATION ON THE CRAY T3D Abstract Only **c61**
Toshihiro Kinoshita and Tsutomu Saito *In* National Aerospace Lab., Special Publication of National Aerospace Laboratory 16 Jun. 1994 p 225-230 In JAPANESE (For primary document see N95-34505 12-02)
Avail: CASI HC A02/MF A03

This paper addresses the performance evaluation of three-dimensional compressible inviscid flow analysis code on the Cray T3D massively parallel processing system. Second-order upwind TVD scheme and Strang-type time splitting method are employed in the analysis code. The method of data decomposition and array redistribution for minimizing the communication cost will be discussed. The outline of T3D system and its programming environments such as programming model and tools will be also given. Author

N95-34536# National Aerospace Lab., Tokyo (Japan).
AN UNSTEADY SIMULATION OF A CENTRIFUGAL COMPRESSOR STAGE USING THE NWT Abstract Only **c34**
Takashi Yamane *In its* Special Publication of National Aerospace Laboratory 16 Jun. 1994 p 231-235 In JAPANESE (For primary document see N95-34505 12-02)
Avail: CASI HC A01/MF A03

Numerical calculations have been performed for the analysis of the impeller/diffuser interaction flow field of a centrifugal compressor using the Numerical Wind Tunnel (NWT) system. The three dimensional unsteady simulation took enormous calculation time but the parallel processing on the NWT solved its problem. The calculation using 16 processor elements (PE) achieved 11 times faster speed than on a single PE. Author

N95-34537# Daiko Ltd. (Japan).
PARALLEL COMPUTATION OF TRANSONIC FLOWS ABOUT AN AIRCRAFT CONFIGURATION USING MULTI-BLOCK STRUCTURED GRIDS Abstract Only
Ryozo Ito and Susumu Takanashi (National Aerospace Lab., Tokyo, Japan.) *In* National Aerospace Lab., Special Publication of National Aerospace Laboratory 16 Jun. 1994 p 237-242 In JAPANESE (For primary document see N95-34505 12-02)
Avail: CASI HC A02/MF A03

Three dimensional Navier-Stokes computation of transonic flows about ONERA-M5 has been carried out using the NAL's parallel vector computer called 'NWT'. the computational space around ONERA-M5 is decomposed into 14 blocks. The code is parallelized in two methods. The first one is sharing the computation for each block to each PE. The second one is combining the first one and the parallelization in each block. The performance of the parallelization is estimated by measuring the cpu-time for solving the Navier-Stokes equations. Validation of the computational results has also been done. Author

N95-34538# Tokyo Noko Univ. (Japan).
VECTOR-PARALLEL SIMULATIONS OF TRANSONIC WIND TUNNEL FLOWS ABOUT A FULLY CONFIGURED MODEL OF AIRCRAFT Abstract Only
Yoko Takakura and Satoru Ogawa (National Aerospace Lab., Tokyo, Japan.) *In* National Aerospace Lab., Special Publication of National Aerospace Laboratory 16 Jun. 1994 p 243-248 In JAPANESE (For primary document see N95-34505 12-02)
Avail: CASI HC A02/MF A03

It has been tried continuously to numerically analyze NAL transonic wind-tunnel flows about a fully configured model of aircraft, ONERA-M5, to investigate the reliability of numerical computations; in these trials a multi-domain technique is used to realize the computations of flows about a complicated configuration, and in each domain thin-layer Navier-Stokes equations are solved by the Chakravarthy-Osher TVD scheme. In this time the simple vector-parallel algorithm of this multi-domain technique on NAL's NWT system is presented and simulations have been performed. Consequently the computed pressure, lift and drag coefficients have agreed well with experimental ones. Regarding the parallel performance, the parallel-computing time has been reduced to the computing time on the domain with the largest number of grid points, and communication time between PE's can be negligible. Author

N95-34539# Kawasaki Heavy Industries Ltd., Tokyo (Japan). Technical Inst.
A LARGE SCALE 3D NAVIER-STOKES ANALYSIS USING NAL-NWT Abstract Only **c34**
Takuji Kishimoto *In* National Aerospace Lab., Special Publication of National Aerospace Laboratory 16 Jun. 1994 p 249-253 In JAPANESE (For primary document see N95-34505 12-02)
Avail: CASI HC A01/MF A03

Parallelization of 3D Navier-Stokes analysis using a structured multi-block grid has been achieved by a domain decomposition method with message passing procedure. Modification of existent solver can be done easily, because added procedures for parallelization are only the domain decomposition routine and the inter domain communication of boundary conditions between each neighboring subdomains, that is message passing procedure, and there is no need to modify main routines. NWT(Numerical Wind Tunnel) of National Aerospace Laboratory(NAL) was used in order to investigate the effect of parallelization. A parallelized flow analysis around alone swept wing using about 1 million grid points and 4PE(Processor Element)s was accelerated about 3 times faster than using single PE. We also got the result that a larger scale flow analysis around complete configuration of ONERA-M5 model using over 5 million grid points and 16PEs was accelerated about 12 times faster than using FACOM VP-400. Author

N95-34540# Kawasaki Heavy Industries Ltd., Tokyo (Japan). Technical Inst.
ROLE OF COMPUTATIONAL FLUID DYNAMICS IN AERONAUTICAL ENGINEERING. NUMBER 12: FORMULATION AND VERIFICATION OF UNI-PARTICLE UPWIND SCHEMES FOR THE EULER EQUATIONS Abstract Only **c34**
Eiji Shima and Tadamasa Jounouchi (National Aerospace Lab., Tokyo, Japan.) *In* National Aerospace Lab., Special Publication of National Aerospace Laboratory 16 Jun. 1994 p 255-260 In JAPANESE (For primary document see N95-34505 12-02)
Avail: CASI HC A02/MF A03

A new approach to construct upwind schemes for the Euler equations is shown. This approach uses a simple flux splitting with the mass flux of some approximate Riemann solver. Two schemes based on this approach, which are SFS2 (Simplified Flux Splitting 2) and SHUS (Simple High-resolution Upwind Scheme), are proposed and are verified by some tests. Both schemes are as simple,robust and accurate for discontinuities and boundary layers as any other existing scheme. Author

N95-34541# Fujitsu Ltd., Tokyo (Japan).
NUMERICAL ANALYSIS AROUND THE WHOLE SST CONFIGURATION Abstract Only **c05**
Tetsuo Yamazaki and Takashi Uchida (Japan Aircraft Development Corp., Tokyo, Japan.) *In* National Aerospace Lab., Special Publication of National Aerospace Laboratory 16 Jun. 1994 p 261-265 In JAPANESE (For primary document see N95-34505 12-02)
Avail: CASI HC A01/MF A03

In designing the Second Generation of Supersonic Transport, the improvement of the lift to drag ratio at cruise condition is one of the most important subjects. This ratio affects the economic viability of the next SST, but there are some phenomena which degrade it. One of these is the wing-nacelle interference. We have applied a Euler method to a SST configuration which have 4 nacelles located under the aft wing. In this result the whole configuration has a higher inviscid lift to drag ratio than the sum of the wing-body configuration and 4 times of only one nacelle. And the inflow Mach number just upstream of a nacelle is less than the free stream Mach number and the flow is inclined, owing to the wing surface pressure. Therefore, it is necessary to investigate the wing-nacelle interference in more detail. Author

N95-34542# National Aerospace Lab., Tokyo (Japan).
APPLICATION OF CFD TECHIQUE FOR HYFLEX AERODYNAMIC DESIGN Abstract Only **c05**
Yukimitsu Yamamoto, Shigeya Watanabe (National Space Development Agency, Tokyo, Japan.), Mitsuo Ishiguro (Mitsubishi Heavy Industries Ltd., Tokyo, Japan.), and Kou Ogasawara (Mitsubishi Heavy Industries Ltd., Tokyo, Japan.) *In its* Special Publication of National Aerospace Laboratory 16 Jun. 1994 p 267-272 In JAPANESE (For primary document see N95-34505 12-02)
Avail: CASI HC A02/MF A03

An overview of the application of CFD technique for the HYFLEX (HYpersonic FLight EXperiment) aerodynamic design by using the numerical simulation codes in the supersonic and hypersonic speed ranges is presented. Roles of CFD required to make up for the short term of development and small amount of the wind tunnel test cases, application in the HYFLEX aerodynamic design and their application methods are described. The procedure of CFD code validation by the experimental data before design application is also presented. Finally, future view and subject of the CFD application for the development of hypersonic flight vehicle is shortly discussed. Author

N95-34543# Saitama Univ., Urawa (Japan). Dept. of Mechanical Engineering.
NUMERICAL SIMULATION OF INTERACTION BETWEEN SHOCK WAVE AND DENSITY INTERFACE Abstract Only **c34**
Yoshiaki Murata, Tetsuro Obara, and Shigeharu Ohyagi *In* National Aerospace Lab., Special Publication of National Aerospace Laboratory 16 Jun. 1994 p 273-278 In JAPANESE (For primary document see N95-34505 12-02)
Avail: CASI HC A02/MF A03

Interactions of the planar shock wave propagating along a backward-facing step region with a density interface are simulated numerically. The time-dependent solutions of the Euler equations were obtained by using a explicit predictor-corrector TVD scheme. A flow field consists of two regions, one is the backward-facing step region filled with gas-2, the other is the region filled with gas-1 above it. A planar shock propagating in gas-1 propagates along the backward-facing step and interacts with the interface separating these two gases with different densities. Two

general cases of interface are considered, which are called as a slow/fast interface and a fast/slow interface. As parameters of calculations, a density ratio of two gases and a shock Mach number were selected. In the case of slow/fast interaction, a shock transmitted in a light gas propagates with higher propagation velocity and, behind the shock, a large vortex is created which mixes two gases. For the fast/slow interaction, a shock transmitted in a heavy gas forms an oblique shock wave whose angle is determined by the density ratio and the interface is more stable in comparison with slow/fast interaction. Author

N95-34544# Fujitsu Ltd., Tokyo (Japan).
COMPUTATIONS OF LOW SPEED FLOW ABOUT SPACE-PLANE Abstract Only
Kisa Matsushima and Susumu Takanashi (National Aerospace Lab., Tokyo, Japan.) *In* National Aerospace Lab., Special Publication of National Aerospace Laboratory 16 Jun. 1994 p 279-284 In JAPANESE (For primary document see N95-34505 12-02)
Avail: CASI HC A02/MF A03

Parallel computation of flow fields around a space-plane has been conducted on the NWT at the National Aerospace Laboratory, aiming to apply the compressible navier-Stokes code we have simulated super/transonic flows to calculate low subsonic flow fields. Computational results show sufficient reliability in terms of predicting aerodynamic forces. Thus, we have come to have a prospect of making the present code a robust flow solver that with modifications can be applied from a low subsonic to a supersonic regime. To realize it, further effort is needed to attain the convergence efficiency of computation and to analyze the mechanism of microscopic flow phenomena. Author

N95-34545# National Aerospace Lab., Tokyo (Japan).
FLOW AND HEAT TRANSFER IN ROTATING CURVED PIPES Abstract Only **c34**
Hiroshi Ishigaki *In its* Special Publication of National Aerospace Laboratory 16 Jun. 1994 p 285-289 In JAPANESE (For primary document see N95-34505 12-02)
Avail: CASI HC A01/MF A03

When a coiled pipe rotates about the coil axis, the effect of rotation interacts with centrifugal and viscous effects to complicate the flow characteristics beyond those seen in stationary curved pipes. Following a previous paper on the flow characteristics, fundamental characteristics of convective heat transfer are studied for fully developed laminar flows through similarity arguments and computational studies. The variation of temperature contours with body force ratio and Prandtl number are shown for two Dean numbers. Empirical formulae for average heat transfer rate are given for wide range of Prandtl numbers. Author

N95-34546# Kyushu Univ., Kasuga (Japan) Dept. of Aeronautics and Astronautics.
NUMERICAL SIMULATIONS OF DYNAMIC STALL PHENOMENA IN LOW SPEED FLOWS Abstract Only
Shigeru Aso and Yuichi Kumamoto *In* National Aerospace Lab., Special Publication of National Aerospace Laboratory 16 Jun. 1994 p 291-296 In JAPANESE (For primary document see N95-34505 12-02)
Avail: CASI HC A02/MF A03

In order to reveal the flow structure and mechanism of dynamic stall around airfoils, these phenomena have been investigated numerically by solving incompressible Navier-Stokes equations with third-order upwind scheme. In this paper, we have calculated separated flows around oscillating airfoils in pitch by moving mesh system. The airfoil used for calculations is NACA0012 and numerical simulations have conducted under Re = 1.0 x 10(exp 3) and 3.5 x 10(exp 4). In case of Re = l.0 x 10(exp 3), we have investigated the influence of time divisions and densities of grids upon aerodynamic characteristics. Time divisions have few influences upon the tendency of hysteresis of C(sub L), but if the number of grid points increases, vibrations of the curves of C(sub L) at pitching down process become large. Further, comparisons between numerical simulations and experiments with a wind tunnel. Quite significant flow patterns due to dynamic stall are revealed. Author

N95-34547# Kyushu Univ., Kasuga (Japan) Dept. of Aeronautics and Astronautics.
NUMERICAL SIMULATION OF UNSTEADY VISCOUS FLOW AROUND AN AIRFOIL WITH OSCILLATING SPOILER Abstract Only
Koji Isogai and Masahiro Yoshida (National Aerospace Lab., Tokyo, Japan.) *In* National Aerospace Lab., Special Publication of National Aerospace Laboratory 16 Jun. 1994 p 297-302 In JAPANESE (For primary document see N95-34505 12-02)
Avail: CASI HC A02/MF A03

Numerical simulations of unsteady viscous flows around an airfoil with oscillating spoiler have been performed using the compressible Navier-Stokes equations. The Yee-Harten Total Variation Diminishing (TVD) scheme and the Baldwin-Lomax algebraic turbulence model are employed. The unsteady pressure distributions on the 16 percent thick supercritical airfoil with oscillating spoiler in low subsonic and transonic Mach numbers have been calculated, being compared with the existing experimental data. Author

N95-34548# Ship Research Inst., Tokyo (Japan).
NUMERICAL SIMULATION OF TWO-DIMENSIONAL PAR-WIG Abstract Only
Nobuyuki Hirata *In* National Aerospace Lab., Special Publication of National Aerospace Laboratory 16 Jun. 1994 p 303-308 In JAPANESE (For primary document see N95-34505 12-02)
Avail: CASI HC A02/MF A03

In the recent trend of super high-speed ships, a PAR-WIG has been paid attention to again. A Power Augmented Ram Wing In Ground effect (= PAR-WIG) is a wing in ground effect, whose lift is enhanced by using the airflow of a thruster, which is placed in the upstream of the wing, so as to create a high ram pressure region under the wing. The PAR effect enables this vehicle to take off and land on at lower speed and supplies that structural weight and engine power can be reduced compared with the conventional WIGs. To understand the aerodynamic characteristics of a PAR-WIG, a two-dimensioinal NS solver for incompressible flow is developed. The solver is based on a finite-volume method whose algorithm is a fractional step method. Through the solver, relations among strength of thrust, high ram pressure region under the wing and aerodynamic forces are considered. Author

N95-34549# National Aerospace Lab., Tokyo (Japan).
DIRECT ANALYSIS OF TRANSONIC ROTOR NOISE WITH CFD TECHNIQUE Abstract Only **c71**
Takashi Aoyama and Shigeru Saito *In its* Special Publication of National Aerospace Laboratory 16 Jun. 1994 p 309-314 In JAPANESE (For primary document see N95-34505 12-02)
Avail: CASI HC A02/MF A03

Three-dimensional Euler equations are directly solved to analyze the High-Speed Impulsive (HSI) noise of a helicopter motor by using CFD technique. The MSI noise is one of the most important sources of helicopter noise. It is generated on the advancing side of a helicopter caused by the shock wave on a blade surface. Although the method which solves the Ffowcs-Williams and Hawkings equation has been often used to analyze the subsonic rotor noise, it doesn't success to predict the transonic rotor noise such as the HSI noise With the advance of CFD technique, the calculation of the HSI noise is recently performed by the combined method of CFD with the Kirchhoff's equation or by the direct simulation using CFD technique. The latter has not been studied enough because huge number of grids are needed to capture the propagation of sound from a blade to an observer located in a far field. So, the powerful supercomputer of NAL, Numerical Wind Tunnel (NWT) is employed to calculate the RSI noise of a non-lifting hovering rotor directly by using the method. The numerical method to solve the governing equation is an implicit finite-difference scheme which utilizes a higher-order upwind scheme based on TVD. As a result, it is observed that the calculated wave form is in very good agreement with an experimental data at sonic cylinder. The agreement is not very good at about three rotor radii but is reasonable at about two rotor radii. Author

N95-34550# National Aerospace Lab., Tokyo (Japan).
DEPENDENCY OF A BOUNDARY LAYER FLOW ON COMPUTATIONAL GRIDS Abstract Only **c34**
Toshiyuki Nomura *In its* Special Publication of National Aerospace Laboratory 16 Jun. 1994 p 315-320 In JAPANESE (For primary

document see N95-34505 12-02)
Avail: CASI HC A02/MF A03

The first step to numerically predict laminar-turbulent transition is taken by the linear stability analysis on a laminar boundary layer. Presently the improvements of high-accuracy schemes as well as computers have enabled Navier-Stokes code to calculate the boundary layer instead of a boundary layer code. It is therefore significant to verify the accuracy of the boundary layer calculated by Navier-Stokes code. By simulating a supersonic flow around an infinite swept cylinder with three kinds of grids which differ in density, the number of cells needed in the boundary layer to obtain the accurate velocity and temperature profiles independent of grid density is investigated. Author

N95-34551# Nagoya Univ., Nagoya (Japan). Dept. of Aeronautical Engineering.
A SIMULATION OF DAMPING PROCESS OF PENDULUM MOTION DUE TO AERODYNAMIC FORCES Abstract Only **c70**
Casmara Nakamura and Yoshiaki Nakamura *In* National Aerospace Lab., Special Publication of National Aerospace Laboratory 16 Jun. 1994 p 321-326 In JAPANESE (For primary document see N95-34505 12-02)
Avail: CASI HC A02/MF A03

A numerical simulation is presented for the flow around a circular cylinder in a free-pendulum motion. In this motion, the aerodynamic forces are exerted on the body and affect the body motion. In this case, the motion will damp out due to its forces. For this problem, the Navier-Stokes equations are solved by a finite difference - finite volume method, where the u-v-p formulation is employed. A multi-grid technique is also employed to solve the pressure Poisson equation. The results are well compared with potential flow solutions. Author

N95-34552# Science Univ. of Tokyo (Japan).
GRID GENERATION AROUND AIRFOIL WITH A FLAP USING BOUNDARY ELEMENT METHOD Abstract Only
Masamichi Iwasa and Mitsunori Yanagizawa *In* National Aerospace Lab., Special Publication of National Aerospace Labo ratory 16 Jun. 1994 p 327-332 In JAPANESE (For primary document see N95-34505 12-02)
Avail: CASI HC A02/MF A03

In many cases, it is very difficult to generate uni-grid around complicated configurations. It has been used that the method for generation of the grid by simulating electric line of force and equipotential surface. But it is difficult to apply to dents in a body. This paper describes a method for generating uni-grid around a airfoil with a flap, having a exceeding dent, by simulating electric line of force and equipotential surface using boundary element method. The grid is mainly generated by dividing panels of wing into rather small panels. Author

N95-34553# National Aerospace Lab., Tokyo (Japan).
FORMATION OF HIGH DENSITY CORES IN MOLECULAR CLOUD Abstract Only **c34**
Toshiya Kimura *In its* Special Publication of National Aerospace Laboratory 16 Jun. 1994 p 333-338 In JAPANESE (For primary document see N95-34505 12-02)
Avail: CASI HC A02/MF A03

This paper presents results of 3D hydrodynamical simulations on formation of high density cores in a molecular cloud. A cubic region of the side of 1pc is considered. Inside the region, the gas is initially uniform and a random velocity field is imposed. The physical properties appropriate to the internal condition of molecular clouds are given. The evolution is numerically followed with special attention to formation of high density cores in the turbulent medium. The effects of the thermal nature of gas and the self-gravity are also examined. The results show that dense and compact cores are formed in a highly disturbed medium. Their physical properties such as size, mass, mass spectrum, etc. are similar to dense cores observed in molecular clouds. Author

N95-34554# Railway Technical Research Inst., Tokyo (Japan).
NUMERICAL SIMULATION OF AERODYNAMIC PROBLEMS IN HIGH SPEED RAILWAYS, PART 2 Abstract Only
Masanobu Iida, Yasuo Yoshida, Tatsuo Maeda, Satoru Ogawa (National Aerospace Lab., Tokyo, Japan.), and Yasuhiro Wada (National Aerospace Lab., Tokyo, Japan.) *In* National Aerospace Lab., Special Publication of National Aerospace Laboratory 16 Jun. 1994 p 339-344 In JAPANESE (For primary document see N95-34505 12-02)
Avail: CASI HC A02/MF A03

Numerical simulation of aerodynamic problems in high speed railways has been performed to investigate applicability of CFD to aerodynamic design of vehicles and ground structures. The first problem treated here is passing-by of two trains in open area. Unsteady 3D Euler simulation using relatively moving grids has been conducted and the result qualitatively agrees with real testing data. The second problem is compression wave generation during train nose entry into the tunnel. Axisymmetric Euler simulation gives quite realistic results on the compression waveform and can be extensively used to optimize area distribution of the train nose for reduction of strength of the pressure wave radiated from the tunnel exit. Author

N95-34555# Tsukuba Univ. (Japan).
TURBULENT SOLITARY WAVE PROPAGATING THROUGH WALL BOUNDARY LAYER Abstract Only **c34**
Burtsitsig Bai, Yuichi Matsuo (National Aerospace Lab., Tokyo, Japan.), and Shunichi Tsuge *In* National Aerospace Lab., Special Publication of National Aerospace Laboratory 16 Jun. 1994 p 345-350 In JAPANESE (For primary document see N95-34505 12-02)
Avail: CASI HC A02/MF A03

A flat plate turbulent Boundary Layer has been investigated numerically by applying turbulence governing equations without any empirical parameters, that originally proposed by Tsuge. Pseudo-compressibility method is employed to make the system of Equations hyperbolic. FDM with Newton Iteration and with the upwind technique is applied to solve fluctuation equations for given velocity profiles. An approximate factorization is used to speed up the convergence. A solitary wave solution of turbulent vortices is obtained in the physical-plus eddy space, Reynolds stress and other turbulence intensities are calculated through simple integrations, and satisfactory agreement with experimental data is observed. Author

N95-34556# SofTek Systems, Inc., Tokyo (Japan).
LARGE SCALE COMPUTING AND VOLUME VISUALIZATION Abstract Only **c61**
Susumu Shirayama *In* National Aerospace Lab., Special Publication of National Aerospace Laboratory 16 Jun. 1994 p 351-356 In JAPANESE (For primary document see N95-34505 12-02)
Avail: CASI HC A02/MF A03

This paper describes several issues about a scientific visualization system utilized in analyzing a flow field obtained by a large scale computing. Firstly, a characteristic of data by the large scale computing is considered. Secondly, we focus on the efficiency of the volume-visualization techniques, and the accuracy of a proposed method is discussed. As a preliminary case, some model fields are visualized by using a Z-slice algorithm on a personal computer system. Author

N95-34557# Mitsubishi Heavy Industries Ltd., Tokyo (Japan).
NUMERICAL SIMULATION OF TWO-DIMENSIONAL COMPRESSIBLE INVISCID FLOW ON UNSTRUCTURED GRID SYSTEM Abstract Only **c34**
Nobuyuki Tsuboi *In* National Aerospace Lab., Special Publication of National Aerospace Laboratory 16 Jun. 1994 p 357-362 In JAPANESE (For primary document see N95-34505 12-02)
Avail: CASI HC A02/MF A03

Two-dimensional Euler equations are solved on an unstructured grid system using the finite volume approach. First order part of convection term is calculated by the Roe scheme with the Roe's approximate Riemann solver. Higher order part of convection term is obtained by MUSCL approach with Barth's limiter or Karman's limiter in order to compare numerical stability and convergence. Time integration is achieved by explicit 2-stage Runge-Kutta method or implicit Jacobi method in order to compare CPU time. The unstructured grid system for NACA 0012 is generated from the structured O-mesh grid system. Computational conditions are Mach number of 0.8 and angle of attack of 1.25 degrees. Numerical stability and convergence with Barth's limiter are better than those with Karman's limiter. CPU time of implicit Jacobi method is less than that of explicit 2-stage Runge-Kutta method when the converged result is obtained. Author

N95-34558# Kyoto Inst. of Tech. (Japan).
PARALLEL COMPUTATION FOR TWO DIMENSIONAL INCOMPRESSIBLE FLOW ON ARRAY OF TRANSPUTERS Abstract Only **c34**
Masanori Obata, Toshihiro Suzuki, and Nobuyuki Satofuka *In* National Aerospace Lab., Special Publication of National Aerospace Laboratory 16 Jun. 1994 p 363-368 In JAPANESE (For primary document see N95-34505 12-02)
Avail: CASI HC A02/MF A03

The two-dimensional incompressible Navier-Stokes equations are solved on a distributed memory parallel computer. The Poisson solver based on a modified successive over-relaxation (SOR) method is implemented on an array of 16 transputers (T805), and it is applied to solve the incompressible Navier-Stokes equations in terms of the vorticity-stream function formulation. The method of lines approach using a rational Runge-Kutta time integration scheme is adopted to solve the vorticity transport equation. As a parallelizing strategy, the domain decomposition technique is used to solve the partial differential equation on a structured grid. The result of the parallelized Poisson solver for 129 x 129 grid points gives high speedup of 15.7 and efficiency of 0.98 of computations of 16 PEs. In the computation of the incompressible Navier-Stokes equations we get an almost linear speedup of approximately 15.96 and corresponding efficiency 0.998 is obtained through the present implementation of the parallel algorithm for 16 transputers. Author

N95-34559# National Aerospace Lab., Tokyo (Japan).
UPWIND SCHEMES FOR THE TWO-DIMENSIONAL EULER EQUATIONS Abstract Only **c34**
Masakazu Tachibana *In its* Special Publication of National Aerospace Laboratory 16 Jun. 1994 p 369-373 In JAPANESE (For primary document see N95-34505 12-02)
Avail: CASI HC A01/MF A03

A genuinely two-dimensional Euler scheme was developed for rectangular grids. This scheme is equivalent to the extension of one-dimensional Steger-Warming scheme to two dimensions. In order to construct the scheme, linearized Euler equations were solved analytically at cell vertexes using Poisson's wave formula. Author

N95-34560# Tokyo Univ. (Japan).
STATIC PRESSURE DROP BY SWIRLING FLOW OF AN INTERNAL COOLING AIR SYSTEM THROUGH A TURBINE SHAFT Abstract Only **c07**
Tadaharu Kishibe and Shojiro Kaji *In* National Aerospace Lab., Special Publication of National Aerospace Laboratory 16 Jun. 1994 p 375-381 In JAPANESE (For primary document see N95-34505 12-02)
Avail: CASI HC A02/MF A03

High thermal efficiency of the gas turbine is dependent on high turbine entry temperature, which is limited by the turbine blade and nozzle guide vane materials. Cooling these components with internal air system allows their environmental operating temperature to exceed their melting point. The cooling air is taken from the compressor and passes through in the hollow turbine shaft. Generally, it is assumed that any troublesome phenomenon by swirling flow does not occur if the cooling air enters the hollow shaft with the relative tangential velocity equal to zero, i.e., the absolute tangential velocity equal to the circumferential speed of the shaft at the air inlet. In this calculation for an internal cooling air system, however, it is observed that unexpectedly even the relative tangential velocity grows as the rotational speed of the shaft increases, and as a result, static pressure drops remarkably. Author

N95-34750# Naval Postgraduate School, Monterey, CA.
AN LDV INVESTIGATION OF SUPPORT STRUCTURE INFLUENCE ON THE FLOW FIELD NEAR THE WINGTIP OF A STOVL CONFIGURATION IN HOVER M.S. Thesis
Edgar R. Enochs Sep. 1994 134 p
(AD-A294126) Avail: CASI HC A07/MF A02

Acquisition phase zero (Concept Exploration) of the Advanced Short Takeoff/ Vertical Land (ASTOYL) aircraft development includes, among other tests, evaluation of forces and moments on a large-scale powered model (LSPM) suspended in the Outdoor Aerodynamic Research Facility (OARF) at the NASA Ames Research Center. This investigation assessed the influence of the OARF support structure upon the flow field through LDV measurements in the vicinity of the struts and the wingtip of a generic flat-plate model mounted in the sub-scale NPS ground effects test rig. The model was a twin subcritical jet configuration with the nozzles arranged in tandem. The test environment was saturation seeded using a smoke generator and LDV measurements were made in the entrained flow. Non-coincident measurements were made to determine the three component mean velocities at points in the region of interest and the component mean and composite mean velocities compared for configurations with struts present and struts removed. Variations were discernible in the component mean velocities between samples both in the same strut configuration and between the struts-installed and struts-removed configurations, but were generally small enough to be considered negligible. DTIC

N95-34763# Brown Univ., Providence, RI. Div. of Applied Mathematics.
HIGH ORDER ACCURACY COMPUTATIONAL METHODS IN AERODYNAMICS USING PARALLEL ARCHITECTURES Final Technical Report, Jan. 1993 - Jan. 1995
David Gottlieb, C. W. Shu, P. Fischer, and W. S. Don 24 Mar. 1995 29 p
(Contract F49620-93-1-0090)
(AD-A294167; AFOSR-95-0344TR) Avail: CASI HC A03/MF A01

In this research we presented the development and application of spectral shock capturing techniques as well as ENO finite difference and finite element methods for realistic problems. For genuinely time dependent problems, special care had to be taken in order to preserve accuracy. Small errors that do not show up in steady state calculations can be amplified and ruin the total accuracy. Time dependent boundary conditions may also pose problems. We addressed those issues in our research efforts. The recent advent of parallel computers poses a special challenge to the users of high-order methods. Issues in parallel computing for the simulations of incompressible and compressible flows has been treated. DTIC

03 AIR TRANSPORTATION AND SAFETY

Includes passenger and cargo air transport operations; and aircraft accidents.

For related information see also *16 Space Transportation* and *85 Urban Technology and Transportation.*

N95-32486# Advisory Group for Aerospace Research and Development, Neuilly-Sur-Seine (France). Mission Systems Panel.
LOW-LEVEL AND NAP-OF-THE-EARTH (NOE) NIGHT OPERATIONS [OPERATION DE NUIT A BASSE ALTITUDE ET EN RASE MOTTES]
Jan. 1995 204 p Presented at the Mission Systems Panel Symposium, Rome, Italy, 25-27 Oct. 1994
(AGARD-CP-563; ISBN-92-836-0009-6) Copyright Avail: CASI HC A10/MF A03

Tactical rotary wing and low-level, fixed wing aircraft operating in high threat areas require improvements in night and adverse weather conditions in order to increase survivability, improve operational performance, and reduce pilot workload. Recent developments and the results of on-going programs suggest that increased automation and optimized integration of sensors, guidance/navigation, control and display systems, and weapons provide approaches to greatly enhanced capability in night operation. The purpose of this symposium is to support the evolutions and envelopment of alternative core structures which will lead to the fielding of effective low-level and N.O.E. night operations systems for fixed and rotary wing aircraft. For individual titles, see N95-32487 through N95-32505.

N95-32487# Bureau des Systemes d'Armes, (France).
NIGHT ATTACK [L'ATTAQUE DE NUIT]
Claude Dortomb *In* AGARD, Low-Level and Nap-of-the-Earth (NOE) Night Operations Jan. 1995 3 p In FRENCH (For primary document see N95-32486 12-03)
Copyright Avail: CASI HC A01/MF A03

The ability to carry out night strikes is sought by all countries. Limited to current budgetary constraints and performance of optoelectronic sensors, nacelle mounted active infrared night vision binoculars are the answer to

this need. From the simplest to the most complex systems, these can be developed at reasonable costs for in-service aircraft. Transl. by CASI

N95-32488# Fabrica Italiana Apparecchiature Radioelettriche S.p.A., Milan (Italy).

AN APPROACH TO SENSOR DATA FUSION FOR FLYING AND LANDING AID PURPOSE

G. Balzarotti, L. Fiori, B. Midollini, and G. Viglialoro *In* AGARD, Low-Level and Nap-of-the-Earth (NOE) Night Operations Jan. 1995 8 p (For primary document see N95-32486 12-03)

Copyright Avail: CASI HC A02/MF A03

Modern aircraft, operating in hostile environments, at night and in adverse weather conditions, are usually equipped with a number of sensors, both active and passive, which separately provide the pilot with data and images and represent a substantial aid during the mission. Novel techniques are currently under development to further improve the effectiveness of the mission by integrating and interpreting the produced data before making them available to the pilot. This paper analyzes the data fusion following a growing integration level criteria. The levels in the integration flow where the fusion is effectively applicable are investigated starting from raw signal (lowest level) up to processed data from sensors, even located on different sites (highest level). Schematically the integration levels considered in the paper will be the following: (1) sensor/pre-processing; (2) processing; (3) display; (4) operative modes; and (5) multiple platforms. Derived from text

N95-32489# Naval Air Warfare Center, China Lake, CA. Targeting Systems Integration Section.

MULTISPECTRAL IMAGE CORRELATION FOR AIR-TO-GROUND TARGETING **c54**

W. R. Ditzler, M. J. Boyd, T. J. Corcoran, M. S. Franklin, J. E. McKnight, H. C. Ottenhoff, R. W. Tyhurst, and M. M. Wirtz *In* AGARD, Low-Level and Nap-of-the-Earth (NOE) Night Operations Jan. 1995 12 p (For primary document see N95-32486 12-03)

Copyright Avail: CASI HC A03/MF A03

A primary cause of failure in tactical air-to-ground missions is the the aircrew fails to find the assigned target. This is the case even for missions against preassigned, large, stationary targets, such as bridges, supply depots, and air-defense sites, for which reconnaissance and satellite images of the target and its surroundings are available for the mission planning process. An important reason for this poor performance is the limited time available for target acquisition, especially when target defences necessitate low-level ingress. During the time a target is visible to aircraft sensors, the aircraft is also visible to the target's defense systems. The time required for air-to-ground targeting with present systems (for example, to lock a targeting FLIR onto an aimpoint is comparable to the response time of air defense systems. Clearly, minimizing the time needed to find and recognize targets is crucial for making attack missions more survivable. Survivability is enhanced if the attack mission can be carried out without the need to 'pop up' to use a targeting sensor. In a typical low-level attack mission, 8-10 s is available for the targeting process, from appearance of the target to weapon release. However, a pilot cannot remove his attention from flying the aircraft for this length of time, especially at night using night-vision systems. Pilots who have tested night-vision systems for low-level flight estimate that 1.5-2.0 s is the maximum allowable time to concentrate on a head-down display under these conditions. A near-term solution to the targeting problem must let the human operator make the final decision. The system described in this paper automates the search for the target (or an offset aimpoint) by sending video from one or more of the aircraft sensors to an image correlator. The correlator finds the best match to an image of the target area, supplied from mission planning data, and displays the resulting target position overlaid on the sensor image. The aircrew is required to look at a head-down display only long enough to confirm of deny the correlator's result. The correlator can then automate the process of locking an image missile seeker onto target. Derived from text

N95-32490*# National Aeronautics and Space Administration. Ames Research Center, Moffett Field, CA.

FLIGHT TEST OF A LOW-ALTITUDE HELICOPTER GUIDANCE SYSTEM WITH OBSTACLE AVOIDANCE CAPABILITY **c04**

Richard E. Zelenka, Raymond F. Clark (Army Command/Control and Systems Integration Directorate, Fort Monmouth, NJ.), and Robert G. Branigan (Army Night Vision Lab., Fort Belvoir, VA.) *In* AGARD, Low-Level and Nap-of-the-Earth (NOE) Night Operations Jan. 1995 10 p (For primary document see N95-32486 12-03)

Copyright Avail: CASI HC A02/MF A03

Military aircraft regularly conduct missions that include low-altitude, near-terrain flight in order to increase covertness and payload effectiveness. Civilian applications include airborne fire fighting, police surveillance, search and rescue, and helicopter emergency medical service. Several fixed-wing aircraft now employ terrain elevation maps and forward-pointed radars to achieve automated terrain following or terrain avoidance flight. Similar systems specialized to helicopters and their flight regime have not received as much attention. A helicopter guidance system relying on digitized terrain elevation maps has been developed that employs airborne navigation, mission requirements, aircraft performance limits, and radar altimeter returns to generate a valley-seeking, low-altitude trajectory between waypoints. The guidance trajectory is symbolically presented to the pilot on a helmet mounted display. This system has been flight tested to 150 ft (45.7 m) above ground level altitude at 80 kts, and is primarily limited by the ability of the pilot to perform manual detection and avoidance of unmapped hazards. In this study, a wide field of view laser radar sensor has been incorporated into this guidance system to assist the pilot in obstacle detection and avoidance, while expanding the system's operational flight envelope. The results from early flight tests of this system are presented. Low-altitude missions to 100 ft (30.5 m) altitude at 80n kts in the presence of unmapped natural and man-made obstacles were demonstrated while the pilot maintained situational awareness and tracking of the guidance trajectory. Further reductions in altitude are expected with continued flight testing. Derived from text

N95-32491# Elmer, Rome (Italy).

HELICOPTER HF COMMUNICATIONS USING THE NVIS MODE **c32**

M. Proia *In* AGARD, Low-Level and Nap-of-the-Earth (NOE) Night Operations Jan. 1995 12 p (For primary document see N95-32486 12-03)

Copyright Avail: CASI HC A03/MF A03

The importance of helicopters in the battlefield scenarios is significantly increasing as the new weaponry and guidance control systems allow use of helicopters in a multiplicity of roles, ranging from anti-tank operations to rapid transportation of men and materials. Missions are often assigned to the helicopters that require flying at close distance from the enemy positions. In these cases, low-altitude flying is necessary for survivability and this type of operation, designated as Nap-Of-Earth (NOE) flying, is a well established helicopter tactic for concealment against enemy fire. In the ordinary modes of operation, radio communications between the helicopter and other platforms in the tactical area are supported by the VHF1 (30 to 88 MHz), VHF2 (108 to 172 MHz)m, and UHF (225 to 400 MHz) frequency bands over line-of-sight (LOS) links. The VHF1 band is used by the helicopter to communicate with ground forces during RECCE missions and to interact with other battlefield units for mission management and briefing. The VHF2 band is dedicated to communications with the Base for ATC purposes, while the UHF band is universally used for Ground-Air-Ground and Air-to-Air links in Air Defense operations. As NOE altitudes for helicopters are typically in the order of a few feet, LOS conditions are seldom achieved due to interposed obstacles (such as vegetation or a hilly landscape) or simply because at NOE altitudes the distance between the communicators may well exceed the LOS range. In this scenario precluding effective use of tactical VHF, helicopter to ground and helicopter to helicopter links can be reliably established over battlefield distances by use of the HF propagation mode known as Near-Vertical - Incidence-Skywave (NVIS), whereby an RF signal with a high angle of incidence (greater than 80 degrees) is reflected by the ionosphere back to earth producing an umbrella-type coverage. By appropriate selection of the operating frequency in 1 to 2 MHz passbands (windows) located in the 2 to 10 MHz range, NVIS provides gapless coverage over distances up to 300 km. Derived from text

N95-32492# Army Communications-Electronics Command, Fort Monmouth, NJ. Space and Terrestrial Communications Directorate.

TACTICAL LOW-LEVEL HELICOPTER COMMUNICATIONS **c32**

Bernard V. Ricciardi, George H. Hagn (SRI International Corp., Arlington, VA.), and Gerald August (SRI International Corp., Menlo Park, CA.) *In* AGARD, Low-Level and Nap-of-the-Earth (NOE) Night Operations Jan. 1995 13 p (For primary document see N95-32486 12-03)

Copyright Avail: CASI HC A03/MF A03

This paper identifies a systems approach to communications requirements, defines a helicopter communications system model, and describes some potential paths for future investigation and development to improve helicopter communications. The primary focus is on external communications to other helicopters and to ground stations.
Derived from text

N95-32493# British Aerospace Aircraft Group, Preston (England). Warton Aerodrome.
OPTIMUM ROUTEING: ANALYTICAL CONSTRAINT OF SEARCH SPACE **c66**
W. G. Semple *In* AGARD, Low-Level and Nap-of-the-Earth (NOE) Night Operations Jan. 1995 10 p (For primary document see N95-32486 12-03)
Copyright Avail: CASI HC A02/MF A03

Algorithms are being developed for route optimization using the geometric constraints imposed on route geometry by zero-gradient conditions on route costs. Two related techniques are under consideration. The first takes a spatial search approach using the geometric constraints to guide the search. The second uses the errors in the constraint equations on a given path to derive an iterative correction. The first technique itself divides into free, or path-aligned propagation, and bound, or grid-aligned propagation. The former enables removal of many terms in the equations, the latter removes the need for complex geometric housekeeping. To date, the techniques have been coded for two-dimensional scalar isotropic cost functions. Work is in hand to progress this to non-isotropic and multi-dimensional cases, especially to cater for representative threat tracking and missile characteristics and for fuel consumption. Results from the code produced so far are extremely encouraging. The principles have been shown to be sound, and full spatial search achieved without combinatorial explosion of computing demand. Fine-grain searches of sizable grids have been completed in less than half a second on a workstation of modest performance. 'Real' cases will in general require dynamic cost density and derivative calculations. Conventional methods can deliver these at sufficient granularity and at a sufficient rate for the present search methods, given that there appears to be scope for the average granularity in the method to be coarsened considerably. For refinement of coarse-grained search output, a fast iterative scheme has been produced. Subsequent development will address extending its stable range of usability. Derived from text

N95-32494# GEC-Marconi Avionics Ltd., Rochester (England).
A TACTICAL NAVIGATION AND ROUTEING SYSTEM FOR LOW-LEVEL FLIGHT **c66**
C. Hewitt and S. A. Broatch *In* AGARD, Low-Level and Nap-of-the-Earth (NOE) Night Operations Jan. 1995 10 p (For primary document see N95-32486 12-03)
Copyright Avail: CASI HC A02/MF A03

Many types of offensive air operations need to be carried out at low level in order to ensure survivability and to maximize the probability of mission success. However, such a flight trajectory is workload intensive and leaves little room for pilot error. It would be highly beneficial if the activities of in-flight route planning, obstacle, threat and terrain avoidance, and time and fuel monitoring could be automated. This paper presents an integrated solution to this automation problem based on the effective exploitation of terrain and mission databases. The requirements of the component parts of this system are presented. These include: (1) an optimum routing algorithm, together with the criteria used in selecting the optimum four dimensional route for all mission scenarios; (2) a ground and obstacle collision avoidance system which enables the pilot to fly low, while providing timely warnings of imminent high terrain and obstacles; and (3) the navigation accuracy required to support the optimum routing and collision avoidance systems. The paper then describes a number of systems that have been developed by GEC-Marconi Avionics with the support of the Defence Research Agency (DRA), UK Ministry of Defence. The first is an optimum routing algorithm which uses terrain and mission databases to generate an optimum route, taking account of threats, terrain, obstacles, time and fuel constraints. A description of a predictive Ground and Obstacle Collision Avoidance Technique (GOCAT) is then presented. This uses a terrain and obstacle database to assess whether the current and future aircraft trajectory is safe. Finally the navigation requirements to support these systems are discussed and a solution based on integrated INS, GPS, Map Referenced Navigation (MRN) and Edge Detection Navigation (EDN) is described. Derived from text

N95-32495# Office National d'Etudes et de Recherches Aerospatiales, Chatillon (France).
AN ORIGINAL NUMERICAL METHOD FOR AUTONOMOUS NAVIGATION [UNE METHODE NUMERIQUE ORIGINALE POUR LA NAVIGATION AUTONOME] **c63**
Hubert Cantalloube *In* AGARD, Low-Level and Nap-of-the-Earth (NOE) Night Operations Jan. 1995 9 p In FRENCH (For primary document see N95-32486 12-03)
Copyright Avail: CASI HC A02/MF A03

A original numerical method associated with classical filtering techniques, image treatment techniques, and the evidence theory is proposed for the automatic engine navigation. The ambiguous observations (confusing reference marks, false alarms, and nondetections) are tolerated. The effectiveness of the algorithm is illustrated with a concrete example.
Transl. by CASI

N95-32496# Defence Research Agency, Farnborough, Hampshire (England).
THE APPLICATION OF HELICOPTER MISSION SIMULATION TO NAP-OF-THE-EARTH OPERATIONS **c66**
P. R. Birkett and D. W. Roden *In* AGARD, Low-Level and Nap-of-the-Earth (NOE) Night Operations Jan. 1995 5 p (For primary document see N95-32486 12-03)
Copyright Avail: CASI HC A01/MF A03

This paper describes some of the system trade-offs and integration issues associated with the next generation of battlefield helicopters operating in the NOE environment. The interactions between weapons, sensors, aircrew and the platform itself are discussed and their influence on the effectiveness of the helicopter as a total system is considered. Finally, an approach to the study of helicopter system integration is presented. The 'multipleman-in-the-loop' mission simulator, HOVERS, is described and its application to a typical trade-off issue discussed. Derived from text

N95-32497*# National Aeronautics and Space Administration. Langley Research Center, Hampton, VA.
A HIGHLY RELIABLE, HIGH PERFORMANCE OPEN AVIONICS ARCHITECTURE FOR REAL TIME NAP-OF-THE-EARTH OPERATIONS **c06**
Richard E. Harper (Draper, Charles Stark Lab., Inc., Cambridge, MA.) and Carl Elks *In* AGARD, Low-Level and Nap-of-the-Earth (NOE) Night Operations Jan. 1995 14 p (For primary document see N95-32486 12-03)
Copyright Avail: CASI HC A03/MF A03

An Army Fault Tolerant Architecture (AFTA) has been developed to meet real-time fault tolerant processing requirements of future Army applications. AFTA is the enabling technology that will allow the Army to configure existing processors and other hardware to provide high throughput and ultrahigh reliability necessary for TF/TA/NOE flight control and other advanced Army applications. A comprehensive conceptual study of AFTA has been completed that addresses a wide range of issues including requirements, architecture, hardware, software, testability, producibility, analytical models, validation and verification, common mode faults, VHDL, and a fault tolerant data bus. A Brassboard AFTA for demonstration and validation has been fabricated, and two operating systems and a flight-critical Army application have been ported to it. Detailed performance measurements have been made of fault tolerance and operating system overheads while AFTA was executing the flight application in the presence of faults.
Derived from text

N95-32498# Alenia Aeronautica, Turin (Italy). System Technology Dept.
AN INTEGRATED SYSTEM FOR AIR TO GROUND OPERATIONS **c66**
Massimo Avalle *In* AGARD, Low-Level and Nap-of-the-Earth (NOE) Night Operations Jan. 1995 10 p (For primary document see N95-32486 12-03)
Copyright Avail: CASI HC A02/MF A03

The following paper describes, at the conceptual level, a possible solution for a system able to meet the hard requirements for attack A/Cs operating at low level into a high threat density scenario. The conceptual study related to this work takes place from a research program related to air to

air engagements, as some concepts mainly related to pilot workload reduction can be tuned up air to ground missions. A research program to deeply analyze the more important functions related to the safe penetration concept could be initiated from this work. Some of the main concepts related to low level A/C operations are overview and possible enhancements related to the technology trend and to possible new functions derived from enhanced system integration are discussed as an introduction for the system description. The main functions forming the system will be described and an overview about the possible involved technologies will be supplied.

Author

N95-32499# Eltro G.m.b.H., Heidelberg (Germany).
LASER BASED OBSTACLE WARNING SENSORS FOR HELICOPTERS
W. Buechtemann and M. Eibert (Dornier Luftfahrt G.m.b.H., Friedrichshafen, Germany.) *In* AGARD, Low-Level and Nap-of-the-Earth (NOE) Night Operations Jan. 1995 8 p (For primary document see N95-32486 12-03)
Copyright Avail: CASI HC A02/MF A03

Helicopters and aircraft in low-level flight have a high risk to strike obstacles, in particular power lines and overhead wires down to the size of telephone wires. This risk increases when flying nap-of-the-earth (N.O.E.), at night and under poor visibility conditions. Existing night vision equipment cannot provide safe detection of these dangerous obstacles. For these reasons there has been, for quite some time, a widely accepted need for reliable means of detecting obstacles, particularly under all acceptable Low-Level and N.O.E. flying conditions. Solutions to this problem, proposed and developed in the past, have been mainly based on millimeter wave technology. More recently, laser based system are being developed which offer good capabilities to solve this task without many of the shortcomings of the radar systems. The laser radar solution, on the other hand, has to prove its adequacy under limited visibility conditions. This paper presents laser radar developments in the thermal infrared (10 micron region) and near infrared spectral regions for helicopter obstacle warning systems. Both Dornier and Eltro have designed, built and demonstrated laser radar sensors for obstacle warning. Eltro has designed and built an experimental laser radar based on CO2-lasers and heterodyne detection. Ranges in excess of 600 m against railway overhead wires and 1100 m against extended targets have been achieved. Dornier has designed, built and flight demonstrated a GaAs laser obstacle warning sensor operating at 0.9 micron. Merits and limitations of these technologies are being discussed.

Derived from text

N95-32500# Army Night Vision Lab., Fort Belvoir, VA.
DEVELOPMENT AND FLIGHT TESTING OF AN OBSTACLE AVOIDANCE SYSTEM FOR US ARMY HELICOPTERS
Sandra L. Holder and Robert G. Branigan *In* AGARD, Low-Level and Nap-of-the-Earth (NOE) Night Operations Jan. 1995 10 p (For primary document see N95-32486 12-03)
Copyright Avail: CASI HC A02/MF A03

Today's Army Aviator must fly both low and fast in order to survive against modern anti-aircraft weapons. Such flight brings him perilously close to wires, poles, trees and other obstacles. Helicopter collisions with such obstacles have been a long-standing concern for the United States Army. In order to address this issue, the Night Vision and Electronic Sensors Directorate (NVESD) has sponsored the development of an Obstacle Avoidance System (OASYS) capable of being integrated onto an aircraft and operated in real time. Under this program, two different systems have been fabricated and delivered. Both systems utilize direct detection laser radar sensors which operate in the eyesafe regime. The two systems differ primarily in the type of laser source used. The first system, developed by Northrop Corporation, utilizes a diode laser operating at 850 nm with an average repetition rate of 64 kHz. The second system, developed by Fibertek Inc., utilizes a diode-pumped solid-state laser operating at 1.54 microns with a repetition rate of 15 kHz. Both systems have been integrated onto helicopters and extensive flight evaluations have been completed. A number of important lessons have been learned regarding the individual technologies involved and obstacle avoidance as a whole. Both systems have been demonstrated to enhance mission effectiveness and flight safety. Furthermore, the technologies have been shown to be mature enough to justify proceeding to an Engineering and Manufacturing Development (EMD) phase in which issues relating to cost, volume and weight are addressed.

Derived from text

N95-32501# Defence Research Agency, Bedford (England).
THE ANGLO-FRENCH COMPACT LASER RADAR DEMONSTRATOR PROGRAMME **c32**
G. M. Hogg, K. Harrison, and S. Minisclou (STTE, Paris, France.) *In* AGARD, Low-Level and Nap-of-the-Earth (NOE) Night Operations Jan. 1995 8 p (For primary document see N95-32486 12-03)
Copyright Avail: CASI HC A02/MF A03

CLARA is an Anglo-French Compact Laser Radar technical demonstrator program. It is a multi-mode CO2 laser radar, the primary mode being cable and obstacle warning, with additional modes including terrain following and a range of targeting modes. The 3 1/2 year program will provide both France and the UK with a podded equipment in 1996. The UK will carry out fixed wing trials and France will fit their pod on a helicopter. The flight trials data are being exchanged between the two countries.

Derived from text

N95-32502# Aeronautica Militare Italiana, Rome.
FIXED WING NIGHT ATTACK MISSIONS: ASSESSMENT IN A FLIGHT SIMULATION ENVIRONMENT **c09**
G. Arpaia, E. Scarabotto, and I. M. Spinoni (Alenia Aeronautica, Turin, Italy.) *In* AGARD, Low-Level and Nap-of-the-Earth (NOE) Night Operations Jan. 1995 12 p (For primary document see N95-32486 12-03)
Copyright Avail: CASI HC A03/MF A03

Transforming a dedicated daytime attack aircraft in an effective night-attack weapon system requires the evaluation of different aircraft and navigation/attack sensor configuration options. Flight Simulation has been considered an appropriate tool to enable preliminary evaluations of these different options. This paper illustrates the results of a first series of evaluations performed on the Alenia Aeronautica AM-X Flight Simulator with participation of Italian Air Force pilots and engineers to evaluate some proposed options for a night-attack version of the Alenia-Aermacchi-Embraer AM-X aircraft. Derived from text

N95-32503# Sextant Avionique, Saint Medard en Jalles (France).
A HELMET MOUNTED DISPLAY FOR NIGHT MISSIONS AT LOW ALTITUDE [UN VISUEL DE CASQUE POUR LA MISSION DE NUIT A BASSE ALTITUDE] **c06**
Jean-Pierre Cursolle, Alain Leger, and Franck Leppert *In* AGARD, Low-Level and Nap-of-the-Earth (NOE) Night Operations Jan. 1995 10 p In FRENCH (For primary document see N95-32486 12-03)
Copyright Avail: CASI HC A02/MF A03

The achievement of air to ground mission in a complex operational context, with bad meteorological conditions and, moreover by night is a very demanding task for the pilot. This mission requests a high situation awareness which can only be reached with specific, accurate and reliable means, such as sensors, displays or controls, perfectly integrated in the aircraft system. The mission can be successfully realized thanks to sensors performances. But, the use of FLIR or I(sup 2)T depends on a lot of conditions such as weather with bad effects on the efficiency. So images must be enhanced with symbols to be fully exploitable. Furthermore, the sensors have to be fully integrated, the efficiency depending on the interfaces such as displays and controls. The third Generation Helmet Mounted Display is an answer to this requirement but has to be fighter pilot customized. The conference will include a few operational requirements recall, the Sextant Gen 3 HMD description and will highlight the first symbology results issued from a ground simulation assessment. Author

N95-32504# Fabrica Italiana Apparecchiature Radioelettriche S.p.A., Milan (Italy).
SIRPH: STEERABLE INFRARED PICTURE ON HELMET MOUNTED DISPLAY **c54**
Giorgio Balzarotti, Lorenzo Fiori, and Beatrice Midollini *In* AGARD, Low-Level and Nap-of-the-Earth (NOE) Night Operations Jan. 1995 10 p (For primary document see N95-32486 12-03)
Copyright Avail: CASI HC A02/MF A03

Helmet Mounted Displays (HMD's) are being paid remarkable attention as an essential aid to pilots of both fixed and rotary wing aircraft: The technological improvements such equipment are experiencing place them in an outstanding position among avionics. A very important role in the success of HMD's is played by the management of man-machine-interface aspects: The way to make the information available, in a useful format, to the pilot must be considered with particular care. A smart example is the

presentation of images from steerable sensors: The head tracking systems have actually achieved a high degree of accuracy, thus allowing a precise control of the Line Of Sight (LOS) of electrooptical vision systems. Therefore, pictures generated by a steerable infrared sensor slaved to the pilot's head movements can be displayed onto the helmet visor, in order to provide the pilot with a substantial aid in day and night, adverse weather conditions, high altitudes down to low level and nap of the earth flight operations. The paper describes the results of a technical analysis performed on a system based on a steerable IR sensor integrated with an advanced HMD for navigation aid purposes. The parameters which lead to an imperfect static or dynamic overlay of the generated IR picture with the external world, as seen by the pilot through the helmet visors, and the effects of such misalignment are analyzed in detail, together with integration aspects and human engineering factors. The analysis has also taken into account the finite angular excursion of the IR sensor LOS, originated by gimbals limits, and the consequent necessary transition to and from the LLTV's integrated within the helmet, suitable to cover all possible head motions, has been investigated. An approach to the problem of the fusion of information generated by the IR sensor and the LLTV's is also reported. Finally, the paper highlights the limits and the constraints of navigation using a steerable IR sensor, with respect to safety aspects. Author

N95-32505# Defence Research Agency, Farnborough, Hampshire (England). Man Machine Integration Dept.

COVERT NIGHT/DAY OPERATIONS FOR ROTORCRAFT (CONDOR) PROGRAMME c66

T. H. Southam *In* AGARD, Low-Level and Nap-of-the-Earth (NOE) Night Operations Jan. 1995 16 p (For primary document see N95-32486 12-03)

Copyright Avail: CASI HC A03/MF A03

CONDOR is a major joint US-UK project that will support a comprehensive demonstration of the functionality of current and future attack helicopters under day/night adverse weather conditions in a nap of the Earth environment. The aim of the program is to investigate the integration of a suite of avionics, sensors and displays for battlefield helicopters and to assess their effectiveness during ingress, egress and attack phases of the mission. The concept features a precision navigation system which together with a steerable sensor coupled visually, via a helmet-position sensing system, to an advanced helmet mounted display with a wide FOV, full colour and laser eye protection enables a virtual outside world overlaid with appropriate flight and mission information to the pilot. The program includes development and building of the advanced hardware, research into the human factors issues connected with their exploitation, symbology development coupled to a detailed application in a full mission scenario. Flight demonstrations are scheduled to take place in both the Lynx at DRA and, with subsequent testing in the U.S., to exploit a new full-authority FBW flight control system with mission configurable control laws. Author

N95-32705# General Accounting Office, Washington, DC. Accounting and Information Management Div.

REPORT TO THE CHAIRMAN, SUBCOMMITTEE ON AVIATION, COMMITTEE ON COMMERCE, SCIENCE, AND TRANSPORTATION, US SENATE. AVIATION SAFETY: DATA PROBLEMS THREATEN FAA STRIDES ON SAFETY ANALYSIS SYSTEM

8 Feb. 1995 31 p

(GAO/AIMD-95-27; B-259097) Avail: CASI HC A03/MF A01; GAO, PO Box 6015, Gaithersburg, MD 20877 HC

Catastrophic aviation events, such as the recent airline crashes, have placed renewed attention on the Federal Aviation Administration's (FAA) oversight of the aviation community's compliance with safety regulations. To meet this challenge, FAA relies on a group of highly professional and committed aviation inspection and certification personnel. However, this group faces an enormous task: overseeing hundreds of domestic airlines and thousands of aircraft and personnel, not to mention the multitudes of other aviation community participants, such as flight training schools. To assist in this endeavor, FAA is acquiring an automated decision support tool, called the Safety Performance Analysis System (SPAS). This system is intended to assist FAA in focusing its limited inspection and certification resources. Because of GAO's long-standing interest in helping FAA improve its inspection and certification programs, GAO reviewed FAA's development and deployment of SPAS to determine (1) whether FAA is effectively managing the acquisition of SPAS, including its data communication network, and (2) the extent to which SPAS will rely on Aviation Safety Analysis System databases and whether FAA is effectively addressing known data quality problems with the databases. Derived from text

N95-32784# General Accounting Office, Washington, DC. Resources, Community, and Economic Development Div.

REPORT TO THE CHAIRMAN, SUBCOMMITTEE ON AVIATION, COMMITTEE ON COMMERCE, SCIENCE, AND TRANSPORTATION, US SENATE. AVIATION SAFETY: FAA CAN BETTER PREPARE GENERAL AVIATION PILOTS FOR MOUNTAIN FLYING RISKS

9 Dec. 1993 67 p

(GAO/RCED-94-15; B-254704) Avail: CASI HC A04/MF A01; GAO, PO Box 6015, Gaithersburg, MD 20877 HC

The FAA's oversight of general aviation safety in mountainous areas is examined. Specifically, the GAO was asked to identify (1) the extent to which mountainous areas present higher risks than nonmountainous areas for general aviation and (2) the actions that FAA is taking and should take to reduce the risks associated with mountain flying and the impact of those actions on general aviation. In addition, GAO was asked to examine the legal and safety issues involved with the prohibition imposed by Pitkin County, Colorado, on general aviation night operations at Aspen Airport. In analyzing National Transportation Safety Board (NTSB) data, GAO found that the general aviation accident rate was (1) nearly 40 percent higher for western states designated by FAA as mountainous than the rate for all other continental states in fiscal year 1992 and (2) 155 percent higher for a group of selected mountain airports than for a group of nonmountain airports with similar levels of flight operations between fiscal years 1983 and 1992. FAA alerts general aviation pilots about the hazards of flying in mountainous areas during the pilot certification process and at subsequent safety seminars. Many of the suggested actions that the FAA could take to more effectively promote mountain flying safety, such as issuing guidance that identifies special mountain airports with difficult operating conditions and recommends routes for takeoffs and landings at those airports, would impose little financial burden on the general aviation industry. Analysis indicates that night operations under visual flight rules at Aspen Airport would be hazardous, in contradiction to the conclusions of the FAA's 1992 study. CASI

N95-32885# General Accounting Office, Washington, DC. Resources, Community, and Economic Development Div.

AVIATION SECURITY: DEVELOPMENT OF NEW SECURITY TECHNOLOGY HAS NOT MET EXPECTATIONS. REPORT TO CONGRESSIONAL REQUESTERS

19 May 1994 59 p

(GAO/RCED-94-142; B-256584) Avail: CASI HC A04/MF A01; GAO, PO Box 6015, Gaithersburg, MD 20877 HC

This report examines the Federal Aviation Administration's (FAA) efforts to develop new equipment for detecting explosives and methods to improve aircraft survivability as mandated by the Aviation Security Improvement Act of 1990. Recommendations are made to ensure that (1) FAA's process for approving new explosive detection equipment can provide the aviation community and the flying public with effective and reliable technology and (2) FAA's research efforts are properly managed to meet the threats to aviation. FAA has made little progress towards meeting the act's goal for deploying new explosive detection systems. Although several devices show promise, technical problems are slowing the development and approval of the devices. Similarly, FAA's efforts to enhance aircraft survivability are promising but are several years from completion. In addition, FAA does not plan to test new explosive detection systems at airports during the certification process. Other identified weaknesses in FAA's security research program are that FAA does not (1) conduct software reviews to evaluate system designs, (2) emphasize integrating different technologies into total systems, or (3) focus sufficient attention on human factors' issues. Purchasing the new security equipment will also place demands on the airlines throughout the next decade. However, FAA lacks a strategy to guide its and the airlines' efforts to implement this equipment. Several issues are identified that need to be resolved before Airport Improvement Program funds can be used for such purposes. CASI

N95-34766*# Nottingham Univ. (England).
A ROSE BY ANY OTHER NAME: CERTIFICATION SEEN AS PROCESS RATHER THAN CONTENT
John R. Wilson *In* Embry-Riddle Aeronautical Univ., Daytona Beach,FL, Human Factors Certification of Advanced Aviation Technologies 1994 p 26-34 (For primary document see N95-34764 12-54)
Avail: CASI HC A02/MF A04

04 AIRCRAFT COMMUNICATIONS AND NAVIGATION

Includes digital and voice communication with aircraft; air navigation systems (satellite and ground based); and air traffic control.

For related information see also *17 Space Communications, Spacecraft Communications, Command and Tracking* and *Communications and Radar.*

N95-33480# Massachusetts Inst. of Tech., Lexington, MA. Lincoln Lab.
GPS-SQUITTER INTERFERENCE ANALYSIS
Vincent A. Orlando and William H. Harman, III 6 Apr. 1995 42 p
(Contracts DTFA01-93-Z-02012; F19628-95-C-0002)
(AD-A293690; ATC-229) Avail: CASI HC A03/MF A01

GPS-Squitter is a system concept that merges the capabilities of Automatic Dependent Surveillance (ADS) and the Mode S beacon radar. The result is an integrated concept for seamless surveillance and data link that permits equipped aircraft to participate in ADS and/or beacon ground environments, offering many possibilities for transition from a beacon to an ADS-based environment. Since GPS-Squitter and its associated data link share the 1030/1090-MHz beacon frequencies with other users (e.g., ground beacon radars and TCAS), there is some level of interaction between the operation of these various systems. One form of interaction is the effect on GPS-Squitter operation caused by the activities of other users. This effect, plus the effect of self-interference of GPS-Squitter Operation, determines the operational capacity of GPS-Squitter. The complementary process is the effect of the GPS-Squitter operation on the other users of the beacon frequencies. This report provides an analysis of the interference to other users of the 1030/1090-MIlz beacon frequencies caused by GPS-Squitter operation. The principal interference effect is channel occupancy on the beacon frequencies that prevents the reception of a desired signal by a receiver. The basis for the analysis is to estimate the channel occupancy on the beacon frequencies and its effect on the operation of victim receivers on those frequencies. The analysis is performed separately for the two frequencies. The analysis of 1030-MHz interference estimates the effect of the 1030-MHz data link activity that may be associated with GPS-Squitter (such as differential correction broadcast and two-away data link) on the operation of a transponder receiver. The 1090-MHz analysis estimates similar interference effects on: (1) a terminal or en route sensor receiver, and (2) a TCAS receiver. DTIC

N95-34562# Massachusetts Inst. of Tech., Cambridge, MA. Aeronautical Systems Lab.
CURRENT ISSUES IN THE DESIGN AND INFORMATION CONTENT OF INSTRUMENT APPROACH CHARTS Final Report, period ending Nov. 1990
R. J. Hansman, Jr. and Mark Mykityshyn Mar. 1995 74 p
(Contract DTRS57-88-C-00078)
(AD-A294752; DOT/FAA/AAR-95/1) Avail: CASI HC A04/MF A01

This report documents an analysis and interview effort conducted to identify common operational errors made using current Instrument Approach Plates (IAP), Standard Terminal Arrival Route (STAR) charts, Standard Instrument Departure (SID) charts, and the preferences of pilots regarding current chart format designs. In addition, pilot preferences or comments relevant to the presentation of IAP information in advanced electronic format were solicited and noted. The analysis included data from prior studies and a variety of accident, incident, and operational error databases. Representatives from flight operation user groups and charting organizations were interviewed to gain insight into operational errors, pilot preferences and the factors which influence chart design. The IAP user groups interviewed consisted primarily of training centers and individuals representing the full spectrum of IAP users (General Aviation, Corporate Aviation, Air Taxi Part 135 Operators, and Air Carrier Part 121 Operators). Cartographic organizations interviewed included Jeppesen Sanderson Inc., NOAA and the FAA. For comparison, a non-US based Carrier and chart provider (KLM) was queried by mail. DTIC

N95-34570# Air Force Inst. of Tech., Wright-Patterson AFB, OH.
THE EFFECTS OF DISPLAY LOCATION AND DIMENSIONALITY ON TAXIWAY NAVIGATION M.S. Thesis
James W. Lasswell 1995 83 p
(AD-A294878; AFIT/CI-95-028) Avail: CASI HC A05/MF A01

This study investigated whether taxiway navigation is best supported by head-up or head-down presentation of either perspective (3-D conformal) or plan-view (2-D nonconformal) route guidance information. Thirty-two pilots taxied in low visibility conditions (300' RVR) in a high-fidelity simulator. Pilots were instructed to maximize speed while maintaining safe control of the aircraft as they taxied along a specified route. Pilots were randomly assigned to either the 2D or 3D display condition. Each subject completed half of the trials with the display in the head-up position, and half with the display in the head-down position. Expected events were presented in both near and far domains, while an unexpected event was presented in the far domain. Results revealed that, while pilots in both groups followed the cleared route with equal success, greater mean taxi speeds were supported by the 2D display, but lateral tracking error showed a slight advantage for the 3D display. A significant number of pilots using the 2D display failed to detect and respond to the unexpected far domain event (ground traffic), resulting in six collisions. The practical and theoretical implications of these results are discussed. DTIC

N95-34797# Battelle Memorial Inst., Columbus, OH.
RESOURCE DOCUMENT FOR THE DESIGN OF ELECTRONIC INSTRUMENT APPROACH PROCEDURE DISPLAYS Final Report, Jul. 1993 - Dec. 1994
Melanie C. Wright and Todd Barlow Mar. 1995 238 p Sponsored by FAA
(AD-A295108; DOT-VNTSC-FAA-95-9; DOT/FAA/RD-95/2) Avail: CASI HC A11/MF A03

Instrument approach procedure (ZAP) charts play a large role in contributing to the success or failure of approaches and landings. Paper ZAP charts have been criticized for excessive clutter, for text sizes that are too small to read, and for inadequate terrain representation. The electronic presentation of approach information may counteract these criticisms by providing automatic or pilot controlled filtering of the information displayed. However, without careful attention to human factors issues early in the design and development of electronic ZAPs (EZAP's), new problems may result. The goal of this project was to develop preliminary guidelines for designers and certifiers of EZAP's to assure that EZAP's help rather than hinder pilots during approach and Landing. To identify potential human factors problems in the design of EZAP's, current paper ZAP charts and the instrument approach task were studied. Pilots were interviewed and literature describing the information requirements of the task and the cognitive implications of the task were reviewed. A cognitive task analysis was performed. Specific features and functions were identified that may be beneficial to an EZAP. Literature was reviewed in the areas of cognitive psychology, human-computer interaction, and aviation to identify design concepts and principles for the design of these features and functions. Guidelines were developed from the design concepts and principles and, finally, prototypes of EZAP's were designed in accordance with the new guidelines. DTIC

N95-32490*# National Aeronautics and Space Administration. Ames Research Center, Moffett Field, CA.
FLIGHT TEST OF A LOW-ALTITUDE HELICOPTER GUIDANCE SYSTEM WITH OBSTACLE AVOIDANCE CAPABILITY
Richard E. Zelenka, Raymond F. Clark (Army Command/Control and Systems Integration Directorate, Fort Monmouth, NJ.), and Robert G. Branigan (Army Night Vision Lab., Fort Belvoir, VA.) *In* AGARD, Low-Level and Nap-of-the-Earth (NOE) Night Operations Jan. 1995 10 p (For primary document see N95-32486 12-03)
Copyright Avail: CASI HC A02/MF A03

N95-33131# Central Research and Development Inst. Elektropribor, Saint Petersburg (Russia).
NAVIGATIONAL TECHNOLOGY OF DUAL USAGE
V. G. Peshekhonov, I. M. Okon, L. P. Nesenyuk, and Yu. P. Belous *In* AGARD, Dual Usage in Military and Commercial Technology in Guidance and Control Mar. 1995 6 p (For primary document see N95-33126 12-31)
Copyright Avail: CASI HC A02/MF A02

N95-33134# Technische Univ., Brunswick (Germany). Inst. fuer Flugfuehrung.
EFFECTS OF THE SPECIFIC MILITARY ASPECTS OF SATELLITE NAVIGATION ON THE CIVIL USE OF GPS/GLONASS
Detlef Kayser and Gunther Schaenzer *In* AGARD, Dual Usage in Military and Commercial Technology in Guidance and Control Mar. 1995 10 p (For primary document see N95-33126 12-31)
Copyright Avail: CASI HC A02/MF A02

N95-33135# Deutsche Forschungsanstalt fuer Luft- und Raumfahrt, Brunswick (Germany). Inst. of Flight Guidance.
THE DLR RESEARCH PROGRAMME ON AN INTEGRATED MULTI SENSOR SYSTEM FOR SURFACE MOVEMENT GUIDANCE AND CONTROL
Kurt Klein *In* AGARD, Dual Usage in Military and Commercial Technology in Guidance and Control Mar. 1995 8 p (For primary document see N95-33126 12-31)
Copyright Avail: CASI HC A02/MF A02

N95-33136# Centre d'Etudes et de Recherches, Toulouse (France). Dept. d'Etudes et de Recherche en Optique.
LOW-LEVEL DATA FUSION FOR LANDING RUNWAYS DETECTION
Laure Sliwa and Xavier Briottet *In* AGARD, Dual Usage in Military and Commercial Technology in Guidance and Control Mar. 1995 11 p (For primary document see N95-33126 12-31)
Copyright Avail: CASI HC A03/MF A02

N95-33140# Lockheed-Fort Worth Co., Fort Worth, TX.
APPLICATION OF ADVANCED SAFETY TECHNIQUE TO RING LASER GYRO INERTIAL NAVIGATION SYSTEM INTEGRATION
James Blaylock, Donald Swihart (Wright Lab., Wright-Patterson AFB, OH.), and Chuck Stribula (Aeronautical Systems Div., Wright-Patterson AFB, OH.) *In* AGARD, Dual Usage in Military and Commercial Technology in Guidance and Control Mar. 1995 10 p (For primary document see N95-33126 12-31)
Copyright Avail: CASI HC A02/MF A02

N95-34770*# Civil Aviation Authority, Farnborough (England).
HUMAN FACTORS CERTIFICATION IN THE DEVELOPMENT OF FUTURE AIR TRAFFIC CONTROL SYSTEMS
Alyson E. Evans *In its* Human Factors Certification of Advanced Aviation Technologies 1994 p 87-96 (For primary document see N95-34764 12-54)
Avail: CASI HC A02/MF A04

N95-34771*# Royal Air Force Inst. of Aviation Medicine, Farnborough (England).
QUALITY ASSURANCE AND RISK MANAGEMENT: PERSPECTIVES ON HUMAN FACTORS CERTIFICATION OF ADVANCED AVIATION SYSTEMS
Robert M. Taylor and Iain S. MacLeod (Aerosystems International, Yeovil, England.) *In* Embry-Riddle Aeronautical Univ., Daytona Beach,FL, Human Factors Certification of Advanced Aviation Technologies 1994 p 97-118 (For primary document see N95-34764 12-54)
Avail: CASI HC A03/MF A04

05 AIRCRAFT DESIGN, TESTING AND PERFORMANCE

Includes aircraft simulation technology.

For related information see also *18 Spacecraft Design, Testing and Performance* and *39 Structural Mechanics*.For land transportation vehicles see *85 Urban Technology and Transportation*.

N95-32699*# National Aeronautics and Space Administration. Ames Research Center, Moffett Field, CA.
FULL-SCALE HINGELESS ROTOR PERFORMANCE AND LOADS
Randall L. Peterson Jun. 1995 829 p
(NASA-TM-110356; A-950069; NAS 1.15:110356) Avail: CASI HC A99/MF A10

A full-scale BO-105 hingeless rotor system was tested in the NASA Ames 40- by 80-Foot Wind Tunnel on the rotor test apparatus. Rotor performance, rotor loads, and aeroelastic stability as functions of both collective and cyclic pitch, tunnel velocity, and shaft angle were investigated. This test was performed in support of the Rotor Data Correlation Task under the U.S. Army/German Memorandum of Understanding on Cooperative Research in the Field of Helicopter Aeromechanics. The primary objective of this test program was to create a data base for full-scale hingeless rotor performance and structural blade loads. A secondary objective was to investigate the ability to match flight test conditions in the wind tunnel. This data base can be used for the experimental and analytical studies of hingeless rotor systems over large variations in rotor thrust and tunnel velocity. Rotor performance and structural loads for tunnel velocities from hover to 170 knots and thrust coefficients (C(sub T)/sigma) from 0.0 to 0.12 are presented in this report. Thrust sweeps at tunnel velocities of 10, 20, and 30 knots are also included in this data set. Author

N95-32904 Old Dominion Univ., Norfolk, VA.
THREE-DIMENSIONAL AERODYNAMIC SHAPE OPTIMIZATION USING DISCRETE SENSITIVITY ANALYSIS Ph.D. Thesis
Gregory Wayne Burgreen 1994 154 p
Avail: Univ. Microfilms Order No. DA9423428

An aerodynamic shape optimization procedure based on discrete sensitivity analysis is extended to treat three-dimensional geometries. The function of sensitivity analysis is to directly couple computational fluid dynamics (CFD) with numerical optimization techniques, which facilitates the construction of efficient direct-design methods. The development of a practical three-dimensional design procedures entails many challenges, such as: (1) the demand for significant efficiency improvements over current design methods; (2) a general and flexible three-dimensional surface representation; and (3) the efficient solution of very large systems of linear algebraic equations. It is demonstrated that each of these challenges is overcome by: (1) employing fully implicit (Newton) methods for the CFD analyses; (2) adopting a Bezier-Bernstein polynomial parameterization of two- and three-dimensional surfaces; and (3) using preconditioned conjugate gradient-like linear system solvers. Whereas each of these extensions independently yields an improvement in computational efficiency, the combined effect of implementing all the extensions simultaneously results in a significant factor of 50 decrease in computational time and a factor of eight reduction in memory over the most efficient design strategies in current use. The new aerodynamic shape optimization procedure is demonstrated in the design of both two- and three-dimensional inviscid aerodynamic problems including a two-dimensional supersonic internal/external nozzle, two-dimensional transonic airfoils (resulting in supercritical shapes), three-dimensional transonic transport wings, and three-dimensional supersonic delta wings. Each design application results in realistic and useful optimized shapes. Dissert. Abstr.

N95-32928*# Arizona State Univ., Tempe, AZ. Dept. of Mechanical and Aerospace Engineering.
DEVELOPMENT OF A COMPOSITE TAILORING PROCEDURE FOR AIRPLANE WING Progress Report
Aditi Chattopadhyay and Sen Zhang 3 Aug. 1995 14 p
(Grant NAG2-908)
(NASA-CR-199081; NAS 1.26:199081) Avail: CASI HC A03/MF A01

The development of a composite wing box section using a higher order-theory is proposed for accurate and efficient estimation of both static

and dynamic responses. The theory includes the effect of through-the-thickness transverse shear deformations which is important in laminated composites and is ignored in the classical approach. The box beam analysis is integrated with an aeroelastic analysis to investigate the effect of composite tailoring using a formal design optimization technique. A hybrid optimization procedure is proposed for addressing both continuous and discrete design variables. Derived from text

N95-33311 California Univ., Davis, CA.
ANALYSIS AND DESIGN METHODOLOGY FOR CHORDWISE DEFORMABLE WINGS Ph.D. Thesis
Yau-Sheun Chang 1993 135 p
Avail: Univ. Microfilms Order No. DA9415898

Structural tailoring concepts have been developed to create wings with elastically produced camber for the purpose of increasing the lift generated by these wings. A new, simple structural model intended for use in aeroelastic tailoring studies of high aspect ratio wings is presented. The model is assumed to behave with Bernoulli-Euler type spanwise bending. Closed form expressions for all stiffnesses and compliances have been obtained by modifying the theory of Rehfield. Two primary and two secondary structural concepts have been created to produce chordwise camber deformations that result in enhanced lift. Two designs have been found that optimize the aerodynamic benefits of these wings. It appears that lift enhancements of sufficient magnitude can be produced to render this type of wing tailoring of practical interest. Two performance studies, one for the maximum chordwise camber curvature and the other for the maximum lift production, have been performed and discussed. Four distinct configuration designs are used for these studies. It has been shown that, with the aggressive utilization of elastic tailoring, increased performance and structural weight savings can be achieved. The influence of camber induced bending divergence on the configuration designs has been investigated and analyzed. The occurrence of a static instability of this type arises because wing bending produces positive camber, which, in turn, produces additional lift, and, hence, increased bending of the wing. For subsonic flight conditions, a bending type instability will not occur. The only instability is the torsional one. Finally, the effects of changing environmental conditions, elevated temperature and humidity, on the effective Poisson ratios and configuration designs for laminated carbon composites have been studied. It should be noted that much care is needed when designing a wing which will be subject to a wide range temperature and moisture extremes.
Dissert. Abstr.

N95-34422# General Accounting Office, Washington, DC. National Security and International Affairs Div.
COMANCHE HELICOPTER: TESTING NEEDS TO BE COMPLETED PRIOR TO PRODUCTION DECISIONS
18 May 1995 30 p
(AD-A294408; GAO/NSIAD-95-112) Avail: CASI HC A03/MF A01

This report presents the results of the GAO review of the Department of the Army's Comanche helicopter program. It is recommended that the Secretary of Defense require the Army to complete operational testing to validate the Comanche's effectiveness and suitability before committing any funds to acquire long-lead production items or enter low-rate initial production. Derived from text

N95-34583# Galaxy Scientific Corp., Pleasantville, NJ.
CORROSION OF FIRE-DAMAGED AIRCRAFT Final Report
William T. Westfield Apr. 1995 31 p
(Contract DTFA03-89-C-0043)
(AD-A294968; DOT/FAA/CT-94/89) Avail: CASI HC A03/MF A01

The Federal Aviation Administration (FAA) Western Pacific Regional Office issued a Significant Activity Report concerning a 5727 that experienced extensive corrosion, well beyond what would have normally been expected for an aircraft with its operational time and cycles. This incident triggered interest in the possible connection between fire, extinguishment, and subsequent increased incidence of corrosion. The FAA Technical Center requested an investigation of the potential for this connection to exist by performing an analysis of available data. Trends of aircraft operational hours, cycles, fire occurrence, and corrosion reports were developed. Data extending from 1974 to the present were accessed from the Aviation Research and Support database and the Service Difficulty Reports (SDRs) database, respectively. Sufficient data to support a connection between fire and subsequent related corrosion were not available. Twenty-two aircraft were analyzed and none exhibited a pattern of corrosion that could definitely be associated with fire smoke or extinguishment. This result was supported by consideration of the intensity of the fire, the extinguishing agent and the time between the occurrence of the fire and the corrosion reports.
DTIC

N95-34793# Army Aeromedical Research Lab., Fort Rucker, AL.
TRANSMITTANCE CHARACTERISTICS OF US ARMY ROTARY-WING AIRCRAFT TRANSPARENCIES Final Report
Sean L. Wentworth, Everette McGowin, III, Rebecca H. Ivey, Clarence E. Rash, and William E. McLean Mar. 1995 40 p
(AD-A295035; USAARL-95-19) Avail: CASI HC A03/MF A01

This report documents a survey of the spectral and luminous transmittance characteristics of transparencies (windscreens) used in currently fielded U.S. Army rotary-wing aircraft. The survey was conducted in two phases. In the first phase, samples of windscreens from each aircraft type were evaluated in the laboratory for phototopic (day) and scotopic (night) luminous transmittance. The spectral transmittance of each sample also was measured. Based on laboratory measurements of unused samples, all windscreens met specifications. However, field measurements on windscreens showed consistent failure of luminous transmittance requirements. This loss of transmittance is attributed to haze resulting from exposure to environmental factors. DTIC

N95-33023*# National Aeronautics and Space Administration. Hugh L. Dryden Flight Research Center, Edwards, CA.
FLIGHT TEST OF A PROPULSION CONTROLLED AIRCRAFT SYSTEM ON THE NASA F-15 AIRPLANE
Frank W. Burcham, Jr. and Trindel A. Maine *In its* An Electronic Workshop on the Performance Seeking Control and Propulsion Controlled Aircraft Results of the F-15 Highly Integrated Digital Electronic Control Flight Research Program Jan. 1995 p 193-221 (For primary document see N95-33009 12-07)
Avail: CASI HC A03/MF A03

N95-33024*# Planning Research Corp., Edwards, CA.
DYNAMIC GROUND EFFECTS FLIGHT TEST OF THE NASA F-15 AIRCRAFT
Stephen Corda *In* NASA. Dryden Flight Research Center, An Electronic Workshop on the Performance Seeking Control and Propulsion Controlled Aircraft Results of the F-15 Highly Integrated Digital Electronic Control Flight Research Program Jan. 1995 p 222-228 (For primary document see N95-33009 12-07)
Avail: CASI HC A02/MF A03

N95-33025*# National Aeronautics and Space Administration. Hugh L. Dryden Flight Research Center, Edwards, CA.
DESIGN CHALLENGES ENCOUNTERED IN THE F-15 PCA FLIGHT TEST PROGRAM
Trindel A. Maine, Frank W. Burcham, Jr., Peter Schaefer (University of Southern California, Los Angeles, CA.), and John Burken *In its* An Electronic Workshop on the Performance Seeking Control and Propulsion Controlled Aircraft Results of the F-15 Highly Integrated Digital Electronic Control Flight Research Program Jan. 1995 p 229-244 (For primary document see N95-33009 12-07)
Avail: CASI HC A03/MF A03

N95-33145# Aerodata Flugmesstechnik G.m.b.H., Brunswick (Germany).
INTEGRATED SPECIAL MISSION FLIGHT MANAGEMENT FOR A FLIGHT INSPECTION AIRCRAFT
A. Redeker and M. Haverland *In* AGARD, Dual Usage in Military and Commercial Technology in Guidance and Control Mar. 1995 3 p (For primary document see N95-33126 12-31)
Copyright Avail: CASI HC A01/MF A02

N95-34506# Princeton Univ., NJ. Dept. of Mechanical and Aerospace Engineering.
REQUIREMENTS AND TRENDS OF COMPUTATIONAL AERODYNAMICS AS A TOOL FOR AIRCRAFT DESIGN
Antony Jameson *In* National Aerospace Lab., Special Publication of

National Aerospace Laboratory 16 Jun. 1994 p 1-49 (For primary document see N95-34505 12-02)
Avail: CASI HC A03/MF A03

N95-34541# Fujitsu Ltd., Tokyo (Japan).
NUMERICAL ANALYSIS AROUND THE WHOLE SST CONFIGURATION Abstract Only
Tetsuo Yamazaki and Takashi Uchida (Japan Aircraft Development Corp., Tokyo, Japan.) *In* National Aerospace Lab., Special Publication of National Aerospace Laboratory 16 Jun. 1994 p 261-265 In JAPANESE (For primary document see N95-34505 12-02)
Avail: CASI HC A01/MF A03

N95-34542# National Aerospace Lab., Tokyo (Japan).
APPLICATION OF CFD TECHIQUE FOR HYFLEX AERODYNAMIC DESIGN Abstract Only
Yukimitsu Yamamoto, Shigeya Watanabe (National Space Development Agency, Tokyo, Japan.), Mitsuo Ishiguro (Mitsubishi Heavy Industries Ltd., Tokyo, Japan.), and Kou Ogasawara (Mitsubishi Heavy Industries Ltd., Tokyo, Japan.) *In its* Special Publication of National Aerospace Laboratory 16 Jun. 1994 p 267-272 In JAPANESE (For primary document see N95-34505 12-02)
Avail: CASI HC A02/MF A03

06 AIRCRAFT INSTRUMENTATION

Includes cockpit and cabin display devices; and flight instruments.

For related information see also *19 Spacecraft Instrumentation* and *35 Instrumentation and Photography.*

N95-32497*# National Aeronautics and Space Administration. Langley Research Center, Hampton, VA.
A HIGHLY RELIABLE, HIGH PERFORMANCE OPEN AVIONICS ARCHITECTURE FOR REAL TIME NAP-OF-THE-EARTH OPERATIONS
Richard E. Harper (Draper, Charles Stark Lab., Inc., Cambridge, MA.) and Carl Elks *In* AGARD, Low-Level and Nap-of-the-Earth (NOE) Night Operations Jan. 1995 14 p (For primary document see N95-32486 12-03)
Copyright Avail: CASI HC A03/MF A03

N95-32503# Sextant Avionique, Saint Medard en Jalles (France).
A HELMET MOUNTED DISPLAY FOR NIGHT MISSIONS AT LOW ALTITUDE [UN VISUEL DE CASQUE POUR LA MISSION DE NUIT A BASSE ALTITUDE]
Jean-Pierre Cursolle, Alain Leger, and Franck Leppert *In* AGARD, Low-Level and Nap-of-the-Earth (NOE) Night Operations Jan. 1995 10 p In FRENCH (For primary document see N95-32486 12-03)
Copyright Avail: CASI HC A02/MF A03

07 AIRCRAFT PROPULSION AND POWER

Includes prime propulsion systems and systems components, e.g., gas turbine engines and compressors; and onboard auxilliary power plants for aircraft.

For related information see also *20 Spacecraft Propulsion and Power, 28 Propellants and Fuels,* and *44 Energy Production and Conversion.*

N95-32636# Allison Engine Co., Indianapolis, IN.
ALLISON ENGINE TESTING CMSX-4(REG SIGN) SINGLE CRYSTAL TURBINE BLADES AND VANES
P. S. Burkholder, M. C. Thomas, D. J. Frasier, J. R. Whetstone, K. Harris (Cannon-Muskegon Corp., MI.), G. L. Erickson (Cannon-Muskegon Corp., MI.), S. L. Sikkenga (Cannon-Muskegon Corp., MI.), and J. M. Eridon (Cannon-Muskegon Corp., MI.) 1995 16 p Presented at the 3rd International Charles Parsons Turbine Conference: Materials Engineering in Turbines and Compressors, Newcastle upon Tyne, UK, 25-27 Apr. 1995
(Contract DE-AC21-93MC-29257)
(DE95-010308; DOE/MC-29257/95/C0452; CONF-950463-1) Avail: CASI HC A03/MF A01

A team approach utilizing simultaneous engineering has been used to develop CMSX-4 turbine airfoil components. CMSX-4 is a nickel-base single crystal superalloy containing 3% (wt) rhenium and a high 71% volume fraction of coherent (gamma)(prime) precipitate strengthening phase. The high level of balanced properties determined by extensive laboratory evaluation has been confirmed during engine testing the Allison AE 2100 and AE 301X engines, with the post-test condition of the components, including advanced Castcool(trademark) vane segments, being excellent. Also uncooled vane segments in CMSX-4 have exceeded engineering expectations. DOE

N95-32916*# National Aeronautics and Space Administration. Lewis Research Center, Cleveland, OH.
LOW-ORDER NONLINEAR DYNAMIC MODEL OF IC ENGINE-VARIABLE PITCH PROPELLER SYSTEM FOR GENERAL AVIATION AIRCRAFT
Jacques C. Richard Jul. 1995 37 p
(RTOP 505-62-50)
(NASA-TM-107006; E-9789; NAS 1.15:107006) Avail: CASI HC A03/MF A01

This paper presents a dynamic model of an internal combustion engine coupled to a variable pitch propeller. The low-order, nonlinear time-dependent model is useful for simulating the propulsion system of general aviation single-engine light aircraft. This model is suitable for investigating engine diagnostics and monitoring and for control design and development. Furthermore, the model may be extended to provide a tool for the study of engine emissions, fuel economy, component effects, alternative fuels, alternative engine cycles, flight simulators, sensors, and actuators. Results show that the model provides a reasonable representation of the propulsion system dynamics from zero to 10 Hertz. Author

N95-32931*# National Aeronautics and Space Administration. Lewis Research Center, Cleveland, OH.
COMBUSTION-ACOUSTIC STABILITY ANALYSIS FOR PREMIXED GAS TURBINE COMBUSTORS
Douglas Darling, Krishnan Radhakrishnan (NYMA, Inc., Brook Park, OH.), Ayo Oyediran (AYT Corp., Brook Park, OH.), and Iizabeth Cowan (Iowa State Univ. of Science and Technology, Ames, IA.) Aug. 1995 10 p Presented at the 31st Joint Propulsion Conference and Exhibit, San Diego, CA, 10-12 Jul. 1995; sponsored by AIAA, ASME, SAE, and ASEE
(Contracts NAS3-27186; NAS3-27571; RTOP 537-02-21)
(NASA-TM-107024; E-9834; NAS 1.15:107024; AIAA Paper 95-2470)
Avail: CASI HC A02/MF A01

Lean, prevaporized, premixed combustors are susceptible to combustion-acoustic instabilities. A model was developed to predict eigenvalues of axial modes for combustion-acoustic interactions in a premixed combustor. This work extends previous work by including variable area and detailed chemical kinetics mechanisms, using the code LSENS. Thus the acoustic equations could be integrated through the flame zone. Linear perturbations were made of the continuity, momentum, energy, chemical species, and state equations. The qualitative accuracy of our approach was checked by examining its predictions for various unsteady heat release rate models. Perturbations in fuel flow rate are currently being added to the model. Author

N95-33009*# National Aeronautics and Space Administration. Hugh L. Dryden Flight Research Center, Edwards, CA.
AN ELECTRONIC WORKSHOP ON THE PERFORMANCE SEEKING CONTROL AND PROPULSION CONTROLLED AIRCRAFT RESULTS OF THE F-15 HIGHLY INTEGRATED DIGITAL ELECTRONIC CONTROL FLIGHT RESEARCH PROGRAM
Sheryll Goecke Powers, comp. Jan. 1995 256 p Workshop held in Edwards, CA, 1993
(NASA-TM-104278; H-2020; NAS 1.15:104278) Avail: CASI HC A12/MF A03

Flight research for the F-15 HIDEC (Highly Integrated Digital Electronic Control) program was completed at NASA Dryden Flight Research Center in the fall of 1993. The flight research conducted during the last two years of the HIDEC program included two principal experiments: (1) performance seeking control (PSC), an adaptive, real-time, on-board optimization of engine, inlet, and horizontal tail position on the F-15; and (2) propulsion

controlled aircraft (PCA), an augmented flight control system developed for landings as well as up-and-away flight that used only engine thrust (flight controls locked) for flight control. In September 1994, the background details and results of the PSC and PCA experiments were presented in an electronic workshop, accessible through the Dryden World Wide Web (http://www.dfrc.nasa.gov/dryden.html) and as a compact disk. For individual titles, see N95-33010 through N95-33025.

N95-33010*# National Aeronautics and Space Administration. Hugh L. Dryden Flight Research Center, Edwards, CA.

AN OVERVIEW OF INTEGRATED FLIGHT-PROPULSION CONTROLS FLIGHT RESEARCH ON THE NASA F-15 RESEARCH AIRPLANE

Frank W. Burcham, Jr., Donald H. Gatlin, and James F. Stewart *In its* An Electronic Workshop on the Performance Seeking Control and Propulsion Controlled Aircraft Results of the F-15 Highly Integrated Digital Electronic Control Flight Research Program Jan. 1995 p 1-28 (For primary document see N95-33009 12-07)

Avail: CASI HC A03/MF A03

The NASA Dryden Flight Research Center has been conducting integrated flight-propulsion control flight research using the NASA F-15 airplane for the past 12 years. The research began with the digital electronic engine control (DEEC) project, followed by the F100 Engine Model Derivative (EMD). HIDEC (Highly Integrated Digital Electronic Control) became the umbrella name for a series of experiments including: the Advanced Digital Engine Controls System (ADECS), a twin jet acoustics flight experiment, self-repairing flight control system (SRFCS), performance-seeking control (PSC), and propulsion controlled aircraft (PCA). The upcoming F-15 project is ACTIVE (Advanced Control Technology for Integrated Vehicles). This paper provides a brief summary of these activities and provides background for the PCA and PSC papers, and includes a bibliography of all papers and reports from the NASA F-15 project. Author

N95-33011*# National Aeronautics and Space Administration. Hugh L. Dryden Flight Research Center, Edwards, CA.

PERFORMANCE SEEKING CONTROL PROGRAM OVERVIEW

John S. Orme *In its* An Electronic Workshop on the Performance Seeking Control and Propulsion Controlled Aircraft Results of the F-15 Highly Integrated Digital Electronic Control Flight Research Program Jan. 1995 p 31-36 (For primary document see N95-33009 12-07)

Avail: CASI HC A02/MF A03

The Performance Seeking Control (PSC) program evolved from a series of integrated propulsion-flight control research programs flown at NASA Dryden Flight Research Center (DFRC) on an F-15. The first of these was the Digital Electronic Engine Control (DEEC) program and provided digital engine controls suitable for integration. The DEEC and digital electronic flight control system of the NASA F-15 were ideally suited for integrated controls research. The Advanced Engine Control System (ADECS) program proved that integrated engine and aircraft control could improve overall system performance. The objective of the PSC program was to advance the technology for a fully integrated propulsion flight control system. Whereas ADECS provided single variable control for an average engine, PSC controlled multiple propulsion system variables while adapting to the measured engine performance. PSC was developed as a model-based, adaptive control algorithm and included four optimization modes: minimum fuel flow at constant thrust, minimum turbine temperature at constant thrust, maximum thrust, and minimum thrust. Subsonic and supersonic flight testing were conducted at NASA Dryden covering the four PSC optimization modes and over the full throttle range. Flight testing of the PSC algorithm, conducted in a series of five flight test phases, has been concluded at NASA Dryden covering all four of the PSC optimization modes. Over a three year period and five flight test phases 72 research flights were conducted. The primary objective of flight testing was to exercise each PSC optimization mode and quantify the resulting performance improvements. Author

N95-33012*# Pratt and Whitney Aircraft, West Palm Beach, FL.

F-15 PROPULSION SYSTEM

Mark Bushman and Steven G. Nobbs (McDonnell-Douglas Corp., Saint Louis, MO.) *In* NASA. Dryden Flight Research Center, An Electronic Workshop on the Performance Seeking Control and Propulsion Controlled Aircraft Results of the F-15 Highly Integrated Digital Electronic Control Flight Research Program Jan. 1995 p 37-40 (For primary document see N95-33009 12-07)

Avail: CASI HC A01/MF A03

A brief description of the NASA F-15 research aircraft propulsion system is given. The F-15 is powered by two PW1128 afterburning turbofan engines which are growth versions of the F100-PW-100 engine. The PW1128 is controlled by a full-authority digital electronic engine control (DEEC). The F-15 inlet is a two-dimensional, three-ramp, external compression design with partially cut back side plates. Each inlet is independently controlled by an electronic air inlet controller (EAIC). CASI

N95-33013*# McDonnell-Douglas Corp., Saint Louis, MO.

PSC ALGORITHM DESCRIPTION

Steven G. Nobbs *In* NASA. Dryden Flight Research Center, An Electronic Workshop on the Performance Seeking Control and Propulsion Controlled Aircraft Results of the F-15 Highly Integrated Digital Electronic Control Flight Research Program Jan. 1995 p 41-60 (For primary document see N95-33009 12-07)

Avail: CASI HC A03/MF A03

An overview of the performance seeking control (PSC) algorithm and details of the important components of the algorithm are given. The onboard propulsion system models, the linear programming optimization, and engine control interface are described. The PSC algorithm receives input from various computers on the aircraft including the digital flight computer, digital engine control, and electronic inlet control. The PSC algorithm contains compact models of the propulsion system including the inlet, engine, and nozzle. The models compute propulsion system parameters, such as inlet drag and fan stall margin, which are not directly measurable in flight. The compact models also compute sensitivities of the propulsion system parameters to change in control variables. The engine model consists of a linear steady state variable model (SSVM) and a nonlinear model. The SSVM is updated with efficiency factors calculated in the engine model update logic, or Kalman filter. The efficiency factors are used to adjust the SSVM to match the actual engine. The propulsion system models are mathematically integrated to form an overall propulsion system model. The propulsion system model is then optimized using a linear programming optimization scheme. The goal of the optimization is determined from the selected PSC mode of operation. The resulting trims are used to compute a new operating point about which the optimization process is repeated. This process is continued until an overall (global) optimum is reached before applying the trims to the controllers. Author

N95-33014*# McDonnell-Douglas Corp., Saint Louis, MO.

PSC IMPLEMENTATION AND INTEGRATION

Steven Nobbs *In* NASA. Dryden Flight Research Center, An Electronic Workshop on the Performance Seeking Control and Propulsion Controlled Aircraft Results of the F-15 Highly Integrated Digital Electronic Control Flight Research Program Jan. 1995 p 61-89 (For primary document see N95-33009 12-07)

Avail: CASI HC A03/MF A03

Hardware and software design of the performance seeking control (PSC) for the NASA F-15 research aircraft are described. The hardware architecture, vehicle management system computer (VMSC), pilot interface, and PSC mode selection are discussed. The PSC software is distributed among the VMSC, central computer, digital electronic engine controls (DEEC's), and electronic air inlet controllers (EAIC's). The major PSC modules, VMSC logic, VMSC channel C memory requirements, VMSC channel C timing, and navigation control indicator (NCI) variables and where they are located are presented. CASI

N95-33015*# National Aeronautics and Space Administration. Hugh L. Dryden Flight Research Center, Edwards, CA.

MINIMUM FUEL MODE EVALUATION

John S. Orme and Steven G. Nobbs (McDonnell-Douglas Corp., Saint Louis, MO.) *In its* An Electronic Workshop on the Performance Seeking Control and Propulsion Controlled Aircraft Results of the F-15 Highly Integrated Digital Electronic Control Flight Research Program Jan. 1995 p 91-98 (For primary document see N95-33009 12-07)

Avail: CASI HC A02/MF A03

The minimum fuel mode of the NASA F-15 research aircraft is designed to minimize fuel flow while maintaining constant net propulsive force (FNP), effectively reducing thrust specific fuel consumption (TSFC), during cruise flight conditions. The test maneuvers were at stabilized flight conditions.

The aircraft test engine was allowed to stabilize at the cruise conditions before data collection initiated; data were then recorded with performance seeking control (PSC) not-engaged, then data were recorded with the PSC system engaged. The maneuvers were flown back-to-back to allow for direct comparisons by minimizing the effects of variations in the test day conditions. The minimum fuel mode was evaluated at subsonic and supersonic Mach numbers and focused on three altitudes: 15,000; 30,000; and 45,000 feet. Flight data were collected for part, military, partial, and maximum afterburning power conditions. The TSFC savings at supersonic Mach numbers, ranging from approximately 4% to nearly 10%, are in general much larger than at subsonic Mach numbers because of PSC trims to the afterburner. Derived from text

N95-33016*# National Aeronautics and Space Administration. Hugh L. Dryden Flight Research Center, Edwards, CA.

MINIMUM FAN TURBINE INLET TEMPERATURE MODE EVALUATION

John S. Orme and Steven G. Nobbs (McDonnell-Douglas Corp., Saint Louis, MO.) *In its* An Electronic Workshop on the Performance Seeking Control and Propulsion Controlled Aircraft Results of the F-15 Highly Integrated Digital Electronic Control Flight Research Program Jan. 1995 p 99-110 (For primary document see N95-33009 12-07)

Avail: CASI HC A03/MF A03

Measured reductions in turbine temperature which resulted from the application of the F-15 performance seeking control (PSC) minimum fan turbine inlet temperature (FTIT) mode during the dual-engine test phase is presented as a function of net propulsive force and flight condition. Data were collected at altitudes of 30,000 and 45,000 feet at military and partial afterburning power settings. The FTIT reductions for the supersonic tests are less than at subsonic Mach numbers because of the increased modeling and control complexity. In addition, the propulsion system was designed to be optimized at the mid supersonic Mach number range. Subsonically at military power, FTIT reductions were above 70 R for either the left or right engines, and repeatable for the right engine. At partial afterburner and supersonic conditions, the level of FTIT reductions were at least 25 R and as much as 55 R. Considering that the turbine operates at or very near its temperature limit at these high power settings, these seemingly small temperature reductions may significantly lengthen the life of the turbine. In general, the minimum FTIT mode has performed well, demonstrating significant temperature reductions at military and partial afterburner power. Decreases of over 100 R at cruise flight conditions were identified. Temperature reductions of this magnitude could significantly extend turbine life and reduce replacement costs. Derived from text

N95-33017*# National Aeronautics and Space Administration. Hugh L. Dryden Flight Research Center, Edwards, CA.

MAXIMUM THRUST MODE EVALUATION

John S. Orme and Steven G. Nobbs (McDonnell-Douglas Corp., Saint Louis, MO.) *In its* An Electronic Workshop on the Performance Seeking Control and Propulsion Controlled Aircraft Results of the F-15 Highly Integrated Digital Electronic Control Flight Research Program Jan. 1995 p 111-120 (For primary document see N95-33009 12-07)

Avail: CASI HC A02/MF A03

Measured reductions in acceleration times which resulted from the application of the F-15 performance seeking control (PSC) maximum thrust mode during the dual-engine test phase is presented as a function of power setting and flight condition. Data were collected at altitudes of 30,000 and 45,000 feet at military and maximum afterburning power settings. The time savings for the supersonic acceleration is less than at subsonic Mach numbers because of the increased modeling and control complexity. In addition, the propulsion system was designed to be optimized at the mid supersonic Mach number range. Recall that even though the engine is at maximum afterburner, PSC does not trim the afterburner for the maximum thrust mode. Subsonically at military power, time to accelerate from Mach 0.6 to 0.95 was cut by between 6 and 8 percent with a single engine application of PSC, and over 14 percent when both engines were optimized. At maximum afterburner, the level of thrust increases were similar in magnitude to the military power results, but because of higher thrust levels at maximum afterburner and higher aircraft drag at supersonic Mach numbers the percentage thrust increase and time to accelerate was less than for the supersonic accelerations. Savings in time to accelerate supersonically at maximum afterburner ranged from 4 to 7 percent. In general, the maximum thrust mode has performed well, demonstrating significant thrust increases at military and maximum afterburner power. Increases of up to 15 percent at typical combat-type flight conditions were identified. Thrust increases of this magnitude could be useful in a combat situation. Author

N95-33018*# National Aeronautics and Space Administration. Hugh L. Dryden Flight Research Center, Edwards, CA.

RAPID DECELERATION MODE EVALUATION

Timothy R. Conners, Steven G. Nobbs (McDonnell-Douglas Corp., Saint Louis, MO.), and John S. Orme *In its* An Electronic Workshop on the Performance Seeking Control and Propulsion Controlled Aircraft Results of the F-15 Highly Integrated Digital Electronic Control Flight Research Program Jan. 1995 p 121-128 (For primary document see N95-33009 12-07)

Avail: CASI HC A02/MF A03

Aircraft with flight capability above 1.4 normally have an RPM lockup or similar feature to prevent inlet buzz that would occur at low engine airflows. This RPM lockup has the effect of holding the engine thrust level at the intermediate power (maximum non-afterburning). For aircraft such as military fighters or supersonic transports, the need exists to be able to rapidly slow from supersonic to subsonic speeds. For example, a supersonic transport that experiences a cabin decompression needs to be able to slow/descend rapidly, and this requirement may size the cabin environmental control system. For a fighter, there may be a desire to slow/descend rapidly, and while doing so to minimize fuel usage and engine exhaust temperature. Both of these needs can be aided by achieving the minimum possible overall net propulsive force. As the intermediate power thrust levels of engines increase, it becomes even more difficult to slow rapidly from supersonic speeds. Therefore, a mode of the performance seeking control (PSC) system to minimize overall propulsion system thrust has been developed and tested. The rapid deceleration mode reduces the engine airflow consistent with avoiding inlet buzz. The engine controls are trimmed to minimize the thrust produced by this reduced airflow, and moves the inlet geometry to degrade the inlet performance. As in the case of the other PSC modes, the best overall performance (in this case the least net propulsive force) requires an integrated optimization of inlet, engine, and nozzle variables. This paper presents the predicted and measured results for the supersonic minimum thrust mode, including the overall effects on aircraft deceleration. Author

N95-33019*# National Aeronautics and Space Administration. Hugh L. Dryden Flight Research Center, Edwards, CA.

PERFORMANCE SEEKING CONTROL EXCITATION MODE

Gerard Schkolnik *In its* An Electronic Workshop on the Performance Seeking Control and Propulsion Controlled Aircraft Results of the F-15 Highly Integrated Digital Electronic Control Flight Research Program Jan. 1995 p 133-142 (For primary document see N95-33009 12-07)

Avail: CASI HC A02/MF A03

Flight testing of the performance seeking control (PSC) excitation mode was successfully completed at NASA Dryden on the F-15 highly integrated digital electronic control (HIDEC) aircraft. Although the excitation mode was not one of the original objectives of the PSC program, it was rapidly prototyped and implemented into the architecture of the PSC algorithm, allowing valuable and timely research data to be gathered. The primary flight test objective was to investigate the feasibility of a future measurement-based performance optimization algorithm. This future algorithm, called AdAPT, which stands for adaptive aircraft performance technology, generates and applies excitation inputs to selected control effectors. Fourier transformations are used to convert measured response and control effector data into frequency domain models which are mapped into state space models using multiterm frequency matching. Formal optimization principles are applied to produce an integrated, performance optimal effector suite. The key technical challenge of the measurement-based approach is the identification of the gradient of the performance index to the selected control effector. This concern was addressed by the excitation mode flight test. The AdAPT feasibility study utilized the PSC excitation mode to apply separate sinusoidal excitation trims to the controls - one aircraft, inlet first ramp (cowl), and one engine, throat area. Aircraft control and response data were recorded using on-board instrumentation and analyzed post-flight. Sensor noise characteristics, axial acceleration performance gradients, and repeatability were determined. Results were compared to pilot comments to assess the ride quality. Flight test results

indicate that performance gradients were identified at all flight conditions, sensor noise levels were acceptable at the frequencies of interest, and excitations were generally not sensed by the pilot. Author

N95-33020*# National Aeronautics and Space Administration. Hugh L. Dryden Flight Research Center, Edwards, CA.

[PERFORMANCE SEEKING CONTROL (PSC) FOR THE F-15 HIGHLY INTEGRATED DIGITAL ELECTRONIC CONTROL (HIDEC) AIRCRAFT] Summary

John S. Orme *In its* An Electronic Workshop on the Performance Seeking Control and Propulsion Controlled Aircraft Results of the F-15 Highly Integrated Digital Electronic Control Flight Research Program Jan. 1995 p 146-156 (For primary document see N95-33009 12-07)

Avail: CASI HC A03/MF A03

The performance seeking control algorithm optimizes total propulsion system performance. This adaptive, model-based optimization algorithm has been successfully flight demonstrated on two engines with differing levels of degradation. Models of the engine, nozzle, and inlet produce reliable, accurate estimates of engine performance. But, because of an observability problem, component levels of degradation cannot be accurately determined. Depending on engine-specific operating characteristics PSC achieves various levels performance improvement. For example, engines with more deterioration typically operate at higher turbine temperatures than less deteriorated engines. Thus when the PSC maximum thrust mode is applied, for example, there will be less temperature margin available to be traded for increasing thrust. Derived from text

N95-33021*# National Aeronautics and Space Administration. Hugh L. Dryden Flight Research Center, Edwards, CA.

BACKGROUND AND PRINCIPLES OF THROTTLES-ONLY FLIGHT CONTROL

Frank W. Burcham, Jr. *In its* An Electronic Workshop on the Performance Seeking Control and Propulsion Controlled Aircraft Results of the F-15 Highly Integrated Digital Electronic Control Flight Research Program Jan. 1995 p 159-169 (For primary document see N95-33009 12-07)

Avail: CASI HC A03/MF A03

There have been many cases in which the crew of a multi-engine airplane had to use engine thrust for emergency flight control. Such a procedure is very difficult, because the propulsive control forces are small, the engine response is slow, and airplane dynamics such as the phugoid and dutch roll are difficult to damp with thrust. In general, thrust increases are used to climb, thrust decreases to descend, and differential thrust is used to turn. Average speed is not significantly affected by changes in throttle setting. Pitch control is achieved because of pitching moments due to speed changes, from thrust offset, and from the vertical component of thrust. Roll control is achieved by using differential thrust to develop yaw, which, through the normal dihedral effect, causes a roll. Control power in pitch and roll tends to increase as speed decreases. Although speed is not controlled by the throttles, configuration changes are often available (lowering gear, flaps, moving center-of-gravity) to change the speed. The airplane basic stability is also a significant factor. Fuel slosh and gyroscopic moments are small influences on throttles-only control. The background and principles of throttles-only flight control are described. Author

N95-33022*# McDonnell-Douglas Corp., Saint Louis, MO.

PROPULSION CONTROLLED AIRCRAFT DESIGN AND DEVELOPMENT

Edward A. Wells and James M. Urnes, Sr. *In* NASA. Dryden Flight Research Center, An Electronic Workshop on the Performance Seeking Control and Propulsion Controlled Aircraft Results of the F-15 Highly Integrated Digital Electronic Control Flight Research Program Jan. 1995 p 170-192 (For primary document see N95-33009 12-07)

Avail: CASI HC A03/MF A03

This paper describes the design, development, and ground testing of the propulsion controlled aircraft (PCA) flight control system. A backup flight control system which uses only engine thrust, the PCA system utilizes collective and differential thrust changes to steer an aircraft that experiences partial or complete failure of the hydraulically actuated control surfaces. The objective of the program was to investigate, in flight, the throttles-only control capability of the F-15, using manual control, and also an augmented PCA mode in which computer-controlled thrust was used for flight control. The objective included PCA operation in up-and-away flight and, if performance was adequate, a secondary objective to make actual PCA landings. The PCA design began with a feasibility study which evaluated many control law designs. The study was done using off-line control analysis, simulation, and on-line manned flight simulator tests. Control laws, cockpit displays, and cockpit controls were evaluated by NASA test pilots. A flight test baseline configuration was selected based on projected flight performance, applicability to transport and fighter aircraft, and funding costs. During the PCA software and hardware development, the initial design was updated as data became available from throttle-only flight experiments conducted by NASA on the F-15. This information showed basic airframe characteristics that were not observed in the F-15 flight simulator and resulted in several design changes. After the primary objectives of the PCA flight testing were accomplished, additional PCA modes of operation were developed and implemented. The evolution of the PCA system from the initial feasibility study, control law design, simulation, hardware-in-the-loop tests, pilot-in-the-loop tests, and ground tests is presented. Author

N95-33023*# National Aeronautics and Space Administration. Hugh L. Dryden Flight Research Center, Edwards, CA.

FLIGHT TEST OF A PROPULSION CONTROLLED AIRCRAFT SYSTEM ON THE NASA F-15 AIRPLANE c05

Frank W. Burcham, Jr. and Trindel A. Maine *In its* An Electronic Workshop on the Performance Seeking Control and Propulsion Controlled Aircraft Results of the F-15 Highly Integrated Digital Electronic Control Flight Research Program Jan. 1995 p 193-221 (For primary document see N95-33009 12-07)

Avail: CASI HC A03/MF A03

Flight tests of the propulsion controlled aircraft (PCA) system on the NASA F-15 airplane evolved as a result of a long series of simulation and flight tests. Initially, the simulation results were very optimistic. Early flight tests showed that manual throttles-only control was much more difficult than the simulation, and a flight investigation was flown to acquire data to resolve this discrepancy. The PCA system designed and developed by MDA evolved as these discrepancies were found and resolved, requiring redesign of the PCA software and modification of the flight test plan. Small throttle step inputs were flown to provide data for analysis, simulation update, and control logic modification. The PCA flight tests quickly revealed less than desired performance, but the extensive flexibility built into the flight PCA software allowed rapid evaluation of alternate gains, filters, and control logic, and within 2 weeks, the PCA system was functioning well. The initial objective of achieving adequate control for up-and-away flying and approaches was satisfied, and the option to continue to actual landings was achieved. After the PCA landings were accomplished, other PCA features were added, and additional maneuvers beyond those originally planned were flown. The PCA system was used to recover from extreme upset conditions, descend, and make approaches to landing. A heading mode was added, and a single engine plus rudder PCA mode was also added and flown. The PCA flight envelope was expanded far beyond that originally designed for. Guest pilots from the USAF, USN, NASA, and the contractor also flew the PCA system and were favorably impressed. Author

N95-33024*# Planning Research Corp., Edwards, CA.

DYNAMIC GROUND EFFECTS FLIGHT TEST OF THE NASA F-15 AIRCRAFT c05

Stephen Corda *In* NASA. Dryden Flight Research Center, An Electronic Workshop on the Performance Seeking Control and Propulsion Controlled Aircraft Results of the F-15 Highly Integrated Digital Electronic Control Flight Research Program Jan. 1995 p 222-228 (For primary document see N95-33009 12-07)

Avail: CASI HC A02/MF A03

Aerodynamic characteristics of an aircraft may significantly differ when flying close to the ground rather than when flying up and away. Recent research has also determined that dynamic effects (i.e., sink rate) influence ground effects (GE). A ground effects flight test program of the F-15 aircraft was conducted to support the propulsion controlled aircraft (PCA) program at the NASA Dryden Flight Research Center. Flight data was collected for 24 landings on seven test flights. Dynamic ground effects data were obtained for low- and high-sink rates, between 0.8 and 6.5 ft/sec, at two approach speed and flap combinations. These combinations consisted of 150 kt with the flaps down (30 deg deflection) and 170 kt with the flaps up (0 deg deflection), both with the inlet ramps in the full-up position. The aerodynamic coefficients caused by ground effects were estimated from the flight data. These ground effects data were correlated

with the aircraft speed, flap setting, and sink rate. Results are compared to previous flight test and wind-tunnel ground effects data for various wings and for complete aircraft. Author

N95-33025*# National Aeronautics and Space Administration. Hugh L. Dryden Flight Research Center, Edwards, CA.
DESIGN CHALLENGES ENCOUNTERED IN THE F-15 PCA FLIGHT TEST PROGRAM **c05**
Trindel A. Maine, Frank W. Burcham, Jr., Peter Schaefer (University of Southern California, Los Angeles, CA.), and John Burken *In its* An Electronic Workshop on the Performance Seeking Control and Propulsion Controlled Aircraft Results of the F-15 Highly Integrated Digital Electronic Control Flight Research Program Jan. 1995 p 229-244 (For primary document see N95-33009 12-07)
Avail: CASI HC A03/MF A03

The NASA Dryden Flight Research Center conducted flight tests of a propulsion-controlled aircraft system on an F-15 airplane. This system was designed to explore the feasibility of providing safe emergency landing capability using only the engines to provide flight control in the event of a catastrophic loss of conventional flight controls. Control laws were designed to control the flight path and bank angle using only commands to the throttles. While the program was highly successful, this paper concentrates on the challenges encountered using engine thrust as the only control effector. Compared to conventional flight control surfaces, the engines are slow, nonlinear, and have limited control effectiveness. This increases the vulnerability of the system to outside disturbances and changes in aerodynamic conditions. As a result, the PCA system had problems with gust rejection. Cross coupling of the longitudinal and lateral axis also occured, primarily as a result of control saturation. The normally negligible effects of inlet airframe interactions became significant with the engines as the control effector. Flight and simulation data are used to illustrate these difficulties. Author

N95-33208*# NYMA, Inc., Brook Park, OH.
NUMERICAL SIMULATION OF SUPERSONIC FLOW USING A NEW ANALYTICAL BLEED BOUNDARY CONDITION Final Report
G. J. Harloff and G. E. Smith AIAA Aug. 1995 21 p
(Contract NAS3-27186; RTOP 505-62-20)
(NASA-CR-198368; E-9807; NAS 1.26:198368) Avail: CASI HC A03/MF A01

A new analytical bleed boundary condition is used to compute flowfields for a strong oblique shock wave/boundary layer interaction with a baseline and three bleed rates at a freestream Mach number of 2.47 with an 8 deg shock generator. The computational results are compared to experimental Pitot pressure profiles and wall static pressures through the interaction region. An algebraic turbulence model is employed for the bleed and baseline cases, and a one equation model is also used for the baseline case where the boundary layer is separated. Author

N95-33250 Defence Science and Technology Organisation, Melbourne (Australia). Airframes and Engines Div.
WATER MODEL TESTS ON THE ALLISON T56 SERIES 3 COMBUSTION SYSTEM
Grant T. McCabe Mar. 1995 31 p Original contains color illustrations.
(DSTO-TR-0139; AR-007-138) Avail: Issuing Activity (DSTO Aeronautical and Maritime Research Lab., GPO Box 4331, Melbourne, Victoria 3001, Australia)

A modification was developed for the combustion system of the Allison T56 Series 3 turboprop engine which has resulted in an engine that has: (1) a lower smoke emission; (2) a lower specific fuel consumption; and (3) a combustor with potentially increased durability or life. In-service testing of the combustor has proven all the above advantages; however, the formation of hard carbon in the combustor and its subsequent release has resulted in increased erosion in the turbine section of the engine. Further development was undertaken to remedy this problem without affecting the overall gains offered by the modification. This report covers part of this work and in particular details flow field investigations made using a water flow model of the combustor liner. A comprehensive understanding of the flow mechanisms within the standard liner, the low smoke modification (LSM) liner, and proposed revisions of the LSM liner has now been obtained. It is anticipated that modifications arising from the present investigation will reduce, if not completely eliminate, hard carbon formation in the revised LSM (RLSM) form. Author

N95-34805 Washington Univ., Seattle, WA.
INVESTIGATION OF STARTING AND IGNITION TRANSIENTS IN THE THERMALLY CHOKED RAM ACCELERATOR Ph.D. Thesis
Edward Alonza Burnham, Jr. 1993 189 p
Avail: Univ. Microfilms Order No. DA9416991

An experimental investigation of the starting transients of the thermally choked ram accelerator is presented. A highly instrumented tube section and instrumentation inserts provide high resolution experimental pressure, luminosity, and electromagnetic data of the starting transients. Detonations are used to estimate induction and reaction times at elevated pressures. Data obtained prior to and following the entrance diaphragm show detailed development of shock systems in both combustible and inert mixtures. With an evacuated launch tube, starting the diffuser is possible at any Mach number above the Kantrowitz Mach number. The detrimental effects and possible solutions of higher launch tube pressures and excessive obturator leakage (blow-by) are discussed. Ignition of a combustible mixture is demonstrated with both perforated and solid obturators. The relative advantages and disadvantages of each are discussed. The source of ignition is identified and discussed. Numerical simulations of various features using Van Leer splitting or advection upwind splitting method (AUSM) are shown and related to experimental observations. Data obtained from these starting experiments enhance the understanding of the ram accelerator, as well as assist in the validation of unsteady, chemically reacting CFD codes.
Dissert. Abstr.

N95-34507# Ishikawajima-Harima Heavy Industries Co. Ltd., Tokyo (Japan).
DESIGN OF SECONDARY FLOW CONTROL CASCADE USING NUMERICAL SIMULATION Abstract Only
Y. Ohkita, H. Kodama, K. Kikuchi (National Aerospace Lab., Tokyo, Japan.), O. Nozaki (National Aerospace Lab., Tokyo, Japan.), and A. Tamura (National Aerospace Lab., Tokyo, Japan.) *In* National Aerospace Lab., Special Publication of National Aerospace Laboratory 16 Jun. 1994 p 51-55 In JAPANESE (For primary document see N95-34505 12-02)
Avail: CASI HC A01/MF A03

N95-34511# Mitsubishi Heavy Industries Ltd., Tokyo (Japan).
VERIFICATION OF TURBINE CASCADE FLOW WITH TIP CLEARANCE Abstract Only
Kunihiro Shimizu, Yoshiaki Miyake, Osamu Nozaki (National Aerospace Lab., Tokyo, Japan.), Kazuo Kikuchi (National Aerospace Lab., Tokyo, Japan.), and Atsuhiro Tamura (National Aerospace Lab., Tokyo, Japan.) *In* National Aerospace Lab., Special Publication of National Aerospace Laboratory 16 Jun. 1994 p 75-80 In JAPANESE (For primary document see N95-34505 12-02)
Avail: CASI HC A02/MF A03

N95-34513# Mitsubishi Heavy Industries Ltd., Tokyo (Japan).
CALCULATION OF SUPERSONIC COMBUSTION IN SCRAMJET ENGINES Abstract Only
Hideyuki Taguchi and Yoshihiro Kawamata (Touhoku Univ., Japan.) *In* National Aerospace Lab., Special Publication of National Aerospace Laboratory 16 Jun. 1994 p 87-92 In JAPANESE (For primary document see N95-34505 12-02)
Avail: CASI HC A02/MF A03

N95-34560# Tokyo Univ. (Japan).
STATIC PRESSURE DROP BY SWIRLING FLOW OF AN INTERNAL COOLING AIR SYSTEM THROUGH A TURBINE SHAFT Abstract Only
Tadaharu Kishibe and Shojiro Kaji *In* National Aerospace Lab., Special Publication of National Aerospace Laboratory 16 Jun. 1994 p 375-381 In JAPANESE (For primary document see N95-34505 12-02)
Avail: CASI HC A02/MF A03

08 AIRCRAFT STABILITY AND CONTROL

Includes aircraft handling qualities; piloting; flight controls; and autopilots.

For related information see also *05 Aircraft Design, Testing and Performance.*

N95-34306# Systems Technology, Inc., Hawthorne, CA.
PROPOSED INCORPORATION OF MISSION-ORIENTED FLYING QUALITIES INTO MIL-STD-1797A Final Report, 15 May 1992 - 15 Aug. 1994
David G. Mitchell, Roger H. Hoh, Bimal L. Aponso, and David H. Klyde Oct. 1994 452 p Prepared in cooperation with HOH Aeronautics, Inc. (Contract F33615-92-C-3604)
(AD-A294211; TR-1291-1; WL-TR-94-3162) Avail: CASI HC A20/MF A04

The effort documented in this report was undertaken to revise the flying qualities military standard, MIL-STD-1797A, in both form and content. It was felt that mission-oriented requirements on new systems would expand the applicability of the standard to all tasks performed in an operational environment. This allows replacement of Flight Phases and reference to aircraft weight with a series of Mission- Task-Elements. Demonstration maneuvers are included to be an independent assessment of handling qualities. Additionally, much of the work done in the definition of flying quality criteria in the twelve years since the MIL-STD was originally proposed has been incorporated. These modifications deal generally with task amplitude, system response type, and control feel system characteristics. Two other important changes are the guidance provided on use of alternative requirements and the linking of flying qualities Levels and the Cooper-Harper Handling Qualities Rating Scale. The results of this effort are expected to be a cornerstone in the process to create MIL-STD-1797B and will be subject to critical review by the aerospace industry as well as a Tri-Service Review Team. DTIC

N95-34806 California Univ., Los Angeles, CA.
A STOCHASTIC ADAPTIVE CONTROL APPLICATION TO FLIGHT SYSTEMS Ph.D. Thesis
Guohua H. Wang 1994 119 p
Avail: Univ. Microfilms Order No. DA9418925

We present the results of our study of stochastic adaptive control theory and its applications to flight control systems. The stochastic adaptive control (SAC) problem of interest may be described as follows: given a stochastic system represented by linear state and observation equations with uncertain parameters, find an adaptive control law which minimizes a quadratic cost functional. We have designed an optimal stochastic adaptive controller for the important class of SAC problems where the system control derivatives are uncertain. Our SAC design incorporates a state and parameter estimator, and a LQG controller, and is automatic (in that it utilizes the state noise process as the identifying excitation). We have established that the parameter estimates converge almost surely, that the adaptive controls are asymptotically optimal, and that the adaptively controlled system is L(sub p) stable. We have also examined, through computer simulations, several important aspects of the practical application of our SAC to the problem of an aircraft being flown in atmospheric turbulence where the gust response in the angle of attack is to be minimized. The results suggest effectively that the parameter estimation algorithm converges so that optimal performance is achieved rapidly, i.e. the gust response in the angle of attack is reduced quickly to the minimum level achievable when the control derivatives are perfectly known. Simulations also indicate that the SAC design performs well in heavy turbulence. In fact, the rate of adaptation increase with the gust noise level. It is further demonstrated that the SAC performs well when the control derivatives vary slowly. Based upon the speed of adaptation, a threshold value of the wind gust intensity, which determines if the SAC can adapt parameter changes in an admissible period of time, is approximated. Finally, some future studies are suggested. Dissert. Abstr.

N95-34772*# University of Central Florida, Orlando, FL.
USER TYPE CERTIFICATION FOR ADVANCED FLIGHT CONTROL SYSTEMS
Richard D. Gilson and David W. Abbott *In* Embry-Riddle Aeronautical Univ., Daytona Beach,FL, Human Factors Certification of Advanced Aviation Technologies 1994 p 119-123 (For primary document see N95-34764 12-54)
Avail: CASI HC A01/MF A04

09 RESEARCH AND SUPPORT FACILITIES (AIR)

Includes airports, hangars and runways; aircraft repair and overhaul facilities; wind tunnels; shock tubes; and aircraft engine test stands.

For related information see also *14 Ground Support Systems and Facilities (Space).*

N95-32759# General Accounting Office, Washington, DC.
FACT SHEET FOR CONGRESSIONAL REQUESTERS. AIRPORT COMPETITION: ESSENTIAL AIR SERVICE SLOTS AT O'HARE INTERNATIONAL AIRPORT
4 Mar. 1994 19 p
(GAO/RCED-94-118FS; B-256330) Avail: CASI HC A03/MF A01; GAO, PO Box 6015, Gaithersburg, MD 20877 HC

This fact sheet responds to a request for information on the availability of air travel between small airports in the Midwest and Chicago's O'Hare International Airport. The Essential Air Service (EAS) program was established in 1978 to guarantee continued service from small airports following deregulation. The program maintains a link between small airports with insufficient enplanements to support service to hub airports, guaranteeing residents of small communities access to the national air travel network. This study found (1) overall service to O'Hare has declined, but some communities have experienced increased service; (2) commuter aviation services in the midwest are becoming increasingly concentrated; (3) fares between small midwestern airports and O'Hare generally are not higher than those to other hubs; (4) airport and airline officials believe O'Hare could accommodate more air traffic through more efficient slot allocation; and (5) improvements at O'Hare are yielding capacity increases. Derived from text

N95-32786# General Accounting Office, Washington, DC. Resources, Community, and Economic Development Div.
REPORT TO THE CHAIRMAN, SUBCOMMITTEE ON TRANSPORTATION AND RELATED AGENCIES, COMMITTEE ON APPROPRIATIONS, US SENATE. AIRPORT IMPROVEMENT PROGRAM: RELIEVER AIRPORT SET-ASIDE FUNDS COULD BE REDIRECTED
30 Jun. 1994 30 p
(GAO/RCED-94-226; B-257609) Avail: CASI HC A03/MF A01; GAO, PO Box 6015, Gaithersburg, MD 20877 HC

A review of a particular set-aside of the Airport Improvement Program (AIP) that provides AIP funds for projects at general aviation airports called 'relievers' is presented. This set-aside was created by Congress to (1) reduce congestion at commercial airports by improving reliever airports and (2) provide general aviation with additional access to airports. FAA does not consider general aviation to be a significant factor in congestion at commercial airports today. Further, FAA and aviation industry group officials consider access to general aviation facilities to be sufficient - and often more than sufficient - in most areas where relievers are located. FAA still plans to continue to designate 5 percent of all AIP funds to add to the $2 billion already set aside since 1982 for reliever airport projects. However, FAA does not know whether funding projects at relievers has actually reduced congestion or improved general aviation access to airports, and it has not analyzed whether the relatively small growth in general aviation traffic projected for the next 12 years justifies the expenditure. It is concluded that reliever airport set-aside funds could be redirected. One option is to reduce the number of airports designated as relievers so that only those that currently have the facilities to accommodate large general aviation aircraft - the only forecasted growth segment of general aviation - would be included in the set-aside. A second option is to eliminate the designation altogether and have these airports compete with all other general aviation airports for general aviation development funds. CASI

N95-32888# General Accounting Office, Washington, DC. Resources, Community, and Economic Development Div.
REPORT TO THE CHAIRMAN, SUBCOMMITTEE ON TRANSPORTATION AND RELATED AGENCIES, COMMITTEE ON APPROPRIATIONS, US SENATE. AIRPORT IMPROVEMENT PROGRAM: THE MILITARY AIRPORT PROGRAM HAS NOT ACHIEVED INTENDED IMPACT
30 Jun. 1994 34 p
(GAO/RCED-94-209; B-256001) Avail: CASI HC A03/MF A01; GAO, PO Box 6015, Gaithersburg, MD 20877 HC

One set-aside of the Airport Improvement Program (AIP) - the Military Airport Program (MAP) - was established in 1990 to assist current and former military airports located in congested metropolitan areas in converting to civilian airports. This report focuses on whether (1) MAP airports were selected in accordance with program goals of enhancing capacity system-wide and providing conversion-related assistance and (2) FAA has effectively allocated MAP funds to ensure that they are having their intended impact. As implemented, MAP is not having its intended impact. Nine of the 12 airports in MAP do not meet key legislatively established program goals. FAA has not established clear criteria to define what it considers a program-related need, identified airports with such needs located near congested metropolitan areas, or developed an effective strategy or plan for allocating program funds among selected airports. As a result, FAA has no basis for assessing the overall impact of MAP investments and determining if selected airports merit continued participation. CASI

N95-34342# Army Armament Research, Development and Engineering Center, Picatinny Arsenal, NJ.
ANECHOIC CHAMBER UPGRADE Final Report, Jan. - Aug. 1994
Steven Weiss and Andrew Leshchyshyn May 1995 21 p
(AD-A294375; ARAED-TR-95009) Avail: CASI HC A03/MF A01

Hardware and software upgrades have been made recently to an anechoic chamber at the Adelphi Laboratory Center (ALC). A new data acquisition system (using Scientific Atlanta equipment) has been installed and connected to a Dell 386 personal computer. This computer has been dedicated to the chamber to be used solely for data acquisition and analysis. The computer can be connected to the ALC facility network so that data can be downloaded to any location within the ALC campus. DTIC

N95-34344# Dayton Univ., OH. Research Inst.
PERCEPTUAL DIMENSIONS OF SIMULATED SCENES RELEVANT FOR VISUAL LOW-ALTITUDE FLIGHT Interim Report, Jun. 1988 - Nov. 1993
James A. Kleiss Apr. 1995 29 p
(Contract F33615-90-C-0005)
(AD-A294385; AL/HR-TR-1994-0170) Avail: CASI HC A03/MF A01

Previous experiments using multidimensional scaling reveal that pilots flying at low altitudes perceive two types of detail in real-world scenes: (1) hills and ridges, and (2) discrete scene elements exemplified by large objects or groups of objects. The present experiments sought to determine the extent to which these types of detail can be effectively rendered in computer- generated flight simulator scenes. In Experiment 1, subjects rated the visual similarity between simulated scenes exhibiting a range of different features. Ratings were analyzed with multidimensional scaling which revealed that subjects perceived variation in three types of detail: (1) texture on the terrain, (2)objects, and (3) hills. Evidence for a dimension related to texture on the terrain arose from comparisons involving completely featureless surfaces which were not represented in real-world scenes. Field of view was reduced in Experiment 2 and results revealed a change in perceived detail. Texture, objects and hills were perceived in scenes, but they were perceived as being a single type of detail contributing to global scene complexity. Taken together, present results indicate that detail important in real-world scenes can be effectively rendered in simulated scenes. Indeed, present scenes exhibited an even richer variety of detail than real-world scenes used previously. Nevertheless, what is important in scenes is not directly related to specific scene features but to more abstract forms of information mediated by those features. DTIC

N95-34362# Dayton Univ., OH. Research Inst.
ALTITUDE CUING EFFECTIVENESS OF TERRAIN TEXTURE CHARACTERISTICS IN SIMULATED LOW-ALTITUDE FLIGHT Final Technical Report, May 1989 - Jan. 1993
Harold D. Warner, Gary L. Serfoss, and David C. Hubbard Mar. 1995 48 p Limited Reproducibility: Document partially illegible
(Contract F33615-90-C-0005)
(AD-A294369; AL/HR-TR-1994-0168) Avail: CASI HC A03/MF A01

Two experiments were conducted to determine the altitude cuing effectiveness of various terrain texture characteristics in simulated low-altitude flight. In Experiment 1, we compared the effects of five different texture conditions, two types of subjects (pilots versus nonpilots), and direction of altitude change (ascent versus descent) on altitude change discriminability. Results indicated that performance varied significantly as a function of texture, pilots were more sensitive than nonpilots to changes in altitude, and simulated descents were easier to discriminate than ascents. Experiment 2 involved an investigation of the effects of four of the five texture conditions previously used, direction of altitude change, and two levels of texture contrast that simulated normal daytime and dawn/dusk lighting on the detection of change in altitude. We again observed that descents were more discriminable than ascents, but unlike the first experiment, performance did not vary as a function of texture. Further, simulated dawn/dusk terrain lighting did not adversely affect performance. DTIC

N95-32426*# Oklahoma Baptist Univ., Shawnee, OK. Div. of Natural Science.
CHARACTERIZING THE FRAGMENTATION RING ON WITNESS PLATES
Yuan-Liang A. Chen *In* NASA. Johnson Space Center, National Aeronautics and Space Administration (NASA)/American Society for Engineering Education (ASEE) Summer Faculty Fellowship Program, 1994, Volume 1 Jul. 1995 11 p (For primary document see N95-32418 12-99)
Avail: CASI HC A03/MF A03

N95-32502# Aeronautica Militare Italiana, Rome.
FIXED WING NIGHT ATTACK MISSIONS: ASSESSMENT IN A FLIGHT SIMULATION ENVIRONMENT
G. Arpaia, E. Scarabotto, and I. M. Spinoni (Alenia Aeronautica, Turin, Italy.) *In* AGARD, Low-Level and Nap-of-the-Earth (NOE) Night Operations Jan. 1995 12 p (For primary document see N95-32486 12-03)
Copyright Avail: CASI HC A03/MF A03

N95-34514# National Aerospace Lab., Tokyo (Japan).
NUMERICAL SIMULATION OF HIGH ENTHALPY SHOCK TUNNEL Abstract Only
Katsuhiro Itoh and Masahiro Takahashi (Queensland Univ., Brisbane, Australia.) *In its* Special Publication of National Aerospace Laboratory 16 Jun. 1994 p 93-98 In JAPANESE (For primary document see N95-34505 12-02)
Avail: CASI HC A02/MF A03

12 ASTRONAUTICS (GENERAL)

For extraterrestrial exploration see *91 Lunar and Planetary Exploration.*

N95-33167* National Aeronautics and Space Administration, Washington, DC.
SHUTTLE TO SPACE STATION. HEART ASSIST IMPLANT. HUBBLE UPDATE. X-30 MOCK-UP (Videotape)
Aug. 1992 Videotape: 15 min. 17 sec. playing time, in color, with sound
(NASA-TM-110837; NONP-NASA-VT-95-63907) Avail: CASI VHS A02/BETA A22

Shuttle to Space Station, Heart Assist Implant, Hubble Update, and X-30 Mockup are the four parts that are discussed in this video. The first part, Shuttle to Space Station, is focussed on the construction and function of the Space Station Freedom. While part two, Heart Assist Implant, discusses a newly developed electromechanical device that helps to reduce heart attack by using electric shocks. Interviews with the co-inventor and patients are also included. Brief introduction to Hubble Telescope, problem behind its poor image quality (mirror aberration), and the plan to correct this problem are the three issues that are discussed in part three, Hubble Update. The last part, part four, reviews the X-30 Mockup designed by the staff and students of Mississippi State University. CASI

13 ASTRODYNAMICS

Includes powered and free-flight trajectories; and orbital and launching dynamics.

No abstracts in this category.

14 GROUND SUPPORT SYSTEMS AND FACILITIES (SPACE)

Includes launch complexes, research and production facilities; ground support equipment, e.g., mobile transporters; and simulators.

For related information see also *09 Research and Support Facilities (Air).*

N95-33030 McMaster Univ., Hamilton (Ontario).
DIVIDING ANNULAR/TWO-PHASE FLOW IN HORIZONTAL T-JUNCTIONS Ph.D. Thesis
John David Ballyk 1993 191 p
(ISBN-0-315-84910-X) Avail: Univ. Microfilms Order No. DANN84910

The results of an experimental and analytical investigation of the separation phenomenon in dividing annular two-phase flow are presented Detailed experiments have been carried out with a steam-water loop to isolate the effect of flow split, inlet quality, inlet mass flux, and branch diameter on the phase and pressure distribution characteristics in horizontal T-junctions. Through the set of measurements made in the experimental program, the phase separation and pressure distribution characteristics were shown to be strongly interdependent. Based on these measurements, a physical model describing the phase separation mechanism is presented. This physical model is then developed mathematically. A model to predict the dividing flow characteristics for annular flow in a T-junction is proposed consisting of mixture and vapor phase continuity equations, two pressure change correlations, and a closure relationship. The pressure change from the inlet through the run of the T is modeled by way of a balance of axial momentum at the junction based on a separated flow assumption. The branch pressure change is modeled using a balance of mechanical energy for the branching flow consisting of reversible and irreversible components. In the development of the branch model, a new equivalent inlet density for the branching flow (rho(sub 1)*) and a two-phase multiplier (Phi*) are defined. The closure relationship links the phase separation characteristics with the junction pressure changes. It involves a balance between pressure and inertia forces within the junction volume defining a dividing surface for each phase between the run and branch flows. The degree of phase redistribution is then determined using a well defined inlet flow distribution. The model is capable of predicting the experimentally observed phase separation characteristics from three independent studies of annular/steam-water and air-water flow in dividing T-junctions.

Dissert. Abstr.

N95-34606# Range Commanders Council, White Sands Missile Range, NM.
RANGE GRAPHICS BENCHMARK
Apr. 1995 31 p
(AD-A293541; RCC-166-95) Avail: CASI HC A03/MF A01

This document details the various avenues available to the government in determining what benchmarks are applicable to the test range community. Areas explored include vendor benchmarks, government developed benchmarks, third party benchmarks, and proposed benchmarks for Data Reduction and Computer Group member ranges. DTIC

15 LAUNCH VEHICLES AND SPACE VEHICLES

Includes boosters; operating problems of launch/space vehicle systems; and reusable vehicles.

For related information see also *20 Spacecraft Propulsion and Power.*

N95-34815# Army Research Lab., Adelphi, MD.
ENVIRONMENT AND CIRCUIT MODEL FOR CAPACITOR-BASED RAIL GUNS Final Report, May - Sep. 1994
William Coburn, Ira Kohlberg (Kohlberg Associates, Inc., Alexandria, VA.), Warren Williams, and Calvin Le Apr. 1995 14 p
(AD-A293455; ARL-TN-46) Avail: CASI HC A03/MF A01

High-power electromagnetic devices such as rail guns require pulse power systems that can generate peak powers between 10(exp 8) and 10(exp 11) W and generate electromagnetic fields whose dominant energy spectrum falls between quasi-dc and tens of kilohertz. These fields may be important for electromagnetic compatibility (EMC), and may also be of concern for environmental and biological effects. This paper summarizes the results of the first phase of a U.S. Army Research Laboratory program that deals with the characterization of the electromagnetic fields produced by laboratory rail guns, the results of which can be scaled to operational size systems. Included are discussions of the pulsed power system, measurement techniques, theoretical models, and selected experimental data. DTIC

N95-33128# Central Research Inst. of Technology and Machine Building, Kaliningrad, Moscow (Russia).
THE CONCEPT OF THE SPACE SYSTEM BASED ON THE ROCKET LAUNCH VEHICLE OF LIGHT-WEIGHT CLASS FOR DIRECT SOUNDING OF LARGE-SCALE NATURAL HAZARDS
V. I. Loukiachtchenko, G. A. Tsyboulskii, A. K. Nedaivoda (Khrunichev State Research and Production Space Center, Moscow, Russia.), V. K. Karrask (Khrunichev State Research and Production Space Center, Moscow, Russia.), A. A. Medvedev (Khrunichev State Research and Production Space Center, Moscow, Russia.), N. A. Meliankov (Khrunichev State Research and Production Space Center, Moscow, Russia.), S. N. Philosophov (Khrunichev State Research and Production Space Center, Moscow, Russia.), and V. P. Karmasin (Nauchno-Proizvodstvennoe Obedinenie Typhoon, Obninsk, Russia.) *In* AGARD, Dual Usage in Military and Commercial Technology in Guidance and Control Mar. 1995 8 p (For primary document see N95-33126 12-31)
Copyright Avail: CASI HC A02/MF A02

16 SPACE TRANSPORTATION

Includes passenger and cargo space transportation, e.g., shuttle operations; and space rescue techniques.

For related information see also *03 Air Transportation and Safety* and *18 Spacecraft Design, Testing and Performance.* For space suits see *54 Man/System Technology and Life Support.*

N95-32539* National Aeronautics and Space Administration. Lyndon B. Johnson Space Center, Houston, TX.
LIFTOFF TO LEARNING: ASSIGNMENT SPACE (Videotape)
27 Mar. 1995 Sponsored by NASA, Washington Videotape: 16 min. 05 sec. playing time, in color, with sound
(NASA-TM-110820; NAS 1.15:110820) Avail: CASI VHS A01/BETA A22

The crew of the STS-58 Space Shuttle Columbia -- Commander John Blaha, Pilot Richard Searfoss, Payload Commander Rhea Seddon, Mission Specialist Shannon Lucid, Mission Specialist David Wolf, and Payload Specialist William McArthur host this educational video (part of the Liftoff to Learning series). The Astronauts help students to understand the importance of safety procedures on Earth as well as in space. They also discuss the effects of microgravity on various experiments in space. CASI

N95-32772# Phillips Lab., Hanscom AFB, MA.
SHUTTLE POTENTIAL AND RETURN ELECTRON EXPERIMENT (SPREE) ELECTROSTATIC ANALYZER (ESA) CALIBRATION REPORT Interim Report

M. R. Oberhardt, D. A. Hardy, W. E. Slutter, J. O. McGarity, and A. Huber 19 Jun. 1994 93 p
(AD-A293026; PL-TR-94-2210; ERP-1155) Avail: CASI HC A05/MF A01

A pair of 260 deg, spherical-plate electrostatic analyzer (ESA) units were designed, built and flown as part of the Shuttle Potential and Return Electron Experiment (SPREE) onboard the Tethered Satellite System 1 (TSS-1). Each ESA simultaneously measured ions and electrons in the energy range of 10 eV to 10 keV over an angular fan of 100 deg by 10 deg. The deflection voltage of the ESAs was logarithmically stepped through 32 channels at a rate of either 8 (fast mode) or 1 slow mode) sweeps/second. The geometric factors for the two units differed by 2 orders of magnitude so that both ambient and perturbed plasma conditions could be measured during the TSS-1 mission. In this report we present the results of the detailed calibration of these ESA's. DTIC

N95-33728* EVKO Productions, Inc., Alexandria, VA.
THE SPACE SHUTTLE: AMERICA'S TEAM REACHING FOR THE FUTURE (Videotape)
[1995] Sponsored by NASA, Washington Videotape: 23 min. 19 sec. playing time, in color, with sound
(NASA-CR-199222; NONP-NASA-VT-95-63906) Avail: CASI VHS A02/BETA A22

This video features the different NASA research centers and their contribution toward NASA's space program. It includes the following research centers: NASA headquarters, Ames Research Center, Goddard Flight Research Center, Jet Propulsion Laboratory, Johnson Space Flight Center, Kennedy Space Flight Center, Langley Research Center, Lewis Research Center, and Marshall Space Flight Center. CASI

N95-34280* National Aeronautics and Space Administration. Lyndon B. Johnson Space Center, Houston, TX.
STS-42 MISSION HIGHLIGHTS RESOURCE TAPE. PART 1 OF 2 (Videotape)
[1992] Videotape: 44 min. playing time, in color, with sound
(NASA-TM-110838; VJSC-1246-Pt-1; NONP-NASA-VT-95-63905) Avail: CASI VHS A02/BETA A22

The mission of STS-42, the first International Microgravity Laboratory (IML-1), is highlighted. The main purpose of this seven-member crews (including Payload specialist Raborto Bondar from Canada and Payload specialist Ulf D. Merbold from Germany) space shuttle was to perform different experiments at microgravity environment. The experiments were focussed on the following two major study areas: (1) life sciences (biorack, biostack, space physiology, mental workload and performance, Microgravity vestibular investigations, etc.); and (2) material sciences (critical point facility, cryostat, fluid experiment system, mercury lodide crystal growth and vapor crystal growth systems). Cargo bay and middeck experiments; earth views (Quebec, Manicougan Reservoir, St. Lawrence River, and Mountain ranges);and orbiter activities are also included. CASI

N95-34281* National Aeronautics and Space Administration. Lyndon B. Johnson Space Center, Houston, TX.
STS-42 MISSION HIGHLIGHTS RESOURCE TAPE. PART 2 OF 2 (Videotape)
[1992] Videotape: 44 min. playing time, in color, with sound
(NASA-TM-110840; VJSC-1246-Pt-2; NONP-NASA-VT-95-64175) Avail: CASI VHS A02/BETA A22

This second part of the STS-42 mission highlights resource tape presents the special events that had happened during the 8 days, 1 hour, 14 minutes, and 45 seconds mission duration. These special events include: phone calls from President Bush, German Officials, and Canadian Officials; special appearance in Super Bowl pre-game events; and in-flight press conference. CASI

17 SPACE COMM., SPACECRAFT COMM., COMMAND & TRACKING

Includes telemetry; space communications networks; astronavigation and guidance; and radio blackout.

For related information see also *04 Aircraft Communications and Navigation* and *32 Communications and Radar.*

N95-34744# RMS Technologies, Inc., Landover, MD.
SPACE PROBE DATA PROCESSING Final Report, 1 Oct. 1990 - 31 Dec. 1994
Eben Hiscock, Robert Rose, and Paul Whitman 31 Dec. 1994 53 p
(Contract F19628-90-C-0193)
(AD-A294124; PL-TR-95-2020) Avail: CASI HC A04/MF A01

This report discusses the design, development, modification and implementation of telemetry data processing techniques and computational routines for processing large volumes of data telemetered from space probes. The original design of the Orbital Data Processing System (ODPS) supported the Combined Release and Radiation Effects Satellite (CRRES) Program. The ODPS was modified to support the Advanced Photovoltaic and Electronics Experiment (APEX) Satellite. The ODPS was again modified to support the Miniature Sensor Technology Integration (MSTI) Satellite Program. The APEX ODPS and the MSTI ODPS were used successfully during the period of this effort. The Telemetry Data Processing System (TDPS) was substantially upgraded during the period of this effort. DTIC

N95-33144# MATRA Marconi Space, Toulouse (France).
GPS-BASED NAVIGATION FOR SPACE APPLICATIONS
C. Champetier, T. Duhamel, and M. Frezet *In* AGARD, Dual Usage in Military and Commercial Technology in Guidance and Control Mar. 1995 9 p (For primary document see N95-33126 12-31)
Copyright Avail: CASI HC A02/MF A02

18 SPACECRAFT DESIGN, TESTING AND PERFORMANCE

Includes satellites; space platforms; space stations; spacecraft systems and components such as thermal and environmental controls; and attitude controls.

For life support systems see *54 Man/System Technology and Life Support.* For related information see also *05 Aircraft Design, Testing and Performance, 39 Structural Mechanics,* and *16 Space Transportation.*

N95-32713# Los Alamos National Lab., NM.
DEVELOPMENT OF A COMPOSITE SATELLITE STRUCTURE FOR FORTE
C. I. Grastataro, T. A. Butler, B. G. Smith, and T. C. Thompson 1995 17 p Presented at the 10th International Conference on Composite Materials, Whistler, Canada, 14-18 Aug. 1995
(Contract W-7405-eng-36)
(DE95-009416; LA-UR-95-1016; CONF-950833-1) Avail: CASI HC A03/MF A01

The Los Alamos National Laboratory (LANL) in partnership with Composite Optics Incorporated (COI) has advanced the development of low-cost, lightweight, composite technology for use in small satellite structures, in this case, for the Fast On-Orbit Recording of Transient Events (FORTE) satellite mission. The use of advanced composites in space applications is well developed, but the application of an all-composite satellite structure has not been achieved until now. This paper investigates the application of composite technology in the design of an all-composite spacecraft structure for small satellites. Engineering analysis and test results obtained from the development of the spacecraft engineering model are also presented. DOE

N95-32884# General Accounting Office, Washington, DC. National Security and International Affairs Div.
SPACE STATION: ESTIMATED TOTAL US FUNDING REQUIREMENTS. REPORT TO CONGRESSIONAL REQUESTERS

Jun. 1995 22 p
(GAO/NSIAD-95-163; B-261547) Avail: CASI HC A03/MF A01; GAO, PO Box 6015, Gaithersburg, MD 20884-6015

This report reviews current estimated costs of the NASA space station, in particular the total U.S. funding requirements for the program and program uncertainties that may affect those requirements. U.S. funds required to design, launch, and operate the International Space Station will total about $94 billion through 2012 (about $77 billion in fiscal year 1995 constant dollars). This total may decrease to the extent NASA accomplishes its goal for achieving station operational efficiencies over the period 2003 to 2012, or efficiencies currently being studied in the space shuttle program materialize. Despite major progress, the program faces formidable challenges in completing all its tasks on schedule and within its budget. The program estimates through fiscal year 1997 show limited annual financial reserves - about 6 percent to 11 percent of estimated costs. Inadequate reserves would hinder program managers' ability to cope with unanticipated technical problems. In addition, the space station's current launch and assembly schedule is ambitious, and the shuttle program may have difficulty supporting it. Moreover, the prime contract target cost could increase if the contractor is unable to negotiate subcontractor agreements for the expected price.

CASI

N95-32903 North Carolina State Univ., Raleigh, NC.
THERMO-CHEMICAL ABLATION OF HEAT SHIELDS UNDER EARTH REENTRY CONDITIONS Ph.D. Thesis
James Anthony Keenan 1994 271 p
Avail: Univ. Microfilms Order No. DA9425472

The process of ablation for earth atmospheric entry is modeled. The flowfield surrounding the ablator is modeled by an extended set of Navier-Stokes equations that include the effects of thermochemical nonequilibrium. This set of equations encompasses the conservation of mass for each chemical species, conservation of momentum, the conservation of vibrational energy, and the conservation of total energy. The heat conduction into the ablator material is modeled by using Fourier's Law of heat conduction and the heat equation. The flowfield and ablator are coupled by a thermochemical ablation model that includes a surface mass balance and a surface energy balance. The ablation model takes into account chemical reactions of the flowfield species with the surface material, surface material acting as a catalytic surface, and sublimation of the surface material. To solve the governing equations for the model, a computational fluid dynamics approach is used where the flowfield is solved using a modified Steger-Warming flux vector splitting scheme and the solid is solved using a centrally differenced scheme. A Gauss-Seidel line relaxation technique is implemented to speed numerical convergence. The flowfield model is verified by comparing to flowfield computations of other researchers and to experimental data. The ablator/heat shield model is validated by a direct comparison between an exact analytical solution and a numerical solution. The thermochemical ablation model is verified by comparing to the experimental results of the Passive Nosetip Technology (PANT) program. The model is used to calculate steady-state ablation data for sphere-cone reentry bodies. Two bodies with nose radii of 0.0127 m and 0.1270 m are tested at a velocity of 8 km/s. The ablator material is selected to be a commercial grade graphite. Due to the ablator selection, the flowfield is limited to 11 chemical species and two internal energy modes. A standard earth atmosphere is selected at altitudes ranging from 40 km to 80 km. The major results concern the thermochemical ablation model. Both oxidation and sublimation mechanisms are evident and are dependent on freestream conditions and the reentry body shape. At low heat flux levels, the primary ablation mechanism is due to oxidation. However, as heat flux increases, sublimation of the graphitic material is the dominant ablation mechanism. Sublimation effects can become strong enough to force-off or blow all flow species away from the body's surface. Several ablation species are present within the surrounding flowfield, but the primary species are CO, C, and CN. The cyano radical, CN, is of most interest since it is often omitted from the species studied in ablation models. Carbon monoxide, CO, is present due to surface oxidation and to flowfield oxygen reacting with sublimation species.

Dissert. Abstr.

N95-33264*# Boeing Defense and Space Group, Seattle, WA.
OPERATION OF THE COMPUTER MODEL FOR MICROENVIRONMENT ATOMIC OXYGEN EXPOSURE
R. J. Bourassa, J. R. Gillis, and P. E. Gruenbaum Aug. 1995 162 p
(Contracts NAS1-18224; NAS1-19247; RTOP 233-03-02-02)
(NASA-CR-198190; NAS 1.26:198190) Avail: CASI HC A08/MF A02

A computer model for microenvironment atomic oxygen exposure has been developed to extend atomic oxygen modeling capability to include shadowing and reflections. The model uses average exposure conditions established by the direct exposure model and extends the application of these conditions to treat surfaces of arbitrary shape and orientation.

Author

N95-33890*# Boeing Defense and Space Group, Seattle, WA.
OPERATION OF THE COMPUTER MODEL FOR MICROENVIRONMENT SOLAR EXPOSURE
J. R. Gillis, R. J. Bourassa, and P. E. Gruenbaum Aug. 1995 165 p
(Contracts NAS1-18224; NAS1-19247; RTOP 233-03-02-02)
(NASA-CR-198189; NAS 1.26:198189) Avail: CASI HC A08/MF A02

A computer model for microenvironmental solar exposure was developed to predict solar exposure to satellite surfaces which may shadow or reflect on one another. This document describes the technical features of the model as well as instructions for the installation and use of the program.

Author (revised)

N95-34493# Air Force Inst. of Tech., Wright-Patterson AFB, OH.
THERMAL CONTROL TECHNOLOGY OF COMMUNICATIONS SATELLITE
Guo Jiurong 13 Apr. 1995 26 p Transl. into ENGLISH from Zhongguo Kongjian Kexue Jishu (China), no. 1, 1990 p 14-20, 45-51 Prepared by Leo Kanner Associates
(Contract F33657-88-D-2188)
(AD-A294249; NAIC-ID(RS)T-0562-93) Avail: CASI HC A03/MF A01

This paper briefly describes status quo and recent prospects on thermal control technology of communications satellites. A discussion of several problems on heat radiators and other thermal control elements is given.

DTIC

N95-34500# Air Force Systems Command, Wright-Patterson AFB, OH. National Air Intelligence Center.
THERMAL DESIGN OF RETURNABLE SATELLITES
Xu Jiwan 25 Apr. 1995 26 p Transl. into ENGLISH from Zhongguo Kongjian Kexue Jishu, China, Nr. 6, 1990 p 49-56
(AD-A294113; NAIC-ID(RS)T-0558-93) Avail: CASI HC A03/MF A01

This introduces China's returnable satellite thermal control design plans. On the basis of the special characteristics of China's returnable type satellites, it describes the applications of thermal inertia methods in thermal design. Comparisons between ground heat experiment data and flight telemetry temperature data clearly show that the two agree together well. Heat control system operations were normal. Satellite body and satellite interior instrument temperatures all fell relatively well into required ranges.

DTIC

N95-32432*# Military Academy, West Point, NY. Dept. of Civil and Mechanical Engineering.
IMPLEMENTATION OF A SINGLE-STAGE-TO-ORBIT (SSTO) MODEL FOR STABILITY AND CONTROL ANALYSIS Final Report
Stephen A. Ingalls *In* NASA. Johnson Space Center, National Aeronautics and Space Administration (NASA)/American Society for Engineering Education (ASEE) Summer Faculty Fellowship Program, 1994, Volume 1 Jul. 1995 14 p (For primary document see N95-32418 12-99)
(Grant NGT-44-005-803)
Avail: CASI HC A03/MF A03

19 SPACECRAFT INSTRUMENTATION

For related information see also *06 Aircraft Instrumentation* and *35 Instrumentation and Photography.*

N95-32593# Lawrence Livermore National Lab., Livermore, CA.
SINGLE EVENT AND TREE LATCHUP MITIGATION FOR A STAR TRACKER SENSOR: AN INNOVATIVE APPROACH TO SYSTEM LEVEL LATCHUP MITIGATION
J. R. Kimbrough, N. J. Colella, R. W. Davis, D. B. Bruener (JAYCOR, San

Diego, CA.), P. G. Coakley (JAYCOR, San Diego, CA.), S. W. Lutjens (JAYCOR, San Diego, CA.), and C. E. Mallori (JAYCOR, San Diego, CA.)
Aug. 1994 14 p
(Contract W-7405-eng-48)
(DE95-010331; UCRL-ID-114325) Avail: CASI HC A03/MF A01

Electronic packages designed for spacecraft should be fault-tolerant and operate without ground control intervention through extremes in the space radiation environment. If designed for military use, the electronics must survive and function in a nuclear radiation environment. This paper presents an innovative 'blink' approach rather than the typical 'operate through' approach to achieve system level latchup mitigation on a prototype star tracker camera. Included are circuit designs, flash x-ray test data, and heavy ion data demonstrating latchup mitigation protecting micro-electronics from current latchup and burnout due to Single Event Latchup (SEL) and Transient Radiation Effects on Electronics (TREE). DOE

20 SPACECRAFT PROPULSION AND POWER

Includes main propulsion systems and components, e.g., rocket engines; and spacecraft auxilliary power sources.

For related information see also *07 Aircraft Propulsion and Power, 28 Propellants and Fuels, 44 Energy Production and Conversion,* and *15 Launch Vehicles and Space Vehicles.*

N95-32396# Ames Lab., IA.
FABRICATION OF IMPROVED SiGe ALLOYS FOR AN 18-COUPLE MODULE TEST
S. Loughin (Martin Marietta Aero and Naval Systems, Baltimore, MD.), J. F. Nakahara (Martin Marietta Aero and Naval Systems, Baltimore, MD.), D. X. Centurioni (Martin Marietta Aero and Naval Systems, Baltimore, MD.), B. A. Cook, and J. L. Harringa 1995 6 p Presented at the 12th Symposium on Space Nuclear Power and Propulsion, Albuquerque, NM, 8-12 Jan. 1995
(Contract W-7405-eng-82)
(DE95-010238; IS-M-813; CONF-950110-20) Avail: CASI HC A02/MF A01

N- and p-type Si(0.78)Ge(0.22) alloys were fabricated to determine if recently reported improvements in the figure-of-merit, Z, could be realized in devices. These will be tested in an 18-couple module to directly compare the performance of these materials with that of standard coarse-grain SiGe used in flight programs. We describe the synthesis by vacuum casting and hot pressing p-type SiGe and mechanical alloying and hot-isostatic pressing n-type SiGe. Improved materials and standard materials are characterized and compared. The integrated average figures-of-merit (573-1273 K) of the improved materials were Z(sub p) = 0.59 x 10(exp -3) K(sup -1) and Z(sub n) = 0.85 x 10(exp -3) K(sup -1) compared with Z(sub p) = 0.52 x 10(exp -1) K(sup -1) and Z(sub n) = 0.76 x 10(exp -3) K(sup -1) for the standard materials. We also report the power factors for improved and standard materials removed from fabricated devices to gain insight as to how subsequent processing impacts performance. DOE

N95-32673*# NYMA, Inc., Brook Park, OH.
PERFORMANCE OF PARTIALLY FLUORINATED POLYIMIDE INSULATION FOR AEROSPACE APPLICATIONS Final Contractor Report
Ahmad N. Hammoud, Mark W. Stavnes, James R. Ide (McDonnell-Douglas Aerospace, Saint Louis, MO.), and Ed Muegge (McDonnell-Douglas Aerospace, Saint Louis, MO.) Cleveland, OH NASA Aug. 1995 6 p Presented at the 1995 Conference on Electrical Insulation and Dielectric Phenomena, Virginia Beach, VA, 22-25 Oct. 1995; sponsored by IEEE Dielectrics and Electrical Insulation Society
(Contracts NAS3-27186; NAS1-18580; RTOP 297-50-00)
(NASA-CR-198372; E-9820; NAS 1.26:198372) Avail: CASI HC A02/MF A01

Polyimide has been used extensively as the primary wiring insulation in commercial planes, military aircraft, and space vehicles due to its low weight, high service temperature, and good dielectric strength. New failure modes, however, have been associated with the use of polyimide because of the susceptibility of the insulation to pyrolization and arc tracking. A new wiring construction utilizing partially fluorinated polyimide insulation has been tested and compared with the standard military polyimide wire. Electrical properties which were investigated include AC corona inception and extinction voltages (sea level and 60,000 feet), time/current to smoke, and wire fusing time. The two constructions were also characterized in terms of their mechanical properties including abrasion resistance, dynamic cut through, and notch propagation. These test efforts and the results obtained are presented and discussed. Author

N95-32755# National Aerospace Lab., Kakuda (Japan). Research Center.
POP TESTS OF STORABLE BIOPROPELLANT LIQUID APOGEE ENGINE
Yukio Kuroda, Makoto Tadano, Masahiro Sato, Kazuo Kusaka, Hideyuki Kobayashi (National Space Development Agency, Tokyo, Japan.), Sigeyasu Iihara (Ishikawajima-Harima Heavy Industries Co. Ltd., Tokyo, Japan.), and Hiroyuki Ban (Ishikawajima-Harima Heavy Industries Co. Ltd., Tokyo, Japan.) Oct. 1994 18 p In JAPANESE
(ISSN 0389-4010)
(NAL-TR-1253) Avail: CASI HC A03/MF A01

A pressure-fed, blowdown, hydrazine/NTO apogee propulsion system had been selected for the ETS-6. One of the problems encountered during the development of the engine was the occurrence of pops (popping) at the higher operating chamber pressures. Pops are irregular high amplitude pressure pulses. It is generally agreed that pops is a liquid spray/gas two-phase explosion triggered by a local explosion near the jet impingement region. The effects of operating parameters on pops observed in the development tests of the apogee engine for the ETS-6 were inconsistent with those reported earlier for single impingement injectors; pops with the apogee engine injectors was more likely to occur at higher chamber pressures, higher injection velocities, and higher propellant temperatures. Pops data were correlated fairly well in chamber pressures (bar-P(sub c)) vs. fuel Reynolds number (R(sub ef)) plane. However, the range of operating parameters for the above correlation were very narrow since they were obtained during injector screening tests for a particular application to the apogee engine. It was also felt that the above correlation was too simplistic to capture any effect of design parameters of multi-element injectors. In the present study, the demarcation between pops and the pops-free region was determined in broader operating ranges and design parameters. The range of bar-P(sub c) and R(sub ef) was extended by exchanging graphite nozzle throat inserts with different throat diameters. The injectors were carefully selected to obtain effects, if any, of (1) film cooling fraction, (2) secondary mixing, and (3) number of elements and/or fuel orifice diameters. It was found that there was a threshold fuel Reynolds number below which no pops were observed at any chamber pressures and that the pops region curve in the bar-P(sub c)-R(sub ef) plane had two branches: upper branches and lower branches. Author

N95-32917*# National Aeronautics and Space Administration. Lewis Research Center, Cleveland, OH.
ADVANCED PROPULSION FOR GEOSTATIONARY ORBIT INSERTION AND NORTH-SOUTH STATION KEEPING
Steven R. Oleson (NYMA, Inc., Brook Park, OH.), Roger M. Myers (NYMA, Inc., Brook Park, OH.), Craig A. Kluever (Missouri Univ., Kansas City, MO.), John P. Riehl, and Francis M. Curran Aug. 1995 18 p Presented at the 31st Joint Propulsion Conference and ExhiBit, San Diego, CA, 10-12 Jul. 1995; sponsored by AIAA, ASME, SAE, and ASEE
(Contract NAS3-27186; RTOP 564-09-20)
(NASA-TM-107018; E-9818; NAS 1.15:107018; AIAA Paper 95-2513)
Avail: CASI HC A03/MF A01

Solar electric propulsion (SEP) technology is currently being used for geostationary satellite station keeping to increase payload mass. Analyses show that advanced electric propulsion technologies can be used to obtain additional increases in payload mass by using these same technologies to perform part of the orbit transfer. In this work three electric propulsion technologies are examined at two power levels for an Atlas 2AS class spacecraft. The on-board chemical propulsion apogee engine fuel is reduced to allow the use of electric propulsion. A numerical optimizer is used to determine the chemical burns which will minimize the electric propulsion transfer time. Results show that for a 1550 kg Atlas 2AS class payload, increases in net mass (geostationary satellite mass less wet propulsion system mass) of 150 to 800 kg are possible using electric propulsion for station keeping, advanced chemical engines for part of the transfer, and

electric propulsion for the remainder of the transfer. Trip times are between one and four months. Author

N95-32932*# Pennsylvania State Univ., University Park, PA. The Propulsion Engineering Research Center.

FUNDAMENTAL PHENOMENA ON FUEL DECOMPOSITION AND BOUNDARY-LAYER COMBUSTION PROCESSES WITH APPLICATIONS TO HYBRID ROCKET MOTORS Semiannual Report

Kenneth K. Kuo, Yeu-Cherng Lu, Martin J. Chiaverini, George C. Harting, David K. Johnson, and Nadir Serin 1995 31 p

(Contract NAS8-39945)

(NASA-CR-199126; NAS 1.26:199126) Avail: CASI HC A03/MF A01

The experimental study on the fundamental processes involved in fuel decomposition and boundary-layer combustion in hybrid rocket motors is continuously being conducted at the High Pressure Combustion Laboratory of The Pennsylvania State University. This research will provide a useful engineering technology base in the development of hybrid rocket motors as well as a fundamental understanding of the complex processes involved in hybrid propulsion. A high-pressure, 2-D slab motor has been designed, manufactured, and utilized for conducting seven test firings using HTPB fuel processed at PSU. A total of 20 fuel slabs have been received from the Mcdonnell Douglas Aerospace Corporation. Ten of these fuel slabs contain an array of fine-wire thermocouples for measuring solid fuel surface and subsurface temperatures. Diagnostic instrumentation used in the test include high-frequency pressure transducers for measuring static and dynamic motor pressures and fine-wire thermocouples for measuring solid fuel surface and subsurface temperatures. The ultrasonic pulse-echo technique as well as a real-time x-ray radiography system have been used to obtain independent measurements of instantaneous solid fuel regression rates. Author

N95-33156*# Georgia Inst. of Tech., Atlanta, GA.

ACTIVELY CONTROLLED SHAFT SEALS FOR AEROSPACE APPLICATIONS Final Contractor Report

Richard F. Salant Cleveland, OH NASA Jul. 1995 192 p

(Grant NAG3-974; RTOP 242-70-04)

(NASA-CR-4678; E-9742; NAS 1.26:4678) Avail: CASI HC A09/MF A02

This study experimentally investigates an actively controlled mechanical seal for aerospace applications. The seal of interest is a gas seal, which is considerably more compact than previous actively controlled mechanical seals that were developed for industrial use. In a mechanical seal, the radial convergence of the seal interface has a primary effect on the film thickness. Active control of the film thickness is established by controlling the radial convergence of the seal interface with a piezoelectric actuator. An actively controlled mechanical seal was initially designed and evaluated using a mathematical model. Based on these results, a seal was fabricated and tested under laboratory conditions. The seal was tested with both helium and air, at rotational speeds up to 3770 rad/sec, and at sealed pressures as high as 1.48 x 10(exp 6) Pa. The seal was operated with both manual control and with a closed-loop control system that used either the leakage rate or face temperature as the feedback. The output of the controller was the voltage applied to the piezoelectric actuator. The seal operated successfully for both short term tests (less than one hour) and for longer term tests (four hours) with a closed-loop control system. The leakage rates were typically 5-15 slm (standard liters per minute), and the face temperatures were generally maintained below 100C. When leakage rate was used as the feedback signal, the setpoint leakage rate was typically maintained within 1 slm. However, larger deviations occurred during sudden changes in sealed pressure. When face temperature was used as the feedback signal, the setpoint face temperature was generally maintained within 3 C, with larger deviations occurring when the sealed pressure changes suddenly. the experimental results were compared to the predictions from the mathematical model. The model was successful in predicting the trends in leakage rate that occurred as the balance ratio and sealed pressure changed, although the leakage rates were not quantitatively predicted with a high degree of accuracy. This model could be useful in providing valuable design information for future actively controlled mechanical seals. Author

N95-33926*# NYMA, Inc., Brook Park, OH. Engineering Services Div.

LIFE TEST OF A XENON HOLLOW CATHODE FOR A SPACE PLASMA CONTRACTOR Final Report

Timothy R. Sarver-Verhey Nov. 1994 7 p Presented at the 1994 Tri-Service/NASA Cathode Workshop, Cleveland, OH, 29-31 Mar. 1994; sponsored by NASA. Lewis Research Center and the Advisory Group on Electron Devices

(Contract NAS3-27186; RTOP 478-43-00)

(NASA-CR-195403; E-9247; NAS 1.26:195403) Avail: CASI HC A02/MF A01

A plasma contacting device using a hollow cathode for plasma production has been baselined for use on the Space Station. This application will require reliable, continuous operation of the cathode at electron emission currents of between 0.75 and 10 A for two years (17,500 hours). In order to validate life-time capability, a hollow cathode, operated in a diode configuration, has been tested for more than 8600 hours of stable discharge operation as of March 30, 1994. This cathode is operated at a steady-state emission current of 12.0 and a fixed xenon flow rate of 4.5 sccm. Discharge voltage and cathode temperature have remained relatively stable at approximately 12.9 V and 1260 C during the test. The test has experienced 7 shutdowns to date. In all instances, the cathode was reignited at about 42 V and resumed stable operation. This test represents the longest demonstration of stable operation of high current (greater than 1A) xenon hollow cathodes reported to date. Author

N95-34302# Air Force Systems Command, Wright-Patterson AFB, OH. National Air Intelligence Center.

THE DEVELOPMENT OF SOME KINDS OF LRE INJECTORS

Yu Yueying 28 Apr. 1995 20 p Transl. into ENGLISH from Journal of Propulsion Technology, no. 4, Aug. 1992 p 15-21

(AD-A294199; NAIC-ID(RS)T-0819-94) Avail: CASI HC A03/MF A01

This article introduces technical problems which appear in the development of several types of liquid rocket engine injectors and ways to solve them. At the same time, analysis was done of dual component centrifugal type injector nozzle flow amount deviations. Inquiries were made into methods of controlling flow amount deviations. A type of body interior cooling system was put forward. Option was made for the use of beveled slot drill rod welded integral type structures. In medium thrust liquid rocket engines, experiments were carried out and preliminary conclusions obtained. DTIC

N95-34625*# Aerojet-General Corp., Sacramento, CA.

SSME POST TEST DIAGNOSTIC SYSTEM: SYSTEMS SECTION Final Contractor Report

Timothy Bickmore Aug. 1995 420 p

(Contract NAS3-25883; RTOP 584-03-11)

(NASA-CR-198375; E-9829; NAS 1.26:198375) Avail: CASI HC A18/MF A04

An assessment of engine and component health is routinely made after each test firing or flight firing of a Space Shuttle Main Engine (SSME). Currently, this health assessment is done by teams of engineers who manually review sensor data, performance data, and engine and component operating histories. Based on review of information from these various sources, an evaluation is made as to the health of each component of the SSME and the preparedness of the engine for another test or flight. The objective of this project - the SSME Post Test Diagnostic System (PTDS) - is to develop a computer program which automates the analysis of test data from the SSME in order to detect and diagnose anomalies. This report primarily covers work on the Systems Section of the PTDS, which automates the analyses performed by the systems/performance group at the Propulsion Branch of NASA Marshall Space Flight Center (MSFC). This group is responsible for assessing the overall health and performance of the engine, and detecting and diagnosing anomalies which involve multiple components (other groups are responsible for analyzing the behavior of specific components). The PTDS utilizes several advanced software technologies to perform its analyses. Raw test data is analyzed using signal processing routines which detect features in the data, such as spikes, shifts, peaks, and drifts. Component analyses are performed by expert systems, which use 'rules-of-thumb' obtained from interviews with the MSFC data analysts to detect and diagnose anomalies. The systems analysis is performed using case-based reasoning. Results of all analyses are stored in a relational database and displayed via an X-window-based

graphical user interface which provides ranked lists of anomalies and observations by engine component, along with supporting data plots for each. Author

N95-32423*# Louisiana Tech Univ., Ruston, LA. Dept. of Electrical Engineering.
MODELING OF DC SPACECRAFT POWER SYSTEMS Final Report
F. C. Berry *In* NASA. Johnson Space Center, National Aeronautics and Space Administration (NASA)/American Society for Engineering Education (ASEE) Summer Faculty Fellowship Program, 1994, Volume 1 Jul. 1995 9 p (For primary document see N95-32418 12-99)
(Grant NGT-44-005-803)
Avail: CASI HC A02/MF A03

23 CHEMISTRY AND MATERIALS (GENERAL)

N95-33835# Sandia National Labs., Albuquerque, NM.
CHARACTERIZATION OF MICROENVIRONMENT POLARITY AND SOLVENT ACCESSIBILITY OF POLYSILSESQUIOXANE XEROGELS BY THE FLUORESCENT PROBE TECHNIQUE
K. J. Shea (California Univ., Irvine, CA.), H. D. Zhu (California Univ., Irvine, CA.), and D. A. Loy 1995 8 p Presented at the American Chemical Society Spring Meeting, Anaheim, CA, 2 Feb. 1995
(Contract DE-AC04-94AL-85000)
(DE95-011874; SAND-95-0932C; CONF-950297-1) Avail: CASI HC A02/MF A01

Poly (1, 4 bis(triethoxysilyl)benzene) (PTESB), a representative of a new type of organic-inorganic hybrid polysilsesquioxane material, was characterized by fluorescence spectroscopy for both microenvironmental polarity and solvent accessibility. A dansyl fluorescent molecule was incorporated into the bulk as well as onto the surface of both PTESB and silica materials. Information about the microenvironment polarity and accessibility of PTESB to various organic solvents was determined and compared to that of silica gel. This study found that both the bulk and surface of PTESB are less polar than that of the silica material. The silica material is accessible to polar solvents and water, while YMB is accessible to polar solvents but not to water. The hydrophobicity of PTESB differentiates these new materials from silica gel. DOE

N95-33848# Los Alamos National Lab., NM.
LATTICE POLYMER AUTOMATA
Steen Rasmussen and Joshua R. Smith (Santa Fe Inst., NM.) 1995 27 p Presented at the Self-organization of Biopolymers, Jena, Germany, 10-13 Apr. 1994 Submitted for publication in Berichte der Bunsen-Gesellschaft fuer Physikalische Chemie
(Contract W-7405-eng-36)
(DE95-011980; LA-UR-95-1543; CONF-9404261-1) Avail: CASI HC A03/MF A01

We present a new style of molecular dynamics and self-assembly simulation, the Lattice Polymer Automaton (LPA). In the LPA all interactions, including electromagnetic forces, are decomposed and communicated via propagating particles, (open 'photons'. The monomer-monomer bondforces, the molecular excluded volume forces, the longer range intermolecular forces, and the polymer-solvent interactions may all be modeled with propagating particles. The LPA approach differs significantly from both of the standard approaches, Monte Carlo lattice methods and Molecular Dynamics simulations. On the one hand, the LPA provides more realism than Monte Carlo methods, because it produces a time series of configurations of a single molecule, rather than a set of casually unrelated samples from a distribution of configurations. The LPA can therefore be used directly to study dynamical properties; one can in fact watch polymers move in real time. On the other hand, the LPA is fully discrete, and therefore much simpler than traditional Molecular Dynamics models, which are continuous and operate on much shorter time scales. Due to this simplicity it is possible to simulate longer real time periods, which should enable the study of molecular self-organization on workstations supercomputers are not needed. DOE

24 COMPOSITE MATERIALS

Includes physical, chemical, and mechanical properties of laminates and other composite materials.

For ceramic materials see *27 Nonmetallic Materials.*

N95-32395# Ames Lab., IA.
A NUMERICAL ANALYSIS OF FRACTURE AND HIGH TEMPERATURE CREEP CHARACTERISTICS OF COMPOSITES WITH DISCONTINUOUS DUCTILE REINFORCEMENTS
S. B. Biner 1994 6 p Presented at the 1994 Fall Meeting of the Materials Research Society (MRS), Boston, MA, 28 Nov. - 2 Dec. 1994
(Contract W-7405-eng-48)
(DE95-010236; IS-M-815; CONF-941144-123) Avail: CASI HC A02/MF A01

Role of material parameters on fracture and creep behavior of discontinuous ductile fiber reinforced brittle matrix composite system was numerically investigated. For simulation of fracture behavior, the ductile fibers were modeled using a constitutive relationship that accounts for strength degradation resulting from nucleation and growth of the voids. The matrix is assumed to be elastic and fails according to requirements of a stress criterion. Results indicate that the contribution of ductile reinforcement to the work of fracture value (toughness) of the composite increases with less exhaustion of its work hardening capacity before the onset of matrix failure. At creep regime, for rigidly bonded interfaces, the creep rate of the composite is not significantly influenced by the material properties of the ductile reinforcing phase due to development of large hydrostatic stress and constrained deformation in the reinforcement. Significant increases in room temperature fracture toughness can be achieved without extensively sacrificing the creep strength by ductile discontinuous reinforcements. DOE

N95-32399# Lawrence Livermore National Lab., Livermore, CA.
METALLIC LAMINATES FOR ENGINE APPLICATIONS
D. R. Lesuer and C. K. Syn Jun. 1994 14 p Presented at the 8th World Ceramic Congress, Florence, Italy, 29 Jun. - 4 Jul. 1994
(Contract W-7405-eng-48)
(DE95-010259; UCRL-JC-115700; CONF-940641-2) Avail: CASI HC A03/MF A01

Laminated metal composites consist of alternating metal (or metal matrix composite) layers that are bonded together. This paper reviews the processing of these materials and the properties relevant to engine applications. These properties include strength, toughness and damping capacity. Laminates can have very attractive properties relative to other structural materials for weight critical applications requiring high stiffness, strength and fracture toughness. The structure-property correlations that determine these properties are described. DOE

N95-32602# Lawrence Livermore National Lab., Livermore, CA.
FRACTURE TOUGHNESS AND TENSILE BEHAVIOR OF MULTI-LAYER LAMINATED METAL COMPOSITE OF Al 6090-25 VOL % SiCp AND Al 5182
C. K. Syn, D. R. Lesuer, and O. D. Sherby (Stanford Univ., CA.) 8 Feb. 1995 8 p
(Contract W-7405-eng-48)
(DE95-011421; UCRL-ID-119966) Avail: CASI HC A02/MF A01

Multilayer laminates of varying volume percentage (from 50-50 to 3-97) of Al 5182 and Al 6090 metal matrix composite containing 25 vol % SiC particulate were made by a press bonding method. The yield and tensile strengths of these laminated metal composites were slightly lower than the rule-of-averages values of the component materials. As the volume fraction of the ductile component decreased from 50% to about 3%, the yield and tensile strengths increased from those of the 50-50 laminates, and the fracture toughness also showed a slightly increasing tendency. The ductility of the laminate was insensitive to the change in volume fraction of the ductile component. Fractography on tensile and fracture toughness tested samples showed that crack propagation in the laminates was blunted by delamination ahead of the growing crack and by plastic deformation in the ductile component. DOE

N95-32711# Japan Atomic Energy Research Inst., Tokyo (Japan). Dept. of Materials Science and Engineering.
EVALUATION OF STRENGTH PROPERTIES OF DEVELOPED SiC/C COMPOSITIONALLY GRADIENT GRAPHITE MATERIALS
Junichi Nakano, Kimio Fujii, and Masami Shindo (Japan Atomic Energy Research Inst., Ibaraki, Japan.) Oct. 1994 29 p In JAPANESE
(DE95-737271; JAERI-Research-94-016) Avail: CASI HC A03/MF A01

To evaluate the influence of surface SiC coating and intermediate SiC/C layers on the mechanical strength of graphite matrix of the developed compositionally gradient graphite materials, which are composed of a surface SiC coating layer, an intermediate SiC/C layer and a graphite matrix, bending and compressive tests were carried out for SiC/C compositionally gradient graphite materials, SiC coated graphite materials, graphite materials with the intermediate SiC/C and virgin graphite materials at room temperature. The results of the tests were discussed in comparison with the specific surface areas which is a measure for the surface condition of samples. For the graphite with the intermediate SiC/C layer, the strength was independent of the Si content in the intermediate SiC/C layer and almost the same as that for the graphite substrate, although the specific surface area increased with an increase in the Si content in the intermediate SiC/C layer. The strength of the surface SiC coated specimens, i.e., SiC/C compositionally gradient graphite materials and SiC coated graphite materials, was about twice as that of the respective substrate, i.e., the graphite with the intermediate SiC/C layer and the virgin graphite. DOE

N95-32775 Harvard Univ., Cambridge, MA.
MICROMECHANICS OF FIBER-REINFORCED CERAMIC COMPOSITES Ph.D. Thesis
Zhiyong Cedric Xia 1994 124 p
Avail: Univ. Microfilms Order No. DA9421984

This thesis presents a micromechanics study of the matrix cracking behavior of fiber-reinforced ceramic composites. Primary efforts are made to understand the overall stress-strain behavior of a cross-ply laminate, with emphasis on developing a complete constitutive law in terms of its constituent properties, which are suitable for continuum damage mechanics applications. Chapter 2 addresses transverse cracking by the tunneling mechanism in the matrix of the 90 deg plies of a cross-ply laminate. Several aspects of the problem are considered, including conditions for the onset of matrix cracking, the evolution of crack spacing, and the construction of the tensile stress-strain behavior of the laminate undergoing progressive matrix cracking in the presence of initial residual stress. The subsequent study where the fully tunneled cracks begin to extend into and across the adjacent 0 deg plies is presented in Chapter 3. The cracking process involves a competition between crack bridging by the fibers in the 0 deg plies and interaction among multiple cracks. Crack bridging is modeled by a line- spring formulation and crack interaction is modeled by two representative doubly periodic crack patterns. The study provides results which enable the tensile stress-strain behavior of the cross-ply laminate to be predicted, and it provides estimates of the maximum stress concentration in the bridging fibers. The line-spring model used in Chapter 3 to characterize matrix crack bridging through the sliding resistance between fibers and matrix is critically examined in Chapter 4. It is found that the distance along the fiber within which sliding occurs is often too large to justify use of the line-spring representation. An LSS model which allows for large scale sliding is proposed and applied to several representative problems. In general, the line-spring model is found to overestimate the stress concentration in critically located fibers. Chapter 5 offers a preliminary study on shear behavior of fiber-reinforced cross-ply laminates. A plane strain model is invoked for this purpose to give some qualitative insights. The differences between shear and tensile responses are discussed, along with a discussion of further work needed in this direction. Dissert. Abstr.

N95-33062# Burton Technologies, Inc., Raleigh, NC.
WEAR RESISTANT COMPOSITE STRUCTURE OF VITREOUS CARBON CONTAINING CONVOLUTED FIBERS Quarterly Report No. 4
R. G. Burton and R. A. Burton 1 May 1995 5 p
(Contract DE-FG01-94CE-15613)
(DE95-011463; DOE/CE-15613/T4) Avail: CASI HC A01/MF A01

This report presents a brief description of the fabrication and advantages of a metal-reinforced carbon composite (MRCC) material which does not require lubrication. MRCC are a new class of material made up of nongraphitic, continuous-phase, unstructured carbon binder and continuous metal fibers. A noteworthy advantage of the MRCC process is that it can be applied not only to small parts, such as bearings and seals, but also to large castings, such as pump bodies and compressor cylinders. The process for manufacturing the MRCC is a simple, single-stage pyrolysis of a resin-formed greenbody, i.e., metal and carbon composite particles held together by binder or resin. Machining can be performed on the greenbody or on the final fired component, depending on required tolerances. The MRCC material offers several desirable features: self-lubricating, impermeable, chemically resistant, lightweight, controllable strength and conductivity, high-temperature tolerance, and good wear performance in both vacuum and dry atmosphere. CASI

N95-33210*# National Aeronautics and Space Administration. Lewis Research Center, Cleveland, OH.
MICROMECHANICS OF COMPOSITES WITH SHAPE MEMORY ALLOY FIBERS IN UNIFORM THERMAL FIELDS
Victor Birman (Missouri Univ., Rolla, MO.), Dimitris A. Saravanos (Ohio Aerospace Inst., Cleveland, OH.), and Dale A. Hopkins Aug. 1995 21 p Presented at the 36th Structures, Structural Dynamics and Materials Conference, New Orleans, LA, 10-13 Apr. 1995; cosponsored by AIAA, ASME, AHS, and ASC
(RTOP 505-63-5B)
(NASA-TM-107011; E-9795; NAS 1.15:107011; AIAA Paper 95-1210)
Avail: CASI HC A03/MF A01

Analytical procedures are developed for a composite system consisting of shape memory alloy fibers within an elastic matrix subject to uniform temperature fluctuations. Micromechanics for the calculation of the equivalent properties of the composite are presented by extending the multi-cell model to incorporate shape memory alloy fibers. A three phase concentric cylinder model is developed for the analysis of local stresses which includes the fiber, the matrix, and the surrounding homogenized composite. The solution addresses the complexities induced by the nonlinear dependence of the in-situ martensite fraction of the fibers to the local stresses and temperature, and the local stresses developed from interactions between the fibers and matrix during the martensitic and reverse phase transformations. Results are presented for a nitinol/epoxy composite. The applications illustrate the response of the composite in isothermal longitudinal loading and unloading, and in temperature induced actuation. The local stresses developed in the composite under various stages of the martensitic and reverse phase transformation are also shown. Author

N95-33309 Michigan Univ., Ann Arbor, MI.
A NEW APPROACH TO FRACTURE OF LAYERED FIBROUS COMPOSITES: EXPERIMENTS AND ANALYSIS Ph.D. Thesis
Seung Jae Song 1994 144 p
Avail: Univ. Microfilms Order No. DA9423321

A mechanics model has been developed to predict mode 1, mode 2 and mixed mode delamination failure of laminated composites. Instead of using the concepts of Linear Elastic Fracture Mechanics, a nonlinear elastic foundation model was employed with a novel characterization of the foundation. The material ahead of the crack tip experiencing 'micro' behavior of high gradients of stress and strain was separated out from the 'macro' behavior of relatively low gradients of stress and strain by replacing it with spring foundations. Two types of mechanics models were developed as categorized by their failure criterions. One is an energy based model and the other is a strength based model. Mode 1 and mode 2 components of the mixed mode failure were represented by nonlinear tension and shear spring foundations, respectively. Mode 1, mode 2 and mixed mode laboratory fracture tests were performed to investigate the material failure ahead of the crack tip and to validate the current models. Two types of fiber-polymeric laminated composite beams were used in the experiment. Double cantilever beam type specimens were used for mode 1 fracture tests and end loaded split type specimens were used for mode 2 and mixed mode fracture tests with appropriate boundary conditions and gripping mechanisms. A finite element method was implemented to simulate the laboratory fracture tests. A finite element which can incorporate material nonlinearities was developed and a corresponding computer code was written for this purpose. The current models reproduced load versus displacement curves obtained from mode 1, mode 2 and mixed mode fracture tests very closely. Also, the energy based model showed an excellent mode separation capability for mixed mode delamination problems. The developed mechanical models can be applied to very general layered composite structures without having

to appeal to complicated mathematical details as long as the failure type is delamination, in which the classical fracture mechanics approaches have difficulties, particularly for mixed mode situations. Dissert. Abstr.

N95-33326 Michigan Univ., Ann Arbor, MI.
RESPONSE AND FAILURE OF THICK COMPOSITE RINGS SUBJECTED TO UNIFORM EXTERNAL HYDROSTATIC PRESSURE OR RADIAL CONTRACTION Ph.D. Thesis
Lei Fu 1994 174 p
Avail: Univ. Microfilms Order No. DA9423183

The behavior of thick S-2 Glass/Epoxy and AS4/PPS composite rings under external uniform hydrostatic pressure or radial contraction is investigated both experimentally and theoretically. A volume controlled pressurization setup was implemented and the rings were pressurized until failure. Test results indicate that for the radius to thickness ratios investigated, the rings are highly elastic and fail through global buckling. The initial postbuckling response is found to be stable and no ply nor fiber level damaged is observed in the unloaded specimens. Information on the compression failure strength of the composite ring specimens is obtained by subjecting the rings to a uniform radial contraction. Composite rings tested in this configuration are found not to be subjected to buckling instabilities. This testing configuration is viewed as a feasible candidate in obtaining the compression failure strength of composites. Unlike the case with straight sided specimens, the failure is not sensitive to parallelism and flatness of the opposing loading surfaces. The experimentally obtained buckling modes and loads in the pressure test are modeled with both a 1-D shear formulation and a 2-D elasticity formulation. The results are compared to typical 1-D formulations in the literature and the effects of thickness on buckling, and the initial postbuckling response is examined. The initial postbuckling responses are stable for all ring thicknesses. For rings with a R/t ratio of less than 10, both the predicted buckling load and the initial postbuckling responses are sensitive to the thickness of the ring. A 1-D twist buckling analysis is readily available, but an analysis for the asymmetric out of plane buckling of thick composite rings is lacking. The modeling of the out of plane buckling of polar and rectilinear orthotropic composite rings is accomplished without assumptions of axisymmetry. Results show that assumptions of symmetry in the buckling modes produces buckling loads that are not minimal in the externally pressurized cases. An envelope of the failure modes of S-2 Glass/Epoxy and AS4/PPS composite rings of various thicknesses is constructed and compared to experimental results. It is found that the experimental results are well modeled by the theories developed here. Dissert. Abstr.

N95-33327 Virginia Polytechnic Inst. and State Univ., Blacksburg, VA.
INTERLAMINAR STRESS ANALYSIS OF DROPPED-PLY LAMINATED PLATES AND SHELLS BY A MIXED METHOD Ph.D. Thesis
Peter Newton Harrison 1994 172 p
Avail: Univ. Microfilms Order No. DA9425574

A mixed method of approximation based on Reissner's variational principle is developed for the linear analysis of interlaminar stresses in laminated composites, with special interest in laminates that contain terminated internal plies (dropped-ply laminates). Two models are derived, one for problems of generalized plane deformation and the other for the axisymmetric response of shells of revolution. A layer-wise approach is taken in which the stress field is assumed with an explicit dependence on the thickness coordinate in each layer. The dependence of the stress field on the thickness coordinate is determined such that the three-dimensional equilibrium equations are satisfied by the approximation. The solution domain is reduced to one dimension by integration through the thickness. Continuity of tractions and displacements between layers is imposed. The governing two-point boundary value problem is composed of a system of both differential and algebraic equations (DAE's) and their associated boundary conditions. Careful evaluation of the system of DAE's was required to arrive at form that allowed application of a one-step finite difference approximation. A two-stage Gauss implicit Runge-Kutta finite difference scheme was used for the solution because of its relatively high degree of accuracy. Patch tests of the two models revealed problems with solution accuracy for the axisymmetric model of a cylindrical shell loaded by internal pressure. Parametric studies of dropped-ply laminate characteristics and their influence on the interlaminar stresses were performed using the generalized plane deformation model. Eccentricity of the middle surface of the laminate through the ply drop-off was found to have a minimal effect on the interlaminar stresses under longitudinal compression, transverse tension, and in-plane shear. A second study found the stiffness change across the ply termination to have a much greater influence on the interlaminar stresses. Correlations between the stiffness ratio of the thick to the thin sections of the laminates and the magnitude of a parameter based on a quadratic delamination criterion were found to be surprisingly good for longitudinal compression and in-plane shear loadings. For laminates with very stiff terminated plies loaded in longitudinal compression, inclusion of a short insert of softer composite material at the end of the dropped plies was found to significantly reduce the interlaminar stresses produced. Dissert. Abstr.

N95-33463 Northwestern Univ., Chicago, IL.
ENHANCED STRESS PROJECTIONS FOR ERROR ESTIMATION AND A SINGULAR FLOATING NODE ELEMENT FOR STATIC AND DYNAMIC FRACTURE Ph.D. Thesis
Ted D. Blacker 1993 137 p
Avail: Univ. Microfilms Order No. DA9415695

This thesis presents two new developments: (1) an enhanced stress recovery method for error estimation, and (2) a new singular element for static and dynamic crack propagation. Applications of these techniques to various problems are presented. Error estimation is an essential task for adaptive analyses using the finite element method. Improvements in the recovery of derivative quantities, e.g. stress and strain, allow for a better approximation of the exact derivatives. It is shown that adding the square of the boundary condition and the equilibrium residual to both local and global stress projection substantially improves the accuracy, but not the rate of convergence. In addition, a new conjoint polynomial for interpolating the local patch stresses is presented which significantly improves the local projection scheme. Several examples are presented which show the utility of these enhancements. A sizing function which uses the estimated error for setting element size for adaptive remeshing is also presented. This sizing function is based on theoretical convergence rates and size gradient controls. The paving meshing algorithm is used to remesh the domain and adaptive iterations are performed. A new singular floating node element has been devised for numerical analysis of static fatigue crack propagation as well as rapid crack propagation in dynamic fracture. A fifth node is added to the edge of the standard 4-node quadrilateral element. This floating node remains at the crack tip as the crack propagates, providing a convenient and accurate method of unzipping the mesh during crack propagation. A variable order singularity has been added to the element. The shape function associated with the floating node can be specified with a great deal of freedom, and several choices for this function were explored. The performance of this element is demonstrated in a static crack analysis, in analysis of dynamic loading with a stationary crack, and in dynamic crack propagation. Dissert. Abstr.

N95-33468 Illinois Univ., Urbana-Champaign, IL.
THE LINEAR ELASTIC BIAXIAL RESPONSE OF PLAIN-WOVEN MESHES Ph.D. Thesis
Christopher George Kocher 1994 157 p
Avail: Univ. Microfilms Order No. DA9416385

Castigliano's second theorem is applied to determine the linear elastic constitutive response of plain-weave meshes under biaxial tension and bending. In-plane force-deflection relations are derived through examining a representative element of the mesh. The analysis includes the contributions of tension, bending, and transverse shear to the complementary energy. An experimental program was implemented to verify the energy method theory. Samples of aluminum, steel, and brass wire mesh were tested quasi-statically under uniaxial tension. The experimental results compare very well with theoretical predictions. An investigation into the nature of the stress distribution in a fiber bundle of a woven composite material was performed using a two dimensional anisotropic theory of elasticity analysis of a laminated curved beam subjected to an arbitrarily oriented in-plane load. Dissert. Abstr.

N95-33704# Los Alamos National Lab., NM.
STRESS RELAXATION IN DISCONTINUOUSLY REINFORCED COMPOSITES
N. Shi and R. J. Arsenault (Maryland Univ., College Park, MD.) 1995 12 p Presented at the Micromechanics and Constitutive Modeling of Composite Materials, Los Angeles, CA, 28-30 Jun. 1995

(Contracts W-7405-eng-36; N00014-91-J-1353)
(DE95-010928; LA-UR-95-1168; CONF-9506181-1) Avail: CASI HC A03/MF A01

It has been observed that in discontinuously-reinforced Al2O3/NiAl composites that as the reinforcement size increases the average density of dislocations generated from the relaxation of the thermal stresses increases, and the corresponding thermal residual stresses slightly decrease. Similar changes result when the reinforcement morphology changes from spheres to short fibers to continuous filaments. The changes of dislocation density and thermal residual stresses with respect to particle size are in contrast to those observed in the SiC/Al counterpart. A previously developed simple model used to explain the SiC/Al data, which was based on prismatic dislocation punching, suggested that the density of the misfit dislocations decreases when the reinforcement size increases. In this investigation, a simple model is proposed to explain the anomaly in the development of thermal residual stresses and the generation of misfit dislocations as a function of the particle size and shape in Al2O3/NiAl composites. As a result of a lack of sufficient independent-slip-systems in low symmetry materials such as NiAl, plastic relaxation of the thermal stresses is severely constrained as compared to fcc Al. As such, plastic relaxation requires collaborative slips in an aggregate of grains. This only occurs when the length scale of the varying misfit thermal stress field is much larger than the average grain size. That is, the mechanism of plastic relaxation becomes operative when the reinforcement size increases. DOE

N95-33710 Ecole Polytechnique, Montreal (Quebec).
LOW VELOCITY IMPACT DAMAGE IN CARBON FIBER/PEEK COMPOSITE LAMINATES Ph.D. Thesis
Hao Wang 1993 206 p
(ISBN-0-315-86546-6) Avail: Univ. Microfilms Order No. DANN86546

This dissertation presents both experimental and analytical investigations on the low velocity impact damage in carbon fiber/ polyetheretherketone (PEEK/Carbon) thermoplastic composite. Emphases of the study were focused on the material properties that may control the extension of impact-induced delamination and transverse crack. The Strength of Materials approach to predict the damage extension was evaluated by a dynamic finite element analysis. A fracture mechanics approach is proposed to characterize the crack growth behavior of impact-induced delamination. Prediction of the delamination size is discussed using the concept of crack arrest toughness. In the crossply laminates studied, it has been found that the thermoplastic material exhibits the same damage modes as that observed in thermoset epoxy composites. Considering the thermal residual stress and the crack constraining mechanism, extension of the transverse cracks could not be predicted by the Strength of Materials approach. On the other hand, the impact-induced delamination results from a Mode 2 dominated unstable fracture and also cannot be described by a Strength of Materials criterion. The delamination occurs under a displacement controlled condition and seems to be arrested at a constant interlaminar fracture energy. The strain energy release rate and delamination arrest toughness of the material control the delamination extension. In addition, the end-loaded-split (ELS) fracture test was conducted to measure the Mode 2 delamination toughness of PEEK/Carbon composite. Large deflection effect on toughness measurement was studied by nonlinear beam theory. Using this test to measure the Mode 2 crack arrest toughness of the material is also discussed. Dissert. Abstr.

N95-33721 Northwestern Univ., Chicago, IL.
INCLUSION MODELS OF TENSILE FRACTURE IN FIBER-REINFORCED BRITTLE-MATRIX COMPOSITES Ph.D. Thesis
Wen-Bin Tsai 1993 141 p
Avail: Univ. Microfilms Order No. DA9415827

Inclusion models of tensile fracture in fiber-reinforced brittle-matrix composites are proposed in this study. Three stages of matrix cracking including initiation of microcracks, propagation of a bridged crack and multiplication of periodic cracks are modeled using the unique approach - Eshelby's equivalent inclusion method. Moreover, the interfacial debonding may occur during matrix cracking and is taken into account by the present analysis. After interfacial debonding initiates, the fiber slides against the friction which is assumed to be constant in chapter 2 and chapter 3. However, the fiber-matrix interfaces are assumed to be Coulomb's friction controlled in chapter 4. Energy release rate and crack resistance are obtained analytically. From the fracture criterion, the equivalence of energy release rate and crack resistance, the critical applied stress is also obtained. On the critical applied stress the effects of material parameters such as interfacial frictional stress, interfacial surface energy, volume fraction of fibers, misfit strain are evaluated. These evaluations are important for the purpose of material design. Finally, it is attempted in chapter 5 to solve the crack-inhomogeneity interaction problem inhomogeneities. First, the formulation of two inhomogeneities without overlapping is derived in detail. When one of the inhomogeneities is the penny-shape crack and the other one is the ellipsoidal inhomogeneity, the interaction energy between the crack and the applied stress and the energy release rate of the crack are evaluated. Based on the framework of this chapter, one can deal with the real configuration including many inhomogeneities in the similar way. Also, the misfit strains due to thermal mismatch, phase transformation et al. can be included in the present analysis with no difficulty. Dissert. Abstr.

N95-34448 Department of the Navy, Washington, DC.
APPARATUS FOR INJECTION MOLDING HIGH-VISCOSITY MATERIALS Patent
Timothy I. Mahoney, inventor (to Navy), Kirk E. Newman, inventor (to Navy), James A. Gusack, inventor (to Navy), and George J. Sallade, inventor (to Navy) 7 Feb. 1995 15 p Filed 7 Apr. 1993
(AD-D017471; US-Patent-5,387,095; US-Patent-Appl-SN-043706; US-Patent-Class-425-145) Avail: US Patent and Trademark Office

An apparatus is introduced for injection molding highly viscous materials in which incoming high-viscosity material flows through a supply conduit and is divided into strands by splitter plates as it flows into an evacuated chamber and is degassed. When the chamber is full, the supply of high-viscosity material is interrupted and the chamber is rotated to an injecting station while another chamber swings to the degassing station for filling. At the injecting Station, a piston is lowered to engage the high-viscosity material in the first chamber, and a mold table is rotated to register a mold with a vacuum shroud and the mold is lifted into the shroud. The piston is further lowered in controlled increments to inject a quantity of high-viscosity material sufficient to fill a mold, then stop in place while the filled mold is removed and empty molds are sequentially inserted for filling. When the chamber has insufficient high-viscosity material remaining to fill another mold, the piston is retracted and the chamber is rotated back to the degassing station while the filled chamber swings to the injecting station for another cycle of loading additional molds. Flow passages for the high-viscosity material, which has a viscosity of at least about 5 kilopoise, have a minimum orifice diameter of at least about 0.5 inch. Flow stagnation and clogging of the high-viscosity material are avoided. Operations such as degassing and injecting can be separately controlled. High driving forces are avoided. Rapid, effective degassing, and enhanced production, are achieved. DTIC

N95-34620 Department of the Navy, Washington, DC.
METHOD OF INSTALLING A METALLIC THREADED INSERT IN A COMPOSITE/RUBBER PANEL Patent
Stanley J. Izdebski, inventor (to Navy) 10 Jan. 1995 5 p Filed 22 Feb. 1994
(AD-D017522; US-Patent-5,380,382; US-Patent-Appl-SN-199927; US-Patent-Class-156-91) Avail: US Patent and Trademark Office

A method of installing a metallic threaded insert in a composite/rubber panel consists of threading a first insert section into a preformed hole in a fiberglass composite panel, and bonding a rubber panel over the fiberglass composite panel. The rubber panel includes an opening which is positioned over the first insert section. A second insert section is threaded onto an elongated positioning panel bolt and then the positioning bolt is threaded into the first insert section. The second insert section is threaded downwardly on the positioning so as to be in adjacent relation to the first insert section, and the opening in the rubber panel is filled with a rubber compound. The rubber compound is cured, preferably at room temperature, to set the second insert section in position and the positioning bolt is threaded out of the first and second insert sections. DTIC

N95-34808 California Univ., Santa Barbara, CA.
FIBER COATINGS FOR BRITTLE MATRIX COMPOSITES Ph.D. Thesis
Janet Beth Davis 1993 164 p
Avail: Univ. Microfilms Order No. DA9419063

The current interest in tough, high-temperature materials has motivated fiber coatings development for ceramic matrix composites. Such coatings

are needed for controlled interface debonding and frictional sliding. The composite investigated in this study was sapphire fiber-reinforced alumina. This system is thermochemically stable for severe use conditions, exhibits little thermal expansion mismatch, and utilizes the excellent strength and creep resistance of sapphire reinforcements. A variety of coating materials was investigated with respect to their ability to satisfy thermochemical and thermomechanical properties criteria as needed for toughness improvement. Few suitable materials were found. The most promising coatings included porous oxides, a few refractory metals, and carbon. These were identified by employing a variety of analytical and mechanical testing techniques to determine the interface chemistry and structure as well as the interfacial fracture energy and sliding resistance. The results indicate that the interfacial properties can be controlled with coatings which can be eliminated from the interface subsequent to composite consolidation. However, these fugitive coatings also contribute to the high temperature strength degradation of sapphire fibers. Such degradation can be minimized by selecting appropriate composite processing conditions, but overcoming fiber strength loss remains an important issue for the use of these composites. Dissert. Abstr.

25 INORGANIC AND PHYSICAL CHEMISTRY

Includes chemical analysis, e.g., chromatography; combustion theory; electrochemistry; and photochemistry.

For related information see also *77 Thermodynamics and Statistical Physics.*.

N95-32394# Ames Lab., IA.
DEVELOPMENT OF IMPROVED p-TYPE Si-20 AT. %Ge BY ADDITION OF FULLERITE
B. A. Cook and J. L. Harringa 1994 6 p Presented at the 13th International Conference on Thermoelectrics, Kansas City, MO, 30 Aug. - 1 Sep. 1994
(Contract W-7405-eng-82)
(DE95-010230; IS-M-811; CONF-940830-3) Avail: CASI HC A02/MF A01

In a series of experiments designed to evaluate the possibility of lowering the lattice thermal conductivity of silicon-germanium alloys through the formation of an inert, intragrannular nanophase, a number of p-type Si-20 at. % Ge alloys, with a nominal doping level of 0.5 at. % boron, were prepared with varying amounts of fullerite, a mixture of 90% C60 + 10% C70 with a particle size of 0.7 nm. The alloys were synthesized by mechanical alloying (MA) and the fullerite was added at various stages of the preparation sequence. Compacts consolidated by hot pressing at temperatures of 1200 to 1265 C were found to be fully dense and homogeneous. Each compact was characterized by Hall effect at room temperature and also by electrical resistivity, Seebeck coefficient, and thermal diffusivity measurements to 1000 C. A reduction in thermal conductivity of up to 22% compared to standard p-type alloys was observed in samples containing 0.8 wt % additions. In this study, a maximum integrated average figure of merit, Z, between 300 and 1000 C of 0.65 x 10(exp -3) /C was obtained, corresponding to 0.4 wt % addition of fullerite. Observation of selected samples by transmission electron microscopy revealed that the fullerite reacted with silicon to form nanophase SiC inclusions. DOE

N95-32540# Ames Lab., IA.
SPIN COUNTING IN DIPOLAR COUPLED SPIN 1/2 SYSTEMS BY MULTIPLE QUANTUM NMR SPECTROSCOPY IN SOLIDS: DEVELOPMENT OF A SINGLE QUANTUM PROPAGATOR AND ITS APPLICATION TO HETEROGENEOUS CATALYSIS Ph.D. Thesis
S. Hwang 10 Feb. 1995 108 p
(Contract W-7405-eng-82)
(DE95-010246; IS-T-1598) Avail: CASI HC A06/MF A02

The ideas behind the development and detection of multiple quantum coherence in ensembles of dipolar coupled spin 1/2 systems are developed. An rf pulse sequence for a single quantum propagator which creates multiple quantum coherence in steps of single quanta was developed and examined for use as a tool for spin counting in solids. Experimental details concerning the manipulations necessary to produce multiple quantum NMR spectra are presented. The multiple quantum (MQ) spin counting was applied to identify reaction intermediates in heterogeneous catalysis. Spin counting was shown to yield an upper limit of n = 6 for strongly bound, rigid intermediates C(m)H(n) in the reaction of ethylene over Ru/SiO2. The results eliminated the possibility of major components of such intermediates being polymer-like coke precursors. A precursor to 2-butene such as Ru-CH2-CH(double bond)CH-CH2-Ru was proposed as one possible intermediate which is in accord with the experimental observations. Another application of multiple quantum spin counting was performed in order to characterize the local structure of silica in supported Ru/SiO2 catalysts. Cab-O-Sil HS5 used as the support in silica supported ruthenium (Ru/SiO2) catalysts was characterized via single and multiple quantum (MQ) H-1 NMR spectroscopy. The samples were studied both in the presence and the absence of ruthenium. Single quantum spin counting of protons on a silica support with and without ruthenium metal indicated that the total number of hydroxyl groups decreased significantly with increasing reduction temperature over the range of 350-530 C. Two different components shown in static H-1 NMR were found to reveal homogeneous and inhomogeneous broadening via spectral hole burning experiments. H-1 MQ-NMR spin counting, based on the number of MQ coherences observed showed the existence of small clusters of proton spins on the silica surface. DOE

N95-32557# Grambling State Univ., LA. Dept. of Physics.
NQR-NMR STUDIES OF HIGHER ALCOHOL SYNTHESIS Cu-Co CATALYSTS Final Technical Progress Report
A. N. Murty 10 Mar. 1995 53 p
(Contract DE-FG22-89PC-89761)
(DE95-010524; DOE/PC-89761/T13) Avail: CASI HC A04/MF A01

In recent years, due to the many technical advantages of using alcohol-gasoline blends, various processes for the production of higher alcohols from synthesis gas have been studied. The intent of this project is to conduct a comprehensive investigation into the nature of the electronic charge distribution in the vicinity of copper and cobalt nuclei in selected higher alcohol synthesis catalyst systems. Any strong perturbation in the orbital electronic charge distribution of Cu and Co is expected to sensitively influence both their catalytic properties and magnetic characteristics. The NMR and magnetic characterization studies undertaken in this investigation attempt to provide a better understanding of the correlation between magnetic and catalytic properties. DOE

N95-32566# Korea Cancer Center Hospital, Seoul (Republic of Korea).
DEVELOPMENT OF ULTRASENSITIVE SPECTROSCOPIC ANALYSIS TECHNOLOGY. DEVELOPMENT OF ATOMIC SPECTROSCOPY TECHNOLOGY
Hyung Ki Cha, Ky Seok Song, Young Joo Rhee, Dae Hyun Baik, Jang Soo Shin, Duck Hyun Kim, Ki Ho Yang, and Jong Hoon Yi Jul. 1994 235 p In KOREAN
(DE95-614352; KAERI/RR-1329/94) Avail: CASI HC A11/MF A03 (US Sales Only)

In this project, three principal techniques are developed. The laser photoionization spectrometry (LAPIS) is used for the ultrasensitive detection for heavy metals such as Pb and Cd. The Laser atomic fluorescence spectrometry is applied to the quantitative analysis of the lanthanide and actinide elements. And the DIAL remote sensing system is used for monitoring the ozone concentration and the atmospheric pollution. A time-of-flight mass spectrometer and a high efficient atomic beam generator were designed and manufactured. Various spectroscopic parameters and optimum analytical condition were investigated. By using the laser fluorescence technique, U, Eu and Sm in solution were quantitatively analyzed. The basic researches for the direct analytical method of solid samples were also carried out. The DIAL system for ozone remote sensing was developed and ozone concentration above Taejon were obtained. DOE

N95-32581*# Alabama Univ., Huntsville, AL. Center for Automation and Robotics.
STUDY OF THE SPACE ENVIRONMENTAL EFFECTS ON SPACECRAFT ENGINEERING MATERIALS Final Report
Susan K. OBrien, Gary L. Workman, and Guy A. Smith 1 May 1995 72 p Original contains color illustrations
(Contract NAS8-38609)
(NASA-CR-199090; NAS 1.26:199090) Avail: CASI HC A04/MF A01; 8 functional color pages

The issue of the effects of the space environment on spacecraft needs to be understood for the long term exposure of structures in space.

In order to better understand the effect of these hostile phenomena on spacecraft, several types of studies are worth performing in order to simulate at some level the effect of the environment. For example the effect of protons and electrons impacting structural materials are easily simulated through experiments using the Van de Graff and Pelletron accelerators currently housed at MSFC. Proton fluxes with energies of 700 KeV - 2.5 MeV can be generated and used to impinge on sample targets to determine the effects of the particles. Also the Environmental Effects Facility at MSFC has the capability to generate electron beams with energies from 700 KeV to 2.5 MeV. These facilities will be used in this research to simulate space environmental effects from energetic particles. Ultraviolet radiation, particularly less than 400 nm wavelength, is less well characterized at this time. The Environmental Effects Facility has a vacuum system dedicated to studying the effects of ultraviolet radiation on specific surface materials. This particular system was assembled in a previous study in order to perform a variety of experiments on materials proposed for the Space Station. That system has continued to function as planned and has been used in carrying out portions of the proposed study.

Derived from text

N95-32615 Institutet foer Vatten-Och Luftvaardsforskning, Stockholm (Sweden).

ENVIRONMENTAL EVALUATION OF LACTATES AS CLEANING AGENTS [RENGOERING MED LAKTATER: MILJOETEKNISK UTVAERDERING]

H. Carlsson, Y. A. Skoeld, S. Janhaell, P. Solyom, and K. Ancker Feb. 1995 45 p In SWAHILI

(PB95-214854; IVL-B-1160) Avail: Issuing Activity (National Technical Information Service (NTIS))

Esters of lactic acid, lactates, have been proposed as an alternative to chlorinated solvents for cleaning purposes. The critical effect from the lactates in the working environment seems to be irritation of skin and mucuos membranes. One single case of contact dermatitis caused by ethyl lactate is reported. The acute toxicity of the lactates is low. Data concerning mutagenicity, reproductive toxicity and potential to cause cancer are few for the lactates. Cleaning of metal parts was studied at one company. The staff was complaining on irritation in the air ways during short working tasks inside or very close to the wash tunnel. Computer models have been used for calculation of the photochemical ozone formation from lactates in the atmosphere. This ozone formation is low comparing with other organic solvents. The lactates have strong odors which may limit the emissions. NTIS

N95-32641# Ames Lab., IA.

THERMAL REARRANGEMENT OF OXYGEN-CONTAINING (OMICRON)-ALLYLTOLUENE DERIVATIVES M.S. Thesis - Iowa State Univ.

Fang Li 10 Feb. 1995 168 p

(Contract W-7405-eng-82)

(DE95-010124; IS-T-1721) Avail: CASI HC A08/MF A02

For several years, workers in the Trahanovsky group have been studying the gas phase thermal reactions of simple organic molecules. The FVP of (Omicron)-allyltoluene involves a novel rearrangement that is proposed to involve a diradical produced by intramolecular hydrogen-atom transfer which undergoes intramolecular coupling to give 2-methylindan. Studies of this rearrangement have been extended to other systems. The two papers in this thesis describe studies of the flash vacuum pyrolysis (FVP) of oxygen-containing (omicron)-allyltoluene derivatives. In the first chapter of this thesis, the results from o-allylbenzaldehyde and related compounds are examined in terms of the intramolecular hydrogen-atom transfer diradical/coupling mechanism. A mechanism which involves an enol intermediate generated by an oxa-1,5 H shift is proposed for formation of naphthalene from the FVP of o-allylbenzaldehyde. In the second chapter more limitations of the formation of the diradicals is revealed. DOE

N95-32671# Argonne National Lab., IL.

DETECTION OF EMISSION SOURCES USING PASSIVE-REMOTE FOURIER TRANSFORM INFRARED SPECTROSCOPY

Jack C. Demirgian, Susan M. Macha, Shauna M. Darby, and John Ditillo (Army Edgewood Arsenal, MD.) 1995 13 p Presented at the 4th International Symposium on Field Screening Methods for Hazardous Wastes and Toxic Chemicals, Las Vegas, NV, 22-24 Feb. 1995

(Contract W-31-109-eng-38)

(DE95-009920; ANL/CMT-ACL/CP-83198; CONF-950209-7) Avail: CASI HC A03/MF A01

The detection and identification of toxic chemicals released in the environment is important for public safety. Passive-remote Fourier transform infrared (FTIR) spectrometers can be used to detect these releases. Their primary advantages are their small size and ease of setup and use. Open-path FTIR spectrometers are used to detect concentrations of pollutants from a fixed frame of reference. These instruments detect plumes, but they are too large and difficult to aim to be used to track a plume to its source. Passive remote FTIR spectrometers contain an interferometer, optics, and a detector. They can be used on tripods and in some cases can be hand-held. A telescope can be added to most units. We discuss the capability of passive-remote FTIR spectrometers to detect the origin of plumes. Low concentration plumes were released using a custom-constructed vaporizer. These plumes were detected with different spectrometers from different distances. Passive-remote spectrometers were able to detect small (10 cm on a side) chemical releases at concentration-pathlengths at the low parts per million-meter (ppm-m) level. DOE

N95-32709# Sandia National Labs., Albuquerque, NM. Engineering Sciences Center.

SOLVING STIFF CHEMISTRY PROBLEMS WITH FIDAP

T. A. Baer and J. R. Torczynski 1995 16 p Presented at the Fluid Dynamics International (FIDAP) Users Conference, Chicago, IL, 30 Apr. - 2 May 1995

(Contract DE-AC04-94AL-85000)

(DE95-011053; SAND-95-0197C; CONF-9504145-1) Avail: CASI HC A03/MF A01

Stiff means high fluid-phase on surface reaction rate relative to transport rate. A method for implementing surface-only species in FIDAP has been demonstrated. The method requires no modifications to the FIDAP source code or custom subroutines but instead relies on a novel application of FIDAP commands. Although the surface species are formally treated as also existing in the fluid phase, concentrations of these species are mathematical unknowns only on the reactive surfaces, rather than throughout the fluid phase, which keeps the problem size manageable. To take full advantage of this capability, however, it is necessary to employ the full Jacobian for the chemical-reaction source terms in the solution algorithm. An implementation of the full Jacobian of chemical-reaction source terms was demonstrated. This approach allows solution of extremely stiff chemically reacting problems. However, the resultant equations are inherently cross coupled: variations of all species simultaneously affect the chemical-reaction source term portions of all the equations. This precludes solution of the system by a straightforward application of a segregated approach which may be the only practical way at present to solve large three-dimensional problems. To circumvent this difficulty, an approach was demonstrated that maintains an approximate form of the cross-species chemical coupling but permits application of a segregated approach. For problems in which convection dominates diffusion, upwinding must be employed to maintain stability. DOE

N95-32804# Florida Univ., Gainesville, FL. Quantum Theory Project.

SOLVENT EFFECTS ON THE ELECTRONIC SPECTRUM OF R HARDT'S DYE

Ricardo Bicca de Alencastro, Joaquim D. daMottaNeto, and Michael C. Zerner 18 Apr. 1995 30 p Submitted for publication in the Intern. J. Quantum Chem.

(Contract N00014-90-J-1608)

(AD-A293667; TR-25) Avail: CASI HC A03/MF A01

The extreme sensitivity of the absorption spectrum to small changes in the medium polarity has made Reichardt's dyes useful molecular probes in the study of micelle/solution interfaces and phospholipid bilayers. This work reports preliminary results of semiempirical quantum chemical calculations on some conformations of 2,6-diphenyl-(2,4,6-triphenyl-1-pyridinium)-N-phenoxide betaine (Reichardt's betaine, RB), which exhibits negative solvatochromic effects. We have used the AM1 Hamiltonian of Dewar in the geometry optimizations, and the Intermediate Neglect of Differential Overlap method parameterized for spectroscopy (INDO/S). For RB, two low lying conformations have been found. The small difference in energy between them suggests that both forms may be present in solution, an observation confirmed by calculations on the spectra using the SCRF

model: the superposition of the calculated spectra for these two forms matches the experimental spectra very well. For non-polar solvents, the general pattern consists of variation of Et(30) concurrent with variation of the dielectric constant. We have also carried out calculations for solvents which form specific (e.g. H-bond) binding to the solute, namely methanol and water, using a supermolecule approach. Our results are in excellent agreement with the experiment and present an accurate description of the spectra. DTIC

N95-32812# Technische Univ., Delft (Netherlands).
STUDY ON TURBULENT FLUCTUATIONS IN DIFFUSION FLAMES USING LASER INDUCED FLUORESCENCE Ph.D. Thesis [STUDIE VAN TURBULENTE FLUCTUATIES IN DIFFUSIEVLAMMEN MET GEBRUIK VAN LASER GEINDUCEERDE FLUORESCENTIE]
Jorrit Ernst deVries 15 Nov. 1994 263 p
(PB95-214425) Avail: CASI HC A12/MF/ A03

Even with the fastest computers of the day, detailed chemistry modelling can only be applied to turbulent flames with simple geometry, and not to flames in industrial furnaces which generally have complex geometries. The power of the laboratory scale turbulent flames we studied is about 25 kW, compared to flame powers used in industry often ranging from 100 kW to several MW. In the Heat Transfer Group, several researchers collaborate to provide a description as complete as possible of turbulent co-current nonpremixed natural gas flames produced by a burner designed in the Heat Transfer Group. In total, we investigated six flames with different conditions. The aims of this study are to provide concentration measurements, including measurements of average concentrations and of quantities describing turbulent fluctuations of the species measured. The effect of turbulence on the concentrations is studied by varying the exit velocities, and the effect of chemistry by varying the exit flow temperature. In addition, we chose to measure NO seeded to the natural gas, to study the mixing of a conserved species by shear layer turbulence. These results uncover the qualities and shortcomings of the current models of turbulent combustion. NTIS

N95-33070# Lawrence Livermore National Lab., Livermore, CA. Applied Superconductivity Group.
BACKGROUND MEETING AND TECHNOLOGY DEMONSTRATION: CHROMIUM ELECTROPLATING OF SUPERCONDUCTOR STRAND
1995 40 p Presented at the Background Meeting and Technology Demonstration: Chromium Electroplating of Superconductor Strand, Livermore, CA, 22 Feb. 1995
(Contract W-7405-eng-48)
(DE95-011736; CONF-950266) Avail: CASI HC A03/MF A01

A meeting concerned with electroplating copper onto superconducting wires was held. Topics of discussion were concerned with the market, strand cleanliness, and an improved rinsing system for the process. DOE

N95-33223# Ohio State Univ., Columbus, OH. Dept. of Physics.
TURBULENCE AND SPATIO-TEMPORAL CHAOS Final Report
C. Jayaprakash and F. Hayot 1995 30 p
(Contract DE-FG02-86ER-13916)
(DE95-012912; DOE/ER-13916/T3) Avail: CASI HC A03/MF A01

Turbulence phenomena encompass many behaviors at many scales, from chaotic behavior at small scales to coherent structures at large scales. The crucial question is how different scales interact. We have sought clues to a general answer by raising the following questions: Can a deterministic chaotic system described by a determininstic partial differential equation (the Kuramoto-Sivashinsky equation) be characterized at large scales by the same static and dynamic scaling exponents that determine a stochastic equation (the Kardar-Parisi-Zhang equation)? Through an extensive numerical study in both one and two dimensions we have concluded that truly, on large scales, the Kuramoto-Sivashinsky and Kardar-Parisi-Zhang equations belong to the same universality class. The procedure (pioneered by Zaleski) involves coarse graining in Fourier space. Through a detailed analysis of its features, and in particular the effective noise-noise correlation, we are able to comprehend the magnitudes of the physical parameters, and in particular estimate the cross-over times from free to interacting behavior. DOE

N95-33224# Colorado Univ., Boulder, CO. Dept. of Chemical Engineering.
ZEOLITE MEMBRANES FOR GAS SEPARATIONS
John Falconer and Richard Noble 1995 6 p Presented at the Natural Gas Research, Development and Demonstration Contractors Review Meeting, Baton Rouge, LA, 4-6 Apr. 1995 Sponsored in part by Chevron Research and Technology Co.
(Contract DE-FG21-90MC-27115)
(DE95-012984; DOE/MC-27115/95/C0478; CONF-950494-20) Avail: CASI HC A02/MF A01

Silicalite-1, a pure silica zeolite, was deposited on a tubular, asymmetric, (gamma)-alumina support. Single gas permeation experiments with N2, CH4, and CO2 were carried out on the membrane. Separation experiments for N2/CH4 mixtures were also conducted. Single-gas permeation of H2 and separation of H2/SF6 mixture were also carried out with the membrane. Composite membranes of silicalite and Ni-SAPO-34 were also fabricated, but no CO2/H2 selectivity was found. It is proposed to use these membranes for methanol synthesis and separation, and for separating H2 from gasification products for use as fuel cell fuel, etc. DOE

N95-33229# Swedish Inst. for Metals Research, Stockholm (Sweden).
PHASE EQUILIBRIA AND PHASE DIAGRAMS IN CARBIDE SYSTEMS
B. Uhrenius, K. Forsen, B. O. Haglund, and I. Andersson Nov. 1993 40 p
(PB95-211348; IM-3058) Avail: CASI HC A03/MF A01

Experimental data on phase equilibria in the systems Co-Ni-W-C, Fe-Ni-W-C, and Co-Ti-W-C are presented. This information involves data on the equilibria between the liquid phase at 1350 C and the tungsten carbide (WC) in the Fe-Ni-W-C system as well as on the solubility of graphite in these liquids. Information on the solubility of graphite in the Co-Ni-W-C liquid is also presented. The major part of this information has earlier been used for phase diagram evaluations made by the ThermoCalc group at the Royal Institute of Technology in Stockholm in collaboration with LTPCM-ENSEEG in Grenoble. NTIS

N95-33242# Helsinki Univ. of Technology, Espoo (Finland). Lab. of Chemical Engineering.
TESTING OF A CARPET CATALYST
Antti Pyhaelahti and Kimmo Klemola 1994 83 p
(ISSN 0358-0776)
(PB95-208492; ISBN-951-22-2343-0; Rept-24) Avail: CASI HC A05/MF A01

The report describes the experiments made with carpet type ion-exchange resin catalyst in a reactive distillation column. The principal feature of the packing is that there can be efficiently combined gas-liquid mass transfer with catalytic action necessary for certain catalytic distillation projects, e.g. the etherification with catalytic distillation. The report contains description of the equipment used and the results achieved during the runs. Three sets of experiments were done. The first set consists of four experiments in which Tert-Amyl-Methyl-Ether (TAME) was decomposed. The system is equilibrium limited and carpet type catalyst was found to be very efficient by reaction rate per catalyst mass basis. NTIS

N95-33243# Norwegian Defence Research Establishment, Kjeller (Norway).
ANALYSIS OF SAMPLES FOR THE FIRST (1994) OPCW ROUND ROBIN INTERLABORATORY COMPARISON TEST
John A. Tornes, Bjorn A. Johnsen, and Aase M. Opstad 2 Nov. 1994 32 p See also N91-32188
(Proj. FFITOX/625/138)
(PB95-210324) Avail: CASI HC A03/MF A01

The Norwegian Defense Research Establishment has participated in a Round Robin interlaboratory exercise and has analyzed samples of soil, water and decontamination liquid. Five compounds related to the Chemical Weapons Convention were identified: methylphosphonic acid, isopropyl hydrogen methylphosphonate, diisopropyl methylphosphonate, pinacolyl hydrogen methylphosphonate and n-butylphosphonic acid. The samples had been prepared by the Lawrence Livermore National Laboratory, and spiked with 500 microgram sample of methylphosphonic acid, diisopropyl methylphosphonate, pinacolyl hydrogen methylphosphonate, n-butylphosphonyl dichloride, thiodiglycol and 1,4-dithiane. Due to unexpected

rapid degradation, only a few laboratories were able to detect thiodiglycol and 1,4-dithiane. NTIS

N95-33265*# National Aeronautics and Space Administration. Lyndon B. Johnson Space Center, Houston, TX.

THIRD INTERNATIONAL WORKSHOP ON ION MOBILITY SPECTROMETRY

John H. Cross, ed. (Krug Life Sciences, Inc., Houston, TX.) Apr. 1995 337 p Proceedings of an International Speciality Conference, Galveston, TX, 16-19 Oct. 1994; sponsored by Lyndon B. Johnson Space Center and KRUG Life Sciences

(NASA-CP-3301; S-799; NAS 1.55:3301) Avail: CASI HC A15/MF A03

Basic research in ion mobility spectrometry has given rise to rapid advancement in hardware development and applications. The Third International Workshop on Ion Mobility Spectrometry (IMS) was held October 16-19, 1994, at Johnson Space Center to provide a forum for investigators to present the most recent results of both basic and applied IMS research. Presenters included manufacturers and various users, including military research organizations and drug enforcement agencies. Thirty papers were given in the following five sessions: Fundamental IMS Studies, Instrument Development, Hyphenated IMS Techniques, Applications, and Data Reduction and Signal Processing. Advances in hardware development, software development, and user applications are described. For individual titles, see N95-33266 through N95-33291.

N95-33266*# Edgewood Research Development and Engineering Center, Aberdeen Proving Ground, MD. Development and Engineering Center.

PROTON AFFINITY DETERMINATIONS AND PROTON-BOUND DIMER STRUCTURE INDICATIONS IN C2 TO C15, (ALPHA), (OMEGA)-ALKYLDIAMINES **c72**

Z. Karpas (Nuclear Research Center, Beer-Sheva, Israel.), C. S. Harden, and P. B. W. Smith (GEO-Centers, Inc., Aberdeen Proving Ground, MD.) *In* NASA. Johnson Space Center, Third International Workshop on Ion Mobility Spectrometry Apr. 1995 p 1-15 (For primary document see N95-33265 12-25)

Avail: CASI HC A03/MF A03

The 'kinetic method' was used to determine the proton affinity (PA) of a,coalkyldiamines from collision induced dissociation (CID) studies of protonated heterodimers. These PA values were consistently lower than those reported in the proton affinity scale. The apparent discrepancy was rationalized in terms of differences in the conformation of the protonated diamine monomers. The minimum energy species, formed by equilibrium proton transfer processes, have a cyclic conformation and the ion charge is shared by both amino-groups which are bridged by the proton. On the other hand, the species formed through dissociation of protonated dimers have a linear structure and the charge is localized on one of the amino-groups. Thus, the difference in the PA values obtained by both methods is a measure of the additional stability acquired by the protonated diamines through cyclization and charge delocalization. The major collision dissociation pathway of the protonated diamine monomers involved elimination of an ammonia moiety. Other reactions observed included loss of the second amino-group and several other bond cleavages. CID of the protonated dimers involved primarily formation of a protonated monomer through cleavage of the weaker hydrogen bond and subsequently loss of ammonia at higher collision energies. As observed from the CID studies, doubly charged ions were also formed from the diamines under conditions of the electrospray ionization. Author

N95-33267*# Environmental Technologies Group, Inc., Baltimore, MD.

THE EFFECTS OF CO2 ON THE NEGATIVE REACTANT IONS OF IMS

Glenn E. Spangler *In* NASA. Johnson Space Center, Third International Workshop on Ion Mobility Spectrometry Apr. 1995 p 16-33 (For primary document see N95-33265 12-25)

Avail: CASI HC A03/MF A03

In the presence of CO2, the negative reactant ions of ion mobility spectrometry (IMS) are ion clusters of CO4(-) and CO3(-). Methyl salicylate is ionized by the CO4(-)(H2O(n))(N2(m)) reactant ions, but not by the CO3(-)(H2O(n))(N2(m)) reactant ions. While the CO4(-) ions are formed by direct association, the CO3(-) ions require additional energy to be formed. The additional energy is provided by either excited neutral gas molecules in a metastable state or UV (ultraviolet) radiation. Author

N95-33268*# Montana State Univ., Bozeman, MT. Dept. of Chemistry.

FUNDAMENTAL STUDIES OF GAS PHASE IONIC REACTIONS BY ION MOBILITY SPECTROMETRY

K. Giles, W. B. Knighton, K. E. Sahlstrom, and E. P. Grimsrud *In* NASA. Johnson Space Center, Third International Workshop on Ion Mobility Spectrometry Apr. 1995 p 34-45 (For primary document see N95-33265 12-25)

Avail: CASI HC A03/MF A03

Ion mobility spectrometry (IMS) provides a promising approach to the study of gas phase ionic reactions in buffer gases at unusually high pressures. This point is illustrated here by studies of the Sn2 nucleophilic displacement reaction, Cl(-) + CH3Br yields Br + CH3Br, using IMS at atmospheric pressure. The equilibrium clustering reaction, Cl(-)(CHCl3)(n - 1) + CHCl3 yields Cl(-)(CHCl3)(n), where n = 1 and 2, and the effect of clustering on the Sn2 reaction with CH3Br have also been characterized by this IMS-based kinetic method. Present problems and anticipated improvements in the application of ion mobility spectrometry to studies of other gas phase ionic processes are discussed. Author

N95-33269*# Institut fuer Spectrochemie und Angewandte Spectroskopie, Dortmund (Germany).

DETERMINATION OF BENZENE, TOLUENE, AND XYLENE BY MEANS OF AN ION MOBILITY SPECTROMETER DEVICE USING PHOTOIONIZATION

J. W. Leonhardt, H. Bensch, D. Berger, M. Nolting (MSA, Berlin, Germany.), and J. I. Baumbach (Institut fuer Spectrochemie und Angewandte Spectroskopie, Dortmund, Germany.) *In* NASA. Johnson Space Center, Third International Workshop on Ion Mobility Spectrometry Apr. 1995 p 49-56 (For primary document see N95-33265 12-25)

Avail: CASI HC A02/MF A03

The continuous monitoring of changes on the quality of ambient air is a field of advantage of ion mobility spectrometry. Benzene, Toluene, and Xylene are substances of special interest because of their toxicity. We present an optimized drift tube for ion mobility spectrometers, which uses photo-ionization tubes to produce the ions to be analyzed. The actual version of this drift tube has a length of 45 mm, an electric field strength established within the drift tube of about 180 V/cm and a shutter-opening-time of 400 mus. With the hydrogen tube used for ionisation a mean flux of 10(exp 12) photons/sq cm s was established for the experiments described. We discuss the results of investigations on Benzene, Toluene, and Xylene in normal used gasoline SUPER. The detection limits obtained with the ion mobility spectrometer developed in co-operation are in the range of 10 ppbv in this case. Normally, charge transfer from Benzene ions to Toluene takes place. Nevertheless the simultaneous determination in mixtures is possible by a data evaluation procedure developed for this case. The interferences found between Xylene and others are rather weak. The ion mobility spectra of different concentrations of gasoline SUPER are attached as an example for the resolution and the detection limit of the instrument developed. Resolution and sensitivity of the system are well demonstrated. A hand-held portable device produced just now is to be tested for special environmental analytical problems in some industrial and scientific laboratories in Germany. Author

N95-33270*# National Aeronautics and Space Administration. Ames Research Center, Moffett Field, CA.

THE MINI-CIDEX GC/IMS: ANALYSIS OF COMETARY ICE AND DUST **c90**

Daniel R. Kojiro, Glenn C. Carle, Donald E. Humphry (Search for Extraterrestrial Intelligence Inst., Mountain View, CA.), Maxine Shao (Search for Extraterrestrial Intelligence Inst., Mountain View, CA.), and Nori Takeuchi (TMA/Norcal, Richmond, CA.) *In* NASA. Johnson Space Center, Third International Workshop on Ion Mobility Spectrometry Apr. 1995 p 57-65 (For primary document see N95-33265 12-25)

Avail: CASI HC A02/MF A03

Comets are recognized as among the most scientifically important objects in the solar system. They are presumed relics of the early primitive material in the solar nebula and are believed to have provided a general enrichment of volatiles to the inner solar system. The Cometary Coma Chemical Composition (C4) Mission, a proposed Discovery-Class Mission, will analyze materials released into the coma, providing information leading to the understanding of the chemical composition and make-up of the cometary nucleus. As one of two scientific instruments in the C4 spacecraft,

an advanced and streamlined version of the Cometary Ice and Dust Experiment (CIDEX), a mini-CIDEX, will employ an X-Ray Fluorescence (XRF) spectrometer to determine bulk elemental composition of cometary dust grains and a Gas Chromatograph/Ion Mobility Spectrometer (GC/IMS) for determination of the molecular composition of dust and ices following stepwise pyrolysis and combustion. A description of the mini-CIDEX IMS will be provided as well as data from analyses conducted using the mini-CIDEX breadboard instrument. Author

N95-33271*# Bulstrode Technology, Hempstead (England).
ENGINEERING APPROACHES AND COMPROMISES IN THE DESIGN OF SMALL ION MOBILITY SPECTROMETERS
R. F. D. Bradshaw *In* NASA. Johnson Space Center, Third International Workshop on Ion Mobility Spectrometry Apr. 1995 p 66-70 (For primary document see N95-33265 12-25)
Avail: CASI HC A01/MF A03

The engineering approaches in the design phase of small portable I.M.S.-based instruments are discussed. The choices available are described, and their effect on instrument dimensions analyzed. Possible future developments are outlined. Author

N95-33272*# Brunel Technical Coll., Bristol (England).
APPLICATION OF NI-63 PHOTO AND CORONA DISCHARGE IONIZATION FOR THE ANALYSIS OF CHEMICAL WARFARE AGENTS AND TOXIC WASTES
J. Stach, J. Adler, M. Brodacki, and H.-R. Doring *In* NASA. Johnson Space Center, Third International Workshop on Ion Mobility Spectrometry Apr. 1995 p 71-78 (For primary document see N95-33265 12-25)
Avail: CASI HC A02/MF A03

Over the past decade, advances in instrumental design and refinements in the understanding of ion molecule reactions at atmospheric pressure enabled the application of Ion Mobility Spectrometry (IMS) as a simple inexpensive and sensitive analytical method for the detection of organic trace compounds. Positive and negative gas-phase ions for ion mobility spectrometry have been produced by a variety of methods, including photo-ionization, laser multi photon ionization, surface ionization, corona discharge ionization. The most common ion source used in ion mobility spectrometry is a radioactive Ni-63 foil which is favored due to simplicity, stability, convenience, and high selectivity. If reactant ions like (H2O(n)H)(+) or (H2O(n)O2)(-) dominate in the reaction region, nearly all kinds of compounds with a given proton or electron affinity; are ionized. However, the radioactivity of the Ni-63 foil is one disadvantage of this ion source that stimulates the development and application of other ionization techniques. In this paper, we report analyses of old chemical warfare agents and toxic wastes using Bruker RAID ion mobility spectrometers. Due to the modular construction of the measuring cell, the spectrometers can be equipped with different ion sources. The combined use of Ni-63, photo- and corona discharge ionization allows the identification of different classes of chemical compounds and yields in most cases comparable results. Derived from text

N95-33273*# Revenue Canada, Ottawa (Ontario). Laboratory and Scientific Services Directorate.
IMS R AND D PROGRAM AT CANADA CUSTOMS
Pierre Pilon, Tony Mungham, Lay-Keow Ng, and Andre Lawrence *In* NASA. Johnson Space Center, Third International Workshop on Ion Mobility Spectrometry Apr. 1995 p 79-93 (For primary document see N95-33265 12-25)
Avail: CASI HC A03/MF A03

Over the last few years, Revenue Canada, in collaboration with Barringer Instruments Limited, has been involved in the development of a field-usable ion mobility spectrometer (IMS) for the detection of drugs of abuse. This work has culminated in the manufacturing and commercialization by Barringer of the Ionscan 350 instruments, now in use by various law enforcement agencies worldwide. Although IMS exhibits a very strong and distinctive response toward some nitrogen containing drugs, e.g., cocaine, like all separation techniques it has inherent limitations, namely moderate resolution and low chemical signal to noise ratio which may affect the reliability of IMS-based drug detectors. A program is in place at the Laboratory and Scientific Services Directorate (LSSD) to investigate the applicability of various digital signal processing (DSP) techniques to IMS output signals. The application of neural network techniques to overlapping IMS peaks is presented. Author

N95-33274*# Institut fuer Spectrochemie und Angewandte Spectroskopie, Dortmund (Germany).
EXCHANGE, INTERPRETATION, AND DATABASE-SEARCH OF ION MOBILITY SPECTRA SUPPORTED BY DATA FORMAT JCAMP-DX
J. I. Baumback, A. N. Davies, A. vonIrmer, and P. H. Lampen *In* NASA. Johnson Space Center, Third International Workshop on Ion Mobility Spectrometry Apr. 1995 p 94-111 (For primary document see N95-33265 12-25)
Avail: CASI HC A03/MF A03

To assist peak assignment in ion mobility spectrometry it is important to have quality reference data. The reference collection should be stored in a database system which is capable of being searched using spectral or substance information. We propose to build such a database customized for ion mobility spectra. To start off with it is important to quickly reach a critical mass of data in the collection. We wish to obtain as many spectra combined with their IMS parameters as possible. Spectra suppliers will be rewarded for their participation with access to the database. To make the data exchange between users and system administration possible, it is important to define a file format specially made for the requirements of ion mobility spectra. The format should be computer readable and flexible enough for extensive comments to be included. In this document we propose a data exchange format, and we would like you to give comments on it. For the international data exchange it is important, to have a standard data exchange format. We propose to base the definition of this format on the JCAMP-DX protocol, which was developed for the exchange of infrared spectra. This standard made by the Joint Committee on Atomic and Molecular Physical Data is of a flexible design. The aim of this paper is to adopt JCAMP-DX to the special requirements of ion mobility spectra. Author

N95-33275*# Environmental Technologies Group, Inc., Baltimore, MD.
THE PINHOLE INTERFACE FOR IMS/MS
Glenn E. Spangler *In* NASA. Johnson Space Center, Third International Workshop on Ion Mobility Spectrometry Apr. 1995 p 115-133 (For primary document see N95-33265 12-25)
Avail: CASI HC A03/MF A03

An important supplementary technique for ion mobility spectrometry (IMS) is mass spectrometry (MS). A mass spectrometer coupled to an ion mobility spectrometer (IMS/MS) can provide significant information on the composition of the ions contributing to an ion mobility peak. On the other hand, the interpretation of IMS/MS results requires knowledge of processes which can occur at the pinhole interface. When the ion composition is a mixture of ion clusters, the observed cluster distribution may not be an accurate representation of the ion clusters in the IMS. Depending on the buffer gas, lower clusters can form by equilibrating with reduced concentrations in the continuum regime of the expansion and larger clusters can form by collisional stabilization in the cooled jet stream. Besides water, nitrogen molecules can also add to the ion clusters. Even though nitrogen is non-polar, this addition is made possible by an ion-induced dipole interaction between the ion and molecule. Author

N95-33276*# Federal Bureau of Investigation, Washington, DC. Laboratory Div.
THE USE OF ION MOBILITY SPECTROMETRY AND GAS CHROMATOGRAPHY/MASS SPECTROMETRY FOR THE DETECTION OF ILLICIT DRUGS ON CLANDESTINE RECORDS
Brian Donnelly, Thomas Jourdan, Dean D. Fetterolf, and James O. Beasley, II *In* NASA. Johnson Space Center, Third International Workshop on Ion Mobility Spectrometry Apr. 1995 p 134-144 (For primary document see N95-33265 12-25)
Avail: CASI HC A03/MF A03

Illicit drug distribution has over the past decade grown tremendously from simple 'drug pushing' where drugs were distributed from poorly organized individuals to today's well organized and well financed drug cartels. This change to a more 'corporate-like' atmosphere has resulted in a greater use of record keeping to monitor the profits generated. The use of record keeping by drug distributors is not restricted to high level drug smugglers but is used at all levels within the distribution network. Dealers at all levels including street dealers are generally 'fronted', given on consignment quantities of drugs that they in turn sell to customers, thereby

requiring the need for records to keep track of drug sales versus liabilities. These records because of their illicit nature are often encrypted to hide the fact that they are indeed records of drug transactions. The creation of a handwritten notation concerning a drug transaction is normally brought on because of a purchase or sale. In a sale, this is commonly accomplished through a consignment, or the designation of a quantity to a customer to whom that amount has been 'fronted'. Because this activity generates a debt, it follows that an accounting for payments made, as well as new transactions completed, is only logical. One of the most common means of representing these is through an 'accounting flow', in which payments are subtracted from a running balance while new sales are added to it. The examination of illicit drug records has been the key to the prosecution of numerous federal, state, and local drug cases for a number of years. The Document Section of the FBI Laboratory, through its Racketeering Records Analysis Unit (RRAU), has been involved in such analytical efforts since 1983. Detailed analytical research brought about an evolution in the systematic approach utilized in the RRAU since that time. The close proximity of the drugs to the records often results in trace drug evidence being transferred to the records. The detection of trace drug residue on surfaces by ion mobility spectrometry (IMS) is well documented in literature. The following procedure will deal primarily with the newer techniques of trace drug analysis and drug record analysis developed by the Chemistry/Toxicology Unit of the FBI Laboratory since the more traditional techniques of latent finger print analysis and document analysis are well known. Derived from text

N95-33277*# Edgewood Research Development and Engineering Center, Aberdeen Proving Ground, MD. Development and Engineering Center.

HAND-PORTABLE GAS CHROMATOGRAPHY-ION MOBILITY SPECTROMETER FOR THE DETERMINATION OF THE FRESHNESS OF FISH

A. Peter Snyder, Charles S. Harden, Dennis M. Davis, Donald B. Shoff, and Waleed M. Maswadeh (GEO-Centers, Inc., Aberdeen Proving Ground, MD.) *In* NASA. Johnson Space Center, Third International Workshop on Ion Mobility Spectrometry Apr. 1995 p 146-166 (For primary document see N95-33265 12-25)

Avail: CASI HC A03/MF A03

A hand-held, portable gas chromatography-ion mobility spectrometer (GC-IMS) device was used to detect the presence of volatile amine compounds in the headspace of decomposing fish. The Food and Drug Administration (FDA) largely relies on olfactory discrimination with respect to fresh and spoiled, frozen and unfrozen fish. The fish are delivered at ship docks on pallets, and each pallet of fish can range from 30-40 thousand dollars in value. Fresh fish were placed in a teflon bag and the direct headspace was interrogated. In the first three days, only low molecular weight volatile amines were detected. On the fourth day, a number of spectral signatures were observed which indicated the presence of 1,5-diaminopentane, cadaverine. Analyses typically took from 0.5-1 minute. Author

N95-33278*# Federal Aviation Administration, Atlantic City, NJ.

GAS CHROMATOGRAPHY/ION MOBILITY SPECTROMETRY AS A HYPHENATED TECHNIQUE FOR IMPROVED EXPLOSIVES DETECTION AND ANALYSIS

Al Mercado and Paul Marsden (Science Applications International Corp., San Diego, CA.) *In* NASA. Johnson Space Center, Third International Workshop on Ion Mobility Spectrometry Apr. 1995 p 168-189 (For primary document see N95-33265 12-25)

Avail: CASI HC A03/MF A03

Ion Mobility Spectrometry (IMS) is currently being successfully applied to the problem of on-line trace detection of plastic and other explosives in airports and other facilities. The methods of sample retrieval primarily consist of batch sampling for particulate residue on a filter card for introduction into the IMS. The sample is desorbed into the IMS using air as the carrier and negative ions of the explosives are detected, some as an adduct with a reagent ion such as Cl(-). Based on studies and tests conducted by different airport authorities, this method seems to work well for low vapor pressure explosives such as RDX and PETN, as well as TNT that are highly adsorptive and can be found in nanogram quantities on contaminated surfaces. Recently, the changing terrorist threat and the adoption of new marking agents for plastic explosives has meant that the sample introduction and analysis capabilities of the IMS must be enhanced in order to keep up with other detector developments. The IMS has sufficient analytical resolution for a few threat compounds but the IMS Plasmogram becomes increasingly more difficult to interpret when the sample mixture gets more complex. Derived from text

N95-33279*# Barringer Research Ltd., Rexdale (Ontario).

ENVIRONMENT APPLICATIONS FOR ION MOBILITY SPECTROMETRY

Robert K. Ritchie and Andreas Rudolph *In* NASA. Johnson Space Center, Third International Workshop on Ion Mobility Spectrometry Apr. 1995 p 193-208 (For primary document see N95-33265 12-25)

Avail: CASI HC A03/MF A03

The detection of environmentally important polychlorinated aromatics by ion mobility spectrometry (IMS) was investigated. Single polychlorinated biphenyl (PCB) isomers (congeners) having five or more chlorine atoms were reliably detected in isooctane solution at levels of 35 ng with a Barringer IONSCAN ion mobility spectrometer operating in negative mode; limits of detection (LOD) were extrapolated to be in the low ng region. Mixtures of up to four PCB congeners, showing characteristic multiple peaks, and complex commercial mixtures of PCBs (Aroclors) were also detected. Detection of Aroclors in transformer oil was suppressed by the presence of the antioxidant BHT (2,6-di-t-butyl4-methylphenol) in the oil. The wood preservative pentachlorophenol (PCP) was easily detected in recycled wood shavings at levels of 52 ppm with the IONSCAN; the LOD was extrapolated to be in the low ppm region. Author

N95-33280*# Texas A&M Univ., Galveston, TX. Environmental Analytical Research Lab.

DIRECT ANALYSIS OF ORGANIC PRIORITY POLLUTANTS BY IMS

C. S. Giam, G. E. Reed, T. L. Holliday, L. Chang, and B. J. Rhodes *In* NASA. Johnson Space Center, Third International Workshop on Ion Mobility Spectrometry Apr. 1995 p 209-213 (For primary document see N95-33265 12-25)

Avail: CASI HC A01/MF A03

Many routine methods for monitoring of trace amounts of atmospheric organic pollutants consist of several steps. Typical steps are: (1) collection of the air sample; (2) trapping of organics from the sample; (3) extraction of the trapped organics; and (4) identification of the organics in the extract by GC (gas chromatography), HPLC (High Performance Liquid Chromatography), or MS (Mass Spectrometry). These methods are often cumbersome and time consuming. A simple and fast method for monitoring atmospheric organics using an IMS (Ion Mobility Spectrometer) is proposed. This method has a short sampling time and does not require extraction of the organics since the sample is placed directly in the IMS. The purpose of this study was to determine the responses in the IMS to organic 'priority pollutants'. Priority pollutants including representative polycyclic aromatic hydrocarbons (PAHs), phthalates, phenols, chlorinated pesticides, and polychlorinated biphenyls (PCB's) were analyzed in both the positive and negative detection mode at ambient atmospheric pressure. Detection mode and amount detected are presented. Author

N95-33281*# Graseby Dynamics Ltd., Watford (England)

AN AMMONIA MONITOR FOR THE WATER INDUSTRY

J. L. Brokenshire and C. A. Cumming *In* NASA. Johnson Space Center, Third International Workshop on Ion Mobility Spectrometry Apr. 1995 p 214-220 (For primary document see N95-33265 12-25)

Avail: CASI HC A02/MF A03

Following the emergence of the European Community as a unified trading and economic entity, the various member states are required to follow certain directives governing their social affairs. Many of these directives concern the quality of the air we breathe, and the water that we use for consumption or in industrial processes. In order to comply with these directives a major overhaul of the water industry in the UK was required. For example, in many coastal towns and resorts there has never been any formal sewage treatment since, traditionally, all waste was dumped at sea through outfall pipes. Because this is no longer acceptable, whole new treatment systems are required. Derived from text

N95-33282*# Coast Guard Research and Development Center, Groton, CT.

THE EFFECT OF SAMPLE HOLDER MATERIAL ON ION MOBILITY SPECTROMETRY REPRODUCIBILITY

J. Richard Jadamec, Chih-Wu Su, Stephen Rigdon (Analysis and Technology,

Inc., New London, CT.), and LaVan Norwood (Tectonic Technologies, Inc., Wethersfield, CT.) *In* NASA. Johnson Space Center, Third International Workshop on Ion Mobility Spectrometry Apr. 1995 p 221-228 (For primary document see N95-33265 12-25)
Avail: CASI HC A02/MF A03

When a positive detection of a narcotic occurs during the search of a vessel, a decision has to be made whether further intensive search is warranted. This decision is based in part on the results of a second sample collected from the same area. Therefore, the reproducibility of both sampling and instrumental analysis is critical in terms of justifying an in depth search. As reported at the 2nd Annual IMS Conference in Quebec City, the U.S. Coast Guard has determined that when paper is utilized as the sample desorption medium for the Barringer IONSCAN, the analytical results using standard reference samples are reproducible. A study was conducted utilizing papers of varying pore sizes and comparing their performance as a desorption material relative to the standard Barringer 50 micron Teflon. Nominal pore sizes ranged from 30 microns down to 2 microns. Results indicate that there is some peak instability in the first two to three windows during the analysis. The severity of the instability was observed to increase as the pore size of the paper is decreased. However, the observed peak instability does not create a situation that results in a decreased reliability or reproducibility in the analytical result. Author

N95-33283*# Coast Guard Research and Development Center, Groton, CT.
A NOVEL APPROACH TO INCREASING COCAINE DETECTION CONFIDENCE UTILIZING ION MOBILITY SPECTROMETRY
J. Richard Jadamec, Chih-Wu Su, Stephen Rigdon (Analysis and Technology, Inc., New London, CT.), and LaVan Norwood (Tectonic Technologies, Inc., Wethersfield, CT.) *In* NASA. Johnson Space Center, Third International Workshop on Ion Mobility Spectrometry Apr. 1995 p 229-244 (For primary document see N95-33265 12-25)
Avail: CASI HC A03/MF A03

When a positive detection of a narcotic occurs during the search of a vessel, a decision has to be made whether further intensive search is warranted. In terms of unwarranted delays of vessels and possible property damage, the accuracy of the analytical determination is very important. Analytical accuracy becomes critical when the data may be used in court actions as evidence. For this purpose, the U.S. Coast Guard has been investigating several confirmatory ion mobility spectrometry (IMS) field methods for the detection and identification of cocaine. This paper presents the findings of our investigations on the use of catalytic pyrolysis and base hydrolysis as confirmatory methods. The catalytic effects of various metals on the pyrolysis reaction are reported. In addition, the effects of several different ion mobility spectrometer sample transfer mediums and varying laboratory conditions on the base hydrolysis of the cocaine molecule are also be reported. Author

N95-33284*# Drug Enforcement Administration, National City, CA. Southwest Lab.
APPLICATION OF THE IONSCAN FOR THE DETECTION OF METHAMPHETAMINE AND EPHEDRINE IN ABONDONED CLANDESTINE LABORATORIES
Patricia A. Brown and Jeffrey H. Comparin *In* NASA. Johnson Space Center, Third International Workshop on Ion Mobility Spectrometry Apr. 1995 p 245-252 (For primary document see N95-33265 12-25)
Avail: CASI HC A02/MF A03

Clandestine methamphetamine laboratories are prevalent in southern California. The most common encountered synthesis results in vapor release, and drug residue being left behind. The suspected manufacturing area can be vacuumed and/or methanol wiped and screened immediately at the lab site using the Ionscan. Positive results are confirmed by obtaining vacuum sweep samples with subsequent analysis at the DEA Laboratory. This procedure has been utilized successfully for identifying methamphetamine and ephedrine from clandestine laboratories that have been abandoned and/or remodeled. Author

N95-33285*# Institute of Forensic Medicine, Berne (Switzerland). Dept. of Forensic Chemistry and Toxicology.
APPLICATION OF ION MOBILITY SPECTROMETRY (IMS) IN FORENSIC CHEMISTRY AND TOXICOLOGY WITH FOCUS ON BIOLOGICAL MATRICES
Werner Bernhard, Thomas Keller, and Priska Regenscheit *In* NASA. Johnson Space Center, Third International Workshop on Ion Mobility Spectrometry Apr. 1995 p 253-258 (For primary document see N95-33265 12-25)
Avail: CASI HC A02/MF A03

The IMS (Ion Mobility Spectroscopy) instrument 'Ionscan' takes advantage of the fact that trace quantities of illicit drugs are adsorbed on dust particles on clothes, in cars and on other items of evidence. The dust particles are collected on a membrane filter by a special attachment on a vacuum cleaner. The sample is then directly inserted into the spectrometer and can be analyzed immediately. We show casework applications of a forensic chemistry and toxicology laboratory. One new application of IMS in forensic chemistry is the detection of psilocybin in dried mushrooms without any further sample preparation. Author

N95-33286*# Edgewood Research Development and Engineering Center, Aberdeen Proving Ground, MD.
DATA COLLECTION IN IMS: IT'S NOT AS EASY AS IT LOOKS
Dennis M. Davis, Waleed Maswadeh (GEO-Centers, Inc., Aberdeen Proving Ground, MD.), Donald B. Shoff, Charles S. Harden, and A. Peter Snyder *In* NASA. Johnson Space Center, Third International Workshop on Ion Mobility Spectrometry Apr. 1995 p 261-273 (For primary document see N95-33265 12-25)
Avail: CASI HC A03/MF A03

Data collection in Ion Mobility Spectrometry (IMS) is not as easy an endeavor as it appears. Despite the advent of high speed personal computers and fast analog-to-digital converters (ADC's), care must be taken to ensure that reliable data are obtained in a timely fashion. This is especially true in hyphenated techniques, e.g. GC-IMS, where the amount of data increases dramatically when gas chromatography-ion mobility spectrometry (GC-IMS) data is being collected. Using the Graseby GC-IMS, with a gate repetition rate of 33 Hz, it is theoretically possible to collect 33 spectra per second. This collection rate is not realistically obtained due to a number of factors. Among these factors are inaccuracy of the timing signal from the IMS, the necessity to store the data, disk input/output limitations, disk operating system limitations, and program overhead. Taking these factors into account, we have achieved a data collection rate of 20 spectra per second. This paper will describe these problems, demonstrate the practical effects these problems present, and present methods for minimizing these effects. Author

N95-33287*# Brunel Technical Coll., Bristol (England).
IMS SOFTWARE DEVELOPMENTS FOR THE DETECTION OF CHEMICAL WARFARE AGENT
St. Klepel, U. Graefenhain, R. Lippe, J. Stach, and V. Starrock (Federal Armed Forces Defense Science, Munster, Germany.) *In* NASA. Johnson Space Center, Third International Workshop on Ion Mobility Spectrometry Apr. 1995 p 274-280 (For primary document see N95-33265 12-25)
Avail: CASI HC A02/MF A03

Interference compounds like gasoline, diesel, burning wood or fuel, etc. are presented in common battlefield situations. These compounds can cause detectors to respond as a false positive or interfere with the detector's ability to respond to target compounds such as chemical warfare agents. To ensure proper response of the ion mobility spectrometer to chemical warfare agents, two special software packages were developed and incorporated into the Bruker RAID-1. The programs suppress interferring signals caused by car exhaust or smoke gases resulting from burning materials and correct the influence of variable sample gas humidity which is important for detection and quantification of blister agents like mustard gas or lewisite. Author

N95-33288*# PCP, Inc., West Palm Beach, FL.
A DIGITAL BOXCAR INTEGRATOR FOR IMS SPECTRA
Martin J. Cohen, Robert M. Stimac, Roger F. Wernlund, and Donald C. Parker (Keystone Applications, Brooklyn, WI.) *In* NASA. Johnson Space Center, Third International Workshop on Ion Mobility Spectrometry Apr. 1995 p 281-296 (For primary document see N95-33265 12-25)
Avail: CASI HC A03/MF A03

When trying to detect or quantify a signal at or near the limit of detectability, it is invariably embeded in the noise. This statement is true for nearly all detectors of any physical phenomena and the limit of detectability, hopefully, occurs at very low signal-to-noise levels. This is

particularly true of IMS (Ion Mobility Spectrometers) spectra due to the low vapor pressure of several chemical compounds of great interest and the small currents associated with the ionic detection process. Gated Integrators and Boxcar Integrators or Averagers are designed to recover fast, repetitive analog signals. In a typical application, a time 'Gate' or 'Window' is generated, characterized by a set delay from a trigger or gate pulse and a certain width. A Gated Integrator amplifies and integrates the signal that is present during the time the gate is open, ignoring noise and interference that may be present at other times. Boxcar Integration refers to the practice of averaging the output of the Gated Integrator over many sweeps of the detector. Since any signal present during the gate will add linearly, while noise will add in a 'random walk' fashion as the square root of the number of sweeps, averaging N sweeps will improve the 'Signal-to-Noise Ratio' by a factor of the square root of N. Derived from text

N95-33289*# Graseby Dynamics Ltd., Watford (England)
SIGNAL PROCESSING FOR ION MOBILITY SPECTROMETERS
S. Taylor, M. Hinton, and R. Turner *In* NASA. Johnson Space Center, Third International Workshop on Ion Mobility Spectrometry Apr. 1995 p 297-311 (For primary document see N95-33265 12-25)
Avail: CASI HC A03/MF A03

Signal processing techniques for systems based upon Ion Mobility Spectrometry will be discussed in the light of 10 years of experience in the design of real-time IMS. Among the topics to be covered are compensation techniques for variations in the number density of the gas - the use of an internal standard (a reference peak) or pressure and temperature sensors. Sources of noise and methods for noise reduction will be discussed together with resolution limitations and the ability of deconvolution techniques to improve resolving power. The use of neural networks (either by themselves or as a component part of a processing system) will be reviewed. Author

N95-33290*# Ohio Univ., Athens, OH. Dept. of Chemistry.
QUANTITATIVE ANALYSIS OF VOLATILE ORGANIC COMPOUNDS USING ION MOBILITY SPECTRA AND CASCADE CORRELATION NEURAL NETWORKS
Peter deB. Harrington and Peng Zheng *In* NASA. Johnson Space Center, Third International Workshop on Ion Mobility Spectrometry Apr. 1995 p 312-333 (For primary document see N95-33265 12-25)
Avail: CASI HC A03/MF A03

Ion Mobility Spectrometry (IMS) is a powerful technique for trace organic analysis in the gas phase. Quantitative measurements are difficult, because IMS has a limited linear range. Factors that may affect the instrument response are pressure, temperature, and humidity. Nonlinear calibration methods, such as neural networks, may be ideally suited for IMS. Neural networks have the capability of modeling complex systems. Many neural networks suffer from long training times and overfitting. Cascade correlation neural networks train at very fast rates. They also build their own topology, that is a number of layers and number of units in each layer. By controlling the decay parameter in training neural networks, reproducible and general models may be obtained. Author

N95-33291*# Institut fuer Spectrochemie und Angewandte Spectroskopie, Dortmund (Germany).
FTP-SERVER FOR EXCHANGE, INTERPRETATION, AND DATABASE-SEARCH OF ION MOBILITY SPECTRA, LITERATURE, PREPRINTS AND SOFTWARE **c82**
J. I. Baumbach and A. vonIrmer *In* NASA. Johnson Space Center, Third International Workshop on Ion Mobility Spectrometry Apr. 1995 p A1-A4 (For primary document see N95-33265 12-25)
Avail: CASI HC A01/MF A03

To assist current discussion in the field of ion mobility spectrometry, at the Institut fur Spectrochemie und angewandte Spektroskopie, Dortmund, start with 4th of December, 1994 work of an FTP-Server, available for all research groups at univerisities, institutes and research worker in industry. We support the exchange, interpretation, and database-search of ion mobility spectra through data format JCAMP-DS (Joint Committee on Atomic and Molecular Physical Data) as well as literature retrieval, pre-print, notice, and discussion board. We describe in general lines the entrance conditions, local addresses, and main code words. For further details, a monthly news report will be prepared for all common users. Internet email address for subscribing is included in document. Author (revised)

N95-33308 Michigan Univ., Ann Arbor, MI.
IGNITION AND COMBUSTION OF CELLULOSIC DUST PARTICLES Ph.D. Thesis
Philip Joseph Austin 1994 234 p
Avail: Univ. Microfilms Order No. DA9423138

Observations of the ignition and combustion process and measurements of the ignition delay, volatile combustion, and char combustion times have been made for several hundred nearly-spherical corncob particles having diameters in the range of 100 micrometers to 2000 micrometers. Experiments were conducted in two stages using different experimental apparatuses, but similar experimental techniques. Initial experiments consisted of volatile and char combustion time measurements for nearly-spherical particles in air at a temperature of 920 K. Analysis of this data focuses on determining the relationship between the burning times and the particle diameter, and shows that the combustion times obey a d-squared law. A study of the effect of particle geometry on the burning times was also conducted using rectangular parallelepiped shaped particles. The results of this study indicate that the volatile combustion time is controlled by heat transfer to the particle. Later experiments consisted of ignition delay, volatile combustion, and char combustion time measurements for several different gas temperatures and oxygen/nitrogen mixtures. Analysis of the volatile and char burning time data focuses on determining the effect of variable particle density on the burning times, and shows that the burning times are proportional to the product of the density with the square of the particle diameter. Analysis of the ignition data focuses on determining the primary ignition mechanism, identifying the conditions for which different ignition/combustion processes occur, and determining the dependence of the ignition delay time on the particle size, particle density, gas temperature, and oxygen concentration. Observations revealed four distinct ignition/combustion processes that involve both the heterogeneous and homogeneous ignition mechanisms. Visual ignition data supports the conclusion that both homogeneous and heterogeneous primary ignition occur with a transition from homogeneous to heterogeneous primary ignition occurring as either the particle size or gas temperature is decreased. Ignition delay times are shown to increase with increasing particle diameter and decreasing gas temperature in accordance with a simple heat transfer model of the ignition process. A more sophisticated model of the ignition process of a pyrolyzing particle is also presented which is shown to agree with the experimental data. Dissert. Abstr.

N95-33328# National Chemicals Inspectorate, Solna (Sweden).
CHEMICAL SUBSTANCES LISTS: A GUIDE TO THE LISTS USED IN THE SWEDISH SUNSET PROJECT. SUPPLEMENT TO REPORT 13/94. SELECTING MULTIPROBLEM CHEMICALS FOR RISK REDUCTION. A PRESENTATION OF THE SWEDISH SUNSET PROJECT
Lars Freij, ed. Jul. 1994 194 p
(ISSN 0284-1185)
(PB95-211272; KEMI-10-94) Copyright Avail: CASI HC A09/MF A03

Many potentially hazardous chemicals are used today. It would be almost impossible to identify and assess them all - not only due to limited resources, but because it would simply take too long. Much work is being done both nationally and internationally to identify hazardous chemicals and to reduce risks connected with their use. Still much more needs to be done. A systematic selection of hazardous substances is one way to focus on the most urgent problem chemicals. Having this approach, the Sunset Project conducted by the Swedish National Chemicals Inspectorate (Kemi) is one contribution to this work. Accordingly, this report is a compilation of brief descriptions of the lists that have been included in the Sunset Project. It does not provide a complete survey of lists of substances concerned with impacts on human health and the environment. NTIS

N95-33330# National Chemicals Inspectorate, Solna (Sweden).
RISK ASSESSMENT OF POLYBROMINATED DIPHENYL ETHERS
Lars Freij, ed. Jul. 1994 53 p
(ISSN 0284-1185)
(PB95-211306; KEMI-9-94) Copyright Avail: CASI HC A04/MF A01

This report has been produced within the frame of the Flame Retardants Project at the National Chemicals Inspectorate, Sweden. The objective of the project is to reduce risks to man and the environment caused by flame retardants. The aim of the report is to provide a basis for evaluation of the need for risk reduction measures on polybrominated diphenyl ethers. NTIS

N95-33392# Rice Univ., Houston, TX.
HIGH-RESOLUTION MAGNETIC IMAGING AND INVESTIGATIONS OF THIN-FILM MAGNETISM WITH SPIN-POLARIZED ELECTRON, ION AND ATOM PROBES Progress Report, 1 Nov. 1994 - 31 Oct. 1995
G. K. Walters and F. B. Dunning Apr. 1995 3 p
(Contract DE-FG03-95ER-45531)
(DE95-012190; DOE/ER-45531/1) Avail: CASI HC A01/MF A01

This is a progress report for the period 1 November, 1994 to 31 October, 1995. Research during this grant year includes: (1) Completion of the Spin-Polarized Electron Energy Loss Spectroscopy (SPEELS) research program; (2) Design of an improved and much more intense metastable atom source that can also be converted to a Rydberg atom beam, for continuing studies utilizing Spin-Polarized Metastable (Atom) Deexcitation Spectroscopy (SPMDS), and to initiate new investigations of interactions of Rydberg atoms with surfaces; and (3) Development of a spin-polarized He(+) ion source for studies of ion-surface interaction dynamics and epitaxially grown magnetic films utilizing Spin-Polarized Ion Neutralization Spectroscopy (SPINS). DOE

N95-33414 Northwestern Univ., Chicago, IL.
TRANSVERSE ACOUSTIC PROPERTIES OF THE B-PHASE OF SUPERFLUID HELIUM THREE Ph.D. Thesis
Geneva F. Moores 1993 110 p
Avail: Univ. Microfilms Order No. DA9415784

In the past several decades, liquid helium three has been fertile ground for both theory and experiment. Nuclear magnetic resonance and ultrasound techniques have been important probes of the superfluid phases. NMR studies of (3)He-B in a strong magnetic field have shown a small frequency shift from the Larmor frequency of the normal phase. We present a theoretical calculation of this g-shift which involves the full field dependent susceptibility and order parameter in (3)He-B, and we compare the results to experiment. Studies of ultrasound in (3)He-B have focused primarily on longitudinal currents. Shear waves, or transverse current modes, are also expected to propagate in both normal and superfluid (3)He, but previous work has considered low frequency dynamics, where the mode is difficult to detect because its phase velocity is comparable to the incoherent quasiparticle background, and it disappears as the gap in the quasiparticle spectrum develops. In this thesis, a thorough examination of this mode in bulk superfluid (3)He-B is given. We show that the mode propagates with low attenuation for frequencies between the imaginary squashing mode frequency and the pair breaking edge at low temperatures where there are very few thermally excited quasiparticles. The transverse acoustic impedance is inherently dependent on the boundary conditions at the wall; we consider (3)He-B in confined geometries near specular and diffuse walls before deriving microscopic boundary conditions to model a transversely oscillating wall. Dissert. Abstr.

N95-33469 Illinois Univ., Urbana-Champaign, IL.
A QUANTUM MONTE CARLO STUDY OF THE HIGH-PRESSURE PHASES OF SOLID HYDROGEN Ph.D. Thesis
Vincent Dominic Natoli 1994 167 p
Avail: Univ. Microfilms Order No. DA9416416

Variational and diffusion Monte Carlo are powerful computational methods which can afford accurate estimates of the ground state properties of quantum many-body problems. We have applied these Monte Carlo methods to the high pressure phases of solid hydrogen to elucidate those parts of the phase diagram where experimental results are inconclusive or lacking. The method allows us to treat both electrons and protons as quantum particles by incorporating them in the trial wavefunction and avoids the Born-Oppenheimer and harmonic approximations. Our trial wavefunction uses single-body solutions from a mean-field calculation coupled with standard pair potential terms to achieve the most accurate results to date. Equally accurate results were realized for calculations in the disparate insulating molecular and metallic atomic regime. We performed a study of the possible ground state structures of the atomic metallic phase of hydrogen which identifies a new family of low energy atomic structures. Another study was done on the molecular phase over the range of pressures (40-180 GPa) where recent experiments have observed spectral discontinuities and other interesting new phenomena. Particular attention was directed to determining the equation of state and orientational ordering. We find that molecular hydrogen adopts a lower symmetry insulating structure over a wide range of pressure. The results of the atomic and molecular studies are combined to draw conclusions about the molecular-atomic transition and other details about the high pressure phase diagram. Dissert. Abstr.

N95-33627# Lawrence Livermore National Lab., Livermore, CA.
GASDYNAMIC MODEL OF TURBULENT COMBUSTION IN AN EXPLOSION
A. L. Kuhl, R. E. Ferguson (Naval Surface Warfare Center, Silver Spring, MD.), K. Y. Chien (Naval Surface Warfare Center, Silver Spring, MD.), J. P. Collins (Naval Surface Warfare Center, Silver Spring, MD.), and A. K. Oppenheim (California Univ., Berkeley. Lawrence Berkeley Lab, CA.) 31 Aug. 1994 17 p Presented at the International Conference on Combustion, Moscow, Russia, 12-17 Sep. 1994
(Contract W-7405-eng-48)
(DE95-010267; UCRL-JC-118333; CONF-9409331-1) Avail: CASI HC A03/MF A01

Proposed here is a gasdynamic model of turbulent combustion in explosions. It is used to investigate turbulent mixing aspects of afterburning found in TNT charges detonated in air. Evolution of the turbulent velocity field was calculated by a high-order Godunov solution of the gasdynamic equations. Adaptive Mesh Refinement (AMR) was used to follow convective-mixing processes on the computational grid. Combustion was then taken into account by a simplified sub-grid model, demonstrating that it was controlled by turbulent mixing. The rate of fuel consumption decayed inversely with time, and was shown to be insensitive to grid resolution. DOE

N95-33629# Oak Ridge National Lab., TN.
A BACKGROUND SUBTRACTION ROUTINE FOR ENHANCING ENERGY-FILTERED PLASMON IMAGES OF MgAl2O4 IMPLANTED WITH Al(+) AND Mg(+) IONS
N. D. Evans, E. A. Kenik, J. Bentley, and S. J. Zinkle 1995 3 p Presented at the 29th Annual Meeting of the Microbeam Analysis Society, Breckenridge, CO, 6-11 Aug. 1995 Prepared in cooperation with Oak Ridge Inst. for Science and Education, TN
(Contracts DE-AC05-84OR-21400; DE-AC05-76OR-00033)
(DE95-012850; CONF-950865-2) Avail: CASI HC A01/MF A01

MgAl2O4, a candidate fusion reactor material, was irradiated with Al(+) or Mg(+) ions to assess the effects of high-dose irradation. Electron energy-loss spectra and energy-filtered plasmon images showed that metallic Al colloids are present in the ion-irradiated regions. This paper shows the subtraction of the spinel plasmon component in images using 15-eV-loss electrons in some detail. DOE

N95-33634# National Chemicals Inspectorate, Solna (Sweden).
SENSITIZING SUBSTANCES
Brita Oredsson and Lars Freij, ed. Feb. 1993 58 p
(ISSN 0284-1185)
(PB95-211256; KEMI-3-93) Copyright Avail: CASI HC A04/MF A01

The aim of the report is to present the basis for classification of a number of sensitizing substances. In part 1, evaluations regarding the sensitizing properties of twelve substances are presented. Four of them have been evaluated with regard to sensitization by inhalation and the remaining eight substances with regard to sensitization by skin contact. The substances are concluded to meet the criteria of the National Chemicals Inspectorate of allergic substances, which is the basis for classification. In part 2, some data regarding the sensitizing properties of eleven substances are presented (in Swedish). Complete evaluations have not been made. NTIS

N95-33705# Babcock and Wilcox Co., Alliance, OH. Research and Development Div.
DEVELOPMENT OF A PROTOTYPE LIGNIN CONCENTRATION SENSOR Final Report
Larry A. Jeffers Nov. 1994 206 p
(Contract DE-FC05-90CE-40905)
(DE95-010951; DOE/CE-40905/57) Avail: CASI HC A10/MF A03

The workscope covered in this report is the first step toward the development of an instrument for the on-line measurement of lignin concentration in wood pulp. This first-step program consisted of a series of laboratory measurements of the fluorescence spectra of well-defined pulp samples. The objective of the program was to develop the data base

necessary to design a field-testable prototype instrument, to define the range of conditions over which the prototype can be expected to provide satisfactory performance, and to provide the background for interpretation of the results obtained when field testing the prototype. DOE

N95-33832# Pacific Northwest Lab., Richland, WA.
THE DEVELOPMENT OF A LARGE-AREA CHEMICAL SENSOR: A NEW PLATFORM FOR SELECTIVE COATINGS
M. Bliss Apr. 1995 5 p
(Contract DE-AC06-76RL-01830)
(DE95-011489; PNL-SA-26144) Avail: CASI HC A01/MF A01

A new chemical sensor is described which applies multiple phenomena to identify and measure the concentration of selectively sorbed molecules in an optical fiber cladding. In addition, the sensor can be manufactured at the rate of several thousand meters per hour. Only a few meters are needed for calibrations and testing, leaving thousands of meters of calibrated sensor for use. The method employs absorption or Raman spectroscopy for verification and quantification. Incorporating various selective materials into the cladding enables the sensor to be used for a variety of chemicals such as various pollutants or chemicals from chemical weapons. Organic phosphates and iodine have been identified as two important classes of compounds related to nuclear weapons proliferation issues. DOE

N95-34021# Lehigh Univ., Bethlehem, PA. Zettlemoyer Center for Surface Studies and Dept. of Chemistry.
SELECTIVE METHANE OXIDATION OVER PROMOTED OXIDE CATALYSTS
Kamil Klier and Richard G. Herman 1995 20 p Presented at the Natural Gas Research, Development and Demonstration Contractors Review Meeting, Baton Rouge, LA, 4-6 Apr. 1995; cosponsored by the Morgantown Energy Technology Center and Southern Univ. and Agricultural and Mechanical Coll.
(Contract DE-FG21-92MC-29228)
(DE95-012319; DOE/MC-29228/95/C0462; CONF-950494-12) Avail: CASI HC A03/MF A01

Principal accomplishments have been achieved in all three areas of selective catalytic oxidation of methane that have been pursued in this research project. These accomplishments are centered on the development of catalyst systems that produce high space time yields of C(sub 2) hydrocarbon products, formaldehyde, and methanol from methane/air mixtures at moderate temperatures and at ambient pressure. The accomplishments can be summarized as the following: the SO4(sup 2-)/SrO/La2O3 catalyst developed here has been further optimized to produce 2 kg of C(sub 2) hydrocarbons/kg catalyst/hr at 550 C; V2O5/SiO2 catalysts have been prepared that produce up to 1.5 kg formaldehyde/kg catalyst/hr at 630 C with CO2 selectivities; and a novel dual bed catalyst system has been designed and tested that produces over 100 g methanol/kg catalyst/hr at 600 C. DOE

N95-34268 California Univ., Berkeley. Lawrence Berkeley Lab, CA. Materials and Chemical Sciences Div.
FUNDAMENTAL STUDIES OF THE MECHANISM OF CATALYTIC REACTIONS WITH CATALYSTS EFFECTIVE IN THE GASIFICATION OF CARBON SOLIDS AND THE OXIDATIVE COUPLING OF METHANE Quarterly Report, 1 Jul. 1994 - 30 Sep. 1994
E. Iglesia, D. L. Perry, and H. Heinemann Sep. 1994 17 p Limited Reproducibility: More than 20% of this document may be affected by microfiche quality
(Contract DE-AC03-76SF-00098)
(DE95-012759; LBL-37027; UC-109) Avail: CASI HC A03

Research continued on the study of catalysts and membrane materials involved in the oxidative coupling of methane and coal gasification processes. Membranes studied and fabricated included Sr-Zr-Y-O, Sr-Zr-Y, and Sr-Ce-Y-O systems. DOE

N95-34287 Department of the Navy, Washington, DC.
ENCAPSULATED DRY ELECTROLYTE COMPOSITION FOR TIME RELEASE INTO A SOLUTE Patent
Andrew V. Smith, inventor (to Navy) 21 Mar. 1995 4 p Filed 30 Sep. 1993
(AD-D017485; US-Patent-5,399,444; US-Patent-Appl-SN-129728; US-Patent-Class-429-70) Avail: US Patent and Trademark Office

A device for delivering a water soluble electrolyte is provided comprising a core of a solid electrolyte composition enclosed by a polymeric coating which is permeable to water. The coating has at least one hole to permit passage of an aqueous solution of the electrolyte. The device is useful to maintain the concentration of an electrolyte composition in an electrochemical apparatus such as a fuel cell or a battery. DTIC

N95-34357# Utah Univ., Salt Lake City, UT.
NATURAL CONVECTION AT MICROELECTRODES
Xiaoping Gao, Jeonghee Lee, and Henry S. White 31 Mar. 1995 21 p
(Contract N00014-94-I-0323)
(AD-A294338; TR-5) Avail: CASI HC A03/MF A01

Steady-state voltammetric currents for Fe(CN)6(-4) oxidation and Fe(CN)6(-3) reduction in 0.2 M KCl solutions are shown to be a function of the orientation of Au and Pt microdisk electrodes (radius = 6.4 to 25 micrometers) with respect to the gravitational field. The observed angular dependencies for the Fe(CN)6(-3/-4) couple are in agreement with theoretical expectations based on electrochemically-generated fluid density gradients within the depletion layer. The results demonstrate that steady-state voltammetric currents measured at microelectrodes are comprised of both diffusional and natural convection mass-transfer fluxes. At 25 micrometers-radius microdisks, natural convection accounts for between 2 and 13% of the total current for redox concentrations between 10 and 500 mM, respectively. The contribution of mass-transfer due to natural convection is shown to rapidly decrease with decreasing electrode size. DTIC

N95-34440# Argonne National Lab., Idaho Falls, ID. Analytical Lab.
ANALYSIS OF METALLIC FUELS BY LASER ABLATION
S. G. Johnson, P. S. Goodall, E. L. Wood, and S. M. Kimbrell (Alaska Univ., Fairbanks, AK.) 1995 11 p Presented at the Photonics West 1995: Advanced Optical Methods for Ultrasensitive Detection, San Jose, CA, 4-10 Feb. 1995
(Contract W-31-109-eng-38)
(DE95-012465; ANL/FE/CP-83609; CONF-950226-50) Avail: CASI HC A03/MF A01

A hot cell-based solid sampling system has been developed for application to the analyses of irradiated materials such as metallic reactor fuel from a nuclear reactor, and radioactive waste forms. This system employs one of two sampling techniques, glow discharge or laser ablation, for introduction of material into one of two instruments for analysis, either a time of flight mass spectrometer or an inductively coupled argon plasma-atomic emission spectrometer (ICP-AES). This paper discusses using ICP-AES for the analysis of major, minor and trace constituents in an unirradiated U-10 wt % Zr metallic reactor fuel. The behavior of highly refractory elements, such as Zr, in the laser ablation process is examined in detail. Additional corroborative data provided via scanning electron microscopy-energy dispersive x-ray fluorescence spectroscopy (SEM-EDS) is presented. DOE

N95-34483# Northwestern Univ., Evanston, IL. Dept. of Physics and Astronomy.
METAL-CERAMIC INTERFACES: OVERLAYER-INDUCED RECONSTRUCTION AND MAGNETISM OF 4d TRANSITION-METAL MONOLAYERS
Ruqian Wu and A. J. Freeman 15 Feb. 1995 4 p Repr. from Physical Review B (Evanston, IL), v. 51, no. 8, 15 Feb. 1995
(Contract DE-FG02-88ER-45372)
(DE95-011543; DOE/ER-45372-8) Avail: CASI HC A01/MF A01

Structural, electronic, and magnetic properties of metal-ceramic interfaces, M/MgO(001) (M = Pd, Rh,and Ru), have been investigated using the full potential linearized augmented-plane-wave method. Ru and Rh monolayers are found to be able to retain large spin magnetic moments on MgO(001) (1.95 mu(sub B) and 1.21 mu(sub B) for Ru and Rh, respectively) -- indicating, in principle, the potential application of MgO(001) as a benign substrate for 4d monolayer magnetism. Significantly, according to our atomic-force determinations, the metal overlayers induce a sizable buckling reconstruction in the interfacial MgO layer, which enhances the M-MgO binding energy by 0.1 eV. The weak M-O interaction is mainly via tail effects; however, it affects the density of states at the Fermi level for Pd/MgO(001) significantly and completely eliminates the small magnetic moment of the free Pd monolayer (0.34 mu(sub B)). DOE

N95-34599# Army Research Lab., Aberdeen Proving Ground, MD.
THE RELATIONSHIP OF CHEMICAL STRUCTURE TO SUPERCRITICAL-FLUID SOLUBILITY AND TO COSOLVENT-MODIFIER PROPERTIES: A LITERATURE REVIEW Final Report, Sep. 1992 - Sep. 1994
M. A. Schroeder, R. A. Fifer, and J. B. Morris Jun. 1995 70 p
(AD-A294933; ARL-TR-745) Avail: CASI HC A04/MF A01

This report describes a literature review on solubility and cosolvent effects in supercritical fluid extraction (SFE). A cosolvent modifier is a second solvent that is added, usually in small (less than 10%) amounts, to a supercritical solvent to enhance the solubility of a solute in that solvent. In general, nonpolar solvents such as ethane tend to most efficiently dissolve nonpolar solutes such as hydrocarbons, while more polar solvents such as CHF3 tend to most efficiently dissolve more polar solutes. Supercritical carbon dioxide (SF-CO2) is a fairly good general solvent. With regard to cosolvent effects, the main correlation seems to be that in order for addition of a given cosolvent to cause a large increase in the solubility of a given solute, there should be a specific interaction (e.g., hydrogen bonding, charge transfer, dipole-dipole interaction, etc.) between the solute and the cosolvent involved. The behavior of HMX and RDX in supercritical fluid chromatography (SFC) and SFE behavior are also summarized. Finally, some suggestions are made as to possible ways of enhancing the extractability of HMX and RDX in supercritical solvents. DTIC

N95-34611# Defence Research Establishment Suffield, Ralston (Alberta).
HIGH RESOLUTION ELECTROSPRAY MASS SPECTROMETRY WITH A MAGNETIC SECTOR INSTRUMENT: ACCURATE MASS MEASUREMENT AND PEPTIDE SEQUENCING
P. A. DAgostino, J. R. Hancock, L. R. Provost, P. D. Semchuk (Alberta Univ., Edmonton, Alberta.), and R. S. Hodges (Alberta Univ., Edmonton, Alberta.) Jan. 1995 38 p
(AD-A293564; DRES-SR-622) Avail: CASI HC A03/MF A01

The accurate molecular weights for a series of thirty-eight unknown synthetic peptides used in research studies involving synthetic vaccines, antibacterial peptides, or the de novo design of helical peptides and proteins were determined with a magnetic sector instrument. All data were obtained with external calibration over a wide mass range during magnetic scanning. Errors between observed and theoretical monoisotopic molecular weights were typically in the 5 to 60 ppm range for the unknowns at sector resolutions between 2500 and 9000 (10% valley). Isotopic clusters for charge states up to +10 were resolved through the use of high sector resolution. Collisional activated dissociation in the electrospray interface afforded production of product ions that enabled either full or partial sequencing of most unknown peptides below 2000 Da. The complete primary sequence for one peptide was determined and the importance of high resolution was demonstrated by the differentiation of lysine from glutamine, two amino acids differing in residue mass by only 0.0364 Da. Two other peptides, with identical monoisotopic masses, but different primary sequences, were differentiated based on their collisional activated dissociation mass spectrometry (CAD/MS) data. DTIC

N95-34615# Minnesota Univ., Minneapolis, MN. Dept. of Chemical Engineering and Material Science.
SI-DEVICE-RELATED INTERFACE RESEARCH Final Report
John H. Weaver 31 Dec. 1994 7 p
(Contract N00014-92-J-1492)
(AD-A293587) Avail: CASI HC A02/MF A01

This program aimed at understanding some of the key materials issues relevant to electronic-device miniaturization. In particular, it focused on understanding atomic scale processes that occur during oxidation and etching of Si surfaces. We used scanning tunneling microscopy to obtain sub-nanometer resolution of the surface structure and photoelectron spectroscopy to obtain chemical information. The initial stages of the project focused on the oxidation of Si(100) with H2O. Subsequent investigations emphasized the interactions of Si(100) with halogen molecules, with parallel investigations of halogen etching of GaAs(110). DTIC

N95-34810# Sun Co., Inc., Marcus Hook, PA. Research and Development Dept.
CATALYTIC CONVERSION OF LIGHT ALKANES: PROOF OF CONCEPT STAGE
James E. Lyons 1995 13 p Presented at the Natural Gas Research, Development and Demonstration Contractors Review Meeting, Baton Rouge, LA, 4-6 Apr. 1995 Sponsored by DOE, the Morgantown Energy Technology Center, and Southern Univ. and Agricultural and Mechanical Coll.
(Contract DE-FC21-90MC-26029)
(DE95-012318; DOE/MC-26029-95-C0461; CONF-950494-14) Avail: CASI HC A03/MF A01

During the stage at which this work ended, our program consisted of two phases which were running concurrently, a research phase and a proof-of-concept phase. The function of the research phase is to design synthesize and perform laboratory tests on new materials in order to enhance the catalytic properties of the suprabiotic systems generated in our laboratories. Increases in catalytic activity and process selectivity as well as extensions of structure-activity relationships are examined. The research phase is intended to provide the process development phases with catalysts having superior properties for light alkane oxidation. The second concurrent phase, is the proof-of-concept phase. In this phase process development of oxidations which have succeeded in the research phase are carried out in a pre-pilot PDU. At the conclusion of the cooperative agreement we were developing a process for the conversion of isobutane to (TBA), We have identified two routes for this transformation: a one-step route directly from isobutane to TBA, and a two-step route in which the isobutane is oxidized first to tert-butyl hydroperoxide and then transformed into TBA catalytically. This paper presents the results of these activities. DOE

N95-34814# Naval Medical Research Inst., Bethesda, MD.
DENSITY, HEAT CAPACITY, VISCOSITY, AND THERMAL CONDUCTIVITY OF MIXTURES OF CO2, He, H2, H2O, N2, AND O2 Technical Report, Oct. 1991 - Jul. 1994
L. D. Homer and S. R. Kayar Jul. 1994 26 p
(NMRDC Proj. MR0-4101)
(AD-A288731; NMRI-94-51) Avail: CASI HC A03/MF A01

The thermodynamic properties of gas mixtures are not always well approximated by the average properties of pure gases weighted by the fractional composition. In order to improve our calculations we have turned to the literature to find formulas said to be useful for calculating the properties of mixtures in the range of temperatures and pressures encountered in human diving. Very little has been published on experimental determinations of properties of mixtures, so we have sought principally to verify that the formulas for mixtures give a good match to data on pure gases. In order to match data on pure gases, the values for the critical temperature (TC) and the critical pressure (PC) for H2 and He were modified. In addition, ad-hoc adjustments have been made to the critical volumes (VC) to make viscosity at low pressures match tables for these two gases. Omega, the acentric factor in the formulas, is taken as zero for all gases. The properties for which we have subroutines are thermal conductivity in watts/meter x degree/ K, viscosity micro poise, density in moles/cu cm, heat capacity in Joules/mole x degree /K, and the vapor pressure of water in torr. DTIC

N95-34509# Tokyo Univ. (Japan).
DSMC METHOD APPLIED FOR REACTING GAS FLOWS Abstract Only
Shigeo Obata and Toshio Nagashima *In* National Aerospace Lab., Special Publication of National Aerospace Laboratory 16 Jun. 1994 p 63-68 In JAPANESE (For primary document see N95-34505 12-02)
Avail: CASI HC A02/MF A03

N95-34510# Saitama Univ., Urawa (Japan). Dept. of Mechanical Engineering.
NUMERICAL STUDY ON STABILIZATION OF A DIFFUSION FLAME OVER A FLAT PLATE
Xiao Wang, Shigeharu Ohyagi, and Tri Agung Rohmat *In* National Aerospace Lab., Special Publication of National Aerospace Laboratory 16 Jun. 1994 p 69-73 (For primary document see N95-34505 12-02)
Avail: CASI HC A01/MF A03

26 METALLIC MATERIALS

Includes physical, chemical, and mechanical properties of metals, e.g., corrosion; and metallurgy.

N95-32382# Sandia National Labs., Albuquerque, NM.
MODELS FOR PREDICTING DAMAGE EVOLUTION IN METAL MATRIX COMPOSITES SUBJECTED TO CYCLIC LOADING
D. H. Allen, L. D. Hurtado, and K. L. E. Helms (Texas A&M Univ., College Station, TX.) 1995 7 p Presented at the International Conference on Computational Engineering Science, Mauna Lani, HI, 30 Jul. - 3 Aug. 1995
(Contract DE-AC04-94AL-85000)
(DE95-007734; SAND-95-0351C; CONF-950788-6) Avail: CASI HC A02/MF A01

A thermomechanical analysis of a continuous fiber metal matrix composite (MMC) subjected to cyclic loading is performed herein. The analysis includes the effects of processing induced residual thermal stresses, matrix inelasticity, and interface cracking. Due to these complexities, the analysis is performed computationally using the finite element method. Matrix inelasticity is modelled with a rate dependent viscoplasticity model. Interface fracture is modelled by the use of a nonlinear interface constitutive model. The problem formulation is summarized, and results are given for a four-ply unidirectional SCS-6/(beta)21S titanium composite under high temperature isothermal mechanical fatigue. Results indicate rate dependent viscoplasticity can be a significant mechanism for dissipating the energy available for damage propagation, thus contributing to improved ductility of the composite. Results also indicate that the model may be useful for inclusion in life prediction methodologies for MMC's. DOE

N95-32400# Oak Ridge National Lab., TN. Metals and Ceramics Div.
STRENGTH, DUCTILITY, AND FRACTURE MODE OF TERNARY FeAl ALLOYS
J. H. Schneibel, E. P. George, E. D. Specht, and J. A. Horton 1994 6 p Presented at the 1994 Fall Meeting of the Materials Research Society (MRS), Boston, MA, 28 Nov. - 2 Dec. 1994
(Contract DE-AC05-84OR-21400)
(DE95-010281; CONF-941144-125) Avail: CASI HC A02/MF A01

The iron aluminides Fe-45Al-5X-0.2B-0.1Zr (at. %), where X stands for the first row transition metals Ti, V, Cr, Mn, Fe, Co, Ni, Cu, were examined at room temperature for strength, ductility, environmental sensitivity, and fracture mode. The extruded materials were annealed at 1273 K to produce similar grain sizes and then at 673 K to reduce the quenched-in vacancies. All alloys were essentially single phase. Their solid-solution strengthening was found to correlate with the atomic size misfit from the lattice parameters. The 'binary' alloy Fe-45Al-0.2B-0.1Zr exhibited predominantly transgranular fracture. Ternary alloying additions with atomic numbers less than that of Fe tended to enhance intergranular fracture, whereas those with atomic numbers higher than that of Fe favored substantial amounts of transgranular fracture. Tensile testing in a partial pressure of dry oxygen increased the ductilities of the ternary alloys only slightly, whereas the ductility of the binary alloy increased from about 8 to about 19%. The ductilities in air correlated inversely with the yield strength. However, those alloys exhibiting substantial amounts of transgranular fracture always showed higher ductilities than those fracturing intergranularly. The fracture results are interpreted in terms of yield strengths and ternary element site occupations. DOE

N95-32474# Carnegie-Mellon Univ., Pittsburgh, PA.
METALLURGICAL AND MATERIALS TRANSACTIONS, VOLUME 25A, NO. 9
Sep. 1994 277 p Repr. from Metallurgical and Materials Transactions (Pittsburgh, PA), v. 25A, no. 9, Sep. 1994 p 1781-2068
(Contract N00014-93-1-0026)
(AD-A293622) Avail: CASI HC A13/MF A03

METALLURGICAL AND MATERIALS TRANSACTIONS publishes contributions on all aspects of research and significant engineering advances in materials science and metallurgy. Metallurgical and Materials Transactions-A publishes contributions on all aspects of physical metallurgy and materials science, with a special emphasis on relationships among the processing, structure, and properties of materials. DTIC

N95-32527# Oak Ridge National Lab., TN.
EFFECT OF HEAT TREATMENT AT 1,150 C ON CREEP RUPTURE PROPERTIES OF A Fe3Al-BASED ALLOY
C. G. McKamey, P. J. Maziasz, and Y. Marrero-Santos (Emilio R. Delgado High School, Corozal, Puerto Rico.) 1994 7 p Presented at the 1994 Fall Meeting of the Materials Research Society (MRS), Boston, MA, 28 Nov. - 2 Dec. 1994
(Contract DE-AC05-84OR-21400)
(DE95-010295; CONF-941144-142) Avail: CASI HC A02/MF A01

The effects of heat treatment at 1,150 C on the creep-rupture properties of a Fe3Al-based alloy were studied. Tests were conducted in air using various test temperatures and stresses. By plotting the data to a power-law equation, the activation energy for creep was determined to be approximately 150 kcal/mole and the creep exponent to be about 8. Optical metallography and scanning electron microscopy of ruptured specimens indicated that failure was in a ductile manner by microvoid coalescence at grain boundaries and triple points. Analytical electron microscopy was used to study characteristics of the microstructure and to identify Zr-rich precipitates that formed during heat treatment or creep testing. These precipitates were found to provide strengthening by pinning dislocations and grain boundaries. DOE

N95-32531# Japan Atomic Energy Research Inst., Tokyo (Japan).
IRRADIATION EXPERIMENTS OF LOW COPPER A533B STEELS FOR REACTOR PRESSURE VESSEL TESTED IN JMTR
Masahide Suzuki, Kunio Onizawa, and Minoru Kizaki (Japan Atomic Energy Research Inst., Ibaraki, Japan.) Sep. 1994 79 p
(DE95-737266; JAERI-Research-94-015) Avail: CASI HC A05/MF A01

Irradiation embrittlement of A533B steels with low copper contents was investigated from the point of dose rate and irradiation temperature effects. Changes of neutron flux in the range from approximately 10(exp 12) to approximately 10(exp 13) n/sq cm/s (E greater than 1 MeV) did not have a significant effect on the embrittlement. Irradiation temperature change of 1 C resulted in the transition temperature shift (Delta T(41J)) of about 1 C and yield stress change (Delta sigma(y)) of about 0.8 MPa. Factors that might affect the embrittlement of low copper steels are also discussed. DOE

N95-32555# Pacific Northwest Lab., Richland, WA.
IRRADIATION-ASSISTED STRESS CORROSION CRACKING CONSIDERATIONS AT TEMPERATURES BELOW 288 C
E. P. Simonen, R. H. Jones, and S. M. Bruemmer Mar. 1995 15 p Presented at the Corrosion 1995: National Association of Corrosion Engineers (NACE) International Annual Conference and Corrosion Show, Orlando, FL, 26-31 Mar. 1995
(Contract DE-AC06-76RL-01830)
(DE95-008940; PNL-SA-25506; CONF-950304-14) Avail: CASI HC A03/MF A01

Irradiation-assisted stress corrosion cracking (IASCC) occurs above a critical neutron fluence in light-water reactor (LWR) water environments at 288 C, but very little information exists to indicate susceptibility as temperatures are reduced. Potential low-temperature behavior is assessed based on the temperature dependencies of intergranular (IG) SCC in the absence of irradiation, radiation-induced segregation (RIS) at grain boundaries and micromechanical deformation mechanisms. IGSCC of sensitized SS in the absence of irradiation exhibits high growth rates at temperatures down to 200 C under conditions of anodic dissolution control, while analysis of hydrogen-induced cracking suggests a peak crack growth rate near 100 C. Hence from environmental considerations, IASCC susceptibility appears to remain likely as water temperatures are decreased. Irradiation experiments and model predictions indicate that RIS also persists to low temperatures. Chromium depletion may be significant at temperatures below 100 C for irradiation doses greater than 10 displacements per atom (dpa). Macromechanical effects of irradiation on strength and ductility are not strongly dependent on temperature below 288 C. However, temperature does significantly affect radiation effects on SS microstructure and micromechanical deformation mechanisms. The critical conditions for material susceptibility to IASCC at low temperatures may be controlled by radiation-induced grain boundary microchemistry, strain localization due to irradiation microstructure and irradiation creep processes. DOE

N95-32591# Sandia National Labs., Albuquerque, NM.
INTERMETALLIC COMPOUND LAYER GROWTH KINETICS IN NON-LEAD BEARING SOLDERS
P. T. Vianco, A. C. Kilgo, and R. Grant 1995 18 p Presented at the ECM 1995 Conference, Las Cruces, NM, 12-15 Mar. 1995
(Contract DE-AC04-94AL-85000)
(DE95-009595; SAND-95-0573C; CONF-9503119-2) Avail: CASI HC A03/MF A01

The introduction of alternative, non-lead bearing solders into electronic assemblies requires a thorough investigation of product manufacturability and reliability. Both of these attributes can be impacted by the excessive growth of intermetallic compound (IMC) layers at the solder/substrate interface. An extensive study has documented the stoichiometry and solid state growth kinetics of IMC layers formed between copper and the lead-free solders: 96.5Sn-3.5Ag (wt.%), 95Sn-5Sb, 100Sn, and 58Bi-42Sn. Aging temperatures were 70-205 C for the Sn-based solders and 55-120 C for the Bi-rich solder. Time periods were 1-400 days for all of the alloys. The Sn/Cu, Sn-Ag/Cu, and Sn-Sb/Cu IMC layers exhibited sub-layers of Cu6Sn5 and Cu3Sn; the latter composition was present only following prolonged aging times or higher temperatures. The total layer growth exhibited a time exponent of n = 0.5 at low temperatures and a value of n = 0.42 at higher temperatures in each of the solder/Cu systems. Similar growth kinetics were observed with the low temperature 58Bi-42Sn solder; however, a considerably more complex sub-layer structure was observed. The kinetic data will be discussed with respect to predicting IMC layer growth based upon solder composition. DOE

N95-32614 National Defence Research Establishment, Stockholm (Sweden). Avdelningen foer Styrning, Material och Undervattenssensorer.
FATIGUE PROPERTIES FOR THE Al-Li ALLOY 2090, PART 3 [UTMATTNINGSEGENSKAPER FOER AL-LI-LEGERINGEN 2090, DEL 3]
C. Bratt and J. Erikson Nov. 1994 19 p In SWAHILI See also PB91-224236
(PB95-214532; F0A-R-94-00052-2.5-SE-Pt-3) Avail: Issuing Activity (National Technical Information Service (NTIS))

Static mechanical properties and fatigue crack propagation behavior for the Al-Li alloy 2090-T84 have been investigated at three temperatures, -50, +20 och + 75 C. For the static properties no significant difference can be seen between the three temperatures, although some evidence is seen for higher failure and yield strength at 50 C compared to room temperature. The fatigue crack propagation behavior is better, lower crack propagation rate (da/dN), higher fatigue threshold (delta K(sub th)) and higher fracture toughness (K(sub)), at -50 C compared to room temperature. At increased temperature (+75 C) the fatigue crack behavior is the same as at room temperature. NTIS

N95-32626# Joint Inst. for Nuclear Research, Dubna (USSR). Lab. of Nuclear Reactions.
ABOUT THE MECHANISM OF HEAVY ION RADIATION INFLUENCE ON THE METALS AT HIGH TEMPERATURE
A. Y. Didyk 1994 14 p In RUSSIAN
(DE95-620943; JINR-R-14-94-333) Avail: CASI HC A03/MF A01 (US Sales Only)

The surface of stainless steel Cr18Ni10Ti irradiated by Xe-129 heavy ions in the temperature interval from 400 up to 650 C is studied. The fluences were changed from 10(exp 15) ion/sq cm up to 2 x 10(exp 16) ion/sq cm. A new effect of needle structure formation with the same form was found. The height of these needles increases with the increasing of the ion fluences. The element composition of the needle structures is very different from the initial stainless steel. The phenomenological model of this phenomenon is discussed. The energy criterion when such effect will take place is introduced. DOE

N95-32638# Ames Lab., IA.
REACTIONS OF TRIFLUOROIODOMETHANE ON METAL SURFACES Ph.D. Thesis - Iowa State Univ.
Mark Jensen 10 Feb. 1995 164 p
(Contract W-7405-eng-82)
(DE95-010122; IS-T-1725) Avail: CASI HC A08/MF A02

Reactions of fluorocarbons are relevant to a number of technological applications. Several surface-sensitive analytical techniques are applied to an investigation of the thermal and electron-induced chemistry of trifluoro-iodomethane (CF3I) on Ru (001) and Ni (100) surfaces. DOE

N95-32648# Ames Lab., IA.
ANGULAR DEPENDENCE OF MAGNETIC PROPERTIES OF STEELS UNDER UNIAXIAL STRESS Ph.D. Thesis - Iowa State Univ.
David A. Kaminski 23 Feb. 1995 131 p
(Contract W-7405-eng-82)
(DE95-010189; IS-T-1633) Avail: CASI HC A07/MF A02

Since stress induces directionally dependent changes in the magnetic properties of steels, there should be a discernable change in behavior of the magnetic properties between a magnetic field applied in a direction coaxial with the stress and a field applied non-coaxial with the direction of applied stress. These changes in magnetic properties could perhaps be used ultimately for nondestructive evaluation of stress magnitude and direction in materials that are in service. This work is intended to advance the understanding and modelling of the angular dependence of magnetic properties under stress. As steel structures in power plants reach the end of their projected life span, the probability of catastrophic failure increases dramatically. To avoid this, there is a need to identify components which are at a risk and replace them. Monitoring of the mechanical stress in component sections is very important. This is particularly true in places where one component is joined to another. It is known that microstructural defects in regions of high stress eventually propagate into cracks, which if further propagated, can become causes of structural failure. The use of magnetic NDE methods to monitor stress would be advantageous because these methods provide measurements of properties which are very sensitive to mechanical stresses. It is well known that the magnetic properties of steels are very strongly affected by mechanical deformation of the material and this has led many experts to suggest that magnetic methods should provide an ideal NDE technique for stress evaluation. A complete development of a predictive model for utilizing the interplay between stress and magnetic properties would be an important step in the development of magnetic NDE methods for measuring stress. DOE

N95-32926 Defence Science and Technology Organisation, Melbourne (Australia). Ship Structures and Material Div.
THE TENSILE FRACTURE BEHAVIOR OF THE WELD METAL OF BIS 812 EMA AND Q1N NAVAL CONSTRUCTION STEELS
I. A. Burch and David S. Saunders Feb. 1995 26 p
(DSTO-RR-0021; AR-009-179) Avail: Issuing Activity (DSTO Aeronautical and Maritime Research Lab., GPO Box 4331, Melbourne, Victoria 3001, Australia)

The tensile properties and tensile fracture behavior of BIS 812 EMA and Q1N naval constructional steel weldments have been studied over a wide range of test temperatures utilizing plain and notched tensile specimens. Under certain conditions 'star' fracture is the preferred fracture mode, rather than the usually observed cup-and-cone type fracture. The propensity for star fracture increases with decreasing temperature and the transition temperature for cup-and-cone to star fracture is reduced by notching. This paper describes the fracture surface features resulting from tensile tests and the conditions under which they occur in these materials. Author

N95-32935 McMaster Univ., Hamilton (Ontario).
LOW STRAIN BEHAVIOUR OF A PARTICULATE REINFORCED ALUMINUM ALLOY Ph.D. Thesis
Stephen Francis Jose Corbin 1993 292 p
(ISBN-0-315-84906-1) Avail: Univ. Microfilms Order No. DANN84906

The primary purpose of this investigation was to examine the strengthening that arises when reinforcing an aluminum alloy with approximately equiaxed shaped SiC particles. The results indicate that the majority of strengthening that is derived from the particles develops at low strains. For a variety of test conditions explored, about 90 percent of the total strengthening derived is developed by a plastic strain of about 0.5 percent. This is primarily a result of the high strain hardening rate which is exhibited by the composite materials during the onset of plastic flow. An examination of the Bauschinger effect in the composites indicates that an internal stress, resulting from inhomogeneous plastic flow, develops rapidly in the low strain regime. Microstructural observations suggest that the nature of this inhomogeneous plastic flow is influenced by the distribution of the SiC particles. Initial plasticity appears to be associated with regions of the microstructure which are relatively particle free. A self-consistent

model, based on Eshelby's equivalent inclusion method, has been developed which is capable of calculating the stress partitioning which occurs between the Al matrix and SiC particles during the elastic/plastic transition and beyond. Excellent quantitative agreement between the experimentally measured elastic modulus and that predicted by the model was achieved. When considering a uniform distribution of second phase particles, the model predicts an increase in the initial strain hardening rate. However, it underestimates the actual strain hardening rate which was measured experimentally. The influence of particle distribution was examined by representing the composite microstructure by a bimodal mixture consisting of a particle rich and particle free phase. The model predicts an increase in the initial strain hardening rate as a result of clustering the microstructure in this way. The magnitude of this increased hardening is comparable to that measured experimentally. Dissert. Abstr.

N95-32936 Oregon Graduate Inst. of Science and Technology, Beaverton, OR.

AN EXPERIMENTAL AND NUMERICAL ANALYSIS OF HYDROGEN ASSISTED CRACKING AND WELDABILITY TEST METHODOLOGY Ph.D. Thesis

Rajesh Manohar Dighde 1993 357 p

Avail: Univ. Microfilms Order No. DA9407519

The preferred method for increasing resistance to hydrogen-assisted cracking (HAC) is the application of an adequate preheating temperature, T(sub ph). The suitability of given welding conditions, including T(sub ph), in avoiding HAC is generally assessed through the use of Tekken and Lehigh weldability restraint tests. The safe welding conditions determined from these tests are then applied in industrial fabrication. It is observed that these safe welding conditions do not always avoid HAC in actual weldments. Therefore, it is necessary to evaluate the weldability testing procedure in its entirety against the more general industrial fabrication practice and understand the inherent differences. The differences arising, at different stages of weldability testing procedure, from weld hydrogen measurement technique, weldability testing procedure, hydrogen diffusion behavior, residual stress development, and dimensional differences in weldability tests and actual weldments were analyzed in detail using an experimental and numerical approach. The weld hydrogen measurement results indicated that the existing hydrogen measurement standards do not measure the weld hydrogen levels in actual weldments, and should, therefore, be modified for use in weldability testing procedure. The Tekken and Lehigh weldability test results suggested that weld induced variation at stress concentration locations strongly influences the HAC tendency and crack propagation behavior. Finite element analysis (FEA) of hydrogen diffusion behavior in weldability tests and actual weld grooves indicated that hydrogen diffusion is a strong function of the groove shape and the weld thermal cycle, and hence, direct applicability of weldability test results to actual weldments can be misleading. Elasto-plastic thermo-mechanical behavior of Tekken and Lehigh weldability tests during welding was carried out using FEA. The heat transfer in these test specimens was highly nonuniform resulting in varying HAC susceptibility along the weld length. The residual stress distribution varied significantly along the weld length due to the slot nature of the groove and restraint variation along the weld length. It was observed from this research work that the existing weldability testing methodology needs to be modified for better applicability to industrial fabrication practice. The weldability tests should be designed so as to simulate weld hydrogen level, welding process variables, hydrogen diffusion, heat transfer, and residual stress level of actual weldments.

Dissert. Abstr.

N95-32958# Westinghouse Hanford Co., Richland, WA.

NITRATE STRESS CORROSION CRACK GROWTH RATE IN PLAIN CARBON STEELS

L. D. Blackburn 3 May 1995 13 p

(Contract DE-AC06-87RL-10930)

(DE95-011689; WHC-SD-WM-ES-349) Avail: CASI HC A03/MF A01

This document summarizes information from the published literature related to the rate of growth of stress corrosion cracks in aqueous solution containing nitrate ions. A simple model for crack growth calculations in waste tanks is suggested. DOE

N95-33063# Lawrence Livermore National Lab., Livermore, CA.

COPPER-DIAMOND COMPOSITE SUBSTRATES FOR ELECTRONIC COMPONENTS

H. L. Davidson (Sun Microsystems, Inc., Mountain View, CA.), Nicholas J. Colella, John A. Kerns, and Daniel Makowiecki 25 Jan. 1995 4 p Presented at the 45th Electronic Components and Technology Conference, Las Vegas, NV, 22-26 May 1995

(Contract W-7405-eng-48)

(DE95-011520; UCRL-JC-118992; CONF-9505121-2) Avail: CASI HC A01/MF A01

High-power density electronic components such as fast microprocessors and power semiconductors are often limited by inability to keep the device junctions below their maximum rated operating temperature. Present high power multichip module and single chip package designs use substrate materials such as silicon nitride or copper tungsten with thermal conductivity in the range of 200 W/m K. We have developed a copper-diamond composite (Dymalloy) with a thermal conductivity of 420 W/m K, better than Cu, and an adjustable coefficient of thermal expansion (CTE, = 5.5 ppm/C at 25 C), compatible with Si and GaAs. Because of the matched CTE, it is possible to use low thermal resistance hard die attach methods. The mechanical properties of the composite also make it attractive as an electronic component substrate material. DOE

N95-33065# Connecticut Univ., Storrs, CT.

SYNCHROTRON RADIATION STUDIES OF LOCAL STRUCTURE AND BONDING IN TRANSITION METAL ALUMINIDES AND RARE EARTH TRANSITION METAL MAGNETIC NITRIDES Final Report, 1 Aug. 1990 - 14 Jul. 1993

J. I. Budnick and D. M. Pease 1995 14 p

(Contract DE-FG02-90ER-45424)

(DE95-011579; DOE/ER-45424/2) Avail: CASI HC A03/MF A01

This technical report discusses the following topics: bonding and near neighbor force constants in NiAl, CoAl, FeAl via temperature dependent EXAFS; alloys formed when Fe or Ga is microalloyed into a NiAl matrix; EXAFS studies of nitrided versus non nitrided Y2Fe17; and transition metal x-ray spectra as related to magnetic moments. DOE

N95-33215# Argonne National Lab., IL. Energy Technology Div.

EFFECT OF LEAD CONTENT ON Bi-2223 FORMATION BY A TWO-POWDER PROCESS

S. E. Dorris, M. A. Pitz, J. T. Dawley, and D. J. Trapp Feb. 1995 11 p Presented at the Annual Meeting and Exhibition of the Minerals, Metals and Materials Society (TMS), Las Vegas, NV, 12-16 Feb. 1995

(Contract W-31-109-eng-38)

(DE95-009889; ANL/ET/CP-83802; CONF-950201-14) Avail: CASI HC A03/MF A01

Decreasing the total lead content from Pb(0.4) to Pb(0.3) significantly stunts Bi-2223 phase development and greatly reduces the critical current density (J(sub c)) of powder-in-tube tapes made by a two-powder process. This effect can be explained on the basis of the solubility limit for lead in 2212. Pb(0.4) samples exceed the solubility limit for lead in 2212, so lead is rejected to create a lead-rich liquid that enhances the kinetics of 2223 formation during heat treatment. By contrast, a liquid does not form in the Pb(0.3) sample because its lead content is below the solubility limit. As a result, 2223 formation is much slower and J(sub c) is much lower in the Pb(0.3) sample. DOE

N95-33217# Oak Ridge National Lab., TN. Metals and Ceramics Div.

EFFECT OF PHASE TRANSFORMATIONS ON THE MECHANICAL PROPERTIES OF A MULTIPHASE ALLOY BASED ON NiAl+Fe

J. A. Horton, C. T. Liu, I. Vergara, and E. P. George 1995 8 p Presented at the Materials Week 1994, Rosemont, I L, 3-7 Oct. 1994

(Contract DE-AC05-84OR-21400)

(DE95-010119; CONF-941016-6) Avail: CASI HC A02/MF A01

The ordered intermetallic NiAl with aluminum levels near 36% undergoes a B2 to martensite transformation and exhibits a shape memory effect under 300 C. Many potential shape memory applications such as actuators in under-the-hood automotive situations require alloys with transition temperatures somewhat above 100 C. Shape memory alloys based on NiAl+Fe have the potential for these and even higher transition temperatures of greater than 150 C. While binary alloys appear inherently brittle, alloying with iron and boron results in two-phase alloys with L1(sub 2) and B2

phases and with about 7% room-temperature tensile ductility. These alloys show a two-way shape memory effect over a range of transition temperatures with austenite peak temperature, Ap, between 100 to 200 C based on composition. Unfortunately, the B2 phase and its low temperature body centered tetragonal martensitic form are not stable and both can transform to Ni5Al3 with a loss in ductility. These alloys with a constant tensile load show a two-way shape recovery of up to 0.6% during temperature cycling between 100 and 250 C. A thorough survey of the shape memory properties of one such alloy with a composition of Ni-25.5 Al-16 Fe-0.12 B (at.%) as a function of prior cold work, tensile loading and other training steps is presented. Nanoindentation was used to independently measure the mechanical properties of the two phases. Repeated cycling of the B2-martensitic phase did not result in a buildup of dislocations in or adjacent to the L1(sub 2) phase. The superlattice dislocation spacing in the L1(sub 2) phase also remained at an expected value of 15 mn after repeated cycling. DOE

N95-33626# California Univ., Berkeley. Lawrence Berkeley Lab, CA. Div. of Materials and Chemical Sciences.
STRUCTURAL INFLUENCES ON THE WORK HARDENING BEHAVIOR OF ALUMINUM Ph.D. Thesis
David Chu Dec. 1994 127 p
(Contract DE-AC03-76SF-00098)
(DE95-011262; LBL-36547; UC-404) Avail: CASI HC A07/MF A02

Effects of various grain and subgrain morphologies on low temperature work hardening of pure Al is studied using tensile tests. Plotting the work hardening rate as a function of true stress, the work hardening is separable into two distinct regimes. Both regimes are approximated by a line Theta = Theta(sub 0) - K(sub 2)sigma, where Theta(sub 0) is theoretical work hardening rate at zero stress and K(sub 2) is related to dynamic recovery rate. The first or early deformation regime exhibits greater values of Theta(sub 0) and K(sub 2) and can extend up to the first 10% strain of tensile deformation. This early deformation regime is contingent on the existence of a pre-existent dislocation substructure from previous straining. The Theta(sub 0) and K(sub 2) associated with the early deformation regime are dependent on the strength and orientation of the pre-existent dislocation substructure relative to the new strain path. At high enough temperatures, this pre-existent dislocation substructure is annealed out, resulting in the near elimination of the early deformation regime. In comparison, the latter regime is dominated by the initial grain and/or subgrain morphology and exhibit lower values of Theta(sub 0) and K(sub 2). The actual value of K(sub 2) in the latter regime is strongly dependent on the existence of a subgrain morphology. Recrystallized or well-annealed microstructures exhibit greater values of K(sub 2) than microstructures that remain partially or fully unrecrystallized. The higher K(sub 2) value is indicative of a more rapid dynamic recovery rate and a greater degree of strain relaxation. The ability to achieve a more relaxed state produces a low-energy cellular dislocation substructure upon deformation. The introduction of subgrains hinders the evolution of a low-energy dislocation cell network, giving way to a more random distribution of the dislocation density. DOE

N95-33653# Lawrence Livermore National Lab., Livermore, CA.
THE 3D METAL FORMING APPLICATIONS OF ALE TECHNIQUES
Richard Couch, Rose McCallen, Ivan Otero, and Richard Sharp 27 Jan. 1995 18 p Presented at the 5th International Conference on Numerical Methods in Industrial Forming Processes (NUMIFORM), Ithaca, NY, 18-21 Jun. 1995 Submitted for publication
(Contract W-7405-eng-48)
(DE95-011745; UCRL-JC-117773; CONF-9506144-3) Avail: CASI HC A03/MF A01

A three-dimensional arbitrary Lagrange-Eulerian (ALE) code is being developed for use as a general purpose tool for metal forming analyses. The focus of the effort is on the processes of forging, extrusion, casting and rolling. The ALE approach was chosen as an efficient way to deal with the large deformations and complicated flows associated with these processes. A prototype version of the software package, ALE3D, exists and is being applied to the enumerated processes. It is a finite element code which treats fluid and elastic-plastic response on an unstructured mesh. The prototype version includes heat transfer and the option of either implicit or explicit time integration of the dynamic equations. The status of the code is described. Several examples of application of the code to typical forming simulations are presented with discussions of the advantages and disadvantages of the ALE approach. DOE

N95-33699# Ames Lab., IA.
MEASUREMENT AND MODELLING OF STRUCTURE SENSITIVE MAGNETIC PROPERTIES OF MATERIAL Ph.D. Thesis
Zhao-Jun Chen 10 Feb. 1995 202 p
(Contract W-7405-eng-82)
(DE95-010126; IS-T-1732) Avail: CASI HC A10/MF A03

Due to the fact that magnetic properties of ferromagnetic materials are highly microstructure sensitive, magnetic non-destructive testing (NDT) techniques for material evaluation have developed very quickly in recent years. This dissertation is mainly focused on the magnetic hysteresis measurement technique. The modelling of structure-sensitive magnetic properties will be discussed first. As a result, the relationship between defect density, the initial permeability and the hysteresis parameter k will be developed. This is followed by the application of magnetic hysteresis measurement techniques in the detection of fatigue damage and creep damage. It will be shown that structure sensitive magnetic properties such as coercivity, remanence, hysteresis loss and initial permeability are very sensitive to material degradation due to fatigue and creep effects. Finally, practical problems in hysteresis measurement will be discussed and techniques to overcome these difficulties will also be presented. DOE

N95-33700 Ames Lab., IA.
THEORY OF MAGNETO-OPTICS AND CIRCULAR MAGNETIC X-RAY DICHROISM Ph.D. Thesis
Xindong Wang 20 Oct. 1994 96 p Limited Reproducibility: More than 20% of this document may be affected by poor print
(Contract W-7405-eng-82)
(DE95-010129; IS-T-1697) Avail: Issuing Activity (Department of Energy (DOE))

This thesis contains three parts. In the first part, before getting into the discussion of magneto-optical properties for the systems under study, the author reviews some background subjects, such as the energy-band theory within the framework of density functional theory, the multiple scattering approach to the solution of band problem and its relation with the LMTO method, an account of the tight-binding LMTO method which we use exclusively in our calculations, the linear response theory and its application to the quantum theory of dielectric constants. In the second part, circular magnetic x-ray dichroism, as a powerful and newly experimental technique for quantitative study of the magnetic properties of materials, is discussed. In the last part, the detailed study of the magneto-optical properties of some transition metals and the so-called half metallic Heusler alloys is presented. DOE

N95-33774 Lehigh Univ., Bethlehem, PA.
MICROSTRUCTURAL STUDIES OF HYDROGEN DAMAGE IN METASTABLE STAINLESS STEELS Ph.D. Thesis
Shuchun Chen 1994 200 p
Avail: Univ. Microfilms Order No. DA9414987

The primary objective of this dissertation is to determine the role of microstructure in hydrogen-induced damage in austenitic stainless steels. Specific attention was focused on the interactions between hydrogen and the austenitic grain, twin boundaries and the matrix, and the associated phase transformations. An experimental program of research was conducted to determine the phase transformation and cracking path in hydrogen charged stainless steels. Normal-purity AISI 304 (Fe18CrYNi) and high-purity 305 (Fe18Cr12Ni) solution-annealet stainless steels were examined. The steels were cathodically charged with hydrogen at 1, 10 and 100 mA/sq cm at room temperature for 5 min. to 32 hours, in an 1N H2SO4 solution with 0.25 g/l of NaAsO2 added as a hydrogen recombination poison. Resultant changes in microstructure and hydrogen damage due to charging and subsequent room temperature aging were studied by x-ray diffraction, optical microscope (in the Nomarski mode), scanning electron microscopy (SEM) and transmission electron microscopy (TEM). A new phase in 805 stainless steel was observed, and was identified as an epsilon(*) (hcp) hydride due to hydrogen charging. Two new phases in 304 stainless steel were found as gamma(*) (fcc) and epsilon(*) hydrides from hydrogen charging. The hydride formation mechaniems during charging were: (1) gamma yields gamma(*) hydride and (2) gamma yields epsilon yields epsilon(*) hydride. These hydrides are unstable and decomposed during

room temperature aging in air. The decomposition mechanisms were: (1) epsilon(*) hydride (hcp) yields expanded epsilon (hcp) phase yields a (bcc) phase; (2) gamma(*) hydride yields gamma phase. The grain and twin boundary cracks were the results of charging and identified as the preferred cracking sites. Transgranular crack initiation and growth accompanied the decomposition of hydrides and were controlled by hydrogen outgassing during room temperature aging. TEM observations of hydrogen induced microstructural changes after charging are consistent with the x-ray diffraction data. Indirect evidence in TEM suggested hydrogen associated with c phase, which may be identified as the epsilon(*) hydride. Dissert. Abstr.

N95-34252 Cincinnati Univ., OH.
INTERFACIAL REACTIONS DURING THE LIQUID INFILTRATION OF TITANIUM MATRIX COMPOSITES Ph.D. Thesis
Sunil Govinda Warrier 1993 137 p
Avail: Univ. Microfilms Order No. DA9416807

A rapid infrared forming process has been developed for the fabrication of ceramic fiber reinforced titanium alloy matrix composites. Using this technique, composites can be fabricated at a low cost into complicated shapes. Compared to the titanium matrix composites fabricated by solid state processes, composites fabricated by this technique exhibit smaller as-fabricated reaction zones and comparable mechanical properties. In order to develop a fundamental understanding of reactions during liquid state processing of titanium matrix composites as well as for determining the potential for commercialization of the rapid infrared forming process, interfacial reactions during processing were thoroughly examined. During the fabrication of carbon fiber reinforced titanium alloy matrix composites, it was observed that the fibers react with the alloy and form a protective TiC layer which prevents the fibers from coming in direct contact with the molten alloy. Further degradation of the fibers was found to be controlled by the diffusion of carbon across the reaction product. A cylindrical model has been proposed to predict the extent of reaction in these composites. In uncoated SiC fiber (SCS-0) reinforced composites, a continuous layer of reaction product did not form at the fiber surface and large areas of the fibers were dissolved by the molten alloy. Examinations revealed that the interface consists of radially propagating scalloped dissolution fronts. A self sustaining exothermic dissolution model has been proposed to explain the observed interface. In SCS-6 fiber reinforced composites, it was found that although a continuous layer of the reaction product does not form, self sustaining exothermic dissolution does not occur. A physical model has been proposed to explain the dissolution of the carbon rich coating in these composites. Dissert. Abstr.

N95-34348# Idaho National Engineering Lab., Idaho Falls, ID.
SPRAY COATING OF METALS. PROOF OF CONCEPT: PHASE 2 Final Report, Mar. 1989 - Sep. 1992
Scott A. Ploger, Ray A. Berry, Patricia B. Hembree, James F. Key, and Lloyd D. Watson Dec. 1994 93 p
(Contract DE-AC07-761D-01570)
(AD-A294393; AL/EQ-TR-1994-52) Avail: CASI HC A05/MF A01

A spray coating technique is being developed to replace electroplating processes at Air Logistics Centers and thereby reduce hazardous wastes. A bench-scale spray system was used to coat low-carbon steel strips with three cobalt-chromium hardfacing alloys. The process shows promise to be a replacement for chromium electroplating. One-dimensional models incorporating the most fundamental aspects of molten metal nebulization and coating deposition provided physical insight on the process. DTIC

N95-34373# Army Armament Research, Development and Engineering Center, Watervliet, NY. Benet Lab.
FRACTURE TOUGHNESS ASSESSMENT OF PRESENT AND FUTURE PRESSURE VESSEL MATERIALS BASED ON CHARPY IMPACT ENERGY AND YIELD STRENGTH Final Technical Report
Edward Troiano and Gregory Vigilante Feb. 1995 14 p
(AD-A294008; ARCCB-TR-95007) Avail: CASI HC A03/MF A01

Several medium and high strength alloys, including AF1410, Inconel 718, PH 13-8 Mo stainless steel, and ASTM A723 high strength low alloy steel, have been heat treated to various strength and toughness levels and evaluated for correlations between fracture toughness and charpy impact energy. The correlations investigated included those by Roffe-Novak and Ault-Wald-Bertolo. Previous work by Kapp and Underwood suggests that for A723 steel the Rolfe-Novak correlation predicts the fracture toughness reasonably well. One potential limitation of their study was that the charpy impact energy was measured at -40 deg F, whereas the toughness was evaluated at room temperature. This study evaluates Charpy impact energy and toughness at both room temperature and at -40 deg F and considers both when utilizing these correlations. Results of this study indicate that the Rolfe-Novak correlation over-predicts the measured fracture toughness at room temperature, and tends to underpredict the measured fracture toughness at 40 deg F. The Ault-Wald-Bertolo correlation, in all but one instance, was a conservative estimate of the measured fracture toughness of the material at both room temperature and 40 deg F. Utilizing the results presented in this study, it is recommended that if a correlation is necessary for estimating the toughness of any of the materials, the Ault-Wald-Bertolo correlation will result in a conservative estimate of toughness. DTIC

N95-34482# Lawrence Livermore National Lab., Livermore, CA.
MULTILAYER THERMOELECTRIC FILMS: A STRATEGY FOR THE ENHANCEMENT OF ZT
Andrew V. Wagner, Ronald J. Foreman, Leslie J. Summers, Troy W. Barbee, Jr., and Joseph C. Farmer Mar. 1995 8 p Presented at the 30th Intersociety Energy Conversion Conference, Orlando, FL, 31 Jul. - 4 Aug. 1995
(Contract W-7405-eng-48)
(DE95-011535; UCRL-JC-120255; CONF-950729-3) Avail: CASI HC A02/MF A01

The relative efficiency of a thermoelectric material is measured in terms of a dimensionless figure of merit, ZT. Although all known thermoelectric materials are believed to have ZT less than or equal to 1, recent theoretical results predict that thermoelectric (devices fabricated as two-dimensional quantum wells (2D QW's) could have ZT greater than or equal to 3. Multilayers with the dimensions of 2D QW's have been synthesized by alternately sputtering Bi(0.9)Sb(0.1) and PbTe(0.8)Se(0.2) onto a moving substrate from a pair of magnetron sources. These materials have been synthesized to test the thermoelectric quantum-well concept and gain insight into relevant transport mechanisms. This work focuses primarily on the scientific issues involved in producing the materials necessary to examine the possibility of enhancing ZT using quantum confinement. The techniques needed to measure the relevant electrical parameters of thermoelectric thin films are developed in this paper. Ultimately, if a quantum well enhancement of thermoelectrics is experimentally observed, devices based on this technology could be used to greatly expand the role of thermoelectrics in power generation and refrigeration. DOE

N95-34821# Aerodyne Research, Inc., Billerica, MA.
INFRARED DETECTION OF CHEMICAL CORROSION ON METAL SURFACE Final Report, 15 Jun. 1994 - 15 Mar. 1995
Qing Dai, Andrew Freeman, and Gary N. Robinson 15 Mar. 1995 35 p
(Contract F49620-94-C-0033)
(AD-A295000; ARI-RR-1117; AFOSR-95-0267TR) Avail: CASI HC A03/MF A01

The sulfuric acid-induced corrosion of smooth (20 A average roughness) aluminum surfaces has been studied in real time using an in situ Fourier transform infrared reflection absorption spectrometer (IRAS) and a quartz crystal microbalance. Submicron-thick, 35 - 55 wt% (5- 12 molal), sulfuric acid films were formed on room temperature metal surfaces by the reaction of gas phase SO3 and H2O vapor in a flowing gas system at a total pressure of approx. 200 Torr. Using changes in spectral features that are linked to the production of Al(3+) as indicators of corrosion, we conclude the rate of corrosion of the metal is strongly enhanced by both higher relative humidities and increased rates of sulfuric acid deposition. Ex situ IRAS measurements on aluminum foils indicated that this technique is suitable for the detection of corrosion on metal surfaces. DTIC

27 NONMETALLIC MATERIALS

Includes physical, chemical, and mechanical properties of plastics, elastomers, lubricants, polymers, textiles, adhesives, and ceramic materials.

For composite materials see *24 Composite Materials.*

N95-32380# Sandia National Labs., Albuquerque, NM.
SHOCK PROPERTIES OF HIGH-STRENGTH CERAMICS
D. E. Grady 1994 6 p Presented at the International Conference on Computational Engineering Science, Mauna Lani, HI, 30 Jul. - 3 Aug. 1995
(Contract DE-AC04-94AL-85000)
(DE95-007731; SAND-94-2869C; CONF-950788-5) Avail: CASI HC A02/MF A01

A broad class of brittle solids subjected to large amplitude shock waves can support substantial shear stress (of order 2-10 GPa) without failing due to the very limited slip systems in these materials. When failure occurs under sufficiently intense shock loading, the effect is usually observed as a wave splitting in the compressive shock front. Because of the high confining stress state associated with the failure event in the shock compression environment, it is no longer certain whether the microstructural processes of deformation are brittle or ductile. Some, although by no means sufficient, evidence supports a brittle deformation mechanism in the materials of interest. The present short paper focuses on two aspects of the transition regime neighboring the HEL in the compressive shock process. First, issues of rate dependence associated with prompt yield under shock compression are not well understood. We report here on observations of wave profile data on ceramics, examining the issue of elastic precursor decay. Also in this study, a number of the experimental observations of failure waves in ceramic materials (principally glass) are surveyed. Some of the principal results are summarized and dynamic failure mechanisms consistent with these results are discussed. DOE

N95-32384# Westinghouse Hanford Co., Richland, WA.
GLASS SCIENCE TUTORIAL: LECTURE NO. 4, COMMERCIAL GLASS MELTING AND ASSOCIATED AIR EMISSION ISSUES
A. A. Kruger Jan. 1995 111 p
(Contract DE-AC06-87RL-10930)
(DE95-007818; WHC-MR-0489) Avail: CASI HC A06/MF A02

This document serves as a manual for a workshop on commercial glass melting and associated air emission issues. Areas covered include: An overview of the glass industry; Furnace design and construction practices; Melting furnace operation; Energy input methods and controls; Air legislation and regulations; Soda lime emission mechanisms; and, Post furnace emission controls. Supporting papers are also included. DOE

N95-32541# Fermi National Accelerator Lab., Batavia, IL.
COATING POWER RF COMPONENTS WITH TIN
M. Kuchnir and E. Hahn Mar. 1995 12 p
(Contract DE-AC02-76CH-03000)
(DE95-010357; FNAL-TM-1928) Avail: CASI HC A03/MF A01

A facility for coating RF power components with thin films of Ti and/or TIN has been in operation for some time at Fermilab supporting the Accelerator Division RF development work and the TESLA program. It has been experimentally verified that such coatings improve the performance of these components as far as withstanding higher electric fields. This is attributed to a reduction in the secondary electron emission coefficient of the surfaces when coated with a thin film containing titanium. The purpose of this Technical Memorandum is to describe the facility and the procedure used. DOE

N95-32552# Case Western Reserve Univ., Cleveland, OH. Dept. of Macromolecular Science.
MOLECULAR ENGINEERING OF LIQUID CRYSTALLINE POLYMERS BY LIVING POLYMERIZATION 30. SYNTHESIS AND LIVIING CATIONIC POLYMERIZATION OF (2R, 3S)-2-FLUORO-3-METHYLPENTYL 4'-(8-VINYLOXYOCTYLOXY) BIPHENYL-4-CARBOXYLATE AND ITS COPOLYMERIZATION WITH (2R, 3S)-2-FLUORO-3-METHYLPENTYL 4'-(11 VINYLOXYUNDECANYLOXYLOXY) BIPHENYL-4-CARBOXYLATE
V. Percec and H. Oda 3 Apr. 1995 28 p
(Contract N00014-89-J-1826)
(AD-A293115) Avail: CASI HC A03/MF A01

The synthesis and 'living' cationic polymerization of (2R, 3S)-2-fluoro-3-methylpentyl 4'-(8-vinyloxyoctyloxy) biphenyl-4-carboxylate (11-8) are described. Poly(11-8)s with degrees of polymerization from 4.3 to 15.7 and polydispersities less than or equal to 1.19 were synthesized and characterized by differential scanning calorimetry (DSC) and thermal optical polarized microscopy. All poly(11-8)s exhibit an enantiotropic S(sub c)* and an unidentified smectic (S(sub 1)) phase. Poly(11-8)s with DP less than or equal to 11.5 exhibit an additional enantiotropic unidentified smectic (S(sub 2)) phase. No S(sub A) phase could be detected in any of poly(11-8)s. The nature of mesophases exhibited by poly(11-8) was confirmed by the investigation of the phase diagram of the copolymers prepared from 11-8 and (2R, 3S)-2-fluoro-3-methylpentyl 4'-(11-vinyloxyundecanyloxy) biphenyl-4 carboxylate (11-11). The S(sub c)* phase of these copolymers displays a continuous dependence of copolymer composition. DTIC

N95-32664# Argonne National Lab., IL.
TESTS OF ADHESIVES USED FOR PLATE BONDING OF ATLAS TILE-CAL HADRON CALORIMETER
Norman F. Hill and Lawrence Kocenko 18 Nov. 1994 6 p
(Contract W-31-109-eng-38)
(DE95-009917; ANL-HEP-TR-94-86) Avail: CASI HC A02/MF A01

At the ATLAS meeting in September, 1994, Argonne agreed to carry out a series of tests of the adhesive used to bond the 25 cm prototype module constructed at CERN. This note reports the results obtained from the lap shear, tensile, and peel tests. Although the results are not complete, the following conclusions are drawn from the results: (1) the strength of the bonds is adequate, if the shear stress requirements are understood; (2) the strength of the bonds is improved by oven curing at elevated temperatures; (3) peel tests are inconclusive, and need further study; (4) other adhesives are also adequate; (5) there is improvement of the bond strength if some glue line is maintained, and this should be optimized; and (6) preparation of the surface (roughening) improves strength.
Derived from text

N95-32694# Army Research Lab., Watertown, MA. Materials Directorate.
INVESTIGATION OF AGING EFFECTS FROM HIGH VOLTAGE PROFILES IN CERAMIC PHASE SHIFTER MATERIALS
S. Stowell, L. C. Sengupta, E. Ngo, M. E. ODay, and R. Lancto Dec. 1994 15 p
(AD-A289985; ARL-TR-653) Avail: CASI HC A03/MF A01

Ceramic composite materials comprised of Ba(0.60)Sr(0.40)TiO3 and Alumina and other non ferroelectric oxides have been fabricated for use in phased array antennas. These composites have shown superior electronic properties and have been incorporated into several antenna designs. However, minimal testing has been accomplished to determine the electrical aging and fatigue caused by the large electric fields required to operate these devices. In this paper, a systematic study of the effect of the application of large fields will he presented. The electronic properties of the BSTO-Oxide composites (pre-voltage application) will be presented and include the dielectric constant, loss tangent, and tunability (change in dielectric constant with applied field). The study of the change in the electronic properties after large voltages applications include results on the electronic aging and fatigue of the material and appropriate conditioning of the material for application in phased array antenna systems. DTIC

N95-32710# Melbourne Univ., Parkville (Australia). School of Physics.
COMPARISON OF LEAD ZIRCONATE TITANATE THIN FILMS ON RUTHENIUM OXIDE AND PLATINUM ELECTRODES
L. A. Bursill (Ecole Polytechnique Federale de Lausanne, Switzerland.), Ian M. Reaney (Ecole Polytechnique Federale de Lausanne, Switzerland.), D. P. Vijay (Virginia Polytechnic Inst. and State Univ., Blacksburg, VA.), and S. B. Desu (Virginia Polytechnic Inst. and State Univ., Blacksburg, VA.) 1994 17 p
(DE95-617597; UM-P-93/74) Avail: CASI HC A03/MF A01 (US Sales Only)

High-resolution and bright- and dark-field transmission electron microscopy are used to characterize and compare the interface structures and microstructure of PZT/RuO2/SiO2/Si and PZT/Pt/ Ti/SiO2/Si ferroelectric thin films, with a view to understanding the improved fatigue characteristics of PZT thin films with RuO2 electrodes. The RuO2/PZT interface consists of a curved pseudoperiodic minimal surface. The interface

is chemically sharp with virtually no intermixing of RuO2 and PZT, as evidenced by the atomic resolution images as well as energy dispersive X-ray analysis. A nanocrystalline pyrochlore phase Pb2ZrTiO(7-x) (x (ne) 1) was found on the top surface of the PZT layer. The PZT/Pt/Ti/SiO2/Si thin film was well-crystallized and showed sharp interfaces throughout. Possible reasons for the improved fatigue characteristics of PZT/RuO2/SiO2/Si thin films are discussed. DOE

N95-32819 Arizona Univ., Tucson, AZ.
PERPENDICULAR MAGNETIC BEHAVIOR OF ULTRA-THIN Co SANDWICHES
Michael H. Wiedmann, Brad N. Engel, Charles M. Falco, and Christian Marliere (Centre National de la Recherche Scientifique, Orsay, France.) 1994 3 p Presented at the 14th International Colloquium on Magnetic Films and Surfaces, Duesseldorf, Germany,29 Aug. - 2 Sep. 1994 Limited Reproducibility: More than 20% of this document may be affected by microfiche quality
(Contract DE-FG03-93ER-45488)
(DE95-010611; DOE/ER-45488/4; CONF-940829-3) Avail: CASI HC A01

We have used in situ polar Kerr effect measurements to study the magnetic properties of MBE-grown X/Co/Y trilayers, where X and Y are combinations of the non-magnetic metals Au, Cu or Pd. Polar hysteresis curves were measured in situ for systematically-varied Co and overlayer Y layer thicknesses 2 Angstrom less than or equal T(sub Co) less than or equal 20 Angstrom and 0 Angstrom less than or equal t(sub Y) less than or equal 100Angstrom. We recently reported that for base layers of Pd or Au that induce a large perpendicular anisotropy, the magnitude of the X/Co/Y perpendicular coercivity is strongly peaked at approximately 1 atomic layer overlayer coverage. However, in the case of Pd overlayers the peak in coercivity is much less pronounced than for the other materials. Here we report further measurements on Pd overlayers confirming the existence of a small peak in coercivity. In addition, we have performed measurements on a 'reversed' layered Cu/Co/Au sandwich where the Cu base layer induces only a weak perpendicular anisotropy. We find similar peaked behavior in the perpendicular coercivity as in our earlier measurements on Au/Co/Cu. DOE

N95-32918*# National Aeronautics and Space Administration. Lewis Research Center, Cleveland, OH.
THE EFFECTS OF ION IMPLANTATION ON THE TRIBOLOGY OF PERFLUOROPOLYETHER-LUBRICATED 440C STAINLESS STEEL COUPLES
Bradley Shogrin (Colorado State Univ., Fort Collins, CO.), William R. Jones, Jr., Paul J. Wilbur (Colorado State Univ., Fort Collins, CO.), Herrera-Fierro Pilar (Ohio Aerospace Inst., Cleveland, OH.), and Don L. Williamson (Colorado School of Mines, Golden, CO.) Aug. 1995 22 p
(RTOP 616-00-00)
(NASA-TM-106965; E-9721; NAS 1.15:106965) Avail: CASI HC A03/MF A01

The lubricating lifetime of thin films of a perfluoropolyether (PFPE) based on hexafluoropropene oxide in the presence of ion implanted 440C stainless steel is presented. Stainless steel discs, either unimplanted or implanted with N2, C, Ti, Ti + N2, or Ti + C had a thin film of PFPE (60-400 A) applied to them reproducibly (+/- 20 percent) and uniformly (+/- 15 percent) using a device developed for this study. The lifetimes of these films were quantified by measuring the number of sliding-wear cycles required to induce an increase in the friction coefficient from an initial value characteristic of the lubricated wear couple to a final, or failure value, characteristic of an unlubricated, unimplanted couple. The tests were performed in a dry nitrogen atmosphere (less than 1 percent RH) at room temperature using a 3 N normal load with a relative sliding speed of 0.05 m/s. The lubricated lifetime of the 440C couple was increased by an order of magnitude by implanting the disc with Ti. Ranked from most to least effective, the implanted species were: Ti; Ti+C; unimplanted; N2; C approximately equals Ti+N2. The mechanism postulated to explain these results involves the formation of a passivating or reactive layer which inhibits or facilitates the production of active sites. The corresponding surface microstructures induced by ion implantation, obtained using x-ray diffraction and conversion electron Mossbauer spectroscopy, ranked from most to least effective in enhancing lubricant lifetime were: amorphous Fe-Cr-Ti; amorphous Fe-Cr-Ti-C + TiC; unimplanted; epsilon-(Fe,Cr)(sub x)N, x = 2 or 3; amorphous Fe-Cr-C approximately equals amorphous Fe-Cr-Ti-N. Author

N95-32919*# National Aeronautics and Space Administration. Lewis Research Center, Cleveland, OH.
SPONTANEOUS DEWETTING OF A PERFLUOROPOLYETHER
Bradley Shogrin, william R. Jones, Jr., and Pilar Herrera-Fierro Aug. 1995 15 p
(RTOP 616-00-00)
(NASA-TM-106964; E-9720; NAS 1.15:106964) Avail: CASI HC A03/MF A01

Eight different production lots of a commercial perfluoropolyether (PFPE) based on hexafluoropropene oxide (HFPO) were applied to polished metal surfaces by spinning. One of the lots repeatedly dewetted from a clean 440C steel surface, forming droplets on the surface, whereas the other seven did not dewet. This dewetting phenomenon also repeatedly occurred on 2024 aluminum and 1018 steel, but not on copper or gold. Fourier transform infrared microspectroscopy (mu-FTIR) was used to determine thickness and uniformity of the PFPE films. The dewetting lot was found to dewet from 440C steel at a film thickness greater than 520 A. A portion of the dewetting lot was heated at 316 C for 12 days in the presence of oxygen and M-50 steel. This fluid did not dewet. Sequentially, samples of the dewetting lot were filtered either with an alumina or a silica cartridge which can remove polar impurities. Neither of the filtered samples dewetted from 440C steel. It was concluded that an unknown impurity, both thermally labile and polar, present at very low concentration and undetected by our analytical techniques (FTIR, proton NMR, or F-19 NMR), was responsible for the dewetting phenomenon. Author

N95-32962# Swedish National Testing and Research Inst., Boras (Sweden).
FOAM SPREAD EXPERIMENTS ON A WATER SURFACE
Martin Dahlberg Jan. 1995 40 p
(ISSN 0284-5172)
(PB95-211025; SP-RAPP-1994:16; ISBN-91-7848-475-8) Avail: CASI HC A03/MF A01

Foam spreading experiments have been carried out in a 20 m diameter half-circular water pool and in a 5 m water channel without any thermal exposure. Maximum foam solution rate was 540 l/min. The foams used were an ordinary synthetic (Detergent) and an aqueous film forming foam (AFFF) concentrate. The foam layer extension and the foam height were recorded, as functions of time. The foam height was at maximum 3-6 cm in the pool, and higher in the channel. At an application rate of 1.5 l/min/sq m the pool was covered with foam in 50 s. The results from the experiments agree well with theoretical predictions as shown in a separate report. NTIS

N95-33079 Aluminum Co. of America, Alcoa Center, PA.
LIGHTWEIGHT ALUMINA REFRACTORY AGGREGATE. PHASE 2: PILOT SCALE DEVELOPMENT
T. G. Swansiger and A. Pearson Nov. 1994 277 p Limited Reproducibility: More than 20% of this document may be affected by microfiche quality
(Contract DE-FC07-89ID-12903)
(DE95-012154; DOE/ID-12903/2; Rept-06-94-27) Avail: CASI HC A13/MF A03

Kilogram quantities of refractory aggregate were prepared from both a paste and a pelletized form of extruder feed material in both bench and pilot-scale equipment. The 99(+)% alumina aggregate exhibited a bulk density approaching 2.5 g/cm(sup 3) and a fired strength slightly lower than fused alumina. Based on initial evaluation by two refractory manufacturers in brick or castable applications, the new aggregate offered adequate strength with thermal conductivity reductions up to 34%, depending on the temperature and application of the new aggregate in these initial trials. The new aggregate was simply substituted for Tabular(TM) in the refractory formulation. Thus, there is room for improvement through formulation optimization with the lightweight aggregate. The new aggregate offers a unique combination of density, strength, and thermal properties not available in current aggregate. To this point in time, technical development has led to a pelletized formulation with borderline physical form leaving the Eirich mixer. The formulation requires further development to provide more latitude for the production of pelletized material without forming paste, while still reducing the bulk density slightly to reach the 2.5

g/cm(sup 3) target. The preferred, pelletized process flowsheet was outlined and a preliminary economic feasibility study performed based on a process retrofit into Alcoa's Arkansas tabular production facilities. Based on an assumed market demand of 20,000 mt/year and an assumed selling price of $0.65/lb (25% more than the current selling price of Tabular(TM), on a volume basis), economics were favorable. Decision on whether to proceed into Phase 3 (full- scale demonstration) will be based on a formal market survey in 1994 October. DOE

N95-33218# Westinghouse Hanford Co., Richland, WA.
GLASS SCIENCE TUTORIAL LECTURE NO. 6: THE MELTING OF SILICATE GLASSES, A REVIEW OF SELECTED TOPICS
E. Lowell Swarts 28 Mar. 1995 154 p Lecture held in Richland, WA, Mar. 1995
(Contract DE-AC06-87RL-10930)
(DE95-010199; WHC-MR-0494) Avail: CASI HC A08/MF A02

This report summarizes a two-day lecture given at Westinghouse Hanford Company in March, 1995 and includes the data used in the presentation. Topics included the special needs of a low-level waste vitrification process, glass melting, mechanisms of the formation of foam, glass refining (bubble removal), and homogenization (reduction of chemical heterogeneity to acceptable levels. DOE

N95-33227# Helsinki Univ. of Technology, Espoo (Finland). Dept. of Chemical Engineering.
POLYMERIZATION OF EPSILON-CAPROLACTONE IN THE PRESENCE OF Oh- OR COOh-GROUPS CONTAINING INITIATORS. COPOLYMERS OF LACTIDE WITH EPSILON-CAPROLACTONE: SYNTHESIS, CHARACTERIZATION AND PROCESSING
T. Karjalainen and M. Hiljanen 1994 50 p See also PB94-135589 and PB95-208229
(ISSN 0785-7144)
(PB95-208211; ISBN-951-22-2262-0) Avail: CASI HC A03/MF A01

Poly(epsilon-caprolactone) is aliphatic, biodegradable and hydrolytically unstable polyester. Polymer degrades both in vivo and in vitro with release of nontoxic degradation products. The polymers of epsilon-caprolactone have been used in medical applications, in blends and as a compatibilizer. The ring-opening polymerization of epsilon-caprolactone with stannous octoate as a catalyst and with hydroxyl end group and acid intiators was studied. The effect of amount of initiator, polymerization time and temperature on polymer product was also studied in this paper. NTIS

N95-33228# Helsinki Univ. of Technology, Espoo (Finland). Dept. of Chemical Engineering.
DMTA STUDIES OF BRANCHING DISTRIBUTION IN POLYETHYLENE
Paul Starck 10 Aug. 1994 26 p See also PB95-208229
(ISSN 0785-7144)
(PB95-208237; ISBN-951-22-2237-X) Avail: CASI HC A03/MF A01

The objective of this study is to present the benefits obtained by using the dynamic mechanical analyzing (DMA) technique in the structure characterization of different polyethylenes. The practical measurement include studies of well characterized (by international round robin work) polyethylenes, some commercial metallocene grades as well as some recent test materials where metallocene catalysts have been used. NTIS

N95-33247# Sandia National Labs., Albuquerque, NM.
PRINTABILITY OF SUBSTRATE AND ABSORBER DEFECTS ON EXTREME ULTRAVIOLET LITHOGRAPHIC MASKS
K. B. Nguyen, A. K. Ray-Chaudhuri, D. A. Tichenor, R. H. Stulen, R. P. Nissen, K. W. Berger, P. H. Paul, D. M. Tennant (Bell Telephone Labs., Inc., Holmdel, NJ.), L. A. Fetter (Bell Telephone Labs., Inc., Holmdel, NJ.), and D. L. Windt (Bell Telephone Labs., Inc., Murray Hill, NJ.) et al 1995 9 p Presented at the SPIE 1995: SPIE Conference on Optics, Electro-optics, and Laser Application in Sci ence, Engineering and Medicine, San Jose, CA, 5-14 Feb. 1995
(Contract DE-AC04-94AL-85000)
(DE95-010916; SAND-95-8554C; CONF-950226-47) Avail: CASI HC A02/MF A01

This paper reports results from a study of defect printability for extreme ultraviolet lithographic masks (EUVL). Imaging experiments were performed with an EUVL mask containing programmed defects. The mask contained defects of different sizes and locations with respect to the absorber patterns. Since an EUVL mask consists of absorber layer patterned above a multilayer-coated substrate, both substrate defects, located below the reflective coating, and absorber defects, located above the reflective coating, were included on the programmed defect mask. The absorber layer was patterned using a process previously described by Tennant et al. Imaging was performed using a 10X Schwarzschild camera operating at 13.4 nm with a numerical aperture of 0.08, corresponding to a Rayleigh resolution of 0.1 gm. This system has an effective exposure field of 0.4 mm diameter. Both positive-tone and negative-tone resists were used. Measurements of the defect-induced linewidth variations on the printed resist lines were performed with scanning electron microscopy (SEM) and atomic force microscopy (AFM). Results show that substrate defects are more printable compared to defects of the same sizes located above the reflective coating. In addition, defects located in the center of a clear region in lines-and-space pattern are more printable compared to those located nearer to the absorber lines. DOE

N95-33329# National Chemicals Inspectorate, Solna (Sweden).
PHTHALIC ACID ESTERS USED AS PLASTIC ADDITIVES. VOLUME 1: ECOTOXICOLOGICAL RISK ASSESSMENT. VOLUME 2: COMPARISONS OF TOXICOLOGICAL EFFECTS
Goeran Lundberg, Charlotte Nilsson, and L. Freij, ed. Aug. 1994 284 p
(ISSN 0284-1185)
(PB95-211280; KEMI-12-94) Copyright Avail: CASI HC A13/MF A03

The Swedish Environmental Research Institute (IVL) has been requested by the Swedish National Chemicals Inspectorate (KEML) to conduct a literature review concerning, risk assessment of phthalic esters used as plastic additives. The review has been fully financed by the Swedish National Chemicals Inspectorate. The risk assessment is evaluated with regard to ecotoxicological similarities and differences between the four phthalic esters DEHP, DINP, DIDP and 610P. NTIS

N95-33405# Pacific Northwest Lab., Richland, WA.
INFLUENCE OF PROCESSING VARIABLES ON THE STRUCTURE AND PROPERTIES OF ZnO FILMS
Gregory J. Exarhos and Shiv K. Sharma (Hawaii Univ., Honolulu, HI.) Apr. 1995 18 p Presented at the 22nd International AVS Conference on Metallurgical Coatings and Thin Films, San Diego, CA, 23-28 Apr. 1995
(Contract DE-AC06-76RL-01830)
(DE95-011494; PNL-SA-25315; CONF-950454-2) Avail: CASI HC A03/MF A01

Zinc oxide films of high optical quality have been deposited onto both silica and silicon substrates using reactive sputtering, pulsed laser deposition, and an aqueous solution based technique. Films have been characterized with respect to crystalline phase and phase stability, surface morphology, and optical response by means of X-ray diffraction, Raman Spectroscopy, Atomic Force Microscopy, optical transmission and ellipsometry measurements. All films studied were of the wurtzite phase, fine-grained, and exhibited varying degrees of c-axis orientation with respect to the substrate normal depending upon deposition conditions. Films showed some degree of residual tensile stress which was inferred from the E(sub 2) Raman line shift relative to the single crystal frequency. The wurtzite phase was found to be stable to temperatures near 800 C, but at higher temperatures, reaction with silica led to evolution of Zn2SiO4 at the interface. Variations in Raman line intensities upon post deposition annealing has been correlated with oxidation of excess zinc in the lattice. DOE

N95-33408# Lawrence Livermore National Lab., Livermore, CA.
MACHINABILITY STUDY OF AERMET 100
Dwight V. Squire, Chol K. Syn, and Bradley L. Fix 8 Feb. 1995 14 p
(Contract W-7405-eng-48)
(DE95-011532; UCRL-ID-119964) Avail: CASI HC A03/MF A01

Machinability of Aermet 100, an ultrahigh strength alloy developed for Navy by Carpenter Technology as a candidate material for aircraft landing gear application, was studied by performing single-point turning tests. Coated and uncoated carbides, ceramic, and cermet cutting tool inserts of a square geometry (SNG 432 type) were used. Round stock workpieces were tested in the as - received, unaged condition and without using any cutting fluid. The turning tests for each tool material were conducted by (1) first establishing the cutting conditions that would allow the continued generation of broken chips during a given cutting test; (2) measuring intermittently the flank wear as a function of cutting time under such established cutting

conditions for discontinuous broken chips; and (3) determining the tool life using the criteria specified in the ISO Standard 3685: 1993(E). Cutting tools except some uncoated carbide and ceramic were used with a mechanical chip breaker to induce chip breakage and avoid the generation of long continuous chips. The results obtained include the optimal cutting conditions for discontinuous chips, tool wear - cutting time curves, and records of tool life and tool failure mode for each tool material. From the measured tool life and cutting conditions, the amount of material removed by each cutting material was calculated. Coated carbide with CVD tri-phase coating showed the longest tool life that exceeded the twelve minute criterion and removed the highest amount of material per tool. Other tools failed by cutting edge chipping and their lives were shorter. DOE

N95-33409# Lawrence Livermore National Lab., Livermore, CA.
FEASIBILITY OF FULLERENE THIN FILMS FOR HIGH-SPEED ALL-OPTICAL SWITCHING
Howard W. H. Lee, Robert S. Hughes, Jr., Jeffrey E. Davis, Charles F. MConaghy, Alex V. Hamza, and Mehdi Balooch May 1994 3 p Presented at the CLEO 1994: Conference on Lasers and Electro-optics, Anaheim, CA, 8-13 May 1994
(Contract W-7405-eng-48)
(DE95-011735; UCRL-JC-116858; CONF-940582-8) Avail: CASI HC A01/MF A01

We measured the optical nonlinearity of fullerene thin films (C60,C70) from 710-850 nm and determined the figure of merit for all-optical switching. We also demonstrated, to our knowledge, the first fullerene-based all-optical switch. DOE

N95-33425# Oak Ridge National Lab., TN.
HIGH-SPEED, LOW-DAMAGE GRINDING OF ADVANCED CERAMICS, PHASE 1 Final Report
J. A. Kovach and S. Malkin (Massachusetts Univ., Amherst, MA.) Mar. 1995 115 p
(Contract DE-AC05-84OR-21400)
(DE95-011241; ORNL/SUB-92-SL807/1) Avail: CASI HC A06/MF A02

In manufacture of structural ceramic components, grinding costs can comprise up to 80% of the entire manufacturing cost. Most of these costs arise from the conventional multistep grinding process with numerous grinding wheels and additional capital equipment, perishable dressing tools, and labor. In an attempt to reduce structural ceramic grinding costs, a feasibility investigation was undertaken to develop a single step, roughing-finishing process suitable for producing high-quality silicon nitride ceramic parts at high material removal rates at lower cost than traditional, multistage grinding. This feasibility study employed combined use of laboratory grinding tests, mathematical grinding models, and characterization of resultant material surface condition. More specifically, this Phase 1 final report provides a technical overview of high-speed, low-damage (HSLD) ceramic grinding and the conditions necessary to achieve the small grain depths of cut necessary for low damage grinding while operating at relatively high material removal rates. Particular issues addressed include determining effects of wheel speed and material removal rate on resulting mode of material removal (ductile or brittle fracture), limiting grinding forces, calculation of approximate grinding zone temperatures developed during HSLD grinding, and developing the experimental systems necessary for determining HSLD grinding energy partition relationships. In addition, practical considerations for production utilization of the HSLD process are also discussed. DOE

N95-33635 Oak Ridge National Lab., TN. Metals and Ceramics Div.
INTERFACIAL COMPOSITION ANALYSIS OF SILICON NITRIDE WHISKER REINFORCED OXYNITRIDE GLASS SYSTEMS
E. Y. Sun, K. B. Alexander, P. F. Becher, and S. L. Hwang 1995 3 p Presented at the 53rd Annual Meeting of Microscopy Society of America, Kansas City, KS, 13-17 Aug. 1995 Limited Reproducibility: More than 20% of this document may be affected by microfiche quality
(Contract DE-AC05-84OR-21400)
(DE95-012895; CONF-950892-5) Avail: CASI HC A01

Scanning transmission electron microscopy combined with energy-dispersive x-ray spectroscopy and parallel-detection electron energy-loss spectroscopy was used to analyze the composition at interfaces in (beta)-Si3N4 whisker reinforced oxy nitride glass systems. DOE

N95-34022# Sandia National Labs., Albuquerque, NM.
ELECTRON BEAM JOINING OF STRUCTURAL CERAMICS
B. N. Turman, S. J. Glass, J. A. Halbleib, D. R. Helmich, and R. E. Loehman Apr. 1995 45 p
(Contract DE-AC04-94AL-85000)
(DE95-012521; SAND-95-0595; UC-704) Avail: CASI HC A03/MF A01

Feasibility of ceramic joining using a high energy (10 MeV) electron beam was studied. The experiments used refractory metals as bonding materials in buried interfaces between Si3N4 pieces. Because the heat capacity of the metal bonding layer is much lower than the ceramic, the metal reaches much higher temperatures than the adjoining ceramic. Using the right combination of beam parameters allows the metal to be melted without causing the adjoining ceramics to melt or decompose. Beam energy deposition and thermal simulations were performed to guide the experiments. Joints were shear tested and interfaces between the metal and the ceramic were examined to identify the bonding mechanism. Specimens joined by electron beams were compared to specimens produced by hot-pressing. Similar reactions occurred using both processes. Reactions between the metal and ceramic produced silicides that bond the metal to the ceramic. The molybdenum silicide reaction products appeared to be more brittle than the platinum silicides. Si3N4 was also joined to Si3N4 directly. The bonding appears to have been produced by the flow of intergranular glass into the interface. Shear strength was similar to the metal bonded specimens. Bend specimens of Si3N4 were exposed to electron beams with similar parameters to those used in joining experiments to determine how beam exposure degrades the strength. Damage was macroscopic in nature with craters being formed by material ablation, and cracking occurring due to excessive thermal stresses. Si was also observed on the surface indicating the Si3N4 was decomposing. Bend strength after exposure was 62% of the as-received strength. No obvious microstructural differences were observed in the material close to the damaged region compared to material in regions far away from the damage. DOE

N95-34282 Virginia Polytechnic Inst. and State Univ., Blacksburg, VA.
ADHESION OF NOVEL HIGH-PERFORMANCE POLYMERS TO CARBON FIBERS: FIBER SURFACE TREATMENT, CHARACTERIZATION, AND MICROBOND SINGLE FIBER PULL-OUT TEST Ph.D. Thesis
Cheryl Lavonne Heisey 1993 309 p
Avail: Univ. Microfilms Order No. DA9419215

The adhesion of carbon fibers to several high performance polymers, including a phosphorus-containing bismaleimite, a cyanate ester resin, and a pyridine-containing thermoplastic, was evaluated using the microbond single fiber pull-out test. The objective was to determine the chemical and mechanical properties of the fiber and the polymer which affect the fiber/polymer adhesion in a given composite system. Fiber/matrix adhesion is of interest since the degree of adhesion and the nature of the fiber/matrix interphase has a major influence on the mechanical properties of a composite. The surface chemical composition, topography, tensile strength, and surface energy of untreated AU-4 and commercially surface treated AS-4 carbon fibers were evaluated using x-ray photoelectron spectroscopy (XPS), scanning electron microscopy (SEM), single fiber tensile tests, and dynamic contact angle analysis. The commercial surface treatment which converted the AU-4 to the AS-4 fiber oxidized the carbon fiber surface. The surface of the AS-4 carbon fiber was further modified using air, oxygen, ammonia, and ethylene plasmas. The AS-4 fiber tow was also characterized following exposure to the aqueous poly(amic acid) solution used to disperse the matrix powder during aqueous suspension prepregging of thermoplastic matrix composites. The air and oxygen plasma treatments significantly oxidized and roughened the surface of the AS-4 carbon fibers. In addition, the air and oxygen plasma increased the polar component of the AS-4 fiber surface energy. The ammonia plasma increased the concentration of nitrogen on the fiber surface, without significantly altering the fiber topography (at a magnification of 50,000X). The atomic oxygen present in the air and oxygen plasma treatments is capable of reacting with both the edge and basal planes in the carbon fiber structure. As a result, the oxygen-containing plasmas progressively ablated the organic material in the carbon fiber surface. Energetic species in the ammonia plasma cleaned the fiber surface and reacted with the carbon fiber surface, increasing the concentration of amine groups in the fiber surface. The ethylene plasma deposited a layer of plasma polymerized polymer on the carbon fiber surface. The AS-4 carbon fibers were coated with poly(amic acid) when the tow was wet with

the aqueous suspension prepregging solution. The carbon fiber adhesion of bis(3-maleimito phenoxy) triphenylphosphine oxide was compared to that of Ciba-Geigy's Matrimid 5292 A/B bismaleimite system. With both bismaleimites, the carbon fiber adhesion increased significantly when the fiber received an oxidative commercial surface treatment or was exposed to an air or ammonia plasma prior to bonding. In contrast, the poly(pyritine-bis A) microbond pull-out test results showed that the carbon fiber adhesion of poly(pyritine-bis A) was not affected by the fiber surface chemical composition, fiber surface energy, or topography. Dissert. Abstr.

N95-34361# Case Western Reserve Univ., Cleveland, OH. Dept. of Macromolecular Science.

FROM LIQUID CRYSTAL POLYMERS CONTAINING CROWN ETHERS TO TAPERED BUILDING BLOCKS CONTAINING CROWN ETHERS WHICH SELF-ASSEMBLE INTO TUBULAR SUPERMOLECULES

V. Percec and G. Johansson 9 May 1995 14 p Submitted for publication in Macromolecular Symposia

(Contract N00014-89-J-1828)

(AD-A294359; Rept-6) Avail: CASI HC A02/MF A01

Molecular recognition directed self-assembly of supramolecular architectures or noncovalent synthesis, and molecular recognition directed self-assembly of transition states or self-synthesis, are two of the most active topics of research in the area of supramolecular chemistry. We are concerned with the use of the simplest endo-receptor i.e., crown ether in the design of two classes of systems. The first one is a system which is externally regulated by molecular recognition processes via a crown ether endo-receptor. This system is based on various classes of liquid-crystalline polymers which exhibit phase transitions that are manipulated by the reversible complexation of the crown ether present in different parts of their repeat unit with metal salts. The information gained from these experiments is then exploited in the design of the second group of systems. This consists of self-assembling building blocks containing various combinations of crown ether as endo-receptor and a tapered group as exo-receptor. Upon complexation with metal salts, these building blocks self-assemble into tubular supramolecular architectures. Therefore, while the first system exhibits molecular recognition directed phase transitions, the second one self-assembles into tubular supramolecular architectures via various molecular recognition processes. These tubular supramolecular architectures display a thermotropic hexagona columnar (phi h) liquid crystalline phase, which enables the structure of the self-assembled supramolecular architecture to be determined by X-ray diffraction experiments. DTIC

N95-34447 Department of the Navy, Washington, DC.

METHOD OF FORMING THIN FILMS ON SUBSTRATES AT LOW TEMPERATURES Patent

Monti E. Aklufi, inventor (to Navy) 21 Mar. 1995 7 p Filed 28 Feb. 1994

(AD-D017470; US-Patent-5,399,388; US-Patent-Appl-SN-207312; US-Patent-Class-427-575) Avail: US Patent and Trademark Office

A method is provided for forming thin films, such as high temperature superconductors, on a surface of a substrate using pulsed microwaves to control substrate temperature. The method includes vaporizing a liquid source to form a series of vapor pulses, irradiating the vapor pulses and a makeup gas with pulsed microwaves, and exposing the surface of the substrate to the irradiated mixture to form a thin film on the surface. The microwaves may be pulsed to coincide with the arrival of the vapor pulses at the substrate, thus reducing the amount of material consumed and the amount of waste. Further, the plasma may be closely confined to the substrate with a dielectric waveguide to reduce the power required for irradiating for mixture and to prevent the formation of stray deposits on surfaces enclosing the substrate. DTIC

N95-34452# State Univ. of New York, Buffalo, NY. Dept. of Chemistry.

SYNTHESIS AND CHARACTERIZATION OF A SERIES OF ORGANOINDIUM-PHOSPHIDES INCLUDING MOLECULAR STRUCTURES OF {(Me3CCH2)2InPEt2)2 AND ((Me3CCH2)2InP(H)(C6H11))3

O. T. Beachley, Jr., John D. Maloney, Michael A. Banks, and Robin D. Rogers (University of Northern Illinois, De Kalb, IL.) 5 Mar. 1995 37 p

(Contract N00014-90-J-1530)

(AD-A293965; TR-41) Avail: CASI HC A03/MF A01

A series of organoindium-phosphides including (Me3CCH2)2InPRR' (R = R' =Et, C6H11; R = C6H11, R' = H; R = Me, R' = Ph) and (Me3SiCH2)2InP(Me)Ph have been prepared and characterized. The characterization data include partial elemental analyses (C, H), 1H and 31P NMR and IR spectral studies, physical properties, cryoscopic molecular weight studies (with the exception of ((Me3CCH2)2InPEt2)2 and ((Me3CCH2)2InP(H)(C6H11))3. The compound (Me3CCH2)2InPEt2 is observed to be a dimer in benzene solution; (Me3CCH2)2InP(H)(C6H11) observed to be a dimer in benzene solution; (Me3CCH2)2InP(H)(C6H11) exists as a dimer-trimer equilibrium mixture whereas (Me3CCH2)2InP(Me)(Ph) and (Me3SiCH2)2InP(Me)(Ph) are trimers. NMR studies are consistent with (Me3CCH2)2InP(C6H11)2 being a dimer in benzene solution but the concentration was too low to confirm the conclusion by cryoscopic molecular weight studies. DTIC

N95-34476# Texas Univ., Austin, TX.

LOW TEMPERATURE GROWTH OF THIN FILMS BY HIGH KINETIC ENERGY SUPERSONIC MOLECULAR BEAMS Final Technical Report, 1 Mar. 1992 - 31 Oct. 1993

Charles B. Mullins and Abdelkrim Sellidj 24 Feb. 1995 8 p

(Contract N00014-92-J-1342)

(AD-A294516) Avail: CASI HC A02/MF A01

This grant initiated our work in low temperature deposition by supersonic jets. The attached draft manuscript details our work in growing GaAs thin films by jets of a single-source precursor and suggest that rapid growth and very smooth films can be attained. DTIC

N95-34494# Southwest Research Inst., San Antonio, TX. Belvoir Fuels and Lubricants Research Facility.

EVALUATION OF HIGH-TEMPERATURE LUBRICANT UNDER CYCLIC OPERATING CONDITIONS Interim Report, Apr. 1993 - Sep. 1994

Edwin A. Frame and Douglas M. Yost May 1995 75 p

(Contract DAAK70-92-C-0059)

(AD-A294444; TFLRF-301) Avail: CASI HC A04/MF A01

The performance of a candidate high-temperature lubricant was determined under cyclic operating conditions of idle, maximum torque, and maximum power at intermediate and high oil temperatures. The results were compared with previous oil performance results obtained during steady-state, high-temperature operation. Operation at the cyclic conditions resulted in approximately twice the piston top groove fill deposits. This result confirmed the need to include cyclic operation requirements in any future high-temperature lubricant specification. DTIC

N95-34502# Naval Undersea Warfare Center, New London, CT.

A MOLECULAR DYNAMICS INVESTIGATION OF THE STRUCTURAL CHARACTERISTICS OF AMORPHOUS AND ANNEALED POLY (VINYLIDENE FLUORIDE) AND VINYLIDENE FLUORIDE - TRIFLUOROETHYLENE COPOLYMERS Final Report

Robert W. Holman and George J. Kavarnos 17 Apr. 1995 29 p

(AD-A294116; NUWC-NL-TR-10857) Avail: CASI HC A03/MF A01

Molecular dynamics (MD) computations predict that the percentage of gauche bonds for poly(vinylidene fluoride) PVDF is greater than that for the 50 mol% copolymer with trifluoroethylene, at high temperature and after annealing. PVDF is enriched in gauche conformations on cooling whereas the copolymer acquires more trans conformations. The MD results are consistent with experimental trends that have been observed for these piezoelectric polymers. DTIC

N95-34563# Air Force Inst. of Tech., Wright-Patterson AFB, OH.

ION ASSISTED DEPOSITION OF ZnS AND MgF2

Gu Pei Fu, Chen Yuming, Hu Xuequn, and Tang Jinfa (Zhejiang Univ., China.) 1 May 1995 17 p Transl. into ENGLISH from Guangxue Xuebao (China), v. 9, no. 9, Sep. 1989 p 815-822

(AD-A294759; NAIC-ID(RS)T-0758-94) Avail: CASI HC A03/MF A01

ZnS and MgF2 films have been prepared by Ar ion assisted deposition. The packing density of MgF2 has been increased from 0.8 to 0.9-0.95 without ion bombardment as determined by the wavelength shift measurement after moisture absorption by filter. It is shown that high energy bombardment (greater than 1 keV) increases the absorption and scattering loss, while the low energy bombardment is shown to increase significantly the abrasion resistance and adherence of film without affecting

the optical properties. Therefore, it will play a very important role in preparing durable coatings for temperature sensitive substrate. DTIC

N95-34596# Texas Univ., Austin, TX. Dept. of Chemistry.
ELEMENTAL FLUORINE BASED SYNTHESES OF PENTAFLUORO PHENYL AND OTHER AROMATIC PERFLUOROPOLYETHER POLYMERS Final Report, 1 Feb. 1992 - 31 Jan. 1995
Richard J. Lagow 31 Jan. 1995 74 p
(Contract F49620-92-J-0104)
(AD-A294930; AFOSR-95-0422TR) Avail: CASI HC A04/MF A01

As an approach to the preparation of organic molecules with very high thermooxidative stability, a study was carried out on the preparation of perfluorinated aromatic compounds by liquid-phase direct fluorination of aromatic hydrocarbon precursors followed by reductive defluorination. Diphenylether was converted to a perfluoro(dicyclohexylether) intermediate, however reductive defluorination afforded perfluoro(benzofuran) rather than perfluoro(diphenylether). By contrast, biphenyl was converted in high yield to perfluoro(dicyclohexyl) which, upon reductive defluorination afforded perfluoro(diphenyl). Diphenyl ketone was converted to perfluoro(dicyclohexyl) ketone, reductive defluorination of which is under investigation. Similarly, the o-, m-, and p- isomers of diphenoxybenzene were successfully fluorinated to the corresponding perfluoro(dicyclohexanoxylcyclohexanes), the reductive defluorination of which is under investigation. DTIC

N95-34614# Hughes Aircraft Co., Tucson, AZ.
ZERO DISCHARGE ORGANIC COATINGS: POWDER PAINT - UV CURABLE PAINT - E-COAT Quarterly Technical Report, Jan. - Mar. 1995
James Leal, Stephen J. Spadafora (Naval Air Warfare Center, Warminster, PA.), Richard D. Granata (Lehigh Univ., Bethlehem, PA.), Steven R. Felstein, and Srini Raghavan (Arizona Univ., Tucson, AZ.) Mar. 1995 30 p
(Contract MDA972-93-C-0020; ARPA Order 9328)
(AD-A293573; ZDOC/9501) Avail: CASI HC A03/MF A01

The Zero Discharge Organic Coatings (ZDOC) R&D project will substantially advance coatings technology through the development of high performance zero-discharge coating systems. Development efforts are proceeding on three coating technologies, powder paint, ultraviolet (UV) curable paint, and electro-coating (E-coat) paint. These three paint technologies offer the potential of high performance coatings with no volatile organic compound (VOC) emissions or hazardous waste generation. These three technologies and their associated application processes will be applicable to a wide variety of military equipment and structures, thereby eliminating volatile organic compound (VOC's) and toxic heavy metals from coatings and painting operations. The ZDOC team of Hughes Aircraft Company, Lehigh University, University of Arizona, and the Naval Air Warfare Center Aircraft Division Warminster offers a blend of experience, expertise, and capabilities in all aspects of organic coatings technology. This quarterly report reviews the team's technical activities and results during the period January-March 1995. DTIC

N95-34649# Pennsylvania State Univ., University Park, PA. Dept. of Chemistry.
MOLECULAR MOTION OF PHOSPHAZENE-BOUND NLO CHROMOPHORES
Harry R. Allcock, Charles E. Cameron, Timothy W. Skloss (Texas A&M Univ., College Station, TX.), Sharon Taylor-Meyers (Texas A&M Univ., College Station, TX.), and Kenneth J. Wynne (Texas A&M Univ., College Station, TX.) 17 Apr. 1995 38 p Submitted for publication in Macromolecules
(Contract N00014-91-J-1194)
(AD-A293526; TR-26) Avail: CASI HC A03/MF A01

The behavior of NLO groups linked to a polyphosphazene chain was studied by solid state NMR spectroscopy. A series of poly(organophosphazenes) was prepared and characterized. Variable-temperature solid state C-13 Nuclear Magnetic Resonance (NMR) spectra indicated that the use of a longer spacer group between the polymer backbone and the aromatic portion of the NLO side group lowered the temperature at which chromophore motion is quenched. This implied that the use of such structures may accelerate the randomization of NLO side group orientation at ambient temperatures following poling. This behavior was mirrored in the solid state variable-temperature 31p NMR spectra, which suggested that side chain and polymer backbone may be coupled. DTIC

N95-34798# Oak Ridge National Lab., TN.
R-CURVE BEHAVIOR OF WHISKER-REINFORCED CERAMIC COMPOSITES
Chun-Hway Hsueh and P. F. Becher 1995 3 p Presented at the 2nd International Conference on High Temperature Ceramic Matrix Composites, Santa Barbara, CA, 21-25 Aug. 1995
(Contract DE-AC05-84OR-21400)
(DE95-012873; CONF-9508127-1) Avail: CASI HC A01/MF A01

Ceramics have attracted great interest for advanced heat engines and industrial applications as a result of their stiffness, light weight, corrosion resistance, and superior performance at high temperatures. However, their utilization in engineering applications is severely limited by their brittleness. One approach toward substantially reducing this brittleness is by incorporating strong whiskers into the ceramic matrix. Studies of whisker-reinforced ceramic composites have shown both rising fracture resistance with crack extension (i.e. R-curve behavior) and a three- to four-fold increase in steady-state toughness. The primary toughening mechanism is bridging of the crack surface by whiskers. This paper discusses the bridging mechanism in detail and presents R-curves for SiC whisker-reinforced Al2O3 composites. DOE

N95-34817# Uniax Corp., Santa Barbara, CA.
INDUSTRIAL PRODUCTS BASED UPON PROCESSIBLE CONDUCTIVE POLYANILINE Final Technical Report, 15 Feb. 1993 - 14 Aug. 1994
Floyd Klavetter Apr. 1995 34 p
(Contract F49620-93-C-0011)
(AD-A294985; AFOSR-95-0418TR) Avail: CASI HC A03/MF A01

From a detailed analysis of the behavior of two general type of organic solvents for conducting polyaniline, we conclude that fully protonated polyaniline (ratio H+/PhN=O.5) can be dissolved in a given organic solvent only in cases where the PANI-(acid)O.5 complex is solvated by an appropriate solvating agent. At least 0.5 moles per PANI unit (PhN) of the solvating agent must be present (this amount is dependent on nature of counterion and solvent, for example for very polar counterion in non-polar solvent this value is 1.0). The solvating agent can be the solvent itself if it has strong hydrogen bonding moieties, an excess amount of protonic acid, or some neutral compound with strong hydrogen bonding moieties which is compatible with the solvent. We have shown clearly that the solution properties (solubility, conformation, etc.) of conducting PANI prepare by counterion induced processibility are strongly dependent on the interactions between the polymer chain, the counterions, and the co-solvent. The solid state properties (conductivity, crystallinity, etc.) of a PANI film processed from such a solution are dependent on the choice of counterion, solvent, and co-solvent. The co-solvent can be removed after processing without altering the solid state properties of the resulting polyaniline films or fibers. DTIC

28 PROPELLANTS AND FUELS

Includes rocket propellants, igniters, and oxidizers; their storage and handling procedures; and aircraft fuels.

For related information see also *07 Aircraft Propulsion and Power*, *20 Spacecraft Propulsion and Power*, and *44 Energy Production and Conversion*.

N95-32563# Institute of Gas Technology, Des Plaines, IL.
GASOLINE FROM NATURAL GAS BY SULFUR PROCESSING Quarterly Report, Oct. 1994 - Dec. 1994
E. J. Erekson and F. Q. Miao Feb. 1995 11 p
(Contract DE-AC22-93PC-92114)
(DE95-010651; DOE/PC-92114/T6) Avail: CASI HC A03/MF A01

This report presents the work performed at the Institute of Gas Technology (IGT) during the sixth program quarter from October to December 31, 1994. The overall objective of this research project is to develop a catalytic process to convert natural gas to liquid transportation fuels. The process consists of two steps that each use catalysts and sulfur-containing intermediates: (1) converting natural gas to CS(sub 2) and (2) converting CS(sub 2) to gasoline-range liquids. Experimental data will be generated to demonstrate the potential of catalysts and the overall process. During this quarter, progress in the following areas has been made: (1) Two catalysts were prepared for the reaction of methane with hydrogen sulfide to produce carbon sulfide; (2) A total of 48 runs with catalysts IGT-MS-109 and

IGT-MS-102 were performed for the methane with hydrogen sulfide reaction; (3) Methane conversion reached 100% at temperatures above 1000 C; (4) For IGT-MS-109 and IGT-MS-102, carbon disulfide was produced, but these catalysts also produced significant amounts of sulfur and carbon. DOE

N95-32605# Los Alamos National Lab., NM.
INVESTIGATION ON DEFLAGRATION TO DETONATION TRANSITION IN POROUS ENERGETIC MATERIALS Final Report
D. Scott Stewart 1995 58 p Prepared in cooperation with Illinois Univ., Urbana, IL
(Contract W-7405-eng-36)
(DE95-011638; LA-SUB-94-172) Avail: CASI HC A04/MF A01

Focus of the work was on deflagration to detonation in porous energetic materials, with some activity on detonation shock dynamics. Both efforts were in direct support of the development of computational models for explosive system design and explosive safety. DOE

N95-33254 Pennsylvania State Univ., University Park, PA.
OBSERVATIONS OF SURFACE STRUCTURE AND REGRESSION BEHAVIOR OF SOLID PROPELLANT STRANDS BURNING UNDER NARROW GAP CONDITIONS Ph.D. Thesis
Richard Field 1993 241 p
Avail: Univ. Microfilms Order No. DA9414278

The combustion of solid propellants in gun applications occurs over a wide range of pressures and other time dependent physical conditions. In highly packed propellant charges with closely spaced propellant grain surfaces, the one-dimensional flame zone structures normally associated with homogeneous and nitramine propellants may be altered. This may affect the overall energy release rate and the burning rate through changes in heat transfer within the combustion wave structure. The objective of this study was to examine the combustion behavior of two closely-spaced propellant surfaces. Strand burning rates were measured at constant pressures while maintaining two burning propellant surfaces at constant separation distances. A constant gap strand burner system was developed. Optical position sensing was used to control two motor-driven stages. Microthermocouples were employed to evaluate the condensed phase and near surface thermal profiles. Comparisons were made of the flame zone and burning surface features of a plastisol double-base and a nitramine propellant. Quartz probe gas sampling from the dark zone of the double-base propellant was demonstrated. A purged-probe method was developed to prevent probe blockage by combustion particulates. The gap burning rates of the double-base propellant at surface separations of 1 mm were essentially unchanged from single strand rates at pressures from 0.6 to 2.7 MPa. Under the counterflow conditions of gap burning, the luminous flame zone cannot form above the burning surface; however, conclusions on the influence of the luminous flame on the burning rate require further evaluation of the radiative properties of the burning surfaces. The burning surface and flame structure of the double-base propellant revealedcomplex, multi-dimendonal structures at the lower pressures. Randomly distributed surface reaction wave formation and propagation within the burning surface was observed The luminous flame exhibited distributed flamelets, which may be due to condensed phase surface residues and the low propellant burning rate. Thermal profiles for the double-base propellant revealed test-to-test non-uniformities at the burning surface, and an apparent temperature-dependent thermal diffusivity in the condensed-phase preheat layer. The surface reaction wave structure of the propellant was concluded to be responsible for poor reproducibility in thermocouple tests.
Dissert. Abstr.

N95-33332# Swedish Transport and Communications Research Board, Stockholm (Sweden).
INTRODUCTIONS OF FFV [INTRODUKTION AV FFV-BILAR]
Ake Brandberg, Lovisa Johansson, and Bengt Saevbark Nov. 1994 84 p In SWEDISH
(ISSN 0282-8014)
(PB95-214656; KFB-1994:11; ISBN-91-88370-70-4) Avail: CASI HC A05/MF A01

The purpose is to describe background, objectives and technique for Fuel Flexible Vehicles (FFV), development status and models for possible introduction in Sweden. The conclusion of the report is that introduction of FFV's using alcohol and gasoline is a possible route to reach the broad market and continued efforts are recommended. The conclusions are based in the facts that tests show reduced emissions damaging health and environment, cold starting can be improved and extended to use of pure alcohols, FFV is a cheap alternative for unchanged use of the automobile, there is opportunity to phase over from fossil to bio-based alcohols, the need of FFV's lasts over a very long period after the introduction. NTIS

N95-33395# Argonne National Lab., IL.
ALTERNATIVE-FUELS TECHNOLOGY: NATURAL GAS VEHICLES AS A WAY TO CURB URBAN AIR POLLUTION
Feb. 1995 12 p Presented at the Society of Automotive Engineers International Congress and Exposition, Detroit, MI,27 Feb. - 2 Mar. 1995
(Contract W-31-109-eng-38)
(DE95-012216; ANL/ES/CP-85765; CONF-950256-6) Avail: CASI HC A03/MF A01

This report describes the use of natural gas as an alternative fuel in various vehicles. Safety and emissions resulting from combustion are briefly discussed. DOE

N95-33702# Los Alamos National Lab., NM.
THE OXIDATION OF ENERGETIC MATERIALS IN SUPERCRITICAL WATER Final Report
S. J. Buelow, D. Allen, G. K. Anderson, F. L. Archuleta, J. H. Atencio, G. T. Baca, W. D. Breshears, T. J. Butenhoff, P. C. DellOrco, and R. B. Dyer et al 3 Apr. 1995 222 p
(Contract W-7405-eng-36)
(DE95-010888; LA-UR-95-1164) Avail: CASI HC A10/MF A03

The objective of this project was to determine the suitability of oxidation in supercritical fluids (SCO), particularly water (SCWO), for disposal of propellants, explosives, and pyrotechnics (PEP's). The SCO studies of PEP's addressed the following issues: The efficiency of destruction of the substrate. The products of destruction contained in the effluents. Whether the process can be conducted safely on a large scale. Whether energy recovery from the process is economically practicable. The information essential for process development and equipment design was also investigated, including issues such as practical throughput of explosives through a SCWO reactor, reactor materials and corrosion, and models for process design and optimization.
DOE

N95-33876*# National Aeronautics and Space Administration. Lewis Research Center, Cleveland, OH.
METALLIZED GELLED PROPELLANTS: OXYGEN/RP-1/ALUMINUM ROCKET COMBUSTION EXPERIMENTS
Bryan Palaszewski and James S. Zakany (NYMA, Inc., Brook Park, OH.) Aug. 1995 34 p Presented at the 31st Joint Propulsion Conference and Exhibit, San Diego, CA, 10-12 Jul. 1995; cosponsored by AIAA, ASME, SAE, and ASEE
(Contract NAS3-27186; RTOP 232-01-00)
(NASA-TM-107025; E-9838; NAS 1.15:107025; AIAA Paper 95-2435)
Avail: CASI HC A03/MF A01

A series of combustion experiments were conducted to measure the specific impulse, Cstar-, and specific-impulse efficiencies of a rocket engine using metallized gelled liquid propellants. These experiments used a small 20- to 40-1bf (89- to 178-N) thrust, modular engine consisting of an injector, igniter, chamber and nozzle. The fuels used were traditional liquid RP-1 and gelled RP-1 with 0-, 5-, and 55-wt% loadings of aluminum and gaseous oxygen was the oxidizer. Ten different injectors were used during the testing: 6 for the baseline 02/RP-1 tests and 4 for the gelled fuel tests which covered a wide range of mixture ratios. At the peak of the Isp versus oxidizer-to-fuel ratio (O/F) data, a range of 93 to 99% Cstar efficiency was reached with ungelled 02/RP-1. A Cstar efficiency range of 75 to 99% was obtained with gelled RP-I (0-wt% RP-1/Al) while the metallized 5-wt% RP-1/Al delivered a Cstar efficiency of 94 to 99% at the peak Isp in the O/F range tested. An 88 to 99% Cstar efficiency was obtained at the peak -Isp of the gelled RP1/Al with 55-wt% Al. Specific impulse efficiencies for the 55-wt% RP-1/Al of 67%-83% were obtained at a 2.4:1 expansion ratio. Injector erosion was evident with the 55-wt% testing, while there was little or no erosion seen with the gelled RP-1 with 0- and 5-wt% Al. A protective layer of gelled fuel formed in the firings that minimized the damage to the rocket injector face. This effect may provide a useful technique for engine cooling. These experiments represent a first step in characterizing the performance of and operational issues with gelled RP-1 fuels. Author

29 MATERIALS PROCESSING

Includes space-based development of products and processes for commercial applications.

For biological materials see *55 Space Biology.*

N95-32718*# National Aeronautics and Space Administration. Lewis Research Center, Cleveland, OH.

NUMERICAL SIMULATION OF HEAT AND MASS TRANSPORT DURING SPACE CRYSTAL GROWTH WITH MEPHISTO

Minwu Yao (Ohio Aerospace Inst., Cleveland, OH.), Raghu Raman (Florida Univ., Gainesville, FL.), and Henry C. deGroh, III Jul. 1995 32 p

(RTOP 674-21-05)

(NASA-TM-107015; E-9800; NAS 1.15:107015) Avail: CASI HC A03/MF A01

The MEPHISTO space experiments are collaborative United States and French investigations aimed at understanding the fundamentals of crystal growth. Microgravity experiments were conducted aboard the USMP-1 and -2 missions on STS-52 and 62 in October 1992 and March 1994 respectively. MEPHISTO is a French designed and built Bridgman type furnace which uses the Seebeck technique to monitor the solid/liquid interface temperature and Peltier pulsing to mark the location and shape of the solid/liquid interface. In this paper the Bridgman growth of Sn-Bi and Bi-Sn under terrestrial and microgravity conditions is modeled using the finite element code, FIDAP*. The numerical model considers fully coupled heat and mass transport, fluid motion and solid/liquid phase changes in the crystal growth process. The primary goals of this work are: to provide a quantitative study of the thermal buoyancy-induced convection in the melt for the two flight experiments; to compare the vertical and horizontal growth configurations and systematically evaluate the effects of various gravity levels on the solute segregation. Numerical results of the vertical and horizontal Bridgman growth configurations are presented. Author

N95-32929*# California Univ., Berkeley, CA. Dept. of Mechanical Engineering.

A FUNDAMENTAL STUDY OF SMOLDERING WITH EMPHASIS ON EXPERIMENTAL DESIGN FOR ZERO-G Final Progress Report

Carlos Fernandez-Pello and Patrick J. Pagni Aug. 1995 276 p

(Grant NAG3-443)

(NASA-CR-198378; NAS 1.26:198378) Avail: CASI HC A13/MF A03

A research program to study smoldering combustion with emphasis on the design of an experiment to be conducted in the space shuttle was conducted at the Department of Mechanical Engineering, University of California, Berkeley. The motivation of the research is the interest in smoldering both as a fundamental combustion problem and as a serious fire risk. Research conducted included theoretical and experimental studies that have brought considerable new information about smolder combustion, the effect that buoyancy has on the process, and specific information for the design of a space experiment. Experiments were conducted at normal gravity, in opposed and forward mode of propagation and in the upward and downward direction to determine the effect and range of influence of gravity on smolder. Experiments were also conducted in microgravity, in a drop tower and in parabolic aircraft flights, where the brief microgravity periods were used to analyze transient aspects of the problem. Significant progress was made on the study of one-dimensional smolder, particularly in the opposed-flow configuration. These studies provided enough information to design a small-scale space-based experiment that was successfully conducted in the Spacelab Glovebox in the June 1992 USML-1/STS-50 mission of the Space Shuttle Columbia. Author

31 ENGINEERING (GENERAL)

Includes vacuum technology; control engineering; display engineering; cryogenics; and fire prevention.

N95-32568# Lawrence Livermore National Lab., Livermore, CA.

RICOR K506B CRYOCOOLER PERFORMANCE DURING THE CLEMENTINE MISSION AND GROUND TESTING

Robert E. Priest, Jeffrey A. Robinson, Thomas L. Clark, Dean R. Hadley, and Noel R. Sewall Sep. 1994 11 p Presented at the 8th International Cryocooler Conference, Vail, CO, 28-30 Jun. 1994 Submitted for publication

(Contract W-7405-eng-48)

(DE95-010683; UCRL-JC-118345; CONF-940665-2) Avail: CASI HC A03/MF A01

Two Ricor K506B Stirling cycle cryocoolers with H-10 control electronics were used on the Clementine spacecraft, one cooling a 256 x 256 InSb infrared detector for the near-infrared (NIR) camera and the other cooling a 128 x 128 HgCdTe focal plane array on the longwave infrared (LWIR) camera. This is the first use of these Ricor Stirling cryocoolers in a space environment. This mission has demonstrated the use of these Clementine lightweight imaging sensors in the demanding environment of space, and has space-qualified this Ricor cryocooler. Moreover, nearly the entire 38 million square kilometers of the Moon's surface was mapped in 11 spectral bands, six in the near-infrared, during the 71 days of lunar mapping. The more than 1.6 million digital images collected are providing-mineral typing scientific data to the international civilian scientific community. The NIR cryocooler operated successfully for a total of 840 hours with 361 on/off cycles. The H-10 electronics provided good focal plane array (FPA) temperature control with a typical operating FPA temperature of 70.3 K and a one-sigma variation of 0.46 K. The thermal environment for the cooler ranged from -23.7 C to 38.2 C. The Ricor cryocooler used on the LWIR camera performed the same during the Clementine mission as it did on the ground. This cryocooler ran for a total of 670 hours with 359 on/off cycles. The H-10 electronics were not able to provide FPA temperature control. This inability to operate at a fixed set point is believed to be caused by a ground difference between the H-10 controller electronics and the FPA temperature sense diode. The FPA temperature varied in proportion to the cryocooler (heat reject) temperature. The FPA temperature during imaging varied from 66.9 K to greater than 85 K. The thermal environment for this cooler ranged from -22.1 C to 41.0 C. DOE

N95-32585# Los Alamos National Lab., NM.

NUMERICAL ANALYSIS OF THE ULTRAPRECISION MACHINING OF COPPER

Robert Stevens, Charles Anderson, Richard Rhorer, and Don Lucca (Oklahoma State Univ., Stillwater, OK.) 1995 6 p Presented at the 8th Annual IPES Meeting, Compiegne, France, 6-12 May 1995

(Contract W-7405-eng-36)

(DE95-007857; LA-UR-95-626; CONF-9505203-1) Avail: CASI HC A02/MF A01

Modeling of the ultraprecision machining process can aid in the understanding of the relative importance of various process parameters and ultimately lead to improved methods of generating ultraprecision surfaces such as those required for metal optics and single crystal microelectronics substrates. Any modeling method should be verified by direct comparison to experimental data. Until recently it has been difficult to accurately measure the cutting edge, or sharpness, of a diamond tool; and therefore, most models have assumed an infinitely sharp cutting tip. With the relatively new technology of the Atomic Force Microscope (AFM), the cutting edge of single crystal diamond tools can be quantitatively described. Ultraprecision machining experiments using an AFM characterized cutting tool and orthogonal geometry have been performed. These experiments have resulted in measured cutting and thrust forces for different depths of cut in copper (Te-Cu: 99.4-99.5% Cu, 0.5-0.6% Te, 4-5 micron grain size, 225 MPa yield strength) with a well characterized diamond tool. By using this actual tool tip geometry the authors have been able to develop a model that can predict cutting and thrust forces for depths of cut on the order of the sharpness of the tool. Forces predicted by this numerical model are compared to the experimentally measured forces. DOE

N95-32785# General Accounting Office, Washington, DC. Resources, Community, and Economic Development Div.

METRIC CONVERSION: FUTURE PROGRESS DEPENDS UPON PRIVATE SECTOR AND PUBLIC SUPPORT. REPORT TO CONGRESSIONAL REQUESTERS

13 Jan. 1994 72 p

(GAO/RCED-94-23; B-238858) Avail: CASI HC A04/MF A01; GAO, PO Box 6015, Gaithersburg, MD 20877 HC

In reviewing federal metric conversion (metrication) activities, the General Accounting Office (GAO) evaluated federal agency activities in (1) establishing metric guidelines and preparing reports on the transition, (2) using the metric system in procurements, (3) using the metric system in

grants and other business activities, and (4) dealing with private sector and public attitudes toward conversion. Since 1990, federal preparations for metric conversion have advanced dramatically, with more than 30 agencies having developed some combination of guidelines, transition plans, and progress reports that indicate a substantially greater commitment to metrication. However, they are still facing serious difficulties in putting their plans into practice. These difficulties include a procurement environment in which most products are nonmetric and in which federal agencies represent too small a share of the total market to stimulate private sector conversion. Mixed progress has been made toward metric conversion in the areas of federal grants and other business activities. Grants for research require the use of the metric system, but such a commitment has not been made for grants in other areas, such as housing and education. Agencies that undertake other business-related activities, such as federal programs involving farmers or highway signs, are concerned about private sector and public resistance to conversion. Now that most agencies have made significant progress in preparing for metric conversion, a broader national dialogue between the government, the private sector, and the public is needed to discuss the next steps in decision-making about metric conversion. CASI

N95-32984# Osaka Univ., Osaka (Japan). Faculty of Engineering.
TECHNOLOGY REPORTS OF THE OSAKA UNIVERSITY, VOL. 45, NOS. 2205-2216
15 Apr. 1995 102 p
(ISSN 0030-6177)
Avail: CASI HC A06/MF A02

These reports from Osaka University include a multitude of disciplines ranging from: mathematics and physics; metallurgy and welding engineering; electrical, electronic, communication, and information system engineering; mechanical engineering; and civil, architectural, environmental, and ocean engineering, and naval architecture. For individual titles, see N95-32985 through N95-32994.

N95-32985# Osaka Univ., Osaka (Japan). Dept. of Nuclear Engineering.
CALCULATIONS OF SPATIAL HIGHER MODES WITHOUT DEFLATION PROCEDURE **c72**
Takeo Nishigori and Toshikazu Takeda *In its* Technology Reports of the Osaka Univ. Vol. 45, Nos. 2205-2216 15 Apr. 1995 p 1-6 (For primary document see N95-32984 12-31)
(Rept-2205) Avail: CASI HC A02/MF A02

A new method is proposed to calculate higher-mode eigenvalues and eigenfunctions of the neutron transport (or diffusion) equation. The method assumes that an approximate eigenvalue is known. It provides a highly efficient way of calculating any higher mode because it does not involve the deflation procedure, which is necessary in the well-known power method in the matrix eigenvalue problem. When applied to the results of the WKB approximation proposed in a previous paper, it reduces the error due to the WKB approximation, giving very accurate eigenvalues and eigenfunctions. Higher modes in a 2D diffusion problem are calculated to demonstrate the effectiveness of the present method. Author

N95-32986# Osaka Univ., Osaka (Japan). Dept. of Applied Physics.
PRACTICAL IMPROVEMENT OF MS-X ALPHA MOLECULAR ORBITAL CALCULATION AS APPLIED TO DISSOCIATION PROCESS OF CO MOLECULE **c72**
Yoshihiro Irokawa, Masatsugu Honjo, Yoshizo Takai, and Ryuichi Shimizu *In its* Technology Reports of the Osaka Univ., Vol. 45, Nos. 2205-2216 15 Apr. 1995 p 7-16 (For primary document see N95-32984 12-31)
(Rept-2206) Avail: CASI HC A02/MF A02

A practical improvement for MS-X alpha molecular orbital method has been proposed, which enables non-muffin-tin (NMT) correction to be achieved with reasonable accuracy. The proposed correction based on the first order perturbation theory allows us to perform the calculations easily without requiring such profound knowledge and experience of complicated calculation procedures as does the highly advanced LMTO or FLAPW methods, though the accuracy is not so much high as these methods. The present approach was applied to CO dissociation processes by calculating the total energy curves of the ground and excited states as a function of bond length. The result has indicated that the present approach describes CO dissociation processes with considerable success, ensuring the practical assist, particularly, for experimentalists. Author

N95-32987# Osaka Univ., Osaka (Japan). Dept. of Welding and Production Engineering.
ANALYSIS OF EVAPORATION IN LASER WELDING **c70**
Isamu Miyamoto *In its* Technology Reports of the Osaka Univ., Vol. 45, Nos. 2205-2216 15 Apr. 1995 p 17-26 (For primary document see N95-32984 12-31)
(Rept-2207) Avail: CASI HC A02/MF A02

The evaporation process in CO2 laser welding was analyzed experimentally on the basis of evaporation and soot deposition rates, light scattering and plasma behavior. Heavier shielding gas results in more soot deposition by carrying the condensed particles to the work surface. At power density, 2-3 x 10(exp 5) W/sq cm), which is just below the critical value for deep penetration welding, the soot deposition becomes heaviest with accompanying violent fluctuation of the light emission of the plasma. A hypothetical mechanism of the soot deposition is proposed; at 2-3 x 10(exp 5) W/sq cm, the molten pool surface is hemispherically depressed by the recoil force of evaporation, and acts like a concave mirror to refocus the reflected laser beam within the plasma plume to heat it up. The adiabatic expansion of the plasma caused by the molten pool motion plays an important role to condense the vapor into the soot. Author

N95-32988# Osaka Univ., Osaka (Japan). Dept. of Electromagnetic Energy Engineering.
MEASUREMENT OF LASER WAVEFRONT USING SHACK HARTMANN METHOD WITH NEW LENS ARRAY **c36**
Geun Young Yoon, Takahisa Jitsuno, Masahiro Nakatsuka, and Sadao Nakai *In its* Technology Reports of the Osaka Univ., Vol. 45, Nos. 2205-2216 15 Apr. 1995 p 27-33 (For primary document see N95-32984 12-31)
(Rept-2208) Avail: CASI HC A02/MF A02

The purpose of this research is the laser wavefront control for the improvement of irradiation uniformity in laser fusion. An active optical system would be introduced as a method of wavefront control. The system measures laser wavefront distortion and controls the wavefront using a deformable mirror just before target irradiation optics. In this paper, the laser wavefront measurement for large optical devices using Shack Hartmann method is reported. Shack Hartmann wavefront sensor needs a lens array composed of small segmented lenses. A new microlens array developed for this measurement is made of optical plastic material. The individual lenses (in total number 900) have the rectangular shape of 300 x 300 sq micron and the focal length of 10 mm. Each lenslet gives the same spot size (60 micron) at the focus with nearly constant peak intensity. A deformable mirror is deformed with appropriate defocus and astigmatism for evaluating the accuracy of wavefront sensor. The difference of lower order Zernike coefficients between our Shack Hartmann wavefront sensor and a Fizeau interferometer is less than lambda/10 (lambda = 632.8 nm). Author

N95-32989# Osaka Univ., Osaka (Japan). Dept. of Electromagnetic Energy Engineering.
CONTROL OF THE LASER BEAM IRRADIATION INTENSITY DISTRIBUTION USING ASPHERICAL MULTI LENS ARRAY AND EDGE-SHAPED PLATES **c36**
Noriaki Nishi, Takahisa Jitsuno, Koji Tsubakimoto, Masahiro Nakatsuka, and Sadao Nakai *In its* Technology Reports of the Osaka Univ., Vol. 45, Nos. 2205-2216 15 Apr. 1995 p 35-42 (For primary document see N95-32984 12-31)
(Rept-2209) Avail: CASI HC A02/MF A02

A new concept for improving the laser intensity distribution on the inertial confinement fusion target using a phase controlled multi lens array has been proposed. The diffraction fringe of an elementary lens was mitigated using an edge-shaped plate of super-gaussian phase profile. Uniform beam profiles were obtained with 7 spherical lenses in one-dimensional array and 37 lenses in two-dimensional array. An aspherical element lens was designed to control the intensity distribution on the target, and the experimental results indicated that Fresnel-Kirrhihof diffraction calculation can be used for predicting the beam profile on the target. Author

N95-32990# Osaka Univ., Osaka (Japan). Dept. of Inst. of Laser Engineering.
MEASUREMENT OF GAIN SATURATION ON Nd: DOPED PHOSPHATE LASER GLASSES **c36**
Masakazu Tada, Noriyuki Tsukino (Kawasaki Heavy Industries Ltd., Tokyo,

Japan.), Tadashi Kanabe, Masahiro Nakatsuka, and Sadao Nakai *In its* Technology Reports of the Osaka Univ., Vol. 45, Nos. 2205-2216 15 Apr. 1995 p 43-48 (For primary document see N95-32984 12-31)
(Rept-2210) Avail: CASI HC A02/MF A02

Saturation of gain was studied in Nd:doped phosphate glasses LHG-8 and LG-760 using the laser beam with wavelength of 1.053 micron and pulse width of 1 ns. Saturation fluence was calculated by use of Frantz-Nodvik equation from the input fluence, the output fluence and the small signal gain. The saturation fluence E(sub s) is related to output fluence E(out), which is E(s) = 3.04 plus 0.149 E(out) J/sq cm in case of LHG-8 and E(s) = 2.70 plus 0.170 E(out) J/sq cm in case of LG-760.
Author

N95-32991# Osaka Univ., Osaka (Japan). Dept. of Mechanical Engineering.
ENHANCEMENT OF POOL BOILING HEAT TRANSFER TO LITHIUM BROMIDE AQUEOUS SOLUTION **c73**
Masuo Kaji, Masahiro Furukawa (Sanyo Electric Co. Ltd., Inabe, Japan.), Takayuki Suyama, and Kotohiko Sekoguchi *In its* Technology Reports of the Osaka Univ., Vol. 45, Nos. 2205-2216 15 Apr. 1995 p 49-58 (For primary document see N95-32984 12-31)
(Rept-2211) Avail: CASI HC A02/MF A02

An experimental study on enhancement of nucleate pool boiling heat transfer by placing a sponge metal, which had a three-dimensional mesh structure like sponge, close to a plain smooth heat transfer surface was conducted to improve the heat transfer performance of the high temperature generator of absorption chiller/heaters. Boiling curves of water and lithium bromide aqueous solution of mass concentration of 55 to 58% at the atmospheric pressure were presented. Heat transfer characteristics were improved by two to three times both for water and lithium bromide aqueous solution when the sponge metal was attached with an appropriate clearance. Three kinds of sponge metals were tested for lithium bromide aqueous solution under a reduced pressure (24 kPa). The sponge metal #6, which had the finest mesh among the three sponge metals, brought about excellent results at lower heat fluxes, but it caused deterioration of heat transfer at higher heat fluxes. For the wide range of heat flux (5 x 10(exp 4) approximately 2 x 10(exp 5) W/m(exp 2), it was found that the sponge metal #4 with the middle fineness was the most suitable and the optimal clearance was in the range of 0.1 approximately 0.5 mm. The employment of sponge metals for enhancing boiling heat transfer is practically excellent, since no special manufacturing is required to mount them on the heated surface.
Author

N95-32992# Osaka Univ., Osaka (Japan). Dept. of Architectural Engineering.
SEISMIC RESPONSE ANALYSIS OF SOIL-STRUCTURE INTERACTION SYSTEMS IN THE TIME DOMAIN **c46**
Kensuke Baba, Kiyeon Park, and Yutaka Inoue *In its* Technology Reports of the Osaka Univ.,Vol. 45, Nos. 2205-2216 15 Apr. 1995 p 59-64 (For primary document see N95-32984 12-31)
(Rept-2212) Avail: CASI HC A02/MF A02

A great number of studies have been reported on the dynamic analysis of soil-structure interaction systems especially in the frequency domain, with a few in the time domain. The present investigation is concerned with the introduction of a practical method for execution of a response analysis of the interacting systems based on the casual conditions along the time axis.
Author (revised)

N95-32993# Osaka Univ., Osaka (Japan). Dept. of Architectural Engineering.
INELASTIC RESPONSE SPECTRA OF A SYSTEM WITH BILINEAR RESTORING CHARACTERISTICS: EFFECT OF PLASTIC-STIFFNESS RATIO **c39**
Woontaek Woo and Yutaka Inoue *In its* Technology Reports of the Osaka Univ., Vol. 45, Nos. 2205-2216 15 Apr. 1995 p 65-73 (For primary document see N95-32984 12-31)
(Rept-2213) Avail: CASI HC A02/MF A02

The characteristics of inelastic response spectra with a bilinear restoring force subjected to artificial earthquake motions are investigated. The influences of the plastic-stiffness ratio of the restoring force and the ductility response ratio of the inelastic response spectra are studied for some of the parameters. A method of estimating the inelastic response spectral from the elastic response spectra is proposed with the revising coefficients in the constant acceleration response region and the constant velocity response region. Results are presented as inelastic response ratios.
Author (revised)

N95-32994# Osaka Univ., Osaka (Japan). Dept. of Naval Architecture and Ocean Engineering.
A NOTE ON SEPARATION PREDICTION OF TWO-DIMENSIONAL TURBULENT BOUNDARY LAYER **c34**
Ichiro Tanaka and Kun Ma *In its* Technology Reports of the Osaka Univ., Vol. 45, Nos. 2205-2216 15 Apr. 1995 p 95-99 (For primary document see N95-32984 12-31)
(Rept-2216) Avail: CASI HC A01/MF A02

Based on the two-dimesional turbulent boundary layer theory developed by Tanaka and Himeno, a simple prediction method of the separation of the two-dimensional turbulent boundary layer with the pressure gradient is presented. The effectiveness of this method is investigated by applying it to several cases of published data from previous experiments. This method is shown to be applicable for practical prediction purposes.
Author (revised)

N95-33126# Advisory Group for Aerospace Research and Development, Neuilly-Sur-Seine (France). Guidance and Control Panel.
DUAL USAGE IN MILITARY AND COMMERCIAL TECHNOLOGY IN GUIDANCE AND CONTROL [TECHNOLOGIES DUALES MILITAIRES ET CIVILES DE GUIDAGE/PILOTAGE]
Mar. 1995 179 p 59th symposium was held in Rome, Italy, 20-21 Oct. 1994
(AGARD-CP-556; ISBN-92-836-1016-4) Copyright Avail: CASI HC A09/MF A02

This volume contains the Technical Evaluation Report and the 19 unclassified papers, presented at the Guidance and Control Panel Symposium held in Pratica di Mare (Rome), Italy, from 20th to 21st October 1994. The papers presented covered the following headings: (1) Dual-use Opportunities and Missions; (2) Navigation Sensors for Dual-use Applications; (3) Multi-sensor Navigation Applied to Dual-uses; (4) Dual-use Technology for Air-Ground Operations; and (5) Dual-use Applications of G&C Technology. For individual titles, see N95-33127 through N95-33145.

N95-33127# Honeywell Technology Center, Minneapolis, MN.
DUAL USE: OPPORTUNITIES, PAYOFFS, AND CHALLENGES **c85**
Thomas Cunningham *In* AGARD, Dual Usage in Military and Commercial Technology in Guidance and Control Mar. 1995 7 p (For primary document see N95-33126 12-31)
Copyright Avail: CASI HC A02/MF A02

Significant payoffs can be achieved by increasing the interaction between military and commercial business and technology communities. This paper describes a few of the opportunities available to practitioners of guidance, navigation and control technologies to work in this dual use world. Examined from the point of view of an engineer who has been solving primarily military problems, it is hoped that the NATO AGARD reader as well as our new friends from the Cooperating Countries will benefit. The paper emphasizes three major themes: (1) Guidance, Navigation, and Control (G, N, and C) technologies and engineers are highly qualified to solve important nonmilitary problems; (2) The use of common solutions to commercial and military problems, from components to systems, has significant cost payoffs to future affordable military systems; and (3) Commercial systems, particularly aviation, offer technology advantages which should be exploited for affordable non-recurring developments and reduced cycle times in future military systems.
Derived from text

N95-33128# Central Research Inst. of Technology and Machine Building, Kaliningrad, Moscow (Russia).
THE CONCEPT OF THE SPACE SYSTEM BASED ON THE ROCKET LAUNCH VEHICLE OF LIGHT-WEIGHT CLASS FOR DIRECT SOUNDING OF LARGE-SCALE NATURAL HAZARDS **c15**
V. I. Loukiachtchenko, G. A. Tsyboulskii, A. K. Nedaivoda (Khrunichev State Research and Production Space Center, Moscow, Russia.), V. K. Karrask (Khrunichev State Research and Production Space Center, Moscow, Russia.), A. A. Medvedev (Khrunichev State Research and Production Space Center, Moscow, Russia.), N. A. Meliankov (Khrunichev State Research and Production Space Center, Moscow, Russia.), S. N. Philosophov

(Khrunichev State Research and Production Space Center, Moscow, Russia.), and V. P. Karmasin (Nauchno-Proizvodstvennoe Obedinenie Typhoon, Obninsk, Russia.) *In* AGARD, Dual Usage in Military and Commercial Technology in Guidance and Control Mar. 1995 8 p (For primary document see N95-33126 12-31)

Copyright Avail: CASI HC A02/MF A02

The report contains the description of proposal on development and use of space system intended for direct (contact) exploration of such natural hazards as, for example, tropical cyclones or ozone hole which are heavy influences on human life activity. This system would be developed on base of Russian (former Soviet) SS-19 ICBM, which should be removed from battle duty according to the START Treaty. Recently developed on the basis that ICBM Russian 'Rockot' launch vehicle can deliver with high accuracy to hazard region up to 50 reentry probes which should transmit the information through space, airborne or sea retransmitters. That efficient collection of information on atmosphere conditions in altitude range of 40...0 kilometers should be the effective tool for investigation of large-scale natural phenomena which are very dangerous for people and economics of Earth. Derived from text

N95-33129# Delphin Central Research Inst., Moscow (Russia).

COMMERCIAL USAGE OF NAVY COMPONENTS DEVELOPED AND MANUFACTURED BY CRI DELFIN **c35**

A. V. Novgorodski and M. V. Chichinadze *In* AGARD, Dual Usage in Military and Commercial Technology in Guidance and Control Mar. 1995 9 p (For primary document see N95-33126 12-31)

Copyright Avail: CASI HC A02/MF A02

Parameters of gyro systems (accuracy, size, power consumption, reliability, etc.) are determined by parameters of the elements of which the gyro unit consists. The elements developed for military equipment meet the utmost requirements. Over the past ten years the 'Delphin' Central Research Institute developed a whole number of elements including a gyro, an accelerometer, a torquer, a slip-ring assembly, etc. to provide a basis for designing gyro systems for military purposes. The conversion made it possible to use these elements in commercial gyro systems. The present paper deals with such elements and systems created on their basis and used for commercial purposes. Derived from text

N95-33130# Saint Petersburg State Electrotechnical Univ., Saint Petersburg (Russia).

SOME RESULTS OF INTERNATIONAL COOPERATION IN MILITARY TO COMMERCIAL CONVERSION OF LASER GYRO TECHNOLOGY **c35**

Yu. V. Filatov, D. P. Loukianov, A. V. Mochalov, R. Probst (Physikalisch-Technische Bundesanstalt, Brunswick, Germany.), R. Rodloff (Deutsche Forschungsanstalt fuer Luft- und Raumfahrt, Brunswick, Germany.), and B. Stieler (Deutsche Forschungsanstalt fuer Luft- und Raumfahrt, Brunswick, Germany.) *In* AGARD, Dual Usage in Military and Commercial Technology in Guidance and Control Mar. 1995 5 p (For primary document see N95-33126 12-31)

Copyright Avail: CASI HC A01/MF A02

The results of military to commercial conversion in the field of laser gyro technology are considered. Laser gyro systems were developed in Russia for military purposes. After some modifications within an international cooperation they are used nowadays also for civil applications as track surveying, deformation measurements of long objects and precision angle and angular rate measurements and angle calibration. Derived from text

N95-33131# Central Research and Development Inst. Elektropribor, Saint Petersburg (Russia).

NAVIGATIONAL TECHNOLOGY OF DUAL USAGE **c04**

V. G. Peshekhonov, I. M. Okon, L. P. Nesenyuk, and Yu. P. Belous *In* AGARD, Dual Usage in Military and Commercial Technology in Guidance and Control Mar. 1995 6 p (For primary document see N95-33126 12-31)

Copyright Avail: CASI HC A02/MF A02

Under the new conditions of defense production conversion and basing on high technologies that were developed for the production of military navigation technology the Central R&D Institute 'Elektropribor' has been developing and starts manufacturing products for civil application. Part of the project is dual usage technology. Three trends of the research are considered in this paper: (1) a gimbaled-type inertial system used to inspect railway tracks and in inertial geodesy; (2) gyrostabilized gravity meter for geological prospecting of oil and gas from ships and planes; and (3) shipborne integrated chartgraphic navigation-controlling system. Derived from text

N95-33132# Draper (Charles Stark) Lab., Inc., Cambridge, MA.

DUAL-USE MICROMECHANICAL INERTIAL SENSORS **c35**

John M. Elwell, Jr. *In* AGARD, Dual Usage in Military and Commercial Technology in Guidance and Control Mar. 1995 6 p (For primary document see N95-33126 12-31)

Copyright Avail: CASI HC A02/MF A02

A new industry, which will provide low-cost silicon-based inertial sensors to the commercial and military markets. is being created. Inertial measurement units are used extensively in military systems, and new versions are expected to find their way into commercial products, such as automobiles, as production costs fall as technology advances. An automotive inertial measurement unit can be expected to perform a complete range of control, diagnostic, and navigation functions. These functions are expected to provide significant active safety, performance, comfort, convenience, and fuel economy advantages to the automotive consumer. An inertial measurement unit applicable to the automobile industry would meet many of the performance requirements for the military in important areas, such as antenna and image stabilization, autopilot control, and the guidance of smart weapons. Such a new industrial base will significantly reduce the acquisition cost of many future tactical weapons systems. An alliance, consisting of the Charles Stark Draper Laboratory and Rockwell International, has been created to develop inertial products for this new industry. Derived from text

N95-33133# Scientific Research Inst. of Mechanical Problems, Kiev (Ukraine).

LASER GYROSCOPY TENDENCIES AND THEIR ANALYSIS OF DEVELOPMENT IN UKRAINE **c35**

Alexander A. Dovbeshko *In* AGARD, Dual Usage in Military and Commercial Technology in Guidance and Control Mar. 1995 11 p (For primary document see N95-33126 12-31)

Copyright Avail: CASI HC A03/MF A02

These papers deal with the theoretical and experimental data analysis approach of the accuracy and characteristics of laser gyroscopes obtained by Ukrainian firms. A theoretical model concerned with the physical phenomena of a ring laser with a 4-mirror resonator is created. Ring lasers are considered continuous, nonlinear self-excited oscillatory systems, that contain a number of limited and spatial nonuniform elements (active medium, diaphragms, mirrors). A model of laser generation that considers the effect of more than 40 resonator and amplifying medium parameters on laser output characteristics (intensity, frequencies difference, locking zone, etc.) was created. The mechanism that determines the mode selection and backscattering light from mirrors and diaphragms influence on the intensity and frequency difference of a traveling-wave in a ring laser is investigated. The mode formation mechanism (caustic or guide, or guide-caustic type) that depends on the resonator type and mirrors' dimension, radius of curvature and the channel shape and its linear dimensions can be achieved with the laser. It is shown, that the connection of the counter waves has a diffractional as well as a interferentional nature and is defined by the parameters of the resonator mirrors and diaphragms as well as by their disposition as to the amplifying medium. Using the latter,the methods and the devices that allow the decrease of the influence of the static zone of the waves lock on the output characteristics in 10-20 times has been created. Proceeding from the created mathematical model, the methods of optimization element composition and parameters of optical-physical scheme of the ring laser and the systems of stabilization and control of the laser generation regime of the laser gyroscope are worked out. The microprocessor systems for the laser gyroscope generation regime support and stabilization of its parameters during experimentation were completed. It is shown experimentally that laser gyroscope with such systems has a null drift 0.005 degree/hour and a random walk 0.003 degree/sq rt (hour). Derived from text

N95-33134# Technische Univ., Brunswick (Germany). Inst. fuer Flugfuehrung.

EFFECTS OF THE SPECIFIC MILITARY ASPECTS OF SATELLITE NAVIGATION ON THE CIVIL USE OF GPS/GLONASS **c04**

Detlef Kayser and Gunther Schaenzer *In* AGARD, Dual Usage in Military

and Commercial Technology in Guidance and Control Mar. 1995 10 p (For primary document see N95-33126 12-31)
Copyright Avail: CASI HC A02/MF A02

Satellite Navigation is one of todays most promising and prospering infrastructure technologies. The performance improvement of this technology in comparison to the 'conventional' terrestrial navigation systems can be seen in almost every aspect, e.g.: (1) accuracy (decimeter level); (2) coverage (worldwide); (3) availability (21 hrs); (4) dimension (4 dimensional navigation (space and time)); and (5) system capacity (unlimited number of users). This led to a widespread application of satellite navigation and an according fast growing figure of satellite navigation equipment in the civil market. Up to now however, the final breakthrough in a lot of commercial applications, like in the aviation industry and in the maritime business, has not been reached. Beside some still unsolved technical aspects, like the integrity problem, the fact that GPS and GLONASS are military systems is one of the main hurdles. This institutional aspect, however, is not only an obstacle from the political point of view, but the military background of GPS/GLONASS led to lot of design features of the system, that have a strong influence on the use of the system in civil applications. This paper will describe details on the different areas in which the military design limits the use of the system. Derived from text

N95-33135# Deutsche Forschungsanstalt fuer Luft- und Raumfahrt, Brunswick (Germany). Inst. of Flight Guidance.
THE DLR RESEARCH PROGRAMME ON AN INTEGRATED MULTI SENSOR SYSTEM FOR SURFACE MOVEMENT GUIDANCE AND CONTROL **c04**
Kurt Klein *In* AGARD, Dual Usage in Military and Commercial Technology in Guidance and Control Mar. 1995 8 p (For primary document see N95-33126 12-31)
Copyright Avail: CASI HC A02/MF A02

Based on the long-term experience in the field of Navigation and Air Traffic Control the Institute of Flight Guidance within the German Aerospace Research Establishment (DLR) is conducting a major effort to develop new solutions, system components and procedures for an integrated Surface Movement Guidance and Control System (SMGCS). In addition to and derived from the work on operational procedures, planning tools and HMI in our institute we are focusing our work on an integrated sensor concept to meet the requirements. SMGCS is to be regarded as an integrated concept that has a clearly defined modular approach to meet the particular requirements of a specific aerodrome. After outlining the conception several years ago a solution for the realization was evaluated in close co-operation with the DFS and the national industry. The objective of DLR research is: (1) to analyze the characteristics and to optimize as far as necessary the sensor candidates (e.g. DGPS, SSR Mode S Multilateration); (2) to evaluate the sensor information integration including data fusion algorithms; (3) to find solutions for the specific SMGCS data exchange problems via RF link; (4) to optimize the whole system loop in order to avoid interference by implementing modules into the system; and (5) to solve airfield operating problems by finding new functions within the SMGCS sensor domain. Although the main goal is the improvement of civil airport traffic, the work meets as well military operation problems. In addition, a lot of knowledge gained in military applications has to be considered. The research activities are funded by the DLR itself. To extend the theoretical and laboratory work to more realistic analysis an Experimental SMGCS is build up at the Braunschweig airport. This ESMGCS has the advantage of being very flexible with respect to the implementation of various subsystems and to tests in a real environment. Braunschweig airport is very suitable for experiments like this due to low traffic density and the available research infrastructure. Part of the ESMGCS will be a test environment that is based on the experiences gained during the MLS competition as well as during the development of the Avionics Flight Test System. Main part of the test environment is a measurement system for computing a reference situation assessment. The backbone of the ESMGCS is a high speed data network on fiber cable basis that connects the peripheral stations around the airfield to the master station. Different sensor subsystems or parts of these will be installed in the peripheral stations. The data fusion and the situation analysis are software processes within the master station. The derived situation information can be handed over to planning tools and to the tower simulator available in the DLR !nstitute of Flight Guidance.
Derived from text

N95-33136# Centre d'Etudes et de Recherches, Toulouse (France). Dept. d'Etudes et de Recherche en Optique.
LOW-LEVEL DATA FUSION FOR LANDING RUNWAYS DETECTION **c04**
Laure Sliwa and Xavier Briottet *In* AGARD, Dual Usage in Military and Commercial Technology in Guidance and Control Mar. 1995 11 p (For primary document see N95-33126 12-31)
Copyright Avail: CASI HC A03/MF A02

Data fusion brings reliability and robustness to both military and commercial systems. Data fusion allows in fact to fully apprehend a situation by using multisensors data redundancy and/or complementarity. The presented piece of work particularly concerns fusion of redundant data just outcoming from electro-optical sensors. The used methods are low-level fusion techniques, only preceded by a calibration step. These fusion techniques take into account the radiometric- and not geometric-data content. This paper is divided in two parts: the theoretical approach, and the guidance application of detecting a potential runway. The theoretical approach, according to the proposed goal, raises two problems. The one of suiting the multisensors' configuration to the mission. And the one of evaluating data at every step from ground reality to fusion. It appears necessary to define quality criteria to evaluate every sensor acquisition within the mission scope. The optimization of these criteria defines the weighted combination at the pixel level of the multispectral images. A priori knowledge of road materials spectral signatures and definition of appropriate quality criteria are necessary to detect roads or runways by pixel fusion. They allow to define the appropriate configuration of spectral bands to merge so that the runway shows up clearly. This paper presents the obtained results from low-level fusion of five broad bands (approximately 100 nm wide). The main advantage of pixel fusion is the saving of processing time. On one hand, the multispectral data process is quick. On the other hand, the landing runway can be detected at long range, in a large field of view.
Derived from text

N95-33137# Eurocopter Deutschland G.m.b.H., Munich (Germany).
HeliRadar: A ROTATING ANTENNA SYNTHETIC APERTURE RADAR FOR HELICOPTER ALLWEATHER OPERATIONS **c32**
W. Kreitmair-Steck and A. P. Wolframm (Deutsche Aerospace A.G., Munich, Germany.) *In* AGARD, Dual Usage in Military and Commercial Technology in Guidance and Control Mar. 1995 8 p (For primary document see N95-33126 12-31)
Copyright Avail: CASI HC A02/MF A02

Today, available radar instruments cannot be applied for flight guidance purposes due to lack of resolution and ground elevation information. On the other side, optical sensors such as infrared systems provide an excellent resolution but are nearly blind at adverse weather conditions such as fog and rain. A new radar technology called ROSAR (Synthetic Aperture Radar based on ROtating antennas) promises to overcome the deficiencies of the traditional radar systems. On the basis of encouraging research work on ROSAR-technology and an investigation of the feasibility of a piloting system based on these ideas, Eurocopter Deutschland and Deutsche Aerospace started a development program called HeliRadar to develop a ROSAR-based piloting system. This device should be able to provide photolike images even under extreme visibility conditions. Details on the investigation and the resulting concepts for synthetic vision based flight guidance at Eurocopter will be given. Following an introduction to the basics of ROSAR-technology, the technical concept of HeliRadar will be presented. The paper concludes with a discussion of the perspectives for civil and military applications. Derived from text

N95-33138# Institute for Precision Instrumentation, Moscow (Russia).
IDENTIFICATION OF TERRAIN IMAGERY WITH UNSTABLE REFLECTIVITY **c43**
Y. A. Kozko and V. V. Saveliev *In* AGARD, Dual Usage in Military and Commercial Technology in Guidance and Control Mar. 1995 7 p (For primary document see N95-33126 12-31)
Copyright Avail: CASI HC A02/MF A02

This paper deals with a problem of comparing two terrestrial images: the observed one obtained with a known device and the reference one that is an idealized picture of a given object. The whole problem is formulated in terms of statistical object identification. The SAR (Synthetic Aperature Radar) imagery main properties based on the analysis of experimental data are pointed out. A zonal SAR image model, signal fluctuation fluctuation

statistics, number of looks, S/N ratio and natural cover fragmentation of terrestrial surfaces is proposed. Based on this model, the adaptive zonal recognition algorithms are built. Their efficiency has been confirmed experimentally in a wide range of zone contrasts and under various seasonal/weather conditions. Derived from text

N95-33139# Moscow Inst. of Aviation Technology (USSR). Simulators and Pilot-Vehicle Lab.

DEVELOPMENT AND APPLICATION OF THE METHODS FOR PILOT-AIRCRAFT SYSTEM RESEARCH TO THE MANUAL CONTROL TASKS OF MODERN VEHICLES **c54**

A. V. Efremov and A. V. Ogloblin *In* AGARD, Dual Usage in Military and Commercial Technology in Guidance and Control Mar. 1995 12 p (For primary document see N95-33126 12-31)

Copyright Avail: CASI HC A03/MF A02

There are discussed the influence of some typical for the modern vehicles features (high frequency phase delay and nonliniarities in flight control system (FCS)) and parameters of input spectral density corresponding to the real piloting tasks on pilot response characteristics. There are developed some new standard characteristics the optimal aircraft dynamics and discomfort frequency response, and demonstrated their efficiency for the several applied tasks in design of FCS and development of requirements to the handling qualities. There are discussed the ways for suppression of pilot limitation parameters and FCS nonlinear and phase delay effects. Derived from text

N95-33140# Lockheed-Fort Worth Co., Fort Worth, TX.

APPLICATION OF ADVANCED SAFETY TECHNIQUE TO RING LASER GYRO INERTIAL NAVIGATION SYSTEM INTEGRATION **c04**

James Blaylock, Donald Swihart (Wright Lab., Wright-Patterson AFB, OH.), and Chuck Stribula (Aeronautical Systems Div., Wright-Patterson AFB, OH.) *In* AGARD, Dual Usage in Military and Commercial Technology in Guidance and Control Mar. 1995 10 p (For primary document see N95-33126 12-31)

Copyright Avail: CASI HC A02/MF A02

This paper documents the application of System-Wide Integrity Management (SWIM) to the integration of H-423 and LN-93 ring laser gyro (RLG) inertial navigation system (INS) units with the F-16 terrain following (TF) system. Safety modeling and mishap rate predictions are presented for F-16 TF with an RLG INS. This paper establishes that the H-423 and LN-93 RLG INS units are both safer for F-16 TF than the predecessor LN-39 gimballed, mechanical-gyro INS. The RLG INS design enhancements described are primarily built-in test (BIT) modifications that were developed as a result of the in-depth SWIM critical signal path analysis. These enhancements are low-cost design improvements to the RLG INS units because they were discovered prior to the manufacturer's final operational flight program (OFP) for the production units. This paper discusses dual-use applications of the RLG INS to other military and civilian functions, with design enhancements resulting from the SWIM process. Other military applications include not only specialized control modes such as TF, but also all other phases of the military flight operations regime, since the INS is always active to provide current aircraft state information. Civilian uses can also benefit from the SWIM process improvement to the RLG INS because accurate, reliable, safe navigation with critical timing along congested air routes, in weather, and in dense traffic terminal areas is of paramount importance for passenger safety. Derived from text

N95-33141# Saint Petersburg Inst. of Aerospace Instrumentation, Saint Petersburg (Russia).

SEA WAVE PARAMETERS, SMALL ALTITUDES AND DISTANCES MEASURERS DESIGN FOR MOVEMENT CONTROL SYSTEMS OF SHIPS, WING-IN-SURFACE EFFECT CRAFTS AND SEAPLANES **c48**

A. V. Nebylov, A. P. Vanayev, and V. V. Chernyavets *In* AGARD, Dual Usage in Military and Commercial Technology in Guidance and Control Mar. 1995 12 p (For primary document see N95-33126 12-31)

Copyright Avail: CASI HC A03/MF A02

Advanced methods and means of controlled sea vehicle moving parameters and sea-way ones measurement are considered. Both directly measuring tasks and possibilities of control quality increasing of displacement and undisplacement ships and sea flying vehicles under conditions of active wave disturbances are analyzed. Design principles, some structural features and expected quality characteristics of device, being developed, for meter altitudes and distances measuring based on special phase radioaltimeter and inertial sensor integration are observed. When functioning in the sea-waves profile tracking mode, high measuring accuracy of sea-way and vehicle vertical moving parameters is provided. The mounting of several devices both on the left and on the right sides of vehicle allows to reconstruct the field of sea wave disturbances and to check roll and pitch parameters and draught or clearance as well. The conditions to be fulfilled for determining the main sea wave spread direction are investigated. Derived from text

N95-33142# Lucas Electronics, Birmingham (England).

THE APPLICATION OF ADA AND FORMAL METHODS TO A SAFETY CRITICAL ENGINE CONTROL SYSTEM **c61**

W. C. Dolman, A. M. Ashdown, and K. J. McCallion (Ministry of Defence, London, England.) *In* AGARD, Dual Usage in Military and Commercial Technology in Guidance and Control Mar. 1995 13 p (For primary document see N95-33126 12-31)

Copyright Avail: CASI HC A03/MF A02

The procurement executive of the UK Ministry of Defense, MoD (PE) identified Ada as the single preferred high level language for the implementation of defense real time operational systems from 1 July 1987. This meant that projects selecting an implementation language after that time must select Ada, unless there are sound and documented reasons for using an alternative. MoD (PE) therefore decided to invite proposals for the High Order Language Demonstrator (HOLD) to examine the applicability of Ada to an aero gas turbine full authority digital engine control (FADEC), and awarded the contract to Lucas Electronics, Birmingham. This paper describes the work carried out by Lucas Electronics on this contract. Derived from text

N95-33143# SPEEL Ltd., Prague (Czechoslovakia).

SOLID-STATE DATA RECORDER, NEXT DEVELOPMENT AND USE **c35**

J. Vidiecan, J. Kozak, K. Horak, and J. Svoboda *In* AGARD, Dual Usage in Military and Commercial Technology in Guidance and Control Mar. 1995 10 p (For primary document see N95-33126 12-31)

Copyright Avail: CASI HC A02/MF A02

The use of data recorders on-board aircraft for crash and later for maintenance and logistic purposes is well known. Due to higher requirements for safety and economy of ground transport vehicles operation, such devices are already used in selected types of these vehicles. The use of new technology - solid-state memories - enables the increase of technical parameters of such recorders (number of registered parameters, MTBF), reduces the mass, space and requirements on technical assistance during operation. In this paper a technical description of such recorders for aircraft and ground based vehicles is given. Also, results of recent applications of these devices and different methods and software for evaluation are also presented. Derived from text

N95-33144# MATRA Marconi Space, Toulouse (France).

GPS-BASED NAVIGATION FOR SPACE APPLICATIONS **c17**

C. Champetier, T. Duhamel, and M. Frezet *In* AGARD, Dual Usage in Military and Commercial Technology in Guidance and Control Mar. 1995 9 p (For primary document see N95-33126 12-31)

Copyright Avail: CASI HC A02/MF A02

We present in this paper a survey of the applications of the GPS (global positioning system) system for spacecraft navigation. The use of the GPS techniques for space missions is a striking example of dual-use of military technology; it can bring vast improvements in performances and, in some cases, for a reduced cost. We only deal in this paper with the functional aspects and performances of GPS uses without addressing the issues of hardware implementation where current developments are leading to an increased miniaturization of the GPS receiver hardware. We start this paper with a general overview of the GPS system and its various uses for space missions. We then focus on four areas where MATRA MARCONI Space has conducted detailed analyses of performances: autonomous navigation for geostationary spacecraft, relative navigation for space rendezvous, differential navigation for landing vehicles, absolute navigation for launchers and reentry vehicles. Derived from text

N95-33145# Aerodata Flugmesstechnik G.m.b.H., Brunswick (Germany).
INTEGRATED SPECIAL MISSION FLIGHT MANAGEMENT FOR A FLIGHT INSPECTION AIRCRAFT **c05**
A. Redeker and M. Haverland *In* AGARD, Dual Usage in Military and Commercial Technology in Guidance and Control Mar. 1995 3 p (For primary document see N95-33126 12-31)
Copyright Avail: CASI HC A01/MF A02

Flight Inspection of military and civil radionavigation aids requires calibration aircraft with a complex mission equipment. The measurement patterns and their flight procedures differ from usual flight procedures, which cannot be performed with normal flight management/autopilot systems. On the other hand there is a requirement for an automatic guidance, in order to increase the reproducibility of calibration results and to assist the crew operating in areas with high traffic density. Special mission flight management systems, which are available on the market, are not an elegant solution for flight inspection applications. The flight inspection system (FIS) contains already all elements of a flight management system (FMS), and the FIS has more comprehensive information on navigational data. The system approach of an integrated FIS/FMS system is presented, where special mission profiles are generated and interfaced to the autopilot. Flight test results and operational experience are reported.
Derived from text

N95-33244# Instituut TNO voor Werktuigkundige Constructies, Delft (Netherlands).
DESIGN OF DEEPWATER PIPELINES
C. G. Langner 1995 34 p Presented at the TNO-IWECO 39th Anniversary Symposium on Underwater Technology, The Hague, Netherlands, 24 May 1984 Prepared in cooperation with Shell Development Co.
(PB95-215109) Avail: CASI HC A03/MF A01

For pipelines to be laid offshore in water depths greater than about 3000 feet, pipe design will be governed primarily by external pressure (collapse) considerations and internal pressure (burst) considerations. The paper presents a set of design criteria for deepwater pipelines, based on results of Shell's Deepwater Pipeline Feasibility Study (1), as well as comparisons with other experimental and theoretical results. The design criteria, in general, establish limits on the wall thickness, yield stress, initial imperfections, and pipe weight, in terms of the maximum internal operating pressure, the maximum external pressure or water depth, and the near-bottom ocean currents. NTIS

N95-33393# Alabama Univ., Birmingham, AL. Dept. of Materials Science and Engineering.
ADVANCED PRECISION EXPENDABLE PATTERN CASTING TECHNOLOGY 1994 Summary Report
May 1995 73 p
(Contract DE-FC07-93ID-13230)
(DE95-012200; DOE/ID-13230/T1) Avail: CASI HC A04/MF A01

Advanced precision expendable pattern casting technology is presented. The following areas are reported on: precision pattern production; pattern coating; sand fill and compaction; pattern gating; mechanical properties; and technology transfer efforts. DOE

32 COMMUNICATIONS AND RADAR

Includes radar; land and global communications; communications theory; and optical communications.

For related information see also *04 Aircraft Communications and Navigation* and *17 Space Communications, Spacecraft Communications, Command and Tracking.* For search and rescue see *03 Air Transportation and Safety,* and *16 Space Transportation.*

N95-32569# Lawrence Livermore National Lab., Livermore, CA.
THREE-DIMENSIONAL GROUND PENETRATING RADAR IMAGING USING SYNTHETIC APERTURE TIME-DOMAIN FOCUSING
Erik M. Johansson and Jeffrey E. Mast Aug. 1994 12 p Presented at the Annual Meeting of the Society of Photo-Optical Instrumentation Engineers, San Diego, CA, 24-29 Jul. 1994 Submitted for publication
(Contract W-7405-eng-48)
(DE95-010731; UCRL-JC-116341; CONF-940723-40) Avail: CASI HC A03/MF A01

This paper discusses a three-dimensional synthetic aperture imaging technique based on time-domain focusing of pulse-echo radar data. We describe the basic image formation process, important data processing issues, and compensation for planar variations in the media. We present a high-resolution volumetric image reconstruction of a concrete test slab and show that we are able to identify steel reinforcing bars in the image. We conclude with a brief comparison of this imaging method with a technique based on diffraction tomography. DOE

N95-32570# Lawrence Livermore National Lab., Livermore, CA.
GENERAL LIMITS ON THE PERFORMANCE OF HIGH POWER RADIATORS
P. Poulsen, P. A. Pincosy, and G. J. Burke Oct. 1994 6 p Presented at the 7th Conference on High Power Microwaves, Monterey, CA, 31 Oct. 1994 Submitted for publication
(Contract W-7405-eng-48)
(DE95-010732; UCRL-JC-117133; CONF-9410341-1) Avail: CASI HC A02/MF A01

Performance of high power radiators of electromagnetic energy can be limited by constraints such as those due to voltage holding, corona power loss, and antenna impedance and efficiency. The issues are addressed in such a way that general limits on the electric field and energy at a distance is obtained as a function of wavelength, pulse duration, and size of the radiating element. We address the relation between the frequency content of the driving pulse and the complex impedance of the antenna; the importance of minimizing the antenna impedance and therefore limiting the antenna input voltage is clearly shown. For example, driving the antenna at a resonance with a simple oscillating waveform is shown to allow the radiation of energy with two to three times the efficiency of a mono-polar pulse input. With this information, the prospects for a successful system design of a given size to deliver a specified amount of radiation to a target at a given distance can be quickly assessed. DOE

N95-32613 National Defence Research Establishment, Linkoeping (Sweden). Avdelningen foer Sensorteknik.
[ACTIVITIES OF THE DIVISION OF MICROWAVE TECHNOLOGY] Annual Report, Fiscal Year 1993 - 1994 [INSTITUTIONEN FOER MIKROVAGSTEKNIK ARSRAPPORT 1993/1994]
W. Asp Jan. 1995 35 p In SWAHILI See also PB94-148079
(PB95-214524; FOA-R-95-00078-3.2-SE) Avail: Issuing Activity (National Technical Information Service (NTIS))

The report gives a brief summary of the activities at the Division of Microwave Technology, Fiscal Year 1993/94. NTIS

N95-32616# Stanford Linear Accelerator Center, Menlo Park, CA.
MINIMUM WAKEFIELD ACHIEVABLE BY WAVEGUIDE DAMPED CAVITY
Xintian E. Lin and Norman M. Kroll 1995 4 p Presented at the Particle Accelerator Conference, Dallas, TX, 1-5 May 1995 Prepared in cooperation with California Univ., San Diego, CA
(Contracts DE-AC03-76SF-00515; DE-FG03-93ER-40759)
(DE95-012100; SU-SLAC-PUB-95-6863; CONF-950512-31) Avail: CASI HC A01/MF A01

The authors use an equivalent circuit to model a waveguide damped cavity. Both exponentially damped and persistent (decay t(sup -3/2)) components of the wakefield are derived from this model. The result shows that for a cavity with resonant frequency a fixed interval above waveguide cutoff, the persistent wakefield amplitude is inversely proportional to the external Q value of the damped mode. The competition of the two terms results in an optimal Q value, which gives a minimum wakefield as a function of the distance behind the source particle. The minimum wakefield increases when the resonant frequency approaches the waveguide cutoff. The results agree very well with computer simulation on a real cavity-waveguide system. DOE

N95-32674*# Ohio State Univ., Columbus, OH. ElectroScience Lab.
X-ANTENNA: A GRAPHICAL INTERFACE FOR ANTENNA ANALYSIS CODES
B. L. Goldstein, E. H. Newman, and H. T. Shamansky Jan. 1995

105 p
(Grant NAG1-1058)
(NASA-CR-199212; NAS 1.26:199212; Rept-722792-8) Avail: CASI HC A06/MF A02

This report serves as the user's manual for the X-Antenna code. X-Antenna is intended to simplify the analysis of antennas by giving the user graphical interfaces in which to enter all relevant antenna and analysis code data. Essentially, X-Antenna creates a Motif interface to the user's antenna analysis codes. A command-file allows new antennas and codes to be added to the application. The menu system and graphical interface screens are created dynamically to conform to the data in the command-file. Antenna data can be saved and retrieved from disk. X-Antenna checks all antenna and code values to ensure they are of the correct type, writes an output file, and runs the appropriate antenna analysis code. Volumetric pattern data may be viewed in 3D space with an external viewer run directly from the application. Currently, X-Antenna includes analysis codes for thin wire antennas (dipoles, loops, and helices), rectangular microstrip antennas, and thin slot antennas. Author

N95-32747 European Space Agency. European Space Research and Technology Center, ESTEC, Noordwijk (Netherlands).
OPEX: SECOND WORKSHOP OF THE OLYMPUS PROPAGATION EXPERIMENTERS. VOLUME 1: REFERENCE BOOK ON ATTENUATION MEASUREMENT AND PREDICTION
J. P. V. Poiares Baptista, ed., P. G. Davies, ed., B. Amaya-Rastburg, F. Barbaliscia, J. Belshaw, G. Brussaard, T. Chung, L. Coevering, B. Danielsson, and F. Dintelmann et al Nov. 1994 186 p Workshop held in Noordwijk, Netherlands, 8-10 Nov. 1994
(ISSN 1022-6656)
(ESA-WPP-083-Vol-1) Avail: Issuing Activity (European Space Agency (ESA))

After the Olympus spacecraft was launched, the original working groups were replaced by new groups, each focusing on a specific aspect of the campaign. The presentation of the results in this set of reports is in 5 volumes; one per working group. Besides presenting results (statistics, etc.) in graphical or tabular form, both the scientific background of the propagation effect and the practical aspects of link planning are addressed. This volume, number 1, gives a summary of all co-polar propagation effects on fixed satellite to earth links. A basic necessity is the knowledge of cumulative statistics of attenuation, both for rain and for non-rainy conditions. Scintillation, fade duration statistics and information needed for impairment restoration (e.g. site diversity) were also the subject of intensive studies. Experiments in different geographical locations give insight into the regional and seasonal differences of rain attenuation and allow validation of existing and new slant path attenuation prediction methods. Derived from text

N95-32748 European Space Agency. European Space Research and Technology Center, ESTEC, Noordwijk (Netherlands).
OPEX SECOND WORKSHOP OF THE OLYMPUS PROPAGATION EXPERIMENTERS. VOLUME 2: REFERENCE BOOK ON DEPOLARISATION
F. Dintelmann, ed., J. Belshaw, ed., A. Paraboni, A. Martellucci, R. Jakoby, M vd. Kamp, and F. Rucker Nov. 1994 102 p Workshop held in Noordwijk, Netherlands, 8-10 Nov. 1994
(ISSN 1022-6656)
(ESA-WPP-083-Vol-2) Avail: Issuing Activity (European Space Agency (ESA))

This is the second volume in the series of 5 to summarize the findings of the OPEX (Olympus Propagation Experimenters) group and to provide up-to-date information on propagation impairments to planners and system designers of satellite communication systems. The scientific goal in the depolarization was to derive the anisotropy of hydrometeors and to evaluate the means of distinguishing the influence of ice and rain particles, respectively, from the orthogonally polarized 20 GHz beacon signal. The system-oriented goal of the analysis effort was to improve the prediction model for cross-polarization due to rain and ice. Derived from text

N95-32749 European Space Agency. European Space Research and Technology Center, ESTEC, Noordwijk (Netherlands).
OPEX SECOND WORKSHOP OF THE OLYMPUS PROPAGATION EXPERIMENTERS. VOLUME 3: REFERENCE BOOK ON RADIOMETRY AND METEOROLOGICAL MEASUREMENTS
F. Barbaliscia, ed., G. Brussaard, A. Hornbostel, J. Lavergnat, C. Mallet, G. Ortgies, F. Murr, A. Martellucci, E. Salonen, and F. Rucker et al Nov. 1994 124 p Workshop held in Noordwijk, Netherlands, 8-10 Nov. 1994
(ISSN 1020-6656)
(ESA-WPP-083-Vol-3) Avail: Issuing Activity (European Space Agency (ESA))

This is the third volume in the series of 5 to summarize the findings of the OPEX (Olympus Propagation Experimenters) group and to provide up-to-date information on propagation impairments to planners and system designers of satellite communication systems. Radiometers have been used in most experiments to establish a reference level for extracting the total tropospheric attenuation. Using radiometers operating at 20 and 30 GHz, it was possible to estimate the total atmospheric water vapor content and liquid (cloud) water content. The report of the radiometry Group also presents retrieval algorithms for liquid water and water vapor. Meteorological measurements included raingauges (to measure the instantaneous rainfall rate), distrometers (to measure the drop-size distribution of rain), ceilometers (to measure the cloud base) and radiosondes (to measure the temperature and pressure profiles of the troposphere). Derived from text

N95-32750 European Space Agency. European Space Research and Technology Center, ESTEC, Noordwijk (Netherlands).
OPEX SECOND WORKSHOP OF THE OLYMPUS PROPAGATION EXPERIMENTERS. VOLUME 4: REFERENCE BOOK ON RADAR
J. P. V. Poiares Baptista, ed., C. Capsoni, M. Chandra, M. DAmico, C. Gloaguen, J. W. F. Goddard, A. R. Holt, A. Hornbostel, A. Kawecki, and E. Kubista et al Nov. 1994 112 p Workshop held in Noordwijk, Netherlands, 8-10 Nov. 1994
(ISSN 1022-6656)
(ESA-WPP-083-Vol-4) Avail: Issuing Activity (European Space Agency (ESA))

This is the fourth volume in the series of 5 to summarize the findings of the OPEX (Olympus Propagation Experimenters) group and to provide up-to-date information on propagation impairments to planners and system designers of satellite communication systems. Meteorological radars were used for propagation research in some sites to observe the geographical extent and spatial structure of precipitation and investigate the microstructure of ice, hail, snow, and rain in individual showers. In this reference book, different melting layer models are presented as well as single particle scattering algorithms, comparisons of different scattering algorithms, and radar calibration procedures. Derived from text

N95-32751 European Space Agency. European Space Research and Technology Center, ESTEC, Noordwijk (Netherlands).
OPEX SECOND WORKSHOP OF THE OLYMPUS PROPAGATION EXPERIMENTERS. VOLUME 5: REFERENCE BOOK ON DATA PROCESSING
J. Belshaw, ed., A. Pawlina, S. Upton, P. Gole, J. Matagne, F. Murr, E. Salonen, A. Hornbostel, M. Willis, and J. Tervonen Nov. 1994 86 p Workshop held in Noordwijk, Netherlands, 8-10 Nov. 1994
(ISSN 1022-6656)
(ESA-WPP-083-Vol-5) Avail: Issuing Activity (European Space Agency (ESA))

This is the last volume in the series of 5 to summarize the findings of the OPEX (Olympus Propagation Experimenters) group and to provide up-to-date information on propagation impairments to planners and system designers of satellite communication systems. This volume summarizes the experiences gained from using the standardized DAPPER (Data Analysis and Processing for Propagation Research) software and briefly lists special applications and so-called user routines. Derived from text

N95-32773# Massachusetts Inst. of Tech., Lexington, MA.
RASSP BENCHMARK 1 TECHNICAL DESCRIPTION. REVISION 1
B. W. Zuerndorfer, J. C. Anderson, R. A. Ford, A. H. Anderson, and G. A. Rocco 25 Jan. 1995 159 p
(Contract F19628-95-C-0002)
(AD-A293030; RASSP-1-REV-1; ESC-TR-95-001) Avail: CASI HC A08/MF A02

This report describes the first in a series of application problems which are intended to measure the performance of a process for rapid prototyping of embedded digital signal processors. The rapid prototyping process is being developed for the ARPA/Tri-Services Rapid Prototyping of Application

Specific Signal Processors (RASSP) program. The first application problem is to develop a virtual prototype for a real time digital signal processor capable of forming images from high resolution synthetic aperture radar data. Details of the application are provided along with design constraints and optimization requirements for the processor. The report also describes product and process metrics which are to be collected to derive measures of process and product performance. The application problem and associated performance metrics comprise what is termed a benchmark technical description. DTIC

N95-32797# Army Research and Development Group (Europe), FPO New York, NY.
CONFERENCE PROCEEDINGS OF MATHEMATICAL METHODS IN ELECTROMAGNETIC THEORY
10 Sep. 1994 540 p Conference held in Kharkov, Ukraine, 7-10 Sep. 1994
(Contract N68171-94-M-6429)
(AD-A291165; R/D-7564-EE-02) Avail: CASI HC A23/MF A04

The proceeding of the 5th Mathematical Methods in Electromagnetic Theory (MMET '94) Conference is presented. The Conference Program contains 116 papers from 14 countries, including 9 invited papers. Technological areas disscuded include: High-frequency Methods; Scattering and Diffraction; Transients and Time-domain Methods; Gratings and Rough Surfaces; Regularization Techniques; Optical Fibers; Open Waveguides and Resonators; Numerical Methods; Inverse and synthesis Problems; Remote Sensing; Antennas, Waveguides, and Discontinuities; and Nonlinear and Exotic Media. CASI

N95-32822*# Michigan Univ., Ann Arbor, MI. Radiation Lab.
SIMULATION OF PATCH AND SLOT ANTENNAS USING FEM WITH PRISMATIC ELEMENTS AND INVESTIGATIONS OF ARTIFICIAL ABSORBER MESH TERMINATION SCHEMES
J. Gong, T. Ozdemir, J Volakis, and M. Nurnberger Jul. 1995 91 p
(Grant NAG1-1478)
(NASA-CR-198974; NAS 1.26:198974; Rept-030601-5-T) Avail: CASI HC A05/MF A01

Year 1 progress can be characterized with four major achievements which are crucial toward the development of robust, easy to use antenna analysis code on doubly conformal platforms. (1) A new FEM code was developed using prismatic meshes. This code is based on a new edge based distorted prism and is particularly attractive for growing meshes associated with printed slot and patch antennas on doubly conformal platforms. It is anticipated that this technology will lead to interactive, simple to use codes for a large class of antenna geometries. Moreover, the codes can be expanded to include modeling of the circuit characteristics. An attached report describes the theory and validation of the new prismatic code using reference calculations and measured data collected at the NASA Langley facilities. The agreement between the measured and calculated data is impressive even for the coated patch configuration. (2) A scheme was developed for improved feed modeling in the context of FEM. A new approach based on the voltage continuity condition was devised and successfully tested in modeling coax cables and aperture fed antennas. An important aspect of this new feed modeling approach is the ability to completely separate the feed and antenna mesh regions. In this manner, different elements can be used in each of the regions leading to substantially improved accuracy and meshing simplicity. (3) A most important development this year has been the introduction of the perfectly matched interface (PMI) layer for truncating finite element meshes. So far the robust boundary integral method has been used for truncating the finite element meshes. However, this approach is not suitable for antennas on nonplanar platforms. The PMI layer is a lossy anisotropic absorber with zero reflection at its interface. (4) We were able to interface our antenna code FEMA—CYL (for antennas on cylindrical platforms) with a standard high frequency code. This interface was achieved by first generating equivalent magnetic currents across the antenna aperture using the FEM code. These currents were employed as the sources in the high frequency code. Derived from text

N95-32892 Technische Univ., Twente (Netherlands). Center for Telematics and Information Technology.
SIMULATION OF A CONNECTIONLESS SERVER FOR b-ISDN
Geert Heijenk 1995 14 p Limited Reproducibility: More than 20% of this document may be affected by microfiche quality
(ISSN 0924-3755)
(PB95-215091; Memo-INF-95-06; TIOS-95/04) Copyright Avail: CASI HC A03

A connectionless service can be provided with the B-ISDN by installing Connectionless Servers (CLSs) in the network. A CLS can either operate in message mode, routing and forwarding cells on a per-packet basis, or in streaming mode, routing and forwarding cells individually. Two simulation programs are described, one for each mode of operation, which allow for the evaluation of a CLS with respect to the delay experienced by cells. NTIS

N95-32925# Department of the Navy, Washington, DC.
ARBITRARY WAVEFORM GENERATOR Patent Application
Maurice Griffin, inventor (to Navy) and Glen Sugawara, inventor (to Navy)
2 Feb. 1995 22 p
(AD-D017451; US-Patent-Appl-SN-382708) Avail: CASI HC A02/MF A01

A system for storing an arbitrary waveform on nonvolatile random access memory (NVRAM) device and generating an analog signal using the NVRAM device is described. A central processing unit is used to synthesize an arbitrary waveform and create a digital representation of the waveform and transfer the digital representation to a microprocessor which, in turn, writes the digital data into an NVRAM device which has been mapped into a portion of the microprocessor address space. The NVRAM device is removed from address space and placed into an independent waveform generation unit. In the waveform generation unit, an address clock provides an address timing signal and a cycle clock provides a transmit signal. Both signals are applied to an address generator. When both signals are present, the address generator generates and transmits to the NVRAM device a new address for each cycle of the address timing signal. In response to each new address generated, the NVRAM devices provides a digital output which is applied to a digital to analog converter. The converter produces a continuous analog output which is smoothed by a filter to produce the arbitrary waveform. DTIC

N95-33033*# Kansas Univ. Center for Research, Inc., Lawrence, KS.
DEVELOPMENT OF AN L-, C-, AND X-BAND RADAR FOR BACKSCATTERING STUDIES OVER VEGETATION
G. Lance Lockhart Feb. 1995 175 p
(Grants NGT-51021; NAG5-2344)
(NASA-CR-199112; NAS 1.26:199112; RSL-10290-1; RSL-10480-2) Avail: CASI HC A08/MF A02

With the recent surge of interest in global change, the impact of different ecosystems on the Earth's carbon budget has become the focus of many scientific studies. Studies have been launched by NASA and other agencies to address this issue. One such study is the Boreal Ecosystem-Atmosphere Study (BOREAS). BOREAS focuses on the boreal ecosystem in Northern Canada. As a part of the BOREAS study, we have developed a helicopter-borne three-band radar system for measuring the scattering coefficient of various stands within the boreal forest. During the summer of 1994 the radar was used at the southern study area (SSA) in Saskatchewan over the young jack pine (YJP), old jack pine (OJP), old black spruce (OBS) and old aspen (OA) sites. The data collected will be used to study the interaction of microwaves with forest canopy. By making use of three different frequency bands the contribution to the backscatter from each of the layers within the canopy can be determined. Using the knowledge gained from these studies, we will develop algorithms to enable more accurate interpretation of SAR images of the boreal region. This report describes in detail the development of the L-, C- and X-band radar system. The first section provides background information and explains the objectives of the boreal forest experiment. The second section describes the design and implementation of the radar system. All of the subsystems of the radar are explained in this section. Next, problems that were encountered during system testing and the summer experiments are discussed. System performance and results are then presented followed by a section on conclusions and further work. Author

N95-33061# Pennsylvania Univ., Philadelphia, PA. Dept. of Electrical Engineering.
RADIATIVE INTERACTIONS WITH MICROMACHINED SURFACES: SPECTRAL POLARIZED EMITTANCE Final Report

Jay N. Zemel 1995 44 p
(Contract DE-FG02-88ER-13964)
(DE95-011455; DOE/ER-13964/T1) Avail: CASI HC A03/MF A01

This report covers work aimed at obtaining additional information on the electromagnetic emissions from heated, microstructured surface. Earlier work had established that thermal emission was a useful means for obtaining broad band information on the electromagnetic properties of these surfaces. Among the earlier results obtained was a demonstration that there was an increased amount of coherent radiation emitted from these structures. Also found was that the nature of the emission was dependent on the carrier concentration of the emitting material as well as the details of the geometry of surface structures. Described in this report is the normal polarized emissivity of undoped silicon gratings of different dimensions measured with a new emissometer. Deep grating fabrication, formation of a titanium silicide layer, and wafer cutting is described. DOE

N95-33152# Massachusetts Inst. of Tech., Lexington, MA.
SPACE-TIME ADAPTIVE PROCESSING FOR AIRBORNE RADAR
James Ward 13 Dec. 1994 179 p
(Contract F19628-95-C-0002)
(AD-A293032; TR-1015; ESC-TR-94-109) Avail: CASI HC A09/MF A02

Future airborne radars will be required to detect targets in an interference background comprised of clutter and jamming. Space-time adaptive processing (STAP) refers to multidimensional adaptive filtering algorithms that simultaneously combine the signals from the elements of an array antenna and the multiple pulses of a coherent radar waveform, to suppress interference and provide target detection. STAP can improve detection of low-velocity targets obscured by mainlobe clutter, detection of targets masked by sidelobe clutter, and detection in combined clutter and jamming environments. This report analyzes a variety of approaches to the STAP problem. Optimum or fully adaptive processing is reviewed. Computational complexity and the need to estimate the interference from a limited amount of available data make fully adaptive STAP impractical. As a result, partially adaptive share-time processors are required. A taxonomy of reduced-dimension STAP algorithms is presented where algorithms are classified based on the type of preprocessor employed. For example, beamspace algorithms use spatial preprocessing, while post-Doppler approaches perform (Doppler) filtering before adaptive processing. In some cases, the special structure of the clutter can be exploited to design preprocessors yielding minimum clutter rank. For each class, either sample-matrix-inversion (SMO) or subspace-based weight computation may be employed. Simulation results are presented to illustrate various performance metrics, including SINR adapted patterns, minimum detectable velocity, and required degrees of freedom. DTIC

N95-33230# National Defence Research Establishment, Linkoeping (Sweden). Dept. of Command and Control Warfare Technology.
FH AND DS SPREAD-SPECTRUM SYSTEMS IN INTERFERENCE-LIMITED HF CHANNELS: A COMPARISON
Gunnar Andersson Dec. 1994 34 p
(ISSN 1104-9154)
(PB95-211439; F0A-R-94-00067-3.5-SE) Avail: CASI HC A03/MF A01

A severe problem with high frequency (HF) transmissions is the large amount of interfering signals from other users of the frequency band. To carry out performance evaluations of HF communication systems, the impact of the narrowband interfering signals therefore has to be considered. Thus, a statistical description of the interfering signals is needed. Based on the Laycock-Gott occupancy model, the probability density function of the received narrowband interference power is derived. The derived statistical interference description is employed in the evaluation of the bit error probability of both a frequency-hopping and a direct-sequence spread-spectrum system. The results show that the large variation of the interference power gives a substantial degradation of spread-spectrum systems, compared to the case of constant interference power. Furthermore, the frequency-hopping system performs better than the direct-sequence system on this interference-limited HF channel. NTIS

N95-33231 National Defence Research Establishment, Linkoeping (Sweden).
DETVAg-90: USE OF GTD FOR WAVE PROPAGATION OVER EARTH [DETVAG-90: ANVAENDNING AV GTD VID VAGUTBREDNING OEVER JORD]
P. Holm Dec. 1994 26 p In SWAHILI See also PB95-141859
(PB95-211447; F0A-R-94-00003-3.5-SE) Avail: Issuing Activity (National Technical Information Service (NTIS))

This is a report within the Detvag-90 project. The aim of the project is to improve the ground wave propagation model Detvag. The model predicts the transmission loss for radio-wave propagation over irregular terrain, and consists of several sub models. Two of these are knife-edge diffraction and smooth spherical earth, which are joined together by square-root model. This square-root model sometime gives poor results, which can be explained by considering the wave-propagation problem as a sum of rays. The square-root model does not sum up different rays (direct ray, reflected and diffracted rays) in a correct way with respect to the phase. A model that does so is GTD. Consequently, this model gives also good results even in those cases where the square-root model fails. NTIS

N95-33322 Purdue Univ., West Lafayette, IN.
ACTIVE NOISE CONTROL IN FINITE LENGTH WAVEGUIDES Ph.D. Thesis
James Dennis Stell 1991 153 p
Avail: Univ. Microfilms Order No. DA9420770

This thesis discusses the performance of active noise control systems in rigid-walled, rectangular waveguides with reflective terminations. The theory is developed such that optimal secondary source strengths can be found to minimize three performance criteria; pressure at a selected set of points within the waveguide, potential energy in a selected volume of the waveguide, and power in the downstream region of the waveguide. Analytical results indicate that for control of a single mode the solution of the minimum pressure problem is identical to the solution of the minimum potential energy or minimum propagating power solutions. Simulation results indicate that by properly locating the secondary sources and the performance sensors the global performance of the minimum pressure solution approaches the optimal performance of the minimum potential energy or minimum power solutions. When these solutions are identical, or similar, a local control strategy is capable of obtaining global control. Guidelines are given for configuring an active control system that minimizes the pressure at a set of performance sensors such that the potential energy and propagating power are also minimized. To avoid the effects of evanescent energy the pressure sensors should be located as far downstream from the secondary sources as possible. The effects of evanescent energy can also be reduced by locating the performance sensors and secondary sources on the nodelines of the most significant evanescent mode. If the waveguide has reflective terminations then frequencies will exist at which the evanescent energy is more significant than at other frequencies. At these frequencies there will be reduced control of potential energy and power using pressure minimization. The number of frequencies of poor control can be reduced by locating the transducers properly; the secondary source should be located as close as possible to the reflecting upstream termination and the performance sensor should be located as close as possible to a reflecting downstream termination. The models used in this thesis are experimentally verified. Issues associated with implementing active noise controllers using digital filters are also discussed in this thesis. The reduction in sound pressure obtained over a frequency band increases logarithmically with filter size. The analytical predictions were also compared to the performance of a commercial active controller. The commercial controller did not perform consistently or as well as predicted due to the complex nature of the waveguide sound control problem. Dissert. Abstr.

N95-33336# Stanford Linear Accelerator Center, Stanford, CA.
A CODE TO COMPUTE THE ACTION-ANGLE TRANSFORMATION FOR A PARTICLE IN AN ABRITRARY POTENTIAL WELL
J. Scott Berg and Robert L. Warnock 1995 4 p Presented at the 16th IEEE Particle Accelerator Conference and International Conference on High Energy Accelerators, Dallas, TX, 1-5 May 1995
(Contract DE-AC03-76SF-00515)
(DE95-012554; SU-SLAC-PUB-95-6839; CONF-950512-70) Avail: CASI HC A01/MF A01

For a Vlasov treatment of longitudinal stability under an arbitrary wake field, with the solution of the Haiessinski equation as the unperturbed distribution, it is important to have the action-angle transformation for the distorted potential well in a convenient form. The authors have written a code that gives the transformation q,p (yields) J, (phi), with q(J,(phi)) as a

Fourier series in (phi), the Fourier coefficients and the Hamiltonian H(J) being spline functions of J in C(sup 2) (having continuous second derivatives). DOE

N95-33379# Argonne National Lab., IL.
COMPUTATIONAL ELECTROMAGNETICS AND PARALLEL DENSE MATRIX COMPUTATIONS
Kimmo Forsman (Tampere Univ. of Technology, Finland.), Lauri Kettunen (Tampere Univ. of Technology, Finland.), William Gropp, and David Levine 1995 6 p Presented at the 7th Society for Industrial and Applied Mathematics (SIAM) Conference on Parallel Processing for Scientific Computing, San Francisco, CA, 15-17 Feb. 1995
(DE95-012286; ANL/MCS/CP-85304; CONF-950212-8) Avail: CASI HC A02/MF A01

We present computational results using CORAL, a parallel, three-dimensional, nonlinear magnetostatic code based on a volume integral equation formulation. A key feature of CORAL is the ability to solve, in parallel, the large, dense systems of linear equations that are inherent in the use of integral equation methods. Using the Chameleon and PSLES libraries ensures portability and access to the latest linear algebra solution technology. DOE

N95-33387# Lawrence Livermore National Lab., Livermore, CA.
BICRITERIA NETWORK DESIGN PROBLEMS
M. V. Marathe, R. Ravi (Princeton Univ., NJ.), R. Sundaram (Massachusetts Inst. of Tech., Cambridge, MA.), S. S. Ravi, D. J. Rosenkrantz, and H. B. Hunt, III 1995 13 p Presented at the International Coloquium on Automata Languages (ICALP 1995), Szeged, Hungary, Jun. 1995
(Contract W-7405-eng-36)
(DE95-012052; LA-UR-95-1411; CONF-9506188-1) Avail: CASI HC A03/MF A01

We study several bicriteria network design problems phrased as follows: given an indirected graph and two minimization objectives with a budget specified on one objective, find a subgraph satisfying certain connectivity requirements that minimizes the second objective subject to the budget on the first. First, we develop a formalism for bicriteria problems and their approximations. Secondly, we use a simple parametric search technique to provide bicriteria approximation algorithms for problems with two similar criteria, where both criteria are the same measure (such as the diameter or the total cost of a tree) but differ only in the cost function under which the measure is computed. Thirdly, we present an (O(log n), O(log n))-approximation algorithm for finding a diameter-constrained minimum cost spanning tree of an undirected graph on n nodes. Finally, for the class of treewidth-bounded graphs, we provide pseudopolynomial-time algorithms for a number of bicriteria problems using dynamic programming. These pseudopolynomial-time algorithms can be converted to fully polynomial-time approximation schemes using a scaling technique. DOE

N95-33497*# Kansas Univ. Center for Research, Inc., Lawrence, KS. Radar Systems and Remote Sensing Lab.
STUDIES OF MICROWAVE SCATTERING AND CANOPY ARCHITECTURE FOR BOREAL FORESTS Annual Progress Report
G. Lance Lockhart and S. P. Gogineni Nov. 1994 17 p
(Grant NAG5-2344)
(NASA-CR-199113; NAS 1.26:199113; RSL-10480-1) Avail: CASI HC A03/MF A01

Our primary objectives during the last year have been to develop a helicopter-borne radar system for measuring microwave backscatter from vegetation and to use this system to study the characteristics of backscatter from the boreal forest. Our research is aimed at refining the current microwave models and using these improvements for more accurate interpretation of SAR data. SAR data are very useful for monitoring the boreal forest region because of the microwave signal's ability to penetrate clouds and to see at night. Meeting these objectives involves several stages of development. The first stage is the design and implementation of a frequency-modulated continuous-wave (FM-CW) radar system with the capability of measuring backscatter at three frequencies and four polarizations at each frequency. These requirements necessitate a twelve-channel radar system. Using three frequencies is advantageous because it allows us to look at different parts of the canopy. For instance, the lower frequency signal penetrates deeper into the canopy and allows us to see the ground while the high frequency signal is scattered more by the leaves and needles and typically does not penetrate to the floor of the forest. We designed the radar starting with the antenna system. We then developed the intermediate frequency (IF) and radio frequency (RF) sections of the radar. Also, the need to collect data from twelve channels during each flight line presented a complex data acquisition problem that we solved by using a high-speed data acquisition board. After construction, the radar was tested at the lab. We performed extensive testing of the IF and RF systems of the radar during this time. Once we were satisfied with the operation of the radar it was shipped to Canada for use in the second intensive field campaign (IFC-2) from July 16 - August 8, 1994. During IFC-2, we collected backscatter data over the experimental sites in the southern study area (SSA). Additionally, we used a ground-based step-frequency radar to measure the reflection coefficient of the forest floor at the old jack pine (OJP) and young jack pine (YJP) sites. The ground-based radar data have been processed and a frew examples are included in this report. we are currently processing the helicopter-borne radar data. Author

N95-33726*# Kansas Univ. Center for Research, Inc., Lawrence, KS. Radar Systems and Remote Sensing Lab.
STUDIES OF MICROWAVE SCATTERING AND CANOPY ARCHITECTURE FOR BOREAL FORESTS Annual Progress Report
G. Lance Lockhart and S. P. Gogineni Aug. 1995 15 p
(Grant NAG5-2344)
(NASA-CR-199114; NAS 1.26:199114; RSL-10480-3) Avail: CASI HC A03/MF A01

This is an annual report on the project titled 'Study of Microwave Scattering and Canopy Architecture for Boreal Forests.' The objectives of our work are to study the interaction of microwave signals with vegetation components and to determine the radar's ability to provide accurate estimates of biophysical parameters such as biomass. Our research is aimed at refining the current microwave models and using these improvements to facilitate more accurate interpretations of SAR (synthetic aperture radar) imagery. Author

N95-33839# Wisconsin Univ., Madison, WI. Space Science and Engineering Center.
DEVELOPMENT OF HIGH SPECTRAL RESOLUTION LIDAR (HSRL) TECHNOLOGY Final Report
Edwin W. Eloranta May 1995 6 p
(Contract DE-FG02-90ER-61058)
(DE95-011906; DOE/ER-61058/3) Avail: CASI HC A02/MF A01

This report describes progress achieved during two years of DOE funding provided by grant DE-FG02-90ER61058. This grant was titled 'Development of High Spectral Resolution Lidar Technology for use in the DOE ARM Program'. Nearly all grant objectives were achieved despite the fact that DOE abruptly cancelled funding after only two years of a planned three year effort. The principal investigator learned of the cancellation only after attempting to determine why third year funding had not arrived. This occurred two weeks into the planned third year. The unexpected loss of funds created destructive dislocations in our research program. This report describes only progress during the two funded years. Subsequent research, funded by other sources, has resulted in High Spectral Lidar System performance well in excess of that proposed in the DOE program. This system has proven its performance in routine observations at the University of Wisconsin and during an extended field deployment as part of a winter storms project in Arizona. DOE

N95-34304# Naval Postgraduate School, Monterey, CA.
SPEAKER IDENTIFICATION USING THE TWO-DIMENSIONAL CEPSTRUM TRANSFORM M.S. Thesis
Ioannis Lelakis Mar. 1995 96 p
(AD-A294204) Avail: CASI HC A05/MF A01

This thesis investigates the application of the two-dimensional cepstrum transform to a speaker identification system. Two distance measures are implemented for identification decision; the Euclidean distance and a weighted two-dimensional cepstral distance. The study considers three words to be tested under several noise levels. The effect of speaking rate during recordings is examined and is shown to be critical. Results show identification rates in the range of 95% to 98.5% for 50 dB signal to noise ratio and 57.65% to 80.7% for 0 dB signal to noise ratio. DTIC

N95-34460# Millitech Corp., South Deerfield, MA.
MONOLITHIC DIODE ARRAYS FOR QUASIOPTICAL MILLIMETER WAVE BEAM STEERING Final Report, 22 Sep. 1994 - 31 Mar. 1995
Ellen L. Moore and Debabani Choudhury 28 Apr. 1995 34 p
(Contract DAAH01-94-C-R263; ARPA Order 5916)
(AD-A294256; Rept-A5017) Avail: CASI HC A03/MF A01

This final report presents the details of the research and design effort for the first phase of a program to produce a monolithic diode array for quasioptical beam steering at millimeter wavelengths. Beam steering is accomplished by adding a linear phase shift across the aperture of an antenna. The quasioptical circuit performing this task comprises a 2-dimensional square metallic mesh on gallium arsenide loaded with Schottky varactor diodes. The mesh is an inductive element and the diodes have a variable capacitance which is controlled by the bias voltage. The phase of a wave transmitted through the monolithic array is changed by an amount determined by the diode capacitance. In this design the beam steering array is a 115 mm diameter mosaic of 12.7 mm x 12.7 mm dies. The array is controlled by a 6 layer drive circuit, which can arbitrarily bias each individual die. The circuit is computer controlled to step the beam in a 4 x 4 point raster pattern. After Phase 2 is completed the beam steering array will be incorporated into existing imaging systems to achieve super-resolution. During Phase 1 we designed the Schottky varactor diodes, mesh circuit, 115 mm beam steering array, and the drive circuit to bias the array. In the final report we show the design of these devices and the DC test results on the diodes. DTIC

N95-34474# Massachusetts Inst. of Tech., Lexington, MA.
THE DEVELOPMENT OF THE AUTOMATIC TARGET RECOGNITION SYSTEM FOR THE UGV/RSTA LADAR Progress Report
Jacques G. Verly, Dan E. Dudgeon, and Richard T. Lacoss 21 Mar. 1995 70 p Limited Reproducibility: Document partially illegible
(Contract F19628-95-C-0002)
(AD-A294090; TR-1006; ESC-TR-94-111) Avail: CASI HC A04/MF A01

This report describes the authors' initial work under ARPA Unmanned Ground Vehicle (UGV) Demo II Program in the reconnaissance, surveillance, and target acquisition (RSTA) area. The task is to develop the automatic target recognition (ATR) system that will process the imagery from the RSTA laser radar (ladar). A real-time demonstration of this capability is scheduled for the 'Demo II' of 1996. All major components of this end-to-end ATR system are discussed, and more details are provided for critical elements that have been built and tested so far. A major topic of interest is the use of sets of azimuth-dependent functional templates and functional template correlation forward-looking ladar data. Other optics are the use of height-limited verticality as an interest image for focusing attention and of the Hough transform for getting a preliminary estimate of target orientation. Because the RSTA ladar remains to be procured and built, the report describes also the alternate sources of data that are begin used to develop and test the system elements built to date. DTIC

N95-34566# Naval Postgraduate School, Monterey, CA.
THE 11TH ANNUAL REVIEW OF PROGRESS IN APPLIED COMPUTATIONAL ELECTROMAGNETICS, VOLUME 1
26 Mar. 1995 668 p Conference held in Monterey, CA, 20-25 Mar. 1995 Limited Reproducibility: Document partially illegible
(AD-A294850) Avail: CASI HC A99/MF A06

Symposium papers are presented under the following sessions: scattering; low frequency; research and engineering framework for computational electromagnetics (CEM); interactive technical sessions on EM theory, validation and interfaces, and EMI/EMC/EMP; optimization techniques in applied electromagnetics; computational electromagnetics applied to ship design; finite difference time domain (FDTD); Berenger's boundary condition; time domain/FDTD; and fast algorithms for computational electromagnetics. CASI

N95-34567# Naval Postgraduate School, Monterey, CA.
THE 11TH ANNUAL REVIEW OF PROGRESS IN APPLIED COMPUTATIONAL ELECTROMAGNETICS, VOLUME 2
25 Mar. 1995 682 p Conference held in Monterey, CA, 20-25 Mar. 1995
(AD-A294851) Avail: CASI HC A99/MF A06

Symposium papers are presented under the following sessions: microwave and guided wave; method of moments (MOM); recent developments in finite difference time domain (FDTD) analysis; propagation; parallelization of EM codes; EM theory; electromagnetic modeling techniques for integrated optics; topics in fractal and wavelet electrodynamics; NEC applications; finite element method (FEM); EM analysis techniques for electrically large cavities; accuracy estimation in electromagnetic modeling; and partial differential equation (PDE) methods in electromagnetics. CASI

N95-34578# Army Engineer Waterways Experiment Station, Vicksburg, MS. Environmental Lab.
GRAYLING 2 INFORMATION BASE FOR GENERATION OF SYNTHETIC THERMAL INFRARED SCENES Final Report
Jerrell R. Ballard, Jr. Nov. 1994 55 p
(AD-A294956; SWOE-94-8) Avail: CASI HC A04/MF A01

Procedures are being developed for the environmental information base component of the Smart Weapons Operability Enhancement/Joint Test and Evaluation Program analytical thermal infrared scene generation procedure at Camp Grayling, MI. Scope is limited to documentation of the information base content and data processing/analysis procedures developed to satisfy other component requirements such as thermal signature modeling, thermal radiance field predictions, and generation of realistic graphic representations of the three dimensional thermal backgrounds. DTIC

N95-34590# Colorado State Univ., Fort Collins, CO.
OPTIMIZATION PROBLEMS IN MULTITARGET/MULTISENSOR TRACKING Final Technical Report
Aubrey B. Poore Jan. 1995 28 p
(Contract F49620-93-1-0133)
(AD-A294978; AFOSR-95-0300TR) Avail: CASI HC A03/MF A01

A multi-sensor multi-target tracker based on the use of near optimal and real-time algorithms for data association has been developed. DTIC

N95-34601# California Inst. of Tech., Pasadena, CA.
SPECTRUM ALLOCATION STRATEGIES FOR COMMUNICATION NETWORKS Final Report, 15 Oct. 1993 - 14 Oct. 1994
Robert J. McEliece 14 Oct. 1994 5 p
(Contract F49620-95-I-0005)
(AD-A294936; AFOSR-95-0388TR) Avail: CASI HC A01/MF A01

Models of multi-user communications systems have been developed and studied. The limits for such systems have been computed by linear programming. DTIC

N95-34749# Massachusetts Inst. of Tech., Cambridge, MA.
NUMERICAL AND SYMBOLIC ALGORITHMS FOR APPLICATION SPECIFIC SIGNAL PROCESSING Semiannual Report, 31 Oct. 1994 - 4 Apr. 1995
Alan V. Oppenheim 8 May 1995 13 p
(Contract N00014-93-1-0686)
(AD-A294125) Avail: CASI HC A03/MF A01

Work by Prof. Oppenheim and his collaborators is summarized here. DTIC

N95-34760# Air Force Systems Command, Wright-Patterson AFB, OH. National Air Intelligence Center.
INMARSAT TT&C AND COMMUNICATIONS NETWORK AND THE BEIJING INMARSAT STATION
Lin Rongle 5 Apr. 1995 18 p Transl. into ENGLISH from Aerospace China, China, no. 171, Jul. 1992 p 41-45
(AD-A294163; NAIC-ID(RS)T-0416-94) Avail: CASI HC A03/MF A01

First, this paper presents a briefing of the basic concepts of the INMARSAT TT&C and communications Network which includes the space segment and the ground segment. The Network consists of the satellite control center, the TT&C stations and the corresponding TT&C subsystems of the INMARSAT satellites. Next, this paper describes the configuration, the functions and the performance indicators of the Beijing INMARSAT TT&C station. Finally, the primary technical characteristics of this station are presented. DTIC

N95-34762# Air Force Systems Command, Wright-Patterson AFB, OH. National Air Intelligence Center.
EXPERIMENTAL INVESTIGATION OF IMPULSE RADAR FOR MITIGATION OF EFFECTS OF RADAR ABSORBING MATERIALS

He Jianguo, Lu Zhongliang, and Su Yi 18 Apr. 1995 13 p Transl. into ENGLISH from Guofang Keji Daxue Xuebao, China, v. 14, no. 3, 1992 p 46-50
(AD-A294166; NAIC-ID(RS)T-0500-94) Avail: CASI HC A03/MF A01

This article uses experimental methods from the two areas of frequency-domain and time-domain to investigate electromagnetic scattering associated with targets coated with wave absorbent materials. Results clearly show that UWB signals have a 10-12dB advantage coping with targets coated with wave absorbent materials as compared to the narrow band signals of conventional radar. The explanation is that ultra wide waveband signals clearly possess excellent capabilities for countering narrow band wave absorbent materials. DTIC

N95-34788# Mitre Corp., McLean, VA. Jason Program Office.
SAR
A. Despain, P. Banks, M. Cornwall, W. Dally, and F. Dyson 20 Apr. 1995 257 p Limited Reproducibility: Document partially illegible
(AD-A295020; JSR-93-170) Avail: CASI HC A12/MF A03

This report (1) explores reformulations of the theory of SAR imaging so as to understand how to improve SAR images, structure parallel algorithms and machine architectures and to see what new SAR applications may be possible, (2) examines the issue of formulating parallel algorithms, (3) examines massive parallel computer architectures to determine the possibilities and limits provided by today's and the future massively parallel processors, (4) explores novel methods enabled by massive computing in SAR computation, (5) considers the role of countermeasures, (6) looks forward to how new SAR systems can be designed to exploit massive computing capabilities, and (7) identifies a number of research issues for future study. Lastly, the report draws conclusions as to the role of massive computing in SAR technology. DTIC

N95-34790 Duke Univ., Durham, NC. Dept. of Computer Science.
DESIGN AND ANALYSIS OF LOSSLESS AND LOSSY DATA COMPRESSION METHODS WITH APPLICATIONS TO COMMUNICATION AND CACHING Final Project Report, 1992 - 1994
Jeffrey S. Vitter 19 Dec. 1994 8 p Limited Reproducibility: More than 20% of this document may be affected by poor print
(Contract F49620-92-J-0515)
(AD-A295025; AFOSR-95-0303TR) Avail: Issuing Activity (Defense Technical Information Center (DTIC))

Summary of Progress: Our work in this one-year project has been very successful. It has revolved around the following three important areas dealing data compression and its applications: (1) the design and analysis of sophisticated methods for prediction based on data compression techniques, with applications to prefetching, caching, and locality management; (2) fast, practical, and code-efficient implementations of arithmetic coding and other coding methods, for use in text and image compression; and (3) new methods for choosing motion vectors yielding substantially better rate-distortion tradeoffs for video compression in videoconferencing applications. DTIC

N95-32491# Elmer, Rome (Italy).
HELICOPTER HF COMMUNICATIONS USING THE NVIS MODE
M. Proia *In* AGARD, Low-Level and Nap-of-the-Earth (NOE) Night Operations Jan. 1995 12 p (For primary document see N95-32486 12-03)
Copyright Avail: CASI HC A03/MF A03

N95-32492# Army Communications-Electronics Command, Fort Monmouth, NJ. Space and Terrestrial Communications Directorate.
TACTICAL LOW-LEVEL HELICOPTER COMMUNICATIONS
Bernard V. Ricciardi, George H. Hagn (SRI International Corp., Arlington, VA.), and Gerald August (SRI International Corp., Menlo Park, CA.) *In* AGARD, Low-Level and Nap-of-the-Earth (NOE) Night Operations Jan. 1995 13 p (For primary document see N95-32486 12-03)
Copyright Avail: CASI HC A03/MF A03

N95-32501# Defence Research Agency, Bedford (England).
THE ANGLO-FRENCH COMPACT LASER RADAR DEMONSTRATOR PROGRAMME
G. M. Hogg, K. Harrison, and S. Minisclou (STTE, Paris, France.) *In* AGARD, Low-Level and Nap-of-the-Earth (NOE) Night Operations Jan. 1995 8 p (For primary document see N95-32486 12-03)
Copyright Avail: CASI HC A02/MF A03

N95-33137# Eurocopter Deutschland G.m.b.H., Munich (Germany).
HeliRadar: A ROTATING ANTENNA SYNTHETIC APERTURE RADAR FOR HELICOPTER ALLWEATHER OPERATIONS
W. Kreitmair-Steck and A. P. Wolframm (Deutsche Aerospace A.G., Munich, Germany.) *In* AGARD, Dual Usage in Military and Commercial Technology in Guidance and Control Mar. 1995 8 p (For primary document see N95-33126 12-31)
Copyright Avail: CASI HC A02/MF A02

33 ELECTRONICS AND ELECTRICAL ENGINEERING

Includes test equipment and maintainability; components, e.g., tunnel diodes and transistors; microminiaturization; and integrated circuitry.

For related information see also *60 Computer Operations and Hardware* and *76 Solid-State Physics.*

N95-32578# Sandia National Labs., Albuquerque, NM.
COBRA ACCELERATOR FOR SANDIA ICF DIODE RESEARCH AT CORNELL UNIVERSITY
David L. Smith, Pete Ingwersen, Lawrence F. Bennett, John D. Boyes, David E. Anderson (Cornell Univ., Ithaca, NY.), John B. Greenly (Cornell Univ., Ithaca, NY.), and Ravi N. Sudan (Cornell Univ., Ithaca, NY.) 1995 4 p Presented at the Particle Accelerator Conference, Dallas, TX, 1-5 May 1995
(Contract DE-AC04-94AL-85000)
(DE95-011018; SAND-94-2966C; CONF-950512-38) Avail: CASI HC A01/MF A01

The new COBRA accelerator is being built in stages at the Laboratory of Plasma Studies in Cornell University where its applications will include extraction diode and ion beam research in support of the light ion inertial confinement fusion (ICF) program at Sandia National Laboratories. The 4- to 5-MV, 125- to 250-kA accelerator is based on a four-cavity inductive voltage adder (IVA) design. It is a combination of new ferromagnetically-isolated cavities and self magnetically insulated transmission line (MITL) hardware and components from existing Sandia and Cornell facilities: Marx generator capacitors, hardware, and power supply from the DEMON facility; water pulse forming lines (PFL) and gas switch from the Subsystem Test Facility (STF); a HERMES-3 intermediate store capacitor (ISC); and a modified ion diode from Cornell's LION. The present accelerator consists of a single modified cavity similar to those of the Sandia SABRE accelerator and will be used to establish an operating system for the first stage initial lower voltage testing. Four new cavities will be fabricated and delivered in the first half of FY96 to complete the COBRA accelerator. COBRA is unique in the sense that each cavity is driven by a single pulse forming line, and the IVA output polarity may be reversed by rotating the cavities 180(degrees) about their vertical axis. The site preparations, tank construction, and diode design and development are taking place at Cornell with growing enthusiasm as this machine becomes a reality. Preliminary results with the single cavity and short positive inner cylinder MITL configuration will soon be available. DOE

N95-32596# California Univ., Berkeley. Lawrence Berkeley Lab, CA. Materials Science Div.
PHOTON ECHOES FROM THE ABSORPTION CONTINUUM OF A SEMICONDUCTOR
S. Glutsch, S. Bar-Ad, M. A. Mycek, D. S. Chemla, and U. Siegner (Marburg Univ., Germany.) Nov. 1994 11 p Presented at the 15th Conference on Lasers and Electro-optics and 5th Quantum Electronics and Laser Science Conference, Baltimore, MD, 21-26 May 1995
(Contract DE-AC03-76SF-00098)
(DE95-011274; LBL-36585; CONF-950540-8) Avail: CASI HC A03/MF A01

The theory of photon echoes has been intensively investigated for interaction-free particles. Numerical calculations for semiconductors excited

at or below the band edge have been reported. A very important configuration for ultrashort-pulse experiments corresponds to excitation in the continuum or simultaneous excitation of bound and continuum states. One can expect marked differences between the response of bound and continuum states. In this report, the authors provide theoretical evidence for a photon echo in a homogeneous broadened semiconductor excited in the absorption spectrum. DOE

N95-32628# Joint Inst. for Nuclear Research, Dubna (USSR).
CATHODE READOUT WITH STRIPPED RESISTIVE DRIFT TUBES
V. N. Bychkov, G. D. Kekelidze, E. A. Novikov, V. D. Peshekhonov, M. D. Shafranov, and V. E. Zhiltsov 1994 11 p Presented at the Vienna Wire Chamber Conference, Austria, Feb. 1995
(DE95-621871; JINR-E-13-94-351) Avail: CASI HC A03/MF A01 (US Sales Only)

A straw tube drift chamber prototype has been constructed and tested. The straw tube material is mylar film covered with carbon layer of resistivity 0.5, 30 and 70 k Ohm/sq. The gas mixture used was Ar/CH4. Both the anode wire and cathode signals were detected in order to study the behaviour of the chamber in the presence of X-ray ionization. The construction and the results of the study are presented. DOE

N95-32629# Joint Inst. for Nuclear Research, Dubna (USSR). Lab. of Nuclear Reactions.
ANALYSIS OF RADIATION DAMAGES OF ELECTRONIC CIRCUITS BY SEPARATE IRRADIATION OF THEIR COMPONENTS WITH A COLLIMATED CHARGED PARTICLE BEAM
W. Wronski and A. Y. Didyk 1994 4 p In POLISH
(DE95-621946; JINR-R-14-94-355) Avail: CASI HC A01/MF A01 (US Sales Only)

Some advantages of the comparative method of studying the radiation damages of electronic devices which includes parameter comparison of irradiated and test samples are shown. The analysis of damages is performed at separate irradiation of the electronic circuit components while its operation in the main regime of the device. The purposeful irradiation is carried out by a well-collimated charged particle beam, in this case the principle of simulation of different types of nuclear radiation in view of their damage abilities is used. Experiments have been performed with the scheme of an electronic digital watch. DOE

N95-32708# Sandia National Labs., Albuquerque, NM.
N-15 HYDROGEN PROFILING OF IC METALLIZATIONS
K. M. Horn and W. F. Filter 1995 6 p Presented at the 9th International Conference on Ion Beam Modification of Materials, Canberra, Australia, 5-10 Feb. 1995
(Contract DE-AC04-94AL-85000)
(DE95-011052; SAND-95-0762C; CONF-950220-9) Avail: CASI HC A02/MF A01

The 6.4 MeV p(N-15, alpha gamma)C-12 resonant nuclear reaction has been used to investigate the role of hydrogen as a contributing factor in the formation of stress-induced voids in very large scale integrated circuit metallizations. Hydrogen profiles were measured from a series of layered structures consisting of aluminum-copper alloy metallizations deposited on borophosphosilicate glass and capped with a variety of commercial passivation materials in order to examine differences in the concentrations and depth distributions of hydrogen within the layered structures. DOE

N95-32714# Los Alamos National Lab., NM.
ANALYSIS OF A HTSC CURRENT LEAD UNDER NONLINEAR HEAT TRANSFER CONDITIONS
D. P. Sekulic, Z. Uzelac, and F. J. Edeskuty 1995 8 p Presented at the International Congress of Refrigeration Meeting, The Hague, Netherlands, 20-25 Aug. 1995
(Contract W-7405-eng-36)
(DE95-009420; LA-UR-95-987; CONF-950890-1) Avail: CASI HC A02/MF A01

The main objective of this paper is to consider the influence of the temperature dependence of the convective heat transfer coefficient on the optimal thermal design of the high temperature superconducting current (HTSCl) part of a cryogenic current lead. In the previous study the analysis of a HTSC lead was performed with the assumption that the heat transfer coefficient between the coolant (boil-off liquid helium) and the lead is finite but constant along the lead. In a present effort the heat transfer coefficient is allowed to vary along die lead causing an additional nonlinearity in the model. Numerically obtained current lead temperature profiles and corresponding helium vapor temperature profiles were used to calculate entropy generation within the lead as a function of the relevant design parameters. It has been demonstrated that additional nonlinearities do not cause a significant change of optimal design parameters. DOE

N95-32808# National Renewable Energy Lab., Golden, CO.
A COMPARISON OF MODELED AND MEASURED ENERGY USE IN HYBRID ELECTRIC VEHICLES
Matthew Cuddy Jan. 1995 8 p Presented at the Society of Automotive Engineers International Congress and Exposition, Detroit, MI,27 Feb. - 2 Mar. 1995
(Contract DE-AC36-83CH-10093)
(DE95-000297; NREL/TP-473-7444; CONF-950256-4) Avail: CASI HC A02/MF A01

CarSim 2.5.4, written by AeroVironment, Inc. of Monrovia, California and SIMPLEV 3.0, written by Idaho National Engineering Laboratory were used to simulate two series-configured hybrid electric vehicles that competed in the 1994 Hybrid Electric Vehicle Challenge. Vehicle speed and battery energy use were measured over a 0.2-km maximum effort acceleration and a 58-km range event. The simulations' predictions are compared to each other and to measured data. A rough uncertainty analysis of the validation is presented. The programs agree with each other to within 5% and with the measured energy data within the uncertainty of the experiment. DOE

N95-32956# Argonne National Lab., IL.
LESSONS LEARNED IN ACQUIRING NEW REGULATIONS FOR SHIPPING ADVANCED ELECTRIC VEHICLE BATTERIES
Gary Henriksen, Carol Hammel (National Renewable Energy Lab., Golden, CO.), and Edward A. Altemos (Winston and Strawn, Washington, DC.) Dec. 1994 10 p Presented at the 12th International Electric Vehicle Symposium, Anaheim, CA, 5-7 Dec. 1994
(Contract W-31-109-eng-38)
(DE95-009908; ANL/CMT/CP-83389; CONF-941221-3) Avail: CASI HC A02/MF A01

In 1990, the Electric and Hybrid Propulsion Division of the US Department of Energy established its ad hoc EV Battery Readiness Working Group to identify regulatory barriers to the commercialization of advanced EV battery technologies and facilitate the removal of these barriers. A Shipping Sub-Working Group (SSWG) was formed to address the regulatory issues associated with the domestic and international shipment of these new battery technologies. The SSWG invites major industrial developers of advanced battery technologies to join as members and work closely with appropriate domestic and international regulatory authorities to develop suitable regulations and procedures for the safe transport of these new battery technologies. This paper describes the domestic and international regulatory processes for the transport of dangerous goods; reviews the status of shipping regulations for sodium-beta and lithium batteries; and delineates the lessons learned to date in this process. The sodium-beta battery family was the first category of advanced EV batteries to be addressed by the SSWG. It includes both sodium/sulfur and sodium/metal chloride batteries. Their efforts led to the establishment of a UN number (UN 3292) in the UN Recommendations, for cold cells and batteries, and establishment of a US Department of Transportation general exemption (DOT-E-10917) covering cold and hot batteries, as well as cold cells. The lessons learned for sodium-beta batteries, over the period of 1990--94, are now being applied to the development of regulations for shipping a new generation of lithium battery technologies (lithium-polymer and lithium-aluminum/iron sulfide batteries). DOE

N95-32968# University of Western Washington, Bellingham, WA.
A THERMOPHOTOVOLTAIC GENERATOR FOR USE IN A LIGHTWEIGHT ELECTRIC CAR: YEAR 1 PROGRESS REPORT
M. R. Seal 1 May 1995 9 p
(Contract DE-FG06-94ER-12149)
(DE95-011355; DOE/ER-12149/T1) Avail: CASI HC A02/MF A01

In the nine months since the start of this project significant progress toward the completion of the tasks scheduled in the first year has been made and in some cases exceeded. A number of unforeseen problems

have been isolated and solved with redesign of components and specification of different materials. This project has been running concurrently with a Phase 1 DOE Green Car SBIR grant to JX Crystals in which WWU is the sub-contractor to do burner design, construction and testing. As a result of this concurrent project, the design of the single burner for the TPV8 which is nearing completion at this time, incorporates the improvements of the Phase 1 Green Car burner. The status of the tasks scheduled for the first nine months of the contract and the current status are shown. DOE

N95-33080 Lawrence Livermore National Lab., Livermore, CA.
QUENCH ANTENNA AND FAST-MOTION INVESTIGATIONS DURING TRAINING OF A 7T DIPOLE MAGNET
A. F. Lietzke, R. Benjegerdes, P. Bish, J. Krywinski, R. Scanlan, R. Schmidt (European Organization for Nuclear Research, Geneva, Switzerland.), and C. Taylor 17 Oct. 1994 4 p Presented at the Applied Superconductivity Conference, Boston, MA, 16-21 Oct. 1994 Limited Reproducibility: More than 20% of this document may be affected by microfiche quality
(Contract DE-AC03-76SF-00098)
(DE95-012371; LBL-35422; CONF-941013-42; SC-MAG-458) Avail: CASI HC A01/MF A01

Equipment was installed to detect fast conductor motion and quench propagation in a 1 meter long superconducting dipole magnet. The fast-motion antenna, centered within the bore of the magnet, used three long dipole coils, mounted end-to-end to span the magnet length. Coil signals were nulled against a neighbor to produce low-ripple signals that were sensitive to local flux changes. A low-microphonic signal was used as an event trigger. Nulling improvements were made for the magnet's coil-imbalance signals for improved cross-correlation information. A quench-propagation antenna was installed to observe current redistribution during quench propagation. It consisted of quadrupole/sextupole coil sets distributed at three axial locations within the bore of the magnet. Signals were interpreted in terms of the radius, angle, orientation, and rate of change of an equivalent dipole. The magnet was cooled to 1.8K to maximize the number of events. Twenty-four fast-motion events occurred before the first quench. The signals were correlated with the magnet-coil imbalance signals. The quench-propagation antenna was installed for all subsequent quenches. Ramp-rate triggered quenches produced adequate signals for analysis, but pole-turn quenches yielded such small signals that angular localization of a quench was not precise. DOE

N95-33404# Superconducting Super Collider Lab., Dallas, TX.
QUENCH PROPAGATION VELOCITY FOR HIGHLY STABILIZED CONDUCTORS
R. G. Mints (Tel-Aviv Univ., Ramat-Aviv, Tel-Aviv, Israel.), T. Ogitsu, and A. Devred 1995 17 p Submitted for publication
(Contract DE-AC35-89ER-40486)
(DE95-011040; SSCL-Preprint-37) Avail: CASI HC A03/MF A01

Quench propagation velocity in conductors having a large amount of stabilizer outside the multifilamentary area is considered. It is shown that the current redistribution process between the multifilamentary area and the stabilizer can strongly effect the quench propagation. A criterion is derived determining the conditions under which the current redistribution process becomes significant, and a model of effective stabilizer area is suggested to describe its influence on the quench propagation velocity. As an illustration, the model is applied to calculate the adiabatic quench propagation velocity for a conductor geometry with a multifilamentary area embedded inside the stabilizer. DOE

N95-33640# Sandia National Labs., Albuquerque, NM. Battery Research Dept.
DESIGN RULES AND REALITY CHECK FOR CARBON-BASED ULTRACAPACITORS
Erhard T. Eisenmann Apr. 1995 17 p
(Contract DE-AC04-94AL-85000)
(DE95-010575; SAND-95-0671) Avail: CASI HC A03/MF A01

Design criteria for carbon-based Ultracapacitors have been determined for specified energy and power requirements, using the geometry of the components and such material properties as density, porosity and conductivity as parameters, while also considering chemical compatibility. This analysis shows that the weights of active and inactive components of the capacitor structure must be carefully balanced for maximum energy and power density. When applied to nonaqueous electrolytes, the design rules for a 5 Wh/kg device call for porous carbon with a specific capacitance of about 30 F/cu cm. This performance is not achievable with pure, electrostatic double layer capacitance. Double layer capacitance is only 5 to 30% of that observed in aqueous electrolyte. Tests also showed that nonaqueous electrolytes have a diminished capability to access micropores in activated carbon, in one case yielding a capacitance of less than 1 F/cu cm for carbon that had 100 F/cu cm in aqueous electrolyte. With negative results on nonaqueous electrolytes dominating the present study, the obvious conclusion is to concentrate on aqueous systems. Only aqueous double layer capacitors offer adequate electrostatic charging characteristics which is the basis for high power performance. There are many opportunities for further advancing aqueous double layer capacitors, one being the use of highly activated carbon films, as opposed to powders, fibers and foams. While the manufacture of carbon films is still costly, and while the energy and power density of the resulting devices may not meet the optimistic goals that have been proposed, this technology could produce true double layer capacitors with significantly improved performance and large commercial potential. DOE

N95-33697# Oak Ridge National Lab., TN. Solid State Div.
THIN-FILM RECHARGEABLE LITHIUM BATTERIES
N. J. Dudney, J. B. Bates, and D. Lubben Nov. 1994 6 p Presented at the Contractor's Coordination Meeting, Dearborn, MI, 24-27 Oct. 1994 Submitted for publication
(Contract DE-AC05-84OR-21400)
(DE95-008975; CONF-9410309-4) Avail: CASI HC A02/MF A01

Small thin-film rechargeable cells have been fabricated with a lithium phosphorus oxynitride electrolyte, Li metal anode, and Li(1-x)Mn2O4 as the cathode film. The cathode films were fabricated by several different techniques resulting in both crystalline and amorphous films. These were compared by observing the cell discharge behavior. Estimates have been made for the scale-up of such a thin-film battery to meet the specifications for the electric vehicle application. The specific energy, energy density, and cycle life are expected to meet the USABC mid-term criteria. However, the areas of the thin-films needed to fabricate such a cell are very large. The required areas could be greatly reduced by operating the battery at temperatures near 100 C or by enhancing the lithium ion transport rate in the cathode material. DOE

N95-33864# Allied-Signal Aerospace Co., Kansas City, MO. Kansas City Div.
CHARACTERIZATION OF DUPONT 9015, AQUEOUS PROCESSABLE DRY FILM PHOTORESIST FOR PRINTED WIRING BOARDS
Steve Goldammer Apr. 1995 75 p
(Contract DE-AC04-76DP-00613)
(DE95-011239; KCP-613-5537) Avail: CASI HC A04/MF A01

This report describes the evaluation of DuPont's Riston 9015, fully aqueous processable dry film photoresist as a mask for gold plating, tin/lead plating, and print and etch patterning for printed circuit board products. DOE

N95-33874*# NYMA, Inc., Brook Park, OH.
IMPROVED L-C RESONANT DECAY TECHNIQUE FOR Q MEASUREMENT OF QUASILINEAR POWER INDUCTORS: NEW RESULTS FOR MPP AND FERRITE POWDERED CORES
Janis M. Niedra and Scott S. Gerber Aug. 1995 13 p
(Contract NAS3-27186; RTOP 233-01-0C)
(NASA-CR-198373; E-9823; NAS 1.26:198373) Avail: CASI HC A03/MF A01

The L-C resonant decay technique for measuring circuit Q or losses is improved by eliminating the switch from the inductor-capacitor loop. A MOSFET switch is used instead to momentarily connect the resonant circuit to an existing voltage source, which itself is gated off during the decay transient. Very reproducible, low duty cycle data could be taken this way over a dynamic voltage range of at least 10:1. Circuit Q is computed from a polynomial fit to the sequence of the decaying voltage maxima. This method was applied to measure the losses at 60 kHz in inductors having loose powder cores of moly permalloy and an Mn-Zn power ferrite. After the copper and capacitor losses are separated out, the resulting specific core loss is shown to be roughly as expected for the MPP powder, but anomalously high for the ferrite powder. Possible causes are mentioned. Author

N95-33915*# Hughes Aircraft Co., Torrance, CA.
A 75 WATT, 59 TO 64 GHz SPACE TWT Final Report
Helen Limburg, Diego Zamora, Jon Davis, and Ivo Tammaru Apr. 1995 43 p
(Contract NAS3-25090; RTOP 506-72-00)
(NASA-CR-195450; E-9529; NAS 1.26:195450) Avail: CASI HC A03/MF A01

The design and performance of a high efficiency 70 Watt, 59 to 64 GHz traveling-wave tube (TWT) is described. This intersatellite communications TWT, designated the Hughes Aircraft Company Model 961HA, employs a coupled-cavity slow-wave structure with a two-step velocity taper and a four-stage isotropic graphite multistage depressed collector (MDC). This TWT achieved outstanding beam transmission, 96% with RF. This is the highest power and widest bandwidth device of this type. The tube has 45 dB of gain and 30% efficiency. This TWT is conduction cooled and weighs 13 lbs. Author

N95-34345# University of Southern California, Marina del Rey, CA.
SELF STRESSING TEST STRUCTURE CELLS Final Technical Report, Jun. 1992 - Mar. 1994
Vance C. Tyree Feb. 1995 106 p
(Contract F30602-91-D-0001)
(AD-A294386; RL-TR-95-18) Avail: CASI HC A06/MF A02

This report addresses the work performed to design on chip reliability prognostics for purposes of monitoring fielded integrated circuits for degradation due to the failure mechanisms of oxide breakdown, electromigration, and hot carrier degradation. The self stressing test structure cells are self-contained standard cells that include the test structure, stressing, and monitoring circuitry and a boundary scan interface to be used with the IEEE 1149.1 boundary scan Test Access Port. The cells have been designed to work within the limitations of a CMOS integrated circuit, i.e., no additional power levels are needed, the cell area has been kept as small as possible, the cells may be incorporated independently from active circuitry, and cells will not degrade chip lifetime. The self stressing cells have been shown to function by simulation, but further study to correlate cell degradation to integrated circuit degradation is required. DTIC

N95-34347# Army Research Lab., Fort Monmouth, NJ.
HIGH RATE RECHARGEABLE LITHIUM CELLS EMPLOYING LITHIUM ION CONDUCTING SOLID ELECTROLYTES Technical Report, Jan. - Dec. 1994
Edward J. Plichta and Wishvender K. Behl Feb. 1995 16 p
(AD-A294390; ARL-TR-421) Avail: CASI HC A03/MF A01

Results are presented on high temperature solid state cells employing 50:50 weight percent lithium germanium vanadium oxide-lithium iodide. The incorporation of lithium iodide in lithium germanium vanadium oxide resulted in higher pellet conductivities and improved the high rate performance of the solid state cells. The cells were comprised of a lithium-aluminum or lithium-silicon alloy as the anode and a CVD thin film of titanium disulfide as the cathode. The cells exhibited an open circuit potential of about 2.1 V at 300 C and could be discharged at current densities up to 0.5 ampere per square centimeter. DTIC

N95-34379# Air Force Systems Command, Wright-Patterson AFB, OH. National Air Intelligence Center.
PROGRAMMABLE REAL-TIME OPTOELECTRONIC HYBRID THRESHOLD LOGIC PROCESSORS
Liu Shutian, Wu Jie, and Li Chunfei 5 Apr. 1995 15 p Transl. into ENGLISH from Zhongguo Jiguang, China, v. 18, no. 10, Oct. 1991 p 760-764
(AD-A294067; NAIC-ID(RS)T-0415-94) Avail: CASI HC A03/MF A01

A programmable real-time optoelectronic hybrid threshold logic processor is presented and the applications of the processors in question to digital optical computing a digital optical signal processing are discussed. DTIC

N95-34425 Department of the Navy, Washington, DC.
CROSSPOINT ANALOG DATA SELECTOR Patent
Chester Fedor, inventor (to Navy) and Kevin C. Fitzpatrick, inventor (to Navy) 14 Mar. 1995 11 p Filed 8 Dec. 1993
(AD-D017482; US-Patent-5,398,239; US-Patent-Appl-SN-169923; US-Patent-Class-370-58) Avail: US Patent and Trademark Office

A crosspoint analog data selector for coupling data received on a predetermined number of input channel lines onto a predetermined lesser number of output channel lines. The crosspoint analog data selector includes a selector section and a control section. The selector section includes two or more crosspoint switch sections, each crosspoint switch section including a predetermined number of input terminals and a predetermined number of output terminals. Each output terminal is individually energizable. Each input terminal is connected to a different input channel line, such that none of the input channel lines are connected to input terminals of multiple crosspoint switch sections. Each output terminal is connected to one of the output channel lines such that each Output channel line is connected to an output terminal of each of the crosspoint switch sections. The control section is responsive to commands to enable the selector section to couple data from a selected input channel line to a selected output channel line. In that operation, the control section (1) initially enables the crosspoint switch sections to de-energize their output terminals connected to the selected output channel line, (2) enables the crosspoint switch section connected to the selected input channel line to connect its input terminal connected thereto to its output terminal connected to the selected output channel line, and (3) enables the crosspoint switch section connected to the selected input channel line to energize its output terminal connected to the selected output channel line. DTIC

N95-34445 Department of the Navy, Washington, DC.
DIAMOND MULTILAYER MULTICHIP MODULE SUBSTRATE Patent
Patrick M. Sullivan, inventor (to Navy) and Pat H. Reaves, inventor (to Navy) 21 Feb. 1995 6 p Filed 16 Mar. 1994
(AD-D017468; US-Patent-5,391,914; US-Patent-Appl-SN-215799; US-Patent-Class-257-635) Avail: US Patent and Trademark Office

Diamond is used as a dielectric layer to separate the metalization layers in multichip module substrates. The diamond has use for both electrical and thermal conclusion. Such multichip module substrates may have a diamond base, or a base constructed from silicon, aluminum altride, molybdenum, or any other material supportive of the nucleation and growth of diamond films. The metalization may be molybdenum or other conductor supportive of the nucleation and growth of diamond films. Using diamond as an interlayer dielectric in a multichip system permits a significant increase in the amount of power that can be dissipated by the system. The diamond does not obstruct the system's metalization, so that routing density can be increased and interconnection length may be decreased, enhancing host chip operation. DTIC

N95-34446 Department of the Navy, Washington, DC.
CHANNEL EQUALIZED DC SQUID FLUX-LOCKED LOOP Patent
Meir Gershenson, inventor (to Navy) and Robert J. McDonald, inventor (to Navy) 7 Feb. 1995 7 p Filed 26 Jul. 1993
(AD-D017469; US-Patent-5,387,864; US-Patent-Appl-SN-095557; US-Patent-Class-324-248) Avail: US Patent and Trademark Office

A DC superconductor quantum interference device (i.e. DC SQUID) is used in a flux-looked loop as a sensitive detector of magnetic flux. Prior art devices of this sort had a transfer function which was frequency-limited by the transfer function of impedance matching circuitry which is used to connect the DC SQUID with the first preamplifier, which amplifies the DC SQUID signal before it is applied to a detector circuit. The present invention corrects this frequency limitation by creating a compensating circuit having a transfer function which is the inverse of that of the impedance matching circuitry and inserting it in the system after the first preamplifier and before the detector circuit. DTIC

N95-34451# Washington Univ., Seattle, WA. Dept. of Physics.
INDIUM MONO-ION OSCILLATOR Final Report, 1993 - 1994
Warren Nagourney and Hans Dehmelt 1995 10 p
(Contract F49620-92-J-0052)
(AD-A293736; AFOSR-95-0320TR) Avail: CASI HC A02/MF A01

During the third (and final) year of the 'Indium Mono-Ion Oscillator' grant, our goal of loading and observing a single indium ion was realized. In order to achieve this result, we relied on the development work of previous years; the 'background suppression system' developed earlier was found to be particularly useful. We also began the design and construction of the all-solid-state 'clock laser' system. Our intent is to replace all of the bulky argon and dye lasers with solid state systems; this will allow

considerable reduction in the size and power consumption of the resulting optical frequency standard. DTIC

N95-34458# Advanced Device Technologies, Inc., Charlottesville, VA.
NOVEL FIELD EFFECT TRANSISTORS FOR LOW POWER ELECTRONICS Final Report, 20 Oct. 1994 - 19 May 1995
William C. Peatman 15 May 1995 20 p
(Contract N00014-94-C-0260)
(AD-A294221; SA-51595) Avail: CASI HC A03/MF A01

The primary objective of this Phase 1 project was to determine the extent of the significant reduction in power consumption of integrated circuits which may be achieved by utilizing a novel sidegate FET technology. The new FET technology eliminates the Narrow Channel Effect (NCE) which is one of the primary factors limiting the minimum power consumption of integrated circuits. By eliminating the NCE, we may scale the device size dramatically and reduce the power-delay product by at least an order of magnitude compared to existing transistor technologies. Additionally, the new FET has two gates which can therefore lead to a significant reduction in the transistor count of IC's, as was demonstrated in a simple NOR gate using only two transistors. Finally, the transistor technology is compatible with fiFET circuits for microwave/digital applications. In this Phase 1 project, the design, fabrication, characterization and modeling of the new transistor was investigated and issues concerning manufacturability were discussed. DTIC

N95-34488# Air Force Systems Command, Wright-Patterson AFB, OH. National Air Intelligence Center.
ENGLAND DEVELOPS WORLD'S FASTEST OPTIC SWITCH BREAKTHROUGH IN HIGH-SPEED COMMUNICATIONS
Sheng Li 5 Apr. 1995 6 p Transl. into ENGLISH from Keji Ribao, Chinese, v. 6, no. 12, 3 p 1992
(AD-A294038; NAIC-ID(RS)T-0402-94) Avail: CASI HC A02/MF A01

England's Gelasige University has successfully developed the world's fastest optical switching device, allowing for a major breakthrough in high-speed communications. This switching device is called a non-linear direct coupler. It is a type of all-optical switch which operates with an extremely short strong laser pulse. The laser pulse is focused on a transistor waveguide and can change the optical properties of the transistor; thus by changing the laser pulse intensity, it is possible to change the light emitted by the transistor, thus changing the size of the switching pulse. DTIC

N95-34565# Carnegie-Mellon Univ., Pittsburgh, PA. Dept. of Computer Science.
BIT-LEVEL ANALYSIS OF AN SRT DIVIDER CIRCUIT
Randal E. Bryant 18 Apr. 1995 11 p
(Contract F33615-93-1-1330)
(AD-A294842; CMU-CS-95-140) Avail: CASI HC A03/MF A01

It is impractical to verify multiplier or divider circuits entirely at the bit-level using ordered binary decision diagrams (BDD's), because the BDD representations for these functions grow exponentially with the word size. It is possible, however, to analyze individual stages of these circuits using BDD's. Such analysis can be helpful when implementing complex arithmetic algorithms. As a demonstration, we show that Intel could have used BDD's to detect erroneous table entries in the Pentium floating point divider. Going beyond verification, we show that bit-level analysis can be used to generate a correct version of the table. DTIC

N95-34581# New Mexico Univ., Albuquerque, NM.
HIGH EFFICIENCY VACUUM AND PLASMA FILLED BACKWARD WAVE OSCILLATORS: A CRITICAL EVALUATION Final Report, 1 Feb. 1994 - 31 Jan. 1995
Edl Shamiloglu, Charles Fleddermann, and John Gahl 24 May 1995 93 p
(Contract F49620-94-1-0087)
(AD-A294963; AFOSR-95-0409TR) Avail: CASI HC A05/MF A01

This report describes the results of research during the first year of a proposed three year project to provide a critical evaluation of the attributes of plasma-filled high power backward-wave oscillators when compared with high efficiency vacuum backward-wave oscillators. Since the direction of the program at the University of New Mexico was altered by the newly initiated MURII triservices funding, only about one third of the originally proposed tasks were accomplished. Nevertheless, important new results have been obtained and will continue to be investigated under the auspices of the MURI program. DTIC

N95-34617 Department of the Navy, Washington, DC.
CONFORMING TUNING COUPLER FOR FLEXTENSIONAL TRANSDUCERS Patent
John D. Maltby, inventor (to Navy) 8 Nov. 1994 12 p Filed 7 Jan. 1993
(AD-D017285; US-Patent-5,363,346; US-Patent-Appl-SN-143893; US-Patent-Class-367-163) Avail: US Patent and Trademark Office

A flextensional transducer includes a stack of driving elements disposed along a linear axis to convert a driving power into vibrational energy. End pieces, disposed at each end of the stack, have outwardly facing arcuate surfaces. A flexural shell, formed into a loop, is disposed to circumscribe the stack and the end pieces to present an elliptical cross-section with the major axis thereof being generally coincident with the stack's linear axis. The shell is reactively coupled to the end pieces at the outwardly facing arcuate surfaces. A plant assembly is positioned between each end piece and the flexural shell for maintaining conformal engagement between portions of the end pieces and the flexural shell. The plant assembly is designed such that its stiffness may be adjusted. DTIC

N95-34618 Department of the Navy, Washington, DC.
OPERATIONAL AMPLIFIER USING BIPOLAR JUNCTION TRANSISTORS IN SILICON-ON-SAPPHIRE Patent
Eric N. Cartagena, inventor (to Navy) 20 Dec. 1994 14 p Filed 20 May 1993
(AD-D017421; US-Patent-5,374,567; US-Patent-Appl-SN-065321; US-Patent-Class-437-31) Avail: US Patent and Trademark Office

A method for fabricating low leakage current bipolar junction transistors of silicon-sapphire for efficient use in operational amplifiers utilizes all implant technology, improved silicon conditioning processing, and low temperature annealing. DTIC

N95-34758# Air Force Systems Command, Wright-Patterson AFB, OH. National Air Intelligence Center.
OPTICAL LOGIC IMPLEMENTATION IN COMPOSITE BILED/BILD CIRCUITS
Shutian Liu, Chunfei Li, and Jie Wu 5 Apr. 1995 15 p Transl. into ENGLISH from Guangxue Xuebao, China, v. 9, no. 11, Nov. 1989 p 983-988
(AD-A294160; NAIC-ID(RS)T-0405-94) Avail: CASI HC A03/MF A01

Utilizing laser diode or light emitting diode hybrid bi-stable circuit composites, optical multistability and optical XOR logic gates as well as R-S flip-flops have been obtained. This type of optoelectronic logic circuitry and very large scale integrated (VLSI) technology are fully compatible. Because this is the case, it is hoped to apply it to optical information processing, optical signals, and optical computing. DTIC

N95-34796# Naval Air Warfare Center, China Lake, CA.
AN INVESTIGATION OF THE CHEMISTRY OF CITRIC ACID IN MILITARY SOLDERING APPLICATIONS
Robin Nissan, Larry Merwin, John Fischer, Jim Smith, and Jerry Maurice Jun. 1995 32 p
(AD-A295042; NAWCWPNS-TP-8199) Avail: CASI HC A03/MF A01

As a result of the phase-out of ozone-depleting chemicals (ODC), the military and its contractors are facing the problem of developing alternative materials and processes which currently employ these materials. Electronics are a particularly challenging problem because efficient removal of post soldering flux residues is critical to the long-term performance of high reliability electronics. The use of water soluble flux offers an attractive option because all cleaning would be accomplished using only water. Until recently, the military has not allowed this type of flux because of the highly corrosive fluxing action usually associated with these materials. However, a new flux ingredient, citric acid, is gaining favor within the electronics manufacturing industry. Citric acid offers excellent fluxing ability, efficient removal of residues with water, and non-ionic flux formulations. This report examines the chemistry of this material under simulated soldering conditions in an effort to gain an improved understanding of thermal reactions and degradation products which may have an effect on long-term reliability of military electronic hardware. DTIC

34 FLUID MECHANICS AND HEAT TRANSFER

Includes boundary layers; hydrodynamics; fluidics; mass transfer; and ablation cooling.

For related information see also *02 Aerodynamics* and *77 Thermodynamics and Statistical Physics.*

N95-32387# Sandia National Labs., Albuquerque, NM.
THREE-DIMENSIONAL NATURAL CONVECTION OF A FLUID WITH TEMPERATURE-DEPENDENT VISCOSITY IN AN ENCLOSURE WITH LOCALIZED HEATING
J. R. Torczynski, J. A. Henderson, T. J. OHern, T. Y. Chu, and T. K. Blanchat 1994 8 p Presented at the National Heat Transfer Conference, Portland, OR, 5-9 Aug. 1995
(Contract DE-AC04-94AL-85000)
(DE95-002606; SAND-94-2516C; CONF-950828-1) Avail: CASI HC A02/MF A01

Three-dimensional natural convection of a fluid in an enclosure is examined. The geometry is motivated by a possible magmaenergy extraction system, and the fluid is a magma simulant and has a highly temperature-dependent viscosity. Flow simulations are performed for enclosures with and without a cylinder, which represents the extractor, using the finite-element code FIDAP (Fluid Dynamics International). The presence of the cylinder completely alters the flow pattern. Flow-visualization and PIV experiments are in qualitative agreement with the simulations. DOE

N95-32454*# MCAT Inst., Moffett Field, CA.
BOUNDARY LAYER TRANSITION STUDIES Final Report, Nov. 1990 - Feb. 1995
Jonathan H. Watmuff San Jose, CA Feb. 1995 49 p Original contains color illustrations
(Contract NCC2-698)
(NASA-CR-198983; NAS 1.26:198983; MCAT-95-12) Avail: CASI HC A03/MF A01; 7 functional color pages

A small-scale wind tunnel previously used for turbulent boundary layer experiments was modified for two sets of boundary layer transition studies. The first study concerns a laminar separation/turbulent reattachment. The pressure gradient and unit Reynolds number are the same as the fully turbulent flow of Spalart and Watmuff. Without the trip wire, a laminar layer asymptotes to a Falkner & Skan similarity solution in the FPG. Application of the APG causes the layer to separate and a highly turbulent and approximately 2D mean flow reattachment occurs downstream. In an effort to gain some physical insight into the flow processes a small impulsive disturbance was introduced at the C(sub p) minimum. The facility is totally automated and phase-averaged data are measured on a point-by-point basis using unprecedently large grids. The evolution of the disturbance has been tracked all the way into the reattachment region and beyond into the fully turbulent boundary layer. At first, the amplitude decays exponentially with streamwise distance in the APG region, where the layer remains attached, i.e. the layer is viscously stable. After separation, the rate of decay slows, and a point of minimum amplitude is reached where the contours of the wave packet exhibit dispersive characteristics. From this point, exponential growth of the amplitude of the disturbance is observed in the detached shear layer, i.e. the dominant instability mechanism is inviscid. A group of large-scale 3D vortex loops emerges in the vicinity of the reattachment. Remarkably, the second loop retains its identify far downstream in the turbulent boundary layer. The results provide a level of detail usually associated with CFD. Substantial modifications were made to the facility for the second study concerning disturbances generated by Suction Holes for laminar flow Control (LFC). The test section incorporates suction through interchangeable porous test surfaces. Detailed studies have been made using isolated holes in the impervious test plate that used to establish the Blasius base flow. The suction is perturbed harmonically and data are averaged on the basis of the phase of the disturbance, for conditions corresponding to strong suction and without suction. The technique was enhanced by using up to nine multiple probes to reduce the experimental run-time. In both cases, 3D contour surfaces in the vicinity of the hole show highly 3D TS waves which fan out in the spanwise direction forming bow-shaped waves downstream. The case without suction has proved useful for evaluating calculation methods. With suction, the perturbations on the centerline are much stronger and decay less rapidly, while the TS waves in the far field are similar to the case without suction. Downstream, the contour surfaces of the TS waves develop spanwise irregularities which eventually form into clumps. The spanwise clumping is evidence of a secondary instability that could be associated with suction vortices. Designers of porous surfaces use Goldsmith's Criterion to minimize cross-stream interactions. It is shown that partial TS wave cancellation is possible, depending on the hole spacing, disturbance frequency and free-stream velocity. New high-performance Constant Temperature Hot-Wire Anemometers were designed and built, based on a linear system theory analysis that can be extended to arbitrary order. The motivation was to achieve the highest possible frequency reponse while ensuring overall system stability. The performance is equal to or superior to commercially available instruments at about 10% of the cost. Details, such as fabrication drawings and a parts list, have been published to enable the instrument to be construced by others. Author

N95-32587# Sandia National Labs., Albuquerque, NM. Material and Structural Mechanics Dept.
ON THE FEASIBILITY OF USING SMOOTHED PARTICLE HYDRODYNAMICS FOR UNDERWATER EXPLOSION CALCULATIONS
J. W. Swegle and S. W. Attaway Feb. 1995 33 p Sponsored by NSWC
(Contract DE-AC04-94AL-85000)
(DE95-008799; SAND-95-0311) Avail: CASI HC A03/MF A01

SPH (Smoothed Particle Hydrodynamics) is a gridless Lagrangian technique which is appealing as a possible alternative to numerical techniques currently used to analyze high deformation impulsive loading events. In the present study, the SPH algorithm has been subjected to detailed testing and analysis to determine the feasibility of using PRONTO/SPH for the analysis of various types of underwater explosion problems involving fluid-structure and shock-structure interactions. Of particular interest are effects of bubble formation and collapse and the permanent deformation of thin walled structures due to these loadings. These are exceptionally difficult problems to model. Past attempts with various types of codes have not been satisfactory. Coupling SPH into the finite element code PRONTO represents a new approach to the problem. Results show that the method is well-suited for transmission of loads from underwater explosions to nearby structures, but the calculation of late time effects due to acceleration of gravity and bubble buoyancy will require additional development, and possibly coupling with implicit or incompressible methods. DOE

N95-32787# Deutsche Forschungsanstalt fuer Luft- und Raumfahrt, Goettingen (Germany). Abt. Operative Planung.
A NONLINEAR VORTEX LATTICE METHOD FOR UNSTEADY FLOW WITH SEPARATED VORTEX
Zheng-yin Ye Dec. 1994 33 p Sponsored by Alexander von Humboldt Foundation
(DLR-FB-94-32; CSD-95-98140) Avail: CASI HC A03/MF A01; DLR, Abt. Operative Planug, D-5114C Cologne, Germany, HC

An improved nonlinear vortex lattice method to simulate steady and unsteady flows for wings with leading edge and/or tip vortex separation at moderate or high angles of attack is presented. A type of vortex lattice shape along the leading edge is introduced and a multistep method for determining the position of the free vortex sheets which move downstream in the flow field is presented. This method can predict much more stable results for wings with leading edge separated vortex when undergoing very rapid and large amplitude movements. The calculated airloads agree well with the experiments. Author

N95-32818# Sandia National Labs., Albuquerque, NM. Engineering Sciences Center.
PINCA: A SCALABLE PARALLEL PROGRAM FOR COMPRESSIBLE GAS DYNAMICS WITH NONEQUILIBRIUM CHEMISTRY
C. C. Wong, F. G. Blottner, J. L. Payne, M. Soetrisno (Amtec Engineering, Inc., Bellevue, WA.), and S. T. Imlay (Amtec Engineering, Inc., Bellevue, WA.) Apr. 1995 273 p
(Contract DE-AC04-94AL-85000)
(DE95-010581; SAND-94-2436) Avail: CASI HC A12/MF A03

This report documents an exploratory research work, funded by the Laboratory Directed Research and Development (LDRD) office at Sandia

National Laboratories, to develop an advanced, general purpose, robust compressible flow solver for handling large, complex, chemically reacting gas dynamics problems. The deliverable of this project, a computer program called PINCA (Parallel INtegrated Computer Analysis) will run on massively parallel computers such as the Intel/Gamma and Intel/Paragon. With the development of this parallel compressible flow solver, engineers will be better able to address large three-dimensional scientific arid engineering problems involving multi-component gas mixtures with finite rate chemistry. These problems occur in high temperature industrial processes, combustion, and hypersonic: reentry of space-crafts. DOE

N95-32898 Lehigh Univ., Bethlehem, PA.
ASYMPTOTIC STRUCTURE OF SUPERSONIC TURBULENT BOUNDARY LAYERS Ph.D. Thesis
Jun He 1994 301 p
Avail: Univ. Microfilms Order No. DA9414994

The problem of high speed two-dimensional turbulent boundary layers is considered. An asymptotic analysis of the compressible boundary layer equations is carried out for large Reynolds numbers and main stream Mach numbers O(1). A self-consistent two-layer asymptotic structure is described wherein the time-mean velocity and total enthalpy are logarithmic within the overlap zone but in terms of the Howarth-Dorodnitsyn variable; the proposed structure leads to a compressible law of the wall for high speed turbulent flows and expressions are obtained relating the friction coefficient and surface heat flux to the slope of the velocity and total enthalpy profiles in the fully turbulent (logarithmic) zone. Representative velocity and total enthalpy profiles are obtained for the inner region of the boundary layer through consideration of typical time-dependent motions within the wall layer. The outer layer profiles are determined from the leading order outer layer equations; simple outer region Boussinesq eddy-viscosity and eddy conductivity turbulence models are formulated to reflect the effects of compressibility of the flow. The conditions for self-similarity in a high-speed boundary layer are examined and a set of self-similar velocity and temperature profiles are obtained for constant pressure flows to test the proposed asymptotic structure and turbulence models; these are combined with wall-layer profiles to form a set of composite profiles valid across the entire boundary layer. A direct comparison with experimental data shows good agreement over a wide range of conditions for flows with and without surface heat transfer. To complete the analysis the case of an adiabatic wall is considered and an expression for the adiabatic wall temperature is derived. It is shown that the asymptotic analysis constrains the types of turbulence closures that can be used to represent the effects of viscous dissipation. A simple algebraic model is proposed and comparisons with measured total enthalpy profile data show good agreement. Dissert. Abstr.

N95-32902 Michigan Univ., Ann Arbor, MI.
NEAR-LIMIT DROP DEFORMATION AND SECONDARY BREAKUP Ph.D. Thesis
Lien-Peng Hsiang 1994 149 p
Avail: Univ. Microfilms Order No. DA9423210

An experimental study of the deformation and breakup of liquid drops subjected to both shock wave and steady disturbances is described, emphasizing effects of Weber number, We, and Ohnesorge number, Oh, for various deformation and breakup regimes. Measurements included pulsed shadowgraphy and holography to find drop deformation and drag properties prior to breakup, as well as drop sizes and velocities after breakup. Simplified phenomenological theories were used to help interpret and correlate the measurements. For shock wave disturbances, drop deformation and breakup regimes were identified in terms of We and Oh: regimes at low Oh included no deformation, nonoscillatory deformation, oscillatory deformation, bag breakup, multimode breakup, and shear breakup as We is increased. For We less than 1000, breakup no longer is possible for Oh greater than 10 while 5 percent deformation no longer is possible for Oh greater than 1000. Unified temporal scaling of deformation and breakup processes was observed in terms of a characteristic breakup time that largely was a function of Oh. Prior to breakup, the drag coefficient evolved from the properties of spheres to those of thin disks as drop deformation progressed. Measurements of drop properties after secondary breakup were limited to low Oh conditions. Drop size distributions after breakup satisfied Simmon's universal root normal distribution function in all three breakup regimes, after removing the core drop from the drop population for shear breakup. The Sauter mean diameter after breakup was correlated successfully, independent of the breakup regime, based on consideration of drop stripping in the shear breakup regime. The size and velocity of the core drop after shear breakup were correlated separately, based on the observation that the end of drop stripping corresponded to a constant Eotvos number. The relative velocities of the drop liquid were significantly reduced during secondary breakup, due both to the large drag coefficients caused by drop deformation and the reduced relaxation times of small drops. These effects were correlated successfully, using phenomenological theory. For steady disturbances, significant drop deformation (roughly 5 percent) began at a We of roughly unity, with the deformation regime ending due to the onset of breakup at We in the range of 10-20. These transitions were relatively unaffected by Oh. Another transition, between dome- and bowl-shaped drops (related to the transition between bag and shear breakup), was correlated mainly in terms of We and Re for present conditions. Drop deformation for steady disturbances was relatively independent of dispersed/continuous phase density ratios but generally was smaller than for shock wave disturbances at comparable conditions due to the absence of overshoot from inertial effects. In contrast, drop drag coefficients, normalized by the drag coefficient of a solid sphere at the same Re, was correlated quite well by the degree of deformation alone. Dissert. Abstr.

N95-32905 Maryland Univ., College Park, MD.
APPLICATION OF VORTICITY TRANSPORT ANALYSIS TO THE DEVELOPMENT OF PHYSICALLY ACCURATE TURBULENCE MODELS Ph.D. Thesis
Joseph John Gorski 1993 216 p
Avail: Univ. Microfilms Order No. DA9425038

Turbulence closure for the Reynolds averaged Navier-Stokes equations, based on vorticity transport theory, is investigated. This is a fundamental investigation to determine what new insights or improvements can be gained by using vorticity transport analysis to model turbulence. Specifically, it is an attempt to develop more physically correct turbulence models than currently available. Direct numerical simulation data for flow in a channel is used to evaluate the modeled terms and set unknown constants. One aspect of this work is the modeling of the enstrophy equation as an alternative to the dissipation rate equation. Although it is shown that the equations are similar, the vorticity transport analysis leads to models for two additional production terms in the enstrophy equation which are not accounted for in conventional kappa-epsilon models. These extra terms had only small affects on the computed mean flow quantities, for the flows calculated here, but they significantly alter the turbulent production and dissipation budgets of the enstrophy equation. A second aspect of this work is the use of the vorticity transport correlation bar-(u(sub i)w(sub j)), as an alternative to the Reynolds stresses for closing the Navier-Stokes equations. General two-dimensional expressions are obtained for the individual vorticity transport correlation terms. This is one of the first practical applications of such a model and results are presented for a channel, flat plate boundary layer, and flow over a hill. The computed mean flow and kinetic energy compares well with the data, and the vorticity transport based results perform better than the conventional Boussinesq eddy viscosity Reynolds stress model near the separated flow region on the leeward side of the hill. Dissert. Abstr.

N95-32907 Illinois Univ., Chicago, IL.
FLOW AND HEAT TRANSFER BEHAVIOR OF NON-NEWTONIAN FLUIDS IN RECTANGULAR DUCTS Ph.D. Thesis
Shixiang Gao 1993 234 p
Avail: Univ. Microfilms Order No. DA9414855

Numerical studies are reported for steady laminar flow and heat transfer behavior of non-Newtonian fluids through rectangular ducts. Both the power law model and the Reiner-Rivlin model are studied. Finite difference methods are developed to obtain the primary flow, the secondary flow (in the case of the Reiner-Rivlin fluid), the friction factor, maximum and minimum wall temperatures, and Nusselt number for the H2 thermal boundary condition for different combinations of heated and adiabatic walls. The power law results are used as the base case against which the friction factors and the heat transfer predictions for the Reiner-Rivlin fluids may be compared. The influence of the second normal stress coefficient, the Reynolds number, the Peclet Number, and the aspect ratio on the flow and heat transfer are considered. In general, the effect of the secondary flow on the primary flow rate and friction factor is found to be negligible and the power law

predictions agree with the Reiner-Rivlin results. In contrast the secondary flow, which is about the order of 10(exp -3) of the primary flow, has a dominant effect on heat transfer, especially for aspect ratios of 0.5 and 1.0. The general behavior of the friction factor and the Nusselt number predicted for the Reiner-Rivlin fluid is found to be in good agreement with experimental results. Dissert. Abstr.

N95-32930*# National Aeronautics and Space Administration. Lewis Research Center, Cleveland, OH.
REVIEW OF COMBUSTION-ACOUSTIC INSTABILITIES
Ayo Oyediran (AYT Corp., Brook Park, OH.), Douglas Darling, and Krishnan Radhakrishnan (NYMA, Inc., Brook Park, OH.) Aug. 1995 12 p Presented ath the 31st Joint Propulsion Conference and Exhibit, San Diego, CA, 10-12 Jul. 1995; sponsored by AIAA, ASME, SAE and ASEE
(Contracts NAS3-27571; NAS3-27186; RTOP 537-02-21)
(NASA-TM-107020; E-9825; NAS 1.15:107020; AIAA Paper 95-2469)
Avail: CASI HC A03/MF A01

Combustion-acoustic instabilities occur when the acoustic energy increase due to the unsteady heat release of the flame is greater than the losses of acoustic energy from the system. The problem of combustion-acoustic instability is a concern in many devices for various reasons, as each device may have a unique mechanism causing unsteady heat release rates and many have unique boundary conditions. To accurately predict and quantify combustion-acoustic stabilities, the unsteady heat release rate and boundary conditions need to be accurately determined. The present review brings together work performed on a variety of practical combustion devices. Many theoretical and experimental investigations of the unsteady heat release rate have been performed, some based on perturbations in the fuel delivery system particularly for rocket instabilities, while others are based on hydrodynamic processes as in ramjet dump combustors. The boundary conditions for rocket engines have been analyzed and measured extensively. However, less work has been done to measure acoustic boundary conditions in many other combustion systems. Author

N95-32934 Michigan Univ., Ann Arbor, MI.
TRANSPORT PHENOMENA IN SUBSONIC AND SUPERSONIC FLOWS IN A DUCT WITH MASS INJECTION Ph.D. Thesis
Shyang-Lin Kuo 1994 218 p
Avail: Univ. Microfilms Order No. DA9423238

Film cooling effects have always been crucial for the engine/rocket/ramjet propulsion systems. Knowing the pressure and temperature distribution of the flow is very important for both system and structural analyses to find optimal design. An efficient time dependent, compressible Navier-Stokes solver using higher order accuracy algorithms employing the finite-volume method is developed. The physics inside the flow field with a cooler secondary mass stream injected into the channel is studied. The results showed that for subsonic main flow, the injected mass stream will bend and accelerate in the downstream direction, creating a region of lower temperature near the downstream walls. This lower temperature region also exists even if there is a heat flux added to the flow system. Therefore, film cooling effect exists for the subsonic flow. For supersonic flow, however, the injected mass flow, instead of bending toward the downstream wall in order to have a cooling effect, is bent toward upstream direction and retards the main flow, resulting in a stagnant flow region. The temperature in the entire flow field is found to increase an appreciable amount even though the temperature in the stagnant region is found to be relatively lower than other areas. Therefore, there is no film cooling effect observed for supersonic flow. These phenomena have been verified by the experimental work. For subsonic flow, the acoustical wave is found to travel forwards and backwards in the field system while the pressure gradient is favorable for the whole flow field. For supersonic flow, there is always an adverse pressure gradient region formed near the walls upstream of the mass-injection location. Inside this adverse pressure gradient region, an air bubble is usually found to exist. The flow interactions between the main stream and secondary stream increase the flow vorticity. This vorticity is found to travel in the downstream direction for subsonic flow. However, for supersonic flow, this vorticity is found to travel in both the upstream and the downstream direction. Dissert. Abstr.

N95-33031 Texas Univ., Austin, TX.
PARALLEL FINITE ELEMENT METHODS AND ITERATIVE SOLUTION TECHNIQUES FOR VISCOUS INCOMPRESSIBLE FLOWS Ph.D. Thesis
Edward Joseph Barragy 1993 312 p
Avail: Univ. Microfilms Order No. DA9413434

The present work is motivated by a desire to map the solution structure of nonlinear systems of partial differential equations (PDE). Of particular interest are viscous flow problems in 2D, possibly with coupled heat transfer or species transport. Due to the nonlinearity of the governing PDE's, many complicated solution structures may arise. These may include sharp layers, multiple solutions, and the possibility of bifurcation. The existence of spurious solutions, arising from insufficiently refined meshes, underscores the need for highly accurate solution procedures. This, in turn, motivates the use of p type finite element discretizations. Continuation techniques have been developed by several authors for the solution of these types of nonlinear problems. These techniques involve the solution of linear algebraic systems arising from a Newton iteration, for many, possibly hundreds, of discrete parameter values. This large computational burden motivates the use of large scale, parallel supercomputing facilities. A study of the impact of high p finite element discretizations as applied to the continuation solution of viscous incompressible flows in two dimensions is presented. The impact of these methods is considered for a Newton type continuation method coupled with gradient type element-by-element (EBE) iterative solvers. Significant issues considered concern the effect of high p on performance for various supercomputing platforms, implementation issues for EBE schemes in a distributed memory setting, and issues of scalability in a distributed memory multiprocessor setting. These issues are examined in conjunction with the development of preconditioners appropriate for high p methods, and the development of bifurcation detection schemes appropriate for high p methods and gradient type solution schemes. Dissert. Abstr.

N95-33059# Royal Inst. of Tech., Stockholm (Sweden). Dept. of Numerical Analysis and Computing Science.
TURBULENCE MODELS IN THE NAVIER-STOKES SIMULATION OF AIRFOIL STALL
Carlos Weber [1993] 63 p Prepared in cooperation with Stockholm Univ., Sweden
(TRITA-NA-9312) Avail: CASI HC A04/MF A01

The low-speed flow around a two-dimensional airfoil near stall has been calculated, using a Navier-Stokes multiblock flow solver with a cell-centered finite volume technique and explicit Runge Kutta time-stepping scheme. Two different turbulence models have been implemented in the code: the Baldwin-Lomax model and the Kappa-Tau model. The computations were carried out for angles of attack of 7.2 degrees, 12.3 degrees, and 13.2 degrees. The latter is hereby close to the stall limit. Comparison of computed data with experimental data show that the Baldwin-Lomax model is in quite good agreement with the experiments, although the wall shear stresses are calculated too small. But it fails to predict the separation zone at high angles of attack and therefore the lift coefficients near stall are over-predicted. Small differences between the medium and fine grid show that the latter might be fine enough to yield sufficient results. During the computations using the Kappa-Tau model several problems with the range of the Kappa- and Tau-values appeared which led to some modifications in the code. The results of the Kappa-Tau model are in rather poor agreement with the experimental data. Nevertheless an improvement of the viscous forces compared to the Baldwin-Lomax model can be seen. The poor results are probably due to the fact that the grid sizes for the Kappa-Tau model are still too coarse and the stretching of the grid is too large. Computations with finer grid sizes have to be carried out to show if the results can be improved. CASI

N95-33255 Akron Univ., Akron, OH.
LAMINAR HEAT TRANSFER FOR POWER-LAW FLUIDS IN THERMAL ENTRANCE REGION OF ANNULAR SECTOR DUCTS Ph.D. Thesis
Rong Ping Hsia 1993 132 p
Avail: Univ. Microfilms Order No. DA9415528

Laminar heat transfer of a power law fluid in the thermal entrance region of an annular sector duct is analyzed. The effect of geometric shape, power law index, axial conduction and viscous dissipation are investigated. Both boundary conditions of uniform temperature and uniform heat flux peripherally are considered. The annular sector duct flow configuration is one of the common arrangements in industry, for example, compact heat exchangers, nuclear reactors and injection molds. The power law fluid is one of the frequently used non-Newtonian heat transferring

media. It is important to understand the details of heat transfer and fluid flow for this type of application. The solution algorithm is based on a finite difference methodology. Numerical experiments are performed and comparisons are made between the results obtained and the existing limiting solutions to ensure the accuracy of the present numerical scheme. In the thermal entrance region, there exists a large difference in Nusselt number for different Peclet numbers. The viscous dissipation effect is stronger in the developing region than in the developed region. It is found that due to the reduction in friction and the increase in heat transfer rates, power law fluids with n less than 1 are better working fluids in heat exchange equipments. Dissert. Abstr.

N95-33256 Alabama Univ., Huntsville, AL.
THERMOCAPILLARY FLOW WITH EVAPORATION AND CONDENSATION AND ITS EFFECT ON LIQUID RETENTION IN LOW-g FLUID ACQUISITION DEVICES Ph.D. Thesis
George Raymond Schmidt 1993 331 p
Avail: Univ. Microfilms Order No. DA9415111

The steady motion, thermal and free surface behavior of a volatile, wetting liquid in microgravity are studied using scaling and numerical techniques. The objective is to determine whether the thermocapillary and two-phase convection arising from thermodynamic non-equilibrium along the porous surfaces of spacecraft liquid acquisition devices could cause the retention failures observed with liquid hydrogen and heated vapor pressurant. The study also examines why these devices seem immune to retention loss when pressurized with heated helium or heated directly through the porous structure. The problem domain consists of a rectangular liquid cavity bounded by a saturated vapor on its upper free surface, and superheated or subcooled via isothermal boundaries on its other three sides. The mathematical model is based on dimensionless parameters representing surface tension, viscosity, thermocapillary stress, vapor recoil and surface non-equilibrium. Flowfield and temperature are calculated using Galerkin-based finite elements with mixed order interpolation functions, a semi-implicit Crank-Nicholson time marching scheme and a SIMPLER pressure/velocity algorithm. The meniscus is solved via a transformation of the normal stress balance. Several heating and convection modes are examined. The basic state, which characterizes the nonlinear influence of contact angle and non-equilibrium on interfacial temperature and stress, indicates an increase in net thermocapillary force with reduced contact angle. This result is confirmed in analyses of single and combined-mode convection which show that highly wetting fluids exhibit large negative and positive dynamic pressure gradients towards the meniscus interline when superheated and subcooled, respectively. First-order and coupled assessments of meniscus deformation indicate that for highly wetting fluids in small pores, pressure and vapor recoil dictate surface morphology. With superheating, these two terms exert the same influence on curvature and promote surface retention. With subcooling, however, the pressure distribution produces a suction that degrades mechanical equilibrium of the surface. This result indicates that thermocapillary induced deformation arising from subcooling and condensation is the likely cause for retention loss. In addition, increasing the level of nonequilibrium by reducing accommodation coefficient suppresses deformation and explains why this failure mode does not occur in instances of direct screen heating or pressurization with a heated inert gas. Dissert. Abstr.

N95-33257 Dayton Univ., OH.
EXPERIMENTAL AND NUMERICAL ANALYSIS OF CONTROLLED IMPINGING LIQUID JETS Ph.D. Thesis
Scott Keith Thomas 1993 126 p
Avail: Univ. Microfilms Order No. DA9412551

An experimental and numerical study of the heat transfer from a heated horizontal disk to a thin film of liquid is described. The liquid was delivered to the disk by a collar arrangement such that the film thickness and radial velocity were known at the outer radius of the collar. This method of delivery is termed as a controlled impinging liquid jet. The mean thickness of a thin liquid film of deionized water with a free surface on a rotating horizontal disk has been measured with a nonintrusive capacitance technique. The measurements were taken when the rotational speed ranged from 0 to 300 rpm and the flow rate varied from 7.0 to 15.0 lpm. When the disk was stationary, a circular hydraulic jump was present on the disk. Upstream from the jump, the film thickness was determined by the inertial and frictional forces on the fluid, and the radial spreading of the film. The surface tension coupled with the curvature at the edge of the disk affected the film thickness downstream from the jump. For the rotating disk, the film thickness was dependent upon the inertial and frictional forces near the center of the disk and the centrifugal forces near the edge of the disk. Flow visualization tests were performed and heat transfer data were collected along the radius of the disk for different volumetric flow rates and inlet temperatures in the supercritical (upstream from the hydraulic jump) and subcritical regions (downstream from the jump). The heat transfer coefficient was found to increase with flow rate when both supercritical and subcritical regions were present on the heated surface. A numerical simulation of this free surface problem was performed, which included the effects of conjugate heat transfer within the heated disk and the liquid. The numerical predictions agree with the experimental results and show that conjugate heat transfer has a significant effect on the local wall temperature and heat transfer coefficient. Dissert. Abstr.

N95-33310 Lehigh Univ., Bethlehem, PA.
THE EFFECT OF INTERACTION ON BOUNDARY-LAYER SEPARATION AND BREAKDOWN Ph.D. Thesis
Kevin Wayne Cassel 1994 274 p
Avail: Univ. Microfilms Order No. DA9414986

It is common in boundary-layer flow at high Reynolds numbers involving separation for an interaction to be provoked between the viscous boundary layer and the inviscid external flow. The effect that this viscous-inviscid interaction has on both steady and unsteady boundary-layer separation is investigated. In part 1 the unsteady boundary-layer separation process is considered in the context of two-dimensional incompressible flow. In regions of adverse streamwise pressure gradient along solid surfaces, it is common for the boundary layer to erupt away from the surface in a narrow streamwise region. Classical noninteracting boundary-layer solutions of such flows breakdown within a finite time, but the thickening boundary layer induces an interaction with the outer inviscid flow during the first interactive stage in order to relieve the singularity. Numerical solutions were obtained of the first interactive stage formulated in Lagrangian coordinates. These results show that the viscous-inviscid interaction causes the flow to become unstable resulting in a breakdown of the first interactive stage. The instability is of a high-frequency inviscid type and is shown to be characterized by large complex wavespeeds. In part 2 separation of a hypersonic boundary layer flowing over a compression ramp is considered both with and without wall cooling. For small ramp angles, the flow in the vicinity of the corner is governed by the triple-deck structure which accounts for the viscous-inviscid interaction. The flow over the compression ramp exhibits separation in the corner for ramp angles above a critical value. Numerical solutions have been obtained for the hypersonic triple deck and show that for larger ramp angles the flow becomes unstable in the form of a stationary wave packet which forms near the corner. Wall cooling was found to have a significant effect upon both the location of separation and the extent of the recirculating-flow region, and it is shown to stabilize or destabilize the instability at high ramp angles depending upon the average Mach number across the boundary layer. Dissert. Abstr.

N95-33340 Virginia Polytechnic Inst. and State Univ., Blacksburg, VA.
LARGE EDDY SIMULATION OF TURBULENT VORTICES AND MIXING LAYERS Ph.D. Thesis
Madhu Kumar Sreedhar 1994 187 p
Avail: Univ. Microfilms Order No. DA9422538

In this dissertation large-eddy simulation (LES) is used to study the transitional and turbulent structures of vortices and free shear layers. The recently developed dynamic model and the basic Smagorinsky model are utilized to model the subgrid-scale (SGS) stress tensor. The dynamic model has many advantages over the existing SGS models. This model has the ability to vary in time and space depending on the local turbulence conditions. This eliminates the need to tune the model constants a priori to suit the flow field being simulated. Three different flow fields are considered. First, the evolution of large-scale turbulent structures in centrifugally unstable vortices is studied. It is found that these structures appear as counter rotating vortex rings encircling the vortex core. The interaction of these structures with the core results in the transfer of angular momentum between the core and the surroundings. The mean tangential velocity decays due to this exchange of angular momentum. Second, the generation and decay of turbulent structures in a vortex with an axial velocity deficit are studied. The presence of a destabilizing wake-like axial velocity field in an otherwise

centrifugally stable vortex results in a very complex flow field. The inflectional instability mechanism of the axial velocity deficit amplifies the initial disturbances and results in the generation of large-scale turbulent structures. These structures appear as branches sprouting out of the vortex core. The breakdown of these structures leads to small-scale motions. But the stabilizing effects of the rotational flow field tend to quench the small-scale motions and the vortex returns to its initial laminar state. The mean axial velocity deficit is weakened, but the mean tangential velocity shows no significant decay. Third, a transitional mixing layer calculation is performed. The growth and breakdown to small scales of vortical structures are studied. Emphasis is given to the identification of late transition structures and their subsequent breakdown. Formation of streamwise vortices in place of the original Kelvin-Helmholtz vortices and the subsequent appearance of hairpin vortices at the edges of the mixing layer mark the completion of transition. The basic Smagorinsky model is also used in the mixing layer simulations. The performance of the dynamic model is compared with the previous results obtained using the basic Smagorinsky model. As expected, the basic Smagorinsky model is found to be more dissipative. Dissert. Abstr.

N95-33389# Argonne National Lab., IL. Materials Science Div.
THE INTERACTION OF VORTICES WITH TWIN BOUNDARIES
G. W. Crabtree, W. K. Kwok, U. Welp, J. Fendrich, C. J. vanderBeek, V. K. Vlasko-Vlasov (Academy of Sciences, USSR, Moscow, USSR.), V. I. Nikitenko (Academy of Sciences, USSR, Moscow, USSR.), D. Gunter, and T. Gardiner 1995 10 p Presented at the NRIM International Seminar on Superconductors in High Magnetic Fields, Tsukuba, Japan, 17-18 Feb. 1995
(Contract W-31-109-eng-38; NSF DMR-91-20000)
(DE95-012079; ANL/MSD/CP-85925; CONF-950292-1) Avail: CASI HC A02/MF A01

Twin boundaries provide a convenient defect for investigating vortex dynamics in superconductors. They occur naturally in YBa2Cu3O7, with well defined planar geometries. They are a strong pinning defect, and at the temperature of the melting transition they are the dominant pinning sites in clean crystals. Twin boundaries are easily seen in polarized light, making their location and number directly observable without special equipment. Finally, they present a highly anisotropic pinning potential to the vortices, creating the possibility of interesting new behavior. In this paper, we describe experiments using twin boundaries to probe two effects in vortex dynamics: a new peak effect in the critical current occurring in the solid state just below the melting transition, and anisotropic pinning by planar defects. DOE

N95-33398*# Cleveland State Univ., OH. University Office of Research and Economic Development.
NUMERICAL THERMAL ANALYSES OF HEAT EXCHANGERS FOR THE STIRLING ENGINE APPLICATION
Mohan Raj Kannapareddy 1995 159 p
(Grant NAG3-955)
(NASA-CR-199120; NAS 1.26:199120) Avail: CASI HC A08/MF A02

The Regenerator, Cooler and Heater for the NASA Space Power Research Engine (SPRE) have been analyzed in detail for laminar, incompressible and oscillatory flow conditions. Each component has been analyzed independently and in detail with the regenerator being modeled as two-parallel-plates channel with a solid wall. The ends of the channel are exposed to two reservoir maintained at different temperature thus providing an axial temperature gradient along the channel. The cooler and heater components have been modeled as circular pipes with isothermal walls. Two different types of thermal boundary conditions have been investigated for the cooler and heater, namely, symmetric and asymmetric temperature inflow. In symmetric temperature inflow the flow enters the channel with the same temperature in throughout the velocity cycle whereas, in asymmetric temperature inflow the flow enters with a different temperature in each half cycle. The study was conducted over a wide range of Maximum Reynolds number (RE(max) varying from 75 to 60000, Valensi number (Va) from 2.5 to 800, and relative amplitude of fluid displacement (A(sub r) from 0.357 to 1.34. A two dimensional Finite volume method based on the SIMPLE algorithm was used to solve the governing partial differential equations. Post processing programs were developed to effectively describe the heat transfer mechanism under oscillatory flows. The computer code was validated by comparing with existing analytical solutions for oscillating flows. The thermal field have been studied with the help of temperature contour and three dimensional plots. The instantaneous friction factor, wall heat flux and heat transfer coefficient have been examined. It has been concluded that in general, the frictional factor and heat transfer coefficient are higher under oscillatory flow conditions when the Valensi number is high. Also, the thermal efficiency decreases for lower A(r) values. Further, the usual steady state definition for the heat transfer coefficient does not seem to be valid. Author

N95-33496*# National Aeronautics and Space Administration. Lewis Research Center, Cleveland, OH.
LOW REYNOLDS NUMBER KAPPA-EPSILON AND EMPIRICAL TRANSITION MODELS FOR OSCILLATORY PIPE FLOW AND HEAT TRANSFER M.S. Thesis
Christopher Bauer Nov. 1993 99 p
(Grant NAGw-955)
(NASA-TM-109785; NAS 1.15:109785) Avail: CASI HC A05/MF A02

Stirling engine heat exchangers are shell-and-tube type with oscillatory flow (zero-mean velocity) for the inner fluid. This heat transfer process involves laminar-transition turbulent flow motions under oscillatory flow conditions. A low Reynolds number kappa-epsilon model, (Lam-Bremhorst form), was utilized in the present study to simulate fluid flow and heat transfer in a circular tube. An empirical transition model was used to activate the low Reynolds number k-e model at the appropriate time within the cycle for a given axial location within the tube. The computational results were compared with experimental flow and heat transfer data for: (1) velocity profiles, (2) kinetic energy of turbulence, (3) skin friction factor, (4) temperature profiles, and (5) wall heat flux. The experimental data were obtained for flow in a tube (38 mm diameter and 60 diameter long), with the maximum Reynolds number based on velocity being Re(sub max) = 11840, a dimensionless frequency (Valensi number) of Va = 80.2, at three axial locations X/D = 16, 30 and 44. The agreement between the computations and the experiment is excellent in the laminar portion of the cycle and good in the turbulent portion. Moreover, the location of transition was predicted accurately. The Low Reynolds Number kappa-epsilon model, together with an empirical transition model, is proposed herein to generate the wall heat flux values at different operating parameters than the experimental conditions. Those computational data can be used for testing the much simpler and less accurate one dimensional models utilized in 1-D Stirling Engine design codes. Author

N95-33606 Illinois Univ., Urbana-Champaign, IL.
VERY LARGE EDDY SIMULATIONS OF SPATIALLY EVOLVING SUPERSONIC TURBULENT SHEAR LAYERS Ph.D. Thesis
Choong Kun Oh 1994 202 p
Avail: Univ. Microfilms Order No. DA9416420

The objective was to further the understanding of the fundamental physical mechanisms which control turbulence and entrainment at different levels of compressibility for supersonic shear flows. Very large eddy simulations (VLES) were performed based on the two-dimensional unsteady Euler equations without any empirical coefficients for turbulence modeling. These equations were used to study the spatially evolving mixing characteristics of unforced, planar, confined shear layers formed by two parallel streams of supersonic air that come into contact after passing over a splitter plate. The computations were performed using the conservative finite element method-flux corrected transport (FEM-FCT) scheme with unstructured adaptive grids. In general, it was found that the highest simulation fidelity was obtained by using a full turbulence spectra consistent with measured turbulent kinetic energy levels and an incompressible wavelength distribution. This model is the most physically consistent and yields the best comparison with the downstream experimental data. The computational investigation noted modifications of organized coherent structures as well asymmetric entrainment, i.e. the high speed fluid is entrained and convoluted to a greater extent than that of the lower speed stream, and their subsequent importance in mixing. The round vortex shape of incompressible circular eddies was modified to an oblique flattened shape with decreased transverse height as convective Mach number (M(sub c)) increases. The high speed side convolutions of organized lumps of fluid are also decreased as M(sub c) increases. However, the overall vortex sizes are only slightly modified, whereas the angular orientation is significantly modified. The merging process is very different as a function of M(sub c): the rotational vortex pairing process at low M(sub c) is modified to a slapping process at high M(sub c). This slapping process,

which results in eddy flattening and oblique angles at higher M(sub c), reduces the degree of coherency. Turbulence statistics of velocity and mixture fraction are also investigated for three different values of M(sub c). The converged peak values of V'(sub rms), f'(sub rms), and Reynolds stress are reduced, while U'(sub rms) peak values remain constant as M(sub c) increases (coherency decreases). Those observations are consistent with experimental results and observations of coherency effects. Dissert. Abstr.

N95-33607 Rutgers - The State Univ., New Brunswick, NJ.
VORTICITY IN SHOCK-ACCELERATED DENSITY-STRATIFIED INTERFACES: AN ANALYTICAL AND COMPUTATIONAL STUDY Ph.D. Thesis
Ravindra Samtaney 1993 248 p
Avail: Univ. Microfilms Order No. DA9412676

Vorticity is deposited due to baroclinicity on the surface of a density stratified interface accelerated by a shock. The circulation deposited on a planar interface may be derived analytically using shock polar analysis. The exact analytical result is valid only for regular refraction (RRR) of the shock at the interface. We present analytical expressions for Gamma', the circulation deposited per unit length of the unshocked interface, within and beyond RRR. The scaling behavior for Gamma' is derived as Gamma' varies as (1 - eta(exp -1/2))(sin alpha)(1 + M(exp -1) + 2 M(exp -2))(M - 1)(gamma(exp 1/2)/gamma + 1) where M is the incident shock Mach number, eta is the density ratio across the interface, alpha is the angle between the shock and the interface, and gamma is the specific heat ratio. The analytical results are validated by quantification (visiometrics) of direct numerical simulations of compressible Euler equations using a second order Godunov method. The discrepancy between the analytical and DNS results increases with increase in alpha and eta. The flow field after the vorticity deposition phase is dominated by coherent vortex structures (CVS) in general and dipolar stratified vortices in particular. The evolution CVS is examined in shock interactions with planar interfaces. The dominant vortex processes are binding and unbinding, merger, and filamentation. Effects of changes in M and eta are examined. Furthermore, secondary baroclinic effects are examined and issues of convergence addressed. The expressions for circulation on planar interfaces are generalized to nonplanar (sinusoidal and circular) interfaces and the analytical models are compared with DNS. The vorticity deposition on a 2D cylindrical bubble surface is asymmetric. The total circulation on the bubble surface is modeled by introducing a 'near-normality' ansatz validated by geometrical shock dynamics. A comparison with existing models in literature is presented. For the sinusoidal interface incompressible vortex paradigms for the growth rate of a single mode are developed. These vortex paradigms provide heuristic bounds on the growth rates. In the nonlinear evolution phase, the vorticity on the interface coalesces to form a coherent patch of vorticity. The analytical expressions for vorticity deposition are extended to three dimensional interface. An incompressible vortex paradigm is presented for the growth rate of a double sine wave interface. A possible mechanism for the discrepancy between 2D and 3D growth rates is the increase in the streamwise vorticity component. Finally, evidence of the occurrence of a vortex reconnection event for a planar interface sinusoidally perturbed in the third direction is presented. Dissert. Abstr.

N95-33698# Los Alamos National Lab., NM.
A COMPARISON OF INTERFACE TRACKING METHODS
Douglas B. Kothe and William J. Rider 27 Mar. 1995 12 p Presented at the 26th American Institute of Aeronautics and Astronautics (AIAA) Computational Fluid Dynamics Conference, San Diego, CA, 19-22 Jun. 1995
(Contract W-7405-eng-36)
(DE95-009481; LA-UR-95-1145; CONF-950634-1) Avail: CASI HC A03/MF A01

In this paper we provide a direct comparison of several important algorithms designed to track fluid interfaces. In the process we propose improved criteria by which these methods are to be judged. We compare and contrast the behavior of the following interface tracking methods: high order monotone capturing schemes, level set methods, volume-of-fluid (VOF) methods, and particle-based (particle-in-cell, or PIC) methods. We compare these methods by first applying a set of standard test problems, then by applying a new set of enhanced problems designed to expose the limitations and weaknesses of each method. We find that the properties of these methods are not adequately assessed until they are tested with flows having spatial and temporal vorticity gradients. Our results indicate that the particle-based methods are easily the most accurate of those tested. Their practical use, however, is often hampered by their memory and CPU requirements. Particle-based methods employing particles only along interfaces also have difficulty dealing with gross topology changes. Full PIC methods, on the other hand, do not in general have topology restrictions. Following the particle-based methods are VOF volume tracking methods, which are reasonably accurate, physically based, robust, low in cost, and relatively easy to implement. Recent enhancements to the VOF methods using multidimensional interface reconstruction and improved advection provide excellent results on a wide range of test problems. DOE

N95-33709 California Univ., Davis, CA.
DIRECT AND LARGE EDDY SIMULATIONS OF THREE DIMENSIONAL ROUND TURBULENT JETS Ph.D. Thesis
Jeffrey Jay Lienau 1994 350 p
Avail: Univ. Microfilms Order No. DA9423903

The turbulent flow in a spatially developing three dimensional incompressible round jet is simulated numerically. High order accurate finite difference methods are developed using compact differencing with formal accuracy varying from second to seventh order in the spatial directions. A large eddy simulation model is used to simulate the effect of the unresolved part of the motion. The spatially developing flow in a round jet is computed starting with the inviscid solution and structural and statistical properties of the flow are established. The Kelvin-Helmholtz instability is induced with small disturbances at the jet pipe. The vortex sheet rolls up into rings that interact and produce a variety of structures. The structures emerging in the development of the flow are analyzed using the local and global properties of kinetic energy and vorticity. It is found that the dynamics of breakdown in the round turbulent jet consists of four mechanisms. The first is the evolution of the vortex rings via the Kelvin Helmholtz instability. The second is the instability of the vorticity between the rings which develops into the braid region. The third is the interaction of the braids with the rings and the final is the transition to turbulent flow. The transport of particles is simulated numerically in the round turbulent jet. The particles investigated were the fluid particles, hexadecane particles ranging in size from 35 to 160 micrometers and vaporizing pentane particles in both heated and nonheated environments. For the heated environments, limiting cases of zero and infinite heat conductivity within the droplet were investigated. Particle dispersion time of flight, average velocity and droplet diameter are presented for the first sixty diameters of the jet and compared to experimental data. The comparisons are good which provides support for the computational results. Dissert. Abstr.

N95-33837 Sandia National Labs., Albuquerque, NM.
EVALUATION OF CONDUCTIVE, RADIATIVE, CHEMICAL, AND CONVECTIVE HEAT TRANSFER IN COMPLEX SYSTEMS USING A FAST-RUNNING, IMPLICIT, LUMPED-CAPACITANCE FORMULATION
Allan S. Benjamin, Ricardo Beraun, Nisa N. Brown, and Martin P. Sherman 1995 12 p Presented at the National Heat Transfer Conference, Portland, OR, 5-9 Aug. 1995 Limited Reproducibility: More than 20% of this document may be affected by microfiche quality
(Contract DE-AC04-94AL-85000)
(DE95-011889; SAND-95-0750C; CONF-950828-9) Avail: Issuing Activity (Department of Energy (DOE))

Accurate finite-element simulation of 3-D nonlinear heat transfer in complex systems may require meshes composed of tens of thousands of finite elements and hours of CPU time on today's fastest computers. To treat applications in which thousands of calculations may be necessary such as for risk assessment or design of high-temperature manufacturing processes, methods are needed which can solve these problems far more efficiently and maintain an acceptably high degree of accuracy. For this purpose, we developed the Thermal Evaluation and Matching Program for Risk Applications (TEMPRA). The primary differentiator between TEMPRA and comparable codes is its numerical formulation, which is designed to be unconditionally stable even with very large time steps, to afford good accuracy even with relatively coarse meshing, and to facilitate benchmarking/calibration through the use of adjustable parameters. Analysis for a sample problem shows that TEMPRA can obtain temperature response solutions with errors of less than 10% using approximately 1/1000 of the computer time required by a typical finite element code. DOE

N95-34284 Howard Univ., Washington, DC.
ON THE NONLINEAR STABILITY OF A NEARBY PARALLEL AND A NON-UNIDIRECTIONAL FLOW Ph.D. Thesis
Pankaj Rai Dwarka 1993 129 p
Avail: Univ. Microfilms Order No. DA9419316

Nonlinear stability of a nearly parallel and a non-unidirectional flow in semi-infinite space with the vertical axis extending to infinity is studied where both flows approach a constant exponentially. We use a weakly nonlinear theory, coupled with the method of multiple scales, to investigate this type of stability. More specifically, we derive the amplitude equation for the asymptotic suction velocity profile, a nearly parallel flow. Two forms of the amplitude equation are obtained: the first form is the Landau-Stuart equation, and the second form includes spatial modulations where the coefficients are integrals. In both forms, the precise formulation of the Landau constant is specified. For the non-unidirectional flow which occurs in geophysical fluid dynamics where large scale effects are dominant, the Ekman boundary layer is considered. As with the nearly parallel suction flow, the amplitude equation is derived for the Ekman boundary layer and explicit expressions are given for the Landau constant and the coefficients of the spatial modulations. Numerical computations are needed to test these results since this study is purely theoretical. Since the region of the flows is semi-infinite, it is reasonable to expect contributions from the continuous spectrum of an operator appearing in the linearized stability equations. For the case of the nearly parallel asymptotic suction velocity profile, the linearized equation, frequently referred to as the modified Orr-Sommerfeld equation, is transformed into an integral equation involving a compact integral operator. A fixed point theorem is then used to conclude that for this flow which decays exponentially to a constant, there are finitely many eigenvalues. A three dimensional theory is then discussed in order to better understand the dynamics of the instability. Dissert. Abstr.

N95-34285 Virginia Polytechnic Inst. and State Univ., Blacksburg, VA.
ANALYSIS AND FINITE ELEMENT APPROXIMATION OF AN OPTIMAL SHAPE CONTROL PROBLEM FOR THE STEADY-STATE NAVIER-STOKES EQUATIONS Ph.D. Thesis
Hongchul Kim 1993 158 p
Avail: Univ. Microfilms Order No. DA9419217

An optimal shape control problem for the steady-state Navier-Stokes equations is considered from an analytical point of view. We examine a rather specific model problem dealing with two-dimensional channel flow of incompressible viscous fluid: we wish to determine the shape of a bump on a part of the boundary in order to minimize the energy dissipation. To formulate the problem in a comprehensive manner, we study some properties of the Navier-Stokes equations. The penalty method is applied to relax the difficulty of dealing with incompressibility in conjunction with domain perturbations and regularity requirements for the solutions. The existence of optimal solutions for the penalized problem is presented. The computation of the shape gradient and its treatment play a central role in the shape sensitivity analysis. To describe the domain perturbation and to derive the shape gradient, we study the material derivative method and related shape calculus. The shape sensitivity analysis using the material derivative method and Lagrange multiplier technique is presented. The use of Lagrange multiplier techniques, from which an optimality system is derived, is justified by applying a method from functional analysis. Finite element discretizations for the domain and discretized description of the problem are given. We study finite element approximations for the weak penalized optimality system. To deal with inhomogeneous essential boundary condition, the framework of a Lagrange multiplier technique is applied. The split formulation decoupling the traction force from the velocity is proposed in conjunction with the penalized optimality system and optimal error estimates are derived.
Dissert. Abstr.

N95-34286 Indiana Univ., Bloomington, IN.
STABILITY OF STEADY STATE SOLUTIONS FOR FORCED NAVIER-STOKES EQUATIONS
Daoping Xu 1993 85 p
Avail: Univ. Microfilms Order No. DA9418847

We prove the asymptotic stability of steady state solutions of the Navier-Stokes equations for one dimensional, nonisentropic, compressible fluid flow subject to an external force. We assume that the initial data is in L(exp 2) and the initial velocity is BV. We show that there exists a unique steady state solution determined by the external force, the total initial mass, and the total initial energy, and we prove that this steady state solution is stable with respect to discontinuous perturbations, in the sense that the time-dependent solutions with the given initial mass and energy tend to the corresponding steady-state solution as time goes to infinity. Dissert. Abstr.

N95-34343# Cambridge Hydrodynamics, Inc., Princeton, NJ.
NUMERICAL STUDIES OF TURBULENT FREE SURFACE FLOWS AND UNSTEADY PROPELLER FLOWS Final Report, 1 Jan. 1990 - 31 Mar. 1995
Steven A. Orszag, Vadim Borue, Ilya Staroselsky, and Yansi Zhang 31 Mar. 1995 62 p
(Contract N00014-90-C-0039)
(AD-A294377) Avail: CASI HC A04/MF A01

Two main problems have been studied, viz. the structure of turbulence near a free surface and the Reynolds-averaged solution of unsteady propeller/hydrofoil flows by the renormalization group (RNG) two-equation turbulence transport model. A variety of free-surface turbulence simulations demonstrate the key modifications in turbulence structure due to the free surface. In addition, we determine the modifications in surface wave spectra due to the turbulence beneath the free surface as typically represented by a renormalized dispersion relation. The results for unsteady hydrofoils show the power of the RNO method in robustly and accurately treating large-scale unsteady and transitional flows, a marked improvement over previous turbulence transport models. DTIC

N95-34437# Lawrence Livermore National Lab., Livermore, CA.
CONSISTENT FINITE-VOLUME DISCRETIZATION OF HYDRODYNAMIC CONSERVATION LAWS FOR UNSTRUCTURED GRIDS
Donald E. Burton 17 Oct. 1994 8 p Presented at the Nuclear Explosives Code Developers Conference (NECDC), Las Vegas, NV, 25-28 Oct. 1994 Submitted for publication
(Contract W-7405-eng-48)
(DE95-011730; UCRL-JC-118788; CONF-9410254-6) Avail: CASI HC A02/MF A01

We consider the conservation properties of a staggered-grid Lagrange formulation of the hydrodynamics equations (SGH). Hydrodynamics algorithms are often formulated in a relatively ad hoc manner in which independent discretizationsare proposed for mass, momentum, energy, and so forth. We show that, once discretizations for mass and momentum are stated, the remaining discretizations are very nearly uniquely determined, so there is very little latitude for variation. As has been known for some time, the kinetic energy discretization must follow directly from the momentum equation; and the internal energy must follow directly from the energy currents affecting the kinetic energy. A fundamental requirement (termed isentropicity) for numerical hydrodynamics algorithms is the ability to remain on an isentrope in the absence of heating or viscous forces and in the limit of small timesteps. We show that the requirements of energy conservation and isentropicity lead to the replacement of the usual volume calculation with a conservation integral. They further forbid the use of higher order functional representations for either velocity or stress within zones or control volumes, forcing the use of a constant stress element and a constant velocity control volume. This, in turn, causes the point and zone coordinates to formally disappear from the Cartesian formulation. The form of the work equations and the requirement for dissipation by viscous forces strongly limits the possible algebraic forms for artificial viscosity. The momentum equation and a center-of-mass definition lead directly to an angular momentum conservation law that is satisfied by the system. With a few straightforward substitutions, the Cartesian formulation can be converted to a multidimensional curvilinear one. The formulation in 2D symmetric geometry preserves rotational symmetry. DOE

N95-34572# Purdue Univ., West Lafayette, IN. School of Aeronautics and Astronautics.
MODELING LIQUID JET ATOMIZATION PROCESSES Final Report, 1 Jul. 1992 - 31 Oct. 1994
Stephen D. Heister 19 Nov. 1994 65 p
(Contract F49620-92-J-0390)
(AD-A294888; AFOSR-95-0397TR) Avail: CASI HC A04/MF A01

This report summarizes efforts in developing an analytic/numerical modeling capability for both steady and unsteady liquid jet atomization processes. The research involves the application of boundary element

methods to model nonlinear deformation of liquid surfaces. An inviscid model has been developed to investigate dynamics of a finite-length jet which includes the presence of the orifice flow passages. In addition, a second model has been developed to simulate gas-phase interactions with the distorting jet surface. Preliminary developments associated with a viscous model are also discussed. DTIC

N95-34597# Iowa State Univ. of Science and Technology, Ames, IA.
NONLINEAR STABILITY OF UNSTEADY VISCOUS FLOW Final Technical Report
A. P. Rothmayer 25 Apr. 1995 98 p
(Contract F49620-92-J-0097)
(AD-A294931; AFOSR-95-0382TR) Avail: CASI HC A05/MF A02

The stability and development of unsteady separation on airfoil leading edges has been investigated. In particular, attention was focused on investigations of 2D unsteady incompressible flow past a parabola at angle of attack which models the leading edge of many airfoils. This study has direct application to leading edge stall (LES) and thin airfoil stall as well as unsteady flow past leading edges. The general character of much of this study allows for application to other classes of unsteady boundary layer flow. DTIC

N95-34752# Princeton Univ., NJ.
STUDIES OF HYPERSONIC BOUNDARY LAYER BEHAVIOR Final Technical Report, 1 Dec. 1992 - 30 Nov. 1994
A. J. Smits, R. B. Miles, and G. L. Brown 2 Apr. 1995 21 p
(Contract F49620-93-1-0064)
(AD-A294137; AFOSR-95-0340TR) Avail: CASI HC A03/MF A01

Here, we present the final technical report on AFOSR Grant F49620-93-0064, Studies Of Hypersonic Boundary Layer Behavior. The grant covered three interrelated research efforts: a study of the structure of hypersonic turbulent boundary layers and shock wave boundary layer interactions, a study of boundary layer transition at supersonic and hypersonic speeds, and the development and application of new optical techniques including filtered Rayleigh scattering and RELIEF to obtain multi-dimensional velocity and density data in the supersonic and hypersonic regimes. The research was performed using the existing facilities in the Applied Physics and Lasers Laboratory and at the Princeton University Gas Dynamics Laboratory. The construction of a new boundary layer facility was also partly supported under this contract. The new facility is designed to operate at Mach numbers from 2 to 8, with a range of Reynolds numbers so that the boundary layer can be laminar or turbulent, at all Mach numbers. It is primarily designed to operate with air (and possibly other gases including nitrogen and SF6) to exploit the new optical techniques and to help isolate specific Mach number and Reynolds number effects. It will be ready for its first trials in May, 1995. DTIC

N95-34800# Oak Ridge National Lab., TN.
QMR METHODS IN COMPUTATIONAL FLUID DYNAMICS
N. M. Nachtigal and B. D. Semeraro 1994 10 p Presented at the International Workshop on Solution Techniques for Large-scale Computational Fluid Dynamics (CFD) Problems, Montreal, Canada, 26-28 Sep. 1994
(Contract DE-AC05-84OR-21400)
(DE95-012889; CONF-9409351-1) Avail: CASI HC A02/MF A01

We examine the application of QMR methods to the solution of linear systems of equations arising from the use of implicit solution methods in computational fluid dynamics. We will deal with implicit finite difference schemes for solving the Euler equations. These schemes may arise from the implicit treatment of the time dependent equations or from the use of Newton's method for the solution of the steady state equations. In both situations it is necessary to solve a large sparse nonsymmetric linear system of equations at each iteration. We will examine the effectiveness of QMR in the solution of these systems. We compare the resulting methods to methods which rely on some other simplifying technique to solve the linear systems. Our goal is to show that the QMR method is a viable alternative to the more ad-hoc schemes for solving implicit computational fluid dynamics problems. DOE

N95-34818# Arnold Engineering Development Center, Arnold AFS, TN.
SUBSCALE STUDY OF ENGINE BELLMOUTH INLET VORTICES IN TEST CELL R1D Final Report, Oct. 1992 - Sep. 1994
James A. Reed and Robert S. Hiers, Jr. May 1995 124 p
(AD-A294993; AEDC-TR-95-5) Avail: CASI HC A06/MF A02

A technology program was conducted in Test Cell R1D concerning bellmouth flow quality. Flow visualization was used to determine the presence of inlet vortices. It was shown that these vortices can be eliminated using a 45-deg conical extension attached to the bellmouth inlet. Design guidelines were developed to assist in determining acceptable cone angles and axial and radial gaps between the conical extension and the bellmouth inlet. DTIC

N95-32425*# Texas A&M Univ., Galveston, TX. Dept. of Maritime Systems Engineering.
UNIFIED APPROACH FOR INCOMPRESSIBLE FLOWS Final Report
Tyne-Hsien Chang *In* NASA. Johnson Space Center, National Aeronautics and Space Administration (NASA)/American Society for Engineering Education (ASEE) Summer Faculty Fellowship Program, 1994, Volume 1 Jul. 1995 9 p (For primary document see N95-32418 12-99)
(Grant NGT-44-005-803)
Avail: CASI HC A02/MF A03

N95-32427*# Illinois Univ., Chicago, IL. Dept. of Mechanical Engineering.
BASELINE EXPERIMENTAL INVESTIGATION OF AN ELECTROHYDRODYNAMICALLY ASSISTED HEAT PIPE Final Report
A. B. Duncan *In* NASA. Johnson Space Center, National Aeronautics and Space Administration (NASA)/American Society for Engineering Education (ASEE) Summer Faculty Fellowship Program, 1994, Volume 1 Jul. 1995 15 p (For primary document see N95-32418 12-99)
(Grant NGT-44-005-803)
Avail: CASI HC A03/MF A03

N95-32994# Osaka Univ., Osaka (Japan). Dept. of Naval Architecture and Ocean Engineering.
A NOTE ON SEPARATION PREDICTION OF TWO-DIMENSIONAL TURBULENT BOUNDARY LAYER
Ichiro Tanaka and Kun Ma *In its* Technology Reports of the Osaka Univ., Vol. 45, Nos. 2205-2216 15 Apr. 1995 p 95-99 (For primary document see N95-32984 12-31)
(Rept-2216) Avail: CASI HC A01/MF A02

N95-34508# Tokyo Univ. (Japan). Graduate School.
A STUDY ON THE CONVERGENCE OF A 3-D EULER CODE FOR CASCADE FLOW CALCULATIONS Abstract Only
Daisaku Masaki and Shojiro Kaji *In* National Aerospace Lab., Special Publication of National Aerospace Laboratory 16 Jun. 1994 p 57-62 In JAPANESE (For primary document see N95-34505 12-02)
Avail: CASI HC A02/MF A03

N95-34512# Ishikawajima-Harima Heavy Industries Co. Ltd., Tokyo (Japan).
A STUDY OF SUPERSONIC MIXING FLOW FIELD WITH RAMP INJECTOR Abstract Only
Yoshiyuki Yamane, Seiichi Sawaguchi, Yasunori Ando, Shigeru Aso (Kyushu Univ., Kasuga, Japan), and Masahiro Fukuda (National Aerospace Lab., Tokyo, Japan.) *In* National Aerospace Lab., Special Publication of National Aerospace Laboratory 16 Jun. 1994 p 81-86 In JAPANESE (For primary document see N95-34505 12-02)
Avail: CASI HC A02/MF A03

N95-34515# Kyoto Univ. (Japan). Graduate School.
ADAPTIVE GRID METHOD USING ELLIPTIC EQUATION FOR COMPRESSIBLE FLOWS Abstract Only
Masashi Yamakawa, Kenichi Matsuno, and Nobuyuki Satofuka *In* National Aerospace Lab., Special Publication of National Aerospace Laboratory 16 Jun. 1994 p 99-104 In JAPANESE (For primary document see N95-34505 12-02)
Avail: CASI HC A02/MF A03

N95-34516# Nagoya Univ., Nagoya (Japan). Dept. of Aeronautical Engineering.
A VARIATION OF THE RIEMANN PROBLEM SOLUTION AND ITS APPLICATION TO IMPLICIT GODUNOV'S SCHEME
Igor Men'shov and Yoshiaki Nakamura *In* National Aerospace Lab., Special Publication of National Aerospace Laboratory 16 Jun. 1994 p 105-110 (For primary document see N95-34505 12-02)
Avail: CASI HC A02/MF A03

N95-34517# Ship Research Inst., Tokyo (Japan).
A MULTIGRID INCOMPRESSIBLE NS SOLVER
Takanori Hino *In* National Aerospace Lab., Special Publication of National Aerospace Laboratory 16 Jun. 1994 p 111-116 (For primary document see N95-34505 12-02)
Avail: CASI HC A02/MF A03

N95-34518*# National Aeronautics and Space Administration. Lewis Research Center, Cleveland, OH.
A FLUX SPLITTING SCHEME WITH HIGH-RESOLUTION AND ROBUSTNESS FOR DISCONTINUITIES
Yasuhiro Wada (National Aerospace Lab., Tokyo, Japan.) and Meng-Sing Liou *In* National Aerospace Lab., Special Publication of National Aerospace Laboratory 16 Jun. 1994 p 117-122 (For primary document see N95-34505 12-02)
Avail: CASI HC A02/MF A03

N95-34519# National Aerospace Lab., Tokyo (Japan). Computational Sciences Div.
CONSTRUCTION AND ANALYSIS OF DIFFERENCE APPROXIMATION FOR SCALAR CONSERVATION LAWS AND ITS CONSISTENCY WITH ENTROPY CONDITION USING BOLTZMANN-LIKE APPROACH
Hideaki Aiso and Toshiyuki Iwamiya *In its* Special Publication of National Aerospace Laboratory 16 Jun. 1994 p 123-128 (For primary document see N95-34505 12-02)
Avail: CASI HC A02/MF A03

N95-34522# Tsukuba Univ. (Japan). Inst. of Engineering Mechanics.
SOLITARY WAVE SOLUTION FOR MIXING-LAYER TURBULENCE
Shunichi Tsuge and Satoru Ogawa (National Aerospace Lab., Tokyo, Japan.) *In* National Aerospace Lab., Special Publication of National Aerospace Laboratory 16 Jun. 1994 p 141-146 (For primary document see N95-34505 12-02)
Avail: CASI HC A02/MF A03

N95-34523# National Aerospace Lab., Tokyo (Japan).
DIRECT NUMERICAL SIMULATION OF COMPRESSIBLE ISOTROPIC TURBULENCE
Yuichi Matsuo and Kiyoshi Yamamoto *In its* Special Publication of National Aerospace Laboratory 16 Jun. 1994 p 147-152 (For primary document see N95-34505 12-02)
Avail: CASI HC A02/MF A03

N95-34526# Mitsubishi Electric Corp., Tokyo (Japan).
NUMERICAL SIMULATION OF FILM COOLING EFFECT AROUND AXISYMMETRIC BODY IN HYPERSONIC FLOW FIELD Abstract Only
Takuji Kurotaki, Yoshiko Nakamura, Ryujiro Kurosaki, Masayuki Katayama, and Shigeru Aso, (Kyushu Univ., Kasuga, Japan) *In* National Aerospace Lab., Special Publication of National Aerospace Laboratory 16 Jun. 1994 p 165-170 In JAPANESE (For primary document see N95-34505 12-02)
Avail: CASI HC A02/MF A03

N95-34527# Kyoto Univ. (Japan). Dept. of Aeronautical Engineering.
STRUCTURE OF WEAK SHOCK WAVES IN BUBBLY LIQUID
Ryuji Ishii and Takeshi Hashimoto (Toyota Motor Co., Tokyo, Japan.) *In* National Aerospace Lab., Special Publication of National Aerospace Laboratory 16 Jun. 1994 p 171-176 (For primary document see N95-34505 12-02)
Avail: CASI HC A02/MF A03

N95-34528# National Aerospace Lab., Tokyo (Japan).
THE EFFECT OF BUOYANCY ON FLOW AND HEAT TRANSFER IN CURVED PIPES Abstract Only
Munekazu Mochizuki and Hiroshi Ishigaki *In its* Special Publication of National Aerospace Laboratory 16 Jun. 1994 p 177-181 In JAPANESE (For primary document see N95-34505 12-02)
Avail: CASI HC A01/MF A03

N95-34529# Kyoto Univ. (Japan).
DIRECT NUMERICAL SIMULATION OF INCOMPRESSIBLE HOMOGENEOUS ISOTROPIC TURBULENCE USING COMPRESSIBLE NAVIER-STOKES EQUATIONS Abstract Only
Hidetoshi Nishida, Makoto Kawamoto, and Yoshimi Torao (Shin-Meiwa Industry Co. Ltd., Japan.) *In* National Aerospace Lab., Special Publication of National Aerospace Laboratory 16 Jun. 1994 p 189-194 In JAPANESE (For primary document see N95-34505 12-02)
Avail: CASI HC A09/MF A03

N95-34530# National Aerospace Lab., Tokyo (Japan).
DIRECT NUMERICAL SIMULATION OF INCOMPRESSIBLE HOMOGENEOUS ISOTROPIC TURBULENCE USING NWT Abstract Only
Kiyoshi Yamamoto, Iwao Hosokawa (University of Electro-Communications, Tokyo, Japan.), and Shin-Ichi Oide (University of Electro-Communications, Tokyo, Japan.) *In its* Special Publication of National Aerospace Laboratory 16 Jun. 1994 p 195-200 In JAPANESE (For primary document see N95-34505 12-02)
Avail: CASI HC A02/MF A03

N95-34531# Tokyo Noko Univ. (Japan).
EFFECT OF SCHEMES ON NUMERICAL SIMULATIONS OF SHOCK WAVE REFLECTION Abstract Only
Fumio Higashino, Yoko Takakura, Masahiro Yoshida (National Aerospace Lab., Tokyo, Japan.), and Satoru Ogawa (National Aerospace Lab., Tokyo, Japan.) *In* National Aerospace Lab., Special Publication of National Aerospace Laboratory 16 Jun. 1994 p 201-206 In JAPANESE (For primary document see N95-34505 12-02)
Avail: CASI HC A02/MF A03

N95-34533# National Aerospace Lab., Tokyo (Japan).
PERFORMANCE EVALUATION OF THE NWT WITH INCOMPRESSIBLE NS CODE Abstract Only
Takashi Nakamura and Masahiro Yoshida *In its* Special Publication of National Aerospace Laboratory 16 Jun. 1994 p 213-218 In JAPANESE (For primary document see N95-34505 12-02)
Avail: CASI HC A02/MF A03

N95-34536# National Aerospace Lab., Tokyo (Japan).
AN UNSTEADY SIMULATION OF A CENTRIFUGAL COMPRESSOR STAGE USING THE NWT Abstract Only
Takashi Yamane *In its* Special Publication of National Aerospace Laboratory 16 Jun. 1994 p 231-235 In JAPANESE (For primary document see N95-34505 12-02)
Avail: CASI HC A01/MF A03

N95-34539# Kawasaki Heavy Industries Ltd., Tokyo (Japan). Technical Inst.
A LARGE SCALE 3D NAVIER-STOKES ANALYSIS USING NAL-NWT Abstract Only
Takuji Kishimoto *In* National Aerospace Lab., Special Publication of National Aerospace Laboratory 16 Jun. 1994 p 249-253 In JAPANESE (For primary document see N95-34505 12-02)
Avail: CASI HC A01/MF A03

N95-34540# Kawasaki Heavy Industries Ltd., Tokyo (Japan). Technical Inst.
ROLE OF COMPUTATIONAL FLUID DYNAMICS IN AERONAUTICAL ENGINEERING. NUMBER 12: FORMULATION AND VERIFICATION OF UNI-PARTICLE UPWIND SCHEMES FOR THE EULER EQUATIONS Abstract Only
Eiji Shima and Tadamasa Jounouchi (National Aerospace Lab., Tokyo, Japan.) *In* National Aerospace Lab., Special Publication of National

Aerospace Laboratory 16 Jun. 1994 p 255-260 In JAPANESE (For primary document see N95-34505 12-02)
Avail: CASI HC A02/MF A03

N95-34543# Saitama Univ., Urawa (Japan). Dept. of Mechanical Engineering.
NUMERICAL SIMULATION OF INTERACTION BETWEEN SHOCK WAVE AND DENSITY INTERFACE Abstract Only
Yoshiaki Murata, Tetsuro Obara, and Shigeharu Ohyagi *In* National Aerospace Lab., Special Publication of National Aerospace Laboratory 16 Jun. 1994 p 273-278 In JAPANESE (For primary document see N95-34505 12-02)
Avail: CASI HC A02/MF A03

N95-34545# National Aerospace Lab., Tokyo (Japan).
FLOW AND HEAT TRANSFER IN ROTATING CURVED PIPES Abstract Only
Hiroshi Ishigaki *In its* Special Publication of National Aerospace Laboratory 16 Jun. 1994 p 285-289 In JAPANESE (For primary document see N95-34505 12-02)
Avail: CASI HC A01/MF A03

N95-34550# National Aerospace Lab., Tokyo (Japan).
DEPENDENCY OF A BOUNDARY LAYER FLOW ON COMPUTATIONAL GRIDS Abstract Only
Toshiyuki Nomura *In its* Special Publication of National Aerospace Laboratory 16 Jun. 1994 p 315-320 In JAPANESE (For primary document see N95-34505 12-02)
Avail: CASI HC A02/MF A03

N95-34553# National Aerospace Lab., Tokyo (Japan).
FORMATION OF HIGH DENSITY CORES IN MOLECULAR CLOUD Abstract Only
Toshiya Kimura *In its* Special Publication of National Aerospace Laboratory 16 Jun. 1994 p 333-338 In JAPANESE (For primary document see N95-34505 12-02)
Avail: CASI HC A02/MF A03

N95-34555# Tsukuba Univ. (Japan).
TURBULENT SOLITARY WAVE PROPAGATING THROUGH WALL BOUNDARY LAYER Abstract Only
Burtsitsig Bai, Yuichi Matsuo (National Aerospace Lab., Tokyo, Japan.), and Shunichi Tsuge *In* National Aerospace Lab., Special Publication of National Aerospace Laboratory 16 Jun. 1994 p 345-350 In JAPANESE (For primary document see N95-34505 12-02)
Avail: CASI HC A02/MF A03

N95-34557# Mitsubishi Heavy Industries Ltd., Tokyo (Japan).
NUMERICAL SIMULATION OF TWO-DIMENSIONAL COMPRESSIBLE INVISCID FLOW ON UNSTRUCTURED GRID SYSTEM Abstract Only
Nobuyuki Tsuboi *In* National Aerospace Lab., Special Publication of National Aerospace Laboratory 16 Jun. 1994 p 357-362 In JAPANESE (For primary document see N95-34505 12-02)
Avail: CASI HC A02/MF A03

N95-34558# Kyoto Inst. of Tech. (Japan).
PARALLEL COMPUTATION FOR TWO DIMENSIONAL INCOMPRESSIBLE FLOW ON ARRAY OF TRANSPUTERS Abstract Only
Masanori Obata, Toshihiro Suzuki, and Nobuyuki Satofuka *In* National Aerospace Lab., Special Publication of National Aerospace Laboratory 16 Jun. 1994 p 363-368 In JAPANESE (For primary document see N95-34505 12-02)
Avail: CASI HC A02/MF A03

N95-34559# National Aerospace Lab., Tokyo (Japan).
UPWIND SCHEMES FOR THE TWO-DIMENSIONAL EULER EQUATIONS Abstract Only
Masakazu Tachibana *In its* Special Publication of National Aerospace Laboratory 16 Jun. 1994 p 369-373 In JAPANESE (For primary document see N95-34505 12-02)
Avail: CASI HC A01/MF A03

35 INSTRUMENTATION AND PHOTOGRAPHY

Includes remote sensors; measuring instruments and gages; detectors; cameras and photographic supplies; and holography.

For aerial photography see *43 Earth Resources and Remote Sensing*. For related information see also *06 Aircraft Instrumentation*, and *19 Spacecraft Instrumentation*.

N95-32687*# NYMA, Inc., Brook Park, OH.
COMPRESSION MASS GAUGE TESTING IN A LIQUID HYDROGEN DEWAR Final Contractor Report
J. M. Jurns and A. C. Rogers (Southwest Research Inst., San Antonio, TX.) Jul. 1995 11 p Presented at the 1995 Cryogenic Engineering Conference, Columbus, OH, 17-21 Jul. 1995; sponsored by Centennial Conferences
(Contracts NAS3-27186; NAS3-25365; RTOP 198-36-60)
(NASA-CR-198366; E-9781; NAS 1.26:198366) Avail: CASI HC A03/MF A01

This paper describes testing that was conducted using a mass gauge in a liquid hydrogen environment. The mass gauge, herein referred to as the 'compressibility gauge,' is being developed as a means to accurately determine the mass of liquid contained in a tank in a low-gravity environment. The concept is based on the thermodynamic principle that the pressure of gas or vapor changes when its volume changes. Previous work has been conducted by Southwest Research Institute in collaboration with NASA Lewis Research Center. This consisted of testing the concept with water and other cryogenic simulant fluids. The purpose of conducting liquid hydrogen tests is to test the concept in actual cryogenic conditions, and address hardware issues that arise in fabricating a test article for use in liquid hydrogen. Author

N95-32900# Lawrence Livermore National Lab., Livermore, CA.
A DUAL, PARALLEL CAVITY FABRY-PEROT INTERFEROMETER
L. L. Steinmetz, D. R. Goosman, and G. R. Avara Aug. 1994 13 p Presented at the 21st International Congress on High Speed Photography and Photonics, Taejon, Korea, Republic of, 29 Aug. - 2 Sep. 1994 Submitted for publication
(Contract W-7405-eng-48)
(DE95-010796; UCRL-JC-116856; CONF-9408148-2) Avail: CASI HC A03/MF A01

Laser Doppler shift velocimetry operating in the fringe mode is widely used to record the velocity history of optically reflective solid objects. When the object is rapidly accelerated, the time resolution of the Fabry-Perot Interferometer (FPI)/streak camera system is frequently inadequate to unambiguously record the data. That is, there is a 'dead time' during which fringes form and expand without producing a resolvable record. To remedy this, we have developed a dual, parallel cavity FPI which produces two sets of fringes at the slit of the recording streak camera. The input mirror of the FPI is a conventional flat while the output mirror is stepped so there are two mirror spacings. The input light is divided by the respective areas of the stepped mirror to form two sets of fringes; a higher quality set of fringes 'A' is used to determine the velocity history while a second set of fringes'B' is used as a 'referee' to determine the number of fringe jumps during the 'dead time'. Since the two sets of fringes are necessarily interleaved, there is a possibility of fringe overlap, i.e., fringes of set A can spatially overlap fringes of set B. To date, two dual cavity FPI's have been successfully constructed and characterized. The theory of operation, details of construction, and the results are described. DOE

N95-32927 Defence Science and Technology Organisation, Melbourne (Australia). Ship Structures and Materials Div.
OPERATIONS MANUAL FOR A COMPACT ELECTROMECHANICAL FATIGUE TESTING MACHINE
Leopold Sponder Dec. 1994 52 p Original contains color illustrations
(DSTO-GD-0036; AR-009-182) Avail: Issuing Activity (DSTO Aeronautical and Maritime Research Lab., GPO Box 4331, Melbourne, Victoria 3001, Australia)

This document gives details of the design and operation of two recently developed load controlled electromechanical shaker systems. These systems have been designed to test materials including composites, alloys, and pure metals with either three or four point bending loads. One system (Mk 1) is designed for room temperature testing only and the other (Mk 2) can

also be used at elevated temperatures. The electronic control and drive circuits include new designs by the author, published designs modified by the author, and circuits developed earlier at AMRL. The loading frame and ancillary hardware were designed and built at AMRL. Author

N95-33206# Oak Ridge National Lab., TN.
AN INSTRUMENT FOR GRAVIMETRIC CALIBRATION OF FLOW DEVICES WITH CORROSIVE GASES
Carl J. Remenyik and James O. Hylton 1995 6 p Presented at the 41st International Instrumentation Symposium, Auora, CO, 7-11 May 1995 (Contract DE-AC05-84OR-21400)
(DE95-009700; CONF-9505201-2) Avail: CASI HC A02/MF A01

An instrument was developed for the calibration of mass flow controllers primarily used in the production of semiconductor wafers. Almost all other types of such calibrators require measurement of temperature, pressure, and volume. This instrument measures the weight of gas collected in a container and makes measuring those thermodynamic variables unnecessary. The need to measure the weight of the gas container is eliminated by submerging it in a liquid (presently water) and balancing its weight with the force of buoyancy. The accuracy of this gravimetric calibrator is unaffected by the pressure and temperature of the gas. The calibrator can also measure reactive, corrosive, and nonideal gases. The container remains connected to the process by a torsion capillary, and a load cell measures the changing gas weight continuously throughout the measuring process. A prototype was designed for gas flows ranging from 1 sccm of hydrogen to 10,000 sccm of tungsten hexafluoride, constructed, tested, and used to calibrate flow devices. Experience with the prototype and results are presented, and plans for further developments are discussed. Design of a version for the flow range from 0.1 sccm to 100 sccm is in progress. DOE

N95-34426 Department of the Navy, Washington, DC.
FLUID DYNAMOMETER HAVING FLUID CHARACTERISTIC POWER ABSORPTION ADJUSTMENT CAPABILITY Patent
James R. Quartarone, inventor (to Navy) 14 Mar. 1995 8 p Filed 29 Mar. 1993
(AD-D017489; US-Patent-5,396,811; US-Patent-Appl-SN-037880; US-Patent-Class-73-862) Avail: US Patent and Trademark Office

A fluid dynamometer is provided for absorbing a range of power output produced by an engine's rotating shaft. Power absorbing characteristics are controlled by adjusting the fluid media characteristics in terms of its temperature and/or its density and viscosity. A tank, containing an energy or power absorbing fluid, receives the rotating shaft. One or more disks, submerged in the fluid and coaxially mounted on the rotating shaft for rotation therewith, cooperate with the fluid to absorb power from the rotating shaft. The disk(s) are sized so that a first specified amount of power from the rotating shaft is absorbed at a calibration temperature of the fluid. Heating and cooling units are provided to respectively heat and cool the fluid. A controller energizes the heating and cooling units in a cooperative fashion to adjust and maintain the fluid at a predetermined temperature value for power absorption at a second specified amount of power produced by the rotating shaft. A fluid composition exchanger may also be provided to alter the power absorbing characteristics by altering the fluid's composition. DTIC

N95-34496# Naval Postgraduate School, Monterey, CA.
A REAL-TIME SINGLE-CAMERA, STEREOSCOPIC VIDEO DEVICE M.S. Thesis
Blake L. Converse Dec. 1994 65 p
(AD-A294105) Avail: CASI HC A04/MF A01

This patent application discloses a real-time, single-camera, stereoscopic video imaging device for use with a standard 60 Hz camera and monitor is being developed The device uses a single objective lens to focus disparate views of the object at the focal plane of the lens. Each view is represented by a set of parallel rays emanating from the object at a specific angle. The lens focuses these parallel rays to a single point at the focal plane These views are then shuttered at the focal plane using a Liquid-Crystal Device (LCD) shutter such that one view at a time is passed to the camera. The camera then transmits alternating video fields (individual TV images) to the monitor, such that alternate fields display stereoscopically-related views of the object being imaged. The user views the monitor using off-the-shelf LCD stereoglasses, modified to allow synchronization with the standard field rate of the camera and monitor. The glasses shutter the light alternately to each eye so that the left eye views the left-hand image and the right eye views the right-hand image. The resulting 3-D image is independent of the user's viewing angle or distance from the monitor. DTIC

N95-33129# Delphin Central Research Inst., Moscow (Russia).
COMMERCIAL USAGE OF NAVY COMPONENTS DEVELOPED AND MANUFACTURED BY CRI DELFIN
A. V. Novgorodski and M. V. Chichinadze *In* AGARD, Dual Usage in Military and Commercial Technology in Guidance and Control Mar. 1995 9 p (For primary document see N95-33126 12-31)
Copyright Avail: CASI HC A02/MF A02

N95-33130# Saint Petersburg State Electrotechnical Univ., Saint Petersburg (Russia).
SOME RESULTS OF INTERNATIONAL COOPERATION IN MILITARY TO COMMERCIAL CONVERSION OF LASER GYRO TECHNOLOGY
Yu. V. Filatov, D. P. Loukianov, A. V. Mochalov, R. Probst (Physikalisch-Technische Bundesanstalt, Brunswick, Germany.), R. Rodloff (Deutsche Forschungsanstalt fuer Luft- und Raumfahrt, Brunswick, Germany.), and B. Stieler (Deutsche Forschungsanstalt fuer Luft- und Raumfahrt, Brunswick, Germany.) *In* AGARD, Dual Usage in Military and Commercial Technology in Guidance and Control Mar. 1995 5 p (For primary document see N95-33126 12-31)
Copyright Avail: CASI HC A01/MF A02

N95-33132# Draper (Charles Stark) Lab., Inc., Cambridge, MA.
DUAL-USE MICROMECHANICAL INERTIAL SENSORS
John M. Elwell, Jr. *In* AGARD, Dual Usage in Military and Commercial Technology in Guidance and Control Mar. 1995 6 p (For primary document see N95-33126 12-31)
Copyright Avail: CASI HC A02/MF A02

N95-33133# Scientific Research Inst. of Mechanical Problems, Kiev (Ukraine).
LASER GYROSCOPY TENDENCIES AND THEIR ANALYSIS OF DEVELOPMENT IN UKRAINE
Alexander A. Dovbeshko *In* AGARD, Dual Usage in Military and Commercial Technology in Guidance and Control Mar. 1995 11 p (For primary document see N95-33126 12-31)
Copyright Avail: CASI HC A03/MF A02

N95-33143# SPEEL Ltd., Prague (Czechoslovakia).
SOLID-STATE DATA RECORDER, NEXT DEVELOPMENT AND USE
J. Vidiecan, J. Kozak, K. Horak, and J. Svoboda *In* AGARD, Dual Usage in Military and Commercial Technology in Guidance and Control Mar. 1995 10 p (For primary document see N95-33126 12-31)
Copyright Avail: CASI HC A02/MF A02

N95-33733*# Hughes Danbury Optical Systems, Inc., CT.
CHARACTERISTICS OF THE HYDICE SENSOR Abstract Only
R. W. Basedow and E. Zalewski *In* JPL, Summaries of the Fifth Annual JPL Airborne Earth Science Workshop. Volume 1: AVIRIS Workshop 23 Jan. 1995 p 9 (For primary document see N95-33730 12-42)
Avail: CASI HC A01/MF A02

N95-33739*# Jet Propulsion Lab., California Inst. of Tech., Pasadena, CA.
AIRBORNE VISIBLE/INFRARED IMAGING SPECTROMETER (AVIRIS) ONBOARD CALIBRATION SYSTEM
Thomas G. Chrien, Mike Eastwood, Robert O. Green, Charles Sarture, Howell Johnson, Chris Chovit, and Pavel Hajek *In its* Summaries of the Fifth Annual JPL Airborne Earth Science Workshop. Volume 1: AVIRIS Workshop 23 Jan. 1995 p 31-32 (For primary document see N95-33730 12-42)
Avail: CASI HC A01/MF A02

N95-33740*# Jet Propulsion Lab., California Inst. of Tech., Pasadena, CA.
NEW CALIBRATION TECHNIQUES FOR THE AIRBORNE VISIBLE/INFRARED IMAGING SPECTROMETER (AVIRIS)

Thomas G. Chrien, Robert O. Green, Chris Chovit, Mike Eastwood, Jessica Faust, Pavel Hajek, Howell Johnson, H. Ian Novack, and Charles Sarture *In its* Summaries of the Fifth Annual JPL Airborne Earth Science Workshop. Volume 1: AVIRIS Workshop 23 Jan. 1995 p 33-34 (For primary document see N95-33730 12-42)
Avail: CASI HC A01/MF A02

N95-33746*# Earth Search Sciences, Inc., Salt Lake City, UT.
A LAYERED APPROACH TO TECHNOLOGY TRANSFER OF AVIRIS BETWEEN EARTH SEARCH SCIENCES, INC. AND THE IDAHO NATIONAL ENGINEERING LABORATORY
James S. Ferguson, JoAnne E. Ferguson, John Peel, III, and Larry Vance *In* JPL, Summaries of the Fifth Annual JPL Airborne Earth Science Workshop. Volume 1: AVIRIS Workshop 23 Jan. 1995 p 51-54 Prepared in cooperation with Idaho National Engineering Lab., Idaho Falls, ID (For primary document see N95-33730 12-42)
Avail: CASI HC A01/MF A02

N95-33751*# Jet Propulsion Lab., California Inst. of Tech., Pasadena, CA.
DETERMINATION OF THE IN-FLIGHT SPECTRAL CALIBRATION OF AVIRIS USING ATMOSPHERIC ABSORPTION FEATURES
Robert O. Green *In its* Summaries of the Fifth Annual JPL Airborne Earth Science Workshop. Volume 1: AVIRIS Workshop 23 Jan. 1995 p 71-74 (For primary document see N95-33730 12-42)
Avail: CASI HC A01/MF A02

N95-33752*# Jet Propulsion Lab., California Inst. of Tech., Pasadena, CA.
AN IMPROVED SPECTRAL CALIBRATION REQUIREMENT FOR AVIRIS
Robert O. Green *In its* Summaries of the Fifth Annual JPL Airborne Earth Science Workshop. Volume 1: AVIRIS Workshop 23 Jan. 1995 p 75-78 (For primary document see N95-33730 12-42)
Avail: CASI HC A01/MF A02

N95-33754*# Jet Propulsion Lab., California Inst. of Tech., Pasadena, CA.
IN-FLIGHT RADIOMETRIC CALIBRATION OF AVIRIS IN 1994
Robert O. Green, James E. Conel (California Univ., Santa Barbara, CA.), Mark Helmlinger (California Univ., Santa Barbara, CA.), Jeannette vandenBosch (California Univ., Santa Barbara, CA.), and Pavel Hajek (California Univ., Santa Barbara, CA.) *In its* Summaries of the Fifth Annual JPL Airborne Earth Science Workshop. Volume 1: AVIRIS Workshop 23 Jan. 1995 p 83-86 (For primary document see N95-33730 12-42)
Avail: CASI HC A01/MF A02

N95-33759*# Jet Propulsion Lab., California Inst. of Tech., Pasadena, CA.
AVIRIS USER'S GUIDE
Howell K. Johnson and Robert O. Green *In its* Summaries of the Fifth Annual JPL Airborne Earth Science Workshop. Volume 1: AVIRIS Workshop 23 Jan. 1995 p 105-108 (For primary document see N95-33730 12-42)
Avail: CASI HC A01/MF A02

N95-33789*# Jet Propulsion Lab., California Inst. of Tech., Pasadena, CA.
AIRBORNE VISIBLE/INFRARED IMAGING SPECTROMETER (AVIRIS): SENSOR IMPROVEMENTS FOR 1994 AND 1995
C. M. Sarture, T. G. Chrien, R. O. Green, M. L. Eastwood, J. J. Raney, and M. A. Hernandez *In its* Summaries of the Fifth Annual JPL Airborne Earth Science Workshop. Volume 1: AVIRIS Workshop 23 Jan. 1995 p 145-148 (For primary document see N95-33730 12-42)
Avail: CASI HC A01/MF A02

N95-33794*# Jet Propulsion Lab., California Inst. of Tech., Pasadena, CA.
THE JPL FIELD EMISSION SPECTROMETER Abstract Only
Simon J. Hook and Anne B. Kahle *In its* Summaries of the Fifth Annual JPL Airborne Earth Science Workshop. Volume 2: TIMS Workshop 23 Jan. 1995 p 17 (For primary document see N95-33789 12-42)
Avail: CASI HC A01/MF A01

N95-33795*# Arizona State Univ., Tempe, AZ. Dept. of Geology.
A CONFLICT OF WATER AND FIRE: REMOTE SENSING IMAGERY OF THE UINKARET VOLCANIC FIELD, GRAND CANYON, ARIZONA
Michael S. Ramsey *In* JPL, Summaries of the Fifth Annual JPL Airborne Earth Science Workshop. Volume 2: TIMS Workshopp 19-23 (SEE N95-33789 12-42) 23 Jan. 1995 (For primary document see N95-33789 12-42)
Avail: CASI HC A01/MF A01

N95-33796*# Jet Propulsion Lab., California Inst. of Tech., Pasadena, CA.
THE 1994 LABORATORY CALIBRATION OF TIMS
Vincent J. Realmuto, Pavel Hajek, Mahadeva P. Sinha, and Thomas G. Chrien *In its* Summaries of the Fifth Annual JPL Airborne Earth Science Workshop. Volume 2: TIMS Workshop 23 Jan. 1995 p 25-28 (For primary document see N95-33789 12-42)
Avail: CASI HC A01/MF A01

N95-33797*# Jet Propulsion Lab., California Inst. of Tech., Pasadena, CA.
THE 1994 TIMS AIRBORNE CALIBRATION EXPERIMENT: CASTAIC LAKE, CALIFORNIA
Vincent J. Realmuto, Simon J. Hook, and Jeannette vandenBosch *In its* Summaries of the Fifth Annual JPL Airborne Earth Science Workshop. Volume 2: TIMS Workshop 23 Jan. 1995 p 29-32 (For primary document see N95-33789 12-42)
Avail: CASI HC A01/MF A01

36 LASERS AND MASERS

Includes parametric amplifiers.
For related information see also *76 Solid-State Physics.*

N95-32472# Department of the Air Force, Wright-Patterson AFB, OH. National Air Intelligence Center.
SUM FREQUENCY GENERATION OF DUAL-WAVELENGTH Nd: YAP LASER IN LIIO3 CRYSTAL
Yuping Zhou (Fujian Inst. of Matter Structure, Fuzhou, China.), Hongyuan Shen (Fujian Inst. of Matter Structure, Fuzhou, China.), Huang Miaoling (Fujian Inst. of Matter Structure, Fuzhou, China.), Lin Wenxiong (Fujian Inst. of Matter Structure, Fuzhou, China.), Zeng Ruirong (Fujian Inst. of Matter Structure, Fuzhou, China.), Yu Guifang (Fujian Inst. of Matter Structure, Fuzhou, China.), Huang Chenghui (Fujian Inst. of Matter Structure, Fuzhou, China.), and Zeng Zhengdong (Fujian Inst. of Matter Structure, Fuzhou, China.) 29 Mar. 1995 9 p Transl. into ENGLISH from Zhongguo Jiguang (China), v. 19, no. 6, Jun. 1992 p 448-450 Prepared by Leo Kanner Associates
(Contract F33657-88-D-2188)
(AD-A293094; NAIC-ID(RS)T-0499-94) Avail: CASI HC A02/MF A01

Based on Sellmeier's equation for LiIO3 crystal, the phase-matched condition for sum-frequency generation of 1.0795 micrometers and 1.3414 micrometers dual wavelength Nd:YAP laser has been calculated. The calculated results agree well with the experimental ones. The CW and pulsed 0.5981 micrometers sum-frequency radiation have been achieved for the first time. DTIC

N95-32571# Lawrence Livermore National Lab., Livermore, CA.
PREDICTED OPERATING CONDITIONS FOR MAINTAINING MODE PURITY IN THE 1MW 200 GHz FOM FREE ELECTRON MASER
M. Caplan, T. Antonsen (Maryland Univ., College Park, MD.), B. Levush (Maryland Univ., College Park, MD.), A. Tulupov (FOM-Inst. voor Plasmafysica, Nieuwegein, Netherlands.), and W. Urbanus (FOM-Inst. voor Plasmafysica, Nieuwegein, Netherlands.) Sep. 1994 13 p Presented at the 16th International Free Electron Laser Conference, Stanford, CA, 21-26 Aug. 1994 Submitted for publication
(Contract W-7405-eng-48)
(DE95-010795; UCRL-JC-118397; CONF-9408146-20) Avail: CASI HC A03/MF A01

A Free Electron Maser (FEM) Oscillator is now under construction at the FOM Institute, (Rijnhuisen) Netherlands with the goal of producing 1MW long pulse to CW microwave output in the range 130 GHz to 250 GHz with, application to plasma heating. A newly developed multi-frequency FEM simulation code (MALT 1D) using the windows approximation in the high gain regime and including AC space charge is used to model possibilities for longitudinal mode completion and resulting non-stationary chaotic output. The code predicts that stationary single frequency output can be obtained by taking advantage of the frequency dependence of the feedback reflection coefficient and by optimizing the gap spacing between the two wiggler sections. DOE

N95-32663# Sandia National Labs., Albuquerque, NM.
INTEGRATION OF DIFFRACTIVE LENSES WITH ADDRESSABLE VERTICAL-CAVITY LASER ARRAYS
M. E. Warren, T. C. Du, J. R. Wendt, G. A. Vawter, R. F. Carson, K. L. Lear, S. P. Kilcoyne, R. P. Schneider, and J. C. Zolper 1995 10 p Presented at the SPIE 1995: SPIE Conference on Optics, Electro-optics, and Laser Application in Science, Engineering and Medicine, San Jose, CA, 5-14 Feb. 1995
(Contract DE-AC04-94AL-85000)
(DE95-009850; SAND-95-0360C; CONF-950226-38) Avail: CASI HC A02/MF A01

An optical interconnection system is being developed to provide vertical, digital data channels for stacked multichip modules. A key component of the system is an array of individually addressable vertical-cavity surface-emitting lasers with diffractive lenses integrated into the substrate to control beam divergence and direction. The lenses were fabricated by direct-write e-beam lithography and reactive ion beam etching into the GaAs substrate. Preliminary device performance data and the design and fabrication issues are discussed. DOE

N95-32683# Sandia National Labs., Albuquerque, NM.
THE EFFECT OF TRAVEL SPEED ON THERMAL RESPONSE IN CO2 LASER WELDING OF SMALL ELECTRONIC COMPONENTS
S. E. Gianoulakis, S. N. Burchett, P. W. Fuerschbach, and G. A. Knorovsky 1995 6 p Presented at the National Heat Transfer Conference, Portland, OR, 5-9 Aug. 1995
(Contract DE-AC04-94AL-85000)
(DE95-006314; SAND-94-3231C; CONF-950828-5) Avail: CASI HC A02/MF A01

A comprehensive three-dimensional numerical investigation of the effect of beat source travel speed on temperatures and resulting thermal stresses was performed for CO2-laser welding. The test specimen was a small thermal battery header containing several stress-sensitive glass-to-metal seals surrounding the electrical connections and a temperature sensitive ignitor located under the header near the center. Predictions of the thermal stresses and temperatures in the battery header were made for several travel speeds of the laser. The travel speeds examined ranged from 10mm/sec to 50mm/sec. The results indicate that faster weld speeds result in lower temperatures and stresses for the same size weld. This is because the higher speed welds are more efficient, requiring less energy to produce a given weld. Less energy absorbed by the workpiece results in lower temperatures, which results in lower stresses. DOE

N95-32702# Department of the Air Force, Wright-Patterson AFB, OH. National Air Intelligence Center.
NEW ADVANCES IN 1341.4 nm Nd:YAP LASERS
Hongyuan Shen (Fujian Inst. of Matter Structure, Fuzhou, China.), Yuping Zhou (Fujian Inst. of Matter Structure, Fuzhou, China.), Li Gansheng (Fujian Inst. of Matter Structure, Fuzhou, China.), Zeng Ruirong (Fujian Inst. of Matter Structure, Fuzhou, China.), Guo Xibin (Fujian Inst. of Matter Structure, Fuzhou, China.), Yu Guifang (Fujian Inst. of Matter Structure, Fuzhou, China.), Huang Chenghui (Fujian Inst. of Matter Structure, Fuzhou, China.), Zheng Zhengdong (Fujian Inst. of Matter Structure, Fuzhou, China.), Lin Wenxiong (Fujian Inst. of Matter Structure, Fuzhou, China.), and Ye Qijin (Fujian Inst. of Matter Structure, Fuzhou, China.) et al 30 Mar. 1995 8 p Transl. into ENGLISH from Zhongguo Jiguang (China), v. 19, no. 11, Nov. 1992 p 812-8114 Prepared by Leo Kanner Associates
(Contract F33657-88-D-2188)
(AD-A293070; NAIC-ID(RS)T-0497-94) Avail: CASI HC A02/MF A01

New results of 1341.4 nm CW laser and pulsed laser have been reported in this paper. Using Nd:YAP rod of phi 8 x 138 mm and phi 1 x 100 mm, at 195.8 W CW radiation and 5.1 J pulsed radiation at 1341.4 nm have been obtained with efficiencies of 1.43% and 2.02% respectively. DTIC

N95-33246# Oak Ridge National Lab., TN. Solid State Div.
LASER ABLATION PLUME THERMALIZATION DYNAMICS IN BACKGROUND GASES STUDIED BY TIME-RESOLVED IMAGING, SPECTROSCOPIC, AND ION PROBE DIAGNOSTICS
David B. Geohegan and A. A. Puretzky Feb. 1995 11 p Presented at the SPIE 1995: SPIE Conference on Optics, Electro-optics, and Laser Application in Sci ence, Engineering and Medicine, San Jose, CA, 5-14 Feb. 1995 Submitted for publication
(Contract DE-AC05-84OR-21400)
(DE95-010277; CONF-950226-37) Avail: CASI HC A03/MF A01

A combination of fast plasma diagnostics are utilized to probe the propagation of laser ablation plumes in vacuum and low-pressure background gases in order to understand key gas dynamic processes relevant to film growth by pulsed laser deposition. During expansion into low-pressure background gases, the ion flux in the plasma plume splits into fast and slow components over a limited range of distances and times. This general effect is presented here for the case of yttrium ablation into argon, a single-element target into an inert gas. Time-resolved optical absorption spectroscopy and optical emission spectroscopy are employed to simultaneously view the populations of both excited and ground states of Y and Y(sup +) for comparison with intensified-CCD photography of the visible plume luminescence and ion flux measurements made with fast ion probes during this phenomenon. These measurements indicate that plume-splitting in background gases is consistent with momentum transfer from an initial, vacuum velocity distribution into a second, slowed velocity distribution initiated by scattering collisions between plume and background gas atoms. The fast distribution is exponentially attenuated in accordance with Beer's law, and the second, slowed distribution coalesces into a stable, propagating shock stucture. DOE

N95-33378# Lawrence Livermore National Lab., Livermore, CA.
ABSOLUTE WAVEFRONT MEASUREMENTS OF HIGH-ENERGY LASER BEAMS IN THE BEAMLET DEMONSTRATION PROJECT FOR THE NATIONAL IGNITION FACILITY
J. Thaddeus Salmon, Erlan S. Bliss, Michael W. Kartz, and Bruno M. VanWonterghem Nov. 1994 10 p Presented at the 15th Conference on Lasers and Electro-optics and 5th Quantum Electronics and Laser Science Conference, Baltimore, MD, 22-26 May 1995
(Contract W-7405-eng-48)
(DE95-012224; UCRL-JC-119004; CONF-950540-10) Avail: CASI HC A02/MF A01

The authors measure the absolute wavefront of Beamlet output pulses and actively correct for slowly varying aberrations present when the power amplifiers are not fired. Provision is also made for active precompensation of pump-induced amplifier aberrations. DOE

N95-33464 Northwestern Univ., Chicago, IL.
LASER-BASED ULTRASONICS BY DUAL-PROBE INTERFEROMETER DETECTION AND NARROW-BAND ULTRASOUND GENERATION Ph.D. Thesis
Jin Huang 1993 160 p
Avail: Univ. Microfilms Order No. DA9415746

Despite the advantages of laser-based ultrasonic (LBU) systems, the overall sensitivity of LBU systems needs to be improved for practical applications. Progress is reported to achieve better LBU detection accuracy and sensitivity for applications with surface waves and Lamb waves. A novel dual-probe laser interferometer has been developed to measure the same signal at two points. The dual-probe interferometer is a modification of a conventional single-probe interferometer in that the reference beam is guided to a second detecting point on the specimen surface to form a differential measurement mode, which measure the difference of the displacements at the two points. This dual-probe interferometer is particularly useful for accurate measurements of the speed and attenuation of surface waves and Lamb waves. The dual-probe interferometer has been applied to obtain accurate measurements of the surface wave speed and attenuation on surfaces of increasing surface roughness. It has also been demonstrated that with an appropriate signal processing method, namely, the power cepstrum method, the dual-probe interferometer is applicable to measure

the local surface wave speed even when the probe separation is so small that the two waveforms in the interferometer output signal overlap in the time domain. Narrow-band signal generation and detection improve the sensitivity of LBU systems. It is proposed to use a diffraction grating to form an array of illuminating strips which form a source of narrowband surface and Lamb waves. The line-array of thermoelastic sources generates narrow-band signals whose frequency and bandwidth can be easily controlled. The optimum line-array parameters, such as width, spacing and the number of lines in the array have been derived theoretically and verified experimentally. Narrow-band signal generation with optimum parameters has been demonstrated. The enhanced LBU system with dual-probe detection and narrowband signal generation has been successfully applied to the detection of cracks emanating from rivet holes in aircraft fuselage panel samples. A compact fiber-optic dual-probe interferometer has also been developed and applied to the above mentioned problem of crack detection. Results agree well with those obtained with a bulk LBU system. Dissert. Abstr.

N95-33470 Northwestern Univ., Chicago, IL.
BIFURCATION ANALYSIS OF MULTIMODE INSTABILITIES IN CLASS B LASERS Ph.D. Thesis
Thomas William Carr 1993 110 p
Avail: Univ. Microfilms Order No. DA9415705

We investigate spatio-temporal instabilities appearing in multimode lasers and large arrays of coupled single-mode lasers. Our bifurcation analysis takes advantage of a small parameter appropriate for class B lasers, such as CO2, semiconductor, and solid state lasers. For the multimode laser, we consider a homogeneously broadened two-level unidirectional ring laser described by a set of partial differential equations called the Maxwell-Bloch equations. We study the branching of periodic traveling wave solutions and determine their bifurcation equations. This is achieved by using the class B limit which allows us to reformulate the original laser equations as a weakly perturbed conservative system. In the vicinity of the Hopf bifurcation point, we obtain an expression for the direction of bifurcation of a single-mode traveling wave solution. The bifurcation is subcritical (supercritical) for low (large) values of the wave number. We develop a higher order analysis to examine the singularity separating these two regimes. In addition, we examine the limits of small and large wavenumber. We show that these limits are singular and require a special analysis of the laser equations. For a particular range of the parameters, two modes may simultaneously become unstable and correspond to a multiple eigenvalue of the linear theory. We then determine conditions for the bifurcation equations and classify the possible bifurcation diagrams. We also consider the case of a large cavity for which the spectrum of unstable modes is considered continuous. We derive an amplitude equation which describes the slow modulation in space and time of a basic traveling wave. Our equation differs from traditional evolution equations in that it contains higher order partial derivatives and nonlinearities. This results from the fact that our basic traveling wave corresponds to a vertical bifurcation. In the second part of the thesis, we concentrate on arrays of coupled lasers which exhibit typical multimode instabilities. In addition to the class B limit, we benefit from the small value of the excess pump current. We derive amplitude equations for the long time evolution of special modes called supermodes. We then determine the stability of these supermodes and the bifurcation diagram. Finally, we compare our results with the exact numerical bifurcation diagram. Dissert. Abstr.

N95-33703# Lawrence Livermore National Lab., Livermore, CA.
TEMPORAL DYNAMICS OF THE MULTI-FREQUENCY SPECTRUM GENERATED BY SELF-PHASE MODULATION OF TWO FREQUENCIES IN SINGLE-MODE FIBER
D. M. Pennington, M. A. Henesian, C. G. Brown, P. M. Danforth, and D. Eimerl Jun. 1994 5 p Presented at the IEEE Lasers and Electro-Optics Society 1994 Annual Meeting, Boston, MA, 31 Oct. - 1 Nov. 1994 Submitted for publication
(Contract W-7405-eng-48)
(DE95-010920; UCRL-JC-117360; CONF-941006-6) Avail: CASI HC A01/MF A01

The authors report the development of a tunable bandwidth source based on self-phase modulation of two frequencies in an optical fiber. A single frequency pulse was obtained by placing a 688 micrometer etalon with finesse = 3.3 in a single mode, single frequency Q-switched ND:YLF oscillator. Angle tuning of the etalon allowed continuous frequency tuning of the oscillator by +/- 2.5 (angstrom) about the central frequency of 10,530.3 (angstrom). Two oscillators were modified and tuned to 10,532.8 (angstrom) and 10,527.8 (angstrom), respectively. Additional tests performed with a 344 (mu)m etalon allowed tuning of +/- 5 (angstrom), but with reduced output energy and stability (+/- 20%); however, pulse to pulse energy fluctuations can be compensated for by the use of a pulse energy regulator if a broader range of tunability is required. The output beams were temporally and spatial overlapped, and shortened to an 11 ns nominally square pulse with a 3 ns rise and fall via a Pockels cell. Two Pockels cells were required to reduce nonlinear effects in the fiber due to prelase signal. The two frequencies were coupled into a 10 m single-mode polarization preserving fiber with a 4.2 x 7.4 micrometer core diameter and an effective mode area of 64 micrometers. The beam energy was recorded at the input and output of the fiber. The output spectrum was recorded with a spectrometer/optical multichannel analyzer, and the temporal pulse shape of each frequency was recorded by spectrally dispersing the far field beam and re-imaging it onto a streak camera. DOE

N95-34308# Air Force Systems Command, Wright-Patterson AFB, OH. National Air Intelligence Center.
HIGH POWER CO2 LASER WINDOWS AND REFLECTION REDUCING COATINGS
G. A. Atanassov and Gu Peifu 10 Apr. 1995 18 p Transl. into ENGLISH from Guangxue Xuebao, China, v. 12, no. 10, Oct. 1992 p 934-940
(AD-A294217; NAIC-ID(RS)T-0760-94) Avail: CASI HC A03/MF A01

This article describes evaluation standards for window materials. In conjunction with that, comparisons were made between the four types of materials Ge, GaAs, ZnSe, and KCl. It was discovered that KCl possesses optimum optical characteristics. In conjunction with this, reflection reducing films associated with good performance were designed and prepared. Measurements were done of their absorption and laser damage threshold values. DTIC

N95-34380# Air Force Systems Command, Wright-Patterson AFB, OH. National Air Intelligence Center.
A MULTI-WAVELENGTH DYE LASER SYSTEM
Tang Xingli and Shang-Guan Cheng 25 Apr. 1995 13 p Transl. into ENGLISH from Guangxue Xuebao, China, v. 12, no. 8, Aug. 1992 p 684-687
(AD-A294068; NAIC-ID(RS)T-0652-93) Avail: CASI HC A03/MF A01

A four-wavelength dye laser system consisted of four dye lasers is developed. Its laser parameters and time characteristic after mixing four beams have been measured. The factors which have an effect on efficient dye laser power are discussed briefly. The total average output power of this system is 8.9 W. DTIC

N95-34466 Oak Ridge National Lab., TN. Solid State Div.
MODELING AND SIMULATION OF PULSED LASER ANNEALING AND ABLATION OF SOLID MATERIALS
C. L. Liu and R. F. Wood Apr. 1995 8 p Presented at the Spring Meeting of the Materials Research Society (MRS), San Francisco, CA, 17-21 Apr. 1995 Limited Reproducibility: More than 20% of this document may be affected by microfiche quality
(Contract DE-AC05-84OR-21400)
(DE95-012888; CONF-950412-14) Avail: CASI HC A02

A previously developed one-dimensional (1D) computational model for heat flow and nonequilibrium phase change phenomena induced by pulsed-laser irradiation has been extended to two-dimensions. The 2D modeling focuses attention on the heat flow from localized sources embedded in an otherwise planar matrix. For example, nucleation events occurring in undercooled liquids such as molten Si formed by pulsed-laser melting of amorphous Si (a-Si) and inhomogeneous absorption due to randomly occurring defects in targets used for pulsed-laser ablation can be treated. Concepts introduced in the 1D modeling, such as the state diagram and the state array are extended to 2D and refined. As an example of the calculations that are now possible, the laser-induced formation and propagation of buried liquid layers are followed in two dimensions for the case of a-Si on a crystalline silicon substrate. It is demonstrated how solid phase growth from individual nucleation sites gives rise to a nearly planar liquid layer propagating through the a-Si. Another example briefly addresses questions related to the early stages of the laser ablation of insulators

such as MgO, where it is believed that the absorption of the laser radiation occurs at localized but extended regions of high concentrations of defects. The 2-D program has been rewritten for massively parallel machines such as the Intel Paragons in ORNL's Center for Computational Sciences by one of us (CLL), thus allowing larger and more accurate calculations for complex systems to be carried out in reasonable times. DOE

N95-34469# Air Force Systems Command, Wright-Patterson AFB, OH. National Air Intelligence Center.

PULSED TUNABLE NARROW-BANDWIDTH DYE LASER, WITH HOLLOW CIRCULAR WAVEGUIDE IN CAVITY

Lu Zhengguo and Zhou Jianying 26 Apr. 1995 14 p Transl. into ENGLISH from Guangxue Xuebao, China, v. 11, no. 9, Sep. 1991 p 844-847

(AD-A294060; NAIC-ID(RS)T-0650-93) Avail: CASI HC A03/MF A01

This paper presents a novel widely tunable, pulsed dye laser with single transverse mode narrow bandwidth which can be constructed by using a grazing- incidence grating in conjunction with a hollow circular dielectric waveguide. The experimental results show that the single transverse mode narrow bandwidth laser output can be obtained while maintaining a high lasing efficiency. The mechanism of the improvement is also discussed in this paper. DTIC

N95-34470# Air Force Systems Command, Wright-Patterson AFB, OH. National Air Inteligence Center.

ATMOSPHERIC ATTENUATION PROPERTIES ASSOCIATED WITH CO2 LASER RADIATION SPECTRA

Ruizhong Rao, Junbo Wang, and Shixiao Yue 26 Apr. 1995 18 p Transl. into ENGLISH from unidentified Chinese language article, p 119-125

(AD-A294061; NAIC-ID(RS)T-0444-93) Avail: CASI HC A03/MF A01

In Aug. 1986, in Chengdu city, we did on-the-spot measurements of attenuation in the atmosphere associated with 40 spectral lines of CO2 laser radiation within oscillation bands 00 deg 1 - 10 deg 0 and 00 deg 1 - 02 deg 0. This article gives general values for various spectral line attenuation coefficients. In conjunction with this, it describes attenuation characteristics. Under the specific conditions of the Chengdu area in August, water vapor absorption and gas aerosol particle absorption along with scattering form the principal components of attenuation. Attenuation coefficients measured in association with various spectral lines can supply beneficial references for CO2 laser atmospheric applications. DTIC

N95-34592# Phillips Lab., Kirtland AFB, NM.

ABLEX: HIGH ALTITUDE LASER PROPAGATION EXPERIMENT

L. D. Weaver and R. R. Butts Aug. 1994 27 p

(AD-A294914; PL-LI-94-27) Avail: CASI HC A03/MF A01

This article describes the Airborne Laser Experiment (ABLEX) project. ABLEX consisted of a set of experiments conducted in December 1992 and January 1993 in which a laser beam was propagated between two aircraft flying at high altitude. In these experiments scintillation patterns resulting from propagation through turbulence were recorded. The purpose of the experiments was to determine the fundamental performance limits of an adaptive optics system which performed phase only compensation as part of an Airborne Laser (ABL) theater missile defense weapon platform. Rather than field a highly complex, and expensive, airborne test-bed equipped with a state-of-the-art adaptive optics system, the physics-limited performance was determined by a novel, and quite simple method. This technique permitted a Strehl determination through measurements of the scintillation patterns resulting from propagation through turbulence. ABLEX was a scaled experiment: the aperture, operating wavelength, range to target, and platform altitude were all chosen such that the optical effects experienced by the propagating laser beam would be identical to those experienced by a high energy laser (HEL) beam. ABLEX was conducted as part of the ABL Risk Reduction program that was carried out in the first phase of the ABL program. DTIC

N95-34619 Department of the Navy, Washington, DC.

METHOD AND APPARATUS FOR LOCKING LASER WAVELENGTH TO AN ATOMIC TRANSITION Patent

Stephen A. Miller, inventor (to Navy) 14 Feb. 1995 13 p Filed 13 Jun. 1994

(AD-D017425; US-Patent-5,390,203; US-Patent-Appl-SN-263206; US-Patent-Class-372-29) Avail: US Patent and Trademark Office

An apparatus and method for stabilizing laser light wavelength relative to a resonant optical absorption works with both continuous wave and pulsed lasers and employs the phenomenon of Zeeman energy level splitting to provide an error signal indicative of both the direction and magnitude of wavelength error. A laser system including a wavelength adjusting means produces laser light at a wavelength which differs by an adjustable amount from a resonant absorption wavelength of a selected substance. A first portion of the laser light is propagated through a right circular polarizing means to provide right circularly polarized (RCP) laser light. RCP laser light is propagated through a first volume occupied by the selected substance, said first volume being disposed in a magnetic field. DTIC

N95-34761# Naval Research Lab., Washington, DC.

EXTREME BROADENING OF STIMULATED RAMAN SCATTERED LIGHT FROM HIGH INTENSITY LASER PLASMA INTERACTIONS Interim Report

A. Ting, K. M. Krushelnick, H. R. Burris, A. Fisher, and C. Manka 2 May 1995 15 p

(AD-A294165; NRL/MR/6790-95-7667) Avail: CASI HC A03/MF A01

High intensity picosecond laser plasma interaction experiments were performed to examine nonlinear scattering mechanisms in field ionized underdense plasmas. Broad and oscillatory spectra were observed for the forward scattered light. The Raman backscattered spectrum showed an extremely broad, supercoptinuum like nature, extending from 450 nm to greater than 1200 nm at incident laser intensities of 2 x 10(exp 18) W/sq cm. Narrow and large amplitude modulations in the spectrum of the backscattered radiation were measured and are attributed to scattering from ion waves. DTIC

N95-34811 Sandia National Labs., Albuquerque, NM.

LASER BEAMING DEMONSTRATIONS AT THE STARFIRE OPTICAL RANGE

Ronald J. Lipinski, Dorothy C. Meister, Stephenson Tucker, Phillip Leatherman (Starfire Optical Range, Kirtland AFB, NM.), Robert Q. Fugate (Starfire Optical Range, Kirtland AFB, NM.), Carl Maes (Starfire Optical Range, Kirtland AFB, NM.), W. Joseph Lange (Starfire Optical Range, Kirtland AFB, NM.), William Cowan (Starfire Optical Range, Kirtland AFB, NM.), Richard A. Cleis (Rockwell Power Systems, Albuquerque, NM.), and James M. Spinhirne (Rockwell Power Systems, Albuquerque, NM.) et al 1995 12 p Presented at the SPIE 1995: SPIE Conference on Optics, Electro-optics, and Laser Application in Sci ence, Engineering and Medicine, San Jose, CA, 5-14 Feb. 1995 Limited Reproducibility: More than 20% of this document may be affected by microfiche quality

(Contract DE-AC04-94AL-85000)

(DE95-007747; SAND-94-2002C; CONF-950226-43) Avail: CASI HC A03

The ability to acquire, track, and accurately direct a laser beam to a satellite is crucial for power-beaming and laser-communications. To assess the state of the art in this area, a team consisting of Air Force Phillips Laboratory, Sandia National Laboratories, and COMSAT Corporation personnel performed some laser beaming demonstrations to various satellites. A ruby laser and a frequency-doubled YAG laser were used with the Phillips Lab Starfire Optical Range (SOR) beam director for this activity. The ruby laser projected 20 J in 6 ms out the telescope with a beam divergence that increased from 1.4 to 4 times the diffraction limit during that time. The doubled YAG projected 0.09 J in 10 ns at 20 Hz. The SOR team demonstrated the ability to move rapidly to a satellite, center it in the telescope, then lock onto it with the tracker, and establish illumination. Several low-earth-orbit satellites with corner-cube retro-reflectors were illuminated at ranges from 1000 to 6000 km with a beam divergence estimated to be about 20 micro radians. The return signal from the ruby laser was collected in a 15-cm telescope, detected by a photomultiplier tube, and recorded at 400 kHz. Rapid variations in intensity (as short at 15 micro s) were noted, which may be due to speckles caused by phase interference from light reflected from different retro-reflectors on the satellite. The return light from the YAG was collected by a 35-cm telescope and detected by an intensified CCD camera. The satellite brightened by about a factor of 30 in the sunlight when the laser was turned on, and dimmed back to normal when the 50-micro radian point-ahead was turned off. The satellite was illuminated at 1 Hz as it entered the earth's shadow and

followed for about 10 seconds in the shadow. In another demonstration, four neighboring GEO satellites were located and centered in succession with a 3.5-m telescope at a rate of about 16 seconds per satellite. DOE

N95-32988# Osaka Univ., Osaka (Japan). Dept. of Electromagnetic Energy Engineering.
MEASUREMENT OF LASER WAVEFRONT USING SHACK HARTMANN METHOD WITH NEW LENS ARRAY
Geun Young Yoon, Takahisa Jitsuno, Masahiro Nakatsuka, and Sadao Nakai *In its* Technology Reports of the Osaka Univ., Vol. 45, Nos. 2205-2216 15 Apr. 1995 p 27-33 (For primary document see N95-32984 12-31)
(Rept-2208) Avail: CASI HC A02/MF A02

N95-32989# Osaka Univ., Osaka (Japan). Dept. of Electromagnetic Energy Engineering.
CONTROL OF THE LASER BEAM IRRADIATION INTENSITY DISTRIBUTION USING ASPHERICAL MULTI LENS ARRAY AND EDGE-SHAPED PLATES
Noriaki Nishi, Takahisa Jitsuno, Koji Tsubakimoto, Masahiro Nakatsuka, and Sadao Nakai *In its* Technology Reports of the Osaka Univ., Vol. 45, Nos. 2205-2216 15 Apr. 1995 p 35-42 (For primary document see N95-32984 12-31)
(Rept-2209) Avail: CASI HC A02/MF A02

N95-32990# Osaka Univ., Osaka (Japan). Dept. of Inst. of Laser Engineering.
MEASUREMENT OF GAIN SATURATION ON Nd: DOPED PHOSPHATE LASER GLASSES
Masakazu Tada, Noriyuki Tsukino (Kawasaki Heavy Industries Ltd., Tokyo, Japan.), Tadashi Kanabe, Masahiro Nakatsuka, and Sadao Nakai *In its* Technology Reports of the Osaka Univ., Vol. 45, Nos. 2205-2216 15 Apr. 1995 p 43-48 (For primary document see N95-32984 12-31)
(Rept-2210) Avail: CASI HC A02/MF A02

37 MECHANICAL ENGINEERING

Includes auxiliary systems (nonpower); machine elements and processes; and mechanical equipment.

N95-32376# Los Alamos National Lab., NM.
BOLT PRELOAD SELECTION FOR PULSED-LOADED VESSEL CLOSURES
T. A. Duffey, B. B. Lewis, and S. M. Bowers 1995 29 p Presented at the Joint ASME/JSME Pressure Vessels and Piping Conference, Honolulu, HI, 23-27 Jul. 1995
(Contract W-7405-eng-36)
(DE95-006346; LA-UR-95-47; CONF-950740-9) Avail: CASI HC A03/MF A01

Bounding, closed-form solutions are developed for selecting the bolt preload for a square, flat plate closure subjected to a pressure pulse load. The solutions consider the limiting case in which preload is primarily dependent on closure bending response as well as the limiting case in which preload depends on elastic bolt response. The selection of bolt preload is illustrated. Also presented in the paper is a detailed finite element analysis of dynamically loaded, bolted circular closure. The responses of the structure, closure, and bolts are included, and results are obtained for various preloads. The analysis illustrates a method of bolt preload modeling for use in general finite element computer programs. DOE

N95-32612 Swedish National Testing and Research Inst., Boras (Sweden).
[TEST METHOD TO MEASURE RESISTANCE TOWARDS FRAGMENTATION BY STUDDED TIRES]
L. Viman Jan. 1995 48 p
(PB95-211017; SP-RAPP-1994:21) Avail: Issuing Activity (National Technical Information Service (NTIS))

In the Nordic countries most cars are equipped with studded tires during the winter. The studs increase the wear on the road surfaces and a special test method has been developed to measure the aggregates' resistance towards fragmentation by studded tires. The method has proven to correlate very well with the actual wear on the road surfaces. The Nordic countries Sweden, Norway and Finland have agreed to propose this method as a European Standard test method. One reason is to be able to set requirements on aggregates to be used in countries where studded tires are allowed. A cross-testing project regarding this Nordic abrasion test for studded tires was set up in order to determine the repeatability and the reproducibility of the methods to become European Standard. NTIS

N95-32675*# Catholic Univ. of America, Washington, DC. School of Engineering and Architecture.
A STUDY OF SPACE-RATED CONNECTORS USING A ROBOT END-EFFECTOR Final Report
Charles C. Nguyen Apr. 1995 27 p
(Grant NAG5-1415)
(NASA-CR-199116; NAS 1.26:199116) Avail: CASI HC A03/MF A01

The main research activities have been directed toward the study of the Robot Operated Materials Processing System (ROMPS), developed at GSFC under a flight project to investigate commercially promising in-space material processes and to design reflyable robot automated systems to be used in the above processes for low-cost operations. The research activities can be divided into two phases. Phase 1 dealt with testing of ROMPS robot mechanical interfaces and compliant device using a Stewart Platform testbed and Phase 2 with computer simulation study of the ROMPS robot control system. This report provides a summary of the results obtained in Phase 1 and Phase 2. Author (revised)

N95-32689*# Auburn Univ., AL. Dept. of Mechanical Engineering.
INFLUENCE OF BACKUP BEARINGS AND SUPPORT STRUCTURE DYNAMICS ON THE BEHAVIOR OF ROTORS WITH ACTIVE SUPPORTS Annual Status Report
George T. Flowers Jun. 1995 39 p
(Grant NAG3-1507)
(NASA-CR-199080; NAS 1.26:199080) Avail: CASI HC A03/MF A01

Progress made in the current year is listed, and the following papers are included in the appendix: Steady-State Dynamic Behavior of an Auxiliary Bearing Supported Rotor System; Dynamic Behavior of a Magnetic Bearing Supported Jet Engine Rotor with Auxiliary Bearings; Dynamic Modelling and Response Characteristics of a Magnetic Bearing Rotor System with Auxiliary Bearings; and Synchronous Dynamics of a Coupled Shaft/Bearing/Housing System with Auxiliary Support from a Clearance Bearing: Analysis and Experiment. For individual titles, see N95-32690 through N95-32693.

N95-32690*# National Aeronautics and Space Administration. Lewis Research Center, Cleveland, OH.
STEADY-STATE DYNAMIC BEHAVIOR OF AN AUXILIARY BEARING SUPPORTED ROTOR SYSTEM
Huajun Xie (Auburn Univ., AL.), George T. Flowers (Auburn Univ., AL.), and Charles Lawrence *In* Auburn Univ., Influence of Backup Bearings and Support Structure Dynamics on the Behavior of Rotors with Active Supports Jun. 1995 11 p Presented at the ASME International Mechanical Engineering Congress and Exposition: Symposium on Nonlinear and Stochastic Dynamics, Chicago, IL, 13-18 Nov. 1994 (For primary document see N95-32689 12-37)
Avail: CASI HC A03/MF A01

This paper investigates the steady-state responses of a rotor system supported by auxiliary bearings in which there is a clearance between the rotor and the inner race of the bearing. A simulation model based upon the rotor of a production jet engine is developed and its steady-state behavior is explored over a wide range of operating conditions for various parametric configurations. Specifically, the influence of rotor imbalance, support stiffness, and damping is studied. It is found that imbalance may change the rotor responses dramatically in terms of frequency contents at certain operating speeds. Subharmonic responses of 2nd order through 10th order are all observed except the 9th order. Chaotic phenomenon is also observed. Jump phenomena (or double-valued responses) of both hard-spring type and soft-spring type are shown to occur at low operating speeds for systems with low auxiliary bearing damping or large clearance even with relatively small imbalance. The effect of friction between the shaft and the inner race of the bearing is also discussed. Author

N95-32691*# Auburn Univ., AL. Dept. of Mechanical Engineering.
DYNAMIC BEHAVIOR OF A MAGNETIC BEARING SUPPORTED JET ENGINE ROTOR WITH AUXILIARY BEARINGS
George T. Flowers, Huajun Xie, and S. C. Sinha *In its* Influence of Backup Bearings and Support Structure Dynamics on the Behavior of Rotors with Active Supports Jun. 1995 6 p Presented at the First Industry/University Symposium on High Speed Transport Vehicles, Greensboro, NC, 4-6 Dec. 1994 (For primary document see N95-32689 12-37)
Avail: CASI HC A02/MF A01

This paper presents a study of the dynamic behavior of a rotor system supported by auxiliary bearings. The steady-state behavior of a simulation model based upon a production jet engine is explored over a wide range of operating conditions for varying rotor imbalance, support stiffness, and damping. Interesting dynamical phenomena, such as chaos, subharmonic responses, and double-valued responses, are presented and discussed. Author

N95-32692*# Auburn Univ., AL. Dept. of Mechanical Engineering.
DYNAMIC MODELLING AND RESPONSE CHARACTERISTICS OF A MAGNETIC BEARING ROTOR SYSTEM WITH AUXILIARY BEARINGS
April M. Free, George T. Flowers, and Victor S. Trent *In its* Influence of Backup Bearings and Support Structure Dynamics on the Behavior of Rotors with Active Supports Jun. 1995 8 p Presented at the 15th Biennial ASME Vibrations Conference, Boston, MA, 17-21 Sep. 1995 (For primary document see N95-32689 12-37)
Avail: CASI HC A02/MF A01

Auxiliary bearings are a critical feature of any magnetic bearing system. They protect the soft iron core of the magnetic bearing during an overload or failure. An auxiliary bearing typically consists of a rolling element bearing or bushing with a clearance gap between the rotor and the inner race of the support. The dynamics of such systems can be quite complex. It is desired to develop a rotordynamic model which describes the dynamic behavior of a flexible rotor system with magnetic bearings including auxiliary bearings. The model is based upon an experimental test facility. Some simulation studies are presented to illustrate the behavior of the model. In particular, the effects of introducing sideloading from the magnetic bearing when one coil fails is studied. Author

N95-32693*# Auburn Univ., AL.
SYNCHRONOUS DYNAMICS OF A COUPLED SHAFT/BEARING/HOUSING SYSTEM WITH AUXILIARY SUPPORT FROM A CLEARANCE BEARING: ANALYSIS AND EXPERIMENT
James L. Lawen, Jr. and George T. Flowers *In its* Influence of Backup Bearings and Support Structure Dynamics on the Behavior of Rotors with Active Supports Jun. 1995 8 p Presented at the International Gas Turbine and Aeroengine Congress and Exposition, Houston, TX, 5-8 Jun. 1995 Submitted for publication in the Transactions of the ASME (For primary document see N95-32689 12-37)
(Grant NGT-70312)
Avail: CASI HC A02/MF A01

This study examines the response of a flexible rotor supported by load sharing between linear bearings and an auxiliary clearance bearing. The objective is to develop a better understanding of the dynamical behavior of a magnetic bearing supported rotor system interacting with auxiliary bearings during a critical operating condition. Of particular interest is the effect of coupling between the bearing/housing and shaft vibration on the rotordynamical responses. A simulation model is developed and a number of studies are performed for various parametric configurations. An experimental investigation is also conducted to compare and verify the rotordynamic behavior predicted by the simulation studies. A strategy for reducing synchronous shaft vibration through appropriate design of coupled shaft/bearing/housing vibration modes is identified. Author

N95-32752 Lehigh Univ., Bethlehem, PA.
THE EFFECT OF LABYRINTH SEALS ON THE DYNAMICS OF TURBOMACHINERY Ph.D. Thesis
Dursun Eser 1994 131 p
Avail: Univ. Microfilms Order No. DA9414991

The gas flow in labyrinth seals is investigated for various geometries commonly found in turbomachinery. Labyrinth seals separate regions of high pressure from low pressure regions and they minimize the leakage of the high pressure gas. Equations governing the leakage rate for multicavity labyrinth seals are derived and their predictions, together with the associated pressure and circumferential velocity distributions, are discussed and compared to experimental results. The detailed three dimensional, axisymmetric, steady flow in a single cavity is investigated by the use of standard computational fluid dynamics (CFD) methods. The results so obtained are in general agreement with published experimental results and indicate that the shear forces applied on the rotor are comparable to the pressure forces acting on it. Small amplitude transverse vibrations of the rotor give rise to a three dimensional, nonaxisymmetric time dependent flow in the labyrinth cavities. Such a flow produces a nonzero net force on the rotor which under certain conditions may have a destabilizing effect. The rotor dynamic stiffness and damping coefficients due to those forces are calculated under the assumption that the flow can be modeled by bulk pressures and azimuthal velocities which are time dependent and nonaxisymmetric. Comparison of the results with experimental data is satisfactory. Dissert. Abstr.

N95-32863# Sandia National Labs., Livermore, CA.
IGNITION AND EARLY SOOT FORMATION IN A DI DIESEL ENGINE USING MULTIPLE 2-D IMAGING DIAGNOSTICS
John E. Dec and Christoph Espey (Pennsylvania State Univ., University Park, PA.) 1995 23 p Presented at the Society of Automotive Engineers International Congress and Exposition, Detroit, MI, 27 Feb. - 2 Mar. 1995
(Contract DE-AC04-94AL-85000)
(DE95-010692; SAND-95-8521-C; CONF-950256-5) Avail: CASI HC A03/MF A01

Combined optical imaging diagnostics in the fuel jet of a direct-injection diesel engine to study the ignition and early soot formation processes. A diesel engine of the 'heavy-duty' size class was operated at a representative medium speed (1200 rpm) operating condition. Two fuels were used, a 42.5 cetane number mixture of the diesel reference fuels and a new low-sooting fuel. Combustion and soot formation are almost identical for both fuels. Ignition and early combustion were studied by imaging the natural chemiluminescence using a calibrated intensified video camera. Early soot development was investigated via luminosity imaging and simultaneous planar imaging of laser-induced incandescence (LII) and elastic scattering. The latter provide relative soot concentrations and particle size distributions. Data show that ignition occurs at multiple points across the downstream region of all the fuel jets prior to first apparent heat release well before any soot luminosity occurs. Quantitative vapor-fuel/air mixture images in the leading portion of the jet are also presented and discussed with respect to the early combustion data. The first soot occurs at random locations, and shortly thereafter, small soot particles develop throughout the cross section of the leading portion of the jet. Data indicate that this soot arises from the fuel-rich premixed burn. Then, significantly larger soot particles appear around the periphery of the jet, presumably from the initial diffusion combustion. By the end of the premixed burn, the soot has developed a distribution pattern of a higher concentration toward the front of the jet and a lower concentration upstream, with the larger-sized soot particles being generally confined to the periphery of the jet. DOE

N95-32906 Case Western Reserve Univ., Cleveland, OH.
INFLUENCE OF NON CLASSICAL FRICTION ON THE RUBBING AND IMPACT BEHAVIOR OF ROTOR DYNAMIC SYSTEMS Ph.D. Thesis
Michael Kent Hagigat 1994 290 p
Avail: Univ. Microfilms Order No. DA9425528

A nonlinear finite element model for simulating the effects of rubbing and impact on rotor dynamics has been developed. The nonlinear model is used to conduct a series of forced transient analyses of a rotating system under the influence of rubbing and impact using the modal and the average acceleration direct numerical integration methods. The modal method is shown to be more efficient than the average acceleration method. The first approach for modeling the friction forces is the application of Coulomb friction law. Simulation results show the rotating system to be unstable for all ranges of Coulomb coefficient of friction. In contrast, experimental results have shown that the system under study is stable under the influence of rubbing and impact for the simulation conditions. A second approach for modeling the friction forces is employed for the purpose of investigating the differences between the experimental and the simulation results. The second approach consists of an artificial simulation

of a stick-slip phenomenon by setting the Coulomb coefficient of friction to a value of zero for certain time intervals. The artificial stick-slip simulation has a stabilizing effect on the system. The third approach for modeling the friction forces is the application of an advanced friction model simulating the stick-slip phenomena. The system appears to be completely stable for a dry metal to metal rubbing and impact condition. The results of the simulation using the advanced friction model are close to experimental results. The surface finish of the contacting metals were found to have a negligible effect on the results of the simulation. Dissert. Abstr.

N95-32915*# Scientific Research Associates, Inc., Glastonbury, CT.
DESIGN OF ETO PROPULSION TURBINE USING CFD ANALYSES Final Report
F. J. deJong, Y. T. Chan, and H. J. Gibeling Apr. 1995 89 p Original contains color illustrations
(Contract NAS8-38865)
(NASA-CR-199085; NAS 1.26:199085; R95-9084-F) Avail: CASI HC A05/MF A01; 5 functional color pages

As one of the activities of the NASA/MSFC Turbine Technology Team, the present effort focused on using CFD in the design and analysis of high performance rocket engine pumps. A three-dimensional Navier-Stokes code was used for various turbine flow field calculations, with emphasis on the tip clearance flow and the associated losses. Both a baseline geometry and an advanced-concept geometry (with a mini-shroud at the blade tip) were studied at several tip clearances. The calculations performed under the present effort demonstrate that a state-of-the-art CFD code can be applied successfully to turbine design and the development of advanced hardware concepts. Author

N95-32924# Department of the Navy, Washington, DC.
SPLIT GASKET ATTACHMENT METHOD STATEMENT OF GOVERNMENT INTEREST Patent Application
Paul E. Moody, inventor (to Navy) 17 Jan. 1995 17 p
(AD-D017443; US-Patent-Appl-SN-375335) Avail: CASI HC A02/MF A01

The present invention relates to a method and hardware for bonding together ends of a sealing strip. The method of the present invention comprises the steps of cutting a slot in both a first end and a second end of a sealing strip, inserting an attachment strip having a plurality of engaging members into the slot cut into the first end, applying adhesive to the second end of the sealing strip, and placing the two ends of the sealing strip into an abutting relationship by inserting the attachment strip into the slot in the second end and sliding the ends together. The hardware used to effect the method includes an alignment guide having a substantially C-shaped channel for receiving the ends of the sealing strip to be joined together. The alignment guide has an end cap associated therewith having one or more slots for receiving a cutting tool for cutting slots in the ends of the sealing strip. The hardware further includes an attachment strip which is used to join the ends of the sealing strip together. DTIC

N95-33179*# National Aeronautics and Space Administration. Lewis Research Center, Cleveland, OH.
EXPERIMENTAL AND ANALYTICAL ASSESSMENT OF THE THERMAL BEHAVIOR OF SPIRAL BEVEL GEARS
Robert F. Handschuh and Thomas P. Kicher (Case Western Reserve Univ., Cleveland, OH.) Aug. 1995 21 p Presented at the 1995 Fall Technical Meeting held in Charleston, SC, 16-18 Oct. 1995; sponsored by the American Gear Manufacturers Assoc.
(RTOP 505-62-36; DA Proj. 1L1-62211-A4-7A)
(NASA-TM-107009; E-9793; NAS 1.15:107009; ARL-TR-852) Avail: CASI HC A03/MF A01

An experimental and analytical study of spiral bevel gears operating in an aerospace environment has been performed. Tests were conducted within a closed loop test stand at NASA Lewis Research Center. Tests were conducted to 537 kW (720 hp) at 14,400 rpm. The effects of various operating conditions on spiral bevel gear steady state and transient temperature are presented. Also, a three-dimensional analysis of the thermal behavior was conducted using a nonlinear finite element analysis computer code. The analysis was compared to the experimental results attained in this study. The results agreed well with each other for the cases compared and were no more than 10 percent different in magnitude. Author

N95-33199*# National Aeronautics and Space Administration. Marshall Space Flight Center, Huntsville, AL.
NASA-WIDE FASTENER TECHNICAL INTERCHANGE MEETING
W. R. Gamwell, comp. Jul. 1995 295 p Meeting held in Huntsville, AL, 15-16 Nov. 1994
(NASA-CP-3308; M-788; NAS 1.55:3308) Avail: CASI HC A13/MF A03

This document summarizes the minutes of the second NASA-Wide Fastener Technical Interchange Meeting (TIM) held November 15-16, 1994, and compiles the viewgraph presentations at the TIM by NASA and contractor personnel. The information in this document may be of value to the NASA and contractor fastener engineering community in determining the fastener controls and initiatives that existed at the time of the TIM. Author

N95-33252 Wayne State Univ., Detroit, MI.
DESIGN AND IMPLEMENTATION OF A TWO-AXIS MICROMANIPULATOR TO ENHANCE THE GRIPPER POSITIONAL ACCURACY OF A SINGLE FLEXIBLE LINK Ph.D. Thesis
Xiaoying Zhang 1994 130 p
Avail: Univ. Microfilms Order No. DA9423774

Accurate and versatile robots are required to perform advanced assembly and manufacturing tasks. To improve the end effector positional accuracy of lightweight robot arms, a two-axis micro-manipulator is mounted between the robot wrist and its manipulator. The rationale is to reduce the wrist sensitivity to the structural deflections of the robotic manipulator. In an attempt to separate the problem of the end-of-arm deflections from the overall control problem of multi-link systems, the micromanipulator is tested on a single flexible link. A laser head with a dual axis photodetector is used to provide direct measurements of the transverse deflections at the free-end of the beam and to detect mechanical inaccuracies caused by manufacturing imperfections and assembly misalignment. The advantages of the integrated system of the micro-manipulator with a single compliant beam are demonstrated and compared to the one without the micro-manipulator for two different control schemes, 'rigid body controller (RBC)' and 'rigid and flexible motion controller (RFMC)'. Both theoretical and experimental results have proven the capability of the micro-manipulator in significantly improving the gripper positional accuracy. Furthermore, it was demonstrated that the micromanipulator tends to complement rather than overlap the effort exerted by the host beam controller. The experimental results have revealed the significant adverse effects of the backlash in gearing on the overall performance of the macro- and micro-manipulators. To address this problem, the dynamic model of the macro- and micro-manipulators is modified to include the dynamics of joint actuators along with the effects of backlash in the indirect drive mechanism of the compliant beam. A general method is developed to handle the dynamic characteristics of backlash in gearing. It entails the derivation of a variable structure model with one auxiliary degree-of-freedom. The latter serves to increase the number of degrees of freedom of the system during the phase of gear separation. A set of rules is generated to define the moments at which the matching gears separate or re-engage. The principle of impulse and momentum is then implemented to compute the discontinuities in the instantaneous angular velocities of the gears immediately after their impact. A 'backlash controller' is introduced to replace the original controller of the beam whenever the backlash is being taken up in one direction or the other. The experimental and numerical results provide a qualitative validation of the backlash model. They investigate the relationships with which the backlash in gearing would interact with both the servo-loop controller and the structural flexibility of the system. In addition, the digital simulations have proven that the 'backlash controller' provides a more viable alternative than the micro-manipulator approach in dealing with the dynamic characteristics of backlash in gearing. Dissert. Abstr.

N95-33323 Auburn Univ., AL.
AN EXPERIMENTAL AND ANALYTICAL INVESTIGATION INTO THE PERFORMANCE OF CENTRIFUGAL PUMPS OPERATING WITH AIR-WATER MIXTURES Ph.D. Thesis
John Douglas Sterrett 1994 320 p
Avail: Univ. Microfilms Order No. DA9420263

An investigation was made into the performance of centrifugal pumps when two-phase non-condensable mixtures of gas and liquid are flowing. This problem is encountered during loss-of-coolant accidents in nuclear reactor systems and in the pumping of oil where natural gas may be

present in the mixture. Analytical and experimental techniques were used to address the issues of scaling between a model and a prototype pump and the validity of the single-phase pump affinity laws when two-phase flows are present. The results from this effort have also provided insight into the physical phenomena which cause the degradation in pump performance. An analytical model for the motion of a single bubble through a pump impeller is provided. The results from this fundamental problem show that the Coriolis and buoyancy forces are important in describing the kinematics of a gas phase. These results show that dynamic similitude is not preserved between a model and prototype impeller when the standard single-phase pump scaling relationships are used. The motion of a single bubble is also shown to be influenced by the magnitude of the pump suction pressure. The results from an extensive series of air-water two phase pump tests are provided. A 1/4 scale pump, modeled after the Savannah River Site K-reactor pumps, was tested over a wide range of pump speeds, flow rates, and suction pressures. These results indicate that the single-phase pump affinity laws are not applicable to two-phase pump flows and that the magnitude of the pump suction pressure is an important quantity in determining the pump performance. A second analytical model is developed for two-phase flow through a pump impeller. The results from this one-dimensional, two-fluid, non-homogeneous streamline model show good agreement with the experimental data. The model results support the experimental data in showing that the single-phase pump affinity relationships are not valid for two-phase pump flows and that dynamic similitude is not maintained between scaled test pumps and prototype pumps under normal pump testing procedures. The results from this model also show that the degradation in prototype pump performance will occur at higher air content than in the smaller scaled test pumps.

Dissert. Abstr.

N95-33701# Sandia National Labs., Livermore, CA. Combustion Research Facility.

THE EFFECTS OF HIGH AMBIENT DENSITY ON DIESEL SPRAY PENETRATION AND SPREAD

J. D. Naber, D. L. Siebers, and K. R. Hencken 1995 6 p Presented at the Combustion Institute and American Flame Research Conference, San Antonio, TX, 23-26 Apr. 1995

(Contracts DE-AC04-94AL-85000; DE-AC04-76DP-00789)

(DE95-010761; SAND-95-8563C; CONF-9504163-1) Avail: CASI HC A02/MF A01

The effects of ambient gas density on diesel spray penetration and spread under (1) non-vaporizing, (2) vaporizing, and (3) combusting conditions were examined. Densities more than a factor of two higher than top-dead-center conditions in current technology diesel engines were considered. The results show that the effects of density on non-vaporizing spray penetration are more significant than previously noted, that vaporization processes decrease penetration and spread, and that combustion processes increase penetration and spread of diesel sprays. DOE

N95-33834# Argonne National Lab., IL. Laser Applications Lab.

THE CHOICE: WELDING WITH CO2 OR Nd:YAG LASERS

Keng H. Leong 1995 9 p Presented at the Automotive Laser Applications Workshop, Dearborn, MI, 6-7 Mar. 1995

(Contract W-31-109-eng-38)

(DE95-011825; ANL/TD/CP-85711; CONF-9503113-2) Avail: CASI HC A02/MF A01

The recent commercial availability of multi-kilowatt Nd:YAG lasers has opened new avenues for rapid laser processing as well as intensified the competition (cost effectiveness) between CO2 and Nd:YAG laser systems. Vendors offering Nd:YAG laser systems may claim lower operating costs (than CO2) and fiberoptic beam delivery flexibility while CO2 systems vendors may emphasize lower capital cost and well established processing requirements and experience. The capital and operating costs of a laser system are impacted by demand and supply economics and technological advances. Frequently the total cost of a workcell using a laser for processing has to be considered rather than the laser system alone. Consequently it is not very practical to approach the selection of a laser system based on its capital cost and estimated operating cost only. This presentation describes a more pragmatic approach to aid the user in the selection of the optimal multi-kilowatt laser system for a particular processing requirement with emphasis on welding. CO2 laser systems are well established on the factory floor. Consequently, emphasis is given to the comparative application of Nd:YAG lasers, process requirements and performance. Requirements for the laser welding of different metals are examined in the context of hardware (laser system and beam delivery) selection and examples of welding speeds that can be achieved using CO2 and Nd:YAG lasers are examined. DOE

N95-33836# Sandia National Labs., Albuquerque, NM.

AN APPLICATION OF MECHANICAL LEVERAGE TO MICRCACTUATION

J. J. Sniegowski and C. Smith (Wisconsin Univ., Madison, WI.) 1994 5 p Presented at the 8th International Conference on Solid-state Sensors and Actuators and 9th Biannual International Conference and Annual European Conference on Solid-state Sensors, Stockholm, Sweden, 25-29 Jan. 1995

(Contract DE-AC04-94AL-85000)

(DE95-011883; SAND-94-3205C; CONF-950650-1) Avail: CASI HC A01/MF A01

Preliminary results on the use of mechanical advantage to convert a short-displacement, high-force actuation mechanism into a long-displacement, medium-force actuator are presented. This micromechanical, mechanically-advantaged actuator is capable of relatively large displacement and force values. The target design values are lever ratio of 17.5:1 leading to a +/- 17.5 micrometers displacement while providing no less than 2.25 micro-N of force throughout actuator's range of motion for an applied voltage of less than 50 volts. The basis for the mechanical advantage is simple levers with fulcrums. DOE

N95-33908*# National Aeronautics and Space Administration. Lewis Research Center, Cleveland, OH.

BENDING STRENGTH MODEL FOR INTERNAL SPUR GEAR TEETH

Michael Savage (Akron Univ., Akron, OH.), K. L. Rubadeux (Akron Univ., Akron, OH.), and H. H. Coe American Institute of Aeronautics and Astronautics, Inc. Jul. 1995 12 p Presented at the 31st Joint Propulsion Conference and Exhibit, San Diego, CA, 10-12 Jul. 1995; cosponsored by AIAA, ASME, SAE, and ASEE

(RTOP 505-62-36; DA Proj. 1L1-62211-A-47-A)

(NASA-TM-107012; E-9797; NAS 1.15:107012; ARL-TR-838) Avail: CASI HC A03/MF A01

Internal spur gear teeth are normally stronger than pinion teeth of the same pitch and face width since external teeth are smaller at the base. However, ring gears which are narrower have an unequal addendum or are made of a material with a lower strength than that of the meshing pinion may be loaded more critically in bending. In this study, a model for the bending strength of an internal gear tooth as a function of the applied load pressure angle is presented which is based on the inscribed Lewis constant strength parabolic beam. The bending model includes a stress concentration factor and an axial compression term which are extensions of the model for an external gear tooth. The geometry of the Lewis factor determination is presented, the iteration to determine the factor is described, and the bending strength J factor is compared to that of an external gear tooth. This strength model will assist optimal design efforts for unequal addendum gears and gears of mixed materials. Author

N95-34449 Department of the Navy, Washington, DC.

ENERGY ABSORPTION DEVICE FOR SHOCK LOADING Patent

C. D. Howard, inventor (to Navy), Donald E. LaGrange, inventor (to Navy), David A. Beatty, inventor (to Navy), and David C. Littman, inventor (to Navy) 28 Feb. 1995 5 p Filed 30 Jun. 1993

(AD-D017476; US-Patent-5,393,016; US-Patent-Appl-SN-083602; US-Patent-Class-244-138) Avail: US Patent and Trademark Office

A shock energy absorbing device provides shock protection for the riser line employed to attach an aerodynamic deceleration device to a primary body during deployment of the system into an airstream. During deployment, for example, by dropping an unopened parachute and attached load or by rocket delivery of the unopened parachute and attached load, the parachute is made to open at a desired altitude whereupon very large shock tension forces are generated which are applied to the line. In order to protect the line from failing under these forces and to reduce the requirement for a bulky, heavy line, a shock absorber is provided in the form of a block having one or more breakable web portions formed therein and through which the riser line is threaded. Upon deployment of the system into an airstream, the shock tension forces operate to fracture

some or all of the breakable web portions thereby dissipating the shock energy generated during deployment and protecting the riser line from failure. DTIC

N95-32421*# Texas Technological Univ., Lubbock, TX. Dept. of Mechanical Engineering.
CERTIFICATION OF A HYBRID PARAMETER MODEL OF THE FULLY FLEXIBLE SHUTTLE REMOTE MANIPULATOR SYSTEM Final Report
Alan A. Barhorst *In* NASA. Johnson Space Center, National Aeronautics and Space Administration (NASA)/American Society for Engineering Education (ASEE) Summer Faculty Fellowship Program, 1994, Volume 1 Jul. 1995 10 p (For primary document see N95-32418 12-99)
(Grant NGT-44-005-803)
Avail: CASI HC A02/MF A03

38 QUALITY ASSURANCE AND RELIABILITY

Includes product sampling procedures and techniques; and quality control.

N95-33209*# National Aeronautics and Space Administration. Lewis Research Center, Cleveland, OH.
THERMOGRAPHIC IMAGING FOR HIGH-TEMPERATURE COMPOSITE MATERIALS: A DEFECT DETECTION STUDY
Don J. Roth, James R. Bodis (Cleveland State Univ., OH.), and Chip Bishop (Bales Scientific, Inc., Walnut Creek, CA.) Jun. 1995 26 p
(RTOP 505-63-12)
(NASA-TM-106950; E-9688; NAS 1.15:106950) Avail: CASI HC A03/MF A01

The ability of a thermographic imaging technique for detecting flat-bottom hole defects of various diameters and depths was evaluated in four composite systems (two types of ceramic matrix composites, one metal matrix composite, and one polymer matrix composite) of interest as high-temperature structural materials. The holes ranged from 1 to 13 mm in diameter and 0.1 to 2.5 mm in depth in samples approximately 2-3 mm thick. The thermographic imaging system utilized a scanning mirror optical system and infrared (IR) focusing lens in conjunction with a mercury cadmium telluride infrared detector element to obtain high resolution infrared images. High intensity flash lamps located on the same side as the infrared camera were used to heat the samples. After heating, up to 30 images were sequentially acquired at 70-150 msec intervals. Limits of detectability based on depth and diameter of the flat-bottom holes were defined for each composite material. Ultrasonic and radiographic images of the samples were obtained and compared with the thermographic images. Author (revised)

N95-34346# Nondestructive Testing Information Analysis Center, San Antonio, TX.
MICROWAVE NONDESTRUCTIVE EVALUATION: STATE-OF-THE-ART REVIEW
R. Zoughi and S. Ganchev Feb. 1995 178 p
(Contract DLA900-90-D-0123)
(AD-A294388; NTIAC-95-01) Avail: CASI HC A09/MF A02

This State-of-the-Art Review contains information on both the fundamental science and general applications of microwave nondestructive evaluation. Chapter contents include: introductory background on microwave and millimeter wave spectra, definition and scope of microwave NDE, dielectric properties of materials, material characterization using microwaves, thickness and disbond measurements, microwave techniques for surface cracks, defect detection in thick composites, and concluding remarks and the future of microwave NDE. The publication contains 553 references to microwave NDE-related papers in the public literature. DTIC

39 STRUCTURAL MECHANICS

Includes structural element design and weight analysis; fatigue; and thermal stress.

For applications see *05 Aircraft Design, Testing and Performance* and *18 Spacecraft Design, Testing and Performance.*

N95-32373# Westinghouse Savannah River Co., Aiken, SC.
ANALYTICAL MODELING OF THE EFFECT OF CRACK DEPTH, SPECIMEN SIZE, AND BIAXIAL STRESS ON THE FRACTURE TOUGHNESS OF REACTOR VESSEL STEELS
Yuh-Jin Chao (South Carolina Univ., Columbia, SC.) and Poh-Sang Lam 1995 19 p Presented at the Joint ASME/JSME Pressure Vessels and Piping Conference, Honolulu, HI, 23-27 Jul. 1995
(Contract DE-AC09-89SR-18035)
(DE95-005886; WSRC-MS-94-0463; CONF-950740-5) Avail: CASI HC A03/MF A01

Fracture, toughness values for A533-B reactor pressure vessel (RPV) steel obtained from test programs at Oak Ridge National Laboratory (ORNL) and University of Kansas (KU) are interpreted using the J-A(sub 2) analytical model. The analytical model is based on the critical stress concept and takes into consideration the constraint effect using the second parameter A(sub 2) in addition to the generally accepted first parameter J which represents the loading level. It is demonstrated that with the constraint level included in the model effects of crack depth (shallow vs deep), specimen size (small vs. large), and loading type (uniaxial vs biaxial) on the fracture toughness from the test programs can be interpreted and predicted. DOE

N95-32381# Sandia National Labs., Albuquerque, NM.
THE ROLE OF DYNAMIC EXPERIMENTATION FOR COMPUTATION ANALYSIS
L. C. Chhabildas and T. G. Trucano 1995 7 p Presented at the International Conference on Computational Engineering Science, Mauna Lani, HI, 30 Jul. - 3 Aug. 1995
(Contract DE-AC04-94AL-85000)
(DE95-007733; SAND-95-0284C; CONF-950788-3) Avail: CASI HC A02/MF A01

In this paper a brief description of dynamic techniques commonly available for determining material property studies is presented. For many impact applications, the material generally experiences a complex loading path. In most cases, the initial loading conditions can be represented by the shock commonly referred to as the Hugoniot state. Subsequent loading or release structure, i.e., off-Hugoniot states would however be dependent on the physical processes dominating the material behavior. The credibility of the material model is tested by the accuracy of predictions of off-Hugoniot states. Experimental techniques commonly used to determine off-Hugoniot states are discussed in this survey. DOE

N95-32385# Los Alamos National Lab., NM.
DUCTILE DAMAGE MODEL WITH VOID COALESCENCE
D. L. Tonks 1995 5 p Presented at the Plasticity and Its Current Applications Symposium, Osaka, Japan, 17-21 Jul. 1995
(Contract W-7405-eng-36)
(DE95-007855; LA-UR-95-619; CONF-9507100-2) Avail: CASI HC A01/MF A01

A general model for ductile damage in metals is presented. It includes damage induced by shear stress as well as damage caused by volumetric tension. Spallation is included as a special case. Strain induced damage is also treated. Void nucleation and growth are included and give rise to strain rate effects. Strain rate effects also arise in the model through elastic release wave propagation between damage centers. Underlying physics of the model is the nucleation, growth, and coalescence of voids in a plastically flowing solid. Implementation of the model in hydrocodes is discussed. DOE

N95-32392# Brookhaven National Lab., Upton, NY.
CYLINDRICAL SHELL BUCKLING THROUGH STRAIN HARDENING
K. Bandyopadhyay, J. Xu, S. Shteyngart, and D. Gupta (Department of Energy, Germantown, MD.) 1995 5 p Presented at the Joint ASME/JSME Pressure Vessels and Piping Conference, Honolulu, HI, 23-27 Jul. 1995

(Contract DE-AC02-76CH-00016)
(DE95-009545; BNL-61540; CONF-950740-25) Avail: CASI HC A01/MF A01

Recently, the authors published results of plastic buckling analysis of cylindrical shells. Ideal elastic-plastic material behavior was used for the analysis. Subsequently, the buckling analysis program was continued with the realistic stress-strain relationship of a stainless steel alloy which does not exhibit a clear yield point. The plastic buckling analysis was carried out through the initial stages of strain hardening for various internal pressure values. The computer program BOSOR5 was used for this purpose. Results were compared with those obtained from the idealized elastic-plastic relationship using the offset stress level at 0.2% strain as the yield stress. For moderate hoop stress values, the realistic stress-grain case shows a slight reduction of the buckling strength. But, a substantial gain in the buckling strength is observed as the hoop stress approaches the yield strength. Most importantly, the shell retains a residual strength to carry a small amount of axial compressive load even when the hoop stress has exceeded the offset yield strength. DOE

N95-32670# Sandia National Labs., Albuquerque, NM.
EVALUATION OF A BRIDGE USING SIMPLIFIED ELEMENT MODELING
C. R. Farrar (Los Alamos National Lab., NM.) and T. A. Duffey (New Mexico Highlands Univ., Las Vegas, NM.) 1995 7 p Presented at the International Association for Bridge and Structural Engineering Symposium, San Francisco, CA, 23-25 Aug. 1995
(Contract W-7405-eng-36)
(DE95-006281; LA-UR-95-320; CONF-950878-1) Avail: CASI HC A02/MF A01

An experimental-numerical comparison of the forced and ambient vibrations Of a multi-span composite plate-girder bridge was performed. The bridge was modeled using a finite element program at three levels of complexity, including a simple 250 DOF model that utilizes a single beam element to represent the entire bridge cross section. Difficulties encountered in the development of the simple model are discussed. The dynamic properties predicted by the simple model were consistent with these measured on the bridge and computed using more detailed finite element models. DOE

N95-32684# Oak Ridge National Lab., TN.
FRACTURE BEHAVIOR OF SHALLOW CRACKS IN FULL-THICKNESS CLAD BEAMS FROM AN RPV WALL SECTION
J. A. Keeney, B. R. Bass, and W. J. McAfee 1995 7 p Presented at the 13th International Conference on Structural Mechanics in Reactor Technology, Porto Alegre, Brazil, 13-18 Aug. 1995
(Contract DE-AC05-84OR-21400)
(DE95-009175; CONF-950804-2) Avail: CASI HC A02/MF A01

A testing program is described that utilizes full-thickness clad beam specimens to quantify fracture toughness for shallow cracks in weld material for which metallurgical conditions are prototypic of those found in reactor pressure vessels (RPV's). The beam specimens are fabricated from an RPV shell segment that includes weld, plate and clad material. Metallurgical factors potentially influencing fracture toughness for shallow cracks in the beam specimens include material gradients and material inhomogeneities in welded regions. The shallow-crack clad beam specimens showed a significant loss of constraint similar to that of other shallow-crack single-edge notch bend (SENB) specimens. The stress-based Dodds-Anderson scaling model appears to be effective in adjusting the test data to account for in-plane loss of constraint for uniaxially tested beams, but cannot predict the observed effects of out-of-plane biaxial loading on shallow-crack fracture toughness. A strain-based dual-parameter fracture toughness correlation (based on plastic zone width) performed acceptably when applied to the uniaxial and biaxial shallow-crack fracture toughness data. DOE

N95-32920 Rutgers - The State Univ., New Brunswick, NJ.
MODAL IDENTIFICATION AND ITS APPLICATIONS TO DAMAGE DETECTION IN VIBRATING STRUCTURES Ph.D. Thesis
Santosh Ratan 1994 169 p
Avail: Univ. Microfilms Order No. DA9421828

The present research is concerned with the development and application of identification of various parameters in a vibrating structure. The various applications of the identification procedures include modification in the modeling of a structure, detecting damages, and knowing a boundary condition in a given structure. This is achieved in two steps: identification of the eigensolution, and using the identified eigensolution to detect cracks and other parameters. The first step is based on the scheme developed by Baruh, Khatri, and Boka. This scheme uses a transient vibration response and the knowledge of the mass properties of the system. The scheme is applied to an experimental data set and it is found that the analytical model of the structure was very close to exact, but a small correction was required. A new concept called 'residue' is introduced to detect cracks in a vibrating structure. Residue is based on the modeled mass and stiffness matrix and the identified eigenvalues and eigenvectors of the structure. This method is successfully applied to a truss structure. A modified definition of 'residue' is proposed for the application of crack detection in a rotating system. This modification is necessary as an extra gyroscopic effect is associated with a rotating system. The modified method is used to detect a crack in rotors. In some practical cases, it is unavoidable that the system's mass properties are incorrectly known. In such situations the crack detection scheme and identification of stiffness properties can be erroneous. To combat this situation a new scheme to identify mass parameters is introduced. This scheme uses approximate mass properties of the system and the identified eigenvalues and eigenvectors of the system. The known mass parameters act as constraints in the identification procedure. Hence, an iterative method is resulted. The method, in conjunction with known constraints, can identify the mass parameters with high accuracy. Finally, these developed methods are applied to more general cases where more than one property of the system are unknown or wrongly known. To handle a general case, a sequential identification scheme is developed where one or more of the identification schemes developed are used in a sequence. This sequence is not known a priori, and depends on the outcome of each step. Several examples are solved in this dissertation to illustrate the ideas and validate the various propositions. Dissert. Abstr.

N95-33068 Lawrence Livermore National Lab., Livermore, CA.
A STUDY OF THE EFFECT OF GRAIN SIZE ON THE BALLISTIC PERFORMANCE OF SILICON CARBIDE
Carl F. Cline Mar. 1995 10 p Presented at the 15th International Symposium on Ballistics, Jerusalem, Israel, 21-24 May 1995 Limited Reproducibility: More than 20% of this document may be affected by microfiche quality
(Contract W-7405-eng-48)
(DE95-011724; UCRL-JC-118421; CONF-950537-5) Avail: CASI HC A02/MF A01

The depth of penetration method was used to ballistically evaluate the performance of silicon carbide as a function of grain size. The hot-pressed silicon carbide was backed by 4340 steel Rc = 35 and impacted by tungsten heavy metal projectiles of L/D = 4 at velocities of 1.6 and 1.75 km/s. The hot-pressed silicon carbide was also compared with reaction-sintered silicon carbide of identical thickness in the current study. Results are compared with data previously reported by others. DOE

N95-33222# Oak Ridge National Lab., TN. Computer Science and Mathematics Div.
ON THE EXPANSION FOR SURFACE DISPLACEMENT IN THE NEIGHBORHOOD OF A CRACK TIP
L. J. Gray and Glaucio H. Paulino (Cornell Univ., Ithaca, NY.) 1995 7 p Presented at the IABEM 1995: International Symposium on Boundary Element Methods, HI, Jul. 1995
(Contract DE-AC05-84OR-21400)
(DE95-012890; CONF-9507128-1) Avail: CASI HC A02/MF A01

It is shown that in the expansion of the crack opening displacement vs distance from the tip, there is no linear term present. This should lead to improved accuracy of the near tip fields and improved stress intensity factor results. The two-dimensional discussion should be able to be carried over to three dimensions. DOE

N95-33253 Oklahoma Univ., Norman, OK.
EXPERIMENTAL INVESTIGATION OF THE SEPARATION OF TEXTURE AND RESIDUAL STRESS INDUCED ANISOTROPY VIA OBLIQUE INCIDENCE ACOUSTOELASTICITY Ph.D. Thesis
Xiang Zhao 1994 136 p
Avail: Univ. Microfilms Order No. DA9422788

The separation of the residual stress effect from the texture-induced intrinsic anisotropy in polycrystalline metals is a major concern in the use

of acousto-elasticity today. In this study, an analytical solution to discriminate the anisotropy in the velocity of ultrasonic wave introduced by residual stresses from those induced by rolling texture via a set of quasi-transverse (QSV) wave velocity measurements using the ultrasonic oblique incidence pulse-echo technique is experimentally investigated. Ultrasonic experiments are performed on aluminum alloy specimens and, with the aid of the least squares technique, the measurements are used by the solution to determine the principal strains caused by residual stresses and the lowest three coefficients of the orientation distribution function. The results show that the ultrasonic measurements are reliable, the characteristics of the changes in velocity caused by residual stresses are consistent with the findings of other experimental work, the constructed ultrasonic pole figures present a satisfactory description of rolling texture, and the correspondence in gross texture with the conventional X-ray pole figures is comparatively good for the aluminum alloy tested. A certain effort is also put on the further development and supplement of the theory of oblique-incidence acousto-elasticity. First, it is proven that with the measured time delay from an oblique incidence measurement, an exact calculation of the phase velocity of the elastic wave propagating in anisotropic media can be obtained. Also, with a sensitivity analysis on the effect of the averaging methods for the determination of aggregate elastic moduli, a new type of averaging method is suggested for polycrystalline metals. Finally, a numerical simulation is conducted to investigate the effect of specimen thickness measurement and it is concluded that a very high degree of measuring accuracy of thickness is not necessary for the solution used in this study.

Dissert. Abstr.

N95-33695 Pennsylvania State Univ., University Park, PA.

CUBIC-B-SPLINE BOUNDARY ELEMENTS FOR TWO-DIMENSIONAL AND AXISYMMETRIC ELASTOSTATICS Ph.D. Thesis

Mounir Blibeche 1993 177 p

Avail: Univ. Microfilms Order No. DA9414244

The purpose of the present work is to develop a new cubic-B-spline boundary element formulation based on a synthesis of existing cubic-B-spline and boundary element method formulations. The proposed formulation is valid for the solution of two-dimensional and axisymmetric elastostatic problems. A new integration technique based on separating singular and non-singular terms in boundary element integrals is also presented. A self-adaptive coordinate transformation of order 2 is used to remove the singularity in the singular terms. Six-point standard Gauss quadrature is used for non-singular integration. The proposed method is implemented in a computer program, BEMCBS, and results are compared to those of the BEASY commercial program using quadratic elements based on piecewise polynomial shape functions, for several numerical examples. Numerical results for two-dimensional and axisymmetric elasticity reveal that cubic-B-spline boundary elements yield sufficient accuracy of less than 5.0 percent relative error for a smaller number of boundary points than quadratic boundary elements based on piecewise polynomials. In addition, cubic-B-splines a yield smooth representation of geometry and problem variables due to their inherit continuity. Even though the present algorithm is limited to static loadings and surface boundary conditions with no body forces, it is well-suited for homogeneous and isotropic media, finite and infinite regions, far-field stresses, and single or multiple boundary domains.

Dissert. Abstr.

N95-33833# Pacific Northwest Lab., Richland, WA.

IMPLICATIONS OF EARLY STAGES IN THE GROWTH OF STRESS CORROSION CRACKING ON COMPONENT RELIABILITY

R. H. Jones and E. P. Simonen Apr. 1995 16 p Presented at the Research Assistant Task Force Conference, Charlotte, NC, 11-13 Apr. 1995

(Contract DE-AC06-76RL-01830)

(DE95-011498; PNL-SA-26120; CONF-9504156-1) Avail: CASI HC A03/MF A01

Environment-induced crack growth generally progresses through several stages prior to component failure. Crack initiation, short crack growth, and stage 1 growth are early stages in crack development that are summarized in this paper. The implications of these stages on component reliability, derive from the extended time that the crack exists in the early stages because crack velocity is slow. The duration of the early stages provides a greater opportunity for corrective action if cracks can be detected. Several important factors about the value of understanding short crack behavior include: (1) life prediction requires a knowledge of the total life cycle of the crack including the early stages; (2) greater reliability is possible if the transition between short and long crack behavior is known component life after this transition is short; and (3) remedial actions are more effective for short than long cracks.

DOE

N95-34427 Department of the Navy, Washington, DC.

DEVICE FOR DAMPENING VIBRATORY MOTION Patent

Chahee P. Cho, inventor (to Navy) and John Y. Hung, inventor (to Navy) 28 Feb. 1995 9 p Filed 6 Oct. 1993

(AD-D017490; US-Patent-5,392,881; US-Patent-Appl-SN-134191; US-Patent-Class-188-267) Avail: US Patent and Trademark Office

There is presented a device for dampening vibratory motion. The device comprises a ferromagnetic housing, a non-magnetic, electrically conductive wall upstanding in the housing, and a plunger assembly. The plunger assembly includes a magnetic body movable in the housing adjacent the wall, and connector structure extending from the body and in communication with a vibratory energy source.

DTIC

N95-34442# Oak Ridge National Lab., TN.

PATTERNS AND PERSPECTIVES IN APPLIED FRACTURE MECHANICS

John G. Merkle, Walter G. Reuter, ed., John H. Underwood, ed., and James C. Newman, Jr., ed. 1994 39 p Presented at the 26th National Symposium on Fracture Mechanics, Idaho Falls, ID, 28-30 Jun. 1994

(Contract DE-AC05-84OR-21400)

(DE95-012844; CONF-9406335-1) Avail: CASI HC A03/MF A01

This lecture begins with a overview of applied fracture mechanics pertinent to safety of pressure vessels. It then progresses to a chronological panorama of experimental and analytical results. To be useful and dependable in safety analysis of real structures, new analysis developments must be physically realistic, which means that they must accurately describe physical cause and effect. Consequently, before mathematical modeling can begin, cause and effect must be established from experimental data. This can be difficult and time consuming, but worth the effort. Accordingly, the theme of this paper is that the search for patterns is constant and vital. This theme is illustrated by the development of small, single-specimen, fracture toughness testing techniques. It is also illustrated by the development, based on two different published large-strain, elastic-plastic, three-dimensional finite-element analyses, of a hypothesis concerning three-dimensional loss of constraint. When a generalization of Irwin's thickness-normalized plastic-zone parameter reaches a value close to 2 pi, the through-thickness contraction strain at the apex of the near-tip logarithmic-spiral slip-line region becomes the dominant negative strain accommodating crack opening. Because slip lines passing from the midplane to the stress-free side surfaces do not have to curve, once these slip lines are established, stresses near the crack tip are only elevated by strain hardening and constraint becomes significantly relaxed. This hypothesis, based on published three-dimensional elastic-plastic analyses, provides a potentially valuable means for gaining additional insight into constraint effects on fracture toughness by considering the roles played by the plastic strains as well as the stresses that develop near a crack tip.

DOE

N95-32420*# Louisiana Tech Univ., Ruston, LA. Dept. of Civil Engineering.

APPLICATION OF IMPACT DAMPERS IN VIBRATION CONTROL OF FLEXIBLE STRUCTURES Final Report

Fred A. Akl and Aamir S. Butt *In* NASA. Johnson Space Center, National Aeronautics and Space Administration (NASA)/American Society for Engineering Education (ASEE) Summer Faculty Fellowship Program, 1994, Volume 1 Jul. 1995 15 p (For primary document see N95-32418 12-99)

(Grant NGT-44-005-803)

Avail: CASI HC A03/MF A03

N95-32993# Osaka Univ., Osaka (Japan). Dept. of Architectural Engineering.

INELASTIC RESPONSE SPECTRA OF A SYSTEM WITH BILINEAR RESTORING CHARACTERISTICS: EFFECT OF PLASTIC-STIFFNESS RATIO

Woontaek Woo and Yutaka Inoue *In its* Technology Reports of the

Osaka Univ., Vol. 45, Nos. 2205-2216 15 Apr. 1995 p 65-73 (For primary document see N95-32984 12-31)
(Rept-2213) Avail: CASI HC A02/MF A02

42 GEOSCIENCES (GENERAL)

N95-33730*# Jet Propulsion Lab., California Inst. of Tech., Pasadena, CA.
SUMMARIES OF THE FIFTH ANNUAL JPL AIRBORNE EARTH SCIENCE WORKSHOP. VOLUME 1: AVIRIS WORKSHOP
Robert O. Green, ed. 23 Jan. 1995 170 p Workshop held in Pasadena, CA, 23-26 Jan. 1995 Contains 35mm color slides as supplement
(Contract NAS7-1260; RTOP 655-81-00)
(NASA-CR-198922; JPL-Publ-95-1-Vol-1; NAS 1.26:198922) Avail: CASI HC A08/MF A02

This publication is the first of three containing summaries for the Fifth Annual JPL Airborne Earth Science Workshop, held in Pasadena, California, on January 23-26, 1995. The main workshop is divided into three smaller workshops as follows: (1) The Airborne Visible/Infrared Imaging Spectrometer (AVIRIS) workshop, on January 23-24. The summaries for this workshop appear in this volume; (2) The Airborne Synthetic Aperture Radar (AIRSAR) workshop, on January 25-26. The summaries for this workshop appear in Volume 3; and (3) The Thermal Infrared Multispectral Scanner (TIMS) workshop, on January 26. The summaries for this workshop appear in Volume 2. For individual titles, see N95-33731 through N95-33773.

N95-33731*# New Hampshire Univ., Durham, NH. Complex Systems Research Center.
HIGH SPECTRAL RESOLUTION REMOTE SENSING OF CANOPY CHEMISTRY **c43**
John D. Aber and Mary E. Martin *In* JPL, Summaries of the Fifth Annual JPL Airborne Earth Science Workshop. Volume 1: AVIRIS Workshop 23 Jan. 1995 p 1-4 (For primary document see N95-33730 12-42)
Avail: CASI HC A01/MF A02

Near infrared laboratory spectra have been used for many years to determine nitrogen and lignin concentrations in plant materials. In recent years, similar high spectral resolution visible and infrared data have been available via airborne remote sensing instruments. Using data from NASA's Airborne visible/Infrared Imaging Spectrometer (AVIRIS) we attempt to identify spectral regions correlated with foliar chemistry at the canopy level in temperate forests. Author

N95-33732*# Phillips Lab., Hanscom AFB, MA.
MODTRAN3: AN UPDATE AND RECENT VALIDATIONS AGAINST AIRBORNE HIGH RESOLUTION INTERFEROMETER MEASUREMENTS **c43**
Gail P. Anderson, Jinxue Wang, and James H. Chetwynd *In* JPL, Summaries of the Fifth Annual JPL Airborne Earth Science Workshop. Volume 1: AVIRIS Workshop 23 Jan. 1995 p 5-8 (For primary document see N95-33730 12-42)
Avail: CASI HC A01/MF A02

MODTRAN, the Moderate Resolution Atmospheric Radiance and Transmittance Model, encompasses all the capabilities of LOWTRAN 7, the widely used 20 cm(exp -1) resolution radiance code, but incorporates a much more sensitive molecular band model with 2 cm(exp -1) resolution. MODTRAN contains many important elements that other band model based radiative transfer codes do not incorporate. It shares with FASCODE: spherical geometry, single and multiple scattering default atmospheric profile descriptors (gases, aerosols, clouds, fogs, and rain), and molecular continua (H2O, CO2, O3, O2, N2). In addition, it can calculate the solar/lunar direct and scattered radiation. MODTRAN3 was released to the general public in November 1994. It has several important features that the previous version, MODTRAN2, does not have. Chloro-fluorocarbon (CFC) and related heavy molecules (whose spectroscopic properties first appear on the HITRAN92 data base as temperature-dependent cross sections) have been incorporated into pseudo-band models, with provision for using both default and user supplied profiles. The addition of SO2 and O2 in the UV, along with upgraded ozone Chappuis bands in the visible is also part of MODTRAN3. An improved multiple scattering algorithm, the DIScrete Ordinate Radiative Transfer (DISORT) has also been incorporated into MODTRAN3. MODTRAN is very fast: simple timing runs of MODTRAN3 vs. FASCOD3 show an improvement of more than a factor of 100 for a typical 500 cm(exp -1) spectral interval and comparable vertical layering. Speed is an important consideration in heating/cooling rates calculations, where a large number of radiative transfer calculations are needed. The MODTRAN3 used in this study is based on HITRAN92, but as mentioned, above, it will be upgraded to HITRAN94 upon its release at the end of 1994. MODTRAN has been adopted by: some researchers in the AVIRIS program as one radiative transfer code to derive surface reflectance from AVIRIS measurements. The accuracy of the code is very important because any errors in the radiative transfer calculation will directly translate into errors in the derived surface reflectance. In this paper, the new solar irradiance calculated by Kurucz, which is adopted in MODTRAN3, will be presented. Recent validations of MODTRAN3 with airborne high resolution interferometer measurements over ocean will be discussed. Good agreement between model calculations and measurements was achieved. Author

N95-33733*# Hughes Danbury Optical Systems, Inc., CT.
CHARACTERISTICS OF THE HYDICE SENSOR Abstract Only **c35**
R. W. Basedow and E. Zalewski *In* JPL, Summaries of the Fifth Annual JPL Airborne Earth Science Workshop. Volume 1: AVIRIS Workshop 23 Jan. 1995 p 9 (For primary document see N95-33730 12-42)
Avail: CASI HC A01/MF A02

In 1992, in an effort to significantly improve knowledge in the field of hyperspectral imagery, the Naval Research Laboratories defined a set of requirements for a new generation sensor. Construction of this instrument, designated HYDICE, has recently been completed at Hughes Danbury Optical Systems. It is currently being flight tested on a Convair 580 operated by ERIM. This paper reports on some of the performance parameters measured to date. The majority of these are derived from laboratory test data. Optomechanical parameters include MTF, spatial co-registration, 'smile', spectral profile and spectral calibration. Detector-related parameters include system responsivity, signal to noise ratio, radiometric stability and gain linearity. The results are compared with the original system performance predictions. Author

N95-33734*# Colorado Univ., Boulder, CO. Center for the Study of Earth from Space.
QUANTITATIVE REMOTE SENSING OF AMMONIUM MINERALS, CEDAR MOUNTAINS, ESMERALDA COUNTY, NEVADA **c43**
William M. Baugh and Fred A. Kruse *In* JPL, Summaries of the Fifth Annual JPL Airborne Earth Science Workshop. Volume 1: AVIRIS Workshop 23 Jan. 1995 p 11-14 (For primary document see N95-33730 12-42)
Avail: CASI HC A01/MF A02

Mineral-bound ammonium (NH4+) was discovered by the U.S. Geological Survey in the southern Cedar Mountains of Esmeralda County, Nevada in 1989. At 10 km in length, this site is 100 times larger than any previously known occurrence in volcanic rocks. The ammonium occurs in two hydrothermally altered, crystal-rich rhyolitic tuff units of Oligocene age, and is both structurally and stratigraphically controlled. This research uses Advanced Visible/Infrared Imaging Spectrometer (AVIRIS) data to quantitatively map the mineral-bound ammonium (buddingtonite) concentration in the altered volcanic rocks. Naturally occurring mineral-bound ammonium is fairly rare; however, it has been found to occur in gold-bearing hydrothermal deposits. Because of this association, it is thought that ammonium may be a useful too in exploration for gold and other metal deposits. Mineral-bound ammonium is produced when an ammonium ion (NH4+) replaces the alkali cation site (usually K+) in the crystal structure of silicate minerals such as feldspars, micas and clays. Buddingtonite is an ammonium feldspar. The ammonium originates in buried organic plant matter and is transported to the host rock by hydrothermal fluids. Ammonium alteration does not produce visible changes in the rock, and it is barely detectable with standard x-ray diffraction methods. It is clearly identified, however, by absorption features in short wave-infrared (SWIR) wavelengths (2.0 - 2.5 micrometers). The ammonium absorption features are believed to be caused by N-H vibrational modes and are analogous to hydroxyl (O-H) vibrational modes, only shifted slightly in wavelength. Buddingtonite absorption features in the near- and SWIR lie at 1.56, 2.02 and 2.12

micrometers. The feature at 2.12 micrometer is the strongest of the three and is the only one used in this study. The southern Cedar Mountains are sparsely vegetated and are an ideal site for a remote sensing study.
Author

N95-33735*# Consiglio Nazionale delle Ricerche, Rome (Italy).
CNR LARA PROJECT, ITALY: AIRBORNE LABORATORY FOR ENVIRONMENTAL RESEARCH **c45**
R. Bianchi, R. M. Cavalli, L. Fiumi, C. M. Marino, and S. Pignatti *In* JPL, Summaries of the Fifth Annual JPL Airborne Earth Science Workshop. Volume 1: AVIRIS Workshop 23 Jan. 1995 p 15-18 (For primary document see N95-33730 12-42)
Avail: CASI HC A01/MF A02

The increasing interest for the environmental problems and the study of the impact on the environment due to antropic activity produced an enhancement of remote sensing applications. The Italian National Research Council (CNR) established a new laboratory for airborne hyperspectral imaging, the LARA Project (Laboratorio Aero per Ricerche Ambientali - Airborne Laboratory for Environmental Research), equipping its airborne laboratory, a CASA-212, mainly with the Daedalus AA5000 MIVIS (Multispectral Infrared and Visible Imaging Spectrometer) instrument. MIVIS's channels, spectral bandwidths, and locations are chosen to meet the needs of scientific research for advanced applications of remote sensing data. MIVIS can make significant contributions to solving problems in many diverse areas such as geologic exploration, land use studies, mineralogy, agricultural crop studies, energy loss analysis, pollution assessment, volcanology, forest fire management and others. The broad spectral range and the many discrete narrow channels of MIVIS provide a fine quantization of spectral information that permits accurate definition of absorption features from a variety of materials, allowing the extraction of chemical and physical information of our environment. The availability of such a hyperspectral imager, that will operate mainly in the Mediterranean area, at the present represents a unique opportunity for those who are involved in environmental studies and land-management to collect systematically large-scale and high spectral-spatial resolution data of this part of the world. Nevertheless, MIVIS deployments will touch other parts of the world, where a major interest from the international scientific community is present. Author

N95-33736*# Colorado Univ., Boulder, CO. Center for the Study of Earth from Space.
USING DARK CURRENT DATA TO ESTIMATE AVIRIS NOISE COVARIANCE AND IMPROVE SPECTRAL ANALYSES **c43**
Joseph W. Boardman *In* JPL, Summaries of the Fifth Annual JPL Airborne Earth Science Workshop. Volume 1: AVIRIS Workshop 23 Jan. 1995 p 19-22 (For primary document see N95-33730 12-42)
Avail: CASI HC A01/MF A02

Starting in 1994, all AVIRIS data distributions include a new product useful for quantification and modeling of the noise in the reported radiance data. The 'postcal' file contains approximately 100 lines of dark current data collected at the end of each data acquisition run. In essence this is a regular spectral-image cube, with 614 samples, 100 lines and 224 channels, collected with a closed shutter. Since there is no incident radiance signal, the recorded DN measure only the DC signal level and the noise in the system. Similar dark current measurements, made at the end of each line are used, with a 100 line moving average, to remove the DC signal offset. Therefore, the pixel-by-pixel fluctuations about the mean of this dark current image provide an excellent model for the additive noise that is present in AVIRIS reported radiance data. The 61,400 dark current spectra can be used to calculate the noise levels in each channel and the noise covariance matrix. Both of these noise parameters should be used to improve spectral processing techniques. Some processing techniques, such as spectral curve fitting, will benefit from a robust estimate of the channel-dependent noise levels. Other techniques, such as automated unmixing and classification, will be improved by the stable and scene-independence noise covariance estimate. Future imaging spectrometry systems should have a similar ability to record dark current data, permitting this noise characterization and modeling. Author

N95-33737*# Jet Propulsion Lab., California Inst. of Tech., Pasadena, CA.
MAPPING TARGET SIGNATURES VIA PARTIAL UNMIXING OF AVIRIS DATA **c43**
Joseph W. Boardman (Colorado Univ., Boulder, CO.), Fred A. Kruse (Colorado Univ., Boulder, CO.), and Robert O. Green *In its* Summaries of the Fifth Annual JPL Airborne Earth Science Workshop. Volume 1: AVIRIS Workshop 23 Jan. 1995 p 23-26 (For primary document see N95-33730 12-42)
Avail: CASI HC A01/MF A02

A complete spectral unmixing of a complicated AVIRIS scene may not always be possible or even desired. High quality data of spectrally complex areas are very high dimensional and are consequently difficult to fully unravel. Partial unmixing provides a method of solving only that fraction of the data inversion problem that directly relates to the specific goals of the investigation. Many applications of imaging spectrometry can be cast in the form of the following question: 'Are my target signatures present in the scene, and if so, how much of each target material is present in each pixel?' This is a partial unmixing problem. The number of unmixing endmembers is one greater than the number of spectrally defined target materials. The one additional endmember can be thought of as the composite of all the other scene materials, or 'everything else'. Several workers have proposed partial unmixing schemes for imaging spectrometry data, but each has significant limitations for operational application. The low probability detection methods described by Farrand and Harsanyi and the foreground-background method of Smith et al are both examples of such partial unmixing strategies. The new method presented here builds on these innovative analysis concepts, combining their different positive attributes while attempting to circumvent their limitations. This new method partially unmixes AVIRIS data, mapping apparent target abundances, in the presence of an arbitrary and unknown spectrally mixed background. It permits the target materials to be present in abundances that drive significant portions of the scene covariance. Furthermore it does not require a priori knowledge of the background material spectral signatures. The challenge is to find the proper projection of the data that hides the background variance while simultaneously maximizing the variance amongst the targets. Author

N95-33738*# MacDonald, Dettwiler and Associates Ltd., Richmond (British Columbia).
COMBINED HYPERSPATIAL AND HYPERSPECTRAL IMAGING SPECTROMETER CONCEPT **c43**
Ian Burke and Harold Zwick *In* JPL, Summaries of the Fifth Annual JPL Airborne Earth Science Workshop. Volume 1: AVIRIS Workshop 23 Jan. 1995 p 27-30 (For primary document see N95-33730 12-42)
Avail: CASI HC A01/MF A02

There is a user need for increasing spatial and spectral resolution in Earth Observation (EO) optical instrumentation. Higher spectral resolution will be achieved by the introduction of spaceborne imaging spectrometers. Higher spatial resolutions of 1 - 3m will be achieved also, but at the expense of sensor redesign, higher communications bandwidth, high data processing volumes, and therefore, at the risk of time delays due to large volume data-handling bottlenecks. This paper discusses a design concept whereby the hyperspectral properties of a spaceborne imaging spectrometer can be used to increase the image spatial resolution, without such adverse cost impact. Author

N95-33739*# Jet Propulsion Lab., California Inst. of Tech., Pasadena, CA.
AIRBORNE VISIBLE/INFRARED IMAGING SPECTROMETER (AVIRIS) ONBOARD CALIBRATION SYSTEM **c35**
Thomas G. Chrien, Mike Eastwood, Robert O. Green, Charles Sarture, Howell Johnson, Chris Chovit, and Pavel Hajek *In its* Summaries of the Fifth Annual JPL Airborne Earth Science Workshop. Volume 1: AVIRIS Workshop 23 Jan. 1995 p 31-32 (For primary document see N95-33730 12-42)
Avail: CASI HC A01/MF A02

The AVIRIS instrument uses an onboard calibration system to provide auxiliary calibration data. The system consist of a tungsten halogen cycle lamp imaged onto a fiber bundle through an eight position filter wheel. The fiber bundle illuminates the back side of the foreoptics shutter during a pre-run and post-run calibration sequence. The filter wheel contains two neutral density filters, five spectral filters and one blocked position. This paper reviews the general workings of the onboard calibrator system and discusses recent modifications. Author

N95-33740*# Jet Propulsion Lab., California Inst. of Tech., Pasadena, CA.

NEW CALIBRATION TECHNIQUES FOR THE AIRBORNE VISIBLE/INFRARED IMAGING SPECTROMETER (AVIRIS) **c35**

Thomas G. Chrien, Robert O. Green, Chris Chovit, Mike Eastwood, Jessica Faust, Pavel Hajek, Howell Johnson, H. Ian Novack, and Charles Sarture *In its* Summaries of the Fifth Annual JPL Airborne Earth Science Workshop. Volume 1: AVIRIS Workshop 23 Jan. 1995 p 33-34 (For primary document see N95-33730 12-42)

Avail: CASI HC A01/MF A02

Recent laboratory calibrations of the Airborne Visible/Infrared Imaging Spectrometer (AVIRIS) include new methods for the characterization of the geometric, spectral, temporal and radiometric properties of the sensor. New techniques are desired in order to: (1) increase measurement accuracy and precision, (2) minimize measurement time and expense, (3) prototype new field and inflight calibration systems, (4) resolve measurement ambiguities, and (5) add new measurement dimensions. One of the common features of these new methods is the use of the full data collection and processing power of the AVIRIS instrument and data facility. This allows the collection of large amounts of calibration data in a short period of time and is well suited to modular data analysis routines. Author

N95-33741*# Geological Survey, Denver, CO.

INITIAL VEGETATION SPECIES AND SENESCIENCE/STRESS INDICATOR MAPPING IN THE SAN LUIS VALLEY, COLORADO USING IMAGING SPECTROMETER DATA **c43**

Roger N. Clark, Trude V. V. King, Cathy Ager, and Gregg A. Swayze *In* JPL, Summaries of the Fifth Annual JPL Airborne Earth Science Workshop. Volume 1: AVIRIS Workshop 23 Jan. 1995 p 35-38 (For primary document see N95-33730 12-42)

Avail: CASI HC A01/MF A02

We analyzed AVIRIS data obtained over agricultural areas in the San Luis Valley of Colorado. The data were acquired on September 3, 1993. A combined method of radiative transfer modeling and ground calibration site reflectance was used to correct the flight data to surface reflectance. This method, called Radiative Transfer Ground Calibration, or RTGC, corrects for variable water vapor in the atmosphere and produces spectra free of artifacts with spectral channel to channel noise approaching the signal to noise of the raw data. The calibration site soil samples were obtained on the day of the overflight and measured on our laboratory spectrometer. The site was near the center of the AVIRIS scene and the spectra of the soil is spectrally bland, especially in the region of the chlorophyll absorption in the visible portion of the spectrum. The center of the scene is located at approximately 106 deg 03' longitude, 37 deg 23' latitude, and the scene covers about 92 square kilometers. This scene is one of 28 in the area for a general project to study the Summitville abandoned mine site, located in the mountains west of the San Luis Valley, and its effects on the surrounding environment. Author

N95-33742*# Geological Survey, Denver, CO.

MAPPING MINERALS, AMORPHOUS MATERIALS, ENVIRONMENTAL MATERIALS, VEGETATION, WATER, ICE AND SNOW, AND OTHER MATERIALS: THE USGS TRICORDER ALGORITHM **c43**

Roger N. Clark and Gregg A. Swayze *In* JPL, Summaries of the Fifth Annual JPL Airborne Earth Science Workshop. Volume 1: AVIRIS Workshop 23 Jan. 1995 p 39-40 (For primary document see N95-33730 12-42)

Avail: CASI HC A01/MF A02

One of the challenges of Imaging Spectroscopy is the identification, mapping and abundance determination of materials, whether mineral, vegetable, or liquid, given enough spectral range, spectral resolution, signal to noise, and spatial resolution. Many materials show diagnostic absorption features in the visual and near infrared region (0.4 to 2.5 micrometers) of the spectrum. This region is covered by the modern imaging spectrometers such as AVIRIS. The challenge is to identify the materials from absorption bands in their spectra, and determine what specific analyses must be done to derive particular parameters of interest, ranging from simply identifying its presence to deriving its abundance, or determining specific chemistry of the material. Recently, a new analysis algorithm was developed that uses a digital spectral library of known materials and a fast, modified-least-squares method of determining if a single spectral feature for a given material is present. Clark et al. made another advance in the mapping algorithm: simultaneously mapping multiple minerals using multiple spectral features. This was done by a modified-least-squares fit of spectral features, from data in a digital spectral library, to corresponding spectral features in the image data. This version has now been superseded by a more comprehensive spectral analysis system called Tricorder. Author

N95-33743*# Jet Propulsion Lab., California Inst. of Tech., Pasadena, CA.

CALIBRATION TO SURFACE REFLECTANCE OF TERRESTRIAL IMAGING SPECTROMETRY DATA: COMPARISON OF METHODS

Abstract Only **c43**

Roger N. Clark (Geological Survey, Denver, CO.), Gregg A. Swayze (Geological Survey, Denver, CO.), Kathy Heidebrecht (Colorado Univ., Boulder, CO.), Robert O. Green, and F. H. Goetz (Colorado Univ., Boulder, CO.) *In its* Summaries of the Fifth Annual JPL Airborne Earth Science Workshop. Volume 1: AVIRIS Workshop 23 Jan. 1995 p 41-42 (For primary document see N95-33730 12-42)

Avail: CASI HC A01/MF A02

Many algorithms for spectral analysis of imaging spectroscopy data of the Earth's surface require that the data be calibrated to surface reflectance. Calibration requires removing instrumental response, solar irradiance, atmospheric transmittance, and atmospheric scattering from the radiance detected at the sensor. Depending on the amount of support data, this can be a formidable task. This paper examines four methods of calibration: (1) a radiative transfer model from the University of Colorado (ATREM: Gao and Goetz, 1990; Gao et al., 1992), (2) a MODTRAN-based method developed at the Jet Propulsion Lab by Green et al., (1191), (3) a ground calibration using known sites as standards, and (4) a combined approach using radiative transfer methods and ground calibration. Data from the Airborne Visual and Infra-Red Imaging Spectrometer (AVIRIS) instrument were evaluated from data sets obtained over multiple years and multiple sites. Author

N95-33744*# Southampton Univ. (England). Dept. of Geography.

CAUSAL CORRELATION OF FOLIAR BIOCHEMICAL CONCENTRATIONS WITH AVIRIS SPECTRA USING FORCED ENTRY LINEAR REGRESSION **c43**

Terence P. Dawson, Paul J. Curran, and John A. Kupiec *In* JPL, Summaries of the Fifth Annual JPL Airborne Earth Science Workshop. Volume 1: AVIRIS Workshop 23 Jan. 1995 p 43-46 (For primary document see N95-33730 12-42)

Avail: CASI HC A01/MF A02

A major goal of airborne imaging spectrometry is to estimate the biochemical composition of vegetation canopies from reflectance spectra. Remotely-sensed estimates of foliar biochemical concentrations of forests would provide valuable indicators of ecosystem function at regional and eventually global scales. Empirical research has shown a relationship exists between the amount of radiation reflected from absorption features and the concentration of given biochemicals in leaves and canopies (Matson et al., 1994, Johnson et al., 1994). A technique commonly used to determine which wavelengths have the strongest correlation with the biochemical of interest is unguided (stepwise) multiple regression. Wavelengths are entered into a multivariate regression equation, in their order of importance, each contributing to the reduction of the variance in the measured biochemical concentration. A significant problem with the use of stepwise regression for determining the correlation between biochemical concentration and spectra is that of 'overfitting' as there are significantly more wavebands than biochemical measurements. This could result in the selection of wavebands which may be more accurately attributable to noise or canopy effects. In addition, there is a real problem of collinearity in that the individual biochemical concentrations may covary. A strong correlation between the reflectance at a given wavelength and the concentration of a biochemical of interest, therefore, may be due to the effect of another biochemical which is closely related. Furthermore, it is not always possible to account for potentially suitable waveband omissions in the stepwise selection procedure. This concern about the suitability of stepwise regression has been identified and acknowledged in a number of recent studies (Wessman et al., 1988, Curran, 1989, Curran et al., 1992, Peterson and Hubbard, 1992, Martine and Aber, 1994, Kupiec, 1994). These studies have pointed to the lack of a physical link between wavelengths chosen by stepwise regression and the biochemical of interest, and this in turn has cast doubts on the use of imaging spectrometry for the estimation of

foliar biochemical concentrations at sites distant from the training sites. To investigate this problem, an analysis was conducted on the variation in canopy biochemical concentrations and reflectance spectra using forced entry linear regression. Author

N95-33745*# Science Applications International Corp., McLean, VA.
MINERALOGIC VARIATIONS IN FLUVIAL SEDIMENTS CONTAMINATED BY MINE TAILINGS AS DETERMINED FROM AVIRIS DATA, COEUR D'ALENE RIVER VALLEY, IDAHO **c43**
W. H. Farrand and Joseph C. Harsanyi (Applied Signal and Image Technology Co., Pasadena, MD.) *In* JPL, Summaries of the Fifth Annual JPL Airborne Earth Science Workshop. Volume 1: AVIRIS Workshop 23 Jan. 1995 p 47-50 (For primary document see N95-33730 12-42)
Avail: CASI HC A01/MF A02

The success of imaging spectrometry in mineralogic mapping of natural terrains indicates that the technology can also be used to assess the environmental impact of human activities in certain instances. Specifically, this paper describes an investigation into the use of data from the Airborne Visible/Infrared Imaging Spectrometer (AVIRIS) for mapping the spread of, and assessing changes in, the mineralogic character of tailings from a major silver and base metal mining district. The area under investigation is the Coeur d'Alene River Valley in northern Idaho. Mining has been going on in and around the towns of Kellogg and Wallace, Idaho since the 1880's. In the Kellogg-Smelterville Flats area, west of Kellogg, mine tailings were piled alongside the South Fork of the Coeur d'Alene River. Until the construction of tailings ponds in 1968 much of these waste materials were washed directly into the South Fork. The Kellogg-Smelterville area was declared an Environmental Protection Agency (EPA) Superfund site in 1983 and remediation efforts are currently underway. Recent studies have demonstrated that sediments in the Coeur d'Alene River and in the northern part of Lake Coeur d'Alene, into which the river flows, are highly enriched in Ag, Cu, Pb, Zn, Cd, Hg, As, and Sb. These trace metals have become aggregated in iron oxide and oxyhydroxide minerals and/or mineraloids. Reflectance spectra of iron-rich tailing materials are shown. Also shown are spectra of hematite and goethite. The broad bandwidth and long band center (near 1 micron) of the Fe(3+) crystal-field band of the iron-rich sediment samples combined with the lack of features on the Fe(3+) -O(2-) charge transfer absorption edge indicates that the ferric oxide and/or oxyhydroxide in these sediments is poorly crystalline to amorphous in character. Similar features are seen in poorly crystalline basaltic weathering products (e.g., palagonites). The problem of mapping and analyzing the downriver occurrences of iron rich tailings in the Coeur d'Alene (CDA) River Valley using remotely sensed data is complicated by the full vegetation cover present in the area. Because exposures of rock and soil were sparse, the data processing techniques used in this study were sensitive to detecting materials at subpixel scales. The methods used included spectral mixture analysis and a constrained energy minimization technique. Author

N95-33746*# Earth Search Sciences, Inc., Salt Lake City, UT.
A LAYERED APPROACH TO TECHNOLOGY TRANSFER OF AVIRIS BETWEEN EARTH SEARCH SCIENCES, INC. AND THE IDAHO NATIONAL ENGINEERING LABORATORY **c35**
James S. Ferguson, JoAnne E. Ferguson, John Peel, III, and Larry Vance *In* JPL, Summaries of the Fifth Annual JPL Airborne Earth Science Workshop. Volume 1: AVIRIS Workshop 23 Jan. 1995 p 51-54 Prepared in cooperation with Idaho National Engineering Lab., Idaho Falls, ID (For primary document see N95-33730 12-42)
Avail: CASI HC A01/MF A02

Since initial contact between Earth Search Sciences, Inc. (ESSI) and the Idaho National Engineering Laboratory (INEL) in February, 1994, at least seven proposals have been submitted in response to a variety of solicitations to commercialize and improve the AVIRIS instrument. These proposals, matching ESSI's unique position with respect to agreements with the National Aeronautics and Space Administration (NASA) and the Jet Propulsion Laboratory (JPL) to utilize, miniaturize, and commercialize the AVIRIS instrument and platform, are combined with the applied engineering of the INEL. Teaming ESSI, NASA/JPL, and INEL with diverse industrial partners has strengthened the respective proposals. These efforts carefully structure the overall project plans to ensure the development, demonstration, and deployment of this concept to the national and international arenas. The objectives of these efforts include: (1) developing a miniaturized commercial, real-time, cost effective version of the AVIRIS instrument; (2) identifying multiple users for AVIRIS; (3) integrating the AVIRIS technology with other technologies; (4) gaining the confidence/acceptance of other government agencies and private industry in AVIRIS; and (5) increasing the technology base of U.S. industry. Author

N95-33747*# Jet Propulsion Lab., California Inst. of Tech., Pasadena, CA.
EVALUATION OF THE PHOTOCHEMICAL REFLECTANCE INDEX IN AVIRIS IMAGERY **c43**
John A. Gamon (California State Univ., Los Angeles, CA.), Dar A. Roberts (California Univ., Santa Barbara, CA.), and Robert O. Green *In its* Summaries of the Fifth Annual JPL Airborne Earth Science Workshop. Volume 1: AVIRIS Workshop 23 Jan. 1995 p 55-58 (For primary document see N95-33730 12-42)
Avail: CASI HC A01/MF A02

In this paper, we evaluate the potential for extracting the 'photochemical reflectance index' (PRI; previously called the 'physiological reflectance index') from AVIRIS data. This index, which is derived from narrow-band reflectance at 531 and 570 nm, has proven to be a useful indicator of photosynthetic function at the leaf and canopy scales. At the leaf level, PRI varies with photosynthetic capacity, radiation-use efficiency, and vegetation type (unpublished data). This finding is consistent with the hypothesis that vegetation types exhibiting chronically reduced photosynthesis during periods of stress (e.g. drought-tolerant evergreens) invest proportionally more in photoprotective processes than vegetation with high photosynthetic capacity (e.g. crops or deciduous perennials). Vertical transects in tropical and boreal forest canopies have indicated declines in PRI associated with downregulation of photosynthesis at the canopy tops under sunny, dry midday conditions (unpublished data). This reduced PRI in upper canopy levels provides a further basis for examining this signal with the 'view from above' afforded by aircraft overflights. Although many factors could confound interpretation of a subtle physiological signal at the landscape scale, we conducted a preliminary examination of PRI extracted from existing, AVIRIS imagery of Stanford University's Jasper Ridge Biological Preserve obtained on the June 2nd, 1992, overflight. The goal was to use the hyperspectral capabilities of AVIRIS to evaluate the potential of this index for obtaining useful physiological data at the landscape scale. The expectation based on leaf- and canopy-level studies was that regions containing vegetation of reduced photosynthetic capacity (e.g. chaparral or evergreen woodland) would exhibit lower PRI values than regions of high capacity (e.g. deciduous woodland). Author

N95-33748*# National Aeronautics and Space Administration. Goddard Space Flight Center, Greenbelt, MD.
CORRECTION OF THIN CIRRUS EFFECTS IN AVIRIS IMAGES USING THE SENSITIVE 1.375-MICRON CIRRUS DETECTING CHANNEL **c43**
Bo-Cai Gao (Universities Space Research Association, Greenbelt, MD.) and Yorman J. Kaufman *In* JPL, Summaries of the Fifth Annual JPL Airborne Earth Science Workshop. Volume 1: AVIRIS Workshop 23 Jan. 1995 p 59-62 (For primary document see N95-33730 12-42)
Avail: CASI HC A01/MF A02

Using spectral imaging data acquired with the Airborne Visible Infrared Imaging Spectrometer (AVIRIS) from an ER-2 aircraft at 20 km altitude during various field programs, it was found that narrow channels near the center of the strong 1.38-micrometer water vapor band are very effective in detecting think cirrus clouds. Based on this observation from AVIRIS data, Gao and Kaufman proposed to put a channel centered at 1.375 micrometers with a width of 30 nm on the Moderate Resolution Imaging Spectrometer (MODIS) for remote sensing of cirrus clouds from space. The sensitivity of the 1.375-micrometer MODIS channel to detect thin cirrus clouds during the day time is expected to be one to two orders of magnitude better than the current infrared emission techniques. As a result, much larger fraction of the satellite data is expected to be identified as being covered by cirrus clouds, some of them so thin that their obscuration of the surface is very small. In order to make better studies of surface reflectance properties, thin cirrus effects must be removed from satellite images. Therefore, there is a need to study radiative properties of thin cirrus clouds, so that a strategy for correction or removal of the thin cirrus effects, similar to the correction of atmospheric aerosol effect, can be formed. In this extended abstract, we describe an empirical approach for

removing/correcting thin cirrus effects in AVIRIS images using channels near 1.375 microns - one step beyond the detection of cirrus clouds using these channels. Author

N95-33749*# National Aeronautics and Space Administration. Goddard Space Flight Center, Greenbelt, MD.

REMOTE SENSING OF SMOKE, CLOUDS, AND RADIATION USING AVIRIS DURING SCAR EXPERIMENTS c43

Bo-Cai Gao (Universities Space Research Association, Greenbelt, MD.), Lorraine Remer (Science Systems and Applications, Inc., Greenbelt, MD.), and Yorman J. Kaufman *In* JPL, Summaries of the Fifth Annual JPL Airborne Earth Science Workshop. Volume 1: AVIRIS Workshop 23 Jan. 1995 p 63-65 (For primary document see N95-33730 12-42)

Avail: CASI HC A01/MF A02

During the past two years, researchers from several institutes joined together to take part in two SCAR experiments. The SCAR-A (Sulfates, Clouds And Radiation - Atlantic) took place in the mid-Atlantic region of the United States in July, 1993. remote sensing data were acquired with the Airborne Visible Infrared Imaging Spectrometer (AVIRIS), the MODIS Airborne Simulator (MAS), and a RC-10 mapping camera from an ER-2 aircraft at 20 km. In situ measurements of aerosol and cloud microphysical properties were made with a variety of instruments equipped on the University of Washington's C-131A research aircraft. Ground based measurements of aerosol optical depths and particle size distributions were made using a network of sunphotometers. The main purpose of SCAR-A experiment was to study the optical, physical and chemical properties of sulfate aerosols and their interaction with clouds and radiation. Sulfate particles are believed to affect the energy balance of the earth by directly reflecting solar radiation back to space and by increasing the cloud albedo. The SCAR-C (Smoke, Clouds And Radiation - California) took place on the west coast areas during September - October of 1994. Sets of aircraft and ground-based instruments, similar to those used during SCAR-A, were used during SCAR-C. Remote sensing of fires and smoke from AVIRIS and MAS imagers on the ER-2 aircraft was combined with a complete in situ characterization of the aerosol and trace gases from the C-131A aircraft of the University of Washington and the Cesna aircraft from the U.S. Forest Service. The comprehensive data base acquired during SCAR-A and SCAR-C will contribute to a better understanding of the role of clouds and aerosols in global change studies. The data will also be used to develop satellite remote sensing algorithms from MODIS on the Earth Observing System. Author

N95-33750*# Jet Propulsion Lab., California Inst. of Tech., Pasadena, CA.

HIGH ACCURACY IN-FLIGHT WAVELENGTH CALIBRATION OF IMAGING SPECTROMETRY DATA c43

Alexander F. H. Goetz (Colorado Univ., Boulder, CO.), Kathleen B. Heidebrecht (Colorado Univ., Boulder, CO.), and Thomas G. Chrien *In its* Summaries of the Fifth Annual JPL Airborne Earth Science Workshop. Volume 1: AVIRIS Workshop 23 Jan. 1995 p 67-70 (For primary document see N95-33730 12-42)

Avail: CASI HC A01/MF A02

Accurate wavelength calibration of imaging spectrometer data is essential if proper atmospheric transmission corrections are to be made to obtain apparent surface reflectance. Accuracies of 0.1 nm are necessary for a 10 nm-sampling instrument in order to match the slopes of the deep atmospheric water vapor features that dominate the 0.7-2.3 micrometer regions. The Airborne Visible/Infrared Imaging Spectrometer (AVIRIS) is calibrated in the laboratory to determine the wavelength position and full-width-half-maximum (FWHM) response for each of the 224 channels The accuracies are limited by the quality of the monochromator used as a source. The accuracies vary from plus or minus to plus or minus 1.5 nm depending on the wavelength region, in general decreasing with increasing wavelength. Green et al. make corrections to the wavelength calibrations by using the known positions of 14 atmospheric absorption features throughout the 0.4-2.5 micrometer wavelength region. These features, having varying width and intensity, were matched to the MODTRAN model with a non-linear least squares fitting algorithm. A complete calibration was developed for all 224 channels by interpolation. Instrument calibration cannot be assumed to be stable to 0.1 nm over a flight season given the rigors of thermal cycling and launch and landing loads. The upcoming sensor HYDICE will require a means for in-flight spectral calibration of each scene because the calibration is both temperature and pressure sensitive. In addition, any sensor using a two-dimensional array has the potential for systematic wavelength shifts as a function of cross-track position, commonly called 'smile'. Therefore, a rapid means for calibrating complete images will be required. The following describes a method for determining instrument wavelength calibration using atmospheric absorption features that is efficient enough to be used for entire images on workstations. This study shows the effect of the surface reflectance on the calibration accuracy and the calibration history for the AVIRIS B spectrometer over the 1992 flight season. Author

N95-33751*# Jet Propulsion Lab., California Inst. of Tech., Pasadena, CA.

DETERMINATION OF THE IN-FLIGHT SPECTRAL CALIBRATION OF AVIRIS USING ATMOSPHERIC ABSORPTION FEATURES c35

Robert O. Green *In its* Summaries of the Fifth Annual JPL Airborne Earth Science Workshop. Volume 1: AVIRIS Workshop 23 Jan. 1995 p 71-74 (For primary document see N95-33730 12-42)

Avail: CASI HC A01/MF A02

Spectral calibration of the Airborne Visible/Infrared Imaging Spectrometer (AVIRIS) as data are acquired in flight is essential to quantitative analysis of the measured upwelling spectral radiance. In each spectrum measured by AVIRIS in flight, there are numerous atmospheric gas absorption bands that drive this requirement for accurate spectral calibration. If the surface and atmospheric properties are measured independently, these atmospheric absorption bands may be used to deduce the in-flight spectral calibration of an imaging spectrometer. Both the surface and atmospheric characteristics were measured for a calibration target during an in-flight calibration experiment held at Lunar Lake, Nevada on April 5, 1994. This paper uses upwelling spectral radiance predicted for the calibration target with the MODTRAN radiative transfer code to validate the spectral calibration of AVIRIS in flight. Derived from text

N95-33752*# Jet Propulsion Lab., California Inst. of Tech., Pasadena, CA.

AN IMPROVED SPECTRAL CALIBRATION REQUIREMENT FOR AVIRIS c35

Robert O. Green *In its* Summaries of the Fifth Annual JPL Airborne Earth Science Workshop. Volume 1: AVIRIS Workshop 23 Jan. 1995 p 75-78 (For primary document see N95-33730 12-42)

Avail: CASI HC A01/MF A02

The Airborne Visible/Infrared Imaging Spectrometer (AVIRIS) measures spectra from 400 to 2500 nm through 224 contiguous spectral channels. These spectra are used to identify and determine the abundances of constituents of the earth's surface and atmosphere through the analysis of spectral molecular absorptions and scattering properties of materials. Spectral calibration of the AVIRIS is required to pursue these determinations, which are based on these fundamental spectral characteristics. The spectral calibration of AVIRIS consists of a description of the spectral response function for each of the 224 spectral channels. The spectral response function of AVIRIS channels was measured in the laboratory and shown to be Gaussian in shape. A subset of nine AVIRIS spectral channels is shown with channel centers at 10 nm intervals and channel shapes of Gaussian form with 10 nm full width and half maximum (FWHM). For AVIRIS the spectral calibration is described by the spectral center and FWHM of a Gaussian function for each channel. Uncertainty in the determination of the spectral center and FWHM for each channel are also reported. This paper presents results from an investigation of the sensitivity of AVIRIS-measured upwelling radiance to errors in spectral calibration. Based on this sensitivity analysis in conjunction with earlier work, an improved spectral calibration requirement for AVIRIS is proposed. Derived from text

N95-33753*# Jet Propulsion Lab., California Inst. of Tech., Pasadena, CA.

MOVEMENT OF WATER VAPOR IN THE ATMOSPHERE MEASURED BY AN IMAGING SPECTROMETER AT ROGERS DRY LAKE, CA c46

Robert O. Green and James E. Conel (California Univ., Santa Barbara, CA.) *In its* Summaries of the Fifth Annual JPL Airborne Earth Science Workshop. Volume 1: AVIRIS Workshop 23 Jan. 1995 p 79-82 (For primary document see N95-33730 12-42)

Avail: CASI HC A01/MF A02

Movement of water as vapor in the atmosphere is a fundamental

process in the Earth's hydrological cycle. Investigations of spatial and time scales of water vapor transport in the atmosphere are important areas of research. Water vapor transmits energy as a function of its abundance across the spectrum. This is shown in the 400- to 2500-nm spectral region where the transmission of the terrestrial atmosphere has been modeled using the MODTRAN radiative transfer code for a range of water vapor abundances. Based on these model results, spectra measured by the Airborne Visible/Infrared Imaging Spectrometer (AVIRIS) have been used to investigate the movement of water vapor at 20-m spatial resolution over an 11-by-30-km area at approximately 15-minute time intervals (1.25 hours total). AVIRIS measures the upwelling spectral radiance from 400 to 2500 nm at 10-nm spectral intervals and collects images of 11-by-up-to-1000 km at 20-m spatial resolution. Data are collected at a rate of 1 km of flight line per 4.5 seconds. A set of five AVIRIS flight lines was acquired in rapid succession over Rogers Dry Lake, CA on May 18, 1993 at 18:59, 19:13, 19:29, 19:47, and 19:59 UTC. Rogers Dry lake is located 2 hours north of Los Angeles, CA at 34.84 degrees north latitude and 117.83 degrees west longitude in the Mojave Desert. Author

N95-33754*# Jet Propulsion Lab., California Inst. of Tech., Pasadena, CA.

IN-FLIGHT RADIOMETRIC CALIBRATION OF AVIRIS IN 1994 **c35**

Robert O. Green, James E. Conel (California Univ., Santa Barbara, CA.), Mark Helmlinger (California Univ., Santa Barbara, CA.), Jeannette vandenBosch (California Univ., Santa Barbara, CA.), and Pavel Hajek (California Univ., Santa Barbara, CA.) *In its* Summaries of the Fifth Annual JPL Airborne Earth Science Workshop. Volume 1: AVIRIS Workshop 23 Jan. 1995 p 83-86 (For primary document see N95-33730 12-42)

Avail: CASI HC A01/MF A02

The AVIRIS sensor must be calibrated at the time it measures spectra from the ER-2 airborne platform in order to achieve research and application objectives that are both quantitative and physically based. However, the operational environment inside the Q-bay of the ER-2 at 20 km altitude differs from that in the AVIRIS laboratory with respect to temperature, pressure, vibration, and high-frequency electromagnetic fields. Experiments at surface calibration targets are used in each flight season to confirm the accuracy of AVIRIS in-flight radiometric calibrations. For these experiments, the MODTRAN radiative transfer code is constrained by using in situ measurements to independently predict the upwelling spectral radiance arriving at AVIRIS for a specific calibration target. AVIRIS calibration is validated in flight by comparing the MODTRAN-predicted radiance to the laboratory-calibrated radiance measured by the AVIRIS sensor for the same time over the calibration target. We present radiometric calibration results for the AVIRIS in-flight calibration experiment held at the beginning of the 1994 flight season. Derived from text

N95-33755*# Jet Propulsion Lab., California Inst. of Tech., Pasadena, CA.

MEASUREMENT OF ATMOSPHERIC WATER VAPOR, LEAF LIQUID WATER AND REFLECTANCE WITH AVIRIS IN THE BOREAL ECOSYSTEM-ATMOSPHERE STUDY: INITIAL RESULTS **c43**

Robert O. Green, James E. Conel, and Dar A. Roberts (California Univ., Santa Barbara, CA.) *In its* Summaries of the Fifth Annual JPL Airborne Earth Science Workshop. Volume 1: AVIRIS Workshop 23 Jan. 1995 p 87-90 (For primary document see N95-33730 12-42)

Avail: CASI HC A01/MF A02

The Airborne Visible/Infrared Imaging Spectrometer (AVIRIS) acquired data as part of the Boreal Ecosystem-Atmosphere Study (BOREAS) in 1994. Flights occurred over the northern study area (NSA) in the region of 56 degrees north latitude and 98.5 degrees west longitude and over the southern study area (SSA) at 54 degrees north latitude and 105 degrees west longitude. These data will be used to directly derive spectral properties of the surface and atmosphere and to provide supporting data for other instruments, models, and experiments in support of the BOREAS objectives. We present a preliminary evaluation of the AVIRIS data collected in BOREAS in terms of the AVIRIS-derived parameters: water vapor, leaf water, and apparent spectral reflectance. Derived from text

N95-33756*# Jet Propulsion Lab., California Inst. of Tech., Pasadena, CA.

MEASUREMENT OF THE SPECTRAL ABSORPTION OF LIQUID WATER IN MELTING SNOW WITH AN IMAGING SPECTROMETER **c43**

Robert O. Green and Jeff Dozier (California Univ., Santa Barbara, CA.) *In its* Summaries of the Fifth Annual JPL Airborne Earth Science Workshop. Volume 1: AVIRIS Workshop 23 Jan. 1995 p 91-94 (For primary document see N95-33730 12-42)

Avail: CASI HC A01/MF A02

Melting of the snowpack is a critical parameter that drives aspects of the hydrology in regions of the earth where snow accumulates seasonally. New techniques for measurement of snow melt over regional scales offer the potential to improve monitoring and modeling of snow-driven hydrological processes. We present the results of measuring the spectral absorption of liquid water in a melting snowpack with the Airborne Visible/Infrared Imaging Spectrometer (AVIRIS). AVIRIS data were acquired over Mammoth Mountain, in east central California on 21 May 1994 at 18:35 UTC. The air temperature at 2926 m on Mammoth Mountain at site A was measured at 15-minute intervals during the day preceding the AVIRIS data acquisition. At this elevation, the air temperature did not drop below freezing the night of May 20 and had risen to 6 degrees Celsius by the time of the overflight on May 21. These temperature conditions support the presence of melting snow at the surface as the AVIRIS data were acquired. Derived from text

N95-33757*# Jet Propulsion Lab., California Inst. of Tech., Pasadena, CA.

VEGETATION SPECIES COMPOSITION AND CANOPY ARCHITECTURE INFORMATION EXPRESSED IN LEAF WATER ABSORPTION MEASURED IN THE 1000 NM AND 2200 SPECTRAL REGION BY AN IMAGING SPECTROMETER **c43**

Robert O. Green and Dar A. Roberts (California Univ., Santa Barbara, CA.) *In its* Summaries of the Fifth Annual JPL Airborne Earth Science Workshop. Volume 1: AVIRIS Workshop 23 Jan. 1995 p 95-98 (For primary document see N95-33730 12-42)

Avail: CASI HC A01/MF A02

Plant species composition and plant architectural attributes are critical parameters required for the measuring, monitoring, and modeling of terrestrial ecosystems. Remote sensing is commonly cited as an important tool for deriving vegetation properties at an appropriate scale for ecosystem studies, ranging from local to regional and even synoptic scales. Classical approaches rely on vegetation indices such as the normalized difference vegetation index (NDVI) to estimate biophysical parameters such as leaf area index or intercepted photosynthetically active radiation (IPAR). Another approach is to apply a variety of classification schemes to map vegetation and thus extrapolate fine-scale information about specific sites to larger areas of similar composition. Imaging spectrometry provides additional information that is not obtainable through broad-band sensors and that may provide improved inputs both to direct biophysical estimates as well as classification schemes. Some of this capability has been demonstrated through improved discrimination of vegetation, estimates of canopy biochemistry, and liquid water estimates from vegetation. We investigate further the potential of leaf water absorption estimated from Airborne Visible/Infrared Imaging Spectrometer (AVIRIS) data as a means for discriminating vegetation types and deriving canopy architectural information. We expand our analysis to incorporate liquid water estimates from two spectral regions, the 1000-nm region and the 2200-nm region. The study was conducted in the vicinity of Jasper Ridge, California, which is located on the San Francisco peninsula to the west of the Stanford University campus. AVIRIS data were acquired over Jasper Ridge, CA, on June 2, 1992, at 19:31 UTC. Spectra from three sites in this image were analyzed. These data are from an area of healthy grass, oak woodland, and redwood forest, respectively. For these analyses, the AVIRIS-measured upwelling radiance spectra for the entire Jasper Ridge scene were transformed to apparent surface reflectance using a radiative transfer code-based inversion algorithm. Derived from text

N95-33758*# California Univ., Davis, CA. Land, Air, and Water Resources.

PROSPECT REDUX **c43**

S. Jacquemoud, S. L. Ustin, J. Verdebout (Joint Research Centre of the European Communities, Ispra, Italy.), G. Schmuck (Joint Research Centre of the European Communities, Ispra, Italy.), G. Andreoli (Joint Research Centre of the European Communities, Ispra, Italy.), and B. Hosgood (Joint

Research Centre of the European Communities, Ispra, Italy.) *In* JPL, Summaries of the Fifth Annual JPL Airborne Earth Science Workshop. Volume 1: AVIRIS Workshop 23 Jan. 1995 p 99-103 (For primary document see N95-33730 12-42)
Avail: CASI HC A01/MF A02

The remote estimation of leaf biochemical content from spaceborne platforms has been the subject of many studies aimed at better understanding of terrestrial ecosystem functioning. The major ecological processes involved in exchange of matter and energy, like photosynthesis, primary production, evaportranspiration, respiration, and decomposition can be related to plant properties e.g., chlorophyll, water, protein, cellulose and lignin contents. As leaves represent the most important plant surfaces interacting with solar energy, a top priority has been to relate optical properties to biochemical constituents. Two different approaches have been considered: first, statistical correlations between the leaf reflectance (or transmittance) and biochemical content, and second, physically based models of leaf scattering and absorption developed using the laws of optics. Recently reviewed by Verdebout et al., the development of models of leaf optical properties has resulted in better understanding of the interaction of light with plant leaves. Present radiative transfer models mainly use chlorophyll and/or water contents as input parameters to calculate leaf reflectance. Inversion of these models allows to retrieve these constituents from spectrophotometric measurements. Conel et al. recently proposed a two-stream Kubelka-Munk model to analyze the influence of protein, cellulose, lignin, and starch on leaf reflectance, but in fact, the estimation of leaf biochemistry from remote sensing is still an open question. In order to clarify it, a laboratory experiment associating visible/infrared spectra of plan leaves both with physical measurements and biochemical analyses was conducted at the Joint Research Center during the summer of 1993. This unique data set has been used to upgrade the PROSPECT model, by including leaf biochemistry. Author

N95-33759*# Jet Propulsion Lab., California Inst. of Tech., Pasadena, CA.
AVIRIS USER'S GUIDE **c35**
Howell K. Johnson and Robert O. Green *In its* Summaries of the Fifth Annual JPL Airborne Earth Science Workshop. Volume 1: AVIRIS Workshop 23 Jan. 1995 p 105-108 (For primary document see N95-33730 12-42)
Avail: CASI HC A01/MF A02

This paper serves as a brief overview of the AVIRIS instrument (Airborne Visible/Infrared Imaging Spectrometer). The AVIRIS sensor collects data that will be used for quantitative characterization of the Earth's surface and atmosphere from geometrically coherent spectroradiometric measurements. This data can be applied to studies in the fields of oceanography, environmental science, snow hydrology, geology, volcanology, soil and land management, atmospheric and aerosol studies, agriculture, and limnology. Applications under development include the assessment and monitoring of environmental hazards such as toxic waste, oil spills, and land/air/water pollution. Mission planning and flight operations are discussed, and recommendations are given regarding the deployment of ground truth experiments. Author

N95-33760*# Colorado Univ., Boulder, CO. Center for the Study of Earth from Space.
INTEGRATION OF AIRSAR AND AVIRIS DATA FOR TRAIL CANYON ALLUVIAL FAN, DEATH VALLEY, CALIFORNIA **c43**
Kathryn S. Kierein-Young *In* JPL, Summaries of the Fifth Annual JPL Airborne Earth Science Workshop. Volume 1: AVIRIS Workshop 23 Jan. 1995 p 109-112 Sponsored by SIR-C project (For primary document see N95-33730 12-42)
(Grant NGT-50728)
Avail: CASI HC A01/MF A02

Combining quantitative geophysical information extracted from the optical and microwave wavelengths provides complementary information about both the surface mineralogy and morphology. This study combines inversion results from two remote sensing instruments, a polarimetric synthetic aperture radar, AIRSAR, and an imaging spectrometer, AVIRIS, for Trail Canyon alluvial fan in Death Valley, California. The NASA/JPL Airborne Synthetic Aperture Radar (AIRSAR) is a quad-polarization, three frequency instrument. AIRSAR collects data at C-band = 5.66 cm, L-band = 23.98 cm, and P-band = 68.13 cm. The data are processed to four-looks and have a spatial resolution of 10 m and a swath width of 12 km. The AIRSAR data used in this study were collected as part of the Geologic Remote Sensing Field Experiment (GRSFE) over Death Valley on 9/14/89. The Airborne Visible/Infrared Imaging Spectrometer (AVIRIS) is a NASA/JPL instrument that flies in an ER-2 aircraft at an altitude of 20 km. AVIRIS uses four spectrometers to collect data in 224 spectral channels from 0.4 micrometer to 2.45 micrometer. The width of each spectral band is approximately 10 nm. AVIRIS collects data with a swath width of 11 km and a pixel size of 20 m. The AVIRIS data used in this study were collected over Death Valley on 5/31/92. Author

N95-33761*# Geological Survey, Denver, CO.
REMOTE MINERAL MAPPING USING AVIRIS DATA AT SUMMITVILLE, COLORADO AND THE ADJACENT SAN JUAN MOUNTAINS **c43**
Trude V. V. King, Roger N. Clark, Cathy Ager, and Gregg A. Swayze *In* JPL, Summaries of the Fifth Annual JPL Airborne Earth Science Workshop. Volume 1: AVIRIS Workshop 23 Jan. 1995 p 113-116 (For primary document see N95-33730 12-42)
Avail: CASI HC A01/MF A02

We have demonstrated the unique utility of imaging spectroscopy in mapping mineral distribution. In the Summitville mining region we have shown that the mine site does not contribute clay minerals to the Alamosa River, but does contribute Fe-bearing minerals. Such minerals have the potential to carry heavy metals. This application illustrates only one specific environmental application of imaging spectroscopy data. For instance, the types of minerals we can map with confidence are those frequently associated with environmental problems related to active and abandoned mine lands. Thus, the potential utility of this technology to the field of environmental science has yet to be fully explored. Author

N95-33762*# EROS Data Center, Sioux Falls, SD.
AIRCRAFT SCANNER DATA AVAILABILITY VIA THE VERSION 0 INFORMATION MANAGEMENT SYSTEM **c82**
G. R. Mah *In* JPL, Summaries of the Fifth Annual JPL Airborne Earth Science Workshop. Volume 1: AVIRIS Workshop 23 Jan. 1995 p 117-120 (For primary document see N95-33730 12-42)
Avail: CASI HC A01/MF A02

As part of the Earth Observing System Data and Information System (EOSDIS) development, NASA and other government agencies have developed an operational prototype of the Information Management System (IMS). The IMS provides access to the data archived at the Distributed Active Archive Centers (DAAC's) that allows users to search through metadata describing the (image) data. Criteria based on sensor name or type, date and time, and geographic location are used to search the archive. Graphical representations of coverage and browse images are available to further refine a user's selection. previously, the EROS Data Center (EDC) DAAC had identified the Advanced SOlid-state Array Spectrometer (ASAS), Airborne Visible and infrared Imaging Spectrometer (AVIRIS), NS-001, and Thermal Infrared Multispectral Scanner (TIMS) as precursor data sets similar to those the DAAC will handle in the Earth Observing System era. Currently, the EDC DAAC staff, in cooperation with NASA, has transcribed TIMS, NS-001, and Thematic Mapper Simulation (TMS) data from Ames Research Center and also TIMS data from Stennis Space Center. During the transcription process, the IMS metadata and browse images were created to populate the inventory at the EDC DAAC. These data sets are now available in the IMS and may be requested from the any of the DAAC's via the IMS. Author

N95-33763*# Instituto Nacional de Pesaciais Espaciais, Sao Jose dos Campos (Brazil).
AN ALGORITHM FOR CHLOROPHYLL USING FIRST DIFFERENCE TRANSFORMATIONS OF AVIRIS REFLECTANCE SPECTRA **c43**
Evlyn Novo, Mary Gastil (Colorado Univ., Boulder, CO.), and John Melack (Colorado Univ., Boulder, CO.) *In* JPL, Summaries of the Fifth Annual JPL Airborne Earth Science Workshop. Volume 1: AVIRIS Workshop 23 Jan. 1995 p 121-124 (For primary document see N95-33730 12-42)
Avail: CASI HC A01/MF A02

Experimental results have shown the existence of a strong relationship between chlorophyll alpha concentration and remote sensing reflectance measured at lake level with a high resolution spectroradiometer. The objective of our study was to investigate the relationship between surface chlorophyll alpha concentration at Mono Lake and water reflectance retrieved

from Airborne Visible - Infrared Imaging Spectrometer (AVIRIS) data obtained in october 7, 1992. AVIRIS data were atmospherically corrected as described by Green et al. A description of the lake-level sampling is found in Melack and Gastil. The relationship between chlorophyll concentration and both the single band reflectance and the first difference transformation of the reflectance spectra for the first 40 AVIRIS spectral bands (400 nm to 740 nm) was examined. The relationship was then used to produce a map of the surface chlorophyll distribution. Author

N95-33764*# Jet Propulsion Lab., California Inst. of Tech., Pasadena, CA.

IMPROVING ALPINE-REGION SPECTRAL UNMIXING WITH OPTIMAL-FIT SNOW ENDMEMBERS **c43**

Thomas H. Painter (California Univ., Santa Barbara, CA.), Dar A. Roberts (California Univ., Santa Barbara, CA.), Robert O. Green, and Jeff Dozier (California Univ., Santa Barbara, CA.) *In its* Summaries of the Fifth Annual JPL Airborne Earth Science Workshop. Volume 1: AVIRIS Workshop 23 Jan. 1995 p 125-128 (For primary document see N95-33730 12-42)

Avail: CASI HC A01/MF A02

Surface albedo and snow-covered-area (SCA) are crucial inputs to the hydrologic and climatologic modeling of alpine and seasonally snow-covered areas. Because the spectral albedo and thermal regime of pure snow depend on grain size, areal distribution of snow grain size is required. Remote sensing has been shown to be an effective (and necessary) means of deriving maps of grain size distribution and snow-covered-area. Developed here is a technique whereby maps of grain size distribution improve estimates of SCA from spectral mixture analysis with AVIRIS data. Author

N95-33765*# California Univ., Davis, CA. Dept. of Land, Air, and Water Resources.

USING FOREGROUND/BACKGROUND ANALYSIS TO DETERMINE LEAF AND CANOPY CHEMISTRY **c43**

J. E. Pinzon, S. L. Ustin, Q. J. Hart, S. Jacquemoud, and M. O. Smith (Washington Univ., Seattle, WA.) *In* JPL, Summaries of the Fifth Annual JPL Airborne Earth Science Workshop. Volume 1: AVIRIS Workshop 23 Jan. 1995 p 129-132 (For primary document see N95-33730 12-42)

Avail: CASI HC A01/MF A02

Spectral Mixture Analysis (SMA) has become a well established procedure for analyzing imaging spectrometry data, however, the technique is relatively insensitive to minor sources of spectral variation (e.g., discriminating stressed from unstressed vegetation and variations in canopy chemistry). Other statistical approaches have been tried e.g., stepwise multiple linear regression analysis to predict canopy chemistry. Grossman et al. reported that SMLR is sensitive to measurement error and that the prediction of minor chemical components are not independent of patterns observed in more dominant spectral components like water. Further, they observed that the relationships were strongly dependent on the mode of expressing reflectance (R, -log R) and whether chemistry was expressed on a weight (g/g) or are basis (g/sq m). Thus, alternative multivariate techniques need to be examined. Smith et al. reported a revised SMA that they termed Foreground/Background Analysis (FBA) that permits directing the analysis along any axis of variance by identifying vectors through the n-dimensional spectral volume orthonormal to each other. Here, we report an application of the FBA technique for the detection of canopy chemistry using a modified form of the analysis. Author

N95-33766*# National Aeronautics and Space Administration. Goddard Space Flight Center, Greenbelt, MD.

AVIRIS SPECTRAL TRAJECTORIES FOR FORESTED AREAS OF THE GIFFORD PINCHOT NATIONAL FOREST **c43**

Donald E. Sabol, Jr. (Washington Univ., Seattle, WA.), Milton O. Smith (Washington Univ., Seattle, WA.), John B. Adams (Washington Univ., Seattle, WA.), Janet H. Zukin (Washington Univ., Seattle, WA.), Compton J. Tucker, Dar A. Roberts (Colorado Univ., Boulder, CO.), and Alan R. Gillespie (Washington Univ., Seattle, WA.) *In* JPL, Summaries of the Fifth Annual JPL Airborne Earth Science Workshop. Volume 1: AVIRIS Workshop 23 Jan. 1995 p 133-136 (For primary document see N95-33730 12-42)

Avail: CASI HC A01/MF A02

A simple mixing model employing reference endmembers (green vegetation, non-photosynthetic vegetation, soil and shade), and using 180 AVIRIS bands, was used to establish an interpretive framework for a forested area in the Pacific Northwest. A regrowth trend, based on changes in the endmember proportions, was defined for conifers that extends from clearcuts to mature forest, and by implication to old growth. Deciduous species within replanted forest plots caused the fractions to be displaced from the main coniferous regrowth trend and to move toward the green vegetation fraction. The results indicate that the spectral information in AVIRIS can be inverted to estimate approximate stand age and relative proportion of deciduous species in the context of the area studied. Using AVIRIS we measured a 3 to 5 percent increase in woody material in old-growth forest, as distinct from other mature forest. This result is consistent with a predicted increase in NPV in old-growth forest, based on field observations. Previous application of the mixing analysis to a TM image of the same area separated old growth based solely on the shade fraction; however the approach required successful removal of shade introduced by topography. Our new results suggest that with the high spectral resolution and high signal-to-noise of AVIRIS images it may be possible to characterize and map old-growth forests in the Northwest using both the NPV fraction and shade. Author

N95-33767*# Howard Univ., Washington, DC. Dept. of Physics.

SUB-PIXEL LOCALIZATION OF HIGHWAYS IN AVIRIS IMAGES **c43**

Yehuda Salu *In* JPL, Summaries of the Fifth Annual JPL Airborne Earth Science Workshop. Volume 1: AVIRIS Workshop 23 Jan. 1995 p 137-140 (For primary document see N95-33730 12-42)

Avail: CASI HC A01/MF A02

Roads and highways show up clearly in many bands of AVIRIS images. A typical lane in the U.S. is 12 feet wide, and the total width of a four lane highway, including 18 feet of paved shoulders, is 19.8 m. Such a highway will cover only a portion of any 20x20 m AVIRIS pixel that it traverses. The other portion of these pixels wil be usually covered by vegetation. An interesting problem is to precisely determine the location of a highway within the AVIRIS pixels that it traverses. This information may be used for alignment and spatial calibration of AVIRIS images. Also, since the reflection properties of highway surfaces do not change with time, and they can be determined once and for all, such information can be of help in calculating and filtering out the atmospheric noise that contaminates AVIRIS measurements. The purpose of this report is to describe a method for sub-pixel localization of highways. Author

N95-33768*# California Univ., Davis, CA. Dept. of Land, Air, and Water Resources.

VALIDATING SPATIAL STRUCTURE IN CANOPY WATER CONTENT USING GEOSTATISTICS **c43**

E. W. Sanderson, M. H. Zhang, S. L. Ustin, E. Rejmankova, and R. S. Haxo *In* JPL, Summaries of the Fifth Annual JPL Airborne Earth Science Workshop. Volume 1: AVIRIS Workshop 23 Jan. 1995 p 141-143 (For primary document see N95-33730 12-42)

Avail: CASI HC A01/MF A02

Heterogeneity in ecological phenomena are scale dependent and affect the hierarchical structure of image data. AVIRIS pixels average reflectance produced by complex absorption and scattering interactions between biogeochemical composition, canopy architecture, view and illumination angles, species distributions, and plant cover as well as other factors. These scales affect validation of pixel reflectance, typically performed by relating pixel spectra to ground measurements acquired at scales of 1m(exp 2) or less (e.g., field spectra, foilage and soil samples, etc.). As image analysis becomes more sophisticated, such as those for detection of canopy chemistry, better validation becomes a critical problem. This paper presents a methodology for bridging between point measurements and pixels using geostatistics. Geostatistics have been extensively used in geological or hydrogeolocial studies but have received little application in ecological studies. The key criteria for kriging estimation is that the phenomena varies in space and that an underlying controlling process produces spatial correlation between the measured data points. Ecological variation meets this requirement because communities vary along environmental gradients like soil moisture, nutrient availability, or topography. Author

N95-33769*# Jet Propulsion Lab., California Inst. of Tech., Pasadena, CA.

AIRBORNE VISIBLE/INFRARED IMAGING SPECTROMETER (AVIRIS): SENSOR IMPROVEMENTS FOR 1994 AND 1995 **c35**

C. M. Sarture, T. G. Chrien, R. O. Green, M. L. Eastwood, J. J. Raney, and M. A. Hernandez *In its* Summaries of the Fifth Annual JPL Airborne

Earth Science Workshop. Volume 1: AVIRIS Workshop 23 Jan. 1995 p 145-148 (For primary document see N95-33730 12-42)
Avail: CASI HC A01/MF A02

AVIRIS is a NASA-sponsored Earth-remote-sensing imaging spectrometer designed, built and operated by the Jet Propulsion Laboratory (JPL). While AVIRIS has been operational since 1989, major improvements have been completed in most of the sensor subsystems during the winter maintenance cycles. As a consequence of these efforts, the capabilities of AVIRIS to reliably acquire and deliver consistently high quality, calibrated imaging spectrometer data continue to improve annually, significantly over those in 1989. Improvements to AVIRIS prior to 1994 have been described previously. This paper details recent and planned improvements to AVIRIS in the sensor task. Author

N95-33770*# Zurich Univ. (Switzerland). Remote Sensing Lab.

EXTRACTION OF OZONE AND CHLOROPHYLL-A DISTRIBUTION FROM AVIRIS DATA **c43**

M. Schaepman, K. I. Itten, D. Schlaepfer, U. Kurer, S. Veraguth, and J. Keller (Paul Scherrer Inst., Villigen, Switzerland.) *In* JPL, Summaries of the Fifth Annual JPL Airborne Earth Science Workshop. Volume 1: AVIRIS Workshop 23 Jan. 1995 p 149-152 (For primary document see N95-33730 12-42)
Avail: CASI HC A01/MF A02

The potential of airborne imaging spectrometry for assessing and monitoring natural resources is studied. Therefore, an AVIRIS scene of the NASA's MacEurope 1991 campaign - acquired in Central Switzerland - is used. The test site consists of an urban area, the Lake Zug with its surrounding fields, the Rigi mountain in the center of the test site, and the Lake of Four Cantons. The region is covered by the AVIRIS flight #910705, run 6 and 7 of the NASA ER-2 aircraft resulting in an average nominal pixel size of about 18 m. Simultaneous to the ER-2 overflight spectroradiometric measurements have been taken in various locations. Preselected reference targets were measured in the field with a GER Mark V spectroradiometer, and radiance measurements were taken to the lake using a Li-Cor LI 1800UW specroradiometer below and above the water surface. A comprehensive meteorological data set was obtained by joining the POLLUMET experiment which carried out measurements to investigate the summer smog in Switzerland on the same day. The quality assessment for the actual data set can be found in detail in Meyer et al. A parametric approach calculating the location of the airplane was used to simulate the observation geometry. This parametric preprocessing procedure, which takes care of effects of flight line and attitude variations as well as the pixel-by-pixel topographic corrections is described in Meyer. Author

N95-33771*# Canada Centre for Remote Sensing, Ottawa (Ontario).

IMPACT OF DIFFERENCES IN THE SOLAR IRRADIANCE SPECTRUM ON SURFACE REFLECTANCE RETRIEVAL WITH DIFFERENT RADIATIVE TRANSFER CODES **c43**

K. Staenz, D. J. Williams (MacDonald, Dettwiler and Associates Ltd., Richmond, British Columbia.), G. Fedosejevs, and P. M. Teillet *In* JPL, Summaries of the Fifth Annual JPL Airborne Earth Science Workshop. Volume 1: AVIRIS Workshop 23 Jan. 1995 p 153-156 (For primary document see N95-33730 12-42)
Avail: CASI HC A01/MF A02

Surface reflectance retrieval from imaging spectrometer data as acquired with the Airborne Visible/Infrared Imaging Spectrometer (AVIRIS) has become important for quantitative analysis. In order to calculate surface reflectance from remotely measured radiance, radiative transfer codes such as 5S and MODTRAN2 play an increasing role for removal of scattering and absorption effects of the atmosphere. Accurate knowledge of the exo-atmospheric solar irradiance (E(sub 0)) spectrum at the spectral resolution of the sensor is important for this purpose. The present study investigates the impact of differences in the solar irradiance function, as implemented in a modified version of 5S (M5S), 6S, and MODTRAN2, and as proposed by Green and Gao, on the surface reflectance retrieved from AVIRIS data. Reflectance measured in situ is used as a basis of comparison. Author

N95-33772*# Geological Survey, Denver, CO.

SPECTRAL IDENTIFICATION OF MINERALS USING IMAGING SPECTROMETRY DATA: EVALUATING THE EFFECTS OF SIGNAL TO NOISE AND SPECTRAL RESOLUTION USING THE TRICORDER ALGORITHM **c43**

Gregg A. Swayze and Roger N. Clark *In* JPL, Summaries of the Fifth Annual JPL Airborne Earth Science Workshop. Volume 1: AVIRIS Workshop 23 Jan. 1995 p 157-158 (For primary document see N95-33730 12-42)
Avail: CASI HC A01/MF A02

The rapid development of sophisticated imaging spectrometers and resulting flood of imaging spectrometry data has prompted a rapid parallel development of spectral-information extraction technology. Even though these extraction techniques have evolved along different lines (band-shape fitting, endmember unmixing, near-infrared analysis, neural-network fitting, and expert systems to name a few), all are limited by the spectrometer's signal to noise (S/N) and spectral resolution in producing useful information. This study grew from a need to quantitatively determine what effects these parameters have on our ability to differentiate between mineral absorption features using a band-shape fitting algorithm. We chose to evaluate the AVIRIS, HYDICE, MIVIS, GERIS, VIMS, NIMS, and ASTER instruments because they collect data over wide S/N and spectral-resolution ranges. The study evaluates the performance of the Tricorder algorithm, in differentiating between mineral spectra in the 0.4-2.5 micrometer spectral region. The strength of the Tricorder algorithm is in its ability to produce an easily understood comparison of band shape that can concentrate on small relevant portions of the spectra, giving it an advantage over most unmixing schemes, and in that it need not spend large amounts of time reoptimizing each time a new mineral component is added to its reference library, as is the case with neural-network schemes. We believe the flexibility of the Tricorder algorithm is unparalleled among spectral-extraction techniques and that the results from this study, although dealing with minerals, will have direct applications to spectral identification in other disciplines. Author

N95-33773*# Arizona State Univ., Tempe, AZ. Dept. of Geology.

PRELIMINARY STUDY OF KELSO DUNES USING AVIRIS, TM, AND AIRSAR **c43**

Pung Xu, Dan G. Blumberg, and Ronald Greeley *In* JPL, Summaries of the Fifth Annual JPL Airborne Earth Science Workshop. Volume 1: AVIRIS Workshop 23 Jan. 1995 p 159-161 (For primary document see N95-33730 12-42)
Avail: CASI HC A01/MF A02

Remote sensing of sand dunes helps in the understanding of aeolian process and provides important information about the regional geologic history, environmental change, and desertification. Remotely sensed data combined with field studies are valuable in studying dune morphology, regional aeolian dynamics, and aeolian depositional history. In particular, active and inactive sands of the Kelso Dunes have been studied using landsat TM and AIRSAR. In this report, we describe the use of AVIRIS data to study the Kelso dunes and to compare the AVIRIS information with that from TM and AIRSAR. Author

N95-33789*# Jet Propulsion Lab., California Inst. of Tech., Pasadena, CA.

SUMMARIES OF THE FIFTH ANNUAL JPL AIRBORNE EARTH SCIENCE WORKSHOP. VOLUME 2: TIMS WORKSHOP

Vincent J. Realmuto, ed. 23 Jan. 1995 52 p Conference held in Pasadena, CA, 23-26 Jan. 1995 Contains 35mm color slides as supplement
(Contract NAS7-1260; RTOP 665-81-00)
(NASA-CR-198923; JPL-Publ-95-1-Vol-2; NAS 1.26:198923) Avail: CASI HC A04/MF A01

This publication is the second volume of the summaries for the Fifth Annual JPL Airborne Earth Science Workshop, held in Pasadena, California, on January 23-26, 1995. The main workshop is divided into three smaller workshops as follows: (1) The Airborne Visible/Infrared Imaging Spectrometer (AVIRIS) workshop on January 23-24. The summaries for this workshop appear in Volume 1; (2) The Airborne Synthetic Aperture Radar (AIRSAR) workshop on January 25-26. The summaries for this workshop appear in volume 3; and (3) The Thermal Infrared Multispectral Scanner (TIMS)

workshop on January 26. The summaries for this workshop appear in this volume. For individual titles, see N95-33790 through N95-33800.

N95-33790*# Jet Propulsion Lab., California Inst. of Tech., Pasadena, CA.

ANALYSES OF TIMS AND AVIRIS DATA, INTEGRATED WITH FIELD AND LABORATORY SPECTRA, FOR LITHOLOGICAL AND MINERALOGICAL INTERPRETATION OF VULCANO ISLAND, ITALY c43

M. Fabrizia Buongiorno (Istituto Nazionale di Geofisica, Rome, Italy.), M. Paola Bogliolo (Istituto Nazionale di Geofisica, Rome, Italy.), Stefano Salvi (Istituto Nazionale di Geofisica, Rome, Italy.), David C. Pieri, and Francesco Geneselli (Istituto Nazionale di Geofisica, Rome, Italy.) *In its* Summaries of the Fifth Annual JPL Airborne Earth Science Workshop. Volume 2: TIMS Workshop 23 Jan. 1995 p 1-4 (For primary document see N95-33789 12-42)

Avail: CASI HC A01/MF A01

Vulcano Island is part of the Eolian archipelago, located about 25 km from the northeast coast of Sicily. The archipelago comprises seven major volcanic islands, two of which are active volcanoes (Vulcano and Stromboli). Vulcano covers an area of about 50 square km, and is about 10 km long. Explosive volcanic activity has predominated in the geological evolution of Vulcano Island, and there is no evidence that this pattern has ceased. Rather, the current situation is one of unrest, so a strict regimen of continuous geophysical and geochemical monitoring has been undertaken over the last decade. Though the year-round population of Vulcano is small (under 1000), during the summer the island becomes a very popular resort, and has thousands of additional tourists at any time throughout the high season, thus substantially increasing the number of people potentially at risk from an explosive eruption or other hazards such as noxious gas emissions (e.g., CO2, H2S, SO2). During the past ten years, remote sensing data have been repetitively acquired with optical and microwave airborne sensors. The present work shows the preliminary results of a study based on the integration of various remote sensing data sets with field spectroscopy, and other laboratory analyses, for the geological and geomorphological mapping of the island. It is hoped that such work will also usefully contribute to the evaluation of the volcanic hazard potential of the islands as well as to the evaluation of the status of its current activity. Derived from text

N95-33791*# Arizona State Univ., Tempe, AZ. Dept. of Geology.

URBAN REMOTE SENSING APPLICATIONS: TIMS OBSERVATIONS OF THE CITY OF SCOTTSDALE c43

Philip R. Christensen, David E. Melendrez, Donald L. Anderson, Victoria E. Hamilton, Melissa L. Wenrich, and Douglas Howard *In* JPL, Summaries of the Fifth Annual JPL Airborne Earth Science Workshop. Volume 2: TIMS Workshop 23 Jan. 1995 p 5-8 (For primary document see N95-33789 12-42)

Avail: CASI HC A01/MF A01

A research program has been initiated between Arizona State University and the City of Scottsdale, Arizona to study the potential applications of TIMS (Thermal Infrared Multispectral Scanner) data for urban scene classification, desert environmental assessment, and change detection. This program is part of a long-term effort to integrate remote sensing observations into state and local planning activities to improve decision making and future planning. Specific test sites include a section of the downtown Scottsdale region that has been mapped in very high detail as part of a pilot program to develop an extensive GIS database. This area thus provides excellent time history of the evolution of the city infrastructure, such as the timing and composition of street repavement. A second area of study includes the McDowell intensive study by state and local agencies to assess potential sites for urban development as well as preservation. These activities are of particular relevance as the Phoenix metropolitan area undergoes major expansion into the surrounding desert areas. The objectives of this study in urban areas are aimed at determining potential applications of TIMS data for classifying and assessing land use and surface temperatures. Land use centers on surface impermeability studies for storm runoff assessment and pollution control. These studies focus on determining the areal abundance of urban vegetation and undeveloped soil. Highly experimental applications include assessment and monitoring of pavement condition. Temperature studies focus on determining swimming pool area and temperature for use in monitoring evaporating and urban water consumption. These activities are of particular relevance as the Phoenix metropolitan area undergoes major expansion into the surrounding desert area. Derived from text

N95-33792*# Arizona State Univ., Tempe, AZ. Dept. of Geology.

FOR GEOLOGICAL INVESTIGATIONS WITH AIRBORNE THERMAL INFRARED MULTISPECTRAL IMAGES: TRANSFER OF CALIBRATION FROM LABORATORY SPECTROMETER TO TIMS AS ALTERNATIVE FOR REMOVING ATMOSPHERIC EFFECTS c43

Kenneth S. Edgett and Donald L. Anderson *In* JPL, Summaries of the Fifth Annual JPL Airborne Earth Science Workshop. Volume 2: TIMS Workshopp 9-12 (SEE N95-33789 12-42) 23 Jan. 1995 (For primary document see N95-33789 12-42)

Avail: CASI HC A01/MF A01

This paper describes an empirical method to correct TIMS (Thermal Infrared Multispectral Scanner) data for atmospheric effects by transferring calibration from a laboratory thermal emission spectrometer to the TIMS multispectral image. The method does so by comparing the laboratory spectra of samples gathered in the field with TIMS 6-point spectra for pixels at the location of field sampling sites. The transference of calibration also makes it possible to use spectra from the laboratory as endmembers in unmixing studies of TIMS data. Derived from text

N95-33793*# Arizona State Univ., Tempe, AZ. Dept. of Geology.

AEROLIAN EROSION, TRANSPORT, AND DEPOSITION OF VOLCANICLASTIC SANDS AMONG THE SHIFTING SAND DUNES, CHRISTMAS LAKE VALLEY, OREGON: TIMS IMAGE ANALYSIS c43

Kenneth S. Edgett, Michael S. Ramsey, and Philip R. Christensen *In* JPL, Summaries of the Fifth Annual JPL Airborne Earth Science Workshop. Volume 2: TIMS Workshop 23 Jan. 1995 p 13-16 (For primary document see N95-33789 12-42)

Avail: CASI HC A01/MF A01

Remote sensing is a tool that, in the context of aeolian studies, offers a synoptic view of a dune field, sand sea, or entire desert region. Blount et al. (1990) presented one of the first studies demonstrating the power of multispectral images for interpreting the dynamic history of an aeolian sand sea. Blount's work on the Gran Desierto of Mexico used a Landsat TM scene and a linear spectral mixing model to show where different sand populations occur and along what paths these sands may have traveled before becoming incorporated into dunes. Interpretation of sand transport paths and sources in the Gran Desierto led to an improved understanding of the origin and Holocene history of the dunes. With the anticipated advent of the EOS-A platform and ASTER thermal infrared capability in 1998, it will become possible to look at continental sand seas and map sand transport paths using 8-12 mu m bands that are well-suited to tracking silicate sediments. A logical extension of Blount's work is to attempt a similar study using thermal infrared images. One such study has already begun by looking at feldspar, quartz, magnetite, and clay distributions in the Kelso Dunes of southern California. This paper describes the geology and application of TIMS image analysis of a less-well known Holocene dune field in south central Oregon using TIMS data obtained in 1991. Derived from text

N95-33794*# Jet Propulsion Lab., California Inst. of Tech., Pasadena, CA.

THE JPL FIELD EMISSION SPECTROMETER Abstract Only c35

Simon J. Hook and Anne B. Kahle *In its* Summaries of the Fifth Annual JPL Airborne Earth Science Workshop. Volume 2: TIMS Workshop 23 Jan. 1995 p 17 (For primary document see N95-33789 12-42)

Avail: CASI HC A01/MF A01

The Jet Propulsion Laboratory (JPL) Field Emission Spectrometer (FES) was built by Designs and Prototypes based on a set of functional requirements supplied by JPL. The instrument has a spectral resolution of 6 wavenumbers (wn) and can acquire spectra from either the Mid Infrared (3-5 mu m) or the Thermal Infrared (8-12 pm) depending on whether the InSb or HgCdTe detector is installed respectively. The instrument consists of an optical head system unit and battery. The optical head which is tripod mounted includes the interferometer and detector dewar assembly. Wavelength calibration of the interferometer is achieved using a Helium-Neon laser diode. The dewar needs replenishing with liquid Nitrogen approximately every four hours. The system unit includes the controls for operation and the computer used for acquiring viewing and processing spectra. Radiometric

calibration is achieved with an external temperature-controlled blackbody that mounts on the fore-optics of the instrument. The blackbody can be set at 5 C increments between 10 and 55 C. The instrument is compact and weighs about 33 kg. Both the wavelength calibration and radiometric calibration of the instrument have been evaluated. The wavelength calibration was checked by comparison of the position of water features in a spectrum of the sky with their position in the output from a high resolution atmospheric model. The results indicatethat the features in the sky spectrum are within 6-8 wn of their position ill the model spectrum. The radiometric calibration was checked by first calibrating the instrument using the external blackbody supplied with the instrument and then measuring the radiance from another external blackbody at a series of temperatures. The temperatures of these radiance spectra were then recovered by inventing Planck's law and the recovered temperatures compared lo the measured blackbody temperature. These results indicate that radiometric calibration is good to 0.5 C over the range of temperatures 10 to 55 C. The results also indicate that the instrument drifts slowly over time and should be recalibrated every 20 to 30 minutes in the field to ensure good radiometric fidelity. The instrument has now been extensively tested in the field in the United States and Australia. These in situ field measurements are being used to validate emissivity spectra recovered from the Thermal Infrared Multispectral Scanner (TIMS) and also the Australian CO2 Laser. The availability of in situ measurements is proving crucial to validation of the spectra derived from the airborne instruments since many natural surfaces cannot be easily transported back to the laboratory. Author

N95-33795*# Arizona State Univ., Tempe, AZ. Dept. of Geology.
A CONFLICT OF WATER AND FIRE: REMOTE SENSING IMAGERY OF THE UINKARET VOLCANIC FIELD, GRAND CANYON, ARIZONA **c35**
Michael S. Ramsey *In* JPL, Summaries of the Fifth Annual JPL Airborne Earth Science Workshop. Volume 2: TIMS Workshopp 19-23 (SEE N95-33789 12-42) 23 Jan. 1995 (For primary document see N95-33789 12-42)
Avail: CASI HC A01/MF A01

The sedimentary geology of the western Grand Canyon consists of gently northeast dipping sandstones, shales, and carbonates. However, due to facies changes within the units, the geomorphology varies from that seen by visitors at the National Park Headquarters. There, the cliff and slope expression of the rocks is replaced in the west by a series of mesas, ridges, and horizontal platforms. The largest of these occurs on the Esplanade Sandstone within the Supai Formation. The Esplanade is formed by slope retreat of the overlying units and resistance to erosion by the underlying limestones. It is onto this platform that the lavas of the Uinkaret Plateau were emplaced. The Uinkaret lava field lies 120 km south of St. George, Utah and is tectonically defined by two major normal faults -- the Hurricane to the west and the Toroweap to the east. The purpose of this investigation was to collect visible, near and thermal infrared data at different periods of the day and year. It is expected that these data will provide the ability to retrieve water temperatures; monitor sediment loads; map and examine any changes in the near shore vegetation communities and understand some of the intricacies of the geology. This paper will serve, to some degree, as a progress report on the Grand Canyon study, since only a fraction of the data has been received and processed thus far. Data from the Thermal Infrared Multispectral Scanner (TIMS) and the Landsat Thematic Mapper simulator (NS001) were acquired simultaneously on April 4, 1994. A second data acquisition occurred on August 27, 1994. Initial analysis of the TIMS data indicates a remarkably noise-free data set with minimal atmospheric attenuation. environments is evident.

Derived from text

N95-33796*# Jet Propulsion Lab., California Inst. of Tech., Pasadena, CA.
THE 1994 LABORATORY CALIBRATION OF TIMS **c35**
Vincent J. Realmuto, Pavel Hajek, Mahadeva P. Sinha, and Thomas G. Chrien *In its* Summaries of the Fifth Annual JPL Airborne Earth Science Workshop. Volume 2: TIMS Workshop 23 Jan. 1995 p 25-28 (For primary document see N95-33789 12-42)
Avail: CASI HC A01/MF A01

This summary describes the spatial, spectral, and radiometric calibration of Thermal Infrared Multispectral Scanner (TIMS) performed at the Jet Propulsion Laboratory (JPL) Thermal Infrared Calibration Facility (TIRCAL) between May and August, 1994. The 1994 calibration of TIMS was the first to make use of the new EXABYTE (8mm helical-scan tape) recording system. With the new recorder, the TIMS data tapes may be read directly on any computer system that has an EXABYTE tape drive. We analyzed the calibration data sets using image processing procedures written in Interactive Data Language. Derived from text

N95-33797*# Jet Propulsion Lab., California Inst. of Tech., Pasadena, CA.
THE 1994 TIMS AIRBORNE CALIBRATION EXPERIMENT: CASTAIC LAKE, CALIFORNIA **c35**
Vincent J. Realmuto, Simon J. Hook, and Jeannette vandenBosch *In its* Summaries of the Fifth Annual JPL Airborne Earth Science Workshop. Volume 2: TIMS Workshop 23 Jan. 1995 p 29-32 (For primary document see N95-33789 12-42)
Avail: CASI HC A01/MF A01

This summary describes the 9 March 1994 Thermal Infrared Multispectral Scanner (TIMS) airborne calibration experiment conducted at Castaic Lake, California. This experiment was a collaborative effort between the TIMS and Advanced Spaceborne Thermal Emission and Reflection Radiometer (ASTER) science teams at the Jet Propulsion Laboratory (JPL). TIMS was flown on the NASA/Ames Research Center C130 with the new retractable air fence installed in the TIMS instrument bay. The purpose of this experiment was to determine if the fence would reduce the air turbulence in the TIMS instrument bay, thereby reducing the errors in calibration caused by wind-blast cooling of the blackbody reference sources internal to TIMS. Previous experiments have indicated that the wind blast effect could cause TIMS to over-estimate surface temperatures by more than 10 C. We have examined the TIMS data from twelve lines flown over Castaic Lake. Four of the lines were flown at an altitude of approximately 2.5 km (MSL), four at an altitude of approximately 6.7 km, and four at approximately 8.3 km. At each altitude there were flights with northern and southern headings, with the aircraft level and at a positive pitch (nose-up attitude). The suite of twelve flights was designed to subject the TIMS/air fence system to different wind conditions and air temperatures. The TIMS flights were supported by a ground-truth team, who measured lake surface temperatures from a boat, and an atmosphere characterization team, who launched an airsonde and measured solar irradiance with a Reagan Sun Photometer. The Reagan measurements were used to construct a time-series of estimates of the total abundance of water vapor in the atmospheric column. These estimates were used to constrain modifications of the airsonde water vapor profile measurements made when processing the TIMS data with a customized version of the MODTRAN radiative transfer code.

Derived from text

N95-33798*# Arizona State Univ., Tempe, AZ. Dept. of Geology.
DISCRIMINATION OF ALKALINITY IN GRANITOID ROCKS: A POTENTIAL TIMS APPLICATION **c43**
Steven W. Ruff *In* JPL, Summaries of the Fifth Annual JPL Airborne Earth Science Workshop. Volume 2: TIMS Workshop 23 Jan. 1995 p 33-36 (For primary document see N95-33789 12-42)
Avail: CASI HC A01/MF A01

In mineral exploration, the ability to distinguish and map petrochemical variations of magmatic rocks can be a useful reconnaissance tool. Alkalinity is one such petrochemical parameter and is used in the characterization of granitoid rocks. In quartz normative plutonic rocks, alkalinity is related to the composition and abundance of feldspars. Together with quartz abundance, knowledge of feldspar modes allows the classification of these igneous rocks according to the Streckeisen diagram. Alternative classification schemes rely on whole rock geochemistry instead of mineral identifications. The relative ease of obtaining whole rock analyses means that geochemical classifications tend to be favored in exploration geology. But the technique of thermal infrared spectroscopy of rocks yields information on mineralogy and is one that can be applied remotely. The goal of the current work then is to establish whether data from TIMS can be used to distinguish the mineralogical variations that relate to alkalinity. An ideal opportunity to test this thesis arises from the work presented in a paper by Dewitt (1989). This paper contains the results of mapping and analysis of Proterozoic plutonic rocks in north-central Arizona. The map resulting from this work delineates plutons according to alkalinity in an effort to establish a trend or polarity in the regional magmatism. Also contained within this paper are brief descriptions of the mineralogy of half of the region's plutons. This combination of mineralogical and geochemical information was the rationale

behind choosing this area as a site for TIMS over flights. A portion of the region centered on the northern Bradshaw Mountains was selected because it contains plutons of all three alkalinity classifications (alkali-calcic, calc-alkalic, and calic) present on DeWitt's map within a relatively small area. The site was flown in August of 1994 and the data received a few days before the writing of this manuscript. Most of this paper is devoted to the description of laboratory based spectroscopy and spectral simulations. These are required to gain insight into the correct procedures for enhancing the relatively small differences in the low spectral resolution TIMS data. Derived from text

N95-33799*# Jet Propulsion Lab., California Inst. of Tech., Pasadena, CA.

TIMS OBSERVATIONS OF SURFACE EMISSIVITY IN HAPEX-Sahel **c43**

Thomas Schmugge (Food and Drug Administration, Bethesda, MD.), Simon Hook, and Anne Kahle *In its* Summaries of the Fifth Annual JPL Airborne Earth Science Workshop. Volume 2: TIMS Workshop 23 Jan. 1995 p 37 (For primary document see N95-33789 12-42)
Avail: CASI HC A01/MF A01

The Thermal Infrared Multispectral Scanner (TIMS) was flown on the NASA C-130 aircraft for a series of 12 flights during HAPEX-Sahel at altitudes ranging from 0.25 to 6 km (0.6 to 15 m resolution). TIMS provides coverage of the 8 to 12 micrometer thermal infrared band in 6 contiguous channels. Thus it is possible to observe the spectral behavior of the surface emissivity over this wavelength interval. Derived from text

N95-33800*# Arizona State Univ., Tempe, AZ. Dept. of Geology.

A FIELD- AND LABORATORY-BASED QUANTITATIVE ANALYSIS OF ALLUVIUM: RELATING ANALYTICAL RESULTS TO TIMS DATA **c43**

Melissa L. Wenrich, Victoria E. Hamilton, and Philip R. Christensen *In* JPL, Summaries of the Fifth Annual JPL Airborne Earth Science Workshop. Volume 2: TIMS Workshop 23 Jan. 1995 p 39-42 (For primary document see N95-33789 12-42)
Avail: CASI HC A01/MF A01

Thermal Infrared Multispectral Scanner (TIMS) data were acquired over the McDowell Mountains northeast of Scottsdale, Arizona during August 1994. The raw data were processed to emphasize lithologic differences using a decorrelation stretch and assigning bands 5, 3, and 1 to red, green, and blue, respectively. Processed data of alluvium flanking the mountains exhibit moderate color variation. The objective of this study was to determine, using a quantitative approach, what environmental variable(s), in the absence of bedrock, is/are responsible for influencing the spectral properties of the desert alluvial surface. Derived from text

N95-33801*# Jet Propulsion Lab., California Inst. of Tech., Pasadena, CA.

SUMMARIES OF THE FIFTH ANNUAL JPL AIRBORNE EARTH SCIENCE WORKSHOP. VOLUME 3: AIRSAR WORKSHOP

Jakob vanZyl, ed. 23 Jan. 1995 63 p Workshop held in Pasadena, CA, 23-26 Jan. 1995 Contains 35mm color slides as supplement
(Contract NAS7-1260; RTOP 665-81-00)
(NASA-CR-198924; JPL-Publ-95-1-Vol-3; NAS 1.26:198924) Avail: CASI HC A04/MF A01

This publication is the third containing summaries for the Fifth Annual JPL Airborne Earth Science Workshop, held in Pasadena, California, on January 23-26, 1995. The main workshop is divided into three smaller workshops as follows: (1) The Airborne Visible/Infrared Imaging Spectrometer (AVIRIS) workshop, on January 23-24. The summaries for this workshop appear in Volume 1; (2) The Airborne synthetic Aperture Radar (AIRSAR) workshop, on January 25-26. The summaries for this workshop appear in this volume; and (3) The Thermal Infrared Multispectral Scanner (TIMS) workshop, on January 26. The summaries for this workshop appear in Volume 2. For individual titles, see N95-33802 through N95-33816.

N95-33802*# Arizona State Univ., Tempe, AZ. Dept. of Geology.

NEW OBSERVATIONS OF BOLIVIAN WIND STREAKS BY JPL AIRBORNE SAR: PRELIMINARY RESULTS **c43**

Dan G. Blumberg and Ronald Greeley *In* JPL, Summaries of the Fifth Annual JPL Airborne Earth Science Workshop. Volume 3: AIRSAR Workshop 23 Jan. 1995 p 1-4 (For primary document see N95-33801 12-42)
Avail: CASI HC A01/MF A01

In 1993 NASA's Jet Propulsion Laboratory Airborne Synthetic Aperture Radar system (AIRSAR) was deployed to South America to collect multi-parameter radar data over pre-selected targets. Among the sites targeted was a series of wind streaks located in the Altiplano of Bolivia. The objective of this investigation is to study the effect of wavelength, polarization, and incidence angle on the visibility of wind streaks in radar data. Because this is a preliminary evaluation of the recently acquired data we will focus on one scene and, thus, only on the effects of wavelength and polarization. Wind streaks provide information on the near-surface prevailing winds and on the abundance of winderodible material, such as sand. The potential for a free-flyer radar system that could provide global radar images in multiple wavelengths, polarizations, and incidence angles requires definition of system parameters for mission planning. Furthermore, thousands of wind streaks were mapped from Magellan radar images of Venus; their interpretation requires an understanding of the interaction of radar with wind streaks and the surrounding terrain. Our experiment was conducted on wind streaks in the Altiplano of Bolivia to address these issues. Derived from text

N95-33803*# Jet Propulsion Lab., California Inst. of Tech., Pasadena, CA.

MEASURING SOIL MOISTURE WITH IMAGING RADARS **c43**

Pascale C. Dubois, Jakob vanZyl, and Ted Engman (National Aeronautics and Space Administration. Goddard Space Flight Center, Greenbelt, MD.) *In its* Summaries of the Fifth Annual JPL Airborne Earth Science Workshop. Volume 3: AIRSAR Workshop 23 Jan. 1995 p 5-8 (For primary document see N95-33801 12-42)
Avail: CASI HC A01/MF A01

An empirical model was developed to infer soil moisture and surface roughness from radar data. The accuracy of the inversion technique is assessed by comparing soil moisture obtained with the inversion technique to in situ measurements. The effect of vegetation on the inversion is studied and a method to eliminate the areas where vegetation impairs the algorithm is described. Derived from text

N95-33804*# Jet Propulsion Lab., California Inst. of Tech., Pasadena, CA.

USE OF TOPSAR DIGITAL ELEVATION DATA TO DETERMINE THE 3-DIMENSIONAL SHAPE OF AN ALLUVIAL FAN **c43**

Tom G. Farr *In its* Summaries of the Fifth Annual JPL Airborne Earth Science Workshop. Volume 3: AIRSAR Workshop 23 Jan. 1995 p 9-12 (For primary document see N95-33801 12-42)
Avail: CASI HC A01/MF A01

Landforms in arid regions record the interplay between tectonic forces and climate. Alluvial fans are a common landform in desert regions where the rate of uplift is greater than weathering or sedimentation. Changes in uplift rate or climatic conditions can lead to isolation of the currently forming fan surface through entrenchment and construction of another fan either further from the mountain front (decreased uplift or increased runoff) or closer to the mountain front (increased uplift or decreased runoff). Thus, many alluvial fans are made up of a mosaic of fan units of different age, some older than 1 million years. For this reason, determination of the stages of fan evolution can lead to a history of uplift and runoff. In an attempt to separate the effects of tectonic (uplift) and climatic (weathering, runoff, sedimentation) processes on the shapes of alluvial fan units, a modified conic equation developed by Troeh (1965) was fitted to TOPSAR digital topographic data for the Trail Canyon alluvial fan in Death Valley, California. This allows parameters for the apex position, slope, and radial curvature to be compared with unit age. Derived from text

N95-33805*# Jet Propulsion Lab., California Inst. of Tech., Pasadena, CA.

ACCURATE ESTIMATION OF SIGMA(EXP 0) USING AIRSAR DATA **c43**

Francesco Holecz and Eric Rignot *In its* Summaries of the Fifth Annual JPL Airborne Earth Science Workshop. Volume 3: AIRSAR Workshop 23 Jan. 1995 p 13-16 Sponsored by Swiss Academy of Science; and the Holderbank Foundation (For primary document see N95-33801 12-42)
Avail: CASI HC A01/MF A01

During recent years signature analysis, classification, and modeling of

Synthetic Aperture Radar (SAR) data as well as estimation of geophysical parameters from SAR data have received a great deal of interest. An important requirement for the quantitative use of SAR data is the accurate estimation of the backscattering coefficient sigma(exp 0). In terrain with relief variations radar signals are distorted due to the projection of the scene topography into the slant range-Doppler plane. The effect of these variations is to change the physical size of the scattering area, leading to errors in the radar backscatter values and incidence angle. For this reason the local incidence angle, derived from sensor position and Digital Elevation Model (DEM) data must always be considered. Especially in the airborne case, the antenna gain pattern can be an additional source of radiometric error, because the radar look angle is not known precisely as a result of the the aircraft motions and the local surface topography. Consequently, radiometric distortions due to the antenna gain pattern must also be corrected for each resolution cell, by taking into account aircraft displacements (position and attitude) and position of the backscatter element, defined by the DEM data. In this paper, a method to derive an accurate estimation of the backscattering coefficient using NASA/JPL AIRSAR data is presented. The results are evaluated in terms of geometric accuracy, radiometric variations of sigma(exp 0), and precision of the estimated forest biomass.

Derived from text

N95-33806*# National Aeronautics and Space Administration. Goddard Space Flight Center, Greenbelt, MD.

REMOTELY SENSED INDICATORS OF HABITAT HETEROGENEITY AND BIOLOGICAL DIVERSITY: A PRELIMINARY REPORT **c43**

Marc Imhoff, Thomas Sisk (Interior Dept., Washington, DC.), Anthony Milne (New South Wales Univ., Kensington, Australia.), Garth Morgan (Defence Science and Technology Organisation, Melbourne, Australia.), and Tony Orr (Defence Science and Technology Organisation, Melbourne, Australia.) *In* JPL, Summaries of the Fifth Annual JPL Airborne Earth Science Workshop. Volume 3: AIRSAR Workshop 23 Jan. 1995 p 17-20 (For primary document see N95-33801 12-42)

Avail: CASI HC A01/MF A01

The relationship between habitat area, spatial dynamics of the landscape, and species diversity is an important theme in population and conservation biology. Of particular interest is how populations of various species are affected by increasing habitat edges due to fragmentation. Over the last decade, assumptions regarding the effects of habitat edges on biodiversity have fluctuated wildly, from the belief that they have a positive effect to the belief that they have a clearly negative effect. This change in viewpoint has been brought about by an increasing recognition of the importance of geographic scale and a reinterpretation of natural history observations. In this preliminary report from an ongoing project, we explore the use of remote sensing technology and geographic information systems to further our understanding of how species diversity and population density are affected by habitat heterogeneity and landscape composition. A primary feature of this study is the investigation of SAR for making more rigorous investigations of habitat structure by exploiting the interaction between radar backscatter and vegetation structure and biomass. A major emphasis will be on the use of SAR data to define relative structural types based on measures of structural consolidation using the vegetation surface area to volume ratio (SA/V). Past research has shown that SAR may be sensitive to this form of structural expression which may affect biodiversity.

Derived from text

N95-33807*# Naval Research Lab., Washington, DC. Remote Sensing Div.

POLARIZATION AND WAVELENGTH DIVERSITIES OF GULF STREAM FRONTS IMAGED BY AIRSAR **c48**

J. S. Lee, R. W. Jansen, G. O. Marmorino, and S. R. Chubb *In* JPL, Summaries of the Fifth Annual JPL Airborne Earth Science Workshop. Volume 3: AIRSAR Workshop 23 Jan. 1995 p 21-24 (For primary document see N95-33801 12-42)

Avail: CASI HC A01/MF A01

During the 1990 Gulf Stream Experiment, NASA/JPL AIRSAR imaged the north edge of the Gulf Stream near the coast of Virginia. Simultaneous in-situ measurements of currents, temperatures, salinities, etc. were made for several crossings of the north edge by the R/V Cape Henlopen. Measurements identified two fronts with shearing and converging flows. The polarimetric SAR images from the fronts showed two bright linear features. One of them corresponds to the temperature front, which separated the warm Gulf Stream water to the south from a cool, freshwater filament to the north. The other line, located about 8 km north of the temperature front, is believed to correspond to the velocity front between the filament and the slope water. At these fronts, wave-current interactions produced narrow bands of steep and breaking waves manifesting higher radar returns in polarimetric SAR images. In general, our AIRSAR imagery shows that the signal-to-clutter ratio of radar cross sections for the temperature front is higher than that of the velocity front. In this paper, we study the polarization and wavelength diversities of radar response of these two fronts using the P-, L-, and C-Band Polarimetric SAR data. The north-south flight path of the AIRSAR crossed the temperature front several times and provided valuable data for analysis. Three individual passes are investigated. We found that for the temperature front, the cross-pol (HV) responses are much higher than co-pol responses (VV and HH), and that P-Band HV has the highest signal to clutter ratio. For the velocity front, the ratio is the strongest in P-Band VV, and it is indistinguishable for all polarizations in C-Band. The radar cross sections for all three polarization (HH, HV, and VV) and for all three bands are modelled using an ocean wave model and a composite Bragg scattering model. In our initial investigations, the theoretical model agrees qualitatively with the AIRSAR observations.

Derived from text

N95-33808*# Jet Propulsion Lab., California Inst. of Tech., Pasadena, CA.

BAYES CLASSIFICATION OF INTERFEROMETRIC TOPSAR DATA

Abstract Only **c43**

T. R. Michel, E. Rodriguez, B. Houshmand, and R. Carande *In its* Summaries of the Fifth Annual JPL Airborne Earth Science Workshop. Volume 3: AIRSAR Workshop 23 Jan. 1995 p 25 (For primary document see N95-33801 12-42)

Avail: CASI HC A01/MF A01

We report the Bayes classification of terrain types at different sites using airborne interferometric synthetic aperture radar (INSAR) data. A Gaussian maximum likelihood classifier was applied on multidimensional observations derived from the SAR intensity, the terrain elevation model, and the magnitude of the interferometric correlation. Training sets for forested, urban, agricultural, or bare areas were obtained either by selecting samples with known ground truth, or by k-means clustering of random sets of samples uniformly distributed across all sites, and subsequent assignments of these clusters using ground truth. The accuracy of the classifier was used to optimize the discriminating efficiency of the set of features that was chosen. The most important features include the SAR intensity, a canopy penetration depth model, and the terrain slope. We demonstrate the classifier's performance across sites using a unique set of training classes for the four main terrain categories. The scenes examined include San Francisco (CA) (predominantly urban and water), Mount Adams (WA) (forested with clear cuts), Pasadena (CA) (urban with mountains), and Antioch Hills (CA) (water, swamps, fields). Issues related to the effects of image calibration and the robustness of the classification to calibration errors are explored. The relative performance of single polarization Interferometric data classification is contrasted against classification schemes based on polarimetric SAR data. Author

N95-33809*# British Columbia Univ., Vancouver (British Columbia).

TERRAIN CLASSIFICATION USING CIRCULAR POLARIMETRIC FEATURES **c43**

David G. Michelson, Ian G. Cumming, and Charles E. Livingstone (Canada Centre for Remote Sensing, Ottawa, Ontario.) *In* JPL Summaries of the Fifth Annual JPL Airborne Earth Science Workshop. Volume 3: AIRSAR Workshop 23 Jan. 1995 p 27-30 (For primary document see N95-33801 12-42)

Avail: CASI HC A01/MF A01

Conventional representations of polarization response are referred to a horizontally and vertically polarized basis. Recent studies by Freeman and Durden, van Zyl, and others suggest that alternative polarimetric features which more easily resolve the contributions of simple scattering mechanisms such as odd-bounce, even-bounce, and diffuse scattering could offer several advantages in terrain classification. The circular polarization covariance matrix is a potential source of such features. In this paper, we derive its relationship to the Stokes matrix, describe some of its properties, and compare the utility of linear and circular polarimetric features in classifying an AIRSAR scene containing urban, park, and ocean terrain. Derived from text

N95-33810*# New Mexico Univ., Albuquerque, NM.
USE OF AIRSAR TO IDENTIFY WOODY SHRUB INVASION AND OTHER INDICATORS OF DESERTIFICATION IN THE JORNADA LTER **c43**

H. Brad Musick, Gerald G. Schaber (Geological Survey, Flagstaff, AZ.), and Carol S. Breed (Geological Survey, Flagstaff, AZ.) *In* JPL, Summaries of the Fifth Annual JPL Airborne Earth Science Workshop. Volume 3: AIRSAR Workshop 23 Jan. 1995 p 31-34 (For primary document see N95-33801 12-42)
Avail: CASI HC A01/MF A01

The replacement of semidesert grassland by woody shrubland is a widespread form of desertification. This change in physiognomy and species composition tends to sharply reduce the productivity of the land for grazing by domestic livestock, increase soil erosion and reduce soil fertility, and greatly alter many other aspects of ecosystem structure and functioning. Remote sensing methods are needed to assess and monitor shrubland encroachment. Detection of woody shrubs at low density would provide a particularly useful baseline on which to access changes, because an initially low shrub density often tends to increase even after cessation of the disturbance (e.g., overgrazing, drought, or fire suppression) responsible for triggering the initial stages of the invasion (Grover and Musick, 1990). Limited success has been achieved using optical remote sensing. In contrast to other forms of desertification, biomass does not consistently decrease with a shift from grassland to shrubland. Estimation of green vegetation amount (e.g., by NDVI) is thus of limited utility, unless the shrubs and herbaceous plants differ consistently in phenology and the area can be viewed during a season when only one of these is green. The objective of this study was to determine if the potential sensitivity of active microwave remote sensing to vegetation structure could be used to assess the degree of shrub invasion of grassland. Polarimetric Airborne Synthetic Aperture Radar (AIRSAR) data were acquired for a semiarid site containing varied mixtures of shrubs and herbaceous vegetation and compared with ground observations of vegetation type and other landsurface characteristics. In this preliminary report we examine the response of radar backscatter intensity to shrub density. The response of other multipolarization parameters will be examined in future work. Derived from text

N95-33811*# Jet Propulsion Lab., California Inst. of Tech., Pasadena, CA.
THE UNIQUE RADAR SCATTERING PROPERTIES OF SILICIC LAVA FLOWS AND DOMES **c43**

Jeffrey J. Plaut, Ellen R. Stofan, Steven W. Anderson (Black Hills State Univ., Spearfish, SD.), and David A. Crown (Pittsburgh Univ., Pittsburgh, PA.) *In its* Summaries of the Fifth Annual JPL Airborne Earth Science Workshop. Volume 3: AIRSAR Workshop 23 Jan. 1995 p 35-38 (For primary document see N95-33801 12-42)
Avail: CASI HC A01/MF A01

Silicic (silica-rich) lava flows, such as rhyolite, rhyodacite, and dacite, possess unique physical properties primarily because of the relatively high viscosity of the molten lava. Silicic flows tend to be thicker than basaltic flows, and the resulting large-scale morphology is typically a steep-sided dome or flow lobe, with aspect ratios (height/length) sometimes approaching unity. The upper surfaces of silicic domes and flows are normally emplaced as relatively cool, brittle slabs that fracture as they are extruded from the central vent areas, and are then rafted away toward the flow margin as a brittle carapace above a more ductile interior layer. This mode of emplacement results in a surface with unique roughness characteristics, which can be well-characterized by multiparameter synthetic aperture radar (SAR) observations. In this paper, we examine the scattering properties of several silicic domes in the Inyo volcanic chain in the Eastern Sierra of California, using AIRSAR and TOPSAR data. Field measurements of intermediate-scale (cm to tens of m) surface topography and block size are used to assess the mechanisms of the scattering process, and to quantify the unique roughness characteristics of the flow surfaces. Derived from text

N95-33812*# Jet Propulsion Lab., California Inst. of Tech., Pasadena, CA.
ON THE POTENTIAL OF LONG WAVELENGTH IMAGING RADARS FOR MAPPING VEGETATION TYPES AND WOODY BIOMASS IN TROPICAL RAIN FORESTS **c43**

Eric J. Rignot, Reiner Zimmermann, and Ram Oren *In its* Summaries of the Fifth Annual JPL Airborne Earth Science Workshop. Volume 3: AIRSAR Workshop 23 Jan. 1995 p 39-41 (For primary document see N95-33801 12-42)
Avail: CASI HC A01/MF A01

In the tropical rain forests of Manu, in Peru, where forest biomass ranges from 4 kg/sq m in young forest succession up to 100 kg/sq m in old, undisturbed floodplain stands, the P-band polarimetric radar data gathered in June of 1993 by the AIRSAR (Airborne Synthetic Aperture Radar) instrument separate most major vegetation formations and also perform better than expected in estimating woody biomass. The worldwide need for large scale, updated biomass estimates, achieved with a uniformly applied method, as well as reliable maps of land cover, justifies a more in-depth exploration of long wavelength imaging radar applications for tropical forests inventories. Derived from text

N95-33813*# Canada Centre for Remote Sensing, Ottawa (Ontario). Applications Div.
LITHOLOGIC CONTROLS ON AIRSAR SIGNATURES OF BEDROCK AND ALLUVIUM, AT LUNAR CRATER, NEVADA **c43**

Benoit Rivard, Marc Dlorio, and Paul Budkewitsch *In* JPL, Summaries of the Fifth Annual JPL Airborne Earth Science Workshop. Volume 3: AIRSAR Workshop 23 Jan. 1995 p 43-46 (For primary document see N95-33801 12-42)
Avail: CASI HC A01/MF A01

Radar backscatter intensity as measured by calibrated synthetic aperture radar (SAR) systems is primarily controlled by three factors: local incidence angle, wavelength-scale roughness, and dielectric permittivity of surface materials. In order to make adequate use of radar observations for geological investigations of surface type, the relationships between lithology and the above characteristics must be adequately understood. In arid terrains weathering signatures (e.g. fracturing, debris grain size and shape, slope characteristics) are controlled to some extent by lithologic characteristics of the parent bedrock. These textural features of outcrops and their associated debris control radar backscatter to varying degrees. The quad-polarization JPL AIRSAR system allows sampling of textures at three distinct wavelength scales: C-band (5.66 cm), L-band (23.98 cm), and P-band (68.13 cm). This paper presents a discussion of AIRSAR data using recent field observations of weathered felsic and basaltic volcanic rock units exposed in the southern part of the Lunar Crater Volcanic Field, in the Pancake Range of central Nevada. The focus is on the relationship of radar backscatter at multiple wavelengths to weathering style and parent bedrock lithology. Derived from text

N95-33814*# Jet Propulsion Lab., California Inst. of Tech., Pasadena, CA.
ESTIMATION OF PENETRATION OF FOREST CANOPIES BY INTERFEROMETRIC SAR MEASUREMENTS Abstract Only **c43**

Ernesto Rodriguez, Thierry R. Michel, and David J. Harding (National Aeronautics and Space Administration. Goddard Space Flight Center, Greenbelt, MD.) *In its* Summaries of the Fifth Annual JPL Airborne Earth Science Workshop. Volume 3: AIRSAR Workshop 23 Jan. 1995 p 47 (For primary document see N95-33801 12-42)
Avail: CASI HC A01/MF A01

In contrast to traditional Synthetic Aperture Radar (SAR), an Interferometric SAR (INSAR) yields two additional measurements: the phase difference and the correlation between the two interferometric channels. The phase difference has been used to estimate topographic height. For homogeneous surfaces, the correlation depends on the system signal-to-noise (SNR) ratio, the interferometer parameters, and the local slope. In the presence of volume scattering, such as that encountered in vegetation canopies, the correlation between the two channels is also dependent on the degree of penetration of the radiation into the scattering medium. In this paper, we propose a method for removing system and slope effects in order to obtain the decorrelation due to penetration alone. The sensitivities and accuracy of the proposed method are determined by Monte Carlo experiments, and we show that the proposed technique has sufficient sensitivity to provide penetration measurements for airborne SAR systems. Next, we provide a theoretical model to estimate the degree of penetration in a way which is independent of the details of the scattering medium. We also present a model for the correlation from non-homogeneous layers. We assess the sensitivity of the proposed inversion technique to these inhomogeneous situations. Finally, we present a comparison of the

interferometric results against in situ data obtained by an airborne laser profilometer which provides a direct measurement of tree height and an estimate of the vegetation density profile in the forested areas around Mt. Adams, WA. Author

N95-33815*# Jet Propulsion Lab., California Inst. of Tech., Pasadena, CA.

REGIONAL MAPPING OF FOREST CANOPY WATER CONTENT AND BIOMASS USING AIRSAR IMAGES OVER BOREAS STUDY AREA

Abstract Only **c43**

Sasan Saatchi, Eric Rignot, and Jakob vanZyl *In its* Summaries of the Fifth Annual JPL Airborne Earth Science Workshop. Volume 3: AIRSAR Workshop 23 Jan. 1995 p 49 (For primary document see N95-33801 12-42)

Avail: CASI HC A01/MF A01

In recent years, monitoring vegetation biomass over various climate zones has become the primary focus of several studies interested in assessing the role of the ecosystem responses to climate change and human activities. Airborne and spaceborne Synthetic Aperture Radar (SAR) systems provide a useful tool to directly estimate biomass due to its sensitivity to structural and moisture characteristics of vegetation canopies. Even though the sensitivity of SAR data to total aboveground biomass has been successfully demonstrated in many controlled experiments over boreal forests and forest plantations, so far, no biomass estimation algorithm has been developed. This is mainly due to the fact that the SAR data, even at lowest frequency (P-band) saturates at biomass levels of about 200 tons/ha, and the structure and moisture information in the SAR signal forces the estimation algorithm to be forest type dependent. In this paper, we discuss the development of a hybrid forest biomass algorithm which uses a SAR derived land cover map in conjunction with a forest backscatter model and an inversion algorithm to estimate forest canopy water content. It is shown that unlike the direct biomass estimation from SAR data, the estimation of water content does not depend on the seasonal and/or environmental conditions. The total aboveground biomass can then be derived from canopy water content for each type of forest by incorporating other ecological information. Preliminary results from this technique over several boreal forest stands indicate that (1) the forest biomass can be estimated with reasonable accuracy, and (2) the saturation level of the SAR signal can be enhanced by separating the crown and trunk biomass in the inversion algorithm. We have used the JPL AIRSAR data over BOREAS southern study area to test the algorithm and to generate regional scale water content and biomass maps. The results are compared with ground data and the sources of errors are discussed. Several SAR images in synoptic modes are used to generate the parameter maps. The maps are then combined to generate mosaic maps over the BOREAS modeling grid. Author

N95-33816*# National Aeronautics and Space Administration. Goddard Space Flight Center, Greenbelt, MD.

APPLICATION OF IEM MODEL ON SOIL MOISTURE AND SURFACE ROUGHNESS ESTIMATION **c43**

Jiancheng Shi (California Univ., Santa Barbara, CA.), J. R. Wang, P. E. ONeill, A. Y. Hsu, and E. T. Engman *In* JPL, Summaries of the Fifth Annual JPL Airborne Earth Science Workshop. Volume 3: AIRSAR Workshop 23 Jan. 1995 p 51-54 (For primary document see N95-33801 12-42)

Avail: CASI HC A01/MF A01

Monitoring spatial and temporal changes of soil moisture are of importance to hydrology, meteorology, and agriculture. This paper reports a result on study of using L-band SAR imagery to estimate soil moisture and surface roughness for bare fields. Due to limitations of the Small Perturbation Model, it is difficult to apply this model on estimation of soil moisture and surface roughness directly. In this study, we show a simplified model derived from the Integral Equation Model for estimation of soil moisture and surface roughness. We show a test of this model using JPL L-band AIRSAR data. Author

43 EARTH RESOURCES AND REMOTE SENSING

Includes remote sensing of earth resources by aircraft and spacecraft; photogrammetry; and aerial photography.

For instrumentation see *35 Instrumentation and Photography.*

N95-32676*# San Diego State Univ., San Diego, CA. Dept. of Geography.

CANOPY REFLECTANCE MODELLING OF SEMIARID VEGETATION Final Report, 1 Jan. 19990 - 31 Dec. 1994

Janet Franklin 1994 31 p

(Grant NAGw-2031)

(NASA-CR-199117; NAS 1.26:199117) Avail: CASI HC A03/MF A01

Three different types of remote sensing algorithms for estimating vegetation amount and other land surface biophysical parameters were tested for semiarid environments. These included statistical linear models, the Li-Strahler geometric-optical canopy model, and linear spectral mixture analysis. The two study areas were the National Science Foundation's Jornada Long Term Ecological Research site near Las Cruces, NM, in the northern Chihuahuan desert, and the HAPEX-Sahel site near Niamey, Niger, in West Africa, comprising semiarid rangeland and subtropical crop land. The statistical approach (simple and multiple regression) resulted in high correlations between SPOT satellite spectral reflectance and shrub and grass cover, although these correlations varied with the spatial scale of aggregation of the measurements. The Li-Strahler model produced estimated of shrub size and density for both study sites with large standard errors. In the Jornada, the estimates were accurate enough to be useful for characterizing structural differences among three shrub strata. In Niger, the range of shrub cover and size in short-fallow shrublands is so low that the necessity of spatially distributed estimation of shrub size and density is questionable. Spectral mixture analysis of multiscale, multitemporal, multispectral radiometer data and imagery for Niger showed a positive relationship between fractions of spectral endmembers and surface parameters of interest including soil cover, vegetation cover, and leaf area index. Author

N95-32707# General Accounting Office, Washington, DC. National Security and International Affairs Div.

REPORT TO THE CHAIRMAN, COMMITTEE ON SCIENCE, HOUSE OF REPRESENTATIVES. NASA'S EARTH OBSERVING SYSTEM: ESTIMATED FUNDING REQUIREMENTS

9 Jun. 1995 15 p

(GAO/NSIAD-95-175; B-261656) Avail: CASI HC A03/MF A01; GAO, PO Box 6015, Gaithersburg, MD 20877 HC

Funding requirements for the Earth Observing System (EOS) baseline program were estimated to be $33 billion for fiscal years 1991-2022. NASA is studying ways to reduce future EOS funding requirements and expects to substantially change the baseline program when these studies are completed in July 1995. Preliminary results of these studies indicate that technology development and operational improvements could reduce annual funding for the second and third satellites in each series by as much as 30%. If NASA were able to reduce annual funding by 30% in future years, the estimated total funding requirement drops to $27 billion. NASA officials believe that further reductions may be possible from increased collaboration with other agencies, international partners, and the commercial sector. Derived from text

N95-32717*# California Univ., Santa Barbara, CA. Inst. for Computational Earth System Science.

LAND SURFACE TEMPERATURE MEASUREMENTS FROM EOS MODIS DATA Semiannual Report, Jan. - Jun. 1995

Zhengming Wan Jun. 1995 16 p

(Contract NAS5-31370)

(NASA-CR-199082; NAS 1.26:199082) Avail: CASI HC A03/MF A01

A significant progress has been made in TIR instrumentation which is required to establish the spectral BRDF/emissivity knowledge base of land-surface materials and to validate the land-surface temperature (LST) algorithms. The SIBRE (spectral Infrared Bidirectional Reflectance and Emissivity) system and a TIR system for measuring spectral directional-hemispherical emissivity have been completed and tested successfully. Optical properties and performance features of key components (including spectrometer, and TIR source) of these systems have been

characterized by integrated use of local standards (blackbody and reference plates). The stabilization of the spectrometer performance was improved by a custom designed and built liquid cooling system. Methods and procedures for measuring spectral TIR BRDF and directional-hemispheric emissivity with these two systems have been verified in sample measurements. These TIR instruments have been used in the laboratory and the field, giving very promising results. The measured spectral emissivities of water surface are very close to the calculated values based on well established water refractive index values in published papers. Preliminary results show that the TIR instruments can be used for validation of the MODIS LST algorithm in homogeneous test sites. The beta-3 version of the MODIS LST software is being prepared for its delivery scheduled in the early second half of this year. Author

N95-32823*# Georgia Inst. of Tech., Atlanta, GA. School of Electrical and Computer Engineering.

AIRBORNE PASSIVE POLARIMETRIC MEASUREMENTS OF SEA SURFACE ANISOTROPY AT 92 GHz

D. B. Kunkee and A. J. Gasiewski [1994] 3 p

(Grant NAG5-1490)

(NASA-CR-197288; NAS 1.26:197288) Avail: CASI HC A01/MF A01

The potential for remote sensing of ocean wave direction using passive polarimetric microwave observations was investigated. A fixed-beam 91.65 GHz polarimetric radiometer was mounted on the NASA DC-8 aircraft during the Tropical Ocean Global Atmosphere/Coupled Ocean Atmosphere Response Experiment (TOGA/COARE January - February 1993). Several experiments were performed during which the DC-8 was flown in constant bank-angle turns at approximately 1.5 km altitude to obtain azimuthal scans of the sea surface at fixed observation angles. Data at 65 deg from nadir are consistent with previous findings using 19 and 37 GHz Special Sensor Microwave Imager (SSM/1) satellite observations and support the claim that a broadband emission mechanism is responsible for the azimuthal brightness signatures. Accordingly, a tilted-facet geometrical optics (GO) model of the surface was developed to investigate emission from deterministic and random striated surfaces. Laboratory measurements of polarimetric emission at 92 GHz from small-amplitude water-waves corroborate this model. Author

N95-32914*# Miami Univ., Coral Gables, FL. Dept. of Physics.

OCEAN OBSERVATIONS WITH EOS/MODIS: ALGORITHM DEVELOPMENT AND POST LAUNCH STUDIES Semi-Annual Report, Jan. - Jul. 1995

Howard R. Gordon 15 Jul. 1995 114 p

(Contract NAS5-31363)

(NASA-CR-198928; NAS 1.26:198928) Avail: CASI HC A06/MF A02

An investigation of the influence of stratospheric aerosol on the performance of the atmospheric correction algorithm was carried out. The results indicate how the performance of the algorithm is degraded if the stratospheric aerosol is ignored. Use of the MODIS 1380 nm band to effect a correction for stratospheric aerosols was also studied. The development of a multi-layer Monte Carlo radiative transfer code that includes polarization by molecular and aerosol scattering and wind-induced sea surface roughness has been completed. Comparison tests with an existing two-layer successive order of scattering code suggests that both codes are capable of producing top-of-atmosphere radiances with errors usually less than 0.1 percent. An initial set of simulations to study the effects of ignoring the polarization of the the ocean-atmosphere light field, in both the development of the atmospheric correction algorithm and the generation of the lookup tables used for operation of the algorithm, have been completed. An algorithm was developed that can be used to invert the radiance exiting the top and bottom of the atmosphere to yield the columnar optical properties of the atmospheric aerosol under clear sky conditions over the ocean, for aerosol optical thicknesses as large as 2. The algorithm is capable of retrievals with such large optical thicknesses because all significant orders of multiple scattering are included. Author (revised)

N95-33407# Lawrence Livermore National Lab., Livermore, CA Isotope Geochemistry Section.

LITHOGENIC AND COSMOGENIC TRACERS IN CATCHMENT HYDROLOGY

Gregory J. Nimz Jan. 1995 55 p

(Contract W-7405-eng-48)

(DE95-011523; UCRL-ID-119659) Avail: CASI HC A04/MF A01

A variety of physical processes affect solute concentrations within catchment waters. The isotopic compositions of the solutes can indicate which processes have determined the observed concentrations. These processes together constitute the physical history of the water, which is one of the primary concerns in hydrology. Many groundwater solutes are derived as a result of interaction between the water and the rock and/or soil within the system. These are termed 'lithogenic' solutes. The isotopic compositions of these solutes provide information regarding rock-water interactions. Many other solutes have their isotopic compositions determined both internally and externally to the catchment system. Important members of this group include solutes that have isotopic compositions produced by atomic particle interactions with other nuclides. The source of the atomic particles can be cosmic radiation (producing 'cosmogenic' nuclides in the atmosphere and land surface), anthropogenic nuclear reactions 'thermonuclear' nuclides), or radioactive and fission decay of naturally-occurring elements, such as U and Th (producing 'in-situ' lithogenic nuclides in the deep subsurface). Current language usage often combines all of the atomic particle-produced nuclides under the heading 'cosmogenic nuclides', and for simplicity we will often follow that usage, although always clearly indicating which variety is being discussed. This paper addresses the processes that affect the lithogenic and cosmogenic solute compositions in groundwater, and how these compositions can therefore be used in integrative ways to understand the physical history of groundwater within a catchment system. DOE

N95-33498*# Woods Hole Research Center, MA.

COMPLETING BELOW-GROUND CARBON BUDGETS FOR PASTURES, RECOVERING FORESTS, AND MATURE FORESTS OF AMAZONIA Second Annual Report, 1 Aug. 1994 - 31 May 1995

Eric A. Davidson, Daniel C. Nepstad, and Susan E. Trumbore (California Univ., Irvine, CA.) 31 May 1995 26 p Original contains color illustrations

(Grant NAGw-3748)

(NASA-CR-199129; NAS 1.26:199129) Avail: CASI HC A03/MF A01; 1 functional color page

This progress report covers the following efforts initiated for the year: year-round monthly soil CO2 flux measurements were started in both primary and secondary forests and in managed and degraded pastures; root sorting and weighing has begun and all four ecosystems at Paragominas have been analyzed through samples; regional modeling of soil water dynamics and minimum rooting depth has been done and the RADAMBRASIL soils database has been digitized and a 20 year record of the precipitation for the region has been produced, along with a hydrological ('bucket-tipping') model that will run within a GIS framework; prototype tension lysimeters have been designed and installed in soil pits to begin assessing the importance of DOC as a source of organic matter in deep soils; and many publications, listed in this document, have resulted from this year's research. Two of the papers published are included with this annual report document. CASI

N95-33849# Los Alamos National Lab., NM.

COOLING TOWER AND PLUME MODELING FOR SATELLITE REMOTE SENSING APPLICATIONS

B. J. Powers 1995 44 p

(Contract W-7405-eng-36)

(DE95-012000; LA-UR-95-1417) Avail: CASI HC A03/MF A01

It is often useful in nonproliferation studies to be able to remotely estimate the power generated by a power plant. Such information is indirectly available through an examination of the power dissipated by the plant. Power dissipation is generally accomplished either by transferring the excess heat generated into the atmosphere or into bodies of water. It is the former method with which we are exclusively concerned in this report. We discuss in this report the difficulties associated with such a task. In particular, we primarily address the remote detection of the temperature associated with the condensed water plume emitted from the cooling tower. We find that the effective emissivity of the plume is of fundamental importance for this task. Having examined the dependence of the plume emissivity in several IR bands and with varying liquid water content and droplet size distributions, we conclude that the plume emissivity, and consequently the plume brightness temperature, is dependent upon not only the liquid water

content and band, but also upon the droplet size distribution. Finally, we discuss models dependent upon a detailed point-by-point description of the hydrodynamics and thermodynamics of the plume dynamics and those based upon spatially integrated models. We describe in detail a new integral model, the LANL Plume Model, which accounts for the evolution of the droplet size distribution. Some typical results obtained from this model are discussed. DOE

N95-34454# Radex, Inc., Bedford, MA.
AN IMPROVED ALGORITHM FOR COMPUTING ALTITUDE DEPENDENT CORRECTED GEOMAGNETIC COORDINATES Scientific Report No. 7
K. H. Bhavnani and C. A. Hein 19 Dec. 1994 23 p
(Contract F19628-93-C-0023)
(AD-A293967; RXR-94112; PL-TR-94-2310) Avail: CASI HC A03/MF A01

An improved algorithm for computing altitude dependent corrected geomagnetic (CGM) coordinates from geocentric coordinates (and, where it exists, the inverse) using spherical harmonics is described. The method uses a tenth order spherical harmonic fit to the direction cosines (a unit vector) in a suitably chosen intermediate, altitude adjusted coordinate system. The need for this auxiliary coordinate system is to avoid convergence problems associated with the discontinuity in the CGM latitude at the magnetic equator at non- zero altitude. Altitude dependence is obtained by computing the spherical harmonic fits to CGM (and inverse) at 0, 300 and 1200 km altitude, and using a quadratic fit to interpolate each coefficient. The new algorithm provides a good representation of the CGM compression around the South Atlantic Anomaly in addition to modeling the increasing discontinuity with altitude at the magnetic equator. Comparisons are provided with previous approaches. Accuracy limitations and consistency between the direct and inverse computations are also discussed. DTIC

N95-33138# Institute for Precision Instrumentation, Moscow (Russia).
IDENTIFICATION OF TERRAIN IMAGERY WITH UNSTABLE REFLECTIVITY
Y. A. Kozko and V. V. Saveliev *In* AGARD, Dual Usage in Military and Commercial Technology in Guidance and Control Mar. 1995 7 p (For primary document see N95-33126 12-31)
Copyright Avail: CASI HC A02/MF A02

N95-33731*# New Hampshire Univ., Durham, NH. Complex Systems Research Center.
HIGH SPECTRAL RESOLUTION REMOTE SENSING OF CANOPY CHEMISTRY
John D. Aber and Mary E. Martin *In* JPL, Summaries of the Fifth Annual JPL Airborne Earth Science Workshop. Volume 1: AVIRIS Workshop 23 Jan. 1995 p 1-4 (For primary document see N95-33730 12-42)
Avail: CASI HC A01/MF A02

N95-33732*# Phillips Lab., Hanscom AFB, MA.
MODTRAN3: AN UPDATE AND RECENT VALIDATIONS AGAINST AIRBORNE HIGH RESOLUTION INTERFEROMETER MEASUREMENTS
Gail P. Anderson, Jinxue Wang, and James H. Chetwynd *In* JPL, Summaries of the Fifth Annual JPL Airborne Earth Science Workshop. Volume 1: AVIRIS Workshop 23 Jan. 1995 p 5-8 (For primary document see N95-33730 12-42)
Avail: CASI HC A01/MF A02

N95-33734*# Colorado Univ., Boulder, CO. Center for the Study of Earth from Space.
QUANTITATIVE REMOTE SENSING OF AMMONIUM MINERALS, CEDAR MOUNTAINS, ESMERALDA COUNTY, NEVADA
William M. Baugh and Fred A. Kruse *In* JPL, Summaries of the Fifth Annual JPL Airborne Earth Science Workshop. Volume 1: AVIRIS Workshop 23 Jan. 1995 p 11-14 (For primary document see N95-33730 12-42)
Avail: CASI HC A01/MF A02

N95-33736*# Colorado Univ., Boulder, CO. Center for the Study of Earth from Space.
USING DARK CURRENT DATA TO ESTIMATE AVIRIS NOISE COVARIANCE AND IMPROVE SPECTRAL ANALYSES
Joseph W. Boardman *In* JPL, Summaries of the Fifth Annual JPL Airborne Earth Science Workshop. Volume 1: AVIRIS Workshop 23 Jan. 1995 p 19-22 (For primary document see N95-33730 12-42)
Avail: CASI HC A01/MF A02

N95-33737*# Jet Propulsion Lab., California Inst. of Tech., Pasadena, CA.
MAPPING TARGET SIGNATURES VIA PARTIAL UNMIXING OF AVIRIS DATA
Joseph W. Boardman (Colorado Univ., Boulder, CO.), Fred A. Kruse (Colorado Univ., Boulder, CO.), and Robert O. Green *In its* Summaries of the Fifth Annual JPL Airborne Earth Science Workshop. Volume 1: AVIRIS Workshop 23 Jan. 1995 p 23-26 (For primary document see N95-33730 12-42)
Avail: CASI HC A01/MF A02

N95-33738*# MacDonald, Dettwiler and Associates Ltd., Richmond (British Columbia).
COMBINED HYPERSPATIAL AND HYPERSPECTRAL IMAGING SPECTROMETER CONCEPT
Ian Burke and Harold Zwick *In* JPL, Summaries of the Fifth Annual JPL Airborne Earth Science Workshop. Volume 1: AVIRIS Workshop 23 Jan. 1995 p 27-30 (For primary document see N95-33730 12-42)
Avail: CASI HC A01/MF A02

N95-33741*# Geological Survey, Denver, CO.
INITIAL VEGETATION SPECIES AND SENESCIENCE/STRESS INDICATOR MAPPING IN THE SAN LUIS VALLEY, COLORADO USING IMAGING SPECTROMETER DATA
Roger N. Clark, Trude V. V. King, Cathy Ager, and Gregg A. Swayze *In* JPL, Summaries of the Fifth Annual JPL Airborne Earth Science Workshop. Volume 1: AVIRIS Workshop 23 Jan. 1995 p 35-38 (For primary document see N95-33730 12-42)
Avail: CASI HC A01/MF A02

N95-33742*# Geological Survey, Denver, CO.
MAPPING MINERALS, AMORPHOUS MATERIALS, ENVIRONMENTAL MATERIALS, VEGETATION, WATER, ICE AND SNOW, AND OTHER MATERIALS: THE USGS TRICORDER ALGORITHM
Roger N. Clark and Gregg A. Swayze *In* JPL, Summaries of the Fifth Annual JPL Airborne Earth Science Workshop. Volume 1: AVIRIS Workshop 23 Jan. 1995 p 39-40 (For primary document see N95-33730 12-42)
Avail: CASI HC A01/MF A02

N95-33743*# Jet Propulsion Lab., California Inst. of Tech., Pasadena, CA.
CALIBRATION TO SURFACE REFLECTANCE OF TERRESTRIAL IMAGING SPECTROMETRY DATA: COMPARISON OF METHODS
Abstract Only
Roger N. Clark (Geological Survey, Denver, CO.), Gregg A. Swayze (Geological Survey, Denver, CO.), Kathy Heidebrecht (Colorado Univ., Boulder, CO.), Robert O. Green, and F. H. Goetz (Colorado Univ., Boulder, CO.) *In its* Summaries of the Fifth Annual JPL Airborne Earth Science Workshop. Volume 1: AVIRIS Workshop 23 Jan. 1995 p 41-42 (For primary document see N95-33730 12-42)
Avail: CASI HC A01/MF A02

N95-33744*# Southampton Univ. (England). Dept. of Geography.
CAUSAL CORRELATION OF FOLIAR BIOCHEMICAL CONCENTRATIONS WITH AVIRIS SPECTRA USING FORCED ENTRY LINEAR REGRESSION
Terence P. Dawson, Paul J. Curran, and John A. Kupiec *In* JPL, Summaries of the Fifth Annual JPL Airborne Earth Science Workshop. Volume 1: AVIRIS Workshop 23 Jan. 1995 p 43-46 (For primary document see N95-33730 12-42)
Avail: CASI HC A01/MF A02

N95-33745*# Science Applications International Corp., McLean, VA.
MINERALOGIC VARIATIONS IN FLUVIAL SEDIMENTS CONTAMINATED BY MINE TAILINGS AS DETERMINED FROM AVIRIS DATA, COEUR D'ALENE RIVER VALLEY, IDAHO

W. H. Farrand and Joseph C. Harsanyi (Applied Signal and Image Technology Co., Pasadena, MD.) *In* JPL, Summaries of the Fifth Annual JPL Airborne Earth Science Workshop. Volume 1: AVIRIS Workshop 23 Jan. 1995 p 47-50 (For primary document see N95-33730 12-42)
Avail: CASI HC A01/MF A02

N95-33747*# Jet Propulsion Lab., California Inst. of Tech., Pasadena, CA.
EVALUATION OF THE PHOTOCHEMICAL REFLECTANCE INDEX IN AVIRIS IMAGERY
John A. Gamon (California State Univ., Los Angeles, CA.), Dar A. Roberts (California Univ., Santa Barbara, CA.), and Robert O. Green *In its* Summaries of the Fifth Annual JPL Airborne Earth Science Workshop. Volume 1: AVIRIS Workshop 23 Jan. 1995 p 55-58 (For primary document see N95-33730 12-42)
Avail: CASI HC A01/MF A02

N95-33748*# National Aeronautics and Space Administration. Goddard Space Flight Center, Greenbelt, MD.
CORRECTION OF THIN CIRRUS EFFECTS IN AVIRIS IMAGES USING THE SENSITIVE 1.375-MICRON CIRRUS DETECTING CHANNEL
Bo-Cai Gao (Universities Space Research Association, Greenbelt, MD.) and Yorman J. Kaufman *In* JPL, Summaries of the Fifth Annual JPL Airborne Earth Science Workshop. Volume 1: AVIRIS Workshop 23 Jan. 1995 p 59-62 (For primary document see N95-33730 12-42)
Avail: CASI HC A01/MF A02

N95-33749*# National Aeronautics and Space Administration. Goddard Space Flight Center, Greenbelt, MD.
REMOTE SENSING OF SMOKE, CLOUDS, AND RADIATION USING AVIRIS DURING SCAR EXPERIMENTS
Bo-Cai Gao (Universities Space Research Association, Greenbelt, MD.), Lorraine Remer (Science Systems and Applications, Inc., Greenbelt, MD.), and Yorman J. Kaufman *In* JPL, Summaries of the Fifth Annual JPL Airborne Earth Science Workshop. Volume 1: AVIRIS Workshop 23 Jan. 1995 p 63-65 (For primary document see N95-33730 12-42)
Avail: CASI HC A01/MF A02

N95-33750*# Jet Propulsion Lab., California Inst. of Tech., Pasadena, CA.
HIGH ACCURACY IN-FLIGHT WAVELENGTH CALIBRATION OF IMAGING SPECTROMETRY DATA
Alexander F. H. Goetz (Colorado Univ., Boulder, CO.), Kathleen B. Heidebrecht (Colorado Univ., Boulder, CO.), and Thomas G. Chrien *In its* Summaries of the Fifth Annual JPL Airborne Earth Science Workshop. Volume 1: AVIRIS Workshop 23 Jan. 1995 p 67-70 (For primary document see N95-33730 12-42)
Avail: CASI HC A01/MF A02

N95-33755*# Jet Propulsion Lab., California Inst. of Tech., Pasadena, CA.
MEASUREMENT OF ATMOSPHERIC WATER VAPOR, LEAF LIQUID WATER AND REFLECTANCE WITH AVIRIS IN THE BOREAL ECOSYSTEM-ATMOSPHERE STUDY: INITIAL RESULTS
Robert O. Green, James E. Conel, and Dar A. Roberts (California Univ., Santa Barbara, CA.) *In its* Summaries of the Fifth Annual JPL Airborne Earth Science Workshop. Volume 1: AVIRIS Workshop 23 Jan. 1995 p 87-90 (For primary document see N95-33730 12-42)
Avail: CASI HC A01/MF A02

N95-33756*# Jet Propulsion Lab., California Inst. of Tech., Pasadena, CA.
MEASUREMENT OF THE SPECTRAL ABSORPTION OF LIQUID WATER IN MELTING SNOW WITH AN IMAGING SPECTROMETER
Robert O. Green and Jeff Dozier (California Univ., Santa Barbara, CA.) *In its* Summaries of the Fifth Annual JPL Airborne Earth Science Workshop. Volume 1: AVIRIS Workshop 23 Jan. 1995 p 91-94 (For primary document see N95-33730 12-42)
Avail: CASI HC A01/MF A02

N95-33757*# Jet Propulsion Lab., California Inst. of Tech., Pasadena, CA.
VEGETATION SPECIES COMPOSITION AND CANOPY ARCHITECTURE INFORMATION EXPRESSED IN LEAF WATER ABSORPTION MEASURED IN THE 1000 NM AND 2200 SPECTRAL REGION BY AN IMAGING SPECTROMETER
Robert O. Green and Dar A. Roberts (California Univ., Santa Barbara, CA.) *In its* Summaries of the Fifth Annual JPL Airborne Earth Science Workshop. Volume 1: AVIRIS Workshop 23 Jan. 1995 p 95-98 (For primary document see N95-33730 12-42)
Avail: CASI HC A01/MF A02

N95-33758*# California Univ., Davis, CA. Land, Air, and Water Resources.
PROSPECT REDUX
S. Jacquemoud, S. L. Ustin, J. Verdebout (Joint Research Centre of the European Communities, Ispra, Italy.), G. Schmuck (Joint Research Centre of the European Communities, Ispra, Italy.), G. Andreoli (Joint Research Centre of the European Communities, Ispra, Italy.), and B. Hosgood (Joint Research Centre of the European Communities, Ispra, Italy.) *In* JPL, Summaries of the Fifth Annual JPL Airborne Earth Science Workshop. Volume 1: AVIRIS Workshop 23 Jan. 1995 p 99-103 (For primary document see N95-33730 12-42)
Avail: CASI HC A01/MF A02

N95-33760*# Colorado Univ., Boulder, CO. Center for the Study of Earth from Space.
INTEGRATION OF AIRSAR AND AVIRIS DATA FOR TRAIL CANYON ALLUVIAL FAN, DEATH VALLEY, CALIFORNIA
Kathryn S. Kierein-Young *In* JPL, Summaries of the Fifth Annual JPL Airborne Earth Science Workshop. Volume 1: AVIRIS Workshop 23 Jan. 1995 p 109-112 Sponsored by SIR-C project (For primary document see N95-33730 12-42)
(Grant NGT-50728)
Avail: CASI HC A01/MF A02

N95-33761*# Geological Survey, Denver, CO.
REMOTE MINERAL MAPPING USING AVIRIS DATA AT SUMMITVILLE, COLORADO AND THE ADJACENT SAN JUAN MOUNTAINS
Trude V. V. King, Roger N. Clark, Cathy Ager, and Gregg A. Swayze *In* JPL, Summaries of the Fifth Annual JPL Airborne Earth Science Workshop. Volume 1: AVIRIS Workshop 23 Jan. 1995 p 113-116 (For primary document see N95-33730 12-42)
Avail: CASI HC A01/MF A02

N95-33763*# Instituto Nacional de Pesaciais Espaciais, Sao Jose dos Campos (Brazil).
AN ALGORITHM FOR CHLOROPHYLL USING FIRST DIFFERENCE TRANSFORMATIONS OF AVIRIS REFLECTANCE SPECTRA
Evlyn Novo, Mary Gastil (Colorado Univ., Boulder, CO.), and John Melack (Colorado Univ., Boulder, CO.) *In* JPL, Summaries of the Fifth Annual JPL Airborne Earth Science Workshop. Volume 1: AVIRIS Workshop 23 Jan. 1995 p 121-124 (For primary document see N95-33730 12-42)
Avail: CASI HC A01/MF A02

N95-33764*# Jet Propulsion Lab., California Inst. of Tech., Pasadena, CA.
IMPROVING ALPINE-REGION SPECTRAL UNMIXING WITH OPTIMAL-FIT SNOW ENDMEMBERS
Thomas H. Painter (California Univ., Santa Barbara, CA.), Dar A. Roberts (California Univ., Santa Barbara, CA.), Robert O. Green, and Jeff Dozier (California Univ., Santa Barbara, CA.) *In its* Summaries of the Fifth Annual JPL Airborne Earth Science Workshop. Volume 1: AVIRIS Workshop 23 Jan. 1995 p 125-128 (For primary document see N95-33730 12-42)
Avail: CASI HC A01/MF A02

N95-33765*# California Univ., Davis, CA. Dept. of Land, Air, and Water Resources.
USING FOREGROUND/BACKGROUND ANALYSIS TO DETERMINE LEAF AND CANOPY CHEMISTRY
J. E. Pinzon, S. L. Ustin, Q. J. Hart, S. Jacquemoud, and M. O. Smith

(Washington Univ., Seattle, WA.) *In* JPL, Summaries of the Fifth Annual JPL Airborne Earth Science Workshop. Volume 1: AVIRIS Workshop 23 Jan. 1995 p 129-132 (For primary document see N95-33730 12-42)
Avail: CASI HC A01/MF A02

N95-33766*# National Aeronautics and Space Administration. Goddard Space Flight Center, Greenbelt, MD.
AVIRIS SPECTRAL TRAJECTORIES FOR FORESTED AREAS OF THE GIFFORD PINCHOT NATIONAL FOREST
Donald E. Sabol, Jr. (Washington Univ., Seattle, WA.), Milton O. Smith (Washington Univ., Seattle, WA.), John B. Adams (Washington Univ., Seattle, WA.), Janet H. Zukin (Washington Univ., Seattle, WA.), Compton J. Tucker, Dar A. Roberts (Colorado Univ., Boulder, CO.), and Alan R. Gillespie (Washington Univ., Seattle, WA.) *In* JPL, Summaries of the Fifth Annual JPL Airborne Earth Science Workshop. Volume 1: AVIRIS Workshop 23 Jan. 1995 p 133-136 (For primary document see N95-33730 12-42)
Avail: CASI HC A01/MF A02

N95-33767*# Howard Univ., Washington, DC. Dept. of Physics.
SUB-PIXEL LOCALIZATION OF HIGHWAYS IN AVIRIS IMAGES
Yehuda Salu *In* JPL, Summaries of the Fifth Annual JPL Airborne Earth Science Workshop. Volume 1: AVIRIS Workshop 23 Jan. 1995 p 137-140 (For primary document see N95-33730 12-42)
Avail: CASI HC A01/MF A02

N95-33768*# California Univ., Davis, CA. Dept. of Land, Air, and Water Resources.
VALIDATING SPATIAL STRUCTURE IN CANOPY WATER CONTENT USING GEOSTATISTICS
E. W. Sanderson, M. H. Zhang, S. L. Ustin, E. Rejmankova, and R. S. Haxo *In* JPL, Summaries of the Fifth Annual JPL Airborne Earth Science Workshop. Volume 1: AVIRIS Workshop 23 Jan. 1995 p 141-143 (For primary document see N95-33730 12-42)
Avail: CASI HC A01/MF A02

N95-33770*# Zurich Univ. (Switzerland). Remote Sensing Lab.
EXTRACTION OF OZONE AND CHLOROPHYLL-A DISTRIBUTION FROM AVIRIS DATA
M. Schaepman, K. I. Itten, D. Schlaepfer, U. Kurer, S. Veraguth, and J. Keller (Paul Scherrer Inst., Villigen, Switzerland.) *In* JPL, Summaries of the Fifth Annual JPL Airborne Earth Science Workshop. Volume 1: AVIRIS Workshop 23 Jan. 1995 p 149-152 (For primary document see N95-33730 12-42)
Avail: CASI HC A01/MF A02

N95-33771*# Canada Centre for Remote Sensing, Ottawa (Ontario).
IMPACT OF DIFFERENCES IN THE SOLAR IRRADIANCE SPECTRUM ON SURFACE REFLECTANCE RETRIEVAL WITH DIFFERENT RADIATIVE TRANSFER CODES
K. Staenz, D. J. Williams (MacDonald, Dettwiler and Associates Ltd., Richmond, British Columbia.), G. Fedosejevs, and P. M. Teillet *In* JPL, Summaries of the Fifth Annual JPL Airborne Earth Science Workshop. Volume 1: AVIRIS Workshop 23 Jan. 1995 p 153-156 (For primary document see N95-33730 12-42)
Avail: CASI HC A01/MF A02

N95-33772*# Geological Survey, Denver, CO.
SPECTRAL IDENTIFICATION OF MINERALS USING IMAGING SPECTROMETRY DATA: EVALUATING THE EFFECTS OF SIGNAL TO NOISE AND SPECTRAL RESOLUTION USING THE TRICORDER ALGORITHM
Gregg A. Swayze and Roger N. Clark *In* JPL, Summaries of the Fifth Annual JPL Airborne Earth Science Workshop. Volume 1: AVIRIS Workshop 23 Jan. 1995 p 157-158 (For primary document see N95-33730 12-42)
Avail: CASI HC A01/MF A02

N95-33773*# Arizona State Univ., Tempe, AZ. Dept. of Geology.
PRELIMINARY STUDY OF KELSO DUNES USING AVIRIS, TM, AND AIRSAR
Pung Xu, Dan G. Blumberg, and Ronald Greeley *In* JPL, Summaries of the Fifth Annual JPL Airborne Earth Science Workshop. Volume 1: AVIRIS Workshop 23 Jan. 1995 p 159-161 (For primary document see N95-33730 12-42)
Avail: CASI HC A01/MF A02

N95-33790*# Jet Propulsion Lab., California Inst. of Tech., Pasadena, CA.
ANALYSES OF TIMS AND AVIRIS DATA, INTEGRATED WITH FIELD AND LABORATORY SPECTRA, FOR LITHOLOGICAL AND MINERALOGICAL INTERPRETATION OF VULCANO ISLAND, ITALY
M. Fabrizia Buongiorno (Istituto Nazionale di Geofisica, Rome, Italy.), M. Paola Bogliolo (Istituto Nazionale di Geofisica, Rome, Italy.), Stefano Salvi (Istituto Nazionale di Geofisica, Rome, Italy.), David C. Pieri, and Francesco Geneselli (Istituto Nazionale di Geofisica, Rome, Italy.) *In its* Summaries of the Fifth Annual JPL Airborne Earth Science Workshop. Volume 2: TIMS Workshop 23 Jan. 1995 p 1-4 (For primary document see N95-33789 12-42)
Avail: CASI HC A01/MF A01

N95-33791*# Arizona State Univ., Tempe, AZ. Dept. of Geology.
URBAN REMOTE SENSING APPLICATIONS: TIMS OBSERVATIONS OF THE CITY OF SCOTTSDALE
Philip R. Christensen, David E. Melendrez, Donald L. Anderson, Victoria E. Hamilton, Melissa L. Wenrich, and Douglas Howard *In* JPL, Summaries of the Fifth Annual JPL Airborne Earth Science Workshop. Volume 2: TIMS Workshop 23 Jan. 1995 p 5-8 (For primary document see N95-33789 12-42)
Avail: CASI HC A01/MF A01

N95-33792*# Arizona State Univ., Tempe, AZ. Dept. of Geology.
FOR GEOLOGICAL INVESTIGATIONS WITH AIRBORNE THERMAL INFRARED MULTISPECTRAL IMAGES: TRANSFER OF CALIBRATION FROM LABORATORY SPECTROMETER TO TIMS AS ALTERNATIVE FOR REMOVING ATMOSPHERIC EFFECTS
Kenneth S. Edgett and Donald L. Anderson *In* JPL, Summaries of the Fifth Annual JPL Airborne Earth Science Workshop. Volume 2: TIMS Workshopp 9-12 (SEE N95-33789 12-42) 23 Jan. 1995 (For primary document see N95-33789 12-42)
Avail: CASI HC A01/MF A01

N95-33793*# Arizona State Univ., Tempe, AZ. Dept. of Geology.
AEROLIAN EROSION, TRANSPORT, AND DEPOSITION OF VOLCANICLASTIC SANDS AMONG THE SHIFTING SAND DUNES, CHRISTMAS LAKE VALLEY, OREGON: TIMS IMAGE ANALYSIS
Kenneth S. Edgett, Michael S. Ramsey, and Philip R. Christensen *In* JPL, Summaries of the Fifth Annual JPL Airborne Earth Science Workshop. Volume 2: TIMS Workshop 23 Jan. 1995 p 13-16 (For primary document see N95-33789 12-42)
Avail: CASI HC A01/MF A01

N95-33798*# Arizona State Univ., Tempe, AZ. Dept. of Geology.
DISCRIMINATION OF ALKALINITY IN GRANITOID ROCKS: A POTENTIAL TIMS APPLICATION
Steven W. Ruff *In* JPL, Summaries of the Fifth Annual JPL Airborne Earth Science Workshop. Volume 2: TIMS Workshop 23 Jan. 1995 p 33-36 (For primary document see N95-33789 12-42)
Avail: CASI HC A01/MF A01

N95-33799*# Jet Propulsion Lab., California Inst. of Tech., Pasadena, CA.
TIMS OBSERVATIONS OF SURFACE EMISSIVITY IN HAPEX-Sahel
Thomas Schmugge (Food and Drug Administration, Bethesda, MD.), Simon Hook, and Anne Kahle *In its* Summaries of the Fifth Annual JPL Airborne Earth Science Workshop. Volume 2: TIMS Workshop 23 Jan. 1995 p 37 (For primary document see N95-33789 12-42)
Avail: CASI HC A01/MF A01

N95-33800*# Arizona State Univ., Tempe, AZ. Dept. of Geology.
A FIELD- AND LABORATORY-BASED QUANTITATIVE ANALYSIS OF ALLUVIUM: RELATING ANALYTICAL RESULTS TO TIMS DATA
Melissa L. Wenrich, Victoria E. Hamilton, and Philip R. Christensen *In* JPL, Summaries of the Fifth Annual JPL Airborne Earth Science Workshop.

Volume 2: TIMS Workshop 23 Jan. 1995 p 39-42 (For primary document see N95-33789 12-42)
Avail: CASI HC A01/MF A01

N95-33802*# Arizona State Univ., Tempe, AZ. Dept. of Geology.
NEW OBSERVATIONS OF BOLIVIAN WIND STREAKS BY JPL AIRBORNE SAR: PRELIMINARY RESULTS
Dan G. Blumberg and Ronald Greeley *In* JPL, Summaries of the Fifth Annual JPL Airborne Earth Science Workshop. Volume 3: AIRSAR Workshop 23 Jan. 1995 p 1-4 (For primary document see N95-33801 12-42)
Avail: CASI HC A01/MF A01

N95-33803*# Jet Propulsion Lab., California Inst. of Tech., Pasadena, CA.
MEASURING SOIL MOISTURE WITH IMAGING RADARS
Pascale C. Dubois, Jakob vanZyl, and Ted Engman (National Aeronautics and Space Administration. Goddard Space Flight Center, Greenbelt, MD.) *In its* Summaries of the Fifth Annual JPL Airborne Earth Science Workshop. Volume 3: AIRSAR Workshop 23 Jan. 1995 p 5-8 (For primary document see N95-33801 12-42)
Avail: CASI HC A01/MF A01

N95-33804*# Jet Propulsion Lab., California Inst. of Tech., Pasadena, CA.
USE OF TOPSAR DIGITAL ELEVATION DATA TO DETERMINE THE 3-DIMENSIONAL SHAPE OF AN ALLUVIAL FAN
Tom G. Farr *In its* Summaries of the Fifth Annual JPL Airborne Earth Science Workshop. Volume 3: AIRSAR Workshop 23 Jan. 1995 p 9-12 (For primary document see N95-33801 12-42)
Avail: CASI HC A01/MF A01

N95-33805*# Jet Propulsion Lab., California Inst. of Tech., Pasadena, CA.
ACCURATE ESTIMATION OF SIGMA(EXP 0) USING AIRSAR DATA
Francesco Holecz and Eric Rignot *In its* Summaries of the Fifth Annual JPL Airborne Earth Science Workshop. Volume 3: AIRSAR Workshop 23 Jan. 1995 p 13-16 Sponsored by Swiss Academy of Science; and the Holderbank Foundation (For primary document see N95-33801 12-42)
Avail: CASI HC A01/MF A01

N95-33806*# National Aeronautics and Space Administration. Goddard Space Flight Center, Greenbelt, MD.
REMOTELY SENSED INDICATORS OF HABITAT HETEROGENEITY AND BIOLOGICAL DIVERSITY: A PRELIMINARY REPORT
Marc Imhoff, Thomas Sisk (Interior Dept., Washington, DC.), Anthony Milne (New South Wales Univ., Kensington, Australia.), Garth Morgan (Defence Science and Technology Organisation, Melbourne, Australia.), and Tony Orr (Defence Science and Technology Organisation, Melbourne, Australia.) *In* JPL, Summaries of the Fifth Annual JPL Airborne Earth Science Workshop. Volume 3: AIRSAR Workshop 23 Jan. 1995 p 17-20 (For primary document see N95-33801 12-42)
Avail: CASI HC A01/MF A01

N95-33808*# Jet Propulsion Lab., California Inst. of Tech., Pasadena, CA.
BAYES CLASSIFICATION OF INTERFEROMETRIC TOPSAR DATA Abstract Only
T. R. Michel, E. Rodriguez, B. Houshmand, and R. Carande *In its* Summaries of the Fifth Annual JPL Airborne Earth Science Workshop. Volume 3: AIRSAR Workshop 23 Jan. 1995 p 25 (For primary document see N95-33801 12-42)
Avail: CASI HC A01/MF A01

N95-33809*# British Columbia Univ., Vancouver (British Columbia).
TERRAIN CLASSIFICATION USING CIRCULAR POLARIMETRIC FEATURES
David G. Michelson, Ian G. Cumming, and Charles E. Livingstone (Canada Centre for Remote Sensing, Ottawa, Ontario.) *In* JPL Summaries of the Fifth Annual JPL Airborne Earth Science Workshop. Volume 3: AIRSAR Workshop 23 Jan. 1995 p 27-30 (For primary document see N95-33801 12-42)
Avail: CASI HC A01/MF A01

N95-33810*# New Mexico Univ., Albuquerque, NM.
USE OF AIRSAR TO IDENTIFY WOODY SHRUB INVASION AND OTHER INDICATORS OF DESERTIFICATION IN THE JORNADA LTER
H. Brad Musick, Gerald G. Schaber (Geological Survey, Flagstaff, AZ.), and Carol S. Breed (Geological Survey, Flagstaff, AZ.) *In* JPL, Summaries of the Fifth Annual JPL Airborne Earth Science Workshop. Volume 3: AIRSAR Workshop 23 Jan. 1995 p 31-34 (For primary document see N95-33801 12-42)
Avail: CASI HC A01/MF A01

N95-33811*# Jet Propulsion Lab., California Inst. of Tech., Pasadena, CA.
THE UNIQUE RADAR SCATTERING PROPERTIES OF SILICIC LAVA FLOWS AND DOMES
Jeffrey J. Plaut, Ellen R. Stofan, Steven W. Anderson (Black Hills State Univ., Spearfish, SD.), and David A. Crown (Pittsburgh Univ., Pittsburgh, PA.) *In its* Summaries of the Fifth Annual JPL Airborne Earth Science Workshop. Volume 3: AIRSAR Workshop 23 Jan. 1995 p 35-38 (For primary document see N95-33801 12-42)
Avail: CASI HC A01/MF A01

N95-33812*# Jet Propulsion Lab., California Inst. of Tech., Pasadena, CA.
ON THE POTENTIAL OF LONG WAVELENGTH IMAGING RADARS FOR MAPPING VEGETATION TYPES AND WOODY BIOMASS IN TROPICAL RAIN FORESTS
Eric J. Rignot, Reiner Zimmermann, and Ram Oren *In its* Summaries of the Fifth Annual JPL Airborne Earth Science Workshop. Volume 3: AIRSAR Workshop 23 Jan. 1995 p 39-41 (For primary document see N95-33801 12-42)
Avail: CASI HC A01/MF A01

N95-33813*# Canada Centre for Remote Sensing, Ottawa (Ontario). Applications Div.
LITHOLOGIC CONTROLS ON AIRSAR SIGNATURES OF BEDROCK AND ALLUVIUM, AT LUNAR CRATER, NEVADA
Benoit Rivard, Marc Dlorio, and Paul Budkewitsch *In* JPL, Summaries of the Fifth Annual JPL Airborne Earth Science Workshop. Volume 3: AIRSAR Workshop 23 Jan. 1995 p 43-46 (For primary document see N95-33801 12-42)
Avail: CASI HC A01/MF A01

N95-33814*# Jet Propulsion Lab., California Inst. of Tech., Pasadena, CA.
ESTIMATION OF PENETRATION OF FOREST CANOPIES BY INTERFEROMETRIC SAR MEASUREMENTS Abstract Only
Ernesto Rodriguez, Thierry R. Michel, and David J. Harding (National Aeronautics and Space Administration. Goddard Space Flight Center, Greenbelt, MD.) *In its* Summaries of the Fifth Annual JPL Airborne Earth Science Workshop. Volume 3: AIRSAR Workshop 23 Jan. 1995 p 47 (For primary document see N95-33801 12-42)
Avail: CASI HC A01/MF A01

N95-33815*# Jet Propulsion Lab., California Inst. of Tech., Pasadena, CA.
REGIONAL MAPPING OF FOREST CANOPY WATER CONTENT AND BIOMASS USING AIRSAR IMAGES OVER BOREAS STUDY AREA Abstract Only
Sasan Saatchi, Eric Rignot, and Jakob vanZyl *In its* Summaries of the Fifth Annual JPL Airborne Earth Science Workshop. Volume 3: AIRSAR Workshop 23 Jan. 1995 p 49 (For primary document see N95-33801 12-42)
Avail: CASI HC A01/MF A01

N95-33816*# National Aeronautics and Space Administration. Goddard Space Flight Center, Greenbelt, MD.
APPLICATION OF IEM MODEL ON SOIL MOISTURE AND SURFACE ROUGHNESS ESTIMATION
Jiancheng Shi (California Univ., Santa Barbara, CA.), J. R. Wang, P. E.

ONeill, A. Y. Hsu, and E. T. Engman *In* JPL, Summaries of the Fifth Annual JPL Airborne Earth Science Workshop. Volume 3: AIRSAR Workshop 23 Jan. 1995 p 51-54 (For primary document see N95-33801 12-42)
Avail: CASI HC A01/MF A01

N95-34233*# Jet Propulsion Lab., California Inst. of Tech., Pasadena, CA.
MULTI-LAYER HOLOGRAPHIC BIFURCATIVE NEURAL NETWORK SYSTEM FOR REAL-TIME ADAPTIVE EOS DATA ANALYSIS Abstract Only
Hua-Kuang Liu, K. S. Huang (University of Southern California, Los Angeles, CA.), and J. Diep *In* Colorado Univ., Applied Information Systems Research Program (AISRP) Workshop 3 Meeting Proceedings 1993 1 p (For primary document see N95-34218 12-82)
Avail: CASI HC A01/MF A03

44 ENERGY PRODUCTION AND CONVERSION

Includes specific energy conversion systems, e.g., fuel cells; global sources of energy; geophysical conversion; and windpower.

For related information see also *07 Aircraft Propulsion and Power, 20 Spacecraft Propulsion and Power,* and *28 Propellants and Fuels.*

N95-32402# Central Research Inst. of Electric Power Industry, Tokyo (Japan).
SOLAR CELL ARRAY DESIGN METHOD FOR PREVENTING POWER REDUCTION DUE TO MODULE OUTPUT FLUCTUATION
H. Kobayashi Apr. 1994 29 p In JAPANESE
(DE95-769745; CRIE-T-93073) Avail: CASI HC A03/MF A01

A discussion was given on the method to design solar cell arrays to minimize reduction in power output from the arrays caused by variance in the output characteristics of solar cell modules. Measurements verified that the variance in solar array modules causes the fluctuation coefficient of the output current to reach 5% as a maximum, and the reduction in the solar cell array output power can reach about 6% as a maximum. Using the arrangement and connection methods of the modules as parameters, the array output voltage/current characteristics were analyzed by using a simulation. As a result, it was found that an arrangement in which the module output current becomes uniform in the portions where the modules are connected in series in the array circuit, and a method to divide the arrays into blocks are the effective solution. Thus, when the interior of the solar cell arrays was divided into three to four blocks in the series direction, and the modules were arranged by using a simple method to consider the orders of the module output current values, the reduction in the solar cell array output was suppressed nearly completely. DOE

N95-32403# New Energy and Industrial Technology Development Organization, Tokyo (Japan).
INVESTIGATION RESEARCH ON INTRODUCING NEW ENERGY TECHNOLOGY, PROMOTING ITS PRACTICAL APPLICATION, AND PROVIDING ITS INSTRUCTION
Mar. 1994 303 p In ENGLISH and JAPANESE
(DE95-769601; NEDO-NP-9322) Avail: CASI HC A14/MF A03

For the purpose of smoothly expediting concrete introduction and utilization of new energy technology, the paper investigates and analyzes various kinds of information, and at the same time studies construction of a system to assist giving smooth technical guidance and consultation. Data are arranged on the insolation amount, mean temperature, maximum/minimum temperature collected from 67 weather observatories in Japan. Calculation is made on the insolation amount, and the generated output which is supposed from the latitude angle and the inclination angle of solar cell modules. Examples of introducing the photovoltaic power generation system, including NEDO, are pigeonholed and classified. There are many restrictive conditions at the time of introduction of the photovoltaic power generation. Relations between kinds of places where the technology is introduced and the related legal system are studied. In case of interconnecting to the power system as on-site power generation facilities, the technology should meet requirements of technology of the system interconnection, and therefore study items and equipment policy in case of low-/high- pressure interconnection are arranged. The assistance system is constructed by databasing the data collected, pigeonholed, and analyzed such above. DOE

N95-32546# New Energy and Industrial Technology Development Organization, Tokyo (Japan).
FEASIBILITY SURVEY ON INTERNATIONAL COOPERATION FOR HIGH EFFICIENCY ENERGY CONVERSION TECHNOLOGY IN FISCAL 1993
Mar. 1994 149 p In JAPANESE
(DE95-769804; NEDO-P-93-57) Avail: CASI HC A07/MF A02

Following cooperative researches on fuel cell jointly conducted by NEDO and EGAT (Electricity Generating Authority of Thailand), the survey on international cooperation relating to high efficiency energy conversion technology was carried out for the ASEAN countries. The paper summed up the results of the survey. The study of the international cooperation is made for the following three items: a program for periodical exchange of information with EGAT, a project for cooperative research on phosphoric acid fuel cell in Indonesia, and a project for cooperative research with EGAT on electric power storage by advanced battery. In Malaysia, which is small in scale of state, part of the Ministry of Energy, Telecommunication and Posts is only in charge of the energy issue. Therefore, the situation is that they cannot answer well to many items of research/development cooperation brought in from Japan. The item of medium- and long-term developmental research in the Philippines is about the problems which are seen subsequently in the Manila metropolitan area where the problem of outage is being settled. Accordingly, it is essential to promote the cooperative research, well confirming policies and systems of the Ministry of Energy and the national electricity corporation. DOE

N95-32551# National Renewable Energy Lab., Golden, CO.
HYBRID2: A VERSATILE MODEL OF THE PERFORMANCE OF HYBRID POWER SYSTEMS
H. James Green and James Manwell (Massachusetts Univ., Amherst, MA.) Apr. 1995 12 p Presented at the 25th Annual Conference and Exhibition on Wind Power, Washington, DC, 26-30 Mar. 1995
(Contract DE-AC36-83CH-10093)
(DE95-004062; NREL/TP-441-7807; CONF-950309-1) Avail: CASI HC A03/MF A01

In 1993, the National Renewable Laboratory (NREL) made an assessment of the available tools from the United States and Europe for predicting the long-term performance of hybrid power systems. By hybrid power the authors mean combinations of two or more power sources wind turbines, photovoltaics (PV), diesel gensets, or other generators into integrated systems for electric power generation in remote locations. Their conclusion was that there was no single, user-friendly tool capable of modeling the full range of hybrid power technologies being considered for the 1990s and beyond. The existing tools were, in particular, lacking flexibility in system configuration and in dispatch of components. As a result, NREL developed a specification for a model, called HYBRID2, for making comparisons of competing technology options on a level playing field. This specification was prepared with a range of potential users in mind including not only the US Department of Energy (DOE) renewable energy programs, but also the US wind industry, technical consultants, international development institutions/banks, and rural electrification programs in developing countries. During 1994, NREL and subcontractor, the University of Massachusetts (UMass), began development of HYBRID2 with funding from the DOE Wind Energy Program. It builds on the wind/diesel model, HYBRID1, developed previously by UMass, and expands that model to accommodate the wider array of technologies used in hybrid power systems. This paper will provide an overview of the model's features, functions, and status. DOE

N95-32575# Los Alamos National Lab., NM.
DESIGN AND TESTING CRITERIA FOR BIPOLAR PLATE MATERIALS FOR PEM FUEL CELL APPLICATIONS
Rodney L. Borup and Nicholas E. Vanderborgh 1995 8 p Presented at the Spring Meeting of the Materials Research Society (MRS), San Francisco, CA, 17-21 Apr. 1995
(Contract W-7405-eng-36)
(DE95-010878; LA-UR-95-1303; CONF-950412-2) Avail: CASI HC A02/MF A01

Bipolar plates for proton exchange membrane (PEM) fuel cells are

currently under development. These plates separate individual cells of the fuel cell stack, and thus must be sufficiently strong to support clamping forces, be electrically conducting, be fitted with flow channels for stack thermal control, be of a low permeability material to separate safely hydrogen and oxygen feed streams, be corrosion resistant, and be fitted with distribution channels to transfer the feed streams over the plate surface. To date, bipolar plate costs dominate stack costs, and therefore future materials need to meet strict cost targets. A first step in the bipolar plate development program is an assessment of design constraints. Such constraints have been estimated and evaluated and are discussed here. Conclusions point to promising advanced materials, such as conductive, corrosion resistant coatings on metal substrates, as candidates for mass production of fuel cell bipolar plates. Possible candidate materials are identified, and testing procedures developed to determine suitability of various materials. DOE

N95-32645# Westinghouse Electric Corp., West Mifflin, PA. Atomic Power Lab.

DESIGN AND OPERATION OF A THERMIONIC CONVERTER IN AIR

M. Harlan Horner (General Atomics Co., San Diego, CA.), Lester L. Begg (General Atomics Co., San Diego, CA.), Joe N. Smith, Jr. (General Atomics Co., San Diego, CA.), Clint B. Geller (Bettis Atomic Power Lab., West Mifflin, PA.), and Joseph E. Kalinowski (Bettis Atomic Power Lab., West Mifflin, PA.) 1995 7 p Presented at the Intersociety Energy Conversion Conference, Orlando, FL, 30 Jul. - 5 Aug. 1995

(Contract DE-AC11-93PN-38195)

(DE95-010151; WAPD-T-3062; CONF-950729-2) Avail: CASI HC A02/MF A01

An electrically heated thermionic converter has been designed, built and successfully tested in air. Several unique features were incorporated in this converter: an integral cesium reservoir, innovative ceramic-to-metal seals, a heat rejection system coupling the collector to a low temperature heat sink and an innovative cylindrical heater filament. The converter was operated for extended periods of time with the emitter at about 1900 K, the collector at about 700 K, and a power density of over 2 w(e)/sq cm. Input power transients were run between 50% and 100% thermal power, at up to 1% per second, without instabilities in performance. DOE

N95-32685# National Renewable Energy Lab., Golden, CO.

TECHNIQUES FOR THE DETERMINATION OF LOCAL DYNAMIC PRESSURE AND ANGLE OF ATTACK ON A HORIZONTAL AXIS WIND TURBINE

D. E. Shipley, M. S. Miller, M. C. Robinson, M. W. Luttges, and D. A. Simms May 1995 57 p

(Contract DE-AC36-83CH-10093)

(DE95-009204; NREL/TP-442-7393) Avail: CASI HC A04/MF A01

Data from the National Renewable Energy Laboratory's Combined Experiment has been utilized to develop techniques for indirectly calculating the instantaneous local dynamic pressure and angle of attack on a horizontal axis wind turbine. First, an analytic model based upon inflow geometry relative to the wind turbine was developed for both parameters. Second, dynamic pressure and angle of attack were inferred from the pressure required to normalize the blade stagnation point to C(sub p) = 1.0. Third, rotor blade pressure profiles were compared to those from wind tunnel tests to determine angle of attack. Test results are shown over a variety of typical inflow conditions and are corroborated by measured data. Differences between the calculated and measured values are also discussed. DOE

N95-32811# Jet Propulsion Lab., California Inst. of Tech., Pasadena, CA.

THERMOELECTRIC MATERIAL DEVELOPMENT Final Report

Jan W. Vandersande, Camillo Allevato, and Thierry Caillat Oct. 1994 41 p

(Contract DE-AI03-89SF-17905)

(DE95-007890; DOE/SF-17905/T8) Avail: CASI HC A03/MF A01

A search was made for improved TE materials that could have higher efficiency than state-of-the-art SiGe alloys used in Radioisotope Thermoelectric Generators. A new family of materials having the skutterudite structure was identified (cubic space group Im3, formula (Fe, Co, Ni)As3. Properties of n-type IrSb3, CoSb3, and their solid solutions were investigated. Pt, Te, Tl, and In were used as dopants. The thermal conductivity was reduced by about 70% for the solid solutions vs the binary compounds. A maximum ZT of about 0.36 was measured on Co-rich solid solutions which is 160% improved over that of the binary compounds. DOE

N95-32813 Netherlands Energy Research Foundation, Petten (Netherlands).

CORROSION OF SEPARATOR PLATE CONSTITUENTS IN MOLTEN CARBONATE [CORROSIE VAN SEPARATORPLAAT-LEGERINGS ELEMENTEN IN GESMOLTEN CARBONAAT]

Jack Vossen 1994 237 p Limited Reproducibility: More than 20% of this document may be affected by microfiche quality

(PB95-214490) Copyright Avail: CASI HC A11

To improve the corrosion resistance of the separator plates, insight in the corrosion behavior of the materials used is necessary. Especially, a detailed knowledge of the dissolution and passivation mechanisms as a function of the electrode potential will be useful. It is very difficult to unravel the corrosion mechanism of commercially available materials because it depends on several factors. Therefore, to obtain a first insight, the corrosion mechanism of pure metals and binary model alloys has been investigated and described in this thesis. The pure metals investigated are gold, nickel and chromium. The alloys that were investigated in this thesis are nickel-chromium, nickel-iron and nickel-aluminium alloys. Some commercially available materials have been investigated as a first attempt to understand the corrosion and passivation mechanisms of more complicated alloys. NTIS

N95-32817# National Renewable Energy Lab., Golden, CO.

DEVICE PHYSICS OF THIN-FILM POLYCRYSTALLINE CELLS AND MODULES Annual Subcontract Report, 6 Dec. 1993 - 5 Dec. 1994

J. R. Sites (Colorado State Univ., Fort Collins, CO.) May 1995 31 p

(Contract DE-AC36-83CH-10093)

(DE95-009209; NREL/TP-451-7709) Avail: CASI HC A03/MF A01

Progress has been made in several applications of device physics to thin-film polycrystalline cells and modules. At the cell level, results include a more quantitative separation of photon losses, the impact of second barriers on cell operation, and preliminary studies of how current-voltage curves are affected by band offsets. Module analysis includes the effects of the typical monolithic, series-connected cell geometry, analytical techniques when only the two module leads are accessible, and the impact of chopping frequency, local defects, and high-intensity beams on laser-scanning measurements. DOE

N95-33153# National Renewable Energy Lab., Golden, CO.

PHOTOVOLTAIC MANUFACTURING TECHNOLOGY (PVMaT) Semiannual Subcontract Report, 31 Mar. - 30 Sep. 1994

W. Holley (Springborn Labs., Inc., Enfield, CT.) Apr. 1995 27 p

(Contract DE-AC36-83CH-10093)

(DE95-004093; NREL/TP-411-7693) Avail: CASI HC A03/MF A01

The following highlights key findings from this reporting period: While 'standard cure' A9918P ethylene vinyl acetate (EVA) encapsulant, laminated between low iron glass, shows significant yellowing after 17 weeks in a xenon-arc Weather-Ometer, 'neat' EVA with no additives shows little or no yellowing after the same exposure. When similar laminates were prepared and exposed in the Weather-Ometer, using A9918P with the Lupersol 101 crosslinker removed from the encapsulant, color development after 10 weeks was reduced by approximately 2/3. This result strongly implicates Lupersol 101 in the discoloration of EVA encapsulant. Similar Weather-Ometer aging studies of other laminates, prepared using EVA with various combinations of the A9918P additives, suggests that EVA discoloration arises primarily from Naugard P and an interaction of Lupersol 101 with Cyasorb UV-531. Transformation products of these additives appear to be giving rise to yellowing, rather than the Elvax 3185 resin itself. When Lupersol TBEC was substituted for Lupersol 101 in the encapsulant (i.e. 'fast cure' 15295P formulation rather than the 'standard cure' A9918P), the rate of yellowing was reduced by a factor of approximately 2.5. Use of a cerium-oxide containing low-iron glass superstrate reduced the rate of yellowing of A9918P EVA by approximately 75%. When laminates were prepared and exposed using 15295P EVA and cerium-oxide containing glass superstrate, there was no visible yellowing. Analytical results show no measurable loss of acetic acid from very browned, field-aged EVA and no evidence of conjugated unsaturation; analysis also reveals the loss of Cyasorb UV-531 in both field-aged and laboratory U.V. aged samples, but

only in the presence of Lupersol 101. This result supports the finding of an interaction of Lupersol 101 with UV-531 as contributing to color formation in the presence of U.V. DOE

N95-33225# National Renewable Energy Lab., Golden, CO.
THE 17TH SYMPOSIUM ON BIOTECHNOLOGY FOR FUELS AND CHEMICALS
1995 206 p Symposium held in Vail, CO, 7-11 May 1995
(Contract DE-AC36-83CH-10093)
(DE95-004054; NREL/SP-420-7849; CONF-950587-Absts) Avail: CASI HC A10/MF A03

This volume contains the abstracts of oral and poster presentations made at the Seventeenth Symposium on Biotechnology for Fuels and Chemicals. Session titles include Thermal, Chemical, and Biological Processing; Applied Biological Research; Bioprocessing Research; Special Topics Discussion Groups; Process Economics and Commercialization; and Environmental Biotechnology. DOE

N95-33383# National Renewable Energy Lab., Golden, CO.
TOMORROW'S ENERGY TODAY FOR CITIES AND COUNTRIES
May 1995 6 p
(Contract DE-AC36-83CH-10093)
(DE95-012464; DOE/GO-10095-086) Avail: CASI HC A02/MF A01

Wind is a proven, cost-effective, and environmentally source of power for public utilities around the country. And with recent technological innovations in wind turbine design, more public utility officials are using this vast renewable energy resource. This paper discusses the usefulness of wind as a source for providing electricity to public utilities. CASI

N95-33400# Pacific Northwest Lab., Richland, WA.
CRADA WITH UNITED SOLAR TECHNOLOGIES AND PACIFIC NORTHWEST LABORATORY (PNL-021): THIN FILM MATERIALSFOR LOW-COST HIGH PERFORMANCE SOLAR CONCENTRATORS Final Project Report
P. M. Martin, J. D. Affinito, M. E. Gross, and W. D. Bennett Mar. 1995 20 p
(Contract DE-AC06-76RL-01830)
(DE95-010423; PNL-10416) Avail: CASI HC A03/MF A01

The objectives of this project were to develop and evaluate promising low-cost dielectric and polymer-protected thin-film reflective metal coatings to be applied to preformed continuously-curved solar reflector panels to enhance their solar reflectance, and to demonstrate protected solar reflective coatings on preformed solar concentrator panels. The opportunity for this project arose from a search by United Solar Technologies (UST) for organizations and facilities capable of applying reflective coatings to large preformed panels. PNL was identified as being uniquely qualified to participate in this collaborative project. DOE

N95-33642# Lawrence Livermore National Lab., Livermore, CA.
UNITIZED REGENERATIVE FUEL CELLS FOR SOLAR RECHARGEABLE AIRCRAFT AND ZERO EMISSION VEHICLES
Fred Mitlitsky, Nicholas J. Colella, and Blake Myers 6 Sep. 1994 8 p Presented at the Fuel Cell Seminar, San Diego, CA, 28 Nov. - 1 Dec. 1994 Submitted for publication
(Contract W-7405-eng-48)
(DE95-010684; UCRL-JC-117130; CONF-941109-3) Avail: CASI HC A02/MF A01

A unitized regenerative fuel cell (URFC) produces power and electrolytically regenerates its reactants using a single stack of reversible cells. URFC'S have been designed for high altitude long endurance (HALE) solar rechargeable aircraft (SRA), zero emission vehicles (ZEV's), hybrid energy storage/propulsion systems for long duration satellites, energy storage for remote (off-grid) power sources, and peak shaving for on-grid applications. URFC's have been considered using hydrogen/oxygen, hydrogen/air, or hydrogen/halogen chemistries. This discussion is limited to the lightweight URFC energy storage system designs for span-loaded HALE SRA using hydrogen/oxygen, and for ZEV's using hydrogen/air with oxygen supercharging. Overlapping and synergistic development and testing opportunities for these two technologies will be highlighted. DOE

N95-33706# Sandia National Labs., Albuquerque, NM.
FATIGUE DAMAGE ESTIMATE COMPARISONS FOR NORTHERN EUROPEAN AND US WIND FARM LOADING ENVIRONMENTS
H. J. Sutherland and N. D. Kelley 1995 10 p Presented at the 25th Annual Conference and Exhibition on Wind Power, Washington, DC, 26-30 Mar. 1995 Prepared in cooperation with National Renewable Energy Lab., Golden, CO
(Contracts DE-AC04-94AL-85000; DE-FC36-86CH-10311)
(DE95-011061; SAND-94-2550C; CONF-950309-6) Avail: CASI HC A02/MF A01

Typical loading histories associated with wind turbine service environments in northern Europe and within a large wind farm in the continental US were recently compared by Kelley using the WISPER (Ten Have) loading standard and its development protocol. In this study, an equivalent load spectrum for a US wind farm was developed by applying the WISPER development protocol to representative service load histories collected from two adjacent turbines operating within a large wind farm in San Gorgonio Pass, California. The results of this study showed that turbines operating in the California wind farm experience many more loading cycles with larger peak-to-peak values for the same mean wind speed classification than their European counterparts. In this paper, the impact of the two WISPER-protocol fatigue-load spectra on service lifetime predictions are used to compare and contrast the impact of the two loading environments with one another. The service lifetime predictions are made using the LIFE2 Fatigue Analysis Code (Sutherland and Schluter), with the fatigue properties of typical fiber glass composite blade materials. Additional analyses, based on rainflow counted time histories from the San Gorgonio turbines, are also used in the comparisons. In general, these results indicate that the WISPER load spectrum from northern European sites significantly underestimates the WISPER protocol load spectrum from a US wind farm site; i.e., the WISPER load spectrum significantly underestimates the number and magnitude of the loads observed at a US wind farm site. The authors conclude that there are fundamental differences in the two service environments. DOE

N95-34359# Ain Shams Univ., Cairo (Egypt).
THE 3RD INTERNATIONAL CONFERENCE ON SOLAR ENERGY STORAGE AND APPLIED PHOTOCHEMISTRY
14 Jan. 1995 160 p Conference held in Cairo, Egypt, 8-14 Jan. 1995
(Contract N68171-94-M-6700)
(AD-A294343) Avail: CASI HC A08/MF A02

This technical report contains abstracts that are presented on the 3rd international conference on solar storage and applied photochemistry. Technological areas discussed include: The rapid deterioration of anthracene laser dyes in chlorinated organic solvents; Photolysis of polyaromatic ethers and thioethers with pendant cyclopentadienyl iron moieties; Photochemical reaction of 4-nitrobenzylidene malononitriles with hydrogen donors; Homogeneous photoinitiated graft copolymerization of 4- vinyl pyridine onto ethyl cellulose; Charge transfer interactions and efficiencies of sensitized singlet oxygen production from substituted biphenyls; Singlet-singlet energy transfer between coumarin 4-water Exciplex and coumarin 314 in aqueous and micellar media; On the photogeneration of pyridylcarbenes; environmental degradation of pesticides under the influence of light; Analytical determination of iron (III): fluorescence quenching technique; Photochemical reactions of dibenzalacetone; The role of inorganic complexes in energy conversion; and Energy transfer from 2,5-distyryl pyrazine(DSP) and 2,5-bis 2(2-naphthyl) vinyl pyrazine(B2NVP) to R6G. DTIC

N95-34360# Ain Shams Univ., Cairo (Egypt).
THE INTERNATIONAL CONFERENCE ON SOLAR ENERGY STORAGE AND APPLIED PHOTOCHEMISTRY
14 Jan. 1995 42 p Conference held in Cairo, Egypt, 8-14 Jan. 1995
(Contract N68171-94-M-6700)
(AD-A294347; R/D-7539-CH-02) Avail: CASI HC A03/MF A01

A bibliography of the international conference on solar energy storage and applied photochemistry is presented. Study areas dicussed include: Nanocrystalline solar cells; scientific principles and economic perspectives; Solar synthesis of hydrogen peroxide; Dye molecules in zeolites as artificial antenna systems; Mechanism of the early steps in photosynthesis; Novel vacuum-uv-(vuv) and uv excimer flow through photorectors for waste water treatment and for wavelengths selective photochemistry; Heterosupramolecular chemistry: an approach to modulating function in

molecular devices; Excited state characteristics and new unactivated C-H bond functionalization photocatalysis by W10O32 (4-); Time-resolved photothermal measurements on biological photoreceptors; Photoinduced proton transfer in substituted pyridines; Photochromic materials: a comprehensive kinetic thermodynamic and photochemical study; Photolysis and thermolysis of acid amides and sulphonamides; mechanistic studies; Studies of photochemical reactions by nuclear spin polarization detected ESR spectroscopy; A non-silver dry processed photographic arts film.

DTIC

N95-34468# Air Force Systems Command, Wright-Patterson AFB, OH. National Air Intelligence Center.

A 30-PAIR THIN FILM THERMOELECTRIC PILE

Shao Qiulin and Han Koulan 26 Apr. 1995 19 p Transl. into ENGLISH from Zidongua Yibiao, China, v. 11, no. 11, 1990 p 24-28

(AD-A294058; NAIC-ID(RS)T-0563-93) Avail: CASI HC A03/MF A01

A thin film thermoelectric pile is an infrared probe element without selectivity with respect to the optical spectrum. The performance indicators of a thermoelectric pile are stable; its structure is firm, sensitivity is high, and response time is short, and the response range of the optical spectrum is wide. A thin film thermoelectric pile can operate at normal temperatures for measuring direct current. The instruments and meters involved do not require additional bias and do not require an adjustment system. Since the pile has its unique advantages, its applications are wide, used as reception elements for noncontact temperature measuring instrumentation, infrared interference alarm instruments, and hot-metal position detectors. DTIC

N95-34481# California Univ., Berkeley. Lawrence Berkeley Lab, CA. Materials Sciences Div.

THIN-FILM ELECTROLYTES FOR REDUCED TEMPERATURE SOLID OXIDE FUEL CELLS

Steven J. Visco, Li-shun Wang, Selmar deSouza, and Lutgard C. deJonghe Nov. 1994 13 p Presented at the 1994 Fall Meeting of the Materials Research Society (MRS), Boston, MA, 27 Nov. - 2 Dec. 1994

(Contract DE-AC03-76SF-00098)

(DE95-011273; LBL-36813; CONF-941144-146) Avail: CASI HC A03/MF A01

Solid oxide fuel cells produce electricity at very high efficiency and have very low to negligible emissions, making them an attractive option for power generation for electric utilities. However, conventional SOFC's are operated at 1000 C or more in order to attain reasonable power density. The high operating temperature of SOFC's leads to complex materials problems which have been difficult to solve in a cost-effective manner. Accordingly, there is much interest in reducing the operating temperature of SOFC's while still maintaining the power densities achieved at high temperatures. There are several approaches to reduced temperature operation including alternative solid electrolytes having higher ionic conductivity than yttria stabilized zirconia, thin solid electrolyte membranes, and improved electrode materials. Given the proven reliability of zirconia-based electrolytes (YSZ) in long-term SOFC tests, the use of stabilized zirconia electrolytes in reduced temperature fuel cells is a logical choice. In order to avoid compromising power density at intermediate temperatures, the thickness of the YSZ electrolyte must be reduced from that in conventional cells (100 to 200 micro m) to approximately 4 to 10 micro m. There are a number of approaches for depositing thin ceramic films onto porous supports including chemical vapor deposition/electrochemical vapor deposition, sol-gel deposition, sputter deposition, etc. In this paper we describe an inexpensive approach involving the use of colloidal dispersions of polycrystalline electrolyte for depositing 4 to 10 micro m electrolyte films onto porous electrode supports in a single deposition step. This technique leads to highly dense, conductive, electrolyte films which exhibit near theoretical open circuit voltages in H2/air fuel cells. These electrolyte films exhibit bulk ionic conductivity, and may see application in reduced temperature SOFC's, gas separation membranes, and fast response sensors. DOE

N95-34656 Rutherford Appleton Lab., Chilton (England). Energy Research Unit.

REVIEW OF THE RESEARCH ACTIVITIES OF THE ENERGY RESEARCH UNIT IN 1994

J. Halliday Jan. 1995 100 p

(PB95-235008; RAL-95-004) Avail: Issuing Activity (National Technical Information Service (NTIS))

The report contains short reviews of the Energy Research Unit's hardware facilities and of its recently completed and ongoing research activities. The Unit was established by the Science and Engineering Research Council (SERC) in the late 1970's to provide university researchers with access to facilities not available within their own institutions. In 1994 a new research council - the Engineering and Physical Sciences Research Council (EPSRC), was created by the Government and took over responsibility for much of SERC's engineering remit, including the support of the facilities provided by the Energy Research Unit. The report reviews the recent research activities of the Unit, and includes all projects active at the end of December 1994 as well as mention of several which have recently been completed.

NTIS

45 ENVIRONMENT POLLUTION

Includes atmospheric, noise, thermal, and water pollution.

N95-32475# Pacific Northwest Lab., Richland, WA.

AN ELECTRONIC DESIGN GUIDELINE FOR INCORPORATING POLLUTION PREVENTION INTO US DEPARTMENT OF ENERGY DESIGN PROJECTS

F. L. Greitzer, B. W. Brown, J. A. Dorsey, J. C. Stitzel, and E. A. Raney (Westinghouse Hanford Co., Richland, WA.) Mar. 1995 11 p Presented at the 1st International Plant Operations and Design Conference, Houston, TX, 21-23 Mar. 1995

(Contract DE-AC06-76RL-01830)

(DE95-008935; PNL-SA-25590; CONF-9503128-1) Avail: CASI HC A03/MF A01

The Pacific Northwest Laboratory has developed a prototype pollution prevention electronic design guideline (EDG) for the U.S. Department of Energy (DOE), Waste Minimization Division (EM-334). The EDG contains a database of 267 opportunities to incorporate pollution prevention features into DOE design projects. Each opportunity provides supporting data that help the decision-maker (designers, engineers, and project managers) evaluate the applicability and potential benefits of implementing pollution prevention in their particular project. The EDG's database was derived from both DOE and non-DOE sources including pollution prevention literature, industrial design personnel, and federal, state, and DOE sources. A key feature of the tool is the integration of photos, illustrations, and documentation to provide easy access to technical information on specific waste minimization opportunities in design. Historically, pollution prevention activities within the U.S. Department of Energy (DOE) have focused on existing process waste streams. However, it is estimated that 70% of the cost over the life of a product is fixed by design (i.e., before the product is constructed or used). In recognition of this pollution prevention opportunity, the DOE has funded the Hanford Site to incorporate it into the design of new products, processes, and facilities across the complex. Hanford Site contractors are now beginning their third year of leading this activity for DOE Headquarters (HQ). DOE

N95-32547# New Energy and Industrial Technology Development Organization, Tokyo (Japan).

TECHNICAL INNOVATION FOR REDUCING EMISSIONS OF GREENHOUSE EFFECT GAS AND SURVEY OF EFFECTS OF CHANGES OF INDUSTRIAL STRUCTURES

31 Mar. 1994 245 p In JAPANESE

(DE95-769808; NEDO-GET-9308) Avail: CASI HC A11/MF A03

The paper evaluates energy utilization efficiency and recycling potential in the industrial sector. Energy conservation in the commercial/residential sector is effective for improvement of energy efficiency of space heating and cooling. In the business sector, heat insulated structure of buildings is increasing, as well as increasing efficiency of heating facilities. In the passenger sector, energy conservation of automobiles is increasing. In the iron and steel industry, energy conservation of 20% was achieved. However, future recovery of exhaust energy needs technical development. The cement industry treats waste from other industrial sectors, aiming at energy conservation. Energy conservation in the petrochemical industry is mainly a combination of process rationalization and increasing of production ability. The electric utility industry tackles the energy conservation issue from the

supply/demand aspect. In the town gas industry, energy conservation is promoted by improvement of energy conversion efficiency and utilization of LNG cold energy. For reference, attached are reports of the Intergovernmental Panel on Climate Change (IPCC). DOE

N95-32553# Argonne National Lab., IL. Material Science Div.
ALTERNATIVE CATALYST AND EXHAUST GAS SENSOR WORK AT ARGONNE NATIONAL LABORATORY
Lennox E. Iton, Victor A. Maroni, Stephen L. Dieckman, Shu-Haw Sheen, and A. C. Raptis 1994 9 p Presented at the Society of Automotive Engineers' Convergence 1994, Detroit, MI, 18-27 Oct. 1994
(Contract W-31-109-eng-38)
(DE95-007138; ANL/ET/CP-85237; CONF-9410256-4) Avail: CASI HC A02/MF A01

Research programs at Argonne National Laboratory in the areas of automobile emissions monitoring and control are described. The mandate to improve automobile efficiency while reducing Pollution requires the development of new catalysts for exhaust emissions control that are capable of functioning efficiently under lean-burn engine operating conditions. It is also desirable that the use of expensive noble metal catalysts be avoided. NO(x) emissions will not be efficiently controlled by the current three-way, supported noble metal catalysts under lean-burn conditions. New catalysts are being sought that could effect the selective catalytic reduction (SCR) of NO(x) by exhaust hydrocarbons in the presence of oxygen. Molecular sieve zeolites of the ZSM-5 and ferrierite types, ion-exchanged with copper ions, are the best of the catalysts known to effect this chemistry, but the mechanism of the SCR is still not understood. In this project the authors will first undertake the investigation of the SCR of NO using model reactions to test postulated mechanistic pathways. Initial experiments have been devised to investigate the possible participation of metal alkyl complexes, metal oxime complexes, N-alkyl-N-nitroso-alkylaminato-metal complexes, and metal nitrile complexes in the zeolites. ANL will also develop microsensors, based on surface acoustic wave (SAW) chemical sensing techniques, and a micro mass-spectrometer (MS) for tailpipe or engine-out emission monitoring. The sensor configurations and sensing techniques of the proposed SAW and micro-MS are described. DOE

N95-32556# Sandia National Labs., Albuquerque, NM. Environmental Characterization Dept.
WINTER SEASON AIR POLLUTION IN EL PASO-CIUDAD JUAREZ. A REVIEW OF AIR POLLUTION STUDIES IN AN INTERNATIONAL AIRSHED
Wayne Einfeld and Hugh W. Church Mar. 1995 166 p
(Contract DE-AC04-94AL-85000)
(DE95-009083; SAND-95-0273) Avail: CASI HC A08/MF A02

This report summarizes a number of research efforts completed over the past 20 years in the El Paso del Norte region to characterize pollution sources and air quality trends. The El Paso del Norte region encompasses the cities of El Paso, Texas and Ciudad Juarez, Chihuahua and is representative of many US-Mexico border communities that are facing important air quality issues as population growth and industrialization of Mexican border communities continue. Special attention is given to a group of studies carried out under special US Congressional funding and administered by the US Environmental Protection Agency. Many of these studies were fielded within the last several years to develop a better understanding of air pollution sources and trends in this typical border community. Summary findings from a wide range of studies dealing with such issues as the temporal and spatial distribution of pollutants and pollution potential from both stationary and mobile sources in both cities are presented. Particular emphasis is given to a recent study in El Paso-Ciudad Juarez that focussed on winter season PM(sub 10)(particles less than 10 micro m diameter) pollution in El Paso-Ciudad Juarez. Preliminary estimates from this short-term study reveal that biomass combustion products and crustal material are significant components of winter season PM(sub 10) in this international border community. DOE

N95-32573# Los Alamos National Lab., NM.
A METHODOLOGY FOR EVALUATING AIR POLLUTION STRATEGIES TO IMPROVE THE AIR QUALITY IN MEXICO CITY
Adrian S. Barrera-Roldan (Instituto Mexicano de Petroleo, Mexico City, Mexico.), Francisco Guzman (Instituto Mexicano de Petroleo, Mexico City, Mexico.), R. Wayne Hardie, and Gary R. Thayer 1995 18 p Presented at the Annual Meeting and Exhibition of the Air and Waste Management Association, Cincinnati, OH, 19-24 Jun. 1994
(Contract W-7405-eng-36)
(DE95-010874; LA-UR-95-1287; CONF-940632-28) Avail: CASI HC A03/MF A01

The Mexico City Air Quality Research Initiative has developed a methodology to assist decision makers in determining optimum pollution control strategies for atmospheric pollutants. The methodology introduces both objective and subjective factors in the comparison of various strategies for improving air quality. Strategies or group of options are first selected using linear programming. These strategies are then compared using Multi-Attribute Decision Analysis. The decision tree for the Multi-Attribute Decision Analysis was generated by a panel of experts representing the organizations in Mexico that are responsible for formulating policy on air quality improvement. Three sample strategies were analyzed using the methodology: one to reduce ozone by 33% using the most cost effective group of options, the second to reduce ozone by 43% using the most cost effective group of options and the third to reduce ozone by 43% emphasizing the reduction of emissions from industrial sources. Of the three strategies, the analysis indicated that strategy 2 would be the preferred strategy for improving air quality in Mexico City. DOE

N95-32668# National Renewable Energy Lab., Golden, CO.
SOLVING WIDESPREAD LOW-CONCENTRATION VOC AIR POLLUTION PROBLEMS: GAS-PHASE PHOTOCATALYTIC OXIDATION ANSWERS THE NEEDS OF MANY SMALL BUSINESSES
C. Lyons, C. Turchi, and D. Gratson Apr. 1995 11 p Presented at the Air and Waste Management Association Meeting, San Antonio, TX, 18-23 Jun. 1995
(Contract DE-AC36-83CH-10093)
(DE95-004059; NREL/TP-473-7569; CONF-950646-16) Avail: CASI HC A03/MF A01

Many small businesses are facing new regulations under the 1990 Amendments to the Clean Air Act. Regulators, as well as the businesses themselves, face new challenges to control small point-source air pollution emissions. An individual business-such as a dry cleaner, auto repair shop, bakery, coffee roaster, photo print shop, or chemical company-may be an insignificant source of air pollution, but collectively, the industry becomes a noticeable source. Often the businesses are not equipped to respond to new regulatory requirements because of limited resources, experience, and expertise. Also, existing control strategies may be inappropriate for these businesses, having been developed for major industries with high volumes, high pollutant concentrations, and substantial corporate resources. Gas-phase photocatalytic oxidation (PCO) is an option for eliminating low-concentration, low-flow-rate emissions of volatile organic compounds (VOC's) from small business point sources. The advantages PCO has over other treatment techniques are presented in this paper. This paper also describes how PCO can be applied to specific air pollution problems. We present our methodology for identifying pollution problems for which PCO is applicable and for reaching the technology's potential end users. PCO is compared to other gas-phase VOC control technologies. DOE

N95-32686# National Renewable Energy Lab., Golden, CO.
ENVIRONMENTAL CHAMBER STUDIES OF ATMOSPHERIC REACTIVITIES OF VOLATILE ORGANIC COMPOUNDS: EFFECTS OF VARYING CHAMBER AND LIGHT SOURCE
W. Carter, D. Luo, I. Malkina, and J. Pierce (California Univ., Riverside, CA.) May 1995 105 p
(Contract DE-AC36-83CH-10093)
(DE95-009225; NREL/TP-425-7621) Avail: CASI HC A06/MF A02

Photochemical oxidant models are essential tools for assessing effects of emissions changes on ground-level ozone formation. Such models are needed for predicting the ozone impacts of increased alternative fuel use. The gas-phase photochemical mechanism is an important component of these models because ozone is not emitted directly, but is formed from the gas-phase photochemical reactions of the emitted volatile organic compounds (VOC's) and oxides of nitrogen NO(x) in air. The chemistry of ground level ozone formation is complex; hundreds of types of VOC's being emitted into the atmosphere, and most of their atmospheric reactions are not completely understood. Because of this, no chemical model can be relied upon to give even approximately accurate predictions unless it has been evaluated by comparing its predictions with experimental data.

Therefore, an experimental and modeling study was conducted to assess how chemical mechanism evaluations using environmental chamber data are affected by the light source and other chamber characteristics. Xenon arc lights appear to give the best artificial representation of sunlight currently available, and experiments were conducted in a new Teflon chamber constructed using such a light source. Experiments were also conducted in an outdoor Teflon Chamber using new procedures to improve the light characterization, and in Teflon chambers using blacklights. These results, and results of previous runs in other chambers, were compared with model predictions using an updated detailed chemical mechanism. The magnitude of the chamber radical source assumed when modeling the previous runs were found to be too high; this has implications in previous mechanism evaluations. Temperature dependencies of chamber effects can explain temperature dependencies in chamber experiments when Ta-300 K, but not at temperatures below that. DOE

N95-32809# National Renewable Energy Lab., Golden, CO.
THE NEXT GENERATION OF AUTOMOBILE EMISSIONS REDUCTION: INNOVATIVE CONTROL OF OFF-CYCLE EMISSIONS
Thomas Potter, F. and Carol E. Lyons Mar. 1995 19 p Presented at the Air and Waste Management Association Meeting, San Antonio, TX, 18-23 Jun. 1995
(Contract DE-AC36-83CH-10093)
(DE95-004057; NREL/TP-473-7570; CONF-950646-8) Avail: CASI HC A03/MF A01

Innovative heat management technologies can reduce emissions from cars by an order of magnitude. Substantial reductions would be realized during cold starts and in evaporative emissions. Such improvements result from a new class of variable-conductance steel vacuum insulations that insulate during one time period and take advantage of beneficial thermal conditions during another. Around a catalytic converter, for example, such control allows heat from one driving cycle to catalyze engine-out emissions occurring at the beginning of the next cycle. As with other more efficient uses of heat in automobiles, reduced complexity and cost are likely compared to supplemental catalyst heating systems. In a similar way, thermal cycling of fuel and the resulting vapor release can be reduced or avoided. Urban air quality could be greatly improved by the wide availability of vehicles using these technologies early in the next century. This paper presents analyses and prototype data supporting the design, operation, and rapid market penetration of internal combustion engine vehicles with significantly lower emissions based on such improved thermal management. Potential implications for fleet emissions are discussed. DOE

N95-32816# EIC, Inc., Norwood, MA.
FIELD RAMAN SPECTROGRAPH FOR ENVIRONMENTAL ANALYSIS
Michael M. Carrabba 1995 8 p Presented at the Opportunity 1995: Environmental Technology Through Small Business, Morgantown, WV, 16-17 Nov. 1994
(Contract DE-AC21-92MC-29108)
(DE95-007969; DOE/MC-29108/95/C0417; CONF-9411149-28) Avail: CASI HC A02/MF A01

The use of Raman Spectroscopy in the screening of soils, ground water, and surface waters for pollutants is described. A probe accessory for conducting surface enhanced Raman Spectroscopy is undergoing testing for dilute chlorinated solvents. DOE

N95-33192# Brookhaven National Lab., Upton, NY. Environmental Chemistry Div.
COMPARISON OF SEASONAL AND ZONAL PATTERNS OF THE DIRECT AND INDIRECT RADIATIVE FORCING OF CLIMATE BY AEROSOLS
R. Wagener and S. E. Schwartz Mar. 1995 5 p Presented at the 5th Atmospheric Radiation Measurement (ARM) Meeting, San Diego, CA, 20-23 Mar. 1995
(Contract DE-AC02-76CH-00016)
(DE95-010896; BNL-60197; CONF-9503140-1) Avail: CASI HC A01/MF A01

Aerosols have a climatically significant influence on the absorption of shortwave radiant energy in the troposphere, both directly through enhanced scattering of sunlight in the absence of clouds and indirectly through their fundamental role in controlling cloud microphysical properties. Quantitative estimates of the magnitudes of both effects are very uncertain. To possibly distinguish these effects, the authors calculated the monthly and zonally averaged forcing for a spatially uniform and seasonally constant perturbation in aerosol and cloud optical properties. DOE

N95-33205# Colorado State Univ., Fort Collins, CO. Dept. of Atmospheric Science.
IMPACT OF CLOUD MICROPHYSICS ON CLOUD-RADIATION INTERACTIONS IN THE CSU GENERAL CIRCULATION MODEL
Laura D. Fowler and David A. Randall 1995 5 p Presented at the 74th American Meteorological Society Annual Meeting, Nashville, TN, 23-28 Jan. 1994
(Contract DE-FG02-91ER-61218)
(DE95-008979; CONF-940115-33) Avail: CASI HC A01/MF A01

Our ability to study and quantify the impact of cloud-radiation interactions in studying global scale climate variations strongly relies upon the ability of general circulation models (GCMs) to simulate the coupling between the spatial and temporal variations of the model-generated cloudiness and atmospheric moisture budget components. In particular, the ability of GCMs to reproduce the geographical distribution of the sources and sinks of the planetary radiation balance depends upon their representation of the formation and dissipation of cloudiness in conjunction with cloud microphysics processes, and the fractional amount and optical characteristics of cloudiness in conjunction with the mass of condensate stored in the atmosphere. A cloud microphysics package which encompasses five prognostic variables for the mass of water vapor, cloud water, cloud ice, rain, and snow has been implemented in the Colorado State University General Circulation Model (CSU GCM) to simulate large-scale condensation processes. Convection interacts with the large-scale environment through the detrainment of cloud water and cloud ice at the top of cumulus towers. The cloud infrared emissivity and cloud optical depth of the model-generated cloudiness are interactive and depend upon the mass of cloud water and cloud ice suspended in the atmosphere. The global atmospheric moisture budget and planetary radiation budget of the CSU GCM obtained from a perpetual January simulation are discussed. Geographical distributions of the atmospheric moisture species are presented. Global maps of the top-of-atmosphere outgoing longwave radiation and planetary albedo are compared against Earth Radiation Budget Experiment (ERBE) satellite data. DOE

N95-33331# State Pollution Control Authority, Oslo (Norway).
POLLUTION IN NORWAY
S. Midtland 1993 55 p
(PB95-214565; TA-995/1993) Avail: CASI HC A04/MF A01

The report describes developments within the agency's fields of responsibility, with particular emphasis on emissions of pollutants, the state of the environment, and anticipated developments. The data are based on reports from industrial enterprises, material flow analyses, modelling, and data from the National Environmental Monitoring Program run by the State Pollution Control Authority. NTIS

N95-33337 New Hampshire Univ., Durham, NH.
MODELING SOIL CLIMATE CONTROLS ON THE EXCHANGE OF TRACE GASES BETWEEN THE TERRESTRIAL BIOSPHERE AND THE ATMOSPHERE Ph.D. Thesis
Stephen Edward Frolking 1993 245 p
Avail: Univ. Microfilms Order No. DA9420564

Soil temperature and moisture profiles (soil climate) have a strong influence on the rate of trace gas exchange between the terrestrial biosphere and the atmosphere through the controls exerted on microbial processes and the physical exchange of gases. Principal controls of biological denitrification in mineral soils are the availability of carbon and nitrogen substrates and the soil anaerobic status. A process-oriented model of decomposition and denitrification in soils (DNDC) was modified to have a more detailed portrayal of these controls. In particular, a diffusive soil gas phase was added, along with a method for determining anaerobic and aerobic fractional volume within a soil profile. The model generally overestimated N2O fluxes when compared to field data from a sandy soil in Costa Rica, but captured the timing and shape of the brief flux episodes. Several modelling shortcomings are discussed, including the nature of the carbon substrates and the nature and dynamics of soil anaerobic fractional volume. Methane flux from wetland soils is generally correlated with soil temperature and depth to water table. A model of peat soil climate was

developed and applied to a small, poor fen in southern New Hampshire. Temperature profiles and ice depth are in good agreement with field data, but depth to water table is more problematic. Field-based flux correlations to soil temperature, depth to water table, and weighted recent precipitation were developed. When used with the wetland soil climate model, much of the seasonal and shorter period flux variability was captured. The model was then driven by local weather data for 1926-1986; flux variability was dependent on both summer season temperatures and summer precipitation patterns. It is estimated that a five-year field study would capture most of the inter-annual variability. Sensitivity of northern peatland methane flux to climate variability was studied by combining data on flux rates, inundation areas, and summer temperature anomalies (1900-1986) for the eight major northern peatland regions. Spatial and temporal variability in summer temperature anomalies caused regional methane flux anomalies to be small, and not likely to provide a strong feedback to initial climate change.

Author

N95-33339 Iowa Univ., Iowa City, IA.

MULTISCALE CHARACTERISTICS AND MODELING OF ATMOSPHERIC METHANE Ph.D. Thesis

Kurtis Gerhardt Paterson 1993 283 p

Avail: Univ. Microfilms Order No. DA9421183

Methane influences the atmospheric radiative balance, ozone cycle, oxidizing capacity, and stratospheric water vapor abundance. Heightening concern, methane concentrations are increasing globally due to increasing emissions, predominantly from human activities. Atmospheric methane measurements over 1983-1989 from twelve stations in the NOAA flask sampling network were used for statistical analysis and model calibration. Methane concentrations are greatest at high northern latitudes and decrease southward. Seasonal cycles are present at all latitudes but greatest at high northern latitudes. Concentrations are increasing at all latitudes, but the rates of increase are decreasing at most stations. Model studies suggest that hydroxyl radical concentrations are increasing in the northern hemisphere and decreasing in the southern hemisphere. The rate of increase in the northern hemisphere is greater than the southern. The rate of increase decreased more rapidly in the northern hemisphere. A six month cycle exists in the northern hemisphere. The methane interhemispheric ratio oscillates annually, but shows no long-term trend. This, plus decreasing atmospheric methane residence times, suggests that the methane hemispheric source ratio decreased throughout the 1980's. Global atmospheric methane concentrations continue to increase, although the rate of increase decreased throughout the 1980's. The global concentration record contains twelve and six month cycles. Removing the latter produces a much smoother seasonal cycle. A global methane mass balance model indicates increasing global hydroxyl radical concentrations contribute significantly to the decreasing methane rate of increase. Decreasing natural sources or increasing soil sinks are needed to achieve mass balance closure. Simulations suggest global methane concentrations will peak in twenty years. Cryogenic Limb Array Etalon Spectrometer methane measurements delineate major transport mechanisms throughout the middle atmosphere. Seasonal patterns suggest the dominance of changing transport in the tropics and chemistry in the polar regions. Methane concentrations are increasing, but rates of increase are confounded by measurement uncertainty. Methanenitrous oxide correlations indicate temporal and spatial variability in stratospheric transport and photochemistry. Fugitive methane emissions can be recovered at low cost or profit to lessen anthropogenic contributions to the global budget. Engineering is needed for successful policy implementation. Atmospheric policies must not be considered in isolation, as impacts may be offsetting. Dissert. Abstr.

N95-33394# Argonne National Lab., IL.

THE NATURE AND FATE OF NATURAL RESINS IN THE GEOSPHERE 6: ANALYSIS OF FOSSIL RESINS FROM AXEL HEIBERG ISLAND CANADIAN ARCTIC

Ken B. Anderson and Ben A. LePage (Alberta Univ., Edmonton, Alberta.) 1995 26 p Presented at the 208th American Chemical Society National Meeting, Washington, DC, 21-25 Aug. 1994

(Contract W-31-109-eng-38)

(DE95-012212; ANL/CHM/CP-85869; CONF-940813-41) Avail: CASI HC A03/MF A01

Ambers are well known and abundant in terrestrial sediments all over the world; however, due largely to the absence of definite morphological characteristics, the precise botanical origin of most amber samples, are at best, often a matter of speculation. This has severely restricted the usefulness of amber in paleobotanical and paleoecological interpretations. The molecular composition and structural characteristics of fossil resins however, may preserve evidence of their botanical origin, which could be of great value in both geochemical, paleobotanical, and paleoenvironmental studies. The remains of a number of exceptionally well-preserved Taxodiaceae-dominated swamp-forest communities have been identified in the sediments of the middle Eocene (45 million years old) Buchanan Lake Formation of Axel Heiberg Island, Canadian Arctic Archipelago. The amber collected from these ancient in situ forests provides a unique opportunity to characterize these resins chemically and taxonomically. Resinite associated with Metasequoia, Pinus and Pseudolarix has been characterized using Pyrolysis-Gas Chromatography-Mass Spectrometry. This method provides a direct analysis of the molecular structure and composition of the resin. In several cases, both bled resin and cone-resin samples have been characterized. The results of these analyses are presented and discussed. The implications of these results for the botanical origins of other ambers represented in the fossil record (including succinite) will also be discussed. DOE

N95-33413# Columbia Univ., New York, NY.

ABSTRACTS OF ORAL AND POSTER SESSIONS

Leonard M. Druyan 1994 22 p Presented at the European Conference on the Global Energy and Water Cycle, London, England, 18-22 Jul. 1994

(Contract DE-FG02-92ER-61477)

(DE95-011951; CONF-9407181-Absts) Avail: CASI HC A03/MF A01

The climate model of the Goddard Institute for Space Studies (GISS GCM) has been used to project the influence of increasing concentrations of greenhouse gases on the future global climate. New parameterizations for the GISS GCM are being developed to improve its depiction of current climate scenarios and to make it more sensitive to the variability of external forcing mechanisms such as sea-surface temperatures (SST), atmospheric aerosols and constituent trace gases. The new moist convection scheme makes cumulus fluxes proportional to vertical thermal instability and computes convective-scale downdrafts whose effect is to prevent excessive drying of the boundary layer by compensating subsidence. The physically-based ground hydrology component improves the land surface sensible and latent heat calculations by explicitly considering transpiration, evaporation from intercepted precipitation, evaporation from bare soil, infiltration, soil water flow and runoff. The revised planetary boundary layer uses a more valid physical model than previously to obtain more realistic near-surface winds and energy budgets. Preliminary results with newer versions of the GCM include a better seasonal migration of the ITCZ and more realistic tropical winds. One of our approaches to model validation is the evaluation of runs forced by globally observed sea-surface temperatures. The presentation will show how model improvements increase the quality of simulated interannual variations in global circulation and tropical rainfall.

DOE

N95-33638# Allied-Signal Aerospace Co., Kansas City, MO. Kansas City Div.

DEVELOPMENT OF ENVIRONMENTALLY CONSCIOUS CLEANING PROCESS FOR LEADLESS CHIP CARRIER ASSEMBLIES Final Report

B. E. Adams Apr. 1995 48 p

(Contract DE-AC04-76DP-00613)

(DE95-010186; KCP-613-5556) Avail: CASI HC A03/MF A01

A cross-functional team of process, product, quality, material, and design lab engineers was assembled to develop an environmentally friendly cleaning process for leadless chip carrier assemblies (LCCAs). Using flush and filter testing, Auger surface analysis, GC-Mass spectrophotometry, production yield results, and electrical testing results over an extended testing period, the team developed an aqueous cleaning process for LCCAs. The aqueous process replaced the Freon vapor degreasing/ultrasonic rinse process.

DOE

N95-33655# Oak Ridge National Lab., TN.

CARBON DIOXIDE INFORMATION ANALYSIS CENTER AND WORLD DATA CENTER: A FOR ATMOSPHERIC TRACE GASES Annual Progress Report

Marvel D. Burtis, comp. (Tennessee Univ., Knoxville, TN.), Robert M. Cushman, Thomas A. Bodan, Sonja B. Jones, Tommy R. Nelson, and

Frederick W. Stoss Mar. 1995 65 p
(Contract DE-AC05-84OR-21400)
(DE95-011769; ORNL/CDIAC-76) Avail: CASI HC A04/MF A01

This report summarizes the activities and accomplishments made by the Carbon Dioxide Information Analysis Center and World Data Center-A for Atmospheric Trace Gases during the fiscal year 1994. Topics discussed in this report include; organization and staff, user services, systems, communications, Collaborative efforts with China, networking, ocean data and activities of the World Data Center-A. DOE

N95-34435# Westinghouse Hanford Co., Richland, WA.
ABCASH PLOTTING PROGRAM USERS GUIDE
G. L. Troyer 25 Apr. 1995 15 p
(Contract DE-AC03-87RL-10930)
(DE95-011652; WHC-SD-EN-CSUD-002) Avail: CASI HC A03/MF A01

The Automated Bar Coding of Air Samples at Hanford (ABCASH) system provides an integrated data collection, sample tracking, and data reporting system for radioactive particulate air filter samples. The ABCASH plotting program provides a graphical trend report for ABCASH of the performance of air sample results. This document provides an operational guide for using the program. Based on sample location identifier and date range, a trend chart of the available data is generated. The trend chart shows radiological activity versus time. General indications of directional trend of the concentrations in air over time may be discerned. Comparison limit set point values are also shown as derived from the ABCASH data base. DOE

N95-34441# Pacific Northwest Lab., Richland, WA.
MULTIMEDIA ENVIRONMENTAL POLLUTANT ASSESSMENT SYSTEM (MEPAS(TRADEMARK)): EXPOSURE PATHWAY AND HUMAN HEALTH IMPACT ASSESSMENT MODELS
D. L. Strenge and P. J. Chamberlain May 1995 177 p
(Contract DE-AC06-76RL-01830)
(DE95-012763; PNL-10523; UC-630) Avail: CASI HC A09/MF A02

The Multimedia Environmental Pollutant Assessment System (MEPAS) provides physics-based models for human health risk assessment for radioactive and hazardous pollutants. MEPAS analyzes pollutant behavior in various media (air, soil, groundwater and surface water) and estimates transport through and between media and exposure and impacts to the environment, to the maximum individual, and to populations. MEPAS includes 25 exposure pathway models, a database with information on more than 650 contaminants, and a sensitivity module that allows for uncertainty analysis. Four major transport pathways are considered in MEPAS: groundwater, overland, surface water, and atmospheric. This report describes the exposure pathway and health impact assessment component of MEPAS, which provides an estimate of health impacts to selected individuals and populations from exposure to pollutants. The exposure pathway analysis starts with pollutant concentration in a transport medium and estimates the average daily dose to exposed individuals from contact with the transport medium or a secondary medium contaminated by the transport medium. The average daily dose is then used to estimate a measure of health impact appropriate to the type of pollutant considered. Discussions of the exposure pathway models include the assumptions and equations used to convert the transport medium concentrations to exposure medium concentrations. The discussion for a given exposure pathway defines the transport pathways leading to the exposure, the special processes considered in determining the pollutant concentration in the exposure medium, and the exposure model used to estimate the average daily dose. Models for the exposure pathway and health impact assessments require definition of several parameters. A summary of the notation used for these parameters is provided. DOE

N95-34591# Cornell Univ., Ithaca, NY.
GEOCHEMICAL, GENETIC, AND PHYSIOLOGICAL CONTROL OF POLLUTANT BIODEGRADATION Final Technical Report, 30 Mar. 1991 - 31 Mar. 1995
Eugene L. Madsen and Leonard W. Lion 12 May 1995 77 p
(Grant AF-AFOSR-0436-91)
(AD-A294902; AFOSR-95-0424TR) Avail: CASI HC A05/MF A01

This project has merged four-research areas (field geochemistry, sorption chemistry microbiology, and molecular biology) in order to understand the behavior of low molecular weight polycyclic aromatic hydrocarbon (PAH) compounds in a contaminated field site. Naphthalene has been transported approximately 400 m via ground-water flow from buried subsurface coal-tar to an organic matter-rich seep area where the water energies at the foot of a hill at a field study site. Gas chromatographic analyses of cores taken from the sediments show naphthalene concentrations in vertical profiles ranging from 0.9 to 45 ug/cu cm. We have tested hypotheses for explaining why naphthalene and phenanthrene persists in seep sediments and found that neither toxicity, nor nutrient limitation, nor the absence of microorganisms or appropriate catabolic genes were the cause of PAH persistence. Despite clear laboratory indications of 02- limited naphthalene metabolism, when H2O2 was added to site sediments in situ in a randomized block design, no discernible naphthalene loss occurred. DTIC

N95-33735*# Consiglio Nazionale delle Ricerche, Rome (Italy).
CNR LARA PROJECT, ITALY: AIRBORNE LABORATORY FOR ENVIRONMENTAL RESEARCH
R. Bianchi, R. M. Cavalli, L. Fiumi, C. M. Marino, and S. Pignatti *In* JPL, Summaries of the Fifth Annual JPL Airborne Earth Science Workshop. Volume 1: AVIRIS Workshop 23 Jan. 1995 p 15-18 (For primary document see N95-33730 12-42)
Avail: CASI HC A01/MF A02

46 GEOPHYSICS

Includes aeronomy; upper and lower atmosphere studies; ionospheric and magnetospheric physics; and geomagnetism.

For space radiation see *93 Space Radiation.*

N95-32455# Helsinki Univ. of Technology, Espoo (Finland). Radio Lab.
OPTIMIZATION OF A MELTING LAYER MODEL IN THE RADAR BACKSCATTER, ATTENUATION, AND PHASE SHIFT CALCULATIONS AT CENTIMETER AND MILLIMETER WAVELENGTHS
Z. Wei Aug. 1994 22 p
(PB95-207189; ISBN-951-22-2228-0) Avail: CASI HC A03/MF A01

This report addresses the optimization of a melting layer model in the radar backscatter, attenuation, and phase shift calculations at centimeter and millimeter wavelengths. The model of a melting layer where snowflakes (snow particles) melt and become raindrops consists of the size distribution of the melting snow particles, the average dielectric function of the melting snow particle, the thickness of a melting layer, and the density of the dry snowflakes on the top of the melting layer. It allows one to formulate and further compute both the radar backscatter and the forward scattering by the melting layer of precipitation. Scattering by single spherical and oblate-spheroidal hydrometeors is computed by applying the well known Mie theory and point matching technique, respectively. On a related point, the differential attenuation and phase shift applied to the depolarization calculations are computed at 5-100 GHz. These can apply not only to the radar remote sensing and satellite-earth communications at present but also to some millimeter wave radar technique and depolarization considerations in the future. NTIS

N95-32599# Geological Survey of Britain, Keyworth (England).
UNITED KINGDOM MINERALS YEARBOOK, 1994. STATISTICAL DATA TO 1993
G. J. Lofty, D. E. Highley, D. G. Bate, J. A. Hillier, and K. A. Linley 1995 92 p
(PB95-207841) Copyright Avail: CASI HC A05/MF A01

This yearbook contains data on mineral production, consumption, and trade, and includes an up-to-date and authoritative commentary on current developments in the mineral industry in the United Kingdom. Contents include chapters on minerals in the national economy, energy minerals, construction and industrial minerals, metals, and commodity summaries. Derived from text

N95-32601# Geological Survey of Britain, Keyworth (England).
WORLD MINERAL STATISTICS, 1988-92. PRODUCTION: EXPORTS: IMPORTS
G. J. Lofty, J. A. Hillier, D. G. Bate, K. A. Linley, and N. E. Hutchinson 1 Nov. 1994 282 p
(PB95-208096; ISBN-0-85272-240-0) Copyright Avail: CASI HC A13/MF A03

The report covers the majority of economically important, and internationally traded, mineral commodities, and for the past two editions has been published in two volumes covering metallic and energy minerals, and nonmetallic minerals. These two volumes have again been amalgamated into this edition. For each commodity constant efforts are made to ensure that as many producing and trading countries as possible are reported and that trade data cover all major traded forms. NTIS

N95-32603# Geological Survey of Britain, Keyworth (England).
WORLD MINERAL PRODUCTION, 1989-93. PRELIMINARY STATISTICS
G. J. Lofty, J. A. Hillier, D. G. Bate, and G. R. Chapman 1995 92 p
(PB95-208104; ISBN-0-85272-241-9) Copyright Avail: CASI HC A05/MF A01

This supplement to World Mineral Statistics has been prepared to give available data on world production of minerals and metals at an earlier date. The data in this supplement comprise updated and revised production statistics for the years 1989-92 and preliminary figures for 1993. NTIS

N95-32697# Lawrence Livermore National Lab., Livermore, CA.
LARGE-EDDY SIMULATION OF THE DEVELOPMENT OF STABLY-STRATIFIED ATMOSPHERIC BOUNDARY LAYERS OVER COOL FLAT SURFACES
Richard T. Cederwall Dec. 1994 6 p Presented at the 11th Symposium on Boundary Layers and Turbulence, Charlotte, NC, 27-31 Mar. 1995
(Contract W-7405-eng-48)
(DE95-009574; UCRL-JC-118405; CONF-950381-2) Avail: CASI HC A02/MF A01

The stable boundary layer (SBL) has received less attention in atmospheric field studies, laboratory experiments, and numerical modeling than other states of the atmospheric boundary layer. The low intensity and potential intermittency of turbulence in the SBL make it difficult to measure and characterize its structure. Large-eddy simulation (LES) offers an approach for simulating the SBL and, in particular, its evolution from the onset of surface cooling. Traditional approaches that involve Reynolds-averaged models of turbulence are not able to simulate the stochastic nature of the intermittent turbulence that is associated with the SBL. LES shows promise in this area through its explicit calculation of turbulent eddies at resolved scales. In the LES approach, the Navier-Stokes equations governing the flow are averaged (filtered) over some small interval, such as one or more cells of the computational grid. The grid size is small enough so that large eddies, which carry most of the turbulent energy, are explicitly calculated. The turbulence associated with the subgrid-scale (SGS) eddies is modeled. In the Reynolds-averaging approach, on the other hand, the turbulence model must account for all scales of turbulence. Thus the advantage of LES is that the choice of turbulence parameterization for the SGS turbulence is not nearly as critical as in the Reynolds-averaged approach. Complications faced by turbulence models, such as anisotropy and pressure-strain correlations, are associated mainly with large, energy-containing eddies. LES offers the potential for more realistic simulations since the more complicated features of turbulence are calculated explicitly. The ability of LES to simulate the stochastic behavior of turbulence makes this approach suitable for developing and testing stochastic models of turbulent diffusion. One of the goals of the present work is to provide stochastic datasets to be used in such studies. DOE

N95-33847# Argonne National Lab., IL. Environmental Research Div.
WAVELET ANALYSIS OF ATMOSPHERIC TURBULENCE STRUCTURES: WHAT CAN WE GAIN FROM THIS NEW TECHNIQUE?
Weigang Gao and Bai-Lian Li (Texas A&M Univ., College Station, TX.) 1995 5 p Presented at the 11th Symposium on Boundary Layers and Turbulence, Charlotte, NC, 27-31 Mar. 1995
(Contract W-31-109-eng-38)
(DE95-011955; ANL/ER/CP-84929; CONF-950381-4) Avail: CASI HC A01/MF A01

The authors examined three specific methods for using the wavelet transform to derive information on the turbulence structure in the atmospheric boundary layer from raw data. The scale-time cross section method yields a qualitative picture of turbulence structures occurring at different times and different scales, the wavelet variance method provides a relatively objective estimate of principal scales associated with organized structures, and the wavelet cross correlation helps in identifying motions that are most important in turbulent transport and spatial coherence. The wavelet analysis can also be used to decompose the data for different scales and to detect coherent structures objectively by using the transform coefficient at the principal scale detected by the variance method (Collineau and Brunet, Coulter and Li). These methods can improve their capability to unfold the data for hidden information that is difficult to obtain from traditional spectral analysis and thus can provide a useful tool for understanding multiscale phenomena in the atmospheric boundary layer. DOE

N95-34214# Brookhaven National Lab., Upton, NY. Environmental Chemistry Div.
ENHANCED SHORTWAVE CLOUD RADIATIVE FORCING DUE TO ANTHROPOGENIC AEROSOLS
S. E. Schwartz and A. Slingo May 1995 46 p Presented at the NATO Advanced Research Workshop on Clouds, Chemistry and Climate, Heidelberg, Germany, 1995 Prepared in cooperation with Meteorological Office, Bracknell, England Submitted for publication in Clouds, Chemistry and Climate
(Contract DE-AC02-76CH-00016)
(DE95-013319; BNL-61815; CONF-950001-1) Avail: CASI HC A03/MF A01

It has been suggested that anthropogenic aerosols in the troposphere can influence the microphysical properties of clouds and in turn their reflectivity, thereby exerting a radiative influence on climate. This article presents the theoretical basis for of this so-called indirect forcing and reviews pertinent observational evidence and climate model calculations of its magnitude and geographical distribution. We restrict consideration to liquid-water clouds. DOE

N95-34283 Wyoming Univ., Laramie, WY.
MODELING SEISMIC WAVE PROPAGATION IN HETEROGENEOUS MATERIALS USING FINITE ELEMENTS Ph.D. Thesis
Curtis Lee Card 1993 138 p
Avail: Univ. Microfilms Order No. DA9418667

A major goal of computational seismology is the fast, accurate solution of the wave equation for perfectly elastic, isotropic, heterogeneous media, especially in the presence of discontinuities in material properties. Such discontinuities are referred to as interfaces. Traditionally, the analysis of finite-difference schemes is limited to very restricted interfaces, such as those that coincide with lines formed by the spatial grid. This work focuses on the construction of difference-like schemes, resulting from application of the finite-element method, that are capable of treating more general interfaces in an efficient manner. These schemes provide concrete procedures for accommodating the wide variety of subsurface structures of exploration interest. Furthermore, like the standard difference schemes, they can be efficiently solved using explicit timestepping techniques. Three schemes for evaluating the integrals resulting from the Galerkin formulation are considered. In the first scheme, these integrals are evaluated using exact quadrature. A rigorous analysis demonstrates this scheme to have optimal order accuracy. However, the zero structure of the mass and stiffness matrices precludes its use in practice, since explicit timestepping procedures for solving such systems are very inefficient. For the second scheme, the preview scheme is modified by using the trapezoid rule to evaluate the Galerkin integrals. In the absence of an interface or when all interfaces coincide with grid lines, this is identical to the standard five-point finite-difference scheme. Otherwise, the stiffness matrices have nine diagonals. Here, use of the trapezoid rule results in the mass matrix being a diagonal matrix, whether or not an interface is present. In one spatial dimension, use of the trapezoid rule to approximate the mass and stiffness matrices preserves O(h squared) accuracy. For two-dimensional problems, use of the trapezoid rule to evaluate only the mass matrix preserves optimal-order accuracy. However, application of the trapezoid rule to both the mass and stiffness matrices results in error estimates of only O(h). The third scheme modifies the second scheme by using a lumping procedure to convert the stiffness matrix into a pentadiagonal matrix. Although, an analysis of this scheme is unavailable, the numerical experiments indicate this to be a reasonable candidate for extending the finite-difference scheme. Finally, we extend the second scheme to the fully elastic case. The results of numerical experiments are included that demonstrate the capabilities of this scheme in the presence of an interface. Dissert. Abstr.

N95-34299# Air Force Systems Command, Wright-Patterson AFB, OH. National Air Intelligence Center.
STIMULATED ROTATIONAL RAMAN SCATTERING OF N2 IN THE ATMOSPHERE
Song Ruhua and Yue Shixiao 7 Apr. 1995 12 p Transl. into ENGLISH from unidentified Chinese language document, p 679-681
(AD-A294195; NAIC-ID(RS)T-0443-93) Avail: CASI HC A03/MF A01

This article generally describes stimulated rotational Raman scattering (SRRS) of N2 in the atmosphere. It summarizes theoretical and experimental research work in the field in question in recent years. In conjunction with this, it carries out discussions on a number of problems which still have not been resolved up to now. DTIC

N95-34613# Aerospace Corp., El Segundo, CA. Technology Operations.
IRON BOLTZMANN FACTOR LIDAR: PROPOSED NEW REMOTE-SENSING TECHNIQUE FOR MESOSPHERIC TEMPERATURE
Jerry A. Gelbwachs 15 Jan. 1995 11 p
(Contract F04701-93-C-0094)
(AD-A293568; TR-94(4925)-1; SMC-TR-95-12) Avail: CASI HC A03/MF A01

We describe a new LIDAR technique for middle atmospheric temperature measurement. The proposed LIDAR exploits the Fe layer in the 80 to 100 km altitude region. Absolute temperatures are inferred by the use of the Maxwell-Boltzmann relationship from the ratio of LIDAR returns from mesospheric Fe atoms excited at 372 and 374 nm, corresponding to the ground-state resonance line and a thermally populated resonance line, respectively. The wavelengths of the new LIDAR are favorable for capturing Rayleigh signals from the middle atmosphere. A simulation indicates that a complete temperature profile from 30 to 100 km can be acquired with the proposed LIDAR by monitoring simultaneously the Rayleigh signals and the Fe fluorescence returns excited by the same transmitter pulse. DTIC

N95-34751# Naval Postgraduate School, Monterey, CA.
TURBULENT HEAT FLUX MEASUREMENTS OVER THE GREENLAND, NORWEGIAN AND BARENTS SEAS M.S. Thesis
Joseph C. Johnson Mar. 1995 91 p
(AD-A294129) Avail: CASI HC A05/MF A01

Turbulent heat fluxes in the Greenland, Norwegian and Barents Seas during March 1988, February and March 1989, November 1991 and January and March 1992 have been calculated with the bulk method using shipboard-based measurements of wind speed, air and sea surface temperatures, relative humidity and atmospheric pressure. The largest mean total turbulent heat flux, near 250 W/sq m, was in the Greenland Sea in March 1989. The Norwegian Sea had mean turbulent heat fluxes of 130 W/sq m, whereas the Barents Sea had the smallest mean turbulent heat fluxes. These results compared satisfactorily with climatological studies of the region. However, this study shows the turbulent heat fluxes to be much smaller than those of a recent study, especially in the northern Greenland and Barents Seas. Additionally, comparison of turbulent heat flux values based on 10 minute averages with fluxes calculated from the averages of the bulk variables for an entire ship's cruise (10-22 days) shows the values to differ by only approximately 5%. DTIC

N95-32992# Osaka Univ., Osaka (Japan). Dept. of Architectural Engineering.
SEISMIC RESPONSE ANALYSIS OF SOIL-STRUCTURE INTERACTION SYSTEMS IN THE TIME DOMAIN
Kensuke Baba, Kiyeon Park, and Yutaka Inoue *In its* Technology Reports of the Osaka Univ.,Vol. 45, Nos. 2205-2216 15 Apr. 1995 p 59-64 (For primary document see N95-32984 12-31)
(Rept-2212) Avail: CASI HC A02/MF A02

N95-33753*# Jet Propulsion Lab., California Inst. of Tech., Pasadena, CA.
MOVEMENT OF WATER VAPOR IN THE ATMOSPHERE MEASURED BY AN IMAGING SPECTROMETER AT ROGERS DRY LAKE, CA
Robert O. Green and James E. Conel (California Univ., Santa Barbara, CA.) *In its* Summaries of the Fifth Annual JPL Airborne Earth Science Workshop. Volume 1: AVIRIS Workshop 23 Jan. 1995 p 79-82 (For primary document see N95-33730 12-42)
Avail: CASI HC A01/MF A02

47 METEOROLOGY AND CLIMATOLOGY

Includes weather forecasting and modification.

N95-32760# General Accounting Office, Washington, DC. Accounting and Information Management Div.
WEATHER FORECASTING: SYSTEMS ARCHITECTURE NEEDED FOR NATIONAL WEATHER SERVICE MODERNIZATION. REPORT TO CONGRESSIONAL REQUESTERS
11 Mar. 1994 41 p
(GAO/AIMD-94-28; B-255498) Avail: CASI HC A03/MF A01; GAO, PO Box 6015, Gaithersburg, MD 20877 HC

The National Weather Service's (NWS) ability to forecast the weather impacts not only the lives and property of every American but also our nation's commerical interests. Catastrophic disasters such as hurricane Andrew and the 'great flood of 1993' demonstrate the importance of providing timely weather forecasts and warnings. To improve the accuracy, timeliness, and efficiency of its weather forecasts and warnings, the National Oceanic and Atmospheric Administration (NOAA), of which NWS is a part, is spending over $4 billion to modernize NWS weather observing, information processing, and communication systems. Given the risks inherent in such a large and complex undertaking, the GAO was requested to review the NWS modernization effort to determine (1) whether NOAA has a systems architecture to guide the development and evolution of the many interrelated subsystems under the modernization, (2) whether there are architectural differences among these subsystems and the impact of any such differences, and (3) whether responsibility for managing the modernization has been clearly assigned. Derived from text

N95-32891# Technische Univ., Delft (Netherlands). Dept. of Sanitary Engineering and Water Management.
RAINGAUGE NETWORK OPTIMIZATION AND GIS: A CASE STUDY OF THE MANANGA BASIN. COMMUNICATIONS OF THE SANITARY ENGINEERING AND WATER MANAGEMENT DIVISION
M. J. vanDijk and T. H. M. Rientjes Oct. 1993 33 p
(ISSN 0169-6246)
(PB95-214284; Rept-58) Avail: CASI HC A03/MF A01

Contents include the following: The Mananga basin; Rainfall analyses; The Mananga river; Cases; Ilwis (Input module, Vector module, Raster module, Tables module, Points module, Output module, Command option, Dos option); Creating the digital elevation model (DEM) (Rasterize, Interpolation, Display and Store, Pixel information, Classification, Colors); Creating the catchment map; Creating the river map; Digital elevation model with river at catchment level; Yearly rainfall of the Mananga basin, (The semivariogram, Kriging, Detrending Kriging); and Network optimization. NTIS

N95-32933*# Utah Univ., Salt Lake City, UT. Dept. of Meterology.
ANALYSES AND FORECASTS WITH LAWS WINDS Final Report, 22 Sep. 1993 - 31 Dec. 1994
Muyin Wang and Jan Paegle Dec. 1994 35 p
(NASA-CR-199134; NAS 1.26:199134; S-12871-F) Avail: CASI HC A03/MF A01

Horizontal fluxes of atmospheric water vapor are studied for summer months during 1989 and 1992 over North and South America based on analyses from European Center for Medium Range Weather Forecasts, US National Meteorological Center, and United Kingdom Meteorological Office. The calculations are performed over 20 deg by 20 deg box-shaped midlatitude domains located to the east of the Rocky Mountains in North America, and to the east of the Andes Mountains in South America. The fluxes are determined from operational center gridded analyses of wind and moisture. Differences in the monthly mean moisture flux divergence determined from these analyses are as large as 7 cm/month precipitable water equivalent over South America, and 3 cm/month over North America. Gridded analyses at higher spatial and temporal resolution exhibit better agreement in the moisture budget study. However, significant discrepancies of the moisture flux divergence computed from different gridded analyses still exist. The conclusion is more pessimistic than Rasmusson's estimate based on station data. Further analysis reveals that the most significant sources of error result from model surface elevation fields, gaps in the data archive, and uncertainties in the wind and specific humidity analyses. Uncertainties in the wind analyses are the most important problem. The

low-level jets, in particular, are substantially different in the different data archives. Part of the reason for this may be due to the way the different analysis models parameterized physical processes affecting low-level jets. The results support the inference that the noise/signal ratio of the moisture budget may be improved more rapidly by providing better wind observations and analyses than by providing better moisture data. Author

N95-33259# Aerospace Corp., El Segundo, CA. Engineering and Technology Group.
IDENTIFICATION OF CRITICAL SUBSTORM-EXPANSION-PHASE PHENOMENA: PROBLEMS ADDRESSABLE WITH GEM OBSERVATIONS
L. R. Lyons 16 Sep. 1994 16 p Reprint from Strategies for the Tail and Substorm Campaign
(Grant NSF ATM-91-20072)
(ATR-94(7270)-1) Avail: CASI HC A03/MF A01

Understanding the physics of the substorm process is currently a crucial topic in magnetospheric physics. Fundamental to this understanding is the determination of what phenomena occur in the magnetosphere during the expansion phase, where these phenomena occur, and how they propagate during the expansion phase. Satellite observations have given us important point measurements of what happens; however there is potential for enhancing the use of ground-based observations to study the substorm phenomena. Such enhanced use of ground-based measurements is already taking place as part of the GEM (Geospace Environment Modeling) boundary-layer campaign and is planned to continue throughout the tail/substorm campaign. This report identifies expansion-phase phenomena observed locally within the nightside magnetosphere and from the ground, believed to be of fundamental importance for understanding large-scale substorm processes. The phenomena observed in situ are related to the phenomena observed from the ground. The primary goal is to identify outstanding questions that could be addressed during the GEM tail/substorm campaign using ground-based data from GEM observing periods in coordination with available satellite observations. Derived from text

N95-33505# Pacific Northwest Lab., Richland, WA.
BALLOON-BORNE RADIOMETER PROFILER: FIELD OBSERVATIONS
W. J. Shaw, C. D. Whiteman, G. A. Anderson, J. M. Alzheimer, J. M. Hubbe, and K. A. Scott Mar. 1995 9 p Presented at the 5th Atmospheric Radiation Measurement (ARM) Meeting, San Diego, CA, 20-23 Mar. 1995
(Contract DE-AC06-76RL-01830)
(DE95-011493; PNL-SA-26034; CONF-9503140-3) Avail: CASI HC A02/MF A01

This project involves the development of the capability of making routine soundings of broadband radiative fluxes and radiative flux divergences to heights of 1500m AGL. Described in this document are radiometers carried on a stabilized platform in a harness inserted in the tetherline of a tethered balloon meteorological sounding system. Field test results are given. DOE

N95-34491# Air Force Systems Command, Wright-Patterson AFB, OH. National Air Intelligence Center.
DIAGNOSIS OF FRONTOGENESIS OF MEIYU FRONT
Yi Bing, Qiao Quanming, and Zhang Li 25 Apr. 1995 22 p Transl. into ENGLISH from unidentified Chinese document, p 92-100
(AD-A294043; NAIC-ID(RS)T-0092-93) Avail: CASI HC A03/MF A01

This article analyzes the frontogenesis processes associated with one instance of Meiyu front. In conjunction with this, use is made of frontogenesis functions and temperature balance equations. Discussions are made of factors influencing Meiyu front formation and maintenance. Results clearly show that sensible heating is the main factor causing the Yangtze-Huai river valley lower layer frontal area to disappear and latent heating as well as deformations associated with horizontal motion are the main factors associated with maintaining the existence of Meiyu fronts. DTIC

N95-34575# HSS, Inc., Bedford, MA.
A TACTICAL PRESENT WEATHER SENSOR FOR AIR FORCE APPLICATIONS Final Report, 1 Dec. 1992 - 30 Sep. 1994
D. F. Hansen and W. K. Shubert 25 Oct. 1994 47 p
(Contract F19628-92-C-0100)
(AD-A294900; PL-TR-94-2287) Avail: CASI HC A03/MF A01

A present weather sensor has been developed for Air Force tactical applications under a Phillips Laboratory Broad Agency Announcement to meet the more general requirement for 'automated fixed/bare based weather sensors.' The present weather sensor design is based on techniques evolved over a period of time by HSS Inc. for the automated measurement of visibility and precipitation. The prototype sensor is a compact, rugged, light weight, single-package instrument capable of measuring visibility and several precipitation parameters (i.e. precipitation type, intensity, and rate of fall). Preliminary tests demonstrate that the performance of the tactical sensor is comparable to that of the performance of the highly regarded larger HSS Inc. present weather sensors. DTIC

N95-34757# Air Force Systems Command, Wright-Patterson AFB, OH. National Air Intelligence Center.
INTRA-ANNUAL AND INTER-ANNUAL RAINFALL VARIABILITY OVER EAST ASIA, SOUTHEAST ASIA, AND SOUTH ASIA
Guangji Yang and Jiaming Liu 25 Apr. 1995 23 p
(AD-A294156; NAIC-ID(RS)T-0094-93) Avail: CASI HC A03/MF A01

This article applied average monthly precipitation data for April-September 1951-1981 and average ten-day data for April-September 1961-1970. It did research on inter-annual and intra-annual changes in precipitation for East Asia, South Asia, and Southeast Asia. It analyzed precipitation differences between eastern and western China as well as the characteristics of Yangtze valley drought and excessive rain. Results point out that there is a constant trend shown in a southwest-northeast direction in association with distributions of areas of large rainfall above 200mm from April to September in East Asia, South Asia, and Southeast Asia. It is closely in line with the direction of movement associated with southwest monsoons. In this belt of heavy rains, three different types of precipitation are included. Besides this, amounts of 10 day precipitation in China's Yangtze-Huai area from July to September harbor quasi periodic oscillation phenomena associated with periods of approximately 20 days. They are completely different from precipitation distributions associated with western China. Precipitation in south and central China has an inverse relationship to El Nino phenomena. Statistical results clearly show that there is only a 23% probability of producing sustained heavy rain and sustained scarce rain on the middle and lower reaches of the Yangtze River in summer. Most years have normal precipitation. Finally, we also discussed circulation factors influencing drought and excessive rain on the middle and lower reaches of the Yangtze River in summer. DTIC

N95-34223*# Colorado Univ., Boulder, CO. Center for Astrodynamics Research.
A LAND-SURFACE TESTBED FOR EOSDIS Abstract Only
William Emery, Jeff Dozier (California Univ., Santa Barbara, CA.), and Paul Rotar (National Center for Atmospheric Research, Boulder, CO.) *In its* Applied Information Systems Research Program (AISRP) Workshop 3 Meeting Proceedings 1993 1 p (For primary document see N95-34218 12-82)
Avail: CASI HC A01/MF A03

48 OCEANOGRAPHY

Includes biological, dynamic, and physical oceanography; and marine resources.

For related information see also *43 Earth Resources and Remote Sensing.*

N95-32545*# National Aeronautics and Space Administration. Goddard Space Flight Center, Greenbelt, MD.
SeaWIFS TECHNICAL REPORT SERIES. VOLUME 15: THE SIMULATED SeaWIFS DATA SET, VERSION 2
Stanford B. Hooker, ed., Elaine R. Firestone, ed. (General Sciences Corp., Laurel, MD.), Watson W. Gregg, Frederick S. Patt (General Sciences Corp., Laurel, MD.), and Robert H. Woodward (General Sciences Corp., Laurel, MD.) Jan. 1994 53 p Original contains color illustrations
(NASA-TM-104566-Vol-15; Rept-94B00041-Vol-15; NAS 1.15:104566-Vol-15) Avail: CASI HC A04/MF A01; 6 functional color pages

This document describes the second version of the simulated SeaWiFS data set. A realistic simulated data set is essential for mission readiness preparations and can potentially assist in all phases of ground support for a future mission. The second version improves on the first version primarily

through additional realism and complexity. This version incorporates a representation of virtually every aspect of the flight mission. Thus, it provides a high-fidelity data set for testing several aspects of the ground system, including data acquisition, data processing, data transfers, calibration and validation, quality control, and mission operations. The data set is constructed for a seven-day period, 25-31 March 1994. Specific features of the data set include Global Area coverage (GAC), recorded Local Area Coverage (LAC), and realtime High Resolution Picture Transmission (HRPT) data for the seven-day period. A realistic orbit, which is propagated using a Brouwer-Lyddane model with drag, is used to simulate orbit positions. The simulated data corresponds to the command schedule based on the orbit for this seven-day period. It includes total (at-satellite) radiances not only for ocean, but for land, clouds, and ice. The simulation also utilizes a high-resolution land-sea mask. It includes the April 1993 SeaWiFS spectral responses and sensor saturation responses. The simulation is formatted according to July 1993 onboard data structures, which include corresponding telemetry (instrument and spacecraft) data. The methods are described and some examples of the output are given. The instrument response functions made available in April 1993 have been used to produce the Version 2 simulated data. These response functions will change as part of the sensor improvements initiated in July-August 1993. Author

N95-32672*# National Aeronautics and Space Administration. Goddard Space Flight Center, Greenbelt, MD.

SeaWiFS TECHNICAL REPORT SERIES. VOLUME 22: PRELAUNCH ACCEPTANCE REPORT FOR THE SeaWiS RADIOMETER

Stanford B. Hooker, ed., Elaine Firestone, R., ed. (General Sciences Corp., Laurel, MD.), Robert A. Barnes (ManTech, Inc., Wallops Island, VA.), William L. Barnes, Wayne E. Esaias, Charles R. McClain, and James G. Acker, ed. (Hughes STX, Inc., Lanham, MD.) Sep. 1994 36 p

(NASA-TM-104566-Vol-22; Rept-94B00126-Vol-22; NAS 1.15:104566-Vol-22) Avail: CASI HC A03/MF A01

The final acceptance, or rejection, of the Sea-viewing Wide field-of-view Sensor (SeaWiFS) will be determined by the instrument's on-orbit operation. There is, however, an extensive set of laboratory measurements describing the operating characteristics of the radiometer. Many of the requirements in the Ocean Color Data Mission (OCDM) specifications can be checked only by laboratory measurements. Here, the calibration review panel (composed of the authors of this technical memorandum) examines the laboratory characterization and calibration of SeaWiFS in the light of the OCDM performance specification. Overall, the performance of the SeaWiFS instrument meets or exceeds the requirements of the OCDM contract in all but a few unimportant details. The detailed results of this examination are presented here by following the outline of the specifications, as found in the Contract. The results are presented in the form of requirements and compliance pairs. These results give conclusions on many, but not all, of the performance specifications. The acceptance of this panel of the performance of SeaWiFS must only be considered as an intermediate conclusion. The ultimate acceptance (or rejection) of the SeaWiFS data set will rely on the measurements made by the instrument on orbit.

Author

N95-32833*# National Aeronautics and Space Administration. Goddard Space Flight Center, Greenbelt, MD.

SeaWiFS TECHNICAL REPORT SERIES. VOLUME 31: STRAY LIGHT IN THE SeaWiFS RADIOMETER

Stanford B. Hooker, ed., Elaine R. Firestone, ed. (General Sciences Corp., Laurel, MD.), James G. Acker, ed. (Hughes STX, Inc., Lanham, MD.), Robert A. Barnes (ManTech, Inc., Wallops Island, VA.), Alan W. Holmes (Santa Barbara Research Center, Goleta, CA.), and Wayne E. Esaias Jul. 1995 79 p

(NASA-TM-104566-Vol-31; Rept-95-B00108-Vol-31; NAS 1.15:104566-Vol-31) Avail: CASI HC A05/MF A01

Some of the measurements from the Sea-viewing Wide Field-of-view Sensor (SeaWiFS) will not be useful as ocean measurements. For the ocean data set, there are procedures in place to mask the SeaWiFS measurements of clouds and ice. Land measurements will also be masked using a geographic technique based on each measurment's latitude and longitude. Each of these masks involves a source of light much brighter than the ocean. Because of stray light in the SeaWiFS radiometer, light from these bright sources can contaminate ocean measurements located a variable number of pixels away from a bright source. In this document, the sources of stray light in the sensor are examined, and a method is developed for masking measurements near bright targets for stray light effects. In addition, a procedure is proposed for reducing the effects of stray light in the flight data from SeaWiFS. This correction can also reduce the number of pixels masked for stray light. Without these corrections, local area scenes must be masked 10 pixels before and after bright targets in the along-scan direction. The addition of these corrections reduces the along-scan masks to four pixels before and after bright sources. In the along-track direction, the flight data are not corrected, and are masked two pixels before and after. Laboratory measurements have shown that stray light within the instrument changes in a direct ratio to the intensity of the bright source. The measurements have also shown that none of the bands show peculiarities in their stray light response. In other words, the instrument's response is uniform from band to band. The along-scan correction is based on each band's response to a 1 pixel wide bright sources. Since these results are based solely on preflight laboratory measurements, their successful implementation requires compliance with two additional criteria. First, since SeaWiFS has a large data volume, the correction and masking procedures must be such that they can be converted into computationally fast algorithms. Second, they must be shown to operate properly on flight data. The laboratory results, and the corrections and masking procedures that derive from them, should be considered as zeroeth order estimates of the effects that will be found on orbit. Author

N95-33410# Lawrence Livermore National Lab., Livermore, CA.

A LOW DIFFRACTION BEAM TECHNIQUE FOR SCANNING IN THE SHALLOW OCEAN

D. Kent Lewis 1 Dec. 1994 8 p Presented at the Inversion Methods in Ocean and Seismic Acoustics Conference, La Spezia, Italy, 27 Jun. - 1 Jul. 1994

(Contract W-7405-eng-48)

(DE95-011742; UCRL-JC-119287; CONF-9406241-2) Avail: CASI HC A02/MF A01

The Localized Wave pulse project has created the concept of highly localized, pulsed wave energy. We have confirmed, and developed the technique in a series of experimental and numerical tests. This technique generates radiation, mechanical or electromagnetic, from an array. LW generation sends a broad frequency bandwidth pulse of energy along the array axis. The pulse has no sidelobes and maintains the frequency bandwidth and pulse amplitude better than any other method proposed to date. Confirmation of the theory by acoustic experiments show that the effect is real, and that the advantages of the technique can be realized in a laboratory environment. Numerical studies have shown that this effect is extendible to the microwave (vector field) and elastodynamic (tensor field) regimes as well as the stratified ocean environment. The main features of the LW beam are: (1) the pulses are broad bandwidth and maintain that bandwidth over their entire working range; (2) the beam generates no side lobes; (3) the LW effect is accomplished in the linear regime, so that small errors in beam generation result in a less effective beam not the loss of the effect; and (4) the beam can be generated using present technology in the acoustic realm. The LW beam has a wide range of applications. As an active source, it offers a unique method of variable beam forming from spatially wide to the narrowest possible beam. Its uses include oceanographic sound velocity profile estimation and attenuation measurements. Since the pulse characteristics are changeable through the source signal parameters, it also offers the possibility of adaptive beam forming in real time. Passively, the LW array can use a wide spatial width listening pattern until something of interest occurs. Instantaneously, the listening pattern could be changed to a very narrow, steerable beam with a broad bandwidth. These uses also apply in the electromagnetic realm.

DOE

N95-34341# Naval Research Lab., Bay Saint Louis, MS.

PROCEEDINGS OF THE ONR/NRL WORKSHOP ON MODELING THE DISPERSION OF NUCLEAR CONTAMINANTS IN THE ARCTIC SEAS Final Report

Ruth H. Preller and Robert Edson 22 Feb. 1995 350 p Workshop held in Monterey, CA, 18-19 Oct. 1994

(AD-A294373; NRL/MR/7322-95-7584) Avail: CASI HC A15/MF A03

A workshop focusing on modeling the dispersion of radionuclides which have been dumped into the Arctic Ocean was held in Monterey, CA, in October 1994. This workshop was sponsored by the Office of Naval

Research and hosted by the Naval Research Laboratory. Over 40 participants attended this meeting during which 23 oral presentations were given. The focus of this workshop was on the existing modeling effort within the Arctic Nuclear Waste Assessment program, complementary data sets and the future direction of these efforts. The goal of the workshop was to foster communication through presentations of ongoing work. The intent was that discussions, brought about by these presentations would help the most important processes, effects, and issues that should be addressed by present and future modeling efforts. DTIC

N95-34372# Naval Postgraduate School, Monterey, CA.
AN EXPERIMENTAL STUDY OF COLLECTIVE SEA STATE MODES OF DEEP WATER SURFACE GRAVITY WAVES M.S. Thesis
Patricia A. Gill Dec. 1994 63 p
(Contract N00014-94-WR-23019)
(AD-A294007) Avail: CASI HC A04/MF A01

Experimental tests of the theory of collective sea state modes of deep water surface gravity waves were made in a 20 meter long, 1.1 meter wide wind-wave tank. First, bursts of broadband wave energy were injected into the upwind end of the tank with a paddle. According to wave turbulence theory and previous experiments, it is expected that the collective mode can be seen as a change in the wind generated background spectral density propagating down the tank. The collective mode is expected to give an anomalous phase shift between the wind generated waves and the lowest tank modes. A series of experiments were conducted to measure the phase of the lowest oscillatory modes of the tank at which increases in the magnitude of wind generated waves occurred. Finally, the surface tension of water in the tank was measured in order to better characterize our system. Although our experiments suggest that the collective mode may indeed exist, the results, so far, remain inconclusive. DTIC

N95-34375# North Carolina State Univ., Raleigh, NC.
ICE-OCEAN FOUR DIMENSIONAL STRUCTURE AND DYNAMICS Annual Report, 31 Mar. 1994 - 31 Mar. 1995
F. Y. Sorrell 31 Mar. 1995 3 p
(Contract N00014-90-J-4128)
(AD-A294017) Avail: CASI HC A01/MF A01

To understand the relationship among underice morphology, ice thickness and the structure of the oceanic boundary layer, an Autonomous Oceanographic Sampling Network is being developed. The purpose of the network is to provide a technique for spatially adaptive sampling capable of resolving evolving gradients with sparsely distributed sensors. Each network consists of a base buoy and a number of Autonomous Oceanographic Vehicles (AUVs) at fixed levels. The base buoy serves as a navigation beacon, energy source, telemetry link and surface sensor platform. Each AUV functions as a subsurface sensor platform, short term data logger and programmable, navigable vessel. The first step has been to use an AUV to define acceptable performance as a subsurface platform, to implement and evaluate schemes/systems for homing and docking with the base buoy, and to conduct tests of the data and power transfer interfaces. DTIC

N95-34457# University of Southern California, Los Angeles, CA.
PHOTOBIOLOGY AND OPTICAL PROPERTIES OF PLANKTONIC AND SEA ICE MICROALGAE IN THE HIGH ARCTIC Final Technical Report
Cornelius W. Sullivan 4 May 1995 54 p
(Contract N00014-88-K-0187)
(AD-A294002) Avail: CASI HC A04/MF A01

Time series studies of the spectral irradiance fields beneath multiyear pack ice were conducted in the Eastern Arctic Basin at 82-83 deg N as part of the Coordinated Eastern Arctic Research Experiment (CEAREX). Particulate matter was collected from the multiyear pack ice as well as first year ice in a refrozen lead. The vertical distribution within the ice and the spectral absorbtion properties of the particulates were determined in order to estimate their contribution to the optical properties of the sea ice. Among the particulates contained in sea ice detritus was common throughout all portions of the pack ice and was the major light absorbing particulate matter in the ice at the time of the observation. Algal cells and mineral-like particulates also were present, yet they contributed to the light-absorbing properties to a lesser extent than the detritus. During early spring, particulate matter contributed little to the bulk attenuation coefficients of the multiyear ice, however, it was estimated to have a more substantial contribution to the attenuation coefficients of first year ice in a refrozen lead. Results of a single stream multilayer radiative transfer model that simulates concentrations of biogenic particulate matter observed in Arctic sea ice indicates that particulate matter within sea ice plays a substantial role in radiative energy transfer and has the potential to seasonally alter spectral irradiance regimes within the ice covered Arctic ocean. DTIC

N95-34461# Army Engineer Waterways Experiment Station, Vicksburg, MS. Environmental Lab.
THE CE-QUAL-ICM THREE-DIMENSIONAL EUTROPHICATION MODEL, RELEASE VERSION 1.0 Final Report
Carl F. Cerco and Thomas Cole Mar. 1995 317 p
(AD-A294258; WES/TR/EL-95-15) Avail: CASI HC A14/MF A03

CE-QUAL-ICM (Release 1.0) is a three-dimensional, time-variable eutrophication model. CE-QUAL-ICM incorporates 22 state variables that include physical properties; multiple forms of algae, carbon, nitrogen, phosphorus, and silica; and dissolved oxygen. The model incorporates a predictive submodel of benthic processes including sediment oxygen demand and sediment-water nutrient flux. Features of the model include the following: operational in one-, two, or three-dimensional configurations; state variables may be individually activated or deactivated; computations may he restarted following interruption; internal averaging of model output over arbitrary intervals; computation and reporting of concentrations, mass transport, kinetics transformations, and mass balances; and debugging aids. The model does not compute hydrodynamics. Flows, diffusion coefficients, and volume must be specified externally and read into the model. The user must provide processors which prepare input files and process output for presentation. CE-QUAL-ICM is coded in ANSI Standard FORTRAN F77 and operates on a variety of platforms including 486 PC, unix work stations, and mainframe supercomputers. DTIC

N95-34594# Arizona State Univ., Flagstaff, AZ.
LABORATORY AND NUMERICAL MODELING OF TOPOGRAPHIC EFFECTS ON TIME-DEPENDENT OCEAN CURRENTS Final Report, 15 Nov. 1988 - 15 Aug. 1995
Don L. Boyer 1 Jun. 1995 9 p
(Contract N00014-89-J-1217)
(AD-A294920) Avail: CASI HC A02/MF A01

The principal goal of this effort was to develop an improved understanding of the physical and biological environment in the vicinity of isolated seamounts. Field experiments and attendant analyses along with numerical modeling and physical simulations of the region in the vicinity of Fieberling Guyot were conducted. The report findings are divided into three sections: ocean current interactions with isolated topography, jets in rotating and stratified fluids, and other physical modeling experiments. DTIC

N95-33141# Saint Petersburg Inst. of Aerospace Instrumentation, Saint Petersburg (Russia).
SEA WAVE PARAMETERS, SMALL ALTITUDES AND DISTANCES MEASURERS DESIGN FOR MOVEMENT CONTROL SYSTEMS OF SHIPS, WING-IN-SURFACE EFFECT CRAFTS AND SEAPLANES
A. V. Nebylov, A. P. Vanayev, and V. V. Chernyavets *In* AGARD, Dual Usage in Military and Commercial Technology in Guidance and Control Mar. 1995 12 p (For primary document see N95-33126 12-31)
Copyright Avail: CASI HC A03/MF A02

N95-33807*# Naval Research Lab., Washington, DC. Remote Sensing Div.
POLARIZATION AND WAVELENGTH DIVERSITIES OF GULF STREAM FRONTS IMAGED BY AIRSAR
J. S. Lee, R. W. Jansen, G. O. Marmorino, and S. R. Chubb *In* JPL, Summaries of the Fifth Annual JPL Airborne Earth Science Workshop. Volume 3: AIRSAR Workshop 23 Jan. 1995 p 21-24 (For primary document see N95-33801 12-42)
Avail: CASI HC A01/MF A01

51 LIFE SCIENCES (GENERAL)

N95-32719*# National Aeronautics and Space Administration. Ames Research Center, Moffett Field, CA.

MINUTES OF THE 12TH JOINT NASA/DARA-DLR LIFE SCIENCES PROGRAM WORKING GROUP MEETING Final Report

Ronald J. White 1994 234 p Meeting held in Moffett Field, CA, 26-27 Oct. 1994

(NASA-TM-110655; NAS 1.15:110655) Avail: CASI HC A11/MF A03

This report contains the final minutes of the 12th Joint NASA/DARA-DLR Life Sciences Program Working Group Meeting and includes the presentations made by participants. For individual titles, see N95-32720 through N95-32731.

N95-32720*# Siegen Univ., (Germany). Dept. of Physics.

PROTON-INDUCED FRAGMENTATION OF CARBON AT ENERGIES BELOW 100 MEV

M. Schmitz, T. Streibel, H. Roecher, J. Dreute, S. E. Hirzebruch, G. Huentrup, and Wolfgang Heinrich *In* NASA. Ames Research Center, Minutes of the 12th Joint NASA/DARA-DLR Life Sciences Program Working Group Meeting 1994 p 1-3 (For primary document see N95-32719 12-51)

Avail: CASI HC A01/MF A03

Radiation effects caused by single cosmic ray particles have been studied for many years in radiobiological experiments for different biological objects and biological end-points. Additionally, single event effects in microelectronic devices have gained large interest. There are two fundamental mechanisms by which a single particle can cause radiation effects. On the one hand, a cosmic ray ion with high linear energy transfer can deposit a high dose along its path. On the other hand, in a nuclear collision, a high dose can be deposited by short range particles emitted from the target nucleus. In low earth orbits a large contribution to target fragmentation events originates from trapped protons which are encountered in the South Atlantic Anomaly. These protons have energies up to a few hundred MeV. We study the fragmentation of C, O and Si nuclei - the target nuclei of biological material and microelectronic devices - in nuclear collisions. Our aim is to measure production cross sections, energy spectra, emission directions and charge correlations of the emitted fragments. The present knowledge concerning these data is rather poor. M. Alurralde et al. have calculated cross sections and average energies of fragments produced from Si using the cascade-evaporation model. D.M. Ngo et al. have used the semiempirical cross section formula of Silberberg and Tsao to calculate fragment yields and the statistical model of Goldhaber to describe the reaction kinematics. Cross sections used in these models have uncertainties within a factor of two. Our data will help to test and improve existing models especially for energies below 300 MeV/nucleon. Charge correlations of fragments emitted in the same interaction are of particular importance, since high doses can be deposited if more than one heavy fragment with a short range is produced. Derived from text

N95-32721*# Deutsche Forschungsanstalt fuer Luft- und Raumfahrt, Cologne (Germany). Radiation Biology Div.

DOSIMETRY OF HEAVY IONS BY USE OF CCD DETECTORS c72

J. U. Schott *In* NASA. Ames Research Center, Minutes of the 12th Joint NASA/DARA-DLR Life Sciences Program Working Group Meeting 1994 p 5-10 (For primary document see N95-32719 12-51)

Avail: CASI HC A02/MF A03

The design and the atomic composition of Charge Coupled Devices (CCD's) make them unique for investigations of single energetic particle events. As detector system for ionizing particles they detect single particles with local resolution and near real time particle tracking. In combination with its properties as optical sensor, particle transversals of single particles are to be correlated to any objects attached to the light sensitive surface of the sensor by simple imaging of their shadow and subsequent image analysis of both, optical image and particle effects, observed in affected pixels. With biological objects it is possible for the first time to investigate effects of single heavy ions in tissue or extinguished organs of metabolizing (i.e. moving) systems with a local resolution better than 15 microns. Calibration data for particle detection in CCD's are presented for low energetic protons and heavy ions. Author

N95-32722*# Justus Liebig-Univ., Giessen (Germany). Cell and Radiation Biophysics.

ESTIMATION OF SPATIALLY RESTRICTED LET USING TRACK STRUCTURE MODELS

J. Kiefer *In* NASA. Ames Research Center, Minutes of the 12th Joint NASA/DARA-DLR Life Sciences Program Working Group Meeting 1994 p 11-13 (For primary document see N95-32719 12-51)

Avail: CASI HC A01/MF A03

The spatial distribution of energy deposition is an important determinant in the formation of biologically significant lesions. It has been widely realized that Linear Energy Transfer (LET) being an average quantity is not sufficient to describe the situation at a submicroscopic scale. To remedy this to some extent 'energy-cut-off' values are sometimes used but since they are related to secondary electron energy and only indirectly to their range they are also not adequate although they may be easily calculated. 'Range-restricted LET' appears to be better but its determination is usually quite involved. Xapsos (1992) suggested a semi-empirical approximation based on a modified Bethe-formula which contains a number of assumption which are difficult to verify. A simpler and easier way is to use existing beam-models which describe energy deposition around an ion's path. They all agree that the energy density (i. e., energy deposited per unit mass) decreases with the inverse square of the distance from the track center. This simple dependence can be used to determine the fraction of total LET which is deposited in a cylinder of a given radius. As an example our own beam model. Energy density depends on distance x (measured in m) from the track center according to the presented formula.

Derived from text

N95-32723*# Justus Liebig-Univ., Giessen (Germany). Cell and Radiation Biophysics.

HEAVY ION INDUCED DNA-DSB IN YEAST AND MAMMALIAN CELLS Status Report

M. Loebrich, S. Ikpeme, and J. Kiefer *In* NASA. Ames Research Center, Minutes of the 12th Joint NASA/DARA-DLR Life Sciences Program Working Group Meeting 1994 p 15-17 (For primary document see N95-32719 12-51)

Avail: CASI HC A01/MF A03

Molecular changes at the DNA are assumed to be the main cause for radiation effects in a number of organisms. During the course of the last decades techniques have been developed for measuring DNA double-strand breaks (dsb), generally assumed to be the most critical DNA lesions. The outcome of all those different approaches portrays a collection of data useful for a theoretical description of radiation action mechanisms. However, in the case of heavy ion induced DNA dsb the picture is not quite clear yet and further projects and strategies have to be developed. The biological systems studied in our group are yeast and mammalian cells. While in the case of yeast cells technical and methodical reasons highlight these organisms mammalian cells reach greater importance when dsb repair studies are performed. In both types of organisms the technique of pulsed-field gel electrophoresis (PFGE) is applied, although with different modifications and evaluation procedures mainly due to the different genome sizes. Derived from text

N95-32724*# Deutsche Forschungsanstalt fuer Luft- und Raumfahrt, Cologne (Germany). Radiation Biology Div.

INACTIVATION, DNA DOUBLE STRAND BREAK INDUCTION AND THEIR REJOINING IN BACTERIAL CELLS IRRADIATED WITH HEAVY IONS

M. Schaefer, H. Zimmermann, and C. Schmitz *In* NASA. Ames Research Center, Minutes of the 12th Joint NASA/DARA-DLR Life Sciences Program Working Group Meeting 1994 p 18-22 (For primary document see N95-32719 12-51)

Avail: CASI HC A01/MF A03

Besides inactivation one of the major interests in our experiments is to study the primary damage in the DNA double strand breaks (DSB) after heavy ion irradiation. These damages lead not only to cell death but also under repair activities to mutations. In further experiments we have investigated the inactivation with two different strains of Deinococcus radiodurans (R1, Rec 30) and the induction of DSB as well as the rejoining of DSB in stationary cells of E. coli (strain B/r) irradiated with radiations of different quality. In the latter case irradiations were done so that the cell survival was roughly at the same level. We measured the DSB using the

pulse field gelelectrophoresis which allows to separate between intact (circular) and damaged (linear) DNA. The irradiated cells were transferred to NB medium and incubated for different times to allow rejoining.

Derived from text

N95-32725*# Gesellschaft fuer Schwerionenforschung m.b.H., Darmstadt (Germany). Biophysics Group.

DNA-DSB IN CHO-K1 CELLS INDUCED BY HEAVY-IONS: BREAK REJOINING AND RESIDUAL DAMAGE (GSI)

G. Taucher-Scholz, J. Heilmann, G. Becher, and G. Kraft *In* NASA. Ames Research Center, Minutes of the 12th Joint NASA/DARA-DLR Life Sciences Program Working Group Meeting 1994 p 23-25 (For primary document see N95-32719 12-51)

Avail: CASI HC A01/MF A03

DNA double strand breaks (DSB's) are the critical lesions involved in cellular effects of ionizing radiation. Therefore, the evaluation of DSB induction in mammalian cells after heavy ion irradiation is an essential task for the assessment of high-LET radiation risk in space. Of particular interest has been the question of how the biological efficiency for the cellular inactivation endpoint relates to the initial lesions (DSBs) at varying LETs. For cell killing, an increased Relative Biological Efficiency (RBE) has been determined for highLET radiation around 100-200 keV/mu m. At higher LET, the RBE's decrease again to values below one for the very heavy particles. At GSI, DSB-induction was measured in CHO-K1 cells following irradiation with accelerated particles covering a wide LET range. The electrophoretic elution of fragmented DNA out of agarose plugs in a constant electrical field was applied for the detection of DSB's. The fraction of DNA retained was determined considering the relative intensities of ethidium bromide fluorescence in the well and in the gel lane. Dose-effect curves were established, from which the RBE for DSB induction was calculated at a fraction of 0.7 of DNA retained In summary, these rejoining studies are in line with an enhanced severity of the DNA DSB's at higher LET's, resulting in a decreased repairability of the induced lesions. However, no information concerning the fidelity of strand breaks rejoining is provided in these studies. To assess correct rejoining of DNA fragments an experimental system involving individual DNA hybridization bands has been set up. In preliminary experiments Sal I generated DNA fragments of 0.9 Mbp were irradiated with xrays and incubated for repair However, restitution of the original signals was not observed, probably due to the high radiation dose necessary for breakage of a fragment of this size. A banding pattern with NotI hybridization signals in a higher MW range (3Mbp) has been obtained by varying the electrophoretic conditions and correct rejoining studies will be further developed in this system. Derived from text

N95-32726*# Gesellschaft fuer Schwerionenforschung m.b.H., Darmstadt (Germany). Biophysics Group.

CHROMOSOMAL DAMAGE OBSERVED IN FIRST POSTIRRADIATION METAPHASES OF REPAIR-PROFICIENT AND -DEFICIENT CELL LINES

S. Ritter, W. Kraft-Weyrather, K. Fussel, E. Kehr, and G. Kraft *In* NASA. Ames Research Center, Minutes of the 12th Joint NASA/DARA-DLR Life Sciences Program Working Group Meeting 1994 p 26-27 (For primary document see N95-32719 12-51)

Avail: CASI HC A01/MF A03

Investigation of radiation induced damage in mutant strains of mammalian cells which show a defect in the rejoining of DNA double strand breaks provides an unique opportunity to examine the role of double strand breaks and the mechanisms of double strand break rejoining in the production of chromosome aberrations. This is particularly important, because there is increasing evidence that the DNA double strand break is the major lesion responsible for the formation of chromosome aberrations. To address this issue, we studied the induction of chromosome aberrations in xrs-5 cells, an x-ray sensitive strain of a Chinese hamster ovary cell line, which shows a defect in the rejoining of double strand breaks and their wild-type parent CHO-cells. Because radiosensitivity depends strongly on cellular age, the experiments were performed with synchronous cells. Derived from text

N95-32727*# Deutsche Forschungsanstalt fuer Luft- und Raumfahrt, Cologne (Germany). Radiation Biology Div.

MUTATION INDUCTION IN BACTERIA AFTER HEAVY ION IRRADIATION

G. Horneck and S. Kozubek (Ceskoslovenska Akademie Ved, Brno.) *In* NASA. Ames Research Center, Minutes of the 12th Joint NASA/DARA-DLR Life Sciences Program Working Group Meeting 1994 p 28-29 (For primary document see N95-32719 12-51)

Avail: CASI HC A01/MF A03

From a compilation of experimental data on the mutagenic effects of heavy ions in bacteria, main conclusions have been drawn as follows: (1) The mutagenic efficacy of heavy ions in bacteria depends on physical and biological variables. Physical variables are the radiation dose, energy and charge of the ion; the biological variables are the bacterial strain, the repair genotype of bacteria, and the endpoint investigated (type of mutation, induction of enzymes related to mutagenesis); (2) The responses on dose or fluence are mainly linear or linear quadratic. The quadratic component, if found for low LET radiation, is gradually reduced with increasing LET; (3) At low values of Z and LET the cross section of mutation induction sigma m (as well as SOS response, sigma sos. and lambda phage induction, sigma lambda versus LET curves can be quite consistently described by a common function which increases up to approximately 100 keV/mu m. For higher LET values, the sigma(m) versus LET curves show the so-called 'hooks' observed also for other endpoints; (4) For light ions (Z is less than or equal to 4), the cross sections mostly decrease with increasing ion energy, which is probably related to the decrease of the specific energy departed by the ion inside the sensitive volume (cell). For ions in the range of Z = 10, sigma(m) is nearly independent on the ion energy. For heavier ions (Z is greater than or equal to 16), sigma(m) increases with the energy up to a maximum or saturation around 10 MeV/u. The increment becomes steeper with increasing atomic number of the ion. It correlates with the increasing track radius of the heavy ion; (5) The mutagenic efficiency per lethal event changes slightly with ion energy, if Z is small indicating a rough correlation between cellular lethality and mutation induction, only. For ions of higher Z this relation increases with energy, indicating a change in the 'mode' of radiation action from 'killing-prone' to 'mutation-prone'; and (6) Repair genotype substantially influences the radiation induced mutagenesis. Different mechanisms of mutation induction and/or different types of biologically significant lesions in wild type cells compared to repair deficient strains are a likely explanation.

Derived from text

N95-32728*# Justus Liebig-Univ., Giessen (Germany). Cell and Radiation Biophysics.

HEAVY ION INDUCED MUTATIONS IN MAMMALIAN CELLS: CROSS SECTIONS AND MOLECULAR ANALYSIS Status Report

U. Stoll, P. Schmidt, E. Schneider, and J. Kiefer *In* NASA. Ames Research Center, Minutes of the 12th Joint NASA/DARA-DLR Life Sciences Program Working Group Meeting 1994 p 30-32 (For primary document see N95-32719 12-51)

Avail: CASI HC A01/MF A03

Our investigations of heavy ion-induced mutations in mammalian cells, which had been begun a few years ago, were systematically continued. For the first time, it was possible to cover a large LET range with a few kinds of ions. To do this, both UNILAC and SIS were used to yield comparable data for a large energy range. This is a necessary condition for a comprehensive description of the influence of such ion parameters as energy and LET. In these experiments, the induced resistance against the poison 6-thioguanin (6-TG), which is linked to the HPRT locus on the genome, is being used as mutation system. In addition to the mutation-induction cross-section measurements, the molecular changes of the DNA are being investigated by means of Multiplex PCR ('Polymerase Chain Reaction') gene amplification. From these experiments we expect further elucidation of the mutation-inducing mechanisms composing the biological action of heavy-ion radiation. Derived from text

N95-32729*# Justus Liebig-Univ., Giessen (Germany). Cell and Radiation Biophysics.

HEAVY ION ACTION ON SINGLE CELLS: CELLULAR INACTIVATION CAPABILITY OF SINGLE ACCELERATED HEAVY IONS

M. Kost, H.-D. Pross, C. Russmann, E. Schneider, J. Kiefer, G. Kraft (Gesellschaft fuer Schwerionenforschung m.b.H., Darmstadt, Germany.), G. Lenz (Gesellschaft fuer Schwerionenforschung m.b.H., Darmstadt, Germany.), and W. Becher (Gesellschaft fuer Schwerionenforschung m.b.H., Darmstadt, Germany.) *In* NASA. Ames Research Center, Minutes of the 12th Joint NASA/DARA-DLR Life Sciences Program Working Group Meeting 1994 p 33-35 (For primary document see N95-32719 12-51)

Avail: CASI HC A01/MF A03

Heavy ions (HZE-particles) constitute an important part of radiation in space. Although their number is small the high amount of energy transferred by individual particles may cause severe biological effects. Their investigation requires special techniques which were tested by experiments performed at the UNILAC at the GSI (Darmstadt). Diploid yeast was used which is a suitable eucaryotic test system because of its resistance to extreme conditions like dryness and vacuum. Cells were placed on nuclear track detector foils and exposed to ions of different atomic number and energy. To assess the action of one single ion on an individual cell, track parameters and the respective colony forming abilities (CFA) were determined with the help of computer aided image analysis. There is mounting evidence that not only the amount of energy deposited along the particle path, commonly given by the LET, is of importance but also the spatial problem of energy deposition at a submicroscopical scale. It is virtually impossible to investigate track structure effects in detail with whole cell populations and (globally applied) high particle fluences. It is, therefore, necessary to detect the action of simple ions in individual cells. The results show that the biological action depends on atomic number and specific energy of the impinging ions, which can be compared with model calculations of recent track structure models. Derived from text

N95-32730*# Deutsche Forschungsanstalt fuer Luft- und Raumfahrt, Cologne (Germany). Radiation Biology Div.

COSMIC HEAVY ION TRACKS IN MESOSCOPIC BIOLOGICAL TEST OBJECTS

R. Facius *In* NASA. Ames Research Center, Minutes of the 12th Joint NASA/DARA-DLR Life Sciences Program Working Group Meeting 1994 p 36-40 (For primary document see N95-32719 12-51)
Avail: CASI HC A01/MF A03

Since more than 20 years ago, when the National Academy of Sciences and the National Research Council of the U.S.A. released their report on 'HZE particle effects in manned spaced flight', it has been emphasized how difficult - if not even impossible - it is to assess their radiobiological impact on man from conventional studies where biological test organisms are stochastically exposed to 'large' fluences of heavy ions. An alternative, competing approach had been realized in the BIOSTACK experiments, where the effects of single cosmic as well as accelerator - heavy ions on individual biological test organisms could be investigated. Although presented from the beginning as the preferable approach for terrestrial investigations with accelerator heavy ions too ('The BIOSTACK as an approach to high LET radiation research'), only recently this insight is gaining more widespread recognition. In space flight experiments, additional constraints imposed by the infrastructure of the vehicle or satellite further impede such investigations. Restrictions concern the physical detector systems needed for the registration of the cosmic heavy ions' trajectories as well as the biological systems eligible as test organisms. Such optimized procedures and techniques were developed for the investigations on chromosome aberrations induced by cosmic heavy ions in cells of the stem meristem of lettuce seeds (Lactuca sativa) and for the investigation of the radiobiological response of Wolffia arriza, which is the smallest flowering (water) plant. The biological effects were studied by the coworkers of the Russian Institute of Biomedical Problems (IBMP) which in cooperation with the European Space Agency ESA organized the exposure in the Biosatellites of the Cosmos series. Since biological investigations and physical measurements of particle tracks had to be performed in laboratories widely separated, the preferred fixed contact between biological test objects and the particle detectors until the geometrical correlation between tracks and organisms has been established could not be maintained. This gave rise to half a dozen of coordinate systems for different measurements which finally had to be related to a single stack reference system. Derived from text

N95-32731*# Justus Liebig-Univ., Giessen (Germany). Cell and Radiation Biophysics.

X-RAY-PROVOKED NON-MENDELIAN TRANSGENERATIONAL ONCODETERMINANTS

A. Anders, C. Fleming, H. Schneider, H. Groeger, E. Schneider, J. Kiefer, and F. Anders *In* NASA. Ames Research Center, Minutes of the 12th Joint NASA/DARA-DLR Life Sciences Program Working Group Meeting 1994 p 41-46 (For primary document see N95-32719 12-51)
Avail: CASI HC A02/MF A03

Cancer is the most important risk of radiation exposure. There is a definite lack of suitable test systems, human epidemiological data are only available for certain radiation types, especially not for charged particles. We use the Xiphophorus model which is genetically well characterized. As a prelude to experiments with heavy ions we report here on results obtained with x-rays to establish the necessary baseline for future studies. Apart from this direct aim we hope to obtain also a better insight in the genetical determination of cancer formation. Derived from text

N95-32901 Colorado Univ., Boulder, CO.

EFFECTS OF GRAVITY AND LIGHT ON PLANT GROWTH AND PERFORMANCE IN NORMAL AND REDUCED GRAVITY Ph.D. Thesis

Alexander Hoehn 1993 307 p
Avail: Univ. Microfilms Order No. DA9423497

Microgravity enables studies of fundamental processes in gravitational biology not possible on Earth. Biological systems are affected directly through gravity-dependent functions in the organism as well as indirectly through microgravity-induced changes in the environment. Microgravity plant growth experiments were conducted using spaceflight hardware developed at the University of Colorado. Seedling development was investigated during five space shuttle missions and was similar for ground and space tests. Indications of reduced growth in spaceflight were found in older, dark-grown seedlings (greater than 5 days). Younger plants (less than 3 days) indicated accelerated growth in space when compared to ground controls. Reduced gravity effects on moisture distribution around plant roots and on the output of incandescent lamps were also investigated. Plant lighting in closed space environments is difficult due to power and heat removal limitations. Stringent safety requirements have to be fulfilled for the human spaceflight environments currently used for orbital plant growth payloads. Light-emitting diodes, LEDs, are a promising alternative for future plant lighting systems because of useful safety, life time, and wavelength characteristics. Currently, only red LEDs provide efficiencies and intensities suitable for plant horticulture use. The narrow spectral output of the LEDs raised questions about plant responses under such lighting conditions. Subsequent growth, using custom-built LED arrays, indicated that additional blue light in the order of 5-10 W/sq m (20-40 micromol photons m(exp -2) s(exp -1)) will be required for nominal plant development. The possible replacement of gravitropic stimulation through phototropism in a reduced gravity environment also was investigated. Earth based experiments using one and two-axis clinostats supplemented microgravity plant growth tests, conducted both in light and darkness. The lack of an adequate plant growth system for longer-term plant growth studies in space led to the definition, design, and manufacturing of the Plant-Module for Autonomous Space Support, P-MASS. P-MASS is designed for a 30 day mission aboard the recoverable COMET-1 payload capsule. A new plant growth facility is being designed as a space shuttle middeck-locker payload, addressing many of the needs identified during plant growth experiments described herein. Adequate lighting systems, two phase fluid handling and atmospheric control are essential for a useful spaceflight horticulture capability. Dissert. Abstr.

N95-33232# Royal Inst. of Tech., Stockholm (Sweden). Dept. of Mathematics.

MATHEMATICAL METHODS APPLIED TO BIOTECHNICAL PROCESSES

Jorge Mari Dec. 1994 106 p
(ISSN 0348-405X)
(PB95-212114; TRITA-MAT-94-43) Avail: CASI HC A06/MF A02

This work describes how to set up models for biotechnical processes and how to study the resulting characteristics from a mathematical viewpoint in order to facilitate the optimization of the processes. A yeast growth process is the main application example. Special care is taken in showing how model reduction techniques may be applicable, and in which way parameter identification may be performed. The optimization of fed-batch processes is studied from a theoretical, numerical and experimental perspective. Finally the role of computer simulations is also exhibited. NTIS

N95-33236# Stockholm Environment Inst., Stockholm (Sweden).

CLEARING-HOUSE MECHANISM TO PROMOTE AND FACILITATE TECHNICAL AND SCIENTIFIC COOPERATION UNDER THE UN CONVENTION ON BIOLOGICAL DIVERSITY

A. Rosemarin 1994 55 p Conference held in Nassau, Bahamas, 22-23 Nov. 1994
(PB95-214557; ISBN-91-88714-05-5) Copyright Avail: CASI HC A04/MF A01

The objective of the Convention on Biological Diversity is the conservation of germplasm, both in situ and ex situ and the sustainable use of biological diversity in a similar manner. Its access to technologies and other development, marketing and financial expertise that will assure mutually equitable arrangements are promoted. These establishment of a clearning house mechanism to promote and facilitate technical and scientificco-operation is envisaged under Article 18 of the Convention on Biodiversity. NTIS

N95-33654# Lawrence Livermore National Lab., Livermore, CA.
PLASMA MEDIATED ABLATION OF BIOLOGICAL TISSUES WITH ULTRASHORT LASER PULSES
A. A. Oraevsky (Rice Univ., Houston, TX.), L. B. DaSilva, M. D. Feit, M. E. Glinsky, B. M. Mammini, K. L. Paquette, M. D. Perry, A. M. Rubenchik, W. Small, IV, and B. C. Stuart 8 Mar. 1995 10 p Presented at the SPIE 1995: SPIE Conference on Optics, Electro-optics, and Laser Application in Science, Engineering and Medicine, San Jose, CA, 4-10 Feb. 1995 Submitted for publication
(Contract W-7405-eng-48)
(DE95-011748; UCRL-JC-120215; CONF-950226-39) Avail: CASI HC A02/MF A01

Plasma mediated ablation of collagen gels and porcine cornea was studied at various laser pulse durations in the range from 350 fs to 1 ns at 1,053 nm wavelength. A time resolved stress detection technique was employed to measure transient stress profiles and amplitudes. Optical microscopy was used to characterize ablation craters qualitatively, while a wide band acoustic transducer helped to quantify tissue mechanical response and the ablation threshold. The ablation threshold was measured as a function of laser pulse duration and linear absorption coefficient. For nanosecond pulses the ablation threshold was found to have a strong dependence on the linear absorption coefficient of the material. As the pulse length decreased into the subpicosecond regime the ablation threshold became insensitive to the linear absorption coefficient. The ablation efficiency was found to be insensitive to both the laser pulse duration and the linear absorption coefficient. High quality ablation craters with no thermal or mechanical damage to surrounding material were obtained with 350 fs laser pulses. The mechanism of optical breakdown at the tissue surface was theoretically investigated. In the nanosecond regime, optical breakdown proceeds as an electron collisional avalanche ionization initiated by thermal seed electrons. These seed electrons are created by heating of the tissue by linear absorption. In the ultrashort pulse range, optical breakdown is initiated by the multiphoton ionization of the irradiated medium (6 photons in case of tissue irradiated at 1,053 nm wavelength), and becomes less sensitive to the linear absorption coefficient. The energy deposition profile is insensitive to both the laser pulse duration and the linear absorption coefficient. DOE

N95-34789# Analytic Sciences Corp., San Antonio, TX.
ULTRASHORT PULSE LASER EFFECTS IN THE PRIMATE EYE Interim Report, Mar. 1993 - Jun. 1994
Clarence P. Cain, Gary D. Noojin, David J. Stolarski, Cynthia A. Toth, and Cheryl D. DiCarlo Nov. 1994 121 p Limited Reproducibility: Document partially illegible
(Contract F33615-92-C-0017)
(AD-A295024; AL/OE-TR-1994-0141) Avail: CASI HC A06/MF A02

Minimum visible lesion (MVL) threshold measurements at the retina for rhesus monkey eyes are reported for femtosecond, picosecond, and nanosecond single laser pulses using visible wavelengths. Estimates of the dose causing 50% probability for damage (ED50) are calculated for 1-hour and 24-hours postexposure as well as the 95% fiducial intervals for ED. The ED values are found to be dependent on both wavelength and pulsewidth, and for a single wavelength are, in general, lower for short pulsewidths, with the exception of values at the shortest pulsewidth of 90 fs at 580 nm. At 90 fs the ED(50) dosages were noted to increase slightly when compared with the 3-ps and 600-fs values, all three delivered at 580-nm wavelength. The 4-ns ED(50) value was more than double the value at 60 ps delivered at 532-nm wavelength. Fluorescein angiography was accomplished at 1-hour and 24-hours postexposure and did not demonstrate lower threshold for damage, which has been the case for MVL's created with longer pulse duration (greater than 1 ns) or for rabbit eyes at the same pulse-widths as measured in our laboratory. DTIC

52 AEROSPACE MEDICINE

Includes physiological factors; biological effects of radiation; and effects of weightlessness on man and animals.

N95-32611 Hopital A. Beclere, Clamart (France). Lab. d'Explorations Fonctionnelles.
NONINVASIVE DETERMINATION OF CARDIAC OUTPUT Final Report [EVALUATION NON-INVASIVE DU DEBIT CARDIAQUE]
P. Escourrou and M. Jaffrin Jan. 1994 24 p In FRENCH Prepared in cooperation with Universite de Technologie de Compiegne, France. Sponsored by Direction des Recherches, Etudes et Techniques, Paris, France. Centre de Documentation de l'Armement
(Contract DRET-91-1215-A)
(PB95-208310) Avail: Issuing Activity (National Technical Information Service (NTIS))

Cardiac output (CO) is an important determinant of the hemodynamic homeostasis during stress conditions. To measure the variations in CO, we applied the pulse contour analysis method to blood pressure derived from the Finapres (Ohmeda). Several circulatory models have been compared for the determination of CO from an aortic micromanometer and from the Finapres. Significant correlations were obtained with mean CO values derived by thermodilution during catheterization. An acquisition system has been implemented on a personal computer (PC) fc· the determination of CO changes during sleep in sleep apnea syndrome and periodic leg movements. This noninvasive tool may be used to evaluate cardiovascular status during stress conditions such as orthostatism, acceleration, hyperthermia, hypovolemia, or stable exercise. NTIS

N95-32666# Joint Inst. for Nuclear Research, Dubna (USSR). Lab. of Nuclear Reactions.
A NOVEL APPROACH TO THE PROBLEM OF HIGHLY-SENSITIVE REGULAR ANALYSIS FOR MAN-MADE PLUTONIUM IN ENVIRONMENT AND HUMAN BODY
Y. T. Chuburkov, V. P. Perelygin, I. Zvara, Z. Szeglowski, S. P. Shtanko, G. V. Buklanov, Y. P. Kharitonov, A. G. Belov, T. P. Drobina, and V. N. Bugrov et al 1994 8 p Submitted for publication in Radiochimica Acta
(DE95-620764; JINR-E-6-94-357) Avail: CASI HC A02/MF A01 (US Sales Only)

A method of determining subpicogram quantities of plutonium in soil, mud, water, plant and animal tissues is proposed. Plutonium is chemically isolated from the samples, while the (alpha)-active Pu-236 is issued to control yield. The plutonium fraction deposited on some backing as well as an uranium containing standard are put in contact with solid state track detectors (SSTD) - foils of polyethyleneterephtalate, and irradiated by thermal neutrons of approximately 10(exp 15)/sq cm fluence. After an appropriate chemical etching, the content of Pu-239 in the samples is determined by scanning fission fragment tracks in the SSTD. To control possible uranium impurities in the plutonium fraction, the latter and the standard (in contact with a fresh SSTD) are bombarded by a high fluence of (gamma)-quanta with energies (less than or equal to) 25 MeV (microtron Bremsstrahlung). We have succeeded in determining the lower limit of U-235 impurities at a level of less than 10(exp -13) g, due to similar photofission cross section of all Pu isotopes. The proposed method provides the determination of Pu-239 content in routine analysis with a sensitivity at a level of 10(exp -13) g/g. More than one hundred assays for Pu-239 content in specimens of above indicated media from Ukraine, Belorussia, Ural region and Germany have been performed. In future, one will hopefully reach a sensitivity of 10(exp -14) - 10(exp -15) g/g. DOE

N95-33200# Uniformed Services Univ. of the Health Sciences, Bethesda, MD. School of Medicine.
TOXIN-MEDIATED TRANSFER AND EXPRESSION OF GENES IN NERVE CELLS Final Report, 3 Jan. 1991 - 30 May 1994
Gregory P. Mueller 12 Oct. 1994 17 p Prepared in cooperation with Maryland Univ., Baltimore, MD.
(Contract ARO-MIPR-122-93)
(AD-A290501; ARO-27890.1-LS) Avail: CASI HC A03/MF A01

This research sought to determine the feasibility of using receptor-mediated gene transfer as a mechanism for introducing the expression of foreign genes in nerve cells. DNA carrier systems were

constructed using neuronal ligands that are rapidly internalized by receptor-mediated endocytosis. These proteins, principally wheat germ agglutinin and tetanus toxin C-fragment, were complexed with high expression reporter genes and applied to nerve cells in vitro, and administered in vivo into rats. Uptake and expression of the reporter genes were analyzed by standard enzymatic and histochemical procedures. While we have demonstrated, for the first time, that cells in brain can internalize and express plasmid DNA, there is no evidence that this process can be made specific through the introduction of a receptor-mediated mechanism. The findings indicate that: (1) receptor-mediated uptake and expression does occur in the central nervous system (CNS), and (2) lysosomal degradation is probably not the underlying basis for our inability to observe expression. From this it may be concluded that receptor-mediated uptake is not an efficient means for directing the expression of foreign genes in nerve cells in vivo. DTIC

N95-34472# New York Univ. Medical Center, New York, NY.
MEASUREMENT AND REGULATION OF CENTRAL NORADRENERGIC RECEPTORS Final Report, 1 Dec. 1991 - 30 Nov. 1994
Eric A. Stone, Sanil J. Mncln, and Yi Zhang 30 Nov. 1994 5 p
(Contract F49620-92-J-0084)
(AD-A294065; AFOSR-95-0338TR) Avail: CASI HC A01/MF A01

Progress was made in a number of areas related to the role of the central noradrenergic system in the behavioral effects of stress. First we established that norepinephrine mediates the persistent anxiety after stress as other have found in various learning paradigms thus linking studies of stress to studies of learned anxiety. Second we showed that a likely factor in this effect is the stimulation of the gene, c-fos, which we found to be stimulated throughout the brain by the noradrenergic system during stress. Third we discovered a new phenomenon caused by stress involving a transient reduction in arousal which causes animals to lose caution in dangerous situations and may be related to temporary desensitization of the brain beta-1 adrenoceptor. Fourth we found that repeated stress in mice causes a progressive decline in nocturnal activity and feeding thus establishing a new animal model of depression which will facilitate studies of the role of the noradrenergic system in behavioral depression. DTIC

N95-34564# Air Force Occupational Measurement Center, Randolph AFB, TX.
AEROSPACE PHYSIOLOGY AFSC 4M0X1
Mar. 1995 110 p
(AD-A294839; AFPT-90-4M0-028) Avail: CASI HC A06/MF A02

This is an Air Force Occupational Measurement Squadron occupational survey report (OSR) of the Aerospace Physiology (AFSC 4M0X1) career ladder. This survey, completed in 1994, is intended to update the current data base and to identify any changes that may have taken place since the last survey in 1988. The AFMAN 36-2108 Specialty Description for this career field states that 3- and 5-skill level members conduct training and testing with aerospace physiology devices. This includes delivering briefings to trainees before hypobaric and hyperbaric chamber flights and dives, as well as acting as inside and outside observer or other related crew positions. Related duties involve instructing and supervising trainees in fitting, adjusting, and caring for oxygen masks and other personal equipment; and briefing students on parasail and proper parachuting techniques, to include landing-fall procedures, swing landing trainer procedures, and parasail procedures. Finally, these personnel maintain and modify aerospace physiology equipment and associated records. DTIC

N95-34573# Naval Postgraduate School, Monterey, CA.
MANAGING TECHNOLOGICAL CHANGE IN A MILITARY TREATMENT FACILITY: A CASE STUDY OF MEDICAL DIAGNOSTIC IMAGING SUPPORT (MDIS) SYSTEM M.S. Thesis
Laura S. Tillery Dec. 1994 187 p
(AD-A294894) Avail: CASI HC A09/MF A02

Picture archiving and communication system (PACS) represents an enormously expensive technological innovation in digital imaging which has the potential to alter the way in which radiology is practiced. The purpose of this thesis is to provide a better understanding of the requirements for PACS technology and the implementation of information systems in medical facilities. The objective of PACS technology is to improve access to radiographic images and reports throughout medical facilities while decreasing the cost of image production and storage. Medical Diagnostic Imaging Support (MDIS) system is the military tri-service project to install PACS in selected U.S. military medical treatment facilities (MTF) in an attempt to create a totally filmless environment. This thesis includes a case study of the implementation of the MDIS system at Madigan Army Medical Center and the change management issues that surround the introduction of an information system in a health care organization. The issues brought forth in this study are derived from two change models in the implementation of information systems. DTIC

N95-34754# Baylor Coll. of Medicine, Houston, TX.
IMMUNOLOGICAL PROTECTION AGAINST BOTULINUM NEUROTOXIN BY A SYNTHETIC VACCINE
M. Z. Atassi 10 Apr. 1995 27 p
(Contract DAMD17-93-C-3159)
(AD-A294146) Avail: CASI HC A03/MF A01

Botulism due to food toxin is caused mainly by seven known serotypes of protein neurotoxins, botulinum neurotoxins (BoNt) produced by clostridium botulinum. BoNts are the most potent toxins and poisons known. The purpose of this work is to design a synthetic peptides vaccine for protection against BoNt. Regions of BoNt/A will be selected for synthesis, based on a number of sequence and conformational parameters and their immunological activities towards anti-BoNt/A antibodies and T cells determined. The immunodominant epitopes will be used as immunogens and those peptides which stimulate BoNt/A-cross reactive antibody and/or T cell responses will then be investigated for their capacity to provide active and passive immunity against BoNt/A challenge. The epitopes that are most protective when employed individually as immunogens will be used, in a mixture and in a multiepitope- carrier conjugate, as a vaccine for both active and passive protection of mice. The synthetic vaccine against BoNt/A will be used as a prototype to prepare synthetic vaccines containing the regions of the other serotypes that are counterparts to the regions found to be most protective on BoNt/A. DTIC

N95-32419*# National Aeronautics and Space Administration. Lyndon B. Johnson Space Center, Houston, TX.
CHARACTERIZATION OF MICROGRAVITY EFFECTS ON BONE STRUCTURE AND STRENGTH USING FRACTAL ANALYSIS
Raj S. Acharya (State Univ. of New York, Buffalo, NY.) and Linda Shackelford *In its* National Aeronautics and Space Administration (NASA)/American Society for Engineering Education (ASEE) Summer Faculty Fellowship Program, 1994, Volume 1 Jul. 1995 15 p (For primary document see N95-32418 12-99)
Avail: CASI HC A03/MF A03

N95-34052# Royal Air Force Inst. of Aviation Medicine, Farnborough (England).
NEGATIVE TO POSITIVE Gz ACCELERATION TRANSITION
A. R. J. Prior *In* AGARD, Current Concepts on G-Protection Research and Development May 1995 8 p (For primary document see N95-34050 12-54)
Copyright Avail: CASI HC A02/MF A02

N95-34056# Air Force Inst. of Aviation and Space Medicine, Moscow (Russia).
INCREASE OF HIGH-SUSTAINED +G(z) TOLERANCE AT THE EXPENSE OF PILOT'S WORKING POSTURE CHANGE
G. P. Stupakov and M. N. Khomenko *In* AGARD, Current Concepts on G-Protection Research and Development May 1995 12 p (For primary document see N95-34050 12-54)
Copyright Avail: CASI HC A03/MF A02

N95-34057# Department of the Air Force, Brooks AFB, TX.
NEW ADVANCES IN PHYSIOLOGICAL MEASUREMENTS DURING HIGH-G: TECHNOLOGY
Ulf I. Balldin *In* AGARD, Current Concepts on G-Protection Research and Development May 1995 10 p (For primary document see N95-34050 12-54)
Copyright Avail: CASI HC A02/MF A02

N95-34058# Defence and Civil Inst. of Environmental Medicine, North York (Ontario).
METHODS FOR MEASURING PHYSIOLOGICAL RESPONSES AND PROTECTION IN MAN EXPOSED TO HIGH +G(z)
F. Buick, E. H. Wood (Mayo Foundation, Rochester, MN.), M. Pecaric, and J. Maloan *In* AGARD, Current Concepts on G-Protection Research and Development May 1995 15 p (For primary document see N95-34050 12-54)
Copyright Avail: CASI HC A03/MF A02

53 BEHAVIORAL SCIENCES

Includes psychological factors; individual and group behavior; crew training and evaluation; and psychiatric research.

N95-34356# Navy Personnel Research and Development Center, San Diego, CA.
EVENT-RELATED POTENTIALS AND ELECTROENCEPHALOGRAMS IN ADAPTIVE OPERATOR TRAINING: RATIONALE AND ANNOTATED BIBLIOGRAPHY Interim Report, 1 Oct. 1992 - Mar. 1993
Leonard J. Trejo, Michelle Mullane, and Jaimee Stewart May 1995 55 p
(AD-A294337; NPRDC-TN-95-3) Avail: CASI HC A04/MF A01

This report presents summaries of research on physiological metrics of learning and memory, task performance, attention, imagery, mental workload, and adaptive training. The focus of the report is on the potential for physiological metrics such as electroencephalograms and event-related potentials to serve as control variables in adaptive operator training. An adaptive training system could use such variables to adapt the frequency and difficulty of training so as to accelerate learning and enhance transfer of training to real-world environments. This report also describes problems in learning and performance of Navy tasks that call for research on adaptive operator training. Such problems include the complexity of current combat systems, individual differences in learning strategies and ability, and poor transfer of training using conventional training methods. An example of bow adaptive training could apply to Navy training is developed for the emitter classification task performed by Navy electronic warfare operators. DTIC

N95-34463# Hartford Univ., CT.
LOCUS OF CONTROL AND COPING STYLE AS STRESS MODERATORS IN ACHIEVEMENT ORIENTED INDIVIDUALS M.S. Thesis
Douglas S. Mulbury May 1995 78 p
(AD-A294275) Avail: CASI HC A05/MF A01

The effects of achievement motivation, locus of control orientation and preferred coping style were investigated for their relationship with subjects reported stress symptoms. Scales for each of these variables were administered to 100 Psychology students at the University of Hartford. The results of these self-reports were analyzed using zero-order correlations and multiple regression analysis. It was predicted that the overall multiple regression coefficient would be significant, as well as the joint effects of locus of control orientation, achievement motive, and preferred coping style on subjects reported stress symptoms. The results indicated a lack of relationship between the independent variables and the dependent variable. An external locus of control orientation was significantly related to higher stress scores and lower achievement orientation. Higher achievement orientation was positively related to the use of active coping styles. Male subjects were slightly but significantly more internally oriented in terms of locus of control than female subjects. The findings were intended to refute the usefulness of the Type A Personality construct in predicting stress-related illness. There is evidence that there are stress moderators that may buffer high achievers from the adverse effects of stress but the relationship is complex and tenuous. DTIC

N95-34609# University of Southern Illinois, Springfield, IL. School of Medicine.
CONCEPTUAL UNDERSTANDING AND STABILITY, AND KNOWLEDGE SHIELDS FOR FENDING OFF CONCEPTUAL CHANGE Final Report, 1988 - 1991
Paul J. Feltovich, Rand J. Spire (Illinois Univ., Urbana-Champaign, IL.), Richard L. Coulson, and Jans F. Adami 31 Dec. 1994 63 p
(Contract N00014-88-K-0077)
(AD-A293555; TR-7) Avail: CASI HC A05/MF A01

The paper reports on the learning of difficult and complex concepts, the characteristics of these concepts that make them difficult for students to learn and understand well, the kind of misconceptions they acquire, and the difficulty of changing these misbeliefs. Mental maneuvers (knowledge shields) learners engage to ward off changing their beliefs are presented and discussed. DTIC

N95-34610# Massachusetts Inst. of Tech., Cambridge, MA. Research Lab. of Electronics.
THE VIRTUAL SAILOR: SYNTHETIC HUMANS FOR VIRTUAL ENVIRONMENTS Final Technical Report, 15 Aug. 1992 - 14 Aug. 1993
David L. Zeltzer 20 Apr. 1995 192 p
(Contract N00014-92-J-4005)
(AD-A293560) Avail: CASI HC A09/MF A02

In many virtual environment (VE) applications, e.g., a VE system for training personnel to perform multiperson maintenance tasks, the VE system must be able to display accurate models of human figures that can perform routine behaviors and adapt to events in the virtual world. In order to achieve such adaptive, task level interaction with virtual actors, it is necessary to model elementary human motor skills. SkillBuilder is a software system for constructing a set of motor behaviors for a virtual actor by designing motor programs for arbitrarily complicated skills. Motor programs are modeled using finite state machines, and we have categorized a set of transition and ending conditions. Using inverse kinematics and automatic collision avoidance, we use SkillBuilder to construct a suite of behaviors for simulating visually guided reaching, grasping, and head/eye tracking motions for a kinematically simulated actor consisting of rigid body parts. All of these actions have been successfully demonstrated in real-time by permitting the user to interact with the virtual environment using a whole-hand input device. DTIC

N95-32422*# Mount Holyoke Coll., South Hadley, MA. Dept. of Biological Sciences.
THE ROLE OF THE VESTIBULAR SYSTEM IN MANUAL TARGET LOCALIZATION Final Report
Susan R. Barry and S. Alyssa Mueller *In* NASA. Johnson Space Center, National Aeronautics and Space Administration (NASA)/American Society for Engineering Education (ASEE) Summer Faculty Fellowship Program, 1994, Volume 1 Jul. 1995 14 p (For primary document see N95-32418 12-99)
(Grant NGT-44-005-803)
Avail: CASI HC A03/MF A03

N95-34053# Air Force Inst. of Aviation and Space Medicine, Moscow (Russia).
SELECTION AND SPECIAL PHYSIOLOGICAL TRAINING OF FLYING PERSONNEL TO HIGH +G(z)-MANEUVERABLE FLIGHTS-MAIN CONCEPT
G. P. Stupakov and M. N. Khomenko *In* AGARD, Current Concepts on G-Protection Research and Development May 1995 15 p (For primary document see N95-34050 12-54)
Copyright Avail: CASI HC A03/MF A02

N95-34059# German Air Force, Koenigsbrueck (Germany). Inst. of Aviation Medicine.
SELECTION AND TRAINING OF MIG-29 AND FUTURE FIGHTER PILOTS
H. Welsch *In* AGARD, Current Concepts on G-Protection Research and Development May 1995 10 p (For primary document see N95-34050 12-54)
Copyright Avail: CASI HC A02/MF A02

N95-34774*# Embry-Riddle Aeronautical Univ., Daytona Beach, FL.
CERTIFICATION OF TRAINING
Richard S. Gibson *In its* Human Factors Certification of Advanced Aviation Technologies 1994 p 137-141 (For primary document see N95-34764 12-54)
Avail: CASI HC A01/MF A04

N95-34775*# Civil Aviation Administration (Sweden).
PRESENTATION OF A SWEDISH STUDY PROGRAM CONCERNING RECRUITMENT, SELECTION AND TRAINING OF STUDENT AIR TRAFFIC CONTROLLERS: THE MRU PROJECT PHASE 1
Rune Haglund *In* Embry-Riddle Aeronautical Univ., Daytona Beach, FL Human Factors Certification of Advanced Aviation Technologies 1994 p 143-161 (For primary document see N95-34764 12-54)
Avail: CASI HC A03/MF A04

54 MAN/SYSTEM TECHNOLOGY AND LIFE SUPPORT

Includes human engineering; biotechnology; and space suits and protective clothing.

For related information see also *16 Space Transportation.*

N95-32535# Lawrence Livermore National Lab., Livermore, CA.
FUNCTIONAL REQUIREMENTS ANALYSIS AND HUMAN MACHINE INTERFACE SPECIFICATIONS FOR HANDHELD METAL DETECTOR WANDS
V. Hoang, C. Hartney, and W. Banks Nov. 1994 110 p
(Contract W-7405-eng-48)
(DE95-009845; UCRL-CR-119401) Avail: CASI HC A06/MF A02

Functional Requirements Analysis (FRA) and Human-Machine-Interface Design Specifications (HMID's) are critical elements in the development of effective security systems. Handheld metal detector wands are currently used by security personnel to detect metal weapons and munitions that might be smuggled onboard an aircraft by terrorists or individuals who intend to do harm to passengers, aircraft, or other air carrier-related targets. The FAA has requested that Lawrence Livermore National Laboratory (LLNL) assist in developing functional requirements for handheld metal detector devices (wands) used at airports. This effort is focused on both defining and assuring adequate functional and human interface designs that are an integral part of airport security operations. In addition to developing functional requirements, LLNL was also requested to examine and review wanding procedures currently used by the airports and air carriers and provide comments, recommendations, and suggestions for enhanced security based upon this review. The phrase 'Human-Machine-Interface' (HMI) is frequently used to describe the characteristics of a system that allows the human to interact and control the machine or system. Equipment used by checkpoint security Pre-Board Screeners (PBS's) during rapid search of passengers must be designed to fit a broad range of anthropometric differences in height, hand size, grip strength, upper body strength, visual. acuity, auditory acuity, and other related human variables. In essence, if there is a high degree of compatibility between the end-user and the equipment, there will be a direct enhancement of total system performance and system operability. Thus, this document may also be used as, a guideline to enhance ergonomic compatibility between the PBS's and the equipment they use. DOE

N95-32688*# California Univ., Los Angeles, CA. Dept. of Chemical Engineering.
MULTIOBJECTIVE OPTIMIZATION OF HYBRID REGENERATIVE LIFE SUPPORT TECHNOLOGIES. TOPIC D: TECHNOLOGY ASSESSMENT Progress Report
Vasilios Manousiouthakis May 1995 27 p
(Grant NAG2-822)
(NASA-CR-199125; NAS 1.26:199125) Avail: CASI HC A03/MF A01

We developed simple mathematical models for many of the technologies constituting the water reclamation system in a space station. These models were employed for subsystem optimization and for the evaluation of the performance of individual water reclamation technologies, by quantifying their operational 'cost' as a linear function of weight, volume, and power consumption. Then we performed preliminary investigations on the performance improvements attainable by simple hybrid systems involving parallel combinations of technologies. We are developing a software tool for synthesizing a hybrid water recovery system (WRS) for long term space missions. As conceptual framework, we are employing the state space approach. Given a number of available technologies and the mission specifications, the state space approach would help design flowsheets featuring optimal process configurations, including those that feature stream connections in parallel, series, or recycles. We visualize this software tool to function as follows: given the mission duration, the crew size, water quality specifications, and the cost coefficients, the software will synthesize a water recovery system for the space station. It should require minimal user intervention. The following tasks need to be solved for achieving this goal: (1) formulate a problem statement that will be used to evaluate the advantages of a hybrid WRS over a single technology WBS; (2) model several WRS technologies that can be employed in the space station; (3) propose a recycling network design methodology (since the WRS synthesis task is a recycling network design problem, it is essential to employ a systematic method in synthesizing this network); (4) develop a software implementation for this design methodology, design a hybrid system using this software, and compare the resulting WRS with a base-case WRS; and (5) create a user-friendly interface for this software tool. Author

N95-33237# National Defence Research Establishment, Stockholm (Sweden). Dept. of Human Sciences.
STIMULUS-RESPONSE COMPATIBILITY
Bengt Bergstroem Dec. 1994 19 p
(ISSN 0014-9154)
(PB95-214722; FOA-R-94-00077-5.2-SE) Avail: CASI HC A03/MF A01

A critical relation in a man-machine system is the operator-workstation interface. The present report reviews the stimulus-response compatibility aspect of this interface. Three kinds of compatibility are recognized: display-control, control-display, and display-central process-control relations. Empirical principles of display-control and control-display compatibility are described. Display-central process-control relations are discussed using a multiple-resource model of information processing. The report concludes with recommendations aimed at system designers and users. NTIS

N95-33312 Virginia Univ., Charlottesville, VA.
THE PRESERVATION OF HUMAN SURROGATES FOR BIOMECHANICAL STUDIES Ph.D. Thesis
Jeff Richard Crandall 1994 285 p
Avail: Univ. Microfilms Order No. DA9415549

Preservation procedures for human surrogates were evaluated based on their ability to maintain the mechanical properties of fresh tissues, to simulate the response of living tissues, and to limit the transmittance of infectious diseases. The biomechanical properties of fresh, frozen, and embalmed hard tissues were obtained from three-point bend tests and analyzed using elastic beam theory. The elastic responses and the relaxation functions of preserved soft tissues were determined from indentation testing and viscoelastic models. Based upon the results from mechanical testing of the tissue specimens, preservation techniques for surrogates were adjusted to provide the response of living humans in an impact environment. Compression tests of preserved surrogates were performed and compared with published values for tensed and untensed volunteers. Combining simulation software and dynamic analysis; the sensitivity of human response to tissue condition was characterized in order to demonstrate the utility of using preservation techniques to adjust the physical properties of human surrogates. Finally, chromatography procedures estimated the distribution and the concentration of chemical disinfectants within embalmed surrogates. The analysis determined that the concentrations of the preservatives were sufficient to neutralize any infectious viruses or bacteria in the tissues. The mechanical test results, simulation work, and chemical analysis indicate that embalming is the preferential preservation method for human surrogates used in biomechanical studies. Dissert. Abstr.

N95-33605 Dayton Univ., OH.
HUMAN PILOTING FACTORS IN THE DESIGN OF CONTROL LAWS FOR PRECISION LANDING Ph.D. Thesis
David John Moorhouse 1993 177 p
Avail: Univ. Microfilms Order No. DA9412549

This research investigates aircraft control law design with two objectives: (1) facilitate precise touchdown through enhanced controllability and (2) improve safety by reducing pilot workload when landing in adverse conditions. Aircraft accidents have happened in windshear conditions that were well within the aircraft performance capability to negotiate safely. A review of such occurrences led to a conviction that pilots were receiving ambiguous response cues. The classical equations of aircraft dynamics were reanalyzed from the viewpoint of how a pilot perceives the dynamic responses and his most likely control response. This new viewpoint shows that an aperiodic

phugoid mode resulting from tight glideslope control gives the appearance of losing speed stability. The analyses were extended to combined effects of pilot control inputs and wind gradient effects. It was shown that a major factor in the ambiguity of the piloting cues is the coupling between airspeed and flight path responses. It was postulated, therefore, that a more effective control law design could be achieved by decoupling of the two responses using airspeed as the reference as opposed to the conventional use of angle of attack. The preceding requirement for decoupling of flight path and airspeed responses was implemented in a flight experiment to demonstrate precision touchdown for a fighter aircraft. The flight results validated the concept under a variety of adverse conditions, including an actual windshear encounter. As part of the larger experiment, the decoupled control laws facilitated a precision touchdown at night with no external lighting or guidance aids with very low pilot workload. Additional analyses were performed using the theory of divided attention, with airspeed control considered as a managerial task and glide slope as a compensatory task. This was developed into an 'imperfect pilot' model to quantify the benefits of augmenting the managerial task. Simulation results using the imperfect pilot model were compared with results from an optimal control formulation. The results were shown to be completely different. It is suggested that the two techniques should be used in a complementary fashion for aircraft design. Dissert. Abstr.

N95-34050# Advisory Group for Aerospace Research and Development, Neuilly-Sur-Seine (France). Aerospace Medical Panel.

CURRENT CONCEPTS ON G-PROTECTION RESEARCH AND DEVELOPMENT [CONCEPTS ACTUELS EN RECHERCHE ET DEVELOPPEMENT POUR LA PROTECTION ANTI-G]

May 1995 128 p Lecture series held in Ohio, 15-16 May 1995, in Koenigsbrueck, Germany, 12-13 Jun. 1995, and in Farnborough, UK, 15-16 Jun. 1995

(AGARD-LS-202; ISBN-92-836-0016-9) Copyright Avail: CASI HC A07/MF A02

A new class of fighter aircraft is emerging that will be operational or in advanced Test and Evaluation (T&E) by 1995. These aircraft (e.g. MiG 31, YF-22, Eurofighter, Rafale) are capable of developing G far in excess of 9G (i.e. 12G will be a realistic capability). The operational envelope of these agile aircraft will depend upon the G protection provided to the aircrew. In response to this challenge, established and new laboratories using human-use centrifuges are developing new aircrew protection methods. These laboratories include Armstrong Laboratory (US), SAM (UK), DCIEM (CA), LAMAS (FR), SAM (RU), KONIGSBRUCK Laboratory (GE) and FOA Laboratory (SW). In 1995, much of this research will have produced prototype flight-worthy equipment/methods with advanced understanding of their physiological bases. This lecture series reviews (1) pathophysiology of high sustained G (9G and above) and (2) recent equipment development and reports on T&E. For individual titles, see N95-34051 through N95-34060.

N95-34051# Armstrong Lab., Brooks AFB, TX. Crew Technology Div.

G-PROTECTION BASIS/ACCELERATION PHYSIOLOGY

J. W. Burns *In* AGARD, Current Concepts on G-Protection Research and Development May 1995 10 p (For primary document see N95-34050 12-54)

Copyright Avail: CASI HC A02/MF A02

Our major objective is to protect the aircrew against the detrimental effects of +Gz by developing and assessing equipment and techniques to enhance high sustained acceleration (+Gz) tolerance, and minimize the hazards of G-LOC. The payoff is reduced pilot fatigue and improved combat effectiveness. To accomplish these objectives it is imperative that we learn as much as possible regarding acceleration physiology and the influence that protective equipment and techniques have on acceleration physiology. Derived from text

N95-34052# Royal Air Force Inst. of Aviation Medicine, Farnborough (England).

NEGATIVE TO POSITIVE Gz ACCELERATION TRANSITION **c52**

A. R. J. Prior *In* AGARD, Current Concepts on G-Protection Research and Development May 1995 8 p (For primary document see N95-34050 12-54)

Copyright Avail: CASI HC A02/MF A02

Sustained negative Gz acceleration is an uncommon stress; it is poorly tolerated by the pilot, the airframe is normally stressed to only -3 Gz, and operationally there is no defined advantage for performing such a maneuver. However, during repeated pulls of high +Gz it is common practice to push negative Gz while regaining aircraft energy prior to another high G turn. During the period of negative G, which might be for only 1 or 2 seconds, there is the rapid development of bradycardia, peripheral vasodilation, and the likelihood of cardiac arrhythmias. In this physiological state the pilot then pulls positive G giving rise to profound changes in cerebral perfusion and a marked reduction in G tolerance. The use of anti-G trousers reduces the magnitude of this effect but there remains a significant lowering of G tolerance which, it is suggested, might contribute to the genesis of G-induced loss of consciousness. Author

N95-34053# Air Force Inst. of Aviation and Space Medicine, Moscow (Russia).

SELECTION AND SPECIAL PHYSIOLOGICAL TRAINING OF FLYING PERSONNEL TO HIGH +G(z)-MANEUVERABLE FLIGHTS-MAIN CONCEPT **c53**

G. P. Stupakov and M. N. Khomenko *In* AGARD, Current Concepts on G-Protection Research and Development May 1995 15 p (For primary document see N95-34050 12-54)

Copyright Avail: CASI HC A03/MF A02

For insurance of the complete and efficient protection of flyers from exposure of high-sustained and rapid onset rate +Gz-acceleration profiles, together with administration of modern sophisticated counter-G technical appliances, individual physiological tolerance of flyer to the effects of high level Gz stress plays an important role. The necessity of practical implementation of methods of determination of Gz acceleration tolerance to high-sustained +Gz-stress for selection are verified, along with carrying-out of special physiological preparation of flyers in order to magnify their tolerance to such effects. The results of study are presented of health and special physiological preparedness on pilot's individual tolerance to high-sustained +Gz-accelerations. The procedure and criteria of determination of pilot's ability to tolerate high level +Gz-accelerations in centrifuge tests for selection to transition and mastering the high performance fighter-aircraft of type MIG-29 and SU-27 are disclosed. The possibility of individual pilot's tolerance to high sustained +Gz-acceleration prediction is proved, based on data of statoergometric functional loading test on special physical trainer 'Statoergometer'. For enhancement of flyers' tolerance to high-sustained +Gz-acceleration the complex of means and ways of special physiological preparation involves carrying-out of ground and simulator training, course of physical training exercises on special trainers, realization of training centrifugation runs, and special infight training in aerobatic sorties. The methodological particularities of carrying-out and efficiency of various kinds of above mentioned special preparation of flyer are analyzed and the probable prospective ways of its further improvement are discussed. Author

N95-34054# Laboratoire de Medecine Aerospatiale, Bretigny-sur-Orge (France).

ANTI-G SUITS **c64**

J. M. Clere, G. Ossard, and M. Kerguelen *In* AGARD, Current Concepts on G-Protection Research and Development May 1995 8 p (For primary document see N95-34050 12-54)

Copyright Avail: CASI HC A02/MF A02

Several improvements were carried out on the anti-G suits and on the anti-G valves. These improvements should enhance G tolerance and pilot effectiveness under G. Most of these improvements need to be applied in operational use and not be simply reserved for the research world. In order to achieve this, these new anti G equipments must be the least cumbersome and intensive for pilots and efforts must be made to ensure their acceptability. Derived from text

N95-34055# Royal Air Force Inst. of Aviation Medicine, Farnborough (England).

POSITIVE PRESSURE BREATHING FOR G PROTECTION (PBG)

A. R. J. Prior *In* AGARD, Current Concepts on G-Protection Research and Development May 1995 16 p (For primary document see N95-34050 12-54)

Copyright Avail: CASI HC A03/MF A02

Modern, high performance, combat aircraft are capable of high sustained +Gz acceleration, at high G onset rates, for which enhanced G protection of the pilot is required if the performance of the aircraft is not to be

limited by the capabilities of the pilot. Given that the pilot is essentially seated upright in the cockpit, the most suitable system of enhanced G protection is that of positive pressure breathing (PBG) with the possible addition of new anti-G trousers having considerably greater bladder coverage than previous garments. PBG used with in-service anti-G trousers reduces pilot fatigue and doubles G endurance. An anti-G straining maneuver (AGSM) is still required as the relaxed G tolerance of the pilot is increased by only 1G. PBG used with full or extended coverage anti-G trousers enables the pilot to tolerate 8G without needing to employ the AGSM and provides a high degree of protection against G-induced loss of conscious. However, the increased bladder coverage of the trousers, and that of the chest counterpressure garment which is probably required for PBG, imposes a higher heat load on the pilot and has a tendency to reduce mobility. In addition, the oxygen mask must be capable of effecting an adequate seal of the PBG pressure against the face without user intervention; furthermore the system must be compatible with helmets containing display and sighting systems and be capable of use with NBC protective systems. Development PBG systems have yet to be fully optimized and their routine use by aircrew requires further assessment particularly with regard to the longer term consequences. Author

N95-34056# Air Force Inst. of Aviation and Space Medicine, Moscow (Russia).

INCREASE OF HIGH-SUSTAINED +G(z) TOLERANCE AT THE EXPENSE OF PILOT'S WORKING POSTURE CHANGE **c52**

G. P. Stupakov and M. N. Khomenko *In* AGARD, Current Concepts on G-Protection Research and Development May 1995 12 p (For primary document see N95-34050 12-54)

Copyright Avail: CASI HC A03/MF A02

This lecture summarizes practical experience and results of theoretical investigations in the field of anti-Gz protection of flyer in high performance fighter-aircraft. The physiological and ergonomical issues are examined of implementation in aerospace flying practice of the anti-G variable geometry seat, which is aimed at the prophylaxy of adverse effects of high sustained, rapid onset rate longitudinal (+Gz), lateral (Gy), and combined (Gz/Gy) accelerations. Presented are the results of estimation of protective efficiency for variable geometry seat, received at multiple centrifuge tests, as well as its advantages with reference to prolonged flights, which were discovered in ground flight simulator experiments. There are elucidated the main physiological particularities of effects of lateral Gy and combined (Gz/Gy) aerial combat maneuvering accelerations. The applicability of variable geometry reclining seat is verified for prevention of some deleterious effects of hypergravitation of flyer's organism. Significant role is shared to physiologo-hygienic aspects of flyer's articulate seat in context with arrangement scheme for flight cabin workstation in high performance fighter aircraft. Author

N95-34057# Department of the Air Force, Brooks AFB, TX.

NEW ADVANCES IN PHYSIOLOGICAL MEASUREMENTS DURING HIGH-G: TECHNOLOGY **c52**

Ulf I. Balldin *In* AGARD, Current Concepts on G-Protection Research and Development May 1995 10 p (For primary document see N95-34050 12-54)

Copyright Avail: CASI HC A02/MF A02

New noninvasive techniques for measuring cardiovascular parameters have been introduced to the acceleration research in centrifuge and in flight in fighter aircraft. Transcranial Doppler blood flow velocity measurements have been used in the centrifuge to detect brain blood flow changes during high G. As probe movements during high G is a problem, a remote control probe system has been developed and tested for better accuracy. Infrared spectrophotometry has been tested during increased G, but further development is required. Ear opacity blood volume measurements of circulatory endpoints during high G has been re-introduced. The use of Finapres or similar equipment to measure finger blood pressure has shown to be a very effective tool in acceleration research, both in the centrifuge and in flight, when used properly. Impedance plethysmography has also shown to be a useful tool in acceleration research. Doppler ultrasound blood flow measurements and echocardiography are difficult to use at high G-level, if new robotic techniques are not developed. Subjective scales for ratings of perceived exertion during testing of G-protecting measures or during centrifuge fatigue studies seem to be valuable tools in acceleration research and may help to avoid the need for maximal tests in the centrifuge and thereby discomfort and injuries. Author

N95-34058# Defence and Civil Inst. of Environmental Medicine, North York (Ontario).

METHODS FOR MEASURING PHYSIOLOGICAL RESPONSES AND PROTECTION IN MAN EXPOSED TO HIGH +G(z) **c52**

F. Buick, E. H. Wood (Mayo Foundation, Rochester, MN.), M. Pecaric, and J. Maloan *In* AGARD, Current Concepts on G-Protection Research and Development May 1995 15 p (For primary document see N95-34050 12-54)

Copyright Avail: CASI HC A03/MF A02

The often-used subjective measurements of +Gz tolerance are inadequate because they are prone to subjective bias and cannot document the time-dependent changes in the reacting physiology. This lecture describes noninvasive, objective measurements used to measure the human subject's physiological status, to monitor physiological reactions in order to compare the +Gz protective value of various +Gz countermeasures, and to measure endpoints which will guide the termination of +Gz exposure. Author

N95-34059# German Air Force, Koenigsbrueck (Germany). Inst. of Aviation Medicine.

SELECTION AND TRAINING OF MIG-29 AND FUTURE FIGHTER PILOTS **c53**

H. Welsch *In* AGARD, Current Concepts on G-Protection Research and Development May 1995 10 p (For primary document see N95-34050 12-54)

Copyright Avail: CASI HC A02/MF A02

With the reunification on 3 Oct. 1990 the German Air Force took possession not only of 24 MiG-29 modern fighter aircraft, but also of the human centrifuge at Koenigsbrueck near Dresden, Saxony. Until now the MiG-29 is the only high performance fighter aircraft of the German Air Force whose pilots need training in a human centrifuge in accordance with the STANAG 3827. The Office of the Surgeon General GAF took the occasion to generate a new basic program for the German Air Force (GAF) not only for the few pilots of the MiG-29, but for the future fighter pilot generation. The program includes the preselection of young pilot candidates on a voluntary basis to exclude candidates without normal physiological cardiovascular reflexes against acceleration forces, the training of student pilots of fighter aircraft before starting fighter pilot school, and the training and qualification program for fighter pilots, for flying the MiG-29 fighter aircraft or other high performance aircraft such as F-16, F-18, and Mirage 2000 as exchange pilots in the USAF, the CAF, or in France. Author

N95-34060# Department of the Air Force, Brooks AFB, TX. Crew Technology Div.

G-PROTECTION CAPABILITIES AND CURRENT G-PROTECTION ISSUES

J. W. Burns *In* AGARD, Current Concepts on G-Protection Research and Development May 1995 8 p (For primary document see N95-34050 12-54)

Copyright Avail: CASI HC A02/MF A02

Acceleration tolerance and protection of female pilots, relationship between time away from +Gz exposure (G-layoff) and a reduced G tolerance, and +Gz-induced loss of consciousness (G-LOC) are discussed. G tolerance and endurance capabilities are reflections of the pilot's strength. While within gender there is a poor correlation (average 0.2) between body size and strength, males as a group are significantly stronger than females. Current +Gz protective equipment has been designed using male anthropometry. Two modifications were made to the anti-G suit to provide a better fit for female pilots: (1) a V-shaped dart in the lumbar restraint material to bring the suit in at the waist and (2) a lowered upper edge of the abdominal bladder below the rib cage in the seated position. Anecdotal information suggests a positive relationship between G-layoff and reduced G tolerance. The reduced endurance observed in this study may reflect the reduced +Gz tolerance reported to follow G-layoff, but they are not related to changes in aerobic or anaerobic metabolism, or relaxed responses to +Gz. The anti-G straining maneuver (AGSM) is a major factor in the maintenance of vision and consciousness for most pilots during high levels of +Gz. G-LOC is unique to the flight maneuvering environment in that it

occurs in healthy aircrew. It is insidiously dangerous because it can happen with little or no warning. Cessation of cerebral blood flow, kinetics and secondary characteristics, and convulsions during G-LOC are discussed.
CASI

N95-34358# Naval Air Warfare Center, Patuxent River, MD.
THE ANVIS HEAD-UP DISPLAY: AN ANALYSIS OF ITS APPLICATION TO NAVAL HELICOPTERS
Dean Peters 28 Feb. 1995 21 p
(AD-A294342) Avail: CASI HC A03/MF A01

Combat Search and Rescue (CSAR) helicopter pilots routinely utilize Night Vision Goggles to enhance visual capabilities during night operations. The Aviator's Night Vision Imaging System (ANVIS) Head-Up Display (HUD), recently tested on the HH-60H Seahawk, provides the capability to display critical flight parameters to the pilots via goggle-mounted display units, thus minimizing headdown time in the cockpit. As more and more naval helicopter missions diversify to include CSAR and CSAR support, devices which effectively enhance night mission pilots. This HUE system and critically analyzes its advantages and limitations for use in Naval helicopters. In addition, ANVIS HUD symbology is examined from a human factors perspective with recommendations for symbology design and placement.
DTIC

N95-34370# Army Medical Research and Development Command, Fort Detrick, MD.
TRI-SERVICE PERSPECTIVES ON MICROCLIMATE COOLING OF PROTECTIVE CLOTHING IN THE HEAT
Kent B. Pandolf Apr. 1995 207 p
(AD-A294005; USAMRMC-T95-10) Avail: CASI HC A10/MF A03

This Tri-Service report evaluates the effectiveness of various microclimate cooling systems in alleviating the thermal burden imposed on our service members by wearing protective clothing in the heat. The report summarizes the findings from studies involving liquid-cooled, air-cooled, and ice-cooled systems conducted by the U.S. Army, U.S. Navy, and the U.S. Air Force. While both liquid- and air-cooled systems are shown to remove significant quantities of body heat, more evidence seems to favor air-cooled systems. In general, most commercially available microclimate cooling systems are shown not to be operationally suitable for the Services' needs. To date, the ideal microclimate cooling system suitable for most military situations has not been developed or identified. However, prediction modeling analyses indicate that with heat extraction rates of 300-400 watt, microclimate cooling can be a significant force multiplier for the Services in most desert and tropic climates.
DTIC

N95-34376# Army Research Lab., Aberdeen Proving Ground, MD.
A COMPARISON OF MONOCULAR, BIOCULAR, AND BINOCULAR NIGHT VISION GOGGLES FOR TRAVERSING OFF-ROAD TERRAIN ON FOOT Final Report
V. G. CuQlock-Knopp, Warren Torgerson, Dawn E. Sipes, Edward Bender, and John O. Merritt Mar. 1995 47 p
(AD-A294018; ARL-TR-747) Avail: CASI HC A03/MF A01

The performance of humans who traversed off-road terrain while wearing monocular, biocular, and binocular night vision goggles was examined. The difficulties that each of 35 male participants encountered while walking through rough terrain and wearing the three types of goggles were scored by independent observers. Participants themselves also rated several qualities of the goggles and ranked the goggles overall. In general, results indicated that the binocular goggle yielded better performance and was preferred to the other two goggles and that the biocular and the monocular goggles showed no consistent difference for any of the four sets of dependent measures.
DTIC

N95-34378# Army Aeromedical Research Lab., Fort Rucker, AL.
OH-58 PILOT DISPLAY UNIT (PDU) SIMULATED CRASH TESTS Final Report
Joseph L. Haley, Jr. and B. J. McEntire Dec. 1994 54 p
(DA Proj. 301-62787-A-878)
(AD-A294049; USAARL-95-10) Avail: CASI HC A04/MF A01

The pilot display unit (PDU) is designed to be placed directly in front of the pilot's eyes in the OH-58 helicopter to provide targeting and a missile status display. The location and the 7-pound mass of the unit creates a potentially hazardous head impact surface. In order to determine the degree of the hazard, a damaged OH-58 cockpit section was exposed to five survivable simulated crashes of moderate to severe impact vectors with an instrumented dummy pilot in the right seat behind the PDU. The cockpit floor was exposed to crash force up to 8 G in the vertical (z) axis and 19 G along the longitudinal (x) axis with velocity changes of 24 fps and 36 fps, respectively. These exposures did not exceed acceptable levels of human tolerance for neck and head forces when a properly fitted flight helmet was worn so that impact occurred on the helmet and not the head.
DTIC

N95-34475# Naval Postgraduate School, Monterey, CA.
ANIMATION WITHIN A MULTIMEDIA TRAINING SYSTEM FOR NIGHT VISION GOGGLES M.S. Thesis
Sean T. Epperson Mar. 1995 56 p
(AD-A294095) Avail: CASI HC A04/MF A01

Night vision goggles (NVG) provide aircrews the ability to perform many daylight operations in the nighttime environment. However, with these enhanced nighttime capabilities many mishaps occur due to aircrews overestimating the capabilities of the goggles. To reduce the risks when using NVG's, increase combat survivability, and increase combat effectiveness, continuous training is needed. A promising training alternative is multimedia. This thesis focuses on the implementation of animation within a computer-based interactive multimedia system to assist in training aircrews who use NVG's. The extent any media such as animation can be implemented to provide effective training through multimedia is largely dependent on adherence to fundamental instructional design principles. This research details the methods and techniques used in the development of animation that is part of the NVG multimedia prototype. Also a description is given of the hardware components and software applications utilized, as well as how the prototype was developed. The findings show that animation is very useful for certain instructional roles and conditions. Animation's most significant uses are in presenting procedural tasks, providing a visual representation of information that cannot be captured by other media, and the principles of operation of NVG's.
DTIC

N95-34489# Army Aeromedical Research Lab., Fort Rucker, AL.
EVALUATING THE POTENTIAL FOR ROTATION AND LOSS OF FLIGHT HELMETS FROM INERTIA AND IMPACT LOADS Final Report
James E. Bruckart and Joseph L. Haley, Jr. Mar. 1995 16 p
(DA Proj. 301-62787-A-878)
(AD-A294041; USAARL-95-20) Avail: CASI HC A03/MF A01

In severe helicopter accidents, flight helmets rotate or sometimes come off the head, triggering wearer injury. This study evaluates rotation potential for new flight helmets. Current and prototype flight helmets (SPH-4B and two versions of the HGU-56) were subjected to three tests. First, rotation was measured with up to a 50-pound upward pull at the rear edge of the helmet on a medium-size headform. Second, angular displacement was measured with a 30-pound force at the side of the helmet. Third, the helmet was placed on a Hybrid 2 headform and Hybrid 3 neck, then mounted on a pendulum test device. The freefalling pendulum was decelerated to produce 16 to 20 G peak acceleration at the neck. Angular displacement of the helmet versus time was measured with high-speed video. The upward pull tests produced 18 to 33 degrees of helmet rotation. Sideward loads produced 13 to 21 degrees of rotation. The pendulum test produced up to 45 degrees forward and up to 25 degrees rearward displacement.
DTIC

N95-34492# Army Aeromedical Research Lab., Fort Rucker, AL.
USER ACCEPTABILITY AND COMFORT OF THE COMMUNICATIONS EARPLUG (CEP) WHEN USED IN THE UH-1 HELICOPTER
Ben T. Mozo, Barbara A. Murphy, and John E. Ribera Feb. 1995 39 p
(DA Proj. 301-6287-A-878)
(AD-A294047; USAARL-95-17) Avail: CASI HC A03/MF A01

Aviators and crewmembers assigned to the crash rescue (FLATIRON) unit at Fort Rucker, Alabama participated in an evaluation of the communications earplug (CEP) in the aviation environment. They were asked to wear the two CEP configurations in combination with their personal SPH-4 helmet for three flights of at least 1 hour duration. One CEP configuration included a foam tip and the other included a premolded triple flange tip. Comments and responses provided by the volunteers showed the CEP, with some modifications, is acceptable for use in the aviation environment. Speech clarity of the CEP was judged to be an improvement

over normal helmet/ear protection by 85 percent of the respondents. The CEP with foam tip was judged to be more comfortable than CEP with the triple flange tip. Comfort was judged to be between comfortable and mildly uncomfortable for the CEP with foam earplug tip. The volunteers rated the CEP as being helpful in achieving their mission. The results of this study show the CEP is comfortable and acceptable to the aviation crewmember. DTIC

N95-34574# Army Aeromedical Research Lab., Fort Rucker, AL.
EVALUATION OF A RETROFIT OH-58 PILOT'S SEAT TO PREVENT BACK INJURY Final Report
Joseph L. Haley, Jr. and Ronald W. Palmer Dec. 1994 87 p
(AD-A294895; USAARL-95-9) Avail: CASI HC A05/MF A01

This report documents the development of pilot and copilot retrofit seats, flight tests and evaluation of the seats based on crash tests, flight tests, and a 5-year usage test in the USAARL OH-58, serial no. 71-207781. The Bell Helicopter Textron (BHT) designed seat consists of a new seat pan, hinged at the forward edge, and attached to 'load-limit' devices at the rear edge. The seat will rotate about its forward edge mount and move downward approximately 5 inches at the rear edge when the impact sink speed of the helicopter is excessive. The 5-inch stroke of the seat occurs while sustaining approximately 12 G on a 50th percentile pilot (1500-lb maximum in the lower lumbar spine). The seats, mounted in a standard OH-58 fuselage, were subjected to simulated 'sink' speeds of 26.5, 29.6, and 32.2 fps. The seats easily prevented 'injury' to the dummy pilots at 26.5 fps, but the seats 'bottomed' against the cyclic control yoke at greater sink speed. DTIC

N95-34577# Army Research Inst. of Environmental Medicine, Natick, MA.
GENERAL PROCEDURE FOR CLOTHING EVALUATIONS RELATIVE TO HEAT STRESS
Leslie Levine, Michael N. Sawka, and Richard R. Gonzalez May 1995 62 p
(AD-A294953; USARIEM-TN-95-5) Avail: CASI HC A04/MF A01

This technical note (TN) describes the recommended biophysical and physiological test procedures for heat stress evaluations of textiles and clothing. The emphasis in this TN is on the human physiological testing, which is required as part of the development and acquisition process for Army materiel, in support of the Health Hazard Assessment (HHA) which is conducted by the U.S. Army Center for Health Promotion and Preventive Medicine, provisional. Biophysical evaluations for clothing include determination of the thermal characteristics for textiles via guarded hot plate tests, and for clothing systems via thermal manikin tests. Mathematical models are used to predict performance for evaluation conditions and/or field use. Human physiological testing for clothing is best done in a controlled laboratory environment, although field trials may also be conducted. Tests must control for confounding variables, and proven test and measurement methods must be employed. DTIC

N95-34616# Rochester Univ., NY. Dept. of Computer Science.
ADAPTIVE DIFFERENTIAL VISUAL FEEDBACK FOR UNCALIBRATED HAND-EYE COORDINATION AND MOTOR CONTROL Technical Report
Martin Jagersand and Randal C. Nelson 14 Dec. 1994 30 p Sponsored by Sverige-Amerika Stiftelsen; and the Fulbright Commission
(Contract N00014-93-1-0221)
(AD-A293607; TR-597) Avail: CASI HC A03/MF A01

We propose and implement a novel method for visual space trajectory planning, and adaptive high degree of freedom (DOF) visual feedback control. The method requires no prior information either about the kinematics of the manipulator, or the placement or calibration of the cameras, and imposes no limitations on the number of degrees of freedom controlled or the number of kind of visual features utilized. The approach provides not only a means of low-level servoing but a means to integrate it with higher level visual space trajectory and task planning. We are thus able to specify and perform complex tasks composed of several primitive behaviors, using both visual servoing and open loop control, where the number of sensed and controlled signals varies during the task. We report experimental results demonstrating a factor of 5 improvement in the repeatability of manipulations using a PUMA arm when comparing visual closed-loop to traditional joint level servoing. We also present experiment statistics showing the advantages of adaptive over nonadaptive control systems, and of using redundant visual information when performing manipulation tasks. Finally, we demonstrate usefulness of the approach by using it to specify and execute complex tasks involving real-world robot manipulation of rigid and nonrigid objects in up to 12 degrees of freedom. The manipulation is performed in the context of a semi-autonomous robot manipulation system. DTIC

N95-34658 Newcastle-upon-Tyne Univ., Newcastle (England).
ANALYSIS OF SAFETY REQUIREMENTS IN THE CONTEXT OF SYSTEM FAULTS AND HUMAN ERRORS
R. deLemos, R. Fields, and A. Saeed Feb. 1995 27 p Prepared in cooperation with York Univ., England
(PB95-236105; TRS-504) Copyright Avail: Issuing Activity (National Technical Information Service (NTIS))

The paper describes an approach to the incremental and iterative analysis of requirements for safety-critical systems. The novel feature of the approach is that properties related to users of safety-critical systems are also considered in the analysis. Safety strategies are developed to ensure that hazard states are avoided and the system's integrity is maintained in the presence of failures in the system components. The approach supports an understanding of human error and the formulation of human error tolerance requirements ensuring that safety is preserved in the presence of user errors. The approach is illustrated with an example from the aerospace industry, and complementary safety strategies that allocate functionality to both the pilot and the computing systems are presented. NTIS

N95-34764*# Embry-Riddle Aeronautical Univ., Daytona Beach, FL. Center for Aviation/Aerospace Research.
HUMAN FACTORS CERTIFICATION OF ADVANCED AVIATION TECHNOLOGIES
John A. Wise, ed., V. David Hopkin, ed. (Civil Aviation Authority, Farnborough, England.), Daniel J. Garland, ed., and L. W. Hennessy, ed. Embry-Riddle Aeronautical Univ. Press 1994 387 p Conference held in Toulouse, France, 19-23 Jul. 1993 Sponsored in cooperation with Eurocontrol, FAA, Direction Generale de l'Aviation Civile, and Research Inst. for Information, Science, and Engineering In Aviation Human Factors Series
(Grant NAG1-1593)
(NASA-CR-199009; NAS 1.26:199009; ISBN-1-884099-03-3) Avail: CASI HC A17/MF A04

Proceedings of the Human Factors Certification of Advanced Aviation Technologies Conference held at the Chateau de Bonas, near Toulouse, France, 19-23 July 1993. For individual titles, see N95-34765 through N95-34787.

N95-34765*# Embry-Riddle Aeronautical Univ., Daytona Beach, FL.
ON THE USE OF THE SYSTEMS APPROACH TO CERTIFY ADVANCED AVIATION TECHNOLOGIES
Mark A. Wise (University of Central Florida, Orlando, FL.) and John A. Wise *In its* Human Factors Certification of Advanced Aviation Technologies 1994 p 15-23 (For primary document see N95-34764 12-54)
Avail: CASI HC A02/MF A04

The field of human factors is as varied and diverse as the human subject itself. But one of its most important applications is the facilitation of safety and efficiency in a particular working environment through the implementation of paradigms known about humans and their working relationship with machines and systems. During the period since World War II (which is often viewed as the birth of Human Factors) no area has been the subject of more human factors research than aviation. And in no time during that epoch is the influence of human factors more important, nor more imperative than it is today. As technology driven designs have been finding their way into the national airspace system (NAS), there has been growing concern within the aviation industry itself, the Federal Aviation Administration (FAA), and the general public for a means by which to certify complex systems and the advanced aviation technologies that will be responsible for transporting, directing, and maintaining our airborne travel. While it is widely agreed human factors certification is desirable, the philosophy that will underlie the approach is debatable. There are, in general, two different approaches to certification: (1) the top-down or systems approach; and, (2) the bottom-up or monadical approach. The top-down approach is characterized by the underlying assumption that certification can be best achieved by looking at the system as a whole, understanding

its objectives and operating environment, then examining the constituent parts. In an aircraft cockpit, this would be accomplished by first examining what the aircraft is supposed to be (e.g., fighter, general aviation, passenger), identifying its operating environment (IFR, VMC, combat, etc.) and looking at the entire working system which includes the hardware, software, liveware and their interactions; then, evaluative measures can be applied to the subsystems (e.g., individual instruments, CRT displays, controls). The bottom-up approach is founded on the philosophy that the whole can be best served by first examining it constituent elements. This approach would perform the above certification completely antithetically, by looking at the individual parts and certifying good human factors applications to those parts under the basic assumption that the whole is equal to the sum of its parts. Author

N95-34766*# Nottingham Univ. (England).
A ROSE BY ANY OTHER NAME: CERTIFICATION SEEN AS PROCESS RATHER THAN CONTENT **c03**
John R. Wilson *In* Embry-Riddle Aeronautical Univ., Daytona Beach,FL, Human Factors Certification of Advanced Aviation Technologies 1994 p 26-34 (For primary document see N95-34764 12-54)
Avail: CASI HC A02/MF A04

Green (1990) believes that the two main factors safeguarding flying from human error are both related to certification and regulation. First is the increasingly proceduralized nature of flying whereby as much as possible is reduced to a rule-based activity. Second is the emphasis placed upon training and competency checking of aircrew in simulators and in the air, both generally and for all particular types of aircraft flown. This leaves, believes Green, other human factors that are relatively unaddressed as yet and which can give rise to human reliability problems. These include: hardware factors and especially pilot/co-pilot relationships; and system factors including fatigue and cost/safety trade-offs. He also, importantly, identifies problems with the integration of the 'electronic crew member' following increased automation. Human reliability failures with artificial intelligence and automation, due to over-reliance on the system fail-safe mechanisms, or to operator under- confidence in the integrity or self-regulating capacity of the system, or to out-of-loop effects, are widely accepted as being due to deficiencies in plant design, planning, management and maintenance more than to 'operator error' - Reason's (1990) latent error or organization pathogens argument. Reliability failures in complex systems are well enough documented to give cause for concern and at least promote a debate on the merits of a full certification program. The purpose of this short paper is to seek out and explore what is valuable in certification, at the least to show that the benefits outweigh the disadvantages and at best to identify positive outcomes perhaps not obtainable in other ways. On both sides of the debate on certification there is general agreement on the need for a better human factors perspective and effort in complex aviation systems design. What is at issue is how this is to be promoted. It is incumbent upon opponents of certification to say how else such promotion be enabled. This is an exploratory and philosophical review, not a focused and specific one, and it will draw upon much that is not firmly in the domain of complex aviation systems. Author

N95-34767*# Federal Aviation Administration, Washington, DC.
A PSYCHOLOGIST'S VIEW OF VALIDATING AVIATION SYSTEMS
Earl S. Stein and Dan Wagner *In* Embry-Riddle Aeronautical Univ., Daytona Beach,FL, Human Factors Certification of Advanced Aviation Technologies 1994 p 46-52 (For primary document see N95-34764 12-54)
Avail: CASI HC A02/MF A04

All systems, no matter what they are designed to do, have shortcomings that may make them less productive than was hoped during the initial development. Such shortcomings can arise at any stage of development: from conception to the end of the implementation life cycle. While systems failure and errors of a lesser magnitude can occur as a function of mechanical or software breakdown, the majority of such problems, in aviation are usually laid on the shoulders of the human operator and, to a lesser extent, on human factors. The operator bears the responsibility and blame even though, from a human factors perspective, error may have been designed into the system. Human factors is not a new concept in aviation. The name may be new, but the issues related to operators in the loop date back to the industrial revolution of the nineteenth century and certainly to the aviation build-up for World War I. During this first global confrontation, military services from all sides discovered rather quickly that poor selection and training led to drastically increased personnel losses. While hardware design became an issue later, the early efforts were primarily focused on increased care in pilot selection and on their training. This actually involved early labor-intensive simulation, using such devices as sticks and chairs mounted on rope networks which could be manually moved in response to control input. The use of selection criteria and improved training led to more viable person-machine systems. More pilots survived training and their first ten missions in the air, a rule of thumb arrived at by experience which predicted ultimate survival better than any other. This rule was to hold through World War II. At that time, personnel selection and training became very sophisticated based on previous standards. Also, many psychologists were drafted into Army Air Corps programs which were geared towards refining the human factor. However, despite the talent involved in these programs and the tremendous build-up of aviation during the war, there were still aircraft designs that were man killers (no sexism implied since all combat pilots were men). One classic design error that was identified fifty years ago was the multipointer altimeter, which could easily be misread especially by a pilot under considerable task load. It has led to flying fully operational aircraft into the terrain. The authors of the research which formally identified this problem put 'Human Errors' in quotes to express their dissatisfaction with the traditional approach to accident investigation. It traditionally places the burden of guilt on the operator. Some of these altimeters still exist in older aircraft to this day. Author

N95-34768*# Eurocontrol Experimental Centre, Bretigny (France).
CERTIFICATION OF TACTICS AND STRATEGIES IN AVIATION
Hartmut Koelman *In* Embry-Riddle Aeronautical Univ., Daytona Beach,FL, Human Factors Certification of Advanced Aviation Technologies 1994 p 54-75 (For primary document see N95-34764 12-54)
Avail: CASI HC A03/MF A04

The paper suggests that the 'tactics and strategies' notion is a highly suitable paradigm to describe the cognitive involvement of human operators in advanced aviation systems (far more suitable than classical functional analysis), and that the workload and situational awareness of operators are intimately associated with the planning and execution of their tactics and strategies. If system designers have muddled views about the collective tactics and strategies to be used during operation, they will produce sub-optimum designs. If operators use unproven and/or inappropriate tactics and strategies, the system may fail. The author wants to make a point that, beyond certification of people or system designs, there may be a need to go into more detail and examine (certify?) the set of tactics and strategies (i.e., the Operational Concept) which makes the people and systems perform as expected. The collective tactics and strategies determine the information flows and situational awareness which exists in organizations and composite human-machine systems. The available infrastructure and equipment (automation) enable these information flows and situational awareness, but are at the same time the constraining factor. Frequently, the tactics and strategies are driven by technology, whereas we would rather like to see a system designed to support an optimized Operational Concept, i.e., to support a sufficiently coherent, cooperative and modular set of anticipation and planning mechanisms. Again, in line with the view of MacLeod and Taylor (1993), this technology driven situation may be caused by the system designer's and operator job designer's over-emphasis on functional analysis (a mechanistic engineering concept), at the expense of a subject which does not seem to be well understood today: the role of the (human cognitive and/or automated) tactics and strategies which are embedded in composite human-machine systems. Research would be needed to arrive at a generally accepted 'planning theory' which can elevate the analysis, description and design of tactics and strategies from today's cottage industry methods to an engineering discipline. The available infrastructure and equipment (automation) enable these information flows and situational awareness, but are at the same time the constraining factor. Frequently, the tactics and strategies are driven by technology, whereas we would rather like to see a system designed to support an optimized Operational Concept, i.e., to support a sufficiently coherent, cooperative and modular set of anticipation and planning mechanisms. Again, in line with the view of MacLeod and Taylor (1993), this technology driven situation may be caused by the system designer's and operator job designer's over-emphasis on functional analysis (a mechanistic engineering concept), at the expense of a subject which does not seem to be well understood

today: the role of the (human cognitive and/or automated) tactics and strategies which are embedded in composite human-machine systems. Research would be needed to arrive at a generally accepted 'planning theory' which can evaluate the analysis, description and design of tactics and strategies from today's cottage industry methods to an engineering discipline. Author

N95-34769*# Eurocontrol Experimental Centre, Bretigny (France).
HUMAN FACTORS CERTIFICATION: A USEFUL CONCEPT?
Alistair Jackson *In* Embry-Riddle Aeronautical Univ., Daytona Beach,FL, Human Factors Certification of Advanced Aviation Technologies 1994 p 79-86 (For primary document see N95-34764 12-54)
Avail: CASI HC A02/MF A04

This paper considers what is involved in certification processes and their relation to human factors aspects of systems. It derives from recognition of a lack of understanding of the processes and purposes of certification. This was encountered when attempting to address the workshop topic by integrating an understanding of human factors with the observed processes of certification. The paper considers what human factors (HF) certification might be and then develops a simple model of the elements of a certification process. It then tries to relate these elements to the needs of the aviation communities and other parties with an interest in the certification of advance aviation technologies. Author

N95-34770*# Civil Aviation Authority, Farnborough (England).
HUMAN FACTORS CERTIFICATION IN THE DEVELOPMENT OF FUTURE AIR TRAFFIC CONTROL SYSTEMS c04
Alyson E. Evans *In its* Human Factors Certification of Advanced Aviation Technologies 1994 p 87-96 (For primary document see N95-34764 12-54)
Avail: CASI HC A02/MF A04

If human factors certification of aviation technologies aims to encompass the wide range of issues which need to be addressed for any new system, then human factors involvement must be present throughout the whole design process in a manner which relates to final certification. A certification process cannot simply be applied to the final product of design. Standards and guidelines will be required by designers at the outset of design for reference in preparing for certification. The most effective use of human factors principles, methods, and measures is made as part of an iterative design process, leading to a system which reflects these as far as possible. This particularly applies where the technology is complex and may be represented by a number of components or sub-systems. Some aspects of the system are best certified during early prototyping, when there is still scope to make changes to software or hardware. At this stage in design, financial and/or time pressures will not rule out the possibility of necessary changes, as may be the case later. Other aspects of the system will be best certified during the final phases of design when the system is in a more complete form and in a realistic environment. Author

N95-34771*# Royal Air Force Inst. of Aviation Medicine, Farnborough (England).
QUALITY ASSURANCE AND RISK MANAGEMENT: PERSPECTIVES ON HUMAN FACTORS CERTIFICATION OF ADVANCED AVIATION SYSTEMS c04
Robert M. Taylor and Iain S. MacLeod (Aerosystems International, Yeovil, England.) *In* Embry-Riddle Aeronautical Univ., Daytona Beach,FL, Human Factors Certification of Advanced Aviation Technologies 1994 p 97-118 (For primary document see N95-34764 12-54)
Avail: CASI HC A03/MF A04

This paper is based on the experience of engineering psychologists advising the U.K. Ministry of Defense (MoD) on the procurement of advanced aviation systems that conform to good human engineering (HE) practice. Traditional approaches to HE in systems procurement focus on the physical nature of the human-machine interface. Advanced aviation systems present increasingly complex design requirements for human functional integration, information processing, and cognitive task performance effectiveness. These developing requirements present new challenges for HE quality assurance (QA) and risk management, requiring focus on design processes as well as on design content or product. A new approach to the application of HE, recently adopted by NATO, provides more systematic ordering and control of HE processes and activities to meet the challenges of advanced aircrew systems design. This systematic approach to HE has been applied by MoD to the procurement of mission systems for the Royal Navy Merlin helicopter. In MoD procurement, certification is a judicial function, essentially independent of the service customer and industry contractor. Certification decisions are based on advice from MoD's appointed Acceptance Agency. Test and evaluation (T&E) conducted by the contractor and by the Acceptance Agency provide evidence for certification. Certification identifies limitations of systems upon release to the service. Evidence of compliance with HE standards traditionally forms the main basis of HE certification and significant non-compliance could restrict release. The systems HE approach shows concern for the quality of processes as well as for the content of the product. Human factors certification should be concerned with the quality of HE processes as well as products. Certification should require proof of process as well as proof of content and performance. QA criteria such as completeness, consistency, timeliness, and compatibility provide generic guidelines for progressive acceptance and certification of HE processes. Threats to the validity of certification arise from problems and assumptions in T&E methods. T&E should seek to reduce the risk of specification non-compliance and certification failure. Author

N95-34772*# University of Central Florida, Orlando, FL.
USER TYPE CERTIFICATION FOR ADVANCED FLIGHT CONTROL SYSTEMS c08
Richard D. Gilson and David W. Abbott *In* Embry-Riddle Aeronautical Univ., Daytona Beach,FL, Human Factors Certification of Advanced Aviation Technologies 1994 p 119-123 (For primary document see N95-34764 12-54)
Avail: CASI HC A01/MF A04

Advanced avionics through flight management systems (FMS) coupled with autopilots can now precisely control aircraft from takeoff to landing. Clearly, this has been the most important improvement in aircraft since the jet engine. Regardless of the eventual capabilities of this technology, it is doubtful that society will soon accept pilotless airliners with the same aplomb they accept driverless passenger trains. Flight crews are still needed to deal with inputing clearances, taxiing, in-flight rerouting, unexpected weather decisions, and emergencies; yet it is well known that the contribution of human errors far exceed those of current hardware or software systems. Thus human errors remain, and are even increasing in percentage as the largest contributor to total system error. Currently, the flight crew is regulated by a layered system of certification: by operation, e.g., airline transport pilot versus private pilot; by category, e.g., airplane versus helicopter; by class, e.g., single engine land versus multi-engine land; and by type (for larger aircraft and jet powered aircraft), e.g., Boeing 767 or Airbus A320. Nothing in the certification process now requires an in-depth proficiency with specific types of avionics systems despite their prominent role in aircraft control and guidance. Author

N95-34773*# Search Technology, Inc., Norcross, GA.
CERTIFY FOR SUCCESS: A METHODOLOGY FOR HUMAN-CENTERED CERTIFICATION OF ADVANCED AVIATION SYSTEMS
Ronald L. Small and William B. Rouse *In* Embry-Riddle Aeronautical Univ., Daytona Beach,FL, Human Factors Certification of Advanced Aviation Rechnologies 1994 p 127-133 (For primary document see N95-34764 12-54)
Avail: CASI HC A02/MF A04

This position paper uses the methodology in Design for Success as a basis for a human factors certification program. The Design for Success (DFS) methodology espouses a multi-step process to designing and developing systems in a human-centered fashion. These steps are as follows: (1) naturalizing - understand stakeholders and their concerns; (2) marketing - understand market-oriented alternatives to meeting stakeholder concerns; (3) engineering - detailed design and development of the system considering tradeoffs between technology, cost, schedule, certification requirements, etc.; (4) system evaluation - determining if the system meets its goal(s); and (5) sales and service - delivering and maintaining the system. Because the main topic of this paper is certification, we will focus our attention on step 4, System Evaluation, since it is the natural precursor to certification. Evaluation involves testing the system and its parts for their correct behaviors. Certification focuses not only on ensuring that the system exhibits the correct behaviors, but ONLY the correct behaviors.
Author

N95-34774*# Embry-Riddle Aeronautical Univ., Daytona Beach, FL.
CERTIFICATION OF TRAINING c53
Richard S. Gibson *In its* Human Factors Certification of Advanced Aviation Technologies 1994 p 137-141 (For primary document see N95-34764 12-54)
Avail: CASI HC A01/MF A04

Training has been around as an informal process for countless years. Most higher order animals require some level of training in hunting, social skills, or other survival related skills to continue their existence beyond early infancy. Much of the training is accomplished through imitation, trial and error, and good luck. In some ways the essentials of training in aviation have not deviated from this original formula a great deal. One of the major changes in aviation and other technical areas is that more complex response chains based on a broader base of knowledge are now required. 'To certify' means many things according to the American Heritage dictionary of the English Language. These meanings range from 'to guarantee as meeting a standard' to 'to declare legally insane'. For this discussion, we will use the definition 'an action taken by some authoritative body that essentially guarantees that the instruction meets some defined standard'. In order to make this certification, the responsible body subjects the educational process, training, training device, or simulator to some type of examination to determine its adequacy or validity. Author

N95-34775*# Civil Aviation Administration (Sweden).
PRESENTATION OF A SWEDISH STUDY PROGRAM CONCERNING RECRUITMENT, SELECTION AND TRAINING OF STUDENT AIR TRAFFIC CONTROLLERS: THE MRU PROJECT PHASE 1 c53
Rune Haglund *In* Embry-Riddle Aeronautical Univ., Daytona Beach, FL Human Factors Certification of Advanced Aviation Technologies 1994 p 143-161 (For primary document see N95-34764 12-54)
Avail: CASI HC A03/MF A04

The Director of the ANS Department has set up an objective for the efficiency of screening and training procedures for air traffic controller students which implies that all students admitted 'shall be considered to have the qualification for - and be given the means of - completing the training'. As a consequence, a study project has been established. It is run by the ANS Department with members from the Swedish CAA, in close cooperation with Uppsala University. Author

N95-34776*# Aerosystems International, Yeovil (England).
DOES HUMAN COGNITION ALLOW HUMAN FACTORS (HF) CERTIFICATION OF ADVANCED AIRCREW SYSTEMS?
Iain S. MacLeod and Robert M. Taylor (Royal Air Force Inst. of Aviation Medicine, Farnborough, England.) *In* Embry-Riddle Aeronautical Univ., Daytona Beach,FL, Human Factors Certification of Advanced Aviation Technologies 1994 p 163-186 (For primary document see N95-34764 12-54)
Avail: CASI HC A03/MF A04

This paper has examined the requirements of HF specification and certification within advanced or complex aircrew systems. It suggests reasons for current inadequacies in the use of HF in the design process, giving some examples in support, and suggesting an avenue towards the improvement of the HF certification process. The importance of human cognition to the operation and performance of advanced aircrew systems has been stressed. Many of the shortfalls of advanced aircrew systems must be attributed to over automated designs that show little consideration on either the mental limits or the cognitive capabilities of the human system component. Traditional approaches to system design and HF certification are set within an over physicalistic foundation. Also, traditionally it was assumed that physicalistic system functions could be attributed to either the human or the machine on a one to one basis. Moreover, any problems associated with the parallel needs, or promoting human understanding alongside system operation and direction, were generally equated in reality by the natural flexibility and adaptability of human skills. The consideration of the human component of a complex system is seen as being primarily based on manifestations of human behavior to the almost total exclusion of any appreciation of unobservable human mental and cognitive processes. The argument of this paper is that the considered functionality of any complex human-machine system must contain functions that are purely human and purely cognitive. Human-machine system reliability ultimately depends on human reliability and dependability and, therefore, on the form and frequency of cognitive processes that have to be conducted to support system performance. The greater the demand placed by an advanced aircraft system on the human component's basic knowledge processes or cognition, rather than on skill, the more insiduous the effects the human may have on that system. This paper discusses one example of an attempt to devise an improved method of specificaiton and certification with relation to the advanced aircrew system, that of the RN Merlin helicopter. The method is realized to have limitations in practice, these mainly associated with the late production of the system specification in relation to the system development process. The need for a careful appreciation of the capabilities and support needs of human cognition within the design process of a complex man machine system has been argued, especially with relation to the concept of system functionality. Unlike the physicalistic Fitts list, a new classification of system functionality is proposed, namely: (1) equipment - system equipment related; (2) cognitive - human cognition related; and (3) associated - necessary combinatin of equipment and cognitive. This paper has not proposed a method for a fuller consideration of cognition within systems design, but has suggested the need for such a method and indicated an avenue towards its development. Finally, the HF certification of advanced aircrew systems is seen as only being possible in a qualified sense until the important functions of human cognition are considered within the system design process. (This paper contains the opinions of its authors and does not necessarily refledt the standpoint of their respective organizations). Author

N95-34777*# Wales Univ. Inst. of Science and Technology, Cardiff (United Kingdom).
PRACTICAL GUIDELINES FOR WORKLOAD ASSESSMENT
Andrew J. Tattersall *In* Embry-Riddle Aeronautical Univ., Daytona Beach,FL, Human Factors Certification of Advanced Aviation Technologies 1994 p 193-206 (For primary document see N95-34764 12-54)
Avail: CASI HC A03/MF A04

The practical problems that might be encountered in carrying out workload evaluations in work settings have been outlined. Different approaches have been distinguished that may determine the type of research design used and provide assistance in the difficult choice between workload assessment techniques. One approach to workload assessment is to examine the short-term consequences of combining various tasks. Theoretical models of attention allocation will underpin specific studies of interference and the consequences of task demand and task conflict for performance. A further approach with a different temporal orientation may lead us to a better understanding of the relationships between work demands and strain through the analysis of individual differences in cognitive control processes. The application of these processes may depend on individual differences in long term styles and short term strategies, but may be used to prevent decrements in work performance under difficult conditions. However, control may attract costs as well as benefits in terms of changes in effective state and physiological activity. Thus, strain associated with work demands may only be measurable in the form of tradeoffs between performance and other domains of individual activity. The methodological implications are to identify patterns of adjustment to workload variations using repeated measures and longitudinal sampling of performance as well as subjective and physiological measures. Possible enhancements to workplace design must take into account these human factors considerations of workload in order to avoid potential decrements in individual performance and associated organizational problems. Author

N95-34778*# University of Eastern Michigan, Ypsilanti, MI.
IS THERE A ROLE FOR A TEST CONTROLLER IN THE DEVELOPMENT OF NEW ATC EQUIPMENT?
Ron Westrum *In* Embry-Riddle Aeronautical Univ., Daytona Beach,FL, Human Factors Certification of Advanced Aviation Technologies 1994 p 221-228 (For primary document see N95-34764 12-54)
Avail: CASI HC A02/MF A04

Earl Wiener points out that human factors problems fixed during the R & D stage are paid for once. When they are not fixed during R & D, they are then paid for every day. How users are involved in the R & D process to assist in developing equipment is a critical issue. Effective involvement can produce real improvements. Ineffective involvement can produce inefficient kludges or systems that are actually dangerous. The underlying problem is the management of information and ideas. To develop a really generative system a great deal would have to change in the way that the FAA innovates. Use of test controllers would solve only some of the

problems. For instance, we have cockpit resource management now for pilots; we may have it soon for controllers. But the management of ideas in the innovation process also needs intellectual resource management. Simply involving users is not enough. Brought in at the wrong point in the development process, users can block or compromise innovation. User involvement must be carefully considered. A test controller may be one solution to this problem. It might be necessary to have several kinds of test controllers (en route versus TRACON, for instance). No doubt further problems would surface in getting test controllers into operation. I would recommend that the FAA engage in a series of case studies of controller involvement in the innovation process. A systematic comparison of effective and ineffective cases would do much to clarify what we ought to do in the future. Unfortunately, I have been unable to find any cases where test controllers have been used. Perhaps we need to create some, to see how they work. Author

N95-34779*# Austrian Road Safety Board (Austria).
TOWARDS A FRAMEWORK OF HUMAN FACTORS CERTIFICATION OF COMPLEX HUMAN-MACHINE SYSTEMS
Birgit Bukasa *In* Embry-Riddle Aeronautical Univ., Daytona Beach, FL Human Factors Certification of Advanced Aviation Technologies 1994 p 229-234 (For primary document see N95-34764 12-54)
Avail: CASI HC A02/MF A04

As far as total automation is not realized, the combination of technical and social components in man-machine systems demands not only contributions from engineers but at least to an equal extent from behavioral scientists. This has been neglected far too long. The psychological, social and cultural aspects of technological innovations were almost totally overlooked. Yet, along with expected safety improvements the institutionalization of human factors is on the way. The introduction of human factors certification of complex man-machine systems will be a milestone in this process. Author

N95-34780*# Baldwin International Services, Heffingen (Luxembourg).
THE SUCCESSFUL MANAGEMENT OF PROGRAMS FOR HUMAN FACTORS CERTIFICATION OF ADVANCED AVIATION TECHNOLOGIES
Rod Baldwin *In* Embry-Riddle Aeronautical Univ., Daytona Beach, FL Human Factors Certification of Advanced Aviation Technologies 1994 p 237-245 (For primary document see N95-34764 12-54)
Avail: CASI HC A02/MF A04

In recent years there have been immense pressures to enact changes on the air traffic control organizations of most states. In addition, many of these states are or have been subject to great political, sociological and economic changes. Consequently, any new schemes must be considered within the context of national or even international changes. Europe has its own special problems, and many of these are particularly pertinent when considering human factors certification programs. Although these problems must also be considered in the wider context of change, it is usually very difficult to identify which forces are pressing in support of human factors aspects and which forces are resisting change. There are a large number of aspects which must be taken into account if human factors certification programs are to be successfully implemented. Certification programs would be new ventures, and like many new ventures it will be essential to ensure that managers have the skills, commitment and experience to manage the programs effectively. However, they must always be aware of the content and the degree of certainty to which the human factors principles can be applied - as Debons and Horne have carefully described. It will be essential to avoid the well known pitfalls which occur in the implementation of performance appraisal schemes. While most appraisal schemes are usually extremely well thought out, they often do not produce good results because they are not implemented properly and staff therefore do not have faith in them. If the manager does not have the commitment and interest in his/her staff as human beings, then the schemes will not be effective. Thus, one aspect of considering human factors certification schemes is within the context of a managed organization. This paper outlines some of the management factors which need to be considered for the air traffic control services. Many of the points received attention during the plenary sessions while others were covered by the working groups when the question arose of how various aspects of human factors certification programs would be managed. Management and organizational issues will certainly need to be included in any frame of reference by those who may be involved in developing certification programs. Author

N95-34781*# Sterling Software, Inc., Dallas, TX.
EVALUATION IN CONTEXT: ATC AUTOMATION IN THE FIELD
Kelly Harwood and Beverly Sanford *In* Embry-Riddle Aeronautical Univ., Daytona Beach, FL Human Factors Certification of Advanced Aviation Technologies 1994 p 247-262 (For primary document see N95-34764 12-54)
Avail: CASI HC A03/MF A04

The process for incorporating advanced technologies into complex aviation systems is as important as the final product itself. This paper described a process that is currently being applied to the development and assessment of an advanced ATC automation system, CTAS. The key element of the process is field exposure early in the system development cycle. The process deviates from current established practices of system development -- where field testing is an implementation endpoint -- and has been deemed necessary by the FAA for streamlining development and bringing system functions to a level of stability and usefulness. Methods and approaches for field assessment are borrowed from human factors engineering, cognitive engineering, and usability engineering and are tailored for the constraints of an operational ATC environment. To date, the focus has been on the qualitative assessment of the match between TMA capabilities and the context for their use. Capturing the users' experience with the automation tool and understanding tool use in the context of the operational environment is important, not only for developing a tool that is an effective problem-solving instrument but also for defining meaningful operational requirements. Such requirements form the basis for certifying the safety and efficiency of the system. CTAS is the first U.S. advanced ATC automation system of its scope and complexity to undergo this field development and assessment process. With the rapid advances in aviation technologies and our limited understanding of their impact on system performance, it is time we opened our eyes to new possibilities for developing, validating, and ultimately certifying complex aviation systems. Author

N95-34782*# International Civil Aviation Organization, Montreal (Quebec).
INTEGRATING HUMAN FACTORS KNOWLEDGE INTO CERTIFICATION: THE POINT OF VIEW OF THE INTERNATIONAL CIVIL AVIATION ORGANIZATION (ICAO)
Daniel Maurino and Vincent Galotti *In* Embry-Riddle Aeronautical Univ., Daytona Beach,FL, Human Factors Certification of Advanced Aviation Technologies 1994 p 264-273 (For primary document see N95-34764 12-54)
Avail: CASI HC A03/MF A04

It is appropriate here to repeat the analogy described in the introduction to this paper which is that: The consideration of human factors requirements during the design stage of advanced, new technology systems may be seen as resting over a three-legged stool. The first leg, the equipment that a system will utilize to achieve its goals, has traditionally attracted ergonomic considerations associated with equipment design, usually centered around 'knobs and dials.' Lately, this view has expanded to include the so-called other important aspect of Human Factor's study which deals with the cognitive, behaviorial and social processes of the human operators. Study in this area must be furthered. The second leg of the stool, the procedures to operate the equipment, however, has been largely unaddressed. Procedures are not inherent to equipment, but must be developed. The importance of proper human factors consideration in the design of procedures can not be overstated. Lastly, the third leg of the stool, the certification of personnel who will operate the equipment, is very much underway, but far from being complete. The real quest now, however, is to integrate these three legs into an indivisible one. Finally, and most importantly, this workshop and its topic are extremely timely in that we are at the dawn of the most ambitious development ever undertaken in international civil aviation. This would allow us the rather unique opportunity to put theory into practice in the near future by ensuring that the concepts developed and furthered by this workshop and the follow-up are implemented in the design and certification of the ICAO future CNS/ATM systems described earlier in this paper. Now is the time to incorporate human factors requirements during the certification processes of these systems. This might act as a test to the feasibility of these ideas. Such endeavors

represent a challenge for the research, engineering, training, operational and regulatory communities. But there is certainly more to be gained by attempting to meet the challenge rather than refraining from progress by decrying the difficulties involved. Author

N95-34783*# Action Recherches Application Matra Irit en Interface Homme Systeme (France).

IMPROVING AIR TRAFFIC CONTROL: PROVING NEW TOOLS OR APPROVING THE JOINT HUMAN-MACHINE SYSTEM?

Irene Gaillard and Marcel Leroux (Centre d'Etudes de la Navigation Aerienne, Toulouse, France.) *In* Embry-Riddle Aeronautical Univ., Daytona Beach, FL Human Factors Certification of Advanced Aviation Technologies 1994 p 275-299 (For primary document see N95-34764 12-54)

Avail: CASI HC A03/MF A04

From the description of a field problem (i.e., designing decision aids for air traffic controllers), this paper points out how a cognitive engineering approach provides the milestones for the evaluation of future joint human-machine systems. Author

N95-34784*# National Aeronautics and Space Administration. Lyndon B. Johnson Space Center, Houston, TX.

CERTIFICATION FOR CIVIL FLIGHT DECKS AND THE HUMAN-COMPUTER INTERFACE

Andrew J. McClumpha (Royal Air Force Inst. of Aviation Medicine, Farnborough, England.) and Marianne Rudisill *In* Embry-Riddle Aeronautical Univ., Daytona Beach,FL, Human Factors Certification of Advanced Aviation Technologies 1994 p 289-299 (For primary document see N95-34764 12-54)

Avail: CASI HC A03/MF A04

This paper will address the issue of human factor aspects of civil flight deck certification, with emphasis on the pilot's interface with automation. In particular, three questions will be asked that relate to this certification process: (1) are the methods, data, and guidelines available from human factors to adequately address the problems of certifying as safe and error tolerant the complex automated systems of modern civil transport aircraft; (2) do aircraft manufacturers effectively apply human factors information during the aircraft flight deck design process; and (3) do regulatory authorities effectively apply human factors information during the aircraft certification process? Author

N95-34785*# Bureau Enquetes Accidents, Paris (France).

SOME INADEQUACIES OF THE CURRENT HUMAN FACTORS CERTIFICATION PROCESS OF ADVANCED AIRCRAFT TECHNOLOGIES

Jean Paries *In* Embry-Riddle Aeronautical Univ., Daytona Beach, FL Human Factors Certification of Advanced Aviation Technologies 1994 p 301-306 (For primary document see N95-34764 12-54)

Avail: CASI HC A02/MF A04

Automation related accidents or serious incidents are not limited to advanced technology aircraft. There is a full history of such accidents with conventional technology aircraft. However, this type of occurrence is far from sparing the newest 'glass cockpit' generation, and it even seems to be a growing contributor to its accident rate. Nevertheless, all these aircraft have been properly certificated according to the relevant airworthiness regulations. Therefore, there is a growing concern that with the technological advancement of air transport aircraft cockpits, the current airworthiness regulations addressing cockpit design and human factors may have reached some level of inadequacy. This paper reviews some aspects of the current airworthiness regulations and certification process related to human factors of cockpit design and focuses on questioning their ability to guarantee the intended safety objectives. Author

N95-34786*# Direction Generale de l'Aviation Civile, Paris (France).

ADVANCED AUTOMATED GLASS COCKPIT CERTIFICATION: BEING WARY OF HUMAN FACTORS

Rene Amalberti and Florence Wilbaux *In* Embry-Riddle Aeronautical Univ., Daytona Beach,FL, Human Factors Certification of Advanced Aviation Technologies 1994 p 309-319 (For primary document see N95-34764 12-54)

Avail: CASI HC A03/MF A04

This paper presents some facets of the French experience with human factors in the process of certification of advanced automated cockpits. Three types of difficulties are described: first, the difficulties concerning the hotly debated concept of human error and its non-linear relationship to risk of accident; a typology of errors to be taken into account in the certification process is put forward to respond to this issue. Next, the difficulties connected to the basically gradual and evolving nature of pilot expertise on a given type of aircraft, which contrasts with the immediate and definitive style of certifying systems. The last difficulties to be considered are those related to the goals of certification itself on these new aircraft and the status of findings from human factor analyses (in particular, what should be done with disappointing results, how much can the changes induced by human factors investigation economically affect aircraft design, how many errors do we need to accumulate before we revise the system, what should be remedied when human factor problems are discovered at the certification stage: the machine? pilot training? the rules? or everything?). The growth of advanced-automated glass cockpits has forced the international aeronautical community to pay more attention to human factors during the design phase, the certification phase and pilot training. The recent creation of a human factor desk at the DGAC-SFACT (Official French services) is a direct consequence of this. The paper is divided into three parts. Part one debates human error and its relationship with system design and accident risk. Part two describes difficulties connected to the basically gradual and evolving nature of pilot expertise on a given type of aircraft, which contrasts with the immediate and definitive style of certifying systems. Part three focuses on concrete outcomes of human factors for certification purposes. Author

N95-34787*# Liege Univ. (Belgium).

BEWARE OF AGENTS WHEN FLYING AIRCRAFT: BASIC PRINCIPLES BEHIND A GENERIC METHODOLOGY FOR THE EVALUATION AND CERTIFICATION OF ADVANCED AVIATION SYSTEMS

Denis Javaux, Michel Masson, and Veronique DeKeyser *In* Embry-Riddle Aeronautical Univ., Daytona Beach,FL, Human Factors Certification of Advanced Aviation Technologies 1994 p 321-345 (For primary document see N95-34764 12-54)

Avail: CASI HC A03/MF A04

There is currently a growing interest in the aeronautical community to assess the effects of the increasing levels of automation on pilots' performance and overall safety. The first effect of automation is the change in the nature of the pilot's role on the flight deck. Pilots have become supervisors who monitor aircraft systems in usual situations and intervene only when unanticipated events occur. Instead of 'hand flying' the airplane, pilots contribute to the control of aircraft by acting as mediators, instructions given to the automation. By eliminating the need for manually controlling normal situations, such a role division has reduced the opportunities for the pilot to acquire experience and skills necessary to safely cope with abnormal events. Difficulties in assessing the state and behavior of automation arise mainly from four factors: (1) the complexity of current systems and consequence mode-related problems; (2) the intrinsic autonomy of automation which is able to fire mode transitions without explicit commands from the pilots; (3) the bad quality of feed-back from the control systems displays and interfaces to the pilots; and (4) the fact that the automation currently has no explicit representation of the current pilots' intentions and strategy. Assuming certification has among its major goals to guarantee the passengers' and pilots' safety and the airplane integrity under normal and abnormal operational conditions, the authors suggest it would be particularly fruitful to come up with a conceptual reference system providing the certification authorities both with a theoretical framework and a list of principles usable for assessing the quality of the equipment and designs under examination. This is precisely the scope of this paper. However, the authors recognize that the conceptual presented is still under development and would thus be best considered as a source of reflection for the design, evaluation and certification processes of advanced aviation technologies. Derived from text

N95-32428*# Tulane Univ., New Orleans, LA. Dept. of Mechanical Engineering.

BICYCLE ERGOMETER INSTRUMENTATION TO DETERMINE MUSCLE AND BONE FORCES DURING EXERCISE Final Report

Fernando Figueroa *In* NASA. Johnson Space Center, National Aeronautics and Space Administration (NASA)/American Society for Engineering Education (ASEE) Summer Faculty Fellowship Program, 1994, Volume 1

Jul. 1995 14 p (For primary document see N95-32418 12-99)
(Grant NGT-44-055-803)
Avail: CASI HC A03/MF A03

N95-32489# Naval Air Warfare Center, China Lake, CA. Targeting Systems Integration Section.
MULTISPECTRAL IMAGE CORRELATION FOR AIR-TO-GROUND TARGETING
W. R. Ditzler, M. J. Boyd, T. J. Corcoran, M. S. Franklin, J. E. McKnight, H. C. Ottenhoff, R. W. Tyhurst, and M. M. Wirtz *In* AGARD, Low-Level and Nap-of-the-Earth (NOE) Night Operations Jan. 1995 12 p (For primary document see N95-32486 12-03)
Copyright Avail: CASI HC A03/MF A03

N95-32504# Fabrica Italiana Apparecchiature Radioelettriche S.p.A., Milan (Italy).
SIRPH: STEERABLE INFRARED PICTURE ON HELMET MOUNTED DISPLAY
Giorgio Balzarotti, Lorenzo Fiori, and Beatrice Midollini *In* AGARD, Low-Level and Nap-of-the-Earth (NOE) Night Operations Jan. 1995 10 p (For primary document see N95-32486 12-03)
Copyright Avail: CASI HC A02/MF A03

N95-33139# Moscow Inst. of Aviation Technology (USSR). Simulators and Pilot-Vehicle Lab.
DEVELOPMENT AND APPLICATION OF THE METHODS FOR PILOT-AIRCRAFT SYSTEM RESEARCH TO THE MANUAL CONTROL TASKS OF MODERN VEHICLES
A. V. Efremov and A. V. Ogloblin *In* AGARD, Dual Usage in Military and Commercial Technology in Guidance and Control Mar. 1995 12 p (For primary document see N95-33126 12-31)
Copyright Avail: CASI HC A03/MF A02

55 SPACE BIOLOGY

Includes exobiology; planetary biology; and extraterrestrial life.

No abstracts in this category.

59 MATHEMATICAL AND COMPUTER SCIENCES (GENERAL)

No abstracts in this category.

60 COMPUTER OPERATIONS AND HARDWARE

Includes hardware for computer graphics, firmware, and data processing.

For components see *33 Electronics and Electrical Engineering.*

N95-32398# Ames Lab., IA.
HINT: A NEW WAY TO MEASURE COMPUTER SPEED
John L. Gustafson and Quinn O. Snell 1995 21 p
(Contract W-7405-eng-82)
(DE95-010245; IS-5109) Avail: CASI HC A03/MF A01

The computing community has long faced the problem of scientifically comparing different computers and different algorithms. When speeds or architectures or methods are very different, it is difficult or misleading to compare by taking the ratio of execution times, keeping all other things fixed. This paper presents a practical and fair approach that provides mathematically sound comparison of computational performance even when the algorithm, the computer, and the precision are changed. The HINT method removes the need for pseudo-work measures such as 'Mflop/s' or 'MIPS'. It is designed to be particularly revealing of memory bandwidth and memory hierarchies. The scalability of HINT allows it to compare computing as slow as hand calculation to computing as fast as the largest supercomputer systems. It ports to every sequential and parallel programming environment with very little effort, permitting fair but low-cost comparison of any architecture capable of digital arithmetic. DOE

N95-32757# Tokyo Univ., Tanashi (Japan). Inst. for Nuclear Study.
VHS-TAPE SYSTEM FOR GENERAL PURPOSE COMPUTER. FOR NEXT GENERATION MASS STORAGE SYSTEM
K. Ukai, M. Takano, M. Shinohara, K. Niki, Y. Suzuki (Tokyo Univ., Japan.), T. Hamada (TEAC Co. Ltd., Saitama, Japan.), and M. Ogawa (Fujitsu Ltd., Tokyo, Japan.) Jul. 1994 24 p In JAPANESE
(DE95-737268; INS-T-529) Avail: CASI HC A03/MF A01

Mass storage is one of the key technology of next generation computer system. A huge amount of data is produced on a field of particle and nuclear physics. These data are raw data of experiments, analysis data, Monte Carlo simulations data, etc. We search a storage device for these data at the point of view of capacity, price, size, transfer speed, etc. We have selected a VHS-tape (12.7 mm-tape, helical scan) from many storage devices. Characteristics of the VHS-tape are as follows; capacity of 14.5 GB, size of 460 cm(sup 3), price of 1,000 yen (S-VHS tape for video use), and 1.996 MB/sec transfer speed at a sustained mode. Last year, we succeeded to operate the VHS-tape system on a workstation as a I/O device with read/write speed of 1.5 MB/sec. We have tested a VHS-tape system by connecting to the channel of the general purpose computer (Fujitsu M-780/10S) in our institute. We obtained a read and write speeds of 1.07 MB/sec and 1.72 MB/sec by FORTRAN test programs, respectively. Read speeds of an open reel tape and a 3480 type cassete tape by the same test programs are 1.13 MB/sec and 2.54 MB/sec, respectively. Speeds of write operation are 1.09 MB/sec and 2.54 MB/sec for the open reel and 3480 cassete tape, respectively. A start motion of the VHS-tape for read/write operations needs about 60 seconds. DOE

N95-32955# Los Alamos National Lab., NM.
OPEN ARCHITECTURE CNC SYSTEM
Jacob Tal (Galil Motion Control, Inc., Sunnyvale, CA.), Aaron A. Lopez, and John M. Edwards 1995 12 p Presented at the 24th Annual Symposium on Incremental Motion Control Systems and Devices, San Jose, CA, 7 Jun. 1995
(Contract W-7405-eng-36)
(DE95-009485; LA-UR-95-1130; CONF-9506169-1) Avail: CASI HC A03/MF A01

In this paper, an alternative solution to the traditional CNC machine tool controller has been introduced. Software and hardware modules have been described and their incorporation in a CNC control system has been outlined. This type of CNC machine tool controller demonstrates that technology is accessible and can be readily implemented into an open architecture machine tool controller. Benefit to the user is greater controller flexibility, while being economically achievable. PC based, motion as well as non-motion features will provide flexibility through a Windows environment. Up-grading this type of controller system through software revisions will keep the machine tool in a competitive state with minimal effort. Software and hardware modules are mass produced permitting competitive procurement and incorporation. Open architecture CNC systems provide diagnostics thus enhancing maintainability, and machine tool up-time. A major concern of traditional CNC systems has been operator training time. Training time can be greatly minimized by making use of Windows environment features. DOE

N95-34301# California Univ., Berkeley, CA.
CONSTRUCTION OF A CONNECTIONIST NETWORK SUPERCOMPUTER Technical Progress Report, 1 Feb. - 30 Apr. 1995
30 Apr. 1995 4 p
(Contract N00014-92-J-1617)
(AD-A294198) Avail: CASI HC A01/MF A01

This report presents a summary of the technical status for the period 2/1/95-4/30/95. In this period we passed a major milestone in the development of connectionist network computers-we completed the design and fabrication of the TO vector microprocessor. We also continued to

make significant progress in system and application software for these systems, in porting neural network algorithms, and in the application of analog auditory preprocessors to speech recognition. DTIC

N95-34453# Illinois Univ. at Urbana-Champaign, Savoy, IL. Coordinated Science Lab.
RECOVERABLE DISTRIBUTED SHARED MEMORY UNDER SEQUENTIAL AND RELAXED CONSISTENCY
Bob Janssens and W. Kent Fuchs May 1995 31 p
(Contract N00014-90-J-1270)
(AD-A293966; UILU-ENG-95-2211; CRHC-95-10) Avail: CASI HC A03/MF A01

Distributed shared memory (DSM) implemented on a cluster of workstations is an increasingly attractive platform for executing parallel scientific applications. Checkpointing and rollback techniques can be used in such a system to allow the computation to progress in spite of the temporary failure of one or more processing nodes. The complexity and overhead inherent in traditional message-passing checkpointing techniques can be reduced by taking advantages of specific properties of DSM. In this paper we show that, if designed correctly, a DSM system only needs to consider a subset of message-passing dependencies for correct rollback. A passive server model of DSM computation is described that allows a loosening of dependency restrictions by considering the events involved in interactions between nodes as atomic. An ownership timestamp scheme is used to eliminate many of the dependencies related to keeping directories consistent. The schemes can be implemented in DSM hardware by simply redesigning the directory at the network interface. Finally, we show that by relaxing the memory consistency model and using lazy release consistency, it is possible to further relax dependency restrictions. DTIC

N95-34462# Texas A&M Univ., College Station, TX. Dept. of Electrical Engineering.
HARDWARE IMPLEMENTATION OF A DESKTOP SUPERCOMPUTER FOR HIGH PERFORMANCE IMAGE PROCESSING Technical Report, 10 Feb. - 1 May 1995
Jose PinedadeGyvez 17 May 1995 23 p
(Contract N00014-94-1-0516)
(AD-A294272; Rept-93-549/5) Avail: CASI HC A03/MF A01

This report presents a CNN monolithic implementation suitable for Very Large Scale Integration. Novel circuit techniques have been investigated, designed and tested for various basic building blocks such as: (1) a transconductance multiplier; (2) a linear resistor based on a multiplier circuit; (3) an OTA based integrator; (4) a hard limiter circuit; and (5) YO circuitry based on Switched Capacitor Techniques. The report addresses both circuit design and layout plan issues. It highlights also the trade-offs among different design parameters including power supplies, dynamic range, area and tolerance. The CNN cell consumes approximately 2.5 mW of power and occupies around 0.25 mm(exp 2) of area. The IC has been sent for fabrication through MOSIS. Preliminary experimental results of some basic building blocks are encouraging. DTIC

N95-34484# Westinghouse Hanford Co., Richland, WA.
CERTIFICATION OF MCNP VERSION 4A FOR WHC COMPUTER PLATFORMS, REVISION 7
L. L. Carter 3 May 1995 72 p
(Contract DE-AC06-87RL-10930)
(DE95-011546; WHC-SD-MP-SWD-30001-Rev-7) Avail: CASI HC A04/MF A01

MCNP is a general-purpose Monte Carlo code that can be used for neutron, photon, or coupled neutron/photon transport, including the capability to calculate eigenvalues for critical systems. The code treats an arbitrary three-dimensional configuration of materials in geometric cells bounded by first- and second-degree surfaces, and some special fourth-degree surfaces (elliptical tori). DOE

N95-34503# Rome Lab., Griffiss AFB, NY.
OPTICAL INTERCONNECTS FOR 3D COMPUTER ARCHITECTURES
Franz Haas, David A. Honey, and Harold F. Bare Dec. 1994 33 p
(AD-A294118; RL-TR-94-227) Avail: CASI HC A03/MF A01

This report details a novel approach for integrating optical interconnects into Air Force computer systems to increase system performance. Computer systems from the average personal desktop models to specialized supercomputers are limited in performance by the electronic wiring used to transport information between processing circuitry. Using light instead of electronics to transport information inside a computer can greatly increase overall system operating speed. A modular optical interconnect architecture was designed and demonstrated which is applicable for use in a variety of computer architectures (multichip module or wafer scale integration). The interconnect scheme uses a diffractive optic to image an array of light emitting diodes (LED's) on one board to a corresponding array of photodetectors on a second board. This optical solution can replace 16 electronic wires running between the two boards. DTIC

N95-34745 Holoplex, Inc., Pasadena, CA.
READ/WRITE MODULE FOR HIGH CAPACITY MEMORY DISK Final Report
Fai Mok 2 Apr. 1995 15 p Limited Reproducibility: More than 20% of this document may be affected by poor print
(Contract F49620-94-C-0089)
(AD-A294946; AFOSR-95-0272TR) Avail: Issuing Activity (Defense Technical Information Center (DTIC))

This SBIR program addresses the tracking and alignment sensitivity issues of a practical holographic storage system. To demonstrate the feasibility of this program, we plan to accomplish the following: (1) Characterize the storage medium; (2) Construct a preliminary tracking system; (3) Study the alignment sensitivity of Fourier transform holograms; (4) Design the final tracking system. After carefully studying potential markets for the holographic storage system, we have decided to use laser diodes as the light source and photopolymer as the recording medium. The decision was based on cost, size, reliability, availability, and convenience. We have decided to modify the tracking mechanism of existing optical disk systems and use it for the 3-D holographic disk system. We have procured a CD-ROM and interfaced it to a PC. We plan to create a preliminary recording medium by lamenating a layer of photopolymer onto a CD-ROM disk. We have partially dissected the CD-ROM. We will obtain tracking signal from the CD-ROM and use it to drive the readout mechanism. (The recording will be performed off-line using another setup.) The readout mechanism is consisted of a laser diode, optics and an output detector. The tracking signal will be used to rotate the holographic disk to a specified location, to synchronize the firing of the laser diode, and to coordinate the capture of the reconstruction by the detector array. We have studied the operation principles, the physical specifications, the logical specifications, and the addressing scheme of CD-ROM. We have learned the interface protocol and acquired the control subroutines library. We are developing computer software to monitor the status and to control the movements of the head of the CD-ROM. DTIC

61 COMPUTER PROGRAMMING AND SOFTWARE

Includes computer programs, routines, alogorithms, and specific applications, e.g., CAD/CAM.

N95-32378# Sandia National Labs., Albuquerque, NM.
APPLICATION OF FUZZY TECHNOLOGY TO RISK-BASED DESIGN AND DECISION PROBLEMS
M. E. Senglaub and A. T. Bahill (Arizona Univ., Tucson, AZ.) 1995 9 p Presented at the Joint ASME/JSME Pressure Vessels and Piping Conference, Honolulu, HI, 23-27 Jul. 1995
(Contract DE-AC04-94AL-85000)
(DE95-006815; SAND-94-2294C; CONF-950740-11) Avail: CASI HC A02/MF A01

A study was undertaken to assess the impact of employing fuzzy technologies in areas of complex weapon system design. The technology was examined for use in a life-cycle cost exercise with the objective of providing a foundation from which to make service life assessments and recommendations on future weapon systems. The issues associated with this problem can be highly subjective and often exhibit a high degree of functional as well as variable uncertainty, ambiguity and noise. The study demonstrated that there is a potential role for the technology, but only in

a hybridized environment not as a stand-alone solution methodology. DOE

N95-32390# Lawrence Livermore National Lab., Livermore, CA.
VISUALIZATION METHODS FOR HIGH-RESOLUTION, TRANSIENT, 3-D, FINITE ELEMENT SITUATIONS
M. A. Christon 10 Jan. 1995 19 p Presented at the International Workshop on Visualization, Paderborn, Germany, 18-20 Jan. 1994
(Contract W-7405-eng-48)
(DE95-009479; UCRL-JC-119879; CONF-9401114-1) Avail: CASI HC A03/MF A01

Scientific visualization is the process whereby numerical data is transformed into a visual form to augment the process of discovery and understanding. Visualizing the data generated by large-scale, transient, three-dimensional finite element simulations poses many challenges due to geometric complexity, the presence of multiple materials and multiple element types, and the inherent unstructured nature of the meshes. In this paper, the direct use of finite element data structures, nodal assembly procedures, and element interpolants for volumetric adaptive surface extraction, surface rendering, vector grids and particle tracing is discussed. A brief description of a 'direct-to-disk' animation system is presented, and case studies which demonstrate the use of isosurfaces, vector plots, cutting planes, reference surfaces and particle tracing are then discussed in the context of several case studies for transient incompressible viscous flow, and acoustic fluid-structure interaction simulations. An overview of the implications of massively parallel computers on visualization is presented to highlight the issues in parallel visualization methodology, algorithms. data locality and the ultimate requirements for temporary and archival data storage and network bandwidth. DOE

N95-32470# Nevada Univ., Las Vegas, NV. Heat Transfer Lab.
A PRELIMINARY EVALUATION OF HISTOGRAM-BASED BINARIZATION ALGORITHMS
Junichi Kanai and Kevin Grover 1995 9 p Presented at the SPIE 1995: SPIE Conference on Optics, Electro-optics, and Laser Application in Science, Engineering and Medicine, San Jose, CA, 5-10 Feb. 1995
(Contract DE-FC08-90NV-10872)
(DE95-009886; CONF-950226-35) Avail: CASI HC A02/MF A01

To date, most Optical Character Recognition (OCR) systems process binary document images, and the quality of the input image strongly affects their performance. Since a binarization process is inherently lossy, different algorithms typically produce different binary images from the same gray scale image. The objective of this research is to study effects of global binarization algorithms on the performance of OCR systems. Several binarization methods were examined: the best fixed threshold value for the data set, the ideal histogram method, and Otsu's algorithm. Four contemporary OCR systems and 50 hard copy pages containing 91,649 characters were used in the experiments. These pages were digitized at 300 dpi and 8 bits/pixel, and 36 different threshold values (ranging from 59 to 199 in increments of 4) were used. The resulting 1,800 binary images were processed by all four OCR systems. All systems made approximately 40% more errors from images generated by Otsu's method than those of the ideal histogram method. Two of the systems made approximately the same number of errors from images generated by the best fixed threshold value and Otsu's method. DOE

N95-32543# Sandia National Labs., Albuquerque, NM.
USERS' MANUAL FOR LEHGC: A LAGRANGIAN-EULERIAN FINITE-ELEMENT MODEL OF HYDROGEOCHEMICAL TRANSPORT THROUGH SATURATED-UNSATURATED MEDIA. VERSION 1.0
G. T. Yeh Mar. 1995 170 p
(Contract DE-AC04-94AL-85000)
(DE95-010513; SAND-93-7081) Avail: CASI HC A08/MF A02

The computer program LEHGC is a Hybrid Lagrangian-Eulerian Finite-Element Model of HydroGeoChemical (LEHGC) Transport Through Saturated-Unsaturated Media. LEHGC iteratively solves two-dimensional transport and geochemical equilibrium equations and is a descendant of HYDROGEOCHEM, a strictly Eulerian finite-element reactive transport code. The hybrid Lagrangian-Eulerian scheme improves on the Eulerian scheme by allowing larger time steps to be used in the advection-dominant transport calculations, causing less numerical dispersion and alleviating the problem of negative concentration, and it also is more computationally efficient. LEHGC is designed for generic application to reactive transport problems associated with such systems as contaminant transport in subsurface media. Input to the program includes the geometry of the system, the spatial distribution of finite elements and nodes, the properties of the media, the potential chemical reactions, and the initial and boundary conditions. Output includes the spatial distribution of chemical element concentrations as a function of time and space and the chemical speciation at user-specified nodes. DOE

N95-32572# Los Alamos National Lab., NM.
INTERVALS IN EVOLUTIONARY ALGORITHMS FOR GLOBAL OPTIMIZATION
Rajendra B. Patil 1995 17 p Presented at the APIC 1995 Conference, El Paso, TX, Mar. 1995 Submitted for publication in the International Journal of Reliable Computing
(Contract W-7405-eng-36)
(DE95-010866; LA-UR-95-1196; CONF-9503135-1) Avail: CASI HC A03/MF A01

Optimization is of central concern to a number of disciplines. Interval Arithmetic methods for global optimization provide us with (guaranteed) verified results. These methods are mainly restricted to the classes of objective functions that are twice differentiable and use a simple strategy of eliminating a splitting larger regions of search space in the global optimization process. An efficient approach that combines the efficient strategy from Interval Global Optimization Methods and robustness of the Evolutionary Algorithms is proposed. In the proposed approach, search begins with randomly created interval vectors with interval widths equal to the whole domain. Before the beginning of the evolutionary process, fitness of these interval parameter vectors is defined by evaluating the objective function at the center of the initial interval vectors. In the subsequent evolutionary process the local optimization process returns an estimate of the bounds of the objective function over the interval vectors. Though these bounds may not be correct at the beginning due to large interval widths and complicated function properties, the process of reducing interval widths over time and a selection approach similar to simulated annealing helps in estimating reasonably correct bounds as the population evolves. The interval parameter vectors at these estimated bounds (local optima) are then subjected to crossover and mutation operators. This evolutionary process continues for predetermined number of generations in the search of the global optimum. DOE

N95-32669# Los Alamos National Lab., NM.
MESSAGE BASED EVENT SPECIFICATION FOR DEBUGGING NONDETERMINISTIC PARALLEL PROGRAMS
S. K. Damohdaran-Kamal and J. M. Francioni 1995 16 p Presented at the 4th IEEE International Symposium on High Performance Distributed Computing, Pentagon City, VA, 1-4 Aug. 1995
(Contract W-7405-eng-36)
(DE95-006169; LA-UR-95-433; CONF-950863-1) Avail: CASI HC A03/MF A01

Portability and reliability of parallel programs can be severely impaired by their nondeterministic behavior. Therefore, an effective means to precisely and accurately specify unacceptable nondeterministic behavior is necessary for testing and debugging parallel programs. In this paper we describe a class of expressions, called Message Expressions that can be used to specify nondeterministic behavior of message passing parallel programs. Specification of program behavior with Message Expressions is easier than pattern based specification techniques in that the former does not require knowledge of run-time event order, whereas that later depends on the user's knowledge of the run-time event order for correct specification. We also discuss our adaptation of Message Expressions for use in a dynamic distributed testing and debugging tool, called mdb, for programs written for PVM (Parallel Virtual Machine). DOE

N95-32715# Los Alamos National Lab., NM.
THE RDB: A PARALLEL, SPATIAL DATABASE FOR THE IES/BTI SYSTEM
K. Carlson and L. Winter 1995 14 p Presented at the Large Spatial Databases (SSD 1995), Portland, ME, 6-9 Aug. 1995
(Contract W-7405-eng-36)
(DE95-009425; LA-UR-95-910; CONF-950889-1) Avail: CASI HC A03/MF A01

The manipulation and representation of spatial data on computers is an important issue in many computer applications. Spatial data, which consists of points, lines, and regions in 2-dimensions, can be difficult to manage efficiently because it is often quite voluminous. For instance, the number of picture elements in even a small digital image is on the order of a million, while the number of locations stored in a terrain database can easily include billions of points. Furthermore, the kinds of operations performed on spatial data -- set operations, insertion, deletion, searches such as 'near' -- are compute intensive, and hence slow unless the data is structured to reflect its underlying topology. Hence a conventional database which is organized on search keys is often not adequate for handling spatial data. The Image Exploitation System, which is an automated image analysis system, has a great need for efficient storage and manipulation of spatial data. The Image Exploitation System is part of the Advanced Research Project Agency's Balanced Technology Initiative and is abbreviated IES/BTI. IES/BTI must process tens to hundreds of megabytes of imagery in a few minutes, and is composed of many independent components which need to access and share spatial data. The system needed an efficient parallel spatial database, hence the motivation for our work on the Region Database, or RDB. The RDB is our attempt to meet the needs of the IES/BTI Cycle 2 system. The RDB provides for storage and retrieval of both raster and vector based spatial data as well as attribute-based retrievals. It also provides facilities for conversion between the two representations of spatial data (raster and vector) and for efficient, parallel boolean operations on vector data. In this paper we discuss the research and development performed to design and implement the RDB. DOE

N95-32716# Los Alamos National Lab., NM.
ON THE MINIMUM WEIGHT STEINER TRIANGULAR TILING PROBLEM
S. Doddi and B. Zhu 1995 7 p Presented at the 7th Canadian Conference on Computation Geometry, Quebec City, Canada, 10-14 Aug. 1995
(Contract W-7405-eng-36)
(DE95-009482; LA-UR-95-1155; CONF-950891-1) Avail: CASI HC A02/MF A01

In this paper, we introduce the Minimum Weight Steiner Triangular Tiling problem, which is a generalization of the Minimum Weight Steiner Triangulation. Contrary to the conjecture of Eppstein that the Minimum Weight Steiner Triangulation of a convex polygon has the property that the Steiner points all lie on the boundary of the polygon, we show that the Steiner points of a Minimum Weight Steiner Triangular Tiling could lie in the interior of a convex polygon. DOE

N95-32765*# Colorado Univ., Boulder, CO. Coll. of Engineering.
A THREE-DIMENSIONAL NONLINEAR TIMOSHENKO BEAM BASED ON THE CORE-CONGRUENTIAL FORMULATION
Luis A. Crivelli and Carlos A. Felippa May 1992 42 p Submitted for publication in the International Journal Numerical Methods in Engineering
(Contract NAG1-756; F49620-87-C-0074; NSF 87-17773)
(NASA-CR-199042; NAS 1.26:199042; CU-CSSC-92-05) Avail: CASI HC A03/MF A01

A three-dimensional, geometrically nonlinear two-node Timoshenkoo beam element based on the total Larangrian description is derived. The element behavior is assumed to be linear elastic, but no restrictions are placed on magnitude of finite rotations. The resulting element has twelve degrees of freedom: six translational components and six rotational-vector components. The formulation uses the Green-Lagrange strains and second Piola-Kirchhoff stresses as energy-conjugate variables and accounts for the bending-stretching and bending-torsional coupling effects without special provisions. The core-congruential formulation (CCF) is used to derived the discrete equations in a staged manner. Core equations involving the internal force vector and tangent stiffness matrix are developed at the particle level. A sequence of matrix transformations carries these equations to beam cross-sections and finally to the element nodal degrees of freedom. The choice of finite rotation measure is made in the next-to-last transformation stage, and the choice of over-the-element interpolation in the last one. The tangent stiffness matrix is found to retain symmetry if the rotational vector is chosen to measure finite rotations. An extensive set of numerical examples is presented to test and validate the present element. Author

N95-32766*# Colorado Univ., Boulder, CO. Center for Space Structures and Controls.
A SURVEY OF PARAMETRIZED VARIATIONAL PRINCIPLES AND APPLICATIONS TO COMPUTATIONAL MECHANICS
Carlos A. Felippa May 1993 47 p Presented at the First International Mechanics Seminar, Grenoble, France, May 1992 Submitted for publication in Computer Methods in Applied Mechanics and Engineering
(Grant NAG1-756)
(NASA-CR-199041; NAS 1.26:199041; CU-CSSC-92-11) Avail: CASI HC A03/MF A01

This survey paper describes recent developments in the area of parametrized variational principles (PVP's) and selected applications to finite-element computational mechanics. A PVP is a variational principle containing free parameters that have no effect on the Euler-Lagrange equations. The theory of single-field PVP's based on gauge functions (also known as null Lagrangians) is a subset of the inverse problem of variational calculus that has limited value. On the other hand, multifield PVP's are more interesting from theoretical and practical standpoints. Following a tutorial introduction, the paper describes the recent construction of multifield PVP's in several areas of elasticity and electromagnetics. It then discusses three applications to finite-element computational mechanics: the derivation of high-performance finite elements, the development of element-level error indicators, and the constructions of finite element templates. The paper concludes with an overview of open research areas. Author

N95-32834*# Institute for Computer Applications in Science and Engineering, Hampton, VA.
TRACKING A TURBULENT SPOT IN AN IMMERSIVE ENVIRONMENT Final Report
David C. Banks and Michael Kelley (Information Science Inst., Arlington, VA.) Jun. 1995 13 p Presented at the 1995 Symposium on Interactive 3D computer graphics
(Contract NAS1-19480; RTOP 505-90-52-01)
(NASA-CR-198179; NAS 1.26:198179; ICASE-95-50) Avail: CASI HC A03/MF A01

We describe an interactive, immersive 3D system called Tracktur, which allows a viewer to track the development of a turbulent flow. Tracktur displays time-varying vortex structures extracted from a numerical flow simulation. The user navigates the space and probes the data within a windy 3D landscape. In order to sustain a constant frame rate, we enforce a fixed polygon budget on the geometry. We supplement the interactive system with interactive, hypertext documentation available on the World Wide Web. In actual use by a fluid dynamicist, the system has yielded new insights into the transition to turbulence in a laminar flow. Author

N95-32937 Pennsylvania Univ., Philadelphia, PA.
OFF-LINE PROGRAMMING USING COMMERICAL CAD SYSTEMS, AND DESIGN CRITERIA FOR MANIPULATORS WITH INHERENT ACCURACY Ph.D. Thesis
Karim Antoun Abdel-Malek 1993 247 p
Avail: Univ. Microfilms Order No. DA9413783

The design of high accuracy manipulators has seen many advances in recent years. Many researchers have discussed correction of the errors in accuracy by use of control optimization and calibration techniques. We discuss the criteria for designing manipulators with inherentally high accuracy. The development, design, and building of a six degree of freedom manipulator is presented. Recommendations concerning cross-sectional shapes, joints, detailed design, prestressing effects, material, dexterous solid angle, as well as other criteria are discussed. Because current teaching methods are inadequate to fully control a high accuracy manipulator, the concept of a graphical interface has been introduced. The interface combines teaching and programming methods. The complexity of a user interface has become extremely important as manipulators and other programmable automation are applied to more industrial applications. Three dimensional visualization is definitely an important aspect of the problem facing a robotics programmer. Often coordinates passed to the manipulator are not easily visualized in space. The introduction of a graphical environment, the 'TR-environment,' reduces the task of visualizing points, orientations, and trajectories. The environment developed here provides the user with an off-line programming method where logic, repetitive tasks, and sensory control can be performed. The environment consists of the integration of commercial CAD packages with computer languages. The program consists

of the so called 'NODES' which define the six generalized coordinates and the state of the end-effector at a point in space. Trajectories in space can be planned by connecting nodes via entities. A special language is associated with nodes where program branching, sensory control, and digital communication can occur. Dissert. Abstr.

N95-33154# Los Alamos National Lab., NM. Computer Research Group.

AUTOMATIC SCRIPT IDENTIFICATION FROM IMAGES USING CLUSTER-BASED TEMPLATES

Judith Hochberg, Lila Kerns, Patrick Kelly, and Timothy Thomas 1995 20 p Presented at the 3rd International Conference on Document, Analysis, and Recognition, Montreal, Canada, 14-16 Aug. 1995

(Contract W-7405-eng-36)

(DE95-006339; LA-UR-95-21; CONF-950869-1) Avail: CASI HC A03/MF A01

We have developed a technique for automatically identifying the script used to generate a document that is stored electronically in bit image form. Our approach differs from previous work in that the distinctions among scripts are discovered by an automatic learning procedure, without any hands-on analysis. We first develop a set of representative symbols (templates) for each script in our database (Cyrillic, Roman, etc.). We do this by identifying all textual symbols in a set of training documents, scaling each symbol to a fixed size, clustering similar symbols, pruning minor clusters, and finding each cluster's centroid. To identify a new document's script, we identify and scale a subset of symbols from the document and compare them to the templates for each script. We choose the script whose templates provide the best match. Our current system distinguishes among the Armenian, Burmese, Chinese, Cyrillic, Ethiopic, Greek, Hebrew, Japanese, Korean, Roman, and Thai scripts with over 90% accuracy. DOE

N95-33193*# National Aeronautics and Space Administration. Hugh L. Dryden Flight Research Center, Edwards, CA.

FORTRAN PROGRAM FOR ANALYZING GROUND-BASED RADAR DATA: USAGE AND DERIVATIONS, VERSION 6.2

Edward A. Haering, Jr. and Stephen A. Whitmore Washington Aug. 1995 69 p

(RTOP 505-68-50)

(NASA-TP-3430; H-1892; NAS 1.60:3430) Avail: CASI HC A04/MF A01

A postflight FORTRAN program called 'radar' reads and analyzes ground-based radar data. The output includes position, velocity, and acceleration parameters. Air data parameters are also provided if atmospheric characteristics are input. This program can read data from any radar in three formats. Geocentric Cartesian position can also be used as input, which may be from an inertial navigation or Global Positioning System. Options include spike removal, data filtering, and atmospheric refraction corrections. Atmospheric refraction can be corrected using the quick White Sands method or the gradient refraction method, which allows accurate analysis of very low elevation angle and long-range data. Refraction properties are extrapolated from surface conditions, or a measured profile may be input. Velocity is determined by differentiating position. Accelerations are determined by differentiating velocity. This paper describes the algorithms used, gives the operational details, and discusses the limitations and errors of the program. Appendices A through E contain the derivations for these algorithms. These derivations include an improvement in speed to the exact solution for geodetic altitude, an improved algorithm over earlier versions for determining scale height, a truncation algorithm for speeding up the gradient refraction method, and a refinement of the coefficients used in the White Sands method for Edwards AFB, California. Appendix G contains the nomenclature. Author

N95-33325 Rensselaer Polytechnic Inst., Troy, NY.

A PROCEDURAL FRAMEWORK FOR DESIGNING LINEAR ORIENTING DEVICES Ph.D. Thesis

Mengyik Yeong 1993 172 p

Avail: Univ. Microfilms Order No. DA9420375

Significant research has been devoted to bringing the design of parts feeding and orientation equipment into the domain of fundamental engineering principles and Computer Aided Design. However, the wealth of research has yet to present a single unifying framework for guiding the task of the designer. The problem faced in designing a feeder for a completely new part is there exists no starting point for the design, and waiting for a prototype part to be developed adds to the design lead time. Although design and analysis tools exists for feeders, a method for initial configuration does not exist. This thesis addresses the problem by proposing a procedural methodology to serve as a method for designing feeding devices. The methodology serves as a guide from the initial design specifications to the final prototype. While the methodology serves as a framework for design, many tools which are needed to synthesize the feeder within the framework of the methodology are also lacking. As integral parts of this thesis, analytical models and a numerical simulation of part-feeder interaction are developed to aid in the task of design. The analytical tools are based on fundamental principles of dynamics and kinematics and developed for three common orienting devices. Simple equations for predicting primary design parameters model the interaction between part and feeder. These models serve as initial design estimates for the task of parametric design. The numerical simulation is an extension into three dimensions of the 2-D variable constraint multibody dynamic model presented by Gilmore and Cipra (1991). This simulation serves the task of iterative design of the feeding device using a CAD representation of a part. Extending the model to three dimensions requires rederiving the fundamental dynamic equations and kinematic constraint equations. The analytical and numerical models are verified by comparing predictions of primary design parameters with experimental data. A simple design case study is used to illustrate the methodology and how initial redesign of a device can be accomplished using a computer simulation. One of the results of the simulation is the importance of friction between the part and feeding device. Dissert. Abstr.

N95-33396*# SRI International Corp., Menlo Park, CA.

FORMAL VERIFICATION OF AN AVIONICS MICROPROCESSOR Final Report

Mandayam Srivas, K. and Steven P. Miller (Rockwell International Corp., Cedar Rapids, IA.) Jul. 1995 106 p

(Contract NAS1-18969; RTOP 505-64-10-13)

(NASA-CR-4682; NAS 1.26:4682; ECU-8200-270) Avail: CASI HC A06/MF A02

Formal specification combined with mechanical verification is a promising approach for achieving the extremely high levels of assurance required of safety-critical digital systems. However, many questions remain regarding their use in practice: Can these techniques scale up to industrial systems, where are they likely to be useful, and how should industry go about incorporating them into practice? This report discusses a project undertaken to answer some of these questions, the formal verification of the AAMPS microprocessor. This project consisted of formally specifying in the PVS language a rockwell proprietary microprocessor at both the instruction-set and register-transfer levels and using the PVS theorem prover to show that the microcode correctly implemented the instruction-level specification for a representative subset of instructions. Notable aspects of this project include the use of a formal specification language by practicing hardware and software engineers, the integration of traditional inspections with formal specifications, and the use of a mechanical theorem prover to verify a portion of a commercial, pipelined microprocessor that was not explicitly designed for formal verification. Author

N95-33624 Sandia National Labs., Albuquerque, NM. Simulation Technology Research Dept.

xdamp: AN IDL(R)-BASED DATA MANIPULATION PROGRAM

William P. Ballard Apr. 1995 56 p Limited Reproducibility: More than 20% of this document may be affected by microfiche quality

(Contract DE-AC04-94AL-85000)

(DE95-011242; SAND-94-2391) Avail: CASI HC A04

The original DAMP (DAta Manipulation Program) was written by Mark Hedemann of Sandia National Laboratories and used the CA-DISSPLA(TM) (available from Computer Associates International, Inc., Garden City, NY) graphics package as its engine. It was used to plot, modify, and otherwise manipulate the one-dimensional data waveforms (data vs time) from a wide variety of accelerators. With the waning of CA-DISSPLA and the increasing popularity of UNIX(R)-based workstations, a replacement was needed. This package uses the IDL(R) software, available from Research Systems Incorporated in Boulder, Colorado, as the engine, and creates a set of widgets to manipulate the data in a manner similar to the original DAMP. IDL is currently supported on a wide variety of UNIX platforms

such as IBM(R) workstations, Hewlett Packard workstations, SUN(R) workstations, Microsoft(R) Windows(TM) computers, Macintosh(R) computers and Digital Equipment Corporation VMS(R) systems. Thus, this program should be portable across many platforms. We have verified operation, albeit with some IDL bugs, on IBM UNIX platforms, DEC Alpha systems, HP 9000/7OO series workstations, and Macintosh computers, both regular and PowerPC(TM) versions. DOE

N95-33652# Lawrence Livermore National Lab., Livermore, CA.
RIGID BODIES FOR METAL FORMING ANALYSIS WITH NIKE3D
Bradley N. Maker 25 Jan. 1995 8 p Presented at the 5th International Conference on Numerical Methods in Industrial Forming Processes (NUMIFORM), Ithaca, NY, 18-21 Jun. 1995
(Contract W-7405-eng-48)
(DE95-011740; UCRL-JC-119862; CONF-9506144-4) Avail: CASI HC A02/MF A01

Perhaps the most common approximation in engineering is that, relative to its neighbors, a system component is structurally rigid. This paper presents a development of the rigid assumption for use in nonlinear, implicit finite element codes. In this method, computational economy is gained by condensing the size of the associated linear system of equations, eliminating the processing of rigid elements, and reducing the overall nonlinearity of the problem. DOE

N95-34349# Naval Postgraduate School, Monterey, CA. Dept. of Operations Research.
BRANCH AND BOUND METHODS FOR SEARCH PROBLEMS
Alan R. Washburn Apr. 1995 35 p
(AD-A294522; NPS-OR-95-003) Avail: CASI HC A03/MF A01

Branch and bound methods for search problems are considered, including hybrid methods that employ multiple bounds. Computational results are reported. DTIC

N95-34371# Army Research Inst. of Environmental Medicine, Natick, MA.
A PROTOTYPE COMPUTER PROGRAM THAT INTEGRATES PREDICTIVE MODELS AND MEDICAL HANDBOOKS FOR ALTITUDE, COLD EXPOSURE, AND HEAT STRESS
Matthew J. Reardon May 1995 143 p
(AD-A294006) Avail: CASI HC A07/MF A02

First, a brief overview is provided of the current state of USARIEM algorithms for predicting the physiologic strain and weather related casualty rates associated with exposure to hot or cold environments. Next, a prototype software program is described that demonstrates the technical feasibility of consolidating numeric models for altitude, cold, and heat strain with operationally oriented handbooks for environmental physiology and medicine. This software program is a unified and dynamic environmental medicine and physiology computer-based tool of potential use for military medical personnel in predeployment analysis, planning, and training. The program's altitude module utilizes a simplified model of hypoxic strain. The altitude model does not yet include closed-loop feedback physiologic mechanisms or altitude illness prediction. These are areas requiring further altitude modeling efforts. The cold strain module's data structures and input-output interfaces were designed for USARIEM's lumped-parameter cold digit model. The heat strain module employs the well-established USARIEM Heat Strain Algorithm with an expanded interface that provides improved flexibility with regard to data entry and display modes. On-line medical handbooks provide narrative, tables, and reference lists. These could be enhanced with interactive tutorials for use in medical training situations. DTIC

N95-34455# Illinois Univ., Urbana, IL. Coordinated Science Lab.
REDUCING CACHE MISSES IN NUMERICAL APPLICATIONS USING DATA RELOCATION AND PREFETCHING
Yoji Yamada, Teresa L. Johnson, Grant E. Haab, John C. Gyllenhaal, Wen-mei W. Hwu, and Josep Torrellas Apr. 1995 31 p Sponsored by Mazda Motor Corp., the National Science Foundation, the Fannie and John Hertz Foundation
(AD-A293978; UILU-ENG-95-2206; CRHC-95-03) Avail: CASI HC A03/MF A01

Numerical applications frequently contain nested loops that process large arrays of data. The execution of these loop structures often produces memory reference patterns that utilize data caches poorly. Indeed, poor reuse of the data, large working set sizes, and frequent non-unit stride accesses all combine to cause many cache misses. To improve cache performance, data copying has been proposed. However, this technique has high overhead. In this paper, instead, we propose a combined hardware and software technique called data relocation and prefetching which eliminates much of the overhead of data copying through the use of special hardware. Furthermore, by relocating the data while performing software prefetch- ing, the overhead of copying the data can be reduced further. This technique performs better than prefetching alone because it reduces cache misses through relocation, and it reduces overhead by prefetching multiple elements at once. The hardware is designed to overlap relocation and prefetching with normal execution, and to highly utilize the available bus bandwidth. Simulation results show that this technique greatly reduces data cache miss rates. As a result, large applications including PERFECT and SPEC benchmarks achieve up to 2.5 times speedup. The hardware support required by this technique has been greatly refined over that presented in an earlier paper. DTIC

N95-34456# Naval Research Lab., Washington, DC.
ON THE VIRTUES OF PARAMETERIZED UNIFORM CROSSOVER
William M. Spears and Kenneth A. DeJong (George Mason Univ., Fairfax, VA.) 1995 7 p
(AD-A293985) Avail: CASI HC A02/MF A01

Traditionally, genetic algorithms have relied upon 1 and 2-point crossover operators. Many recent empirical studies, however, have shown the benefits of higher numbers of crossover points. Some of the most intriguing recent work has focused on uniform crossover, which involves on the average L/2 crossover points for strings of length L. Theoretical results suggest that, from the view of hyperplane sampling disruption, uniform crossover has few redeeming features. However, a growing body of experimental evidence suggests otherwise. In this paper, we attempt to reconcile these opposing views of uniform crossover and present a framework for understanding its virtues. DTIC

N95-34580# Naval Postgraduate School, Monterey, CA.
IMAGE COMPRESSION SCHEME FOR NETWORK TRANSMISSION M.S. Thesis
Lim Seng Mar. 1995 66 p
(AD-A294959) Avail: CASI HC A04/MF A01

In this thesis a scheme is proposed for still image compression for realtime transmission over a packet switched network. A layered image compression scheme based on the quad tree decomposition technique (QTD) is developed. The image is decomposed into three layers, where layers are added to a base image to incrementally improve the quality of the reconstructed image. The performance of the QTD is enhanced by adding a DCT algorithm with adaptive bit allocation and a region of interest methodology. The quad tree is then extended to a nona tree whereby pixel blocks of size 3 x 3 are processed instead of 2 x 2. Results are presented to provide a visual subjective perception of the proposed scheme. Depending on the number of layers transmitted, the compression gains range from 60:1 to 18:1. It is shown that the proposed scheme exhibits graceful degradation of the reconstructed image and some error tolerant capabilities. DTIC

N95-34582# Kestrel Inst., Palo Alto, CA.
AUTOMATED SUPPORT FOR SOFTWARE ENGINEERING Final Report
Douglas R. Smith 13 Mar. 1995 42 p
(Contract F49620-91-C-0073)
(AD-A294965; AFOSR-95-0269TR) Avail: CASI HC A03/MF A01

The key idea of this project is that parameterized theories and various operations on them provide a uniform conceptual foundation for software engineering. The broad objectives of this project are (1) to show how well-understood concepts of mathematical logic apply to software engineering; (2) to identify and automate the basic operations on theories that underlie and support formal approaches to software system development and evolution; and (3) to demonstrate a higher and more broadly applicable level of software automation than has previously been achieved. DTIC

N95-34598# Rice Univ., Houston, TX.
SOME ISSUES IN NONLINEAR PROGRAMMING ALGORITHMS FOR PROBLEMS WITH SIMULATION CONSTRAINTS Final Technical Report, 1 Mar. 1993 - 28 Feb. 1995

John E. Dennis, Jr., Richard A. Tapia, and Virginia J. Torczon 13 Apr. 1995 24 p
(Contract F49620-93-1-0212)
(AD-A294932; AFOSR-95-0386TR) Avail: CASI HC A03/MF A01

Many large-scale optimization problems can be formulated as nonlinear programming problems where the constraints represent systems governed by partial differential equations. This deceptively simple observation allows for a wealth of possibilities in the development of optimization methods applicable to such problems. This is a vast area of research on problems of importance to the nations environment, economy, and defense. The work reported here had as its goal the development and evaluation of a number of different optimization strategies for problems with simulation constraints. Specifically, the work focused on applying direct search methods to and developing interior-point algorithms for problems of this form. DTIC

N95-34604# Texas Univ., El Paso, TX.
TOWARDS A FORMALISM FOR PROGRAM GENERATION 1995 Final Report, 1 Feb. 1993 - 28 Feb. 1995
Daniel E. Cooke 28 Feb. 1995 32 p
(Contract F49620-93-1-0152)
(AD-A294941; AFOSR-95-0416TR) Avail: CASI HC A03/MF A01

BagL is a formal, general purpose language which provides for database, event-driven, and scientific computing in a uniform level of representation. In BagL a problem solver is not required to provide the algorithmic detail in a problem solution. Instead the problem solver describes the solution directly by specifying, via a meta-structure, the data structures which will hold results useful in solving the problem. A meta-structure is a very general abstraction configurable into any imaginable data structure, where a data structure is viewed as a database; a CRT screen or report layout; or a classical data structure such as a stack, a queue, ect. BagL provides a platform to specify the contents and the form of a data structure. BagL is an improvement over current programming paradigms in that it provides for a natural platform to exploit data flow parallelisms and because it eliminates much of the technical complexity of problem solving including: decisions about data structures; decisions about how control structures are to interact with data structures; decisions about how one converts an external structure to an internal structure and vice versa; input-output decisions, in general; decisions about a parallelisms; decisions about control structures in general. DTIC

N95-34605# California Univ., Berkeley, CA.
NON-SMOOTH OPTIMIZATION ALGORITHMS, SYSTEM THEORY AND SOFTWARE TOOLS Final Report, 1 Mar. 1993 - 28 Feb. 1995
Elijah Polak 28 Apr. 1995 5 p
(Contract F49620-93-1-0165)
(AD-A294944; Rept-442427-22525; AFOSR-95-0384TR) Avail: CASI HC A01/MF A01

The broad research objective of this project was the development of optimization algorithms and related system-theoretic aspects for the integrated design of flexible structures and their control systems, and shape design. DTIC

N95-34612# Rochester Univ., NY. Dept. of Computer Science.
THREE-DIMENSIONAL RECOGNITION VIA TWO-STAGE ASSOCIATIVE MEMORY Technical Report
Randal C. Nelson 16 Jan. 1995 20 p
(Contracts MDA972-92-J-1012; N00014-93-1-0221)
(AD-A293567; TR-565) Avail: CASI HC A03/MF A01

We describe a method of 3-D object recognition based on two stage use of a general purpose associative memory and a principal views representation. The basic idea is to make use of semi-invariant objects called keys. A key is any robustly extractable feature that has sufficient information content to specify a 2-D configuration of an associated object (location, scale, orientation) plus sufficient additional parameters to provide efficient indexing and meaningful verification. The recognition system utilizes an associative memory organized so that access via a key feature evokes associated hypotheses for the identity and configuration of all objects that could have produced it. These hypothesis are fed into a second stage associative memory, which maintains a probabilistic estimate of the likelihood of each hypothesis based on statistics about the occurrence of the keys in the primary database. Because it is based on a merged percept of local features rather than global properties, the method is robust to occlusion and background clutter, and does not require prior segmentation. Entry of objects into the memory is an active, automatic procedure. We have implemented a version of the system that allows arbitrary definitions for key features. Experiments using keys based on perceptual groups of line segments are reported. Good results were obtained on a database derived from approximately 150 images representing different views of seven polyhedral objects. DTIC

N95-34655 Newcastle-upon-Tyne Univ., Newcastle (England). Dept. of Computing Science.
SLEEP SETS METHOD FOR PARTIAL ORDER VERIFICATION OF CONCURRENT SYSTEMS
M. Koutny and M. Pietkiewicz-Koutny Feb. 1995 22 p
(PB95-236121; TRS-495) Copyright Avail: Issuing Activity (National Technical Information Service (NTIS))

The authors discuss one of the versions of the 'sleep sets' method proposed to reduce the computational effort involved in state space research. They identify some of the problems in previous algorithms which use sleep sets to implement an efficient search of the state space of a concurrent system. NTIS

N95-34813# Lawrence Livermore National Lab., Livermore, CA.
THE DEVELOPMENT OF A DISTRIBUTED COMPUTING ENVIRONMENT FOR THE DESIGN AND MODELING OF PLASMA SPECTROSCOPY EXPERIMENTS
J. K. Nash, W. G. Eme, R. W. Lee, and J. M. Salter (South Gosforth Computer Systems Ltd., Newcastle-upon-Tyne, England.) Oct. 1994 51 p Presented at the 6th International Workshop on Radiative Properties of Hot Dense Matter, Sarasota, FL, 31 Oct. - 4 Nov. 1994 Submitted for publication
(Contract W-7405-eng-48)
(DE95-011725; UCRL-JC-119826; CONF-9410314-3) Avail: CASI HC A04/MF A01

The design and analysis of plasma spectroscopy experiments can be significantly complicated by relatively routine computational tasks arising from the massive amount of data encountered in the experimental design and analysis stages of the work. Difficulties in obtaining, computing, manipulating and visualizing the information represent not simply an issue of convenience -- they have a very real limiting effect on the final quality of the data and on the potential for arriving at meaningful conclusions regarding an experiment. We describe ongoing work in developing a portable UNIX environment shell with the goal of simplifying and enabling these activities for the plasma-modeling community. Applications to the construction of atomic kinetics models and to the analysis of x-ray transmission spectroscopy will be shown. DOE

N95-32429*# Wyoming Univ., Laramie, WY. Dept. of Computer Science.
VALIDATION OF SPACE/GROUND ANTENNA CONTROL ALGORITHMS USING A COMPUTER-AIDED DESIGN TOOL Final Report
Rex E. Gantenbein *In* NASA. Johnson Space Center, National Aeronautics and Space Administration (NASA)/American Society for Engineering Education (ASEE) Summer Faculty Fellowship Program, 1994, Volume 1 Jul. 1995 12 p (For primary document see N95-32418 12-99)
(Grant NGT-44-005-803)
Avail: CASI HC A03/MF A03

N95-33007# Melbourne Univ., Parkville (Australia). Dept. of Computer Science.
A DECLARATIVE DEBUGGER FOR A LOGICAL-FUNCTIONAL LANGUAGE
Lee Naish and Tim Barbour *In* Defence Science and Technology Organisation, Industrial and Engineering Applications of Artificial Intelligence and Expert Systems: Invited and Additional Papers May 1995 p 91-98 (For primary document see N95-32995 12-63)
Avail: Issuing Activity (DSTO Aeronautical and Maritime Research Lab., PO Box 4331, Melbourne, Victoria 3001, Australia)

N95-33142# Lucas Electronics, Birmingham (England).
THE APPLICATION OF ADA AND FORMAL METHODS TO A SAFETY CRITICAL ENGINE CONTROL SYSTEM

W. C. Dolman, A. M. Ashdown, and K. J. McCallion (Ministry of Defence, London, England.) *In* AGARD, Dual Usage in Military and Commercial Technology in Guidance and Control Mar. 1995 13 p (For primary document see N95-33126 12-31)
Copyright Avail: CASI HC A03/MF A02

N95-34225*# National Aeronautics and Space Administration. Ames Research Center, Moffett Field, CA.
CONSTRUCTION OF AN ADVANCED SOFTWARE TOOL FOR PLANETARY ATMOSPHERIC MODELING Abstract Only
Peter Friedland, Richard M. Keller, Christopher P. McKay, Michael H. Sims, and David E. Thompson *In* Colorado Univ., Applied Information Systems Research Program (AISRP) Workshop 3 Meeting Proceedings 1993 1 p (For primary document see N95-34218 12-82)
Avail: CASI HC A01/MF A03

N95-34226*# National Aeronautics and Space Administration. Goddard Space Flight Center, Greenbelt, MD.
EXPERIMENTER'S LABORATORY FOR VISUALIZED INTERACTIVE SCIENCE Abstract Only
Elaine R. Hansen (Colorado Univ., Boulder, CO.), Marjorie K. Klemp (Colorado Univ., Boulder, CO.), Sally W. Lasater (Colorado Univ., Boulder, CO.), Marti R. Szczur, and Joseph B. Klemp (National Center for Atmospheric Research, Boulder, CO.) *In* Colorado Univ., Applied Information Systems Research Program (AISRP) Workshop 3 Meeting Proceedings 1993 1 p (For primary document see N95-34218 12-82)
Avail: CASI HC A01/MF A03

N95-34535# Cray Research Japan, Tokyo (Japan).
PROGRAM DEVELOPING ENVIRONMENT AND A CFD APPLICATION ON THE CRAY T3D Abstract Only
Toshihiro Kinoshita and Tsutomu Saito *In* National Aerospace Lab., Special Publication of National Aerospace Laboratory 16 Jun. 1994 p 225-230 In JAPANESE (For primary document see N95-34505 12-02)
Avail: CASI HC A02/MF A03

N95-34556# SofTek Systems, Inc., Tokyo (Japan).
LARGE SCALE COMPUTING AND VOLUME VISUALIZATION Abstract Only
Susumu Shirayama *In* National Aerospace Lab., Special Publication of National Aerospace Laboratory 16 Jun. 1994 p 351-356 In JAPANESE (For primary document see N95-34505 12-02)
Avail: CASI HC A02/MF A03

62 COMPUTER SYSTEMS

Includes computer networks and special application computer systems.

N95-32374# Sandia National Labs., Albuquerque, NM.
THE DEVELOPMENT AND APPLICATION OF MASSIVELY PARALLEL SOLID MECHANICS CODES
M. McGlaun, A. Robinson, and J. Peery 1995 6 p Presented at the International Conference on Computational Engineering Science, Mauna Lani, HI, 30 Jul. - 3 Aug. 1995
(Contract DE-AC04-94AL-85000)
(DE95-006307; SAND-95-0095C; CONF-950788-1) Avail: CASI HC A02/MF A01

Computational physicists at Sandia National Laboratories have moved the Eulerian CTH code, and the arbitrary-Lagrangian-Eulerian ALEGRA code to distributed memory parallel computers. CTH is a three-dimensional solid mechanics code used for large-deformation, shock wave analysis. ALEGRA is a three-dimensional arbitrary Lagrangian-Eulerian solid-mechanics code used for coupled large-deformation, shock and structural mechanics problems. This paper discusses our experiences moving the codes to parallel computers, the algorithms we used and our experiences running the codes. DOE

N95-32383# Sandia National Labs., Albuquerque, NM.
SIMULATION OF HYPERVELOCITY IMPACT ON MASSIVELY PARALLEL SUPERCOMPUTER
H. E. Fang 1994 7 p Presented at the International Conference on Computational Engineering Science, Mauna Lani, HI, 30 Jul. - 3 Aug. 1995
(Contract DE-AC04-94AL-85000)
(DE95-007735; SAND-94-2637C; CONF-950788-7) Avail: CASI HC A02/MF A01

Hypervelocity impact studies are important for debris shield and armor/anti-armor research and development. Numerical simulations are frequently performed to complement experimental studies, and to evaluate code accuracy. Parametric computational studies involving material properties, geometry and impact velocity can be used to understand hypervelocity impact processes. These impact simulations normally need to address shock wave physics phenomena, material deformation and failure, and motion of debris particles. Detailed, three-dimensional calculations of such events have large memory and processing time requirements. At Sandia National Laboratories, many impact problems of interest require tens of millions of computational cells. Furthermore, even the inadequately resolved problems often require tens or hundred of Cray CPU hours to complete. Recent numerical studies done by Grady and Kipp at Sandia using the Eulerian shock wave physics code CTH demonstrated very good agreement with many features of a copper sphere-on-steel plate oblique impact experiment, fully utilizing the compute power and memory of Sandia's Cray supercomputer. To satisfy requirements for more finely resolved simulations in order to obtain a better understanding of the crater formation process and impact ejecta motion, the numerical work has been moved from the shared-memory Cray to a large, distributed-memory, massively parallel supercomputing system using PCTH, a parallel version of CTH. The current work is a continuation of the studies, but done on Sandia's Intel 1840-processor Paragon X/PS parallel computer. With the great compute power and large memory provided by the Paragon, a highly detailed PCTH calculation has been completed for the copper sphere impacting steel plate experiment. Although the PCTH calculation used a mesh which is 4.5 times bigger than the original Cray setup, it finished in much less CPU time. DOE

N95-32415# Lawrence Livermore National Lab., Livermore, CA. Methods Development Group.
THE FUTURE OF FINITE ELEMENT APPLICATIONS ON MASSIVELY PARALLEL SUPERCOMPUTERS
Mark A. Christon 5 Jul. 1994 21 p
(Contract W-7405-eng-48)
(DE95-011659; UCRL-ID-118354) Avail: CASI HC A03/MF A01

The current focus in large scale scientific computing is upon parallel supercomputers. While still relatively unproven, these machines are being slated for production-oriented, general purpose supercomputing applications. The promise, of course, is to use massively parallel computers to venture further into scientific realisms by performing computations with anywhere from 10(exp 6) to 10(exp 9) grid points thereby, in principle, obtaining a deeper understanding of physical processes. In approaching this brave new world of computing with finite element applications, many technical issues become apparent. This paper attempts to reveal some of the applications-oriented issues which are facing code developers and ultimately the users of engineering and scientific applications on parallel supercomputers, but which seem to be remaining unanswered by vendors, researchers and centralized computing facilities. At risk is the fundamental way in which analysis is performed in a production sense, and the insight into physical problems which results. while at first this treatise may seem to advocate traditional register-to-register vector supercomputers, the goal of this paper is simply an attempt to point out what is missing from the massively parallel computing picture not only for production finite element applications, but also for grand challenge problems. the limiting issues for the use of FEM applications on parallel supercomputers are centered about the need for adequate disk space, archival storage, high bandwidth networks, and continued software development for mesh generation, scientific visualization, linear equation solvers and parallel input/output. DOE

N95-32558# Sandia National Labs., Albuquerque, NM. Infrastructure and Networking Research Dept.
CONGESTION CONTROL OVER ATM LOCAL AREA NETWORKS

Helen Chen, Chien Fang, and James Hutchins Mar. 1995 22 p
(Contract DE-AC04-94AL-85000)
(DE95-010343; SAND-95-8218) Avail: CASI HC A03/MF A01

Asynchronous Transfer Mode (ATM) has emerged as a standard which offers integration of different classes of service as well as scalability in terms of network size and speed. While the early focus on ATM was mainly on wide-area networks, the driving force behind this new technology is increasingly coming from local-area applications. The need for an ATM LAN to support existing protocols (e.g., TCP/IP) transparently is key to its adoption in the local-area environment. In traditional shared medium LANS, congestion control on the medium is handled by medium access control (MAC) protocol. Once a network device gains access to the shared medium, it has the full bandwidth to itself. Other contending network devices must wait until the shared medium becomes free. In ATM LANS, the MAC protocol is removed, and as a result the congestion control it provides is also removed. Each network device can transmit at the full link bandwidth, and can thus potentially cause congestion at some output ports of an ATM switch. This report presents some simulation results and demonstrates the importance of congestion control in ATM networks. First, we show the effects of cell loss on TCP performance in a congested ATM LAN. When congestion results in switch buffer overflow, cells are dropped. The effect of a small cell loss rate is found to translate into a much larger TCP packet retransmission rate, resulting in poor TCP performance. Secondly, we will describe a credit-based, per virtual circuit, per hop flow control algorithm proposed by Digital Equipment Corporation (DEC). We show that when flow control is employed, cell loss and TCP retransmissions are eliminated, resulting in greatly improved TCP performance. DOE

N95-32580 Rochester Univ., NY. Dept. of Computer Science.
DISTRIBUTED SHARED MEMORY FOR NEW GENERATION NETWORKS
Leonidas I. Kontothanassis and Michael L. Scott 27 Mar. 1995 19 p Limited Reproducibility: More than 20% of this document may be affected by poor print
(Contract N00014-92-J-1801; NSF CDA-88-22724; ARPA Order 8930)
(AD-A293722; TR-578) Avail: Issuing Activity (Defense Technical Information Center (DTIC))

Shared memory is widely believed to provide an easier programming model than message passing for expressing parallel algorithms. Distributed shared memory (DSM) systems provide the illusion of shared memory on top of standard message passing hardware at very low implementation cost but provide acceptable performance on only a limited class of applications. We study the main sources of overhead found in software-coherent distributed shared-memory systems and argue that recent revolutionary changes in network technology now allow us to design protocols that minimize such overheads and that approach the performance of full hardware coherence. Specifically we claim that memory-mapped network interfaces that support a global physical address space can greatly improve the performance of DSM systems. To support this claim we study a variety of coherence protocols that can take advantage of the global physical address space and compare their performance with the best known protocol for pure message passing hardware. For the programs in our application suite, protocols taking advantage of the new hardware features improve performance by at least 50% and by as much as an order of magnitude. DTIC

N95-32582# Pacific Northwest Lab., Richland, WA. Molecular Science Research Center.
VISUALIZATION OF PARALLEL MOLECULAR DYNAMICS SIMULATION ON A REMOTE VISUALIZATION PLATFORM
Tong-Yee Lee (Washington State Univ., Pullman, WA.), C. S. Raghavendra (Washington State Univ., Pullman, WA.), and John B. Nicholas Sep. 1994 7 p Presented at the GVIS 1994: Graphics and Visualization Conference, Richland, WA, 8 Sep. 1994
(Contract DE-AC06-76RL-01830)
(DE95-007806; PNL-SA-24897; CONF-9409278-4) Avail: CASI HC A02/MF A01

Visualization requires high performance computers. In order to use these shared high performance computers located at national centers, the authors need an environment for remote visualization. Remote visualization is a special process that uses computing resources and data that are physically distributed over long distances. In their experimental environment, a parallel raytracer is designed for the rendering task. It allows one to efficiently visualize molecular dynamics simulations represented by three dimensional ball-and-stick models. Different issues encountered in creating their platform are discussed, such as I/O, load balancing, and data distribution. DOE

N95-32771# Los Alamos National Lab., NM.
HIGH PERFORMANCE SYSTEMS
Manuel B. Vigil, comp. Mar. 1995 195 p Presented at the Conference on High Speed Computing, Gleneden Beach, OR, 18-21 Apr. 1994
(Contract W-7405-eng-36)
(DE95-009523; LA-12930-C; CONF-9404252) Avail: CASI HC A09/MF A03

This document provides a written compilation of the presentations and viewgraphs from the 1994 Conference on High Speed Computing given at the High Speed Computing Conference, High Performance Systems, held at Gleneden Beach, Oregon, on April 18 through 21, 1994. DOE

N95-32815# Norwegian Defence Research Establishment, Kjeller (Norway).
BASIS IMAGE PROCESSOR Pr5210: CORRELATOR TECHNICAL DESCRIPTION
Bjorn Rudberg 25 Aug. 1994 210 p
(Proj. FFI/566-E/139)
(PB95-222485; FFI/RAPPORT-94/03544) Copyright Avail: CASI HC A10/MF A03

A dedicated hardware correlator is incorporated in the BASIS image processing system. Correlation, which is typically used in template matching, is calculated in search windows across the image. Alternatively, correlation may be computed in independent locations of the image. Subsampling is introduced to cover larger areas of the image. A technical description of the module is given in volume 1 of the report whereas detailed block diagrams, programmable logic information, component listings etc., are given in volume 2. NTIS

N95-32820 Stanford Linear Accelerator Center, Stanford, CA.
PROCEEDINGS OF THE REXX SYMPOSIUM FOR DEVELOPERS AND USERS
Jul. 1994 268 p Presented at the REXX Symposium for Developers and Users, Boston, MA, 1-3 May 1994 Limited Reproducibility: More than 20% of this document may be affected by microfiche quality
(Contract DE-AC03-76SF-00515)
(DE95-010668; SU-SLAC-447; CONF-9405161; UC-405) Avail: CASI HC A12

This conference has become the premier event for exchanging REXX technical information, and people were impressed with how much REXX has spread since the last Symposium. This year the conference sponsors welcomed implementations for new platforms and continued growth in numbers of users and in importance of uses. One of the most popular sessions was 'Object-Oriented Extensions', given by Simon Nash of IBM. Also IBM gave the first public demonstration of their Object REXX for Windows. And the attendees continued the Symposium tradition of contributing software and making diskettes available for all. The Symposium served as a springboard for the REXX Language Association (RexxLA) which will help promote the use of the language. RexxLA held its first public meeting in conjunction with this year's REXX Symposium. DOE

N95-32967 California Univ., Berkeley. Lawrence Berkeley Lab, CA. Information and Computing Sciences Div.
FAST APPROXIMATION OF SELF-SIMILAR NETWORK TRAFFIC
Vern Paxson Jan. 1995 14 p Presented at the SIGCOMM 1995, Boston, MA, 30 Aug. - 2 Sep. 1995 Limited Reproducibility: More than 20% of this document may be affected by microfiche quality
(Contract DE-AC03-76SF-00098)
(DE95-011271; LBL-36750; CONF-9508118-1) Avail: CASI HC A03

Recent network traffic studies argue that network arrival processes are much more faithfully modeled using statistically self-similar processes instead of traditional Poisson processes (LTWW94a, PF94). One difficulty in dealing with self-similar models is how to efficiently synthesize traces (sample paths) corresponding to self-similar traffic. We present a fast Fourier transform method for synthesizing approximate self-similar sample paths and assess its performance and validity. We find that the method is as fast or faster than existing methods and appears to generate a closer

approximation to true self-similar sample paths than the other known fast method (Random Midpoint Displacement). We then discuss issues in using such synthesized sample paths for simulating network traffic, and how an approximation used by our method can dramatically speed up evaluation of Whittle's estimator for H, the Hurst parameter giving the strength of long-range dependence present in a self-similar time series. DOE

N95-33403# Lawrence Livermore National Lab., Livermore, CA. Advanced Computing Lab.
COST-EFFECTIVE DATA-PARALLEL LOAD BALANCING
Charles D. Hansen (Washington Univ., Seattle, WA.) and James P. Ahrens 1995 17 p Presented at the International Conference on Parallel Processing, Madison, WI, 14-18 Aug. 1995
(Contract W-7405-eng-36)
(DE95-010985; LA-UR-95-1462; CONF-9508112-1) Avail: CASI HC A03/MF A01

Load balancing algorithms improve a program's performance on unbalanced datasets, but can degrade performance on balanced datasets, because unnecessary load redistributions occur. This paper presents a cost-effective data-parallel load balancing algorithm which performs load redistributions only when the possible savings outweigh the redistribution costs. Experiments with a data-parallel polygon renderer show a performance improvement of up to a factor of 33 on unbalanced datasets and a maximum performance loss of only 27 percent on balanced datasets when using this algorithm. DOE

N95-33639# Fermi National Accelerator Lab., Batavia, IL.
COLLABORATING OVER THE WEB: LIBRARIES AND LABORATORIES OR THE LIBRARIAN AND THE WEBMASTER
Paula Garrett and David J. Ritchie Mar. 1995 19 p Presented at the AusWeb 1995: Australian WWW Conference, New South Wales, Australia, 29 Apr. - 2 May 1995
(Contract DE-AC02-76CH-03000)
(DE95-010572; FNAL/C-95/056; CONF-9504144-1) Avail: CASI HC A03/MF A01

Fermilab (HREF1) has been using World Wide Web (HREF2) (WWW) servers and browsers for the past several years. The purpose has been to allow information sharing within internationally dispersed teams of large collaborations of high energy physics experimenters and to make possible the easy dissemination of information by support groups who work with those collaborations. That is, the purpose has been in fact that for which was created at CERN (HREF3) beginning in March 1989. In the remainder of this paper, we describe the architecture of the Laboratory and Library servers, discuss the goals, the implications of those goals, the drivers of structure and content, and the effect of these factors on the architecture. Comparisons are made. The implications for Libraries within organizations are described. The application to large Libraries which begin to have multiple servers within their own organization (e.g., one in reference, one in cataloging, one in circulation) is made. The broader implications are discussed. DOE

N95-33643 Lawrence Livermore National Lab., Livermore, CA.
PROCEEDINGS: HIGH PERFORMANCE FUNCTIONAL COMPUTING
A. P. W. Boehm, ed. (Colorado State Univ., Fort Collins, CO.) and John T. Feo, ed. Apr. 1995 238 p Presented at the High Performance Functional Computing, Denver, CO, 9-11 Apr. 1995 Limited Reproducibility: More than 20% of this document may be affected by microfiche quality
(Contract W-7405-eng-48)
(DE95-010736; CONF-9504126) Avail: CASI HC A11

The discipline of functional programming offers the advantage of writing programs for concurrent execution with a guarantee of determinacy, first introduced in (Karp/Miller 1966), the property that all runs of the program on an asynchronous interpreter will yield identical results. The absence of this guarantee in most other approaches to programming for parallel computers leads to programs that are needlessly large, hard to understand, and troublesome to debug. Nevertheless, the ability to express nondeterminacy appears to be essential in writing programs for certain kinds of applications: transactions systems that respond to inputs that arrive asynchronously from several sources; heuristic search problems where the extensive available parallelism can be exploited only if speculative execution is performed, leading to nondeterminacy; and other tasks where use of nondeterminate mechanisms may be shown to yield programs having greater efficiency than purely functional programs for the same tasks. DOE

N95-33838# Sandia National Labs., Albuquerque, NM.
A RECONFIGURABLE OPTOELECTRONIC INTERCONNECT TECHNOLOGY FOR MULTI-PROCESSOR NETWORKS
Yin-Chen Lu (New Mexico Univ., Albuquerque, NM.), Julian Cheng (New Mexico Univ., Albuquerque, NM.), J. C. Zolper, and J. Klem 1995 5 p Presented at the 45th Electronic Components and Technology Conference, Las Vegas, NV, 22-26 May 1995
(Contract DE-AC04-94AL-85000)
(DE95-011895; SAND-95-0753C; CONF-9505121-3) Avail: CASI HC A01/MF A01

This paper describes a new optical interconnect architecture and the integrated optoelectronic circuit technology for implementing a parallel, reconfigurable, multiprocessor network. The technology consists of monolithic array's of optoelectronic switches that integrate vertical-cavity surface-emitting lasers with three-terminal heterojunction phototransistors, which effectively combined the functions of an optical transceiver and an optical spatial routing switch. These switches have demonstrated optical switching at 200 Mb/s, and electrical-to-optical data conversion at greater than 500 Mb/s, with a small-signal electrical-to-optical modulation bandwidth of approximately 4 GHz. DOE

N95-33852# Texas Univ., Austin, TX. Fusion Research Center.
AN OBJECT-ORIENTED DECOMPOSITION OF THE ADAPTIVE-hp FINITE ELEMENT METHOD
J. C. Wiley 13 Dec. 1994 16 p Presented at the 2nd Conference on Object-Oriented Numerics (OONSKI 1994), Sun River, OR, 24 Apr. 1994
(Contract DE-FG05-88ER-53266)
(DE95-012142; DOE/ER-53266/50; FRCR-454; CONF-9404121-4) Avail: CASI HC A03/MF A01

Adaptive-hp methods are those which use a refinement control strategy driven by a local error estimate to locally modify the element size, h, and polynomial order, p. The result is an unstructured mesh in which each node may be associated with a different polynomial order and which generally require complex data structures to implement. Object-oriented design strategies and languages which support them, e.g., C++, help control the complexity of these methods. Here an overview of the major classes and class structure of an adaptive-hp finite element code is described. The essential finite element structure is described in terms of four areas of computation each with its own dynamic characteristics. Implications of converting the code for a distributed-memory parallel environment are also discussed. DOE

N95-34340# Minnesota Univ., Minneapolis, MN.
PARALLEL SOLUTION OF LARGE-SCALE NONLINEAR OPTIMIZATION Final Report, 1 Feb. 1991 - 30 Jun. 1994
J. B. Rosen 8 Nov. 1994 4 p
(Grant AF-AFOSR-0147-91)
(AD-A294372) Avail: CASI HC A01/MF A01

A new global optimization algorithm has been developed and applied to molecular structure computation. In addition, this report discusses a structure preserving total least squares method and its application to parameter estimation. DTIC

N95-34584# Ohio State Univ., Columbus, OH.
PROTOCOL ENGINEERING FOR BROADBAND NETWORKS Final Report, 1 Jun. 1991 - 31 Aug. 1994
Ming T. Liu 1 Apr. 1995 158 p Limited Reproducibility: Document partially illegible
(Contract DAAL03-91-G-0093)
(AD-A294969; ARO-28467.27-EL) Avail: CASI HC A08/MF A02

The final report summarizes the research results obtained, covering five areas in protocol engineering and distributed systems. The five areas are (1) protocol conversion; (2) conformance testing; (3) multimedia protocols; (4) high-speed packet switches; and (5) distributed control. For each area of research, the problems under investigation are first described, and then the major results obtained are summarized. A total of 28 publications, including 4 Ph.D. dissertations, 6 journal publications and 18 publications in international conference proceedings, have been credited to the contract.

In the appendix, six reprints that were not included in two previous progress reports, are included in the final report. DTIC

N95-34587 Carnegie-Mellon Univ., Pittsburgh, PA. School of Computer Science.
EXPERIENCES USING DCE AND CORBA TO BUILD TOOLS FOR CREATING HIGHLY-AVAILABLE DISTRIBUTED SYSTEMS
E. N. Elnozahy, V. Ratan, and M. E. Segal Feb. 1995 14 p
(Grant NSF CCR-94-10116)
(AD-A294973; CMU-CS-95-117) Avail: Issuing Activity (Defense Technical Information Center (NTIS))

Open Distributed Processing (ODP) systems simplify the task of building portable distributed applications that can interoperate even when running on heterogeneous platforms. In this paper, we report on our experience in augmenting an ODP system with tools that allow developers to build highly available distributed objects with little or no additional programming effort. Our tools are implemented within the context of the DCE and CORBA standards for distributed computing. We describe the system that we built and how the combination of DCE and CORBA often helped our efforts and sometimes impeded them. Based on our laboratory experiences, we conclude that these standards generally have a good potential for developing tools for high availability that are portable and applicable to a variety of applications in a distributed computing environment. This potential, however, is hampered by several shortcomings and problems in the specifications of the standards. Such problems could impede other developers and researchers who plan to use these standards. We discuss these problems and suggest solutions to them. DTIC

N95-34603# Georgia Inst. of Tech., Atlanta, GA.
STOCHASTIC NETWORK PROCESSES Final Report, 1 Jan. - 31 Dec. 1994
Richard F. Serfozo 27 Mar. 1995 6 p
(Contract F49620-94-1-0034; AF-AFOSR-0093-91)
(AD-A294939; AFOSR-95-0415TR) Avail: CASI HC A02/MF A01

The general theme of our research has been to develop stochastic network processes for modeling the movement of discrete units in networks. Primary examples are the movement of parts and supplies in manufacturing plants and in distribution systems and the movement of data packets and telephone calls in computer and telecommunications networks. The distinguishing feature of our research is the emphasis on the next generation of intelligent networks that will be the backbone of our manufacturing and computer systems. In these networks, the processing of units at the nodes and the routing of units typically depend dynamically on the actual network congestion, and units move concurrently (e.g. batch processing). Most of the present theory of stochastic network processes is for unintelligent networks in which the nodes operate independently, the routes of units are independent, and the units move one-at-a-time. Our goal is to provide an understanding of these more complex intelligent networks by describing their stochastic behavior. DTIC

N95-34532# National Aerospace Lab., Tokyo (Japan).
ELEMENTARY BENCHMARKS OF THE NWT COMPUTER SYSTEM AND PROGRAM PERFORMANCE
Shigeki Hatayama *In its* Special Publication of National Aerospace Laboratory 16 Jun. 1994 p 207-212 (For primary document see N95-34505 12-02)
Avail: CASI HC A02/MF A03

N95-34534# Fujitsu Ltd., Tokyo (Japan). Parallel Computing Research Center.
HIGHLY PARALLEL COMPUTER AP1000: ARCHITECTURE AND BASIC SOFTWARE Abstract Only
Hiroyuki Sato *In* National Aerospace Lab., Special Publication of National Aerospace Laboratory 16 Jun. 1994 p 219-224 In JAPANESE (For primary document see N95-34505 12-02)
Avail: CASI HC A03/MF A03

63 CYBERNETICS

Includes feedback and control theory, artificial intelligence, robotics and expert systems.

For related information see also *54 Man/System Technology and Life Support.*

N95-32375# Los Alamos National Lab., NM.
OFF-TRAINING-SET ERROR FOR THE GIBBS AND THE BAYES OPTIMAL GENERALIZERS
T. Grossman, E. Knill, and D. Wolpert (Santa Fe Inst., NM.) 3 Jan. 1995 10 p Presented at the ACM Conference on Computational Learning Theory, Santa Cruz, CA, Jul. 1995
(Contract W-7405-eng-36)
(DE95-006344; LA-UR-95-38; CONF-950778-1) Avail: CASI HC A02/MF A01

In this paper we analyze the average off-training-set behavior of the Bayes-optimal and Gibbs learning algorithms. We do this by exploiting the concept of refinement, which concerns the relationship between probability distributions. For non-uniform sampling distributions the expected off training-set error for both learning algorithms can rise with, training set size. However we show in this paper that for uniform sampling and either algorithm, the expected error is a non-increasing function of training set size. For uniform sampling distributions, we also characterize the priors for which the expected error of the Bayes-optimal algorithm stays constant. In addition we show that when the target function is fixed, expected off-training-set error can increase with training set size if and only if the expected error averaged over all targets decreases with training set size. Our results hold for arbitrary noise and arbitrary loss functions. DOE

N95-32386# Los Alamos National Lab., NM.
TRAINING NEURAL NETWORKS USING SEQUENTIAL EXTENDED KALMAN FILTERING
E. S. Plumer 1995 7 p Presented at the 1995 World Congress on Neural Networks, Washington, DC, Jul. 1995
(Contract W-7405-eng-36)
(DE95-007874; LA-UR-95-423; CONF-950789-1) Avail: CASI HC A02/MF A01

Recent work has demonstrated the use of the extended Kalman filter (EKF) as an alternative to gradient-descent backpropagation when training multi-layer perceptrons. The EKF approach significantly improves convergence properties but at the cost of greater storage and computational complexity. Feldkamp et al. have described a decoupled version of the EKF which preserves the training advantages of the general EKF but which reduces the storage and computational requirements. This paper reviews the general and decoupled EKF approaches and presents sequentialized versions which provide further computational savings over the batch forms. The usefulness of the sequentialized EKF algorithms is demonstrated on a pattern classification problem. DOE

N95-32476# Joint Inst. for Nuclear Research, Dubna (USSR).
A CHOICE OF INPUT VARIABLES FOR A MULTILAYER PERCEPTRON
A. Y. Bonyushkina, P. V. Zrelov, and V. V. Ivanov 1994 12 p In RUSSIAN
(DE95-623573; JINR-R-10-94-363) Avail: CASI HC A03/MF A01 (US Sales Only)

In the paper some aspects of multilayer perceptron (MLP) application to the problem of classifying the events presented by empirical samples of a finite volume are considered. The results of the MLP learning for various forms of the input data are analyzed and the reasons leading to the effect of an instantaneous learning of the MLP and rise of the neural network are investigated for the case when the input data are presented in a form of variational series. The problem of hidden layer neuron reduction without raising the recognition error is discussed. DOE

N95-32533# Sandia National Labs., Albuquerque, NM.
ON BOOTSTRAPPING LOCAL SEARCH WITH TRAIL-MARKERS
Pang C. Chen 1995 15 p Presented at the 14th International Joint Conference on Artificial Intelligence, Montreal, Canada, 20-25 Aug. 1995
(Contract DE-AC04-94AL-85000)
(DE95-009835; SAND-95-0673C; CONF-950834-1) Avail: CASI HC A03/MF A01

We identify a general framework for search called bootstrap search, which is defined as global search using only a local search procedure along with some memory for learning intermediate subgoals. We present a simple algorithm for bootstrap search, and provide some initial theory on their performance. In our theoretical analysis, we develop a random digraph problem model and use it to make some performance predictions and comparisons. We also use it to provide some techniques for approximating the optimal resource bound on the local search to achieve the best global search. We validate our theoretical results with empirical demonstration on the 15-puzzle. We show how to reduce the cost of a global search by 2 orders of magnitude using bootstrap search. We also demonstrate a natural but not widely recognized connection between search costs and the lognormal distribution. To further illustrate our algorithm's generality and effectiveness, we also apply it to robot path planning, and demonstrate a phenomenon of over-learning. DOE

N95-32627# Joint Inst. for Nuclear Research, Dubna (USSR).
APPLICATION OF DEFORMABLE TEMPLATES FOR RECOGNIZING TRACKS DETECTED WITH HIGH PRESSURE DRIFT TUBES
S. Baginyan, S. Baranov, A. Glazov, and G. Ososkov 1994 14 p
(DE95-621870; JINR-E-10-94-328) Avail: CASI HC A03/MF A01 (US Sales Only)

The modification of the deformable template method (DTM) application to the problem of track finding and track parameter determination for data detected with high pressure drift tubes (HPDT) in the design of ATLAS for the muon spectrometer experiment is proposed. Our DTM applications consist of two parts, according to two stages of the study. The first part relates to the stage of HPDT study on the CERN muon beam (BEAM-TEST) with the simplest one-prong events without noise signals, where the main obstacle is the left-right ambiguities for each tube. In the second part more complicated HPDT data are to be handled with noise signals. It was shown that the suggested DTM development solves the problem of track recognition and track parameter determination for both noiseless and noise data. Results are obtained on the real beam test data and on data simulating the muon spectrometer on the basis of HPDT. DOE

N95-32659*# Jet Propulsion Lab., California Inst. of Tech., Pasadena, CA.
A DECADE OF NEURAL NETWORKS: PRACTICAL APPLICATIONS AND PROSPECTS
Sabrina Kemeny, ed. and Anil Thakoor, ed. 1 Oct. 1994 16 p Workshop held in Pasadena, CA, 11-13 May, 1994; sponsored by DOD
(Contract NAS7-1260; RTOP 888-00-01-00-01)
(NASA-CR-198867; JPL-Publ-94-25; NAS 1.26:198867) Avail: CASI HC A03/MF A01

On May 11-13, 1994, JPL's Center for Space Microelectronics Technology (CSMT) hosted a neural network workshop entitled, 'A Decade of Neural Networks: Practical Applications and Prospects,' sponsored by DOD and NASA. The past ten years of renewed activity in neural network research has brought the technology to a crossroads regarding the overall scope of its future practical applicability. The purpose of the workshop was to bring together the sponsoring agencies, active researchers, and the user community to formulate a vision for the next decade of neural network research and development prospects, with emphasis on practical applications. Of the 93 participants, roughly 15% were from government agencies, 30% were from industry, 20% were from universities, and 35% were from Federally Funded Research and Development Centers (FFRDC's). Author

N95-32767*# Cincinnati Univ., OH. Dept. of Electrical and Computer Engineering.
GENETIC ALGORITHMS AS GLOBAL RANDOM SEARCH METHODS Final Report
Charles C. Peck and Atam P. Dhawan 21 Feb. 1995 65 p
(Contract NCC3-308)
(NASA-CR-199088; NAS 1.26:199088) Avail: CASI HC A04/MF A01

Genetic algorithm behavior is described in terms of the construction and evolution of the sampling distributions over the space of candidate solutions. This novel perspective is motivated by analysis indicating that that schema theory is inadequate for completely and properly explaining genetic algorithm behavior. Based on the proposed theory, it is argued that the similarities of candidate solutions should be exploited directly, rather than encoding candidate solution and then exploiting their similarities. Proportional selection is characterized as a global search operator, and recombination is characterized as the search process that exploits similarities. Sequential algorithms and many deletion methods are also analyzed. It is shown that by properly constraining the search breadth of recombination operators, convergence of genetic algorithms to a global optimum can be ensured. Author

N95-32768*# Sverdrup Technology, Inc., Brook Park, OH.
GENETIC ALGORITHM BASED INPUT SELECTION FOR A NEURAL NETWORK FUNCTION APPROXIMATOR WITH APPLICATIONS TO SSME HEALTH MONITORING Final Report
Charles C. Peck, Atam P. Dhawan, and Claudia M. Meyer 1991 8 p
Prepared in cooperation with Cincinnati Univ., OH
(Contract NCC3-308)
(NASA-CR-199089; NAS 1.26:199089) Avail: CASI HC A02/MF A01

A genetic algorithm is used to select the inputs to a neural network function approximator. In the application considered, modeling critical parameters of the space shuttle main engine (SSME), the functional relationship between measured parameters is unknown and complex. Furthermore, the number of possible input parameters is quite large. Many approaches have been used for input selection, but they are either subjective or do not consider the complex multivariate relationships between parameters. Due to the optimization and space searching capabilities of genetic algorithms they were employed to systematize the input selection process. The results suggest that the genetic algorithm can generate parameter lists of high quality without the explicit use of problem domain knowledge. Suggestions for improving the performance of the input selection process are also provided. Author

N95-32995 Defence Science and Technology Organisation, Melbourne (Australia). Aeronautical and Maritime Research Lab.
INDUSTRIAL AND ENGINEERING APPLICATIONS OF ARTIFICIAL INTELLIGENCE AND EXPERT SYSTEMS: INVITED AND ADDITIONAL PAPERS
Graham F. Forsyth, ed. and Moonis Ali, ed. (Southwest Texas State Univ., San Marcos, TX.) May 1995 116 p Presented at the 8th International Conference, Melbourne, Australia, 6-8 Jun. 1995
(DSTO-GD-0051; AR-009-257) Copyright Avail: Issuing Activity (DSTO Aeronautical and Maritime Research Lab., PO Box 4331, Melbourne, Victoria 3001, Australia)

Invited and additional papers not included in the Proceedings of the Eighth International Conference on Industrial and Engineering Applications of Artificial Intelligence and Expert Systems are presented. The papers present a spectrum of new ideas, issues, and practicum, addressing the needs of real-life applied systems. Topics include adaptive architectures, case-based reasoning, computer aided manufacturing, diagnosis, fuzzy logic and control, image analysis, knowledge acquisition, knowledge-based systems, model-based reasoning, modeling, and software engineering. For individual titles, see N95-32996 through N95-33008.

N95-32996# Hong Kong Polytechnic, Kowloon (Hong Kong). Dept. of Electronic Engineering.
TRAINING AND RECOGNITION OF CANTONESE PHONEMES BY BACKPROPAGATION THROUGH TIME
K. K. Shin, J. C. H. Poon, and K. C. Li *In* Defence Science and Technology Organisation, Industrial and Engineering Applications of Artificial Intelligence and Expert Systems: Invited and Additional Papers 1-7 (SEE N95-32995 12-63) May 1995 (For primary document see N95-32995 12-63)
Avail: Issuing Activity (DSTO Aeronautical and Maritime Research Lab., PO Box 4331, Melbourne, Victoria 3001, Australia)

Neural networks have received considerable attention in the area of speech recognition. Networks that model time and temporal variation have also been proposed for continuous speech recognition. The technique of time-delay neural network, backpropagation through time, and its application to Cantonese phonemes are presented in detail. Author

N95-32997# University of Technology, Victoria (Australia). Dept. of Computer and Mathemtical Sciences.
INCORPORATING DISTRIBUTED PROBLEM SOLVING TECHNIQUE INTO A CASE-BASED SYSTEM

S. K. Wong, A. Kalam, and C. H. C. Leung *In* Defence Science and Technology Organisation, Industrial and Engineering Applications of Artificial Intelligence and Expert Systems: Invited and Additional Papers May 1995 p 9-16 (For primary document see N95-32995 12-63)
Avail: Issuing Activity (DSTO Aeronautical and Maritime Research Lab., PO Box 4331, Melbourne, Victoria 3001, Australia)

This paper presents an object based architecture that uses cooperating and distributed agents in a case-based framework. The proposed architecture incorporates agents into a case-based system to achieve better coordination. An agent corresponds to a knowledge-based entity. This architecture consists of set of entities and agents organized in a federated structure, which are managed and coordinated by the facilitator and controller modules respectively. This architecture is applied in the development of a case-based system to design, analyze, and assess power system protection schemes (CAPP). Part of the system has already been implemented and the results obtained thus far indicate that the proposed framework appears to offer substantial advantages over conventional approaches. Author

N95-32998# Wollongong Univ. (Australia).
KNOWLEDGE-BASED SYSTEM FOR METALLURGICAL GRADE DESIGN
S. S. Shivathaya, X. D. Fang, and J. G. Williams (Broken Hill Proprietary, Port Kembla, Australia.) *In* Defence Science and Technology Organisation, Industrial and Engineering Applications of Artificial Intelligence and Expert Systems: Invited and Additional Papers May 1995 p 17-26 (For primary document see N95-32995 12-63)
Avail: Issuing Activity (DSTO Aeronautical and Maritime Research Lab., PO Box 4331, Melbourne, Victoria 3001, Australia)

Knowledge-based system development for metallurgical grade design in steel making is a complex task, due to the difficulties faced in the knowledge elicitation process and due to the interrelationship of many factors in steel making process. This paper discusses the first stage of metallurgical grade design system which deals with the determination of the steel making aim chemistry. If an attempt is made to design aim chemistry based on the mathematical approach of utilizing the empirical models between various design parameters, it would result in unrealistic design because relationships between various design parameters are not always linear. Therefore it is inevitable to apply the knowledge based approach along with the mathematical approach to deal with this complex task. The approach put forward is a hybrid approach, where the knowledge base is applied at every stage of the design process to utilize the expert as well as the heuristic knowledge of metallurgists to obtain designs which are realistic and which take account of the various limitations and constraints encountered in steel making. Knowledge elicitation approach developed includes the use of a codification scheme, paper models, and noninterview techniques. The metallurgical grade design is also characterized by extensive utilization of the grade history database which contains performance data for various steel grades and thickness combinations. The inputs to the system are through interactive dialog sessions and the basic inputs consist of the material standards, size, quantity, tonnage, end use, and the customer special requirements. These basic inputs along with the numerous rules in the knowledge bases as well as the mathematical modeling enable the effective design of the steel making aim chemistry. Author

N95-32999# Technical Univ. of Budapest (Hungary). Dept. of Manufacturing Engineering.
MONITORING OF THE CUTTING OPERATIONS USING FUZZY LOGIC
Tibor Szalay, Sandor Markos, and Imre Meszaros *In* Defence Science and Technology Organisation, Industrial and Engineering Applications of Artificial Intelligence and Expert Systems: Invited and Additional Papers May 1995 p 27-30 Sponsored by National Research Foundation, Hungary (For primary document see N95-32995 12-63)
Avail: Issuing Activity (DSTO Aeronautical and Maritime Research Lab., PO Box 4331, Melbourne, Victoria 3001, Australia)

In the case of monitoring and control of many industrial processes more than one attribute is measured and these attributes provide different information about the monitored process. Because of difference in the information acquired from the process and the large number of monitored attributes, new control methods are required. The results of our research in process monitoring are reported. In order to solve the problems of the acquisition of the different signals of different sensors and real time processing of those we apply the efficient artificial intelligence method of fuzzy logic. After the fuzzy processing of the experimental data we gained a three dimensional inference matrix which can be qualified the tool wear and the surface roughness based on the measured cutting force and the adjusted feed. Author

N95-33000# Telstra Research Labs., Clayton (Australia). Artificial Intelligence Systems Section.
AN EFFICIENT INFERENCE ENGINE FOR INTERACTIVE FAULT DIAGNOSIS IN A HELPDESK APPLICATION
Ming Zhao, Chris Leckie, Muriel deBeler, and Chris Rowles *In* Defence Science and Technology Organisation, Industrial and Engineering Applications of Artificial Intelligence and Expert Systems: Invited and Additional Papers May 1995 p 31-40 (For primary document see N95-32995 12-63)
Avail: Issuing Activity (DSTO Aeronautical and Maritime Research Lab., PO Box 4331, Melbourne, Victoria 3001, Australia)

This paper presents work on an interactive fault diagnosis expert system for a Helpdesk application. An efficient knowledge representation and inference algorithm is proposed which takes into consideration the factors that no multiple instances exist in human fault report, the diagnosis sequence is unpredictable, and the inference engine is passive in an event-driven environment. A lattice data structure is designed for knowledge representation, which is generated automatically from a script of decision rules. The inference engine works in a transaction-like style, reasoning on the lattice. It can either guide the inference sequence or respond to the input to any decision node. Author

N95-33001# University of Technology, Victoria (Australia). Dept. of Electrical and Electronic Engineering.
AN ALTERNATIVE REASONING METHOD
Omar Ghanayem *In* Defence Science and Technology Organisation, Industrial and Engineering Applications of Artificial Intelligence and Expert Systems: Invited and Additional Papers May 1995 p 41-45 (For primary document see N95-32995 12-63)
Avail: Issuing Activity (DSTO Aeronautical and Maritime Research Lab., PO Box 4331, Melbourne, Victoria 3001, Australia)

An alternative reasoning method is presented which considers the sides of convex membership functions used for input and output parameters in the fuzzy system. Considering the left, right, and center of the membership function during fuzzification or defuzzification would allow better use of the available knowledge about the system and thus limit the nonlinearities introduced by the reasoning process. Comparison between the proposed and the classical reasoning methods is demonstrated using different number of membership functions, implemented on a single input single output fuzzy system, and in the design of a fuzzy logic based power system stabilizer for a synchronous generator connected to an infinite bus through a transmission line. Author

N95-33002# North Carolina Agricultural and Technical State Univ., Greensboro, NC. Dept. of Electrical Engineering.
A GENERAL SOLUTION TO OBJECT MATCHING PROBLEMS BY USING THE MULTIRESOLUTION APPROXIMATION
Jung H. Kim, Sung H. Yoon (North Carolina State Univ., Raleigh, NC.), Winser E. Alexander (North Carolina State Univ., Raleigh, NC.), Eui H. Park, and Celestin Ntuen *In* Defence Science and Technology Organisation, Industrial and Engineering Applications of Artificial Intelligence and Expert Systems: Invited and Additional Papers May 1995 p 47-56 (For primary document see N95-32995 12-63)
(Contract N00600-93-K-2051; FAA-93-G-012)
Avail: Issuing Activity (DSTO Aeronautical and Maritime Research Lab., PO Box 4331, Melbourne, Victoria 3001, Australia)

This paper proposes the multiresolution approximation approach to obtaining good representations which can be used for matching of objects. We define a continuous multiresolution approximation (CMA) in terms of the continuous wavelet transform. The CMA is an extended version of the multiresolution approximation related to the discrete wavelet transform. The theory of the CMA enables us to generate good representations to solve object matching problems. Low resolution approximations of an original boundary are obtained by applying the continuous wavelet transform to a boundary of an object. We compute curvature functions of the approximations and find zero crossings of the curvature functions to construct the proposed representations. The proposed representations can be used to solve several types of matching problems. The properties of the representations such as

validity, efficiency, and reliability are investigated. We conclude the representations are suitable for the matching of objects in the presence of occlusion, scale, and noise. Author

N95-33003# Instituto Technologico y de Estudios Superiores de Monterrey, (Mexico).

INDUCTION OF DEPENDENCY STRUCTURES FROM DATA AND ITS APPLICATION TO OZONE PREDICTION

L. Enrique Sucar, Joaquin Perez-Brito, and J. Carlos Ruiz-Suarez (Instituto Politecnico Nacional, Merida, Mexico.) *In* Defence Science and Technology Organisation, Industrial and Engineering Applications of Artificial Intelligence and Expert Systems: Invited and Addtional Papers May 1995 p 57-63 (For primary document see N95-32995 12-63)

Avail: Issuing Activity (DSTO Aeronautical and Maritime Research Lab., PO Box 4331, Melbourne, Victoria 3001, Australia)

We propose an algorithm for structure learning in predictive expert systems based on a probabilistic network representation. The idea is to have the 'simplest' structure with acceptable predictive capability. The algorithm starts by building a tree structure by measuring mutual information between pairs of variables, and then it adds links as necessary to obtain certain predictive performance. We have applied it for ozone prediction in Mexico City. We obtained, as a first approximation, a tree-structured dependency model. We observe that even with only three parameters, its estimations are quite good. A causal network representation and the structure learning techniques produced some interesting results. Firstly, we got some insight into the dependency structure of the phenomena. Secondly, we got an indication of which are the important variables for ozone forecasting. Thirdly, this dependency information could be used for improving other prediction techniques, such as neural networks. Author

N95-33004# Wollongong Univ. (Australia). Dept. of Mechanical Engineering.

HOTQUA: AN EXPERT SYSTEM PROTOTYPE FOR QUALITY MONITORING IN A ROLLING MILL

X. Yao, A. K. Tieu, X. D. Fang, and D. Frances (Broken Hill Proprietary, Port Kembla, Australia.) *In* Defence Science and Technology Organisation, Industrial and Engineering Applications of Artificial Intelligence and Expert Systems: Invited and Additional Papers May 1995 p 65-70 (For primary document see N95-32995 12-63)

Avail: Issuing Activity (DSTO Aeronautical and Maritime Research Lab., PO Box 4331, Melbourne, Victoria 3001, Australia)

HOTQUA, an expert system prototype which was developed to monitor the quality situation when rolling hot steel at a hot strip mill and to advise operators to take actions for optimal quality control, is described. This system is integrated with not only the traditional part-heuristic knowledge, but also with neural networks and statistical analysis for dynamic modeling of the relationships between the quality and the key rolling process variables. It is intended that this expert system is suitable for all quality items of a hot strip mill. A case study is presented here for width quality. G2 system is used as a shell for the development of HOTQUA. Author

N95-33005# Dalian Inst. of Tech. (China). School of Chemical Engineering.

THE METHOD OF MODEL-BASED REASONING AND APPLICATION OF AN INTELLIGENT ADAPTIVE OBSERVER ON THE INTEGRATED PROCESS

Wen-Bao Dong and Ning-Bin Cai *In* Defence Science and Technology Organisation, Industrial and Engineering Applications of Artificial Intelligence and Expert Systems: Invited and Additional Papers May 1995 p 71-79 (For primary document see N95-32995 12-63)

Avail: Issuing Activity (DSTO Aeronautical and Maritime Research Lab., PO Box 4331, Melbourne, Victoria 3001, Australia)

On the basis of study of the on-line identifier and adaptive observer of the linear time-invariant multiple input, multiple output (MIMO) discrete systems, an improved methods with discounted measurement of stochastic Newton algorithm (MDM-SNA) is adopted to study the method of model-based reasoning and application of an intelligent adaptive observer on the integrated complex distillation process. First the intelligent adaptive observer can select automatically a decomposition method of integrated process system and data processing pattern according to different production scheduling, and then carry out the model-based reasoning to get observation. The satisfied results are obtained in the industrial application. Author

N95-33006# De Montfort Univ., Milton Keynes (England). Artificial Intelligence Group.

CONCEPTUAL, CAUSAL AND NUMERICAL MODELLING AND ANALYSIS OF PHYSICAL SYSTEMS

S. Xia *In* Defence Science and Technology Organisation, Industrial and Engineering Applications of Artificial Intelligence and Expert Systems: Invited and Additional Papers May 1995 p 81-89 (For primary document see N95-32995 12-63)

Avail: Issuing Activity (DSTO Aeronautical and Maritime Research Lab., PO Box 4331, Melbourne, Victoria 3001, Australia)

An appropriate model is essential in analyzing a dynamic physical system satisfactorily and it can be constructed through using a correct perspective, approximation, and abstraction. The perspective, approximation, and abstraction information of a model can be characterized by the concepts, cause-effect connections, and numerical relationships contained in the model. We use three levels of model - conceptual, causal, and numerical models - to describe a physical system and apply qualitative reasoning to examine the conceptual and causal properties of the system. Multiple levels of model representation and automatic transformation between different levels of model are the two important concepts of this work. Three case studies have been presented to demonstrate the advantages of this approach and it has been shown that multiple levels of modeling and analysis is not only possible but also necessary. Author

N95-33007# Melbourne Univ., Parkville (Australia). Dept. of Computer Science.

A DECLARATIVE DEBUGGER FOR A LOGICAL-FUNCTIONAL LANGUAGE **c61**

Lee Naish and Tim Barbour *In* Defence Science and Technology Organisation, Industrial and Engineering Applications of Artificial Intelligence and Expert Systems: Invited and Additional Papers May 1995 p 91-98 (For primary document see N95-32995 12-63)

Avail: Issuing Activity (DSTO Aeronautical and Maritime Research Lab., PO Box 4331, Melbourne, Victoria 3001, Australia)

Logic and functional programming languages have many advantages and there is a growing trend to develop languages which incorporate both these paradigms. One of the disadvantages of such languages is that the execution mechanisms are so complex that traditional debugging methods are difficult to use. Declarative debugging techniques have been successfully applied to Prolog and more recently functional languages. They allow programs to be debugged using only knowledge of the declarative semantics, hiding the details of the execution from the programmer. We describe a declarative debugger for a combined logic and functional programming language, NUE-Prolog. The debugger combines both existing and new algorithms. The main new algorithm is for declarative debugging of functions which for some inputs are not well-defined (typically resulting in a runtime error). The algorithms can easily be adapted to other logic and functional languages. Author

N95-33008# Commonwealth Scientific and Industrial Research Organization, Highett, Victoria (Australia). Div. of Building, Construction, and Engineering.

EXPERT SYSTEMS AND ARTIFICIAL INTELLIGENCE APPLICATIONS IN ENGINEERING DESIGN AND INSPECTION

Ron Sharpe, Jacek Gibert, and Stephen Oakes *In* Defence Science and Technology Organisation, Industrial and Engineering Applications of Artificial Intelligence and Expert Systems: Invited and Additional Papers May 1995 p 99-109 (For primary document see N95-32995 12-63)

Avail: Issuing Activity (DSTO Aeronautical and Maritime Research Lab., PO Box 4331, Melbourne, Victoria 3001, Australia)

The CSIRO Division of Building, Construction, and Engineering (CSIRO DBCE) provides the major Australian source of science and technology required to service the needs of Australia's construction and related engineering sectors. Close links to Australian industry enable the division to identify industry needs and potential applications for new scientific knowledge and to apply this knowledge through collaborative research activities. The paper presents three representative examples of the way in which advanced artificial intelligence (AI) techniques are currently being applied for engineering design and inspection. The first is the Windloader expert system used to determine wind forces on structures to comply with the Australian Standard AS 1170.2. The second is the BCAider expert system for the Building Code of Australia (BCA), which is now used by

over 500 architects, engineers, regulators, and fire authorities. The PIRAT system (Pipe Inspection Real-time Assessment Technique) is a patented robotic inspection system which moves through a sewer system assessing pipe conditions through a combination of machine vision and artificial intelligence. Derived from text

N95-33060# Department of Energy, Pittsburgh, PA. Energy Technology Center.
HIGH-TECH CONTROLS FOR ENERGY AND ENVIRONMENT
Samuel J. Biondo, ed. and Charles J. Drummond, ed. 1995 168 p Presented at the Adaptive Control Systems Technology Symposium on High-tech Controls for Energy and Environment, Pittsburgh, PA, 24-25 Oct. 1994; sponsored by IEEE Neural Networks Council, NRL, Electric Power Research Inst., and US Bureau of Mines
(DE95-004011; CONF-9410201) Avail: CASI HC A08/MF A02

This document contains reports which were presented at a symposium for adaptive control systems. Topics were concerned with fuzzy logic, genetic algorithms, adaptive processes control, nonlinear component analysis, and processes control and efficiency applied to reducing nitrogen oxides emissions to a column flotation unit. Individual reports (22 reports) are processed separately for the data bases. DOE

N95-33212# Los Alamos National Lab., NM.
FUNCTION APPROXIMATION USING ADAPTIVE AND OVERLAPPING INTERVALS
Rajendra B. Patil 1995 15 p Presented at the APIC 1995, El Paso, TX, Mar. 1995
(Contract W-7405-eng-36)
(DE95-010865; LA-UR-95-1224; CONF-9503135-2) Avail: CASI HC A03/MF A01

A problem common to many disciplines is to approximate a function given only the values of the function at various points in input variable space. A method is proposed for approximating a function of several to one variable. The model takes the form of weighted averaging of overlapping basis functions defined over intervals. The number of such basis functions and their parameters (widths and centers) are automatically determined using given training data and a learning algorithm. The proposed algorithm can be seen as placing a nonuniform multidimensional grid in the input domain with overlapping cells. The non-uniformity and overlap of the cells is achieved by a learning algorithm to optimize a given objective function. This approach is motivated by the fuzzy modeling approach and a learning algorithms used for clustering and classification in pattern recognition. The basics of why and how the approach works are given. Few examples of nonlinear regression and classification are modeled. The relationship between the proposed technique, radial basis neural networks, kernel regression, probabilistic neural networks, and fuzzy modeling is explained. Finally advantages and disadvantages are discussed. DOE

N95-33214# Sandia National Labs., Albuquerque, NM.
GLOBALLY STABLE FEEDBACK LAWS FOR NEAR-MINIMUM-FUEL AND NEAR-MINIMUM-TIME POINTING MANEUVERS FOR A LANDMARK-TRACKING SPACECRAFT
Hanspeter Schaub, Rush D. Robinett, and John L. Junkins 1995 12 p Presented at the American Institute of Aeronautics and Astronautics/American Aeronautics Society Astrodynamics Conference, Halifax, Canada, 7-10 Aug. 1995
(Contract DE-AC04-94AL-85000)
(DE95-009867; SAND-95-0720C; CONF-9508109-1) Avail: CASI HC A03/MF A01

Utilizing unique properties of a recently developed set of attitude parameters, the modified Rodrigues parameters, we develop feedforward/feedback type control laws that globally control a spacecraft undergoing large nonlinear motions, using three or more reaction wheels. The method is suitable for tracking given smooth reference trajectories that spline smoothly into a target state or pure spin motion; these reference trajectories may be exact or approximate solutions of the system equations of motion. In particular, we illustrate the ideas using both near-minimum-time and near-minimum fuel rotations about Euler's principal rotation axis, with parameterization of the sharpness of the control switching for each class of reference maneuvers. Lyapunov stability theory is used to prove rigorous stability of closed loop motion in the end game, and qualified Lyapunov stability during the large nonlinear path tracking portion of the closed loop tracking error dynamics. The methodology is illustrated by designing example control laws for a prototype landmark tracking spacecraft; simulations are reported that show this approach to be attractive for practical applications. The inputs to the reference trajectory are designed with user-controlled sharpness of all control switches, to enhance the trackability of the reference maneuvers in the presence of structural flexibility. DOE

N95-33307 Toronto Univ. (Ontario).
MOTION AND FORCE CONTROL OF COORDINATED ROBOTS Ph.D. Thesis
Yan-Ru Hu 1993 193 p
(ISBN-0-315-86323-4) Avail: Univ. Microfilms Order No. DANN86323

The objective of this research is to develop motion and force control methods for coordinated robots. The robots are assumed to grasp rigidly an object, and the purpose of the cooperating control is to regulate the object motion, the contact force between the object and environment, with which it comes in contact, and the internal force, which does not contribute to the object motion and contact force. The control problem is defined in a system-theoretical framework, where desired trajectories of motion and forces are tracked asymptotically. In this research, both joint redundant and nonredundant robots are considered. Four motion and force control problems are defined and solved: (1) motion and force control of coordinated robots in the presence of model uncertainty; (2) control of redundant robots in the presence of obstacles in the environment; (3) optimal control of redundant robots; and (4) motion and force control of robots in the presence of joint flexibility. The proposed control of motion and force in the presence of uncertainty is developed based on an adaptive scheme. The adaptive control is used to estimate the unknown constant parameters of the robots, the object, and the environment. Based on Lyapunov stability theory, asymptotic convergence of the motion, contact and internal force errors, and of the parameter errors is obtained. The problem of control in the presence of obstacles is addressed by defining the extended task space. This space is formed by the regular task subspace and the constraint subspace. Using the method developed for coordinated nonredundant robots, a solution to motion and force control in the presence of obstacles is proposed. The optimal control problem focuses on minimizing torque loading at the joints of coordinated redundant robots. Both, locally and globally optimal control laws are developed. Using analytical tools, asymptotic stability of the system is proven. The control problem of nonredundant robots is also extended to the case of joint flexibility. A unified controller is developed to regulate the motion, the contact and internal forces, and the joint elastic force, and to distribute the load between the robots. Experimental work has also been conducted to examine the proposed motion and force control scheme for coordinated nonredundant robots. The experimental setup consists of two commercial robots, and custom designed software and hardware for coordinated control of both arms. The experiment has confirmed the results of the theoretical analysis. Dissert. Abstr.

N95-33324 Cleveland State Univ., OH.
SELF-ORGANIZING NEURAL NETWORK AND ITS APPLICATIONS TO VISION-GUIDED ROBOT MOTION COORDINATION Ph.D. Thesis
An-Jen Yang 1993 170 p
Avail: Univ. Microfilms Order No. DA9418115

Artificial neural networks have been investigated in almost all aspects of robotic theories and implementations, such as robotic kinematics, path planning, robot arm dynamics, and position and force control problems. A new idea for vision-motor controlled robots to learn the vision-robot coordination using self-organizing neural network (SONN) has been recently explored, where a robot learns by observing its trial movements without external supervisor. Although this approach is still in the introductory stage, it has demonstrated the potential to develop a flexible, self-organizing robot neural controller. The main objective of this study is to improve the SONN learning algorithm for vision-guided robot coordination. A new strategy to improve the adaptability and convergence of the Kohonen self-organizing neural network is proposed and a new learning algorithm to acquire the desired coordination among multiple mappings based on SONN is presented. With the proposed adaptability improvement algorithm, the network can adapt to the change of robot workspace or the vision system. With the new learning strategy of SONN, the desired robot coordination maps, such as for obstacle and singularity free robot motion, can be obtained. Another SONN application, neural trajectory interpolator based on coordination map, is proposed, which provided better performance than the incremental

trajectory interpolator based on resolved motion rate control method. The computer simulations and analysis for the proposed algorithms are included. The significance of this study is the development of a different method in obtaining the vision-machine coordination, and an alternate approach to the traditional machine dependent tedious calibration process. A vision-guided machine can learn how to perform difficult tasks using solely two cameras (equivalent to two human eyes). More importantly, a pretrained machine system can properly function in real time. Dissert. Abstr.

N95-33399# Technische Univ., Delft (Netherlands). Dept. of Technical Mathematics and Informatics.

POPOV THEORY BASED APPROACH TO DIGITAL H(INFINITY)-CONTROL WITH MEASUREMENT-FEEDBACK FOR PRITCHARD-SALAMON SYSTEMS

Florin Dan Barb, Vlad Ionescu (Institutul Politehnic din Bucharest, Romania.), and Willem deKoning 1994 47 p

(ISSN 0922-5641)

(PB95-218111; Rept-94-12) Copyright Avail: CASI HC A03/MF A01

In the paper the authors deal with the digital output measurement-feedback H-infinity control problem for Pritchard-Salamon infinite-dimensional systems with unbounded input and output operators. A discrete Popov theory based solution is given in terms of the solvability of Kalman-Szego-Popov-Yakubovitch systems associated to the equivalent discrete-time, time-invariant system obtained by lifting the T-periodically continuous-time system. NTIS

N95-33604 Case Western Reserve Univ., Cleveland, OH.

NONHOLONOMIC CONTROL OF COUPLED SPATIAL MULTIBODY SYSTEMS Ph.D. Thesis

Chih-Keng Chen 1993 134 p

Avail: Univ. Microfilms Order No. DA9416194

This dissertation is concerned with dynamic modeling, controllability, and control synthesis of coupled multibody systems. The systems are configured as open kinematic chains and with large angle motions in three dimensional space. The angular momentum preserving reorientation problem is of interest here. This has applications in multibody satellites and space robotics, and in the understanding of the classical cat fall problem. A coordinate free representation of the dynamics of a multibody system, composed of rigid bodies connected by ball-in-socket joints without kinematic loops, is derived. The conservation of angular momentum results in a nonholonomic constraint. Important properties of nonholonomic systems are discussed. Controllability is explored in a coordinate free form. Local coordinate results can then be easily derived. A sufficient condition for strong accessibility and small time local controllability (STLC) is derived. We give a nonsmooth feedback control law to control the absolute orientation of two-body system. This synthesis approach is based on a path planning method: multicycle joint motion. We prove that the applicability of the control synthesis using linear motions along a closed relative angle path requires controllability condition to be satisfied. The computer simulation results illustrate the convergent property of this control design. Results presented here are a nontrivial extension of previous work on planar systems. All results can be extended to tree connected multibody systems and can be applied to many mechanical system with nonholonomic constraint. Dissert. Abstr.

N95-33712 Oregon State Univ., Corvallis, OR.

NONLINEAR ADAPTIVE CONTROL OF HIGHLY MANEUVERABLE HIGH PERFORMANCE AIRCRAFT Ph.D. Thesis

Sul Cho 1993 125 p

Avail: Univ. Microfilms Order No. DA9413708

This thesis presents an effective control design methodology using a one-step-ahead prediction adaptive control law and an adaptive control law based on a Lyapunov function. These control laws were applied to a highly maneuverable, high performance aircraft, in particular, a modified F/A-18. An adaptive controller is developed to maneuver an aircraft at a high angle of attack even if the aircraft is required to fly over a highly nonlinear flight regime. The adaptive controller is based on linear, bilinear, and nonlinear prediction models with input constraints. It is shown that the linear, bilinear, and nonlinear adaptive controllers can be constructed to minimize the given cost function or Lyapunov function with respect to the control input at each step. The control is calculated such that the system follows the reference trajectory, and such that control signal remains within its constraints. From several simulation results, the nonlinear controller is more effective than the linear controller as the angle of attack is increased. This thesis shows that nonlinear control can be utilized effectively to control high performance aircraft such as the F-18 aircraft for rapid maneuvers with large changes in angle of attack even if the nonlinear feedback controller operates with a higher-order (more delay terms) linear model reference. Dissert. Abstr.

N95-33713 Cincinnati Univ., OH.

IDENTIFICATION OF FLEXIBLE STRUCTURES UNDER CLOSED LOOP CONTROL Ph.D. Thesis

Albert Bernard Bosse 1993 121 p

Avail: Univ. Microfilms Order No. DA9416772

The focus is the development of methods for estimating open loop plant Markov parameters (i.e., impulse response functions) for multivariable flexible structures whose feedback control systems continue to operate during the data acquisition phase of identification experiments. Since all the approaches to closed loop identification considered here require the application of disturbance inputs to the system, in addition to the controls, special consideration is given to the minimization of these disturbances so that a major deterioration in controller performance can be avoided. To minimize the disruption caused by the disturbance inputs, two measures were developed in connection with the direct identification algorithm which indicate where additional disturbances must be applied and also whether the current input levels are adequate for the unique determination of system Markov parameters. One approach to the closed loop identification problem, called control signal perturbation, is a traditional closed loop identification approach that directly estimates the open loop plant Markov parameters using knowledge of both the disturbance and control inputs. A second approach, called extraction, is an indirect approach that estimates Markov parameters for the closed loop system, which are subsequently used to extract Markov parameters for the open loop plant using knowledge of the disturbance inputs and controller dynamics. The procedures developed for closed loop identification are demonstrated using analytical model data, and evaluated using experimental data for a flexible 4.6 meter space truss equipped with proof-mass actuators and accelerometers. Dissert. Abstr.

N95-33714 Cincinnati Univ., OH.

A ROBUST CONTROL SYSTEM FOR EXACT TRAJECTORY TRACKING Ph.D. Thesis

Yonghua Wei 1993 164 p

Avail: Univ. Microfilms Order No. DA9416808

The goal is to develop a method of designing robust control systems for trajectory tracking problems, such as those encountered in the design of industrial manipulators or robots. Inverse controllers are chosen for the trajectory tracking control problem, and are discussed in discrete time form, continuous time domain, and in the frequency domain. The relationship between exact tracking ability and the controllability of the system is proved in the discrete time case. The implementation of inverse controllers in continuous form is presented for many cases of tracking problems. The robustness of the closed loop system is studied. A new combined system of LQ-optimal full state feedback and an inverse controller is suggested for trajectory tracking problems. Several state observers are discussed for use in trajectory tracking when the full states are not available directly. The problem of observers with loop transfer recovery for a second order system is discussed in particular. A new method of function estimator design for some second order systems and nonregular systems to reach approximate LTR is presented. Three examples are used to demonstrate the control schemes and the observer design method. Dissert. Abstr.

N95-34467# Naval Research Lab., Washington, DC.

TOWARDS FRIENDLIER USER INTERFACES FOR EXPERT SYSTEMS

Elaine Marsh 1995 10 p

(AD-A294056) Avail: CASI HC A02/MF A01

Much research in computational linguistics and artificial intelligence has gone into characterizing natural language discourse structures, developing discourse models, and using these to develop more useful natural language interfaces to databases and expert systems. However, this knowledge about the nature of discourse has not been used to any advantage in graphical expert system interfaces. This paper proposes that discourse elements and discourse models used in the world of natural language understanding can be extended to graphical expert system interfaces, promoting continuity

of interactions and allowing relationships among interactions to be exploited, redundancy reduced, operations tracked, and higher-level operations recognized. DTIC

N95-34473# Naval Research Lab., Washington, DC.
ADAPTIVE STRATEGY SELECTION FOR CONCEPT LEARNING
William M. Spears and Diana F. Gordon 1995 16 p
(AD-A294086) Avail: CASI HC A03/MF A01

In this paper, we explore the use of genetic algorithms (GA's) to construct a system called GABIL that continually learns and refines concept classification rules from its interaction with the environment. The performance of this system is compared with that of two other concept learners (NEWGEM and C4.5) on a suite of target concepts. From this comparison, we identify strategies responsible for the success of these concept learners. We then implement a subset of these strategies within GABIL to produce a multistrategy concept learner. Finally, this multistrategy concept learner is further enhanced by allowing the GA's to adaptively select the appropriate strategies. DTIC

N95-34495# Navy Center for Applied Research in Artificial Intelligence, Washington, DC.
IMPROVING THE COMPREHENSIBILITY, ACCURACY, AND GENERALITY OF REACTIVE PLANS
Diana F. Gordon 1995 10 p
(AD-A294104) Avail: CASI HC A02/MF A01

This paper describes a method for improving the comprehensibility, accuracy, and generality of reactive plans. A reactive plan is a set of reactive rules. Our method involves two phases, formulate explanations of execution traces, and generate new reactive rules from the explanations. The explanation phase involves translating the execution trace of a reactive planner into an abstract language, and then using Explanation Based Learning to identify general strategies within the abstract trace. The rule generation phase consists of taking a subset of the explanations and using these explanations to generate a set of new reactive rules to add to the original set for the purpose of performance improvement. DTIC

N95-34497# Navy Center for Applied Research in Artificial Intelligence, Washington, DC.
CONDITIONS FOR IMPLICIT PARALLELISM
John J. Grefenstette 1995 10 p
(AD-A294110) Avail: CASI HC A02/MF A01

Many interesting varieties of genetic algorithms have been designed and implemented in the last fifteen years. One way to improve our understanding of genetic algorithms is to identify properties that are invariant across these seemingly different versions. This paper focuses on invariants among genetic algorithms that differ along two dimensions: the way user-defined objective function is mapped to a fitness measure, and the way the fitness measure is used to assign offspring to parents. A genetic algorithm is called admissible if it meets what seem to be the weakest reasonable requirements along these dimensions. It is shown that any admissible genetic algorithm exhibits a form of implicit parallelism. DTIC

N95-34499# Navy Center for Applied Research in Artificial Intelligence, Washington, DC.
IS THE GENETIC ALGORITHM A COOPERATIVE LEARNER?
Helen G. Cobb 1995 20 p
(AD-A294112) Avail: CASI HC A03/MF A01

This paper begins to explore an analogy between the usual competitive learning metaphor presented in the genetic algorithm (GA) literature and the cooperative learning metaphor discussed by Clearwater, Huberman, and Hogg. In a blackboard cooperative learning paradigm, agents share partial results with one another through a common blackboard. By occasionally accessing the blackboard for a partial solution, an agent can dramatically increase its speed in finding the overall solution to a problem. The study of Clearwater et al. shows that the resulting speed distribution among the agents is lognormal. The GA can also be described in terms of an analogous cooperative learning paradigm. Unlike the blackboard learner, the GA shares information by copying and recombining the solutions of the agents. This method of communication slows down the propagation of useful information to agents. The slower propagation of information is necessary because the GA cannot directly evaluate parts of a solution or partial solutions. The extent to which the GA is cooperative also depends on the choice of heuristics used to modify the canonical GA. The few test cases presented in this paper suggest that the GA may at times yield an approximately lognormal distribution or a mixture of lognormal distributions. While the results look promising, more analysis of the algorithm's overall process is required. DTIC

N95-34501# Navy Center for Applied Research in Artificial Intelligence, Washington, DC.
EXPLANATIONS OF EMPIRICALLY DERIVED REACTIVE PLANS
Diana F. Gordon and John J. Grefenstette 1995 7 p
(AD-A294114) Avail: CASI HC A02/MF A01

Given an adequate simulation model of the task environment and payoff function that measures the quality of partially successful plans, competition-based heuristics such as genetic algorithms can develop high performance reactive rules for interesting sequential decision tasks. We have previously described an implemented system, called SAMUEL, for learning reactive plans and have shown that the system can successfully learn rules for a laboratory scale tactical problem. In this paper, we describe a method for deriving explanations to justify the success of such empirically derived rule sets. The method consists of inferring plausible subgoals and then explaining how the reactive rules trigger a sequence of actions (i.e., a strategy) to satisfy the subgoals. DTIC

N95-34593# David Sarnoff Research Center, Princeton, NJ.
HYBRID PYRAMID/NEURAL NETWORK VISION SYSTEM Research and Development Status Report, 1 Mar. - 31 May 1995
John Pearson, Paul Sajda, and Clay Spence 31 May 1995 10 p
(Contract N00014-93-C-0202; ARPA Order A418)
(AD-A294919) Avail: CASI HC A02/MF A01

An artificial problem was constructed and described in the last report. During this quarter, another, more difficult, artificial problem was constructed. As before, the objects to be found and some potential false positives each have component patterns. Each positive has two different component patterns chosen from three types. In addition, the rectangles which form the objects and the sub-patterns all have artificial shadows added (Figure 1). The angle of the shadow is randomly-chosen. The potential false positive objects either have two component patterns of the same type, or only one pattern of some type, and one or both of the component patterns may not have a shadow. Thus the pattern tree must detect all three types of components with shadows to be able to detect a positive. As in the previous simpler problem, the positives and potential false-positives are 18-by-11 pixel rectangles, but now their brightness is randomly-chosen between 136 to 247. The sub-patterns have a brightness that is independently chosen at random from the same range, but both patterns (if there are two in an object) have the same brightness. The component patterns are three-by-three x, +, and square patterns. DTIC

N95-34600# Virginia Polytechnic Inst. and State Univ., Blacksburg, VA.
THEORY AND APPLICATION OF HOMOTOPY TECHNIQUES IN NONLINEAR PROGRAMMING AND CONTROL SYSTEMS Final Report, 1 May 1994 - 30 Apr. 1995
Layne T. Watson 28 Apr. 1995 8 p
(Contract F49620-92-J-0236)
(AD-A294934; AFOSR-95-0387TR) Avail: CASI HC A02/MF A01

The objective of this project was to derive global convergence theorems and practical numerical algorithms for probability-one homotopies in the area of constrained optimization, large sparse unstructured systems of nonlinear equations, H2 control design and analysis, and H 2/H infinity disturbance and rejection controls. The emphasis was on useful convergence theorems expressed in terms of conditions on the original problem rather than conditions on the derived problem. Important applications were considered as a guide to what theoretical questions should be asked. DTIC

N95-34602# Carnegie-Mellon Univ., Pittsburgh, PA. School of Computer Science.
EVERYDAY BELIEVABILITY
Garrett A. Pelton and Jill F. Lehman Mar. 1995 14 p
(Contract F33615-93-1-1330)
(AD-A294938; CMU-CS-95-133) Avail: CASI HC A03/MF A01

Believable Agents must be able to handle a large number of goals, opportunistically acting on them while maintaining a focus of purpose.

They also must be able to operate over long life times without significant performance degradations. We describe in this paper a method of managing an agent's goals so that the agent can make progress on as many goals as possible, without spending undue time considering goals that it can't make progress on. The key part of this method is a way of specializing and generalizing the set of perceptual cues that are used to bring a goal into consideration by the agent. The method is described via a simple example. DTIC

N95-34742# Virginia Univ., Charlottesville, VA.
CONTROL OF INITIALIZATION BIAS IN QUEUEING SIMULATIONS USING QUEUEING APPROXIMATIONS M.S. Thesis
Patrick J. Delaney May 1995 126 p
(AD-A294121) Avail: CASI HC A07/MF A02

The most widely used methodology of initialization bias control is that of data truncation. The idea is that the stochastic nature of the random variables will ultimately produce observations which are more representative of the steady-state of the system after a period of transience. The initial transient observations which bias an estimate are not representative of the steady state characteristics and can be deleted or thrown away. From that point in the output sequence to the end, the estimate will be less biased than taking the entire output sequence average. While these control methodologies are commonly known as heuristics, they do serve a purpose to provide the decision maker with the best possible information by doing the best they can with an output sequence. This research focuses on producing a good estimate from sequentially correlated simulation output data. I evaluate the use of proven accurate queueing approximations to stochastically set the initial queue length from the approximated steady state distribution to derive a better estimate than empty and idle, without the use of pilot runs. I also evaluate how point approximations can assist in controlling the bias in output estimates of a desired performance parameter through four truncation heuristics. The end result is a less biased and more accurate estimator of the expected wait in a queueing model. DTIC

N95-34807 Catholic Univ. of America, Washington, DC.
TRAJECTORY PLANNING AND CONTROL OF KINEMATICALLY REDUNDANT ROBOTIC MANIPULATORS Ph.D. Thesis
Zhen-Lei Zhou 1994 175 p
Avail: Univ. Microfilms Order No. DA9418591

This dissertation dealt with the development of trajectory planning schemes and advanced control schemes for kinematically redundant robotic manipulators (KRRM), classified as manipulators whose number of joints is greater than the dimension of the workspace. A globally optimal joint trajectory planning scheme was developed by applying the Pontryagin's minimum principle. This is an off-line optimization scheme which employed the shooting method to numerically solve the associated two point boundary value problem, and thereby to optimally resolve the KRRM redundancy. KRRM joint limits were taken into account by two considerable methods, the penalty function method and the state space augmentation method. Using the above methods, the singularity avoidance, joint limit, avoidance and motion conservativity at position/joint level were achieved simultaneously on the resultant optimal joint trajectories. The output of the optimal trajectory planning scheme is a set of desired joint control points satisfying the trajectory optimalities. An error-based direct adaptive control scheme was developed in order to deal with considerable uncertainties in KRRM dynamic model, including highly nonlinear and coupled dynamic equations, joint friction, gear backlashes, sudden payload changes, and other external disturbances. The adaptation scheme is obtained using the Lyapunov theorem and the concept of model reference adaptive control. This control scheme was developed in joint space and consists of a proportional feedback term, a derivative feedback term, and a feedforward compensator. The developed scheme is very computationally efficient as compared to existing model-based adaptive control schemes because it does not require the manipulator dynamics. In order to evaluate the above developed trajectory planning and adaptive control schemes, intensive computer simulations were performed on a three degree-of-freedom planar KRRM model considered for two-dimensional tasks. Several study cases were conducted with the desired joint trajectories generated by the optimal trajectory planning scheme, serving as the reference inputs to the adaptive control scheme. Computer simulation results showed that conservative trajectories avoiding joint limits and singularities were generated by the globally optimal trajectory planner. Simulation results also manifested that the developed adaptive control scheme was able to successfully react to sudden changes in payload, dynamic uncertainties, and time-varying manipulator parameters.
Dissert. Abstr.

N95-32433*# Houston Univ., TX. Dept. of Mathematics.
SCANNERS, OPTICAL CHARACTER READERS, CYRILLIC ALPHABET AND RUSSIAN TRANSLATIONS Final Report
Gordon G. Johnson *In* NASA. Johnson Space Center, National Aeronautics and Space Administration (NASA)/American Society for Engineering Education (ASEE) Summer Faculty Fellowship Program, 1994, Volume 1 Jul. 1995 5 p (For primary document see N95-32418 12-99)
(Grant NGT-44-005-308)
Avail: CASI HC A01/MF A03

N95-32434*# Rice Univ., Houston, TX. Dept. of Mechanical Engineering and Materials Science.
NUMERICAL SOLUTION OF DIFFERENTIAL EQUATIONS BY ARTIFICIAL NEURAL NETWORKS Final Report
Andrew J. Meade, Jr. *In* NASA. Johnson Space Center, National Aeronautics and Space Administration (NASA)/American Society for Engineering Education (ASEE) Summer Faculty Fellowship Program, 1994, Volume 1 Jul. 1995 13 p (For primary document see N95-32418 12-99)
(Grant NGT-44-005-803)
Avail: CASI HC A03/MF A03

N95-32495# Office National d'Etudes et de Recherches Aerospatiales, Chatillon (France).
AN ORIGINAL NUMERICAL METHOD FOR AUTONOMOUS NAVIGATION [UNE METHODE NUMERIQUE ORIGINALE POUR LA NAVIGATION AUTONOME]
Hubert Cantalloube *In* AGARD, Low-Level and Nap-of-the-Earth (NOE) Night Operations Jan. 1995 9 p In FRENCH (For primary document see N95-32486 12-03)
Copyright Avail: CASI HC A02/MF A03

64 NUMERICAL ANALYSIS

Includes iteration, difference equations, and numerical approximation.

N95-32388# Oak Ridge National Lab., TN.
A POSTERIORI POINTWISE ERROR ESTIMATES FOR THE BOUNDARY ELEMENT METHOD
G. H. Paulino (Cornell Univ., Ithaca, NY.), L. J. Gray, and V. Zarikian (University of Central Florida, Orlando, FL.) Jan. 1995 39 p
(Contract DE-AC05-84OR-21400)
(DE95-008099; ORNL/TM-12820) Avail: CASI HC A03/MF A01

This report presents a new approach for a posteriori pointwise error estimation in the boundary element method. The estimator relies upon the evaluation of hypersingular integral equations, and is therefore intrinsic to the boundary integral equation approach. This property allows some theoretical justification by mathematically correlating the exact and estimated errors. A methodology is developed for approximating the error on the boundary as well as in the interior of the domain. In the interior, error estimates for both the function and its derivatives (e.g. potential and interior gradients for potential problems, displacements and stresses for elasticity problems) are presented. Extensive computational experiments have been performed for the two dimensional Laplace equation on interior domains, employing Dirichlet and mixed boundary conditions. The results indicate that the error estimates successfully track the form of the exact error curve. Moreover, a reasonable estimate of the magnitude of the actual error is also obtained. DOE

N95-32389# State Univ. of New York, Stony Brook, NY. Dept. of Applied Mathematics and Statistics.
FIFTH INTERNATIONAL CONFERENCE ON HYPERBOLIC PROBLEMS, THEORY, NUMERICS, APPLICATIONS: ABSTRACTS
1994 111 p Presented at the 5th International Conference on Hyperbolic Problems, Stony Brook, NY, Jun. 1994

(Contract DE-FG02-94ER-25195)
(DE95-008173; CONF-9406279-Absts) Avail: CASI HC A06/MF A02

The conference demonstrated that hyperbolic problems and conservation laws play an important role in many areas including industrial applications and the studying of elasto-plastic materials. Among the various topics covered in the conference, the authors mention: the big bang theory, general relativity, critical phenomena, deformation and fracture of solids, shock wave interactions, numerical simulation in three dimensions, the level set method, multidimensional Riemann problem, application of the front tracking in petroleum reservoir simulations, global solution of the Navier-Stokes equations in high dimensions, recent progress in granular flow, and the study of elastic plastic materials. The authors believe that the new ideas, tools, methods, problems, theoretical results, numerical solutions and computational algorithms presented or discussed at the conference will benefit the participants in their current and future research. DOE

N95-32479# Joint Inst. for Nuclear Research, Dubna (USSR). Lab. of Theoretical Physics.

THE METHOD OF INTEGRATION OF THE NONLINEAR SCHROEDINGER EQUATION WITH A SOURCE

V. K. Melnikov 1994 30 p In RUSSIAN Submitted for publication in the Bulletin of the Technical Univ. of Istanbul
(DE95-623601; JINR-R-2-94-226) Avail: CASI HC A03/MF A01 (US Sales Only)

It is shown that the nonlinear Schroedinger equation with a source can be investigated by the inverse scattering method for the Dirac operator if the source is represented as the Fourier integral over the eigenfunctions of the so-called generating operator. The conditions are found under which the nonlinear Schroedinger equation with a source has a pure soliton solution. The obtained results are relevant to some problems of plasma physics and solid state physics. DOE

N95-32523# International Centre for Theoretical Physics, Trieste (Italy).

MAXIMUM PRINCIPLE FOR SUBSOLUTIONS OF DEGENERATE ELLIPTIC OPERATORS

Mythily Ramaswamy (Tata Inst. of Fundamental Research, Bangalore, India.) and S. Ramaswamy Sep. 1994 10 p
(DE95-613373; IC-94/266) Avail: CASI HC A02/MF A01 (US Sales Only)

The maximum principle for classical and viscosity subsolutions of a general degenerate elliptic linear second order operator with second and first order terms alone on bounded open subsets is proved under various assumptions on the coefficients. A general sufficient condition is given when the coefficients are continuous. A counter example is also given to show that the maximum principle is not valid even for classical subsolutions of degenerate elliptic operators in general. DOE

N95-32559# Lawrence Livermore National Lab., Livermore, CA.

DIFFERENCING THE DIFFUSION EQUATION ON UNSTRUCTURED MESHES IN 2-D

Todd S. Palmer 24 Oct. 1994 11 p
(Contract W-7405-eng-48)
(DE95-010410; UCRL-ID-119045) Avail: CASI HC A03/MF A01

During the last few years, there has been an increased effort to devise robust transport differencings for unstructured meshes, specifically arbitrarily connected grids of polygons. Adams has investigated unstructured mesh discretization techniques for the even- and odd-parity forms of the transport equation, and for the more traditional first-order form. Conversely, development of unstructured mesh diffusion methods has been lacking. While Morel, Kershaw, Shestakov and others have done a great deal of work on diffusion schemes for logically-rectangular grids, to the author's knowledge there has been no work on discretizations of the diffusion equation on unstructured meshes of polygons. In this paper, the authors introduce a point-centered diffusion differencing for two-dimensional unstructured meshes. They have designed the method to have the following attractive properties: (1) the scheme is equivalent to the standard five-point point-centered scheme on an orthogonal mesh; (2) the method preserves the homogeneous linear solution; (3) the method gives second-order accuracy; (4) they have strict conservation within the control volume surrounding each point; and (5) the numerical solution converges to the exact result as the mesh is refined, regardless of the smoothness of the mesh. A potential disadvantage of the method is that the diffusion matrix is asymmetric, in general. DOE

N95-32609# Joint Inst. for Nuclear Research, Dubna (USSR). Lab. of Theoretical Physics.

CAMPBELL-HAUSDORFF FORMULA AND ALGEBRAS WITH OPERATOR

O. M. Khudaverdyan (Erivan State Univ., Erivan, Armenia.) 1994 11 p Submitted for publication in Letters in Mathematical Physics
(DE95-623635; JINR-E-2-94-356) Avail: CASI HC A03/MF A01 (US Sales Only)

Some new classes of algebras are introduced and in these algebras Campbell-Hausdorff like formula is established. The application of these constructions to the problem of the connectivity of the Feynman graphs corresponding to the Green functions in Quantum Field Theory is described. DOE

N95-32889# Royal Inst. of Tech., Stockholm (Sweden). Dept. of Mathematics.

ASSOCIATIVE INTEGRAL FORMULAS AND DEFORMATIONS OF YANGIANS

A. A. Stolin Nov. 1994 18 p
(PB95-212189; TRITA-MAT-1994-0042) Avail: CASI HC A03/MF A01

Let g be a simple Lie algebra over C (the set of complex numbers). Let c(2) belonging to g x(circled) g be an invariant element, which is unique up to a scalar factor. Then c(2)/u is the famous rational solution of the classical Yang-Baxter equation (CYBE). The corresponding quantum object is called Yangian and is a deformation of the co-commutative Hopf algebra U(g(u)). NTIS

N95-32890# Royal Inst. of Tech., Stockholm (Sweden). Dept. of Mathematics.

COUNTEREXAMPLE TO THE LIEB-THIRRING CONJECTURE CONCERNING THE MOMENTS OF THE EIGENVALUES OF THE SCHROEDINGER OPERATOR

Ari Laptev Jan. 1995 12 p
(PB95-212197; TRITA-MAT-1995-0004) Avail: CASI HC A03/MF A01

We give an example of a Schrodinger operator whose first eigenvalue lambda(sub 1) satisfies the inequality lambda(sub 1) is greater than 1.0733L(sub 1,3, sup cl) integral of V(sup 5/2)dx. NTIS

N95-32893 Technische Univ., Delft (Netherlands). Faculty of Technical Mathematics and Informatics.

SUM OF FRACTIONAL DERIVATIVES AND m-ACCRETIVE OPERATORS

P. Clement and S. O. Londen 1994 15 p Limited Reproducibility: More than 20% of this document may be affected by microfiche quality
(ISSN 0922-5641)
(PB95-215307; Rept-94-68) Copyright Avail: CASI HC A03

The authors study an abstract integrodifferential equation in a real Hilbert space H. The scalar-valued kernel k is assumed to be locally integrable, positive and nonincreasing on R(+). Although this is not explicitly assumed, the main interest lies in the case where k(0+) = infinity. The goal is to obtain the existence of a unique strong solution. NTIS

N95-33058# International Centre for Theoretical Physics, Trieste (Italy).

TRACING A PLANAR ALGEBRAIC CURVE

Fa Lai Chen (China Scientific and Technical Univ., Hofei, China.), Yu Yu Feng, and Jernej Kozak (Ljubljana Univ., Yugoslavia.) Sep. 1994 15 p
(DE95-613375; IC-94/279) Avail: CASI HC A03/MF A01 (US Sales Only)

An algorithm that determines a real algebraic curve is outlined. Its basic step is to divide the plane into subdomains that include only simple branches of the algebraic curve without singular points. Each of the branches is then stably and efficiently traced in the particular subdomain. Except for the tracing, the algorithm requires only a couple of simple operations on polynomials that can be carried out exactly if the coefficients are rational, and the determination of zeros of several polynomials of one variable. DOE

N95-33233# Royal Inst. of Tech., Stockholm (Sweden). Dept. of Mathematics.
BOUNDARY AND LENS RIGIDITY OF LORENTZIAN SURFACES
Lars Andersson, Mattias Dahl, and Ralph Howard Dec. 1994 26 p Prepared in cooperation with South Carolina Univ. and the Swedish Natural Science Research Council Sponsored in part by the Wallenberg Foundation, the Swedish Academy of Sciences, and the Crafoord Foundation
(PB95-212163; TRITA-MAT-1994-0045) Avail: CASI HC A03/MF A01

Let g be a Lorentzian metric on the plane R(sup 2) that agrees with the standard metric g(sub 0) = -dx(squared) + dy(squared) outside a compact set and so that there are no conjugate points along any time-like geodesic of (R(sup 2), g). Then (R(sup 2), g) and (R(sup 2), g(sub 0)) are isometric. Further, if (M, g) and (M*, g*) are two dimensional compact time oriented Lorentzian manifolds with space-like boundaries and so that all time-like geodesics of (M, g) maximize the distances between their points and ((M, g) and M*, g*) are 'boundary isometric' then there is a conformal diffeomorphism between (M, g) and (M*, g*) and they have the same areas. Similar results hold in higher dimensions under an extra assumption on the volumes of the manifolds. NTIS

N95-33234# Royal Inst. of Tech., Stockholm (Sweden). Dept. of Mathematics.
LIEB-THIRRING CONSTANTS L(SUB GAMMA,1) FOR GAMMA GREATER THAN OR EQUAL TO 1/2
Timo Weidl Jan. 1995 12 p
(PB95-212171; TRITA-MAT-1995-0005) Avail: CASI HC A03/MF A01

Let E(sub i, sup H) denote the negative eigenvalues of the one-dimensional Schroedinger operator Hu := -u(double prime) - Vu, V greater than or equal to 0, on L(sub 2)(R). We prove this inequality: summation over i of (absolute value of E(sub i, sup H))(sup gamma) less than or equal to L(sub gamma,1) (the integral over R of V(sup gamma+ 1/2)(x)dx), for the 'limit' case gamma = 1/2. This will imply improved estimates for the best constants L(sub gamma, 1) as 1/2 is less than gamma less than 3/2. NTIS

N95-33248# EG and G Mound Applied Technologies, Miamisburg, OH.
OPERATIONAL EQUATIONS FOR THREE-DIMENSIONAL DATA
Gary L. Silver 12 Apr. 1995 17 p
(Contract DE-AC24-88DP-43495)
(DE95-011332; MLM-3810) Avail: CASI HC A03/MF A01

Three categories of easy-to-use, nonlinear equations for rectangular prisms are presented: (1) polynomial equations of the second degree, (2) an equation using the hyperbolic and circular functions, and (3) equations using simple exponentials. All of the methods are new; they are based on operational calculus. DOE

N95-33500*# Institute for Computer Applications in Science and Engineering, Hampton, VA.
A UNIFIED MULTIGRID SOLVER FOR THE NAVIER-STOKES EQUATIONS ON MIXED ELEMENT MESHES Final Report
D. J. Mavriplis and V. Venkatakrishnan Jul. 1995 27 p Submitted for publication in International Journal of Computational Fluid Dynamics
(Contract NAS1-19480; RTOP 505-90-52)
(NASA-CR-198183; NAS 1.26:198183; ICASE-95-53) Avail: CASI HC A03/MF A01

A unified multigrid solution technique is presented for solving the Euler and Reynolds-averaged Navier-Stokes equations on unstructured meshes using mixed elements consisting of triangles and quadrilaterals in two dimensions, and of hexahedra, pyramids, prisms, and tetrahedra in three dimensions. While the use of mixed elements is by no means a novel idea, the contribution of the paper lies in the formulation of a complete solution technique which can handle structured grids, block structured grids, and unstructured grids of tetrahedra or mixed elements without any modification. This is achieved by discretizing the full Navier-Stokes equations on tetrahedral elements, and the thin layer version of these equations on other types of elements, while using a single edge-based data-structure to construct the discretization over all element types. An agglomeration multigrid algorithm, which naturally handles meshes of any types of elements, is employed to accelerate convergence. An automatic algorithm which reduces the complexity of a given triangular or tetrahedral mesh by merging candidate triangular or tetrahedral elements into quadrilateral or prismatic elements is also described. The gains in computational efficiency afforded by the use of non-simplicial meshes over fully tetrahedral meshes are demonstrated through several examples. Author

N95-33727*# Institute for Computer Applications in Science and Engineering, Hampton, VA.
KRYLOV METHODS FOR COMPRESSIBLE FLOWS Final Report
M. D. Tidriri Jun. 1995 32 p Submitted for publication in Computer Methods in Applied Mechanics and Engineering
(Contract NAS1-19480; RTOP 505-90-52-01)
(NASA-CR-198176; NAS 1.26:198176; ICASE-95-48) Avail: CASI HC A03/MF A01

We investigate the application of Krylov methods to compressible flows, and the effect of implicit boundary conditions on the implicit solution of nonlinear problems. Two defect-correction procedures, namely, approximate factorization (AF) for structured grids and ILU/GMRES for general grids, are considered. Also considered here are Newton-Krylov matrix-free methods that we combined with the use of mixed discretization schemes in the implicitly defined Jacobian and its preconditioner. Numerical experiments that show the performance of our approaches are then presented. Author

N95-34377# Rockwell International Corp., Thousand Oaks, CA. Science Center.
EFFICIENT TIME DOMAIN SOLUTIONS OF MAXWELL'S EQUATIONS FOR AEROSPACE SYSTEMS Final Report, 1 Sep. 1993 - 10 Mar. 1995
Vijaya Shankar, W. Hally, C. Rowell, and A. Tohammaian 17 Apr. 1995 108 p
(Contract F49620-93-C-0066)
(AD-A294019; AFOSR-95-0341TR) Avail: CASI HC A06/MF A02

This report contains the development of an unstructured grid-based finite-volume integration scheme for solving the time-domain Maxwell's equations to study a myriad of problems in electromagnetics. The principal application of this technology is the prediction of radar cross section (RCS) of low observable platforms. DTIC

N95-34803 Washington Univ., Seattle, WA.
UNCERTAINTY ANALYSIS USING STOCHASTIC FINITE ELEMENTS Ph.D. Thesis
Tushar Dasharath Fadale 1993 133 p
Avail: Univ. Microfilms Order No. DA9417007

A technique is developed for the finite element method to analyze systems exhibiting uncertainties and to determine the effect of these uncertainties on the system's response. The uncertainties are classified based on their causes and are modeled as random fields for consistent mathematical manipulation. There are two broad approaches to analyze systems with uncertainties. One is the more expensive statistical approach while the other is a nonstatistical approach. The merits and demerits of both these approaches are discussed. The first/second order, second moment technique, a nonstatistical approach, is chosen for implementation in the finite element method. This modified finite element method is referred to as the stochastic finite element method. The computational aspect of the stochastic finite element, as compared to the conventional deterministic finite element, is discussed. The stochastic finite element code was validated using the Monte Carlo technique of random sampling. Finally the application of stochastic finite elements is demonstrated through two case studies, one for sensitivity analysis and the other for optimal experimental design. Dissert. Abstr.

N95-34054# Laboratoire de Medecine Aerospatiale, Bretigny-sur-Orge (France).
ANTI-G SUITS
J. M. Clere, G. Ossard, and M. Kerguelen *In* AGARD, Current Concepts on G-Protection Research and Development May 1995 8 p (For primary document see N95-34050 12-54)
Copyright Avail: CASI HC A02/MF A02

65 STATISTICS AND PROBABILITY

Includes data sampling and smoothing; Monte Carlo method; and stochastic processes.

N95-32391# Los Alamos National Lab., NM.
APPROACHES TO IMPLEMENTING DETERMINISTIC MODELS IN A PROBABILISTIC FRAMEWORK
D. V. Talbott 1995 8 p Presented at the Joint ASME/JSME Pressure Vessels and Piping Conference, Honolulu, HI, 23-27 Jul. 1995
(Contract W-7405-eng-36)
(DE95-009483; LA-UR-95-1117; CONF-950740-21) Avail: CASI HC A02/MF A01

The increasing use of results from probabilistic risk assessments in the decision-making process makes it ever more important to eliminate simplifications in probabilistic models that might lead to conservative results. One area in which conservative simplifications are often made is modeling the physical interactions that occur during the progression of an accident sequence. This paper demonstrates and compares different approaches for incorporating deterministic models of physical parameters into probabilistic models; parameter range binning, response curves, and integral deterministic models. An example that combines all three approaches in a probabilistic model for the handling of an energetic material (i.e. high explosive, rocket propellant,...) is then presented using a directed graph model. DOE

N95-32624# Joint Inst. for Nuclear Research, Dubna (USSR).
BOGOLYUBOV LECTURES
1994 215 p Presented at the International Bogolyubov Memorial Meeting, Dubna, Russia, 19-21 Aug. 1993
(DE95-620495; JINR-94-55; CONF-9308260) Avail: CASI HC A10/MF A03 (US Sales Only)

The papers of the International Bogolyubov Memorial Meeting at Dubna in August 19-21, 1993 are given. The meeting pays special attention to problems of kinetic theory, polaron theory, multiparticle distribution functions in problems of statistical mechanics and other aspects of modern physics. DOE

N95-33220# Lawrence Livermore National Lab., Livermore, CA.
A COMPARISON OF RISK ASSESSMENT TECHNIQUES FROM QUALITATIVE TO QUANTITATIVE
Thomas J. Altenbach 13 Feb. 1995 24 p Presented at the Joint ASME/JSME Pressure Vessels and Piping Conference, Honolulu, HI, 23-27 Jul. 1995
(Contract W-7405-eng-48)
(DE95-011430; UCRL-JC-118794; CONF-950740-36) Avail: CASI HC A03/MF A01

Risk assessment techniques vary from purely qualitative approaches, through a regime of semi-qualitative to the more traditional quantitative. Constraints such as time, money, manpower, skills, management perceptions, risk result communication to the public, and political pressures all affect the manner in which risk assessments are carried out. This paper surveys some risk matrix techniques, examining the uses and applicability for each. Limitations and problems for each technique are presented and compared to the others. Risk matrix approaches vary from purely qualitative axis descriptions of accident frequency vs consequences, to fully quantitative axis definitions using multi-attribute utility theory to equate different types of risk from the same operation. DOE

66 SYSTEMS ANALYSIS

Includes mathematical modeling; network analysis; and operations research.

N95-32758# General Accounting Office, Washington, DC. National Security and International Affairs Div.
REPORT TO CONGRESSIONAL COMMITTEES. B-1B BOMBER: EVALUATION OF AIR FORCE REPORT ON B-1B OPERATIONAL READINESS ASSESSMENT
18 Jul. 1995 23 p
(GAO/NSIAD-95-151; B-261347) Avail: CASI HC A03/MF A01; GAO, PO Box 6015, Gaithersburg, MD 20877 HC

The Air Force was required to test the operational readiness rate of one B-1B bomber wing if the wing was provided the planned complement of spare parts, maintenance equipment and manpower, and logistics support equipment. The tests -- referred to as the B-1B Operational Readiness Assessment (ORA) -- were conducted from 1 June 1994 through 30 November 1994. The ORA test plan was complete and comprehensive. Further, the ORA was conducted in accordance with the test plan. The ORA demonstrated that, given a full complement of spare parts, equipment, and manpower, the Air Force could achieve and sustain a 75% mission capable rate for the B-1B. But, the ORA was not exclusively used to project the cost of sustaining the entire B-1B fleet at that rate. At the completion of the ORA, the mission capable rate for the B-1B fleet was about 65%. The Air Force believes that the completion of ongoing initiatives in progress and the continued funding for spare parts and repairs will increase the fleet mission capable rate to 72%. The Air Force estimates that for an additional $11.19 million for management actions and reliability and maintainability improvements, the B-1B fleet has the potential to achieve and sustain a 75% mission capable rate by 2000. The GAO believes the $11.19 million estimate, which was based on various modeling techniques, is optimistic. Neither the GAO nor the Air Force can predict how successful the ongoing or planned initiatives will be. Therefore, the potential cost to achieve and sustain a 75% mission capable rate for the B-1B is still not known. Derived from text

N95-32807# General Accounting Office, Washington, DC. National Security and International Affairs Div.
REPORT TO CONGRESSIONAL COMMITTEES. AIR FORCE FIGHTERS: MORE RELIANCE ON RESERVES INCREASES THE NEED TO KNOW THEIR CAPABILITIES
9 May 1994 48 p
(GAO/NSIAD-94-86; B-255905) Avail: CASI HC A03/MF A01; GAO, PO Box 6015, Gaithersburg, MD 20877 HC

This report discusses the relative capabilities of active and reserve Air Force fighter forces and the adequacy of current reporting mechanisms to identify differences between those forces. This review assesses the Air National Guard and Air Force Reserve capability for more rapid and direct involvement in future conflicts and the differences between active and reserve fighter forces' capabilities as indicated by Air Force assessments. This review finds the reserve force's fighter aircraft units generally less capable in terms of their aircraft, level of training, and availability than corresponding active fighter aircraft units. The capability of reserve fighter forces to deploy and fight upon arrival is unclear because current Air Force indicators do not uniformly assess the relative capabilities of reserve and active units. The Air Force's Status of Resources and Training System (SORTS) and other assessments indicate reserve forces are as prepared as active forces to meet future contingencies; however, several factors that these assessments do not measure could affect decisions about crises response, missions, and training. Derived from text

N95-32886# General Accounting Office, Washington, DC. National Security and International Affairs Div.
REPORT TO THE HONORABLE WILLIAM V. ROTH, JR., US SENATE. NAVAL AVIATION: F/A-18 E/F ACQUISITION STRATEGY
Aug. 1994 10 p
(GAO/NSIAD-94-194; B-248882) Avail: CASI HC A02/MF A01; GAO, PO Box 6015, Gaithersburg, MD 20877 HC

This study determines whether the DOD's acquisition regulations permitted classification of the F/A-18E/F program as a major modification rather than a new program to avoid the more rigorous review, analysis, and documentation required to justify a new program. The Under Secretary of Defense for Acquisition, on May 12, 1992, approved the Navy's October 1991 request that the F/A-18E/F development be designated as a major modification of its existing F/A-18C/D, instead of a new program. He decided that acquisition regulations did not require a Cost and Operational Effectiveness Analysis (COEA) for this modification, and he waived certain live fire testing requirements. The decisions were based on (1) Navy analyses that indicated the E/F development was a low to moderate risk and (2) recommendations made by the Conventional Systems Committee of the Defense Acquisition Board (DAB). Applicable defense acquisition regulations allow management discretion in these matters for the purpose of minimizing

development time and reducing cost. No conclusion is made at this point whether the decisions made thus far will have a positive or negative effect on the program. CASI

N95-33263# General Accounting Office, Washington, DC. National Security and International Affairs Div.
REPORT TO THE CHAIRMAN, COMMITTEE ON ARMED SERVICES, US SENATE. STRATEGIC BOMBER: ISSUES RELATING TO THE B-1B'S AVAILABILITY AND ABILITY TO PERFORM CONVENTIONAL MISSIONS
10 Jan. 1994 17 p
(GAO/NSIAD-94-81; B-256104) Avail: CASI HC A03/MF A01; GAO, PO Box 6015, Gaithersburg, MD 20877 HC

This report reviews issues concerning the B-1B bomber as its operational orientation shifts from nuclear to conventional missions. It focuses on (1) the operational status of the B-1B fleet and (2) the impact of engine problems and structural cracks found on the aircraft on the availability of B-1Bs. Derived from text

N95-33875*# National Aeronautics and Space Administration. Ames Research Center, Moffett Field, CA.
A RELATIONAL METRIC, ITS APPLICATION TO DOMAIN ANALYSIS, AND AN EXAMPLE ANALYSIS AND MODEL OF A REMOTE SENSING DOMAIN
Michael W. McGreevy Jul. 1995 61 p
(RTOP 199-06-30)
(NASA-TM-110358; A-950075; NAS 1.15:110358) Avail: CASI HC A04/MF A01

An objective and quantitative method has been developed for deriving models of complex and specialized spheres of activity (domains) from domain-generated verbal data. The method was developed for analysis of interview transcripts, incident reports, and other text documents whose original source is people who are knowledgeable about, and participate in, the domain in question. To test the method, it is applied here to a report describing a remote sensing project within the scope of the Earth Observing System (EOS). The method has the potential to improve the designs of domain-related computer systems and software by quickly providing developers with explicit and objective models of the domain in a form which is useful for design. Results of the analysis include a network model of the domain, and an object-oriented relational analysis report which describes the nodes and relationships in the network model. Other products include a database of relationships in the domain, and an interactive concordance. The analysis method utilizes a newly developed relational metric, a proximity-weighted frequency of co-occurrence. The metric is applied to relations between the most frequently occurring terms (words or multiword entities) in the domain text, and the terms found within the contexts of these terms. Contextual scope is selectable. Because of the discriminating power of the metric, data reduction from the association matrix to the network is simple. In addition to their value for design, the models produced by the method are also useful for understanding the domains themselves. They can, for example, be interpreted as models of presence in the domain. Author

N95-32493# British Aerospace Aircraft Group, Preston (England). Warton Aerodrome.
OPTIMUM ROUTEING: ANALYTICAL CONSTRAINT OF SEARCH SPACE
W. G. Semple *In* AGARD, Low-Level and Nap-of-the-Earth (NOE) Night Operations Jan. 1995 10 p (For primary document see N95-32486 12-03)
Copyright Avail: CASI HC A02/MF A03

N95-32494# GEC-Marconi Avionics Ltd., Rochester (England).
A TACTICAL NAVIGATION AND ROUTEING SYSTEM FOR LOW-LEVEL FLIGHT
C. Hewitt and S. A. Broatch *In* AGARD, Low-Level and Nap-of-the-Earth (NOE) Night Operations Jan. 1995 10 p (For primary document see N95-32486 12-03)
Copyright Avail: CASI HC A02/MF A03

N95-32496# Defence Research Agency, Farnborough, Hampshire (England).
THE APPLICATION OF HELICOPTER MISSION SIMULATION TO NAP-OF-THE-EARTH OPERATIONS
P. R. Birkett and D. W. Roden *In* AGARD, Low-Level and Nap-of-the-Earth (NOE) Night Operations Jan. 1995 5 p (For primary document see N95-32486 12-03)
Copyright Avail: CASI HC A01/MF A03

N95-32498# Alenia Aeronautica, Turin (Italy). System Technology Dept.
AN INTEGRATED SYSTEM FOR AIR TO GROUND OPERATIONS
Massimo Availe *In* AGARD, Low-Level and Nap-of-the-Earth (NOE) Night Operations Jan. 1995 10 p (For primary document see N95-32486 12-03)
Copyright Avail: CASI HC A02/MF A03

N95-32505# Defence Research Agency, Farnborough, Hampshire (England). Man Machine Integration Dept.
COVERT NIGHT/DAY OPERATIONS FOR ROTORCRAFT (CONDOR) PROGRAMME
T. H. Southam *In* AGARD, Low-Level and Nap-of-the-Earth (NOE) Night Operations Jan. 1995 16 p (For primary document see N95-32486 12-03)
Copyright Avail: CASI HC A03/MF A03

67 THEORETICAL MATHEMATICS

Includes topology and number theory.

No abstracts in this category.

70 PHYSICS (GENERAL)

For precision time and time interval (PTTI) see *35 Instrumentation and Photography;* for geophysics, astrophysics or solar physics see *46 Geophysics, 90 Astrophysics,* or *92 Solar Physics.*

N95-32397# Ames Lab., IA.
ANISOTROPIC MAGNETIZATION OF HoNi2B2C
P. C. Canfield, B. K. Cho, D. C. Johnston, and M. F. Hundley (Los Alamos National Lab., NM.) 1994 6 p Presented at the 1994 Fall Meeting of the Materials Research Society (MRS), Boston, MA, 28 Nov. - 2 Dec. 1994
(Contract W-7405-eng-82)
(DE95-010239; IS-M-816; CONF-941144-124) Avail: CASI HC A02/MF A01

Anisotropic, temperature dependent magnetization measurements on single crystals of HoNi2B2C indicate that there is a cascade of magnetic transitions in zero and low applied magnetic fields. Comparison of the temperature dependence of the specific heat and d((chi)T)/dT data shows a remarkable agreement in the low field limit, supporting the use of d((chi)T)/dT as a method of determining the magnetic transition temperatures as a function of applied field. The magnetic transition temperatures determined by this analysis are remarkably sensitive to the applied field and highly anisotropic. Comparison to similar data for ErNi2B2C show that the sensitivity and anisotropy a re common features. These data emphasize the importance of anisotropic measurements of field dependent properties on single crystal samples, since the application of a magnetic field to a polycrystalline sample will effectively broaden the transition temperatures. DOE

N95-32525# International Centre for Theoretical Physics, Trieste (Italy).
PROBE TRANSPARENCY IN A TWO-LEVEL MEDIUM EMBEDDED BY A SQUEEZED VACUUM
S. Swain and P. Zhou Aug. 1994 22 p
(DE95-614123; IC-94/243) Avail: CASI HC A03/MF A01 (US Sales Only)

Effect of the detuning on the probe absorption spectra of a two-level

system with and without a classically driven field in a squeezed vacuum is investigated. For a strong squeezing, there is a threshold which determines the positions and widths of the absorption peaks, for the squeezed parameter M. In a large detuning, the spectra exhibit some resemblance to the Fano spectrum. The squeezing-induced transparency occurs at the frequency 2 omega(sub L) - omega(sub A) in the minimum-uncertainty squeezed vacuum. This effect is not phase-sensitive. DOE

N95-33292 Illinois Univ., Urbana-Champaign, IL.
DESIGN AND ANALYSIS OF TRANSIENT NONLINEAR COUPLED SYSTEMS Ph.D. Thesis
Panagiotis Michaleris 1994 139 p
Avail: Univ. Microfilms Order No. DA9416407

Techniques for efficient and systematic design and analysis of transient nonlinear coupled problems are presented. This class of problems includes systems with history dependent material response, e.g. plasticity. The traditional finite element analysis is combined with sensitivity analysis and numerical optimization to obtain a systematic design algorithm. Sensitivities for a generalized response function are formulated with respect to design parameters, i.e. shape, applied loads, prescribed initial and boundary conditions, and material properties. The generalized response functional depends on the design parameters both explicitly and implicitly through the system's response, e.g. temperature, heat flux, displacement, plastic hardening, stress, strain and reaction forces. Analytic sensitivities are formulated via both the direct differentiation and adjoint methods. The formulations are particularized to the case of rate-independent elasto-plasticity. Analytic sensitivities for weakly coupled thermo-elasto-plastic systems are computed with the finite element method by implementing the direct differentiation method. The solution process for the transient nonlinear coupled problems uses the Newton-Raphson iteration method so that analytic design sensitivities may be readily evaluated. The formulation is particularized to elasto-plastic and weakly coupled thermo-elasto-plastic systems by implementing the algorithmic tangent operator. A systematic numerical approach to compute the algorithmic tangent operator is formulated that facilitates systematic and modular computer implementation. A simple one-dimensional problem with an analytical solution is studied to demonstrate the adjoint and direct differentiation sensitivity evaluation for rate-independent elasto-plasticity. The finite element method is used to perform the weakly coupled thermo-elasto-plasticity analysis and sensitivity analysis for more complicated problems. The sensitivity computations are compared with expensive finite difference approximations for verification purposes. The analysis and sensitivity analysis capabilities are combined with numerical optimization to optimize the design of a butt weldment with respect to both manufacturing and service life aspects. Dissert. Abstr.

N95-33415 George Mason Univ., Fairfax, VA.
MODELING AND INFERENCE WITH FRACTIONAL BROWNIAN MOTION AND FRACTIONAL GAUSSIAN NOISE Ph.D. Thesis
Winston Chih Chow 1994 167 p
Avail: Univ. Microfilms Order No. DA9417922

Stochastic modeling in the form of stochastic differential equations driven by Gaussian white noise or its corresponding standard Brownian motion (also called Wiener process) has been extensively studied. Parametric estimators have been developed for certain parameters in some forms of stochastic differential equations driven by standard Brownian motion (Wiener process). However, some real-life processes exhibit noise processes that are not represented accurately by Gaussian white noise or its corresponding standard Brownian motion. An alternate model is the fractional Brownian motion and its corresponding fractional Gaussian noise. This process can be used to represent some real-life processes more accurately than the conventionally used Gaussian white noise process. The objective of the research is to find optimal estimators for finite and infinite dimensional parameters for certain representative stochastic differential equations that are driven by fractional Gaussian noise, instead of the conventional Gaussian white noise process. This work is useful in information technology because it will provide statistical estimators for mathematical models driven by fractional Gaussian noise that represent some physical system or phenomena more accurately than its corresponding model driven by Gaussian white noise. In particular, physical processes that contain random noise that exhibit long term, slowly decreasing dependencies with low frequency, slowly decreasing spectral power are candidates for modeling with stochastic differential equations where the noise process is fractional Gaussian noise. For example, river discharges may tend to exhibit groups of low and high periods and thus exhibit long term dependencies. Also, signals produced by the motion of objects in water such as submarines possess an uncountably infinite number of frequencies over an interval. These frequencies being uncountably infinite in number over an interval can be modeled by a process with slowly decreasing spectral power. Also, the correlation between occurrences of these signals during two different times decreases as the difference in time increases, meaning that they possess long term decreasing dependencies. Dissert. Abstr.

N95-34269# California Univ., Berkeley. Lawrence Berkeley Lab, CA. Accelerator and Fusion Research Div.
THE BEAM ENVELOPE EQUATION-SYSTEMATIC SOLUTION FOR A PERIODIC QUADRUPOLE LATTICE WITH SPACE CHARGE
Edward P. Lee Apr. 1995 22 p
(Contract DE-AC03-76SF-00098)
(DE95-012761; LBL-37050; UC-414) Avail: CASI HC A03/MF A01

Many approximate solutions for matched beam envelope functions with space charge have been developed; they generally have errors of 2-10% for the parameters of interest and cannot be reliably improved. The new, systematic approach described here provides the K-V envelope functions to high accuracy as a power series in the quadrupole gradient. A useful simplification results from defining the sum and difference of the envelope radii; S = (a+b)/2 varies only slightly with distance z along the system axis, and D = (a-b)/2 contains most of the envelope oscillations. To solve the coupled equations for S and D, the quadrupole strength K(z) is turned on by replacing K with alpha K(sub 1) and letting alpha increase continuously from 0 to 1. It is found that S and D may be expanded in even and odd powers of alpha, respectively. Equations for the coefficients of powers of alpha are then solved successively by integration in z. The periodicity conditions and tune integration close the calculation. Simple low order results are typically accurate to 1% or better. DOE

N95-34477 Advanced Fuel Research, Inc., East Hartford, CT.
NOVEL FERROELECTRIC HETEROSTRUCTURES FOR HIGH-DENSITY DRAMS Final Report, 1-30 Apr. 1995
Pang-Jen Kung and David B. Fenner 25 May 1995 25 p
(Contract DAAH04-94-C-00021)
(AD-A294517; AFR-529025) Avail: Issuing Activity (Defense Technical Information Center (NTIS))

In pursuit of oxide ferroelectric materials in perovskite phases with high dielectric constants used as storage capacitor dielectrics in new-generation dynamic random access memories (DRAM's), development of the process for fabricating film capacitors in planar structures of small dimensions is a central issue of great importance. From the point of view of device performance, such effort includes not only the deposition of epitaxial ferroelectric films but also the integration of associated top and bottom electrodes. The objective of the present study is, therefore, to explore the feasibility of a process based on all oxide materials for dielectrics and electrodes. As such, thin, epitaxial ferroelectric films (FE) including BaTiO3, (Ba, Sr)TiO3, and Pb(Zr, Ti)O3 stacked in a multilayer structure of M/FE/M/B, where M is the conducting oxide electrode and B is the oxide buffer layer, have been successfully grown in this work by pulsed laser deposition on Si(100) wafers. Scanning electron microscopy, X-ray diffractometry, and transmission electron microscopy were employed to characterize these multilayer films for their morphology, crystallinity, and microstructure, respectively. Dielectric constants, leakage, hysteresis loops, remanent polarization, saturation voltage, and fatigue were measured to study the device potential. Our findings have provided valuable information on the realization of oxide ferroelectric film capacitors applied in DRAM's, but more work is still needed to improve the fatigue behavior and understand the microstructure-related device physics. DTIC

N95-32987# Osaka Univ., Osaka (Japan). Dept. of Welding and Production Engineering.
ANALYSIS OF EVAPORATION IN LASER WELDING
Isamu Miyamoto *In its* Technology Reports of the Osaka Univ., Vol. 45, Nos. 2205-2216 15 Apr. 1995 p 17-26 (For primary document see N95-32984 12-31)
(Rept-2207) Avail: CASI HC A02/MF A02

N95-34551# Nagoya Univ., Nagoya (Japan). Dept. of Aeronautical Engineering.
A SIMULATION OF DAMPING PROCESS OF PENDULUM MOTION DUE TO AERODYNAMIC FORCES Abstract Only
Casmara Nakamura and Yoshiaki Nakamura *In* National Aerospace Lab., Special Publication of National Aerospace Laboratory 16 Jun. 1994 p 321-326 In JAPANESE (For primary document see N95-34505 12-02)
Avail: CASI HC A02/MF A03

71 ACOUSTICS

Includes sound generation, transmission and attenuation.
For noise pollution see *45 Environmental Pollution.*

N95-32836*# NYMA, Inc., Brook Park, OH.
COMPUTATION OF NOISE RADIATION FROM TURBOFANS: A PARAMETRIC STUDY Final Contractor Report
M. Nallasamy Cleveland, OH NASA Jul. 1995 37 p Original contains color illustrations
(Contract NAS3-27186; RTOP 538-03-11)
(NASA-CR-198359; E-9747; NAS 1.26:198359) Avail: CASI HC A03/MF A01; 7 functional color pages

This report presents the results of a parametric study of the turbofan far-field noise radiation using a finite element technique. Several turbofan noise radiation characteristics of both the inlet and the aft ducts have been examined through the finite element solutions. The predicted far-field principal lobe angle variations with duct Mach number and cut-off ratio compare very well with the available analytical results. The solutions also show that the far-field lobe angle is only a function of cut-off ratio, and nearly independent of the mode number. These results indicate that the finite element codes are well suited for the prediction of noise radiation characteristics of a turbofan. The effects of variations in the aft duct geometry are examined. The ability of the codes to handle ducts with acoustic treatments is also demonstrated. Author

N95-33251 Iowa State Univ. of Science and Technology, Ames, IA.
STRUCTURAL WAVE PROPAGATION AND SOUND RADIATION STUDY THROUGH TIME AND SPATIAL PROCESSING Ph.D. Thesis
Ruey-Chang Wei 1994 150 p
Avail: Univ. Microfilms Order No. DA9424274

This work explores new usages of experimental and analysis tools to study the relationship between the wave propagation and sound radiation in a structure with inhomogeneities. The focus of the research is to develop and test new and merged techniques. The analysis tools used in the research include: time domain analysis, k-space analysis, and wave speed tracking. With the time domain analysis, one can study the response of any synthetic excitation with only one set of experimental data. The k-space analysis provides insight into locating areas on a vibrating structure that radiate sound to the acoustic farfield. The wave speed tracking technique was developed to estimate the phase speed of propagating waves in a structure. In addition, the reflection coefficient of a boundary can be computed from the wave speed tracking results. The chirp signal, used in the experiments, provides a concentrated power signal which can excite every mode in the interested frequency range. In addition, the transient property of the chirp signal also provides information in the time domain. A very consistent experimental setup and a repeatable experimental procedure were designed and tested to minimize the errors caused by the setup or mishandling of the equipment. A plate equation with a spatially distributed stress was used to model a structure with inhomogeneities. The results of simulations show that the spatially distributed stress can change the amplitude and wave numbers of the waves in the plate. A HY-80 steel beam with a T-bar welded to it was investigated experimentally with the proposed tools. The Tbar shows a significant contribution to the radiated sound power, and the existence of the T-bar decreases the phase speed of the propagating waves around the T-bar by 4 percent to 7 percent. The heat treatment did not have much influence on the sound radiation or wave phase speed change in this study. The experimental results have proven that the proposed techniques are very useful in the study of wave propagation and sound radiation for structures. Dissert. Abstr.

N95-33694 Kentucky Univ., Lexington, KY.
ADVANCED BOUNDARY ELEMENT METHODS IN AEROACOUSTICS AND ELASTODYNAMICS Ph.D. Thesis
Li Lee 1994 128 p
Avail: Univ. Microfilms Order No. DA9423025

In the first part of this dissertation, advanced boundary element methods (BEM) are developed for acoustic radiation in the presence of subsonic flows. A direct boundary integral formulation is first introduced for acoustic radiation in a uniform flow. This new formulation uses the Green's function derived from the adjoint operator of the governing differential equation. Therefore, it requires no coordinate transformation. This direct BEM formulation is then extended to acoustic radiation in a nonuniform-flow field. All the terms due to the nonuniform-flow effect are taken to the right-hand side and treated as source terms. The source terms result in a domain integral in the standard boundary integral formulation. The dual reciprocity method is then used to convert the domain integral into a number of boundary integrals. The second part of this dissertation is devoted to the development of advanced BEM algorithms to overcome the multi-frequency and nonuniqueness difficulties in steady-state elastodynamics. For the multi-frequency difficulty, two different interpolation schemes, borrowed from recent developments in acoustics, are first extended to elastodynamics to accelerate the process of matrix re-formation. Then, a hybrid scheme that retains only the merits of the two different interpolation schemes is suggested. To overcome the nonuniqueness difficulty, an enhanced CHIEF (Combined Helmholtz Integral Equation Formulation) method using a linear combination of the displacement and the traction boundary integral equations on the surface of a small interior volume is proposed. Numerical examples are given to demonstrate all the advanced BEM formulations. Dissert. Abstr.

N95-33719 Texas Univ., Austin, TX.
HIGH-ORDER TAYLOR-GALERKIN AND ADAPTIVE hp-METHODS FOR HYPERBOLIC SYSTEMS WITH APPLICATION TO STRUCTURAL ACOUSTICS Ph.D. Thesis
Andrzej Jerzy Safjan 1993 259 p
Avail: Univ. Microfilms Order No. DA9413592

In the present work general high-order hp-adaptive finite element methods for solving wave propagation problems characterized by linear hyperbolic systems of equations are studied. Particular emphasis is placed on problems of radiation and scattering of transient acoustic signals, propagation of stress waves in elastic solids, and on problems of interaction of an acoustic fluid with an elastic structure. A new family of stable high order Taylor Galerkin (TG) methods is developed for the numerical solutions of first- as well as second-order hyperbolic systems. It is shown that a multi-stage process can be used that produces schemes of order at most 2s for s-stages, each of which involves the solution of a well-posed second-order system of elliptic like equations. For such systems, the use of hp-schemes can exhibit exponential convergence rates and, therefore, the present approach may exploit a major attribute of h-p methods. A detailed stability analysis is provided for the case of linear systems which establishes choices of parameters that result in unconditionally stable schemes. Temporal as well as spatial a priori error estimates are derived. An a posteriori error estimation procedure is also presented which leads to estimates of both the spatial and temporal approximation error. In addition, an adaptive algorithm is developed which employs an hp-adaptive finite element method for controlling the spatial errors. The problem of radiation boundary conditions at the boundary of computational domain is also addressed. An application of the techniques of Enquist and Majda to TG schemes is developed Applications to linear transient acoustics problems, problems in elastodynamics and elastic scattering are presented. Very little oscillation of solutions in the vicinity of wave fronts is observed. h-p Methods are designed to manipulate the mesh size h and the local spectral order p of the approximations so as to approximately minimize the number of degrees of freedom required to produce a solution with specified accuracy. Several numerical experiments are described. These include two dimensional radiation and scattering problems, and detailed calculations of scattering of a plane acoustical wave by an elastic shell. Dissert. Abstr.

N95-33831*# McDonnell-Douglas Aerospace, Long Beach, CA.
FAN NOISE PREDICTION ASSESSMENT Final Report
Paul H. Bent May 1995 37 p

(Contract NAS1-20103; RTOP 538-03-11-01)
(NASA-CR-195051; NAS 1.26:195051; CRAD-9310-TR-0128) Avail: CASI HC A03/MF A01

This report is an evaluation of two techniques for predicting the fan noise radiation from engine nacelles. The first is a relatively computational intensive finite element technique. The code is named ARC, an abbreviation of Acoustic Radiation Code, and was developed by Eversman. This is actually a suite of software that first generates a grid around the nacelle, then solves for the potential flowfield, and finally solves the acoustic radiation problem. The second approach is an analytical technique requiring minimal computational effort. This is termed the cutoff ratio technique and was developed by Rice. Details of the duct geometry, such as the hub-to-tip ratio and Mach number of the flow in the duct, and modal content of the duct noise are required for proper prediction. Author

N95-34289 Department of the Navy, Washington, DC.
ACOUSTIC-OPTIC SOUND VELOCITY PROFILER Patent
George C. Connolly, inventor (to Navy) 3 Jan. 1995 7 p Filed 25 Mar. 1994
(AD-D017487; US-Patent-5,379,270; US-Patent-Appl-SN-217816; US-Patent-Class-367-128) Avail: US Patent and Trademark Office

An apparatus and method for determining the velocity of sound propagation in a fluid as a function of position in the fluid along an axis. A wave of acoustic energy is transmitted along the axis to produce a disturbance that moves in the medium at the velocity of sound. A laser generator transmits a light pulse substantially along the axis through the fluid medium. As the light passes through the disturbance, light backscatters in a characteristic pattern that a detector senses for analysis to provide information concerning the distance traveled and the time of travel for the acoustic wave through the fluid medium and to provide a profile of output characteristic, such as the speed of sound in the medium, as a function of position in the medium. DTIC

N95-34424 Department of the Navy, Washington, DC.
VERTICAL VELOCITY AMBIGUITY RESOLUTION METHOD Patent
Robert L. Winje, inventor (to Navy) 10 Jan. 1995 7 p Filed 9 May 1988
(AD-D017481; US-Patent-5,381,384; US-Patent-Appl-SN-191454; US-Patent-Class-367-89) Avail: US Patent and Trademark Office

The present invention relates to a method of resolving an ambiguity in the estimation of vertical velocity of a moving underwater or surface vehicle. Three acoustic pulses are successively transmitted. They are received by a series of detectors located on the vehicle. The time difference between correlated first and second received pulses is measured. The time difference between correlated first and third received pulses is also measured. The phase shifts between the three transmitted pulses and three received pulses is measured. This information is used to determine the vertical velocity of the vehicle. DTIC

N95-34444 Department of the Navy, Washington, DC.
ACOUSTIC ATTENUATION AND VIBRATION DAMPING MATERIALS Patent
William B. Cushman, inventor (to Navy) and Gerald B. Thomas, inventor (to Navy) 21 Mar. 1995 12 p Filed 25 Jan. 1994
(AD-D017465; US-Patent-5,400,296; US-Patent-Appl-SN-186058; US-Patent-Class-367-1) Avail: US Patent and Trademark Office

A means of enhancing the acoustic attenuation and vibration damping of a material by embedding high characteristic acoustic impedance particles, low characteristic acoustic impedance particles, or both high and low characteristic acoustic impedance particles within the matrix of the material is disclosed. The mass of the resultant material may be very low while retaining excellent acoustic attenuation, vibration damping, and structural characteristics. When particles with mis-matched characteristic acoustic impedances are embedded within the matrix of a material that can support shearing loads, propagating acoustic energy that encounters the particles of the instant invention is partially reflected in random directions. That is, the propagating energy is diffused. As the propagation vectors and modes of acoustic energy are effectively randomized, the probability of localized energy absorption and damping is increased. We present acoustic attenuation and vibration damping data for some representative examples of the instant invention and other commercially available materials. DTIC

N95-34595# Washington Univ., Seattle, WA.
UNDERWATER ACOUSTIC FIELD EXTRAPOLATION: THEORY AND SENSITIVITY ANALYSIS
Warren L. Fox Mar. 1995 151 p
(AD-A294925; APL-UW-TR-9501) Avail: CASI HC A08/MF A02

In some underwater acoustic applications, it is desirable to predict what an acoustic field will be at some distance away from a source. Numerical modeling based on environmental parameters (e.g., sound speed, bathymetry, sediment properties) is one possibility, but the amount of environmental information necessary for accurate long-range modeling is often beyond what is realistically measurable. Actual acoustic measurements are another possibility, but our knowledge of the fields is then limited to the points in the ocean where the sources and receivers are located. We present a hybrid method for predicting acoustic fields that takes limited acoustic measurements and extrapolates them over short ranges using modeled fields. The measured and modeled fields are combined in an integral formulation via a specialization of Huygens' principle. The basic theoretical formulation is stated and analyzed using the theory of normal modes. The formulation leads directly to modal-dependent (grazing angle dependent) obliquity factors, which are canceled to first order by averaging with a range derivative-based extrapolation. Sensitivity of the algorithm to the higher order components of the obliquity factors is studied. As with other model-based algorithms, environmental mismatch can degrade the results. The algorithm's sensitivity to mismatch in water column sound speed and sediment sound speed, attenuation, and density are studied via a perturbational approach. Since the algorithm explicitly contains an integral and the measured field is collected at discrete locations, numerical quadrature techniques are studied. It is shown how undersampling can degrade the quality of the extrapolated fields, and how the spatial sampling required for reliable extrapolation can be obtained. DTIC

N95-34549# National Aerospace Lab., Tokyo (Japan).
DIRECT ANALYSIS OF TRANSONIC ROTOR NOISE WITH CFD TECHNIQUE Abstract Only
Takashi Aoyama and Shigeru Saito *In its* Special Publication of National Aerospace Laboratory 16 Jun. 1994 p 309-314 In JAPANESE (For primary document see N95-34505 12-02)
Avail: CASI HC A02/MF A03

72 ATOMIC AND MOLECULAR PHYSICS

Includes atomic structure, electron properties, and molecular spectra.

N95-32379# Fermi National Accelerator Lab., Batavia, IL.
PRODUCTION ASYMMETRIES IN x(SUB f) AND P(SUP 2)(SUB t) FOR D(SUP +/-) MESONS
T. Carter Nov. 1994 6 p Presented at the Electronic Materials Conference, Boulder, CO, 22-24 Jun. 1994
(Contract DE-AC02-76CH-03000)
(DE95-007207; FNAL/C-94/383; CONF-940616-91) Avail: CASI HC A02/MF A01

We present differences in leading and non-leading charged D meson production as a doubly-differential function of both P(sup 2)(sub t) and (chi)(integral). Comparisons to specific models are made. This information is from the analysis of half the data from Fermilab experiment E791, taken during the 1991-2 fixed target run with a 500 GeV/c (pi)(sup -) beam incident on a segmented target. DOE

N95-32393# Puerto Rico Univ., Mayaguez.
CHARM DECAYS AND HIGH ENERGY PHOTOPRODUCTION
Jan. 1995 13 p
(Contract DE-FG05-94ER-40842)
(DE95-010165; DOE/ER-40842/T1) Avail: CASI HC A03/MF A01

The activities during the first nine months of the three-year grant period have concentrated on the development of computer resources both hardware and software as well as the design of a muon detector for Fermilab Experiment E831. An important related activity has been a successful search of funds to complement the resources provided by this grant and permit the involvement of additional personnel as well as a much-better leveraged impact of the funds provided. Grant funds were the main providers

of a new computer system which is dedicated to the High Energy Physics group at Mayaguez. This system can be considered a minimum configuration to carry out the simulation and analysis loads of E831. The bulk of the software development has been directed at developing a Monte Carlo simulation for E831 in particular the E831 muon detector. DOE

N95-32404# Tokyo Univ., Tanashi (Japan). Inst. for Nuclear Study.
DOUBLE-STRANGENESS FIVE-BODY SYSTEM
Khin Swe Myint (Mandalay Univ., Mandalay, Myanmar.) and Yoshinori Akaishi Sep. 1994 25 p
(DE95-737277; INS-1055) Avail: CASI HC A03/MF A01

We perform theoretical analysis on the structure and decay of a double-strangeness five-body system which consists of (Lambda Lambda)H-5 and (Xi)H-5 states. In this S = -2 five-body system the thresholds of the t(Lambda)(Lambda) channel and the alpha(Xi)(-) channel come closer with only 8.51 MeV difference. We treat both bound and resonant states of the three-body channels t(Lambda)(Lambda) and tp(Xi)(-) by applying a complex rotation method. It is found that there is a bound (Lambda Lambda)H-5 state with 6.3 MeV below the threshold of t + Lambda + Lambda. In the Xi(-) channel a resonant (Xi)H-5 state appears at 1.7 MeV below the threshold of alpha + Xi(-). Though the existence of this state is ensured by the Coulomb interaction, it is a 'halo' nuclear state rather than an atomic state as judged from its size. The conversion width of this state is 0.2 MeV which is extremely narrow. It is also found that Xi mixing into the (Lambda Lambda)H-5 ground state is small with 1.0 %. For the (Lambda Lambda)H-5 state, the weak decay to the alpha + Sigma(-) final state produces a high mono-energetic Sigma(-) with branching ratio of 5.5 %. Thus the Sigma(-) with discrete energy would become a clear signature of the forming of the Lambda Lambda hypernucleus. DOE

N95-32406# Joint Inst. for Nuclear Research, Dubna (USSR). Lab. of Theoretical Physics.
THE Q(2)-DEPENDENCE OF THE GROSS-LLEWELLYN SMITH SUM RULE AND OF THE PARTON DISTRIBUTIONS
A. L. Kataev (European Organization for Nuclear Research, Geneva, Switzerland.) and A. V. Sidorov 1994 10 p Presented at the International Seminar Quarks 1994, Vladimir, Russia, May 1994
(DE95-623678; JINR-E-2-94-344) Avail: CASI HC A02/MF A01 (US Sales Only)

We describe the results of our recent work on the determination of the value of the parameter (Lambda) and of the Q(sup 2)-dependence of the Gross-Llewellyn Smith (GLS) sum rule from the experimental data of the CCFR collaboration on neutrino-nucleon deep inelastic scattering, using the Jacobi polynomials QCD analysis. The new information on the Q(sup 2)-dependence of the parton distributions is presented. DOE

N95-32407# Joint Inst. for Nuclear Research, Dubna (USSR). Lab. of Theoretical Physics.
ISGUR-WISE FUNCTION AND POLARIZATION CHARACTERISTICS OF LAMBDA(SUB b)-BARYON
M. A. Ivanov and V. E. Lyubovitskij 1994 11 p In RUSSIAN Submitted for publication in Pis'ma v Zhurnal Ehksperimental'noj i Teoreticheskoj Fiziki
(DE95-623696; JINR-R-2-94-325) Avail: CASI HC A03/MF A01 (US Sales Only)

In connection with planned experiments devoted to investigation of semileptonic decays of beauty baryons Isgur-Wise function and polarization characteristics of Lambda(sub b) baryon are calculated in the framework of diquark model with taking into account of infrared behaviour of heavy quark. DOE

N95-32477# Joint Inst. for Nuclear Research, Dubna (USSR). Lab. of Theoretical Physics.
PHYSICS OF THE CEM92M CODE
S. G. Mashnik 1994 14 p Presented at the NEA Nuclear Science Committee Meeting on Intermediate Energy Nuclear Data, Paris, France, 30 May - 1 Jun. 1994
(DE95-623579; JINR-E-2-94-352) Avail: CASI HC A03/MF A01 (US Sales Only)

The code CEM92M is intended for calculation of reaction, elastic, fission and total cross sections; nuclear fissilities; excitation functions; nuclide distributions; energy and angular spectra; double differential cross sections; mean multiplicities, mean energies and production cross sections for n, p, d, t, He-3, He-4, pi(sup -), pi(sup 0) and (pi)+ emitted in nucleon-and pion-induced reactions using the Cascade-Exciton Model (CEM) of nuclear reactions. The main assumptions of the CEM are given. A large variety of nucleon-, pion- and (gamma)-induced reactions in the bombarding energy range of 0-3000 MeV have been analyzed and evaluated with it. It is shown that the CEM adequately describes nuclear reactions at intermediate energies, has one of the best predictive powers as compared to other available modern models and may be used for evaluation of medium energy nuclear data for science and applications. Further development and improvement of the code CEM92M are discussed. DOE

N95-32481# Academy of Sciences (USSR), Novosibirsk (USSR).
VACUUM POLARIZATION CORRECTION TO THE POSITRONIUM DECAY RATE
A. P. Burichenko and D. Yu. Ivanov 1993 7 p
(DE95-614164; BUDKERINP-93-64; IYaF-93-64) Avail: CASI HC A02/MF A01 (US Sales Only)

Correction of approximately alpha(exp 2) to the positronium decay rate, induced by one-loop vacuum polarization diagram, are calculated. Their relative values are 0.4468(3) (alpha/pi)(exp 2) for para- and 0.960(3) (alpha/pi)(exp 2) for orthopositronium. DOE

N95-32484# Brookhaven National Lab., Upton, NY. National Nuclear Data Center.
EVALUATED NUCLEAR STRUCTURE DATA FILE
J. K. Tuli 1995 18 p Presented at the Conference and International Symposium on Radionuclide Metrology and Its Applications, Paris, France, 15-19 May 1995
(Contract DE-AC02-76CH-00016)
(DE95-011343; BNL-60875; CONF-950563-1) Avail: CASI HC A03/MF A01

The Evaluated Nuclear Structure Data File (ENSDF) contains the evaluated nuclear properties of all known nuclides. These properties are derived both from nuclear reaction and radioactive decay measurements. All experimental data are evaluated to create the adopted properties for each nuclide. ENSDF, together with other numeric and biographic files, can be accessed on-line through the INTERNET or modem. Some of the databases are also available on the World Wide Web. The structure and the scope of ENSDF are presented along with the on-line access system of the National Nuclear Data Center at Brookhaven National Laboratory. DOE

N95-32524# International Centre for Theoretical Physics, Trieste (Italy).
A STUDY OF LUMINESCENCE AND ABSORPTION SPECTRA OF GaP
H. M. M. Mansour (Cairo Univ., Egypt.), M. Mounir, and S. M. AbdelWahab (Ain Shams Univ., Cairo, Egypt.) Aug. 1994 17 p
(DE95-614122; IC-94/221) Avail: CASI HC A03/MF A01 (US Sales Only)

Experimental luminescence and absorption spectra of GaP at room temperature are presented. A theoretical analysis has been performed on the luminescence and absorption spectra in GaP. The experimental data are in good agreement with the theoretical results. DOE

N95-32529# Japan Atomic Energy Research Inst., Tokyo (Japan).
HYDROGEN FORMATION IN METALS AND ALLOYS DURING FUSION REACTOR OPERATION
Sergei Zimin (Japan Atomic Energy Research Inst., Ibaraki, Japan.), Hideyuki Takatsu, and Seiji Mori Aug. 1994 25 p
(DE95-737224; JAERI-Tech-94-013) Avail: CASI HC A03/MF A01

The results of neutron transport calculations of the hydrogen formation based on the JENDL gas-production cross section file are discussed for some metals and alloys, namely V-51, Cr, Fe, Ni, Mo, austenitic stainless steel (Ti modified 316SS:PCA), ferritic steel (Fe-8Cr-2W:F82H) and the vanadium-base alloy (V-5Cr-5Ti). Impact of the steel fraction in steel/water homogeneous blanket/shield compositions on the hydrogen formation rate in above-mentioned metals and alloys is discussed both for the hydrogen formation in the first wall and the blanket/shield components. The results obtained for the first wall are compared with those for the helium formation obtained at JAERI by the same calculational conditions. Hydrogen formation rates at the first wall having V-51, Cr, Fe, Ni and Mo are larger than those of helium by 3-8 times. DOE

N95-32542# Brookhaven National Lab., Upton, NY.
COMPARISON OF THE WANG AND WACHSMUTH MODELS FOR (PI) PRODUCTION WITH MEASUREMENTS AT 12 GeV/c
R. C. Fernow Mar. 1995 11 p Presented at the 13th Congress of the Association for Radiation Protection Science and Technology, Strasbourg, France, 6-8 Nov. 1984
(Contract DE-AC02-76CH-00016)
(DE95-010417; BNL-61578; CONF-8411210-7) Avail: CASI HC A03/MF A01

The author converted the invariant cross section measurements of Blobel et al at 12 GeV/c into the form d(exp 2)sigma/d Omega dp as a function of the LAB total momentum p and p(T). The author then adjusted the parameters of the pion production models of Wang and of Wachsmuth-Hagedorn-Ranft to obtain the best fit to the data. Neither model gave a statistically accurate fit to the data. DOE

N95-32544# Stanford Linear Accelerator Center, Menlo Park, CA.
STUDY OF THE TRAPPED MODES AT THE VACUUM PORTS
S. Heifets and G. Stupakov Jan. 1995 16 p
(Contract DE-AC03-76SF-00515)
(DE95-010570; SU-SLAC/AP-98) Avail: CASI HC A03/MF A01

Pumping ports in PEP-II vacuum chamber will be shielded with slots cut in the walls of the beam pipe. The number of slots n(s), their length l, and width w are defined by the required pumping conductance. The present design has 40 slots around the stainless steel round pipe in the straight sections, and, for the rectangular copper chamber of the arcs, there are 18 slots placed in upper and lower decks. Here we want to address two potential problems related to the slots: radiation of the TE HOM-s through the slots, and generation of the trapped modes. DOE

N95-32554# Gosudarstvennyi Komitet po Ispolzovaniyu Atomnoi Energii, Protvino (USSR).
SCALING LAW FOR THE UPSILON(4S) YIELDS BAR-BB AND PSI(3770) YIELDS BAR-DD DECAY CONSTANTS FROM EFFECTIVE SUM RULES
V. V. Kiselev 1994 12 p
(DE95-620538; IHEP-94-3) Avail: CASI HC A03/MF A01 (US Sales Only)

The sum rules for exclusive production of heavy meson pairs in e(+)e(-) annihilation are used to evaluate the Upsilon(4S) yields bar-BB and psi(3770) yields bar-DD decay widths. Infinitely heavy quark limit is discussed, and the scaling law for the quarkonium-meson coupling constant is derived. The bar-BB pair contribution into the leptonic constant f(sub Upsilon(4S)) is estimated. DOE

N95-32564# Kansas State Univ., Manhattan, KS.
LOW ENERGY COLLISIONS INVOLVING MULTIPLY CHARGED IONS
W. Wu, J. P. Giese, and C. L. Cocke 1994 5 p Presented at the Department of Energy Basic Energy Sciences Atomic Physics Workshop, Lexington, KY, 14-15 Oct. 1994
(Contract DE-FG02-86ER-13491)
(DE95-010911; DOE/ER-13491/742; CONF-9410198-2) Avail: CASI HC A01/MF A01

This report contains summary of papers that are presented at the Department of Energy Basic Energy Sciences Atomic Physics Workshop. The following titles are included: Direct ionization of He by low velocity highly charged projectiles; Q-value and cross section ratios for electron capture from Ar by Xe(30+) for projectile velocities between 0.3 and 1.0 a.u.; experimental velocity dependence of charge capture cross sections for slow, highly charged ions with a rydberg target; development of a sodium rydberg target for use in collision with slow highly charged ions; Nanometer-size surface modification produce by single, low energy, highly charged ions; Charge exchange in large angle scattering of C(4+) and C(6+) on He; Electron capture from C60 by slow multiply charged ions; and Ion-ion collisions. CASI

N95-32567# Stanford Linear Accelerator Center, Stanford, CA.
IMPEDANCE STUDY FOR THE PEP-2 B-FACTORY
S. Heifets, K. Ko, C. Ng, X. Lin, A. Chao, G. Stupakov, M. Zolotorev, J. Seeman, U. Wienands, and C. Perkins et al Mar. 1995 90 p Prepared in cooperation with the Univ. of Technology, Darmstadt, Germany and Lawrence Livermore Lab.
(Contract DE-AC03-76SF-00515)
(DE95-010569; SU-SLAC/AP-99) Avail: CASI HC A05/MF A01

The paper summarizes results on the impedance study of the PEP-2 B-factory. DOE

N95-32574# Los Alamos National Lab., NM.
SEMI-ANALYTIC COMPUTATION OF THE DRIVEN FIELDS IN RIGHT CIRCULAR CYLINDRICAL MICROWAVE APPLICATORS
Eric M. Nelson, Robert J. Kares, and Ray M. Stringfield 1995 3 p Presented at the 30th Annual Microwave Symposium, Denver, CO, 9-12 Jul. 1995
(Contract W-7405-eng-36)
(DE95-010875; LA-UR-95-1288; CONF-9507121-1) Avail: CASI HC A01/MF A01

A semi-analytic technique for computing the driven fields in a pillbox microwave applicator composed of concentric right circular cylinders (e.g., load, tube and air regions) is described. The fields are driven by idealized apertures on the cavity wall. A modal expansion of the driven fields provides insight about thermal energy deposition in the load. DOE

N95-32576# Los Alamos National Lab., NM.
BEHAVIOR OF STRUCTURAL AND TARGET MATERIALS IRRADIATED IN SPALLATION NEUTRON ENVIRONMENTS
James F. Stubbins (Illinois Univ., Urbana, IL.), M. Wichsler (North Carolina State Univ., Raleigh, NC.), Michael J. Bordon (North Carolina State Univ., Raleigh, NC.), and Walter F. Sommer (Illinois Univ., Urbana, IL.) 1995 11 p Presented at the Accelerator-driven Transmutation Technology (ADTT) Conference, Las Vegas, NV, 24-29 Jul. 1995 Submitted for publication
(Contract W-7405-eng-36)
(DE95-010879; LA-UR-95-1312; CONF-950777-3) Avail: CASI HC A03/MF A01

This paper describes considerations for selection of structural and target materials for accelerator-driven neutron sources. Due to the operating constraints of proposed accelerator-driven neutron sources, the criteria for selection are different than those commonly applied to fission and fusion systems. Established irradiation performance of various alloy systems is taken into account in the selection criteria. Nevertheless, only limited materials performance data are available which specifically related to neutron energy spectra anticipated for spallation sources. DOE

N95-32577# Los Alamos National Lab., NM.
IN SITU ION-BEAM ANALYSIS AND MODIFICATION OF SOL-GEL ZIRCONIA THIN FILMS
Timothy Edge Levine (Cornell Univ., Ithaca, NY.), Ning Yu, Padma Kodali, Kevin C. Walter, Michael Nastasi, Joseph R. Tesmer, Carl J. Maggiore, and James W. Mayer (Arizona State Univ., Tempe, AZ.) 1995 14 p Presented at the 9th International Conference on Ion Beam Modification of Materials, Canberra, Australia, 5-10 Feb. 1995
(Contract W-7405-eng-36)
(DE95-010994; LA-UR-95-1436; CONF-950220-7) Avail: CASI HC A03/MF A01

We report the investigation of ion-beam-induced densification of sol-gel zirconia thin films via in situ ion backscattering spectrometry. We have irradiated three regions of a sample with neon, argon, and krypton ions. For each ion species, a series of irradiation and analysis steps were performed using an interconnected 3 MV tandem accelerator. The technique offers the advantages of minimizing the variation of experimental parameters and sequentially monitoring the densification phenomenon with increasing ion dose. DOE

N95-32583# Los Alamos National Lab., NM. Theoretical Div.
FADDEEV CALCULATIONS OF p(MU)+p COLLISIONS: EFFECT OF HYPERFINE SPLITTING ON THE CROSS SECTIONS
Chi-Yu Hu (California State Univ., Long Beach, CA.), A. Kvitsinsky (California State Univ., Long Beach, CA.), and J. S. Cohen 1995 27 p Presented at the 19th International Conference on the Physics of Electronic and the Atomic Collisions, Whistler, Canada, 26 Jul. - 1 Aug. 1995
(Contract W-7405-eng-36)
(DE95-007838; LA-UR-95-790; CONF-950706-1) Avail: CASI HC A03/MF A01

The Faddeev equations, modified to remove long-range coupling between different channels, are solved in the total-angular-momentum representation

for p(mu) + p collisions. S-wave elastic and hyperfine-transition cross sections are calculated with and without explicit inclusion of the hyperfine splitting (Delta)E. For hyperfine quenching the simpler approach without hyperfine splitting is found adequate at collision energies above about (Delta)E, but for elastic scattering it becomes adequate at somewhat higher energies. The present cross sections tend to fall in between earlier calculations done using a large Standard adiabatic expansion and those done using a two-state improved adiabatic expansion, but are closer to the former. DOE

N95-32584# Los Alamos National Lab., NM.
PROGRESS TOWARDS ANTIHYDROGEN PRODUCTION BY THE REACTION OF COLD ANTIPROTONS WITH POSITRONIUM ATOMS
M. Charlton (University Coll., London, England.), G. Laricchia (University Coll., London, England.), B. I. Deutch (Aarhus Univ., Denmark.), X. Feng (Aarhus Univ., Denmark.), J. S. Hangst (Aarhus Univ., Denmark.), P. Hvelplund (Aarhus Univ., Denmark.), H. Knudsen (Aarhus Univ., Denmark.), J. P. Merrison (Aarhus Univ., Denmark.), E. Uggerhoj (Aarhus Univ., Denmark.), and M. H. Holzscheiter et al 1995 10 p Presented at the Low-energy Antiproton Physics, Bled, 12-17 Sep. 1994
(Contract W-7405-eng-36)
(DE85-007850; LA-UR-95-728; CONF-9409264-2) Avail: CASI HC A02/MF A01

An experiment aimed at producing antihydrogen atoms by the reaction of cold antiprotons stored in a Penning trap with injected ground state positronium atoms is described. The apparatus developed in an attempt to observe the charge conjugate reaction using proton projectiles is discussed. Technically feasible upgrades to this apparatus are identified which may allow, in conjunction with the PS200 trap, antihydrogen production at LEAR. DOE

N95-32610# Joint Inst. for Nuclear Research, Dubna (USSR). Lab. of Nuclear Reactions.
DAMAGE FORMATION IN SILICON IRRADIATED BY HEAVY IONS WITH ENERGY MORE THAN 1 MeV/a.m.u.
M. A. Adawi (Nuclear Research Center, Cairo, Egypt.) and A. Y. Didyk 1994 11 p Presented at the Symposium on Advances in Materials Science, Cairo, Egypt, 1994
(DE95-623968; JINR-E-14-94-334) Avail: CASI HC A03/MF A01 (US Sales Only)

The experimental data of the optical reflection coefficient along the projective range of ions Ar-40 (46,3 MeV) and Ne-22 (26,7 MeV) are presented. The change of silicon lattice constants irradiated by heavy ions was studied with the use of X-ray diffraction method. The estimations of the track diameter for different ions are carried out. DOE

N95-32617# Washington Univ., Seattle, WA. Inst. for Nuclear Theory.
INTRINSIC CHARM CONTRIBUTION TO DOUBLE QUARKONIUM HADROPRODUCTION
R. Vogt and S. J. Brodsky (Stanford Linear Accelerator Center, Stanford, CA.) 1995 10 p
(Contracts DE-FG06-90ER-40561; DE-AC03-76SF-00098; DE-AC03-76SF-00515)
(DE95-012170; DOE/ER-40561/190) Avail: CASI HC A02/MF A01

Double J/(psi) production has been observed by the NA3 collaboration in (pi)N and pN collisions with a cross section of the order of 20-30 pb. The (psi)(psi) pairs measured in (pi)(sup (minus)) nucleus interactions at 150 and 280 GeV/c are observed to carry an anomalously large fraction of the projectile momentum in the laboratory frame, x(sub (psi)(psi)) greater than or equal to 0.6 at 150 GeV/c and greater than or equal to 0.4 at 280 GeV/c. We postulate that these forward (psi)(psi) pairs are created by the materialization of Fock states in the projectile containing two pairs of intrinsic c(bar c) quarks. We calculate the overlap of the charmonium states with the (bar u)dc(bar c)c(bar c) Fock state as described by the intrinsic charm model and find that the (pi)(sup (minus))N (yields) (psi)(psi) longitudinal momentum and invariant mass distributions are both well reproduced. We also discuss double J/(psi) production in pN interactions and the implications for other heavy quarkonium production channels in QCD. DOE

N95-32619# California Univ., Berkeley. Lawrence Berkeley Lab, CA. Nuclear Science Div.
QCD MECHANISMS FOR DOUBLE QUARKONIUM AND OPEN HEAVY MESON HADROPRODUCTION
R. Vogt 1995 30 p Prepared in cooperation with Washington Univ., Seattle, WA
(Contracts DE-FG06-90ER-40561; DE-AC03-76SF-00098)
(DE95-012171; DOE/ER-40561/191) Avail: CASI HC A03/MF A01

Double J/(psi) production on the order of 20-30 pb has been observed by the NA3 collaboration. These (psi)(psi) pairs, measured in (pi)(sup (minus))N interactions at 150 and 280 GeV/c and in pN interactions at 400 GeV/c, carry a large fraction of the projectile momentum, x(sub (psi)(psi)) greater than or equal to 0.6 for the 150 GeV/c beam and greater than or equal to 0.4 at 280 GeV/c. We examine several sources of (psi)(psi) pair production within QCD, including (Omicron)((alpha)(sub s)(sup 4)) (psi)(psi) production, leading-twist b(bar b) production and decay, and the materialization of heavy-quark Fock states in the projectile. We estimate the production cross section and the single and double J/(psi) momentum and mass distributions for each, comparing the results with the NA3 data, and predict (psi)(psi) production in pN interactions at 800 GeV/c, accessible to current fixed-target experiments. We also discuss the observable implications of open heavy meson pair production from the intrinsic heavy quark Fock states. DOE

N95-32621# State Univ. of New York, Stony Brook, NY.
CHIRAL RESTORATION IN HOT AND/OR DENSE MATTER
G. E. Brown and M. Rho (Commissariat a l'Energie Atomique, Gif-sur-Yvette, France.) 1995 65 p
(Contracts DE-FG06-90ER-40561; DE-FG02-88ER-40388)
(DE95-012176; DOE/ER-40561/195) Avail: CASI HC A04/MF A01

Chiral restoration phase transition in hot and/or dense hadronic matter is discussed in terms of the BR scaling based on chiral symmetry and scale anomaly of QCD. The precise connection between the scalar field that figures in the trace anomaly and the sigma field that figures in the linear sigma model is established. It is suggested that in hot and/or dense medium, the nonlinear sigma model linearizes with the help of a dilaton to a linear (sigma) model with medium-renormalized constants. The relevance of Georgi's vector symmetry and/or Weinberg's 'mended symmetry' in chiral restoration is pointed out. Some striking consequences for relativistic heavy-ion collisions and dense matter in compact stars following stellar collapse are discussed. DOE

N95-32622# Melbourne Univ., Parkville (Australia). School of Physics.
DOPPLERON RESONANCES IN THE DIFFRACTION OF ATOMS BY AN EVANESCENT FIELD
John E. Murphy, Lloyd C. L. Hollenberg, and Andrew E. Smith (Monash Univ., Clayton, Australia.) 1994 16 p
(DE95-619190; UM-P-93/85) Avail: CASI HC A03/MF A01 (US Sales Only)

The diffracted intensities of sodium atoms by a standing evanescent light wave near the three doppleron resonance are calculated using a multi-slice technique. This calculation predicts a sharp dip in the reflected intensity of the specular beam for a detuning slightly below resonance. Such phenomena has been observed experimentally and can be understood using the dressed state picture. DOE

N95-32623# Melbourne Univ., Parkville (Australia). School of Physics.
INVERSION OF ELECTRON-WATER ELASTIC SCATTERING DATA
A. Lun, X. J. Chen, L. J. Allen, and K. Amos 1994 33 p
(DE95-619323; UM-P-93/101) Avail: CASI HC A03/MF A01 (US Sales Only)

Fixed energy inverse scattering theory has been used to analyse the differential cross-sections for the elastic scattering of electrons from water molecules. Both semiclassical (WKB) and fully quantal inversion methods have been used with data taken in the energy range 100 to 1000 eV. Constrained to be real, the local inversion potentials are found to be energy dependent; a dependence that can be interpreted as the local equivalence of true nonlocality in the actual interaction. DOE

N95-32625# Joint Inst. for Nuclear Research, Dubna (USSR). Lab. of Nuclear Reactions.
THE STRUCTURE OF ION TRACK IN SOLIDS PRODUCED BY IONS WITH HIGH LEVEL INELASTIC ENERGY LOSSES
A. Y. Didyk 1994 14 p
(DE95-620942; JINR-E-14-94-365) Avail: CASI HC A03/MF A01 (US Sales Only)

The phenomenological model of the track formation processes under the heavy ion passing through the materials is introduced. This model is based on the scanning tunneling and electronic microscopy experimental data about the direct and indirect observation of crater parameters on the surfaces obtained after the surface researches of diamond single crystals and stainless steel irradiated by Ar-40, Kr-84 and Xe-129 ions. The energy and temperature criteria when crater formation under the heavy ion irradiation takes place are introduced. DOE

N95-32630# Joint Inst. for Nuclear Research, Dubna (USSR). Lab. of High Energy.
ON APPLICATION OF WAVELET ANALYSIS TO SEPARATION OF SECONDARY PARTICLES FROM NUCLEUS-NUCLEUS INTERACTIONS
S. V. Afanasev, M. V. Altajskij, and Y. G. Zhestkov 1994 14 p Submitted for publication in Nuovo Cimento
(DE95-623572; JINR-E-2-94-337) Avail: CASI HC A03/MF A01 (US Sales Only)

We apply wavelet analysis for separation of secondary particle from different channels of d + Au (yields) ... reaction. Using the data obtained in the experiments at Nuclotron (Dubna) in March 1994 at deuteron momentum of 3.8 GeV/c, we found 4 different regions in the time-of-flight vs energy loss plot. DOE

N95-32632# Melbourne Univ., Parkville (Australia). School of Physics.
THE NON-RELATIVISTIC CHARGED BOSE GAS IN A MAGNETIC FIELD. PART 1: FORMALISM
Victor Kowalenko and N. E. Frankel 1994 27 p
(DE95-619696; UM-P-93/78) Avail: CASI HC A03/MF A01 (US Sales Only)

The polarisation tensor for the non-relativistic charged Bose gas (CBG) in a uniform magnetic field (B) is derived by using a gauge-independent second-quantised Hamiltonian approach in the random phase or one loop approximation. The tensor's gauge invariant and symmetry properties are used to develop expressions for the dielectric tensor, the longitudinal dielectric response function and the transverse dielectric response functions corresponding to photon propagation perpendicular and parallel to the magnetic field, so that detailed examinations of both the longitudinal and transverse properties of the system at T=0 K and at finite temperature may follow. DOE

N95-32650# Oak Ridge National Lab., TN. Physics Div.
THE FULLY CORRELATED TWO-ELECTRON PROBLEM ON A NUMERICAL LATTICE
David R. Schultz 1994 10 p Presented at the 4th U.S./Mexico Joint Symposium on Atomic and Molecular Physics, San Juan Del Rio, Mexico, 7-10 Dec. 1994
(Contract DE-AC05-84OR-21400)
(DE95-010280; CONF-941268-1) Avail: CASI HC A02/MF A01

A technique for solving the time-dependent Schroedinger equation on a numerical lattice is described for the fully correlated two-electron, one-center problem. First applications of the method are briefly summarized here, including the demonstration of its ability to accurately reproduce static solutions for the helium atom, describe the time dependence of the autoionization of a doubly excited state of helium, and to explore the treatment of electron impact of atomic hydrogen. DOE

N95-32651# Brookhaven National Lab., Upton, NY.
STRANGENESS FROM HADRONIC PROCESSES
Y. Pang (Columbia Univ., New York, NY.), T. J. Schlagel, S. H. Kahana, and D. E. Kahana (State Univ. of New York, Stony Brook, NY.) 1995 14 p Presented at the Strangeness in Hadronic Matter Conference, Tucson, AZ, 3-7 Jan. 1995
(Contracts DE-AC02-76CH-00016; DE-AC02-91ER-40651; DE-FG02-93ER-40768)
(DE95-010311; BNL-61583; CONF-950172-2) Avail: CASI HC A03/MF A01

Large amounts of experimental data on strangeness production in nucleon-nucleon and in pion-nucleon collisions, and data on hadronic scattering of strange particles, make it possible to calculate, with accuracy, the hadronic contribution to the strangeness production in nucleus-nucleus reactions. The relativistic cascade model ARC, relying on the experimental measurements of elementary hadron-hadron interactions, successfully predicted many single particle spectra in Au + Au collisions at BNL-AGS, including those of strange mesons K(sup (+-)). DOE

N95-32652# Brookhaven National Lab., Upton, NY.
TARGETS AND MAGNETIC ELEMENTS FOR PION COLLECTION IN MUON COLLIDER DRIVERS
R. C. Fernow, J. C. Gallardo, Y. Y. Lee, R. B. Palmer, D. R. Winn, D. V. Neuffer (Continuous Electron Beam Accelerator Facility, Newport New, VA.), and Y. Torun Mar. 1995 13 p Presented at the 2nd Workshop on Physics Potential and Development of Mu(+) Mu(-) Colliders, Sausalito, CA, 17-19 Nov. 1994
(Contract DE-AC02-76CH-00016)
(DE95-010316; BNL-61575; CONF-9411210-5) Avail: CASI HC A03/MF A01

The authors review quasi-achromatic magnetic focusing elements which collect pions produced in a target for transport into a (pi) yields (mu) decay channel, with features appropriate to the development of high energy muon colliders. They discuss how the collection and target requirements of a muon collider are different from and similar to existing secondary particle collection systems. They briefly discuss target technology issues. DOE

N95-32654# Brookhaven National Lab., Upton, NY. Center for Accelerator Physics.
A POSSIBLE IONIZATION COOLING EXPERIMENT AT THE AGS
R. C. Fernow, J. C. Gallardo, R. B. Palmer, D. R. Winn (Fairfield Univ., CT.), and D. V. Neuffer (Continuous Electron Beam Accelerator Facility, Newport New, VA.) Mar. 1995 16 p Presented at the 2nd Workshop on Physics Potential and Development of Mu(+) Mu(-) Colliders, Sausalito, CA, 17-19 Nov. 1994
(Contract DE-AC02-76CH-00016)
(DE95-010317; BNL-61577; CONF-9411210-6) Avail: CASI HC A03/MF A01

Ionization cooling may play an important role in reducing the phase space density of muons for a future muon-muon collider. The authors describe possible transverse and longitudinal emittance cooling experiments that utilize the capabilities of the AGS at Brookhaven National Laboratory. DOE

N95-32703# Gosudarstvennyi Komitet po Ispolzovaniyu Atomnoi Energii, Leningrad (USSR).
SEARCH FOR N(SUB (PHI))(1960) BARYON
M. Ya. Balatz, I. M. Belyaev, and V. A. Dorofeev 1993 15 p
(DE95-619290; IHEP-OEF-93-97) Avail: CASI HC A03/MF A01 (US Sales Only)

In the experiments at the SPHINX facility in the 70 GeV proton beam of the IHEP accelerator the diffractive production reactions p + N (yields) (Sigma(1385)(0)K(+)) + N and p + N yields (Sigma(1385)(0)K(+)) + N + (neutral particles) were studied. In the effective mass spectra of the (Sigma(1385)(0)K(+)) system in these processes there were no signals from the anomalously narrow baryon state N(sub phi)(1960), which had been observed earlier in the measurement at the BIS-2 setup. DOE

N95-32704# Gosudarstvennyi Komitet po Ispolzovaniyu Atomnoi Energii, Serpukhov (USSR).
FOUR HEAVY QUARK AND BOUND STATE PRODUCTION IN THE e(+)e(-) YIELDS Q + (BAR-Q' + Q' + BAR-Q AND e(+)e(-) YIELDS (Q(BAR-Q')) + Q' + BAR-Q PROCESSES IN Z(SUP 0)-BOSON POLE
V. V. Kiselev, A. K. Likhoded, and M. V. Shevlyagin (Moscow Inst. of Physics and Technology, Moscow, Russia.) 1994 31 p Submitted for publication in Yad. Phys.
(DE95-620533; IHEP-94-10) Avail: CASI HC A03/MF A01 (US Sales Only)

In the frame of the QCD perturbation theory and nonrelativistic model

of heavy quarkonium the cross-sections of four heavy quark production in e(+)e(-) annihilation, as well as the cross-sections of the associative production of the 1S- and 2S-wave (QQ-bar('))-mesons in the e(+)e(-) yields (QQ-bar(')) + Q(') + Q-bar process are calculated. Basing on the assumption of the quark-hadron duality the number of the Lambda(bc)-hyperon expected for LEP experiments is estimated. The fragmentation functions of b-quark into B(c)(B(c)(*))-meson, c- and b-quarks into eta(c)(psi)- and (eta)(b)(Upsilon)-mesons, respectively, are obtained. DOE

N95-32763# Kansas State Univ., Manhattan, KS.
HIGH ENERGY COLLISIONS INVOLVING MULTIPLY CHARGED IONS
K. L. Wong, W. Wu, E. C. Montenegro, I. Ben-Itzhak, C. L. Cocke, J. P. Giese, and P. Richard 1994 5 p Presented at the Department of Energy Basic Energy Sciences Atomic Physics Workshop, Lexington, KY, 14-15 Oct. 1994
(Contract DE-FG02-86ER-13491)
(DE95-010912; DOE/ER-13491/741; CONF-9410198-3) Avail: CASI HC A01/MF A01

Eight abstracts cover the following areas: single capture and transfer ionization in collisions of Cl(q+) projectile ions; charge-state q-dependence of zero degree BEE (binary encounter electrons) production in 30 MeV O(q+) + H2, He, Ne, and O2; charge-state dependence of BEE cross sections and peak energies; experimental separation of electron-electron and electron-nuclear contributions to ionization of fast hydrogen-like ions colliding with He; diffraction structure in the doubly differential cross section for electron emission; electron emission angle dependence of the violation of q(exp 2) scaling of the DDCS for BEE emission for F(q+) (3 less than or equal to q less than or equal to 9) on H2; ion molecule collisions; and mean lifetimes of long lived doubly charged molecular ions. DOE

N95-32796# Joint Inst. for Nuclear Research, Dubna (USSR).
A STUDY OF THE A DEPENDENCE OF THE DEEP INELASTIC SCATTERING OF LEPTONS AND IMPLICATIONS FOR UNDERSTANDING OF THE EMC EFFECT
G. I. Smirnov 1994 12 p
(DE95-613711; JINR-D-1-94-278) Avail: CASI HC A03/MF A01 (US Sales Only)

It is suggested to determine the A dependence of distortions of the nucleon structure function F(sub 2)(x) by summing the distortions over the interval (x(sub 1), x(sub 2)). It was found from the analysis of the data on deep inelastic scattering of muons and electrons from nuclei that the A dependence of distortion magnitudes obtained in each of the three regions under study, namely shadowing, anti shadowing and the EMC effect region, follow the same functional form, being different in the normalizing factor only. All the available data give evidence for the saturation of the distortion magnitude with rising A. DOE

N95-32806# Gosudarstvennyi Komitet po Ispolzovaniyu Atomnoi Energii, Leningrad (USSR).
THE (PI)(YIELDS)e(NU)(GAMMA) DECAY IN CHIRAL PERTURBATION THEORY
Y. Y. Komachenko and R. N. Rogalev 1994 8 p
(DE95-619269; IHEP-94-15) Avail: CASI HC A02/MF A01 (US Sales Only)

We calculate the electromagnetic correction to (pi)(yields)e(nu)(gamma) form factors within the Chiral Perturbation Theory. This correction does not explain the discrepancy between the theoretical and experimental spectra of the (pi)(yields)e(nu)(gamma) decay. However, the expression we obtain indicates that there exists a tensorial interaction with coupling constant f(sub T)(approx)10(exp -7)-10(exp -6) in the effective weak hamiltonian. We also estimate f(sub T) within the Standard Model. There is a good agreement between the ChPT and SM. DOE

N95-32814 Rutherford Appleton Lab., Chilton (England).
ENGIN MINI-MANUAL. VERSION 1.5
J. S. Wright Jan. 1995 44 p
(PB95-216095; RAL-95-017) Avail: Issuing Activity (National Technical Information Service (NTIS))

The document is designed to get you started planning and executing your experiment and analysing your data. You will also find useful the PUNCH mini-guide which describes the operation of the ISIS VAX cluster and other computing facilities, and the GENIE manual which describes the functions of GENIE, a language for display and manipulation of ISIS histogram data. These are both obtainable from the computer support office. If you want to go more deeply into the refinement of your data, you should obtain a copy of 'Profile Analysis of Neutron Powder Diffraction Data at ISIS', RAL report 92-032, by W. I. F. David, R. M. Ibberson and J. C. Matthewman, usually available from Richard Ibberson. NTIS

N95-32921# Polish Academy of Sciences, Warsaw (Poland). Inst. of Basic Problems of Technology.
PROPAGATION OF SPATIAL SOLITONS GENERATED BY GAUSSIAN BEAMS IN A NON-LINEAR KERR MEDIUM [PROPAGACJA SOLITONOW PRZESTRZENNYCH GENEROWANYCH WIAZKAMI GAUSSA W NIELINIOWYM OSRODKU KERRA]
Dariusz Burak Sep. 1995 116 p In POLISH
(ISSN 0208-5658)
(IFTR-9/1995) Avail: CASI HC A06/MF A02

##e author analyzes the propagation of light space solitons (first and second order) generated by Gauss-Hermit beams of the fundamental and second orders in a non-linear Kerr medium. The author numerically determines the relationship of the parameters of the excited solitons to the parameters of the initial Gauss-Hermit beams. The author analytically determines the threshold amplitudes required for the generation of a soliton of any order using excitation by a fundamental Gauss beam. The author discovered self-focusing of the initial beams in the near field, followed by the generation of soliton beams in the far field. The author determined the parameters of a fundamental Gauss beam necessary for its self confinement in a Kerr medium (propagation without a change in shape) and for maximum conversion of its power to a soliton beam. The excitation of a Kerr medium by a second order Gauss-Hermit beam may only result in the generation of an even number of solitons. In this case, below the threshold amplitude, the initial beam is subject to non-linear diffraction, while above the threshold amplitude it generates two solitons which are propagated symmetrically in directions from the axis of propagation of the coordinate system. The relative angle of propagation of the solitons decreases with an increase in the amplitude of the initial beam, up to the generation of a pulsating soliton. The author has developed a variational approximation of the non-linear propagation of zero- and second-order Gauss Hermit beams. The author determines the form of the soliton in a variational approximation of a fundamental-order Gauss beam. The author analytically determines the approximate parameters of a first-order soliton generated by a Gauss beam. The author discusses the agreement between the variational approximation of propagation and an exact (numerical) solution of a propagation equation. The author demonstrates that the propagation of second order solitons may be quite adequately approximated by the propagation of a second-order Gauss-Hermit beam with variationally defined parameters. Author

N95-32965# Georgia State Univ., Atlanta, GA.
LIGHT PARTICLE EMISSION IN HEAVY ION REACTIONS Progress Report for 1994 - 1995
E. H. Howell, Xiaochun He, G. A. Petitt, and Ziyang Zhang 1995 25 p
(Contract DE-FG05-84ER-40162)
(DE95-010727; DOE/ER-40162/T8) Avail: CASI HC A03/MF A01

This report discusses the following topics: PHENIX RD94 R&D: PISA/PISORP code development; level-1 trigger rate simulation study for PHENIX muon arm; mu/tau discrimination performanc of PHENIX muon arm; and mu/tau discrimination performance of RD45 ca rimeter. DOE

N95-32966# Kansas State Univ., Manhattan, KS. J.H. MacDonald Lab.
THE MEAN LIFETIMES OF THE 2p(SIGMA) LOWEST BOUND STATE OF HeH(2+) AND ITS ISOTOPES
B. D. Esry (Colorado Univ., Boulder, CO.), I. Ben-Itzhak, Z. Chen, C. D. Lin, J. P. Bouhnik (Technion - Israel Inst. of Engineering, Haifa, Israel.), I. Gertner (Technion - Israel Inst. of Engineering, Haifa, Israel.), B. Rosner (Technion - Israel Inst. of Engineering, Haifa, Israel.), and O. Heber (Weizmann Inst. of Science, Rehovot, Israel.) 1995 2 p Presented at the 19th International Conference on the Physics of Electronic and the Atomic Collisions, Whistler, Canada, 26 Jul. - 1 Aug. 1995
(Contract DE-FG02-86ER-13491)
(DE95-010812; DOE/ER-13491/772; CONF-950706-5) Avail: CASI HC A01/MF A01

The HeH(2+) molecular ion is bound in its first excited electronic state (2p(sigma)) in spite of the strong nuclear repulsion. This state decays by spontaneous electronic dipole transition to the repulsive ground state (1s(sigma)). Its mean life is of the order of a few nsec, and thus none of the molecular ions are detected directly. Fragment-fragment coincidences are used determine that the HeH(2+) have passed a small analyzer next to the target cell. Recently, we have determine the mean lifetime of (4)HeH(2+) from the measured number of molecular ions as a function of their flight time from the target cell to the exit of the analyzer. The data was consistent with our model calculations which involved contributions form many vibrational states with different decay rate, however a single exponential fit was also consistent with the data. Derived from text

N95-33171# Gosudarstvennyi Komitet po Ispolzovaniyu Atomnoi Energii, Leningrad (USSR).
STUDY OF THE p + N YIELDS (SIGMA(0)K(+)) + N REACTION AT E(SUB P) 70 GeV
D. V. Vavilov, V. A. Viktorov, and S. V. Golovkin 1994 7 p
(DE95-619273; IFVE-OEF-94-6) Avail: CASI HC A02/MF A01 (US Sales Only)

The reaction p + N yields (Sigma(0)K(+)) + N has been studied at the SPHINX Facility with the IHEP 70 GeV proton beam. In the mass spectrum M(Sigma(0)K(+)) for a coherent diffraction process a distinct peak with the mass M = 1999 +/- 7 MeV and width Gamma = 91 +/- 17 MeV is observed alongside with the near threshold structure with M(approx equal) 1800 MeV. DOE

N95-33201# Stanford Linear Accelerator Center, Stanford, CA.
VIRTUAL EFFECTS OF PHYSICS BEYOND THE STANDARD MODEL
J. L. Hewett Apr. 1995 6 p Presented at the 4th International Conference on Physics Beyond the Standard Model, Lake Tahoe, CA 13-18 Dec. 1994
(Contract DE-AC03-76SF-00515)
(DE95-012499; SLAC-PUB-95-6822; CONF-941251-4) Avail: CASI HC A02/MF A01

The author examines the indirect effect of new physics on a variety of processes in the B system, such as the Z yields b(bar b) vertex, the decays B yields X(sub s) gamma and B yields X(sub s)l(+)l(-), and CP violation. DOE

N95-33203# Brookhaven National Lab., Upton, NY. Physics Dept.
HADRON DISTRIBUTIONS AT HIGHER RAPIDITY USING THE BRAHMS FORWARD SPECTROMETER
Bruce Moskowitz 1995 10 p Presented at the 11th International Conference on Ultra-relativistic Nucleus-nucleus Collisions, Monterey, CA, 9-13 Jan. 1995
(Contract DE-AC02-76CH-00016)
(DE95-008861; BNL-61518; CONF-950127-10) Avail: CASI HC A02/MF A01

Different conditions, and therefore different physics, are expected to exist over the range of rapidities at RHIC. The BRAHMS Forward Spectrometer will measure identified hadron distributions up to y = 4, giving it a unique place in the RHIC experimental program. DOE

N95-33219# Lawrence Livermore National Lab., Livermore, CA.
OBSERVATION OF KLM DIELECTRONIC RECOMBINATION RESONANCES IN HIGHLY CHARGED URANIUM IONS
David Knapp and John Tanis (University of Western Michigan, Kalamazoo, MI.) 14 Sep. 1994 7 p Presented at the 7th International Conference on Physics of Highly Charged Ions, Vienna, Austria, 19-23 Sep. 1994
(Contract W-7405-eng-48)
(DE95-010266; UCRL-JC-118724; CONF-940922-8) Avail: CASI HC A02/MF A01

We have observed the KLM and higher (Delta)n (ge) 1 dielectronic recombination resonances in highly charged (near-heliumlike) uranium ions. The resonances were observed via photon emission from ions trapped in an electron beam ion trap (EBIT). As the energy of the electron beam was swept over the resonances, characteristic radiation from dielectronic recombination was recorded in photon detectors. DOE

N95-33226# Joint Inst. for Nuclear Research, Dubna (USSR). Lab. of High Energy.
THE PROBLEM 4/3 AS A CONSEQUENCE OF CONTRACTED LENGTH NON-COVARIANCE
V. N. Streltsov 1994 3 p
(DE95-623628; JINR-D-2-94-331) Avail: CASI HC A01/MF A01 (US Sales Only)

It is emphasized that the known non-covariance of the energy and the momentum of the electromagnetic field of a moving charge is a direct consequence of the generally accepted definition of dimensions of moving objects. As known, according to this definition the longitudinal sizes contract. DOE

N95-33241# Kansas State Univ., Manhattan, KS. Dept. of Physics.
CDW-EIS CALCULATION OF LONGITUDINAL MOMENTUM DISTRIBUTION IN SINGLE IONIZATION OF HELIUM BY NI(24+) IONS
V. D. Rodriguez (Buenos Aires Univ., Argentina.), Y. D. Wang, and C. D. Lin 1995 2 p Presented at the 19th International Conference on the Physics of Electronic and the Atomic Collisions, Whistler, Canada, 26 Jul. - 1 Aug. 1995
(Contract DE-FG02-86ER-13491)
(DE95-010816; DOE/ER-13491/776; CONF-950706-17) Avail: CASI HC A01/MF A01

The calculation of a longitudinal momentum distribution with the single ionization of helium by a nickel ion is discussed in this short communication. This development has allowed new opportunities to study ion-atom collision physics. In this work, the continuum-distored-wave- eikonal-initial state (CDW-EIS) method to study this distribution is applied. DOE

N95-33245# Stanford Linear Accelerator Center, Stanford, CA.
SEARCHING FOR NEW PHYSICS WITH CHARM
J. L. Hewett 1995 7 p Presented at the LAFEX International School in High Energy Physics, Rio de Janeiro, Brazil, 20 Feb. 1995
(Contract DE-AC03-76SF-00515)
(DE95-012498; SLAC-PUB-95-6821; CONF-950285-2) Avail: CASI HC A02/MF A01

The author considers the prospect of using the charm system as a laboratory for probing new physics. The theoretical expectations for rare charm meson decays, D(sup 0) - (bar D)(sup 0), and charm quark asymmetries in Z decays are examined in the Standard Model. The effects of new physics from several classes of nonstandard dynamical models are summarized for these phenomena. DOE

N95-33370# Kansas State Univ., Manhattan, KS.
VELOCITY DEPENDENCE OF IONIZATION AND EXCITATION OF HYDROGEN MOLECULES BY FAST PROTON IMPACT
I. Ben-Itzhak, Vidhya Krishnamurthi, K. D. Carnes, H. Aliabadi, H. Knudsen, U. Mikkelsen (Aarhus Univ., Denmark.), and B. D. Esry (Colorado Univ., Boulder, CO.) 1995 2 p Presented at the 19th International Conference on the Physics of Electronic and the Atomic Collisions, Whistler, Canada, 26 Jul. - 1 Aug. 1995
(Contract DE-FG02-86ER-13491)
(DE95-010818; DOE/ER-13491/770; CONF-950706-15) Avail: CASI HC A01/MF A01

The collisions between fast protons and hydrogen molecules has been studied over a wide range of impact velocities (6-23 a.u.) using the coincidence time-of-flight technique. The ratio of double- to single-ionization (DI/SI) approaches a constant value at high velocities indicating that double ionization is due to e-e interactions. In addition, the ratio is about half of the value measured for a He target. This difference between the two targets is due to the single ionization cross section for hydrogen being larger than that for He. The double ionization cross section, however, is similar for both targets. DOE

N95-33371# Kansas State Univ., Manhattan, KS. J.R. Macdonald Lab.
STATE-SELECTIVE SINGLE ELECTRON CAPTURE CROSS SECTIONS IN He(EXP 2+) + Li(2s) AND Li(*)(2p) COLLISIONS
R. Shingal, C. P. Bhalla, and S. R. Grabbe 1995 2 p Presented at the 19th International Conference on the Physics of Electronic and the Atomic Collisions, Whistler, Canada, 26 Jul. - 1 Aug. 1995
(Contract DE-FG02-86ER-13491)

(DE95-010819; DOE/ER-13491/769; CONF-950706-14) Avail: CASI HC A01/MF A01

It has been well established that charge transfer processes are of considerable importance in thermonuclear fusion research. Motivated by the recent studies of doubly charged ions with ground state and laser excited Li targets, we have calculated single electron capture cross sections from Li(2s), Li(*)(2p Sigma), and Li(*)(2p Pi) initial states into He(+) (n = 3,4,5,6) final states. These calculations have been carried out for impact energies ranging from 1.0 to 84.0 KeV using a 96-state atomic orbital (AO) close coupling calculation. DOE

N95-33372# Kansas State Univ., Manhattan, KS. J.R. Macdonald Lab.
AN ION-ION COLLISIONS SYSTEM AT KSU
C. Y. Chen, A. Landers, J. P. Giese, F. Melchert, P. Richard, C. L. Cocke, and M. P. Stockli 1995 2 p Presented at the 19th International Conference on the Physics of Electronic and the Atomic Collisions, Whistler, Canada, 26 Jul. - 1 Aug. 1995
(Contract DE-FG02-86ER-13491)
(DE95-010820; DOE/ER-13491/768; CONF-950706-13) Avail: CASI HC A01/MF A01

An ion-ion collisions facility has been built at Kansas State University (KSU) to study electron capture processes between two multiply charged ions. While the study of ion-ion collisions is still young compared to ion-atom and electron-atom collisions, a considerable amount of research has been done on systems where both of the beams were composed of singly or doubly charged ions. Only a few ion-ion collisions experiments have used two multiply charged ions. We hope to systematically extend these studies to higher charged ions by studying one and two electron transfer along various isoelectronic sequences. DOE

N95-33374# Kansas State Univ., Manhattan, KS.
ELECTRON-ELECTRON INTERACTION IN THE IONIZATION OF HYDROGENLIKE PROJECTILES BY He
W. Wu, K. L. Wong, E. C. Montenegro, R. Ali, C. Y. Chen, C. L. Cocke, R. Doerner (Johann-Wolfgang-Goethe-Univ., Frankfurt am Main, Germany.), V. Frohne, J. P. Giese, and V. Mergel (Johann-Wolfgang-Goethe-Univ., Frankfurt am Main, Germany.) et al 1995 2 p Presented at the 19th International Conference on the Physics of Electronic and the Atomic Collisions, Whistler, Canada, 26 Jul. - 1 Aug. 1995
(Contract DE-FG02-86ER-13491)
(DE95-010822; DOE/ER-13491/765; CONF-950706-11) Avail: CASI HC A01/MF A01

The ionization of a fast hydrogenlike projectile in a collision with a light target can be caused by the interaction of the projectile electron with either the target nucleus or with one of its electrons. Attempts to isolate the latter contribution to projectile electron loss has been the focus of many recent experimental efforts. A particularly clean separation of the electron-electron (ee) mechanism from the more conventional electron-nuclear (eN) is possible through the measurement of the longitudinal momentum, p(upsilon) transferred to the recoil ion in the collision. While the eN process throws the recoil ion forward with a momentum given by P(z) = Q/v, the recoil ion views the ee process as a spectator and receives almost no p(z) in that case. Here Q is the sum of the projectile electron binding energy and the final energy of that electron in its parent reference frame, and v is the projectile velocity. In this experiment we have used recoil momentum spectroscopy to separate the ee and eN contributions to the ionization of fast hydrogenlike O and F ions by He, and have constructed models for the quantitative interpretation of the momentum distributions. DOE

N95-33375# Stanford Linear Accelerator Center, Menlo Park, CA.
PROBING NEW PHYSICS IN B PENGUINS
J. L. Hewett Feb. 1995 4 p Presented at the 1994 International Workshop on B Physics, Physics Beyond the Standard Model At the B Factory, Nagoya, Japan, 26-28 Oct. 1994
(Contract DE-AC03-76SF-00515)
(DE95-012494; SU-SLAC-PUB-95-6782; CONF-9410248-3) Avail: CASI HC A01/MF A01

Constraints placed on physics beyond the Standard Model from the recent CLEO observation of the inclusive decay B yields X(s)gamma are summarized. Further searches for new physics using the process B yields X(s)l(+)l(-) are discussed. DOE

N95-33380# California Univ., Berkeley. Lawrence Berkeley Lab, CA.
DEVELOPMENT OF SILICON DRIFT DETECTORS FOR STRANGENESS MEASUREMENTS
G. Odyniec, B. Krieger, D. Krofcheck, D. Lewak, R. ODonnel, M. Partlan, J. T. Walton, and N. W. Wang Feb. 1995 12 p Presented at the Strangeness in Hadronic Matter Conference, Tucson, AZ, 4-6 Jan. 1995
(Contract DE-AC03-76SF-00098)
(DE95-012366; LBL-36908; CONF-950172-3; UC-414) Avail: CASI HC A03/MF A01

Detection of multi-strange and charm particles requires precise measurements of the secondary vertices close to the interaction point and the decay products of strange and charm particles. This presents an unprecedented challenge for relativistic heavy ion experiments, where multiplicity reaches thousands of final state particles per collision. Development of affordable technology for realizing high spatial resolution and low mass vertex detectors has become the ultimate goal of many R&D projects in major laboratories. In this paper we present preliminary results on silicon drift detectors fabricated for the first time on p-type silicon substrates. These detectors were designed, fabricated and tested recently at LBL and show very interesting properties which make their use in future experiments very likely. DOE

N95-33623# Los Alamos National Lab., NM.
INDIRECT MEASUREMENTS OF HYDROGEN: THE DEFICIT METHOD FOR A MANY-COMPONENT SYSTEM
Timothy E. Levine (Cornell Univ., Ithaca, NY.), Ning Yu, Padma Kodali, Kevin C. Walter, Michael Nastasi, Joseph R. Tesmer, Carl J. Maggiore, and James W. Mayer (Arizona State Univ., Tempe, AZ.) 1995 6 p Presented at the Applications of Ion Beam Analysis Workshop, Sydney, Australia, 1-3 Feb. 1995
(Contract W-7405-eng-36)
(DE95-010993; LA-UR-95-1437; CONF-950220-8) Avail: CASI HC A02/MF A01

We have developed a simple technique for determining hydrogen atomic fraction from the ion backscattering spectrometry (IBS) signals of the remaining species. This technique uses the surface heights of various IBS signals in the form of a linear matrix equation. We apply this technique to in situ analysis of ion-beam-induced densification of sol-gel zirconia thin films, where hydrogen is the most volatile species during irradiation. Attendant errors are discussed with an emphasis on stopping powers and Bragg's rule. DOE

N95-33850# Brookhaven National Lab., Upton, NY. Physics Dept.
OVERVIEW OF RARE K DECAYS
Laurence Littenberg 1995 24 p Presented at the 2nd International Workshop on Heavy Quark Physics in Fixed Targets, Charlottesville, VA, 6-10 Oct. 1994
(Contract DE-AC02-76CH-00016)
(DE95-012081; BNL-61775; CONF-9410285-3) Avail: CASI HC A03/MF A01

The status and future prospects of searches for and studies of forbidden and highly suppressed K decays are reviewed. Here the author discusses three areas of recent activity in rare K decay. These are lepton-flavor violating decays, which are entirely forbidden in the Standard Model, K(sub S) (yields) (pi)(+)(pi)(-) (pi)(sup 0), which is of interest from the point of view of CP-violation, and 'one loop' decays of the form K(sup 0,(+-)) (yields) ((pi)(sup 0,(+-)))l(bar l), that can throw light on Standard Model CP-violation and determine parameters such as V(sub td). DOE

N95-33854# Washington Univ., Seattle, WA. Inst. for Nuclear Theory.
WEE PARTONS IN LARGE NUCLEI: FROM VIRTUAL DREAM TO HARD REALITY
Raju Venugopalan 1995 17 p Presented at the 11th International Conference on Ultra-relativistic Nucleus-nucleus Collisions, Monterey, CA, 9-13 Jan. 1995
(Contract DE-FG06-90ER-40561)
(DE95-012168; DOE/ER-40561/188; CONF-950127-7) Avail: CASI HC A03/MF A01

We construct a weak coupling, many body theory to compute parton distributions in large nuclei for x much less than A(sup -1/3). The wee partons are highly coherent, non-Abelian Weizsaecker-Williams fields. Radiative corrections to the classical results axe discussed. The parton

distributions for a single nucleus provide the initial conditions for the dynamical evolution of matter formed in ultrarelativistic nuclear collisions.
DOE

N95-33855# Washington Univ., Seattle, WA. Inst. for Nuclear Theory.
QCD AND HADRON STRUCTURE
D. B. Kaplan 1995 11 p Presented at the Nuclear Theory Town Meeting, Argonne, IL, 29-30 Jul. 1995
(Contract DE-FG06-90ER-40561)
(DE95-012173; DOE/ER-40561/176; CONF-9507126-1) Avail: CASI HC A03/MF A01

I give a brief and selective overview of QCD as it pertains to determining hadron structure, and the relevant directions in this field for nuclear theory. This document is intended to start discussion about priorities, not end it.
DOE

N95-34212# Argonne National Lab., IL.
PARALLEL MOLECULAR DYNAMICS: COMMUNICATION REQUIREMENTS FOR MASSIVELY PARALLEL MACHINES
Valerie E. Taylor (Northwestern Univ., Evanston, IL.), Rick L. Stevens, and Kathryn E. Arnold 1995 8 p Presented at the Frontiers 1995: A Workshop on Future Directions of Massively Parallel Processing, McLean, VA, 6-9 Feb. 1995
(Contract W-31-109-eng-38)
(DE95-012948; ANL/MCS/CP-84761; CONF-9502101-2) Avail: CASI HC A02/MF A01

Molecular mechanics and dynamics are becoming widely used to perform simulations of molecular systems from large-scale computations of materials to the design and modeling of drug compounds. In this paper we address two major issues: a good decomposition method that can take advantage of future massively parallel processing systems for modest-sized problems in the range of 50,000 atoms and the communication requirements needed to achieve 30 to 40% efficiency on MPPs. We analyzed a scalable benchmark molecular dynamics program executing on the Intel Touchstone Deleta parallelized with an interaction decomposition method. Using a validated analytical performance model of the code, we determined that for an MPP with a four-dimensional mesh topology and 400 MHz processors the communication startup time must be at most 30 clock cycles and the network bandwidth must be at least 2.3 GB/s. This configuration results in 30 to 40% efficiency of the MPP for a problem with 50,000 atoms executing on 50,000 processors.
DOE

N95-34350# Pennsylvania Univ., Philadelphia, PA. Dept. of Chemistry.
THE COMPUTATION OF ELECTRON TRANSFER RATES: THE NONADIABATIC INSTANTON SOLUTION Technical Report, May 1994 - 1995
Jianshu Cao, Camilla Minichino, and Gregory A. Voth 30 May 1995 32 p
(Contract N00014-92-J-1243)
(AD-A294523; TR-11) Avail: CASI HC A03/MF A01

A computational theory for determining electron transfer rate constants is formulated based on an instanton expression for the quantum rate and the self-consistent solution of the imaginary time nonadiabatic steepest descent approximation. The theory obtains the correct asymptotic behavior for the electron transfer rate constant in the nonadiabatic cases, and it smoothly bridges between those two limits for intermediate couplings. Furthermore, no assumptions regarding the form of the diabatic states can be included in the calculations. The method thereby holds considerable promise for computing electron transfer rate constants in realistic condensed phase systems.
DTIC

N95-34355# Kansas State Univ., Manhattan, KS. J. R. MacDonald Lab.
MEAN LIFETIME MEASUREMENTS OF (3)He(4)He2+
I. Ben-Itzhak, Z. Chen, C. D. Lin, J. P. Bouhnik (Technion - Israel Inst. of Tech., Haifa, Israel.), I. Gertner (Technion - Israel Inst. of Tech., Haifa, Israel.), B. Rosner (Technion - Israel Inst. of Tech., Haifa, Israel.), O. Heber (Weizmann Inst. of Science, Rehovot, Israel.), and D. Zajfman (Weizmann Inst. of Science, Rehovot, Israel.) 1995 4 p Presented at the 19th International Conference on the Physics of Electronic and the Atomic Collisions, Whistler, Canada, 26 Jul. - 1 Aug. 1995
(Contract DE-FG02-86ER-13491)
(DE95-010813; DOE/ER-13491/773; CONF-950706-4) Avail: CASI HC A01/MF A01

A beam of 0.9 MeV (3)He(4)He+ molecular ions was directed through a target cell containing a thin target of Argon gas. The reaction products emerging from the target cell were analyzed by an electrostatic deflector and detected by a surface barrier detector. The decay rates of many rovibrational states of (3)He(4)He2+ were calculated using the phase shift method in order to find the states which had been detected.
CASI

N95-34423 Centro di Cultura Scientifica A. Volto, Como (Italy).
ATOMS IN STRONG FIELDS Final Technical Report
Giulio Casati Apr. 1995 28 p Limited Reproducibility: More than 20% of this document may be affected by poor print
(Contract N68171-94-M-5310)
(AD-A294589; R/D-7184-MA-01/ENV) Avail: Issuing Activity (Defense Technical Information Center (DTIC))

The response of a bound electron to an external monochromatic field is a complicated process, that gives rise to a variety of phenomena. This problem has proven much richer than could be suspected at the origins of quantum mechanics. This is hardly surprising, because at the root of its richness lies the full complicacy of classical nonlinear dynamics that only in recent times we have begun to explore. In 1974 Bayfield and Koch found that the ionization of highly excited hydrogen atoms by microwaves fields has a threshold character with respect to field strength: it is very small at very small intensity but it increases abruptly at a certain threshold intensity. This was found to be an essentially classical phenomenon, the observed threshold being practically the same as the classical threshold above which the classical dynamics of the electron becomes chaotic. Chaotic ionization was extensively investigated in the 80's, both experimentally and theoretically.
DTIC

N95-34650 Rutherford Appleton Lab., Oxford (England).
REMARKS ON THE KARMEN ANOMALY
V. Barger, R. G. N. Phillips, and S. Sarkar Mar. 1995 15 p Prepared in cooperation with Wisconsin Univ., Madison, WI, and Oxford Univ., Oxford, England
(Contract DE-FG02-95ER-40896)
(PB95-234977; RAL-95-026) Avail: Issuing Activity (National Technical Information Service (NTIS))

A recently reported anomaly in the time structure of signals in the KARMEN neutrino detector suggests the decay of a new particle x, produced in pi(+) yields (mu(+))x with mass M(sub x) = 33.9 MeV. The authors discuss the constraints and difficulties in interpreting x as a neutrino. The authors show that a mainly-sterile neutrino scenario is tenable, within narrow constraints on the mixing parameters, but it predicts that appreciable numbers of other x-decay events with different origins and time structures should also be observable in the KARMEN detector. Such x-decay events should also be found in the LSND experiment and may be relevant to the search for (bar-nu)(sub mu) yields (bar-nu)(sub e) oscillations. Derived from text

N95-34657 Rutherford Appleton Lab., Chilton (England). ISIS Facility.
INTERNATIONAL MEETING ON MUON SCIENCE
G. H. Eaton Mar. 1995 347 p Meeting held in Abingdon, England, 5-7 Dec. 1994
(PB95-236014; RAL-95-023) Avail: Issuing Activity (National Technical Information Service (NTIS))

The proceeding of the Internation Meeting on Muon Science is presented. Session topics include the following: ISIS Muon Facilities; Condensed Matter Science; Slow Muons; Muonium Spectroscopy; Muon Catalyzed Fusion and Exotic Atoms; Neutrinos and Fundamental Particle Physics; ISIS Visit and Summary. A partial listing of titles of papers includes the following: The ISIS European Muon Facility; The Installation and Build of the RIKEN Facility; Optical and Infra-red Spectroscopy in Semiconductors; Muon State Dynamics in Silicon; The KEK Ultra Slow Muon Facility; Very Slow Polarized Muons; Laser Spectroscopy of Muonic Atoms; Pulsed VUV lasers for Muonium Resonant Ionization; Laser Spectroscopy at Pulsed and DC Muon Beams; Muon Experiments with a Pulsed Source; Neutrino Physics at LAMPF.
NTIS

N95-34819# Champlain Technology, Inc., West Palm Beach, FL.
STRUCTURE AND DYNAMICS OF EXCITED ATOMS Final Report, 15 Nov. 1989 - 14 Nov. 1994

Thomas F. Gallagher Mar. 1995 15 p
(Grant AF-AFOSR-0036-90)
(AD-A294997; AFOSR-95-0289TR) Avail: CASI HC A03/MF A01

During the five year period of grant AFOSR-90-0036 we have worked on two different kinds of projects, microwave multiphoton processes and resonant collisional energy transfer. Both kinds of experiments are carried out with highly excited, or Rydberg atoms, which allow us to do quantitative experiments giving insights which would be difficult or impossible to obtain in other systems. For example, our experiments on microwave multiphoton excitation and ionization have demonstrated that the Floquet, or dressed state, approach provides an accurate description of the evolution of atomic systems in intense radiation pulses. The understanding derived from our microwave experiments resolved a controversy about how laser multiphoton ionization through intermediate resonances occurred. In the two following sections of this report we describe the collision experiments and the microwave multiphoton experiments. DTIC

N95-32424*# Houston Univ.-Clear Lake, Houston, TX. Dept. of Natural and Applied Sciences.
IMAGE ANALYSIS USED TO COUNT AND MEASURE ETCHED TRACKS FROM IONIZING RADIATION
George E. Blanford and Cindy K. Schulz *In* NASA. Johnson Space Center, Houston, National Aeronautics and Space Administration NASA)/American Society for Engineering Education (ASEE) Summer Faculty Fellowship Program, 1994, Volume 1 Jul. 1995 13 p (For primary document see N95-32418 12-99)
Avail: CASI HC A03/MF A03

N95-32721*# Deutsche Forschungsanstalt fuer Luft- und Raumfahrt, Cologne (Germany). Radiation Biology Div.
DOSIMETRY OF HEAVY IONS BY USE OF CCD DETECTORS
J. U. Schott *In* NASA. Ames Research Center, Minutes of the 12th Joint NASA/DARA-DLR Life Sciences Program Working Group Meeting 1994 p 5-10 (For primary document see N95-32719 12-51)
Avail: CASI HC A02/MF A03

N95-32985# Osaka Univ., Osaka (Japan). Dept. of Nuclear Engineering.
CALCULATIONS OF SPATIAL HIGHER MODES WITHOUT DEFLATION PROCEDURE
Takeo Nishigori and Toshikazu Takeda *In its* Technology Reports of the Osaka Univ. Vol. 45, Nos. 2205-2216 15 Apr. 1995 p 1-6 (For primary document see N95-32984 12-31)
(Rept-2205) Avail: CASI HC A02/MF A02

N95-32986# Osaka Univ., Osaka (Japan). Dept. of Applied Physics.
PRACTICAL IMPROVEMENT OF MS-X ALPHA MOLECULAR ORBITAL CALCULATION AS APPLIED TO DISSOCIATION PROCESS OF CO MOLECULE
Yoshihiro Irokawa, Masatsugu Honjo, Yoshizo Takai, and Ryuichi Shimizu *In its* Technology Reports of the Osaka Univ., Vol. 45, Nos. 2205-2216 15 Apr. 1995 p 7-16 (For primary document see N95-32984 12-31)
(Rept-2206) Avail: CASI HC A02/MF A02

N95-33266*# Edgewood Research Development and Engineering Center, Aberdeen Proving Ground, MD. Development and Engineering Center.
PROTON AFFINITY DETERMINATIONS AND PROTON-BOUND DIMER STRUCTURE INDICATIONS IN C2 TO C15, (ALPHA),(OMEGA)-ALKYLDIAMINES
Z. Karpas (Nuclear Research Center, Beer-Sheva, Israel.), C. S. Harden, and P. B. W. Smith (GEO-Centers, Inc., Aberdeen Proving Ground, MD.) *In* NASA. Johnson Space Center, Third International Workshop on Ion Mobility Spectrometry Apr. 1995 p 1-15 (For primary document see N95-33265 12-25)
Avail: CASI HC A03/MF A03

73 NUCLEAR AND HIGH-ENERGY PHYSICS

Includes elementary and nuclear particles; and reactor theory. For space radiation see *93 Space Radiation.*

N95-32411# Brookhaven National Lab., Upton, NY.
CRYSTALLINE BEAM PROPERTIES AS PREDICTED FOR THE STORAGE RINGS ASTRID AND TSR
Jie Wei, Xiao-Ping Li (Biosym Technologies, Inc., San Diego, CA.), and Andrew Sessler (California Univ., Berkeley. Lawrence Berkeley Lab, CA.) 1995 4 p Presented at the Particle Accelerator Conference, Dallas, TX, 1-5 May 1995
(Contracts DE-AC02-76CH-00016; DE-AC03-76SF-00098)
(DE95-011557; BNL-61158; CONF-950512-48) Avail: CASI HC A01/MF A01

During recent years, significant progress has been made in understanding the formation of crystalline beams in circular accelerators and storage rings. No crystalline beam exists in a constant gradient storage ring, but in an alternating gradient (AG) ring crystalline beams exist at all densities as long as the beam energy is smaller than the transition energy of the machine. The ground-state structure depends upon the machine lattice property, the beam energy, and the beam intensity (line density). At low density, the ground state is a one-dimensional (1D) chain with particles equally spaced along the azimuthal axis. As the density increases, the ground state first becomes a 2D zig zag in the plane of weaker transverse focusing, and then becomes 3D single- and multi-shell helices. The maximum spatial density of the crystal, on the other hand, is determined only by the machine lattice property and beam energy, independent of the beam intensity. Employing a previously developed formalism, the authors have performed ground-state and melting calculations of the expected crystalline beams in ion storage rings ASTRID and TSR. DOE

N95-32413# Brookhaven National Lab., Upton, NY.
THE EFFECT AND CORRECTION OF COUPLING GENERATED BY THE RHIC TRIPLET QUADRUPOLES
F. Pilat, S. Peggs, S. Tepikian, D. Trbojevic, and J. Wei 1995 4 p Presented at the Particle Accelerator Conference, Dallas, TX, 1-5 May 1995
(Contract DE-AC02-76CH-00016)
(DE95-011562; BNL-61165; CONF-950512-58) Avail: CASI HC A01/MF A01

This study explores the possibility of operating the nominal RHIC coupling correction system in local decoupling mode, where a subset of skew quadrupoles are independently set by minimizing the coupling as locally measured by beam position monitors. The goal is to establish a correction procedure for the skew quadrupole errors in the interaction region triplets that does not rely on a priori knowledge of the individual errors. After a description of the present coupling correction scheme envisioned for RHIC, the basics of the local decoupling method will be briefly recalled in the context of its implementation in the TEAPOT simulation code as well as operationally. The method is then applied to the RHIC lattice: a series of simple tests establish that single triplet skew quadrupole errors can be corrected by local decoupling. More realistic correction schemes are then studied in order to correct distributed sources of skew quadrupole errors: the machine can be decoupled either by pure local decoupling or by a combination of global (minimum tune separation) and local decoupling. The different correction schemes are successively validated and evaluated by standard RHIC simulation runs with the complete set of errors and corrections. The different solutions and results are finally discussed together with their implications for the hardware. DOE

N95-32414# Brookhaven National Lab., Upton, NY.
LINEAR ORBIT PARAMETERS FOR THE EXACT EQUATIONS OF MOTION
G. Parzen 1995 4 p Presented at the Particle Accelerator Conference, Dallas, TX, 1-5 May 1995
(Contract DE-AC02-76CH-00016)
(DE95-011567; BNL-61170; CONF-950512-63) Avail: CASI HC A01/MF A01

This paper defines the beta function and other linear orbit parameters using the exact equations of motion. The beta, alpha and psi functions are redefined using the exact equations. Expressions are found for the transfer

matrix and the emittance. The differential equations for eta = x/beta(exp 1/2) is found. New relationships between alpha, beta, psi and nu are derived. DOE

N95-32416# Los Alamos National Lab., NM.
UNEXPECTED MATCHING INSENSITIVITY IN DTL OF GTA ACCELERATOR
V. W. Yuan, J. D. Gilpatrick, K. F. Johnson, W. P. Lysenko, D. P. Rusthoi, O. R. Sander, M. Smith, and R. Weiss 1995 4 p Presented at the Particle Accelerator Conference, Dallas, TX, 1-5 May 1995
(Contract W-7405-eng-36)
(DE95-011984; LA-UR-95-1524; CONF-950512-65) Avail: CASI HC A01/MF A01

The Intertank Matching Section (IMS) of the Ground Test Accelerator (GTA) contains four variable-field quadrupoles (VFQ's) and is designed to match beam exiting the Radio-Frequency Quadrupole to the first tank of the Drift-tube LINAC (DTL-1). By varying the VFQ field strengths to create a range of beam mismatches at the entrance to DTL-1, one can test the sensitivity of the DTL-1 output beam to variations in the DTL-1 input beam. Experimental studies made during commissioning of the GTA indicate an unexpected result: the beam exiting DTL-1 shows little variation for a range of mismatches produced at the entrance. Results of the experiment and simulation studies are presented. DOE

N95-32483# Department of Energy, Washington, DC. Office of Energy Research.
MATERIALS SCIENCES PROGRAMS: FISCAL YEAR 1994
Apr. 1995 183 p
(DE95-011248; DOE/ER-0648) Avail: CASI HC A09/MF A02

The Division of Materials Sciences is located within the DOE in the Office of Basic Energy Sciences. The Division of Materials Sciences is responsible for basic research and research facilities in strategic materials science topics of critical importance to the mission of the Department and its Strategic Plan. Materials Science is an enabling technology. The performance parameters, economics, environmental acceptability and safety of all energy generation, conversion, transmission and conservation technologies are limited by the properties and behavior of materials. The Materials Sciences programs develop scientific understanding of the synergistic relationship amongst the synthesis, processing, structure, properties, behavior, performance and other characteristics of materials. Emphasis is placed on the development of the capability to discover technologically, economically, and environmentally desirable new materials and processes, and the instruments and national user facilities necessary for achieving such progress. Materials Sciences sub-fields include physical metallurgy, ceramics, polymers, solid state and condensed matter physics, materials chemistry, surface science and related disciplines where the emphasis is on the science of materials. This report includes program descriptions for 458 research programs including 216 at 14 DOE National Laboratories, 242 research grants (233 for universities), and 9 Small Business Innovation Research (SBIR) Grants. The report is divided into eight sections. Section A contains all Laboratory projects, Section B has all contract research projects, Section C has projects funded under the SBIR Program, Section D describes the Center of Excellence for the Synthesis and Processing of Advanced Materials and E has information on major user facilities. F contains descriptions of other user facilities; G, a summary of funding levels; and H, indices characterizing research projects. DOE

N95-32485# Brookhaven National Lab., Upton, NY.
ESTIMATION OF COLLECTIVE INSTABILITIES IN RHIC
W. W. MacKay, M. Blaskiewicz, D. Deng, V. Mane, S. Peggs, A. Ratti, J. Rose, T. J. Shea, and J. Wei 1995 3 p Presented at the Particle Accelerator Conference, Dallas, TX, 1-5 May 1995
(Contract DE-AC02-76CH-00016)
(DE95-011347; BNL-61173; CONF-950512-52) Avail: CASI HC A01/MF A01

The authors have estimated the broadband impedance in RHIC to be absolute value of(Z/n) less than 1.2 Omega for frequencies above 100 MHz. The Z/n threshold is set for Au(79+) ions at transition with an estimated 10% growth in emittance for Z/n = 1.5 Omega. They summarize the sources of broad and narrow band impedances in RHIC and investigate the multibunch instability limits throughout the machine cycle. The largest contribution to the broadband impedance comes from the abort and injection kickers. Since RHIC is designed to accelerate fully stripped ions from H(+) up to Au(79+) they give results for both protons and gold ions; other ions should give results somewhere between these two extremes. All ion species are expected to be stable during storage. At lower energies damping systems and chromaticity corrections will limit any growth to acceptable levels during the short time it takes to inject and accelerate the beams. DOE

N95-32606# Stanford Linear Accelerator Center, Menlo Park, CA.
SUMMARY OF THE IMPEDANCE WORKING GROUP
A. W. Chao 1995 13 p Presented at the Collective Effects in Large Hadron Collider, Montreux, Switzerland, 17-22 Oct. 1994
(Contract DE-AC03-76SF-00515)
(DE95-012095; SU-SLAC-PUB-95-6732; CONF-9410315-2) Avail: CASI HC A03/MF A01

The impedance working group concentrated on the LHC design during the workshop. They look at the impedance contributions of liner, beam position monitors, shielded bellows, experimental chambers, superconducting cavities, recombination chambers, space charge, kickers, and the resistive wall. The group concluded that the impedance budgeting and the conceptual designs of the vacuum chamber components looked basically sound. It also noted, not surprisingly, that a large amount of studies are to be carried out further, and it ventured to give a partial list of these studies. DOE

N95-32607# Stanford Linear Accelerator Center, Menlo Park, CA.
TRANSVERSE MULTIBUNCH INSTABILITIES FOR NON-RIGID BUNCHES
J. Scott Berg and Ronald D. Ruth 1995 4 p Presented at the Particle Accelerator Conference, Dallas, TX, 1-5 May 1995
(Contract DE-AC03-76SF-00515)
(DE95-012098; SU-SLAC-PUB-95-6830; CONF-950512-35) Avail: CASI HC A01/MF A01

In this paper, the authors present a method for computing growth rates and frequency shifts of a beam containing multiple non-rigid bunches. With this approach, they calculate non-rigid multibunch effects which can impact phenomena which are traditionally treated as single-bunch effects, such as the transverse mode-coupling instability. This approach is important for high current storage rings such as PEP-2 at SLAC (the B-Factory) which have very strong interbunch forces. Typical calculations treat multibunch and single bunch effects separately, and thus eliminate important interactions between the two. To illustrate the technique, the authors calculate growth rates and frequency shifts using PEP-2 as an example. DOE

N95-32608# Stanford Linear Accelerator Center, Menlo Park, CA.
FAST FEEDBACK FOR LINEAR COLLIDERS
L. Hendrickson, C. Adolphsen, S. Allison, T. Gromme, P. Grossberg, T. Himel, K. Krauter, R. MacKenzie, M. Minty, and R. Sass et al 1995 6 p Presented at the Particle Accelerator Conference, Dallas, TX, 1-5 May 1995
(Contract DE-AC03-76SF-00515)
(DE95-012099; SU-SLAC-PUB-95-6861; CONF-950512-32) Avail: CASI HC A02/MF A01

A fast feedback system provides beam stabilization for the SLC. As the SLC is in some sense a prototype for future linear colliders, this system may be a prototype for future feedbacks. The SLC provides a good base of experience for feedback requirements and capabilities as well as a testing ground for performance characteristics. The feedback system controls a wide variety of machine parameters throughout the SLC and associated experiments, including regulation of beam position, angle, energy, intensity and timing parameters. The design and applications of the system are described, in addition to results of recent performance studies. DOE

N95-32647# Westinghouse Electric Corp., West Mifflin, PA. Bettis Atomic Power Lab.
INTEGRAL CESIUM RESERVOIR: DESIGN AND TRANSIENT OPERATION
Joe N. Smith, Jr. (General Atomics Co., San Diego, CA.), M. Harlan Horner (General Atomics Co., San Diego, CA.), Lester L. Begg (General Atomics Co., San Diego, CA.), and William J. Wrobleski (Bettis Atomic Power Lab., West Mifflin, PA.) 1995 7 p Presented at the Intersociety Energy Conversion Conference, Orlando, FL, 30 Jul. - 5 Aug. 1995

(Contract DE-AC11-93PN-38195)
(DE95-010152; WAPD-T-3066; CONF-950729-1) Avail: CASI HC A02/MF A01

An electrically heated thermionic converter has been designed built and successfully tested in air. One of the unique features of this converter was an integral cesium reservoir thermally coupled to the emitter. The reservoir consisted of fifteen cesiated graphite pins located in pockets situated in the emitter lead with thermal coupling to the emitter, collector and the emitter terminal; there were no auxiliary electric heaters on the reservoir. Test results are described for conditions in which the input thermal power to the converter was ramped up and down between 50% and 100% of full power in times as short as 50 sec, with data acquisition occurring every 12 sec. During the ramps the emitter and collector temperature profiles. the reservoir temperature and the electric output into a fixed load resistor are reported. The converter responded promptly to the power ramps without excessive overshoot and with no tendency to develop instabilities. This is the rust demonstration of the performance of a cesium-graphite integral reservoir in a fast transient. DOE

N95-32657# Stanford Linear Accelerator Center, Menlo Park, CA.
BEAM-BASED MAGNETIC ALIGNMENT OF THE FINAL FOCUS TEST BEAM

P. Tenenbaum, D. Burke, R. Helm, J. Irwin, P. Raimondi (Stanford Univ., CA.), K. Oide (National Lab. for High Energy Physics, Tsukuba, Japan.), and K. Floettmann (Deutsches Elektronen-Synchrotron, Hamburg, Germany.) 1995 3 p Presented at the Particle Accelerator Conference, Dallas, TX, 1-5 May 1995
(Contract DE-AC03-76SF-00515)
(DE95-012096; SU-SLAC-PUB-95-6769; CONF-950512-33) Avail: CASI HC A01/MF A01

In order to optimize tunability and backgrounds in linear collider final focus systems, it is necessary to align strong quadrupole and sextupole magnets with beam-based measurements. Algorithms for alignment have been used successfully on the Final Focus Test Beam (FFTB) beamline at SLAC. Quadrupole magnets were aligned using a shunt technique, with resolutions from 50 microns down to 700 nanometers. Sextupole magnets were aligned by moving the magnets transverse to the beam and observing the kick on downstream beam position monitors. This procedure resulted in sextupole misalignment resolutions of 5 to 20 microns. All magnets were then moved into aligned positions via remote-controlled stages capable of sub-micron resolution. Details of the fitting algorithms, results of the measurement, and potential improvements in the system are discussed. DOE

N95-32665# Argonne National Lab., IL.
EFFICIENCY OF MODIFIED UA1 JET RECONSTRUCTION ALGORITHM IN PP, PA AND AA COLLISIONS AT STAR

B. Christie (Brookhaven National Lab., Upton, NY.) and K. Shestermanov (Gosudarstvennyi Komitet po Ispolzovaniyu Atomnoi Energii, Protvino, USSR.) 1995 11 p
(Contract W-31-109-eng-38)
(DE95-009918; ANL-HEP-TR-95-11) Avail: CASI HC A03/MF A01

The efficiency of a modified UA1 jet reconstruction algorithm and the reconstructed jet's P(sub T) resolution in PP, PA, and AA events using the STAR detector has been studied. The HIJING and PYTHIA event generators, full GEANT simulations, and the Time Projection Chamber (TPC) Analysis Shell (TAS) have been used. DOE

N95-32712# Japan Atomic Energy Research Inst., Tokyo (Japan). Dept. of Material Development.
LOW-ENERGY ION-BEAM DEPOSITION APPARATUS EQUIPPED WITH SURFACE ANALYSIS SYSTEM

Hideki Ohno (Meisei Univ., Tokyo, Japan.), Yasushi Aoki, and Siro Nagai Oct. 1994 51 p In JAPANESE
(DE95-737272; JAERI-Research-94-018) Avail: CASI HC A04/MF A01

A sophisticated apparatus for low energy ion beam deposition (IBD) was installed at Takasaki Radiation Chemistry Research Establishment of JAERI in March 1991. The apparatus is composed of an IBD system and a real time/in-situ surface analysis system for diagnosing deposited thin films. The IBD system provides various kinds of low energy ion down to 10 eV with current density of 10 micro A/sq cm and irradiation area of 15 x 15 sq mm. The surface analysis system consists of RHEED, AES, ISS and SIMS. This report describes the characteristics and the operation procedure of the apparatus together with some experimental results on depositing thin carbon films. DOE

N95-32960# Los Alamos National Lab., NM. Prepared in cooperation with CKW Nuclear Consulting, Los Alamos, NM
TECHNICAL SUPPORT IN THE AREA OF THEORETICAL SUPPORT OF NUCLEAR PREEQUILIBRIUM Final Report, Jul. 1992 - Sep. 1994

Constance Kalbach Walker 18 Jan. 1995 102 p
(Contract W-7405-eng-36)
(DE95-011617; LA-SUB-95-22) Avail: CASI HC A06/MF A02

The work performed under this subcontract is part of a longer term effort to develop a 'global preequilibrium package' for the calculations of continuum energy spectra and angular distributions from light particle reactions with nuclei based on the exciton model. This package will ultimately include the computer code PRECO-E and a global set of input parameters that will permit the calculation of reactions with reasonable accuracy and without the introduction of adjustable parameter values. The code PRECO-E is to be suitable for inclusion in the general Hauser-Feshbach code GNASH developed and used by Group T-2. Task 2(a) calls for updating the shell-corrected particle-hole state densities used in PRECO-E. That work was begun in FY92 and completed in the current fiscal year. Revised state densities have been compared with the results of the exact counting of states as well as with published state densities obtained from more realistic sets of single particle states. Task 2(b) covers the implementation of these modified state densities, in the investigator's code PRECO-E and comparisons with measured energy spectra. This work was carried out entirely within FY94. DOE

N95-33064# Lawrence Livermore National Lab., Livermore, CA.
THE USES OF ELECTRON BEAM ION TRAPS IN THE STUDY OF HIGHLY CHARGED IONS

David A. Knapp 2 Nov. 1994 25 p Presented at the NATO Advanced Study Institute: Physics With Multiply Charged Ions, Cargese, Corsica, 18-30 Jul. 1994
(Contract W-7405-eng-48)
(DE95-011537; UCRL-JC-119193; CONF-9407166-2) Avail: CASI HC A03/MF A01

The Electron Beam Ion Trap (EBIT) is a relatively new tool for the study of highly charged ions. Its development has led to a variety of new experimental opportunities; measurements have been performed with EBITs using techniques impossible with conventional ion sources or storage rings. The author highlights the various experimental techniques developed and the results obtained using the EBIT and higher-energy Super-EBIT built at the Lawrence Livermore National Laboratory. The EBIT employs a high-current-density electron beam to trap, ionize, and excite a population of ions. The ions can be studied in situ or extracted from the trap for external experiments. The trapped ions form an ionization-state equilibrium determined by the relative ionization and recombination rates. Ions of several different elements may simultaneously be present in the trap. The ions are nearly at rest, and, for most systems, all in their ground-state configurations. The electron-ion interaction energy has a narrow distribution and can be varied over a wide range. We have used the EBIT devices for the measurement of electron-ion interactions, ion structure, ion-surface interactions, and the behavior of low-density plasmas. DOE

N95-33067 Brookhaven National Lab., Upton, NY.
EFFECTS OF ENHANCED CHROMATIC NONLINEARITY DURING THE AGS GAMMA(T)-JUMP

J. Wei, J. M. Brennan, L. A. Ahrens, M. M. Blaskiewicz, D. P. Deng, W. W. MacKay, S. Peggs, T. Satogata, D. Trbojevic, and A. Warner et al 1995 4 p Presented at the Particle Accelerator Conference, Dallas, TX, 1-5 May 1995 Limited Reproducibility: More than 20% of this document may be affected by microfiche quality
(Contract DE-AC02-76CH-00016)
(DE95-011703; BNL-61755; CONF-950512-116) Avail: CASI HC A01

The gamma(sub t)-jump de-signed to reduce the bunch self-field mismatch and intensity loss during the AGS transition crossing can cause significant orbit and lattice distortions and dramatically enhance chromatic nonlinear effects. Employing a low-intensity, small emittance proton bunch crossing transition with the gamma(sub t)-jump quadrupoles excited, we found that the nonlinear momentum-compaction factor alpha(sub 1) increases from

2.2 to about 90 in the presence of the gamma(sub t)-jump. On the other hand, this enhancement can be effectively suppressed by properly exciting the chromaticity sextupoles, reducing alpha(sub 1) from 90 to 16. The experimental measurement agrees well with computer simulations using MAD and TIBETAN. DOE

N95-33204# Brookhaven National Lab., Upton, NY.
BEAM DYNAMICS GROUP SUMMARY
S. Peggs 1994 8 p Presented at the Collective Effects in Large Hadron Collider, Montreux, Switzerland, 17-22 Oct. 1994
(Contract DE-AC02-76CH-00016)
(DE95-008865; BNL-61527; CONF-9410315-3) Avail: CASI HC A02/MF A01

This paper summarizes the activities of the beam dynamics working group of the LHC Collective Effects Workshop that was held in Montreux in 1994. It reviews the presentations that were made to the group, the discussions that ensued, and the consensuses that evolved. DOE

N95-33333# Stanford Linear Accelerator Center, Stanford, CA.
THE PEP-2 PROJECT-WIDE DATABASE
A. Chan, S. Calish, G. Crane, I. MacGregor, S. Meyer, J. Wong, and A. Weinstein (Lawrence Livermore National Lab., Livermore, CA.) May 1995 3 p Presented at the 16th IEEE Particle Accelerator Conference and International Conference on High Energy Accelerators, Dallas, TX, 1-5 May 1995
(Contracts DE-AC03-76SF-00515; W-7405-eng-48)
(DE95-012512; SU-SLAC-PUB-95-6896; CONF-950512-75) Avail: CASI HC A01/MF A01

The PEP-2 Project Database is a tool for monitoring the technical and documentation aspects of this accelerator construction. It holds the PEP-2 design specifications, fabrication and installation data in one integrated system. Key pieces of the database include the machine parameter list, magnet and vacuum fabrication data. CAD drawings, publications and documentation, survey and alignment data and property control. The database can be extended to contain information required for the operations phase of the accelerator and detector. Features such as viewing CAD drawing graphics from the database will be implemented in the future. This central Oracle database on a UNIX server is built using ORACLE Case tools. Users at the three collaborating laboratories (SLAC, LBL, LLNL) can access the data remotely, using various desktop computer platforms and graphical interfaces. DOE

N95-33335# Stanford Linear Accelerator Center, Stanford, CA.
NONLINEAR ANALYSES OF STORAGE RING LATTICES USING ONE-TURN MAPS
Y. T. Yan, J. Irwin, and T. Chen May 1995 3 p Presented at the 16th IEEE Particle Accelerator Conference and International Conference on High Energy Accelerators, Dallas, TX, 1-5 May 1995
(Contract DE-AC03-76SF-00515)
(DE95-012515; SU-SLAC-PUB-95-6903; CONF-950512-72) Avail: CASI HC A01/MF A01

Using normalized one-turn resonance-basis Lie generators in conjunction with an action-angle tracking algorithm (nPB tracking), the authors have been able to better understand the relationship between the dynamic aperture and lattice nonlinearities. Tunes, tune shifts with amplitude and/or energy, and resonance strengths may be freely changed to probe their individual impact on the dynamic aperture. Fast beam-beam simulations can be performed with the inclusion of nonlinear lattice effects. Examples from studies of the PEP-2 lattices are given. DOE

N95-33338# Stanford Linear Accelerator Center, Stanford, CA.
EMITTANCE AND ENERGY CONTROL IN THE NLC MAIN LINACS
C. Adolphsen, K. L. F. Bane, K. Kubo, T. Raubenheimer, R. D. Ruth, K. A. Thompson, and F. Zimmermann 1995 3 p Presented at the 16th IEEE Particle Accelerator Conference and International Conference on High Energy Accelerators, Dallas, TX, 1-5 May 1995
(Contract DE-AC03-76SF-00515)
(DE95-012556; SU-SLAC-PUB-95-6845; CONF-950512-68) Avail: CASI HC A01/MF A01

The authors discuss tolerances and correction schemes needed to control single- and multi-bunch emittance in the NLC main linacs. Specifications and design of emittance diagnostic stations will be presented. Trajectory correction schemes appropriate to simultaneously controlling the emittance of a multibunch train and the emittance of individual bunches within the train will be discussed. The authors discuss control of bunch-to-bunch energy spread using a ramped RF pulse generated by phase-modulating the SLED-2 input. Tolerances on ions, wake fields, quadrupole alignment, and accelerating structure alignment will be given. DOE

N95-33376# Stanford Linear Accelerator Center, Stanford, CA.
EMITTANCE GROWTH DUE TO DECOHERENCE AND WAKEFIELDS
M. G. Minty, A. W. Chao, and W. L. Spence May 1995 3 p Presented at the Particle Accelerator Conference, Dallas, TX, 1-5 May 1995
(Contract DE-AC03-76SF-00515)
(DE95-012495; SU-SLAC-PUB-95-6815; CONF-950512-91) Avail: CASI HC A01/MF A01

Suddenly induced coherent centroid oscillations about the closed orbit will decohere due to nonlinearities in the magnetic optics - at the expense of a stored beam's emittance. Collective effects mediated by the vacuum chamber wakefield and dependent on the beam current, can however damp the coherent oscillations-ameliorating the emittance growth. Closed form expressions for both the beam centroid and the beam size are obtained in the absence of collective effects. Simultaneous turn-by-turn measurements of beam centroid and size in the SLC damping ring are presented, and the importance and intricacy of collective effects is discussed. DOE

N95-33377# Stanford Linear Accelerator Center, Stanford, CA.
INJECTION ENVELOPE MATCHING IN STORAGE RINGS
M. G. Minty and W. L. Spence May 1995 3 p Presented at the Particle Accelerator Conference, Dallas, TX, 1-5 May 1995
(Contract DE-AC03-76SF-00515)
(DE95-012496; SU-SLAC-PUB-95-6816; CONF-950512-90) Avail: CASI HC A01/MF A01

The shape and size of the transverse phase space injected into a storage ring can be deduced from turn-by-turn measurements of the transient behavior of the beam envelope in the ring. Envelope oscillations at 2 x the beta-tron frequency indicate the presence of a beta-mismatch, while envelope oscillations at the beta-tron frequency are the signature of a dispersion function mismatch. Experiments in injection optimization using synchrotron radiation imaging of the beam and a fast-gated camera at the SLC damping rings are reported. DOE

N95-33385# Stanford Linear Accelerator Center, Stanford, CA.
A MAP FOR THE THICK BEAM-BEAM INTERACTION
J. Irwin and T. Chen 1995 3 p Presented at the Particle Accelerator Conference and the International Conference on High Energy Accelerators, Dallas, TX, 1-5 May 1995; sponsored by IEEE
(Contract DE-AC03-76SF-00515)
(DE95-012561; SU-SLAC-PUB-95-6888; CONF-950512-96) Avail: CASI HC A01/MF A01

The authors give a closed-form expression for the thick beam-beam interaction for a small disruption parameter, as typical in electron-positron storage rings. The dependence on transverse angle and position of the particle trajectory as well as the longitudinal position of collision and the waist-modified shape of the beam distribution are included. Large incident angles, as are present for beam-halo particles or for large crossing-angle geometry, are accurately represented. The closed-form expression is well approximated by polynomials times the complex error function. Comparisons with multi-slice representations show even the first order terms are more accurate than a five slice representation, saving a factor of 5 in computation time. DOE

N95-33406# Fermi National Accelerator Lab., Batavia, IL.
CDF RESULTS ON Z(GAMMA) PRODUCTION
Robert G. Wagner (Argonne National Lab., IL.) Apr. 1995 6 p Presented at the International Symposium on Vector Boson Interactions, Los Angeles, CA, 2 Feb. 1995
(Contract W-31-109-eng-38)
(DE95-011500; FNAL/C-95/062-E; ANL-HEP-CP-95-20; CONF-950287-3)
Avail: CASI HC A02/MF A01

Results on Z(sub (gamma)) production observed by the Collider Detector at Fermilab (CDF) from the Tevatron Collider Run Ib and preliminary results

from 36/pb of integrated luminosity from Run Ib. Both the Run Ia and Ib results are consistent with expectations from the Standard Model. DOE

N95-33504# California Univ., Berkeley. Lawrence Berkeley Lab, CA.
A FINAL-FOCUS MAGNET FOR PEP-2
C. E. Taylor, S. Caspi, and N. Saho (Agency of Industrial Science and Technology, Ibaraki, Japan.) 17 Oct. 1994 4 p Presented at the Applied Superconductivity Conference, Boston, MA, 17-21 Oct. 1994
(Contract DE-AC03-76SF-00098)
(DE95-012372; LBL-35421; CONF-941013-41; SC-MAG-457; UC-414)
Avail: CASI HC A01/MF A01

A compact quadrupole magnet has been designed for the final-focus of the 3GeV (times) 9GeV PEP II B-factory collider being built at SLAC. The magnet system must fit within the particle detector, has no iron, and consists of four nested separately controlled magnets: a two-layer 11.95 T/m quadrupole; a horizontal dipole; a vertical dipole; and a 1.5T solenoid. The 1.1 m long magnet must produce a highly uniform quadrupole field in the 120 mm ID beam pipe. The cryostat is 140 mm ID. (warm), 314 mm OD, and approximately 1.5 m long. The very compact cryogenic suspension system using Ti alloy plates is designed to withstand large forces due to interaction between the field of the detector solenoid and the four nested magnets. Cryogenic services and magnet leads are provided through a single flexible transfer line approximately 4m long. DOE

N95-33720 Superconducting Super Collider Lab., Dallas, TX.
RAMP-RATE SENSITIVITY OF SSC DIPOLE MAGNET PROTOTYPES
A. Devred and T. Ogitsu Jul. 1994 129 p Submitted for publication to Particle Accelerators
(Contract DE-AC35-89ER-40486)
(DE95-011162; SSCL-Preprint-568) Avail: CASI HC A07/MF A02

One of the major achievements of the magnet R&D program for the Superconducting Super Collider (SSC) is the fabrication and test of a series of 20 5-cm aperture, 15-m long dipole magnet prototypes. The ramp rate sensitivity of these magnets appears to fall in at least two categories that can be correlated to the manufacturer and production batch of the strands used for the inner-coil cables. The first category, referred to as type-A, is characterized by a strong quench current degradation at high ramp rates, usually accompanied by large distortions of the multipole fields and large energy losses. The second category, referred to as type-B, is characterized by a sudden drop of quench current at low ramp rates, followed by a much milder degradation at larger rates. The multipole fields of the type-B magnets show little ramp-rate sensitivity, and the energy losses are smaller than for the type-A magnets. The behavior of the Type-A magnets can be explained in terms of inter-strand eddy currents arising from low and non-uniform resistances at the crossovers between the strands of the two-layer Rutherford-type cable. Anomalies in the transport-current repartition among the cable strands are suggested as a possible cause for the type-B behavior. The origins of these anomalies have not yet been clearly identified. The SSC project was canceled by decision of the United States Congress on October 21, 1994. DOE

N95-34023# Stanford Linear Accelerator Center, Stanford, CA.
THE EFFECT OF PHASE ADVANCE ERRORS BETWEEN INTERACTION POINTS ON BEAM HALOS
T. Chen, J. Irwin, and R. H. Siemann 1995 3 p Presented at the IEEE Particle Accelerator Conference and International Conference on High Energy Accelerators, Dallas, TX, 1-5 May 1995
(Contract DE-AC03-76SF-00515)
(DE95-012559; SU-SLAC-PUB-95-6886; CONF-950512-94) Avail: CASI HC A01/MF A01

Phase advance errors between interaction points (IP) break the symmetry of multi-IP colliders. This symmetry breaking introduces new, lower order resonances which may chance the halo from the beam-beam interaction dramatically. The mechanism of introducing new resonances is discussed. Simulation results showing the changes due to phase advance errors are presented. Simulation results are compared with experimental measurements at VEPP-2M. DOE

N95-34024# Stanford Linear Accelerator Center, Stanford, CA.
STUDIES OF HALO DISTRIBUTIONS UNDER BEAM-BEAM INTERACTION
T. Chen, J. Irwin, and R. H. Siemann 1995 3 p Presented at the 16th IEEE Particle Accelerator Conference and International Conference on High Energy Accelerators, Dallas, TX, 1-5 May 1995
(Contract DE-AC03-76SF-00515)
(DE95-012560; SU-SLAC-PUB-95-6887; CONF-950512-95) Avail: CASI HC A01/MF A01

The halo distribution due to the beam-beam interaction in circular electron-positron colliders is simulated with a program which uses a technique that saves a factor of hundreds to thousands of CPU time. The distribution and the interference between the beam-beam interaction and lattice nonlinearities has been investigated. The effects on the halo distribution due to radiation damping, misalignment at the collision point and chromatic effect are presented. DOE

N95-34439# California Univ., Berkeley. Lawrence Berkeley Lab, CA. Accelerator and Fusion Research Div.
HEAVY IONS ACCELERATION IN RF WELLS OF 2-FREQUENCY ELECTROMAGNETIC FIELD AND IN THE INVERTED FEL
A. I. Dzergach, V. S. Kabanov, M. G. Nikulin, and S. V. Vinogradov Mar. 1995 26 p
(Contract DE-AC03-76SF-00098)
(DE95-012439; LBL-36842; UC-414) Avail: CASI HC A03/MF A01

Last results of the study of heavy ions acceleration by electrons trapped in moving two-frequency 3-D RF wells are described. A linearized theoretical model of ions acceleration in a polarized spheroidal plasmoid is proposed. The equilibrium state of this plasmoid is described by the modified microcanonical distribution of the „Courant-Snyder invariant ('quasienergy' of electrons). Some new results of computational simulation of the acceleration process are given. The method of computation takes into account the given cylindrical field E(sub 011)(phi,r,z) and the self fields of electrons and ions. The results of the computation at relatively short time intervals confirm the idea and estimated parameters of acceleration. The heavy ion accelerator using this principle may be constructed with the use of compact cm band iris-loaded and biperiodical waveguides with double-sided two-frequency RF feeding. It can accelerate heavy ions with a charge number Z(sub i) from small initial energies approximately 50 keV/a.u. with the rate approximately Z(sub i) (center dot) 10 MeV/m. Semirelativistic ions may be accelerated with similar rate also in the inverted FEL. DOE

N95-34651 Rutherford Appleton Lab., Oxford (England).
TRACK FINDING AND FITTING IN THE H1 FORWARD TRACK DETECTOR
S. Burke, R. C. W. Henderson, S. J. Maxfield, J. V. Morris, and G. D. Patel Mar. 1995 55 p Prepared in cooperation with Lancaster Univ., England, Liverpool Univ., England, and Glasgow Univ., Scotland
(PB95-234985; RAL-95-037) Avail: Issuing Activity (National Technical Information Service (NTIS))

The tracking environment in the H1 Forward Track Detector, where the hit multiplicity from proton fragments is high, is particularly hostile. The techniques and software which have been developed for pattern recognition and Kalman fitting of charged particle tracks in this region are described in detail. NTIS

N95-34653 Rutherford Appleton Lab., Oxford (England).
ANALYTIC APPROACH TO SMALL x STRUCTURE FUNCTIONS
J. R. Forshaw, R. G. Roberts, and R. S. Thorne Mar. 1995 24 p
(PB95-236030; RAL-95-035) Avail: Issuing Activity (National Technical Information Service (NTIS))

We present a method for the analytic solution of small x structure functions. The essential small x logorithms are summed to all orders in the anomalous dimensions and coefficient functions. Although we work at leading logarithmic accuracy, the method is general enough to allow the systematic inclusion of sub-leading logarithms. Results and predictions are presented for the gluon density, and the structure functions F(sub 2)(x,Q(sup 2)) and F(sub L)(x,Q(sup 2)). We find that corrections to the simple double logarithmic calculation are important in the HERA range and obtain good fits to all available data. NTIS

N95-32991# Osaka Univ., Osaka (Japan). Dept. of Mechanical Engineering.
ENHANCEMENT OF POOL BOILING HEAT TRANSFER TO LITHIUM BROMIDE AQUEOUS SOLUTION
Masuo Kaji, Masahiro Furukawa (Sanyo Electric Co. Ltd., Inabe, Japan.),

Takayuki Suyama, and Kotohiko Sekoguchi *In its* Technology Reports of the Osaka Univ., Vol. 45, Nos. 2205-2216 15 Apr. 1995 p 49-58 (For primary document see N95-32984 12-31)
(Rept-2211) Avail: CASI HC A02/MF A02

74 OPTICS

Includes light phenomena; and optical devices.
For lasers see *36 Lasers and Masers.*

N95-32658# Stanford Linear Accelerator Center, Menlo Park, CA.
BEAM-BASED OPTICAL TUNING OF THE FINAL FOCUS TEST BEAM
P. Tenenbaum (Stanford Linear Accelerator Center, Stanford, CA.), D. Burke (Stanford Linear Accelerator Center, Stanford, CA.), S. Hartman (Stanford Linear Accelerator Center, Stanford, CA.), R. Helm (Stanford Linear Accelerator Center, Stanford, CA.), J. Irwin (Stanford Linear Accelerator Center, Stanford, CA.), R. Iverson (Stanford Linear Accelerator Center, Stanford, CA.), P. Raimondi (Stanford Linear Accelerator Center, Stanford, CA.), W. Spence (Stanford Linear Accelerator Center, Stanford, CA.), V. Bharadwaj (Fermi National Accelerator Lab., Batavia, IL.), and M. Halling (Fermi National Accelerator Lab., Batavia, IL.) et al 1995 4 p Presented at the Particle Accelerator Conference, Dallas, TX, 1-5 May 1995
(Contract DE-AC03-76SF-00515)
(DE95-012097; SU-SLAC-PUB-95-6770; CONF-950512-34) Avail: CASI HC A01/MF A01

In order to reduce the SLAC 46.6 GeV beam to submicron sizes, the Final Focus Test Beam (FFTB) must meet tight tolerances on many aberrations. These aberrations include: mismatch and coupling of the incoming beam; dispersion; chromaticity; lattice errors in the chromatic correction sections; lattice coupling; and residual sextupole content in the quadrupoles. In order to address these aberrations, the authors have developed a procedure which combines trajectory analysis, use of intermediate wire scanners, and a pair of novel beam size monitors at the IP. This procedure allows the FFTB IP spot to be reduced to sizes under 100 nanometers. DOE

N95-32660# Department of the Air Force, Wright-Patterson AFB, OH. National Air Intelligence Center.
STUDY OF LIQUID CRYSTAL SPATIAL LIGHT MODULATOR APPLICATION TO HADAMARD TRANSFORM SPECTROMETER: A FAST AND ACCURATE DECODING METHOD
Bingquan B. Zhang and Fengfei Bi (Sushou Univ., Sushou, China.) 27 Mar. 1995 12 p Transl. into ENGLISH from Guangxue Xuebao (China), v. 12, no. 7, Jul. 1992 p 1-7 Prepared by Scitran Company
(AD-A293087; NAIC-ID (RS) T-0404-94) Avail: CASI HC A03/MF A01

A study is made on liquid crystal spatial light modulators (LC-SLM), used as a stationary encoding mask of Hadamard transform spectrometer (HTS), and thus a fast and accurate decoding method is proposed. The improvement is given in terms of root-mean-square of the signal-to-noise ratio produced by the LC-SLM mask. DTIC

N95-32662# Harvard Univ., Cambridge, MA.
X-RAY STANDING WAVE INTERFEROMETRY-OPTICS AT 1 ANGSTROM WITH APPLICATIONS TO SURFACE AND MATERIAL SCIENCES Final Report
J. L. Smith 1995 10 p
(Contract DE-FG02-89ER-45399)
(DE95-009688; DOE/ER-45399/T1) Avail: CASI HC A02/MF A01

The goal is to advance basic knowledge in x-ray optics by continuing to apply and refine x-ray standing wave interferometric methods of studying crystal surfaces and by developing new x-ray optical methods to probe matter. This report is divided into two sections outlining the accomplishments made first in the area of applying crystal optics to the study of crystal surfaces, and secondly in the more general area of developing new crystal optics. DOE

N95-32701# Department of the Air Force, Wright-Patterson AFB, OH. National Air Intelligence Center.
HIGH-RESOLUTION TeO2 ACOUSTO-OPTICAL DEFLECTOR FOR MILLIMETER-WAVE SPECTROMETER
Binghuo Xu (Shanghai Inst. of Ceramics, China.), Guozhen Zhao (Shanghai Inst. of Ceramics, China.), Huian Bian (Shanghai Inst. of Ceramics, China.), Haiqun Chu (Shanghai Inst. of Ceramics, China.), and Jianhui Jin (Shanghai Inst. of Ceramics, China.) 22 Feb. 1995 15 p Transl. into ENGLISH from Yingyong Jiguang (China), v. 8, no. 6, Dec. 1988 p 10 Prepared by Leo Kanner Associates
(AD-A293054; NAIC-ID(RS)T-0412-94) Avail: CASI HC A03/MF A01

This paper introduces high resolution TeO2 deflector for mm-wave radio spectrometer. We have developed mm-wave acousto-optic radio spectrometer using these devices; it has 17.5 KHz frequency resolution, 13 MHz bandwidth and the system drift is +/- 0.03 channel per hour. DTIC

N95-32923# Department of the Navy, Washington, DC.
A FIBER-OPTIC CONNECTOR Patent Application
Gregory H. Ames, inventor (to Navy) and Roger L. Morency, inventor (to Navy) 25 Nov. 1994 24 p
(AD-D017424; US-Patent-Appl-SN-345957) Avail: CASI HC A02/MF A01

This invention relates to fiber-optics connectors. The connector comprises a plurality of ferrules, each of the ferrules having extending centrally therethrough a single optical fiber. The connector further includes structure abutting at least a portion of the ferrules for exercising a radially compressive force on the ferrules for urging the ferrules into a configuration in which said bodies are co-parallel and nested so as to form a stable bundle which in transverse section is substantially axisymmetrical, and retaining the ferrules in the configuration. The connector still further includes alignment structure for angular positioning of said bodies in said connector in said transverse section about a nominal longitudinal axis of said bundle for registry of the connector with a second connector of complementary configuration. DTIC

N95-32957# Air Force Inst. of Tech., Wright-Patterson AFB, OH.
APPLICATIONS OF ORGANIC AND POLYMER NONLINEAR OPTICAL MATERIALS IN OPTICS COMPUTATIONS
Maocong Sun (Shandong Univ., Jinan, China.), Suling Ji (Shandong Univ., Jinan, China.), and Chunfei Li (Harbin Industrial Univ., Harbin, China.) 27 Mar. 1995 21 p Transl. into ENGLISH from Wuli (China), v. 20, no. 6, Jun. 1991 p 361-365 Prepared by Leo Kanner Associates
(Contract F33657-88-D-2188)
(AD-A293088; NAIC-ID(RS)T-0407-94) Avail: CASI HC A03/MF A01

Organic and polymer nonlinear optical materials have good properties in optics, structure, and mechanics. At present, such materials are undergoing rapid development. This article emphasizes presenting some typical organic and polymer nonlinear optical materials, describes the optical bistability devices, optical power restraining units, spatial optical modulators, and optical waveguides fabricated from these materials. By comparing the organic crystals and semiconductor devices of the same categories, the article reports on the potential priorities and application prospects in the field of optics computations by using these organic and polymer nonlinear materials. DTIC

N95-33239# National Defence Research Establishment, Linkoeping (Sweden). Dept. of Command and Control Warfare Technology.
CADIR: A MODEL FOR GENERATING INFRARAD IMAGES
Lars Berglund and Carl Hedberg Nov. 1994 56 p
(Proj. 547352) (ISSN 1104-9154)
(PB95-222956; FOA-R-94-00059-3.6-SE) Avail: CASI HC A04/MF A01

This report describes a computer model which is used for the generation of images of different kinds of objects within the infrared wavelength bands. A description of the computer model and the geometric and radiometric calculations to support it is given. Some examples of images that can be produced are shown. An object's geometry is defined by triangles organized in a modular structure, which makes it possible to handle objects with moving parts. The possibility to use and define transparent surfaces enables models with plumes. The radiometric model handles both transparent and reflective surfaces. NTIS

N95-33381# California Univ., Berkeley. Lawrence Berkeley Lab, CA.
A FIBER OPTIC STRAIN MEASUREMENT AND QUENCH LOCALIZATION FOR USE IN SUPERCONDUCTING ACCELERATOR DIPOLE MAGNETS
Johannes M. vanOort, Ronald M. Scanlan, and Herman H. J. tenKate

(Technische Hogeschool, Twente, Netherlands.) 17 Oct. 1994 4 p Presented at the Applied Superconductivity Conference, Boston, MA, 17-21 Oct. 1994
(Contract DE-AC03-76SF-00098)
(DE95-012370; LBL-35426; SC-MAG-462; CONF-941013-43) Avail: CASI HC A01/MF A01

A novel fiber-optic measurement system for superconducting accelerator magnets is described. The principal component is an extrinsic Fabry-Perot Interferometer to determine localized strain and stress in coil windings. The system can be used either as a sensitive relative strain measurement system or as an absolute strain detector. Combined, one can monitor the mechanical behaviour of the magnet system over time during construction, long time storage and operation. The sensing mechanism is described, together with various tests in laboratory environments. The test results of a multichannel test matrix to be incorporated first in the dummy coils and then in the final version of a 13T Nb3Sn accelerator dipole magnet are presented. Finally, the possible use of this system as a quench localization system is proposed. DOE

N95-33411# Lawrence Livermore National Lab., Livermore, CA.
PHASE CONTROL AND MEASUREMENT OF ULTRASHORT OPTICAL PULSES
A. Sullivan, W. E. White, K. C. Chu (California Univ., Davis, CA.), and J. P. Heritage (California Univ., Davis, CA.) 10 Feb. 1995 8 p Presented at the SPIE 1995: SPIE Conference on Optics, Electro-optics, and Laser Application in Science, Engineering and Medicine, San Jose, CA, 4-10 Feb. 1995
(Contract W-7405-eng-48)
(DE95-011746; UCRL-JC-120006; CONF-950226-40) Avail: CASI HC A02/MF A01

We have used the Direct Optical Spectral Phase Measurement (DOSPM) technique to characterize the cubic phase tuning ability of our pulse stretcher. We have compared the measured phase to the phase determined from cross-correlation measurements. DOE

N95-33506# Lawrence Livermore National Lab., Livermore, CA.
OPTICAL PULSE GENERATION USING FIBER LASERS AND INTEGRATED OPTICS
R. B. Wilcox, D. F. Browning, S. C. Burkhart, and B. W. VanWonterghem 27 Mar. 1995 7 p Presented at the 1995 International Conference on Integrated Optics and Optical Fibre Communications, Tokyo, Japan, 26-30 Jun. 1995 Submitted for publication
(Contract W-7405-eng-48)
(DE95-011517; UCRL-JC-120517; CONF-9506179-1) Avail: CASI HC A02/MF A01

We have demonstrated an optical pulse forming system using fiber and integrated optics, and have designed a multiple-output system for a proposed fusion laser facility. Our approach is an advancement over previous designs for fusion lasers, and an unusual application of fiber lasers and integrated optics. DOE

N95-33651# Lawrence Livermore National Lab., Livermore, CA.
MULTIPLE-BEAM PULSE SHAPING AND PREAMPLIFICATION
R. B. Wilcox, B. W. VanWonterghem, S. C. Burkhart, and J. M. Davin 9 Nov. 1994 10 p Presented at the International Atomic Energy Agency (IAEA) Technical Committee Meeting on Drivers for Inertial Confinement Fusion, Paris, France, 14-18 Nov. 1994 Submitted for publication
(Contract W-7405-eng-48)
(DE95-011738; UCRL-JC-117491; CONF-9411152-4) Avail: CASI HC A02/MF A01

Glass fusion laser systems typically use a master oscillator-power amplifier (MOPA) architecture, where control of the optical pulse temporal and spatial parameters is accomplished mainly in the master oscillator and low power optics. The pulses from this low power 'front end' are amplified in the power amplifier, which modifies the pulse shape temporally and spatially. Nonlinear frequency conversion crystals following the amplifier further change the pulse before it reaches the target. To effectively control the optical pulse on target for different types of experiments, and compensate for nonlinearity in the preceding optics, the front end system must be versatile enough to easily control many pulse parameters over a large range. The front end pulse generation system described in this article represents a new approach to this problem. The proposed National Ignition Facility (NIF) has 192 beamlines, each of which requires an input pulse of up to 12 Joules in around 4 ns equivalent square pulse length. Considerations of laser architecture for supplying each of these beamlines from a central oscillator system were crucial in the design of the front end. Previous lasers have used bulk optics to split a single oscillator signal and report beams to multiple amplifier chains. A key idea in the current design is to replace bulk optic transport with fibers, eliminating large opto-mechanical subsystems. Another important concept is convenient pulse forming using low voltage integrated optic modulators. The integrated optic and fiber optic concepts resulted in the current pulse generation designs for NEF. An important advantage is that each of the beamlines can have an independently controlled temporal pulse shape, which provides for precise balance of instantaneous power on target. DOE

N95-34020# Lawrence Livermore National Lab., Livermore, CA.
DISCRETE MODELING OF OPTICAL PULSE PROPAGATION IN NONLINEAR MEDIA Final Report
Richard W. Ziolkowski 1995 12 p Prepared in cooperation with Arizona Univ., Tucson, AZ
(Contract W-7405-eng-36)
(DE95-011515; UCRL-CR-112910-2) Avail: CASI HC A03/MF A01

With the continuing and heightened interest in nonlinear semiconductor and optically integrated devices, more accurate and realistic numerical simulations of these devices and systems are in demand. Such calculations provide a testbed in which one can investigate new basic and engineering concepts, materials, and device configurations before they are fabricated. This encourages multiple concept and design iterations that result in enhanced performances and system integrations of those devices. They also provide a framework in which one can interpret complex experimental results and suggest further diagnostics or alternate protocols. Thus the time from device conceptualization to fabrication and testing could be enormously improved with numerical simulations that incorporate more realistic models of the linear and nonlinear material responses and the actual device geometries. The authors have successfully developed a finite difference time domain method that simulates the propagation of ultra-short optical pulses in nonlinear materials which can be described with a linear Lorentz dispersion model, an instantaneous nonlinear Kerr model and a retarded nonlinear Raman model. They have used this NL-FDTD method to model and characterize several ultra-short optical pulse configurations including linear and nonlinear optical waveguides that could be used as all-optical output couplers and beam steerers. DOE

N95-34288 Department of the Navy, Washington, DC.
METHOD FOR MAKING FIBER-OPTIC BUNDLE COLLIMATOR ASSEMBLY Patent
Gregory H. Ames, inventor (to Navy) and Thomas J. Gryk, inventor (to Navy) 21 Mar. 1995 8 p Filed 8 Aug. 1994
(AD-D017486; US-Patent-5,400,429; US-Patent-Appl-SN-287028; US-Patent-Class-385-147) Avail: US Patent and Trademark Office

A method for making a fiber-optic bundle collimator assembly, comprising the steps of assembling side by side a multiplicity of first bodies of cylindrical configuration and equal diameter and applying uniform compressive force to the first bodies to force the first bodies into a predictable hexagonal pattern of minimum diameter. Additional bodies of cylindrical configuration and having diameters equal to the diameters of the first bodies are inserted on each of the sides of the bundle of first bodies with each of the additional bodies abutting two of the first bodies. A plurality of the first bodies is then removed from the bundle. Each of the removed first bodies is replaced with a pair of cylindrically-shaped second bodies having diameters equal to the diameters of the first bodies, with one of the pair protruding from the bundle on a first face thereof and another of the pair protruding from the bundle on a second face thereof. A clamp is applied to exposed portions of the second bodies at one of the bundle first and second faces, to force the second bodies into an attitude parallel to each other, the second bodies causing the first bodies to align parallel to the second bodies and parallel to each other. An outer ring of the first bodies is locked in place and a second plurality of first bodies is removed from the bundle. A plurality of optical fiber bearing ferrules is inserted in the place of the removed first bodies. DTIC

N95-34297# Air Force Systems Command, Wright-Patterson AFB, OH. National Air Intelligence Center.
INFLUENCE OF CO2 CONTINUOUS LASER PREPROCESSED SUBSTRATES ON OPTICAL THIN FILM DAMAGE THRESHOLDS
Wu Zhouling, Gao Yang, Fan Zhengxiu, and Wang Zhijiang 26 Apr. 1995 17 p Transl. into ENGLISH from Hongwai Yanjiju, China, v. 9, no. 5, May 1990 p 329-335
(AD-A294190; NAIC-ID(RS)T-0648-93) Avail: CASI HC A03/MF A01

As far as experimental research into the influences of CO2 laser preprocessed substrates on optical thin film damage threshold values is concerned, it was discovered that, with regard to single layer films and antireflective coatings, radiation pretreatment causes threshold values to clearly go up. At their highest, they reach 5 times those not radiation treated. However, on high reflection films, radiation pretreatment has no great influence. Using repetition frequency pulse photothermal deflection techniques, real time studies were done of corresponding relationships associated with light absorption and damage. Using pulsed time resolved light deflection technology, precise determinations were made of the locations associated with the occurrence of initial damage on samples in depth and direction. Making use of continuous modulation light deflection techniques - combining Nomarski optical microscope analysis of damage morphology - a number of significant conclusions were reached. DTIC

N95-34298# Air Force Systems Command, Wright-Patterson AFB, OH. National Air Intelligence Center.
TiO2/SiO2 AND ZrO2/SiO2 MULTILAYER MEDIA FILM OPTICAL LOSS AND LASER DAMAGE STUDY
Zhouling Wu and Zhengxiu Fan 11 Apr. 1995 11 p Transl. into ENGLISH from Zhongguo Jiguang, China, v. 16, no. 8, Aug. 1989 p 468-470
(AD-A294192; NAIC-ID(RS)T-0641-93) Avail: CASI HC A03/MF A01

Taking TiO2/SiO2 and ZrO2/SiO2 multilayer media films as examples, measurements were done, with different technical conditions and different film system structures, of thin film sample optical losses as well as laser loss threshold values. At the same time, preliminary research and discussion was done with regard to experimental results. DTIC

N95-34300# Syracuse Univ., NY.
QUANTUM CYLINDER FIBER LIGHT AMPLIFIER Final Technical Report, Mar. 1993 - 1994
Philipp Kornreich Feb. 1995 25 p
(Contract F30602-93-C-0019)
(AD-A294197; RL-TR-95-20) Avail: CASI HC A03/MF A01

The objective of this effort was to fabricate and test Quantum Cylinder Fiber Light Amplifiers (QCyFLA). These devices are to be used for optical amplification. During the course of this effort, we were able to fabricate and test devices as planned. Test results were not the same as the theoretical predictions. New devices will be fabricated using a wide gap semiconductor against the glass. This should shift the absorption edge to the predicted wavelength. DTIC

N95-34303# Air Force Systems Command, Wright-Patterson AFB, OH. National Air Intelligence Center.
USING PHOTOTHERMAL DEFLECTION TECHNIQUES FOR STUDYING THE ATTENUATIONS OF GUIDED WAVES PROPAGATED IN OPTICAL THIN FILMS
Xu Liu 5 Apr. 1995 18 p Transl. into ENGLISH from Yiqi Yibiao Xuebao, China, v. 13, no. 3, Aug. 1992 p 233-239
(AD-A294203; NAIC-ID(RS)T-0753-94) Avail: CASI HC A03/MF A01

A new experimental system, utilizing photothermal deflection techniques, does test measurements of guided wave propagation attenuation in optical thin films. Lessons are drawn from propagation attenuation in wave guidance optics in order to characterize the losses and qualities associated with high quality optical thin films. Experimental results clearly show that attenuation coefficients are capable of very sensitively and completely reflecting thin film properties and quality. DTIC

N95-34305# Air Force Systems Command, Wright-Patterson AFB, OH. National Air Intelligence Center.
SUCCESSFUL DEVELOPMENT OF FIRST-GENERATION LASER DEVICE; MARKING CHINA'S OPTOELECTRONIC TECHNOLOGY AT WORLD CLASS LEVEL
18 Apr. 1995 6 p Transl. into ENGLISH from Keji Ribao, China, no. 228, 1991 p 9
(AD-A294206; NAIC-ID(RS)T-0836-94) Avail: CASI HC A02/MF A01

Bell Laboratories has developed the world's first optical information processor. Its core device is a self-excited electrooptical effect apparatus array of symmetric operation. After being developed in the United States, this high-technology device was successfully developed by China's scientists,thus making the fact that China's optoelectronic technology is among the most advanced in the world. Author (DTIC)

N95-34307# Air Force Systems Command, Wright-Patterson AFB, OH. National Air Intelligence Center.
RECENT DEVELOPMENTS IN MARITIME TECHNOLOGY RESEARCH INSTITUTE ACOUSTO-OPTICAL TECHNOLOGY RESEARCH
Yu Liansheng 5 Apr. 1995 20 p Transl. into ENGLISH from Yingyong Shengxue, China, v. 8, no. 6, Nov. 1989 p 24-28
(AD-A294215; NAIC-ID(RS)T-0372-94) Avail: CASI HC A03/MF A01

This article introduces recent developments in acoustic technology research at our institute in the last five years. Contents include: acousto-optical interaction theory research; acousto-optical device manufacturing technology research; acousto-optical device test measurement method research; partial acousto-optical devices, as well as applied research. DTIC

N95-34309# Air Force Systems Command, Wright-Patterson AFB, OH. National Air Intelligence Center.
USING OPTICAL INTERFERENCE METHODS TO MEASURE ACOUSTO-OPTICAL DEVICE THERMAL EFFECTS
Xu Binghuo and Zhao Guozhen 5 Apr. 1995 15 p Transl. into ENGLISH from Yingyong Shengxue, China, v. 8, no. 6, Nov. 1989 p 19-23
(AD-A294219; NAIC-ID(RS)T-0398-94) Avail: CASI HC A03/MF A01

This article introduces methods for using optical interference methods to measure acousto-optical device thermal effects and acousto-optical deflection device test measurement results on PbMoO4 and ZF6 glass. At the same time, it introduces good acousto-optical deviation device heat dispersion systems. DTIC

N95-34374# Southampton Univ. (England).
EFFICIENT POCKEL'S MODULATORS IN OPTICAL FIBERS Final Report, 15 Sep. 1992 - 14 Mar. 1995
P. G. Kazansky and P. S. Russell 31 Mar. 1995 47 p
(Contract F49620-92-J-0480; AF-AFOSR-0018-92)
(AD-A294009) Avail: CASI HC A03/MF A01

The main aim of this project was to study the feasibility of using thermal poling of glasses as a means of realizing efficient electro-optic modulators in optical fibers. We found that substantial spreading out of the second-order nonlinearity beyond the boundaries of the positive electrode occurs, and also showed that implantation of electrons erases the second-order nonlinearity in thermally poled glass. This erasure technique holds much promise as a versatile new means of realizing complex patterns for advanced electro-optic modulators. We proposed a mechanism for the thermal poling process based on a frozen-in space charge field; this model explains both our own and other recorded experimental results. Ge doping of silica glass observed to enhance both thermal poling (in combination with $^{-}$OH doping) and electron beam poling effects. Effective values of second-order nonlinearity as high as 0.2 pm/V were obtained in Ge-doped silica fibres. This value is approx. 200 times higher than ever previously reported in these optical fibres. The use of thermal poling in vacuum to improve in reproducibility and quality of the induced second-order susceptibility was proposed and experimentally demonstrated. Strong electro-acousto-optic transduction in thermally poled fibre was observed. Phase shift at resonance as high as 1 radian was obtained at applied fields of 0.3 V/microns. A value of electrooptic coefficient of 0.05 pm/V was experimentally measured. This value is about 25 times higher then previously reported in silica fibres and may be increased by optimization of poling conditions. DTIC

N95-34459# Air Force Inst. of Tech., Wright-Patterson AFB, OH.
TRIPLE INVARIANT OPTICAL PATTERN RECOGNITION USING CIRCULAR HARMONIC SYNTHETIC FILTERS
Yang Baotang and Cheng Yu 15 Apr. 1995 13 p Transl. into ENGLISH from Zhongguo Jiguang (China), v. 18, no. 8, Aug. 1991 p

615-619 Prepared by Leo Kanner Associates
(Contract F33657-84-D-0165)
(AD-A294253; NAIC-ID(RS)T-0392-94) Avail: CASI HC A03/MF A01

This article, on the foundation of circular harmonic filter algorithms, combines synthetic discrimination functions to put forward circular harmonic synthetic filters. It solves traditional problems of matched space filters with input target geometrical distortions. On synthetic filters, computer simulations and optical correlation experiments were carried out. Results clearly showed that circular harmonic synthetic filters possess relatively strong triple invariant optical pattern recognition capabilities. DTIC

N95-34471# Air Force Systems Command, Wright-Patterson AFB, OH. National Air Intelligence Center.
EFFECT OF PROPAGATION ATTENUATION OF THIN FILM WAVEGUIDE ON OPTICAL THIN FILM LOSSES
Liu Xu, Tang Jinfa, and E. Pelletier 28 Apr. 1995 16 p Transl. into ENGLISH from Guangzue Xuebao, China, v. 12, no. 4, Apr. 1992 p 348-352
(AD-A294064; NAIC-ID(RS)T-0761-94) Avail: CASI HC A03/MF A01

Theoretical analysis of three fundamental deficiencies of optical thin films is studied: the effect of the extinction coefficient of the refractive index, surface roughness effects, and refractive index nonuniformity on the propagation attenuation of thin film waveguides. Based on different deficiencies in the propagation attenuation of different guide nodes in optical thin films, the article presents a method of distinguishing absorption and scattering losses in thin films. DTIC

N95-34480# Oak Ridge National Lab., TN.
FABRICATION OF OPTICAL CHANNEL WAVEGUIDES IN THE GaAs/AlGaAs SYSTEM BY MeV ION BEAM BOMBARDMENT
T. Taylor (Alabama A & M Univ., Normal, AL.), D. Ila (Alabama A & M Univ., Normal, AL.), R. L. Zimmerman (Alabama A & M Univ., Normal, AL.), P. R. Ashley (Army Missile Command, Redstone Arsenal, AL.), and D. B. Poker (Oak Ridge National Lab., TN.) 1994 7 p Presented at the 1994 Fall Meeting of the Materials Research Society (MRS), Boston, MA, 28 Nov. - 2 Dec. 1994
(Contract DE-AC05-84OR-21400)
(DE95-008973; CONF-941144-156) Avail: CASI HC A02/MF A01

We have fabricated optical channel waveguides in planar GaAs/AlGaAs waveguides using 10 MeV oxygen ions at a fluence of 3 x 10(exp 13) and 3 x 10(exp 14) ions/cm(sup 2). Although disordering of GaAs/AlGaAs quantum well structures has previously been reported, to the best of the authors' knowledge the fabrication of channel waveguides using high energy oxygen bombardment has not been demonstrated in this material system. This technique may provide a totally new concept of localized material modifications in GaAs/AlGaAs waveguides by creating compositional disordered regions that act as optical confinement channels. The masking technique used to provide selective disordering of the planar waveguide structures will be presented. Optical measurements were performed on the channel waveguides at a wavelength of 1.3 micro m. DOE

N95-34490# Air Force Systems Command, Wright-Patterson AFB, OH. National Air Intelligence Center.
STUDY OF A LARGE OPTICAL/INFRARED TELESCOPE SCHEME
Zhou Bifang and Zhao Peiqian 19 Apr. 1995 19 p Transl. into ENGLISH from Tianwen Xuebao, China, v. 33, no. 2, Jun. 1992 p 212-219
(AD-A294042; NAIC-ID(RS)T-0742-94) Avail: CASI HC A03/MF A01

In this paper, the study of a scheme of a large telescope array is presented. As an example, a large telescope scheme consisting of six 2.16m telescopes, based on the 2.16m optical telescope completed last year is studied. It can be operated both in visible and IR wavelength regions in three modes: (1) as a unit 2.16m telescope which can be operated at the prime focus, Cassegrain focus, and Coude focus; (2) as an incoherent array for the visible array wavelength region; and (3) as a phase array. In section 2, a preliminary design for an incoherent telescope array is given. Six fibers, each with a length of about 20 in and a core diameter of 65 micrometers are used to link the prime focus and the beam transfer system. Six fibers are also used to guide the light beam to a common detector. DTIC

N95-34498# Colorado Univ., Boulder, CO. Dept. of Electrical and Computer Engineering.
OPTICAL PROPERTIES OF LITHIUM NIOBATE WAVEGUIDES, AND PRISM COUPLING FOR OPTIMIZING WAVEGUIDE FABRICATION
25 Apr. 1995 210 p
(Contracts N00014-92-J-1190; DAAL03-92-G-0289)
(AD-A294111; ECE/GWOL/68) Avail: CASI HC A10/MF A03

I investigated the accuracy and precision of effective index of refraction measurements using prism coupling. I found that the coupling gap's geometry is critical to predicting the accuracy and resolution of measurements. I provide experimental evidence that there are advantages to using high coupling pressures that yield long coupling lengths. I present and evaluate an experimental technique aimed at reducing the effects of perturbation and find that it may not be applicable to all situations. I extend a previous model of prism coupling to include a finite coupling length. Also, I introduce an alternative model of prism coupling based upon a local normal-mode expansion and present its preliminary numerical results. I have observed more extraordinary polarized guide modes near cut-off in Ti in-diffused lithium niobate planar waveguides than are predicted by Ti in-diffusion models. I also observe these nearly cut-off modes in lithium niobate specimens fabricated without Ti under a variety of diffusion atmospheres. Values of the effective index of these nearly cut-off modes found do not agree with those calculated. DTIC

N95-34504# Physical Optics Corp., Torrance, CA.
PHOTONIC BAND GAP STRUCTURES ON POLYMER MATERIALS FOR MICROSTRUCTURE WAVEGUIDES AND HIGH-SPEED INTERCONNECTS Final Report, 2 Aug. 1994 - 20 Feb. 1995
Michael Wang Mar. 1995 40 p
(Contract F30602-94-C-0193)
(AD-A294119) Avail: CASI HC A03/MF A01

Physical Optics Corporation (POC) proposed a new concept of creating photonic band gaps on optical waveguides for the realization of low loss bands. These low loss bands are particularly useful for the realization of high density optical interconnection networks for multi-chip modules and other single-board high-speed functional circuits. In the Phase I program, POC focused on the structures that can be used to construct waveguide photonic band gap structures, namely 2-D and 1-D PBG structures. The understanding of these structures and a theoretical study of their contributions to optical beam confinement have been achieved. We further examined their operational properties, including polarization dependence and material index differential requirements. Beam confinement conditions for a large range of off-axis beam angles have been identified between two 1-D PBG structures, which is the basis for the construction of low loss waveguide bands. This strong beam confinement for large angle off-axis beams is not achievable in conventional optical waveguides based on total internal reflection. The applications of the waveguide PBG structures include high density optical interconnect buses, waveguide filters, micro-ring tunable filters and lasers, switches, and integrated wavelength division multiplexers. DTIC

N95-34571# Minnesota Univ., Minneapolis, MN. Dept. of Chemistry.
ULTRAFAST NEAR-FIELD SCANNING OPTICAL MICROSCOPY (NSOM) OF EMERGING DISPLAY TECHNOLOGY MEDIA: SOLID STATE ELECTRONIC STRUCTURE AND DYNAMICS
Paul F. Barbara 31 May 1995 12 p
(Contract N00014-89-J-1746)
(AD-A294879) Avail: CASI HC A03/MF A01

The main focus is the further development and application of NSOM to studies of the local photophysical and photochemical properties of complex nanostructured materials. We are directly involved in the currently-rapid advance of NSOM methodologies and are especially interested in ultrafast time-resolved applications of NSOM. Our ultrafast NSOM currently allows for picosecond (and in the near futurer, femtosecond) time resolution to be obtained with nanometer-scale spatial resolution. In our experiments we are addressing questions pertaining to variations in excited state lifetimes, charge and energy transfer rates, and charge and energy transfer distances and directionality in highly nanostructured materials. These results are being employed along with static imaging and polarization-dependent imaging, as well as static spectroscopic measurements, to provide invaluable information on how nanoscale structural variations lead to variations in the important

local photophysical and photochemical properties of numerous technologically-important, nanostructured samples. DTIC

N95-34576# Oregon State Univ., Corvallis, OR.
COMPARISON OF THEORETICAL PREDICTIONS WITH FIELD OBSERVATIONS FOR A SIMPLE FORWARD SCATTERING SENSOR
James C. Kitchen and J. R. Zaneveld 4 Nov. 1994 21 p
(Contract N00014-92-C-6015)
(AD-A294948; NRL/CR/7410-94-0028) Avail: CASI HC A03/MF A01

Field measurements with a simple 660 nm forward scattering sensor were analyzed by means of a three-layered sphere model of light scattering. The scattering sensor measures a value that represents the scattering function multiplied by a weighting function The geometry of the scattering sensor determines the weighting function. A model was developed that determines the weighting function based on sensor geometry. For the sensor tested the weighting function peaks at 27 degrees with a FWHM of 22 degrees. Measurements with the device were made off the Oregon coast and off San Diego. The device tested displayed segmented linear relationships with the particulate beam attenuation coefficient at 660% and the particulate total scattering coefficient at 488 nm as a function of depth. The slope of the correlation with the particulate beam attenuation coefficient changed by a factor of five over a depth range of 125 meters. DTIC

N95-34579# Texas Technological Univ., Lubbock, TX.
ACCURACY ENHANCEMENT IN OPTICAL COMPUTING Final Technical Report
John F. Walkup and Thomas F. Krile 30 Jan. 1995 41 p
(Grant AF-AFOSR-0192-91)
(AD-A294958; AFOSR-95-0285TR) Avail: CASI HC A03/MF A01

Investigations of techniques for describing and enhancing the accuracy of optical linear algebra processors have been conducted. Significant accomplishments include: (1) showing that error correcting codes can improve processor accuracy and developing criteria which such codes need to possess in order to be suitable for this task; (2) developing a system model incorporating device dynamic range for better quantitative assessment of error correcting code performance; (3) completing a detailed study of the combination of digital partitioning and Modified Multilevel Hamming Codes to achieve high accuracy computation, including scaling properties and effects on processor throughput. DTIC

N95-34758# Air Force Systems Command, Wright-Patterson AFB, OH. National Air Intelligence Center.
APPLIED RESEARCH ON LIQUID CRYSTAL SPATIAL MODULATORS IN HADAMARD TRANSFORM SPECTROMETERS. QUICK AND ACCURATE DECODING METHODS
Zhang Bingquan and Bi Fengfei 1994 9 p
(AD-A294152; NAIC-ID(RS)T-0388-94) Avail: CASI HC A02/MF A01

This article studies liquid crystal spatial light modulator (LC-SLM) functioning as a fixed, unmoving encoding mask applied in Hadamard transform spectrometers (HTS). It puts forward a fast and accurate decoding method, and offers improvements in root mean square signal to noise ratios associated with liquid crystal spatial light modulators. DTIC

N95-34759# Air Force Systems Command, Wright-Patterson AFB, OH. National Air Intelligence Center.
DEVELOPMENT OF 1.06 MICRON HIGH EFFICIENCY ANTIREFLECTIVE COATING
Fan Ruiying and Lu Yuemei 26 Apr. 1995 17 p Transl. into ENGLISH from Zhongguo Jiguang, China, v. 11, no. 11, Nov. 1984 p 686-690
(AD-A294161; NAIC-ID(RS)T-0646-93) Avail: CASI HC A03/MF A01

This article carries out analyses of errors associated with two layer antireflective coatings. It points out that two layer antireflective coatings associated with non lambda/4 stacks have more stable optical properties than lambda 4 stacks. Using Ta2O5 and SiO2 to act as film materials, two layer antireflective coatings were prepared on Kg glass substrate. The single surface reflectivity was below 0.03%, and laser damage threshold values were greater than 7 GW/sq cm (laser light wave length 1.06 micron, pulse width 1 ns). DTIC

N95-34791# Arizona Univ., Tucson, AZ.
MULTILAYER OPTICS FOR SOFT X-RAYS Final Technical Report, 1 Apr. 1993 - 30 Sep. 1994
Charles M. Falco and Jon M. Slaughter 15 Nov. 1994 8 p
(Contract F49620-93-1-0201)
(AD-A295030; AFOSR-95-0315TR) Avail: CASI HC A02/MF A01

We have shown that high quality Be films may be grown on alpha-Al2O3 Si(111) and Ge(111) consistent with the relative lattice mismatches, films grown on Si(111) are of higher quality than those grown on alpha-Al2O3, and those grown on Ge(111) are of the highest quality. The epitaxial Be films grown on Ge during this grant period are the best quality Be films that we or anyone else have ever produced. Growth of these high quality films is a significant step toward single crystal heterostructures containing Be. Such Be-containing structures may be useful, not only in EUV optics, but also in IR optics electronic devices, and studies of thin-film superconductivity. We have been successful in growing epitaxial Co-on-Be, and Ge-on-Be, but not in making Co/Be or Ge/Be superlattices. In both cases the problem is related to limitations of our equipment. To pursue this work further would require an upgrade to our MBE apparatus. Our very recent successes with sputter-deposited Y- and B4C-based multilayers show that there is still much to be gained by studying and optimizing the growth of carefully chosen new material pairs. DTIC

75 PLASMA PHYSICS

Includes magnetohydrodynamics and plasma fusion.

For ionospheric plasmas see *46 Geophysics*. For space plasmas see *90 Astrophysics*.

N95-32401 Argonne National Lab., IL. Fusion Power Program.
SUMMARY REPORT FOR ITER TASK NO. T226B: EVALUATION OF ITER DISRUPTION EROSION
A. Hassanein, P. Rockett, and J. Hunter Feb. 1995 41 p Limited Reproducibility: More than 20% of this document may be affected by microfiche quality
(Contract W-31-109-eng-38)
(DE95-010402; ANL/FPP/TM-280) Avail: Issuing Activity (Department of Energy (DOE))

The behavior of divertor materials during a major disruption in a tokamak reactor is very important to successful and reliable operation of the device. Erosion of material surfaces due to a thermal energy dump can severely limit the lifetimes of plasma-facing components and thus diminish the reactor's economic feasibility. A comprehensive numerical model has been developed and used in this analysis, which includes all major physical processes taking place during plasma/material interactions. Models to account for material thermal evolution, plasma/vapor interaction physics, and models for hydrodynamic radiation transport in the developed vapor cloud above the exposed surface are implemented in a self-consistent manner to realistically assess disruption damage. The extent of self-protection from the developed vapor cloud in front of the incoming plasma particles is critically important in determining the overall disruption lifetime. Models to study detailed effects of the strong magnetic field on the behavior of the vapor cloud and on the net erosion rate have also been developed and analyzed. Candidate materials such as beryllium and carbon are considered in this analysis. The dependence of divertor disruption lifetime on disruption physics and reactor conditions is analyzed and discussed. In addition, material erosion from melting of plasma-facing components during a tokamak disruption is also a serious problem that limits reactor operation and economical reactor lifetime. In particular, metallic low-Z components such as Be will be subjected to severe melting during disruptions and edge localized modes (ELM's). Loss of the developed melt layer will critically shorten the lifetime of these components, severely contaminate the plasma, and seriously inhibit successful and reliable operation of the reactor. In this study mechanisms responsible for melt-layer loss during a disruption are also modeled and evaluated. DOE

N95-32406# Japan Atomic Energy Research Inst., Tokyo (Japan).
DEVELOPMENT AND TRIAL MANUFACTURING OF 1/2-SCALE PARTIAL MOCK-UP OF BLANKET BOX STRUCTURE FOR FUSION EXPERIMENTAL REACTOR

Toshiyuki Hashimoto, Hideyuki Takatsu, and Satoshi Sato (Japan Atomic Energy Research Inst., Ibaraki, Japan.) Jul. 1994 78 p In JAPANESE
(DE95-737184; JAERI-Tech-94-009) Avail: CASI HC A05/MF A01

Conceptual design of breeding blanket has been discussed during the CDA (Conceptual Design Activities) of ITER (International Thermonuclear Experimental Reactor). Structural concept of breeding blanket is based on box structure integrated with first wall and shield, which consists of three coolant manifolds for first wall, breeding and shield regions. The first wall must have cooling channels to remove surface heat flux and nuclear heating. The box structure includes plates to form the manifolds and stiffening ribs to withstand enormous electromagnetic load, coolant pressure and blanket internal (purge gas) pressure. A 1/2-scale partial model of the blanket box structure for the outboard side module near midplane is manufactured to estimate the fabrication technology, i.e. diffusion bonding by HIP (Hot Isostatic Pressing) and EBW (Electron Beam Welding) procedure. Fabrication accuracy is a key issue to manufacture first wall panel because bending deformation during HIP may not be small for a large size structure. Data on bending deformation during HIP was obtained by preliminary manufacturing of HIP elements. For the shield structure, it is necessary to reduce the welding strain and residual stress of the weldment to establish the fabrication procedure. Optimal shape of the parts forming the manifolds, welding locations and welding sequence have been investigated. In addition, preliminary EBW tests have been performed in order to select the EBW conditions, and fundamental data on built-up shield have been obtained. Especially, welding deformation by joining the first wall panel to the shield has been measured, and total deformation to build-up shield by EBW has been found to be smaller than 2 mm. Consequently, the feasibility of fabrication technologies has been successfully demonstrated for a 1m-scaled box structure including the first wall with cooling channels by means of HIP, EBW and TIG (Tungsten Inert Gas arc)-welding. DOE

N95-32409# Japan Atomic Energy Research Inst., Tokyo (Japan).
DESIGN CONCEPT OF A CRYOGENIC DISTILLATION COLUMN CASCADE FOR A ITER SCALE FUSION REACTOR
Toshihiko Yamanishi, Mikio Enoeda, and Kenji Okuno (Japan Atomic Energy Research Inst., Ibaraki, Japan.) Jul. 1994 37 p
(DE95-737185; JAERI-Tech-94-011) Avail: CASI HC A03/MF A01

A column cascade has been proposed for the fuel cycle of a ITER scale fusion reactor. The proposed cascade consists of three columns and has significant features: either top or bottom product is prior to the other for each column; it is avoided to withdraw side streams as products or feeds of down stream columns; and there is no recycle steam between the columns. In addition, the product purity of the cascade can be maintained against the changes of flow rates and compositions of feed streams just by adjusting the top and bottom flow rates. The control system has been designed for each column in the cascade. A key component in the prior product stream was selected, and the analysis method of this key component was proposed. The designed control system never brings instability as long as the concentration of the key component is measured with negligible time lag. The time lag for the measurement considerably affects the stability of the control system. A significant conclusion by the simulation in this work is that permissible time for the measurement is about 0.5 hour to obtain stable control. Hence, the analysis system using the gas chromatography is valid for control of the columns. DOE

N95-32410# Japan Atomic Energy Research Inst., Tokyo (Japan).
STABILITY ANALYSIS OF EXTERNAL KINK MODE FOR ITER L-MODE PROFILE PLASMAS
Shinji Tokuda and Takahisa Ozeki (Japan Atomic Energy Research Inst., Ibaraki, Japan.) Sep. 1994 21 p
(DE95-737207; JAERI-Research-94-013) Avail: CASI HC A03/MF A01

A stability analysis is made for the n = 1 external kink mode (n: toroidal mode number) to the predicted ITER L-mode profiles. The beta limit (g(sub T)) for this kink mode is sufficiently higher than the design value of g(sub T) = 2.0-2.4 for the L-mode profiles in case of the assumed current profile even with a finite but small edge current. However, in case of q(sub 0) less than unity (q(sub 0): safety factor on the magnetic axis) the beta limit for the kink mode is significantly reduced; g(sub T) is 1.0 for q(sub 0) = 0.8 without a conducting wall. A conducting wall located near the mid-plane has a stronger stabilizing effect than a wall located near the null point. DOE

N95-32417# Japan Atomic Energy Research Inst., Tokyo (Japan).
TRANSPORT STUDIES OF TOKAMAK PLASMAS IN JT-60 DEVICE
Hiroshi Shirai (Japan Atomic Energy Research Inst., Ibaraki, Japan.) Aug. 1994 257 p
(DE95-737227; JAERI-Research-94-001) Avail: CASI HC A12/MF A03

In order to study the magnetic flux exchange at the sawtooth crash, the nonlinear evolution of the tearing mode with poloidal mode number m=1 and toroidal mode number n=1 in the presence of two or three resonant surfaces satisfying q=m/n=1 is examined. It is clarified that whether the local magnetic flux exchange or the internal disruption occurs depends on the initial profile of helical flux function phi(0). Light impurities such as carbon and oxygen and metal impurities such as titanium and molybdenum cause dominant radiation loss in the high density regime and give rise to major disruption. Increasing density by gas puffing while keeping the impurity content constant, the density limit of ohmically heated plasmas is studied. The numerically obtained operational diagram or Hugill diagram, qualitatively agrees well with that obtained in the experiment. Characteristics of global parameter dependence of JT-60 plasmas in both ohmic heating phase and neutral beam heating phase have been studied by using the models of electron and ion thermal diffusivities, chi(e) and chi(i). The predicted T(e) profile and the energy confinement time, tau(E), show good agreement with experimental data in the medium line for both ohmic heating and neutral beam heating phase. The power degradation of energy confinement time (tau(E)(exp th) proportional to P(abs)(exp -1/2)) is also reproduced. Ion temperature profiles of neutral beam heated phase of JT-60 have been simulated by using a chi(i) model based on eta(i) mode turbulence and the drift wave turbulence. In case of TFTR L-mode plasmas, the simulated T(i) profiles become flatter than experimental data. In the high T(i) plasmas of JT-60 and supershot plasmas of TFTR, the predicted T(i) profiles become broader compared with the experimental results. DOE

N95-32507# Academy of Sciences (USSR), Novosibirsk (USSR). Inst. Yadernoj Fiziki.
BERNSTEIN-GREEN-KRUSKAL WAVE. 2: THE INTERACTION WITH THE LANGMUIR WAVE. STOCHASTIC PHENOMENA
N. S. Buchelnikova and B. N. Lazeev 1993 54 p
(DE95-614202; IYF-93-98) Avail: CASI HC A04/MF A01 (US Sales Only)

The interaction of the Bernstein-Green-Kruskal (BGK) wave (N = 1) with the Langmuir wave was studied in numerical experiments. It was shown that the interaction leads to the stochastic instability (the formation of the stochastic layers) or to the large scale stochasticity. The evolution of the large scale stochasticity is accompanied by the secondary nonlinear effects, which lead to the increase of the amplitude of the BGK and Langmuir waves and to the increase of the Chirikov parameter. The final stage of the large scale stochasticity evolution is the formation of a new quasi-stationary structure on the phase plane, which includes the region of stochastic motion. It was shown that the BGK wave itself is unstable due to the interaction with the Langmuir waves excited by the electric field of the electron density distribution in the BGK wave, which leads to the stochastic instability or the large scale stochasticity. DOE

N95-32508# Academy of Sciences (USSR), Novosibirsk (USSR). Inst. Yadernoj Fiziki.
CONVERSION OF THE BERNSTEIN-GREEN-KRUSKAL WAVE ON THE DENSITY PERTURBATION, PART 1
N. S. Buchelnikova and B. N. Lazeev 1994 25 p
(DE95-614203; IYF-94-48) Avail: CASI HC A03/MF A01 (US Sales Only)

The interaction of the BGK-wave with sinusoidal density perturbation in the one-dimensional plasma with fixed ions was studied in numerical experiments (PIC-method). It was shown, that this interaction, like the case of the Langmuir wave, leads to the conversion into the direct and backward Langmuir waves with the wave numbers N = N(sub e) +/- beta N(sub i), beta = 1,2,3... The dynamical description the conversion shows itself in the modulation of the electric field and in the localization of the energy in the density cavities. DOE

N95-32509# Academy of Sciences (USSR), Novosibirsk (USSR). Inst. Yadernoj Fiziki.
CONVERSION OF THE BERNSTEIN-GREEN-KRUSKAL WAVE ON THE DENSITY PERTURBATION, PART 3
N. S. Buchelnikova and B. N. Lazeev 1994 32 p
(DE95-614205; IYF-94-50) Avail: CASI HC A03/MF A01 (US Sales Only)

The interaction of the BGK-wave with sinusoidal density perturbation in the one-dimensional plasma with fixed ions was studied in numerical experiments (PIC-method). The results are compared with works where the cases with other parameters of the BGK-wave and the density perturbation were studied. It was shown that this interaction in all the cases leads to the conversion into direct and backward Langmuir waves with the wave numbers N = N(sub e) +/- beta N(sub i), beta = 1,2,3... and in the case N(sub i) = N(sub e) into the direct waves N = N(sub e) +/- beta N(sub i), like the case of the Langmuir wave conversion. But the evolution of the conversion is different. In all the cases the electrons, trapped in the BGK-wave, stabilize the wave and prevent the conversion. DOE

N95-32510# Academy of Sciences (USSR), Novosibirsk (USSR). Inst. Yadernoj Fiziki.
CONVERSION OF THE BERNSTEIN-GREEN-KRUSKAL WAVE ON THE DENSITY PERTURBATION, PART 4
N. S. Buchelnikova and B. N. Lazeev 1994 29 p
(DE95-614206; IYF-94-51) Avail: CASI HC A03/MF A01 (US Sales Only)

The interaction of the BGK-wave with sinusoidal density perturbation in the one-dimensional plasma with fixed ions was studied in numerical experiments (PIC-method). It was shown that this interaction leads to the conversion into the direct and backward Langmuir waves with the wave numbers N = N(sub e) +/- beta N(sub i), beta = 1,2,3... In the cases with n-tilde/n(sub 0) approx. 0,6 - 0,9 the wide spectrum of the conversion modes is excited up to beta approx. 8 during one plasma period. In these cases the main role is played by the large scale stochasticity of the electron motion which shows itself in the region of the cross trapping regions of the short-wavelength conversion modes. The energy of the BGK-wave is transferred through the long-wavelength conversion modes into the short-wavelength modes, where it is absorbed by the plasma electrons. As a result, the electric field energy is damped and the BGK-wave is destroyed. DOE

N95-32536 Lawrence Livermore National Lab., Livermore, CA.
EXPERIMENTAL STUDY OF THE PROCESSES IN THE EXPANDER OF THE AXISYMMETRIC MIRROR DEVICE
A. A. Ivanov, A. V. Anikeev, and P. A. Bagryansky (Academy of Sciences, USSR, Novosibirsk, USSR.) Sep. 1994 35 p Limited Reproducibility: More than 20% of this document may be affected by microfiche quality
(Contract W-7405-eng-48)
(DE95-009846; UCRL-CR-118994) Avail: CASI HC A03

This work was devoted to studying the plasma flow in the expander region, of a gas-dynamic trap. A knowledge of processes occurring in this region is essential in two aspects. The first is that the plasma flowing out the central cell eventually comes into direct contact with -material wall thus depositing the energy from the central cell to the end wall. Since the longitudinal energy losses dominate in MHD-stable regimes of confinement, the data on an energy transport in the expander is important in estimations of the prospective of gas-dynamic trap as well as the other open-ended systems. It might also be useful for studies of a plasma-wall interaction in other systems where a plasma is inherently in contact with the wall, for example, for the divertors of tokamaks. The second aspect is that the parameters of the plasma flow, in the case of gas-dynamic trap, determine the contribution of the expander to the MHD-stability of the entire trap. The paper is organized as follows. The description of the GDT device and its operational regimes and a description of the diagnostics which have been used in the experiments are given. The methods of measurements of plasma parameters are also given. A simple model of the plasma flow in the expander region of a gas-dynamic trap which was used in an analysis of the experimental data is presented. The experimental results obtained in the course of this work are presented and discussed. Our conclusions regarding the comparison of the theoretical predictions and the experimental data are summarized. DOE

N95-32560# Academy of Sciences (USSR), Novosibirsk (USSR).
ON THE PARAXIAL EQUILIBRIUM OF THE FINITE (BETA) PLASMA IN OPEN MAGNETIC CONFIGURATIONS
I. M. Lanskij 1993 8 p
(DE95-614170; BUDKERINP-93-96; IYaF-93-96) Avail: CASI HC A02/MF A01 (US Sales Only)

Paraxial equilibrium of the finite (beta) plasma in the magnetic mirror is considered. The upper (beta) limit is established, upwards of which a current layer is generated in plasma, and, as a consequence, a small longitudinal scale-length occurs in the problem. The latter leads to the violation of the paraxial equilibrium. Results are applicable to various plasma configurations with the mirror confinement. DOE

N95-32561# Academy of Sciences (USSR), Novosibirsk (USSR).
RADIAL ELECTRIC FIELD MEASUREMENT IN A TOKAMAK BY THE INJECTION OF A PULSED NEUTRAL BEAM
V. I. Davydenko, A. A. Ivanov, A. N. Karpushov, D. D. Ryutov, R. Pozzoli, and M. Rome 1994 22 p
(DE95-614176; BUDKERINP-94-1; IYaF-94-1) Avail: CASI HC A03/MF A01 (US Sales Only)

The detection of the profile of the radial electric field of a tokamak by the perpendicular injection of a pulsed neutral beam into the plasma is analyzed. The method is based on the measurement of the toroidal precession velocity of the thus formed ion population. The toroidal drift is caused by the curvature of the magnetic field lines and by the electric field. For the separation of these two effects, the use of a beam with two energy fractions is studied. The application of this diagnostic scheme in a real tokamak is considered. DOE

N95-32562# China Nuclear Information Centre, Beijing (China).
STUDY OF IMPURITY CONCENTRATIONS BY VUV SPECTROSCOPY ON HL-1
Cuixian Luo, Kehua Li, Yushan Liu, Quanming Wang, and Wenlin Yuan Jul. 1993 10 p
(DE95-614186; CNIC-00784; SIP-0066) Avail: CASI HC A02/MF A01 (US Sales Only)

The impurity concentrations in HL-1 were determined by VUV spectroscopy. The absolute calibration of VUV spectrometer by the branching ratio technique and a SITCODE impurity transport code developed in SWIP for interpreting the spectroscopic measurements are described. In order to obtain these results easily on a shot-to-shot basis at the end of each discharge, a simplified fast evaluation method is introduced. The evaluation of the impurity concentrations in HL-1 discharges with and without carbonization, pump limiter and edge polarization are discussed. DOE

N95-32565# Japan Atomic Energy Research Inst., Tokyo (Japan).
IRRADIATION TESTS OF CRITICAL COMPONENTS FOR REMOTE HANDLING IN GAMMA RADIATION ENVIRONMENT
Henjiro Obara, Satoshi Kakudate, Kiyoshi Oka (Japan Atomic Energy Research Inst., Ibaraki, Japan.), Kazuyuki Furuya, Kou Taguchi, Eisuke Tada, Kiyoshi Shibanuma, Yoshinao Ohkawa, Yousuke Morita, and Noriko Yokoo et al Aug. 1994 81 p
(DE95-737223; JAERI-Tech-94-003) Avail: CASI HC A05/MF A01

Since the fusion power core of a D-T fusion reactor will be highly activated once it starts operation, personnel access will be prohibited so that assembly and maintenance of the components in the reactor core will have to be totally conducted by remote handling technology. Fusion experimental reactors such as ITER require unprecedented remote handling equipments which are tolerable under gamma radiation of more than 10(exp 6) R/h. For this purpose, the Japan Atomic Energy Research Institute (JAERI) has been developing radiation hard components for remote handling purpose and a number of key components have been tested over 10(exp 9) rad at a radiation dose rate of around 10(exp 6) R/h, using Gamma Ray Radiation Test Facility in JAERI-Takasaki Establishment. This report summarizes the irradiation test results and the latest status of AC servo motor, potentiometer, optical elements, lubricant, sensors and cables, which are key elements of the remote handling system. DOE

N95-32588# Idaho National Engineering Lab., Idaho Falls, ID.
FUSION SAFETY PROGRAM ANNUAL REPORT, FISCAL YEAR 1994
Glen R. Longhurst, Lee C. Cadwallader, Thomas J. Dolan, J. Stephen Herring, Kathryn A. McCarthy, Brad J. Merrill, Chester C. Motloch, and

David A. Petti Mar. 1995 62 p
(Contract DE-AC07-94ID-13223)
(DE95-006872; INEL-95/0002) Avail: CASI HC A04/MF A01

This report summarizes the major activities of the Fusion Safety Program in fiscal year 1994. The Idaho National Engineering Laboratory (INEL) is the designated lead laboratory and Lockheed Idaho Technologies Company is the prime contractor for this program. The Fusion Safety Program was initiated in 1979. Activities are conducted at the INEL, at other DOE laboratories, and at other institutions, including the University of Wisconsin. The technical areas covered in this report include tritium safety, beryllium safety, chemical reactions and activation product release, safety aspects of fusion magnet systems, plasma disruptions, risk assessment failure rate data base development, and thermalhydraulics code development and their application to fusion safety issues. Much of this work has been done in support of the International Thermonuclear Experimental Reactor (ITER). Also included in the report are summaries of the safety and environmental studies performed by the Fusion Safety Program for the Tokamak Physics Experiment and the Tokamak Fusion Test Reactor and of the technical support for commercial fusion facility conceptual design studies. A major activity this year has been work to develop a DOE Technical Standard for the safety of fusion test facilities. DOE

N95-32592# General Atomics Co., San Diego, CA.
RECENT RESULTS FROM THE D3-D TOKAMAK AND IMPLICATIONS FOR FUTURE DEVICES
J. L. Luxon et al Feb. 1995 31 p Presented at the 18th European Symposium on Fusion Technology, Karlsruhe, Germany, 22-26 Aug. 1994
(Contracts DE-AC03-89ER-51114; DE-AC05-84OR-21400; W-7405-eng-48; DE-AC04-76DP-00789)
(DE95-009605; GA-A-21814; CONF-940843-18) Avail: CASI HC A03/MF A01

Improvements to the D3-D tokamak have led to significant new research results and enhanced performance. These results provide important inputs to the design of next generation divertor systems including the upgrade of the D3-D divertor. The use of graphite for the plasma facing components and careful wall preparation has enabled the routine achievement of regimes of enhanced energy confinement. In elongated discharges, triangularity has been found to be important in attaining good discharge performance as measured by the product of the normalized plasma pressure and the energy confinement time, (beta)(tau)(sub E) This constrains the design of the divertor configuration (X-point location). Active pumping of the divertor region using an in-situ toroidal cryogenic pump has demonstrated control of the plasma density in H-mode discharges and allowed the dependence of confinement on plasma density and current to be separately determined. Helium removal from the plasma edge sufficient to achieve effective ash removal in reactor discharges has also been demonstrated using this pumping configuration. The reduction of the heat flux to the divertor plates has been demonstrated using two different techniques to increase the radiation in the boundary regions of the plasma and thus reduce the heat flux to the divertor plates; deuterium gas injection has been used to create a strongly radiating localized zone near the X-point, and impurity (neon) injection to enhance the radiation from the plasma mantle. Precise shaping of the plasma current profile has been found to be important in achieving enhanced tokamak performance. Transiently shaped current profiles have been used to demonstrate regimes of plasmas with high beta and good confinement. Control of the current profile also is important to sustaining the plasma in the Very High (VH)-mode of energy confinement. DOE

N95-32656# General Atomics Co., San Diego, CA.
D3-D POWER SUPPLY, DESIGN, AND DEVELOPMENT
A. Nerem Feb. 1995 5 p Presented at the International Power Electronics Conference, Yokohama, Japan, 3-7 Apr. 1995
(Contract DE-AC03-89ER-51114)
(DE95-009603; GA-A-21957; CONF-9504138-1) Avail: CASI HC A01/MF A01

An overview of the D3-D power supply system with information details concerning the configuration, power ratings, acquisition costs, and cost scaling relevant to the design of ITER and other tokamaks is presented. The power supplies for the D3-D tokamak were installed and commissioned during the late 1970's and the beginning of the 1980's. Several upgrades have been implemented during the last two years to solve increasing reliability problems encountered as the equipment aged, to provide enhanced operational flexibilities, and to enable operation at the higher power levels needed to provide experimental data relevant to the ITER and TPX design activities. These upgrades ranged from redesign of the power supply control systems to the replacement of vacuum circuit breakers which had become unreliable in service. A new interlock and protection system has also been implemented using the latest programmable logic controllers (PLC) and computer technology. These upgrades have been highly successful and are described to provide insight to many issues in the specification of high power converters. Power supply models used in the design of the D3-D Plasma Control System are also described along with model verification test data. These models are being used in the development of a new advanced plasma control system for the D3-D tokamak. Recent operational experience and results are presented. DOE

N95-32756# General Atomics Co., San Diego, CA.
OPTIMIZED PROFILES FOR IMPROVED CONFINEMENT AND STABILITY IN THE DIII-D TOKAMAK
T. S. Taylor, H. StJohn, A. D. Turnbull, Y. R. Lin-Liu, K. H. Burrell, V. Chan, M. S. Chu, J. R. Ferron, L. L. Lao, and R. J. LaHaye et al Feb. 1995 11 p Presented at the 21st EPS Conference on Controlled Fusion and Plasma Physics, Montpellier, France, 27 Jun. - 1 Jul. 1994
(Contracts DE-AC03-89ER-51114; DE-AC05-84OR-21400)
(DE95-009606; GA-A-21757; CONF-9406270-8) Avail: CASI HC A03/MF A01

Simultaneous achievement of high energy confinement, tau(sub E), and high plasma, beta, leads to an economically attractive compact tokamak fusion reactor. High confinement enhancement, H = tau(sub E)/tau(sub E-ITER89P) = 4, and high normalized beta, beta(sub N) = beta/(I/aB) = 6%-m-T/MA, have been obtained in DIII-D experimental discharges. These improved confinement and/or improved stability limits are observed in several DIII-D high performance operational regimes: VH-mode, high (ell)(sub i) H-mode, second stable core, and high beta poloidal. The authors have identified several important features of the improved performance in these discharges: details of the plasma shape, toroidal rotation or ExB flow profile, q profile and current density profile, and pressure profile. From the improved physics understanding of these enhanced performance regimes, they have developed operational scenarios which maintain the essential features of the improved confinement and which increase the stability limits using localized current profile control. The stability limit is increased by modifying the interior safety factor profile to be nonmonotonic with high central q, while maintaining the edge current density consistent with the improved transport regimes and the high edge bootstrap current. They have calculated high beta equilibria with beta(sub N) = 6.5, stable to ideal n = 1 kinks and stable to ideal ballooning modes. The safety factor at the 95% flux surface is 6, the central q value is 3.9 and the minimum in q is 2.6. The current density profile is maintained by the natural profile of the bootstrap current, and a modest amount of electron cyclotron current drive. DOE

N95-32770# Academy of Sciences (USSR), Novosibirsk (USSR). Inst. Yadernoj Fiziki.
HF-STABILIZATION OF PLASMA WITH SHARP BOUNDARY
I. A. Kotelnikov and S. G. Yakovchenko 1994 27 p
(DE95-614207; IYF-94-66) Avail: CASI HC A03/MF A01 (US Sales Only)

The effect of HF natural oscillations of a plasma filament in a conducting cylindrical housing on the flute disturbance stability is investigated. Flute development leads to HF oscillation frequency (omega) variation connected with the energy W variation by the condition of constancy of the adiabatic invariant W/(omega) = const. The last is conserved owing to relative slow variations of flute disturbances. The adiabatic approximation used permits one to obtain simple criteria for flute instability stabilization by a HF field. HF oscillations of a plasma with a sharp boundary are considered. DOE

N95-32838 Massachusetts Univ., Lowell, MA.
MID-LATITUDE IONOSPHERIC PLASMA DRIFT: A COMPARISON OF DIGITAL IONOSONDE AND INCOHERENT SCATTER RADAR MEASUREMENTS AT MILLSTONE HILL Ph.D. Thesis
Terence William Bullett 1994 324 p
Avail: Univ. Microfilms Order No. DA9423779

A successful validation of the Digisonde drift technique was performed by comparing local ionospheric plasma drift velocity vectors measured by

a Digisonde 256 digital ionosonde and a UHF incoherent scatter radar co-located at Millstone Hill (42 deg N, 71 deg 30' W) in Massachusetts, USA. The Digisonde drift technique uses imaging Doppler interferometry, measuring amplitude and phase Doppler spectra of ionospherically reflected signals across an array of receive antennas and processing these as line of sight ionospheric velocity vectors. Line of sight velocities of sufficient orthogonality are combined to calculate 3 dimensional ionospheric plasma drift vectors with 5 minutes resolution. A total of 145 hours of simultaneous radar and ionosonde drift vectors from 4 experiments are presented and compared. Geographically aligned, bottom side F-region (200-350 km) velocity components measured by each system were correlated. East-west velocities correlate to plus 0.90, north-south components to plus 0.67 and vertical components to plus 0.51. The Digisonde drift technique works best during moderately disturbed nighttime conditions, and those conditions are the emphasis of the work. The relative smoothness of the daytime mid-latitude ionosphere reduces the technique's ability to measure horizontal drifts. Dissert. Abstr.

N95-33066# Lawrence Livermore National Lab., Livermore, CA.
ENERGY AND TECHNOLOGY REVIEW
W. A. Bookless, ed. and D. Wheatcraft, ed. Mar. 1995 25 p Repr. from Energy and Technology Review (Springfield, VA), Mar. 1995
(Contract W-7405-eng-48)
(DE95-011686; UCRL-52000-95-3) Avail: CASI HC A03/MF A01

This journal contains two feature articles. The first article reports on the background, design, and capabilities of the Portable Tritium Processing System currently being used to clean up and decontaminate the Laboratory's Tritium Facility. The second article discusses the development of a x-ray lasers as a probe to obtain high-resolution images of high-density plasmas produced at the Nova laser facility. Finally, two research programs are highlighted. They are silicon microcomponents and modern technology for advanced military training. DOE

N95-33216# Washington Univ., Seattle, WA. Aerospace and Energetics Research Program.
TRAP: TOKAMAK REFUELING BY ACCELERATED PLASMOIDS Annual Progress Report No. 3, 7 Aug. 1994 - 6 Aug. 1995
Alan L. Hoffman and John T. Slough 1995 17 p
(Contract DE-FG06-92ER-54176)
(DE95-009925; DOE/ER-54176/T1) Avail: CASI HC A03/MF A01

This is the annual progress report for the period August 7, 1994 to August 6, 1995. This project is to demonstrate the ability to generate, accelerate, and inject plasmoids into a tokamak type magnetic geometry with the purpose being plasma fueling. The hardware has been assembled and constructed. Early test results have shown some unexpected problems which have been addressed. These and other delivery problems have extended the assembly phase and the authors are requesting a six month extension to allow adequate time for experimentation with the apparatus. DOE

N95-33221# Wisconsin Univ., Madison, WI.
THE EFFECT OF COLLISIONALITY AND DIAMAGNETISM ON THE PLASMA DYNAMO
H. Ji (Princeton Univ., NJ.), Y. Yagi (Electrotechnical Lab., Tsukuba, Japan.), K. Hattori (Electrotechnical Lab., Tsukuba, Japan.), Y. Hirano (Electrotechnical Lab., Tsukuba, Japan.), T. Shimada (Electrotechnical Lab., Tsukuba, Japan.), Y. Maejima (Electrotechnical Lab., Tsukuba, Japan.), K. Hayase (Electrotechnical Lab., Tsukuba, Japan.), A. F. Almagri, S. C. Prager, and J. S. Sarff et al 28 Apr. 1995 17 p
(Contract DE-FG02-85ER-53198)
(DE95-012409; DOE/ER-53198/259) Avail: CASI HC A03/MF A01

Fluctuation-induced dynamo forces are measured over a wide range of electron collisionality in the edge of TPE-1RM20 Reversed-Field Pinch (RFP). In the collisionless region the Magnetohydrodynamic (MHD) dynamo alone can sustain the parallel current, while in the collisional region a new dynamo mechanism resulting from the fluctuations in the electron diamagnetic drift becomes dominant. A comprehensive picture of the RFP dynamo emerges by combining with earlier results from MST and REPUTE RFPs. DOE

N95-33391 Texas Univ., Austin, TX.
STUDIES OF IMPURITY MODE AND ITG MODE IN TOROIDAL PLASMAS
J. Q. Dong (Southwest Inst. of Physics, Sichuan, China.) and W. Horton Apr. 1995 37 p Limited Reproducibility: More than 20% of this document may be affected by microfiche quality
(Contract DE-FG05-80ET-53088)
(DE95-012134; DOE/ET-53088/703; IFSR-703) Avail: CASI HC A03

The impurity mode and eta(sub i) mode driven by impurity ions with outwardly peaked density profiles, just as it is at the boundary of tokamak plasmas, and the ion temperature gradient, respectively, are studied in high temperature toroidal plasmas. The gyrokinetic theory is applied and finite Larmor radius effects of both hydrogenic and impurity ions are included. It is found that the impurity mode is enhanced by the ion temperature gradient. In addition, the impurity ions with outwardly peaked density profiles are demonstrated to have destabilizing effects on the eta(sub i) mode. These two modes are strongly coupled to each other so that it is impossible to distinguish between them when both the driving mechanisms are strong enough to drive the corresponding mode unstable independently. The correlation of the results with nonlinear simulations and the experimental observations are discussed. DOE

N95-33412# Sandia National Labs., Albuquerque, NM.
HIGH RATE DRY ETCHING OF GaN, AlN AND InN IN ECR Cl2/CH4/H2/Ar PLASMAS
C. B. Vartuli (Florida Univ., Gainesville, FL.), S. J. Pearton (Florida Univ., Gainesville, FL.), C. R. Abernathy (Florida Univ., Gainesville, FL.), R. J. Shul, S. P. Kilcoyne, M. Hagerott Crawford, A. J. Howard, and J. E. Parmeter 1995 6 p Presented at the Spring Meeting of the Materials Research Society (MRS), San Francisco, CA, 17-21 Apr. 1995
(Contract DE-AC04-94AL-85000)
(DE95-011872; SAND-95-0936C; CONF-950412-12) Avail: CASI HC A02/MF A01

Etch rates for binary nitrides in ECR Cl2/CH4/H2/ Ar are reported as a function of temperature, RF-bias, microwave power, pressure and relative gas proportions. GaN etch rates remain relatively constant from 30 to 125 C and then increase to a maximum of 2340 angstrom/min at 170 C. The AlN etch rate decreases throughout the temperature range studied with a maximum of 960 angstrom/min at 30 C. When CH4 is removed from the plasma chemistry, the GaN and InN etch rates are slightly lower, with less dramatic changes with temperature. The surface composition of the III-V nitrides remains unchanged over the temperatures studied. The GaN and InN rates increase significantly with RF power, and the fastest rates for all three binaries are obtained at 2 mTorr. Surface morphology is smooth for GaN over a wide range of conditions, whereas InN surfaces are more sensitive to plasma parameters. DOE

N95-33619# Korea Cancer Center Hospital, Seoul (Republic of Korea).
DEVELOPMENT OF TOKAMAK EXPERIMENT TECHNOLOGY: A STUDY ON THE NUCLEAR FUSION REACTOR
Kwang Won Lee, Chul Kew Hwang, Sang Ryul In, Sung Kyu Kim, Byung Hoon Oh, Seung Ho Jeong, Bong Guen Hong, Jae Sung Yoon, Byung Joo Yoon, and Woo Sup Song et al Jul. 1994 211 p In KOREAN
(DE95-614255; KAERI/RR-1363/93) Avail: CASI HC A10/MF A03 (US Sales Only)

Overall test operation of KT-1 tokamak has been done with the modified power supplies and constructed plasma position feedback control system. The achieved plasma parameters of KT-1 are Ip (plasma current) greater than 15 kA (9ms) and Td (plasma current sustaining time) greater than 12 ms (7.5 kA) until now. Instrumentations for the carbonization/boronization are also equipped and applied to the first boronization of invessel components of KT-1 tokamak. As a preliminary treatment of the 1st wall of tokamak vacuum torus, RG discharge cleaning has been done. Plasma qualities have been improved by discharge cleaning. In addition, helicon plasma device is designed succeeding exploitation of the first wall conditioning program which are all for the development of conditioning technology of 1st wall facing the plasma. As a part of the development program on the plasma monitoring technologies, conceptual design study on the FIR interferometer- polarimeter is accomplished. Parallel to these experimental activities, an effort has been made in designing the operating scenario of poloidal field system of KT-2 tokamak. DOE

N95-33696# Texas Univ., Austin, TX. Inst. for Fusion Studies.
MORE ON CORE-LOCALIZED TOROIDAL ALFVEN EIGENMODES
H. L. Berk, J. vanDam, D. Borba (Joint European Torus Project, Abingdon, England.), J. Candy (Joint European Torus Project, Abingdon, England.), G. T. A. Huysmans (Joint European Torus Project, Abingdon, England.), and S. Sharapov (Joint European Torus Project, Abingdon, England.) Feb. 1995 20 p
(Contract DE-FG05-80ET-53088)
(DE95-010857; DOE/ET-53088/695; IFSR-695) Avail: CASI HC A03/MF A01

A novel type of ideal toroidal Alfven eigenmode, localized in the low-shear core region of a tokamak plasma, is shown to exist, whose frequency is near the upper continuum of the toroidal Alfven gap. This mode converts to a kinetic-type toroidal Alfven eigenmode above a critical threshold that depends on aspect ratio, pressure gradient, and shear. Opposite to the usual ideal toroidal Alfven eigenmode, this new mode is peaked in amplitude on the small-major-radius side of the plasma. DOE

N95-33851# Sandia National Labs., Albuquerque, NM.
UNIFIED MODEL OF THE RF PLASMA SHEATH
Merle E. Riley May 1995 35 p
(Contract DE-AC04-94AL-85000)
(DE95-012114; SAND-95-0775) Avail: CASI HC A03/MF A01

By developing an approximation to the first integral of the Poisson equation, one can obtain solutions for the voltage-current characteristics of a radio-frequency (RF) plasma sheath that are valid over the whole range of inertial response of the ions to an imposed RF voltage or current-specified conditions. The theory adequately reproduces the time-dependent voltage-current characteristics of the two extreme cases corresponding to the Lieberman RF sheath theory and the Metze-Ernie-Oskam theory. Contained within the approximation is a time constant which controls the amount of ion response to the RF electric field. A prescription is given for determining this ion relaxation time constant, which also determines the time-dependent ion impact energy on the electrode surface. DOE

N95-33853# Texas Univ., Austin, TX. Fusion Research Center.
SINGLE LANGMUIR PROBE CHARACTERISTIC IN A MAGNETIZED PLASMA AT THE TEXT TOKAMAK Ph.D. Thesis
Stefan Jachmich May 1995 65 p
(Contract DE-FG03-94ER-54241)
(DE95-012144; DOE/ER-54241/138; FRCR-456) Avail: CASI HC A04/MF A01

A single Langmuir probe tip was used at TEXT-Upgrade to obtain I-V characteristics in a magnetized plasma. Noisy data were reduced by a boxcar-averaging routine. Unexpected effects, namely nonsaturation of ion current, hysterises in the characteristics and I(V)-data were observed, which are in disagreement to the common single probe model. A double probe model allows parameterization of the I(V) curves and to determine the plasma properties in the scrape-off layer. It is shown in this model that a Langmuir probe does perturb the local space potential in the plasma. Comparisons were made with the triple probe technique of measuring temperatures. The nonsaturation of ion current leads to an error in the triple probe technique of order 20%. DOE

N95-33873# Instituto Nacional de Pesaciais Espaciais, Sao Jose dos Campos (Brazil). Ministry of Science and Technology.
TOKAMAK ETE CIRCUITS: ANALYSIS AND SPECIFICATIONS [ANALISE E ESPECIFICACAO DOS CIRCUITOS DO TOKAMAK ETE]
Luis Filipe deF.P.W.Barbosa and Edson DelBosco Jun. 1994 56 p In PORTUGUESE
(INPE-5573-PRP/182) Avail: CASI HC A04/MF A01

Plasma is a set of neutral and charged particles that satisfies given criteria and is called a quasi-neutral set of particles. Plasma consists of electrons and ions produced through the ionization of atoms and molecules. The recombination of electrons and ions causes the plasma to emit radiation. This radiation may or may not be visible. If the radiation occurs within the visible spectrum, the light's color will depend upon the kind of gas to used. For instance, if hydrogen is used, the plasma's color will be blue. The objective of the plasma physics is the study of ionized and macroscopically neutral gaseous systems. These are systems composed of a large number of charged particles, distributed inside a (macroscopic) volume where the same amount of positive and negative charges exist. The greatest problem encountered was due to the necessary high power utilized in the Tokamak device. The Brazilian-made switches were not suitable to function normally under high I(exp 2)t. These switches relied upon capacitor banks, where more problems had arisen in the slower banks than in the faster ones. Consequently, imported equipment was used, including ignitrons for the circuits of the ohmic transformer, and thyristors and power diodes for the circuits of the toroidal field coil. All capacitor banks that have been mentioned so far are electrolytic and Brazilian-made. The same analysis could not be carried out for the ohmic circuit because of an unexpected physical effect. The trigger of the bank C2 had been sending a current to the switch S1, affecting the switch opening. The utilization of other devices, such as a saturated inductor, an open-capacitor or a vacuum break, should be considered to assist in this switch opening. Author

N95-34436# General Atomics Co., San Diego, CA.
INERTIAL CONFINEMENT FUSION TARGET COMPONENT FABRICATION AND TECHNOLOGY DEVELOPMENT SUPPORT Annual Report, 1 Oct. 1993 - 30 Sep. 1994
Martin Hoppe, ed. Apr. 1995 158 p
(Contract DE-AC03-91SF-18601)
(DE95-011655; GA-A21966) Avail: CASI HC A08/MF A02

On December 30, 1990, the US Department of Energy entered into a contract with General Atomics (GA) to be the Inertial Confinement Fusion (ICF) Target Component Fabrication and Technology Development Support contractor. During the period, GA was assigned 17 tasks in support of the Inertial Confinement Fusion program and its laboratories. This year they achieved full production capabilities for the micromachining, dimensional characterization and gold plating of hohlraums. They fabricated and delivered 726 gold-plated mandrels of 27 different types to LLNL and 48 gold-plated mandrels of two different types to LANL. They achieved full production capabilities in composite capsule production and delivered in excess of 240 composite capsules. They continuously work to improve performance and capabilities. They were also directed to dismantle, remove, and disposition all equipment at the previous contractor (KMSF) that had radioactive contamination levels low enough that they could be exposed to the general public without radiological constraints. GA was also directed to receive and store the tritium fill equipment. They assisted LANL in the development of techniques for characterization of opaque targets. They developed deuterated and UV-opaque polymers for use by the University of Rochester's Laboratory for Laser Energetics (UR/LLE) and devised a triple-orifice droplet generator to demonstrate the controlled-mass nature of the microencapsulation process. The ICF program is anticipating experiments at NIF and the Omega Upgrade. Both facilities will require capsules containing layered D2 or D-T fuel. They continued engineering and assembly of equipment for a cryogenic target handling system for UR/LLE that will fill, transport, layer, and characterize targets filled with cryogenic deuterium or deuterium-tritium fuel, and insert these cryogenic targets into the OMEGA Upgrade target chamber for laser implosion experiments. DOE

N95-34586# Clark Univ., Worcester, MA. Dept. of Mathematics and Computer Science.
MATHEMATICAL MODELLING IN PLASMA PHYSICS Final Report, 1 Jun. 1993 - 30 Sep. 1994
Natalia Sternberg 30 Sep. 1994 7 p
(Grant AF-AFOSR-0233-91)
(AD-A294972; AFOSR-95-0288TR) Avail: CASI HC A02/MF A01

The investigator was able to give a complete mathematical analysis for a self-consistent dynamic model for RF sheaths in the frequency range between the ion and electron plasma frequencies for arbitrary collision parameters arid arbitrary RF sheath voltages. Based on the above analysis, the investigator developed an algorithm which permits a complete numerical solution of the problem in its full generality without any restrictive assumptions. Using the developed algorithm, the investigator has computed the sheath characteristics for Argon and Helium. The computed results were compared with those found in known RF sheath theories and with those obtained experimentally at GTE Laboratories for a wide range of discharge conditions. It was found that our mathematical model matches the experiment better than any of the existing models. It is most complete and generalized model for the RF sheath in capacitive RF discharges. DTIC

N95-34824# National Inst. for Fusion Science, Nagoya (Japan).
APPLICATION OF GRATING POLARIZER TO 106.4GHz ECH SYSTEM ON HELIOTRON-E
K. Nagasaki, A. Isayama (Kyoto Univ., Japan.), and A. Ejiri Jan. 1995 31 p Submitted for publication
(ISSN 0915-633X)
(NIFS-334) Avail: CASI HC A03/MF A01

A grating polarizer with rectangular grooves is designed for 106.4GHz electron cyclotron heating (ECH) system on th Heliotron-E helical device. The polarizer is installed on mirrors of waveguide miter bends. In oversized waveguides, the HE(sub 11) mode can be treated by the plane wave theory. The polarization of the reflected wave is calculated as a function of the groove parameters and the mirror rotation angle. When launching the ECH power to fusion devices with moderate or strong magnetic shear such as heliotron/torsatron configuration, we should take into account the change of the wave polarization through the plasma. The effect of the magnetic shear can be investigated by using the polarizer. The dependence of the absorbed power on the mirror rotation angle are presented. Author

N95-34812# Northrop Grumman Corp., Princeton, NJ. Advanced Technology and Development Center.
HIGH BETA AND SECOND STABILITY REGION TRANSPORT AND STABILITY ANALYSIS
M. H. Hughes and M. W. Phillips Mar. 1995 17 p
(Contract DE-FG02-89ER-51124)
(DE95-011298; DOE/ER-51124/20) Avail: CASI HC A03/MF A01

This report summarizes MHD equilibrium and stability studies carried out at Northrop Grumman's Advanced Technology and Development Center during the 12 month period starting March 1, 1994. Progress is reported in both ideal and resistive MHD modeling of TFTR plasmas. The development of codes to calculate the significant effects of highly anisotropic pressure distributions is discussed along with results from this model. DOE

76 SOLID-STATE PHYSICS

Includes superconductivity.

For related information, see also *33 Electronics and Electrical Engineering* and *36 Lasers and Masers.*

N95-32377# Oak Ridge National Lab., TN.
MAGNETIC EXCITATIONS IN A RANDOM EXCHANGE SYSTEM Fe(x)Mn(1-x)TiO3
H. Kawano (Tokyo Univ., Japan.), H. Yoshizawa (Tokyo Univ., Japan.), R. M. Nicklow, and A. Ito (Ochanomizu Women's Univ., Tokyo, Japan.) 24 Aug. 1994 10 p Presented at the Neutron Scattering, Sendai, Japan, 11-14 Oct. 1994
(Contract DE-AC05-84OR-21400)
(DE95-006626; CONF-9410165-13) Avail: CASI HC A02/MF A01

In order to examine the influence of exchange frustration on spin wave excitations, inelastic neutron scattering experiments have been performed on a random exchange system Fe(x)Mn(1-x)TiO3 with x = 0.00, 0.10, 0.25 and 0.33. For all three mixed systems, the magnetic excitation spectra consist of two components: a well-defined spin wave component and a broad damped component. The latter can be well fitted to a spectral weight function for a damped harmonic oscillator. DOE

N95-32480# Joint Inst. for Nuclear Research, Dubna (USSR). Lab. of Theoretical Physics.
TRANSPARENT POTENTIAL PERTURBATIONS ON LATTICES AND IN THE PERIODICAL STRUCTURES. ELEMENTS OF THE QUALITATIVE THEORY OF WAVE MOTION OVER THE CHANNELS
B. N. Zakharev and A. I. Pashnev 1994 11 p
(DE95-623602; JINR-R-4-94-335) Avail: CASI HC A03/MF A01 (US Sales Only)

It is shown that the peculiarities of the wave motion over the discrete variable 'n' do not permit to construct the local potential v(n) transparent for all energies of the allowed zone. Every local potential well bends the allowed zone in the plane 'E, n' and necessitates the lowering of its upper boundary (the appearance of the effective barrier hanging from above) what gives strong reflection of waves. To remove the hindering prominence of the forbidden zone into the allowed one it is possible to use the minimal nonlocality: the potential u(n) on the neighbor diagonals of the matrix finite-difference Hamiltonian. Together the soliton-like potentials constitute the reflectionless system. Different transparent systems are demonstrated by means of instructive illustrations. In the periodical potentials the matching conditions of functions on the neighbor intervals (periods) play the part of minimal nonlocality. DOE

N95-32532# Los Alamos National Lab., NM.
TEM INVESTIGATION ON THE LOW TEMPERATURE PHASE OF HfV2
Fuming Chu and T. E. Mitchell 1995 3 p Presented at the 53rd Annual Meeting of Microscopy Society of America, Kansas City, KS, 13-17 Aug. 1995
(Contract W-7405-eng-36)
(DE95-009500; LA-UR-95-1027; CONF-950892-1) Avail: CASI HC A01/MF A01

HfV2, a particularly attractive C15 Laves phase structural material, undergoes a structural transformation at 115 K. A tentative reciprocal lattice for low-temperature HfV2 based on a combination of selected area diffraction patterns is illustrated. The results reveal structural characteristics inconsistent with earlier claims by other investigators. Further and detailed studies are under way, using a combination of CBED and synchrotron diffraction to determine the low-temperature structure's crystal symmetry, lattice parameters, and atomic positions. DOE

N95-32579# Sandia National Labs., Albuquerque, NM.
SMOOTHING DURING ION-ASSISTED GROWTH BY TRANSIENT ION BEAM-INDUCED DEFECTS
B. K. Kellerman, E. Chason, J. A. Floro, S. T. Picraux, and J. M. White (Texas Univ., Austin, TX.) 1995 7 p Presented at the Spring Meeting of the Materials Research Society (MRS), San Francisco, CA, 17-21 Apr. 1995
(Contract DE-AC04-94AL-85000)
(DE95-011021; SAND-95-0850C; CONF-950412-7) Avail: CASI HC A02/MF A01

Several studies have shown that the surface morphology can be smoother during simultaneous ion bombardment and growth than during growth alone. Ion-induced adatoms and surface vacancies are believed to be responsible for essentially reversing the surface roughening produced during growth. However, the atomistic mechanism for the smoothing effect has been difficult to determine. Measurements of ion-induced point defect production indicate that a large number of defects exist temporarily on the surface, but at typical growth temperatures the defects have sufficient mobility to recombine and annihilate. The authors propose that this ion-induced transient surface defect population can play a significant role in modifying the dynamic surface morphology. The authors have developed Monte Carlo simulations of growth and defect diffusion to model the interaction between growth atoms and ion-induced defects. The simulations support a dynamic surface smoothing mechanism that involves the destabilization of adatom islands by the transient ion-induced defects. DOE

N95-32586# Argonne National Lab., IL.
CONVERSION OF HOLES INTO REDUCING SPECIES ON SURFACE MODIFIED SMALL-PARTICLE TiO2
O. I. Micic, A. E. Ostafin, T. Rajh, J. J. Sabelko, M. C. Thurnauer, D. M. Tiede, and Y. Zhang 1995 12 p Presented at the 5th International Symposium on Chemical Oxidation, Nashville, TN, 15-17 Feb. 1995
(Contract W-31-109-eng-38)
(DE95-008282; ANL/CHM/CP-84094; CONF-950241-3) Avail: CASI HC A03/MF A01

Complexation of colloidal titanium dioxide nanoparticles (40 (angstrom)) by cysteine as a surface derivative was investigated by electron paramagnetic resonance (EPR) and infra-red (diffusion reflectance infra-red Fourier Transform DRIFT) spectroscopies. It was found that cysteine strongly binds to the colloid surface. The authors have demonstrated with EPR spectroscopy that cysteine modifies the TiO2 surface with formation of new trapping sites where photogenerated electrons and holes are localized. Illumination of cysteine modified TiO2 at 77K resulted in formation of a sulfur centered radical observed by EPR spectroscopy at 200 K. Upon addition of lead ions, a new complex of cysteine that bridges surface titanium atoms and lead ions was detected by IR spectroscopy. Illumination of lead/cysteine modified TiO2 did not result in the formation of sulfur

centered radical, but symmetrical, lattice defect type EPR signal for trapped holes was observed. However, addition of methanol to this system resulted in the formation of (center dot)CH2OH radical following illumination at 8.2 K. After the temperature was raised to 120 K, doubling of the signal associated with electrons trapped at particle surface (Ti(3)(sub surf)) was observed. On further increase of the temperature to 200 K the EPR signal for trapped electrons disappeared as a result of the reduction of Pb(2+) ions, and metallic lead was observe d to precipitate. Conversion of photogenerated holes into trapped electrons due to the presence of methanol doubles the yield of trapped electrons that can reduce Pb(2+). Direct reduction of Pb(2+) ions by (center dot)CH2OH radical on TiO2 was not detected. DOE

N95-32588# Sandia National Labs., Albuquerque, NM. Optical Systems and Image Processing Dept.

FREQUENCY RESPONSE OF A TeO2 SLOW SHEAR WAVE ACOUSTO-OPTIC CELL EXPOSED TO RADIATION

Ireena A. Erteza, David C. Craft, K. Terry Stalker, E. W. Taylor (Phillips Lab., Kirtland AFB, NM.), M. A. Kelley (Phillips Lab., Kirtland AFB, NM.), A. D. Sanchez (Phillips Lab., Kirtland AFB, NM.), S. P. Chapman (Phillips Lab., Kirtland AFB, NM.), D. M. Craig (Phillips Lab., Kirtland AFB, NM.), and E. Kinsley (Phillips Lab., Kirtland AFB, NM.) 1994 12 p Presented at the SPIE International Symposium on Aerospace/Defense Sensing and Dual-use Photonics, Orlando, FL, 17-21 Apr. 1995 Sponsored by DNA

(Contract DE-AC04-94AL-85000)

(DE95-009588; SAND-94-2519C; CONF-950472-5) Avail: CASI HC A03/MF A01

Radiation testing of photonic components is not new, however component level testing to date has not completely addressed quantities which are important to system behavior. One characteristic that is of particular importance for optical processing systems is the frequency response. In this paper, the authors present the results of the analysis of data from an experiment designed to provide a preliminary understanding of the effects of radiation on the frequency response of acousto-optic devices. The goal is to present possible physical mechanisms responsible for the radiation effects and to discuss the effects on signal processing functionality. The experiment discussed in this paper was designed by Sandia National Laboratories (SNL) and performed by SNL and Phillips Laboratory (PL) personnel at White Sands Missile Range (WSMR). In the experiment, a TeO2 slow shear-wave acousto-optic cell was exposed to radiation from the WSMR linear accelerator. The TeO2 cell was placed in an experimental configuration which allowed swept frequency diffracted power measurements to be taken during radiation exposure and recovery. A series of exposures was performed. Each exposure consisted of between 1 to 800, 1 microsec radiation pulses (yielding exposures of 2.25 kRad(Si) to 913 kRad(Si)), followed by recovery time. At low total and cumulative doses, the bandshape of the frequency response (i.e. diffracted power vs. frequency) remained almost identical during and after radiation. At the higher exposures, however, the amplitude and width of the frequency response changed as the radiation continued, but returned to the original shape slowly after the radiation stopped and recovery proceeded. It is interesting to note that the location of the Bragg degeneracy does not change significantly with radiation. In this paper, the authors discuss these effects, and they discuss the effect on the signal processing functionality. DOE

N95-32590# Sandia National Labs., Albuquerque, NM.

MECHANISM(S) FOR THE SUPPRESSION OF THE SWITCHABLE POLARIZATION IN PZT AND BaTiO3

William L. Warren, Duane Dimos, Bruce A. Tuttle, Gordon E. Pike, Mark V. Raymond, Robert D. Nasby, R. Ramesh (Bell Communications Research, Inc., Red Bank, NJ.), and Joseph T. Evans, Jr. (Radiant Technologies, Inc., Albuquerque, NM.) 1995 15 p Presented at the 1994 Fall Meeting of the Materials Research Society (MRS), Boston, MA, 28 Nov. - 2 Dec. 1994

(Contract DE-AC04-94AL-85000)

(DE95-009589; SAND-95-0567C; CONF-941144-121) Avail: CASI HC A03/MF A01

Switchable polarization can be significantly suppressed in ferroelectric (FE) materials by optical, thermal, and electrical processes. The thermal process can occur by either annealing the FE in a reducing environment or by heating it in air to 100 C while impressing a bias near the switching threshold. The optical process occurs while biasing the FE near the switching threshold and illuminating with bandgap light. And the electrical suppression effect occurs by subjecting the FE to repeated polarization reversals. Using electron paramagnetic resonance, polarization-voltage measurements, and charge injection scenarios, the authors have been able to elucidate both electronic and ionic trapping effects that lead to a suppression in the amount of switchable polarization in FE materials. The relative roles of electronic and ionic effects in the same material can depend on the stress condition. For instance, in oxidized BaTiO3 crystals, optical and thermal suppressions occur by electronic domain pinning; electrical fatigue in the BaTiO3 crystals also appears to involve electronic charge trapping, however, it is suggested that these electronic traps are further stabilized by nearby ionic defects. In sol-gel PZT thin films with either Pt, RuO2, or La-Sr-Co-O electrodes it appears that the polarization suppression induced by electrical fatigue, a temperature/bias combination, or a light/bias combination are all primarily due to the trapping of electronic charge carriers to first order. DOE

N95-32594# Sandia National Labs., Albuquerque, NM.

HIGH RESISTIVITY InAlN BY NITROGEN OR OXYGEN IMPLANTATION

J. C. Zolper, S. J. Pearton (Florida Univ., Gainesville, FL.), C. R. Abernathy (Florida Univ., Gainesville, FL.), and C. B. Vartuli (Florida Univ., Gainesville, FL.) 1995 6 p Presented at the Spring Meeting of the Materials Research Society (MRS), San Francisco, CA, 17-21 Apr. 1995 Sponsored in part by AFOSR

(Contract DE-AC04-94AL-85000; NSF DMR-95-36533)

(DE95-011023; SAND-94-2795C; CONF-950412-5) Avail: CASI HC A02/MF A01

The authors report on the isolation properties of In(0.75)Al(0.25)N implanted with either N or O for several doses and post-implant anneal temperatures. Sheet resistance versus anneal temperature data are reported for the various implants with a maximum sheet resistance of (approximately) 1 x 10(exp 9) (Omega)/(open square)achieved for a high dose N-implant annealed at 600 or 700 C and (approximately) 5 x 10(exp 8) (Omega)/(open square) achieved for a high dose O-implant annealed at 600 C. These sheet resistances correspond to a greater than three order of magnitude increase over the as-grown values. The compensating defect level for the highest resistance N-implanted sample has an estimate ionization level 580 meV below the conduction band edge. Implant isolation of InAlN is also compared to oxygen implant isolation of In(x)Ga(1-x)N, where only a 50 to 100 fold increase in sheet resistance is observed, to study the effect of Al in the isolation scheme. DOE

N95-32595# Sandia National Labs., Albuquerque, NM.

THE GROWTH AND OPTIMIZATION OF InPSb/InGaAs/InAsS(LC B STRAINED-LAYER SUPERLATTICE EMITTERS BY METAL ORGANIC CHEMICAL VAPOR DEPOSITION

R. M. Biefeld and S. R. Kurtz 1995 6 p Presented at the Spring Meeting of the Materials Research Society (MRS), San Francisco, CA, 17-21 Apr. 1995

(Contract DE-AC04-94AL-85000)

(DE95-011057; SAND-94-2758C; CONF-950412-1) Avail: CASI HC A02/MF A01

The authors have prepared InAsSb/InGaAs strained-layer superlattices (SLS's) and InPSb confinement layers using metal-organic chemical vapor deposition (MOCVD) for use as infrared emitters. X-ray diffraction was used to determine lattice matching as well as composition and structure of the SLS's. Photoluminescence linewidth and intensity were used as a measure of the quality of the structures. Typical FWHM were less than 10 meV. The presence of interface layers were indicated by broadened X-ray diffraction peaks for samples grown under non-optimized conditions. Two types of interfacial layers apparently due to a difference in composition at the interfaces were observed with transmission electron microscopy (TEM). The width of the X-ray peaks can be explained by a variation of the interfacial layer thicknesses. Optimized growth resulted in SLS's with narrow X-ray peaks and high radiative efficiency. Room temperature LED's operating between 4-5 micrometers have been prepared. DOE

N95-32598# Argonne National Lab., IL. Materials Science Div.

EPITAXIAL Pb(Zr(x)Ti(1-x))O3/SrR(LC UO3 ((LC)X = 0, 0.35, 0.65) MULTILAYER THIN FILMS ON S(LC)RT(LC)IO3(100) AND M(LC)GO(100) PREPARED BY MOCVD AND RF SPUTTERING

C. M. Foster, R. Csencsits, P. M. Baldo, G. R. Bai, Z. Li, L. E. Rehn, L. A. Wills, and R. Hiskes Feb. 1995 13 p Presented at the North American Conference on Smart Structures and Materials, San Diego, CA, 26 Feb. - 3 Mar. 1995
(Contract W-31-109-eng-38)
(DE95-008288; ANL/MSD/CP-83776; CONF-950228-6) Avail: CASI HC A03/MF A01

Epitaxial SrRuO3 thin films were deposited on SrTiO3(100) and MgO(100) substrates by RF sputtering for use as bottom electrodes and epitaxial buffer layers. On these conductive substrates, epitaxial Pb(Zr(x)Ti(1-x))O3 (PZT; x = 0.35,0.65) and PbTiO3 (PT; x = 0) thin films were deposited by metalorganic chemical vapor deposition (MOCVD). X-ray diffraction (XRD), RBS channeling (RBS), transmission electron microscopy (TEM) and optical waveguiding were used to characterize the phase, microstructure, defect structure, refractive index, and film thickness of the deposited films. The PZT and PT films were epitaxial and c-axis oriented. 90(degree) domains, interfacial misfit dislocations and threading dislocations were the primary structural defects, and the films showed as high as a 70% RBS channeling reduction. Ferroelectric hysteresis and dielectric measurements of epitaxial PZT ferroelectric capacitor structures formed using evaporated Ag top electrode showed: a remanent polarization of 46.2 micro C/cm(exp 2), a coercivefield of 54.9 kV/cm, a dielectric constant of 410, a bipolar resistivity approximately 5.8 x 10(exp 9) Omega-cm at a field of 275 kV/cm, and a breakdown strength greater than 400 kV/cm. Cyclic fatigue measurements showed that the remanent polarization was maintained greater than 10(exp 9) cycles. DOE

N95-32600# California Univ., Berkeley. Lawrence Berkeley Lab, CA. Materials Science Div.
OBSERVATION OF INTRABAND COHERENCE IN THE NONLINEAR OPTICAL RESPONSE OF GALLIUM ARSENIDE
S. Bar-Ad, S. Glutsch, M. A. Mycek, D. S. Chemla, and U. Siegner (Marburg Univ., Germany.) Nov. 1994 6 p Presented at the 15th Conference on Lasers and Electro-optics and 5th Quantum Electronics and Laser Science Conference, Baltimore, MD, 21-26 May 1995
(Contract DE-AC03-76SF-00098)
(DE95-011281; LBL-36586; CONF-950540-9) Avail: CASI HC A02/MF A01

We show that magnetic-field-induced modulation of the intraband density matrix elements produces new resonances in the power spectra of ultrashort-pulse four-wave mixing in semiconductors. DOE

N95-32631# Joint Inst. for Nuclear Research, Dubna (USSR).
THE INTERRELATION OF A Z(3) GAUGE THEORY ON FLAT LATTICES AND A SPIN-1 BEG MODEL
N. S. Ananikyan and R. R. Shcherbakov (Academy of Sciences of the Armenian SSR, Erivan, Armenia.) 1994 6 p Submitted for publication in Physics Letters A
(DE95-623634; JINR-E-2-94-306) Avail: CASI HC A02/MF A01 (US Sales Only)

A Z(3) gauge model with double plaquette representation of the action on the flat triangular and square lattices is constructed. It is reduced to the spin-1 Blume-Emery-Griffiths (BEG) model. An Ising-type critical line of a second-order phase transition is found. DOE

N95-32640# Ames Lab., IA.
SYNTHESIS OF POTENTIAL NEW Zintl PHASES M.S. Thesis - Iowa State Univ.
Jason Harp 10 Feb. 1995 40 p
(Contract W-7405-eng-82)
(DE95-010123; IS-T-1727) Avail: CASI HC A03/MF A01

This work has shown that addition of a transition metal interstitial atom, Z, into Ae5Tt3Z (Ae = Sr, Ba; Tt = Sn, Pb) does not stabilize a Mn5Si3-type structure as in the Ca--Pb system. The products that resulted from these reaction were invariably the same as those seen in the binary systems. Apparently, the Cr5B3, Pu31Pt20, and W5Si3 structure types found in these systems do not have holes in their structures which might allow an interstitial atom to be incorporated into the structure. It is evident that the inverse Cr5B3 structure of La3Sn3InGe, La3Sn2In2Ge, and La3SnIn3Ge characterized in this work is seen when the composition yields compounds that will be either electron deficient as are La3In4Ge, La3SnIn3Ge, and La3Sn3In2Ge or electron precise as is La3Sn3InGe. The structure is destabilized if more electrons are added to the system. This helps to explain why La3Sn4Ge does not exhibit this structure type. In other words this structure is more stable when electron deficient. Perhaps as more electrons are added to the system and more negative charge accumulates on the In/Sn site, anti-bonding levels become populated or electrostatic repulsions contribute to the destabilization of the anionic network. DOE

N95-32643# Ames Lab., IA.
PHOTOEMISSION STUDY OF SOME NOVEL MATERIALS: RARE EARTH/TRANSITION METAL INTERFACE, Ba*(0.6)*K*(0.4)*BiO3* AND AlPdMn Ph.D. Thesis - Iowa State Univ.
Xilin Wu 10 Feb. 1995 97 p
(Contract W-7405-eng-82)
(DE95-010125; IS-T-1695) Avail: CASI HC A05/MF A02

Synchrotron radiation photoemission spectroscopy and low energy electron diffraction (LEED) are applied to explore several novel materials: (1) Ce epitaxial growth on W (110) surfaces; (2) Eu epitaxial growth on Ta (110) surfaces; (3) Sm epitaxial growth on Ta (110) surfaces; (4) quasicrystalline AlPdMn; and (5) superconducting Ba(1-x)K(x)BiO3. In the case of rare earth overlayers on transition metal surface, resonance photoemission spectroscopy is used to enhance the 4f features. The metal surface phase transition is investigated on an atomic-scale. In the case of quasicrystalline AlPdMn and superconducting Ba(1-x)K(x)BiO3 the electronic structures are investigated by angle-resolved photoemission. DOE

N95-32677# Wien Univ. (Austria).
THE 8TH WINTERSCHOOL ON NEW DEVELOPMENTS IN SOLID STATE PHYSICS
Nov. 1994 184 p Repr. from Semiconductor Science and Technology (Bristol, England), v. 9, no. 11S, Nov. 1994 Conference held in Mauterndorf, Austria, 14-18 Feb. 1994
(Grant NSF DMR-91-2497) (ISSN 0268-1242)
(AD-A290163) Avail: CASI HC A09/MF A02

The Eighth International Winterschool on New Developments in Solid State Physics, entitled 'Interaction and Scattering Phenomena in Nanostructures', was held in Mauterndorf Castle, Salzburg, Austria on 14-18 February 1994. A total of 69 papers (including posters) were presented at the meeting. The 28 invited papers are printed in this volume. As usual, it was intended to have the most recent highlights in low dimensional physics presented at this meeting. The main topics were: Composite fermions and fractional quantum Hall effect; Mesoscopic transport and chaos; Low dimensional tunnelling; Wires: Spectroscopy and lasing action; Bloch oscillations and ultrafast phenomena; Coupled quantum wells and superlattices; Si/SiGe heterostructures; and Microcavities. DTIC

N95-32695# Ibis Associates, Inc., Wellesley, MA.
CVD DIAMOND COST ANALYSIS UPDATE Quarterly Report, No. 4
1994 4 p
(Contract N00014-93-C-2044)
(AD-A289990) Avail: CASI HC A01/MF A01

Progress for IBIS Associates in the fourth quarter of 1994 includes discussion with 3M and Research Triangle Institute regarding their radio frequency (RF) CVD diamond deposition technology. Although modeling this technology has not been accomplished, the non-disclosure agreements have been taken care of. IBIS awaits feedback on the schedules of 3M and RTI contacts for modeling to proceed. Also accomplished in the fourth quarter of 1994 was initial discussion with Torch Temed (Arava, Israel) concerning the economics of their DC arcjet CVD diamond deposition technology. IBIS intends to follow up with 3M and RF and analyze the economics of their CVD diamond process. DTIC

N95-32698# China Nuclear Information Centre, Beijing (China).
THE EFFECTS OF H(+) IMPLANTS ON YBa2Cu3O7 SUPERCONDUCTING MATERIALS
Chenglin Luo (Nanjing Normal Univ., Nanjing, China.), Guoqiang Pan (Nanjing Univ., China.), Ming Han (Nanjing Univ., China.), and Guanghou Wang (Nanjing Univ., China.) Sep. 1993 13 p
(DE95-614466; CNIC-00779; NNU-0001) Avail: CASI HC A03/MF A01

The variations of microstructure and electrical properties of Y-Ba-Cu-O with and without H(+) implantation have been studied by scanning electron microscope, x-ray diffraction and IR spectrum techniques. The results have shown that these variations are directly relative to the intrinsic quality of

YBa2Cu3O7. Microstructural change is responsible for the variations of electrical properties of YBa2Cu3O7 superconductor. The Cu-H bond formed by H(+) implanted into YBa2Cu3O7 is not a key factor for these variations. DOE

N95-32810# Argonne National Lab., IL.
YBa2Cu3O(7-X) 45 DEG (001) TILT GRAIN BOUNDARIES INDUCED BY CONTROLLED LOW-ENERGY SPUTTERING OF MgO SUBSTRATES: TRANSPORT PROPERTIES AND ATOMIC-SCALE STRUCTURE
Boris V. Vuchic, Karl L. Merkle, Jeffrey W. Funkhouser, D. Bruce Bucholz (Northwestern Univ., Evanston, IL.), Kenneth A. Dean (Northwestern Univ., Evanston, IL.), Robert P. H. Chang (Northwestern Univ., Evanston, IL.), and Laurence D. Marks (Northwestern Univ., Evanston, IL.) Oct. 1994 5 p Presented at the Applied Superconductivity Conference, Boston, MA, 16-21 Oct. 1994
(Contract W-31-109-eng-38; NSF DMR-91-20000)
(DE95-005826; ANL/MSD/CP-82574; CONF-941013-36) Avail: CASI HC A01/MF A01

Grain boundaries can act as weak links in the high (Tc) materials. If properly controlled, these grain boundaries can be used in various device applications. We have been able to reproducibly form 45 deg (001) tilt grain boundary junctions in YBa2Cu3O(7-x) thin films. The films were grown on MgO substrates using a pre-growth substrate treatment. A low energy broad beam Argon ion source was used to irradiate a select region of (100) MgO substrates. The film on the milled portion of the substrate grows predominantly with a grain orientation rotated 45 deg about the c-axis with respect to the grain on the unmilled portion. Backscattered electron Kikuchi patterns have been used to confirm that the rotation occurs across the entire milled portion of the substrate. Transport properties of these films are discussed and related to high resolution electron microstructural and microchemical analyses of the grain boundaries. This technique has potential use in device applications as a method for controlled grain boundary engineering. DOE

N95-32959 Ames Lab., IA.
PEAK EFFECT AND FLUX PINNING IN YBa2Cu3O(7-(DELTA)) SINGLE CRYSTALS M.S. Thesis
Paul Panetta 10 Feb. 1995 88 p Limited Reproducibility: More than 20% of this document may be affected by microfiche quality
(Contract W-7405-eng-82)
(DE95-010126; IS-T-1702) Avail: CASI HC A05

Oxygen annealing studies have been carried out for YBa2Cu3O7-delta single crystals in order to determine the factors controlling the magnetic field dependence of the flux pinning and critical current densities as a function of oxygen content (7-delta). A 300 C anneal removes much of the damage introduced either during crystal growth or by proton irradiation, but it does not permit substantial oxygen uptake to improve the bulk superfluid density. Anneals at 400 C result in substantial oxygen uptake accompanied by an overall enhancement in critical current densities with changes in both the overall superfluid density as well as the pinning effects of oxygen defect clusters. Anneals at 500 and 550 C result in a depletion of oxygen content and a resulting overall diminution of critical current densities. The 'fishtail' shape can be systematically controlled by first adding and then removing oxygen. A model based on the formation and destruction of oxygen point defects and clusters of oxygen defects describes the data rather well. DOE

N95-33213# Sandia National Labs., Albuquerque, NM.
GROWTH AND CHARACTERIZATION OF HETEROSTRUCTURES AND INFRARED EMITTERS WITH COMPRESSED InAsSb LAYERS
S. R. Kurtz, R. M. Biefeld, L. R. Dawson, D. M. Follstaedt, K. C. Baucom, and A. J. Howard Apr. 1995 17 p
(Contract DE-AC04-94AL-85000)
(DE95-009828; SAND-95-0560) Avail: CASI HC A03/MF A01

An overview is presented of work on strained InAsSb heterostructures and infrared emitters. InAsSb/InGaAs strained-layer superlattices (SLS) and InAsSb quantum wells were grown by metal-organic chemical vapor deposition and characterized using magneto-photoluminescence. LEDs and lasers with InAsSb heterostructure active regions are described. DOE

N95-33235# Technische Univ., Delft (Netherlands).
SUPERCRITICAL CRYSTALLIZATION: THE RESs-PROCESS AND THE GAS-PROCESS Ph.D. Thesis
Edwin M. Berends 27 Sep. 1994 287 p
(PB95-214482; ISBN-90-9007-495-3) Avail: CASI HC A13/MF A03

This Doctoral Ph.D. thesis describes the development of two novel crystallization processes utilizing supercritical fluids either as a solvent, the RESS-process, or as an anti-solvent, the GAS-process. In th RESS-process precipitation of the solute is performed by expansion of the solution over a nozzle to produce ultra-fine, monodisperse particles without any solvent inclusions. In the GAS-process a high pressure gas is dissolved into the liquid phase solvent, where it causes a volumetric expansion of this liquid solvent and lowers the equilibrium solubility. Particle size, particle size distribution and other particle characteristics such as their shape, internal structure and the residual amount of solvent in the particles are expected to be influenced by the liquid phase expansion profile. NTIS

N95-33240# Oak Ridge National Lab., TN.
COMBINING THE QMR METHOD WITH FIRST PRINCIPLES ELECTRONIC STRUCTURE CODES
Noel M. Nachtigal, William A. Shelton, and George M. Stocks Apr. 1995 16 p
(Contract DE-AC05-84OR-21400)
(DE95-009927; ORNL/TM-12873) Avail: CASI HC A03/MF A01

First principles methods are used to aid the metallurgist in the investigation and design of new materials. However, these methods suffer from an O(N3) scaling which restricts the problem sizes that can be addressed. By incorporating the QMR (quasi-minimal residual) method into a first principles algorithm the authors are able to attain O(N) scaling for the problem sizes of interest. This advancement will provide researchers with the necessary tools to treat large systems. DOE

N95-33373# Kansas State Univ., Manhattan, KS.
IMPACT-PARAMETER DEPENDENT L-K VACANCY-TRANSFER IN COLLISIONS OF Ni(23+) WITH Ge SOLID TARGETS
M. Jaeger, M. Schulz (Missouri Univ., Rolla, MO.), T. Kandler, A. Warczak, H. Braeuning (Johann-Wolfgang-Goethe-Univ., Frankfurt am Main, Germany.), A. Demian (Johann-Wolfgang-Goethe-Univ., Frankfurt am Main, Germany.), M. Damrau (Johann-Wolfgang-Goethe-Univ., Frankfurt am Main, Germany.), A. El-Sadek (Johann-Wolfgang-Goethe-Univ., Frankfurt am Main, Germany.), K. Freitag (Bonn Univ., Germany.), and J. Ulrich (Johann-Wolfgang-Goethe-Univ., Frankfurt am Main, Germany.) et al 1995 2 p Presented at the 19th International Conference on the Physics of Electronic and the Atomic Collisions, Whistler, Canada, 26 Jul. - 1 Aug. 1995
(Contract DE-FG02-86ER-13491)
(DE95-010821; DOE/ER-13491/766; CONF-950706-12) Avail: CASI HC A01/MF A01

It is commonly accepted that the mechanism of 2p pi-2p alpha rotational coupling is responsible for K-vacancy production in slow, nearly symmetric ion-atomn collisions, where the MO (molecular orbital) model can be applied. Initial vacancies present in the the 2p pi orbital can be transferred by a coriolis coupling into the 2p alpha MO. This is followed by a 2p alpha-1s alpha vacancy sharing process (radial coupling) that distributes the vacancies between the K-shells on both collision partners on the outgoing part of the collision. Based on theoretical calculations of Taulbjerg et al, a distinct dependence of the K-shell excitation probability (P(K)) on the impact parameter b is predicted. Using Ni(23+) projectiles from the UNILAC accelerator at GSI and solid Ge targets, P(K)(b) were determined by a coincidence measurement between characteristic x-rays and deflected projectiles. DOE

N95-33382# Argonne National Lab., IL.
THEORETICAL DYNAMICAL STUDIES OF METAL CLUSTERS AND CLUSTER-LIGAND SYSTEMS
J. Jellinek 1995 36 p Presented at the NATO Advanced Study Institute on Metal-ligand Interactions: Structure and Reactivity, Cetraro, Italy, 4-16 Sep. 1994
(Contract W-31-109-eng-38)
(DE95-012461; ANL/CHM/CP-83703; CONF-9409347-1) Avail: CASI HC A03/MF A01

In what follows we use the term cluster to designate a cohesive

group of like atoms (molecules), i.e., bare ('neei', 'naked')clusters.More generally, the term is also used for organo- and inorganometallic compounds, i.e., ligated clusters. Although the approaches and techniques used by the various disciplines to study metal-ligand interactions are quite different, many of the central subjects and issues are common for them. The common subjects include possible geometric structures and isomeric forms, structural (isomerization) transitions, stability, fluxionality, structure-reactivity correlation (or lack of it), role of coordination, etc. However, the precise interpretation of these issues and the details emphasized by the different disciplines are dictated by the nature of the objects studied and may not, therefore, be identical. For example, questions regarding structures, isomerization transitions, fluxionality or even melting of metal clusters refer to the state and properties of the metal network itself. The same questions, when asked in connection with organo- and inorganometallic compounds, often refer to the arrangements and rearrangements of the ligands attached to a metal framework of a fixed structure. Of course, when required, the state of and changes in the metal framework are considered as well. The fields of metal-containing molecular compounds, surface science, and physics and chemistry of clusters furnish complementary information on a broad variety of metal-ligand systems. A comprehensive understanding of the nature and properties of these systems, as defined by the type and number of metal atoms and ligands involved, can be achieved only through a mutual awareness of and continuing progress in all of these research areas. DOE

N95-33386# Los Alamos National Lab., NM.
MAGNETOSTRICTION AND THERMAL EXPANSION OF THE KONDO SEMICONDUCTOR Ce3Bi4Pt3
M. F. Hundley, J. J. Neumeier, J. D. Thompson, A. Lacerda, and P. C. Canfield (Ames Lab., IA.) 1995 7 p Presented at the 2nd Physical Phenomena At High Magnetic Fields Conference, Tallahassee, FL, 6-9 May 1995
(Contract W-7405-eng-36)
(DE95-011975; LA-UR-95-1555; CONF-9505186-1) Avail: CASI HC A02/MF A01

We report dilatometric thermal expansion (alpha) and magnetostriction (lambda) measurements on the Kondo semiconductor Ce3Bi4Pt3 and its non-magnetic analog L&3Bi4Pt3 in fields to 100 kOe. The magnetic contribution to the thermal expansion of Ce3Bi4Pt3 displays a broad maximum centered at 50 K, close to the temperature where the 4f specific heat is a maximum. The linear magnetostriction is anomalously large in Ce3Bi4Pt3, with values that are characteristic of mixed-valent compounds (lambda(perpendicular) = 3.26 x 10(exp -5), (lambda(parallel) = -6.24 x 10(exp -5) in 100 kOe at 4 K). The volume magnetostriction is positive and a factor of ten smaller than the linear coefficients (lambda(sub V) = 2.75 x 10(exp -6) in 100 kOe at 4 K). The volume magnetostriction is temperature-dependent, and peaks at 50 K. The data are considered in terms of a Grueneisen analysis that links the temperature-dependent magnetic susceptibility, thermal expansion, magnetostriction, bulk modulus, and specific heat of Ce3Bi4Pt3 via temperature-dependent electronic and magnetic scaling parameters. DOE

N95-33401# Los Alamos National Lab., NM.
CRYSTALLINE-AS-DEPOSITED CaGa2S4: Ce VIA LOW-TEMPERATURE METAL-ORGANIC CHEMICAL VAPOR DEPOSITION
David C. Smith, John A. Samuels, Brent F. Espinoza, Elizabeth Apen, Nathaniel M. Peachey, Robert C. Dye, Richard T. Tuenge (Planar Systems, Inc., Beaverton, OR.), Christian F. Schaus (Planar Systems, Inc., Beaverton, OR.), and Christopher N. King (Planar Systems, Inc., Beaverton, OR.) 1995 5 p Presented at the SID 1995: Society for InformationDisplay, Orlando, FL, 21-26 May 1995 Sponsored in part by the Advanced Research Projects Agency
(Contract W-7405-eng-36)
(DE95-010883; LA-UR-95-1181; CONF-9505157-2) Avail: CASI HC A01/MF A01

A metal-organic chemical vapor deposition (MOCVD) process for the growth of crystalline-as-deposited cerium doped calcium thiogallate (CaGa2S4:Ce) at substrate temperatures less than 600 C has been developed. Blue-green electroluminescence was observed with a luminance of approx. 2 cd/sq m at 40 volts above threshold using 60 Hz drive frequency. Threshold voltages were approximately 200 V. DOE

N95-33628# California Univ., Berkeley. Lawrence Berkeley Lab, CA.
SIZE, SHAPE, AND CRYSTALLINITY OF LUMINESCENT STRUCTURES IN OXIDIZED Si NANOCLUSTERS AND H-PASSIVATED POROUS Si
S. Schuppler, M. A. Marcus, Y. H. Xie, T. D. Harris, W. L. Brown, Y. J. Chabal, P. J. Szajowski, S. L. Friedman, s0401118, D. L. Adler (Illinois Univ., Urbana-Champaign, IL.), and F. M. Ross et al Nov. 1994 9 p Presented at the 1994 Fall Meeting of the Materials Research Society (MRS), Boston, MA, 28 Nov. - 2 Dec. 1994
(Contract DE-AC03-76SF-00098)
(DE95-012322; LBL-36909; CONF-941144-157) Avail: CASI HC A02/MF A01

Near-edge and extended x-ray absorption fine structure measurements from a wide variety of H-passivated porous Si samples and oxidized Si nanocrystals, combined with electron microscopy, ir-absorption, alpha-recoil, and luminescence emission data, provide a consistent structural picture of the species responsible for the luminescence observed in these systems. For luminescent porous Si samples peaking in the visible region, i. e., less than or equal 700nm, their mass-weighted-average structures are determined here to be particles - not wires, whose short-range character is crystalline - not amorphous, and whose dimensions - typically less than 15 angstrom - are significantly smaller than previously reported or proposed. These results depend only on sample luminescence behavior, not on sample preparation details, and thus have general implications in describing the mechanism responsible for visible luminescence in porous silicon. New results are also presented which demonstrate that the observed luminescence is unrelated to either the photo-oxidized Si species in porous Si or the interfacial suboxide species in the Si nanocrystals. DOE

N95-33636# Argonne National Lab., IL.
EPITAXIAL Pb(Zr(0.40)Ti(0.60))O3/SrRuO3 AND PbTiO3/SrRuO3 MULTILAYER THIN FILMS PREPARED BY MOCVD AND RF SPUTTERING
C. M. Foster, R. Csencsits, P. M. Baldo, G. R. Bai, Z. Li, L. E. Rehn, L. A. Wills (Hewlett-Packard Co., Palo Alto, CA.), R. Hiskes (Hewlett-Packard Co., Palo Alto, CA.), D. Dimos (Sandia National Labs., Albuquerque, NM.), and M. B. Sinclair (Sandia National Labs., Albuquerque, NM.) Dec. 1994 7 p Presented at the 1994 Fall Meeting of the Materials Research Society (MRS), Boston, MA, 28 Nov. - 2 Dec. 1994
(Contracts W-31-109-eng-38; DE-AC04-94AL-85000)
(DE95-007146; ANL/MSD/CP-83373; SAND-95-1145C; CONF-941144-148) Avail: CASI HC A02/MF A01

Epitaxial SrRuO3 thin films were deposited by RF sputtering on SrTiO3 or MgO substrates for use as underlying electrodes. On these conductive substrates, epitaxial Pb(Zr(0.35)Ti(0.65))O3 (PZT) and PbTiO3 (PT) thin films were, deposited by metalorganic chemical vapor deposition (MOCVD). X-ray diffraction (XRD), RBS channeling (RBS), transmission electron microscopy (TEM) and optical waveguiding were used to characterize phase, microstructure, defect structure, refractive index, and film thickness of the deposited films. The PZT and PT films were epitaxial and c-axis oriented. 90 deg domains, interfacial misfit dislocations and dislocations and threading dislocations were the primary structural defects, and the films showed a 70% RBS channeling reduction. Hysteresis and dielectric measurements of epitaxial PZT ferroelectric capacitor structures formed using evaporated Ag or ITO glass top electrode showed: a remanent polarization of 46.2 mC/sq cm, a coercive field of 54.9 KV/cm, a dielectric constant of 410, a bipolar resistivity of approximately 5.8 x 10(exp 9) (Omega)-cm at a field of 275 KV/cm, and a breakdown strength of greater than 400 KV/cm. DOE

N95-33637# Ames Lab., IA.
OPTICAL ANISOTROPY OF (110) SURFACES OF Ag AND Cu Ph.D. Thesis
Zai Chen 20 Oct. 1994 106 p Prepared in cooperation with Iowa State Univ. of Science and Technology, Ames, IA
(Contract W-7405-eng-82)
(DE95-010130; IS-T-1714) Avail: CASI HC A06/MF A02

A reflectance-difference spectroscopy (RD) system was designed and built to study the anisotropic optical response of the (110) surfaces of silver and copper. Results of the RD spectra are described. DOE

N95-33641# Arizona Univ., Tucson, AZ. Dept. of Physics.
UNUSUAL BEHAVIOR IN THE MAGNETIC ANISOTROPY OF ULTRA-THIN Co SANDWICHES: THE ROLE OF Au UNDERLAYERS

Christian Marliere, Brad N. Engel, and Charles M. Falco 1994 7 p Presented at the 14th International Colloquium on Magnetic Films and Surfaces, Duesseldorf, Germany, 29 Aug. - 2 Sep. 1994
(Contract DE-FG03-93ER-45488)
(DE95-010612; DOE/ER-45488/5; CONF-940829-4) Avail: CASI HC A02/MF A01

We have used it situ polar Kerr effect measurements to study tile magnetic anisotropy of X/Co/Y sandwich structures grown by MBE on Cu(111) buffers, where X and Y are variable thicknesses of Au. For fixed values of Y and in the case of an underlayer wedge, e.g. variable X value, we have found a sharp minimum in both coercive field and perpendicular anisotropy at approximately 1 atomic layer of the Au underlayer. This anisotropy behavior is opposite to that of an Au overlayer deposited on a Co film, i.e. variable Y and fixed X. DOE

N95-33650# Lawrence Livermore National Lab., Livermore, CA. Lab. for Experimental Astrophysics.
LOW-ENERGY RESPONSE OF SUPERCONDUCTING TUNNEL JUNCTION X-RAY SPECTROMETERS
S. E. Labov, L. H. Hiller, C. A. Mears, M. Frank, H. Netel, F. Azgui, and A. T. Barfknecht (Conductus, Inc., Sunnyvale, CA.) 9 Dec. 1994 6 p Presented at the Applied Superconductivity Conference, Boston, MA, 16-21 Oct. 1994 Submitted for publication in IEEE Trans. Appl. Superconductivity
(Contract W-7405-eng-48)
(DE95-011733; UCRL-JC-119291; CONF-941013-37) Avail: CASI HC A02/MF A01

Thin film structures incorporating metallic superconducting layers and tunnel junctions can be configured as low-energy X-ray spectrometers. We present results obtained when low-energy X-rays are absorbed in niobium films coupled to aluminum layers that serve as quasiparticle traps in an Nb/Al/Al2O3/Al/Nb tunnel junction X-ray detector. The linearity of the pulse height as a function of energy is discussed along with the energy dependence of the observed resolution and its relation to the broadening mechanisms. A resolution of 14 eV at 1 keV has been measured with our detector cooled to 0.3 K. DOE

N95-33865# California Univ., Berkeley. Lawrence Berkeley Lab, CA. Materials Sciences Div.
CHARGE-TRANSFER GAP CLOSURE IN TRANSITION-METAL HALIDES UNDER PRESSURE
Anthony L. Chen and Peter Y. Yu Jan. 1995 30 p Submitted for publication in Quantum Theory of Real Materials
(Contract DE-AC03-76SF-00098)
(DE95-011268; LBL-36696; UC-404) Avail: CASI HC A03/MF A01

Insulator-to-metal transition induced by pressure has been studied in three transition metal iodides: NiI2, CoI2 and FeI2 using optical absorption and resistivity measurements at room temperature. Comparisons between the results obtained by these two techniques suggested that the closure of the charge-transfer gap is the principal mechanism responsible for the insulator-to-metal transition in these materials. DOE

N95-33880# California Univ., Berkeley. Lawrence Berkeley Lab, CA. Materials Sciences Div.
QUANTUM MECHANICAL CAPACITANCE IN A SCANNING TUNNELING MICROSCOPE
D. Botkin (California Univ., Berkeley, CA.), S. Weiss, D. F. Ogletree, M. Salmeron, and D. S. Chemla (California Univ., Berkeley, CA.) Feb. 1995 7 p Presented at the Ultrafast Electronics and Optoelectronics Symposium, Dana Point, CA, Mar. 1995
(Contract DE-AC03-76SF-00098)
(DE95-011272; LBL-36845; CONF-9503146-1; UC-400) Avail: CASI HC A02/MF A01

The nature of the ultrafast response of the tunnel junction in a scanning tunneling microscope is discussed. DOE

N95-34213# Oak Ridge National Lab., TN.
EFFECT OF THE COLONY MICROSTRUCTURE ON TRANSPORT CRITICAL CURRENT OF HIGH-J(c) Tl-1223 THICK FILMS
A. Goyal, E. D. Specht, D. M. Kroeger, D. K. Christen, J. E. Tkaczyk (General Electric Co., Schenectady, NY.), J. A. DeLuca (General Electric Co., Schenectady, NY.), and J. A. Sutliff (General Electric Co., Schenectady, NY.) 1995 3 p Presented at the International Workshop on Superconductivity: Controlled Processing of High Temperature Superconductors - Fundamentals and Applications, Maui, HI, 18-21 Jun. 1995
(Contract DE-AC05-84OR-21400)
(DE95-013049; CONF-950637-2) Avail: CASI HC A01/MF A01

High J(c), polycrystalline, TlBa2Ca2Cu3O(6 + x) thick films on poly-YSZ substrates were examined by x-ray microdiffraction, electron microscopy, and electron backscatter diffraction. The superconducting phase was formed by vapor phase thallination. X-ray phi scans were used to study the local and macroscopic in-plane texture. Electron Backscatter Kikuchi Diffraction was used to discern the grains structure within the colonies. Figure shows results of a limiting path calculation of J(c) vs colony mosaic. DOE

N95-34215# Argonne National Lab., IL. Materials Science and Chemistry Div.
IN SITU SURFACE ROUGHNESS MEASUREMENT DURING PECVD DIAMOND FILM GROWTH
C. D. Zuiker, D. M. Gruen, and A. R. Krauss 1995 7 p Presented at the 4th International Symposium on Diamond Materials, Reno, NV, 21-26 May 1995
(Contract W-31-109-eng-38)
(DE95-013411; ANL/CHM/CP-85037; CONF-9505192-2) Avail: CASI HC A02/MF A01

To investigate the development of surface morphology and bulk optical attenuation in diamond films, we have followed diamond film growth on silicon by in-situ laser reflection interferometry in a microwave plasma chemical vapor deposition system. A model for the interpretation of the reflectivity data in terms of film thickness, rms surface roughness and bulk losses due to scattering and absorption is presented. Results are compared with ex situ measurements of these quantities and found to be in good agreement. DOE

N95-34438# Lawrence Livermore National Lab., Livermore, CA. High Temperature Div.
MEASUREMENTS OF CROSS SECTIONS AND RESONANCE STRUCTURES FOLLOWING ELECTRON-IMPACT EXCITATION/IONIZATION OF Ne-LIKE Kr AND Xe
D. Schneider, D. DeWitt, D. A. Knapp, K. J. Reed, and M. H. Chen 28 Sep. 1994 15 p Presented at the 13th International Conference on the Application of Accelerators in Research and Industry, Denton, TX, 7-10 Nov. 1994 Submitted for publication
(Contract W-7405-eng-48)
(DE95-011731; UCRL-JC-112929; CONF-941129-25) Avail: CASI HC A03/MF A01

We report high-resolution measurements of electron impact excitation and ionization cross sections for the Na-like ions Kr(25+) and Xe(43+). Ions with ionization states centered on the Na-like configurations were produced in an electron beam ion trap (EBIT) using electrons with energies below the L shell ionization thresholds. The Na-like ions were exposed to an electron beam with an energy between 3 and 7 keV. The Na- and Ne-like ions were then extracted and their intensities measured as a function of the electron beam energy. Theoretical ionization cross sections were calculated using relativistic distorted wave methods. Complex resonance structures that appear in the computed cross sections are observed in the experimental results. These results are the first experimental observation of resonant-excitation-double-autoionization (REDA) in highly charged high-Z ions. DOE

N95-34443# Oak Ridge National Lab., TN.
LASER INDUCED DIFFUSION OF ION-IMPLANTED BISMUTH IN FUSED SILICA
Seung Y. Park (Vanderbilt Univ., Nashville, TN.), Robert A. Weeks (Vanderbilt Univ., Nashville, TN.), and Raymond A. Zuhr 1994 13 p Presented at the 5th International Otto Schott Colloquium, Jena, Germany, 11-14 Jul. 1994
(Contract DE-AC05-84OR-21400)
(DE95-012869; CONF-9407184-1) Avail: CASI HC A03/MF A01

The near surface regions of optical grade fused silica discs (Spectrosil A) were modified by implantation with bismuth ions at 160 and 320 keV and at room temperature. The glasses implanted with a nominal dose of 6 x 10(exp 16) Bi(2+) ions/sq cm were subsequently annealed with a 5 eV

KrF pulsed excimer laser and by a furnace in oxygen atmosphere. Rutherford backscattering and optical absorption were measured before and after the anneals. Backscattering profiles after laser anneal showed shifts of the profiles toward the surface with decrease in retained dose. We attribute the diffusion of bismuth to Soret effect. Profiles of furnace annealed samples showed that the diffusion was both toward and away from the surface.
DOE

N95-34450# Los Alamos National Lab., NM.
DEVELOPMENT OF LOCAL SHEAR BANDS AND ORIENTATION GRADIENTS IN fcc POLYCRYSTALS
A. J. Beaudoin, Jr. (Reynolds Metals Co., Richmond, VA.), H. Mecking (Technische Univ., Hamburg, Germany.), and U. F. Kocks 1995 7 p Presented at the 5th International Conference on Numerical Methods in Industrial Forming Processes (NUMIFORM), Ithaca, NY, 18-21 Jun. 1995
(Contract W-7405-eng-36)
(DE95-012072; LA-UR-95-1319; CONF-9506144-6) Avail: CASI HC A02/MF A01

A finite element formulation which derives constitutive response from crystal plasticity theory is used to examine localized deformation in fcc polycrystals. The polycrystals are simple, idealized arrangements of grains. Localized deformations within individual grains lead to the development of domains that are separated by boundaries of high misorientation. Shear banding is seen to occur on a microscopic scale of grain dimensions. The important consequences of these simulations are that the predicted local inhomogeneities are meeting various requirements which make them possible nucleation sites for recrystallization.
DOE

N95-34465# Oak Ridge National Lab., TN. Solid State Div.
FORMATION OF ARTIFICIALLY-LAYERED HIGH-TEMPERATURE SUPERCONDUCTORS USING PULSED-LASER DEPOSITION
D. P. Norton, B. C. Chakoumakos, and J. D. Budai Mar. 1995 4 p Presented at the 3rd International Conference on Laser Ablation (COLA 1995), Strasbourg, France, 22-26 May 1995
(Contract DE-AC05-84OR-21400)
(DE95-012884; CONF-9505219-1) Avail: CASI HC A01/MF A01

Pulsed-laser deposition has been used to synthesize artificially-layered high-temperature superconductors. Novel thin-film SrCuO2/BaCuO2 superlattices have been synthesized which superconduct at temperatures as high as 70 K. These results demonstrate that pulsed-laser deposition and epitaxial stabilization can be effectively used to engineer artificially-layered thin-film materials.
DOE

N95-34478# Pennsylvania State Univ., University Park, PA.
DEVELOPMENT OF THIN FILM DIAMOND BASED INTEGRATED CIRCUIT TECHNOLOGY Final Report, 1 Jan. 1992 - 31 Dec. 1994
Andrzej Badzian and Gennady Gildenblat 31 Dec. 1994 12 p
(Contract N00014-92-J-1421)
(AD-A294519) Avail: CASI HC A03/MF A01

In the portion of this project funded by BMDO/IST, we have been developing the elements of a diamond based semiconductor technology for high temperature applications. The approach is centered around incorporating a Schottky barrier contact and MOS field effect transistor using diamond films prepared by microwave plasma chemical vapor deposition (MPACVD). The experimental basis for this research is the successful fabrication in our laboratory of the world's first Schottky diodes with PACVD diamond base. These devices have characteristics similar to their counterparts fabricated using single crystal synthetic diamond prepared by high pressure methods. This has required a detailed understanding and control of the deposition process at it relates to the chemical purity and structural perfection of the resulting single crystal diamond films, in addition, detailed characterization of the films has allowed for meaningful preparation characterization electronic property relations. The ultimate goal of the proposed research is to fabricate transistors on single crystal heteroepitaxial diamond and to fabricate small scale integrated circuit operational at 400-500 C.
DTIC

N95-34485# Cornell Univ., Ithaca, NY.
NUCLEATION, PROPAGATION, ELECTRONIC LEVELS AND ELIMINATION OF MISFIT DISLOCATIONS IN 3-5 SEMICONDUCTOR INTERFACES Final Report
G. P. Watson and M. Matragrano Mar. 1995 279 p
(Contract DE-FG02-86ER-45278)
(DE95-011595; DOE/ER-45278/T2) Avail: CASI HC A13/MF A03

This report discusses the following topics: strained layer defects; the structural and electronic characteristics of misfit dislocations; requirements for the growth of high quality, low defect density InGaAs strained epitaxial layers; the isolation and nucleation of misfit dislocations in strained epitaxial layers grown on patterned, ion-damaged GaAs; the effect of pattern substrate trench depth on misfit dislocation density; the thermal stability of lattice mismatched InGaAs grown on patterned GaAs; misfit dislocations in ZnSe strained epitaxial layers grown on patterned GaAs; and the measurement of deep level states caused by misfit dislocations in InGaAs/GaAs grown on patterned GaAs substrates.
DOE

N95-34486# Sandia National Labs., Albuquerque, NM.
FUNDAMENTAL SURFACE CHEMISTRY OF GaAs OMVPE
J. R. Creighton and C. M. Truong 1995 8 p Presented at the US/Japan Workshop on Atomic Scale Mechanisms of Epitaxial Growth, Honolulu, HI, 10-12 May 1995
(Contract DE-AC04-94AL-85000)
(DE95-011606; SAND-95-0848C; CONF-9505216-1) Avail: CASI HC A02/MF A01

Organometallic and hydride compounds are widely used as precursors for the epitaxial growth of GaAs and other compound semiconductors. These precursors are most commonly used to perform organometallic vapor phase epitaxy (OMVPE) and also in related deposition techniques such as atomic layer epitaxy (ALE) and metalorganic molecular beam epitaxy (MOMBE). We have investigated the surface chemical properties of these precursors on GaAs(100) using a variety of surface science diagnostics. Results have shed light on the mechanisms of precursor decomposition which lead to film growth and carbon doping. For instance, kinetics of trimethylgallium (TMGa) decomposition on the Ga-rich and As-rich surfaces, measured by TPD, are in semiquantitative agreement with ALE results; indicating that the dominant growth mechanism during ALE is heterogeneous. Furthermore, there is no compelling evidence for the production of methane (CH4) on the GaAs surface when TMGa and arsine (AsH3) are coadsorbed.
DOE

N95-34568# Conductus, Inc., Sunnyvale, CA.
PROPERTIES OF HIGH-T(SUB c) JOSEPHSON JUNCTIONS WITH Y(0.7)Ca(0.3)Ba2Cu3O(7-DELTA) BARRIER LAYERS
L. Antognazza, B. H. Moeckly, T. H. Geballe, and K. Char 20 Mar. 1995 33 p
(Contracts N00014-93-C-2054; F49620-93-C-0058)
(AD-A294852) Avail: CASI HC A03/MF A01

We report the use of Y(0.7)Ca(0.3)Ba2Cu3O(7-delta) as an epitaxial barrier between YBa2CuO(7-delta) (YBCO) electrodes in high-T(sub c) superconductor-normal-superconductor (SNS) edge junctions. Ca-doped YBCO is an overdoped version of YBCO, and it has an excellent lattice and thermal expansion match with YBCO. We show that these junctions exhibit clean interfaces with resistances smaller than 10(exp -10) ohm sq cm. We present the temperature dependence of the critical current density J(sub c) and the junction resistance R(sub n) for junctions with 200 A, 400 A, and 600 A thick barriers of Y(0.7)Ca(0.3)Ba2Cu3O(7-delta). As the temperature decreases the resistance of the junction decreases faster than the resistance calculated from the resistivity of a Y(0.7)Ca(0.3)Ba2Cu3O(7-delta) film. We analyze our data by considering various possibilities for the microstructure in the barrier region. We discuss the ideal conventional proximity effect, diffusion between the barriers and the electrodes, and doping fluctuations inside the barrier. We find that combinations of these ideas explain the observed behavior with reasonable parameters.
DTIC

N95-34569# Massachusetts Inst. of Tech., Cambridge, MA. Dept. of Electrical Engineering and Computer Science.
FABRICATION TECHNOLOGY AND MEASUREMENT OF COUPLED QUANTUM DOT DEVICES Final Report, 1 Nov. 1991 - 31 Jan. 1995
Dimitri A. Antoniadis, Henry I. Smith, and Martin Burkhardt 31 Jan. 1995 170 p
(Contract F49620-92-J-0064)
(AD-A294853; AFOSR-95-0398TR) Avail: CASI HC A08/MF A02

This report describes the fabrication and measurement of planar

tunneling devices. X-ray lithography was used to define gate patterns in order to achieve lateral electrostatic confinement in a two dimensional electron gas. Technologies were developed for the printing of features with linewidth of 50 nm and below, a lithographic resolution which is necessary for the fabrication of narrow tunneling barriers. Development of technologies such as this can also be used for large scale fabrication of silicon and GaAs devices and circuits with critical dimensions of 100 nm and below. Quantum dots in which the capacitances to the dot were minimized were fabricated using high resolution lithography. Decreased capacitances to the dot increase the charging energy of a quantum dot, making it possible to observe single electron effects at elevated temperatures. The conductance of a device, featuring eight electrodes to control size and shape of a quantum dot, was measured in a Heliox insertion probe at a temperature of 300 mK. Measurements of several quantum dot sizes were performed and the results were discussed. The same device was biased to produce two unequal quantum dots in series. The results are discussed and compared with theoretical predictions. DTIC

N95-34588# Astralux, Inc., Boulder, CO.
GROWTH OF GaN SINGLE-CRYSTAL BOULES Final Report
Moeljanto Leksono and Jaques I. Pankova 20 Mar. 1995 8 p
(Contract F49620-94-C-0067)
(AD-A294976; AFOSR-95-0411TR) Avail: CASI HC A02/MF A01

The first step in growing a GaN boule was to demonstrate the possibility of growing GaN from elemental Ga and ammonia on a substrate. Although GaN crystals were obtained the diffusion rate of gas vapor was too high. A number of other problems was uncovered and their solution was conceived. Several changes to the deposition system were made, but to succeed, a more radical redesign is needed. This new design will be proposed as a first task during Phase 2. The Phase 1 work has been a very useful experience that uncovered valuable insights. DTIC

N95-34607# Army Research Lab., Fort Monmouth, NJ.
POISSON'S RATIO FOR TETRAGONAL CRYSTALS
Arthur Ballato Mar. 1995 13 p
(AD-A293544; ARL-TR-423) Avail: CASI HC A03/MF A01

General expressions for Poisson's ratio are derived for tetragonal crystals; simplified forms are given for cases involving symmetry directions. Poisson's ratio, nu, is defined for isotropic media as the quotient of lateral contraction to longitudinal extension arising from application of a simple tensile stress; in most materials, this dimensionless number is positive. In crystals, nu takes on different values, depending on the directions of stress and strain chosen. The ratio finds application in a variety of areas of applied elasticity and solid mechanics, for example, as indication of the mechanical coupling between various vibrational modes of motion. DTIC

N95-34608# Army Research Lab., Fort Monmouth, NJ.
POISSON'S RATIO FOR CUBIC CRYSTALS
Arthur Ballato Mar. 1995 14 p
(AD-A293549; ARL-TR-425) Avail: CASI HC A03/MF A01

General expressions for Poisson's ratio are derived for cubic crystals; simplified forms are given for cases involving symmetry directions. Crystals of cubic symmetry include many of the binary semiconductor systems with the piezoelectric zincblende structure, such as GaAs and related alloys. These are extremely important for high technology applications such as cellular radio and microwave collision avoidance radar. All cubic classes have the same elastic matrix scheme, so for our purposes it is not necessary to distinguish between the cubic point groups. The cubic elastic matrix scheme is identical in form to that of isotropic substances; the difference is that for isotropic materials the shear coefficient (s(sub 44) or c(sub 44)) is related to the two other independent coefficients, whereas in cubic crystals it is a third independent quantity. DTIC

N95-34755# Pittsburgh Univ., Pittsburgh, PA.
SURFACE CHEMISTRY OF DIAMOND SINGLE CRYSTALS Final Report, 15 Mar. 1992 - 14 Mar. 1995
John T. Tates, Jr. 21 Apr. 1995 21 p
(Contract F49620-92-J-0192)
(AD-A294150; AFOSR-95-0333TR) Avail: CASI HC A03/MF A01

Diamond(100) was studied as a substrate for the adsorption of atomic hydrogen and fluorine. Both surface C-H bonds and surface C-F bonds are of importance in the tribological use of diamond film coating. A new and facile method for depositing surface fluorine on diamond has been developed. The method involves the photochemical dissociation of perfluoroalkyl iodide molecules depositing C(n)F(2n+1) groups on the diamond. These groups, upon thermal dissociation, produce surface C-F groups on the diamond. A patent application is being researched on this new method. DTIC

N95-34792# Arizona Univ., Tucson, AZ.
GROWTH AND STRUCTURE OF MBE-DEPOSITED IRIDIUM SILICIDE Final Technical Report, 1 Apr. 1991 - 31 Mar. 1994
Charles M. Falco 10 Jan. 1995 14 p
(Grant AF-AFOSR-0220-91)
(AD-A295033; AFOSR-95-0284TR) Avail: CASI HC A03/MF A01

This report describes accomplishments made during the previous three years on a research program to prepare iridium silicide films by Molecular Beam Epitaxy-MBE, and characterize their physical and chemical structure in detail as a function of preparation conditions using the wide variety of probes available in our laboratory. By use of our MBE growth techniques we were able to form pure IrSi3 films at temperatures as low as 450 C, which is almost 200 C lower than previously reported. We also found a previously-unreported c-axis epitaxial IrSi3 growth mode at approx. 700 C, found that the IrSi3 epitaxy on Si(111) was dominated by a Mode B* orientation which had not previously been reported in the literature, as well as showed that the epitaxial growth of IrSi3 on Si(111) was superior to that on Si(100). Measurements made at Rome Laboratory found that the Schottky barrier height of the IrS3 film on Si(111) was considerably larger than that on Si(100) substrates. We also studied in detail the growth and structure of five different types of iridium silicide films: co-deposited and reacted IrSi, co-deposited Ir3Si4, reacted IrSi3, co-deposited IrSi3, and pure Ir reacted on hot Si substrates. This allowed us to form a previously-unreported silicide, Ir3Si4, and identify six epitaxial growth modes of Ir3Si4 crystallites with the Si(100) surface. DTIC

N95-34795# Minnesota Univ., Minneapolis, MN.
THE GROWTH OF ULTRATHIN EPITAXIAL INTERMETALLIC FILMS
P. I. Cohen 2 Dec. 1994 14 p
(Grant AF-AFOSR-0494-89)
(AD-A295037; AFOSR-95-0312TR) Avail: CASI HC A03/MF A01

FeAl has been grown on psuedomorphic AlAs films on GaAs substrates. The growth was characterized by in situ reflection high energy electron diffraction, transmission electron diffraction, and electron channeling. Procedures for the growth of high quality films were developed and the detects analyzed. It was found that a low temperature nucleation followed by a high temperature anneal and low temperature growth gave strong layer by layer growth. RHEED intensity oscillations were observed for the first time in a metal aluminide system, allowing for precise control over ultrathin films. The first metal aluminides grown using metal organics were prepared. The results indicated that though there were advantages to this procedure, it was necessary to use full chemical beam epitaxy to avoid carbon contamination. The first measurement of critical thickness was made. GaAs was grown on top of FeAl films. The construction of a scanning tunneling microscope was begun. DTIC

N95-34799# Oak Ridge National Lab., TN.
HIGHLY DOPED p-ZnTe FILMS AND QUANTUM WELL STRUCTURES GROWN BY NONEQUILIBRIUM PULSED LASER ABLATION
D. H. Lowndes, C. M. Rouleau, J. D. Budai, D. B. Geohegan, and J. W. McCamy (Harvard Univ., Cambridge, MA.) 1995 3 p Presented at the 11th International Conference on the Electronic Properties of Two Dimensional Systems, Nottingham, 7-11 Aug. 1995
(Contract DE-AC05-84OR-21400)
(DE95-012885; CONF-950820-1) Avail: CASI HC A01/MF A01

Highly p-doped ZnTe films have been grown on semi-insulating GaAs (001) and unintentionally doped (p-type) GaSb (001) substrates by pulsed KrF (248 nm) excimer laser ablation of a ZnTe target through an N2 ambient, without the use of any assisting (DC or AC) plasma source. Free hole concentrations in the mid-10(exp 19) cm(exp -3) to greater than 10(exp 20) cm(exp -3) range have been obtained. This appears to be the first time that any wide band gap (E(sub g) greater than or equal to 2 eV) II-VI compound (or other) semiconductor has been impurity-doped from the gas phase by pulsed-laser ablation (PLA). The maximum carrier

concentrations also may be the highest obtained for ZnTe by any method thus far. Because pulsed laser deposition is inherently digital, attractive deposition rates can be combined with precise control of layer thickness in epitaxial multilayered structures. Typical deposition conditions are less than 0.5 (angstrom) per laser pulse, with crystalline quality governed by tradeoffs between substrate temperature, pulse repetition rate, and the focused pulsed laser energy density. PLA's capability for growth of very thin epitaxial layers is being exploited and studied through growth of doped heteroepitaxial quantum well structures in the nearly lattice-matched ZnTe/CdSe//GaSb(substrate) system. Results obtained from growth and characterization of heterostructures in this system will be presented. DOE

N95-34802# Oak Ridge National Lab., TN.
STATIC DISPLACEMENTS OF ATOMS IN CRYSTALLINE METALLIC SOLID SOLUTIONS
C. Sparks, G. Ice, X. Jiang (Sandia National Labs., Albuquerque, NM.), and P. Zschack 1994 8 p Presented at the 1994 Fall Meeting of the Materials Research Society (MRS), Boston, MA, 28 Nov. - 2 Dec. 1994
(Contract DE-AC05-84OR-21400)
(DE95-012893; CONF-941144-158) Avail: CASI HC A02/MF A01

Measurement of diffuse x-ray scattering from binary crystalline solid solutions at more than one x-ray energy is a sensitive probe of the average interatomic distance between neighboring pairs of atoms. Deviations of these bond distances by as little as 0.001 (angstrom) are easily detected in the diffuse scattering from binary alloys consisting of atoms nearby in the periodic table and/or where x-ray energies chosen near their absorption edges can change the scattering contrast. Individual bond distances (AA, AB and BB) are recovered out to several near neighbor shells by combining three scattering measurements at x-ray energies chosen for maximum and minimum contrast. Average bond distances recovered from four metal alloys Fe(77.5)Ni(22.5), Fe(46.5)Ni(53.5), Cr(47)Fe(53) and Cr(20)Ni(80) are discussed. The authors find that the interatomic distances measured for these alloys give interesting insights to atomic displacements in solid solutions. Nearest neighbor bond distances are not well represented by phenomenological models based on pure element atomic size and concentration dependence of the lattice constants. Radial and nonradial displacements are recovered from these measurements of diffuse scattering. DOE

N95-34820# Utah Univ., Salt Lake City, UT.
USE OF D2 TO ELUCIDATE OMVPE GROWTH MECHANISMS Final Report, 1 Dec. 1990 - 1 May 1994
Gerald B. Stringfellow 1 May 1994 10 p
(Grant AF-AFOSR-0059-91)
(AD-A294999; AFOSR-95-0278TR) Avail: CASI HC A02/MF A01

The research concentrated on two important areas of organometallic vapor phase epitaxial growth: (1) A study of the pyrolysis reactions and rates for five new antimony precursors: trivinylantimony (TVSb), triisopropylantimony (TIPSb), Triallylantimony (TASb), tertiarybutyldimethyl-antimony (TBDMSb), and diisopropylantimonyhydride (DIPSbH). They have been compared with the standard precursor, trimethylantimony (TMSb). The pyrolysis temperatures for TIPSb, TASb, TBDMSb, and DIPSbH are all much lower than for TVSb, which is similar to TMSb. The pyrolysis mechanisms are surprisingly dissimilar; and (2) The effect of adding tertiarybutyl radicals (from azo-t-butane pyrolysis) on the low temperature growth of GaAs using trimethylgallium (TMGa) and arsine. The pyrolysis of both precursors is stimulated by t-butyl radicals. The growth rate at 450 C is found to be enhanced by a factor of 6, giving good morphology layers. The properties of the layers were studied using X-ray diffraction, photoluminescence, and Raman spectroscopy. DTIC

N95-34822# Virginia Univ., Charlottesville, VA.
ELECTRON AND HOLE TRANSPORT IN COMPOUND SEMICONDUCTORS Final Report
Michael Shur 1995 3 p
(Contract F49620-92-J-0393)
(AD-A295003; AFOSR-95-0308TR) Avail: CASI HC A01/MF A01

We investigated transport properties of InSb and GaSb. We implemented an algorithm for electron-electron scattering in the Monte Carlo simulator, and used this simulator to study the effect of electron-electron scattering at relatively low electric fields. We also developed a program for the calculation of the electron velocity and electron temperature as functions of an electric field. This calculation was based on the moment and energy balance equations. We applied this program to study the heating and drift velocity of electrons in InSb. This method is less time consuming than the Monte Carlo method and more suitable for the implementation in device simulators. We have also calculated numerically the low field mobility due to acoustic and optical phonons, obtaining excellent agreement with our Monte Carlo simulations. Based on these studies, we wrote a program for the calculation of mobilities in all cubic semiconductors and their alloys. The program assumes spherical bands, but accounts for carrier degeneracy, non-parabolicity, and varying screening length. (It can be easily modified to account for non-parabolicity.) DTIC

77 THERMODYNAMICS AND STATISTICAL PHYSICS

Includes quantum mechanics; theoretical physics; and Bose and Fermi statistics.

For related information see also *25 Inorganic and Physical Chemistry* and *34 Fluid Mechanics and Heat Transfer.*

N95-32405# Joint Inst. for Nuclear Research, Dubna (USSR). Lab. of Theoretical Physics.
NJL MODEL WITH NONPERTURBATIVE DEPENDENCE ON GLUON CONDENSATE
M. Nagy (Slovak Academy of Sciences, Bratislava, Czechoslovakia.), S. Sawada (Nagoya Univ., Nagoya, Japan.), and M. K. Volkov 1994 4 p Submitted for publication in Modern Physics Letters A
(DE95-623677; JINR-E-2-94-339) Avail: CASI HC A01/MF A01 (US Sales Only)

The gap equation in constant or homogeneous background SU(3) color field is investigated by using the Schwinger method. It is shown that the parameters of the NJL model are close to the values obtained within chiral perturbation theory in the G(sup 2)-approximation where G(sup 2) is the gluon condensate. DOE

N95-32478# Joint Inst. for Nuclear Research, Dubna (USSR). Lab. of Theoretical Physics.
GENERAL-COVARIANT QUANTUM MECHANICS OF DIRAC PARTICLE IN CURVED SPACE-TIMES
E. A. Tagirov 1994 16 p
(DE95-623600; JINR-E-2-94-323) Avail: CASI HC A03/MF A01 (US Sales Only)

A general covariant analog of the standard non-relativistic Quantum Mechanics with relativistic corrections in normal geodesic frames in the general Riemannian space-time is constructed for the Dirac particle. Not only the Pauli equation with hermitian Hamiltonian and the pre-Hilbert structure of space of its solutions but also the matrix elements of hermitian operators of momentum, (curvilinear) spatial coordinates and spin of the particle are deduced as general-covariant asymptotic approximation in c(sup -2), c being the velocity of light, to their naturally determined general-relativistic pre images. It is shown that the Hamiltonian in the Pauli equation originated by the Dirac equation is unitary equivalent to the operator of energy, originated by the metric energy-momentum tensor of the spinor field. Commutation and other properties of the observables connected with the considered change of geometrical background of Quantum Mechanics are briefly discussed. DOE

N95-32661# Air-Conditioning and Refrigeration Technology Inst., Inc., Arlington, VA.
THERMOPHYSICAL PROPERTIES OF HCFC ALTERNATIVES Quarterly Report, 1 Oct. 1994 - 31 Dec. 1994
W. M. Haynes (National Inst. of Standards and Technology, Boulder, CO.) Jan. 1995 12 p
(Contract DE-FG02-91CE-23810)
(DE95-009635; DOE/CE-23810/51A; ARTI-660-50800) Avail: CASI HC A03/MF A01

Numerous fluids and fluid mixtures have been identified as promising alternatives to the HCFC refrigerants, but, for many of them, reliable thermodynamic data do not exist. In particular, reliable thermodynamic properties data and models are needed to predict the performance of the

new refrigerants in heating and cooling equipment and to design and optimize equipment to be reliable and energy efficient. The objective of this project is to measure, with high accuracy, selected thermodynamic properties data for two pure refrigerants and nine refrigerant blends; these data will be used to fit equations of state and other property models which can be used in equipment design. The new data will fill in gaps in the existing data and resolve problems and differences that exist in and between existing data sets. Most of the studied fluids and blends are potential replacements for HCFC-22 and/or R502; in addition, one pure fluid and one blend are potential replacements for CFC-13 in low temperature refrigeration applications. DOE

N95-32667# Joint Inst. for Nuclear Research, Dubna (USSR). Lab. of Theoretical Physics.

ZERO MODES OF GAUSS CONSTRAINT IN GAUGELESS REDUCTION OF YANG-MILLS THEORY

A. Khvedelidze (Academy of Sciences of the Georgian SSR, Tbilisi, Georgia.) and V. Pervushin 1994 19 p Submitted for publication in Helvetica Physica Acta

(DE95-623676; JINR-E-2-94-332) Avail: CASI HC A03/MF A01 (US Sales Only)

The physical variables for pure Yang-Mills theory in four-dimensional Minkowski space-time are constructed without using a gauge-fixing condition by the explicit resolving of the non-Abelian Gauss constraint and by the Bogolyubov transformation that diagonalizes the kinetic term in reduced action (action on constraint shell). As a result, the reduced action is expressed in terms of gauge invariant field variables including an additional global (only time-dependent) one, describing zero mode dynamics of the Gauss constraint. This additional variable reflects the symmetry group of topologically nontrivial transformations remaining after the reduction. (It gives also the characteristic of the Gribov ambiguity from the point of view of the gauge fixing method). The perturbation theory in terms of quasiparticles with the new stable vacuum, which is defined through the zero mode configuration, is proposed. It was shown that the averaging of Green's functions for quasiparticles over the global variable describes the mechanism of color confinement. DOE

N95-32961# Joint Inst. for Nuclear Research, Dubna (USSR). Lab. of Theoretical Physics.

SPIN EFFECTS IN HIGH ENERGY PHOTON-HADRON SCATTERING IN QCD

S. V. Goloskokov and O. A. Listopadov (Scorina Univ., Gomel, Belarus.) 1994 8 p Submitted for publication in Yadernaya Fizika

(DE95-623679; JINR-E-2-94-348) Avail: CASI HC A02/MF A01 (US Sales Only)

The spin effects at high energies and momenta transferred, absolute value of t greater than 1 GeV(sup 2) are analyzed for quark-photon scattering. The energy independence of the ratio of spin-flip and spin-non-flip amplitudes in the same alpha(sub s) order of QCD is obtained. It is shown that the contribution of the spin-dependent quark-pomeron vertex to the spin-flip amplitude is intensified by off-mass-shell effects in the quark loop. As a result, the magnitude of this amplitude can reach 20-30% from spin-non-flip one. The dependence of the cross-section on the form factor and alpha(sub s, sup 3), spin-non-flip contributions are observed. DOE

N95-33202# Texas Univ., Austin, TX. Center for Particle Physics.

TOP QUARK SIGNATURES IN EXTENDED COLOR THEORIES

D. A. Dicus, B. Dutta (Oklahoma State Univ., Stillwater, OK.), and S. Nandi (Oklahoma State Univ., Stillwater, OK.) Dec. 1994 27 p

(Contracts DE-FG03-93ER-40757; DE-FG02-94ER-40852)

(DE95-007099; DOE/ER-40757/059) Avail: CASI HC A03/MF A01

We consider the implications of an extended color group, SU (3)(sub I) x SU (3)(sub II), spontaneously broken to SU (3)(sub c) at a TeV or lower scale, for the hadronic colliders. The associated massive color octet gauge bosons (the colorons) can enhance the t(bar t) pair production at the Tevatron collider. At the LHC, the colorons can be pair produced, each decaying to a t(bar t) pair. This gives rise to anomalous multi W production. DOE

N95-33313 Harvard Univ., Cambridge, MA.

COSMOLOGICAL CONSEQUENCES OF TOPOLOGICAL AND GEOMETRIC PHENOMENA IN FIELD THEORIES Ph.D. Thesis

Sean Michael Carroll 1993 177 p

Avail: Univ. Microfilms Order No. DA9412319

Several issues at the nexus of particle physics, gravitation and cosmology are studied. One set of questions involves observational consequences of alternative theories of gravity. Two related theories are examined, featuring pseudoscalar gravitational fields; one has a unique status as a theory satisfying the Weak Equivalence Principle but not the Einstein Equivalence Principle, while the other is a simple model with propagating torsion. Experimental constraints on each theory are discussed. Another question centers around the creation of closed timelike curves in general relativity. Explicit obstacles to the creation of such time machines are demonstrated in an exactly solvable (2 + 1)-dimensional model. The final chapter studies the appearance of textures and topological defects in theories with spontaneously broken symmetries. By computing the homotopy groups of the vacuum manifolds in the theories under consideration, it is revealed which theories predict textures and defects. Dissert. Abstr.

N95-33388# Los Alamos National Lab., NM. Theoretical Div.

NONEQUILIBRIUM PROBLEMS IN QUANTUM FIELD THEORY AND SCHWINGER'S CLOSED TIME PATH FORMALISM

Fred Cooper 1995 18 p Presented at the International Symposium on Unified Symmetry: In the Small and in the Large, Miami, FL, 2-5 Feb. 1995

(Contract W-7405-eng-36)

(DE95-012056; LA-UR-95-1375; CONF-950299-1) Avail: CASI HC A03/MF A01

We review the closed time path formalism of Schwinger using a path integral approach. We apply this formalism to the study of pair production from strong external fields as well as the time evolution of a nonequilibrium chiral phase transition. In 1961 in his classic paper 'Brownian Motion of a Quantum Particle,' Schwinger solved the formidable technical problem of how to use the action principle to study initial value problems. Previously, the action principle was formulated to study only transition matrix elements from an earlier time to a later time. The elegant solution of this problem was the invention of the closed time path (CTP) formalism. This formalism was first used to study field theory problems by Mahanthappa and Bakshi. With the advent of supercomputers, it has now become possible to use this formalism to numerically solve important field theory questions which are presented as initial value problems. Two of these problems we shall review here. They are: (1) The time evolution of the quark-gluon plasma; and (2) Dynamical evolution of a non-equilibrium chiral phase transition following a relativistic heavy ion collision. DOE

N95-34211# General Electric Co., Schenectady, NY.

SOLUBILITY BEHAVIOR OF QUARTZ AND CORUNDUM IN SUPERCRITICAL WATER: A QUANTITATIVE THERMODYNAMIC INTERPRETATION

S. E. Ziemniak May 1995 28 p

(Contract DE-AC12-76SN-00052)

(DE95-012294; KAPL-4790) Avail: CASI HC A03/MF A01

Dissolution reaction equilibria for (alpha)-quartz (SiO2) and corundum ((alpha)-Al2O3) in pure, supercritical water are quantified using a density-dependent thermodynamic model. The database of existing solubility literature for (alpha)-quartz (0.2-10 kb, 200-575 C) is shown to be consistent with the presence of two hydrolyzed Si(IV) ion forms: Si(OH)4(aq) and Si2O(OH)6(aq); the corundum database (1-20 kb, 400-700 C) is consistent with Al(OH)3(aq) and Al(OH)4(exp -)). A third Si(IV) ion hydroxocomplex, Si2O2(OH)5(exp -), is indicated at lower pressures (0.03-0.10 kb). The characteristic sigmoidal nature of the solubility isobars is explained by dimerization of Si(OH)4(aq) (at high densities) or the formation of anionic hydrolysis products, Si2O2(OH)5(exp -) and Al(OH)4(exp -)), in the low density region (p less than 0.01 gm/cc). By means of the evaluated equilibria, thermochemical properties of Si2O(OH)6(aq) and Si2O2(OH)5(exp -) are made available for the first time. DOE

N95-34464# Alabama Univ., Tuscaloosa, AL. Dept. of Mathematics.

PENETRABLE WEDGE ANALYSIS

Robert W. Scharstein and Anthony M. Davis 1 Jul. 1994 40 p

(Contract N00014-93-1-6014)

(AD-A294276; BER-611-162; NRL-CR/7181-94-0008) Avail: CASI HC A03/MF A01

Two complementary analyses of the time-harmonic scattering by a penetrable wedge are presented. The distance from the apex (appropriately scaled by the wavenumber in the exterior region) of the exciting line source is the single length scale in this infinite-domain boundary value problem. The work summarized herein represents two mathematical approaches (among a series of candidates) to solve this important scattering problem and to visualize the wave physics. DTIC

N95-34585# Princeton Univ., NJ.
ELECTRONIC PROCESSES IN HETEROSTRUCTURES, STRAINED-LAYER MATERIALS, AND LATERALLY PATTERNED STRUCTURES Final Technical Report, 30 Sep. 1991 - 29 Sep. 1994
D. C. Tsui 29 Sep. 1994 5 p
(Grant AF-AFOSR-0365-91)
(AD-A294970; AFOSR-95-0281TR) Avail: CASI HC A01/MF A01

This report summarizes the research accomplishments under contract AFOSR-91-0353 at Princeton University. It has three parts: (1) submillimeter wave response of laterally patterned quantum structures; (2) energy structure of two-dimensional holes; and (3) detection of the composite fermions in fractional quantum Hall effect. DTIC

N95-34589# Notre Dame Univ., IN. Dept. of Electrical Engineering.
QUANTUM TRANSPORT Final Report, 15 Mar. 1991 - 14 Aug. 1994
Craig S. Lent, Wolfgang Porod, Supriyo Bandyopadhyay, and Gary H. Bernstein 15 Aug. 1994 28 p
(Grant AF-AFOSR-0211-91)
(AD-A294977; AFOSR-95-0280TR) Avail: CASI HC A03/MF A01

During the period March 15, 1991 to August 14, 1994, research carried out by the Nanostructures Group in the Department of Electrical Engineering at Notre Dame was concerned with a variety of quantum transport in mesoscopic structures. This research was funded by the Air Force Office of Scientific Research under Grant No. AFOSR-91-0211. The major issues examined included quantum transport in high magnetic fields and modulated channels, Coulomb coupled quantum dot systems, transmission resonances and zeroes in resonant transport, self-consistent Hartree calculations of transport, lateral quantum wires an pn-junction formation, quantum magnetotransport in disordered systems, magnetoelectric states in quantum wires, anomalous magnetoresistance, electromigration, collision retardation and phonon effects in hot-electron transport, spin-polarized single electronics, single-particle lifetimes in quasi-1D structures, quantum transport experiments in metals, the mesoscopic photovoltaic effect, and new techniques for fabricating quantum structures in semiconductors. DTIC

N95-34652 Rutherford Appleton Lab., Oxford (England).
PROCEEDINGS OF THE SCHOOL FOR YOUNG HIGH ENERGY PHYSICISTS
J. Flynn, I. G. Halliday, R. G. Roberts, G. M. Shore, and K. J. Peach Mar. 1995 245 p Conference held in Abingdon, England, 5-17 Sep. 1994
(PB95-234993; RAL-95-033) Avail: Issuing Activity (National Technical Information Service (NTIS))

Forty-six young experimental particle physicists students attended the 1994 Summer School, held as usual in Coseners House in Abingdon in early September. The lecture courses given and published in these proceedings are the following: Quantum Field Theory -- Canonical and Path Integral Approaches; Introduction to Quantum Electrodynamics and Quantum Chromodynamics; The Standard Model; and Topics in Standard Model Phenomenology. NTIS

N95-34654 National Physical Lab., Teddington (England).
FIRST NPL CALORIMETRY WORKSHOP
1995 336 p Workshop held on 12-14 Oct. 1994
(PB95-236063) Avail: Issuing Activity (National Technical Information Service (NTIS))

The proceeding of the 1st NPL Calorimetry Workshop is presented. Subject areas discussed include: A sealed water calorimeter for measuring absorbed doses; Water calorimetry, Model and experiment; The development of a standard based on water calorimetry for absorbed dose to water; Comparison of water calorimeter with reference ionization chamber dosimetry in high-energy photon and proton beams; Water calorimeter dosimetry for clinical proton beams; Measurement principles and experimental setup for determining the heat defect of water for high-energy protons, deuterons and alpha-particles; An ice calorimeter for medium energy x-ray dosimetry; UK photon-beam primary standard graphite calorimeter; Changes of the electrical calibration factor observed for the NMi graphite calorimeter; State-of-the-art of calorimetry at LPRI; Calorimeters for absorbed dose standards or reference dosimeters for radiotherapy: Comparisons with other methods; Development of a megavoltage dosimetry calibration system based on graphite calorimetry; Progress on the NPL graphite calorimeter for electron beam radiotherapy; The NIST graphite calorimeter for the calibration of higher energy electron beams. NTIS

80 SOCIAL SCIENCES (GENERAL)

Includes educational matters.

N95-34479# Naval Postgraduate School, Monterey, CA.
DEVELOPING MULTIMEDIA INSTRUCTIONAL SYSTEMS: AN EXAMPLE APPLICATION FOR TRAINING IN NIGHT VISION GOGGLES M.S. Thesis
Francisco Q. Meza Mar. 1995 58 p
(AD-A294521) Avail: CASI HC A04/MF A01

The purpose of this thesis is to implement a computer system for Night Vision Goggles based on appropriate design principles for the development of instructional multimedia systems. Multimedia has tremendous potential to enhance computer-based instruction. The design of any effective instructional multimedia application, however, must incorporate instructional, multimedia, and system design principles. This thesis explores cognitive learning theories, media selection, and the use of a developmental model for creating multimedia systems. This thesis concludes that the presentation of material must complement the internal learning processes of a user and the right combination of media must be used to present the content. The designers of an application must adopt a systems approach, also. This paper employs examples from a multimedia application that provides instruction on the use of night vision goggles. The application allows the user to interactively determine the sequence and pace of instruction. The application makes use of a pull-down menu for quick access to menu selections, includes question and answer sessions to test a user's learning, and full-motion video, text, audio, and graphics be used in combination, or independently, to present the content. DTIC

N95-34743# Pittsburgh Univ., Pittsburgh, PA. Dept. of Computer Science.
A MODEL OF LONG TERM LEARNING: INTEGRATION OF KNOWLEDGE ACQUISITION AND KNOWLEDGE COMPILATION Final Technical Report, 1 Jul. 1992 - 15 Nov. 1993
Kurt VanLehn 5 May 1995 9 p
(Contract N00014-92-J-1945)
(AD-A294123) Avail: CASI HC A02/MF A01

This report describes progress toward constructing a unified, computer-based model of all the major phenomena in cognitive skill acquisition. An extensive review of the literature was completed and published, along with several new analyses of important but hitherto neglected aspects of cognitive skill. However, the computational embodiment of the theory was only partially implemented during the 15 months of funding, and more work is needed. DTIC

81 ADMINISTRATION AND MANAGEMENT

Includes management planning and research.

N95-32706# General Accounting Office, Washington, DC. National Security and International Affairs Div.
AEROSPACE GUIDANCE AND METROLOGY CENTER: COST GROWTH AND OTHER FACTORS AFFECT CLOSURE AND PRIVATIZATION. REPORT TO CONGRESSIONAL REQUESTERS
9 Dec. 1994 16 p
(GAO/NSIAD-95-60; B-259135) Avail: CASI HC A03/MF A01; GAO, PO Box 6015, Gaithersburg, MD 20877 HC

Selected issues were reviewed related to the implementation of maintenance depot closures and realignments resulting from prior Defense Base Closure and Realignment Commission (BRAC) decisions. The

Aerospace Guidance and Metrology Center (AGMC) at Newark Air Force Base (AFB), Ohio, is one of the activities being covered by this review. Unlike other depot closures, the Newark AFB/AGMC implementation plan provides for continuing to perform the same missions at this facility after closure -- largely as a privatized operation, although the Air Force would retain ownership of mission-related equipment valued at about $326 million. The justification of closing Newark AFB/AGMC is not clear. To date, the closure of Newark AFB/AGMC is the only depot closure where almost all of the work may be privatized in place. As such, it merits careful consideration before implementation proceeds. There are a number of issues associated with this privatization that are barriers to its implementation. Also, some projected costs are rising, while others are yet to be determined.

Derived from text

N95-32887# Comptroller General of the United States, Washington, DC.
ANNUAL REPORT TO THE CHAIRMAN, HOUSE AND SENATE COMMITTEES ON APPROPRIATIONS. STATUS OF OPEN RECOMMENDATIONS: IMPROVING OPERATIONS OF FEDERAL DEPARTMENTS AND AGENCIES
14 Jan. 1994 244 p
(GAO/OP-94-1; B-205879) Avail: CASI HC A11/MF A03; GAO, PO Box 6015, Gaithersburg, MD 20877 HC

This is our annual report on the status of open recommendations resulting from the General Accounting Office's (GAO) audits, evaluations, and other review work in federal departments and agencies. To encourage prompt, responsive actions on our recommendations, we systematically follow-up on them and annually report on their status. Derived from text

N95-33907# General Accounting Office, Washington, DC. Program Evaluation and Methodology Div.
REPORT TO THE RANKING MINORITY MEMBER, COMMITTEE ON GOVERNMENT OPERATIONS, HOUSE OF REPRESENTATIVES. PAPERWORK REDUCTION: REPORTED BURDEN HOUR INCREASES REFLECT NEW ESTIMATES, NOT ACTUAL CHANGES
6 Dec. 1993 22 p
(GAO/PEMD-94-3; B-233451.5) Avail: CASI HC A03/MF A01; GAO, PO Box 6015, Gaithersburg, MD 20884-6015 HC

This report addresses four questions in regards to the burden of federal paperwork for the period 1987-92: (1) how has the paperwork burden changed over time; (2) what factors account for the observed changes; (3) have some groups been differentially affected; and (4) have the reasons for information collection changed? Reported burden hours increased 261 percent, from over 1.8 billion hours to nearly 6.6 billion hours, between 1987 and 1992. Most of this change (3.4 billion of the 4.8 billion hour change) is accounted for by Department of Treasury reestimates of the time spent in dealing with burdens rather than by imposition of actual new burdens. Some increases in the estimated paperwork burden resulted from new requirements. Analyses show an apparent decline in the proportion of information collections that placed a burden on entities the Office of Management and Budget (OMB) describes as 'businesses or other institutions' from 33 percent in 1987 to 6 percent in 1992. However, the apparent decline seems to reflect a shift in the way population is reported rather than an actual reduction in the proportion of collections affecting businesses. The major reason for collecting information, what OMB calls 'regulatory or compliance requirements,' rose from 77 percent of all collections in 1987 to 95 percent in 1992. But here again, the seeming increase for this category reflects primarily the Treasury reestimate of time needed to deal with the compliance burden, not an actual change in the distribution of collection purposes. Derived from text

N95-34354*# National Aeronautics and Space Administration, Washington, DC.
ISSUES IN NASA PROGRAM AND PROJECT MANAGEMENT
Francis T. Hoban, ed., Edward J. Hoffman, ed., and William M. Lawbaugh, ed. 1995 65 p
(NASA-SP-6101(09); NAS 1.21:6101(09)) Avail: CASI HC A04/MF A01

This volume is the ninth in an ongoing series on aerospace project management at NASA. Articles in this volume cover evolution of NASA cost estimating; SAM 2; National Space Science Program: strategies to maximize science return; and human needs, motivation, and results of the NASA culture surveys. A section on resources for NASA managers rounds out the publication. Author

N95-34487# Army Research Lab., Adelphi, MD.
FOCUS OF ATTENTION IN DECISION SUPPORT SYSTEMS
John O. Gurney, Jr., Elaine Marsh, and Kenneth Wauchope 12 May 1995 17 p
(AD-A294037) Avail: CASI HC A03/MF A01

In this paper we have described three decision support systems with graphical user interfaces. We have illustrated that interactions with such systems can be improved with the addition of natural language interfaces. NLIs can be added to systems after the initial develop- development phase without loss of functionality. Furthermore we have shown that a hybrid natural language and graphical user interface with multi-modal capability improves access to decision aids more than either one independently. We have also shown that natural language interfaces can help a user maintain his focus of attention in complex situations. A natural language interface to a decision support system has a number of important advantages. A natural language interface is especially useful in recognizing what the user is thinking about at the time of interaction, i.e. identifying the user's focus of attention. It provides a way for the user to maintain focus on his problem without distraction. A natural languages interpreter can access the system for the user and assemble a relevant, well-focused response. A NLI allows the user flexibility of expression. This is important if the user does not know how to say what he intends in the GUI format. NLIs can handle complex focus spaces since focus is readily conveyed through natural language. In fact, natural language may be the only way it can be readily handled. Finally, and importantly, natural language interfaces can handle a user's counterfactual thinking. Because of the complexity and power anticipated in next generation decision support systems, natural language interface technology warrants a closer look. It can serve to help the user manage complex and quantitatively massive amounts of information in a natural and easily-easily expressible way. DTIC

N95-32431*# Houston Univ., TX. Dept. of Industrial Engineering.
THE BACKGROUND AND THEORY OF INTEGRATED RISK MANAGEMENT Final Report
John L. Hunsucker *In* NASA. Johnson Space Center, National Aeronautics and Space Administration (NASA)/American Society for Engineering Education (ASEE) Summer Faculty Fellowship Program, 1994, Volume 1 Jul. 1995 13 p (For primary document see N95-32418 12-99)
(Grant NGT-44-005-803)
Avail: CASI HC A03/MF A03

82 DOCUMENTATION AND INFORMATION SCIENCE

Includes information management; information storage and retrieval technology; technical writing; graphic arts; and micrography.

For computer documentation see *61 Computer Programming and Software.*

N95-32412# Brookhaven National Lab., Upton, NY.
THE RHIC TRANSFER LINE CABLE DATABASE
E. H. Scholl and T. Satogata 1995 3 p Presented at the Particle Accelerator Conference, Dallas, TX, 1-5 May 1995
(Contract DE-AC02-76CH-00016)
(DE95-011560; BNL-61162; CONF-950512-55) Avail: CASI HC A01/MF A01

A cable database was created to facilitate and document installation of cables and wiring in the RHIC project, as well as to provide a data source to track possible wiring and signal problems. The eight tables of this relational database, currently implemented in Sybase, contain information ranging from cable routing to attenuation of individual wires. This database was created in a hierarchical scheme under the assumption that cables contain wires -- each instance of a cable has one to many wires associated with it. This scheme allows entry of information pertinent to individual wires while only requiring single entries for each cable. Relationships to other RHIC databases are also discussed. DOE

N95-32471# Nevada Univ., Las Vegas, NV. Information Science Research Inst.
PREDICTION OF OCR ACCURACY USING SIMPLE IMAGE FEATURES

Luis R. Blando, Junichi Kanai, and Thomas A. Nartker 1995 18 p Presented at the SPIE 1995: SPIE Conference on Optics, Electro-optics, and Laser Application in Science, Engineering and Medicine, San Jose, CA, 5-10 Feb. 1995
(Contract DE-FC08-90NV-10872)
(DE95-009887; CONF-950226-34) Avail: CASI HC A03/MF A01

A classifier for predicting the character accuracy of a given page achieved by any Optical Character Recognition (OCR) system is presented. This classifier is based on measuring the amount of white speckle, the amount of character fragments, and overall size information in the page. No output from the OCR system is used. The given page is classified as either good quality (i.e., high OCR accuracy expected) or poor (i.e., low OCR accuracy expected). Six OCR systems processed two different sets of test data: a set of 439 pages obtained from technical and scientific documents and a set of 200 pages obtained from magazines. For every system, approximately 85% of the pages in each data set were correctly predicted. The performance of this classifier is also compared with the ideal-case performance of a prediction method based upon the number of reject markers in OCR generated text. In several cases, this method matched or exceeded the performance of the reject based approach. DOE

N95-32482# Department of Energy, Washington, DC. Energy Information Administration.
ANNUAL REPORT TO CONGRESS 1994: ENERGY INFORMATION ADMINISTRATION
Apr. 1995 83 p
(DE95-011240; DOE/EIA-0173(94)) Avail: CASI HC A05/MF A01

During 1994, EIA's main goal was to assure its data and analyses were of the highest quality, relevant to its customers' needs, and easily accessible. Efforts to ensure product relevance and quality consisted of conducting new or modified surveys, issuing new information products, revising existing products to include data and analyses desired by EIA's customers, and eliminating products that no longer meet customer needs. Efforts to improve access to energy information consisted of several electronic dissemination initiatives, including Internet services, the Energy Information Highway, and the Energy Emergency Notebook. These activities are discussed in detail in the first two sections of this report. In addition to maintaining its traditional energy information base, EIA plays an important role in developing new information resources required by policymakers and legislators around the world. Examples include data on alternative fuels and greenhouse gas emissions. DOE

N95-32883*# National Aeronautics and Space Administration. Langley Research Center, Hampton, VA.
NASA/DOD AEROSPACE KNOWLEDGE DIFFUSION RESEARCH PROJECT. PAPER 50: FROM STUDENT TO ENTRY-LEVEL PROFESSIONAL: EXAMINING THE ROLE OF LANGUAGE AND WRITTEN COMMUNICATIONS IN THE REACCULTURATION OF AEROSPACE ENGINEERING STUDENTS
Thomas E. Pinelli, Rebecca O. Barclay (Rensselaer Polytechnic Inst., Troy, NY.), Michael L. Keene (Tennessee Univ., Knoxville, TN.), John M. Kennedy (Indiana Univ., Bloomington, IN.), and Laura F. Hecht (Indiana Univ., Bloomington, IN.) 1995 13 p Repr. from Technical Communication, v. 42, no. 3, 1995 p 492-502
(NASA-TM-110834; NAS 1.15:110834) Avail: CASI HC A03/MF A01

When students graduate and enter the world of work, they must make the transition from an academic to a professional knowledge community. Kenneth Bruffee's model of the social construction of knowledge suggests that language and written communication play a critical role in the reacculturation process that enables successful movement from one knowledge community to another. We present the results of a national (mail) survey that examined the technical communications abilities, skills, and competencies of 1,673 aerospace engineering students, who represent an academic knowledge community. These results are examined within the context of the technical communications behaviors and practices reported by 2,355 aerospace engineers and scientists employed in government and industry, who represent a professional knowledge community that the students expect to join. Bruffee's claim of the importance of language and written communication in the successful transition from an academic to a professional knowledge community is supported by the responses from the two communities we surveyed. Implications are offered for facilitating the reacculturation process of students to entry-level engineering professionals. Author

N95-32922*# National Aeronautics and Space Administration. Goddard Space Flight Center, Greenbelt, MD.
NASA WIDE ELECTRONIC PUBLISHING SYSTEM: ELECTRONIC PRINTING AND DUPLICATING. STAGE 3 EVALUATION REPORT
Richard C. Tuey, Fred W. Moore (National Aeronautics and Space Administration, Washington, DC.), and Christine A. Ryan (National Aeronautics and Space Administration. Langley Research Center, Hampton, VA.) Jun. 1995 39 p
(NASA-TM-104620; Rept-95B00094; NAS 1.15:104620) Avail: CASI HC A03/MF A01

The report is presented in four sections: The Introduction describes the duplicating configuration under evaluation and the Background contains a chronological description of the evaluation segmented by phases 1 and 2. This section includes the evaluation schedule, printing and duplicating requirements, storage and communication requirements, electronic publishing system configuration, existing processes and proposed processes, billing rates, costs and productivity analysis, and the return on investment based upon the data gathered to date. The third section contains the phase 1 comparative cost and productivity analysis. This analysis demonstrated that LaRC should proceed with a 90-day evaluation of the DocuTech and follow with a phase 2 cycle to actually demonstrate that the proposed system would meet the needs of LaRC's printing and duplicating requirements, benchmark results, cost comparisons, benchmark observations, and recommendations. These are documented after the recommendations. Author

N95-33198# Advisory Group for Aerospace Research and Development, Neuilly-Sur-Seine (France).
AGARD INDEX OF PUBLICATIONS: 1992-1994 [AGARD INDEX DES PUBLICATIONS 1992-1994]
Jul. 1995 503 p
(AGARD-INDEX-92-94; ISBN-92-836-1019-9) Copyright Avail: CASI HC A22/MF A04

This volume provides abstracts and indexes for AGARD unclassified publications published during the period 1992-1994. Full bibliographical citations and abstracts for all the documents in this publication are given in the abstract section, which is organized in the major subject divisions and specific categories used by NASA in abstract journals and bibliographies. The major subject divisions are listed, together with a note for each that defines its scope and provides any cross-references. Category breaks in the abstract section are identified by category number and title, and a scope note. Within each category, the abstracts are arranged by series and year. Six indexes - Subject (based on NASA Thesaurus nomenclature), Personal Author, Corporate Source, Panel, Report/Accession Number, and Accession Number - are included. Sample entries are shown on the first page of each index. This publication was sponsored by the Technical Information Committee of AGARD (TIC), and compiled by NASA's Center for AeroSpace Information (CASI). Author

N95-33238# Technische Univ., Twente (Netherlands). Dept. of Computer Science.
FORMALIZATION AND REPRESENTATION OF A PRODUCT-DRIVEN APPROACH TO METHOD ASSEMBLY FOR SITUATIONAL SYSTEMS DEVELOPMENT
Frank Harmsen and Sjaak Brinkkemper Dec. 1994 26 p
(ISSN 0924-3755)
(PB95-215190; Memo-INF-94-75) Copyright Avail: CASI HC A03/MF A01

The paper deals with the issue of assembling situational methods out of method fragments, stored in a method base. Starting point of the assembly is the set of development results to be delivered by applying the situational method. Then, activities to produce these results are selected and assembled into a situational method. Method fragments are represented in the Method Engineering language (MEL), of which an overview is given. Products are all described in terms of a so-called Methodology Data Model (MDM), being the foundation of the method base. A set of formalized method quality rules is given. Concepts and relationships of this MDM are manipulated by operations of MEL. NTIS

N95-33240*# National Aeronautics and Space Administration, Washington, DC.
NASA DIRECTIVES MASTER LIST AND INDEX
10 Mar. 1995 116 p
(NHB-1410.13O; NAS 1.18:1410.13O) Avail: CASI HC A06/MF A02

This handbook sets forth in two parts, Master List of Management Directives and Index to NASA Management Directives, the following information for the guidance of users of the NASA Management Directives System. Chapter 1 contains introductory information material on how to use this handbook. Chapter 2 is a complete master list of agencywide management directives, describing each directive by type, number, effective date, expiration date, title, and organization code of the office responsible for the directive. Chapter 3 includes a consolidated numerical list of all delegations of authority and a breakdown of such delegation by the office or center to which special authority is assigned. Chapter 4 sets forth a consolidated list of all NASA handbooks (NHB's) and important footnotes covering the control and ordering of such documents. Chapter 5 is a consolidated list of NASA management directives applicable to the Jet Propulsion Laboratory. Chapter 6 is a consolidated list of NASA regulations published in the Code of Federal Regulations. Chapter 7 is a consolidated list of NASA regulations published in Title 14 of the Code of Federal Regulations. Complementary manuals to the NASA Management Directives System are described in Chapter 8. The second part contains an in depth alphabetical index to all NASA management directives other than handbooks, most of which are indexed by titles only. Derived from text

N95-33334 Toronto Univ. (Ontario).
AN EMPIRICAL INVESTIGATION OF THE SEMANTIC WARRANTS EXERCISED IN THESAURUS CONSTRUCTION Ph.D. Thesis
Blake Fleming Michae Wilson 1993 188 p
(ISBN-0-315-86393-5) Avail: Univ. Microfilms Order No. DANN86393

The primary objective of this thesis is to characterize and compare the thesaurus vocabularies generated by exercising in two subject fields (Social Work and Aerospace Engineering) each of the three semantic warrants: literary warrant, user warrant, and consensus. A determination of how each warrant constrains the selection of terms and thereby shapes the thesaurus vocabulary in made on the basis of differences among the vocabularies generated. The fact that the chosen fields lie at opposite ends of an abstract-concrete conceptual continuum makes it possible to test two hypothesis: that vocabulary commonality and that terminological precision would be significantly higher in the concrete field (Aerospace Engineering) than in the abstract field (Social Work). A vocabulary representing literary warrant sources was compiled in each field from terms in journal abstracts. A vocabulary representing user warrant sources was compiled in each field from terms in nonnegotiated search requests and profiles. A vocabulary representing published sources of consensus was compiled from dictionaries in each field. Terms in the literary warrant and user warrant vocabularies were ranked by their frequency of entailment in dictionary definitions. The three vocabularies were compiled within each field on the basis of: rankings assigned to shared terms (a rank-order correlation coefficient was used as an index of association between rankings); the commonality between pairs of vocabularies (match and compatibility ratios were used); and precision of each vocabulary (a measure of synonymy and a parallel measure of were used). The results of the statistical analysis indicate that the two subject fields do not differ significantly in vocabulary commonality and in precision when comparisons are made without regard for warrant. These findings lead to the rejection of the two hypothesis tested. However, statistically significant differences were found between the warrant vocabularies within each field. Possible explanations of these findings are evaluated and the implication for thesaurus construction are discussed. Dissert. Abstr.

N95-33402# Westinghouse Savannah River Co., Aiken, SC.
INCORPORATING BIBLIOGRAPHIC INFORMATION INTO A SPATIAL DATA QUERY SYSTEM FOR THE SAVANNAH RIVER SITE
David J. Cowen (South Carolina Univ., Columbia, SC.), John R. Jensen (South Carolina Univ., Columbia, SC.), Cynthia V. MacCharles (South Carolina Univ., Columbia, SC.), William N. Holliday (South Carolina Univ., Columbia, SC.), Timothy R. White (South Carolina Univ., Columbia, SC.), and Halkard E. Mackey, Jr. 1995 14 p Presented at the Annual Meeting of Society of Photogrammetry and Remote Sensing, Charlotte, NC, 27 Mar. - 2 Apr. 1995
(Contract DE-AC09-89SR-18035)
(DE95-010965; WSRC-MS-95-0031; CONF-9503141-1) Avail: CASI HC A03/MF A01

Over the past two years the Environmental Sciences Section of the Westinghouse Savannah River Company and the University of South Carolina have developed a full-featured spatial data query system for the Savannah River Site. This Environmental Data Atlas, which operates across multiple platforms, is designed to provide scientists with easy access to a wide range of GIS and remote sensing data resources. This paper describes the method that has been developed to extend the Environmental Data Atlas to incorporate bibliographical data. The bibliographic search function was determined by the scientists to be an extremely important enhancement that will enable them to utilize geographic keys to locate obscure references and databases. The method uses a hot-link function to launch a parsing algorithm by pointing to geographic features. The parsing algorithm efficiently sorts through a list of references based on the keyword associated with the feature. The matched bibliographical entries are formatted into a text file that is displayed in a scrollable window. Any graphics associated with the actual reference can also be scanned and linked to an additional hot link. An additional parsing system was used to automatically create the bibliographical database from a comprehensive CD-ROM version of the Environmental Information Document prepared by the Environmental Sciences Section. This extensive digital reference represents a summary of much of the recent ecological information available on the site. The methods used in this system are directly linked to a commercially available software and provide a universal approach to establishing a geographically based document retrieval system. DOE

N95-33711 North Dakota State Univ. of Agriculture and Applied Science, Fargo, ND.
PERFORMANCE ANALYSIS OF COMBINED CONCURRENCY CONTROL AND COMMIT PROTOCOLS IN DISTRIBUTED DATABASE SYSTEMS Ph.D. Thesis
Shahrzad Amirsoleymani 1993 158 p
Avail: Univ. Microfilms Order No. DA9413144

Many concurrency control and commit algorithms have been proposed for use in distributed database systems. These protocols have a direct impact on performance in the distributed setting. The purpose of this research was to develop a simulation model to study the behavior and compare the performance of integrated concurrency control (CC) and commit protocols in distributed database management systems (DDBMS). Algorithm concurrency control and commit protocols are intimately related; earlier performance studies of DDBMS have ignored the interaction between different concurrency control and commit protocols. Using a bad combination of CC and commit protocol causes the degradation of global system performance. This is mainly due to the interaction between CC and commit protocols. In this research, various combinations of concurrency control and commit protocols in DDBMS were tested. The purpose was to rank all combinations of concurrency control and commit mechanisms based on the response time and throughput of the system. The study was undertaken for a variety of environments which differ in number of data items in the database, arrival rate of transactions at each site, type of transactions, transaction length, and data connection. The best commit protocol for each concurrency control protocol was found in each environment. The system was studied under normal operation and in the presence of site failure due to hardware or software unreliability. The simulation results show that there is an interaction between the CC and commit protocols. Dissert. Abstr.

N95-33722 Vanderbilt Univ., Nashville, TN.
REPRESENTING INCOMPLETE KNOWLEDGE IN RELATIONAL DATABASES Ph.D. Thesis
Gilford Taera Hapanyengwi 1993 157 p
Avail: Univ. Microfilms Order No. DA9416486

Ways of representing and analyzing incomplete information in relational database systems are explored. The relationship between different types of singular, i.e., special, data values is studied. Two new singular values are introduced and the use of a defeasible universal quantifier as a singular value is explored. Other singular values which have been covered in the literature are also reviewed, and emphasis is placed on how all the singular values relate to one another. A singular value see other is introduced. This singular value has an associated function for every attribute in which

it can occur. The function indicates where the value which replaces see other comes from. The associated value can come from within the same tuple, from another tuple or from another relation. The previous work has used the closed world assumption, i.e., assertions not known to be true must be assumed to be false. We now consider the singular value open A set of rules which produces a three valued logic equivalent to the possible worlds is presented. Using this set of rules a tuple can be tested to determine its sign. The idea of partially opening a relation or a database leads to one of partially or fully closing the database. A singular value closure is presented. This singular value together with an underlying open world assumption allows for flexibility in dealing with information represented in a relation. Instead of requiring the closed world assumption on the whole database, closing parts of the database is possible. To achieve a finer granularity the closure singular value is made defeasible by atomic attribute values. An algebra is developed to handle relations allowing the closure singular value. The universal quantifier is presented as a singular value. A database allowing for the universal quantifier and atomic values is presented. To achieve proper representation the universal quantifier is made defeasible. Different ways of resolving conflicts are looked at. Considering a tuple with fewer universal quantifiers to be the dominating tuple is one such way. Contradictions are resolved by inserting the intersection tuple of the contradicting tuples. Algorithms to determine the sign of a tuple and for inserting new tuples are presented. Also given are algorithms to handle the basic operations of the relational algebra. Ways of enhancing relations with the universal quantifier are suggested. These include allowing for subclasses in the attribute domains which result in a finer granularity for the consideration of the universal quantifier. Having weights on tuples is also considered as a way of assigning priorities to the tuples instead of using the number of the universal quantifiers in a tuple. Finally, having signs on attributes is shown to give a more specific representation of individual tuples. Dissert. Abstr.

N95-34217*# National Aeronautics and Space Administration. Langley Research Center, Hampton, VA.

NASA/DOD AEROSPACE KNOWLEDGE DIFFUSION RESEARCH PROJECT. REPORT 33: THE TECHNICAL COMMUNICATIONS PRACTICES OF US AEROSPACE ENGINEERS AND SCIENTISTS: RESULTS OF THE PHASE 1 AIAA MAIL SURVEY

Thomas E. Pinelli, Rebecca O. Barclay (Rensselaer Polytechnic Inst., Troy, NY.), and John M. Kennedy (Indiana Univ., Bloomington, IN.) Sep. 1995 52 p

(RTOP 505-90-00)

(NASA-TM-110180; NAS 1.15:110180) Avail: CASI HC A04/MF A01

The U.S. government technical report is a primary means by which the results of federally funded research and development (R&D) are transferred to the U.S. aerospace industry. However, little is known about this information product in terms of its actual use, importance, and value in the transfer of federally funded R&D. To help establish a body of knowledge, the U.S. government technical report is being investigated as part of the NASA/DOD Aerospace Knowledge Diffusion Research Project. In this report, we summarize the literature on technical reports and provide a model that depicts the transfer of federally funded aerospace R&D via the U.S. government technical report. We present results from our investigation of aerospace knowledge diffusion vis-a-vis the U.S. government technical report, and present the results of research that investigated aerospace knowledge diffusion vis-a-vis the technical communications practices of U.S. aerospace engineers and scientists who are members of the American Institute of Aeronautics and Astronautics (AIAA). Author

N95-34218*# Colorado Univ., Boulder, CO. Lab. for Atmospheric and Space Physics.

APPLIED INFORMATION SYSTEMS RESEARCH PROGRAM (AISRP) WORKSHOP 3 MEETING PROCEEDINGS Final Report

1993 235 p Workshop held in Boulder, CO, 3-6 Aug. 1993 Sponsored by NASA, Washington

(NASA-CR-199103; NAS 1.26:199103) Avail: CASI HC A11/MF A03

The third Workshop of the Applied Laboratory Systems Research Program (AISRP) met at the Univeristy of Colorado's Laboratory for Atmospheric and Space Physics in August of 1993. The presentations were organized into four sessions: Artificial Intelligence Techniques; Scientific Visualization; Data Management and Archiving; and Research and Technology. For individual titles, see N95-34219 through N95-34243.

N95-34219*# Texas A&M Univ., College Station, TX. Climate Systems Research Program.

AN INTERACTIVE ENVIRONMENT FOR THE ANALYSIS OF LARGE EARTH OBSERVATION AND MODEL DATA SETS Abstract Only

Kenneth P. Bowman, John E. Walsh (Illinois Univ., Urbana, IL.), and Robert B. Wilhelmson (Illinois Univ., Urbana, IL.) *In* Colorado Univ., Applied Information Systems Research Program (AISRP) Workshop 3 Meeting Proceedings 1993 1 p (For primary document see N95-34218 12-82)

Avail: CASI HC A01/MF A03

We propose to develop an interactive environment for the analysis of large Earth science observation and model data sets. We will use a standard scientific data storage format and a large capacity (greater than 20 GB) optical disk system for data management; develop libraries for coordinate transformation and regridding of data sets; modify the NCSA X Image and X DataSlice software for typical Earth observation data sets by including map transformations and missing data handling; develop analysis tools for common mathematical and statistical operations; integrate the components described above into a system for the analysis and comparison of observations and model results; and distribute software and documentation to the scientific community. Author

N95-34220*# National Center for Atmospheric Research, Boulder, CO.

INTERACTIVE INTERFACE FOR NATIONAL CENTER FOR ATMOSPHERIC RESEARCH (NCAR) GRAPHICS Abstract Only

William Buzbee and Robert L. Lackman *In* Colorado Univ., Applied Information Systems Research Program (AISRP) Workshop 3 Meeting Proceedings 1993 1 p (For primary document see N95-34218 12-82)

Avail: CASI HC A01/MF A03

NCAR Graphics is a FORTRAN 77 library of over 30 high-level graphics modules which are heavily used by science and engineering researchers at over 1500 sites world-wide including many universities and government agencies. These Earth science oriented modules now have a FORTRAN callable subroutine interface which excludes their use by non-programming researchers. This proposal outlines the development of a fully interactive 'point and click' menu-based interface using the prevailing toolkit standard for the X-Window System. Options for direct output to the display window and/or output to a computer Graphics Metafile (CGM) will be provided. X, PEX, and PHIGS will be implemented as the underlying windowing and graphics standards. Associated meteorological and geometric data sets would exploit the network extended NASA Common Data Format, netCDF. Author

N95-34221*# Boston Univ., Boston, MA. Center for Space Physics.

DEVELOPMENT OF A TOOL-SET FOR SIMULTANEOUS, MULTI-SITE OBSERVATIONS OF ASTRONOMICAL OBJECTS Abstract Only **c89**

Supriya Chakrabarti, J. Garrett Jernigan (California Univ., Berkeley, CA.), and Herman L. Marshall (California Univ., Berkeley, CA.) *In* Colorado Univ., Applied Information Systems Research Program (AISRP) Workshop 3 Meeting Proceedings 1993 1 p (For primary document see N95-34218 12-82)

Avail: CASI HC A01/MF A03

A network of ground and space based telescopes can provide continuous observation of astronomical objects. In a 'Target of Opportunity' scenario triggered by the system, any telescope on the network may request supporting observations. We propose to develop a set of data collection and display tools to support these observations. We plan to demonstrate the usefulness of this toolset for simultaneous multi-site observations of astronomical targets. Possible candidates for the proposed demonstration include the Extreme Ultraviolet Explorer, International Ultraviolet Explorer, ALEXIS, and sounding rocket experiments. Ground based observations, operated by the University of California, Berkeley; the Jet Propulsion Laboratory; and Fairborn Observatory, Mesa, Arizona will be used to demonstrate the proposed concept. Although the demonstration will involve astronomical investigations, these tools will be applicable to a large number of scientific disciplines. the software tools and systems developed as a result of our work will be made available to the scientific community. Author

N95-34222*# California Inst. of Tech., Pasadena, CA. Dept. of Astronomy.

MULTIVARIATE STATISTICAL ANALYSIS SOFTWARE TECHNOLOGIES FOR ASTROPHYSICAL RESEARCH INVOLVING LARGE DATA BASES Abstract Only **c90**

George Djorgovski *In* Colorado Univ., Applied Information Systems Research Program (AISRP) Workshop 3 Meeting Proceedings 1993 1 p (For primary document see N95-34218 12-82)

Avail: CASI HC A01/MF A03

The existing and forthcoming data bases from NASA missions contain an abundance of information whose complexity cannot be efficiently tapped with simple statistical techniques. Powerful multivariate statistical methods already exist which can be used to harness much of the richness of these data. Automatic classification techniques have been developed to solve the problem of identifying known types of objects in multiparameter data sets, in addition to leading to the discovery of new physical phenomena and classes of objects. We propose an exploratory study and integration of promising techniques in the development of a general and modular classification/analysis system for very large data bases, which would enhance and optimize data management and the use of human research resource. Author

N95-34223*# Colorado Univ., Boulder, CO. Center for Astrodynamics Research.

A LAND-SURFACE TESTBED FOR EOSDIS Abstract Only **c47**

William Emery, Jeff Dozier (California Univ., Santa Barbara, CA.), and Paul Rotar (National Center for Atmospheric Research, Boulder, CO.) *In its* Applied Information Systems Research Program (AISRP) Workshop 3 Meeting Proceedings 1993 1 p (For primary document see N95-34218 12-82)

Avail: CASI HC A01/MF A03

We propose to develop an on-line data distribution and interactive display system for the collection, archival, distribution and analysis of operational weather satellite data for applications in land surface studies. A 1,000 square km scene of the western U.S. (centered on the Colorado Rockies) will be extracted from Advanced Very High Resolution Radiometer (AVHRR) imagery collected from morning and afternoon passes of the NOAA polar-orbiters at the direct readout stations operated by CU/CCAR. All five channels of these AVHRR data will be navigated and map registered at CU/CCAR and then be transferred to NCAR for storage in an on-line data system. Software will also be available at NCAR to process and navigate the raw AVHRR data as needed. A display workstation software, based on a Macintosh II computer, will be developed that will display and further process the AVHRR data for studies of vegetation monitoring and snowpack assessment. Various options of presently used techniques for both vegetation and snowpack monitoring will be implemented in the workstation software to provide the individual investigator with the freedom to interact with the satellite image data. The display software will be freely distributed online to interested investigators, and the AVHRR data will be made available on-line to anyone interested. In addition, potential users will be sought out and connected to the on-line data archive. This experiment with an active on-line archive and interactive analysis systems will provide experience with a small scale EOSDIS. Author

N95-34224*# Jet Propulsion Lab., California Inst. of Tech., Pasadena, CA.

GEOGRAPHIC INFORMATION SYSTEM FOR FUSION AND ANALYSIS OF HIGH-RESOLUTION REMOTE SENSING AND GROUND DATA Abstract Only

Anthony Freeman, Jo Bea Way, Pascale DuBois, and Franz Leberl (Vexcel Corp., Boulder, CO.) *In* Colorado Univ., Applied Information Systems Research Program (AISRP) Workshop 3 Meeting Proceedings 1993 2 p (For primary document see N95-34218 12-82)

Avail: CASI HC A01/MF A03

We seek to combine high-resolution remotely sensed data with models and ground truth measurements, in the context of a Geographical Information System (GIS), integrated with specialized image processing software. We will use this integrated system to analyze the data from two Case Studies, one at a boreal forest site, the other a tropical forest site. We will assess the information content of the different components of the data, determine the optimum data combinations to study biogeophysical changes in the forest, assess the best way to visualize the results, and validate the models for the forest response to different radar wavelengths/polarizations. During the 1990's, unprecedented amounts of high-resolution images from space of the Earth's surface will become available to the applications scientist from the LANDSAT/TM series, European and Japanese ERS-1 satellites, RADARSAT and SIR-C missions. When the Earth Observation Systems (EOS) program is operational, the amount of data available for a particular site can only increase. The interdisciplinary scientist, seeking to use data from various sensors to study his site of interest, may be faced with massive difficulties in manipulating such large data sets, assessing their information content, determining the optimum combinations of data to study a particular parameter, visualizing his results and validating his model of the surface. The techniques to deal with these problems are also needed to support the analysis of data from NASA's current program of Multi-sensor Airborne Campaigns, which will also generate large volumes of data. In the Case Studies outlined in this proposal, we will have somewhat unique data sets. For the Bonanza Creek Experimental Forest (Case 1) calibrated DC-8 SAR (Synthetic Aperture Radar) data and extensive ground truth measurement are already at our disposal. The data set shows documented evidence to temporal change. The Belize Forest Experiment (Case 2) will produce calibrated DC-8 SAR and AVIRIS data, together with extensive measurements on the tropical rain forest itself. The extreme range of these sites, one an Arctic forest, the other a tropical rain forest, has been deliberately chosen to find common problems which can lead to generalized observations and unique problems with data which raise issues for the EOS System. Author

N95-34225*# National Aeronautics and Space Administration. Ames Research Center, Moffett Field, CA.

CONSTRUCTION OF AN ADVANCED SOFTWARE TOOL FOR PLANETARY ATMOSPHERIC MODELING Abstract Only **c61**

Peter Friedland, Richard M. Keller, Christopher P. McKay, Michael H. Sims, and David E. Thompson *In* Colorado Univ., Applied Information Systems Research Program (AISRP) Workshop 3 Meeting Proceedings 1993 1 p (For primary document see N95-34218 12-82)

Avail: CASI HC A01/MF A03

Scientific model-building can be a time intensive and painstaking process, often involving the development of large complex computer programs. Despite the effort involved, scientific models cannot be distributed easily and shared with other scientists. In general, implemented scientific models are complicated, idiosyncratic, and difficult for anyone but the original scientist/programmer to understand. We propose to construct a scientific modeling software tool that serves as an aid to the scientist in developing, using and sharing models. The proposed tool will include an interactive intelligent graphical interface and a high-level domain-specific modeling language. As a testbed for this research, we propose to develop a software prototype in the domain of planetary atmospheric modeling. Author

N95-34226*# Canada Centre for Remote Sensing, Victoria (British Columbia).

SYSTEM OF EXPERTS FOR INTELLIGENT DATA MANAGEMENT (SEIDAM) Abstract Only

David G. Goodenough, Joji Iisaka, and Ko Fung (Canada Centre for Remote Sensing, Ottawa, Ontario.) *In* Colorado Univ., Applied Information Systems Research Program (AISRP) Workshop 3 Meeting Proceedings 1993 1 p (For primary document see N95-34218 12-82)

Avail: CASI HC A01/MF A03

A proposal to conduct research and development on a system of expert systems for intelligent data management (SEIDAM) is being developed. CCRS has much expertise in developing systems for integrating geographic information with space and aircraft remote sensing data and in managing large archives of remotely sensed data. SEIDAM will be composed of expert systems grouped in three levels. At the lowest level, the expert systems will manage and integrate data from diverse sources, taking account of symbolic representation differences and varying accuracies. Existing software can be controlled by these expert systems, without rewriting existing software into an Artificial Intelligence (AI) language. At the second level, SEIDAM will take the interpreted data (symbolic and numerical) and combine these with data models. at the top level, SEIDAM will respond to user goals for predictive outcomes given existing data. The SEIDAM Project will address the research areas of expert systems, data management, storage and retrieval, and user access and interfaces. Author

N95-34227*# Jet Propulsion Lab., California Inst. of Tech., Pasadena, CA.

KNOWLEDGE-BASED ASSISTANCE FOR SCIENCE VISUALIZATION AND ANALYSIS USING LARGE DISTRIBUTED DATABASES Abstract Only

Thomas H. Handley, Jr., Allan S. Jacobson, Richard J. Doyle, and Donald J. Collins *In* Colorado Univ., Applied Information Systems Research Program (AISRP) Workshop 3 Meeting Proceedings 1993 1 p (For primary document see N95-34218 12-82)

Avail: CASI HC A01/MF A03

Within this decade, the growth in complexity of exploratory data analysis and the sheer volume of space data require new and innovative approaches to support science investigators in achieving their research objectives. To date, there have been numerous efforts addressing the individual issues involved in inter-disciplinary, multi-instrument investigations. However, while successful in small scale, these efforts have not proven to be open and scalable. This proposal addresses four areas of significant need: scientific visualization and analysis; science data management; interactions in a distributed, heterogeneous environment; and knowledge-based assistance for these functions. The fundamental innovation embedded with this proposal is the integration of three automation technologies, namely, knowledge-based expert systems, science visualization and science data management. This integration is based on concept called the DataHub. With the DataHub concept, NASA will be able to apply a more complete solution to all nodes of a distributed system. Both computation nodes and interactive nodes will be able to effectively and efficiently use the data services (address, retrieval, update, etc.) with a distributed, interdisciplinary information system in a uniform and standard way. This will allow the science investigators to concentrate on their scientific endeavors, rather than to involve themselves in the intricate technical details of the systems and tools required to accomplish their work. Thus, science investigators need not be programmers. The emphasis will be on the definition and prototyping of system elements with sufficient detail to enable data analysis and interpretation leading to publishable scientific results. In addition, the proposed work includes all the required end-to-end components and interfaces to demonstrate the completed concept. Author

N95-34228*# National Aeronautics and Space Administration. Goddard Space Flight Center, Greenbelt, MD.

EXPERIMENTER'S LABORATORY FOR VISUALIZED INTERACTIVE SCIENCE Abstract Only **c61**

Elaine R. Hansen (Colorado Univ., Boulder, CO.), Marjorie K. Klemp (Colorado Univ., Boulder, CO.), Sally W. Lasater (Colorado Univ., Boulder, CO.), Marti R. Szczur, and Joseph B. Klemp (National Center for Atmospheric Research, Boulder, CO.) *In* Colorado Univ., Applied Information Systems Research Program (AISRP) Workshop 3 Meeting Proceedings 1993 1 p (For primary document see N95-34218 12-82)

Avail: CASI HC A01/MF A03

The science activities of the 1990's will require the analysis of complex phenomena and large diverse sets of data. In order to meet these needs, we must take advantage of advanced user interaction techniques: modern user interface tools; visualization capabilities; affordable, high performance graphics workstations; and interoperatable data standards and translator. To meet these needs, we propose to adopt and upgrade several existing tools and systems to create an experimenter's laboratory for visualized interactive science. Intuitive human-computer interaction techniques have already been developed and demonstrated at the University of Colorado. A Transportable Applications Executive (TAE+), developed at GSFC, is a powerful user interface tool for general purpose applications. A 3D visualization package developed by NCAR provides both color-shaded surface displays and volumetric rendering in either index or true color. The Network Common Data Form (NetCDF) data access library developed by Unidata supports creation, access and sharing of scientific data in a form that is self-describing and network transparent. The combination and enhancement of these packages constitutes a powerful experimenter's laboratory capable of meeting key science needs of the 1990's. This proposal encompasses the work required to build and demonstrate this capability. Author

N95-34229*# Massachusetts Inst. of Tech., Cambridge, MA.

TOPOGRAPHY FROM SHADING AND STEREO Abstract Only

Berthold P. Horn and Michael Caplinger (Arizona State Univ., Tempe, AZ.) *In* Colorado Univ., Applied Information Systems Research Program (AISRP) Workshop 3 Meeting Proceedings 1993 1 p (For primary document see N95-34218 12-82)

Avail: CASI HC A01/MF A03

Methods exploiting photometric information in images that have been developed in machine vision can be applied to planetary imagery. Present techniques, however, focus on one visual cue, such as shading or binocular stereo, and produce results that are either not very accurate in an absolute sense or provide information only at few points on the surface. We plan to integrate shape from shading, binocular stereo and photometric stereo to yield a robust system for recovering detailed surface shape and surface reflectance information. Such a system will be useful in producing quantitative information from the vast volume of imagery being received, as well as in helping visualize the underlying surface. The work will be carried out on a popular computing platform so that it will be easily accessible to other workers. Author

N95-34230*# Jet Propulsion Lab., California Inst. of Tech., Pasadena, CA.

A DISTRIBUTED SYSTEM FOR VISUALIZING AND ANALYZING MULTIVARIATE AND MULTIDISCIPLINARY DATA Abstract Only

Allan S. Jacobson, Mark Allen, Michael Bailey, Ronald Blom, Leo Blume, and Lee Elson *In* Colorado Univ., Applied Information Systems Research Program (AISRP) Workshop 3 Meeting Proceedings 1993 1 p (For primary document see N95-34218 12-82)

Avail: CASI HC A01/MF A03

THe Linked Windows Interactive Data System (LinkWinds) is being developed with NASA support. The objective of this proposal is to adapt and apply that system in a complex network environment containing elements to be found by scientists working multidisciplinary teams on very large scale and distributed data sets. The proposed three year program will develop specific visualization and analysis tools, to be exercised locally and remotely in the LinkWinds environment, to demonstrate visual data analysis, interdisciplinary data analysis and cooperative and interactive televisualization and analysis of data by geographically separated science teams. These demonstrators will involve at least two science disciplines with the aim of producing publishable results. Author

N95-34231*# Maryland Univ., College Park, MD. Center for Ocean-Land-Atmosphere Studies.

THE GRID ANALYSIS AND DISPLAY SYSTEM (GRADS): A PRACTICAL TOOL FOR EARTH SCIENCE VISUALIZATION Abstract Only

James L. Kinter, III *In* Colorado Univ., Applied Information Systems Research Program (AISRP) Workshop 3 Meeting Proceedings 1993 1 p (For primary document see N95-34218 12-82)

Avail: CASI HC A01/MF A03

We propose to develop and enhance a workstation based grid analysis and display software system for Earth science dataset browsing, sampling and manipulation. The system will be coupled to a supercomputer in a distributed computing environment for near real-time interaction between scientists and computational results. Author

N95-34232*# Jet Propulsion Lab., California Inst. of Tech., Pasadena, CA.

PLANETARY DATA ANALYSIS AND DISPLAY SYSTEM: A VERSION OF PC-McIDAS Abstract Only

Sanjay S. Limaye (Wisconsin Univ., Madison, WI.), L. A. Sromovsky (Wisconsin Univ., Madison, WI.), R. S. Saunders, and Michael Martin *In* Colorado Univ., Applied Information Systems Research Program (AISRP) Workshop 3 Meeting Proceedings 1993 1 p (For primary document see N95-34218 12-82)

Avail: CASI HC A01/MF A03

We propose to develop a system for access and analysis of planetary data from past and future space missions based on an existing system, the PC-McIDAS workstation. This system is now in use in the atmospheric science community for access to meteorological satellite and conventional weather data. The proposed system would be usable not only by planetary atmospheric researchers but also by the planetary geologic community. By providing the critical tools of an efficient system architecture, newer applications and customized user interfaces can be added by the end user within such a system. Author

N95-34233*# Jet Propulsion Lab., California Inst. of Tech., Pasadena, CA.
MULTI-LAYER HOLOGRAPHIC BIFURCATIVE NEURAL NETWORK SYSTEM FOR REAL-TIME ADAPTIVE EOS DATA ANALYSIS Abstract Only **c43**
Hua-Kuang Liu, K. S. Huang (University of Southern California, Los Angeles, CA.), and J. Diep *In* Colorado Univ., Applied Information Systems Research Program (AISRP) Workshop 3 Meeting Proceedings 1993 1 p (For primary document see N95-34218 12-82)
Avail: CASI HC A01/MF A03

Optical data processing techniques have the inherent advantage of high data throughout, low weight and low power requirements. These features are particularly desirable for onboard spacecraft in-situ real-time data analysis and data compression applications. the proposed multi-layer optical holographic neural net pattern recognition technique will utilize the nonlinear photorefractive devices for real-time adaptive learning to classify input data content and recognize unexpected features. Information can be stored either in analog or digital form in a nonlinear photofractive device. The recording can be accomplished in time scales ranging from milliseconds to microseconds. When a system consisting of these devices is organized in a multi-layer structure, a feedforward neural net with bifurcating data classification capability is formed. The interdisciplinary research will involve the collaboration with top digital computer architecture experts at the University of Southern California. Author

N95-34234*# Space Telescope Science Inst., Baltimore, MD.
DEVELOPMENT OF AN EXPERT DATA REDUCTION ASSISTANT Abstract Only
Glenn E. Miller, Mark D. Johnston, and Robert J. Hanisch *In* Colorado Univ., Applied Information Systems Research Program (AISRP) Workshop 3 Meeting Proceedings 1993 1 p (For primary document see N95-34218 12-82)
Avail: CASI HC A01/MF A03

We propose the development of an expert system tool for the management and reduction of complex datasets. the proposed work is an extension of a successful prototype system for the calibration of CCD (charge coupled device) images developed by Dr. Johnston in 1987. (ref.: Proceedings of the Goddard Conference on Space Applications of Artificial Intelligence). The reduction of complex multi-parameter data sets presents severe challenges to a scientist. Not only must a particular data analysis system be mastered, (e.g. IRAF/SDAS/MIDAS), large amounts of data can require many days of tedious work and supervision by the scientist for even the most straightforward reductions. The proposed Expert Data Reduction Assistant will help the scientist overcome these obstacles by developing a reduction plan based on the data at hand and producing a script for the reduction of the data in a target common language. Author

N95-34235*# Maryland Univ., College Park, MD.
VIEWCACHE: AN INCREMENTAL POINTER-BASED ACCESS METHOD FOR AUTONOMOUS INTEROPERABLE DATABASES Abstract Only
N. Roussopoulos and Timos Sellis *In* Colorado Univ., Applied Information Systems Research Program (AISRP) Workshop 3 Meeting Proceedings 1993 1 p (For primary document see N95-34218 12-82)
Avail: CASI HC A01/MF A03

One of the biggest problems facing NASA today is to provide scientists efficient access to a large number of distributed databases. Our pointer-based incremental data base access method, VIEWCACHE, provides such an interface for accessing distributed datasets and directories. VIEWCACHE allows database browsing and search performing inter-database cross-referencing with no actual data movement between database sites. This organization and processing is especially suitable for managing Astrophysics databases which are physically distributed all over the world. Once the search is complete, the set of collected pointers pointing to the desired data are cached. VIEWCACHE includes spatial access methods for accessing image datasets, which provide much easier query formulation by referring directly to the image and very efficient search for objects contained within a two-dimensional window. We will develop and optimize a VIEWCACHE External Gateway Access to database management systems to facilitate database search. Author

N95-34236*# Hughes Aircraft Co., Culver City, CA.
ADVANCED DATA VISUALIZATION AND SENSOR FUSION: CONVERSION OF TECHNIQUES FROM MEDICAL IMAGING TO EARTH SCIENCE Abstract Only
Richard C. Savage, Chin-Tu Chen (Chicago Univ., Chicago, IL.), Charles Pelizzari (Chicago Univ., Chicago, IL.), and Veerabhadran Ramanathan (Chicago Univ., Chicago, IL.) *In* Colorado Univ., Applied Information Systems Research Program (AISRP) Workshop 3 Meeting Proceedings 1993 1 p (For primary document see N95-34218 12-82)
Avail: CASI HC A01/MF A03

Hughes Aircraft Company and the University of Chicago propose to transfer existing medical imaging registration algorithms to the area of multi-sensor data fusion. The University of Chicago's algorithms have been successfully demonstrated to provide pixel by pixel comparison capability for medical sensors with different characteristics. The research will attempt to fuse GOES (Geostationary Operational Environmental Satellite), AVHRR (Advanced Very High Resolution Radiometer), and SSM/I (Special Sensor Microwave Imager) sensor data which will benefit a wide range of researchers. The algorithms will utilize data visualization and algorithm development tools created by Hughes in its EOSDIS (Earth Observation SystemData/Information System) prototyping. This will maximize the work on the fusion algorithms since support software (e.g. input/output routines) will already exist. The research will produce a portable software library with documentation for use by other researchers. Author

N95-34237*# Brandeis Univ., Waltham, MA. Dept. of Computer Science.
HIGH PERFORMANCE COMPRESSION OF SCIENCE DATA Abstract Only
James A. Storer and Martin Cohn *In* Colorado Univ., Applied Information Systems Research Program (AISRP) Workshop 3 Meeting Proceedings 1993 1 p (For primary document see N95-34218 12-82)
Avail: CASI HC A01/MF A03

In the future, NASA expects to gather over a tera-byte per day of data requiring space for levels of archival storage. Data compression will be a key component in systems that store this data (e.g., optical disk and tape) as well as in communications systems (both between space and Earth and between scientific locations on Earth). We propose to develop algorithms that can be a basis for software and hardware systems that compress a wide variety of scientific data with different criteria for fidelity/bandwidth tradeoffs. The algorithmic approaches we consider are specially targeted for parallel computation where data rates of over 1 billion bits per second are achievable with current technology. Author

N95-34238*# Science Applications International Corp., McLean, VA. Lab. for Atmospheric and Space Sciences.
SAVS: A SPACE ANALYSIS AND VISUALIZATION SYSTEM Abstract Only
Edward P. Szuszczewicz, Alan Mankofsky, and Charles C. Goodrich (Maryland Univ., College Park, MD.) *In* Colorado Univ., Applied Information Systems Research Program (AISRP) Workshop 3 Meeting Proceedings 1993 1 p (For primary document see N95-34218 12-82)
Avail: CASI HC A01/MF A03

We propose to develop, test, demonstrate, and deliver to NASA a powerful and versatile data acquisition, manipulation, analysis and visualization system which will enhance scientific capabilities in the display and interpretation of diverse and distributed data within an integrated user-friendly environment. Our approach exploits existing technologies and combines three major elements into an easy-to-use interactive package: (1) innovative visualization software; (2) advanced database techniques; and (3) a rich set of mathematical and image processing tools. Visualization capabilities will include one-, two-, and three-dimensinal displays, along with animation, compression, warping and slicing functions. Analysis tools will include generic mathematical and statistical techniques along with the ability to use large scale models for interactive interpretation of large volume data sets. Our system will be implemented on Sun and EC UNIX workstations and on the Stardent Graphics Supercomputer. Our final deliverable will include complete documentation and a NASA/NSF-CDAW/SUN-DIAL campaign demonstration. Author

N95-34239*# National Aeronautics and Space Administration. Goddard Space Flight Center, Greenbelt, MD.

A SPATIAL ANALYSIS AND MODELING SYSTEM (SAMS) FOR ENVIRONMENT MANAGEMENT Abstract Only

Fran Stetina, John Hill (Houston Advanced Research Center, The Woodlands, TX.), Paul Chan (Science Applications International Corp., Greenbelt, MD.), Robert Jaske (Federal Emergency Management Agency, Denver, CO.), and Gilbert Rochon (Dillard Univ., New Orleans, LA.) *In* Colorado Univ., Applied Information Systems Research Program (AISRP) Workshop 3 Meeting Proceedings 1993 1 p (For primary document see N95-34218 12-82)

Avail: CASI HC A01/MF A03

This is a proposal to develop a uniform global environmental data gathering and distribution system to support the calibration and validation of remotely sensed data. SAMS is based on an enhanced version of FEMA's Integrated Emergency Management Information Systems and the Department of Defense's Air land Battlefield Environment Software Systems. This system consists of state-of-the-art graphics and visualization techniques, simulation models, database management and expert systems for conducting environmental and disaster preparedness studies. This software package will be integrated into various Landsat and UNEP-GRID stations which are planned to become direct readout stations during the EOS (Earth Observing System) timeframe. This system would be implemented as a pilot program to support the Tropical Rainfall Measuring Mission (TRMM). This will be a joint NASA-FEMA-University-Industry project. Author

N95-34240*# National Aeronautics and Space Administration. Goddard Space Flight Center, Greenbelt, MD.

A DISTRIBUTED ANALYSIS AND VISUALIZATION SYSTEM FOR MODEL AND OBSERVATIONAL DATA Abstract Only

Robert Wilhelmson (Illinois Univ., Urbana, IL.) and Steven Koch *In* Colorado Univ., Applied Information Systems Research Program (AISRP) Workshop 3 Meeting Proceedings 1993 1 p (For primary document see N95-34218 12-82)

Avail: CASI HC A01/MF A03

The objective of this proposal is to develop an integrated and distributed analysis and display software system which can be applied to all areas of the Earth System Science to study numerical model and earth observational data from storm to global scale. This system will be designed to be easy to use, portable, flexible and easily extensible and designed to adhere to current and emerging standards whenever possible. It will provide an environment for visualization of the massive amounts of data generated from satellites and other observational field measurements and from model simulations during or after their execution. Two- and three-dimensional animation will also be provided. This system will be based on a widely used software package from NASA called GEMPAK and prototype software for three-dimensional interactive displays built at NCSA. The underlying foundation of the system will be a set of software libraries which can be distributed across a UNIX based supercomputer and workstations. Author

N95-34241*# Jet Propulsion Lab., California Inst. of Tech., Pasadena, CA.

DataHub: SCIENCE DATA MANAGEMENT IN SUPPORT OF INTERACTIVE EXPLORATORY ANALYSIS

Thomas H. Handley, Jr. and Mark R. Rubin *In* Colorado Univ., Applied Information Systems Research Program (AISRP) Workshop 3 Meeting Proceedings 1993 11 p (For primary document see N95-34218 12-82)

Avail: CASI HC A03/MF A03

The DataHub addresses four areas of significant needs: scientific visualization and analysis; science data management; interactions in a distributed, heterogeneous environment; and knowledge-based assistance for these functions. The fundamental innovation embedded within the DataHub is the integration of three technologies, viz. knowledge-based expert systems, science visualization, and science data management. This integration is based on a concept called the DataHub. With the DataHub concept, science investigators are able to apply a more complete solution to all nodes of a distributed system. Both computational nodes and interactives nodes are able to effectively and efficiently use the data services (access, retrieval, update, etc), in a distributed, interdisciplinary information system in a uniform and standard way. This allows the science investigators to concentrate on their scientific endeavors, rather than to involve themselves in the intricate technical details of the systems and tools required to accomplish their work. Thus, science investigators need not be programmers. The emphasis on the definition and prototyping of system elements with sufficient detail to enable data analysis and interpretation leading to information. The DataHub includes all the required end-to-end components and interfaces to demonstrate the complete concept. Author

N95-34242*# Jet Propulsion Lab., California Inst. of Tech., Pasadena, CA.

DataHub SPONSORED ANALYSIS

An Van Tran and Donald J. Collins *In* Colorado Univ., Applied Information Systems Research Program (AISRP) Workshop 3 Meeting Proceedings 1993 8 p (For primary document see N95-34218 12-82)

Avail: CASI HC A02/MF A03

The primary productivity of phytoplankton in the ocean is largely responsible for the assimilation of carbon into the oceanic environment, and thus in part the removal of carbon from the atmosphere. Because the ocean is thought to be a primary sink for atmospheric carbon, the basin wide and global distribution of oceanic primary productivity is of central importance in the global budget of carbon. To understand the global productivity of the oceans, the interactions between the physical and biological structures must be known. To address the broader context of the primary productivity of the sea, the physical and biological processes and their variability, including changes in water mass, incident irradiance, nutrients, and consequent formation of blooms of different species of marine phytoplankton and bacteria must be studied. In this investigation, we will use time series of the pigment distributions, taken from the Coastal Zone Color Scanner (CZCS), and of the sea-surface temperature, taken from the NOAA Advanced Very High Resolution Radiometer (AVHRR). These time series will be examined to determine the spatial and temporal statistics of productivity, including the interannual variations that occur in productivity caused by variations in the physical environment. For this task we have chosen to use monthly composite global maps created from the satellite imagery. Derived from text

N95-34243*# Aerospace Corp., El Segundo, CA.

A DISTRIBUTED Clips IMPLEMENTATION: dClips

Y. Philip Li *In* Colorado Univ., Applied Information Systems Research Program (AISRP) Workshop 3 Meeting Proceedings 1993 5 p (For primary document see N95-34218 12-82)

Avail: CASI HC A01/MF A03

A distributed version of the Clips language, dClips, was implemented on top of two existing generic distributed messaging systems to show that: (1) it is easy to create a coarse-grained parallel programming environment out of an existing language if a high level messaging system is used; and (2) the computing model of a parallel programming environment can be changed easily if we change the underlying messaging system. dClips processes were first connected with a simple master-slave model. A client-server model with intercommunicating agents was later implemented. The concept of service broker is being investigated. Author

N95-34420# Army Cold Regions Research and Engineering Lab., Hanover, NH.

BIBLIOGRAPHY ON COLD REGIONS SCIENCE AND TECHNOLOGY: VOLUME 48, PART 1

Stuart G. Hibben, ed. 1994 284 p

(AD-A293988) Avail: CASI HC A13/MF A03

This bibliopgraphy is a continuing publication of the Cold Regions Bibliography Project in the Science and Technology Division of the Library of Congress. The present volume contains material accessioned between October 1993 and September 1994. It contains full citations of 5642 items, in many cases with abstracts. Indexing for the volume is issued as Volume 48, Part 2. CASI

N95-34421# Army Cold Regions Research and Engineering Lab., Hanover, NH.

BIBLIOGRAPHY ON COLD REGIONS SCIENCE AND TECHNOLOGY: VOLUME 48, PART 2

Stuart G. Hibben, ed. 1994 402 p

(AD-A293993) Avail: CASI HC A18/MF A04

This bibliopgraphy is a continuing publication of the Cold Regions Bibliography Project in the Science and Technology Division of the Library

of Congress. The present volume contains the author and subject indexes to material accessioned between October 1993 and September 1994. The full citations are contained in the companion volume, issued as Volume 48, Part 1. CASI

N95-34794# Army War Coll., Carlisle Barracks, PA.
A CURRICULUM FOR STRATEGY IN THE INFORMATION AGE: CHAOS IN A NEW ERA Strategy Research Project
Dennis K. Miner 1995 56 p
(AD-A295036) Avail: CASI HC A04/MF A01

The information age is much more than digitization. It will bring with it a new culture, one based on a different ideology than the familiar materialism. For strategists to be adequately equipped for this huge paradigm shift, they will require new knowledge and be able to apply it in both worlds simultaneously. Since the entire world is not going through these paradigm shifts, this duality of thought will be required for the foreseeable future. With scientific proof now in hand that the future will remain unpredictable, we must accept the responsibility associated with terminating the quest for certainty. New techniques are required for developing strategy in the information age. Highly skilled practitioners of strategy are essential. When we recruit a fresh young American into the military, we do not expect that person to immediately go to combat. We give that recruit tools and teach him or her how to use them. After individual training is satisfactorily completed, we train them to perform as part of a team. Preparing strategists for their new missions is no less important than training new recruits. The curriculum that I have proposed in this paper would guide the students through the three levels of thinking and hopefully expand their mental capacities for working with indeterminism. I think implementing such a program is likely to produce as high a quality strategist as we observe in the tactical quality of our soldiers. DTIC

N95-34801# Oak Ridge National Lab., TN.
THE DESIGN OF SCALABLE SOFTWARE LIBRARIES FOR DISTRIBUTED MEMORY CONCURRENT COMPUTERS
J. Choi, D. W. Walker, and J. J. Dongarra 1994 9 p Presented at the Parallel Processing Symposium, Cancun, Mexico, 26-29 Apr. 1994
(Contract DE-AC05-84OR-21400)
(DE95-012891; CONF-940451-2) Avail: CASI HC A02/MF A01

This paper describes the design of ScaLAPACK, a scalable software library for performing dense and banded linear algebra computations on distributed memory concurrent computers. The specification of the data distribution has important consequences for interprocessor communication and load balance, and hence is a major factor in determining performance and scalability of the library routines. The block cyclic data distribution is adopted as a simple, yet general-purpose, way of decomposing block-partitioned matrices. Distributed memory versions of the Level 3 BLAS provide an easy and convenient way of implementing the ScaLAPACK routines. DOE

N95-34804 State Univ. of New York, Stony Brook, NY.
A DOCUMENT ANALYSIS SYSTEM Ph.D. Thesis
Jiangying Zhou 1993 114 p
Avail: Univ. Microfilms Order No. DA9417795

Building a fully automated document processing system remains a challenging problem for researchers. The work presented in this thesis expands the document image processing techniques in two aspects: (1) how to decompose a document page into subregions which represent coherent components such as text, graphics, and photographs, without the knowledge on the specific layout model, and (2) how to describe character shapes. Using the geometry properties of background white spaces we have found a way to avoid a costly skew correction in the separation of columns in a document image. An efficient segmentation is thus achieved in the presence of severe tilt. In a study of an important special case of block classification, an interesting blend of theoretical analysis and practical experiments shows that a faster linear algorithm can be devised using properties of the across scanlines correlation to separate photographic regions from text/line-drawing regions. We proposed a hierarchical description method of curve shapes. The method is a result of the work that has been directed towards improving performance of an OCR system. As an application of the description method, we proposed a machine printed character recognition system. We demonstrated that the scheme is very powerful in both encompassing wide variations in the shape of individual characters and in discerning characters of similar shapes. Dissert. Abstr.

N95-34816# Mitre Corp., McLean, VA. Jason Program Office.
SECURITY AND PRIVACY IN THE NII
P. Weinberger, C. Callan, W. Dally, A. Peterson, and W. Press 23 Feb. 1995 39 p Sponsored by ARPA
(AD-A293475; JSR-94-150) Avail: CASI HC A03/MF A01

The National Information Infrastructure (NII) is a vast undertaking to provide a web of networks, computers and databases to communication and information throughout the country. One of the more difficult topics is privacy and security on the NII. These are areas that are crucial to making the NII fully useful for government and for commerce. The JASON study examined technical issues of security and privacy and came to the conclusion that the problems are policy and not technical in nature. That is, the technology exists to provide security and privacy services on the NII but that issues of what services and their implementation must be resolved. The report suggests some steps that ARPA can make to help resolve the policy issues. DTIC

N95-32430*# Southern Methodist Univ., Dallas, TX. Dept. of Electrical Engineering.
THE COMPOSITE CLASSIFICATION PROBLEM IN OPTICAL INFORMATION PROCESSING Final Report
Eric B. Hall *In* NASA. Johnson Space Center, National Aeronautics and Space Administration (NASA)/American Society for Engineering Education (ASEE) Summer Faculty Fellowship Program, 1994, Volume 1 Jul. 1995 13 p (For primary document see N95-32418 12-99)
(Grant NGT-44-005-803)
Avail: CASI HC A03/MF A03

N95-33291*# Institut fuer Spectrochemie und Angewandte Spectroskopie, Dortmund (Germany).
FTP-SERVER FOR EXCHANGE, INTERPRETATION, AND DATABASE-SEARCH OF ION MOBILITY SPECTRA, LITERATURE, PREPRINTS AND SOFTWARE
J. I. Baumbach and A. vonIrmer *In* NASA. Johnson Space Center, Third International Workshop on Ion Mobility Spectrometry Apr. 1995 p A1-A4 (For primary document see N95-33265 12-25)
Avail: CASI HC A01/MF A03

N95-33762*# EROS Data Center, Sioux Falls, SD.
AIRCRAFT SCANNER DATA AVAILABILITY VIA THE VERSION 0 INFORMATION MANAGEMENT SYSTEM
G. R. Mah *In* JPL, Summaries of the Fifth Annual JPL Airborne Earth Science Workshop. Volume 1: AVIRIS Workshop 23 Jan. 1995 p 117-120 (For primary document see N95-33730 12-42)
Avail: CASI HC A01/MF A02

83 ECONOMICS AND COST ANALYSIS

Includes cost effectiveness studies.

N95-33069*# National Aeronautics and Space Administration, Washington, DC.
BUDGET ESTIMATES: FISCAL YEAR 1994. VOLUME 1: AGENCY SUMMARY
1994 357 p
(NASA-TM-110815; NAS 1.15:110815) Avail: CASI HC A16/MF A03

The NASA FY 1994 budget request of $15,265 million concentrates on (1) investing in the development of new technologies including a particularly aggressive program in aeronautical technology to improve the competitive position of the United States, through shared involvement with industry and other government agencies; (2) continuing the nation's premier program of space exploration, to expand our knowledge of the solar system and the universe as well as the earth; and (3) providing safe and assured access to space using both the space shuttle and expendable launch vehicles. Budget estimates are presented for (1) research and development, including space station, space transportation capability development, space science and applications programs, space science, life and microgravity sciences and applications, mission to planet earth, space research and

technology, commercial programs, aeronautics technology programs, safety and mission quality, academic programs, and tracking and data advanced systems; and (2) space operations, including space transportation programs, launch services, and space communications. CASI

N95-33081*# National Aeronautics and Space Administration, Washington, DC.
BUDGET ESTIMATES: FISCAL YEAR 1994. VOLUME 2: CONSTRUCTION OF FACILITIES
1994 233 p
(NASA-TM-110816; NAS 1.15:110816) Avail: CASI HC A11/MF A03

The Construction of Facilities (CoF) appropriation provides contractual services for the repair, rehabilitation, and modification of existing facilities; the construction of new facilities and the acquisition of related collateral equipment; the acquisition or condemnation of real property; environmental compliance and restoration activities; the design of facilities projects; and advanced planning related to future facilities needs. Fiscal year 1994 budget estimates are broken down according to facility location of project and by purpose. CASI

N95-33082*# National Aeronautics and Space Administration, Washington, DC.
BUDGET ESTIMATES: FISCAL YEAR 1994. VOLUME 3: RESEARCH AND PROGRAM MANAGEMENT
1994 192 p
(NASA-TM-110817; NAS 1.15:110817) Avail: CASI HC A09/MF A02

The research and program management (R&PM) appropriation provides the salaries, other personnel and related costs, and travel support for NASA's civil service workforce. This FY 1994 budget funds costs associated with 23 623 full-time equivalent (FTE) work years. Budget estimates are provided for all NASA centers by categories such as space station and new technology investments, space flight programs, space science, life and microgravity sciences, advanced concepts and technology, center management and operations support, launch services, mission to planet earth, tracking and data programs, aeronautical research and technology, and safety, reliability, and quality assurance. CASI

84 LAW, POLITICAL SCIENCE AND SPACE POLICY

Includes NASA appropriation hearings; aviation law; space law and policy; international law; international cooperation; and patent policy.

No abstracts in this category.

85 URBAN TECHNOLOGY AND TRANSPORTATION

Includes applications of space technology to urban problems; technology transfer; technology assessment; and surface and mass transportation.

For related information see also *03 Air Transportation and Safety, 16 Space Transportation,* and *44 Energy Production and Conversion.*

N95-33489*# National Aeronautics and Space Administration. John F. Kennedy Space Center, Cocoa Beach, FL.
LOGISTICS OPERATIONS MANAGEMENT CENTER: MAINTENANCE SUPPORT BASELINE (LOMC-MSB)
R. Kurrus and F. Stump 3 Jan. 1995 53 p Revised
(NASA-TM-110624; NAS 1.15:110624; K-SS-12.12-Rev-A) Avail: CASI HC A04/MF A01

The Logistics Operations Management Center Maintenance Support Baseline is defined. A historical record of systems, applied to and deleted from, designs in support of future management and/or technical analysis is provided. All Flight elements, Ground Support Equipment, Facility Systems and Equipment and Test Support Equipment for which LOMC has responsibilities at Kennedy Space Center and other locations are listed. International Space Station Alpha Program documentation is supplemented. The responsibility of the Space Station Launch Site Support Office is established. Derived from text

N95-33127# Honeywell Technology Center, Minneapolis, MN.
DUAL USE: OPPORTUNITIES, PAYOFFS, AND CHALLENGES
Thomas Cunningham *In* AGARD, Dual Usage in Military and Commercial Technology in Guidance and Control Mar. 1995 7 p (For primary document see N95-33126 12-31)
Copyright Avail: CASI HC A02/MF A02

88 SPACE SCIENCES (GENERAL)

No abstracts in this category.

89 ASTRONOMY

Includes radio, gamma-ray, and infrared astronomy, and astrometry.

N95-32835*# Applied Research Corp., Landover, MD.
ROSAT SURVEY OF EMISSION FROM Be STARS Final Report
Carol Grady 16 Sep. 1993 35 p
(Grant NAG5-1580)
(NASA-CR-199086; NAS 1.26:199086; ARC-R93-210) Avail: CASI HC A03/MF A01

ROSAT pointed observations of bright, classical Be stars have demonstrated that detection of soft x-rays at a level expected for normal B stars of comparable T(sub eff) and luminosity is anti-correlated with the presence of episodes of enhanced mass ejection and formation of a dense, moderately ionized equatorial circumstellar disk. At epochs of lower than average disk column density, x-ray flaring has been detected in 2 Be stars, lambda Eri and pi Aqr. Author

N95-32837 California Univ., Riverside, CA.
GAMMA RAY IMAGING OF THE CRAB AND VALE REGIONS WITH THE UCR DOUBLE-COMPTON TELESCOPE Ph.D. Thesis
Abderrezak Sarmouk 1994 183 p
Avail: Univ. Microfilms Order No. DA9422897

Results are presented for a new imaging technique applied to the reconstruction of celestial gamma-ray source images. This algorithm uses an expectation maximization maximum likelihood method (EMML) and is applied to the UCR double Compton telescope. First, this technique is used with simulated data and preflight calibration data. It is then applied to the Crab pulsar/Nebula, and Vela regions. These data were collected in 1988 from Alice Springs, Australia and in 1989 from Fort Summer, NM. An excess of 1200 counts from the Crab has been detected at 4 sigma in the energy range 1-30 MeV, 920 counts at 3.1 sigma in the energy range1-5 MeV and 202 counts at 7 sigma in the energy range 5-10 MeV. The total measured flux from 1-30 MeV is (2.0 +/- 0.5) x 10(exp -3) photons/(sq cm.s). Pulsar analysis was also performed. The pulsed flux in the energy range 1-30 MeV is equal to (1.4 plus or minus 0.4) x 10(exp -4) photons/(sq cm.s) Only upper limits for the pulsed flux have been placed in the individual energy ranges of 5-10 MeV and 10-30 MeV. Our results are compared with other experiments. The Vela region image shows an excess of 575 counts in the energy range 1.1-30 MeV at 2.7 sigma 340 counts at 2.4 sigma in the energy range 1.1-5 MeV and 130 counts from 5 to 10 MeV at 2.2 sigma. No excess is seen above 10 MeV.The total flux for the energy range 1.1 to 30 MeV is equal to (1.0 plus or minus 0.4) x 10(exp -3) photons/(sq cm.s). The Vela pulsed flux in the energy range 1.1 to 30 MeV is equal to (3.5 +/- 1.4) x 10(exp -4) photons/(sq cm.s). The ratio

is pulsed flux to total flux in the energy range 1.3-30 MeV, is found to be equal to 0.35 plus or minus 0.2. Dissert. Abstr.

N95-34753# Air Force Inst. of Tech., Wright-Patterson AFB, OH.
RR LYRAE VARIABLE STARS IN THE CCD/TRANSIT INSTRUMENT SURVEY Ph.D. Thesis
Charles J. Wetterer Jul. 1995 375 p
(AD-A294138; AFIT/CI/CIA-95-002D) Avail: CASI HC A16/MF A03

RR Lyrae variable stars have long been recognized as important tools in probing the mass, chemical distribution and kinematics of the Galaxy from the inner recesses of the nuclear bulge to the outer environs of the distant Galactic halo. This dissertation chronicles an RR Lyrae variable star survey from a thorough description of the initial observations with the CCD/Transit Instrument (CTI), to an examination of RR Lyrae space density and the Galactic mass using the discovered RR Lyrae stars. The RR Lyrae space density as a function f Galactocentric distance is shown to be a power-law function (R-3 to -3.5) and consistent with an ellipsoidal distribution in the nuclear bulge and more spherically symmetric distribution in the Galactic halo. The unique area of the CTI survey and comparison to other RR Lyrae surveys verifies this function is valid throughout the Galactic halo and over the range of Galactocentric distances sampled (0.6 less than R less than 40 kpc). Local underdensities and overdensities of RR Lyrae stars are discussed, including a possible resonance with the Magallenic Clouds (R 50 kpc). DTIC

N95-34221*# Boston Univ., Boston, MA. Center for Space Physics.
DEVELOPMENT OF A TOOL-SET FOR SIMULTANEOUS, MULTI-SITE OBSERVATIONS OF ASTRONOMICAL OBJECTS Abstract Only
Supriya Chakrabarti, J. Garrett Jernigan (California Univ., Berkeley, CA.), and Herman L. Marshall (California Univ., Berkeley, CA.) *In* Colorado Univ., Applied Information Systems Research Program (AISRP) Workshop 3 Meeting Proceedings 1993 1 p (For primary document see N95-34218 12-82)
Avail: CASI HC A01/MF A03

90 ASTROPHYSICS

Includes cosmology; celestial mechanics; space plasmas; and interstellar and interplanetary gases and dust.

For related information see also *75 Plasma Physics*.

N95-32597# Lawrence Livermore National Lab., Livermore, CA.
STATUS OF THE LARGE-SCALE DARK-MATTER AXION SEARCH
K. vanBibber, C. Hagmann, W. Stoeffl, E. Daw, L. Rosenberg, P. Sikivie, N. Sullivan, D. Tanner, D. Moltz, and R. Tighe et al Sep. 1994 15 p Presented at the International Conference on Critique of the Source of Dark Matter in the Universe, Bel Air, CA, 16-18 Feb. 1994
(Contracts W-7405-eng-48; DE-AC03-76SF-00098; DE-AC02-76CH-03000; DE-FC02-94ER-40818; DE-FG05-86ER-40272; DE-FG02-90ER-40560)
(DE95-008828; UCRL-JC-118357; CONF-9402136-1) Avail: CASI HC A03/MF A01

If axions constitute the dark matter of our galactic halo they can be detected by their conversion into monochromatic microwave photons in a high-Q microwave cavity permeated by a strong magnetic field. A large-scale experiment is under construction at LLNL to search for halo axions in the mass range 1.3 - 13 (mu)eV, where axions may constitute closure density of the universe. The search builds upon two pilot efforts at BNL and the University of Florida in the late 1980's, and represents a large improvement in power sensitivity (approximately) 50 both due to the increase in magnetic volume (B(sup 2)V = 14 T(sup 2)m(sup 3)), and anticipated total noise temperature T(sub n) (approximately) 3K. This search will also mark the first use of multiple power-combined cavities to extend the mass range accessible by this technique. Data will be analyzed in two parallel streams. In the first, the resolution of the power spectrum will be sufficient to resolve the expected width of the overall axion line, (approximately)(bigcirc) (1kHz). In the second, the resolution will be (bigcirc)(0.01-1 Hz) to look for extremely narrow substructure reflecting the primordial phase-space of the axions during infall. This experiment will be the first to have the required sensitivity to detect axions, for plausible axion models. DOE

N95-32913*# Washington Univ., Saint Louis, MO. Dept. of Physics.
ANALYSIS OF LDEF EXPERIMENT AO187-2 CHEMICAL AND ISOTOPIC MEASUREMENTS OF MICROMETEOROIDS BY SECONDARY ION MASS SPECTROMETRY Final Report
Ernst Zinner [1995] 88 p
(Grant NAG1-1174)
(NASA-CR-198849; NAS 1.26:198849) Avail: CASI HC A05/MF A01

#Experiment AO187-2, that was flown on board the Long Duration Exposure Facility(LDEF), was designed to measure the chemical and isotopic compositions of interplanetary dust impinging on the spacecraft from outer space. Information on the nature and composition of orbital debris was also anticipated. The spacecraft maintained a constant orientation with respect to its velocity vector thereby defining leading and trailing edges that faced respectively into and away from the direction of motion. Arrays of individual capture cells each 80.8 sq cm in size and totaling 237 in number were exposed on both the leading and trailing edges of LDEF. Each cell consisted of a pure Ge target surface slightly separated from a thin (2.5 micrometers) metallized plastic 'entrance foil.' The basic concept was that incoming projectiles would penetrate the foil, strike the Ge target plate at high velocity producing a vapor-liquid cloud that would re-deposit material on the underside of the plastic foil. This material would then be analyzed using the sensitive surface analysis technique of Secondary Ion Mass Spectrometry (SIMS). In practice, most of the plastic entrance foils failed during the extended period of orbital exposure probably due to a combination of UV embrittlement, large densities of impact events and (for the leading edge) the effects of atomic oxygen erosion in orbit. However the foils failed gradually and most remained in place on the capture cells for a significant fraction of the duration of the flight . Because most of the impactors were small (less than 10 micrometers) they were heated and dispersed in traversing the entrance foils producing clouds of molten droplets and vapor that produced easily identifiable 'extended impacts' on the Ge target plates. Fortunately, it proved possible to make ion probe measurements of projectile compositions from material deposited on the Ge in the extended impact structures. Derived from text

N95-33211# Los Alamos National Lab., NM. Earth and Environmental Sciences Div.
HISTORICAL DETECTION OF ATMOSPHERIC IMPACTS BY LARGE BOLIDES USING ACOUSTIC-GRAVITY WAVES
Douglas O. ReVelle 1995 24 p Presented at the International Conference on Near-earth Objects, New York, NY, 24-26 Apr. 1995
(Contract W-7405-eng-36)
(DE95-010864; LA-UR-95-1263; CONF-9504147-1) Avail: CASI HC A03/MF A01

During the period from about 1960 to the early 1980's a number of large bolides (meteor-fireballs) entered the atmosphere which were sufficiently large to generate blast waves during their drag interaction with the air. For example, the remnant of the blast wave from a single kiloton class event was subsequently detected by up to six ground arrays of microbarographs which were operated by the U.S. Air Force during this pre-satellite period. Data have also been obtained from other sources during this period as well and are also discussed in this summary of the historical data. The Air Force data have been analyzed in terms of their observable properties in order to infer the influx rate of NEO's (near-Earth objects) in the energy range from 0.2 to 1100 kt. The determined influx is in reasonable agreement with that determined by other methods currently available such as Rabinowitz, Ceplecha, and by Chapman and Morrison despite the fact that due to sampling deficiencies only a portion of the 'true' flux of large bodies has been obtained by this method, i.e., only sources at relatively low elevations have been detected. Thus the weak, fragile cometary bodies which do not penetrate the atmosphere as deeply are less likely to have been sampled by this type of detection system. Future work using the proposed C.T.B.T. (Comprehensive Test Ban Treaty) global scale infrasonic network will be likely to improve upon this early estimate of the global influx of NEO's considerably. DOE

N95-33261*# Computer Sciences Corp., Calverton, MD.
COMPTON OBSERVATORY OBSERVATIONS OF CLUSTERS OF GALAXIES AND EXTRAGALACTIC RADIO SOURCES Final Report
Mar. 1995 8 p
(NASA Order S-93074-E)

(NASA-CR-189431; NAS 1.26:189431; RHPU-0474) Avail: CASI HC A02/MF A01

This task involved the investigation of the emission of clusters of galaxies, particularly those which contain extended radio emission, in the gamma-ray region of the spectrum. Observations were made of several clusters using the Compton Observatory EGRET instrument. For each cluster a measured flux or upper limit on the gamma-ray flux was obtained. In only one case, Abell 2199, was there a significant measured flux. This source is spatially confused with a know blazar in the field of view. The observation is consistent with all emissions being from the blazar. Author

N95-33262*# Computer Sciences Corp., Calverton, MD.
BERYLLIUM AND BORON ABUNDANCES IN POPULATION II STARS Final Report
Mar. 1995 5 p
(NASA Order S-97228-E)
(NASA-CR-189434; NAS 1.26:189434; RHPU-0429) Avail: CASI HC A01/MF A01

The scientific focus of this program was to undertake UV spectroscopic abundance analyses of extremely metal poor stars with attention to determining abundances of light elements such as beryllium and boron. The abundances are likely to reflect primordial abundances within the early galaxy and help to constrain models for early galactic nucleosynthesis. The general metal abundances of these stars are also important for understanding stellar evolution. Author

N95-33625# California Univ., Berkeley. Lawrence Berkeley Lab, CA. Engineering Div.
ADVANCED FAR INFRARED DETECTOR AND DOUBLE DONOR STUDIES IN Ge M.S. Thesis
Christopher S. Olsen Dec. 1994 93 p
(Contracts NASw-17605; DE-AC03-76SF-00098)
(DE95-011261; LBL-36619; UC-404) Avail: CASI HC A05/MF A01

This has application to astronomy and astrophysics. Selenium in Ge has been studied with a doping technique which limits complex formation. Only one ionization level has been found to correspond to selenium, which presumably occupies a substitutional site. This level is extremely unstable and its concentration decreases after annealing at 400 C. Future work is planned to anneal the fast neutron damage before much selenium has formed in the (sup 74/76)Ge samples. It is expected that the observed selenium level can be better characterized and the missing selenium level is more likely to be discovered if other defects are removed before (sup 77)Se formation. DOE

N95-34216# Texas Univ., Austin, TX. Fusion Research Center.
SINUOUS OSCILLATIONS AND STEADY WARPS OF POLYTROPIC DISKS
N. J. Balmforth and E. A. Spiegel (Columbia Univ., New York, NY.) May 1995 22 p Submitted for publication
(Contract DE-FG05-80ET-53088)
(DE95-013473; DOE/ET-53088/706; IFSR-706) Avail: CASI HC A03/MF A01

In an asymptotic development of the equations governing the equilibria and linear stability of rapidly rotating polytropes we employed the slender aspect of these objects to reduce the three-dimensional partial differential equations to a somewhat simpler, ordinary integro-differential form. The earlier calculations dealt with isolated objects that were in centrifugal balance, that is the centrifugal acceleration of the configuration was balanced largely by self gravity with small contributions from the pressure gradient. Another interesting situation is that in which the polytrope rotates subject to externally imposed gravitational fields. In astrophysics, this is common in the theory of galactic dynamics because disks are unlikely to be isolated objects. The dark halos associated with disks also provide one possible explanation of the apparent warping of many galaxies. If the axis of the highly flattened disk is not aligned with that of the much less flattened halo, then the resultant torque of the halo gravity on the disk might provide a nonaxisymmetric distortion or disk warp. Motivated by these possibilities we shall here build models of polytropic disks of small but finite thickness which are subjected to prescribed, external gravitational fields. First we estimate how a symmetrical potential distorts the structure of the disk, then we examine its sinuous oscillations to confirm that they freely decay, hence suggesting that a warp must be externally forced. Finally, we consider steady warps of the disk plane when the axis of the disk does not coincide with that of the halo. DOE

N95-34561# Oregon Univ., Eugene, OR. Dept. of Physics.
HIGH SPEED VARIABILITY IN X-RAY BINARY SYSTEMS Final Report, 15 Mar. 1994 - 14 Mar. 1995
James N. Imamura 1 May 1995 3 p
(Contract N00014-94-G-0012)
(AD-A294634) Avail: CASI HC A01/MF A01

Portions of this work were performed in collaboration with Drs. M. Wolff and K. Wood of the Naval Research Laboratory. We are engaged in a long-term project to develop numerical models for the high-speed variability seen in the energy output of the x-ray binary systems, in general, and for the white dwarf x-ray binary systems known as the AM Herculis objects (from hereon the AM Her objects), in particular, and to develop modern tools for the analysis of time series data. DTIC

N95-33270*# National Aeronautics and Space Administration. Ames Research Center, Moffett Field, CA.
THE MINI-CIDEX GC/IMS: ANALYSIS OF COMETARY ICE AND DUST
Daniel R. Kojiro, Glenn C. Carle, Donald E. Humphry (Search for Extraterrestrial Intelligence Inst., Mountain View, CA.), Maxine Shao (Search for Extraterrestrial Intelligence Inst., Mountain View, CA.), and Nori Takeuchi (TMA/Norcal, Richmond, CA.) *In* NASA. Johnson Space Center, Third International Workshop on Ion Mobility Spectrometry Apr. 1995 p 57-65 (For primary document see N95-33265 12-25)
Avail: CASI HC A02/MF A03

N95-34222*# California Inst. of Tech., Pasadena, CA. Dept. of Astronomy.
MULTIVARIATE STATISTICAL ANALYSIS SOFTWARE TECHNOLOGIES FOR ASTROPHYSICAL RESEARCH INVOLVING LARGE DATA BASES Abstract Only
George Djorgovski *In* Colorado Univ., Applied Information Systems Research Program (AISRP) Workshop 3 Meeting Proceedings 1993 1 p (For primary document see N95-34218 12-82)
Avail: CASI HC A01/MF A03

91 LUNAR AND PLANETARY EXPLORATION

Includes planetology; and manned and unmanned flights.

For spacecraft design or space stations see *18 Spacecraft Design, Testing and Performance.*

N95-32700*# National Aeronautics and Space Administration. Ames Research Center, Moffett Field, CA.
REDUCTION AND ANALYSIS OF SEASONS 15 AND 16 (1991 - 1992) PIONEER VENUS RADIO OCCULATION DATA AND CORRELATIVE STUDIES WITH OBSERVATIONS OF THE NEAR INFRARED EMISSION OF VENUS Technical Report, 1 Apr. 1992 - 31 May 1995
Jon M. Jenkins 31 May 1995 17 p
(Contract NCC2-753)
(NASA-CR-199071; NAS 1.26:199071) Avail: CASI HC A03/MF A01

In this study, we sought to characterize variations in the abundance and distribution of subcloud H2SO4(g) in the Venus atmosphere by using a number of 13cm radio occultation measurements conducted with the Pioneer Venus Orbiter near the inferior conjunction of 1991. A total of ten data sets were examined and analyzed, producing vertical profiles of temperature and pressure in the neutral atmosphere, and sulfuric acid vapor abundance below the main cloud layer. Two of the vertical profiles of the abundance of H2SO4(g) were correlated with NIR images of the night side of Venus made during the same period of time by Boris Ragent (under a separate PVO Guest Investigator Grant). Initially, we had hoped that the combination of these two different types of data would make it possible to constrain or identify the composition of the large particles causing the features observed in the NIR images. However, the sparseness of the radio occultation data set, combined with the sparseness of the NIR data set (one image per day over an 8 day period) made it impossible to draw strong conclusions. Considered on their own, however, the

parameters retrieved from the radio occultation experiments are valuable science products. Derived from text

N95-33390# Texas Univ., Austin, TX. Inst. for Fusion Studies.
NONLINEAR SYMMETRIC STABILITY OF PLANETARY ATMOSPHERES
J. C. Bowman and T. G. Shepherd (Toronto Univ., Ontario.) Nov. 1994 32 p
(Contract DE-FG05-80ET-53088)
(DE95-012133; DOE/ET-53088/669; IFSR-669) Avail: CASI HC A03/MF A01

The energy-Casimir method is applied to the problem of symmetric stability in the context of a compressible, hydrostatic planetary atmosphere with a general equation of state. Linear stability criteria for symmetric disturbances to a zonally symmetric baroclinic flow are obtained. In the special case of a perfect gas the results of Stevens (1983) are recovered. Nonlinear stability conditions are also obtained that, in addition to implying linear stability, provide an upper bound on a certain positive-definite measure of disturbance amplitude. DOE

92 SOLAR PHYSICS

Includes solar activity, solar flares, solar radiation and sunspots.
For related information see *93 Space Radiation.*

N95-32963 National Geophysical Data Center, Boulder, CO.
SOLAR-GEOPHYSICAL DATA NUMBER 607, MARCH 1995. PART 1 (PROMPT REPORTS). DATA FOR JANUARY, FEBRUARY 1995 AND LATE DATA
Helen E. Coffey, ed. Mar. 1995 131 p See also PB95-200853 and Part 2, PB95-216800 Limited Reproducibility: More than 20% of this document may be affected by microfiche quality
(ISSN 0038-0911)
(PB95-216388; SGD-607-PT-1; LC-79-640375) Avail: CASI HC A07

Late data and January and February 1995 solar and geophysical data reports are contained in this report and include: Solar-Terrestrial Environment; IUWDS Alert Periods (Advance and Worldwide); Solar Activity Indices; Solar Flares; Solar Radio Emission; Stanford Mean Solar Magnetic Field; and GOES-7 Daily Electron Fluence. NTIS

N95-32964# National Geophysical Data Center, Boulder, CO.
SOLAR-GEOPHYSICAL DATA NUMBER 607, MARCH 1995: PART 2 (COMPREHENSIVE REPORTS). DATA FOR SEPTEMBER 1994 AND MISCELLANEOUS
Helen E. Coffey, ed. Mar. 1995 69 p See also PB95-200861 and Part 1, PB95-216388
(ISSN 0038-0911)
(PB95-216800; SGD-607-PT-2; LC-79-640375) Avail: CASI HC A04/MF A01

The Solar-geophysical data for September 1994 and other miscellaneous data are feature and include: Part II (Comprehensive Reports)-Detailed Index for 1994-95; Data for September 1994; Miscellaneous Data including Total Solar Irradiance ERBS Oct 84-Dec 94; Solar UV SOLSTICE Data Oct 91-Sep 94; Lyman-alpha HI121.6nm; 200-205 nm Integrated Flux; Ca II 393.3 nm Core-to-wing Ratio; and Mg II 280.0 nm Core-to-wing Ratio. NTIS

93 SPACE RADIATION

Includes cosmic radiation; and inner and outer earth's radiation belts.
For biological effects of radiation see *52 Aerospace Medicine.* For theory see *73 Nuclear and High-Energy Physics.*

N95-33499*# Columbia Univ., New York, NY. Dept. of Astronomy and Physics.
GRO: STUDIES OF HIGH ENERGY PULSARS WITH EGRET Annual Status Report, 15 Jul. 1994 - 14 Jul. 1995
Malvin Ruderman Jul. 1995 18 p
(Grant NAG5-2016)
(NASA-CR-199130; NAS 1.26:199130) Avail: CASI HC A03/MF A01

A reported e(+/-) annihilation line from the Crab pulsar is described on in this annual report, along with a astronomical model that was investigated theoretically and that displays all of the following properties discovered about this line:very strong (approximately 10(exp 40)e(+/-) annihilations/sec); redshifted (by about 70 KeV relative to mc(exp 2) = 511 KeV); and very narrow (width approximately 10 KeV). A draft of the paper based on this research entitled, 'Pair production in the magnetosphere of the Crab pulsar and a pulsed e(+/-) annihilation gamma-ray line' is included. CASI

N95-33916*# George Mason Univ., Fairfax, VA.
TIME CORRELATIONS BETWEEN LOW AND HIGH ENERGY GAMMA RAYS FROM DISCRETE SOURCES Final Report
R. W. Ellsworth 1 May 1995 22 p
(Grant NAG5-1567)
(NASA-CR-199214; NAS 1.26:199214) Avail: CASI HC A03/MF A01

Activities covered the following areas: (1) continuing analysis of the Cygnus Experiment data on the shadowing of cosmic rays by the moon and sun, which led to a direct confirmation of the angular resolution of the CYGNUS EAS array; and (2) development of analysis methods for the daily search overlapping with EGRET targets. To date, no steady emission of ultrahigh energy (UHE) gamma rays from any source has been detected by the Cygnus Experiment, but some evidence for sporadic emission had been found. Upper limits on steady fluxes from 49 sources in the northern hemisphere have been published. In addition, a daily search of 51 possible sources over the interval April 1986 to June 1992 found no evidence for emission. From these source lists, four candidates were selected for comparison with EGRET data. Derived from text

99 GENERAL

N95-32418*# National Aeronautics and Space Administration. Lyndon B. Johnson Space Center, Houston, TX.
NATIONAL AERONAUTICS AND SPACE ADMINISTRATION (NASA)/AMERICAN SOCIETY FOR ENGINEERING EDUCATION (ASEE) SUMMER FACULTY FELLOWSHIP PROGRAM, 1994, VOLUME 1
Richard Bannerot and Donn G. Sickorez Jul. 1995 202 p Fellowship Program held in Houston, TX
(Grant NGT-44-001-800)
(NASA-CR-188410; NAS 1.26:188410) Avail: CASI HC A10/MF A03

The JSC NASA/ASEE Summer Faculty Fellowship Program was conducted by Texas A&M University and JSC. The objectives of the program, which began nationally in 1964 and at JSC in 1965 are to: (1) further the professional knowledge of qualified engineering and science faculty members, (2) stimulate an exchange of ideas between participants and NASA, (3) enrich and refresh the research and teaching activities of participants' institutions, and (4) contribute to the research objectives of the NASA centers. Each faculty fellow spent at least 10 weeks at JSC engaged in a research project in collaboration with a NASA JSC colleague. This document is a compilation of the final reports on the research projects completed by the faculty fellows during the summer of 1994. For individual titles, see N95-32419 through N95-32434.

N95-32419*# National Aeronautics and Space Administration. Lyndon B. Johnson Space Center, Houston, TX.
CHARACTERIZATION OF MICROGRAVITY EFFECTS ON BONE STRUCTURE AND STRENGTH USING FRACTAL ANALYSIS c52
Raj S. Acharya (State Univ. of New York, Buffalo, NY.) and Linda Shackelford *In its* National Aeronautics and Space Administration (NASA)/American Society for Engineering Education (ASEE) Summer Faculty Fellowship Program, 1994, Volume 1 Jul. 1995 15 p (For primary document see N95-32418 12-99)
Avail: CASI HC A03/MF A03

The effect of micro-gravity on the musculoskeletal system has been well studied. Significant changes in bone and muscle have been shown after long term space flight. Similar changes have been demonstrated due to bed rest. Bone demineralization is particularly profound in weight bearing bones. Much of the current techniques to monitor bone condition use bone mass measurements. However, bone mass measurements are not

reliable to distinguish Osteoporotic and Normal subjects. It has been shown that the overlap between normals and osteoporosis is found for all of the bone mass measurement technologies: single and dual photon absorptiometry, quantitative computed tomography and direct measurement of bone area/volume on biopsy as well as radiogrammetry. A similar discordance is noted in the fact that it has not been regularly possible to find the expected correlation between severity of osteoporosis and degree of bone loss. Structural parameters such as trabecular connectivity have been proposed as features for assessing bone conditions. In this report, we use fractal analysis to characterize bone structure. We show that the fractal dimension computed with MRI images and X-Ray images of the patella are the same. Preliminary experimental results show that the fractal dimension computed from MRI images of vertebrae of human subjects before bedrest is higher than during bedrest. Author

N95-32420*# Louisiana Tech Univ., Ruston, LA. Dept. of Civil Engineering.

APPLICATION OF IMPACT DAMPERS IN VIBRATION CONTROL OF FLEXIBLE STRUCTURES Final Report **c39**

Fred A. Akl and Aamir S. Butt *In* NASA. Johnson Space Center, National Aeronautics and Space Administration (NASA)/American Society for Engineering Education (ASEE) Summer Faculty Fellowship Program, 1994, Volume 1 Jul. 1995 15 p (For primary document see N95-32418 12-99)

(Grant NGT-44-005-803)

Avail: CASI HC A03/MF A03

Impact dampers belong to the category of passive vibration devices used to attenuate the vibration of discrete and continuous systems. An impact damper generally consists of a mass which is allowed to travel freely between two defined stops. Under the right conditions, the vibration of the structure to which the impact damper is attached will cause the mass of the impact damper to strike the structure. Previous analytical and experimental research work on the effect of impact dampers in attenuating the vibration of discrete and continuous systems have demonstrated their effectiveness. It has been shown in this study that impact dampers can increase the intrinsic damping of a lightly-damped flexible structure. The test structure consists of a slender flexible beam supported by a pin-type support at one end and supported by a linear helical flexible spring at another location. Sinusoidal excitation spanning the first three natural frequencies was applied in the horizontal plane. The orientation of the excitation and the test structure in the horizontal plane minimizes the effect of gravity on the behavior of the test structure. The excitation was applied using a linear sine sweep technique. The span of the test structure, the mass of the impact damper, the distance of travel, and the location of the impact damper along the span of the test structure were varied. The damping ratio are estimated for sixty test configurations. The results show that the impact damper significantly increases the damping ratio of the test structure. Statistical analysis of the results using the method of multiple linear regression indicates that a reasonable fit has been accomplished. It is concluded that additional experimental analysis of flexible structures in microgravity environment is needed in order to achieve a better understanding of the behavior of impact damper under conditions of microgravity. Numerical solution of the behavior of flexible structures equipped with impact dampers is also needed to predict stresses and deformations under operating conditions of microgravity in space applications. Author

N95-32421*# Texas Technological Univ., Lubbock, TX. Dept. of Mechanical Engineering.

CERTIFICATION OF A HYBRID PARAMETER MODEL OF THE FULLY FLEXIBLE SHUTTLE REMOTE MANIPULATOR SYSTEM Final Report **c37**

Alan A. Barhorst *In* NASA. Johnson Space Center, National Aeronautics and Space Administration (NASA)/American Society for Engineering Education (ASEE) Summer Faculty Fellowship Program, 1994, Volume 1 Jul. 1995 10 p (For primary document see N95-32418 12-99)

(Grant NGT-44-005-803)

Avail: CASI HC A02/MF A03

The development of high fidelity models of mechanical systems with flexible components is in flux. Many working models of these devices assume the elastic motion is small and can be superimposed on the overall rigid body motion. A drawback associated with this type of modeling technique is that it is required to regenerate the linear modal model of the device if the elastic motion is sufficiently far from the base rigid motion. An advantage to this type of modeling is that it uses NASTRAN modal data which is the NASA standard means of modal information exchange. A disadvantage to the linear modeling is that it fails to accurately represent large motion of the system, unless constant modal updates are performed. In this study, which is a continuation of a project started last year, the drawback of the currently used modal snapshot modeling technique is addressed in a rigorous fashion by novel and easily applied means.

Author

N95-32422*# Mount Holyoke Coll., South Hadley, MA. Dept. of Biological Sciences.

THE ROLE OF THE VESTIBULAR SYSTEM IN MANUAL TARGET LOCALIZATION Final Report **c53**

Susan R. Barry and S. Alyssa Mueller *In* NASA. Johnson Space Center, National Aeronautics and Space Administration (NASA)/American Society for Engineering Education (ASEE) Summer Faculty Fellowship Program, 1994, Volume 1 Jul. 1995 14 p (For primary document see N95-32418 12-99)

(Grant NGT-44-005-803)

Avail: CASI HC A03/MF A03

Astronauts experience perceptual and sensory-motor disturbances during spaceflight and immediately after return to the 1-g environment of Earth. During spaceflight, sensory information from the eyes, limbs and vestibular organs is reinterpreted by the central nervous system so that astronauts can produce appropriate body movements in microgravity. Alterations in sensory-motor function may affect eye-head-hand coordination and, thus, the crewmember's ability to manually locate objects in extrapersonal space. Previous reports have demonstrated that crewmembers have difficulty in estimating joint and limb position and in pointing to memorized target positions on orbit and immediately postflight. One set of internal cues that may assist in the manual localization of objects is information from the vestibular system. This system contributes to our sense of the body's position in space by providing information on head position and movement and the orientation of the body with respect to gravity. Research on the vestibular system has concentrated on its role in oculo-motor control. Little is known about the role that vestibular information plays in manual motor control, such as reaching and pointing movements. Since central interpretation of vestibular information is altered in microgravity, it is important to determine its role in this process. This summer, we determined the importance of vestibular information in a subject's ability to point accurately toward a target in extrapersonal space. Subjects were passively rotated across the earth-vertical axis and then asked to point back to a previously-seen target. In the first paradigm, the subjects used both visual and vestibular cues for the pointing response, while, in the second paradigm, subjects used only vestibular information. Subjects were able to point with 85 percent accuracy to a target using vestibular information alone. We infer from this result that vestibular input plays a role in the spatial programming of manual responses. Author

N95-32423*# Louisiana Tech Univ., Ruston, LA. Dept. of Electrical Engineering.

MODELING OF DC SPACECRAFT POWER SYSTEMS Final Report **c20**

F. C. Berry *In* NASA. Johnson Space Center, National Aeronautics and Space Administration (NASA)/American Society for Engineering Education (ASEE) Summer Faculty Fellowship Program, 1994, Volume 1 Jul. 1995 9 p (For primary document see N95-32418 12-99)

(Grant NGT-44-005-803)

Avail: CASI HC A02/MF A03

Future spacecraft power systems must be capable of supplying power to various loads. This delivery of power may necessitate the use of high-voltage, high-power dc distribution systems to transmit power from the source to the loads. Using state-of-the-art power conditioning electronics such as dc-dc converters, complex series and parallel configurations may be required at the interface between the source and the distribution system and between the loads and the distribution system. This research will use state-variables to model and simulate a dc spacecraft power system. Each component of the dc power system will be treated as a multiport network, and a state model will be written with the port voltages as the inputs. The state model of a component will be solved independently from the other components using its state transition matrix. A state-space averaging method

is developed first in general for any dc-dc switching converter, and then demonstrated in detail for the particular case of the boost power stage. General equations for both steady-state (dc) and dynamic effects (ac) are obtained, from which important transfer functions are derived and applied to a special case of the boost power stage. Author

N95-32424*# Houston Univ.-Clear Lake, Houston, TX. Dept. of Natural and Applied Sciences.

IMAGE ANALYSIS USED TO COUNT AND MEASURE ETCHED TRACKS FROM IONIZING RADIATION **c72**

George E. Blanford and Cindy K. Schulz *In* NASA. Johnson Space Center, Houston, National Aeronautics and Space Administration NASA)/American Society for Engineering Education (ASEE) Summer Faculty Fellowship Program, 1994, Volume 1 Jul. 1995 13 p (For primary document see N95-32418 12-99)

Avail: CASI HC A03/MF A03

We have developed techniques to use digitized scanning electron micrographs and computer image analysis programs to measure track densities in lunar soil grains and plastic dosimeters. Tracks in lunar samples are formed by highly ionizing solar energetic particles and cosmic rays during near surface exposure on the Moon. The track densities are related to the exposure conditions (depth and time). Distributions of the number of grains as a function of their track densities can reveal the modality of soil maturation. We worked on two samples identified for a consortium study of lunar weathering effects, 61221 and 67701. They were prepared by the lunar curator's staff as polished grain mounts that were etched in boiling 1 N NaOH for 6 h to reveal tracks. We determined that backscattered electron images taken at 10 percent contrast and approximately 50 percent brightness produced suitable high contrast images for analysis. We used the NIH Image program to cut out areas that were unsuitable for measurement such as edges, cracks, etc. We ascertained a gray-scale threshold of 25 to separate tracks from background. We used the computer to count everything that was two pixels or greater in size and to measure the area to obtain track densities. We found an excellent correlation with manual measurements for track densities below 1 x 10(exp 8) cm(exp -2). For track densities between 1 x 10(exp 8) cm(exp -2) to 1 x 10(exp 9) cm(exp -2) we found that a regression formula using the percentage area covered by tracks gave good agreement with manual measurements. We determined the track density distributions for 61221 and 67701. Sample 61221 is an immature sample, but not pristine. Sample 67701 is a submature sample that is very close to being fully mature. Because only 10 percent of the grains have track densities less than 10(exp 9) cm(exp -2), it is difficulty to determine whether the sample matured in situ or is a mixture of a mature and a submature soil. Although our analysis of plastic dosimeters is at an early stage of development, results are encouraging. The dosimeter was etched in 6.25 N NaOH at 70 deg C for 16 h. We took 200x secondary electron images of the sample and used the NIH Image software to count and measure major and minor diameters of the etched tracks. We calculated the relative track etch rate from a formula that relates it to the major and minor diameters. We made a histogram of the number of tracks versus their relative etch rate. The relative track etching rate is proportional to the linear energy transfer of the particle. With appropriate calibration experiments, the histogram could be used to calculate the radiation dose. Author

N95-32425*# Texas A&M Univ., Galveston, TX. Dept. of Maritime Systems Engineering.

UNIFIED APPROACH FOR INCOMPRESSIBLE FLOWS Final Report **c34**

Tyne-Hsien Chang *In* NASA. Johnson Space Center, National Aeronautics and Space Administration (NASA)/American Society for Engineering Education (ASEE) Summer Faculty Fellowship Program, 1994, Volume 1 Jul. 1995 9 p (For primary document see N95-32418 12-99)

(Grant NGT-44-005-803)

Avail: CASI HC A02/MF A03

A unified approach for solving incompressible flows has been investigated in this study. The numerical CTVD (Centered Total Variation Diminishing) scheme used in this study was successfully developed by Sanders and Li for compressible flows, especially for the high speed. The CTVD scheme possesses better mathematical properties to damp out the spurious oscillations while providing high-order accuracy for high speed flows. It leads us to believe that the CTVD scheme can equally well apply to solve incompressible flows. Because of the mathematical difference between the governing equations for incompressible and compressible flows, the scheme can not directly apply to the incompressible flows. However, if one can modify the continuity equation for incompressible flows by introducing pseudo-compressibility, the governing equations for incompressible flows would have the same mathematical characters as compressible flows. The application of the algorithm to incompressible flows thus becomes feasible. In this study, the governing equations for incompressible flows comprise continuity equation and momentum equations. The continuity equation is modified by adding a time-derivative of the pressure term containing the artificial compressibility. The modified continuity equation together with the unsteady momentum equations forms a hyperbolic-parabolic type of time-dependent system of equations. Thus, the CTVD schemes can be implemented. In addition, the physical and numerical boundary conditions are properly implemented by the characteristic boundary conditions. Accordingly, a CFD code has been developed for this research and is currently under testing. Flow past a circular cylinder was chosen for numerical experiments to determine the accuracy and efficiency of the code. The code has shown some promising results. Author

N95-32426*# Oklahoma Baptist Univ., Shawnee, OK. Div. of Natural Science.

CHARACTERIZING THE FRAGMENTATION RING ON WITNESS PLATES **c09**

Yuan-Liang A. Chen *In* NASA. Johnson Space Center, National Aeronautics and Space Administration (NASA)/American Society for Engineering Education (ASEE) Summer Faculty Fellowship Program, 1994, Volume 1 Jul. 1995 11 p (For primary document see N95-32418 12-99)

Avail: CASI HC A03/MF A03

Hole-saw ring patterns on the witness plate are studied systematically. Aluminum alloy 1100 and 6061, inconel, teflon, and lead of different thicknesses were utilized for target material. The ring patterns are observed at D(sub p)/T = 1.98 to 4.02 for aluminum 1100 target, at D(sub p)/T = 1.55 to 10.51 for aluminum 6061 target, at D(sub p)/T = 4.41 to 9 98 for inconel target, at D(sub p)/T = 1.33 to 3.94 for teflon target, and at D(subp)/T = 12.5 to 20.89 for lead target. The ring diameter showed a decreasing trend when D(sub p)/T ratio increased. An analytical model is introduced. The crater distributions on the ring were investigated. The majority of the craters are in the neighborhood of 1100 micrometers to 1400 micrometers size. Many broken string like craters were observed on the ring as well as inside the ring. Author

N95-32427*# Illinois Univ., Chicago, IL. Dept. of Mechanical Engineering.

BASELINE EXPERIMENTAL INVESTIGATION OF AN ELECTROHYDRODYNAMICALLY ASSISTED HEAT PIPE Final Report **c34**

A. B. Duncan *In* NASA. Johnson Space Center, National Aeronautics and Space Administration (NASA)/American Society for Engineering Education (ASEE) Summer Faculty Fellowship Program, 1994, Volume 1 Jul. 1995 15 p (For primary document see N95-32418 12-99)

(Grant NGT-44-005-803)

Avail: CASI HC A03/MF A03

The increases in power demand and associated thermal management requirements of future space programs such as potential Lunar/Mars missions will require enhancing the operating efficiencies of thermal management devices. Currently, the use of electrohydrodynamically (EHD) assisted thermal control devices is under consideration as a potential method of increasing thermal management system capacity. The objectives of the currently described investigation included completing build-up of the EHD-Assisted Heat Pipe Test bed, developing test procedures for an experimental evaluation of the unassisted heat pipe, developing an analytical model capable of predicting the performance limits of the unassisted heat pipe, and obtaining experimental data which would define the performance characteristics of the unassisted heat pipe. The information obtained in the currently proposed study will be used in order to provide extensive comparisons with the EHD-assisted performance observations to be obtained during the continuing investigation of EHD-Assisted heat transfer devices. Through comparisons of the baseline test bed data and the EHD assisted test bed data, accurate insight into the performance enhancing characteristics of EHD augmentation may be obtained. This may lead to optimization,

development, and implementation of EHD technology for future space programs. Author

N95-32428*# Tulane Univ., New Orleans, LA. Dept. of Mechanical Engineering.

BICYCLE ERGOMETER INSTRUMENTATION TO DETERMINE MUSCLE AND BONE FORCES DURING EXERCISE Final Report **c54**

Fernando Figueroa *In* NASA. Johnson Space Center, National Aeronautics and Space Administration (NASA)/American Society for Engineering Education (ASEE) Summer Faculty Fellowship Program, 1994, Volume 1 Jul. 1995 14 p (For primary document see N95-32418 12-99)
(Grant NGT-44-055-803)
Avail: CASI HC A03/MF A03

It is hypothesized that bone loss experienced by astronauts in zero gravity conditions may be curtailed by appropriate exercise. According to Wolf's law, bone regenerates when muscles produce stresses by pulling on the bone during daily activity and/or exercise on Earth. to use this theory to prevent or decrease bone loss, one needs to quantify musculoskeletal loads and relate them to bone density changes. In the context of the space program, it is desirable to determine musculoskeletal loads during exercise (using the bicycle ergometer in this case) so that one may make similar measurements on Earth and in space. In this manner, load measurements on Earth may be used as reference to generate similar loads during exercise in space. The work reported in this document entails a musculoskeletal load measurement system that, when complete, will provide forces at muscle insertion points and other contact points, on bone. This data will be used by Dr. Beth A. Todd, who is also a SSF working with Dr. Shackelford, as input to a finite element model of bone sections to determine stress distributions. A bicycle ergometer has been instrumented to measure parameters needed to determine musculoskeletal forces during exercise. A primary feature of the system is its compactness. It uses small/light sensors without line-of-sight requirements. The system developed includes sensors, signal processing, a data acquisition system, and software to collect the data. The sensors used include optical encoders to measure position and orientation of the pedal (foot), accelerometers to determine kinematic parameters of the shank and thigh, load cells to measure pedal forces on the sagittal plane, and EMG probes to measure muscle activity. The signals are processed using anti-aliasing filters and amplifiers. The sensors' output is digitized using 30 channels of a board mounted inside a 486 class PC. A program sets the data acquisition parameters and collects data during a time period specified by the user. The data is put directly into a file on the hard disk in binary form. The 30 channels are sampled at 200 KHz, and each 30 channel scan is done at a rate of 1000 Hz. The instrumented ergometer has been flown in the KC-135 zero-gravity (zero-g) flight to collect information needed to determine musculoskeletal forces under these conditions. Similar information has been collected in 1-g conditions for comparision with the results from the zero-g case. At this time, the sets of data from both experiments are being processed. An existing methodology will be used to determine the kinematic parameters of the shank and thigh using accelerometer and encoder data. This methodology was developed during the fellow's previous NASA/ASEE fellowship and thanks to a Director's Grant. In the future, a methodology to determine the musculoskeletal forces using Newton's Law of Motion and optimization techniques will be developed to determine forces exerted by particular muscles. Author

N95-32429*# Wyoming Univ., Laramie, WY. Dept. of Computer Science.

VALIDATION OF SPACE/GROUND ANTENNA CONTROL ALGORITHMS USING A COMPUTER-AIDED DESIGN TOOL Final Report **c61**

Rex E. Gantenbein *In* NASA. Johnson Space Center, National Aeronautics and Space Administration (NASA)/American Society for Engineering Education (ASEE) Summer Faculty Fellowship Program, 1994, Volume 1 Jul. 1995 12 p (For primary document see N95-32418 12-99)
(Grant NGT-44-005-803)
Avail: CASI HC A03/MF A03

The validation of the algorithms for controlling the space-to-ground antenna subsystem for Space Station Alpha is an important step in assuring reliable communications. These algorithms have been developed and tested using a simulation environment based on a computer-aided design tool that can provide a time-based execution framework with variable environmental parameters. Our work this summer has involved the exploration of this environment and the documentation of the procedures used to validate these algorithms. We have installed a variety of tools in a laboratory of the Tracking and Communications division for reproducing the simulation experiments carried out on these algorithms to verify that they do meet their requirements for controlling the antenna systems. In this report, we describe the processes used in these simulations and our work in validating the tests used. Author

N95-32430*# Southern Methodist Univ., Dallas, TX. Dept. of Electrical Engineering.

THE COMPOSITE CLASSIFICATION PROBLEM IN OPTICAL INFORMATION PROCESSING Final Report **c82**

Eric B. Hall *In* NASA. Johnson Space Center, National Aeronautics and Space Administration (NASA)/American Society for Engineering Education (ASEE) Summer Faculty Fellowship Program, 1994, Volume 1 Jul. 1995 13 p (For primary document see N95-32418 12-99)
(Grant NGT-44-005-803)
Avail: CASI HC A03/MF A03

Optical pattern recognition allows objects to be recognized from their images and permits their positional parameters to be estimated accurately in real time. The guiding principle behind optical pattern recognition is that a lens focusing a beam of coherent light modulated with an image produces the two-dimensinal Fourier transform of that image. When the resulting output is further transformed by the matched filter corresponding to the original image, one obtains the autocorrelation function of the original image, which has a peak at the origin. Such a device is called an optical correlator and may be used to recognize the locate the image for which it is designed. (From a practical perspective, an approximation to the matched filter must be used since the spatial light modulator (SLM) on which the filter is implemented usually does not allow one to independently control both the magnitude and phase of the filter.) Generally, one is not just concerned with recognizing a single image but is interested in recognizing a variety of rotated and scaled views of a particular image. In order to recognize these different views using an optical correlator, one may select a subset of these views (whose elements are called training images) and then use a composite filter that is designed to produce a correlation peak for each training image. Presumably, these peaks should be sharp and easily distinguishable from the surrounding correlation plane values. In this report we consider two areas of research regarding composite optical correlators. First, we consider the question of how best to choose the training images that are used to design the composite filter. With regard to quantity, the number of training images should be large enough to adequately represent all possible views of the targeted object yet small enough to ensure that the resolution of the filter is not exhausted. As for the images themselves, they should be distinct enough to avoid numerical difficulties yet similar enough to avoid gaps in which certain views of the target will be unrecognized. One method that we introduce to study this problem is called probing and involves the creation of the artificial imagery. The second problem we consider involves the clasification of the composite filter's correlation plane data. In particular, we would like to determine not only whether or not we are viewing a training image, but, in the former case, we would like to determine which training image is being viewed. This second problem is investigated using traditional M-ary hypothesis testing techniques. Author

N95-32431*# Houston Univ., TX. Dept. of Industrial Engineering.

THE BACKGROUND AND THEORY OF INTEGRATED RISK MANAGEMENT Final Report **c81**

John L. Hunsucker *In* NASA. Johnson Space Center, National Aeronautics and Space Administration (NASA)/American Society for Engineering Education (ASEE) Summer Faculty Fellowship Program, 1994, Volume 1 Jul. 1995 13 p (For primary document see N95-32418 12-99)
(Grant NGT-44-005-803)
Avail: CASI HC A03/MF A03

While all good managers have always considered risk in their decision making, only recently have formal programs to do so been introduced. This report covers the logical structure behind the formulation of an integrated risk management plan (IRM). Included in the report are factors forcing the development of a formal plan to consider risk, the basic objective or purpose of an IRM, and desirable traits of such a plan. The report moves on to a discussion of background issues, seeks to formalize some definitions,

and then discusses required information on threats. The report concludes with the steps for an IRM. Author

N95-32432*# Military Academy, West Point, NY. Dept. of Civil and Mechanical Engineering.
IMPLEMENTATION OF A SINGLE-STAGE-TO-ORBIT (SSTO) MODEL FOR STABILITY AND CONTROL ANALYSIS Final Report **c18**
Stephen A. Ingalls *In* NASA. Johnson Space Center, National Aeronautics and Space Administration (NASA)/American Society for Engineering Education (ASEE) Summer Faculty Fellowship Program, 1994, Volume 1 Jul. 1995 14 p (For primary document see N95-32418 12-99)
(Grant NGT-44-005-803)
Avail: CASI HC A03/MF A03

Three NASA centers: Marshall Space Flight Center (MSFC), Langley Research Center (LaRC), and Johnson Space Center (JSC) are currently involved in studying a family of single-stage- and two-stage-to-orbit (SSTO/TSTO) vehicles to serve as the next generation space transportation system (STS). A rocketed winged-body is the current focus. The configuration (WB001) is a vertically-launched, horizontally-landing system with circular cross-section. Preliminary aerodynamic data was generated by LaRC and is a combination of wind-tunnel data, empirical methods, and Aerodynamic Preliminary Analysis System-(APAS) generated values. JSC's efforts involve descent trajectory design, stability analysis, and flight control system synthesis. Analysis of WB001's static stability indicates instability in 'tuck' (C(sub mu) less than 0: Mach = 0.30, alpha greater than 3.25 deg; Mach = 0.60, alpha greater than 8.04), an unstable dihedral effects (C(sub l(beta)) greater than 0: Mach = 30,alpha less than 12 deg.; Mach = 0.60, alpha less than 10.00 deg.), and, most significantly, an unstable weathercock stability derivative, C(sub n(beta)), at all angles of attack and subsonic Mach numbers. Longitudinal trim solutions for Mach = 0.30 and 0.60 indicate flight path angle possibilities ranging from around 12 (M = 0.30) to slightly over 20 degrees at Mach = 0.60. Trim angles of attack increase from 6.24 at Mach 0.60 and 10,000 feet to 17.7 deg. at Mach 0.30, sea-level. Lateral trim was attempted for a design cross-wind of 25.0 knots. The current vehicle aerodynamic and geometric characteristics will only yield a lateral trim solution at impractical tip-fin deflections (approximately equal to 43 deg.) and bank angles (21 deg.). A study of the lateral control surfaces, tip-fin controllers for WB001, indicate increased surface area would help address these instabilities, particularly the deficiency in C(sub n(beta)), but obviously at the expense of increased vehicle weight. Growth factors of approximately 7 were determined using a design C(sub n(beta)) of 0.100/radian (approximate subsonic values for the orbiter). Author

N95-32433*# Houston Univ., TX. Dept. of Mathematics.
SCANNERS, OPTICAL CHARACTER READERS, CYRILLIC ALPHABET AND RUSSIAN TRANSLATIONS Final Report **c63**
Gordon G. Johnson *In* NASA. Johnson Space Center, National Aeronautics and Space Administration (NASA)/American Society for Engineering Education (ASEE) Summer Faculty Fellowship Program, 1994, Volume 1 Jul. 1995 5 p (For primary document see N95-32418 12-99)
(Grant NGT-44-005-308)
Avail: CASI HC A01/MF A03

The writing of code for capture, in a uniform format, of bit maps of words and characters from scanner PICT files is presented. The coding of Dynamic Pattern Matched for the identification of the characters, words and sentences in preparation for translation is discussed. Author

N95-32434*# Rice Univ., Houston, TX. Dept. of Mechanical Engineering and Materials Science.
NUMERICAL SOLUTION OF DIFFERENTIAL EQUATIONS BY ARTIFICIAL NEURAL NETWORKS Final Report **c63**
Andrew J. Meade, Jr. *In* NASA. Johnson Space Center, National Aeronautics and Space Administration (NASA)/American Society for Engineering Education (ASEE) Summer Faculty Fellowship Program, 1994, Volume 1 Jul. 1995 13 p (For primary document see N95-32418 12-99)
(Grant NGT-44-005-803)
Avail: CASI HC A03/MF A03

Conventionally programmed digital computers can process numbers with great speed and precision, but do not easily recognize patterns or imprecise or contradictory data. Instead of being programmed in the conventional sense, artificial neural networks (ANN's) are capable of self-learning through exposure to repeated examples. However, the training of an ANN can be a time consuming and unpredictable process. A general method is being developed by the author to mate the adaptability of the ANN with the speed and precision of the digital computer. This method has been successful in building feedforward networks that can approximate functions and their partial derivatives from examples in a single iteration. The general method also allows the formation of feedforward networks that can approximate the solution to nonlinear ordinary and partial differential equations to desired accuracy without the need of examples. It is believed that continued research will produce artificial neural networks that can be used with confidence in practical scientific computing and engineering applications. Author

N95-32473# Air Force Office of Scientific Research, Bolling AFB, Washington, DC.
AIR FORCE OFFICE OF SCIENTIFIC RESEARCH. RESEARCH PROPOSAL Quarterly Report No. 3, Jul. - Sep. 1994
Sep. 1994 70 p
(AD-A293401; AFOSR-TR-95-0257) Avail: CASI HC A04/MF A01

This research proposal status report is published quarterly (March, June, September, and December) by the Air Force Office of Scientific Research (AFOSR). It lists all the research proposals received by AFOSR during the past six months along with the action taken (initiated, declined, or withdrawn). The report is divided into two parts. The Institution Index lists proposals alphabetically by institution. This is followed by a more detailed listing by Directorate, and by Program Manager within the Directorate.
Derived from text

N95-32538# European Space Agency, Paris (France).
ESA BULLETIN, NUMBER 82
Bruce Battrick, ed., Duc Guyenne, ed., and Clare Mattok, ed. The Netherlands May 1995 144 p Original contains color illustrations
(ISSN 0376-4265)
Avail: CASI HC A07/MF A02

The following articles are contained: Has Space a Future?; LEDA -- a First Step in ESA's Lunar Exploration Initiative; Future Perspectives for Europe in Space; Three Missions, Three Launches, Six Spacecraft for Science in 1995; Ulysses Explores the South Pole of the Sun; Microgravity Research During Aircraft Parabolic Flights: the 20 ESA Campaigns; The First Parabolic Flight Campaign for Students; Ballistocraft: a Novel Facility for Microgravity Research; The Atmospheric Reentry Demonstrator (ARD); Research Associations for the Development of Industrial Use of Space: The RADIUS Program; Towards Automatic Product Generation for Meteosat Images; Agency Law and Practice in the Protection of Inventions; and ERS Product Assurance and Quality Control. CASI

N95-32805# European Space Agency, Paris (France).
EUROPEAN SPACE AGENCY 1994 ANNUAL REPORT [AGENCE SPATIALE EUROPEENNE 1994 RAPPORT ANNUEL]
B. Battrick, ed., T. D. Guyenne, ed., and J. J. Hunt, ed. The Netherlands 1995 115 p Original contains color illustrations
(ISSN 0258-025X)
Avail: CASI HC A06/MF A02

The financial resources, activities, means (ESTEC, ESOC, and ESRIN), and human resources of the European Space Agency in 1994 are reviewed. Milestones include the first imaged received from ESA's Faint-Object Camera and NASA's Wide-Field Planetary Camera following the servicing mission to correct the Hubble Space Telescope optics; the cooperation agreement signed with the Republic of Poland; Meteosat-6 experiences anomalies; Russia's signing the Inter-Governmental Agreement (IGA) on the International Space Station; Finland signs agreement for accession to the ESA convention; the successful launch of Arian V64, V65, V66, V67, V68, and V69; the Ulysses space probe reaches the south pole of the Sun; the cooperation agreement with the Russian Space Agency (RKA); and the discovery by the Hubble Space Telescope of one of the smallest stars in the universe (G1623b). CASI

N95-33042*# National Aeronautics and Space Administration. Marshall Space Flight Center, Huntsville, AL.
RESEARCH AND TECHNOLOGY 1994: ANNUAL REPORT OF THE MARSHALL SPACE FLIGHT CENTER

1994 287 p
(NASA-TM-108470; NAS 1.15:108470) Avail: CASI HC A13/MF A03

This report summarizes the technology transfer, advanced studies, and research and technology programs efforts now in progress at the Marshall Space Flight Center (MSFC). Advanced studies include space science, space systems, space transportation, and research. Research programs include Earth system science, space physics, solar physics, astrophysics, and microgravity science and applications. Technology programs include avionics, diagnostic and inspection system, materials and manufacturing processes, mission operations, propulsion and fluid management, structures and dynamics, systems analysis and integration, and environments. CASI

N95-33384* National Aeronautics and Space Administration. Lyndon B. Johnson Space Center, Houston, TX.
TWENTY-FIVE YEARS OF PROGRESS. PART 1: BIRTH OF NASA. PART 2: THE MOON-A GOAL (Videotape)
[1984] Sponsored by NASA, Washington Videotape: 60 min. playing time, in color, with sound
(NASA-TM-110819; NAS 1.15:110819; NONP-NASA-VT-95-61007; CMP-178-0045B) Avail: CASI VHS A02/BETA A22

Historical footage (1958 - 1983) concerning NASA's Space Program, is reviewed in this two-part video. Host, Lynn Bondurant describes the birth of NASA and its accomplishments through the years. Part one contains: the launch of Russian satellite Sputnik on October 4,1957; the first dog (Soviet) in space; NACA Space Research, Explorer-6; and still photographs of various Space projects. Tiros one experimental weather satellite, Microgravity simulators, Eco 1 passive communications satellite, and the first U.S. manned spaceflight Mercury are included in part two. The seven Mercury astronauts are: Captain Donald Slayton, Lt. Commander Allen Shepard, Lt. Commander Walter Schirra, Captain Virgil Grissom, Lt. Col. John Glen Jr., Captain Leroy Cooper Jr, and Lt. Malcolm Scott Carpenter. Also included are an ongoing interview (throughout the video) with NASA's first Administrator Keith Glennon, the first flight in 1961 with Eanus the Monkey, President Kennedy's speech in Washington about the Space Program, Project Gemini - the 2-manned space flight, and the near disastrous recovery of Virgil Grissom from splash down. CASI

SUBJECT INDEX

Typical Subject Index Listing

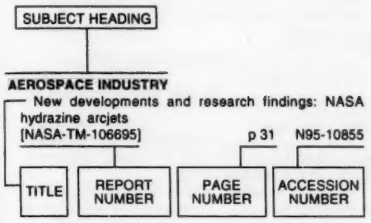

The subject heading is a key to the subject content of the document. Titles, report numbers, and accession numbers of pertinent documents are provided under each subject heading. When the title is insufficiently descriptive of the document content, a title extension is added, separated from the title by three hyphens. The report number helps to indicate the type of document cited (e.g., NASA report, NASA translation, NASA contractor report). The accession number is the number by which the document abstracts are arranged in this journal and by which the document is sold or requested. The page number helps you locate the citation in the abstract section. The titles, with title extensions if present, are arranged under each subject heading in ascending accession number order. The subject headings have been selected from the latest revision of the *NASA Thesaurus*.

A

ABERRATION
Beam-based optical tuning of the Final Focus Test Beam
|DE95-012097| p 3215 N95-32658

ABLATION
Thermo-chemical ablation of heat shields under Earth reentry conditions p 3059 N95-32903
Glass science tutorial lecture no. 6: The melting of silicate glasses, a review of selected topics
|DE95-010199| p 3084 N95-33218
Plasma mediated ablation of biological tissues with ultrashort laser pulses
|DE95-011748| p 3164 N95-33654

ABLATIVE MATERIALS
Thermo-chemical ablation of heat shields under Earth reentry conditions p 3059 N95-32903

ABRASION RESISTANCE
Performance of partially fluorinated polyimide insulation for aerospace applications
|NASA-CR-198372| p 3060 N95-32673
Ion assisted deposition of ZnS and MgF2
|AD-A294759| p 3086 N95-34563

ABSORBENTS
Alternative catalyst and exhaust gas sensor work at Argonne National Laboratory
|DE95-007138| p 3152 N95-32553

ABSORBERS (MATERIALS)
Experimental investigation of impulse radar for mitigation of effects of radar absorbing materials
|AD-A294166| p 3100 N95-34762

ABSORPTION
Fluid dynamometer having fluid characteristic power absorption adjustment capability
|AD-D017489| p 3116 N95-34426

ABSORPTION CROSS SECTIONS
State-selective single electron capture cross sections in He(exp 2+) + Li(2s) and Li(*)(2p) collisions
|DE95-010819| p 3207 N95-33371

ABSORPTION SPECTRA
A study of luminescence and absorption spectra of GaP
|DE95-614122| p 3202 N95-32524
Probe transparency in a two-level medium embedded by a squeezed vacuum
|DE95-614123| p 3198 N95-32525
Photon echoes from the absorption continuum of a semiconductor
|DE95-011274| p 3101 N95-32596
Solvent effects on the electronic spectrum of R hardt's dye
|AD-A293667| p 3067 N95-32804
A digital boxcar integrator for IMS spectra p 3072 N95-33288
FTP-Server for exchange, interpretation, and database-search of ion mobility spectra, literature, preprints and software p 3073 N95-33291
Size, shape, and crystallinity of luminescent structures in oxidized Si nanoclusters and H-passivated porous Si
|DE95-012322| p 3229 N95-33628
Measurement of the spectral absorption of liquid water in melting snow with an imaging spectrometer p 3133 N95-33756
Extraction of ozone and chlorophyll-A distribution from AVIRIS data p 3136 N95-33770
Spectral identification of minerals using imaging spectrometry data: Evaluating the effects of signal to noise and spectral resolution using the tricorder algorithm p 3136 N95-33772
Charge-transfer gap closure in transition-metal halides under pressure
|DE95-011268| p 3230 N95-33865
Photobiology and optical properties of planktonic and sea ice microalgae in the high arctic
|AD-A294002| p 3160 N95-34457
Atmospheric attenuation properties associated with CO2 laser radiation spectra
|AD-A294061| p 3120 N95-34470

ABSORPTION SPECTROSCOPY
The development of a large-area chemical sensor: A new platform for selective coatings
|DE95-011489| p 3075 N95-33832

ABSTRACTS
Fifth International Conference on Hyperbolic Problems, Theory, Numerics, Applications: Abstracts
|DE95-008173| p 3194 N95-32389

ABUNDANCE
Beryllium and Boron abundances in population II stars
|NASA-CR-189434| p 3247 N95-33262

ACCELERATION PROTECTION
Current Concepts on G-Protection Research and Development
|AGARD-LS-202| p 3168 N95-34050
G-protection basis/acceleration physiology p 3168 N95-34051
Anti-G suits p 3168 N95-34054
Positive pressure breathing for G protection (PBG) p 3168 N95-34055
Increase of High-sustained +G(z) tolerance at the expense of pilot's working posture change p 3165 N95-34056
G-protection capabilities and current G-protection issues p 3169 N95-34060

ACCELERATION STRESSES (PHYSIOLOGY)
Negative to positive Gz acceleration transition p 3165 N95-34052

ACCELERATION TOLERANCE
G-protection basis/acceleration physiology p 3168 N95-34051
Negative to positive Gz acceleration transition p 3165 N95-34052
Selection and special physiological training of flying personnel to high +G(z)-maneuverable flights-main concept p 3166 N95-34053
Positive pressure breathing for G protection (PBG) p 3168 N95-34055
Increase of High-sustained +G(z) tolerance at the expense of pilot's working posture change p 3165 N95-34056
Methods for measuring physiological responses and protection in man exposed to high +G(z) p 3166 N95-34058
Selection and training of MiG-29 and future fighter pilots p 3166 N95-34059
G-protection capabilities and current G-protection issues p 3169 N95-34060

ACCELERATORS
Crystalline beam properties as predicted for the storage rings ASTRID and TSR
|DE95-011557| p 3210 N95-32411
VHS-tape system for general purpose computer. For next generation mass storage system
|DE95-737268| p 3177 N95-32757
A fiber optic strain measurement and quench localization for use in superconducting accelerator dipole magnets
|DE95-012370| p 3215 N95-33381
xdamp: An IDL(R)-based Data Manipulation Program
|DE95-011242| p 3181 N95-33624

ACCELEROMETERS
Commercial usage of Navy components developed and manufactured by CRI Delfin p 3092 N95-33129
Dual-use micromechanical inertial sensors p 3092 N95-33132

ACCEPTABILITY
User acceptability and comfort of the communications earplug (CEP) when used in the UH-1 helicopter
|AD-A294047| p 3170 N95-34492

ACCESS CONTROL
Congestion control over ATM local area networks
|DE95-010343| p 3184 N95-32558

ACCUMULATORS
Design and operation of a thermionic converter in air
|DE95-010151| p 3149 N95-32645
Integral cesium reservoir: Design and transient operation
|DE95-010152| p 3211 N95-32647

ACCURACY
The role of dynamic experimentation for computation analysis
|DE95-007733| p 3125 N95-32381
Prediction of OCR accuracy using simple image features
|DE95-009887| p 3236 N95-32471
Accuracy enhancement in optical computing
|AD-A294958| p 3219 N95-34579

ACHIEVEMENT
Locus of control and coping style as stress moderators in achievement oriented individuals
|AD-A294275| p 3166 N95-34463

ACOUSTIC ATTENUATION
Acoustic attenuation and vibration damping materials
|AD-D017465| p 3201 N95-34444

ACOUSTIC FREQUENCIES
High-resolution TeO2 acousto-optical deflector for millimeter-wave spectrometer
|AD-A293054| p 3215 N95-32701

ACOUSTIC IMPEDANCE
Acoustic attenuation and vibration damping materials
|AD-D017465| p 3201 N95-34444

ACOUSTIC MEASUREMENT
Underwater acoustic field extrapolation: Theory and sensitivity analysis
|AD-A294925| p 3201 N95-34595

ACOUSTIC PROPERTIES
Transverse acoustic properties of the B-phase of superfluid helium three p 3074 N95-33414

ACOUSTIC SCATTERING
Penetrable wedge analysis
|AD-A294276| p 3234 N95-34464

ACOUSTIC VELOCITY
Structural wave propagation and sound radiation study through time and spatial processing p 3200 N95-33251
Acoustic-optic sound velocity profiler
|AD-D017487| p 3201 N95-34289
Underwater acoustic field extrapolation: Theory and sensitivity analysis
|AD-A294925| p 3201 N95-34595

ACOUSTICS
High-order Taylor-Galerkin and adaptive hp-methods for hyperbolic systems with application to structural acoustics p 3200 N95-33719
Underwater acoustic field extrapolation: Theory and sensitivity analysis
|AD-A294925| p 3201 N95-34595
ACOUSTO-OPTICS
Frequency response of a TeO2 slow shear wave acousto-optic cell exposed to radiation
|DE95-009586| p 3226 N95-32589
High-resolution TeO2 acousto-optical deflector for millimeter-wave spectrometer
|AD-A293054| p 3215 N95-32701
Acoustic-optic sound velocity profiler
|AD-D017487| p 3201 N95-34289
Recent developments in maritime technology research institute acousto-optical technology research
|AD-A294215| p 3217 N95-34307
Using optical interference methods to measure acousto-optical device thermal effects
|AD-A294219| p 3217 N95-34309
ACTINIDE SERIES
Development of ultrasensitive spectroscopic analysis technology. Development of atomic spectroscopy technology
|DE95-614352| p 3066 N95-32566
ACTIVE CONTROL
Actively controlled shaft seals for aerospace applications
|NASA-CR-4678| p 3061 N95-33156
Active noise control in finite length waveguides p 3098 N95-33322
ACTIVITY (BIOLOGY)
DataHub sponsored analysis p 3243 N95-34242
ACTUATORS
Actively controlled shaft seals for aerospace applications
|NASA-CR-4678| p 3061 N95-33156
Effect of phase transformations on the mechanical properties of a multiphase alloy based on NiAl + Fe
|DE95-010119| p 3079 N95-33217
A digital boxcar integrator for IMS spectra p 3072 N95-33288
An application of mechanical leverage to microactuation
|DE95-011883| p 3124 N95-33836
Explanations of empirically derived reactive plans
|AD-A294114| p 3193 N95-34501
ADA (PROGRAMMING LANGUAGE)
The application of Ada and formal methods to a safety critical engine control system p 3094 N95-33142
ADAPTATION
High-order Taylor-Galerkin and adaptive hp-methods for hyperbolic systems with application to structural acoustics p 3200 N95-33719
ADAPTIVE CONTROL
High-tech controls for energy and environment
|DE95-004011| p 3191 N95-33060
Motion and force control of coordinated robots
|ISBN-0-315-86323-4| p 3191 N95-33307
Nonlinear adaptive control of highly maneuverable high performance aircraft p 3192 N95-33712
Multi-layer holographic bifurcative neural network system for real-time adaptive EOS data analysis p 3148 N95-34233
Adaptive differential visual feedback for uncalibrated hand-eye coordination and motor control
|AD-A293607| p 3171 N95-34616
A stochastic adaptive control application to flight systems p 3055 N95-34806
ADAPTIVE FILTERS
Space-time adaptive processing for airborne radar
|AD-A293032| p 3098 N95-33152
ADAPTIVE OPTICS
ABLEX: High altitude laser propagation experiment
|AD-A294914| p 3120 N95-34592
ADDITIVES
Development of improved p-type Si-20 at. %Ge by addition of fullerite
|DE95-010230| p 3066 N95-32394
Measurement of gain saturation on Nd: Doped phosphate laser glasses
|REPT-2210| p 3090 N95-32990
Phthalic acid esters used as plastic additives. Volume 1: Ecotoxicological risk assessment. Volume 2: Comparisons of toxicological effects
|PB95-211280| p 3084 N95-33329
Advanced far infrared detector and double donor studies in Ge
|DE95-011261| p 3247 N95-33625
Properties of high-T(sub c) Josephson junctions with Y(0.7)Ca(0.3)Ba2Cu3O(7-delta) barrier layers
|AD-A294852| p 3231 N95-34568
ADHESION
Adhesion of novel high-performance polymers to carbon fibers: Fiber surface treatment, characterization, and microbond single fiber pull-out test p 3085 N95-34282
ADHESIVE BONDING
Tests of adhesives used for plate bonding of ATLAS tile-cal hadron calorimeter
|DE95-009917| p 3082 N95-32664
Split gasket attachment method statement of government interest
|AD-D017443| p 3123 N95-32924
ADHESIVES
Tests of adhesives used for plate bonding of ATLAS tile-cal hadron calorimeter
|DE95-009917| p 3082 N95-32664
ADSORPTION
Smoothing during ion-assisted growth by transient ion beam-induced defects
|DE95-011021| p 3225 N95-32579
Surface chemistry of diamond single crystals
|AD-A294150| p 3232 N95-34755
ADSORPTIVITY
Gas chromatography/ion mobility spectrometry as a hyphenated technique for improved explosives detection and analysis p 3071 N95-33278
AEROACOUSTICS
Computation of noise radiation from turbofans: A parametric study
|NASA-CR-198359| p 3200 N95-32836
Review of combustion-acoustic instabilities
|NASA-TM-107020| p 3108 N95-32930
Combustion-acoustic stability analysis for premixed gas turbine combustors
|NASA-TM-107024| p 3050 N95-32931
Advanced boundary element methods in aeroacoustics and elastodynamics p 3200 N95-33694
Fan noise prediction assessment
|NASA-CR-195051| p 3200 N95-33831
AERODYNAMIC BRAKES
Wind turbine trailing edge aerodynamic brakes
|DE95-004061| p 3033 N95-32548
AERODYNAMIC CHARACTERISTICS
Calculation for aerodynamic characteristics on delta wing with leading-edge separated vortex effect using boundary element method p 3037 N95-34524
Sidewall-effect of the wind tunnel on the estimation of the aerodynamic characteristics of a delta wing p 3037 N95-34525
Numerical simulation of two-dimensional PAR-WIG p 3040 N95-34548
AERODYNAMIC COEFFICIENTS
Dynamic ground effects flight test of the NASA F-15 aircraft p 3049 N95-33024
AERODYNAMIC CONFIGURATIONS
The Anglo-French Compact Laser Radar demonstrator programme p 3045 N95-32501
Three-dimensional aerodynamic shape optimization using discrete sensitivity analysis p 3048 N95-32904
Analysis and design methodology for chordwise deformable wings p 3049 N95-33311
AERODYNAMIC DRAG
Wind turbine trailing edge aerodynamic brakes
|DE95-004061| p 3033 N95-32548
Drag measurements of an axisymmetric nacelle mounted on a flat plate at supersonic speeds
|NASA-TM-4660| p 3034 N95-32821
Near-limit drop deformation and secondary breakup p 3107 N95-32902
AERODYNAMIC FORCES
SOFIA 2 model telescope wind tunnel test report
|NASA-TM-110668| p 3033 N95-32764
Energy absorption device for shock loading
|AD-D017476| p 3124 N95-34449
Computations of low speed flow about space-plane p 3040 N95-34544
A simulation of damping process of pendulum motion due to aerodynamic forces p 3041 N95-34551
AERODYNAMIC INTERFERENCE
Numerical analysis around the whole SST configuration p 3039 N95-34541
AERODYNAMIC LOADS
Full-scale hingeless rotor performance and loads
|NASA-TM-110356| p 3048 N95-32699
AERODYNAMIC NOISE
Computation of noise radiation from turbofans: A parametric study
|NASA-CR-198359| p 3200 N95-32836
Fan noise prediction assessment
|NASA-CR-195051| p 3200 N95-33831
Direct analysis of transonic rotor noise with CFD technique p 3040 N95-34549
AERODYNAMIC STABILITY
Full-scale hingeless rotor performance and loads
|NASA-TM-110356| p 3048 N95-32699
AERODYNAMIC STALLING
Turbulence models in the Navier-Stokes simulation of airfoil stall
|TRITA-NA-9312| p 3108 N95-33059
Numerical simulations of dynamic stall phenomena in low speed flows p 3040 N95-34546
AERODYNAMICS
Requirements and trends of computational aerodynamics as a tool for aircraft design p 3034 N95-34506
Hypersonic CFD analysis for the aerothermodynamic design of HOPE p 3036 N95-34520
Application of CFD techique for HYFLEX aerodynamic design p 3039 N95-34542
Numerical simulation of aerodynamic problems in high speed railways, part 2 p 3041 N95-34554
High order accuracy computational methods in aerodynamics using parallel architectures
|AD-A294167| p 3042 N95-34763
AEROELASTICITY
Full-scale hingeless rotor performance and loads
|NASA-TM-110356| p 3048 N95-32699
Development of a composite tailoring procedure for airplane wing
|NASA-CR-199081| p 3048 N95-32928
Analysis and design methodology for chordwise deformable wings p 3049 N95-33311
AERONAUTICAL ENGINEERING
Role of computational fluid dynamics in aeronautical engineering. Number 12: Formulation and verification of uni-particle upwind schemes for the Euler equations p 3039 N95-34540
AERONAUTICS
AGARD index of publications: 1992-1994
|AGARD-INDEX-92-94| p 3237 N95-33198
AEROSOLS
Ocean observations with EOS/MODIS: Algorithm development and post launch studies
|NASA-CR-198928| p 3143 N95-32914
Comparison of seasonal and zonal patterns of the direct and indirect radiative forcing of climate by aerosols
|DE95-010896| p 3153 N95-33192
Remote sensing of smoke, clouds, and radiation using AVIRIS during SCAR experiments p 3132 N95-33749
AVIRIS user's guide p 3117 N95-33759
Development of High Spectral Resolution Lidar (HSRL) technology
|DE95-011906| p 3099 N95-33839
Enhanced shortwave cloud radiative forcing due to anthropogenic aerosols
|DE95-013319| p 3156 N95-34214
Atmospheric attenuation properties associated with CO2 laser radiation spectra
|AD-A294061| p 3120 N95-34470
AEROSPACE ENGINEERING
NASA/DOD Aerospace Knowledge Diffusion Research Project. Paper 50: From student to entry-level professional: Examining the role of language and written communications in the reacculturation of aerospace engineering students
|NASA-TM-110834| p 3237 N95-32883
AGARD index of publications: 1992-1994
|AGARD-INDEX-92-94| p 3237 N95-33198
NASA/DOD Aerospace Knowledge Diffusion Research Project. Report 33: The technical communications practices of US aerospace engineers and scientists: Results of the phase 1 AIAA mail survey
|NASA-TM-110180| p 3239 N95-34217
AEROSPACE ENVIRONMENTS
Ricor K506B cryocooler performance during the Clementine mission and ground testing
|DE95-010683| p 3089 N95-32568
Study of the space environmental effects on spacecraft engineering materials
|NASA-CR-199090| p 3066 N95-32581
Single event and TREE latchup mitigation for a star tracker sensor: An innovative approach to system level latchup mitigation
|DE95-010331| p 3059 N95-32593
AEROSPACE MEDICINE
Current Concepts on G-Protection Research and Development
|AGARD-LS-202| p 3168 N95-34050
G-protection basis/acceleration physiology p 3168 N95-34051
Negative to positive Gz acceleration transition p 3165 N95-34052
Selection and special physiological training of flying personnel to high +G(z)-maneuverable flights-main concept p 3166 N95-34053
Positive pressure breathing for G protection (PBG) p 3168 N95-34055
Increase of High-sustained +G(z) tolerance at the expense of pilot's working posture change p 3165 N95-34056

New advances in physiological measurements during high-G: Technology p 3165 N95-34057
Methods for measuring physiological responses and protection in man exposed to high +G(z) p 3166 N95-34058
G-protection capabilities and current G-protection issues p 3169 N95-34060
STS-42 mission highlights resource tape. Part 1 of 2 | NASA-TM-110838 | p 3058 N95-34280

AEROSPACE PLANES
Computations of low speed flow about space-plane p 3040 N95-34544

AEROSPACE SYSTEMS
Research and technology 1994: Annual report of the Marshall Space Flight Center | NASA-TM-108470 | p 3252 N95-33042
Efficient time domain solutions of Maxwell's equations for aerospace systems | AD-A294019 | p 3196 N95-34377
Aerospace physiology AFSC 4M0X1 | AD-A294839 | p 3165 N95-34564

AEROTHERMOCHEMISTRY
Thermo-chemical ablation of heat shields under Earth reentry conditions p 3059 N95-32903

AEROTHERMODYNAMICS
Special publication of National Aerospace Laboratory | NAL-SP-27 | p 3034 N95-34505
Hypersonic CFD analysis for the aerothermodynamic design of HOPE p 3036 N95-34520

AFFINITY
Proton affinity determinations and proton-bound dimer structure indications in C2 to C15, (alpha),(omega)-alkyldiamines p 3069 N95-33266

AGGREGATES
Test method to measure resistance towards fragmentation by studded tires | PB95-211017 | p 3121 N95-32612

AGING (MATERIALS)
Investigation of aging effects from high voltage profiles in ceramic phase shifter materials | AD-A289985 | p 3082 N95-32694
Microstructural studies of hydrogen damage in metastable stainless steels p 3080 N95-33774

AH-64 HELICOPTER
Army aviation: Modernization strategy needs to be reassessed. Report to Congressional requestors | GAO/NSIAD-95-9 | p 3033 N95-32783

AIR CONDITIONING
Technical innovation for reducing emissions of greenhouse effect gas and survey of effects of changes of industrial structures | DE95-769808 | p 3151 N95-32547

AIR COOLING
Tri-service perspectives on microclimate cooling of protective clothing in the heat | AD-A294005 | p 3170 N95-34370
Static pressure drop by swirling flow of an internal cooling air system through a turbine shaft p 3042 N95-34560

AIR DEFENSE
Helicopter HF communications using the NVIS mode p 3043 N95-32491
An integrated system for air to ground operations p 3044 N95-32498
Report to Congressional Committees. Air Force fighters: More reliance on reserves increases the need to know their capabilities | GAO/NSIAD-94-86 | p 3197 N95-32807

AIR DUCTS
Computation of noise radiation from turbofans: A parametric study | NASA-CR-198359 | p 3200 N95-32836

AIR FLOW
Energy absorption device for shock loading | AD-D017476 | p 3124 N95-34449

AIR NAVIGATION
Flight test of a low-altitude helicopter guidance system with obstacle avoidance capability p 3043 N95-32490
A tactical navigation and routeing system for low-level flight p 3044 N95-32494
The Anglo-French Compact Laser Radar demonstrator programme p 3045 N95-32501
SIRPH: Steerable infrared picture on helmet mounted display p 3045 N95-32504

AIR POLLUTION
Winter season air pollution in El Paso-Ciudad Juarez. A review of air pollution studies in an international airshed | DE95-009083 | p 3152 N95-32556
A methodology for evaluating air pollution strategies to improve the air quality in Mexico City | DE95-010874 | p 3152 N95-32573
Solving widespread low-concentration VOC air pollution problems: Gas-phase photocatalytic oxidation answers the needs of many small businesses | DE95-004059 | p 3152 N95-32668
Detection of emission sources using passive-remote Fourier Transform Infrared spectroscopy | DE95-009920 | p 3067 N95-32671
Induction of dependency structures from data and its application to ozone prediction p 3190 N95-33003
Direct analysis of organic priority pollutants by IMS p 3071 N95-33280
An ammonia monitor for the water industry p 3071 N95-33281
Multiscale characteristics and modeling of atmospheric methane p 3154 N95-33339
Alternative-fuels technology: Natural gas vehicles as a way to curb urban air pollution | DE95-012216 | p 3088 N95-33395
ABCASH plotting program users guide | DE95-011652 | p 3155 N95-34435

AIR QUALITY
Winter season air pollution in El Paso-Ciudad Juarez. A review of air pollution studies in an international airshed | DE95-009083 | p 3152 N95-32556
A methodology for evaluating air pollution strategies to improve the air quality in Mexico City | DE95-010874 | p 3152 N95-32573
Solving widespread low-concentration VOC air pollution problems: Gas-phase photocatalytic oxidation answers the needs of many small businesses | DE95-004059 | p 3152 N95-32668
The next generation of automobile emissions reduction: Innovative control of off-cycle emissions | DE95-004057 | p 3153 N95-32809

AIR SAMPLING
Direct analysis of organic priority pollutants by IMS p 3071 N95-33280
ABCASH plotting program users guide | DE95-011652 | p 3155 N95-34435

AIR TRAFFIC
Fact sheet for Congressional requesters. Airport competition: Essential air service slots at O'Hare International Airport | GAO/RCED-94-118FS | p 3055 N95-32759
Report to the Chairman, Subcommittee on Transportation and Related Agencies, Committee on Appropriations, US Senate. Airport Improvement Program: Reliever airport set-aside funds could be redirected | GAO/RCED-94-226 | p 3055 N95-32786

AIR TRAFFIC CONTROL
The DLR research programme on an integrated multi sensor system for surface movement guidance and control p 3048 N95-33135
GPS-Squitter interference analysis | AD-A293690 | p 3047 N95-33480
Human Factors Certification of Advanced Aviation Technologies | NASA-CR-199009 | p 3171 N95-34764
Human factors certification in the development of future air traffic control systems p 3048 N95-34770
Is there a role for a test controller in the development of new ATC equipment? p 3174 N95-34778
The successful management of programs for human factors certification of advanced aviation technologies p 3175 N95-34780
Evaluation in context: ATC automation in the field p 3175 N95-34781
Improving air traffic control: Proving new tools or approving the joint human-machine system? p 3176 N95-34783

AIR TRAFFIC CONTROLLERS (PERSONNEL)
Presentation of a Swedish study program concerning recruitment, selection and training of student air traffic controllers: The MRU project phase 1 p 3167 N95-34775
Improving air traffic control: Proving new tools or approving the joint human-machine system? p 3176 N95-34783

AIR TRANSPORTATION
Report to the Chairman, Subcommittee on Aviation, Committee on Commerce, Science, and Transportation, US Senate. Aviation safety: Data problems threaten FAA strides on safety analysis system | GAO/AIMD-95-27 | p 3046 N95-32705
Fact sheet for Congressional requesters. Airport competition: Essential air service slots at O'Hare International Airport | GAO/RCED-94-118FS | p 3055 N95-32759
Current issues in the design and information content of instrument approach charts | AD-A294752 | p 3047 N95-34562

AIR WATER INTERACTIONS
An experimental study of collective sea state modes of deep water surface gravity waves | AD-A294007 | p 3160 N95-34372

AIRBORNE EQUIPMENT
Helicopter HF communications using the NVIS mode p 3043 N95-32491
Studies of microwave scattering and canopy architecture for boreal forests | NASA-CR-199113 | p 3099 N95-33497
High spectral resolution remote sensing of canopy chemistry p 3128 N95-33731
MODTRAN3: An update and recent validations against airborne high resolution interferometer measurements p 3128 N95-33732
Quantitative remote sensing of ammonium minerals, Cedar Mountains, Esmeralda County, Nevada p 3128 N95-33734
CNR LARA project, Italy: Airborne laboratory for environmental research p 3129 N95-33735
Mapping target signatures via partial unmixing of AVIRIS data p 3129 N95-33737
Combined hyperspatial and hyperspectral imaging spectrometer concept p 3129 N95-33738
Airborne Visible/Infrared Imaging Spectrometer (AVIRIS) onboard calibration system p 3116 N95-33739
New calibration techniques for the Airborne Visible/Infrared Imaging Spectrometer (AVIRIS) p 3116 N95-33740
Initial vegetation species and senescience/stress indicator mapping in the San Luis Valley, Colorado using imaging spectrometer data p 3130 N95-33741
A layered approach to technology transfer of AVIRIS between Earth Search Sciences, Inc. and the Idaho National Engineering Laboratory p 3117 N95-33746
Determination of the in-flight spectral calibration of AVIRIS using atmospheric absorption features p 3117 N95-33751
An improved spectral calibration requirement for AVIRIS p 3117 N95-33752
Movement of water vapor in the atmosphere measured by an imaging spectrometer at Rogers Dry Lake, CA p 3132 N95-33753
In-flight radiometric calibration of AVIRIS in 1994 p 3117 N95-33754
Measurement of atmospheric water vapor, leaf liquid water and reflectance with AVIRIS in the Boreal Ecosystem-Atmosphere Study: Initial results p 3133 N95-33755
Measurement of the spectral absorption of liquid water in melting snow with an imaging spectrometer p 3133 N95-33756
Vegetation species composition and canopy architecture information expressed in leaf water absorption measured in the 1000 nm and 2200 spectral region by an imaging spectrometer p 3133 N95-33757
AVIRIS user's guide p 3117 N95-33759
Integration of AIRSAR and AVIRIS data for Trail Canyon alluvial fan, Death Valley, California p 3134 N95-33760
Remote mineral mapping using AVIRIS data at Summitville, Colorado and the adjacent San Juan Mountains p 3134 N95-33761
An algorithm for chlorophyll using first difference transformations of AVIRIS reflectance spectra p 3134 N95-33763
The 1994 TIMS airborne calibration experiment: Castaic Lake, California p 3117 N95-33797

AIRBORNE LASERS
ABLEX: High altitude laser propagation experiment | AD-A294914 | p 3120 N95-34592

AIRBORNE RADAR
Space-time adaptive processing for airborne radar | AD-A293032 | p 3098 N95-33152
Accurate estimation of sigma(exp 0) using AIRSAR data p 3139 N95-33805
Bayes classification of interferometric TOPSAR data p 3140 N95-33808

AIRBORNE/SPACEBORNE COMPUTERS
PSC implementation and integration p 3051 N95-33014

AIRCRAFT ACCIDENTS
Report to the Chairman, Subcommittee on Aviation, Committee on Commerce, Science, and Transportation, US Senate. Aviation Safety: FAA can better prepare general aviation pilots for mountain flying risks | GAO/RCED-94-15 | p 3046 N95-32784
Evaluating the potential for rotation and loss of flight helmets from inertia and impact loads | AD-A294041 | p 3170 N95-34489

AIRCRAFT CONFIGURATIONS
Low-Level and Nap-of-the-Earth (NOE) night operations | AGARD-CP-563 | p 3042 N95-32486
Flight test of a low-altitude helicopter guidance system with obstacle avoidance capability p 3043 N95-32490
Parallel computation of transonic flows about an aircraft configuration using multi-block structured grids p 3039 N95-34537

AIRCRAFT CONSTRUCTION MATERIALS
Machinability study of Aermet 100 | DE95-011532 | p 3084 N95-33408

AIRCRAFT CONTROL
An Electronic Workshop on the Performance Seeking, Control and Propulsion Controlled Aircraft Results of the F-15 Highly Integrated Digital Electronic Control Flight Research Program
| NASA-TM-104278 | p 3050 N95-33009
An overview of integrated flight-propulsion controls flight research on the NASA F-15 research airplane p 3051 N95-33010
Performance seeking control program overview p 3051 N95-33011
PSC algorithm description p 3051 N95-33013
PSC implementation and integration p 3051 N95-33014
Performance seeking control excitation mode p 3052 N95-33019
Background and principles of throttles-only flight control p 3053 N95-33021
Propulsion Controlled Aircraft design and development p 3053 N95-33022
Flight test of a propulsion controlled aircraft system on the NASA F-15 airplane p 3049 N95-33023
Design challenges encountered in the F-15 PCA flight test program p 3049 N95-33025
Human piloting factors in the design of control laws for precision landing p 3167 N95-33605
Nonlinear adaptive control of highly maneuverable high performance aircraft p 3192 N95-33712
Beware of agents when flying aircraft: Basic principles behind a generic methodology for the evaluation and certification of advanced aviation systems p 3176 N95-34787
A stochastic adaptive control application to flight systems p 3055 N95-34806

AIRCRAFT DESIGN
Three-dimensional aerodynamic shape optimization using discrete sensitivity analysis p 3048 N95-32904
Propulsion Controlled Aircraft design and development p 3053 N95-33022
Special publication of National Aerospace Laboratory | NAL-SP-27 | p 3034 N95-34505
Requirements and trends of computational aerodynamics as a tool for aircraft design p 3034 N95-34506
Numerical analysis around the whole SST configuration p 3039 N95-34541
Application of CFD techique for HYFLEX aerodynamic design p 3039 N95-34542
An LDV investigation of support structure influence on the flow field near the wingtip of a STOVL configuration in hover
| AD-A294126 | p 3042 N95-34750
Certification for civil flight decks and the human-computer interface p 3176 N95-34784
Some inadequacies of the current human factors certification process of advanced aircraft technologies p 3176 N95-34785
Advanced automated glass cockpit certification: Being wary of human factors p 3176 N95-34786

AIRCRAFT ENGINES
F-15 propulsion system p 3051 N95-33012
Minimum fan turbine inlet temperature mode evaluation p 3052 N95-33016
The application of Ada and formal methods to a safety critical engine control system p 3094 N95-33142

AIRCRAFT ICING
Investigation of water droplet trajectories within the NASA icing research tunnel
| NASA-TM-107023 | p 3034 N95-32769

AIRCRAFT INSTRUMENTS
Integrated special mission flight management for a flight inspection aircraft p 3049 N95-33145

AIRCRAFT LANDING
Dynamic ground effects flight test of the NASA F-15 aircraft p 3049 N95-33024
Design challenges encountered in the F-15 PCA flight test program p 3049 N95-33025
Machinability study of Aermet 100
| DE95-011532 | p 3084 N95-33408
Human piloting factors in the design of control laws for precision landing p 3167 N95-33605

AIRCRAFT MAINTENANCE
Report to Congressional Committees. B-1B bomber: Evaluation of Air Force report on B-1B operational readiness assessment
| GAO/NSIAD-95-151 | p 3197 N95-32758
Report to the Chairman, Committee on Armed Services, US Senate. Strategic Bomber: Issues relating to the B-1B's availability and ability to perform conventional missions
| GAO/NSIAD-94-81 | p 3198 N95-33263

AIRCRAFT MANEUVERS
Negative to positive Gz acceleration transition p 3165 N95-34052

AIRCRAFT MODELS
Low-order nonlinear dynamic model of IC engine-variable pitch propeller system for general aviation aircraft
| NASA-TM-107006 | p 3050 N95-32916

AIRCRAFT NOISE
Direct analysis of transonic rotor noise with CFD technique p 3040 N95-34549

AIRCRAFT PERFORMANCE
Performance seeking control excitation mode p 3052 N95-33019
Flight test of a propulsion controlled aircraft system on the NASA F-15 airplane p 3049 N95-33023

AIRCRAFT PILOTS
Selection and special physiological training of flying personnel to high +G(z)-maneuverable flights-main concept p 3166 N95-34053
Increase of High-sustained +G(z) tolerance at the expense of pilot's working posture change p 3165 N95-34056
Selection and training of MiG-29 and future fighter pilots p 3166 N95-34059
G-protection capabilities and current G-protection issues p 3169 N95-34060
The ANVIS head-up display: An analysis of its application to naval helicopters
| AD-A294342 | p 3170 N95-34358
Human Factors Certification of Advanced Aviation Technologies
| NASA-CR-199009 | p 3171 N95-34764
A rose by any other name: Certification seen as process rather than content p 3047 N95-34766
A psychologist's view of validating aviation systems p 3172 N95-34767
Certification of tactics and strategies in aviation p 3172 N95-34768
Certification of training p 3166 N95-34774
Does human cognition allow Human Factors (HF) certification of advanced aircrew systems? p 3174 N95-34776
Advanced automated glass cockpit certification: Being wary of human factors p 3176 N95-34786
Beware of agents when flying aircraft: Basic principles behind a generic methodology for the evaluation and certification of advanced aviation systems p 3176 N95-34787

AIRCRAFT PRODUCTION COSTS
Report to Congressional Committees. B-2 bomber: Cost to complete 20 aircraft is uncertain
| GAO/NSIAD-94-217 | p 3033 N95-32782

AIRCRAFT SAFETY
Report to the Chairman, Subcommittee on Aviation, Committee on Commerce, Science, and Transportation, US Senate. Aviation safety: Data problems threaten FAA strides on safety analysis system
| GAO/AIMD-95-27 | p 3046 N95-32705
Report to the Chairman, Subcommittee on Aviation, Committee on Commerce, Science, and Transportation, US Senate. Aviation Safety: FAA can better prepare general aviation pilots for mountain flying risks
| GAO/RCED-94-15 | p 3046 N95-32784
Aviation security: Development of new security technology has not met expectations. Report to Congressional requesters
| GAO/RCED-94-142 | p 3046 N95-32885
Current issues in the design and information content of instrument approach charts
| AD-A294752 | p 3047 N95-34562
The effects of display location and dimensionality on taxiway navigation
| AD-A294878 | p 3047 N95-34570
Corrosion of fire-damaged aircraft
| AD-A294968 | p 3049 N95-34583
Human Factors Certification of Advanced Aviation Technologies
| NASA-CR-199009 | p 3171 N95-34764
On the use of the systems approach to certify advanced aviation technologies p 3171 N95-34765
A rose by any other name: Certification seen as process rather than content p 3047 N95-34766
User type certification for advanced flight control systems p 3055 N95-34772
Towards a framework of human factors certification of complex human-machine systems p 3175 N95-34779
Integrating human factors knowledge into certification: The point of view of the Internationanl Civil Aviation Organization (ICAO) p 3175 N95-34782
Some inadequacies of the current human factors certification process of advanced aircraft technologies p 3176 N95-34785
Beware of agents when flying aircraft: Basic principles behind a generic methodology for the evaluation and certification of advanced aviation systems p 3176 N95-34787

AIRCRAFT STRUCTURES
Development of a composite tailoring procedure for airplane wing
| NASA-CR-199081 | p 3048 N95-32928

AIRCRAFT SURVIVABILITY
Aviation security: Development of new security technology has not met expectations. Report to Congressional requesters
| GAO/RCED-94-142 | p 3046 N95-32885

AIRFIELD SURFACE MOVEMENTS
The effects of display location and dimensionality on taxiway navigation
| AD-A294878 | p 3047 N95-34570

AIRFOILS
Allison engine testing CMSX-4(reg sign) single crystal turbine blades and vanes
| DE95-010308 | p 3050 N95-32636
Turbulence models in the Navier-Stokes simulation of airfoil stall
| TRITA-NA-9312 | p 3108 N95-33059
Special publication of National Aerospace Laboratory | NAL-SP-27 | p 3034 N95-34505
Numerical solutions of inviscid and viscous flows about airfoils by TVD method p 3036 N95-34521
Numerical simulations of dynamic stall phenomena in low speed flows p 3040 N95-34546
Numerical simulation of unsteady viscous flow around an airfoil with oscillating spoiler p 3040 N95-34547
Grid generation around airfoil with a flap using boundary element method p 3041 N95-34552
Nonlinear stability of unsteady viscous flow
| AD-A294931 | p 3113 N95-34597

AIRLINE OPERATIONS
Fact sheet for Congressional requesters. Airport competition: Essential air service slots at O'Hare International Airport
| GAO/RCED-94-118FS | p 3055 N95-32759

AIRPORT SECURITY
Functional requirements analysis and human machine interface specifications for handheld metal detector wands
| DE95-009845 | p 3167 N95-32535
Aviation security: Development of new security technology has not met expectations. Report to Congressional requesters
| GAO/RCED-94-142 | p 3046 N95-32885

AIRPORTS
Fact sheet for Congressional requesters. Airport competition: Essential air service slots at O'Hare International Airport
| GAO/RCED-94-118FS | p 3055 N95-32759
Report to the Chairman, Subcommittee on Transportation and Related Agencies, Committee on Appropriations, US Senate. Airport Improvement Program: Reliever airport set-aside funds could be redirected
| GAO/RCED-94-226 | p 3055 N95-32786
Report to the Chairman, Subcommittee on Transportation and Related Agencies, Committee on Appropriations, US Senate. Airport Improvement Program: The Military Airport Program has not achieved intended impact
| GAO/RCED-94-209 | p 3056 N95-32888

AIRSPEED
Human piloting factors in the design of control laws for precision landing p 3167 N95-33605

ALBEDO
Improving alpine-region spectral unmixing with optimal-fit snow endmembers p 3135 N95-33764

ALCOHOLS
NQR-NMR studies of higher alcohol synthesis Cu-Co catalysts
| DE95-010524 | p 3066 N95-32557
Introductions of FFV
| PB95-214656 | p 3088 N95-33332
Catalytic conversion of light alkanes: Proof of concept stage
| DE95-012318 | p 3076 N95-34810

ALGAE
Photobiology and optical properties of planktonic and sea ice microalgae in the high arctic
| AD-A294002 | p 3160 N95-34457

ALGEBRA
Campbell-Hausdorff formula and algebras with operator
| DE95-623635 | p 3195 N95-32609
Tracing a planar algebraic curve
| DE95-613375 | p 3195 N95-33058
Accuracy enhancement in optical computing
| AD-A294958 | p 3219 N95-34579

ALGORITHMS
Off-training-set error for the Gibbs and the Bayes optimal generalizers
| DE95-006344 | p 3187 N95-32375
Training neural networks using sequential extended Kalman filtering
| DE95-007874 | p 3187 N95-32386

HINT: A new way to measure computer speed
| DE95-010245 | p 3177 N95-32398
Validation of space/ground antenna control algorithms using a computer-aided design tool
p 3183 N95-32429
A preliminary evaluation of histogram-based binarization algorithms
| DE95-009886 | p 3179 N95-32470
Optimum Routeing: Analytical constraint of search space p 3044 N95-32493
On bootstrapping local search with trail-markers
| DE95-009835 | p 3187 N95-32533
Intervals in evolutionary algorithms for global optimization
| DE95-010866 | p 3179 N95-32572
On the feasibility of using smoothed particle hydrodynamics for underwater explosion calculations
| DE95-008799 | p 3106 N95-32587
Beam-based magnetic alignment of the final focus test beam
| DE95-012096 | p 3212 N95-32657
On the Minimum Weight Steiner Triangular Tiling Problem
| DE95-009482 | p 3180 N95-32716
Land surface temperature measurements from EOS MODIS data
| NASA-CR-199082 | p 3142 N95-32717
Ocean observations with EOS/MODIS: Algorithm development and post launch studies
| NASA-CR-198928 | p 3143 N95-32914
Fast approximation of self-similar network traffic
| DE95-011271 | p 3185 N95-32967
PSC algorithm description p 3051 N95-33013
Tracing a planar algebraic curve
| DE95-613375 | p 3195 N95-33058
Function approximation using adaptive and overlapping intervals
| DE95-010865 | p 3191 N95-33212
Combining the QMR method with first principles electronic structure codes
| DE95-009927 | p 3228 N95-33240
Nonlinear analyses of storage ring lattices using one-turn maps
| DE95-012515 | p 3213 N95-33335
Bicriteria network design problems
| DE95-012052 | p 3099 N95-33387
Cubic-B-spline boundary elements for two-dimensional and axisymmetric elastostatics p 3127 N95-33695
A comparison of interface tracking methods
| DE95-009481 | p 3111 N95-33698
Mapping minerals, amorphous materials, environmental materials, vegetation, water, ice and snow, and other materials: The USGS tricorder algorithm
p 3130 N95-33742
Calibration to surface reflectance of terrestrial imaging spectrometry data: Comparison of methods
p 3130 N95-33743
High accuracy in-flight wavelength calibration of imaging spectrometry data p 3132 N95-33750
An algorithm for chlorophyll using first difference transformations of AVIRIS reflectance spectra
p 3134 N95-33763
Spectral identification of minerals using imaging spectrometry data: Evaluating the effects of signal to noise and spectral resolution using the tricorder algorithm
p 3136 N95-33772
High performance compression of science data
p 3242 N95-34237
Parallel solution of large-scale nonlinear optimization
| AD-A294372 | p 3186 N95-34340
Branch and bound methods for search problems
| AD-A294522 | p 3182 N95-34349
An improved algorithm for computing altitude dependent Corrected GeoMagnetic coordinates
| AD-A293967 | p 3144 N95-34454
Image compression scheme for network transmission
| AD-A294959 | p 3182 N95-34580
Optimization problems in multitarget/multisensor tracking
| AD-A294978 | p 3100 N95-34590
Some issues in nonlinear programming algorithms for problems with simulation constraints
| AD-A294932 | p 3182 N95-34598
Towards a formalism for program generation 1995
| AD-A294941 | p 3183 N95-34604
Non-smooth optimization algorithms, system theory and software tools
| AD-A294944 | p 3183 N95-34605
Numerical and symbolic algorithms for application specific signal processing
| AD-A294125 | p 3100 N95-34749
SAR
| AD-A295020 | p 3101 N95-34788
Electron and hole transport in compound semiconductors
| AD-A295003 | p 3233 N95-34822

ALIGNMENT
Beam-based magnetic alignment of the final focus test beam
| DE95-012096 | p 3212 N95-32657
Read/write module for high capacity memory disk
| AD-A294946 | p 3178 N95-34745

ALIPHATIC HYDROCARBONS
Field Raman spectrograph for environmental analysis
| DE95-007969 | p 3153 N95-32816

ALKALINITY
Discrimination of alkalinity in granitoid Rocks: A potential TIMS application p 3138 N95-33798

ALKANES
Catalytic conversion of light alkanes: Proof of concept stage
| DE95-012318 | p 3076 N95-34810

ALLERGIC DISEASES
Chemical substances lists: A guide to the lists used in the Swedish Sunset Project. Supplement to report 13/94. Selecting multiproblem chemicals for risk reduction. A presentation of the Swedish Sunset Project
| PB95-211272 | p 3073 N95-33328
Sensitizing substances
| PB95-211256 | p 3074 N95-33634

ALLOYING
Development of improved p-type Si-20 at. %Ge by addition of fullerite
| DE95-010230 | p 3066 N95-32394
Fabrication of improved SiGe alloys for an 18-couple module test
| DE95-010238 | p 3060 N95-32396
Knowledge-based system for metallurgical grade design p 3189 N95-32998
Effect of phase transformations on the mechanical properties of a multiphase alloy based on NiAl + Fe
| DE95-010119 | p 3079 N95-33217

ALLOYS
Hydrogen formation in metals and alloys during fusion reactor operation
| DE95-737224 | p 3202 N95-32529

ALLUVIUM
Integration of AIRSAR and AVIRIS data for Trail Canyon alluvial fan, Death Valley, California
p 3134 N95-33760
A field- and laboratory-based quantitative analysis of alluvium: Relating analytical results to TIMS data
p 3139 N95-33800
Use of TOPSAR digital elevation data to determine the 3-dimensional shape of an alluvial fan
p 3139 N95-33804
Lithologic controls on AIRSAR signatures of bedrock and alluvium, at Lunar Crater, Nevada
p 3141 N95-33813

ALTERNATING DIRECTION IMPLICIT METHODS
Unified approach for incompressible flows
p 3113 N95-32425

ALTITUDE
Sea wave parameters, small altitudes and distances measurers design for movement control systems of ships, wing-in-surface effect crafts and seaplanes
p 3094 N95-33141

ALTITUDE CONTROL
Altitude cuing effectiveness of terrain texture characteristics in simulated low-altitude flight
| AD-A294369 | p 3056 N95-34362

ALTITUDE TOLERANCE
A prototype computer program that integrates predictive models and medical handbooks for altitude, cold exposure, and heat stress
| AD-A294006 | p 3182 N95-34371

ALUMINIDES
Strength, ductility, and fracture mode of ternary FeAl alloys
| DE95-010281 | p 3077 N95-32400

ALUMINUM
Effect of phase transformations on the mechanical properties of a multiphase alloy based on NiAl + Fe
| DE95-010119 | p 3079 N95-33217
Structural influences on the work hardening behavior of aluminum
| DE95-011262 | p 3080 N95-33626
A background subtraction routine for enhancing energy-filtered plasmon images of MgAl2O4 implanted with Al(+) and Mg(+) ions
| DE95-012850 | p 3074 N95-33629
Metallized gelled propellants: Oxygen/RP-1/aluminum rocket combustion experiments
| NASA-TM-107025 | p 3088 N95-33876
Infrared detection of chemical corrosion on metal surface
| AD-A295000 | p 3081 N95-34821

ALUMINUM ALLOYS
Characterizing the fragmentation ring on witness plates p 3056 N95-32426
Effect of heat treatment at 1,150 C on creep rupture properties of a Fe3Al-based alloy
| DE95-010295 | p 3077 N95-32527
Fatigue properties for the Al-Li alloy 2090, part 3
| PB95-214532 | p 3078 N95-32614
Low strain behaviour of a particulate reinforced aluminum alloy
| ISBN-0-315-84906-1 | p 3078 N95-32935
Synchrotron radiation studies of local structure and bonding in transition metal aluminides and rare earth transition metal magnetic nitrides
| DE95-011579 | p 3079 N95-33065
Experimental investigation of the separation of texture and residual stress induced anisotropy via oblique incidence acoustoelasticity p 3126 N95-33253

ALUMINUM ARSENIDES
The growth of ultrathin epitaxial intermetallic films
| AD-A295037 | p 3232 N95-34795

ALUMINUM GALLIUM ARSENIDES
Fabrication of optical channel waveguides in the GaAs/AlGaAs system by MeV ion beam bombardment
| DE95-008973 | p 3218 N95-34480

ALUMINUM NITRIDES
High rate dry etching of GaN, AlN and InN in ECR Cl2/CH4/H2/Ar plasmas
| DE95-011872 | p 3223 N95-33412

ALUMINUM OXIDES
Investigation of aging effects from high voltage profiles in ceramic phase shifter materials
| AD-A289985 | p 3082 N95-32694
Lightweight alumina refractory aggregate. Phase 2: Pilot scale development
| DE95-012154 | p 3083 N95-33079
Solubility behavior of quartz and corundum in supercritical water: A quantitative thermodynamic interpretation
| DE95-012294 | p 3234 N95-34211
Fiber coatings for brittle matrix composites
p 3065 N95-34808

AMAZON REGION (SOUTH AMERICA)
Completing below-ground carbon budgets for pastures, recovering forests, and mature forests of Amazonia
| NASA-CR-199129 | p 3143 N95-33498

AMBIGUITY
Application of fuzzy technology to risk-based design and decision problems
| DE95-006815 | p 3178 N95-32378
Application of deformable templates for recognizing tracks detected with High Pressure Drift Tubes
| DE95-621870 | p 3188 N95-32627
Zero modes of Gauss constraint in gaugeless reduction of Yang-Mills theory
| DE95-623676 | p 3234 N95-32667

AMINES
Hand-portable gas chromatography-ion mobility spectrometer for the determination of the freshness of fish p 3071 N95-33277

AMMONIA
Proton affinity determinations and proton-bound dimer structure indications in C2 to C15, (alpha),(omega)-alkyldiamines p 3069 N95-33266
An ammonia monitor for the water industry
p 3071 N95-33281
Growth of GaN single-crystal boules
| AD-A294976 | p 3232 N95-34588

AMMONIUM COMPOUNDS
Quantitative remote sensing of ammonium minerals, Cedar Mountains, Esmeralda County, Nevada
p 3128 N95-33734

AMORPHOUS MATERIALS
Size, shape, and crystallinity of luminescent structures in oxidized Si nanoclusters and H-passivated porous Si
| DE95-012322 | p 3229 N95-33628
Mapping minerals, amorphous materials, environmental materials, vegetation, water, ice and snow, and other materials: The USGS tricorder algorithm
p 3130 N95-33742
A molecular dynamics investigation of the structural characteristics of amorphous and annealed poly (Vinylidene fluoride) and vinylidene fluoride - trifluoroethylene copolymers
| AD-A294116 | p 3086 N95-34502

AMPLIFICATION
Measurement of gain saturation on Nd: Doped phosphate laser glasses
| REPT-2210 | p 3090 N95-32990

ANALOG DATA
A digital boxcar integrator for IMS spectra
p 3072 N95-33288
Crosspoint analog data selector
| AD-D017482 | p 3104 N95-34425

ANALOGIES
Phthalic acid esters used as plastic additives. Volume 1: Ecotoxicological risk assessment. Volume 2: Comparisons of toxicological effects
| PB95-211280 | p 3084 N95-33329

Is the genetic algorithm a cooperative learner?
[AD-A294112] p 3193 N95-34499
ANALYTICAL CHEMISTRY
Application of Ion Mobility Spectrometry (IMS) in forensic chemistry and toxicology with focus on biological matrices p 3072 N95-33285
ANECHOIC CHAMBERS
Anechoic chamber upgrade
[AD-A294375] p 3056 N95-34342
ANGLE OF ATTACK
Techniques for the determination of local dynamic pressure and angle of attack on a horizontal axis wind turbine
[DE95-009204] p 3149 N95-32685
A nonlinear vortex lattice method for unsteady flow with separated vortex
[DLR-FB-94-32] p 3106 N95-32787
ANGULAR DISTRIBUTION
Technical support in the area of theoretical support of nuclear preequilibrium
[DE95-011617] p 3212 N95-32960
ANGULAR MOMENTUM
Faddeev calculations of p(mu)+p collisions: Effect of hyperfine splitting on the cross sections
[DE95-007838] p 3203 N95-32583
ANISOTROPIC MEDIA
Experimental investigation of the separation of texture and residual stress induced anisotropy via oblique incidence acoustoelasticity p 3126 N95-33253
ANISOTROPY
Anisotropic magnetization of HoNi2B2C
[DE95-010239] p 3198 N95-32397
Perpendicular magnetic behavior of ultra-thin Co sandwiches
[DE95-010611] p 3083 N95-32819
Airborne passive polarimetric measurements of sea surface anisotropy at 92 GHz
[NASA-CR-197288] p 3143 N95-32823
Experimental investigation of the separation of texture and residual stress induced anisotropy via oblique incidence acoustoelasticity p 3126 N95-33253
Optical anisotropy of (110) surfaces of Ag and Cu
[DE95-010130] p 3229 N95-33637
Unusual behavior in the magnetic anisotropy of ultra-thin Co sandwiches: The role of Au underlayers
[DE95-010612] p 3229 N95-33641
ANNEALING
Mechanism(s) for the suppression of the switchable polarization in PZT and BaTiO3
[DE95-009589] p 3226 N95-32590
A molecular dynamics investigation of the structural characteristics of amorphous and annealed poly (Vinylidene fluoride) and vinylidene fluoride - trifluoroethylene copolymers
[AD-A294116] p 3086 N95-34502
ANNIHILATION REACTIONS
GRO: Studies of high energy pulsars with EGRET
[NASA-CR-199130] p 3248 N95-33499
ANNULAR FLOW
Dividing annular/two-phase flow in horizontal T-junctions
[ISBN-0-315-84910-X] p 3057 N95-33030
ANODES
Thin-film rechargeable lithium batteries
[DE95-008975] p 3103 N95-33697
ANOMALIES
Chiral restoration in hot and/or dense matter
[DE95-012176] p 3204 N95-32621
ANTENNA ARRAYS
Investigation of aging effects from high voltage profiles in ceramic phase shifter materials
[AD-A289985] p 3082 N95-32694
ANTENNA DESIGN
Validation of space/ground antenna control algorithms using a computer-aided design tool p 3183 N95-32429
X-Antenna: A graphical interface for antenna analysis codes
[NASA-CR-199212] p 3095 N95-32674
Monolithic diode arrays for quasioptical millimeter wave beam steering
[AD-A294256] p 3100 N95-34460
ANTENNA FEEDS
Simulation of patch and slot antennas using FEM with prismatic elements and investigations of artificial absorber mesh termination schemes
[NASA-CR-198974] p 3097 N95-32822
ANTENNA RADIATION PATTERNS
X-Antenna: A graphical interface for antenna analysis codes
[NASA-CR-199212] p 3095 N95-32674
Simulation of patch and slot antennas using FEM with prismatic elements and investigations of artificial absorber mesh termination schemes
[NASA-CR-198974] p 3097 N95-32822
Anechoic chamber upgrade
[AD-A294375] p 3056 N95-34342
ANTENNAS
Quench antenna and fast-motion investigations during training of a 7T dipole magnet
[DE95-012371] p 3103 N95-33080
ANTIMONY
Use of D2 to elucidate OMVPE growth mechanisms
[AD-A294999] p 3233 N95-34820
ANTIMONY ALLOYS
Multilayer thermoelectric films: A strategy for the enhancement of ZT
[DE95-011535] p 3081 N95-34482
ANTIPROTONS
Progress towards antihydrogen production by the reaction of cold antiprotons with positronium atoms
[DE95-007850] p 3204 N95-32584
ANTIRADAR COATINGS
Experimental investigation of impulse radar for mitigation of effects of radar absorbing materials
[AD-A294166] p 3100 N95-34762
ANTIREFLECTION COATINGS
High power CO2 laser windows and reflection reducing coatings
[AD-A294217] p 3119 N95-34308
Development of 1.06 micron high efficiency antireflective coating
[AD-A294161] p 3219 N95-34759
ANXIETY
Measurement and regulation of central noradrenergic receptors
[AD-A294065] p 3165 N95-34472
APOGEE BOOST MOTORS
Pop tests of storable biopropellant liquid apogee engine
[NAL-TR-1253] p 3060 N95-32755
APPLICATIONS OF MATHEMATICS
On the virtues of parameterized uniform crossover
[AD-A293985] p 3182 N95-34456
Spectrum allocation strategies for communication networks
[AD-A294936] p 3100 N95-34601
APPLICATIONS PROGRAMS (COMPUTERS)
X-Antenna: A graphical interface for antenna analysis codes
[NASA-CR-199212] p 3095 N95-32674
Solving stiff chemistry problems with FIDAP
[DE95-011053] p 3067 N95-32709
OPEX Second Workshop of the OLYMPUS Propagation Experimenters. Volume 5: Reference book on data processing
[ESA-WPP-083-VOL-5] p 3096 N95-32751
FORTRAN program for analyzing ground-based radar data: Usage and derivations, version 6.2
[NASA-TP-3430] p 3181 N95-33193
Operation of the computer model for microenvironment atomic oxygen exposure
[NASA-CR-198190] p 3059 N95-33264
IMS software developments for the detection of chemical warfare agent p 3072 N95-33287
The 3D metal forming applications of ALE techniques
[DE95-011745] p 3080 N95-33653
Studies of microwave scattering and canopy architecture for boreal forests
[NASA-CR-199114] p 3099 N95-33726
Impact of differences in the solar irradiance spectrum on surface reflectance retrieval with different radiative transfer codes p 3136 N95-33771
Operation of the computer model for microenvironment solar exposure
[NASA-CR-198189] p 3059 N95-33890
Experimenter's laboratory for visualized interactive science p 3184 N95-34228
Advanced data visualization and sensor fusion: Conversion of techniques from medical imaging to Earth science p 3242 N95-34236
High performance compression of science data p 3242 N95-34237
A distributed analysis and visualization system for model and observational data p 3243 N95-34240
Multimedia Environmental Pollutant Assessment System (MEPAS(trademark)): Exposure pathway and human health impact assessment models
[DE95-012763] p 3155 N95-34441
The virtual sailor: Synthetic humans for virtual environments
[AD-A293560] p 3166 N95-34610
APPROPRIATIONS
Annual report to the Chairman, House and Senate Committees on Appropriations. Status of open recommendations: Improving operations of federal departments and agencies
[GAO/OP-94-1] p 3236 N95-32887
APPROXIMATION
Estimation of spatially restricted LET using track structure models p 3161 N95-32722
Practical improvement of MS-X alpha molecular orbital calculation as applied to dissociation process of CO molecule
[REPT-2206] p 3090 N95-32986
Function approximation using adaptive and overlapping intervals
[DE95-010865] p 3191 N95-33212
Construction and analysis of difference approximation for scalar conservation laws and its consistency with entropy condition using Boltzmann-like approach p 3036 N95-34519
Control of initialization bias in queueing simulations using queueing approximations
[AD-A294121] p 3194 N95-34742
Numerical and symbolic algorithms for application specific signal processing
[AD-A294125] p 3100 N95-34749
AQUEOUS SOLUTIONS
Enhancement of pool boiling heat transfer to lithium bromide aqueous solution
[REPT-2211] p 3091 N95-32991
Influence of processing variables on the structure and properties of ZnO films
[DE95-011494] p 3084 N95-33405
Encapsulated dry electrolyte composition for time release into a solute
[AD-D017485] p 3075 N95-34287
ARC JET ENGINES
Advanced propulsion for geostationary orbit insertion and north-south station keeping
[NASA-TM-107018] p 3060 N95-32917
ARCHIPELAGOES
Analyses of TIMS and AVIRIS data, integrated with field and laboratory spectra, for lithological and mineralogical interpretation of Vulcano Island, Italy p 3137 N95-33790
ARCHITECTURE (COMPUTERS)
The future of finite element applications on massively parallel supercomputers
[DE95-011659] p 3184 N95-32415
A highly reliable, high performance open avionics architecture for real time Nap-of-the-Earth operations p 3044 N95-32497
Development and flight testing of an Obstacle Avoidance System for US Army helicopters p 3045 N95-32500
VHS-tape system for general purpose computer. For next generation mass storage system
[DE95-737268] p 3177 N95-32757
Weather Forecasting: Systems architecture needed for National Weather Service modernization. Report to Congressional requesters
[GAO/AIMD-94-28] p 3157 N95-32760
Open architecture CNC system
[DE95-009485] p 3177 N95-32955
Planetary data analysis and display system: A version of PC-MIDAS p 3241 N95-34232
Multi-layer holographic bifurcative neural network system for real-time adaptive EOS data analysis p 3148 N95-34233
Construction of a connectionist network supercomputer
[AD-A294198] p 3177 N95-34301
Optical interconnects for 3D computer architectures
[AD-A294118] p 3178 N95-34503
Highly parallel computer AP1000: Architecture and basic software p 3038 N95-34534
High order accuracy computational methods in aerodynamics using parallel architectures
[AD-A294167] p 3042 N95-34763
ARCTIC OCEAN
Proceedings of the ONR/NRL workshop on modeling the dispersion of nuclear contaminants in the arctic seas
[AD-A294373] p 3159 N95-34341
ARCTIC REGIONS
Photobiology and optical properties of planktonic and sea ice microalgae in the high arctic
[AD-A294002] p 3160 N95-34457
ARGON LASERS
Indium mono-ion oscillator
[AD-A293736] p 3104 N95-34451
ARID LANDS
Canopy reflectance modelling of semiarid vegetation
[NASA-CR-199117] p 3142 N95-32676
ARITHMETIC
Intervals in evolutionary algorithms for global optimization
[DE95-010866] p 3179 N95-32572
ARITHMETIC AND LOGIC UNITS
Bit-level analysis of an SRT divider circuit
[AD-A294842] p 3105 N95-34565
ARMED FORCES (UNITED STATES)
Aerospace Guidance and Metrology Center: Cost growth and other factors affect closure and privatization. Report to Congressional requesters
[GAO/NSIAD-95-60] p 3235 N95-32706

Army aviation: Modernization strategy needs to be reassessed. Report to Congressional requestors
[GAO/NSIAD-95-9] p 3033 N95-32783
Report to Congressional Committees. Air Force fighters: More reliance on reserves increases the need to know their capabilities
[GAO/NSIAD-94-86] p 3197 N95-32807
Tri-service perspectives on microclimate cooling of protective clothing in the heat
[AD-A294005] p 3170 N95-34370
A prototype computer program that integrates predictive models and medical handbooks for altitude, cold exposure, and heat stress
[AD-A294006] p 3182 N95-34371
Aerospace physiology AFSC 4M0X1
[AD-A294839] p 3165 N95-34564

ARMOR

A study of the effect of grain size on the ballistic performance of silicon carbide
[DE95-011724] p 3126 N95-33068

ARPA COMPUTER NETWORK

Security and privacy in the NII
[AD-A293475] p 3244 N95-34816

ARTIFICIAL INTELLIGENCE

Training neural networks using sequential extended Kalman filtering
[DE95-007874] p 3187 N95-32386
Numerical solution of differential equations by artificial neural networks p 3194 N95-32434
An original numerical method for autonomous navigation p 3044 N95-32495
On bootstrapping local search with trail-markers
[DE95-009835] p 3187 N95-32533
Industrial and Engineering Applications of Artificial Intelligence and Expert Systems: Invited and additional papers
[DSTO-GD-0051] p 3188 N95-32995
Incorporating distributed problem solving technique into a case-based system p 3188 N95-32997
Monitoring of the cutting operations using fuzzy logic p 3189 N95-32999
An alternative reasoning method p 3189 N95-33001
Induction of dependency structures from data and its application to ozone prediction p 3190 N95-33003
The method of model-based reasoning and application of an intelligent adaptive observer on the integrated process p 3190 N95-33005
Expert systems and artificial intelligence applications in engineering design and inspection p 3190 N95-33008
Applied Information Systems Research Program (AISRP) Workshop 3 meeting proceedings
[NASA-CR-199103] p 3239 N95-34218
System of experts for intelligent data management (SEIDAM) p 3240 N95-34226
Development of an expert data reduction assistant p 3242 N95-34234
Towards friendlier user interfaces for expert systems
[AD-A294056] p 3192 N95-34467
Conditions for implicit parallelism
[AD-A294110] p 3193 N95-34497
Everyday believability
[AD-A294938] p 3193 N95-34602
A document analysis system p 3244 N95-34804

ARTIFICIAL SATELLITES

Development of a composite satellite structure for FORTE
[DE95-009416] p 3058 N95-32713
Thermal design of returnable satellites
[AD-A294113] p 3059 N95-34500
Space probe data processing
[AD-A294124] p 3058 N95-34744
Laser beaming demonstrations at the Starfire Optical Range
[DE95-007747] p 3120 N95-34811

ASIA

Intra-annual and inter-annual rainfall variability over East Asia, Southeast Asia, and South Asia
[AD-A294156] p 3158 N95-34757

ASPECT RATIO

Flow and heat transfer behavior of non-Newtonian fluids in rectangular ducts p 3107 N95-32907

ASPHERICITY

Control of the laser beam irradiation intensity distribution using aspherical multi lens array and edge-shaped plates
[REPT-2209] p 3090 N95-32989

ASSEMBLY

Method for making fiber-optic bundle collimator assembly
[AD-D017486] p 3216 N95-34288

ASSESSMENTS

Fusion Safety Program annual report, fiscal year 1994
[DE95-008872] p 3221 N95-32588
A comparison of risk assessment techniques from qualitative to quantitative
[DE95-011430] p 3197 N95-33220
Phthalic acid esters used as plastic additives. Volume 1: Ecotoxicological risk assessment. Volume 2: Comparisons of toxicological effects
[PB95-211280] p 3084 N95-33329
Risk assessment of polybrominated diphenyl ethers
[PB95-211306] p 3073 N95-33330
Evaluation of conductive, radiative, chemical, and convective heat transfer in complex systems using a fast-running, implicit, lumped-capacitance formulation
[DE95-011889] p 3111 N95-33837

ASTRONAUTS

The role of the vestibular system in manual target localization p 3166 N95-32422
Bicycle ergometer instrumentation to determine muscle and bone forces during exercise p 3176 N95-32428
Liftoff to learning: Assignment space
[NASA-TM-110820] p 3057 N95-32539
Twenty-five years of progress. Part 1: Birth of NASA. Part 2: The Moon-a goal
[NASA-TM-110819] p 3253 N95-33384

ASTRONOMICAL OBSERVATORIES

Development of a tool-set for simultaneous, multi-site observations of astronomical objects p 3239 N95-34221

ASTRONOMICAL PHOTOMETRY

Topography from shading and stereo p 3241 N95-34229

ASTROPHYSICS

The mini-CIDEX GC/IMS: Analysis of cometary ice and dust p 3069 N95-33270
Advanced far infrared detector and double donor studies in Ge
[DE95-011261] p 3247 N95-33625
Sinuous oscillations and steady warps of polytropic disks
[DE95-013473] p 3247 N95-34216
Multivariate statistical analysis software technologies for astrophysical research involving large data bases p 3240 N95-34222

ASYMMETRY

Production asymmetries in x(sub f) and P(sup 2)(sub t) for D(sup +/-) mesons
[DE95-007207] p 3201 N95-32379
Zeolite membranes for gas separations
[DE95-012984] p 3068 N95-33224

ASYMPTOTIC METHODS

Sinuous oscillations and steady warps of polytropic disks
[DE95-013473] p 3247 N95-34216

ASYMPTOTIC PROPERTIES

Stability of steady state solutions for forced Navier-Stokes equations p 3112 N95-34286
The computation of electron transfer rates: The nonadiabatic instanton solution
[AD-A294523] p 3209 N95-34350

ASYMPTOTIC SERIES

The computation of electron transfer rates: The nonadiabatic instanton solution
[AD-A294523] p 3209 N95-34350
Structure of weak shock waves in bubbly liquid p 3037 N95-34527

ATLANTIC OCEAN

Turbulent heat flux measurements over the Greenland, Norwegian and Barents seas
[AD-A294129] p 3157 N95-34751

ATMOSPHERIC ATTENUATION

Optimization of a melting layer model in the radar backscatter, attenuation, and phase shift calculations at centimeter and millimeter wavelengths
[PB95-207189] p 3155 N95-32455
OPEX: Second Workshop of the OLYMPUS propagation experimenters. Volume 1: Reference book on attenuation measurement and prediction
[ESA-WPP-083-VOL-1] p 3096 N95-32747
High accuracy in-flight wavelength calibration of imaging spectrometry data p 3132 N95-33750
Determination of the in-flight spectral calibration of AVIRIS using atmospheric absorption features p 3117 N95-33751
Atmospheric attenuation properties associated with CO2 laser radiation spectra
[AD-A294061] p 3120 N95-34470

ATMOSPHERIC BOUNDARY LAYER

Large-eddy simulation of the development of stably-stratified atmospheric boundary layers over cool flat surfaces
[DE95-009574] p 3156 N95-32697
Wavelet analysis of atmospheric turbulence structures: What can we gain from this new technique?
[DE95-011955] p 3156 N95-33847
On the nonlinear stability of a nearby parallel and a non-unidirectional flow p 3112 N95-34284

ATMOSPHERIC CHEMISTRY

Development of High Spectral Resolution Lidar (HSRL) technology
[DE95-011906] p 3099 N95-33839
Enhanced shortwave cloud radiative forcing due to anthropogenic aerosols
[DE95-013319] p 3156 N95-34214

ATMOSPHERIC CIRCULATION

Large-eddy simulation of the development of stably-stratified atmospheric boundary layers over cool flat surfaces
[DE95-009574] p 3156 N95-32697
Nonlinear symmetric stability of planetary atmospheres
[DE95-012133] p 3248 N95-33390
Abstracts of oral and poster sessions
[DE95-011951] p 3154 N95-33413

ATMOSPHERIC COMPOSITION

Modeling soil climate controls on the exchange of trace gases between the terrestrial biosphere and the atmosphere p 3153 N95-33337
Multiscale characteristics and modeling of atmospheric methane p 3154 N95-33339
Abstracts of oral and poster sessions
[DE95-011951] p 3154 N95-33413
Carbon Dioxide Information Analysis Center and World Data Center: A for Atmospheric trace gases
[DE95-011769] p 3154 N95-33655

ATMOSPHERIC CORRECTION

Ocean observations with EOS/MODIS: Algorithm development and post launch studies
[NASA-CR-198928] p 3143 N95-32914
Correction of thin cirrus effects in AVIRIS images using the sensitive 1.375-micron cirrus detecting channel p 3131 N95-33748
High accuracy in-flight wavelength calibration of imaging spectrometry data p 3132 N95-33750
Extraction of ozone and chlorophyll-A distribution from AVIRIS data p 3136 N95-33770
Impact of differences in the solar irradiance spectrum on surface reflectance retrieval with different radiative transfer codes p 3136 N95-33771
For geological investigations with airborne thermal infrared multispectral images: Transfer of calibration from laboratory spectrometer to TIMS as alternative for removing atmospheric effects p 3137 N95-33792

ATMOSPHERIC EFFECTS

Analysis and design methodology for chordwise deformable wings p 3049 N95-33311
Correction of thin cirrus effects in AVIRIS images using the sensitive 1.375-micron cirrus detecting channel p 3131 N95-33748
For geological investigations with airborne thermal infrared multispectral images: Transfer of calibration from laboratory spectrometer to TIMS as alternative for removing atmospheric effects p 3137 N95-33792

ATMOSPHERIC GENERAL CIRCULATION MODELS

Impact of cloud microphysics on cloud-radiation interactions in the CSU general circulation model
[DE95-008979] p 3153 N95-33205

ATMOSPHERIC MODELS

Optimization of a melting layer model in the radar backscatter, attenuation, and phase shift calculations at centimeter and millimeter wavelengths
[PB95-207189] p 3155 N95-32455
Ocean observations with EOS/MODIS: Algorithm development and post launch studies
[NASA-CR-198928] p 3143 N95-32914
Identification of critical substorm-expansion-phase phenomena: Problems addressable with GEM observations
[ATR-94(7270)-1] p 3158 N95-33259
Multiscale characteristics and modeling of atmospheric methane p 3154 N95-33339
MODTRAN3: An update and recent validations against airborne high resolution interferometer measurements p 3128 N95-33732
Construction of an advanced software tool for planetary atmospheric modeling p 3184 N95-34225

ATMOSPHERIC MOISTURE

OPEX Second Workshop of the OLYMPUS Propagation Experimenters. Volume 3: Reference book on radiometry and meteorological measurements
[ESA-WPP-083-VOL-3] p 3096 N95-32749
OPEX Second Workshop of the OLYMPUS Propagation Experimenters. Volume 4: Reference book on radar
[ESA-WPP-083-VOL-4] p 3096 N95-32750
Analyses and forecasts with LAWS winds
[NASA-CR-199134] p 3157 N95-32933
Impact of cloud microphysics on cloud-radiation interactions in the CSU general circulation model
[DE95-008979] p 3153 N95-33205
Movement of water vapor in the atmosphere measured by an imaging spectrometer at Rogers Dry Lake, CA p 3132 N95-33753

Measurement of atmospheric water vapor, leaf liquid water and reflectance with AVIRIS in the Boreal Ecosystem-Atmosphere Study: Initial results p 3133 N95-33755

ATMOSPHERIC PHYSICS

Identification of critical substorm-expansion-phase phenomena: Problems addressable with GEM observations
| ATR-94(7270)-1 | p 3158 N95-33259

Applied Information Systems Research Program (AISRP) Workshop 3 meeting proceedings
| NASA-CR-199103 | p 3239 N95-34218

Stimulated rotational Raman scattering of N2 in the atmosphere
| AD-A294195 | p 3157 N95-34299

ATMOSPHERIC PRESSURE

Fundamental studies of gas phase ionic reactions by ion mobility spectrometry p 3069 N95-33268

Turbulent heat flux measurements over the Greenland, Norwegian and Barents seas
| AD-A294129 | p 3157 N95-34751

ATMOSPHERIC RADIATION

Impact of cloud microphysics on cloud-radiation interactions in the CSU general circulation model
| DE95-008979 | p 3153 N95-33205

Balloon-borne radiometer profiler: Field observations
| DE95-011493 | p 3158 N95-33505

ATMOSPHERIC REFRACTION

FORTRAN program for analyzing ground-based radar data: Usage and derivations, version 6.2
| NASA-TP-3430 | p 3181 N95-33193

ATMOSPHERIC SCATTERING

Comparison of seasonal and zonal patterns of the direct and indirect radiative forcing of climate by aerosols
| DE95-010896 | p 3153 N95-33192

ATMOSPHERIC SOUNDING

Iron Boltzmann factor LIDAR: Proposed new remote-sensing technique for mesospheric temperature
| AD-A293568 | p 3157 N95-34613

ATMOSPHERIC TEMPERATURE

Iron Boltzmann factor LIDAR: Proposed new remote-sensing technique for mesospheric temperature
| AD-A293568 | p 3157 N95-34613

ATMOSPHERIC TURBULENCE

Large-eddy simulation of the development of stably-stratified atmospheric boundary layers over cool flat surfaces
| DE95-009574 | p 3156 N95-32697

Wavelet analysis of atmospheric turbulence structures: What can we gain from this new technique?
| DE95-011955 | p 3156 N95-33847

ATOMIC BEAMS

High-resolution magnetic imaging and investigations of thin-film magnetism with spin-polarized electron, ion and atom probes
| DE95-012190 | p 3074 N95-33392

ATOMIC COLLISIONS

High energy collisions involving multiply charged ions
| DE95-010912 | p 3206 N95-32763

CDW-EIS calculation of longitudinal momentum distribution in single ionization of helium by Ni(24+) ions
| DE95-010816 | p 3207 N95-33241

State-selective single electron capture cross sections in He(exp 2+) + Li(2s) and Li(*)(2p) collisions
| DE95-010819 | p 3207 N95-33371

Impact-parameter dependent L-K vacancy-transfer in collisions of Ni(23+) with Ge solid targets
| DE95-010821 | p 3228 N95-33373

ATOMIC ENERGY LEVELS

Probe transparency in a two-level medium embedded by a squeezed vacuum
| DE95-614123 | p 3198 N95-32525

ATOMIC EXCITATIONS

Impact-parameter dependent L-K vacancy-transfer in collisions of Ni(23+) with Ge solid targets
| DE95-010821 | p 3228 N95-33373

ATOMIC FORCE MICROSCOPY

Influence of processing variables on the structure and properties of ZnO films
| DE95-011494 | p 3084 N95-33405

ATOMIC PHYSICS

Low energy collisions involving multiply charged ions
| DE95-010911 | p 3203 N95-32564

ATOMIC SPECTRA

Spin counting in dipolar coupled spin 1/2 systems by multiple quantum NMR spectroscopy in solids: Development of a single quantum propagator and its application to heterogeneous catalysis
| DE95-010246 | p 3066 N95-32540

Development of ultrasensitive spectroscopic analysis technology Development of atomic spectroscopy technology
| DE95-614352 | p 3066 N95-32566

Exchange, interpretation, and database-search of ion mobility spectra supported by data format JCAMP-DX p 3070 N95-33274

ATOMIC STRUCTURE

A Study of the A dependence of the deep inelastic scattering of leptons and implications for understanding of the EMC effect
| DE95-613711 | p 3206 N95-32796

Combining the QMR method with first principles electronic structure codes
| DE95-009927 | p 3228 N95-33240

Nucleation, propagation, electronic levels and elimination of misfit dislocations in 3-5 semiconductor interfaces
| DE95-011595 | p 3231 N95-34485

Static displacements of atoms in crystalline metallic solid solutions
| DE95-012893 | p 3233 N95-34802

ATOMIZING

Near-limit drop deformation and secondary breakup p 3107 N95-32902

ATOMS

Smoothing during ion-assisted growth by transient ion beam-induced defects
| DE95-011021 | p 3225 N95-32579

Atoms in strong fields
| AD-A294589 | p 3209 N95-34423

ATTACK AIRCRAFT

Fixed wing night attack missions: Assessment in a Flight Simulation environment p 3045 N95-32502

Covert Night/Day Operations for Rotorcraft (CONDOR) programme p 3046 N95-32505

Comanche helicopter: Testing needs to be completed prior to production decisions
| AD-A294408 | p 3049 N95-34422

ATTENUATION COEFFICIENTS

Atmospheric attenuation properties associated with CO2 laser radiation spectra
| AD-A294061 | p 3120 N95-34470

Effect of propagation attenuation of thin film waveguide on optical thin film losses
| AD-A294064 | p 3218 N95-34471

ATTITUDE (INCLINATION)

YBa2Cu3O(7-x) 45 deg (001) tilt grain boundaries induced by controlled low-energy sputtering of MgO substrates: Transport properties and atomic-scale structure
| DE95-005826 | p 3228 N95-32810

Globally stable feedback laws for near-minimum-fuel and near-minimum-time pointing maneuvers for a landmark-tracking spacecraft
| DE95-009867 | p 3191 N95-33214

AUGMENTATION

Enhancement of pool boiling heat transfer to lithium bromide aqueous solution
| REPT-2211 | p 3091 N95-32991

AUSTENITIC STAINLESS STEELS

Hydrogen formation in metals and alloys during fusion reactor operation
| DE95-737224 | p 3202 N95-32529

Microstructural studies of hydrogen damage in metastable stainless steels p 3080 N95-33774

AUTOIONIZATION

The fully correlated two-electron problem on a numerical lattice
| DE95-010280 | p 3205 N95-32650

AUTOMATA THEORY

Lattice Polymer Automata
| DE95-011980 | p 3062 N95-33848

AUTOMATIC CONTROL

A tactical navigation and routeing system for low-level flight p 3044 N95-32494

Evaluation in context: ATC automation in the field p 3175 N95-34781

Beware of agents when flying aircraft: Basic principles behind a generic methodology for the evaluation and certification of advanced aviation systems p 3176 N95-34787

AUTOMATIC PILOTS

An original numerical method for autonomous navigation p 3044 N95-32495

Integrated special mission flight management for a flight inspection aircraft p 3049 N95-33145

AUTOMATIC WEATHER STATIONS

A tactical present weather sensor for Air Force applications
| AD-A294900 | p 3158 N95-34575

AUTOMOBILE FUELS

Gasoline from natural gas by sulfur processing
| DE95-010651 | p 3087 N95-32563

AUTOMOBILES

Alternative catalyst and exhaust gas sensor work at Argonne National Laboratory
| DE95-007138 | p 3152 N95-32553

The next generation of automobile emissions reduction: Innovative control of off-cycle emissions
| DE95-004057 | p 3153 N95-32809

Introductions of FFV
| PB95-214656 | p 3088 N95-33332

Alternative-fuels technology: Natural gas vehicles as a way to curb urban air pollution
| DE95-012216 | p 3088 N95-33395

AUTONOMOUS NAVIGATION

An original numerical method for autonomous navigation p 3044 N95-32495

GPS-based navigation for space applications p 3058 N95-33144

AUTONOMY

VIEWCACHE: An incremental pointer-based access method for autonomous interoperable databases p 3242 N95-34235

AUTOROTATION

HeliRadar: A rotating antenna synthetic aperture radar for helicopter allweather operations p 3093 N95-33137

AVIONICS

A highly reliable, high performance open avionics architecture for real time Nap-of-the-Earth operations p 3044 N95-32497

AXIAL FLOW

Experimental study of the processes in the expander of the axisymmetric mirror device
| DE95-009846 | p 3221 N95-32536

AXIAL MODES

Combustion-acoustic stability analysis for premixed gas turbine combustors
| NASA-TM-107024 | p 3050 N95-32931

AXIAL STRESS

Analytical modeling of the effect of crack depth, specimen size, and biaxial stress on the fracture toughness of reactor vessel steels
| DE95-005886 | p 3125 N95-32373

AXISYMMETRIC BODIES

Numerical simulation of film cooling effect around axisymmetric body in hypersonic flow field p 3037 N95-34526

B

B STARS

ROSAT survey of emission from Be stars
| NASA-CR-199086 | p 3245 N95-32835

B-1 AIRCRAFT

Report to Congressional Committees. B-1B bomber: Evaluation of Air Force report on B-1B operational readiness assessment
| GAO/NSIAD-95-151 | p 3197 N95-32758

Report to the Chairman, Committee on Armed Services, US Senate. Strategic Bomber: Issues relating to the B-1B's availability and ability to perform conventional missions
| GAO/NSIAD-94-81 | p 3198 N95-33263

B-2 AIRCRAFT

Report to Congressional Committees. B-2 bomber: Cost to complete 20 aircraft is uncertain
| GAO/NSIAD-94-217 | p 3033 N95-32782

BACK INJURIES

Evaluation of a retrofit OH-58 pilot's seat to prevent back injury
| AD-A294895 | p 3171 N95-34574

BACKGROUND NOISE

Space-time adaptive processing for airborne radar
| AD-A293032 | p 3098 N95-33152

BACKSCATTERING

Optimization of a melting layer model in the radar backscatter, attenuation, and phase shift calculations at centimeter and millimeter wavelengths
| PB95-207189 | p 3155 N95-32455

In situ ion-beam analysis and modification of sol-gel zirconia thin films
| DE95-010994 | p 3203 N95-32577

Development of an L-, C-, and X-band radar for backscattering studies over vegetation
| NASA-CR-199112 | p 3097 N95-33033

Studies of microwave scattering and canopy architecture for boreal forests
| NASA-CR-199113 | p 3099 N95-33497

Indirect measurements of hydrogen: The deficit method for a many-component system
| DE95-010993 | p 3208 N95-33623

Accurate estimation of sigma(exp 0) using AIRSAR data p 3139 N95-33805

Remotely sensed indicators of habitat heterogeneity and biological diversity: A preliminary report p 3140 N95-33806

Lithologic controls on AIRSAR signatures of bedrock and alluvium, at Lunar Crater, Nevada p 3141 N95-33813

Regional mapping of forest canopy water content and biomass using AIRSAR images over BOREAS study area p 3142 N95-33815

Development of High Spectral Resolution Lidar (HSRL) technology
| DE95-011906 | p 3099 N95-33839

BACKWARD FACING STEPS
Numerical simulation of interaction between shock wave and density interface p 3039 N95-34543
BACKWARD WAVES
Conversion of the Bernstein-Green-Kruskal wave on the density perturbation, part 1
| DE95-614203 | p 3220 N95-32508
Conversion of the Bernstein-Green-Kruskal wave on the density perturbation, part 3
| DE95-614205 | p 3221 N95-32509
Conversion of the Bernstein-Green-Kruskal wave on the density perturbation, part 4
| DE95-614206 | p 3221 N95-32510
High efficiency vacuum and plasma filled backward wave oscillators: A critical evaluation
| AD-A294963 | p 3105 N95-34581
BACTERIA
Inactivation, DNA double strand break induction and their rejoining in bacterial cells irradiated with heavy ions p 3161 N95-32724
Mutation induction in bacteria after heavy ion irradiation p 3162 N95-32727
BACTERIOPHAGES
Mutation induction in bacteria after heavy ion irradiation p 3162 N95-32727
BALLOON SOUNDING
Balloon-borne radiometer profiler: Field observations
| DE95-011493 | p 3158 N95-33505
BALLOON-BORNE INSTRUMENTS
Balloon-borne radiometer profiler: Field observations
| DE95-011493 | p 3158 N95-33505
BALLOONING MODES
High beta and second stability region transport and stability analysis
| DE95-011298 | p 3225 N95-34812
BANDWIDTH
HINT: A new way to measure computer speed
| DE95-010245 | p 3177 N95-32398
Temporal dynamics of the multi-frequency spectrum generated by self-phase modulation of two frequencies in single-mode fiber
| DE95-010920 | p 3119 N95-33703
BARENTS SEA
Turbulent heat flux measurements over the Greenland, Norwegian and Barents seas
| AD-A294129 | p 3157 N95-34751
BARIUM COMPOUNDS
Investigation of aging effects from high voltage profiles in ceramic phase shifter materials
| AD-A289985 | p 3082 N95-32694
Formation of artificially-layered high-temperature superconductors using pulsed-laser deposition
| DE95-012884 | p 3231 N95-34465
BARIUM OXIDES
Effect of the colony microstructure on transport critical current of high-J(c) Tl-1223 thick films
| DE95-013049 | p 3230 N95-34213
BARIUM TITANATES
Mechanism(s) for the suppression of the switchable polarization in PZT and BaTiO3
| DE95-009589 | p 3226 N95-32590
BAROCLINITY
Vorticity in shock-accelerated density-stratified interfaces: An analytical and computational study p 3111 N95-33607
BARRIER LAYERS
Properties of high-T(sub c) Josephson junctions with Y(0.7)Ca(0.3)Ba2Cu3O(7-delta) barrier layers
| AD-A294852 | p 3231 N95-34568
BARYONS
Isgur-Wise function and polarization characteristics of Lambda(sub b)-baryon
| DE95-623696 | p 3202 N95-32407
Search for N(sub (phi))(1960) baryon
| DE95-619290 | p 3205 N95-32703
BATHYMETERS
Underwater acoustic field extrapolation: Theory and sensitivity analysis
| AD-A294925 | p 3201 N95-34595
BAUSCHINGER EFFECT
Low strain behaviour of a particulate reinforced aluminum alloy
| ISBN-0-315-84906-1 | p 3078 N95-32935
BAYES THEOREM
Off-training-set error for the Gibbs and the Bayes optimal generalizers
| DE95-006344 | p 3187 N95-32375
The composite classification problem in optical information processing p 3244 N95-32430
Induction of dependency structures from data and its application to ozone prediction p 3190 N95-33003
Bayes classification of interferometric TOPSAR data p 3140 N95-33808
BEACONS
OPEX Second Workshop of the OLYMPUS Propagation Experimenters. Volume 2: Reference book on depolarisation
| ESA-WPP-083-VOL-2 | p 3096 N95-32748
BEAM CURRENTS
Emittance growth due to decoherence and wakefields
| DE95-012495 | p 3213 N95-33376
Injection envelope matching in storage rings
| DE95-012496 | p 3213 N95-33377
BEAM INJECTION
Unexpected matching insensitivity in DTL of GTA accelerator
| DE95-011984 | p 3211 N95-32416
Estimation of collective instabilities in RHIC
| DE95-011347 | p 3211 N95-32485
Radial electric field measurement in a tokamak by the injection of a pulsed neutral beam
| DE95-614176 | p 3221 N95-32561
Injection envelope matching in storage rings
| DE95-012496 | p 3213 N95-33377
A map for the thick beam-beam interaction
| DE95-012561 | p 3213 N95-33385
BEAM INTERACTIONS
Unexpected matching insensitivity in DTL of GTA accelerator
| DE95-011984 | p 3211 N95-32416
A map for the thick beam-beam interaction
| DE95-012561 | p 3213 N95-33385
The effect of phase advance errors between interaction points on beam halos
| DE95-012559 | p 3214 N95-34023
Studies of halo distributions under beam-beam interaction
| DE95-012560 | p 3214 N95-34024
BEAMFORMING
Impedance study for the PEP-2 B-factory
| DE95-010569 | p 3203 N95-32567
Transverse multibunch instabilities for non-rigid bunches
| DE95-012098 | p 3211 N95-32607
Targets and magnetic elements for pion collection in muon collider drivers
| DE95-010316 | p 3205 N95-32652
A low diffraction beam technique for scanning in the shallow ocean
| DE95-011742 | p 3159 N95-33410
BEAMS (RADIATION)
Summary of the impedance working group
| DE95-012095 | p 3211 N95-32606
Fast feedback for linear colliders
| DE95-012099 | p 3211 N95-32608
Effects of enhanced chromatic nonlinearity during the AGS gamma(t)-jump
| DE95-011703 | p 3212 N95-33067
A low diffraction beam technique for scanning in the shallow ocean
| DE95-011742 | p 3159 N95-33410
BEDROCK
Lithologic controls on AIRSAR signatures of bedrock and alluvium, at Lunar Crater, Nevada p 3141 N95-33813
BELLOWS
Summary of the impedance working group
| DE95-012095 | p 3211 N95-32606
BENDING
Analysis and design methodology for chordwise deformable wings p 3049 N95-33311
The linear elastic biaxial response of plain-woven meshes p 3064 N95-33468
Bending strength model for internal spur gear teeth
| NASA-TM-107012 | p 3124 N95-33908
BENDING MOMENTS
Design of deepwater pipelines
| PB95-215109 | p 3095 N95-33244
BENZENE
Determination of Benzene, Toluene, and Xylene by means of an ion mobility spectrometer device using photoionization p 3069 N95-33269
BERYLLIUM
Fusion Safety Program annual report, fiscal year 1994
| DE95-008872 | p 3221 N95-32588
Beryllium and Boron abundances in population II stars
| NASA-CR-189434 | p 3247 N95-33262
BETA PARTICLES
On the paraxial equilibrium of the finite (beta) plasma in open magnetic configurations
| DE95-614170 | p 3221 N95-32560
BETAINES
Solvent effects on the electronic spectrum of R hardt's dye
| AD-A293667 | p 3067 N95-32804
BIAS
Mechanism(s) for the suppression of the switchable polarization in PZT and BaTiO3
| DE95-009589 | p 3226 N95-32590
Control of initialization bias in queueing simulations using queueing approximations
| AD-A294121 | p 3194 N95-34742
BIBLIOGRAPHIES
AGARD index of publications: 1992-1994
| AGARD-INDEX-92-94 | p 3237 N95-33198
Incorporating bibliographic information into a spatial data query system for the Savannah River Site
| DE95-010965 | p 3238 N95-33402
Bibliography on cold regions science and technology: Volume 48, part 1
| AD-A293988 | p 3243 N95-34420
Bibliography on cold regions science and technology: Volume 48, part 2
| AD-A293993 | p 3243 N95-34421
BIDIRECTIONAL REFLECTANCE
Land surface temperature measurements from EOS MODIS data
| NASA-CR-199082 | p 3142 N95-32717
BINARY ALLOYS
Strength, ductility, and fracture mode of ternary FeAl alloys
| DE95-010281 | p 3077 N95-32400
Corrosion of separator plate constituents in molten carbonate
| PB95-214490 | p 3149 N95-32813
Effect of phase transformations on the mechanical properties of a multiphase alloy based on NiAl + Fe
| DE95-010119 | p 3079 N95-33217
BINARY DATA
A preliminary evaluation of histogram-based binarization algorithms
| DE95-009886 | p 3179 N95-32470
Synthesis of potential new Zintl phases
| DE95-010123 | p 3227 N95-32640
Bit-level analysis of an SRT divider circuit
| AD-A294842 | p 3105 N95-34565
BINARY STARS
High speed variability in x-ray binary systems
| AD-A294634 | p 3247 N95-34561
BINDING ENERGY
Synchrotron radiation studies of local structure and bonding in transition metal aluminides and rare earth transition metal magnetic nitrides
| DE95-011579 | p 3079 N95-33065
Theoretical dynamical studies of metal clusters and cluster-ligand systems
| DE95-012461 | p 3228 N95-33382
BINOCULAR VISION
A comparison of monocular, biocular, and binocular night vision goggles for traversing off-road terrain on foot
| AD-A294018 | p 3170 N95-34376
BIOCHEMISTRY
Causal correlation of foliar biochemical concentrations with AVIRIS spectra using forced entry linear regression p 3130 N95-33744
Prospect redux p 3133 N95-33758
Measurement and regulation of central noradrenergic receptors
| AD-A294065 | p 3165 N95-34472
BIODEGRADATION
The 17th Symposium on Biotechnology for Fuels and Chemicals
| DE95-004054 | p 3150 N95-33225
Phthalic acid esters used as plastic additives. Volume 1: Ecotoxicological risk assessment. Volume 2: Comparisons of toxicological effects
| PB95-211280 | p 3084 N95-33329
Geochemical, genetic, and physiological control of pollutant biodegradation
| AD-A294902 | p 3155 N95-34591
BIODYNAMICS
The preservation of human surrogates for biomechanical studies p 3167 N95-33312
The virtual sailor: Synthetic humans for virtual environments
| AD-A293560 | p 3166 N95-34610
BIOINSTRUMENTATION
New advances in physiological measurements during high-G: Technology p 3165 N95-34057
Methods for measuring physiological responses and protection in man exposed to high + G(z) p 3166 N95-34058
BIOLOGICAL DIVERSITY
Clearing-house mechanism to promote and facilitate technical and scientific cooperation under the UN Convention on Biological Diversity
| PB95-214557 | p 3163 N95-33236
Remotely sensed indicators of habitat heterogeneity and biological diversity: A preliminary report p 3140 N95-33806
BIOLOGICAL EFFECTS
Heavy ion action on single cells: Cellular inactivation capability of single accelerated heavy ions p 3162 N95-32729

Cosmic heavy ion tracks in mesoscopic biological test objects p 3163 N95-32730
BIOLOGICAL MODELS (MATHEMATICS)
Estimation of spatially restricted LET using track structure models p 3161 N95-32722
A prototype computer program that integrates predictive models and medical handbooks for altitude, cold exposure, and heat stress
|AD-A294006| p 3182 N95-34371
The virtual sailor: Synthetic humans for virtual environments
|AD-A293560| p 3166 N95-34610
BIOMASS
Accurate estimation of sigma(exp 0) using AIRSAR data p 3139 N95-33805
On the potential of long wavelength imaging radars for mapping vegetation types and woody biomass in tropical rain forests p 3141 N95-33812
Regional mapping of forest canopy water content and biomass using AIRSAR images over BOREAS study area p 3142 N95-33815
BIOPHYSICS
General procedure for clothing evaluations relative to heat stress
|AD-A294953| p 3171 N95-34577
BIOPROCESSING
The 17th Symposium on Biotechnology for Fuels and Chemicals
|DE95-004054| p 3150 N95-33225
BIOSPHERE
Modeling soil climate controls on the exchange of trace gases between the terrestrial biosphere and the atmosphere p 3153 N95-33337
BIOTECHNOLOGY
The 17th Symposium on Biotechnology for Fuels and Chemicals
|DE95-004054| p 3150 N95-33225
Mathematical methods applied to biotechnical processes
|PB95-212114| p 3163 N95-33232
BIPOLAR TRANSISTORS
Operational amplifier using bipolar junction transistors in silicon-on-sapphire
|AD-D017421| p 3105 N95-34618
BIPOLARITY
Design and testing criteria for bipolar plate materials for PEM fuel cell applications
|DE95-010878| p 3148 N95-32575
BISMUTH
Laser induced diffusion of ion-implanted bismuth in fused silica
|DE95-012869| p 3230 N95-34443
BISMUTH ALLOYS
Multilayer thermoelectric films: A strategy for the enhancement of ZT
|DE95-011535| p 3081 N95-34482
BISMUTH COMPOUNDS
Magnetostriction and thermal expansion of the Kondo semiconductor Ce3Bi4Pt3
|DE95-011975| p 3229 N95-33386
BISMUTH OXIDES
Effect of lead content on Bi-2223 formation by a two-powder process
|DE95-009889| p 3079 N95-33215
BLACKOUT (PHYSIOLOGY)
G-protection capabilities and current G-protection issues p 3169 N95-34060
BLANKETS (FUSION REACTORS)
Hydrogen formation in metals and alloys during fusion reactor operation
|DE95-737224| p 3202 N95-32529
BLOCK DIAGRAMS
Basis Image Processor Pr5210: Correlator technical description
|PB95-222485| p 3185 N95-32815
BLOOD FLOW
New advances in physiological measurements during high-G: Technology p 3165 N95-34057
BLOOD PRESSURE
Noninvasive determination of Cardiac Output
|PB95-208310| p 3164 N95-32611
New advances in physiological measurements during high-G: Technology p 3165 N95-34057
BLOOD VOLUME
New advances in physiological measurements during high-G: Technology p 3165 N95-34057
BLUNT BODIES
A variation of the Riemann Problem solution and its application to implicit Godunov's scheme p 3036 N95-34516
BO-105 HELICOPTER
Full-scale hingeless rotor performance and loads
|NASA-TM-110356| p 3048 N95-32699
BOEING 747 AIRCRAFT
SOFIA 2 model telescope wind tunnel test report
|NASA-TM-110668| p 3033 N95-32764
BOLIDES
Historical detection of atmospheric impacts by large bolides using acoustic-gravity waves
|DE95-010864| p 3246 N95-33211
BOLIVIA
New observations of Bolivian wind streaks by JPL Airborne SAR: Preliminary results p 3139 N95-33802
BOLTED JOINTS
Method of installing a metallic threaded insert in a composite/rubber panel
|AD-D017522| p 3065 N95-34620
BOLTS
Bolt preload selection for pulsed-loaded vessel closures
|DE95-006346| p 3121 N95-32376
BOLTZMANN TRANSPORT EQUATION
Construction and analysis of difference approximation for scalar conservation laws and its consistency with entropy condition using Boltzmann-like approach p 3036 N95-34519
BONDED JOINTS
Tests of adhesives used for plate bonding of ATLAS tile-cal hadron calorimeter
|DE95-009917| p 3082 N95-32664
BONDING
Fracture toughness and tensile behavior of multi-layer laminated metal composite of Al 6090-25 vol % SiCp and Al 5182
|DE95-011421| p 3062 N95-32602
Surface chemistry of diamond single crystals
|AD-A294150| p 3232 N95-34755
BONES
Characterization of microgravity effects on bone structure and strength using fractal analysis p 3165 N95-32419
Bicycle ergometer instrumentation to determine muscle and bone forces during exercise p 3176 N95-32428
BORON
Development of improved p-type Si-20 at. %Ge by addition of fullerite
|DE95-010230| p 3066 N95-32394
Effect of phase transformations on the mechanical properties of a multiphase alloy based on NiAl + Fe
|DE95-010119| p 3079 N95-33217
Beryllium and Boron abundances in population II stars
|NASA-CR-189434| p 3247 N95-33262
BOSONS
Top quark signatures in extended color theories
|DE95-007099| p 3234 N95-33202
BOULES
Growth of GaN single-crystal boules
|AD-A294976| p 3232 N95-34588
BOUNDARIES
Bolt preload selection for pulsed-loaded vessel closures
|DE95-006346| p 3121 N95-32376
A posteriori pointwise error estimates for the boundary element method
|DE95-008099| p 3194 N95-32388
BOUNDARY CONDITIONS
Review of combustion-acoustic instabilities
|NASA-TM-107020| p 3108 N95-32930
Boundary and lens rigidity of Lorentzian surfaces
|PB95-212163| p 3196 N95-33233
The effect of buoyancy on flow and heat transfer in curved pipes p 3037 N95-34528
BOUNDARY ELEMENT METHOD
A posteriori pointwise error estimates for the boundary element method
|DE95-008099| p 3194 N95-32388
Advanced boundary element methods in aeroacoustics and elastodynamics p 3200 N95-33694
Cubic-B-spline boundary elements for two-dimensional and axisymmetric elastostatics p 3127 N95-33695
Calculation for aerodynamic characteristics on delta wing with leading-edge separated vortex effect using boundary element method p 3037 N95-34524
Grid generation around airfoil with a flap using boundary element method p 3041 N95-34552
Modeling liquid jet atomization processes
|AD-A294888| p 3112 N95-34572
BOUNDARY LAYER COMBUSTION
Numerical study on stabilization of a diffusion flame over a flat plate p 3035 N95-34510
BOUNDARY LAYER CONTROL
Boundary layer transition studies
|NASA-CR-198983| p 3106 N95-32454
Numerical simulation of supersonic flow using a new analytical bleed boundary condition
|NASA-CR-198368| p 3054 N95-33208
BOUNDARY LAYER FLOW
Asymptotic structure of supersonic turbulent boundary layers p 3107 N95-32898
Dependency of a boundary layer flow on computational grids p 3040 N95-34550
BOUNDARY LAYER SEPARATION
A note on separation prediction of two-dimensional turbulent boundary layer
|REPT-2216| p 3091 N95-32994
The effect of interaction on boundary-layer separation and breakdown p 3109 N95-33310
Calculation for aerodynamic characteristics on delta wing with leading-edge separated vortex effect using boundary element method p 3037 N95-34524
BOUNDARY LAYER TRANSITION
Boundary layer transition studies
|NASA-CR-198983| p 3106 N95-32454
Dependency of a boundary layer flow on computational grids p 3040 N95-34550
Studies of hypersonic boundary layer behavior
|AD-A294137| p 3113 N95-34752
BOUNDARY LUBRICATION
The effects of ion implantation on the tribology of perfluoropolyether-lubricated 440C stainless steel couples
|NASA-TM-106965| p 3083 N95-32918
BOUNDARY VALUE PROBLEMS
Penetrable wedge analysis
|AD-A294276| p 3234 N95-34464
BOX BEAMS
Development of a composite tailoring procedure for airplane wing
|NASA-CR-199081| p 3048 N95-32928
BRAIN
Measurement and regulation of central noradrenergic receptors
|AD-A294065| p 3165 N95-34472
BRANCHING (MATHEMATICS)
Bifurcation analysis of multimode instabilities in class B lasers p 3119 N95-33470
BREADBOARD MODELS
A highly reliable, high performance open avionics architecture for real time Nap-of-the-Earth operations p 3044 N95-32497
BRIDGES
Evaluation of a bridge using simplified element modeling
|DE95-006281| p 3126 N95-32670
BRIDGMAN METHOD
Numerical simulation of heat and mass transport during space crystal growth with MEPHISTO
|NASA-TM-107015| p 3089 N95-32718
BRIGHTNESS
SeaWiFS technical report series. Volume 31: Stray light in the SeaWiFS radiometer
|NASA-TM-104566-VOL-31| p 3159 N95-32833
BRIGHTNESS TEMPERATURE
TIMS observations of surface emissivity in HAPEX-Sahel p 3139 N95-33799
A field- and laboratory-based quantitative analysis of alluvium: Relating analytical results to TIMS data p 3139 N95-33800
Cooling tower and plume modeling for satellite remote sensing applications
|DE95-012000| p 3143 N95-33849
BRITTLE MATERIALS
Inclusion models of tensile fracture in fiber-reinforced brittle-matrix composites p 3065 N95-33721
BRITTLENESS
Shock properties of high-strength ceramics
|DE95-007731| p 3082 N95-32380
A numerical analysis of fracture and high temperature creep characteristics of composites with discontinuous ductile reinforcements
|DE95-010236| p 3062 N95-32395
Effect of phase transformations on the mechanical properties of a multiphase alloy based on NiAl + Fe
|DE95-010119| p 3079 N95-33217
R-curve behavior of whisker-reinforced ceramic composites
|DE95-012873| p 3087 N95-34798
BROADBAND
Protocol engineering for broadband networks
|AD-A294969| p 3186 N95-34584
BROADCASTING
GPS-Squitter interference analysis
|AD-A293690| p 3047 N95-33480
BROKEN SYMMETRY
Probing new physics in B Penguins
|DE95-012494| p 3208 N95-33375
The effect of phase advance errors between interaction points on beam halos
|DE95-012559| p 3214 N95-34023
BROMIDES
Enhancement of pool boiling heat transfer to lithium bromide aqueous solution
|REPT-2211| p 3091 N95-32991
BROWNIAN MOVEMENTS
Nonequilibrium problems in Quantum Field Theory and Schwinger's closed time path formalism
|DE95-012056| p 3234 N95-33388

Modeling and inference with fractional Brownian motion and fractional Gaussian noise p 3199 N95-33415

BUBBLES

Glass science tutorial lecture no. 6: The melting of silicate glasses, a review of selected topics
|DE95-010199| p 3084 N95-33218

An experimental and analytical investigation into the performance of centrifugal pumps operating with air-water mixtures p 3123 N95-33323

Structure of weak shock waves in bubbly liquid p 3037 N95-34527

BUCKLING

Cylindrical shell buckling through strain hardening
|DE95-009545| p 3125 N95-32392

BUFFERS (CHEMISTRY)

Fundamental studies of gas phase ionic reactions by ion mobility spectrometry p 3069 N95-33268

BUNCHING

Transverse multibunch instabilities for non-rigid bunches
|DE95-012098| p 3211 N95-32607

Effects of enhanced chromatic nonlinearity during the AGS gamma(t)-jump
|DE95-011703| p 3212 N95-33067

BUNDLES

Method for making fiber-optic bundle collimator assembly
|AD-D017486| p 3216 N95-34288

BUOYANCY

A fundamental study of smoldering with emphasis on experimental design for zero-G
|NASA-CR-198378| p 3089 N95-32929

The effect of buoyancy on flow and heat transfer in curved pipes p 3037 N95-34528

BURNERS

Observations of surface structure and regression behavior of solid propellant strands burning under narrow gap conditions p 3088 N95-33254

BURNING TIME

Ignition and combustion of cellulosic dust particles p 3073 N95-33308

BUSHINGS

Dynamic modelling and response characteristics of a magnetic bearing rotor system with auxiliary bearings p 3122 N95-32692

BYPASSES

Beam-based magnetic alignment of the final focus test beam
|DE95-012096| p 3212 N95-32657

C

C BAND

Polarization and wavelength diversities of Gulf Stream fronts imaged by AIRSAR p 3140 N95-33807

CADMIUM TELLURIDES

Device physics of thin-film polycrystalline cells and modules
|DE95-009209| p 3149 N95-32817

CALCIUM OXIDES

Glass science tutorial lecture no. 6: The melting of silicate glasses, a review of selected topics
|DE95-010199| p 3084 N95-33218

Effect of the colony microstructure on transport critical current of high-J(c) Tl-1223 thick films
|DE95-013049| p 3230 N95-34213

CALCIUM SULFIDES

Crystalline-as-deposited CaGa2S4: Ce via low-temperature metal-organic chemical vapor deposition
|DE95-010883| p 3229 N95-33401

CALIBRATING

SeaWiFS technical report series. Volume 22: Prelaunch acceptance report for the SeaWFS radiometer
|NASA-TM-104566-VOL-22| p 3159 N95-32672

Shuttle Potential and Return Electron Experiment (SPREE) electrostatic analyzer (ESA) calibration report
|AD-A293026| p 3057 N95-32772

An instrument for gravimetric calibration of flow devices with corrosive gases
|DE95-009700| p 3116 N95-33206

Airborne Visible/Infrared Imaging Spectrometer (AVIRIS) onboard calibration system p 3116 N95-33739

New calibration techniques for the Airborne Visible/Infrared Imaging Spectrometer (AVIRIS) p 3116 N95-33740

Initial vegetation species and senescience/stress indicator mapping in the San Luis Valley, Colorado using imaging spectrometer data p 3130 N95-33741

Calibration to surface reflectance of terrestrial imaging spectrometry data: Comparison of methods p 3130 N95-33743

High accuracy in-flight wavelength calibration of imaging spectrometry data p 3132 N95-33750

Determination of the in-flight spectral calibration of AVIRIS using atmospheric absorption features p 3117 N95-33751

An improved spectral calibration requirement for AVIRIS p 3117 N95-33752

In-flight radiometric calibration of AVIRIS in 1994 p 3117 N95-33754

For geological investigations with airborne thermal infrared multispectral images: Transfer of calibration from laboratory spectrometer to TIMS as alternative for removing atmospheric effects p 3137 N95-33792

The JPL Field Emission Spectrometer p 3117 N95-33794

The 1994 laboratory calibration of TIMS p 3117 N95-33796

The 1994 TIMS airborne calibration experiment: Castaic Lake, California p 3117 N95-33797

CALIFORNIA

Preliminary study of Kelso Dunes using AVIRIS, TM, and AIRSAR p 3136 N95-33773

CALORIMETERS

First NPL Calorimetry Workshop
|PB95-236063| p 3235 N95-34654

CAMERAS

A real-time single-camera, stereoscopic video device
|AD-A294105| p 3116 N95-34496

CAMPBELL-HAUSDORFF SERIES

Campbell-Hausdorff formula and algebras with operator
|DE95-623635| p 3195 N95-32609

CANADA

IMS R and D program at Canada customs p 3070 N95-33273

CANCELLATION

Development of High Spectral Resolution Lidar (HSRL) technology
|DE95-011906| p 3099 N95-33839

CANCER

X-ray-provoked non-Mendelian transgenerational oncodeterminants p 3163 N95-32731

CANOPIES (VEGETATION)

Canopy reflectance modelling of semiarid vegetation
|NASA-CR-199117| p 3142 N95-32676

Development of an L-, C-, and X-band radar for backscattering studies over vegetation
|NASA-CR-199112| p 3097 N95-33033

Studies of microwave scattering and canopy architecture for boreal forests
|NASA-CR-199113| p 3099 N95-33497

Studies of microwave scattering and canopy architecture for boreal forests
|NASA-CR-199114| p 3099 N95-33726

High spectral resolution remote sensing of canopy chemistry p 3128 N95-33731

Causal correlation of foliar biochemical concentrations with AVIRIS spectra using forced entry linear regression p 3130 N95-33744

Evaluation of the photochemical reflectance index in AVIRIS imagery p 3131 N95-33747

Vegetation species composition and canopy architecture information expressed in leaf water absorption measured in the 100C ..m and 2200 spectral region by an imaging spectrometer p 3133 N95-33757

Using foreground/background analysis to determine leaf and canopy chemistry p 3135 N95-33765

Validating spatial structure in canopy water content using geostatistics p 3135 N95-33768

Estimation of penetration of forest canopies by Interferometric SAR measurements p 3141 N95-33814

Regional mapping of forest canopy water content and biomass using AIRSAR images over BOREAS study area p 3142 N95-33815

CANYONS

Integration of AIRSAR and AVIRIS data for Trail Canyon alluvial fan, Death Valley, California p 3134 N95-33760

CAPACITANCE

Experimental and numerical analysis of controlled impinging liquid jets p 3109 N95-33257

Design rules and reality check for carbon-based ultracapacitors
|DE95-010575| p 3103 N95-33640

Quantum mechanical capacitance in a scanning tunneling microscope
|DE95-011272| p 3230 N95-33880

CAPACITORS

Design rules and reality check for carbon-based ultracapacitors
|DE95-010575| p 3103 N95-33640

CAPILLARY FLOW

Thermocapillary flow with evaporation and condensation and its effect on liquid retention in low-g fluid acquisition devices p 3109 N95-33256

CARBIDES

Phase equilibria and phase diagrams in carbide systems
|PB95-211348| p 3068 N95-33229

Machinability study of Aermet 100
|DE95-011532| p 3084 N95-33408

CARBON

Cathode readout with stripped resistive drift tubes
|DE95-621871| p 3102 N95-32628

Low-energy Ion-Beam Deposition apparatus equipped with surface analysis system
|DE95-737272| p 3212 N95-32712

Proton-induced fragmentation of carbon at energies below 100 MeV p 3161 N95-32720

Wear resistant composite structure of vitreous carbon containing convoluted fibers
|DE95-011463| p 3063 N95-33062

Proton affinity determinations and proton-bound dimer structure indications in C2 to C15, (alpha),(omega)-alkyldiamines p 3069 N95-33266

Completing below-ground carbon budgets for pastures, recovering forests, and mature forests of Amazonia
|NASA-CR-199129| p 3143 N95-33498

Design rules and reality check for carbon-based ultracapacitors
|DE95-010575| p 3103 N95-33640

The growth of ultrathin epitaxial intermetallic films
|AD-A295037| p 3232 N95-34795

CARBON DIOXIDE

Glass science tutorial lecture no. 6: The melting of silicate glasses, a review of selected topics
|DE95-010199| p 3084 N95-33218

Zeolite membranes for gas separations
|DE95-012984| p 3068 N95-33224

The effects of CO2 on the negative reactant ions of IMS p 3069 N95-33267

Completing below-ground carbon budgets for pastures, recovering forests, and mature forests of Amazonia
|NASA-CR-199129| p 3143 N95-33498

Carbon Dioxide Information Analysis Center and World Data Center: A for Atmospheric trace gases
|DE95-011769| p 3154 N95-33655

The choice: Welding with CO2 or Nd:YAG lasers
|DE95-011825| p 3124 N95-33834

The relationship of chemical structure to supercritical-fluid solubility and to cosolvent-modifier properties: A literature review
|AD-A294933| p 3076 N95-34599

Density, heat capacity, viscosity, and thermal conductivity of mixtures of CO2, He, H2, H2O, N2, and O2
|AD-A288731| p 3076 N95-34814

CARBON DIOXIDE LASERS

Laser based obstacle warning sensors for helicopters p 3045 N95-32499

The Anglo-French Compact Laser Radar demonstrator programme p 3045 N95-32501

The effect of travel speed on thermal response in CO2 laser welding of small electronic components
|DE95-006314| p 3118 N95-32683

Analysis of evaporation in laser welding
|REPT-2207| p 3090 N95-32987

The choice: Welding with CO2 or Nd:YAG lasers
|DE95-011825| p 3124 N95-33834

Influence of CO2 continuous laser preprocessed substrates on optical thin film damage thresholds
|AD-A294190| p 3217 N95-34297

High power CO2 laser windows and reflection reducing coatings
|AD-A294217| p 3119 N95-34308

Atmospheric attenuation properties associated with CO2 laser radiation spectra
|AD-A294061| p 3120 N95-34470

CARBON FIBER REINFORCED PLASTICS

Adhesion of novel high-performance polymers to carbon fibers: Fiber surface treatment, characterization, and microbond single fiber pull-out test p 3085 N95-34282

CARBON FIBERS

Low velocity impact damage in carbon fiber/PEEK composite laminates
|ISBN-0-315-86546-6| p 3065 N95-33710

Interfacial reactions during the liquid infiltration of titanium matrix composites p 3081 N95-34252

Adhesion of novel high-performance polymers to carbon fibers: Fiber surface treatment, characterization, and microbond single fiber pull-out test p 3085 N95-34282

CARBON MONOXIDE

Practical improvement of MS-X alpha molecular orbital calculation as applied to dissociation process of CO molecule
|REPT-2206| p 3090 N95-32986

CARBON STEELS

Nitrate stress corrosion crack growth rate in plain carbon steels
|DE95-011689| p 3079 N95-32958

CARBON 12
N-15 hydrogen profiling of IC metallizations
[DE95-011052] p 3102 N95-32708
CARBON 13
Molecular motion of phosphazene-bound NLO chromophores
[AD-A293526] p 3087 N95-34649
CARBONATES
Corrosion of separator plate constituents in molten carbonate
[PB95-214490] p 3149 N95-32813
CARBOXYLATES
Molecular engineering of liquid crystalline polymers by Living polymerization 30. Synthesis and Living cationic polymerization of (2R, 3S)-2-Fluoro-3-methylpentyl 4'-(8-Vinyloxyoctyloxy) Biphenyl-4-carboxylate and its copolymerization with (2R, 3S)-2-Fluoro-3-methylpentyl 4'-(11 Vinyloxyundecanyloxy) biphenyl-4-carboxylate --- carboxylate and its copolymerization with (2R, 3S)-2-Fluoro-3-methylpentyl 4-(11-Vinyloxyundecanyloxy) biphenyl-4-Carboxylate
[AD-A293115] p 3082 N95-32552
CARDIAC OUTPUT
Noninvasive determination of Cardiac Output
[PB95-208310] p 3164 N95-32611
New advances in physiological measurements during high-G: Technology p 3165 N95-34057
CARDIOVASCULAR SYSTEM
Shuttle to Space Station. Heart assist implant. Hubble update. X-30 mock-up
[NASA-TM-110837] p 3056 N95-33167
CASCADE CONTROL
Quantitative analysis of volatile organic compounds using ion mobility spectra and cascade correlation neural networks p 3073 N95-33290
CASCADE FLOW
Design of secondary flow control cascade using numerical simulation p 3034 N95-34507
A study on the convergence of a 3-D Euler code for cascade flow calculations p 3034 N95-34508
Verification of turbine cascade flow with tip clearance p 3035 N95-34511
CASTIGLIANO VARIATIONAL THEOREM
The linear elastic biaxial response of plain-woven meshes p 3064 N95-33468
CASTING
Fabrication of improved SiGe alloys for an 18-couple module test
[DE95-010238] p 3060 N95-32396
Advanced precision expendable pattern casting technology
[DE95-012200] p 3095 N95-33393
The 3D metal forming applications of ALE techniques
[DE95-011745] p 3080 N95-33653
CATALYSIS
Spin counting in dipolar coupled spin 1/2 systems by multiple quantum NMR spectroscopy in solids: Development of a single quantum propagator and its application to heterogeneous catalysis
[DE95-010246] p 3066 N95-32540
Selective methane oxidation over promoted oxide catalysts
[DE95-012319] p 3075 N95-34021
Fundamental studies of the mechanism of catalytic reactions with catalysts effective in the gasification of carbon solids and the oxidative coupling of methane
[DE95-012759] p 3075 N95-34268
CATALYSTS
Alternative catalyst and exhaust gas sensor work at Argonne National Laboratory
[DE95-007138] p 3152 N95-32553
NQR-NMR studies of higher alcohol synthesis Cu-Co catalysts
[DE95-010524] p 3066 N95-32557
Gasoline from natural gas by sulfur processing
[DE95-010651] p 3087 N95-32583
Testing of a carpet catalyst
[PB95-208492] p 3068 N95-33242
Characterization of microenvironment polarity and solvent accessibility of polysilsesquioxane xerogels by the fluorescent probe technique
[DE95-011874] p 3062 N95-33835
Selective methane oxidation over promoted oxide catalysts
[DE95-012319] p 3075 N95-34021
Fundamental studies of the mechanism of catalytic reactions with catalysts effective in the gasification of carbon solids and the oxidative coupling of methane
[DE95-012759] p 3075 N95-34268
Catalytic conversion of light alkanes: Proof of concept stage
[DE95-012318] p 3076 N95-34810
CATALYTIC ACTIVITY
Reactions of trifluoriodomethane on metal surfaces
[DE95-010122] p 3078 N95-32638
Testing of a carpet catalyst
[PB95-208492] p 3068 N95-33242
CATHETERIZATION
Noninvasive determination of Cardiac Output
[PB95-208310] p 3164 N95-32611
CATHODE RAY TUBES
Towards a formalism for program generation 1995
[AD-A294941] p 3183 N95-34604
CATHODES
Cathode readout with stripped resistive drift tubes
[DE95-621871] p 3102 N95-32628
Thin-film rechargeable lithium batteries
[DE95-008975] p 3103 N95-33697
CAUCHY PROBLEM
Fifth International Conference on Hyperbolic Problems, Theory, Numerics, Applications: Abstracts
[DE95-008173] p 3194 N95-32389
A variation of the Riemann Problem solution and its application to implicit Godunov's scheme p 3036 N95-34516
A flux splitting scheme with high-resolution and robustness for discontinuities p 3036 N95-34518
CAVITIES
COBRA accelerator for Sandia ICF diode research at Cornell University
[DE95-011018] p 3101 N95-32578
Status of the large-scale dark-matter axion search
[DE95-008828] p 3246 N95-32597
Minimum wakefield achievable by waveguide damped cavity
[DE95-012100] p 3095 N95-32616
A dual, parallel cavity Fabry-Perot interferometer
[DE95-010796] p 3115 N95-32900
Elementary benchmarks of the NWT computer system and program performance p 3038 N95-34532
CAVITY RESONATORS
Minimum wakefield achievable by waveguide damped cavity
[DE95-012100] p 3095 N95-32616
Pulsed tunable narrow-bandwidth dye laser, with hollow circular waveguide in cavity
[AD-A294060] p 3120 N95-34469
CD-ROM
Read/write module for high capacity memory disk
[AD-A294946] p 3178 N95-34745
CELESTIAL BODIES
Time correlations between low and high energy gamma rays from discrete sources
[NASA-CR-199214] p 3248 N95-33916
CELLS (BIOLOGY)
Minutes of the 12th Joint NASA/DARA-DLR Life Sciences Program Working Group Meeting
[NASA-TM-110655] p 3161 N95-32719
Heavy ion induced DNA-DSB in yeast and mammalian cells p 3161 N95-32723
Inactivation, DNA double strand break induction and their rejoining in bacterial cells irradiated with heavy ions p 3161 N95-32724
DNA-DSB in CHO-K1 cells induced by heavy-ions: Break rejoining and residual damage (GSI) p 3162 N95-32725
Chromosomal damage observed in first postirradiation metaphases of repair-proficient and -deficient cell lines p 3162 N95-32726
Heavy ion induced mutations in mammalian cells: Cross sections and molecular analysis p 3162 N95-32728
CELLULOSE
A fundamental study of smoldering with emphasis on experimental design for zero-G
[NASA-CR-198378] p 3089 N95-32929
Ignition and combustion of cellulosic dust particles p 3073 N95-33308
Prospect redux p 3133 N95-33758
CENTRAL NERVOUS SYSTEM
The role of the vestibular system in manual target localization p 3166 N95-32422
Toxin-mediated transfer and expression of genes in nerve cells
[AD-A290501] p 3164 N95-33200
Measurement and regulation of central noradrenergic receptors
[AD-A294065] p 3165 N95-34472
CENTRIFUGAL COMPRESSORS
An unsteady simulation of a centrifugal compressor stage using the NWT p 3038 N95-34536
CENTRIFUGAL FORCE
Sinuous oscillations and steady warps of polytropic disks
[DE95-013473] p 3247 N95-34216
Flow and heat transfer in rotating curved pipes p 3040 N95-34545
CENTRIFUGAL PUMPS
An experimental and analytical investigation into the performance of centrifugal pumps operating with air-water mixtures p 3123 N95-33323
CEPSTRAL ANALYSIS
Speaker identification using the two-dimensional cepstrum transform
[AD-A294204] p 3099 N95-34304
CERAMIC BONDING
Electron beam joining of structural ceramics
[DE95-012521] p 3085 N95-34022
CERAMIC FIBERS
Interfacial reactions during the liquid infiltration of titanium matrix composites p 3081 N95-34252
CERAMIC MATRIX COMPOSITES
Micromechanics of fiber-reinforced ceramic composites p 3063 N95-32775
R-curve behavior of whisker-reinforced ceramic composites
[DE95-012873] p 3087 N95-34798
Fiber coatings for brittle matrix composites p 3065 N95-34808
CERAMICS
Shock properties of high-strength ceramics
[DE95-007731] p 3082 N95-32380
Materials sciences programs: Fiscal year 1994
[DE95-011248] p 3211 N95-32483
Design and operation of a thermionic converter in air
[DE95-010151] p 3149 N95-32645
Investigation of aging effects from high voltage profiles in ceramic phase shifter materials
[AD-A289985] p 3082 N95-32694
High-speed, low-damage grinding of advanced ceramics, phase 1
[DE95-011241] p 3085 N95-33425
Thin-film electrolytes for reduced temperature solid oxide fuel cells
[DE95-011273] p 3151 N95-34481
Metal-ceramic interfaces: Overlayer-induced reconstruction and magnetism of 4d transition-metal monolayers
[DE95-011543] p 3075 N95-34483
CERIUM
Crystalline-as-deposited CaGa2S4: Ce via low-temperature metal-organic chemical vapor deposition
[DE95-010883] p 3229 N95-33401
CERIUM COMPOUNDS
Magnetostriction and thermal expansion of the Kondo semiconductor Ce3Bi4Pt3
[DE95-011975] p 3229 N95-33386
CERTIFICATION
Report to the Chairman, Subcommittee on Aviation, Committee on Commerce, Science, and Transportation, US Senate. Aviation safety: Data problems threaten FAA strides on safety analysis system
[GAO/AIMD-95-27] p 3046 N95-32705
NASA-Wide Fastener Technical Interchange Meeting
[NASA-CP-3308] p 3123 N95-33199
Human Factors Certification of Advanced Aviation Technologies
[NASA-CR-199009] p 3171 N95-34764
On the use of the systems approach to certify advanced aviation technologies p 3171 N95-34765
A rose by any other name: Certification seen as process rather than content p 3047 N95-34766
A psychologist's view of validating aviation systems p 3172 N95-34767
Certification of tactics and strategies in aviation p 3172 N95-34768
Human factors certification: A useful concept? p 3173 N95-34769
Human factors certification in the development of future air traffic control systems p 3048 N95-34770
Quality assurance and risk management: Perspectives on Human Factors Certification of Advanced Aviation Systems p 3048 N95-34771
User type certification for advanced flight control systems p 3055 N95-34772
Certify for success: A methodology for human-centered certification of advanced aviation systems p 3173 N95-34773
Certification of training p 3166 N95-34774
Does human cognition allow Human Factors (HF) certification of advanced aircrew systems? p 3174 N95-34776
Practical guidelines for workload assessment p 3174 N95-34777
Towards a framework of human factors certification of complex human-machine systems p 3175 N95-34779
The successful management of programs for human factors certification of advanced aviation technologies p 3175 N95-34780
Evaluation in context: ATC automation in the field p 3175 N95-34781
Integrating human factors knowledge into certification: The point of view of the Internatioanal Civil Aviation Organization (ICAO) p 3175 N95-34782
Certification for civil flight decks and the human-computer interface p 3176 N95-34784

Some inadequacies of the current human factors certification process of advanced aircraft technologies
p 3176 N95-34785
Advanced automated glass cockpit certification: Being wary of human factors p 3176 N95-34786
Beware of agents when flying aircraft: Basic principles behind a generic methodology for the evaluation and certification of advanced aviation systems
p 3176 N95-34787

CESIUM
Design and operation of a thermionic converter in air
[DE95-010151] p 3149 N95-32645
Integral cesium reservoir: Design and transient operation
[DE95-010152] p 3211 N95-32647

CHANGE DETECTION
Urban remote sensing applications: TIMS observations of the City of Scottsdale p 3137 N95-33791

CHANNEL FLOW
Analysis and finite element approximation of an optimal shape control problem for the steady-state Navier-Stokes equations p 3112 N95-34285

CHANNEL NOISE
Using dark current data to estimate AVIRIS noise covariance and improve spectral analyses
p 3129 N95-33736

CHANNELS (DATA TRANSMISSION)
Fabrication of optical channel waveguides in the GaAs/AlGaAs system by MeV ion beam bombardment
[DE95-008973] p 3218 N95-34480

CHAOS
Turbulence and spatio-temporal chaos
[DE95-012912] p 3068 N95-33223
A curriculum for strategy in the information age: Chaos in a new era
[AD-A295036] p 3244 N95-34794

CHARACTER RECOGNITION
A preliminary evaluation of histogram-based binarization algorithms
[DE95-009886] p 3179 N95-32470
Prediction of OCR accuracy using simple image features
[DE95-009887] p 3236 N95-32471
A document analysis system p 3244 N95-34804

CHARACTERIZATION
DMTA studies of branching distribution in polyethylene
[PB95-208237] p 3084 N95-33228
Characterization of DuPont 9015, aqueous processable dry film photoresist for printed wiring boards
[DE95-011239] p 3103 N95-33864
Synthesis and characterization of a series of organoindium-phosphides including molecular structures of ((Me3CCH2)2InPEt2)2 and ((Me3CCH2)2InP(H)(C6H11))3
[AD-A293965] p 3086 N95-34452

CHARGE COUPLED DEVICES
Dosimetry of heavy ions by use of CCD detectors
p 3161 N95-32721
RR lyrae variable stars in the CCD/Transit instrument survey
[AD-A294138] p 3246 N95-34753

CHARGE TRANSFER
State-selective single electron capture cross sections in He(exp 2+) + Li(2s) and Li(*)(2p) collisions
[DE95-010819] p 3207 N95-33371
Charge-transfer gap closure in transition-metal halides under pressure
[DE95-011268] p 3230 N95-33865

CHARGED PARTICLES
Transport studies of tokamak plasmas in JT-60 device
[DE95-737227] p 3220 N95-32417
Low energy collisions involving multiply charged ions
[DE95-010911] p 3203 N95-32564
Analysis of radiation damages of electronic circuits by separate irradiation of their components with a collimated charged particle beam
[DE95-621946] p 3102 N95-32629
The beam envelope equation-systematic solution for a periodic quadrupole lattice with space charge
[DE95-012761] p 3199 N95-34269
Track finding and fitting in the H1 forward track detector
[PB95-234985] p 3214 N95-34651

CHARM (PARTICLE PHYSICS)
Intrinsic charm contribution to double quarkonium hadroproduction
[DE95-012170] p 3204 N95-32617
Four heavy quark and bound state production in the e(+)e(-) yields Q + (bar-Q' + Q' + bar-Q and e(+)e(-) yields (Q(bar-Q')) + Q' + bar-Q processes in Z(sup 0)-boson pole
[DE95-620533] p 3205 N95-32704
Searching for new physics with charm
[DE95-012498] p 3207 N95-33245
Development of silicon drift detectors for strangeness measurements
[DE95-012366] p 3208 N95-33380

CHARPY IMPACT TEST
Irradiation experiments of low copper A533B steels for reactor pressure vessel tested in JMTR
[DE95-737266] p 3077 N95-32531

CHARRING
Ignition and combustion of cellulosic dust particles
p 3073 N95-33308

CHARTS
Current issues in the design and information content of instrument approach charts
[AD-A294752] p 3047 N95-34562
Resource document for the design of electronic instrument approach procedure displays
[AD-A295108] p 3047 N95-34797

CHECKOUT
A declarative debugger for a logical-functional language p 3183 N95-33007
SSME Post Test Diagnostic System: Systems Section
[NASA-CR-198375] p 3061 N95-34625

CHEMICAL ANALYSIS
Analysis of LDEF experiment AO187-2 chemical and isotopic measurements of micrometeoroids by secondary ion mass spectrometry
[NASA-CR-198849] p 3246 N95-32913
Third International Workshop on Ion Mobility Spectrometry
[NASA-CP-3301] p 3069 N95-33265
The effect of sample holder material on ion mobility spectrometry reproducibility p 3071 N95-33282
Application of the ionscan for the detection of methamphetamine and ephedrine in abondoned clandestine laboratories p 3072 N95-33284
IMS software developments for the detection of chemical warfare agent p 3072 N95-33287
The nature and fate of natural resins in the geosphere 6: Analysis of fossil resins from Axel Heiberg Island Canadian Arctic
[DE95-012212] p 3154 N95-33394
The development of a large-area chemical sensor: A new platform for selective coatings
[DE95-011489] p 3075 N95-33832

CHEMICAL BONDS
Synchrotron radiation studies of local structure and bonding in transition metal aluminides and rare earth transition metal magnetic nitrides
[DE95-011579] p 3079 N95-33065

CHEMICAL COMPOSITION
Users' manual for LEHGC: A Lagrangian-Eulerian finite-element model of HydroGeoChemical transport through saturated-unsaturated media. Version 1.0
[DE95-010513] p 3179 N95-32543
A novel approach to the problem of highly-sensitive regular analysis for man-made plutonium in environment and human body
[DE95-620764] p 3164 N95-32666
Effect of lead content on Bi-2223 formation by a two-powder process
[DE95-009889] p 3079 N95-33215
Glass science tutorial lecture no. 6: The melting of silicate glasses, a review of selected topics
[DE95-010199] p 3084 N95-33218
The mini-CIDEX GC/IMS: Analysis of cometary ice and dust p 3069 N95-33270
Application of Ni-63 photo and corona discharge ionization for the analysis of chemical warfare agents and toxic wastes p 3070 N95-33272
The relationship of chemical structure to supercritical-fluid solubility and to cosolvent-modifier properties: A literature review
[AD-A294933] p 3076 N95-34599
Growth and structure of MBE-Deposited iridium silicide
[AD-A295033] p 3232 N95-34792

CHEMICAL COMPOUNDS
Analysis of samples for the first (1994) OPCW round robin interlaboratory comparison test
[PB95-210324] p 3068 N95-33243
Chemical substances lists: A guide to the lists used in the Swedish Sunset Project. Supplement to report 13/94. Selecting multiproblem chemicals for risk reduction. A presentation of the Swedish Sunset Project
[PB95-211272] p 3073 N95-33328
Sensitizing substances
[PB95-211256] p 3074 N95-33634

CHEMICAL EQUILIBRIUM
Phase equilibria and phase diagrams in carbide systems
[PB95-211348] p 3068 N95-33229

CHEMICAL PROPERTIES
Sensitizing substances
[PB95-211256] p 3074 N95-33634

CHEMICAL REACTIONS
Fusion Safety Program annual report, fiscal year 1994
[DE95-008872] p 3221 N95-32588
Reactions of trifluoroiodomethane on metal surfaces
[DE95-010122] p 3078 N95-32638
PINCA: A scalable parallel program for compressible gas dynamics with nonequilibrium chemistry
[DE95-010581] p 3106 N95-32818
Turbulence and spatio-temporal chaos
[DE95-012912] p 3068 N95-33223
Fundamental studies of gas phase ionic reactions by ion mobility spectrometry p 3069 N95-33268

CHEMICAL REACTORS
Coating power RF components with TiN
[DE95-010357] p 3082 N95-32541
Fundamental studies of the mechanism of catalytic reactions with catalysts effective in the gasification of carbon solids and the oxidative coupling of methane
[DE95-012759] p 3075 N95-34268

CHEMICAL WARFARE
Application of Ni-63 photo and corona discharge ionization for the analysis of chemical warfare agents and toxic wastes p 3070 N95-33272
IMS software developments for the detection of chemical warfare agent p 3072 N95-33287
High resolution electrospray mass spectrometry with a magnetic sector instrument: Accurate mass measurement and peptide sequencing
[AD-A293564] p 3076 N95-34611

CHEMILUMINESCENCE
Ignition and early soot formation in a DI diesel engine using multiple 2-D imaging diagnostics
[DE95-010692] p 3122 N95-32863

CHEMISORPTION
Si-device-related interface research
[AD-A293587] p 3076 N95-34615

CHESAPEAKE BAY (US)
The CE-QUAL-ICM three-dimensional eutrophication model, release version 1.0
[AD-A294258] p 3160 N95-34461

CHINA
Successful development of first-generation laser device; marking China's optoelectronic technology at world class level
[AD-A294206] p 3217 N95-34305
Thermal design of returnable satellites
[AD-A294113] p 3059 N95-34500
Intra-annual and inter-annual rainfall variability over East Asia, Southeast Asia, and South Asia
[AD-A294156] p 3158 N95-34757

CHIPS
Development of environmentally conscious cleaning process for leadless chip carrier assemblies
[DE95-010186] p 3154 N95-33638

CHIPS (ELECTRONICS)
Copper-diamond composite substrates for electronic components
[DE95-011520] p 3079 N95-33063
Recent developments in maritime technology research institute acousto-optical technology research
[AD-A294215] p 3217 N95-34307
Self stressing test structure cells
[AD-A294386] p 3104 N95-34345
Diamond multilayer multichip module substrate
[AD-D017468] p 3104 N95-34445
Optical interconnects for 3D computer architectures
[AD-A294118] p 3178 N95-34503

CHLORINATION
Environmental evaluation of lactates as cleaning agents
[PB95-214854] p 3067 N95-32615
Field Raman spectrograph for environmental analysis
[DE95-007969] p 3153 N95-32816

CHLOROFLUOROCARBONS
Thermophysical properties of HCFC alternatives
[DE95-009635] p 3233 N95-32661

CHLOROPHYLLS
Prospect redux p 3133 N95-33758
An algorithm for chlorophyll using first difference transformations of AVIRIS reflectance spectra
p 3134 N95-33763
Extraction of ozone and chlorophyll-A distribution from AVIRIS data p 3136 N95-33770
DataHub sponsored analysis p 3243 N95-34242

CHOKED FLOW
Investigation of starting and ignition transients in the thermally choked ram accelerator p 3054 N95-34805

CHROMIUM
Background meeting and technology demonstration: Chromium electroplating of superconductor strand
[DE95-011736] p 3068 N95-33070

CHROMIUM ALLOYS
Static displacements of atoms in crystalline metallic solid solutions
[DE95-012893] p 3233 N95-34802

CHROMOPHORES
Molecular motion of phosphazene-bound NLO chromophores
[AD-A293526] p 3087 N95-34649

CHROMOSOMES
Heavy ion induced DNA-DSB in yeast and mammalian cells p 3161 N95-32723
Inactivation, DNA double strand break induction and their rejoining in bacterial cells irradiated with heavy ions p 3161 N95-32724
DNA-DSB in CHO-K1 cells induced by heavy-ions: Break rejoining and residual damage (GSI) p 3162 N95-32725
Chromosomal damage observed in first postirradiation metaphases of repair-proficient and -deficient cell lines p 3162 N95-32726
Cosmic heavy ion tracks in mesoscopic biological test objects p 3163 N95-32730

CIRCUIT BOARDS
Characterization of DuPont 9015, aqueous processable dry film photoresist for printed wiring boards [DE95-011239] p 3103 N95-33864
Hardware implementation of a desktop supercomputer for high performance image processing [AD-A294272] p 3178 N95-34462

CIRCUIT BREAKERS
D3-D power supply, design, and development [DE95-009603] p 3222 N95-32656

CIRCUITS
Analysis of radiation damages of electronic circuits by separate irradiation of their components with a collimated charged particle beam [DE95-621946] p 3102 N95-32629
Optical interconnects for 3D computer architectures [AD-A294118] p 3178 N95-34503
Photonic band gap structures on polymer materials for microstructure waveguides and high-speed interconnects [AD-A294119] p 3218 N95-34504
Environment and circuit model for capacitor-based rail guns [AD-A293455] p 3057 N95-34815

CIRCULAR CYLINDERS
Semi-analytic computation of the driven fields in right circular cylindrical microwave applicators [DE95-010875] p 3203 N95-32574
A simulation of damping process of pendulum motion due to aerodynamic forces p 3041 N95-34551

CIRCULAR POLARIZATION
Terrain classification using circular polarimetric features p 3140 N95-33809

CIRCULAR TUBES
Low Reynolds number kappa-epsilon and empirical transition models for oscillatory pipe flow and heat transfer [NASA-TM-109785] p 3110 N95-33496

CIRCULATION
Noninvasive determination of Cardiac Output [PB95-208310] p 3164 N95-32611

CIRRUS CLOUDS
Correction of thin cirrus effects in AVIRIS images using the sensitive 1.375-micron cirrus detecting channel p 3131 N95-33748

CITRIC ACID
An investigation of the chemistry of citric acid in military soldering applications [AD-A295042] p 3105 N95-34796

CIVIL AVIATION
Report to the Chairman, Subcommittee on Aviation, Committee on Commerce, Science, and Transportation, US Senate. Aviation safety: Data problems threaten FAA strides on safety analysis system [GAO/AIMD-95-27] p 3046 N95-32705
Fact sheet for Congressional requesters. Airport competition: Essential air service slots at O'Hare International Airport [GAO/RCED-94-118FS] p 3055 N95-32759
Report to the Chairman, Subcommittee on Transportation and Related Agencies, Committee on Appropriations, US Senate. Airport Improvement Program: Reliever airport set-aside funds could be redirected [GAO/RCED-94-226] p 3055 N95-32786
Report to the Chairman, Subcommittee on Transportation and Related Agencies, Committee on Appropriations, US Senate. Airport Improvement Program: The Military Airport Program has not achieved intended impact [GAO/RCED-94-209] p 3056 N95-32888
Human Factors Certification of Advanced Aviation Technologies [NASA-CR-199009] p 3171 N95-34764
Human factors certification in the development of future air traffic control systems p 3048 N95-34770
Integrating human factors knowledge into certification: The point of view of the Internationanl Civil Aviation Organization (ICAO) p 3175 N95-34782
Certification for civil flight decks and the human-computer interface p 3176 N95-34784

CLADDING
Fracture behavior of shallow cracks in full-thickness clad beams from an RPV wall section [DE95-009175] p 3126 N95-32684
The development of a large-area chemical sensor: A new platform for selective coatings [DE95-011489] p 3075 N95-33832

CLAMPS
Design and testing criteria for bipolar plate materials for PEM fuel cell applications [DE95-010878] p 3148 N95-32575

CLASSIFICATIONS
Training neural networks using sequential extended Kalman filtering [DE95-007874] p 3187 N95-32386
Prediction of OCR accuracy using simple image features [DE95-009887] p 3236 N95-32471
Sensitizing substances [PB95-211256] p 3074 N95-33634
Fatigue damage estimate comparisons for northern European and US wind farm loading environments [DE95-011061] p 3150 N95-33706
Urban remote sensing applications: TIMS observations of the City of Scottsdale p 3137 N95-33791
Discrimination of alkalinity in granitoid Rocks: A potential TIMS application p 3138 N95-33798

CLEANERS
Environmental evaluation of lactates as cleaning agents [PB95-214854] p 3067 N95-32615

CLEANING
Development of environmentally conscious cleaning process for leadless chip carrier assemblies [DE95-010186] p 3154 N95-33638
An investigation of the chemistry of citric acid in military soldering applications [AD-A295042] p 3105 N95-34796

CLEARANCES
Verification of turbine cascade flow with tip clearance p 3035 N95-34511

CLIMATE
Comparison of seasonal and zonal patterns of the direct and indirect radiative forcing of climate by aerosols [DE95-010896] p 3153 N95-33192
Abstracts of oral and poster sessions [DE95-011951] p 3154 N95-33413

CLIMATE CHANGE
Pollution in Norway [PB95-214565] p 3153 N95-33331
Regional mapping of forest canopy water content and biomass using AIRSAR images over BOREAS study area p 3142 N95-33815
Enhanced shortwave cloud radiative forcing due to anthropogenic aerosols [DE95-013319] p 3156 N95-34214

CLIMATE MODELS
Impact of cloud microphysics on cloud-radiation interactions in the CSU general circulation model [DE95-008979] p 3153 N95-33205
Abstracts of oral and poster sessions [DE95-011951] p 3154 N95-33413
Enhanced shortwave cloud radiative forcing due to anthropogenic aerosols [DE95-013319] p 3156 N95-34214

CLIMATOLOGY
Abstracts of oral and poster sessions [DE95-011951] p 3154 N95-33413
Turbulent heat flux measurements over the Greenland, Norwegian and Barents seas [AD-A294129] p 3157 N95-34751

CLINICAL MEDICINE
Conceptual understanding and stability, and knowledge shields for fending off conceptual change [AD-A293555] p 3166 N95-34609

CLOCKS
Indium mono-ion oscillator [AD-A293736] p 3104 N95-34451

CLOSED ECOLOGICAL SYSTEMS
Multiobjective optimization of hybrid regenerative life support technologies. Topic D: Technology Assessment [NASA-CR-199125] p 3167 N95-32688

CLOSTRIDIUM BOTULINUM
Immunological protection against botulinum neurotoxin by a synthetic vaccine [AD-A294146] p 3165 N95-34754

CLOSURES
Bolt preload selection for pulsed-loaded vessel closures [DE95-006346] p 3121 N95-32376
Aerospace Guidance and Metrology Center: Cost growth and other factors affect closure and privatization. Report to Congressional requesters [GAO/NSIAD-95-60] p 3235 N95-32706

CLOTHING
General procedure for clothing evaluations relative to heat stress [AD-A294953] p 3171 N95-34577

CLOUD COVER
Impact of cloud microphysics on cloud-radiation interactions in the CSU general circulation model [DE95-008979] p 3153 N95-33205

CLOUD PHYSICS
Impact of cloud microphysics on cloud-radiation interactions in the CSU general circulation model [DE95-008979] p 3153 N95-33205
Remote sensing of smoke, clouds, and radiation using AVIRIS during SCAR experiments p 3132 N95-33749

CLOUDS (METEOROLOGY)
Comparison of seasonal and zonal patterns of the direct and indirect radiative forcing of climate by aerosols [DE95-010896] p 3153 N95-33192
Enhanced shortwave cloud radiative forcing due to anthropogenic aerosols [DE95-013319] p 3156 N95-34214

CLUSTERS
The pinhole interface for IMS/MS p 3070 N95-33275

CLUTTER
Space-time adaptive processing for airborne radar [AD-A293032] p 3098 N95-33152
Resource document for the design of electronic instrument approach procedure displays [AD-A295108] p 3047 N95-34797

CMOS
Self stressing test structure cells [AD-A294386] p 3104 N95-34345

COAL GASIFICATION
Fundamental studies of the mechanism of catalytic reactions with catalysts effective in the gasification of carbon solids and the oxidative coupling of methane [DE95-012759] p 3075 N95-34268

COALESCING
Ductile damage model with void coalescence [DE95-007855] p 3125 N95-32385

COATING
Evaluation of strength properties of developed SiC/C compositionally gradient graphite materials [DE95-737271] p 3063 N95-32711
Printability of substrate and absorber defects on extreme ultraviolet lithographic masks [DE95-010916] p 3084 N95-33247
Advanced precision expendable pattern casting technology [DE95-012200] p 3095 N95-33393
CRADA with United Solar Technologies and Pacific Northwest Laboratory (PNL-021): Thin film materialsfor low-cost high performance solar concentrators [DE95-010423] p 3150 N95-33400
Zero discharge organic coatings: Powder paint - UV curable paint - E-coat [AD-A293573] p 3087 N95-34614
Fiber coatings for brittle matrix composites p 3065 N95-34808

COATINGS
Evaluation of strength properties of developed SiC/C compositionally gradient graphite materials [DE95-737271] p 3063 N95-32711
Machinability study of Aermet 100 [DE95-011532] p 3084 N95-33408
The development of a large-area chemical sensor: A new platform for selective coatings [DE95-011489] p 3075 N95-33832
Ion assisted deposition of ZnS and MgF2 [AD-A294759] p 3086 N95-34563
Experimental investigation of impulse radar for mitigation of effects of radar absorbing materials [AD-A294166] p 3100 N95-34762

COBALT
Perpendicular magnetic behavior of ultra-thin Co sandwiches [DE95-010611] p 3083 N95-32819
Unusual behavior in the magnetic anisotropy of ultra-thin Co sandwiches: The role of Au underlayers [DE95-010612] p 3229 N95-33641

COBALT COMPOUNDS
NQR-NMR studies of higher alcohol synthesis Cu-Co catalysts [DE95-010524] p 3066 N95-32557

COCKPITS
Certification for civil flight decks and the human-computer interface p 3176 N95-34784
Some inadequacies of the current human factors certification process of advanced aircraft technologies p 3176 N95-34785
Advanced automated glass cockpit certification: Being wary of human factors p 3176 N95-34786

CODING
Optimum Routeing: Analytical constraint of search space p 3044 N95-32493

Design and analysis of lossless and lossy data compression methods with applications to communication and caching
[AD-A295025] p 3101 N95-34790

COEFFICIENT OF FRICTION
Influence of non classical friction on the rubbing and impact behavior of rotor dynamic systems
p 3122 N95-32906

COGNITION
On bootstrapping local search with trail-markers
[DE95-009835] p 3187 N95-32533
Conceptual understanding and stability, and knowledge shields for fending off conceptual change
[AD-A293555] p 3166 N95-34609
Does human cognition allow Human Factors (HF) certification of advanced aircrew systems?
p 3174 N95-34776

COGNITIVE PSYCHOLOGY
Conceptual understanding and stability, and knowledge shields for fending off conceptual change
[AD-A293555] p 3166 N95-34609
Resource document for the design of electronic instrument approach procedure displays
[AD-A295108] p 3047 N95-34797

COHERENT LIGHT
The composite classification problem in optical information processing p 3244 N95-32430

COHESION
Theoretical dynamical studies of metal clusters and cluster-ligand systems
[DE95-012461] p 3228 N95-33382

COLD TOLERANCE
A prototype computer program that integrates predictive models and medical handbooks for altitude, cold exposure, and heat stress
[AD-A294006] p 3182 N95-34371

COLD WORKING
Recent developments in maritime technology research institute acousto-optical technology research
[AD-A294215] p 3217 N95-34307

COLLAGENS
Plasma mediated ablation of biological tissues with ultrashort laser pulses
[DE95-011748] p 3164 N95-33654

COLLIMATORS
ENGIN mini-manual. Version 1.5
[PB95-218095] p 3206 N95-32814
Method for making fiber-optic bundle collimator assembly
[AD-D017486] p 3216 N95-34288

COLLISION AVOIDANCE
A tactical navigation and routeing system for low-level flight p 3044 N95-32494
Laser based obstacle warning sensors for helicopters
p 3045 N95-32499

COLLISIONS
Faddeev calculations of p(mu)+p collisions: Effect of hyperfine splitting on the cross sections
[DE95-007838] p 3203 N95-32583
Intrinsic charm contribution to double quarkonium hadroproduction
[DE95-012170] p 3204 N95-32617
High energy collisions involving multiply charged ions
[DE95-010912] p 3206 N95-32763
The effect of collisionality and diamagnetism on the plasma dynamo
[DE95-012409] p 3223 N95-33221
Wee partons in large nuclei: From virtual dream to hard reality
[DE95-012168] p 3208 N95-33854
Quantum transport
[AD-A294977] p 3235 N95-34589

COLLOIDS
Conversion of holes into reducing species on surface modified small-particle TiO2
[DE95-008282] p 3225 N95-32586

COLOR
Beam-based optical tuning of the Final Focus Test Beam
[DE95-012097] p 3215 N95-32658

COLUMBIA (ORBITER)
Liftoff to learning: Assignment space
[NASA-TM-110820] p 3057 N95-32539

COMBINATORIAL ANALYSIS
Optimum Routeing: Analytical constraint of search space p 3044 N95-32493

COMBUSTIBLE FLOW
Combustion-acoustic stability analysis for premixed gas turbine combustors
[NASA-TM-107024] p 3050 N95-32931
Calculation of supersonic combustion in SCRAMJET engines p 3035 N95-34513

COMBUSTION
Ignition and early soot formation in a DI diesel engine using multiple 2-D imaging diagnostics
[DE95-010692] p 3122 N95-32863
A fundamental study of smoldering with emphasis on experimental design for zero-G
[NASA-CR-198378] p 3089 N95-32929
Ignition and combustion of cellulosic dust particles
p 3073 N95-33308
DSMC method applied for reacting gas flows
p 3035 N95-34509

COMBUSTION CHAMBERS
Combustion-acoustic stability analysis for premixed gas turbine combustors
[NASA-TM-107024] p 3050 N95-32931
Water model tests on the Allison T56 series 3 combustion system
[DSTO-TR-0139] p 3054 N95-33250
A study of supersonic mixing flow field with ramp injector p 3035 N95-34512

COMBUSTION PHYSICS
A fundamental study of smoldering with emphasis on experimental design for zero-G
[NASA-CR-198378] p 3089 N95-32929
Review of combustion-acoustic instabilities
[NASA-TM-107020] p 3108 N95-32930
Fundamental phenomena on fuel decomposition and boundary-layer combustion processes with applications to hybrid rocket motors
[NASA-CR-199126] p 3061 N95-32932
The effects of high ambient density on diesel spray penetration and spread
[DE95-010761] p 3124 N95-33701

COMBUSTION STABILITY
Pop tests of storable biopropellant liquid apogee engine
[NAL-TR-1253] p 3060 N95-32755
Review of combustion-acoustic instabilities
[NASA-TM-107020] p 3108 N95-32930
Combustion-acoustic stability analysis for premixed gas turbine combustors
[NASA-TM-107024] p 3050 N95-32931

COMET NUCLEI
The mini-CIDEX GC/IMS: Analysis of cometary ice and dust p 3069 N95-33270

COMETARY ATMOSPHERES
The mini-CIDEX GC/IMS: Analysis of cometary ice and dust p 3069 N95-33270

COMETS
The mini-CIDEX GC/IMS: Analysis of cometary ice and dust p 3069 N95-33270

COMMAND AND CONTROL
Dual Usage in Military and Commercial Technology in Guidance and Control
[AGARD-CP-556] p 3091 N95-33126
The DLR research programme on an integrated multi sensor system for surface movement guidance and control p 3048 N95-33135

COMMAND GUIDANCE
Dual Usage in Military and Commercial Technology in Guidance and Control
[AGARD-CP-556] p 3091 N95-33126
Low-level data fusion for landing runways detection
p 3048 N95-33136

COMMERCE
Commercial usage of Navy components developed and manufactured by CRI Delfin p 3092 N95-33129
Some results of international cooperation in military to commercial conversion of laser gyro technology
p 3092 N95-33130
Effects of the specific military aspects of satellite navigation on the civil use of GPS/GLONASS
p 3048 N95-33134
Hand-portable gas chromatography-ion mobility spectrometer for the determination of the freshness of fish p 3071 N95-33277

COMMERCIAL AIRCRAFT
Report to the Chairman, Subcommittee on Aviation, Committee on Commerce, Science, and Transportation, US Senate. Aviation safety: Data problems threaten FAA strides on safety analysis system
[GAO/AIMD-95-27] p 3046 N95-32705
Beware of agents when flying aircraft: Basic principles behind a generic methodology for the evaluation and certification of advanced aviation systems
p 3176 N95-34787

COMMUNICATION
Validation of space/ground antenna control algorithms using a computer-aided design tool
p 3183 N95-32429
Bicriteria network design problems
[DE95-012052] p 3099 N95-33387

COMMUNICATION EQUIPMENT
A 75 watt, 59 to 64 GHz space TWT
[NASA-CR-195450] p 3104 N95-33915
England develops world's fastest optic switch breakthrough in high-speed communications
[AD-A294038] p 3105 N95-34488

COMMUNICATION NETWORKS
Congestion control over ATM local area networks
[DE95-010343] p 3184 N95-32558
OPEX: Second Workshop of the OLYMPUS propagation experimenters. Volume 1: Reference book on attenuation measurement and prediction
[ESA-WPP-083-VOL-1] p 3096 N95-32747
Simulation of a connectionless server for b-ISDN
[PB95-215091] p 3097 N95-32892
Spectrum allocation strategies for communication networks
[AD-A294936] p 3100 N95-34601
INMARSAT TT&C and communications network and the Beijing INMARSAT Station
[AD-A294163] p 3100 N95-34760

COMMUNICATION SATELLITES
Twenty-five years of progress. Part 1: Birth of NASA. Part 2: The Moon-a goal
[NASA-TM-110819] p 3253 N95-33384
Thermal control technology of communications satellite
[AD-A294249] p 3059 N95-34493

COMMUTATION
General-covariant Quantum Mechanics of Dirac particle in curved space-times
[DE95-623600] p 3233 N95-32478

COMPACTING
Development of improved p-type Si-20 at. %Ge by addition of fullerite
[DE95-010230] p 3066 N95-32394
Advanced precision expendable pattern casting technology
[DE95-012200] p 3095 N95-33393

COMPARISON
Analysis of samples for the first (1994) OPCW round robin interlaboratory comparison test
[PB95-210324] p 3068 N95-33243

COMPATIBILITY
Design rules and reality check for carbon-based ultracapacitors
[DE95-010575] p 3103 N95-33640

COMPETITION
The choice: Welding with CO2 or Nd:YAG lasers
[DE95-011825] p 3124 N95-33834

COMPLEX SYSTEMS
Application of fuzzy technology to risk-based design and decision problems
[DE95-006815] p 3178 N95-32378
Quantitative analysis of volatile organic compounds using ion mobility spectra and cascade correlation neural networks p 3073 N95-33290
Evaluation of conductive, radiative, chemical, and convective heat transfer in complex systems using a fast-running, implicit, lumped-capacitance formulation
[DE95-011889] p 3111 N95-33837
Human Factors Certification of Advanced Aviation Technologies
[NASA-CR-199009] p 3171 N95-34764
On the use of the systems approach to certify advanced aviation technologies p 3171 N95-34765
A rose by any other name: Certification seen as process rather than content p 3047 N95-34766
A psychologist's view of validating aviation systems
p 3172 N95-34767
Certification of tactics and strategies in aviation
p 3172 N95-34768
Human factors certification: A useful concept?
p 3173 N95-34769
Human factors certification in the development of future air traffic control systems p 3048 N95-34770
Quality assurance and risk management: Perspectives on Human Factors Certification of Advanced Aviation Systems p 3048 N95-34771
Certify for success: A methodology for human-centered certification of advanced aviation systems
p 3173 N95-34773
Does human cognition allow Human Factors (HF) certification of advanced aircrew systems?
p 3174 N95-34776
Practical guidelines for workload assessment
p 3174 N95-34777
Towards a framework of human factors certification of complex human-machine systems p 3175 N95-34779
Evaluation in context: ATC automation in the field
p 3175 N95-34781
Integrating human factors knowledge into certification: The point of view of the internationanl Civil Aviation Organization (ICAO) p 3175 N95-34782
Improving air traffic control: Proving new tools or approving the joint human-machine system?
p 3176 N95-34783
Certification for civil flight decks and the human-computer interface p 3176 N95-34784

COMPONENT RELIABILITY
Implications of early stages in the growth of stress corrosion cracking on component reliability
[DE95-011498] p 3127 N95-33833
An investigation of the chemistry of citric acid in military soldering applications
[AD-A295042] p 3105 N95-34796
COMPOSITE MATERIALS
Materials sciences programs: Fiscal year 1994
[DE95-011248] p 3211 N95-32483
Investigation of aging effects from high voltage profiles in ceramic phase shifter materials
[AD-A289985] p 3082 N95-32694
Evaluation of strength properties of developed SiC/C compositionally gradient graphite materials
[DE95-737271] p 3063 N95-32711
Development of a composite satellite structure for FORTE
[DE95-009416] p 3058 N95-32713
Micromechanics of fiber-reinforced ceramic composites p 3063 N95-32775
Thermographic imaging for high-temperature composite materials: A defect detection study
[NASA-TM-106950] p 3125 N95-33209
Microwave nondestructive evaluation: State-of-the-Art review
[AD-A294386] p 3125 N95-34346
Inertial confinement fusion target component fabrication and technology development support
[DE95-011655] p 3224 N95-34436
Apparatus for injection molding high-viscosity materials
[AD-D017471] p 3065 N95-34448
Method of installing a metallic threaded insert in a composite/rubber panel
[AD-D017522] p 3065 N95-34620
COMPOSITE STRUCTURES
Response and failure of thick composite rings subjected to uniform external hydrostatic pressure or radial contraction p 3064 N95-33326
Interlaminar stress analysis of dropped-ply laminated plates and shells by a mixed method
p 3064 N95-33327
Method of installing a metallic threaded insert in a composite/rubber panel
[AD-D017522] p 3065 N95-34620
COMPOSITION (PROPERTY)
The growth and optimization of InPSb/InGaAs/InAsSb strained-layer superlattice emitters by metal organic chemical vapor deposition
[DE95-011057] p 3226 N95-32595
Lithogenic and cosmogenic tracers in catchment hydrology
[DE95-011523] p 3143 N95-33407
COMPRESSED GAS
Supercritical crystallization: The RESs-process and the GAS-process
[PB95-214482] p 3228 N95-33235
COMPRESSIBILITY
Shock properties of high-strength ceramics
[DE95-007731] p 3082 N95-32380
Compression mass gauge testing in a liquid hydrogen dewar
[NASA-CR-198366] p 3115 N95-32687
Very large eddy simulations of spatially evolving supersonic turbulent shear layers p 3110 N95-33606
COMPRESSIBLE BOUNDARY LAYER
Asymptotic structure of supersonic turbulent boundary layers p 3107 N95-32898
COMPRESSIBLE FLOW
PINCA: A scalable parallel program for compressible gas dynamics with nonequilibrium chemistry
[DE95-010581] p 3106 N95-32818
Krylov methods for compressible flows
[NASA-CR-198176] p 3196 N95-33727
Stability of steady state solutions for forced Navier-Stokes equations p 3112 N95-34286
Direct numerical simulation of compressible isotropic turbulence p 3037 N95-34523
Program developing environment and a CFD application on the Cray T3D p 3038 N95-34535
Numerical simulation of two-dimensional compressible inviscid flow on unstructured grid system
p 3041 N95-34557
COMPRESSION TESTS
Response and failure of thick composite rings subjected to uniform external hydrostatic pressure or radial contraction p 3064 N95-33326
COMPRESSION WAVES
Numerical simulation of aerodynamic problems in high speed railways, part 2 p 3041 N95-34554
COMPRESSORS
Design of secondary flow control cascade using numerical simulation p 3034 N95-34507
COMPUTATION
The role of dynamic experimentation for computation analysis
[DE95-007733] p 3125 N95-32381
High performance systems
[DE95-009523] p 3185 N95-32771
COMPUTATIONAL ASTROPHYSICS
GRO: Studies of high energy pulsars with EGRET
[NASA-CR-199130] p 3248 N95-33499
COMPUTATIONAL CHEMISTRY
Solving stiff chemistry problems with FIDAP
[DE95-011053] p 3067 N95-32709
COMPUTATIONAL ELECTROMAGNETICS
Simulation of patch and slot antennas using FEM with prismatic elements and investigations of artificial absorber mesh termination schemes
[NASA-CR-198974] p 3097 N95-32822
The 11th Annual Review of Progress in Applied Computational Electromagnetics, volume 1
[AD-A294850] p 3100 N95-34566
The 11th Annual Review of Progress in Applied Computational Electromagnetics, volume 2
[AD-A294851] p 3100 N95-34567
COMPUTATIONAL FLUID DYNAMICS
Unified approach for incompressible flows
p 3113 N95-32425
Large-eddy simulation of the development of stably-stratified atmospheric boundary layers over cool flat surfaces
[DE95-009574] p 3156 N95-32697
Solving stiff chemistry problems with FIDAP
[DE95-011053] p 3067 N95-32709
Thermo-chemical ablation of heat shields under Earth reentry conditions p 3059 N95-32903
Three-dimensional aerodynamic shape optimization using discrete sensitivity analysis p 3048 N95-32904
Application of vorticity transport analysis to the development of physically accurate turbulence models
p 3107 N95-32905
Design of ETO propulsion turbine using CFD analyses
[NASA-CR-199085] p 3123 N95-32915
Parallel finite element methods and iterative solution techniques for viscous incompressible flows
p 3108 N95-33031
Turbulence models in the Navier-Stokes simulation of airfoil stall
[TRITA-NA-9312] p 3108 N95-33059
Numerical simulation of supersonic flow using a new analytical bleed boundary condition
[NASA-CR-198368] p 3054 N95-33208
A unified multigrid solver for the Navier-Stokes equations on mixed element meshes
[NASA-CR-198183] p 3196 N95-33500
Very large eddy simulations of spatially evolving supersonic turbulent shear layers p 3110 N95-33606
Direct and large eddy simulations of three dimensional round turbulent jets p 3111 N95-33709
Krylov methods for compressible flows
[NASA-CR-198176] p 3196 N95-33727
Numerical studies of turbulent free surface flows and unsteady propeller flows
[AD-A294377] p 3112 N95-34343
Consistent finite-volume discretization of hydrodynamic conservation laws for unstructured grids
[DE95-011730] p 3112 N95-34437
Special publication of National Aerospace Laboratory
[NAL-SP-27] p 3034 N95-34505
Requirements and trends of computational aerodynamics as a tool for aircraft design
p 3034 N95-34506
A study on the convergence of a 3-D Euler code for cascade flow calculations p 3034 N95-34508
A study of supersonic mixing flow field with ramp injector p 3035 N95-34512
Calculation of supersonic combustion in SCRAMJET engines p 3035 N95-34513
Adaptive grid method using elliptic equation for compressible flows p 3035 N95-34515
A variation of the Riemann Problem solution and its application to implicit Godunov's scheme
p 3036 N95-34516
A multigrid incompressible NS solver
p 3036 N95-34517
A flux splitting scheme with high-resolution and robustness for discontinuities p 3036 N95-34518
Construction and analysis of difference approximation for scalar conservation laws and its consistency with entropy condition using Boltzmann-like approach
p 3036 N95-34519
Hypersonic CFD analysis for the aerothermodynamic design of HOPE p 3036 N95-34520
Numerical solutions of inviscid and viscous flows about airfoils by TVD method p 3036 N95-34521
Direct numerical simulation of incompressible homogeneous isotropic turbulence using compressible Navier-Stokes equations p 3037 N95-34529
Direct numerical simulation of incompressible homogeneous isotropic turbulence using NWT
p 3038 N95-34530
Performance evaluation of the NWT with incompressible NS code p 3038 N95-34533
Program developing environment and a CFD application on the Cray T3D p 3038 N95-34535
Parallel computation of transonic flows about an aircraft configuration using multi-block structured grids
p 3039 N95-34537
Vector-parallel simulations of transonic wind tunnel flows about a fully configured model of aircraft
p 3039 N95-34538
A large scale 3D Navier-Stokes analysis using NAL-NWT p 3039 N95-34539
Role of computational fluid dynamics in aeronautical engineering. Number 12: Formulation and verification of uni-particle upwind schemes for the Euler equations
p 3039 N95-34540
Application of CFD techique for HYFLEX aerodynamic design p 3039 N95-34542
Computations of low speed flow about space-plane
p 3040 N95-34544
Numerical simulations of dynamic stall phenomena in low speed flows p 3040 N95-34546
Numerical simulation of unsteady viscous flow around an airfoil with oscillating spoiler p 3040 N95-34547
Direct analysis of transonic rotor noise with CFD technique p 3040 N95-34549
Dependency of a boundary layer flow on computational grids p 3040 N95-34550
A simulation of damping process of pendulum motion due to aerodynamic forces p 3041 N95-34551
Numerical simulation of aerodynamic problems in high speed railways, part 2 p 3041 N95-34554
Large scale computing and volume visualization
p 3041 N95-34556
Numerical simulation of two-dimensional compressible inviscid flow on unstructured grid system
p 3041 N95-34557
Upwind schemes for the two-dimensional Euler equations p 3042 N95-34559
Modeling liquid jet atomization processes
[AD-A294888] p 3112 N95-34572
QMR methods in computational fluid dynamics
[DE95-012889] p 3113 N95-34800
COMPUTATIONAL GRIDS
Large-eddy simulation of the development of stably-stratified atmospheric boundary layers over cool flat surfaces
[DE95-009574] p 3156 N95-32697
Simulation of patch and slot antennas using FEM with prismatic elements and investigations of artificial absorber mesh termination schemes
[NASA-CR-198974] p 3097 N95-32822
Gasdynamic model of turbulent combustion in an explosion
[DE95-010267] p 3074 N95-33627
Krylov methods for compressible flows
[NASA-CR-198176] p 3196 N95-33727
Adaptive grid method using elliptic equation for compressible flows p 3035 N95-34515
A multigrid incompressible NS solver
p 3036 N95-34517
Hypersonic CFD analysis for the aerothermodynamic design of HOPE p 3036 N95-34520
Direct numerical simulation of incompressible homogeneous isotropic turbulence using NWT
p 3038 N95-34530
Performance evaluation of the NWT with incompressible NS code p 3038 N95-34533
Vector-parallel simulations of transonic wind tunnel flows about a fully configured model of aircraft
p 3039 N95-34538
Role of computational fluid dynamics in aeronautical engineering. Number 12: Formulation and verification of uni-particle upwind schemes for the Euler equations
p 3039 N95-34540
Numerical simulations of dynamic stall phenomena in low speed flows p 3040 N95-34546
Dependency of a boundary layer flow on computational grids p 3040 N95-34550
Grid generation around airfoil with a flap using boundary element method p 3041 N95-34552
Numerical simulation of aerodynamic problems in high speed railways, part 2 p 3041 N95-34554
Upwind schemes for the two-dimensional Euler equations p 3042 N95-34559
COMPUTER AIDED DESIGN
Validation of space/ground antenna control algorithms using a computer-aided design tool
p 3183 N95-32429
X-Antenna: A graphical interface for antenna analysis codes
[NASA-CR-199212] p 3095 N95-32674

Multiobjective optimization of hybrid regenerative life support technologies. Topic D: Technology Assessment
[NASA-CR-199125] p 3167 N95-32688
Three-dimensional aerodynamic shape optimization using discrete sensitivity analysis p 3048 N95-32904
Expert systems and artificial intelligence applications in engineering design and inspection p 3190 N95-33008
A procedural framework for designing linear orienting devices p 3181 N95-33325
The PEP-2 project-wide database
[DE95-012512] p 3213 N95-33333
The 11th Annual Review of Progress in Applied Computational Electromagnetics, volume 1
[AD-A294850] p 3100 N95-34566
Non-smooth optimization algorithms, system theory and software tools
[AD-A294944] p 3183 N95-34605
A model of long term learning: Integration of knowledge acquisition and knowledge compilation
[AD-A294123] p 3235 N95-34743
Numerical and symbolic algorithms for application specific signal processing
[AD-A294125] p 3100 N95-34749

COMPUTER ANIMATION
Animation within a multimedia training system for night vision goggles
[AD-A294095] p 3170 N95-34475

COMPUTER ASSISTED INSTRUCTION
A prototype computer program that integrates predictive models and medical handbooks for altitude, cold exposure, and heat stress
[AD-A294006] p 3182 N95-34371
Animation within a multimedia training system for night vision goggles
[AD-A294095] p 3170 N95-34475
Developing multimedia instructional systems: An example application for training in night vision goggles
[AD-A294521] p 3235 N95-34479

COMPUTER GRAPHICS
Visualization of parallel molecular dynamics simulation on a remote visualization platform
[DE95-007806] p 3185 N95-32582
The RDB: A parallel, spatial database for the IES/BTI system
[DE95-009425] p 3179 N95-32715
Tracking a turbulent spot in an immersive environment
[NASA-CR-198179] p 3180 N95-32834
Open architecture CNC system
[DE95-009485] p 3177 N95-32955
xdamp: An IDL(R)-based Data Manipulation Program
[DE95-011242] p 3181 N95-33624
Interactive interface for National Center for Atmospheric Research (NCAR) graphics p 3239 N95-34220
Experimenter's laboratory for visualized interactive science p 3184 N95-34228
SAVS: A Space Analysis and Visualization System p 3242 N95-34238
ABCASH plotting program users guide
[DE95-011652] p 3155 N95-34435
Towards friendlier user interfaces for expert systems
[AD-A294056] p 3192 N95-34467
Range graphics benchmark
[AD-A293541] p 3057 N95-34606
The development of a distributed computing environment for the design and modeling of plasma spectroscopy experiments
[DE95-011725] p 3183 N95-34813

COMPUTER INFORMATION SECURITY
Security and privacy in the NII
[AD-A293475] p 3244 N95-34816

COMPUTER NETWORKS
Distributed shared memory for new generation networks
[AD-A293722] p 3185 N95-32580
Visualization of parallel molecular dynamics simulation on a remote visualization platform
[DE95-007806] p 3185 N95-32582
Proceedings of the REXX symposium for developers and users
[DE95-010668] p 3185 N95-32820
Fast approximation of self-similar network traffic
[DE95-011271] p 3185 N95-32967
FTP-Server for exchange, interpretation, and database-search of ion mobility spectra, literature, preprints and software p 3073 N95-33291
Bicriteria network design problems
[DE95-012052] p 3099 N95-33387
Collaborating over the Web: Libraries and laboratories or the Librarian and the Webmaster
[DE95-010572] p 3186 N95-33639
A distributed system for visualizing and analyzing multivariate and multidisciplinary data p 3241 N95-34230
Recoverable distributed shared memory under sequential and relaxed consistency
[AD-A293966] p 3178 N95-34453
Stochastic network processes
[AD-A294939] p 3187 N95-34603

COMPUTER PROGRAMMING
The future of finite element applications on massively parallel supercomputers
[DE95-011659] p 3184 N95-32415
Optimum Routeing: Analytical constraint of search space p 3044 N95-32493
Third International Workshop on Ion Mobility Spectrometry
[NASA-CP-3301] p 3069 N95-33265
Proceedings: High performance functional computing
[DE95-010736] p 3186 N95-33643
Construction of a connectionist network supercomputer
[AD-A294198] p 3177 N95-34301
Conditions for implicit parallelism
[AD-A294110] p 3193 N95-34497
Automated support for software engineering
[AD-A294965] p 3182 N95-34582

COMPUTER PROGRAMS
Cylindrical shell buckling through strain hardening
[DE95-009545] p 3125 N95-32392
Charm decays and high energy photoproduction
[DE95-010165] p 3201 N95-32393
Scanners, optical character readers, Cyrillic alphabet and Russian translations p 3194 N95-32433
Optimum Routeing: Analytical constraint of search space p 3044 N95-32493
Study of impurity concentrations by VUV spectroscopy on HL-1
[DE95-614186] p 3221 N95-32562
Message based event specification for debugging nondeterministic parallel programs
[DE95-006169] p 3179 N95-32669
PINCA: A scalable parallel program for compressible gas dynamics with nonequilibrium chemistry
[DE95-010581] p 3106 N95-32818
Proceedings of the REXX symposium for developers and users
[DE95-010668] p 3185 N95-32820
Open architecture CNC system
[DE95-009485] p 3177 N95-32955
Technical support in the area of theoretical support of nuclear preequilibrium
[DE95-011617] p 3212 N95-32960
Computational electromagnetics and parallel dense matrix computations
[DE95-012286] p 3099 N95-33379
Anechoic chamber upgrade
[AD-A294375] p 3056 N95-34342
A prototype computer program that integrates predictive models and medical handbooks for altitude, cold exposure, and heat stress
[AD-A294006] p 3182 N95-34371
ABCASH plotting program users guide
[DE95-011652] p 3155 N95-34435
Reducing cache misses in numerical applications using data relocation and prefetching
[AD-A293978] p 3182 N95-34455
Certification of MCNP Version 4A for WHC computer platforms, revision 7
[DE95-011546] p 3178 N95-34484
A study on the convergence of a 3-D Euler code for cascade flow calculations p 3034 N95-34508
Verification of turbine cascade flow with tip clearance p 3035 N95-34511
A study of supersonic mixing flow field with ramp injector p 3035 N95-34512
Calculation of supersonic combustion in SCRAMJET engines p 3035 N95-34513
Numerical solutions of inviscid and viscous flows about airfoils by TVD method p 3036 N95-34521
Elementary benchmarks of the NWT computer system and program performance p 3038 N95-34532
Performance evaluation of the NWT with incompressible NS code p 3038 N95-34533
Highly parallel computer AP1000: Architecture and basic software p 3038 N95-34534
Program developing environment and a CFD application on the Cray T3D p 3038 N95-34535
Application of CFD techique for HYFLEX aerodynamic design p 3039 N95-34542
Optimization problems in multitarget/multisensor tracking
[AD-A294978] p 3100 N95-34590
Non-smooth optimization algorithms, system theory and software tools
[AD-A294944] p 3183 N95-34605
Track finding and fitting in the H1 forward track detector
[PB95-234985] p 3214 N95-34651

COMPUTER SYSTEMS DESIGN
A highly reliable, high performance open avionics architecture for real time Nap-of-the-Earth operations p 3044 N95-32497
An integrated system for air to ground operations p 3044 N95-32498
Development and flight testing of an Obstacle Avoidance System for US Army helicopters p 3045 N95-32500
Fixed wing night attack missions: Assessment in a Flight Simulation environment p 3045 N95-32502
High performance systems
[DE95-009523] p 3185 N95-32771
An interactive environment for the analysis of large Earth observation and model data sets p 3239 N95-34219
A land-surface testbed for EOSDIS p 3158 N95-34223
A distributed analysis and visualization system for model and observational data p 3243 N95-34240
Construction of a connectionist network supercomputer
[AD-A294198] p 3177 N95-34301

COMPUTER SYSTEMS PERFORMANCE
Distributed shared memory for new generation networks
[AD-A293722] p 3185 N95-32580
High performance systems
[DE95-009523] p 3185 N95-32771
Cost-effective data-parallel load balancing
[DE95-010985] p 3186 N95-33403
Performance analysis of combined concurrency control and commit protocols in distributed database systems p 3238 N95-33711
Elementary benchmarks of the NWT computer system and program performance p 3038 N95-34532
Range graphics benchmark
[AD-A293541] p 3057 N95-34606

COMPUTER SYSTEMS PROGRAMS
The future of finite element applications on massively parallel supercomputers
[DE95-011659] p 3184 N95-32415
Formal verification of an avionics microprocessor
[NASA-CR-4682] p 3181 N95-33396
The design of scalable software libraries for distributed memory concurrent computers
[DE95-012891] p 3244 N95-34801

COMPUTER TECHNIQUES
NASA wide electronic publishing system: Electronic printing and duplicating. Stage 3 evaluation report
[NASA-TM-104620] p 3237 N95-32922
Automatic script identification from images using cluster-based templates
[DE95-006339] p 3181 N95-33154
The 1994 laboratory calibration of TIMS p 3117 N95-33796
A model of long term learning: Integration of knowledge acquisition and knowledge compilation
[AD-A294123] p 3235 N95-34743

COMPUTER VISION
Self-organizing neural network and its applications to vision-guided robot motion coordination p 3191 N95-33324
Three-dimensional recognition via two-stage associative memory
[AD-A293567] p 3183 N95-34612
Adaptive differential visual feedback for uncalibrated hand-eye coordination and motor control
[AD-A293607] p 3171 N95-34616

COMPUTERIZED SIMULATION
Solar cell array design method for preventing power reduction due to module output fluctuation
[DE95-769745] p 3148 N95-32402
The effect and correction of coupling generated by the RHIC triplet quadrupoles
[DE95-011562] p 3210 N95-32413
The application of helicopter mission simulation to Nap-of-the-Earth operations p 3044 N95-32496
Fixed wing night attack missions: Assessment in a Flight Simulation environment p 3045 N95-32502
Predicted operating conditions for maintaining mode purity in the 1MW 200 GHz FOM Free Electron Maser
[DE95-010795] p 3117 N95-32571
Visualization of parallel molecular dynamics simulation on a remote visualization platform
[DE95-007806] p 3185 N95-32582
Evaluation of a bridge using simplified element modeling
[DE95-006281] p 3126 N95-32670
Numerical simulation of heat and mass transport during space crystal growth with MEPHISTO
[NASA-TM-107015] p 3089 N95-32718
A comparison of modeled and measured energy use in hybrid electric vehicles
[DE95-000297] p 3102 N95-32808
Simulation of a connectionless server for b-ISDN
[PB95-215091] p 3097 N95-32892
Mathematical methods applied to biotechnical processes
[PB95-212114] p 3163 N95-33232
CADIR: A model for generating infrarad images
[PB95-222956] p 3215 N95-33239

Operation of the computer model for microenvironment atomic oxygen exposure
[NASA-CR-198190] p 3059 N95-33264
The preservation of human surrogates for biomechanical studies p 3167 N95-33312
A procedural framework for designing linear orienting devices p 3181 N95-33325
Nonlinear analyses of storage ring lattices using one-turn maps
[DE95-012515] p 3213 N95-33335
A comparison of interface tracking methods
[DE95-009481] p 3111 N95-33698
Operation of the computer model for microenvironment solar exposure
[NASA-CR-198189] p 3059 N95-33890
Studies of halo distributions under beam-beam interaction
[DE95-012560] p 3214 N95-34024
Parallel molecular dynamics: Communication requirements for massively parallel machines
[DE95-012948] p 3209 N95-34212
Heavy ions acceleration in RF wells of 2-frequency electromagnetic field and in the inverted FEL
[DE95-012439] p 3214 N95-34439
Triple invariant optical pattern recognition using circular harmonic synthetic filters
[AD-A294253] p 3217 N95-34459
Improving the comprehensibility, accuracy, and generality of reactive plans
[AD-A294104] p 3193 N95-34495
Explanations of empirically derived reactive plans
[AD-A294114] p 3193 N95-34501
Requirements and trends of computational aerodynamics as a tool for aircraft design p 3034 N95-34506
Design of secondary flow control cascade using numerical simulation p 3034 N95-34507
Calculation of supersonic combustion in SCRAMJET engines p 3035 N95-34513
Direct numerical simulation of compressible isotropic turbulence p 3037 N95-34523
Numerical simulation of film cooling effect around axisymmetric body in hypersonic flow field p 3037 N95-34526
Direct numerical simulation of incompressible homogeneous isotropic turbulence using compressible Navier-Stokes equations p 3037 N95-34529
Direct numerical simulation of incompressible homogeneous isotropic turbulence using NWT p 3038 N95-34530
Effect of schemes on numerical simulations of shock wave reflection p 3038 N95-34531
Application of CFD techique for HYFLEX aerodynamic design p 3039 N95-34542
Numerical simulation of interaction between shock wave and density interface p 3039 N95-34543
Numerical simulation of unsteady viscous flow around an airfoil with oscillating spoiler p 3040 N95-34547
Numerical simulation of two-dimensional PAR-WIG p 3040 N95-34548
Numerical simulation of aerodynamic problems in high speed railways, part 2 p 3041 N95-34554
Large scale computing and volume visualization p 3041 N95-34556
Everyday believability
[AD-A294938] p 3193 N95-34602
The virtual sailor: Synthetic humans for virtual environments
[AD-A293560] p 3166 N95-34610
Control of initialization bias in queueing simulations using queueing approximations
[AD-A294121] p 3194 N95-34742
A model of long term learning: Integration of knowledge acquisition and knowledge compilation
[AD-A294123] p 3235 N95-34743
High order accuracy computational methods in aerodynamics using parallel architectures
[AD-A294167] p 3042 N95-34763

COMPUTERS
Charm decays and high energy photoproduction
[DE95-010165] p 3201 N95-32393
HINT: A new way to measure computer speed
[DE95-010245] p 3177 N95-32398
Study on turbulent fluctuations in diffusion flames using laser induced fluorescence
[PB95-214425] p 3068 N95-32812
xdamp: An IDL(R)-based Data Manipulation Program
[DE95-011242] p 3181 N95-33624
Evaluation of conductive, radiative, chemical, and convective heat transfer in complex systems using a fast-running, implicit, lumped-capacitance formulation
[DE95-011889] p 3111 N95-33837
Reducing cache misses in numerical applications using data relocation and prefetching
[AD-A293978] p 3182 N95-34455
Optical interconnects for 3D computer architectures
[AD-A294118] p 3178 N95-34503

COMSAT PROGRAM
Laser beaming demonstrations at the Starfire Optical Range
[DE95-007747] p 3120 N95-34811

CONCENTRATION (COMPOSITION)
Fracture toughness and tensile behavior of multi-layer laminated metal composite of Al 6090-25 vol % SiCp and Al 5182
[DE95-011421] p 3062 N95-32602
Causal correlation of foliar biochemical concentrations with AVIRIS spectra using forced entry linear regression p 3130 N95-33744
Encapsulated dry electrolyte composition for time release into a solute
[AD-D017485] p 3075 N95-34287

CONCENTRIC CYLINDERS
Semi-analytic computation of the driven fields in right circular cylindrical microwave applicators
[DE95-010875] p 3203 N95-32574

CONCRETES
Investigation research on introducing new energy technology, promoting its practical application, and providing its instruction
[DE95-769801] p 3148 N95-32403

CONCURRENT PROCESSING
Performance analysis of combined concurrency control and commit protocols in distributed database systems p 3238 N95-33711
Sleep sets method for partial order verification of concurrent systems
[PB95-236121] p 3183 N95-34655

CONDENSATES
NJL Model with nonperturbative dependence on gluon condensate
[DE95-623677] p 3233 N95-32405

CONDENSING
Rigid bodies for metal forming analysis with NIKE3D
[DE95-011740] p 3182 N95-33652

CONDUCTION BANDS
High resistivity InAlN by nitrogen or oxygen implantation
[DE95-011023] p 3226 N95-32594

CONDUCTIVE HEAT TRANSFER
Thermo-chemical ablation of heat shields under Earth reentry conditions p 3059 N95-32903
Structure of weak shock waves in bubbly liquid p 3037 N95-34527

CONDUCTIVITY
High rate rechargeable lithium cells employing lithium ion conducting solid electrolytes
[AD-A294390] p 3104 N95-34347

CONDUCTORS
Quench antenna and fast-motion investigations during training of a 7T dipole magnet
[DE95-012371] p 3103 N95-33080
Diamond multilayer multichip module substrate
[AD-D017469] p 3104 N95-34445

CONFERENCES
Fifth International Conference on Hyperbolic Problems, Theory, Numerics, Applications: Abstracts
[DE95-008173] p 3194 N95-32389
Low-Level and Nap-of-the-Earth (NOE) night operations
[AGARD-CP-563] p 3042 N95-32486
Minutes of the 12th Joint NASA/DARA-DLR Life Sciences Program Working Group Meeting
[NASA-TM-110655] p 3161 N95-32719
High performance systems
[DE95-009523] p 3185 N95-32771
Conference proceedings of mathematical methods in electromagnetic theory
[AD-A291165] p 3097 N95-32797
Proceedings of the REXX symposium for developers and users
[DE95-010668] p 3185 N95-32820
Industrial and Engineering Applications of Artificial Intelligence and Expert Systems: Invited and additional papers
[DSTO-GD-0051] p 3188 N95-32995
Dual Usage in Military and Commercial Technology in Guidance and Control
[AGARD-CP-556] p 3091 N95-33126
The 17th Symposium on Biotechnology for Fuels and Chemicals
[DE95-004054] p 3150 N95-33225
Third International Workshop on Ion Mobility Spectrometry
[NASA-CP-3301] p 3069 N95-33265
Proceedings: High performance functional computing
[DE95-010736] p 3186 N95-33643
Summaries of the Fifth Annual JPL Airborne Earth Science Workshop. Volume 1: AVIRIS Workshop
[NASA-CR-198922] p 3128 N95-33730
Summaries of the Fifth Annual JPL Airborne Earth Science Workshop. Volume 2: TIMS Workshop
[NASA-CR-198923] p 3136 N95-33789
Summaries of the Fifth Annual JPL Airborne Earth Science Workshop. Volume 3: AIRSAR Workshop
[NASA-CR-198924] p 3139 N95-33801
Applied Information Systems Research Program (AISRP) Workshop 3 meeting proceedings
[NASA-CR-199103] p 3239 N95-34218
Proceedings of the ONR/NRL workshop on modeling the dispersion of nuclear contaminants in the arctic seas
[AD-A294373] p 3159 N95-34341
Special publication of National Aerospace Laboratory
[NAL-SP-27] p 3034 N95-34505
The 11th Annual Review of Progress in Applied Computational Electromagnetics, volume 1
[AD-A294850] p 3100 N95-34566
The 11th Annual Review of Progress in Applied Computational Electromagnetics, volume 2
[AD-A294851] p 3100 N95-34567
Proceedings of the School for Young High Energy Physicists
[PB95-234993] p 3235 N95-34652
First NPL Calorimetry Workshop
[PB95-236063] p 3235 N95-34654
Human Factors Certification of Advanced Aviation Technologies
[NASA-CR-199009] p 3171 N95-34764

CONFINEMENT
Transport studies of tokamak plasmas in JT-60 device
[DE95-737227] p 3220 N95-32417
Recent results from the D3-D tokamak and implications for future devices
[DE95-009605] p 3222 N95-32592
The growth and optimization of InPSb/InGaAs/InAsSb strained-layer superlattice emitters by metal organic chemical vapor deposition
[DE95-011057] p 3226 N95-32595
Optimized profiles for improved confinement and stability in the DIII-D tokamak
[DE95-009606] p 3222 N95-32756

CONGENERS
Environment applications for ion mobility spectrometry p 3071 N95-33279

CONGESTION
Congestion control over ATM local area networks
[DE95-010343] p 3184 N95-32558

CONGRESSIONAL REPORTS
Annual report to Congress 1994: Energy Information Administration
[DE95-011240] p 3237 N95-32482
Report to the Chairman, Subcommittee on Aviation, Committee on Commerce, Science, and Transportation, US Senate. Aviation safety: Data problems threaten FAA strides on safety analysis system
[GAO/AIMD-95-27] p 3046 N95-32705
Aerospace Guidance and Metrology Center: Cost growth and other factors affect closure and privatization. Report to Congressional requesters
[GAO/NSIAD-95-60] p 3235 N95-32706
Report to the Chairman, Committee on Science, House of Representatives. NASA's Earth Observing System: Estimated funding requirements
[GAO/NSIAD-95-175] p 3142 N95-32707
Report to Congressional Committees. B-1B bomber: Evaluation of Air Force report on B-1B operational readiness assessment
[GAO/NSIAD-95-151] p 3197 N95-32758
Fact sheet for Congressional requesters. Airport competition: Essential air service slots at O'Hare International Airport
[GAO/RCED-94-118FS] p 3055 N95-32759
Weather Forecasting: Systems architecture needed for National Weather Service modernization. Report to Congressional requesters
[GAO/AIMD-94-28] p 3157 N95-32760
Report to Congressional Committees. B-2 bomber: Cost to complete 20 aircraft is uncertain
[GAO/NSIAD-94-217] p 3033 N95-32782
Army aviation: Modernization strategy needs to be reassessed. Report to Congressional requestors
[GAO/NSIAD-95-9] p 3033 N95-32783
Report to the Chairman, Subcommittee on Aviation, Committee on Commerce, Science, and Transportation, US Senate. Aviation Safety: FAA can better prepare general aviation pilots for mountain flying risks
[GAO/RCED-94-15] p 3046 N95-32784
Metric conversion: Future progress depends upon private sector and public support. Report to Congressional requesters
[GAO/RCED-94-23] p 3089 N95-32785
Report to the Chairman, Subcommittee on Transportation and Related Agencies, Committee on Appropriations, US Senate. Airport Improvement Program: Reliever airport set-aside funds could be redirected
[GAO/RCED-94-226] p 3055 N95-32786

Report to Congressional Committees. Air Force fighters: More reliance on reserves increases the need to know their capabilities
[GAO/NSIAD-94-86] p 3197 N95-32807
Space Station: Estimated total US funding requirements. Report to Congressional Requesters
[GAO/NSIAD-95-163] p 3058 N95-32884
Aviation security: Development of new security technology has not met expectations. Report to Congressional requesters
[GAO/RCED-94-142] p 3046 N95-32885
Report to the Honorable William V. Roth, Jr., US Senate. Naval aviation: F/A-18 E/F acquisition strategy
[GAO/NSIAD-94-194] p 3197 N95-32886
Annual report to the Chairman, House and Senate Committees on Appropriations. Status of open recommendations: Improving operations of federal departments and agencies
[GAO/OP-94-1] p 3236 N95-32887
Report to the Chairman, Subcommittee on Transportation and Related Agencies, Committee on Appropriations, US Senate. Airport Improvement Program: The Military Airport Program has not achieved intended impact
[GAO/RCED-94-209] p 3056 N95-32888
Report to the Chairman, Committee on Armed Services, US Senate. Strategic Bomber: Issues relating to the B-1B's availability and ability to perform conventional missions
[GAO/NSIAD-94-81] p 3198 N95-33263
Report to the Ranking Minority Member, Committee on Government Operations, House of Representatives. Paperwork reduction: Reported burden hour increases reflect new estimates, not actual changes
[GAO/PEMD-94-3] p 3236 N95-33907
Comanche helicopter: Testing needs to be completed prior to production decisions
[AD-A294408] p 3049 N95-34422

CONIFERS
AVIRIS spectral trajectories for forested areas of the Gifford Pinchot National Forest p 3135 N95-33766

CONJUGATES
Progress towards antihydrogen production by the reaction of cold antiprotons with positronium atoms
[DE95-007850] p 3204 N95-32584

CONNECTORS
A fiber-optic connector
[AD-D017424] p 3215 N95-32923
Device for dampening vibratory motion
[AD-D017490] p 3127 N95-34427

CONSERVATION
Differencing the diffusion equation on unstructured meshes in 2-D
[DE95-010410] p 3195 N95-32559
Remotely sensed indicators of habitat heterogeneity and biological diversity: A preliminary report p 3140 N95-33806

CONSERVATION LAWS
Fifth International Conference on Hyperbolic Problems, Theory, Numerics, Applications: Abstracts
[DE95-008173] p 3194 N95-32389
Consistent finite-volume discretization of hydrodynamic conservation laws for unstructured grids
[DE95-011730] p 3112 N95-34437
Construction and analysis of difference approximation for scalar conservation laws and its consistency with entropy condition using Boltzmann-like approach p 3036 N95-34519

CONSISTENCY
Recoverable distributed shared memory under sequential and relaxed consistency
[AD-A293966] p 3178 N95-34453

CONSTRUCTION
Investigation research on introducing new energy technology, promoting its practical application, and providing its instruction
[DE95-769801] p 3148 N95-32403
A thermophotovoltaic generator for use in a lightweight electric car: Year 1 progress report
[DE95-011355] p 3102 N95-32968
Budget estimates: Fiscal year 1994. Volume 2: Construction of facilities
[NASA-TM-110816] p 3245 N95-33081
The PEP-2 project-wide database
[DE95-012512] p 3213 N95-33333
Indium mono-ion oscillator
[AD-A293736] p 3104 N95-34451

CONSTRUCTION INDUSTRY
Expert systems and artificial intelligence applications in engineering design and inspection p 3190 N95-33008

CONTACT DERMATITIS
Environmental evaluation of lactates as cleaning agents
[PB95-214854] p 3067 N95-32615

CONTACTORS
Life test of a xenon hollow cathode for a space plasma contractor
[NASA-CR-195403] p 3061 N95-33926

CONTAMINANTS
Winter season air pollution in El Paso-Ciudad Juarez. A review of air pollution studies in an international airshed
[DE95-009083] p 3152 N95-32556
Solving widespread low-concentration VOC air pollution problems: Gas-phase photocatalytic oxidation answers the needs of many small businesses
[DE95-004059] p 3152 N95-32668
Field Raman spectrograph for environmental analysis
[DE95-007969] p 3153 N95-32816
Direct analysis of organic priority pollutants by IMS p 3071 N95-33280
Pollution in Norway
[PB95-214565] p 3153 N95-33331
Geochemical, genetic, and physiological control of pollutant biodegradation
[AD-A294902] p 3155 N95-34591

CONTAMINATION
Mineralogic variations in fluvial sediments contaminated by mine tailings as determined from AVIRIS data, Coeur D'Alene River Valley, Idaho p 3131 N95-33745
ABCASH plotting program users guide
[DE95-011652] p 3155 N95-34435
Geochemical, genetic, and physiological control of pollutant biodegradation
[AD-A294902] p 3155 N95-34591

CONTINUITY EQUATION
Unified approach for incompressible flows p 3113 N95-32425

CONTINUOUS RADIATION
Sum frequency generation of dual-wavelength Nd: YAP laser in LiIO3 crystal
[AD-A293094] p 3117 N95-32472
Predicted operating conditions for maintaining mode purity in the 1MW 200 GHz FOM Free Electron Maser
[DE95-010795] p 3117 N95-32571
New advances in 1341.4 nm Nd:YAP lasers
[AD-A293070] p 3118 N95-32702

CONTINUOUS WAVE LASERS
New advances in 1341.4 nm Nd:YAP lasers
[AD-A293070] p 3118 N95-32702
Influence of CO2 continuous laser preprocessed substrates on optical thin film damage thresholds
[AD-A294190] p 3217 N95-34297
High power CO2 laser windows and reflection reducing coatings
[AD-A294217] p 3119 N95-34308

CONTINUOUS WAVE RADAR
Studies of microwave scattering and canopy architecture for boreal forests
[NASA-CR-199113] p 3099 N95-33497

CONTRACT MANAGEMENT
Budget estimates: Fiscal year 1994. Volume 2: Construction of facilities
[NASA-TM-110816] p 3245 N95-33081
NASA directives master list and index
[NHB-1410.13O] p 3238 N95-33249

CONTRACTION
Response and failure of thick composite rings subjected to uniform external hydrostatic pressure or radial contraction p 3064 N95-33326

CONTRACTORS
Fusion Safety Program annual report, fiscal year 1994
[DE95-008872] p 3221 N95-32588
An investigation of the chemistry of citric acid in military soldering applications
[AD-A295042] p 3105 N95-34796

CONTROL
Emittance and energy control in the NLC main linacs
[DE95-012556] p 3213 N95-33338

CONTROL BOARDS
Dual Usage in Military and Commercial Technology in Guidance and Control
[AGARD-CP-556] p 3091 N95-33126

CONTROL EQUIPMENT
Baseline experimental investigation of an electrohydrodynamically assisted heat pipe p 3113 N95-32427
Development of tokamak experiment technology: A study on the nuclear fusion reactor
[DE95-614255] p 3223 N95-33619

CONTROL SYSTEMS DESIGN
An alternative reasoning method p 3189 N95-33001
Propulsion Controlled Aircraft design and development p 3053 N95-33022
Development and application of the methods for pilot-aircraft system research to the manual control tasks of modern vehicles p 3094 N95-33139
Application of advanced safety technique to ring laser gyro inertial navigation system integration p 3048 N95-33140
Sea wave parameters, small altitudes and distances measurers design for movement control systems of ships, wing-in-surface effect crafts and seaplanes p 3094 N95-33141
Motion and force control of coordinated robots
[ISBN-0-315-86323-4] p 3191 N95-33307
Nonholonomic control of coupled spatial multibody systems p 3192 N95-33604
Human piloting factors in the design of control laws for precision landing p 3167 N95-33605
Nonlinear adaptive control of highly maneuverable high performance aircraft p 3192 N95-33712
A robust control system for exact trajectory tracking p 3192 N95-33714
Proposed incorporation of mission-oriented flying qualities into MIL-STD-1797A
[AD-A294211] p 3055 N95-34306
Non-smooth optimization algorithms, system theory and software tools
[AD-A294944] p 3183 N95-34605

CONTROL THEORY
Optimum Routeing: Analytical constraint of search space p 3044 N95-32493
Globally stable feedback laws for near-minimum-fuel and near-minimum-time pointing maneuvers for a landmark-tracking spacecraft
[DE95-009867] p 3191 N95-33214
Identification of flexible structures under closed loop control p 3192 N95-33713
A model of long term learning: Integration of knowledge acquisition and knowledge compilation
[AD-A294123] p 3235 N95-34743
A stochastic adaptive control application to flight systems p 3055 N95-34806

CONTROLLABILITY
Propulsion Controlled Aircraft design and development p 3053 N95-33022
Design challenges encountered in the F-15 PCA flight test program p 3049 N95-33025
Nonholonomic control of coupled spatial multibody systems p 3192 N95-33604
Human piloting factors in the design of control laws for precision landing p 3167 N95-33605
A robust control system for exact trajectory tracking p 3192 N95-33714

CONTROLLERS
Actively controlled shaft seals for aerospace applications
[NASA-CR-4678] p 3061 N95-33156
Design and implementation of a two-axis micromanipulator to enhance the gripper positional accuracy of a single flexible link p 3123 N95-33252
Active noise control in finite length waveguides p 3098 N95-33322
Self-organizing neural network and its applications to vision-guided robot motion coordination p 3191 N95-33324
Identification of flexible structures under closed loop control p 3192 N95-33713
Is there a role for a test controller in the development of new ATC equipment? p 3174 N95-34778

CONVECTION
Thermocapillary flow with evaporation and condensation and its effect on liquid retention in low-g fluid acquisition devices p 3109 N95-33256

CONVECTIVE HEAT TRANSFER
Analysis of a HTSC current lead under nonlinear heat transfer conditions
[DE95-009420] p 3102 N95-32714
Evaluation of conductive, radiative, chemical, and convective heat transfer in complex systems using a fast-running, implicit, lumped-capacitance formulation
[DE95-011889] p 3111 N95-33837
Flow and heat transfer in rotating curved pipes p 3040 N95-34545

CONVERGENCE
Training neural networks using sequential extended Kalman filtering
[DE95-007874] p 3187 N95-32386
Differencing the diffusion equation on unstructured meshes in 2-D
[DE95-010410] p 3195 N95-32559
Genetic algorithms as global random search methods
[NASA-CR-199088] p 3188 N95-32767
An improved algorithm for computing altitude dependent Corrected GeoMagnetic coordinates
[AD-A293967] p 3144 N95-34454
A study on the convergence of a 3-D Euler code for cascade flow calculations p 3034 N95-34508
Theory and application of homotopy techniques in nonlinear programming and control systems
[AD-A294934] p 3193 N95-34600

COOLING
Ricor K506B cryocooler performance during the Clementine mission and ground testing
[DE95-010683] p 3089 N95-32568
A possible ionization cooling experiment at the AGS
[DE95-010317] p 3205 N95-32654
Cooling tower and plume modeling for satellite remote sensing applications
[DE95-012000] p 3143 N95-33849

COOLING SYSTEMS
Enhancement of pool boiling heat transfer to lithium bromide aqueous solution
[REPT-2211] p 3091 N95-32991
The development of some kinds of LRE injectors
[AD-A294199] p 3061 N95-34302
Tri-service perspectives on microclimate cooling of protective clothing in the heat
[AD-A294005] p 3170 N95-34370
Static pressure drop by swirling flow of an internal cooling air system through a turbine shaft p 3042 N95-34560

COORDINATE TRANSFORMATIONS
Poisson's ratio for tetragonal crystals
[AD-A293544] p 3232 N95-34607
Poisson's ratio for cubic crystals
[AD-A293549] p 3232 N95-34608

COORDINATES
An improved algorithm for computing altitude dependent Corrected GeoMagnetic coordinates
[AD-A293967] p 3144 N95-34454

COPOLYMERS
Photovoltaic Manufacturing Technology (PVMaT)
[DE95-004093] p 3149 N95-33153
Polymerization of epsilon-caprolactone in the presence of OH- or COOh-groups containing initiators. Copolymers of lactide with epsilon-caprolactone: Synthesis, characterization and processing
[PB95-208211] p 3084 N95-33227
A molecular dynamics investigation of the structural characteristics of amorphous and annealed poly (Vinylidene fluoride) and vinylidene fluoride - trifluoroethylene copolymers
[AD-A294116] p 3086 N95-34502

COPPER
Irradiation experiments of low copper A533B steels for reactor pressure vessel tested in JMTR
[DE95-737266] p 3077 N95-32531
Alternative catalyst and exhaust gas sensor work at Argonne National Laboratory
[DE95-007136] p 3152 N95-32553
Numerical analysis of the ultraprecision machining of copper
[DE95-007857] p 3089 N95-32585
Intermetallic compound layer growth kinetics in non-lead bearing solders
[DE95-009595] p 3078 N95-32591
Copper-diamond composite substrates for electronic components
[DE95-011520] p 3079 N95-33063
Background meeting and technology demonstration: Chromium electroplating of superconductor strand
[DE95-011736] p 3068 N95-33070
Combining the QMR method with first principles electronic structure codes
[DE95-009927] p 3228 N95-33240
Optical anisotropy of (110) surfaces of Ag and Cu
[DE95-010130] p 3229 N95-33637
Unusual behavior in the magnetic anisotropy of ultra-thin Co sandwiches: The role of Au underlayers
[DE95-010612] p 3229 N95-33641

COPPER COMPOUNDS
NQR-NMR studies of higher alcohol synthesis Cu-Co catalysts
[DE95-010524] p 3066 N95-32557

COPPER OXIDES
Effect of the colony microstructure on transport critical current of high-J(c) Tl-1223 thick films
[DE95-013049] p 3230 N95-34213
Formation of artificially-layered high-temperature superconductors using pulsed-laser deposition
[DE95-012884] p 3231 N95-34465

CORES
Formation of high density cores in molecular cloud p 3041 N95-34553

CORONAS
General limits on the performance of high power radiators
[DE95-010732] p 3095 N95-32570

CORRECTION
SeaWiFS technical report series. Volume 31: Stray light in the SeaWiFS radiometer
[NASA-TM-104566-VOL-31] p 3159 N95-32833
Wee partons in large nuclei: From virtual dream to hard reality
[DE95-012166] p 3208 N95-33854

CORRELATION
A posteriori pointwise error estimates for the boundary element method
[DE95-008099] p 3194 N95-32388
Causal correlation of foliar biochemical concentrations with AVIRIS spectra using forced entry linear regression p 3130 N95-33744
Estimation of penetration of forest canopies by Interferometric SAR measurements p 3141 N95-33814
Fracture toughness assessment of present and future pressure vessel materials based on Charpy impact energy and yield strength
[AD-A294008] p 3081 N95-34373

CORRELATORS
Basis Image Processor Pr5210: Correlator technical description
[PB95-222485] p 3185 N95-32815

CORROSION
Corrosion of fire-damaged aircraft
[AD-A294968] p 3049 N95-34583
An investigation of the chemistry of citric acid in military soldering applications
[AD-A295042] p 3105 N95-34796
Infrared detection of chemical corrosion on metal surface
[AD-A295000] p 3081 N95-34821

CORROSION PREVENTION
Zero discharge organic coatings: Powder paint - UV curable paint - E-coat
[AD-A293573] p 3087 N95-34614

CORROSION RESISTANCE
Corrosion of separator plate constituents in molten carbonate
[PB95-214490] p 3149 N95-32813

COSMIC DUST
Characterizing the fragmentation ring on witness plates p 3056 N95-32426

COSMIC RAY SHOWERS
Time correlations between low and high energy gamma rays from discrete sources
[NASA-CR-199214] p 3248 N95-33916

COSMIC RAYS
Minutes of the 12th Joint NASA/DARA-DLR Life Sciences Program Working Group Meeting
[NASA-TM-110655] p 3161 N95-32719
Proton-induced fragmentation of carbon at energies below 100 MeV p 3161 N95-32720
Cosmic heavy ion tracks in mesoscopic biological test objects p 3163 N95-32730

COSMOLOGY
Cosmological consequences of topological and geometric phenomena in field theories p 3234 N95-33313
Lithogenic and cosmogenic tracers in catchment hydrology
[DE95-011523] p 3143 N95-33407

COST ANALYSIS
CVD diamond cost analysis update
[AD-A289990] p 3227 N95-32695
Aerospace Guidance and Metrology Center: Cost growth and other factors affect closure and privatization. Report to Congressional requesters
[GAO/NSIAD-95-60] p 3235 N95-32706
Report to the Chairman, Committee on Science, House of Representatives. NASA's Earth Observing System: Estimated funding requirements
[GAO/NSIAD-95-175] p 3142 N95-32707

COST EFFECTIVENESS
Summary report for ITER Task No. T226B: Evaluation of ITER disruption erosion
[DE95-010402] p 3219 N95-32401
NASA wide electronic publishing system: Electronic printing and duplicating. Stage 3 evaluation report
[NASA-TM-104620] p 3237 N95-32922
Cost-effective data-parallel load balancing
[DE95-010985] p 3186 N95-33403
The choice: Welding with CO2 or Nd:YAG lasers
[DE95-011825] p 3124 N95-33834

COST ESTIMATES
Space Station: Estimated total US funding requirements. Report to Congressional Requesters
[GAO/NSIAD-95-163] p 3058 N95-32884
Budget estimates: Fiscal year 1994. Volume 1: Agency summary
[NASA-TM-110815] p 3244 N95-33069
Budget estimates: Fiscal year 1994. Volume 2: Construction of facilities
[NASA-TM-110816] p 3245 N95-33081
Budget estimates: Fiscal year 1994. Volume 3: Research and program management
[NASA-TM-110817] p 3245 N95-33082

COST REDUCTION
The next generation of automobile emissions reduction: Innovative control of off-cycle emissions
[DE95-004057] p 3153 N95-32809
High-speed, low-damage grinding of advanced ceramics, phase 1
[DE95-011241] p 3085 N95-33425
The choice: Welding with CO2 or Nd:YAG lasers
[DE95-011825] p 3124 N95-33834

COSTS
Training neural networks using sequential extended Kalman filtering
[DE95-007874] p 3187 N95-32386
D3-D power supply, design, and development
[DE95-009603] p 3222 N95-32656

COUPLED MODES
Transverse multibunch instabilities for non-rigid bunches
[DE95-012098] p 3211 N95-32607

COUPLERS
A fiber-optic connector
[AD-D017424] p 3215 N95-32923
England develops world's fastest optic switch breakthrough in high-speed communications
[AD-A294038] p 3105 N95-34488

COUPLINGS
Conforming tuning coupler for flextensional transducers
[AD-D017285] p 3105 N95-34617

COVARIANCE
Using dark current data to estimate AVIRIS noise covariance and improve spectral analyses p 3129 N95-33736

CRAB NEBULA
Gamma ray imaging of the Crab and Vale regions with the UCR double-Compton telescope p 3245 N95-32837
GRO: Studies of high energy pulsars with EGRET
[NASA-CR-199130] p 3248 N95-33499

CRACK BRIDGING
Micromechanics of fiber-reinforced ceramic composites p 3063 N95-32775
Inclusion models of tensile fracture in fiber-reinforced brittle-matrix composites p 3065 N95-33721

CRACK INITIATION
Inclusion models of tensile fracture in fiber-reinforced brittle-matrix composites p 3065 N95-33721
Implications of early stages in the growth of stress corrosion cracking on component reliability
[DE95-011498] p 3127 N95-33833

CRACK OPENING DISPLACEMENT
On the expansion for surface displacement in the neighborhood of a crack tip
[DE95-012890] p 3126 N95-33222

CRACK PROPAGATION
Fatigue properties for the Al-Li alloy 2090, part 3
[PB95-214532] p 3078 N95-32614
Fracture behavior of shallow cracks in full-thickness clad beams from an RPV wall section
[DE95-009175] p 3126 N95-32684
Nitrate stress corrosion crack growth rate in plain carbon steels
[DE95-011689] p 3079 N95-32958
On the expansion for surface displacement in the neighborhood of a crack tip
[DE95-012890] p 3126 N95-33222
Enhanced stress projections for error estimation and a singular floating node element for static and dynamic fracture p 3064 N95-33463
Low velocity impact damage in carbon fiber/PEEK composite laminates
[ISBN-0-315-86546-6] p 3065 N95-33710
Microstructural studies of hydrogen damage in metastable stainless steels p 3080 N95-33774
Implications of early stages in the growth of stress corrosion cracking on component reliability
[DE95-011498] p 3127 N95-33833

CRACK TIPS
On the expansion for surface displacement in the neighborhood of a crack tip
[DE95-012890] p 3126 N95-33222
Patterns and perspectives in applied fracture mechanics
[DE95-012844] p 3127 N95-34442

CRACKING (FRACTURING)
Micromechanics of fiber-reinforced ceramic composites p 3063 N95-32775
An experimental and numerical analysis of hydrogen assisted cracking and weldability test methodology p 3079 N95-32936
Inclusion models of tensile fracture in fiber-reinforced brittle-matrix composites p 3065 N95-33721
R-curve behavior of whisker-reinforced ceramic composites
[DE95-012873] p 3087 N95-34798

CRACKS
Analytical modeling of the effect of crack depth, specimen size, and biaxial stress on the fracture toughness of reactor vessel steels
[DE95-005886] p 3125 N95-32373

Fracture behavior of shallow cracks in full-thickness clad beams from an RPV wall section
| DE95-009175 | p 3126 N95-32684
Modal identification and its applications to damage detection in vibrating structures p 3126 N95-32920
Low velocity impact damage in carbon fiber/PEEK composite laminates
| ISBN-0-315-86546-6 | p 3065 N95-33710
Microstructural studies of hydrogen damage in metastable stainless steels p 3080 N95-33774

CRASH INJURIES
Evaluation of a retrofit OH-58 pilot's seat to prevent back injury
| AD-A294895 | p 3171 N95-34574

CRASH LANDING
Evaluation of a retrofit OH-58 pilot's seat to prevent back injury
| AD-A294895 | p 3171 N95-34574

CRASHES
OH-58 pilot display unit (PDU) simulated crash tests
| AD-A294049 | p 3170 N95-34378

CRASHWORTHINESS
Evaluation of a retrofit OH-58 pilot's seat to prevent back injury
| AD-A294895 | p 3171 N95-34574

CRATERS
The structure of ion track in Solids produced by ions with high level inelastic energy losses
| DE95-620942 | p 3205 N95-32625

CRAY COMPUTERS
Simulation of hypervelocity impact on massively parallel supercomputer
| DE95-007735 | p 3184 N95-32383
Program developing environment and a CFD application on the Cray T3D p 3038 N95-34535

CREEP PROPERTIES
A numerical analysis of fracture and high temperature creep characteristics of composites with discontinuous ductile reinforcements
| DE95-010236 | p 3062 N95-32395

CREEP RUPTURE STRENGTH
Effect of heat treatment at 1,150 C on creep rupture properties of a Fe3Al-based alloy
| DE95-010295 | p 3077 N95-32527

CREEP TESTS
Effect of heat treatment at 1,150 C on creep rupture properties of a Fe3Al-based alloy
| DE95-010295 | p 3077 N95-32527

CREWS
User acceptability and comfort of the communications earplug (CEP) when used in the UH-1 helicopter
| AD-A294047 | p 3170 N95-34492

CROSS CORRELATION
Reduction and analysis of seasons 15 and 16 (1991 - 1992) Pioneer Venus radio occulation data and correlative studies with observations of the near infrared emission of Venus
| NASA-CR-199071 | p 3247 N95-32700

CROSS POLARIZATION
OPEX Second Workshop of the OLYMPUS Propagation Experimenters. Volume 2: Reference book on depolarisation
| ESA-WPP-083-VOL-2 | p 3096 N95-32748

CROSS SECTIONS
Faddeev calculations of p(mu)+p collisions: Effect of hyperfine splitting on the cross sections
| DE95-007838 | p 3203 N95-32583

CROSSINGS
Polarization and wavelength diversities of Gulf Stream fronts imaged by AIRSAR p 3140 N95-33807

CRRES (SATELLITE)
Space probe data processing
| AD-A294124 | p 3058 N95-34744

CRUISING FLIGHT
Minimum fuel mode evaluation p 3051 N95-33015

CRYOGENIC EQUIPMENT
Compression mass gauge testing in a liquid hydrogen dewar
| NASA-CR-198366 | p 3115 N95-32687
Solvent effects on the electronic spectrum of R hardt's dye
| AD-A293667 | p 3067 N95-32804
The JPL Field Emission Spectrometer p 3117 N95-33794

CRYOGENIC FLUID STORAGE
Compression mass gauge testing in a liquid hydrogen dewar
| NASA-CR-198366 | p 3115 N95-32687

CRYOGENICS
Design concept of a cryogenic distillation column cascade for a ITER scale fusion reactor
| DE95-737185 | p 3220 N95-32409
Recent results from the D3-D tokamak and implications for future devices
| DE95-009605 | p 3222 N95-32592
Analysis of a HTSC current lead under nonlinear heat transfer conditions
| DE95-009420 | p 3102 N95-32714
A final-focus magnet for PEP-2
| DE95-012372 | p 3214 N95-33504
Synthesis and characterization of a series of organoindium-phosphides including molecular structures of ((Me3CCH2)2InPEt2)2 and ((Me3CCH2)2InP(H)(C6H11))3
| AD-A293965 | p 3086 N95-34452

CRYPTOGRAPHY
Security and privacy in the NII
| AD-A293475 | p 3244 N95-34816

CRYSTAL DISLOCATIONS
Nucleation, propagation, electronic levels and elimination of misfit dislocations in 3-5 semiconductor interfaces
| DE95-011595 | p 3231 N95-34485

CRYSTAL GROWTH
Metallurgical and Materials Transactions, volume 25A, no. 9
| AD-A293622 | p 3077 N95-32474
Peak effect and flux pinning in YBa2Cu3O(7-(delta)) single crystals
| DE95-010126 | p 3228 N95-32959
Magnetostriction and thermal expansion of the Kondo semiconductor Ce3Bi4Pt3
| DE95-011975 | p 3229 N95-33386
Highly doped p-ZnTe films and quantum well structures grown by nonequilibrium pulsed laser ablation
| DE95-012885 | p 3232 N95-34799

CRYSTAL LATTICES
TEM investigation on the low temperature phase of HfV2
| DE95-009500 | p 3225 N95-32532

CRYSTAL OPTICS
X-ray standing wave interferometry-optics at 1 angstrom with applications to surface and material sciences
| DE95-009688 | p 3215 N95-32662

CRYSTAL STRUCTURE
Metallurgical and Materials Transactions, volume 25A, no. 9
| AD-A293622 | p 3077 N95-32474
TEM investigation on the low temperature phase of HfV2
| DE95-009500 | p 3225 N95-32532
Size, shape, and crystallinity of luminescent structures in oxidized Si nanoclusters and H-passivated porous Si
| DE95-012322 | p 3229 N95-33628
Charge-transfer gap closure in transition-metal halides under pressure
| DE95-011268 | p 3230 N95-33865
Formation of artificially-layered high-temperature superconductors using pulsed-laser deposition
| DE95-012884 | p 3231 N95-34465
Static displacements of atoms in crystalline metallic solid solutions
| DE95-012893 | p 3233 N95-34802

CRYSTAL SURFACES
X-ray standing wave interferometry-optics at 1 angstrom with applications to surface and material sciences
| DE95-009688 | p 3215 N95-32662

CRYSTALLINITY
Crystalline beam properties as predicted for the storage rings ASTRID and TSR
| DE95-011557 | p 3210 N95-32411
Size, shape, and crystallinity of luminescent structures in oxidized Si nanoclusters and H-passivated porous Si
| DE95-012322 | p 3229 N95-33628
Static displacements of atoms in crystalline metallic solid solutions
| DE95-012893 | p 3233 N95-34802

CRYSTALLIZATION
Supercritical crystallization: The RESs-process and the GAS-process
| PB95-214482 | p 3228 N95-33235

CRYSTALS
Sum frequency generation of dual-wavelength Nd: YAP laser in LiIO3 crystal
| AD-A293094 | p 3117 N95-32472
Multiple-beam pulse shaping and preamplification
| DE95-011738 | p 3216 N95-33651
Development of local shear bands and orientation gradients in fcc polycrystals
| DE95-012072 | p 3231 N95-34450
Growth of GaN single-crystal boules
| AD-A294976 | p 3232 N95-34588
Poisson's ratio for tetragonal crystals
| AD-A293544 | p 3232 N95-34607
Poisson's ratio for cubic crystals
| AD-A293549 | p 3232 N95-34608

CUBIC LATTICES
Poisson's ratio for cubic crystals
| AD-A293549 | p 3232 N95-34608

CUES
Everyday believability
| AD-A294938 | p 3193 N95-34602

CURING
Photovoltaic Manufacturing Technology (PVMaT)
| DE95-004093 | p 3149 N95-33153
Zero discharge organic coatings: Powder paint - UV curable paint - E-coat
| AD-A293573 | p 3087 N95-34614

CURRENT DENSITY
Peak effect and flux pinning in YBa2Cu3O(7-(delta)) single crystals
| DE95-010126 | p 3228 N95-32959
Effect of lead content on Bi-2223 formation by a two-powder process
| DE95-009889 | p 3079 N95-33215
Properties of high-T(sub c) Josephson junctions with Y(0.7)Ca(0.3)Ba2Cu3O(7-delta) barrier layers
| AD-A294852 | p 3231 N95-34568

CURVE FITTING
Tracing a planar algebraic curve
| DE95-613375 | p 3195 N95-33058
High accuracy in-flight wavelength calibration of imaging spectrometry data p 3132 N95-33750

CUTTING
Numerical analysis of the ultraprecision machining of copper
| DE95-007857 | p 3089 N95-32585
Monitoring of the cutting operations using fuzzy logic p 3189 N95-32999

CYCLES
Fatigue damage estimate comparisons for northern European and US wind farm loading environments
| DE95-011061 | p 3150 N95-33706
Corrosion of fire-damaged aircraft
| AD-A294968 | p 3049 N95-34583

CYCLIC ACCELERATORS
Studies of halo distributions under beam-beam interaction
| DE95-012560 | p 3214 N95-34024

CYCLIC LOADS
Models for predicting damage evolution in metal matrix composites subjected to cyclic loading
| DE95-007734 | p 3077 N95-32382
Operations manual for a compact electromechanical fatigue testing machine
| DSTO-GD-0036 | p 3115 N95-32927
Evaluation of high-temperature lubricant under cyclic operating conditions
| AD-A294444 | p 3086 N95-34494

CYLINDRICAL BODIES
Semi-analytic computation of the driven fields in right circular cylindrical microwave applicators
| DE95-010875 | p 3203 N95-32574
Design and operation of a thermionic converter in air
| DE95-010151 | p 3149 N95-32645
Method for making fiber-optic bundle collimator assembly
| AD-D017486 | p 3216 N95-34288

CYLINDRICAL SHELLS
Cylindrical shell buckling through strain hardening
| DE95-009545 | p 3125 N95-32392

CYSTEINE
Conversion of holes into reducing species on surface modified small-particle TiO2
| DE95-008282 | p 3225 N95-32586

D

DAMAGE
Models for predicting damage evolution in metal matrix composites subjected to cyclic loading
| DE95-007734 | p 3077 N95-32382
Ductile damage model with void coalescence
| DE95-007855 | p 3125 N95-32385
Damage formation in silicon irradiated by heavy ions with energy more than 1 MeV/a.m.u.
| DE95-623968 | p 3204 N95-32610
Microstructural studies of hydrogen damage in metastable stainless steels p 3080 N95-33774

DAMAGE ASSESSMENT
Modal identification and its applications to damage detection in vibrating structures p 3126 N95-32920
Fatigue damage estimate comparisons for northern European and US wind farm loading environments
| DE95-011061 | p 3150 N95-33706

DAMPING
Metallic laminates for engine applications
| DE95-010259 | p 3062 N95-32399
A simulation of damping process of pendulum motion due to aerodynamic forces p 3041 N95-34551

DARK MATTER
Status of the large-scale dark-matter axion search
| DE95-008828 | p 3246 N95-32597

DATA ACQUISITION
Production asymmetries in x(sub f) and P(sup 2)(sub t) for D(sup +/-) mesons
[DE95-007207] p 3201 N95-32379
SeaWiFS technical report series. Volume 15: The simulated SesWiFS data set, version 2
[NASA-TM-104566-VOL-15] p 3158 N95-32545
Data collection in IMS: It's not as easy as it looks p 3072 N95-33286
Report to the Ranking Minority Member, Committee on Government Operations, House of Representatives. Paperwork reduction: Reported burden hour increases reflect new estimates, not actual changes
[GAO/PEMD-94-3] p 3236 N95-33907
Anechoic chamber upgrade
[AD-A294375] p 3056 N95-34342
Crosspoint analog data selector
[AD-D017482] p 3104 N95-34425

DATA BASE MANAGEMENT SYSTEMS
The RDB: A parallel, spatial database for the IES/BTI system
[DE95-009425] p 3179 N95-32715
FTP-Server for exchange, interpretation, and database-search of ion mobility spectra, literature, preprints and software p 3073 N95-33291
Incorporating bibliographic information into a spatial data query system for the Savannah River Site
[DE95-010965] p 3238 N95-33402
Performance analysis of combined concurrency control and commit protocols in distributed database systems p 3238 N95-33711
An interactive environment for the analysis of large Earth observation and model data sets p 3239 N95-34219
A land-surface testbed for EOSDIS p 3158 N95-34223
System of experts for intelligent data management (SEIDAM) p 3240 N95-34226
Knowledge-based assistance for science visualization and analysis using large distributed databases p 3241 N95-34227
The Grid Analysis and Display System (GRADS): A practical tool for Earth science visualization p 3241 N95-34231
Planetary data analysis and display system: A version of PC-McIDAS p 3241 N95-34232
Development of an expert data reduction assistant p 3242 N95-34234
VIEWCACHE: An incremental pointer-based access method for autonomous interoperable databases p 3242 N95-34235
SAVS: A Space Analysis and Visualization System p 3242 N95-34238
A Spatial Analysis and Modeling System (SAMS) for environment management p 3243 N95-34239
DataHub: Science data management in support of interactive exploratory analysis p 3243 N95-34241

DATA BASES
The RHIC transfer line cable database
[DE95-011560] p 3236 N95-32412
An electronic design guideline for incorporating pollution prevention into US Department of Energy design projects
[DE95-008935] p 3151 N95-32475
Evaluated nuclear structure data file
[DE95-011343] p 3202 N95-32484
Full-scale hingeless rotor performance and loads
[NASA-TM-110356] p 3048 N95-32699
The RDB: A parallel, spatial database for the IES/BTI system
[DE95-009425] p 3179 N95-32715
Exchange, interpretation, and database-search of ion mobility spectra supported by data format JCAMP-DX p 3070 N95-33274
FTP-Server for exchange, interpretation, and database-search of ion mobility spectra, literature, preprints and software p 3073 N95-33291
The PEP-2 project-wide database
[DE95-012512] p 3213 N95-33333
Representing incomplete knowledge in relational databases p 3238 N95-33722
Evaluation of the photochemical reflectance index in AVIRIS imagery p 3131 N95-33747
Multivariate statistical analysis software technologies for astrophysical research involving large data bases p 3240 N95-34222
VIEWCACHE: An incremental pointer-based access method for autonomous interoperable databases p 3242 N95-34235
Towards friendlier user interfaces for expert systems
[AD-A294056] p 3192 N95-34467
Adaptive strategy selection for concept learning
[AD-A294086] p 3193 N95-34473
Grayling 2 information base for generation of synthetic thermal infrared scenes
[AD-A294956] p 3100 N95-34578
Towards a formalism for program generation 1995
[AD-A294941] p 3183 N95-34604

DATA COLLECTION PLATFORMS
Data collection in IMS: It's not as easy as it looks p 3072 N95-33286

DATA COMPRESSION
High performance compression of science data p 3242 N95-34237
Design and analysis of lossless and lossy data compression methods with applications to communication and caching
[AD-A295025] p 3101 N95-34790

DATA LINKS
OPEX: Second Workshop of the OLYMPUS propagation experimenters. Volume 1: Reference book on attenuation measurement and prediction
[ESA-WPP-083-VOL-1] p 3096 N95-32747

DATA MANAGEMENT
Aircraft scanner data availability via the version 0 Information Management System p 3134 N95-33762
Applied Information Systems Research Program (AISRP) Workshop 3 meeting proceedings
[NASA-CR-199103] p 3239 N95-34218
Knowledge-based assistance for science visualization and analysis using large distributed databases p 3241 N95-34227
Recoverable distributed shared memory under sequential and relaxed consistency
[AD-A293966] p 3178 N95-34453
Is the genetic algorithm a cooperative learner?
[AD-A294112] p 3193 N95-34499
Numerical and symbolic algorithms for application specific signal processing
[AD-A294125] p 3100 N95-34749

DATA PROCESSING
Visualization methods for high-resolution, transient, 3-D, finite element situations
[DE95-009479] p 3179 N95-32390
Prediction of OCR accuracy using simple image features
[DE95-009887] p 3236 N95-32471
A choice of input variables for a multilayer perceptron
[DE95-623573] p 3187 N95-32476
SeaWiFS technical report series. Volume 15: The simulated SesWiFS data set, version 2
[NASA-TM-104566-VOL-15] p 3158 N95-32545
Three-dimensional ground penetrating radar imaging using synthetic aperture time-domain focusing
[DE95-010731] p 3095 N95-32569
On the Minimum Weight Steiner Triangular Tiling Problem
[DE95-009482] p 3180 N95-32716
OPEX Second Workshop of the OLYMPUS Propagation Experimenters. Volume 5: Reference book on data processing
[ESA-WPP-083-VOL-5] p 3096 N95-32751
VHS-tape system for general purpose computer. For next generation mass storage system
[DE95-737268] p 3177 N95-32757
Operational equations for three-dimensional data
[DE95-011332] p 3196 N95-33248
Mapping target signatures via partial unmixing of AVIRIS data p 3129 N95-33737
New calibration techniques for the Airborne Visible/Infrared Imaging Spectrometer (AVIRIS) p 3116 N95-33740
An interactive environment for the analysis of large Earth observation and model data sets p 3239 N95-34219
Knowledge-based assistance for science visualization and analysis using large distributed databases p 3241 N95-34227
Experimenter's laboratory for visualized interactive science p 3184 N95-34228
Planetary data analysis and display system: A version of PC-McIDAS p 3241 N95-34232
Advanced data visualization and sensor fusion: Conversion of techniques from medical imaging to Earth science p 3242 N95-34236
SAVS: A Space Analysis and Visualization System p 3242 N95-34238
Reducing cache misses in numerical applications using data relocation and prefetching
[AD-A293978] p 3182 N95-34455
Optical interconnects for 3D computer architectures
[AD-A294118] p 3178 N95-34503
Space probe data processing
[AD-A294124] p 3058 N95-34744

DATA PROCESSING EQUIPMENT
Space probe data processing
[AD-A294124] p 3058 N95-34744

DATA RECORDERS
Solid-state data recorder, next development and use p 3094 N95-33143

DATA REDUCTION
Annual report to Congress 1994: Energy Information Administration
[DE95-011240] p 3237 N95-32482
Reduction and analysis of seasons 15 and 16 (1991 - 1992) Pioneer Venus radio occulation data and correlative studies with observations of the near infrared emission of Venus
[NASA-CR-199071] p 3247 N95-32700
FORTRAN program for analyzing ground-based radar data: Usage and derivations, version 6.2
[NASA-TP-3430] p 3181 N95-33193
Third International Workshop on Ion Mobility Spectrometry
[NASA-CP-3301] p 3069 N95-33265
Development of an expert data reduction assistant p 3242 N95-34234

DATA SIMULATION
Application of deformable templates for recognizing tracks detected with High Pressure Drift Tubes
[DE95-621870] p 3188 N95-32627

DATA STORAGE
Arbitrary waveform generator
[AD-D017451] p 3097 N95-32925
An interactive environment for the analysis of large Earth observation and model data sets p 3239 N95-34219
High performance compression of science data p 3242 N95-34237

DATA STRUCTURES
Visualization methods for high-resolution, transient, 3-D, finite element situations
[DE95-009479] p 3179 N95-32390
An efficient inference engine for interactive fault diagnosis in a helpdesk application p 3189 N95-33000
Induction of dependency structures from data and its application to ozone prediction p 3190 N95-33003
An object-oriented decomposition of the adaptive-hp finite element method
[DE95-012142] p 3186 N95-33852
Towards a formalism for program generation 1995
[AD-A294941] p 3183 N95-34604

DATA SYSTEMS
The PEP-2 project-wide database
[DE95-012512] p 3213 N95-33333
Aircraft scanner data availability via the version 0 Information Management System p 3134 N95-33762
A distributed system for visualizing and analyzing multivariate and multidisciplinary data p 3241 N95-34230
A Spatial Analysis and Modeling System (SAMS) for environment management p 3243 N95-34239

DATA TRANSMISSION
Visualization of parallel molecular dynamics simulation on a remote visualization platform
[DE95-007806] p 3185 N95-32582
VHS-tape system for general purpose computer. For next generation mass storage system
[DE95-737268] p 3177 N95-32757
The design of scalable software libraries for distributed memory concurrent computers
[DE95-012891] p 3244 N95-34801

DAYTIME
SIRPH: Steerable infrared picture on helmet mounted display p 3045 N95-32504

DEACTIVATION
Inactivation, DNA double strand break induction and their rejoining in bacterial cells irradiated with heavy ions p 3161 N95-32724
DNA-DSB in CHO-K1 cells induced by heavy-ions: Break rejoining and residual damage (GSI) p 3162 N95-32725
Heavy ion action on single cells: Cellular inactivation capability of single accelerated heavy ions p 3162 N95-32729

DEATH VALLEY (CA)
Integration of AIRSAR and AVIRIS data for Trail Canyon alluvial fan, Death Valley, California p 3134 N95-33760

DEBONDING (MATERIALS)
Fiber coatings for brittle matrix composites p 3065 N95-34808

DEBRIS
Simulation of hypervelocity impact on massively parallel supercomputer
[DE95-007735] p 3184 N95-32383

DECAY
Improved L-C resonant decay technique for Q measurement of quasilinear power inductors: New results for MPP and ferrite powdered cores
[NASA-CR-198373] p 3103 N95-33874

DECAY RATES
Vacuum polarization correction to the positronium decay rate
[DE95-614164] p 3202 N95-32481

Mean lifetime measurements of (3)He(4)He2+
[DE95-010813] p 3209 N95-34355

DECELERATION
Rapid deceleration mode evaluation
p 3052 N95-33018

DECISION MAKING
Approaches to implementing deterministic models in a probabilistic framework
[DE95-009483] p 3197 N95-32391
The background and theory of integrated risk management p 3236 N95-32431
An electronic design guideline for incorporating pollution prevention into US Department of Energy design projects
[DE95-008935] p 3151 N95-32475
Report to the Chairman, Subcommittee on Aviation, Committee on Commerce, Science, and Transportation, US Senate. Aviation safety: Data problems threaten FAA strides on safety analysis system
[GAO/AIMD-95-27] p 3046 N95-32705
Speaker identification using the two-dimensional cepstrum transform
[AD-A294204] p 3099 N95-34304
Focus of attention in decision support systems
[AD-A294037] p 3236 N95-34487
Control of initialization bias in queueing simulations using queueing approximations
[AD-A294121] p 3194 N95-34742
A model of long term learning: Integration of knowledge acquisition and knowledge compilation
[AD-A294123] p 3235 N95-34743

DECISION THEORY
An original numerical method for autonomous navigation p 3044 N95-32495
A methodology for evaluating air pollution strategies to improve the air quality in Mexico City
[DE95-010874] p 3152 N95-32573
Adaptive strategy selection for concept learning
[AD-A294086] p 3193 N95-34473
Improving the comprehensibility, accuracy, and generality of reactive plans
[AD-A294104] p 3193 N95-34495
Explanations of empirically derived reactive plans
[AD-A294114] p 3193 N95-34501

DECOMPOSITION
Prospect redux p 3133 N95-33758
An object-oriented decomposition of the adaptive-hp finite element method
[DE95-012142] p 3186 N95-33852
Image compression scheme for network transmission
[AD-A294959] p 3182 N95-34580

DECONTAMINATION
Energy and Technology Review
[DE95-011686] p 3223 N95-33066

DECOUPLING
The effect and correction of coupling generated by the RHIC triplet quadrupoles
[DE95-011562] p 3210 N95-32413

DEEP WATER
Design of deepwater pipelines
[PB95-215109] p 3095 N95-33244
An experimental study of collective sea state modes of deep water surface gravity waves
[AD-A294007] p 3160 N95-34372

DEFECTS
Smoothing during ion-assisted growth by transient ion beam-induced defects
[DE95-011021] p 3225 N95-32579
Printability of substrate and absorber defects on extreme ultraviolet lithographic masks
[DE95-010916] p 3084 N95-33247
The interaction of vortices with twin boundaries
[DE95-012079] p 3110 N95-33389
Measurement and modelling of structure sensitive magnetic properties of material
[DE95-010128] p 3080 N95-33699
Microwave nondestructive evaluation: State-of-the-Art review
[AD-A294388] p 3125 N95-34346
Nucleation, propagation, electronic levels and elimination of misfit dislocations in 3-5 semiconductor interfaces
[DE95-011595] p 3231 N95-34485

DEFENSE PROGRAM
Air force office of scientific research. Research proposal
[AD-A293401] p 3252 N95-32473

DEFLAGRATION
Investigation on deflagration to detonation transition in porous energetic materials
[DE95-011638] p 3088 N95-32605

DEFLECTION
Using photothermal deflection techniques for studying the attenuations of guided waves propagated in optical thin films
[AD-A294203] p 3217 N95-34303

DEFLECTORS
High-resolution TeO2 acousto-optical deflector for millimeter-wave spectrometer
[AD-A293054] p 3215 N95-32701

DEFLUORINATION
Elemental fluorine based syntheses of pentafluoro phenyl and other aromatic perfluoropolyether polymers
[AD-A294930] p 3087 N95-34596

DEFORMATION
Simulation of hypervelocity impact on massively parallel supercomputer
[DE95-007735] p 3184 N95-32383
On the feasibility of using smoothed particle hydrodynamics for underwater explosion calculations
[DE95-008799] p 3106 N95-32587
Application of deformable templates for recognizing tracks detected with High Pressure Drift Tubes
[DE95-621870] p 3188 N95-32627
Associative integral formulas and deformations of Yangians
[PB95-212189] p 3195 N95-32889
Near-limit drop deformation and secondary breakup
p 3107 N95-32902
Analysis and design methodology for chordwise deformable wings p 3049 N95-33311
Interlaminar stress analysis of dropped-ply laminated plates and shells by a mixed method
p 3064 N95-33327
Development of local shear bands and orientation gradients in fcc polycrystals
[DE95-012072] p 3231 N95-34450
Grid generation around airfoil with a flap using boundary element method p 3041 N95-34552

DEGASSING
Apparatus for injection molding high-viscosity materials
[AD-D017471] p 3065 N95-34448

DEGRADATION
Ramp-rate sensitivity of SSC dipole magnet prototypes
[DE95-011162] p 3214 N95-33720
Self stressing test structure cells
[AD-A294386] p 3104 N95-34345
Everyday believability
[AD-A294938] p 3193 N95-34602

DEGREES OF FREEDOM
Evaluation of a bridge using simplified element modeling
[DE95-006281] p 3126 N95-32670

DELAMINATING
A new approach to fracture of layered fibrous composites: Experiments and analysis
p 3063 N95-33309
Low velocity impact damage in carbon fiber/PEEK composite laminates
[ISBN-0-315-86546-6] p 3065 N95-33710

DELTA WINGS
Calculation for aerodynamic characteristics on delta wing with leading-edge separated vortex effect using boundary element method p 3037 N95-34524
Sidewall-effect of the wind tunnel on the estimation of the aerodynamic characteristics of a delta wing
p 3037 N95-34525

DENSIFICATION
In situ ion-beam analysis and modification of sol-gel zirconia thin films
[DE95-010994] p 3203 N95-32577

DENSITY MEASUREMENT
Image analysis used to count and measure etched tracks from ionizing radiation p 3210 N95-32424

DEOXYRIBONUCLEIC ACID
Minutes of the 12th Joint NASA/DARA-DLR Life Sciences Program Working Group Meeting
[NASA-TM-110655] p 3161 N95-32719
Heavy ion induced DNA-DSB in yeast and mammalian cells p 3161 N95-32723
Inactivation, DNA double strand break induction and their rejoining in bacterial cells irradiated with heavy ions
p 3161 N95-32724
DNA-DSB in CHO-K1 cells induced by heavy-ions: Break rejoining and residual damage (GSI)
p 3162 N95-32725
Chromosomal damage observed in first postirradiation metaphases of repair-proficient and -deficient cell lines
p 3162 N95-32726
Heavy ion induced mutations in mammalian cells: Cross sections and molecular analysis p 3162 N95-32728
Toxin-mediated transfer and expression of genes in nerve cells
[AD-A290501] p 3164 N95-33200

DEPENDENCE
Velocity dependence of ionization and excitation of hydrogen molecules by fast proton impact
[DE95-010818] p 3207 N95-33370

DEPLOYMENT
Report to the Chairman, Committee on Armed Services, US Senate. Strategic Bomber: Issues relating to the B-1B's availability and ability to perform conventional missions
[GAO/NSIAD-94-81] p 3198 N95-33263
Development of High Spectral Resolution Lidar (HSRL) technology
[DE95-011906] p 3099 N95-33839

DEPOLARIZATION
OPEX Second Workshop of the OLYMPUS Propagation Experimenters. Volume 2: Reference book on depolarisation
[ESA-WPP-083-VOL-2] p 3096 N95-32748
Development of High Spectral Resolution Lidar (HSRL) technology
[DE95-011906] p 3099 N95-33839

DEPOSITION
Background meeting and technology demonstration: Chromium electroplating of superconductor strand
[DE95-011736] p 3068 N95-33070
Low temperature growth of thin films by high kinetic energy supersonic molecular beams
[AD-A294516] p 3086 N95-34476
Fundamental surface chemistry of GaAs OMVPE
[DE95-011606] p 3231 N95-34486

DEPTH
Analytical modeling of the effect of crack depth, specimen size, and biaxial stress on the fracture toughness of reactor vessel steels
[DE95-005886] p 3125 N95-32373

DEPTH MEASUREMENT
N-15 hydrogen profiling of IC metallizations
[DE95-011052] p 3102 N95-32708

DERIVATION
Thermal rearrangement of oxygen-containing (omicron)-allyltoluene derivatives
[DE95-010124] p 3067 N95-32641

DESCENT TRAJECTORIES
Implementation of a Single-Stage-To-Orbit (SSTO) model for stability and control analysis
p 3059 N95-32432

DESERTIFICATION
Use of AIRSAR to identify woody shrub invasion and other indicators of desertification in the Jornada LTER
p 3141 N95-33810

DESERTS
Aerolian erosion, transport, and deposition of volcaniclastic sands among the shifting sand dunes, Christmas Lake Valley, Oregon: TIMS image analysis
p 3137 N95-33793

DESIGN ANALYSIS
Functional requirements analysis and human machine interface specifications for handheld metal detector wands
[DE95-009845] p 3167 N95-32535
Open architecture CNC system
[DE95-009485] p 3177 N95-32955
Sea wave parameters, small altitudes and distances measurers design for movement control systems of ships, wing-in-surface effect crafts and seaplanes
p 3094 N95-33141
Design of deepwater pipelines
[PB95-215109] p 3095 N95-33244
Engineering approaches and compromises in the design of small ion mobility spectrometers
p 3070 N95-33271
Design and analysis of transient nonlinear coupled systems p 3199 N95-33292
The PEP-2 project-wide database
[DE95-012512] p 3213 N95-33333
Bicriteria network design problems
[DE95-012052] p 3099 N95-33387
Design rules and reality check for carbon-based ultracapacitors
[DE95-010575] p 3103 N95-33640
Hardware implementation of a desktop supercomputer for high performance image processing
[AD-A294272] p 3178 N95-34462

DETECTION
Low-level data fusion for landing runways detection
p 3048 N95-33136
Determination of Benzene, Toluene, and Xylene by means of an ion mobility spectrometer device using photoionization p 3069 N95-33269
IMS R and D program at Canada customs
p 3070 N95-33273
The use of ion mobility spectrometry and gas chromatography/mass spectrometry for the detection of illicit drugs on clandestine records p 3070 N95-33276
Gas chromatography/ion mobility spectrometry as a hyphenated technique for improved explosives detection and analysis p 3071 N95-33278
A novel approach to increasing cocaine detection confidence utilizing ion mobility spectrometry
p 3072 N95-33283

Application of the ionscan for the detection of methamphetamine and ephedrine in abondoned clandestine laboratories p 3072 N95-33284
IMS software developments for the detection of chemical warfare agent p 3072 N95-33287
A fiber optic strain measurement and quench localization for use in superconducting accelerator dipole magnets
[DE95-012370] p 3215 N95-33381

DETECTORS
The development of a large-area chemical sensor: A new platform for selective coatings
[DE95-011489] p 3075 N95-33832

DETERGENTS
Foam spread experiments on a water surface
[PB95-211025] p 3083 N95-32962

DETERMINANTS
Noninvasive determination of Cardiac Output
[PB95-208310] p 3164 N95-32611

DETONABLE GAS MIXTURES
Investigation of starting and ignition transients in the thermally choked ram accelerator p 3054 N95-34805

DETONATION
Investigation on deflagration to detonation transition in porous energetic materials
[DE95-011638] p 3088 N95-32605
Investigation of starting and ignition transients in the thermally choked ram accelerator p 3054 N95-34805

DETONATION WAVES
Historical detection of atmospheric impacts by large bolides using acoustic-gravity waves
[DE95-010864] p 3246 N95-33211

DEUTERIUM COMPOUNDS
Inertial confinement fusion target component fabrication and technology development support
[DE95-011655] p 3224 N95-34436

DEUTERONS
On application of wavelet analysis to separation of secondary particles from nucleus-nucleus interactions
[DE95-623572] p 3205 N95-32630

DIAGNOSIS
An efficient inference engine for interactive fault diagnosis in a helpdesk application
p 3189 N95-33000
Diagnosis of frontogenesis of Meiyu front
[AD-A294043] p 3158 N95-34491
Managing technological change in a military treatment facility: A case study of medical diagnostic imaging support (MDIS) system
[AD-A294894] p 3165 N95-34573

DIAMAGNETISM
The effect of collisionality and diamagnetism on the plasma dynamo
[DE95-012409] p 3223 N95-33221

DIAMINES
Proton affinity determinations and proton-bound dimer structure indications in C2 to C15, (alpha),(omega)-alkyldiamines p 3069 N95-33266

DIAMOND FILMS
CVD diamond cost analysis update
[AD-A289990] p 3227 N95-32695
In situ surface roughness measurement during PECVD diamond film growth
[DE95-013411] p 3230 N95-34215
Development of thin film diamond based integrated circuit technology
[AD-A294519] p 3231 N95-34478
Surface chemistry of diamond single crystals
[AD-A294150] p 3232 N95-34755

DIAMONDS
Numerical analysis of the ultraprecision machining of copper
[DE95-007857] p 3089 N95-32585
The structure of ion track in Solids produced by ions with high level inelastic energy losses
[DE95-620942] p 3205 N95-32625
CVD diamond cost analysis update
[AD-A289990] p 3227 N95-32695
Copper-diamond composite substrates for electronic components
[DE95-011520] p 3079 N95-33063
Diamond multilayer multichip module substrate
[AD-D017468] p 3104 N95-34445
Surface chemistry of diamond single crystals
[AD-A294150] p 3232 N95-34755

DICHROISM
Theory of magneto-optics and circular magnetic x-ray dichroism
[DE95-010129] p 3080 N95-33700

DIELECTRIC PROPERTIES
Microwave nondestructive evaluation: State-of-the-Art review
[AD-A294388] p 3125 N95-34346

DIELECTRICS
Diamond multilayer multichip module substrate
[AD-D017468] p 3104 N95-34445
Novel ferroelectric heterostructures for high-density DRAMS
[AD-A294517] p 3199 N95-34477

DIESEL ENGINES
Ignition and early soot formation in a DI diesel engine using multiple 2-D imaging diagnostics
[DE95-010692] p 3122 N95-32863
The effects of high ambient density on diesel spray penetration and spread
[DE95-010761] p 3124 N95-33701
Evaluation of high-temperature lubricant under cyclic operating conditions
[AD-A294444] p 3086 N95-34494

DIETHYL HYDROGEN PHOSPHITE (DEHP)
Phthalic acid esters used as plastic additives. Volume 1: Ecotoxicological risk assessment. Volume 2: Comparisons of toxicological effects
[PB95-211280] p 3084 N95-33329

DIFFERENTIAL EQUATIONS
Numerical solution of differential equations by artificial neural networks p 3194 N95-32434
Sum of fractional derivatives and m-accretive operators
[PB95-215307] p 3195 N95-32893
Modeling and inference with fractional Brownian motion and fractional Gaussian noise p 3199 N95-33415

DIFFRACTION
Doppleron resonances in the diffraction of atoms by an evanescent field
[DE95-619190] p 3204 N95-32622

DIFFRACTION PROPAGATION
Propagation of spatial solitons generated by Gaussian beams in a non-linear Kerr medium
[IFTR-9/1995] p 3206 N95-32921

DIFFRACTIVE OPTICS
Integration of diffractive lenses with addressable vertical-cavity laser arrays
[DE95-009850] p 3118 N95-32663

DIFFUSION
Differencing the diffusion equation on unstructured meshes in 2-D
[DE95-010410] p 3195 N95-32559
Conversion of holes into reducing species on surface modified small-particle TiO2
[DE95-008282] p 3225 N95-32586
Growth of GaN single-crystal boules
[AD-A294976] p 3232 N95-34588

DIFFUSION FLAMES
Study on turbulent fluctuations in diffusion flames using laser induced fluorescence
[PB95-214425] p 3068 N95-32812
Numerical study on stabilization of a diffusion flame over a flat plate p 3035 N95-34510

DIFFUSION WELDING
Development and trial manufacturing of 1/2-scale partial mock-up of blanket box structure for fusion experimental reactor
[DE95-737184] p 3219 N95-32408

DIGITAL COMPUTERS
Numerical solution of differential equations by artificial neural networks p 3194 N95-32434
Multi-layer holographic bifurcative neural network system for real-time adaptive EOS data analysis
p 3148 N95-34233
Programmable real-time optoelectronic hybrid threshold logic processors
[AD-A294067] p 3104 N95-34379

DIGITAL DATA
Use of TOPSAR digital elevation data to determine the 3-dimensional shape of an alluvial fan
p 3139 N95-33804

DIGITAL ELECTRONICS
Novel field effect transistors for low power electronics
[AD-A294221] p 3105 N95-34458

DIGITAL INTEGRATORS
A digital boxcar integrator for IMS spectra
p 3072 N95-33288

DIGITAL SYSTEMS
RASSP benchmark 1 technical description. Revision 1
[AD-A293030] p 3096 N95-32773
An Electronic Workshop on the Performance Seeking Control and Propulsion Controlled Aircraft Results of the F-15 Highly Integrated Digital Electronic Control Flight Research Program
[NASA-TM-104278] p 3050 N95-33009
An overview of integrated flight-propulsion controls flight research on the NASA F-15 research airplane
p 3051 N95-33010
Performance seeking control program overview
p 3051 N95-33011
Formal verification of an avionics microprocessor
[NASA-CR-4682] p 3181 N95-33396
Popov theory based approach to digital H(infinity)-control with measurement-feedback for Pritchard-Salamon systems
[PB95-218111] p 3192 N95-33399
Novel field effect transistors for low power electronics
[AD-A294221] p 3105 N95-34458

DIGITAL TECHNIQUES
IMS R and D program at Canada customs
p 3070 N95-33273
A curriculum for strategy in the information age: Chaos in a new era
[AD-A295036] p 3244 N95-34794

DIGITAL TO ANALOG CONVERTERS
Arbitrary waveform generator
[AD-D017451] p 3097 N95-32925

DIMENSIONAL MEASUREMENT
Cosmic heavy ion tracks in mesoscopic biological test objects p 3163 N95-32730

DIMENSIONLESS NUMBERS
Near-limit drop deformation and secondary breakup
p 3107 N95-32902
Multilayer thermoelectric films: A strategy for the enhancement of ZT
[DE95-011535] p 3081 N95-34482

DIMERS
Proton affinity determinations and proton-bound dimer structure indications in C2 to C15, (alpha),(omega)-alkyldiamines p 3069 N95-33266

DIODES
COBRA accelerator for Sandia ICF diode research at Cornell University
[DE95-011018] p 3101 N95-32578

DIPHENYL COMPOUNDS
Risk assessment of polybrominated diphenyl ethers
[PB95-211306] p 3073 N95-33330

DIRAC EQUATION
General-covariant Quantum Mechanics of Dirac particle in curved space-times
[DE95-623600] p 3233 N95-32478

DIRECT CURRENT
Channel equalized DC squid flux-locked loop
[AD-D017469] p 3104 N95-34446
A 30-pair thin film thermoelectric pile
[AD-A294058] p 3151 N95-34468

DIRECTIONAL CONTROL
Control of the laser beam irradiation intensity distribution using aspherical multi lens array and edge-shaped plates
[REPT-2209] p 3090 N95-32989
Sea wave parameters, small altitudes and distances measurers design for movement control systems of ships, wing-in-surface effect crafts and seaplanes
p 3094 N95-33141

DIRECTIVITY
Fan noise prediction assessment
[NASA-CR-195051] p 3200 N95-33831

DISCONTINUITY
A flux splitting scheme with high-resolution and robustness for discontinuities p 3036 N95-34518

DISCRIMINATION
Using foreground/background analysis to determine leaf and canopy chemistry p 3135 N95-33765

DISKS
Sinuous oscillations and steady warps of polytropic disks
[DE95-013473] p 3247 N95-34216
Fluid dynamometer having fluid characteristic power absorption adjustment capability
[AD-D017489] p 3116 N95-34426

DISPLACEMENT
An application of mechanical leverage to microactuation
[DE95-011883] p 3124 N95-33836

DISPLAY DEVICES
An approach to sensor data fusion for flying and landing aid purpose p 3043 N95-32488
Multispectral image correlation for air-to-ground targeting p 3043 N95-32489
A helmet mounted display for night missions at low altitude p 3045 N95-32503
Magnetostriction and thermal expansion of the Kondo semiconductor Ce3Bi4Pt3
[DE95-011975] p 3229 N95-33386
A land-surface testbed for EOSDIS
p 3158 N95-34223
The Grid Analysis and Display System (GRADS): A practical tool for Earth science visualization
p 3241 N95-34231
Planetary data analysis and display system: A version of PC-McIDAS p 3241 N95-34232
SAVS: A Space Analysis and Visualization System
p 3242 N95-34238
A distributed analysis and visualization system for model and observational data p 3243 N95-34240
OH-58 pilot display unit (PDU) simulated crash tests
[AD-A294049] p 3170 N95-34378
The effects of display location and dimensionality on taxiway navigation
[AD-A294878] p 3047 N95-34570

Towards a formalism for program generation 1995
[AD-A294941] p 3183 N95-34604
Resource document for the design of electronic instrument approach procedure displays
[AD-A295108] p 3047 N95-34797

DISRUPTING
Fusion Safety Program annual report, fiscal year 1994
[DE95-008872] p 3221 N95-32588

DISSIPATION
Laminar heat transfer for power-law fluids in thermal entrance region of annular sector ducts
p 3108 N95-33255
Cooling tower and plume modeling for satellite remote sensing applications
[DE95-012000] p 3143 N95-33849

DISSOLVING
Solubility behavior of quartz and corundum in supercritical water: A quantitative thermodynamic interpretation
[DE95-012294] p 3234 N95-34211
The relationship of chemical structure to supercritical-fluid solubility and to cosolvent-modifier properties: A literature review
[AD-A294933] p 3076 N95-34599

DISTANCE
Sea wave parameters, small altitudes and distances measurers design for movement control systems of ships, wing-in-surface effect crafts and seaplanes
p 3094 N95-33141

DISTILLATION
Design concept of a cryogenic distillation column cascade for a ITER scale fusion reactor
[DE95-737185] p 3220 N95-32409
The method of model-based reasoning and application of an intelligent adaptive observer on the integrated process p 3190 N95-33005
Testing of a carpet catalyst
[PB95-208492] p 3068 N95-33242

DISTORTION
A code to compute the action-angle transformation for a particle in an abritrary potential well
[DE95-012554] p 3098 N95-33336

DISTRIBUTED PROCESSING
Distributed shared memory for new generation networks
[AD-A293722] p 3185 N95-32580
Visualization of parallel molecular dynamics simulation on a remote visualization platform
[DE95-007806] p 3185 N95-32582
Incorporating distributed problem solving technique into a case-based system p 3188 N95-32997
Performance analysis of combined concurrency control and commit protocols in distributed database systems
p 3238 N95-33711
A distributed system for visualizing and analyzing multivariate and multidisciplinary data
p 3241 N95-34230
The Grid Analysis and Display System (GRADS): A practical tool for Earth science visualization
p 3241 N95-34231
A distributed analysis and visualization system for model and observational data p 3243 N95-34240
DataHub: Science data management in support of interactive exploratory analysis p 3243 N95-34241
A distributed Clips implementation: dClips
p 3243 N95-34243
Recoverable distributed shared memory under sequential and relaxed consistency
[AD-A293966] p 3178 N95-34453
Experiences using DCE and CORBA to build tools for creating highly-available distributed systems
[AD-A294973] p 3187 N95-34587
The design of scalable software libraries for distributed memory concurrent computers
[DE95-012891] p 3244 N95-34801
The development of a distributed computing environment for the design and modeling of plasma spectroscopy experiments
[DE95-011725] p 3183 N95-34813

DISTRIBUTION FUNCTIONS
Production asymmetries in x(sub f) and P(sup 2)(sub t) for D(sup +/-) mesons
[DE95-007207] p 3201 N95-32379
Hadron distributions at higher rapidity using the BRAHMS forward spectrometer
[DE95-008861] p 3207 N95-33203
Wee partons in large nuclei: From virtual dream to hard reality
[DE95-012168] p 3208 N95-33654

DIURNAL VARIATIONS
Analyses and forecasts with LAWS winds
[NASA-CR-199134] p 3157 N95-32933

DIVERTERS
Summary report for ITER Task No. T226B: Evaluation of ITER disruption erosion
[DE95-010402] p 3219 N95-32401
Experimental study of the processes in the expander of the axisymmetric mirror device
[DE95-009846] p 3221 N95-32536
Recent results from the D3-D tokamak and implications for future devices
[DE95-009605] p 3222 N95-32592
Drag measurements of an axisymmetric nacelle mounted on a flat plate at supersonic speeds
[NASA-TM-4660] p 3034 N95-32821

DIVIDING (MATHEMATICS)
Bit-level analysis of an SRT divider circuit
[AD-A294842] p 3105 N95-34565

DIVING (UNDERWATER)
Density, heat capacity, viscosity, and thermal conductivity of mixtures of CO2, He, H2, H2O, N2, and O2
[AD-A288731] p 3076 N95-34814

DOCUMENTATION
The use of ion mobility spectrometry and gas chromatography/mass spectrometry for the detection of illicit drugs on clandestine records p 3070 N95-33276

DOCUMENTS
A document analysis system p 3244 N95-34804

DOMAINS
A relational metric, its application to domain analysis, and an example analysis and model of a remote sensing domain
[NASA-TM-110358] p 3198 N95-33875
Development of local shear bands and orientation gradients in fcc polycrystals
[DE95-012072] p 3231 N95-34450

DOPED CRYSTALS
Synchrotron radiation studies of local structure and bonding in transition metal aluminides and rare earth transition metal magnetic nitrides
[DE95-011579] p 3079 N95-33065
Crystalline-as-deposited CaGa2S4: Ce via low-temperature metal-organic chemical vapor deposition
[DE95-010883] p 3229 N95-33401
Optical pulse generation using fiber lasers and integrated optics
[DE95-011517] p 3216 N95-33506
Efficient pockel's modulators in optical fibers
[AD-A294009] p 3217 N95-34374
Highly doped p-ZnTe films and quantum well structures grown by nonequilibrium pulsed laser ablation
[DE95-012885] p 3232 N95-34799

DOPPLER EFFECT
A dual, parallel cavity Fabry-Perot interferometer
[DE95-010796] p 3115 N95-32900

DOSAGE
High resistivity InAlN by nitrogen or oxygen implantation
[DE95-011023] p 3226 N95-32594
Multimedia Environmental Pollutant Assessment System (MEPAS(trademark)): Exposure pathway and human health impact assessment models
[DE95-012763] p 3155 N95-34441

DOSIMETERS
Dosimetry of heavy ions by use of CCD detectors
p 3161 N95-32721

DRAG
Historical detection of atmospheric impacts by large bolides using acoustic-gravity waves
[DE95-010864] p 3246 N95-33211

DREAMS
Wee partons in large nuclei: From virtual dream to hard reality
[DE95-012168] p 3208 N95-33854

DRIFT RATE
Electron and hole transport in compound semiconductors
[AD-A295003] p 3233 N95-34822

DROP SIZE
Investigation of water droplet trajectories within the NASA icing research tunnel
[NASA-TM-107023] p 3034 N95-32769
Near-limit drop deformation and secondary breakup
p 3107 N95-32902
Cooling tower and plume modeling for satellite remote sensing applications
[DE95-012000] p 3143 N95-33849

DROPS (LIQUIDS)
Investigation of water droplet trajectories within the NASA icing research tunnel
[NASA-TM-107023] p 3034 N95-32769
Near-limit drop deformation and secondary breakup
p 3107 N95-32902

DROUGHT
Intra-annual and inter-annual rainfall variability over East Asia, Southeast Asia, and South Asia
[AD-A294156] p 3158 N95-34757

DRUGS
IMS R and D program at Canada customs
p 3070 N95-33273
The use of ion mobility spectrometry and gas chromatography/mass spectrometry for the detection of illicit drugs on clandestine records p 3070 N95-33276
Application of Ion Mobility Spectrometry (IMS) in forensic chemistry and toxicology with focus on biological matrices p 3072 N95-33285
Parallel molecular dynamics: Communication requirements for massively parallel machines
[DE95-012948] p 3209 N95-34212

DRYING
Solving widespread low-concentration VOC air pollution problems: Gas-phase photocatalytic oxidation answers the needs of many small businesses
[DE95-004059] p 3152 N95-32668
Spontaneous dewetting of a perfluoropolyether
[NASA-TM-106964] p 3083 N95-32919

DUCTED FLOW
Flow and heat transfer behavior of non-Newtonian fluids in rectangular ducts p 3107 N95-32907
Transport phenomena in subsonic and supersonic flows in a duct with mass injection p 3108 N95-32934
Laminar heat transfer for power-law fluids in thermal entrance region of annular sector ducts
p 3108 N95-33255

DUCTILITY
Ductile damage model with void coalescence
[DE95-007855] p 3125 N95-32385
A numerical analysis of fracture and high temperature creep characteristics of composites with discontinuous ductile reinforcements
[DE95-010236] p 3062 N95-32395
Strength, ductility, and fracture mode of ternary FeAl alloys
[DE95-010281] p 3077 N95-32400

DUFFING DIFFERENTIAL EQUATION
Numerical solution of differential equations by artificial neural networks p 3194 N95-32434

DUNES
Preliminary study of Kelso Dunes using AVIRIS, TM, and AIRSAR p 3136 N95-33773
Aerolian erosion, transport, and deposition of volcaniclastic sands among the shifting sand dunes, Christmas Lake Valley, Oregon: TIMS image analysis
p 3137 N95-33793

DUST
The mini-CIDEX GC/IMS: Analysis of cometary ice and dust p 3069 N95-33270
Ignition and combustion of cellulosic dust particles
p 3073 N95-33308

DWARF STARS
High speed variability in x-ray binary systems
[AD-A294634] p 3247 N95-34561

DYE LASERS
A multi-wavelength dye laser system
[AD-A294068] p 3119 N95-34380
Indium mono-ion oscillator
[AD-A293736] p 3104 N95-34451
Pulsed tunable narrow-bandwidth dye laser, with hollow circular waveguide in cavity
[AD-A294060] p 3120 N95-34469

DYES
Solvent effects on the electronic spectrum of R hardt's dye
[AD-A293667] p 3067 N95-32804

DYNAMIC CHARACTERISTICS
Evaluation of a bridge using simplified element modeling
[DE95-006281] p 3126 N95-32670

DYNAMIC CONTROL
Self-organizing neural network and its applications to vision-guided robot motion coordination
p 3191 N95-33324
Nonholonomic control of coupled spatial multibody systems p 3192 N95-33604
Trajectory planning and control of kinematically redundant robotic manipulators p 3194 N95-34807

DYNAMIC LOADS
The role of dynamic experimentation for computation analysis
[DE95-007733] p 3125 N95-32381
Application of impact dampers in vibration control of flexible structures p 3127 N95-32420
Evaluation of a bridge using simplified element modeling
[DE95-006281] p 3126 N95-32670

DYNAMIC MODELS
Certification of a hybrid parameter model of the fully flexible Shuttle Remote Manipulator System
p 3125 N95-32421
Influence of backup bearings and support structure dynamics on the behavior of rotors with active supports
[NASA-CR-199080] p 3121 N95-32689
Steady-state dynamic behavior of an auxiliary bearing supported rotor system p 3121 N95-32690

Dynamic behavior of a magnetic bearing supported jet engine rotor with auxiliary bearings
p 3122 N95-32691
Dynamic modelling and response characteristics of a magnetic bearing rotor system with auxiliary bearings
p 3122 N95-32692
Synchronous dynamics of a coupled shaft/bearing/housing system with auxiliary support from a clearance bearing: Analysis and experiment
p 3122 N95-32693
Low-order nonlinear dynamic model of IC engine-variable pitch propeller system for general aviation aircraft
|NASA-TM-107006| p 3050 N95-32916
Conceptual, causal and numerical modelling and analysis of physical systems p 3190 N95-33006
Large eddy simulation of turbulent vortices and mixing layers p 3109 N95-33340
Mathematical modelling in plasma physics
|AD-A294972| p 3224 N95-34586

DYNAMIC PRESSURE
Techniques for the determination of local dynamic pressure and angle of attack on a horizontal axis wind turbine
|DE95-009204| p 3149 N95-32685

DYNAMIC PROGRAMMING
Bicriteria network design problems
|DE95-012052| p 3099 N95-33387

DYNAMIC RANGE
Accuracy enhancement in optical computing
|AD-A294958| p 3219 N95-34579

DYNAMIC RESPONSE
Dynamic modelling and response characteristics of a magnetic bearing rotor system with auxiliary bearings
p 3122 N95-32692
Inelastic response spectra of a system with bilinear restoring characteristics: Effect of plastic-stiffness ratio
|REPT-2213| p 3091 N95-32993

DYNAMIC STABILITY
Transport studies of tokamak plasmas in JT-60 device
|DE95-737227| p 3220 N95-32417
Beam dynamics group summary
|DE95-008865| p 3213 N95-33204

DYNAMIC STRUCTURAL ANALYSIS
Influence of backup bearings and support structure dynamics on the behavior of rotors with active supports
|NASA-CR-199080| p 3121 N95-32689
Synchronous dynamics of a coupled shaft/bearing/housing system with auxiliary support from a clearance bearing: Analysis and experiment
p 3122 N95-32693
Development of a composite tailoring procedure for airplane wing
|NASA-CR-199081| p 3048 N95-32928

DYNAMICAL SYSTEMS
Conceptual, causal and numerical modelling and analysis of physical systems p 3190 N95-33006

DYNAMOMETERS
Fluid dynamometer having fluid characteristic power absorption adjustment capability
|AD-D017489| p 3116 N95-34426

E

EAR PROTECTORS
User acceptability and comfort of the communications earplug (CEP) when used in the UH-1 helicopter
|AD-A294047| p 3170 N95-34492

EARTH ATMOSPHERE
Modeling soil climate controls on the exchange of trace gases between the terrestrial biosphere and the atmosphere p 3153 N95-33337

EARTH GRAVITATION
Numerical simulation of heat and mass transport during space crystal growth with MEPHISTO
|NASA-TM-107015| p 3089 N95-32718

EARTH IONOSPHERE
Mid-latitude ionospheric plasma drift: A comparison of digital ionosonde and incoherent scatter radar measurements at Millstone Hill p 3222 N95-32838

EARTH MAGNETOSPHERE
Identification of critical substorm-expansion-phase phenomena: Problems addressable with GEM observations
|ATR-94(7270)-1| p 3158 N95-33259

EARTH OBSERVATIONS (FROM SPACE)
European Space Agency 1994 annual report
p 3252 N95-32805
Combined hyperspatial and hyperspectral imaging spectrometer concept p 3129 N95-33738
An interactive environment for the analysis of large Earth observation and model data sets p 3239 N95-34219
Geographic information system for fusion and analysis of high-resolution remote sensing and ground data
p 3240 N95-34224

EARTH OBSERVING SYSTEM (EOS)
Report to the Chairman, Committee on Science, House of Representatives. NASA's Earth Observing System: Estimated funding requirements
|GAO/NSIAD-95-175| p 3142 N95-32707
Land surface temperature measurements from EOS MODIS data
|NASA-CR-199082| p 3142 N95-32717
Ocean observations with EOS/MODIS: Algorithm development and post launch studies
|NASA-CR-198928| p 3143 N95-32914
Aircraft scanner data availability via the version 0 Information Management System p 3134 N95-33762
A relational metric, its application to domain analysis, and an example analysis and model of a remote sensing domain
|NASA-TM-110358| p 3198 N95-33875

EARTH ORBITAL ENVIRONMENTS
Shuttle Potential and Return Electron Experiment (SPREE) electrostatic analyzer (ESA) calibration report
|AD-A293026| p 3057 N95-32772
Operation of the computer model for microenvironment atomic oxygen exposure
|NASA-CR-198190| p 3059 N95-33264
Operation of the computer model for microenvironment solar exposure
|NASA-CR-198189| p 3059 N95-33890

EARTH RADIATION BUDGET
Impact of cloud microphysics on cloud-radiation interactions in the CSU general circulation model
|DE95-008979| p 3153 N95-33205

EARTH RESOURCES
Clearing-house mechanism to promote and facilitate technical and scientific cooperation under the UN Convention on Biological Diversity
|PB95-214557| p 3163 N95-33236
Extraction of ozone and chlorophyll-A distribution from AVIRIS data p 3136 N95-33770

EARTH SCIENCES
Summaries of the Fifth Annual JPL Airborne Earth Science Workshop. Volume 1: AVIRIS Workshop
|NASA-CR-198922| p 3128 N95-33730
Summaries of the Fifth Annual JPL Airborne Earth Science Workshop. Volume 2: TIMS Workshop
|NASA-CR-198923| p 3136 N95-33789
Summaries of the Fifth Annual JPL Airborne Earth Science Workshop. Volume 3: AIRSAR Workshop
|NASA-CR-198924| p 3139 N95-33801
An interactive environment for the analysis of large Earth observation and model data sets p 3239 N95-34219
The Grid Analysis and Display System (GRADS): A practical tool for Earth science visualization
p 3241 N95-34231
Advanced data visualization and sensor fusion: Conversion of techniques from medical imaging to Earth science p 3242 N95-34236
A distributed analysis and visualization system for model and observational data p 3243 N95-34240

EARTH SURFACE
Canopy reflectance modelling of semiarid vegetation
|NASA-CR-199117| p 3142 N95-32676
A land-surface testbed for EOSDIS
p 3158 N95-34223

EARTHQUAKES
Inelastic response spectra of a system with bilinear restoring characteristics: Effect of plastic-stiffness ratio
|REPT-2213| p 3091 N95-32993

EAST GERMANY
Minutes of the 12th Joint NASA/DARA-DLR Life Sciences Program Working Group Meeting
|NASA-TM-110655| p 3161 N95-32719
The DLR research programme on an integrated multi sensor system for surface movement guidance and control p 3048 N95-33135

ECHOES
Photon echoes from the absorption continuum of a semiconductor
|DE95-011274| p 3101 N95-32596

ECONOMIC ANALYSIS
Summary report for ITER Task No. T226B: Evaluation of ITER disruption erosion
|DE95-010402| p 3219 N95-32401
Lightweight alumina refractory aggregate. Phase 2: Pilot scale development
|DE95-012154| p 3083 N95-33079

ECONOMICS
World mineral statistics, 1988-92. Production: Exports: Imports
|PB95-208096| p 3155 N95-32601

ECONOMY
United Kingdom minerals yearbook, 1994. Statistical data to 1993
|PB95-207841| p 3155 N95-32599
World mineral production, 1989-93. Preliminary statistics
|PB95-208104| p 3156 N95-32603

ECOSYSTEMS
Development of an L-, C-, and X-band radar for backscattering studies over vegetation
|NASA-CR-199112| p 3097 N95-33033
Completing below-ground carbon budgets for pastures, recovering forests, and mature forests of Amazonia
|NASA-CR-199129| p 3143 N95-33498
Carbon Dioxide Information Analysis Center and World Data Center: A for Atmospheric trace gases
|DE95-011769| p 3154 N95-33655
Prospect redux p 3133 N95-33758
Use of AIRSAR to identify woody shrub invasion and other indicators of desertification in the Jornada LTER
p 3141 N95-33810
Regional mapping of forest canopy water content and biomass using AIRSAR images over BOREAS study area p 3142 N95-33815

EDGE DETECTION
A tactical navigation and routeing system for low-level flight p 3044 N95-32494
A general solution to object matching problems by using the multiresolution approximation p 3189 N95-33002

EDUCATION
Training neural networks using sequential extended Kalman filtering
|DE95-007874| p 3187 N95-32386
Investigation research on introducing new energy technology, promoting its practical application, and providing its instruction
|DE95-769801| p 3148 N95-32403
National Aeronautics and Space Administration (NASA)/American Society for Engineering Education (ASEE) Summer Faculty Fellowship Program, 1994, volume 1
|NASA-CR-188410| p 3248 N95-32418
Liftoff to learning: Assignment space
|NASA-TM-110820| p 3057 N95-32539
Developing multimedia instructional systems: An example application for training in night vision goggles
|AD-A294521| p 3235 N95-34479
Aerospace physiology AFSC 4M0X1
|AD-A294839| p 3165 N95-34564
Conceptual understanding and stability, and knowledge shields for fending off conceptual change
|AD-A293555| p 3166 N95-34609
Proceedings of the School for Young High Energy Physicists
|PB95-234993| p 3235 N95-34652
Presentation of a Swedish study program concerning recruitment, selection and training of student air traffic controllers: The MRU project phase 1
p 3167 N95-34775
A curriculum for strategy in the information age: Chaos in a new era
|AD-A295036| p 3244 N95-34794

EIGENVALUES
Counterexample to the lieb-thirring conjecture concerning the moments of the eigenvalues of the Schroedinger operator
|PB95-212197| p 3195 N95-32890
Calculations of spatial higher modes without deflation procedure
|REPT-2205| p 3090 N95-32985

EIGENVECTORS
Calculations of spatial higher modes without deflation procedure
|REPT-2205| p 3090 N95-32985

EKMAN LAYER
On the nonlinear stability of a nearby parallel and a non-unidirectional flow p 3112 N95-34284

ELASTIC DEFORMATION
A three-dimensional nonlinear Timoshenko beam based on the core-congruential formulation
|NASA-CR-199042| p 3180 N95-32765
The linear elastic biaxial response of plain-woven meshes p 3064 N95-33468

ELASTIC MEDIA
Modeling seismic wave propagation in heterogeneous materials using finite elements p 3156 N95-34283

ELASTIC SCATTERING
Faddeev calculations of p(mu)+p collisions: Effect of hyperfine splitting on the cross sections
|DE95-007838| p 3203 N95-32583
Inversion of electron-water elastic scattering data
|DE95-619323| p 3204 N95-32623
Spin effects in high energy photon-hadron scattering in QCD
|DE95-623679| p 3234 N95-32961

ELASTIC WAVES
Experimental investigation of the separation of texture and residual stress induced anisotropy via oblique incidence acoustoelasticity p 3126 N95-33253

ELASTODYNAMICS
Advanced boundary element methods in aeroacoustics and elastodynamics p 3200 N95-33694

High-order Taylor-Galerkin and adaptive hp-methods for hyperbolic systems with application to structural acoustics p 3200 N95-33719

ELASTOPLASTICITY

Fifth International Conference on Hyperbolic Problems, Theory, Numerics, Applications: Abstracts
|DE95-008173| p 3194 N95-32389

Patterns and perspectives in applied fracture mechanics
|DE95-012844| p 3127 N95-34442

ELASTOSTATICS

Cubic-B-spline boundary elements for two-dimensional and axisymmetric elastostatics p 3127 N95-33695

ELECTRIC BATTERIES

A comparison of modeled and measured energy use in hybrid electric vehicles
|DE95-000297| p 3102 N95-32808

Lessons learned in acquiring new regulations for shipping advanced electric vehicle batteries
|DE95-009908| p 3102 N95-32956

Thin-film rechargeable lithium batteries
|DE95-008975| p 3103 N95-33697

Encapsulated dry electrolyte composition for time release into a solute
|AD-D017485| p 3075 N95-34287

ELECTRIC CONNECTORS

Crosspoint analog data selector
|AD-D017482| p 3104 N95-34425

ELECTRIC CORONA

Performance of partially fluorinated polyimide insulation for aerospace applications
|NASA-CR-198372| p 3060 N95-32673

Application of Ni-63 photo and corona discharge ionization for the analysis of chemical warfare agents and toxic wastes p 3070 N95-33272

ELECTRIC CURRENT

Quench propagation velocity for highly stabilized conductors
|DE95-011040| p 3103 N95-33404

Using dark current data to estimate AVIRIS noise covariance and improve spectral analyses p 3129 N95-33736

ELECTRIC DISCHARGES

Application of Ni-63 photo and corona discharge ionization for the analysis of chemical warfare agents and toxic wastes p 3070 N95-33272

ELECTRIC FIELDS

Radial electric field measurement in a tokamak by the injection of a pulsed neutral beam
|DE95-614176| p 3221 N95-32561

General limits on the performance of high power radiators
|DE95-010732| p 3095 N95-32570

Electron and hole transport in compound semiconductors
|AD-A295003| p 3233 N95-34822

ELECTRIC GENERATORS

HYBRID2: A versatile model of the performance of hybrid power systems
|DE95-004062| p 3148 N95-32551

A thermophotovoltaic generator for use in a lightweight electric car: Year 1 progress report
|DE95-011355| p 3102 N95-32968

ELECTRIC HYBRID VEHICLES

A comparison of modeled and measured energy use in hybrid electric vehicles
|DE95-000297| p 3102 N95-32808

ELECTRIC MOTOR VEHICLES

A comparison of modeled and measured energy use in hybrid electric vehicles
|DE95-000297| p 3102 N95-32808

A thermophotovoltaic generator for use in a lightweight electric car: Year 1 progress report
|DE95-011355| p 3102 N95-32968

ELECTRIC POTENTIAL

Physics of the CEM92M Code
|DE95-623579| p 3202 N95-32477

General limits on the performance of high power radiators
|DE95-010732| p 3095 N95-32570

COBRA accelerator for Sandia ICF diode research at Cornell University
|DE95-011018| p 3101 N95-32578

An application of mechanical leverage to microactuation
|DE95-011883| p 3124 N95-33836

Unified model of the RF plasma sheath
|DE95-012114| p 3224 N95-33851

Improved L-C resonant decay technique for Q measurement of quasilinear power inductors: New results for MPP and ferrite powdered cores
|NASA-CR-198373| p 3103 N95-33874

Monolithic diode arrays for quasioptical millimeter wave beam steering
|AD-A294256| p 3100 N95-34460

ELECTRICAL ENGINEERING

Quantum transport
|AD-A294977| p 3235 N95-34589

ELECTRICAL FAULTS

Self stressing test structure cells
|AD-A294386| p 3104 N95-34345

ELECTRICAL INSULATION

Performance of partially fluorinated polyimide insulation for aerospace applications
|NASA-CR-198372| p 3060 N95-32673

ELECTRICAL MEASUREMENT

Radial electric field measurement in a tokamak by the injection of a pulsed neutral beam
|DE95-614176| p 3221 N95-32561

Fabrication technology and measurement of coupled quantum dot devices
|AD-A294853| p 3231 N95-34569

ELECTRICAL RESISTIVITY

Development of improved p-type Si-20 at. %Ge by addition of fullerite
|DE95-010230| p 3066 N95-32394

High resistivity InAlN by nitrogen or oxygen implantation
|DE95-011023| p 3226 N95-32594

Cathode readout with stripped resistive drift tubes
|DE95-621871| p 3102 N95-32628

Charge-transfer gap closure in transition-metal halides under pressure
|DE95-011268| p 3230 N95-33865

Properties of high-T(sub c) Josephson junctions with Y(0.7)Ca(0.3)Ba2Cu3O(7-delta) barrier layers
|AD-A294852| p 3231 N95-34568

ELECTRICITY

Feasibility survey on international cooperation for high efficiency energy conversion technology in fiscal 1993
|DE95-769804| p 3148 N95-32546

Tomorrow's energy today for cities and countries
|DE95-012464| p 3150 N95-33383

ELECTRO-OPTICAL EFFECT

Successful development of first-generation laser device; marking China's optoelectronic technology at world class level
|AD-A294206| p 3217 N95-34305

ELECTRO-OPTICS

SIRPH: Steerable infrared picture on helmet mounted display p 3045 N95-32504

Low-level data fusion for landing runways detection p 3048 N95-33136

Efficient pockel's modulators in optical fibers
|AD-A294009| p 3217 N95-34374

Programmable real-time optoelectronic hybrid threshold logic processors
|AD-A294067| p 3104 N95-34379

ELECTROACOUSTIC TRANSDUCERS

High-resolution TeO2 acousto-optical deflector for millimeter-wave spectrometer
|AD-A293054| p 3215 N95-32701

Conforming tuning coupler for flextensional transducers
|AD-D017285| p 3105 N95-34617

ELECTROCHEMICAL CELLS

High rate rechargeable lithium cells employing lithium ion conducting solid electrolytes
|AD-A294390| p 3104 N95-34347

ELECTROCHEMISTRY

Corrosion of separator plate constituents in molten carbonate
|PB95-214490| p 3149 N95-32813

Encapsulated dry electrolyte composition for time release into a solute
|AD-D017485| p 3075 N95-34287

ELECTRODEPOSITION

Zero discharge organic coatings: Powder paint - UV curable paint - E-coat
|AD-A293573| p 3087 N95-34614

ELECTRODES

Comparison of lead zirconate titanate thin films on ruthenium oxide and platinum electrodes
|DE95-617597| p 3082 N95-32710

Corrosion of separator plate constituents in molten carbonate
|PB95-214490| p 3149 N95-32813

Epitaxial Pb(Zr(0.40)Ti(0.60))O3/SrRuO3 and PbTiO3/SrRuO3 multilayer thin films prepared by MOCVD and RF sputtering
|DE95-007146| p 3229 N95-33636

High rate rechargeable lithium cells employing lithium ion conducting solid electrolytes
|AD-A294390| p 3104 N95-34347

Natural convection at microelectrodes
|AD-A294338| p 3075 N95-34357

ELECTRODYNAMICS

The 11th Annual Review of Progress in Applied Computational Electromagnetics, volume 2
|AD-A294851| p 3100 N95-34567

ELECTROENCEPHALOGRAPHY

Event-related potentials and electroencephalograms in adaptive operator training: Rationale and annotated bibliography
|AD-A294337| p 3166 N95-34356

ELECTROHYDRODYNAMICS

Baseline experimental investigation of an electrohydrodynamically assisted heat pipe p 3113 N95-32427

ELECTROLUMINESCENCE

Crystalline-as-deposited CaGa2S4: Ce via low-temperature metal-organic chemical vapor deposition
|DE95-010883| p 3229 N95-33401

ELECTROLYTES

Thin-film rechargeable lithium batteries
|DE95-008975| p 3103 N95-33697

ELECTROMAGNETIC ABSORPTION

Probe transparency in a two-level medium embedded by a squeezed vacuum
|DE95-614123| p 3198 N95-32525

Comparison of seasonal and zonal patterns of the direct and indirect radiative forcing of climate by aerosols
|DE95-010896| p 3153 N95-33192

Operation of the computer model for microenvironment solar exposure
|NASA-CR-198189| p 3059 N95-33890

Influence of CO2 continuous laser preprocessed substrates on optical thin film damage thresholds
|AD-A294190| p 3217 N95-34297

Photobiology and optical properties of planktonic and sea ice microalgae in the high arctic
|AD-A294002| p 3160 N95-34457

ELECTROMAGNETIC COMPATIBILITY

The 11th Annual Review of Progress in Applied Computational Electromagnetics, volume 1
|AD-A294850| p 3100 N95-34566

Environment and circuit model for capacitor-based rail guns
|AD-A293455| p 3057 N95-34815

ELECTROMAGNETIC FIELDS

The Problem 4/3 as a consequence of contracted length non-covariance
|DE95-623628| p 3207 N95-33226

Emittance growth due to decoherence and wakefields
|DE95-012495| p 3213 N95-33376

Computational electromagnetics and parallel dense matrix computations
|DE95-012286| p 3099 N95-33379

Atoms in strong fields
|AD-A294589| p 3209 N95-34423

Heavy ions acceleration in RF wells of 2-frequency electromagnetic field and in the inverted FEL
|DE95-012439| p 3214 N95-34439

Environment and circuit model for capacitor-based rail guns
|AD-A293455| p 3057 N95-34815

ELECTROMAGNETIC INTERACTIONS

Impact of cloud microphysics on cloud-radiation interactions in the CSU general circulation model
|DE95-008979| p 3153 N95-33205

ELECTROMAGNETIC INTERFERENCE

FH and DS spread-spectrum systems in interference-limited HF channels: A comparison
|PB95-211439| p 3098 N95-33230

Using optical interference methods to measure acousto-optical device thermal effects
|AD-A294219| p 3217 N95-34309

ELECTROMAGNETIC PULSES

Phase control and measurement of ultrashort optical pulses
|DE95-011746| p 3216 N95-33411

Discrete modeling of optical pulse propagation in nonlinear media
|DE95-011515| p 3216 N95-34020

Influence of CO2 continuous laser preprocessed substrates on optical thin film damage thresholds
|AD-A294190| p 3217 N95-34297

ELECTROMAGNETIC RADIATION

Environment and circuit model for capacitor-based rail guns
|AD-A293455| p 3057 N95-34815

ELECTROMAGNETIC SCATTERING

Conference proceedings of mathematical methods in electromagnetic theory
|AD-A291165| p 3097 N95-32797

The 11th Annual Review of Progress in Applied Computational Electromagnetics, volume 1
|AD-A294850| p 3100 N95-34566

Experimental investigation of impulse radar for mitigation of effects of radar absorbing materials
|AD-A294166| p 3100 N95-34762

ELECTROMAGNETIC WAVE TRANSMISSION

The 11th Annual Review of Progress in Applied Computational Electromagnetics, volume 2
|AD-A294851| p 3100 N95-34567

ELECTROMAGNETISM
Conference proceedings of mathematical methods in electromagnetic theory
| AD-A291165 | p 3097 N95-32797
Efficient time domain solutions of Maxwell's equations for aerospace systems
| AD-A294019 | p 3196 N95-34377
The 11th Annual Review of Progress in Applied Computational Electromagnetics, volume 1
| AD-A294850 | p 3100 N95-34566

ELECTROMECHANICAL DEVICES
Baseline experimental investigation of an electrohydrodynamically assisted heat pipe
p 3113 N95-32427
Operations manual for a compact electromechanical fatigue testing machine
| DSTO-GD-0036 | p 3115 N95-32927

ELECTROMIGRATION
Self stressing test structure cells
| AD-A294386 | p 3104 N95-34345
Quantum transport
| AD-A294977 | p 3235 N95-34589

ELECTRON ACCELERATORS
The effect of phase advance errors between interaction points on beam halos
| DE95-012559 | p 3214 N95-34023
Studies of halo distributions under beam-beam interaction
| DE95-012560 | p 3214 N95-34024

ELECTRON BEAM WELDING
Development and trial manufacturing of 1/2-scale partial mock-up of blanket box structure for fusion experimental reactor
| DE95-737184 | p 3219 N95-32408
Electron beam joining of structural ceramics
| DE95-012521 | p 3085 N95-34022

ELECTRON BEAMS
The uses of Electron Beam Ion Traps in the study of highly charged ions
| DE95-011537 | p 3212 N95-33064
The effect of phase advance errors between interaction points on beam halos
| DE95-012559 | p 3214 N95-34023
Studies of halo distributions under beam-beam interaction
| DE95-012560 | p 3214 N95-34024

ELECTRON CAPTURE
Low energy collisions involving multiply charged ions
| DE95-010911 | p 3203 N95-32564
State-selective single electron capture cross sections in He(exp 2+) + Li(2s) and Li(*)(2p) collisions
| DE95-010819 | p 3207 N95-33371
An ion-ion collisions system at KSU
| DE95-010820 | p 3208 N95-33372

ELECTRON CYCLOTRON HEATING
Application of grating polarizer to 106.4GHz ECH system on Heliotron-E
| NIFS-334 | p 3225 N95-34624

ELECTRON DIFFRACTION
TEM investigation on the low temperature phase of HfV2
| DE95-009500 | p 3225 N95-32532
Photoemission study of some novel materials: Rare earth/transition metal interface, Ba*(0.6)*K*(0.4)*BiO3* and AlPdMn
| DE95-010125 | p 3227 N95-32643
The growth of ultrathin epitaxial intermetallic films
| AD-A295037 | p 3232 N95-34795

ELECTRON ENERGY
Estimation of spatially restricted LET using track structure models p 3161 N95-32722
High-resolution magnetic imaging and investigations of thin-film magnetism with spin-polarized electron, ion and atom probes
| DE95-012190 | p 3074 N95-33392
Electron and hole transport in compound semiconductors
| AD-A295003 | p 3233 N95-34822

ELECTRON IMPACT
Measurements of cross sections and resonance structures following electron-impact excitation/ionization of Na-like Kr and Xe
| DE95-011731 | p 3230 N95-34438

ELECTRON ORBITALS
State-selective single electron capture cross sections in He(exp 2+) + Li(2s) and Li(*)(2p) collisions
| DE95-010819 | p 3207 N95-33371

ELECTRON OSCILLATIONS
Predicted operating conditions for maintaining mode purity in the 1MW 200 GHz FOM Free Electron Maser
| DE95-010795 | p 3117 N95-32571
Injection envelope matching in storage rings
| DE95-012496 | p 3213 N95-33377

ELECTRON PARAMAGNETIC RESONANCE
Conversion of holes into reducing species on surface modified small-particle TiO2
| DE95-008282 | p 3225 N95-32586
Mechanism(s) for the suppression of the switchable polarization in PZT and BaTiO3
| DE95-009589 | p 3226 N95-32590

ELECTRON PLASMA
Mathematical modelling in plasma physics
| AD-A294972 | p 3224 N95-34586

ELECTRON PROBES
High-resolution magnetic imaging and investigations of thin-film magnetism with spin-polarized electron, ion and atom probes
| DE95-012190 | p 3074 N95-33392

ELECTRON STATES
The mean lifetimes of the 2p(sigma) lowest bound state of HeH(2+) and its isotopes
| DE95-010812 | p 3206 N95-32966

ELECTRON TRANSFER
An ion-ion collisions system at KSU
| DE95-010820 | p 3208 N95-33372
The computation of electron transfer rates: The nonadiabatic instanton solution
| AD-A294523 | p 3209 N95-34350
Electron and hole transport in compound semiconductors
| AD-A295003 | p 3233 N95-34822

ELECTRON TRANSITIONS
The mean lifetimes of the 2p(sigma) lowest bound state of HeH(2+) and its isotopes
| DE95-010812 | p 3206 N95-32966
Method and apparatus for locking laser wavelength to an atomic transition
| AD-D017425 | p 3120 N95-34619

ELECTRON TUNNELING
Quantum mechanical capacitance in a scanning tunneling microscope
| DE95-011272 | p 3230 N95-33880

ELECTRON-ION RECOMBINATION
Observation of KLM dielectronic recombination resonances in highly charged uranium ions
| DE95-010266 | p 3207 N95-33219

ELECTRONIC EQUIPMENT
Solid-state data recorder, next development and use
p 3094 N95-33143
An investigation of the chemistry of citric acid in military soldering applications
| AD-A295042 | p 3105 N95-34796

ELECTRONIC EQUIPMENT TESTS
Is there a role for a test controller in the development of new ATC equipment? p 3174 N95-34778

ELECTRONIC MAIL
Security and privacy in the NII
| AD-A293475 | p 3244 N95-34816

ELECTRONIC PACKAGING
Copper-diamond composite substrates for electronic components
| DE95-011520 | p 3079 N95-33063

ELECTRONIC PUBLISHING
NASA wide electronic publishing system: Electronic printing and duplicating. Stage 3 evaluation report
| NASA-TM-104620 | p 3237 N95-32922

ELECTRONS
Conversion of holes into reducing species on surface modified small-particle TiO2
| DE95-008282 | p 3225 N95-32586
Inversion of electron-water elastic scattering data
| DE95-619323 | p 3204 N95-32623
Synthesis of potential new Zintl phases
| DE95-010123 | p 3227 N95-32640
Electron-electron interaction in the ionization of hydrogenlike projectiles by He
| DE95-010822 | p 3208 N95-33374
Tokamak ETE circuits: Analysis and specifications
| INPE-5573-PRP/182 | p 3224 N95-33873
Electron and hole transport in compound semiconductors
| AD-A295003 | p 3233 N95-34822

ELECTROPLATING
Background meeting and technology demonstration: Chromium electroplating of superconductor strand
| DE95-011736 | p 3068 N95-33070
Characterization of DuPont 9015, aqueous processable dry film photoresist for printed wiring boards
| DE95-011239 | p 3103 N95-33864
Spray coating of metals. Proof of concept: Phase 2
| AD-A294393 | p 3081 N95-34348

ELECTROSTATIC PROBES
Shuttle Potential and Return Electron Experiment (SPREE) electrostatic analyzer (ESA) calibration report
| AD-A293026 | p 3057 N95-32772
Single Langmuir probe characteristic in a magnetized plasma at the TEXT tokamak
| DE95-012144 | p 3224 N95-33853

ELECTROSTATICS
Design rules and reality check for carbon-based ultracapacitors
| DE95-010575 | p 3103 N95-33640

ELEMENTARY EXCITATIONS
Zero modes of Gauss constraint in gaugeless reduction of Yang-Mills theory
| DE95-623676 | p 3234 N95-32667

ELEMENTARY PARTICLE INTERACTIONS
The Q(2)-dependence of the Gross-Llewellyn Smith sum rule and of the parton distributions
| DE95-623678 | p 3202 N95-32406
Track finding and fitting in the H1 forward track detector
| PB95-234985 | p 3214 N95-34651
Analytic approach to small x structure functions
| PB95-236030 | p 3214 N95-34653

ELEMENTARY PARTICLES
Double-strangeness five-body system
| DE95-737277 | p 3202 N95-32404
Lithogenic and cosmogenic tracers in catchment hydrology
| DE95-011523 | p 3143 N95-33407

ELEVATION
Use of TOPSAR digital elevation data to determine the 3-dimensional shape of an alluvial fan
p 3139 N95-33804

ELLIPSOIDS
RR lyrae variable stars in the CCD/Transit instrument survey
| AD-A294138 | p 3246 N95-34753

ELLIPTIC DIFFERENTIAL EQUATIONS
Maximum principle for subsolutions of degenerate elliptic operators
| DE95-613373 | p 3195 N95-32523
High-order Taylor-Galerkin and adaptive hp-methods for hyperbolic systems with application to structural acoustics p 3200 N95-33719
Adaptive grid method using elliptic equation for compressible flows p 3035 N95-34515

EMBRITTLEMENT
Irradiation experiments of low copper A533B steels for reactor pressure vessel tested in JMTR
| DE95-737266 | p 3077 N95-32531

EMBRYOS
X-ray-provoked non-Mendelian transgenerational oncodeterminants p 3163 N95-32731

EMERGENCIES
Background and principles of throttles-only flight control p 3053 N95-33021

EMISSION SPECTRA
Reduction and analysis of seasons 15 and 16 (1991 - 1992) Pioneer Venus radio occulation data and correlative studies with observations of the near infrared emission of Venus
| NASA-CR-199071 | p 3247 N95-32700
Correction of thin cirrus effects in AVIRIS images using the sensitive 1.375-micron cirrus detecting channel
p 3131 N95-33748
The JPL Field Emission Spectrometer
p 3117 N95-33794

EMISSIVITY
Radiative interactions with micromachined surfaces: Spectral polarized emittance
| DE95-011455 | p 3097 N95-33061
TIMS observations of surface emissivity in HAPEX-Sahel p 3139 N95-33799

EMITTANCE
A possible ionization cooling experiment at the AGS
| DE95-010317 | p 3205 N95-32654
Proton-induced fragmentation of carbon at energies below 100 MeV p 3161 N95-32720
Radiative interactions with micromachined surfaces: Spectral polarized emittance
| DE95-011455 | p 3097 N95-33061
Emittance and energy control in the NLC main linacs
| DE95-012556 | p 3213 N95-33338
Emittance growth due to decoherence and wakefields
| DE95-012495 | p 3213 N95-33376

EMITTERS
The growth and optimization of InPSb/InGaAs/InAsSb strained-layer superlattice emitters by metal organic chemical vapor deposition
| DE95-011057 | p 3226 N95-32595
Integral cesium reservoir: Design and transient operation
| DE95-010152 | p 3211 N95-32647
Growth and characterization of heterostructures and infrared emitters with compressed InAsSb layers
| DE95-009828 | p 3228 N95-33213

ENCAPSULATING
Photovoltaic Manufacturing Technology (PVMaT)
| DE95-004093 | p 3149 N95-33153

ENCLOSURE
Three-dimensional natural convection of a fluid with temperature-dependent viscosity in an enclosure with localized heating
[DE95-002606] p 3106 N95-32387
END EFFECTORS
A study of space-rated connectors using a robot end-effector
[NASA-CR-199116] p 3121 N95-32675
Design and implementation of a two-axis micromanipulator to enhance the gripper positional accuracy of a single flexible link p 3123 N95-33252
END-TO-END DATA SYSTEMS
The development of the automatic target recognition system for the UGV/RSTA LADAR
[AD-A294090] p 3100 N95-34474
ENERGETIC PARTICLES
Dosimetry of heavy ions by use of CCD detectors p 3161 N95-32721
ENERGY ABSORPTION
Energy absorption device for shock loading
[AD-D017476] p 3124 N95-34449
ENERGY BANDS
Theory of magneto-optics and circular magnetic x-ray dichroism
[DE95-010129] p 3080 N95-33700
ENERGY BUDGETS
Electron and hole transport in compound semiconductors
[AD-A295003] p 3233 N95-34822
ENERGY CONSERVATION
Technical innovation for reducing emissions of greenhouse effect gas and survey of effects of changes of industrial structures
[DE95-769808] p 3151 N95-32547
ENERGY CONSUMPTION
High-tech controls for energy and environment
[DE95-004011] p 3191 N95-33060
ENERGY CONVERSION EFFICIENCY
Feasibility survey on international cooperation for high efficiency energy conversion technology in fiscal 1993
[DE95-769804] p 3148 N95-32546
ENERGY DISSIPATION
Impedance study for the PEP-2 B-factory
[DE95-010569] p 3203 N95-32567
The structure of ion track in Solids produced by ions with high level inelastic energy losses
[DE95-620942] p 3205 N95-32625
Analysis and finite element approximation of an optimal shape control problem for the steady-state Navier-Stokes equations p 3112 N95-34285
ENERGY DISTRIBUTION
An experimental study of collective sea state modes of deep water surface gravity waves
[AD-A294007] p 3160 N95-34372
ENERGY GAPS (SOLID STATE)
Mechanism(s) for the suppression of the switchable polarization in PZT and BaTiO3
[DE95-009589] p 3226 N95-32590
Charge-transfer gap closure in transition-metal halides under pressure
[DE95-011268] p 3230 N95-33865
ENERGY LEVELS
Nucleation, propagation, electronic levels and elimination of misfit dislocations in 3-5 semiconductor interfaces
[DE95-011595] p 3231 N95-34485
ENERGY METHODS
Glass science tutorial: Lecture no. 4, commercial glass melting and associated air emission issues
[DE95-007818] p 3082 N95-32384
The linear elastic biaxial response of plain-woven meshes p 3064 N95-33468
ENERGY POLICY
Annual report to Congress 1994: Energy Information Administration
[DE95-011240] p 3237 N95-32482
ENERGY REQUIREMENTS
Design rules and reality check for carbon-based ultracapacitors
[DE95-010575] p 3103 N95-33640
ENERGY SPECTRA
Physics of the CEM92M Code
[DE95-623579] p 3202 N95-32477
Gamma ray imaging of the Crab and Vale regions with the UCR double-Compton telescope p 3245 N95-32837
Technical support in the area of theoretical support of nuclear preequilibrium
[DE95-011617] p 3212 N95-32960
Inelastic response spectra of a system with bilinear restoring characteristics: Effect of plastic-stiffness ratio
[REPT-2213] p 3091 N95-32993
ENERGY STORAGE
Unitized Regenerative Fuel Cells for solar rechargeable aircraft and zero emission vehicles
[DE95-010684] p 3150 N95-33642
The 3rd international conference on solar energy storage and applied photochemistry
[AD-A294343] p 3150 N95-34359
The international conference on solar energy storage and applied photochemistry
[AD-A294347] p 3150 N95-34360
Review of the research activities of the Energy Research Unit in 1994
[PB95-235008] p 3151 N95-34656
ENERGY TECHNOLOGY
Investigation research on introducing new energy technology, promoting its practical application, and providing its instruction
[DE95-769801] p 3148 N95-32403
The 3rd international conference on solar energy storage and applied photochemistry
[AD-A294343] p 3150 N95-34359
The international conference on solar energy storage and applied photochemistry
[AD-A294347] p 3150 N95-34360
Review of the research activities of the Energy Research Unit in 1994
[PB95-235008] p 3151 N95-34656
ENERGY TRANSFER
Estimation of spatially restricted LET using track structure models p 3161 N95-32722
Heavy ion action on single cells: Cellular inactivation capability of single accelerated heavy ions p 3162 N95-32729
The 3rd international conference on solar energy storage and applied photochemistry
[AD-A294343] p 3150 N95-34359
Photobiology and optical properties of planktonic and sea ice microalgae in the high arctic
[AD-A294002] p 3160 N95-34457
Structure and dynamics of excited atoms
[AD-A294997] p 3209 N95-34819
ENGINE CONTROL
PSC implementation and integration p 3051 N95-33014
The application of Ada and formal methods to a safety critical engine control system p 3094 N95-33142
ENGINE DESIGN
The development of some kinds of LRE injectors
[AD-A294199] p 3061 N95-34302
Design of secondary flow control cascade using numerical simulation p 3034 N95-34507
ENGINE INLETS
F-15 propulsion system p 3051 N95-33012
Minimum fan turbine inlet temperature mode evaluation p 3052 N95-33016
Fan noise prediction assessment
[NASA-CR-195051] p 3200 N95-33831
Subscale study of engine bellmouth inlet vortices in test cell R1D
[AD-A294993] p 3113 N95-34818
ENGINE NOISE
Computation of noise radiation from turbofans: A parametric study
[NASA-CR-198359] p 3200 N95-32836
Fan noise prediction assessment
[NASA-CR-195051] p 3200 N95-33831
ENGINE TESTS
Allison engine testing CMSX-4(reg sign) single crystal turbine blades and vanes
[DE95-010308] p 3050 N95-32636
Maximum thrust mode evaluation p 3052 N95-33017
SSME Post Test Diagnostic System: Systems Section
[NASA-CR-198375] p 3061 N95-34625
ENGINEERING
National Aeronautics and Space Administration (NASA)/American Society for Engineering Education (ASEE) Summer Faculty Fellowship Program, 1994, volume 1
[NASA-CR-188410] p 3248 N95-32418
ENGINEERS
NASA/DOD Aerospace Knowledge Diffusion Research Project. Paper 50: From student to entry-level professional: Examining the role of language and written communications in the reacculturation of aerospace engineering students
[NASA-TM-110834] p 3237 N95-32883
ENTHALPY
Numerical simulation of high enthalpy shock tunnel p 3035 N95-34514
ENTRAINMENT
Very large eddy simulations of spatially evolving supersonic turbulent shear layers p 3110 N95-33606
ENVIRONMENT EFFECTS
Users' manual for LEHGC: A Lagrangian-Eulerian finite-element model of HydroGeoChemical transport through saturated-unsaturated media. Version 1.0
[DE95-010513] p 3179 N95-32543
The CE-QUAL-ICM three-dimensional eutrophication model, release version 1.0
[AD-A294258] p 3160 N95-34461
Environment and circuit model for capacitor-based rail guns
[AD-A293455] p 3057 N95-34815
ENVIRONMENT MANAGEMENT
Clearing-house mechanism to promote and facilitate technical and scientific cooperation under the UN Convention on Biological Diversity
[PB95-214557] p 3163 N95-33236
A Spatial Analysis and Modeling System (SAMS) for environment management p 3243 N95-34239
ENVIRONMENT MODELS
Identification of critical substorm-expansion-phase phenomena: Problems addressable with GEM observations
[ATR-94(7270)-1] p 3158 N95-33259
The CE-QUAL-ICM three-dimensional eutrophication model, release version 1.0
[AD-A294258] p 3160 N95-34461
ENVIRONMENT POLLUTION
Multimedia Environmental Pollutant Assessment System (MEPAS(trademark)): Exposure pathway and human health impact assessment models
[DE95-012763] p 3155 N95-34441
ENVIRONMENT PROTECTION
An electronic design guideline for incorporating pollution prevention into US Department of Energy design projects
[DE95-008935] p 3151 N95-32475
Winter season air pollution in El Paso-Ciudad Juarez. A review of air pollution studies in an international airshed
[DE95-009083] p 3152 N95-32556
Environment applications for ion mobility spectrometry p 3071 N95-33279
ENVIRONMENT SIMULATION
Study of the space environmental effects on spacecraft engineering materials
[NASA-CR-199090] p 3066 N95-32581
Operation of the computer model for microenvironment atomic oxygen exposure
[NASA-CR-198190] p 3059 N95-33264
ENVIRONMENTAL LABORATORIES
The concept of the space system based on the Rocket launch vehicle of light-weight class for direct sounding of large-scale natural hazards p 3057 N95-33128
ENVIRONMENTAL MONITORING
An electronic design guideline for incorporating pollution prevention into US Department of Energy design projects
[DE95-008935] p 3151 N95-32475
Field Raman spectrograph for environmental analysis
[DE95-007969] p 3153 N95-32816
High-tech controls for energy and environment
[DE95-004011] p 3191 N95-33060
Environment applications for ion mobility spectrometry p 3071 N95-33279
An ammonia monitor for the water industry p 3071 N95-33281
Pollution in Norway
[PB95-214565] p 3153 N95-33331
Completing below-ground carbon budgets for pastures, recovering forests, and mature forests of Amazonia
[NASA-CR-199129] p 3143 N95-33498
Studies of microwave scattering and canopy architecture for boreal forests
[NASA-CR-199114] p 3099 N95-33726
CNR LARA project, Italy: Airborne laboratory for environmental research p 3129 N95-33735
Mineralogic variations in fluvial sediments contaminated by mine tailings as determined from AVIRIS data, Coeur D'Alene River Valley, Idaho p 3131 N95-33745
Measurement of atmospheric water vapor, leaf liquid water and reflectance with AVIRIS in the Boreal Ecosystem-Atmosphere Study: Initial results p 3133 N95-33755
Measurement of the spectral absorption of liquid water in melting snow with an imaging spectrometer p 3133 N95-33756
Vegetation species composition and canopy architecture information expressed in leaf water absorption measured in the 1000 nm and 2200 spectral region by an imaging spectrometer p 3133 N95-33757
Extraction of ozone and chlorophyll-A distribution from AVIRIS data p 3136 N95-33770
ENVIRONMENTAL SURVEYS
Mineralogic variations in fluvial sediments contaminated by mine tailings as determined from AVIRIS data, Coeur D'Alene River Valley, Idaho p 3131 N95-33745

ENVIRONMENTAL TESTS
Study of the space environmental effects on spacecraft engineering materials
| NASA-CR-199090 | p 3066 N95-32581

ENZYMES
Mutation induction in bacteria aft,r heavy ion irradiation p 3162 N95-32727
The 17th Symposium on Biotechnology for Fuels and Chemicals
| DE95-004054 | p 3150 N95-33225

EOS DATA AND INFORMATION SYSTEM
Aircraft scanner data availability via the version 0 Information Management System p 3134 N95-33762
A land-surface testbed for EOSDIS p 3158 N95-34223
Multi-layer holographic bifurcative neural network system for real-time adaptive EOS data analysis p 3148 N95-34233

EPITAXY
Epitaxial Pb(Zr(x)Ti(1-x))O3/SrRuO3 (x = 0, 0.35, 0.65) multilayer thin films on SrTiO3(100) and MgO(100) prepared by MOCVD and RF sputtering
| DE95-008288 | p 3226 N95-32598
Photoemission study of some novel materials: Rare earth/transition metal interface, Ba*(0.6)*K*(0.4)*BiO3* and AlPdMn
| DE95-010125 | p 3227 N95-32643
Epitaxial Pb(Zr(0.40)Ti(0.60))O3/SrRuO3 and PbTiO3/SrRuO3 multilayer thin films prepared by MOCVD and RF sputtering
| DE95-007146 | p 3229 N95-33636
Novel ferroelectric heterostructures for high-density DRAMS
| AD-A294517 | p 3199 N95-34477
Multilayer optics for soft x-rays
| AD-A295030 | p 3219 N95-34791
The growth of ultrathin epitaxial intermetallic films
| AD-A295037 | p 3232 N95-34795
Use of D2 to elucidate OMVPE growth mechanisms
| AD-A294999 | p 3233 N95-34820

EPOXY MATRIX COMPOSITES
Response and failure of thick composite rings subjected to uniform external hydrostatic pressure or radial contraction p 3064 N95-33326

EQUATIONS OF MOTION
Linear orbit parameters for the exact equations of motion
| DE95-011567 | p 3210 N95-32414
Diagnosis of frontogenesis of Meiyu front
| AD-A294043 | p 3158 N95-34491

EQUATIONS OF STATE
Nonlinear symmetric stability of planetary atmospheres
| DE95-012133 | p 3248 N95-33390

EQUIPMENT SPECIFICATIONS
Grayling 2 information base for generation of synthetic thermal infrared scenes
| AD-A294956 | p 3100 N95-34578

EQUIVALENCE
Inversion of electron-water elastic scattering data
| DE95-619323 | p 3204 N95-32623

EQUIVALENT CIRCUITS
Minimum wakefield achievable by waveguide damped cavity
| DE95-012100 | p 3095 N95-32616

ERGOMETERS
Bicycle ergometer instrumentation to determine muscle and bone forces during exercise p 3176 N95-32428

EROSION
Summary report for ITER Task No. T226B: Evaluation of ITER disruption erosion
| DE95-010402 | p 3219 N95-32401
Water model tests on the Allison T56 series 3 combustion system
| DSTO-TR-0139 | p 3054 N95-33250
A conflict of water and fire: Remote sensing imagery of the Unkaret Volcanic Field, Grand Canyon, Arizona p 3117 N95-33795

ERROR ANALYSIS
A posteriori pointwise error estimates for the boundary element method
| DE95-008099 | p 3194 N95-32388
FH and DS spread-spectrum systems in interference-limited HF channels: A comparison
| PB95-211439 | p 3098 N95-33230
Enhanced stress projections for error estimation and a singular floating node element for static and dynamic fracture p 3064 N95-33463
An improved spectral calibration requirement for AVIRIS p 3117 N95-33752
An object-oriented decomposition of the adaptive-hp finite element method
| DE95-012142 | p 3186 N95-33852
Uncertainty analysis using stochastic finite elements p 3196 N95-34803

ERROR CORRECTING CODES
Accuracy enhancement in optical computing
| AD-A294958 | p 3219 N95-34579

ERROR SIGNALS
Method and apparatus for locking laser wavelength to an atomic transition
| AD-D017425 | p 3120 N95-34619

ERRORS
Off-training-set error for the Gibbs and the Bayes optimal generalizers
| DE95-006344 | p 3187 N95-32375
A posteriori pointwise error estimates for the boundary element method
| DE95-008099 | p 3194 N95-32388
Beam-based optical tuning of the Final Focus Test Beam
| DE95-012097 | p 3215 N95-32658
The 1994 TIMS airborne calibration experiment: Castaic Lake, California p 3117 N95-33797
Evaluation of conductive, radiative, chemical, and convective heat transfer in complex systems using a fast-running, implicit, lumped-capacitance formulation
| DE95-011889 | p 3111 N95-33837

ESCHERICHIA
Inactivation, DNA double strand break induction and their rejoining in bacterial cells irradiated with heavy ions p 3161 N95-32724

ESTERS
Environmental evaluation of lactates as cleaning agents
| PB95-214854 | p 3067 N95-32615
Phthalic acid esters used as plastic additives. Volume 1: Ecotoxicological risk assessment. Volume 2: Comparisons of toxicological effects
| PB95-211280 | p 3084 N95-33329

ESTIMATING
A posteriori pointwise error estimates for the boundary element method
| DE95-008099 | p 3194 N95-32388
Estimation of spatially restricted LET using track structure models p 3161 N95-32722

ETALONS
Temporal dynamics of the multi-frequency spectrum generated by self-phase modulation of two frequencies in single-mode fiber
| DE95-010920 | p 3119 N95-33703

ETCHING
High rate dry etching of GaN, AlN and InN in ECR Cl2/CH4/H2/Ar plasmas
| DE95-011872 | p 3223 N95-33412
Characterization of DuPont 9015, aqueous processable dry film photoresist for printed wiring boards
| DE95-011239 | p 3103 N95-33864
Si-device-related interface research
| AD-A293587 | p 3076 N95-34615

ETHANE
The relationship of chemical structure to supercritical-fluid solubility and to cosolvent-modifier properties: A literature review
| AD-A294933 | p 3076 N95-34599

ETHERS
Testing of a carpet catalyst
| PB95-208492 | p 3068 N95-33242
Risk assessment of polybrominated diphenyl ethers
| PB95-211306 | p 3073 N95-33330
From liquid crystal polymers containing crown ethers to tapered building blocks containing crown ethers which self-assemble into tubular supermolecules
| AD-A294359 | p 3086 N95-34361

ETHYL ALCOHOL
The 17th Symposium on Biotechnology for Fuels and Chemicals
| DE95-004054 | p 3150 N95-33225

EUCLIDEAN GEOMETRY
Speaker identification using the two-dimensional cepstrum transform
| AD-A294204 | p 3099 N95-34304

EUKARYOTES
Heavy ion action on single cells: Cellular inactivation capability of single accelerated heavy ions p 3162 N95-32729

EULER EQUATIONS OF MOTION
Users' manual for LEHGC: A Lagrangian-Eulerian finite-element model of HydroGeoChemical transport through saturated-unsaturated media. Version 1.0
| DE95-010513 | p 3179 N95-32543
Special publication of National Aerospace Laboratory
| NAL-SP-27 | p 3034 N95-34505
A study on the convergence of a 3-D Euler code for cascade flow calculations p 3034 N95-34508
A flux splitting scheme with high-resolution and robustness for discontinuities p 3036 N95-34518
Effect of schemes on numerical simulations of shock wave reflection p 3038 N95-34531
Role of computational fluid dynamics in aeronautical engineering. Number 12: Formulation and verification of uni-particle upwind schemes for the Euler equations p 3039 N95-34540
Numerical analysis around the whole SST configuration p 3039 N95-34541
Direct analysis of transonic rotor noise with CFD technique p 3040 N95-34549
Numerical simulation of aerodynamic problems in high speed railways, part 2 p 3041 N95-34554
Upwind schemes for the two-dimensional Euler equations p 3042 N95-34559

EULER-LAGRANGE EQUATION
A survey of parametrized variational principles and applications to computational mechanics
| NASA-CR-199041 | p 3180 N95-32766

EUROPE
HYBRID2: A versatile model of the performance of hybrid power systems
| DE95-004062 | p 3148 N95-32551
The successful management of programs for human factors certification of advanced aviation technologies p 3175 N95-34780
Improving air traffic control: Proving new tools or approving the joint human-machine system? p 3176 N95-34783

EUROPEAN SPACE AGENCY
ESA Bulletin, Number 82 p 3252 N95-32538
European Space Agency 1994 annual report p 3252 N95-32805

EUROPEAN SPACE PROGRAMS
ESA Bulletin, Number 82 p 3252 N95-32538

EUTROPHICATION
The CE-QUAL-ICM three-dimensional eutrophication model, release version 1.0
| AD-A294258 | p 3160 N95-34461

EVANESCENCE
Doppleron resonances in the diffraction of atoms by an evanescent field
| DE95-619190 | p 3204 N95-32622

EVAPORATION
Analysis of evaporation in laser welding
| REPT-2207 | p 3090 N95-32987
Thermocapil'ary flow with evaporation and condensation and its effect on liquid retention in low-g fluid acquisition devices p 3109 N95-33256

EXCIMER LASERS
Highly doped p-ZnTe films and quantum well structures grown by nonequilibrium pulsed laser ablation
| DE95-012885 | p 3232 N95-34799

EXCITATION
Magnetic excitations in a random exchange system Fe(x)Mn(1-x)TiO3
| DE95-006626 | p 3225 N95-32377
The fully correlated two-electron problem on a numerical lattice
| DE95-010280 | p 3205 N95-32650
The mean lifetimes of the 2p(sigma) lowest bound state of HeH(2+) and its isotopes
| DE95-010812 | p 3206 N95-32966
Measurements of cross sections and resonance structures following electron-impact excitation/ionization of Na-like Kr and Xe
| DE95-011731 | p 3230 N95-34438
Structure and dynamics of excited atoms
| AD-A294997 | p 3209 N95-34819

EXCITONS
Technical support in the area of theoretical support of nuclear preequilibrium
| DE95-011617 | p 3212 N95-32960

EXHAUST EMISSION
Alternative catalyst and exhaust gas sensor work at Argonne National Laboratory
| DE95-007138 | p 3152 N95-32553
The next generation of automobile emissions reduction: Innovative control of off-cycle emissions
| DE95-004057 | p 3153 N95-32809

EXHAUST GASES
Alternative catalyst and exhaust gas sensor work at Argonne National Laboratory
| DE95-007138 | p 3152 N95-32553

EXPERIMENT DESIGN
A fundamental study of smoldering with emphasis on experimental design for zero-G
| NASA-CR-198378 | p 3089 N95-32929
Using photothermal deflection techniques for studying the attenuations of guided waves propagated in optical thin films
| AD-A294203 | p 3217 N95-34303
The development of a distributed computing environment for the design and modeling of plasma spectroscopy experiments
| DE95-011725 | p 3183 N95-34813

EXPERIMENTATION
STS-42 mission highlights resource tape. Part 1 of 2
| NASA-TM-110838 | p 3058 N95-34280

STS-42 mission highlights resource tape. Part 2 of 2
[NASA-TM-110840] p 3058 N95-34281

EXPERT SYSTEMS

An original numerical method for autonomous navigation p 3044 N95-32495

Industrial and Engineering Applications of Artificial Intelligence and Expert Systems: Invited and additional papers
[DSTO-GD-0051] p 3188 N95-32995

An efficient inference engine for interactive fault diagnosis in a helpdesk application
p 3189 N95-33000

Induction of dependency structures from data and its application to ozone prediction p 3190 N95-33003

HOTQUA: An expert system prototype for quality monitoring in a rolling mill p 3190 N95-33004

Expert systems and artificial intelligence applications in engineering design and inspection p 3190 N95-33008

System of experts for intelligent data management (SEIDAM) p 3240 N95-34226

Knowledge-based assistance for science visualization and analysis using large distributed databases
p 3241 N95-34227

Development of an expert data reduction assistant
p 3242 N95-34234

A Spatial Analysis and Modeling System (SAMS) for environment management p 3243 N95-34239

DataHub: Science data management in support of interactive exploratory analysis p 3243 N95-34241

Towards friendlier user interfaces for expert systems
[AD-A294056] p 3192 N95-34467

SSME Post Test Diagnostic System: Systems Section
[NASA-CR-198375] p 3061 N95-34625

EXPLOSIONS

Gasdynamic model of turbulent combustion in an explosion
[DE95-010267] p 3074 N95-33627

EXPLOSIVES

Aviation security: Development of new security technology has not met expectations. Report to Congressional requesters
[GAO/RCED-94-142] p 3046 N95-32885

The oxidation of energetic materials in supercritical water
[DE95-010888] p 3088 N95-33702

EXPOSURE

Image analysis used to count and measure etched tracks from ionizing radiation p 3210 N95-32424

Study of the space environmental effects on spacecraft engineering materials
[NASA-CR-199090] p 3066 N95-32581

Multimedia Environmental Pollutant Assessment System (MEPAS(trademark)): Exposure pathway and human health impact assessment models
[DE95-012763] p 3155 N95-34441

EXTRACTION

Three-dimensional natural convection of a fluid with temperature-dependent viscosity in an enclosure with localized heating
[DE95-002606] p 3106 N95-32387

Visualization methods for high-resolution, transient, 3-D, finite element situations
[DE95-009479] p 3179 N95-32390

COBRA accelerator for Sandia ICF diode research at Cornell University
[DE95-011018] p 3101 N95-32578

The relationship of chemical structure to supercritical-fluid solubility and to cosolvent-modifier properties: A literature review
[AD-A294933] p 3076 N95-34599

EXTRAGALACTIC RADIO SOURCES

Compton Observatory observations of clusters of galaxies and extragalactic radio sources
[NASA-CR-189431] p 3246 N95-33261

EXTRAPOLATION

Underwater acoustic field extrapolation: Theory and sensitivity analysis
[AD-A294925] p 3201 N95-34595

EXTRATERRESTRIAL RADIATION

Single event and TREE latchup mitigation for a star tracker sensor: An innovative approach to system level latchup mitigation
[DE95-010331] p 3059 N95-32593

EXTREME ULTRAVIOLET RADIATION

Multilayer optics for soft x-rays
[AD-A295030] p 3219 N95-34791

EXTREMELY HIGH FREQUENCIES

A 75 watt, 59 to 64 GHz space TWT
[NASA-CR-195450] p 3104 N95-33915

EXTRUDING

The 3D metal forming applications of ALE techniques
[DE95-011745] p 3080 N95-33653

EYE (ANATOMY)

Ultrashort pulse laser effects in the primate eye
[AD-A295024] p 3164 N95-34789

F

F STARS

Beryllium and Boron abundances in population II stars
[NASA-CR-189434] p 3247 N95-33262

F-15 AIRCRAFT

An Electronic Workshop on the Performance Seeking Control and Propulsion Controlled Aircraft Results of the F-15 Highly Integrated Digital Electronic Control Flight Research Program
[NASA-TM-104278] p 3050 N95-33009

An overview of integrated flight-propulsion controls flight research on the NASA F-15 research airplane
p 3051 N95-33010

Performance seeking control program overview
p 3051 N95-33011

F-15 propulsion system p 3051 N95-33012

PSC algorithm description p 3051 N95-33013

PSC implementation and integration
p 3051 N95-33014

Minimum fuel mode evaluation p 3051 N95-33015

Minimum fan turbine inlet temperature mode evaluation p 3052 N95-33016

Maximum thrust mode evaluation
p 3052 N95-33017

Performance seeking control excitation mode
p 3052 N95-33019

Performance seeking control (PSC) for the F-15 highly integrated digital electronic control (HIDEC) aircraft
p 3053 N95-33020

Propulsion Controlled Aircraft design and development
p 3053 N95-33022

Flight test of a propulsion controlled aircraft system on the NASA F-15 airplane p 3049 N95-33023

Dynamic ground effects flight test of the NASA F-15 aircraft p 3049 N95-33024

Design challenges encountered in the F-15 PCA flight test program p 3049 N95-33025

F-16 AIRCRAFT

Application of advanced safety technique to ring laser gyro inertial navigation system integration
p 3048 N95-33140

F-18 AIRCRAFT

Report to the Honorable William V. Roth, Jr., US Senate. Naval aviation: F/A-18 E/F acquisition strategy
[GAO/NSIAD-94-194] p 3197 N95-32886

FABRICATION

Fabrication of improved SiGe alloys for an 18-couple module test
[DE95-010238] p 3060 N95-32396

Investigation of aging effects from high voltage profiles in ceramic phase shifter materials
[AD-A289985] p 3082 N95-32694

Development of silicon drift detectors for strangeness measurements
[DE95-012366] p 3208 N95-33380

Thin-film rechargeable lithium batteries
[DE95-008975] p 3103 N95-33697

Ramp-rate sensitivity of SSC dipole magnet prototypes
[DE95-011162] p 3214 N95-33720

Characterization of DuPont 9015, aqueous processable dry film photoresist for printed wiring boards
[DE95-011239] p 3103 N95-33864

Interfacial reactions during the liquid infiltration of titanium matrix composites p 3081 N95-34252

Inertial confinement fusion target component fabrication and technology development support
[DE95-011655] p 3224 N95-34436

Fabrication of optical channel waveguides in the GaAs/AlGaAs system by MeV ion beam bombardment
[DE95-008973] p 3218 N95-34480

Optical properties of lithium niobate waveguides, and prism coupling for optimizing waveguide fabrication
[AD-A294111] p 3218 N95-34498

Fabrication technology and measurement of coupled quantum dot devices
[AD-A294853] p 3231 N95-34569

Operational amplifier using bipolar junction transistors in silicon-on-sapphire
[AD-D017421] p 3105 N95-34618

FABRY-PEROT INTERFEROMETERS

A dual, parallel cavity Fabry-Perot interferometer
[DE95-010796] p 3115 N95-32900

A fiber optic strain measurement and quench localization for use in superconducting accelerator dipole magnets
[DE95-012370] p 3215 N95-33381

FADDEEV EQUATIONS

Faddeev calculations of p(mu)+p collisions: Effect of hyperfine splitting on the cross sections
[DE95-007838] p 3203 N95-32583

FAILURE

Shock properties of high-strength ceramics
[DE95-007731] p 3082 N95-32380

Simulation of hypervelocity impact on massively parallel supercomputer
[DE95-007735] p 3184 N95-32383

Response and failure of thick composite rings subjected to uniform external hydrostatic pressure or radial contraction p 3064 N95-33326

Transmittance characteristics of US Army rotary-wing aircraft transparencies
[AD-A295035] p 3049 N95-34793

Resource document for the design of electronic instrument approach procedure displays
[AD-A295108] p 3047 N95-34797

FAILURE MODES

Machinability study of Aermet 100
[DE95-011532] p 3084 N95-33408

FANS (LANDFORMS)

Use of TOPSAR digital elevation data to determine the 3-dimensional shape of an alluvial fan
p 3139 N95-33804

Lithologic controls on AIRSAR signatures of bedrock and alluvium, at Lunar Crater, Nevada
p 3141 N95-33813

FAR FIELDS

Computation of noise radiation from turbofans: A parametric study
[NASA-CR-198359] p 3200 N95-32836

Propagation of spatial solitons generated by Gaussian beams in a non-linear Kerr medium
[IFTR-9/1995] p 3206 N95-32921

FAR INFRARED RADIATION

Advanced far infrared detector and double donor studies in Ge
[DE95-011261] p 3247 N95-33625

FAR ULTRAVIOLET RADIATION

Study of impurity concentrations by VUV spectroscopy on HL-1
[DE95-614186] p 3221 N95-32562

FAST FOURIER TRANSFORMATIONS

Numerical and symbolic algorithms for application specific signal processing
[AD-A294125] p 3100 N95-34749

FAST NEUTRONS

Hydrogen formation in metals and alloys during fusion reactor operation
[DE95-737224] p 3202 N95-32529

FASTENERS

NASA-Wide Fastener Technical Interchange Meeting
[NASA-CP-3308] p 3123 N95-33199

FATIGUE (MATERIALS)

Fatigue properties for the Al-Li alloy 2090, part 3
[PB95-214532] p 3078 N95-32614

Enhanced stress projections for error estimation and a singular floating node element for static and dynamic fracture p 3064 N95-33463

Fatigue damage estimate comparisons for northern European and US wind farm loading environments
[DE95-011061] p 3150 N95-33706

FATIGUE TESTING MACHINES

Operations manual for a compact electromechanical fatigue testing machine
[DSTO-GD-0036] p 3115 N95-32927

FAULT DETECTION

Modal identification and its applications to damage detection in vibrating structures p 3126 N95-32920

Thermographic imaging for high-temperature composite materials: A defect detection study
[NASA-TM-106950] p 3125 N95-33209

FAULT TOLERANCE

A highly reliable, high performance open avionics architecture for real time Nap-of-the-Earth operations
p 3044 N95-32497

Single event and TREE latchup mitigation for a star tracker sensor: An innovative approach to system level latchup mitigation
[DE95-010331] p 3059 N95-32593

Image compression scheme for network transmission
[AD-A294959] p 3182 N95-34580

Analysis of safety requirements in the context of system faults and human errors
[PB95-236105] p 3171 N95-34658

FEASIBILITY

Feasibility survey on international cooperation for high efficiency energy conversion technology in fiscal 1993
[DE95-769804] p 3148 N95-32546

On the feasibility of using smoothed particle hydrodynamics for underwater explosion calculations
[DE95-008799] p 3106 N95-32587

Design of deepwater pipelines
[PB95-215109] p 3095 N95-33244

Read/write module for high capacity memory disk
[AD-A294946] p 3178 N95-34745

FEASIBILITY ANALYSIS

The concept of the space system based on the Rocket launch vehicle of light-weight class for direct sounding of large-scale natural hazards p 3057 N95-33128

A novel approach to increasing cocaine detection confidence utilizing ion mobility spectrometry
p 3072 N95-33283

FEDERAL BUDGETS
Report to Congressional Committees. B-2 bomber: Cost to complete 20 aircraft is uncertain
| GAO/NSIAD-94-217 | p 3033 N95-32782
Army aviation: Modernization strategy needs to be reassessed. Report to Congressional requestors
| GAO/NSIAD-95-9 | p 3033 N95-32783
Report to the Chairman, Subcommittee on Transportation and Related Agencies, Committee on Appropriations, US Senate. Airport Improvement Program: Reliever airport set-aside funds could be redirected
| GAO/RCED-94-226 | p 3055 N95-32786
Space Station: Estimated total US funding requirements. Report to Congressional Requesters
| GAO/NSIAD-95-163 | p 3058 N95-32884
Annual report to the Chairman, House and Senate Committees on Appropriations. Status of open recommendations: Improving operations of federal departments and agencies
| GAO/OP-94-1 | p 3236 N95-32887
Report to the Chairman, Subcommittee on Transportation and Related Agencies, Committee on Appropriations, US Senate. Airport Improvement Program: The Military Airport Program has not achieved intended impact
| GAO/RCED-94-209 | p 3056 N95-32888
Budget estimates: Fiscal year 1994. Volume 1: Agency summary
| NASA-TM-110815 | p 3244 N95-33069
Budget estimates: Fiscal year 1994. Volume 2: Construction of facilities
| NASA-TM-110816 | p 3245 N95-33081
Budget estimates: Fiscal year 1994. Volume 3: Research and program management
| NASA-TM-110817 | p 3245 N95-33082

FEEDBACK
Fast feedback for linear colliders
| DE95-012099 | p 3211 N95-32608
Globally stable feedback laws for near-minimum-fuel and near-minimum-time pointing maneuvers for a landmark-tracking spacecraft
| DE95-009867 | p 3191 N95-33214

FEEDBACK CONTROL
Fast feedback for linear colliders
| DE95-012099 | p 3211 N95-32608
Popov theory based approach to digital H(infinity)-control with measurement-feedback for Pritchard-Salamon systems
| PB95-218111 | p 3192 N95-33399
Nonholonomic control of coupled spatial multibody systems p 3192 N95-33604
Development of tokamak experiment technology: A study on the nuclear fusion reactor
| DE95-614255 | p 3223 N95-33619
Nonlinear adaptive control of highly maneuverable high performance aircraft p 3192 N95-33712
Identification of flexible structures under closed loop control p 3192 N95-33713
A robust control system for exact trajectory tracking
p 3192 N95-33714
Adaptive differential visual feedback for uncalibrated hand-eye coordination and motor control
| AD-A293607 | p 3171 N95-34616

FEEDERS
A procedural framework for designing linear orienting devices p 3181 N95-33325

FEEDFORWARD CONTROL
Multi-layer holographic bifurcative neural network system for real-time adaptive EOS data analysis
p 3148 N95-34233

FEMALES
G-protection capabilities and current G-protection issues p 3169 N95-34060

FERRITES
Improved L-C resonant decay technique for Q measurement of quasilinear power inductors: New results for MPP and ferrite powdered cores
| NASA-CR-198373 | p 3103 N95-33874

FERROELECTRICITY
Mechanism(s) for the suppression of the switchable polarization in PZT and BaTiO3
| DE95-009589 | p 3226 N95-32590
Epitaxial Pb(Zr(x)Ti(1-x))O3/SrRuO3 (x = 0, 0.35, 0.65) multilayer thin films on SrTiO3(100) and MgO(100) prepared by MOCVD and RF sputtering
| DE95-008288 | p 3226 N95-32598
Investigation of aging effects from high voltage profiles in ceramic phase shifter materials
| AD-A289985 | p 3082 N95-32694
Comparison of lead zirconate titanate thin films on ruthenium oxide and platinum electrodes
| DE95-617597 | p 3082 N95-32710
Novel ferroelectric heterostructures for high-density DRAMS
| AD-A294517 | p 3199 N95-34477

FERROMAGNETIC MATERIALS
Measurement and modelling of structure sensitive magnetic properties of material
| DE95-010128 | p 3080 N95-33699
Device for dampening vibratory motion
| AD-D017490 | p 3127 N95-34427

FEYNMAN DIAGRAMS
The (pi)(yields)e(nu)(gamma) decay in chiral perturbation theory
| DE95-619269 | p 3206 N95-32806

FIBER COMPOSITES
Models for predicting damage evolution in metal matrix composites subjected to cyclic loading
| DE95-007734 | p 3077 N95-32382
A numerical analysis of fracture and high temperature creep characteristics of composites with discontinuous ductile reinforcements
| DE95-010236 | p 3062 N95-32395
Micromechanics of fiber-reinforced ceramic composites p 3063 N95-32775
Wear resistant composite structure of vitreous carbon containing convoluted fibers
| DE95-011463 | p 3063 N95-33062
Micromechanics of composites with shape memory alloy fibers in uniform thermal fields
| NASA-TM-107011 | p 3063 N95-33210
A new approach to fracture of layered fibrous composites: Experiments and analysis
p 3063 N95-33309
Low velocity impact damage in carbon fiber/PEEK composite laminates
| ISBN-0-315-86546-6 | p 3065 N95-33710
Inclusion models of tensile fracture in fiber-reinforced brittle-matrix composites p 3065 N95-33721
Interfacial reactions during the liquid infiltration of titanium matrix composites p 3081 N95-34252
Fiber coatings for brittle matrix composites
p 3065 N95-34808

FIBER OPTICS
Conference proceedings of mathematical methods in electromagnetic theory
| AD-A291165 | p 3097 N95-32797
A fiber-optic connector
| AD-D017424 | p 3215 N95-32923
A fiber optic strain measurement and quench localization for use in superconducting accelerator dipole magnets
| DE95-012370 | p 3215 N95-33381
Feasibility of fullerene thin films for high-speed all-optical switching
| DE95-011735 | p 3085 N95-33409
Method for making fiber-optic bundle collimator assembly
| AD-D017486 | p 3216 N95-34288
Quantum cylinder fiber light amplifier
| AD-A294197 | p 3217 N95-34300

FIBER PULLOUT
Adhesion of novel high-performance polymers to carbon fibers: Fiber surface treatment, characterization, and microbond single fiber pull-out test p 3085 N95-34282

FIBER-MATRIX INTERFACES
Inclusion models of tensile fracture in fiber-reinforced brittle-matrix composites p 3065 N95-33721
Adhesion of novel high-performance polymers to carbon fibers: Fiber surface treatment, characterization, and microbond single fiber pull-out test p 3085 N95-34282
Fiber coatings for brittle matrix composites
p 3065 N95-34808

FIELD EFFECT TRANSISTORS
Novel field effect transistors for low power electronics
| AD-A294221 | p 3105 N95-34458
Development of thin film diamond based integrated circuit technology
| AD-A294519 | p 3231 N95-34478

FIELD EMISSION
The JPL Field Emission Spectrometer
p 3117 N95-33794

FIELD OF VIEW
SeaWiFS technical report series. Volume 22: Prelaunch acceptance report for the SeaWFS radiometer
| NASA-TM-104566-VOL-22 | p 3159 N95-32672
SeaWiFS technical report series. Volume 31: Stray light in the SeaWiFS radiometer
| NASA-TM-104566-VOL-31 | p 3159 N95-32833

FIELD STRENGTH
Atoms in strong fields
| AD-A294589 | p 3209 N95-34423

FIELD THEORY (PHYSICS)
Transparent potential perturbations on lattices and in the periodical structures. Elements of the Qualitative Theory of Wave Motion Over the Channels
| DE95-623602 | p 3225 N95-32480
Cosmological consequences of topological and geometric phenomena in field theories
p 3234 N95-33313
Nonequilibrium problems in Quantum Field Theory and Schwinger's closed time path formalism
| DE95-012056 | p 3234 N95-33388

FIGHTER AIRCRAFT
Current Concepts on G-Protection Research and Development
| AGARD-LS-202 | p 3168 N95-34050
Selection and training of MiG-29 and future fighter pilots p 3166 N95-34059

FIGURE OF MERIT
Fabrication of improved SiGe alloys for an 18-couple module test
| DE95-010238 | p 3060 N95-32396
Feasibility of fullerene thin films for high-speed all-optical switching
| DE95-011735 | p 3085 N95-33409
Multilayer thermoelectric films: A strategy for the enhancement of ZT
| DE95-011535 | p 3081 N95-34482

FILM COOLING
Transport phenomena in subsonic and supersonic flows in a duct with mass injection p 3108 N95-32934
Numerical simulation of film cooling effect around axisymmetric body in hypersonic flow field
p 3037 N95-34526

FILM THICKNESS
Experimental and numerical analysis of controlled impinging liquid jets p 3109 N95-33257
Epitaxial Pb(Zr(0.40)Ti(0.60))O3/SrRuO3 and PbTiO3/SrRuO3 multilayer thin films prepared by MOCVD and RF sputtering
| DE95-007146 | p 3229 N95-33636

FINANCIAL MANAGEMENT
Budget estimates: Fiscal year 1994. Volume 1: Agency summary
| NASA-TM-110815 | p 3244 N95-33069
NASA directives master list and index
| NHB-1410.13O | p 3238 N95-33249

FINE STRUCTURE
Size, shape, and crystallinity of luminescent structures in oxidized Si nanoclusters and H-passivated porous Si
| DE95-012322 | p 3229 N95-33628

FINITE DIFFERENCE THEORY
Differencing the diffusion equation on unstructured meshes in 2-D
| DE95-010410 | p 3195 N95-32559
Direct and large eddy simulations of three dimensional round turbulent jets p 3111 N95-33709
Discrete modeling of optical pulse propagation in nonlinear media
| DE95-011515 | p 3216 N95-34020
Modeling seismic wave propagation in heterogeneous materials using finite elements p 3156 N95-34283
Numerical study on stabilization of a diffusion flame over a flat plate p 3035 N95-34510
Numerical simulation of film cooling effect around axisymmetric body in hypersonic flow field
p 3037 N95-34526
Direct analysis of transonic rotor noise with CFD technique p 3040 N95-34549
A simulation of damping process of pendulum motion due to aerodynamic forces p 3041 N95-34551
The 11th Annual Review of Progress in Applied Computational Electromagnetics, volume 1
| AD-A294850 | p 3100 N95-34566
The 11th Annual Review of Progress in Applied Computational Electromagnetics, volume 2
| AD-A294851 | p 3100 N95-34567
High order accuracy computational methods in aerodynamics using parallel architectures
| AD-A294167 | p 3042 N95-34763
QMR methods in computational fluid dynamics
| DE95-012889 | p 3113 N95-34800

FINITE ELEMENT METHOD
Models for predicting damage evolution in metal matrix composites subjected to cyclic loading
| DE95-007734 | p 3077 N95-32382
Three-dimensional natural convection of a fluid with temperature-dependent viscosity in an enclosure with localized heating
| DE95-002606 | p 3106 N95-32387
Visualization methods for high-resolution, transient, 3-D, finite element situations
| DE95-009479 | p 3179 N95-32390
The future of finite element applications on massively parallel supercomputers
| DE95-011659 | p 3184 N95-32415
Certification of a hybrid parameter model of the fully flexible Shuttle Remote Manipulator System
p 3125 N95-32421

Users' manual for LEHGC: A Lagrangian-Eulerian finite-element model of HydroGeoChemical transport through saturated-unsaturated media. Version 1.0
[DE95-010513] p 3179 N95-32543
Predicted operating conditions for maintaining mode purity in the 1MW 200 GHz FOM Free Electron Maser
[DE95-010795] p 3117 N95-32571
Evaluation of a bridge using simplified element modeling
[DE95-006281] p 3126 N95-32670
Numerical simulation of heat and mass transport during space crystal growth with MEPHISTO
[NASA-TM-107015] p 3089 N95-32718
A three-dimensional nonlinear Timoshenko beam based on the core-congruential formulation
[NASA-CR-199042] p 3180 N95-32765
A survey of parametrized variational principles and applications to computational mechanics
[NASA-CR-199041] p 3180 N95-32766
Conference proceedings of mathematical methods in electromagnetic theory
[AD-A291165] p 3097 N95-32797
Simulation of patch and slot antennas using FEM with prismatic elements and investigations of artificial absorber mesh termination schemes
[NASA-CR-198974] p 3097 N95-32822
Computation of noise radiation from turbofans: A parametric study
[NASA-CR-198359] p 3200 N95-32836
Influence of non classical friction on the rubbing and impact behavior of rotor dynamic systems
p 3122 N95-32906
Parallel finite element methods and iterative solution techniques for viscous incompressible flows
p 3108 N95-33031
Design and analysis of transient nonlinear coupled systems p 3199 N95-33292
Enhanced stress projections for error estimation and a singular floating node element for static and dynamic fracture p 3064 N95-33463
The 3D metal forming applications of ALE techniques
[DE95-011745] p 3080 N95-33653
Low velocity impact damage in carbon fiber/PEEK composite laminates
[ISBN-0-315-86546-6] p 3065 N95-33710
High-order Taylor-Galerkin and adaptive hp-methods for hyperbolic systems with application to structural acoustics p 3200 N95-33719
Fan noise prediction assessment
[NASA-CR-195051] p 3200 N95-33831
An application of mechanical leverage to microactuation
[DE95-011883] p 3124 N95-33836
Evaluation of conductive, radiative, chemical, and convective heat transfer in complex systems using a fast-running, implicit, lumped-capacitance formulation
[DE95-011889] p 3111 N95-33837
An object-oriented decomposition of the adaptive-hp finite element method
[DE95-012142] p 3186 N95-33852
Modeling seismic wave propagation in heterogeneous materials using finite elements p 3156 N95-34283
Analysis and finite element approximation of an optimal shape control problem for the steady-state Navier-Stokes equations p 3112 N95-34285
Development of local shear bands and orientation gradients in fcc polycrystals
[DE95-012072] p 3231 N95-34450
The 11th Annual Review of Progress in Applied Computational Electromagnetics, volume 2
[AD-A294851] p 3100 N95-34567
High order accuracy computational methods in aerodynamics using parallel architectures
[AD-A294167] p 3042 N95-34763
Uncertainty analysis using stochastic finite elements
p 3196 N95-34803

FINITE VOLUME METHOD

Turbulence models in the Navier-Stokes simulation of airfoil stall
[TRITA-NA-9312] p 3108 N95-33059
Numerical thermal analyses of heat exchangers for the stirling engine application
[NASA-CR-199120] p 3110 N95-33398
Efficient time domain solutions of Maxwell's equations for aerospace systems
[AD-A294019] p 3196 N95-34377
Consistent finite-volume discretization of hydrodynamic conservation laws for unstructured grids
[DE95-011730] p 3112 N95-34437
A variation of the Riemann Problem solution and its application to implicit Godunov's scheme
p 3036 N95-34516
A multigrid incompressible NS solver
p 3036 N95-34517
Numerical simulation of two-dimensional PAR-WIG
p 3040 N95-34548
A simulation of damping process of pendulum motion due to aerodynamic forces p 3041 N95-34551

FIRE EXTINGUISHERS

Foam spread experiments on a water surface
[PB95-211025] p 3083 N95-32962

FIRE FIGHTING

Foam spread experiments on a water surface
[PB95-211025] p 3083 N95-32962

FIRES

Remote sensing of smoke, clouds, and radiation using AVIRIS during SCAR experiments p 3132 N95-33749
Corrosion of fire-damaged aircraft
[AD-A294968] p 3049 N95-34583

FISHES

Hand-portable gas chromatography-ion mobility spectrometer for the determination of the freshness of fish p 3071 N95-33277

FISSION

Physics of the CEM92M Code
[DE95-623579] p 3202 N95-32477

FIXED WINGS

Fixed wing night attack missions: Assessment in a Flight Simulation environment p 3045 N95-32502

FLAME PROPAGATION

Turbulence and spatio-temporal chaos
[DE95-012912] p 3068 N95-33223

FLAME RETARDANTS

Risk assessment of polybrominated diphenyl ethers
[PB95-211306] p 3073 N95-33330

FLAME STABILITY

Numerical study on stabilization of a diffusion flame over a flat plate p 3035 N95-34510

FLAMES

Study on turbulent fluctuations in diffusion flames using laser induced fluorescence
[PB95-214425] p 3068 N95-32812
Observations of surface structure and regression behavior of solid propellant strands burning under narrow gap conditions p 3088 N95-33254

FLAPS (CONTROL SURFACES)

Grid generation around airfoil with a flap using boundary element method p 3041 N95-34552

FLAT PLATES

Bolt preload selection for pulsed-loaded vessel closures
[DE95-006346] p 3121 N95-32376
Numerical study on stabilization of a diffusion flame over a flat plate p 3035 N95-34510
Turbulent solitary wave propagating through wall Boundary Layer p 3041 N95-34555

FLAT SURFACES

Large-eddy simulation of the development of stably-stratified atmospheric boundary layers over cool flat surfaces
[DE95-009574] p 3156 N95-32697

FLEXIBILITY

HYBRID2: A versatile model of the performance of hybrid power systems
[DE95-004062] p 3148 N95-32551
D3-D power supply, design, and development
[DE95-009603] p 3222 N95-32656

FLEXIBLE BODIES

Application of impact dampers in vibration control of flexible structures p 3127 N95-32420
Certification of a hybrid parameter model of the fully flexible Shuttle Remote Manipulator System
p 3125 N95-32421
Identification of flexible structures under closed loop control p 3192 N95-33713

FLEXIBLE SPACECRAFT

A three-dimensional nonlinear Timoshenko beam based on the core-congruential formulation
[NASA-CR-199042] p 3180 N95-32765

FLIGHT CHARACTERISTICS

Proposed incorporation of mission-oriented flying qualities into MIL-STD-1797A
[AD-A294211] p 3055 N95-34306

FLIGHT CLOTHING

Current Concepts on G-Protection Research and Development
[AGARD-LS-202] p 3168 N95-34050
G-protection basis/acceleration physiology
p 3168 N95-34051
Anti-G suits p 3168 N95-34054
Positive pressure breathing for G protection (PBG)
p 3168 N95-34055
The ANVIS head-up display: An analysis of its application to naval helicopters
[AD-A294342] p 3170 N95-34358
OH-58 pilot display unit (PDU) simulated crash tests
[AD-A294049] p 3170 N95-34378
Evaluating the potential for rotation and loss of flight helmets from inertia and impact loads
[AD-A294041] p 3170 N95-34489

FLIGHT CONTROL

Implementation of a Single-Stage-To-Orbit (SSTO) model for stability and control analysis
p 3059 N95-32432
A highly reliable, high performance open avionics architecture for real time Nap-of-the-Earth operations
p 3044 N95-32497
An Electronic Workshop on the Performance Seeking Control and Propulsion Controlled Aircraft Results of the F-15 Highly Integrated Digital Electronic Control Flight Research Program
[NASA-TM-104278] p 3050 N95-33009
An overview of integrated flight-propulsion controls flight research on the NASA F-15 research airplane
p 3051 N95-33010
Performance seeking control program overview
p 3051 N95-33011
PSC implementation and integration
p 3051 N95-33014
Background and principles of throttles-only flight control p 3053 N95-33021
Propulsion Controlled Aircraft design and development
p 3053 N95-33022
Flight test of a propulsion controlled aircraft system on the NASA F-15 airplane p 3049 N95-33023
Design challenges encountered in the F-15 PCA flight test program p 3049 N95-33025
Development and application of the methods for pilot-aircraft system research to the manual control tasks of modern vehicles p 3094 N95-33139
Human piloting factors in the design of control laws for precision landing p 3167 N95-33605
Proposed incorporation of mission-oriented flying qualities into MIL-STD-1797A
[AD-A294211] p 3055 N95-34306
Thermal design of returnable satellites
[AD-A294113] p 3059 N95-34500
User type certification for advanced flight control systems p 3055 N95-34772
A stochastic adaptive control application to flight systems p 3055 N95-34806

FLIGHT CREWS

Animation within a multimedia training system for night vision goggles
[AD-A294095] p 3170 N95-34475
User type certification for advanced flight control systems p 3055 N95-34772
Does human cognition allow Human Factors (HF) certification of advanced aircrew systems?
p 3174 N95-34776

FLIGHT HAZARDS

Report to the Chairman, Subcommittee on Aviation, Committee on Commerce, Science, and Transportation, US Senate. Aviation Safety: FAA can better prepare general aviation pilots for mountain flying risks
[GAO/RCED-94-15] p 3046 N95-32784

FLIGHT INSTRUMENTS

The effects of display location and dimensionality on taxiway navigation
[AD-A294878] p 3047 N95-34570

FLIGHT MANAGEMENT SYSTEMS

Integrated special mission flight management for a flight inspection aircraft p 3049 N95-33145
On the use of the systems approach to certify advanced aviation technologies p 3171 N95-34765
Certification of tactics and strategies in aviation
p 3172 N95-34768

FLIGHT OPERATIONS

Low-Level and Nap-of-the-Earth (NOE) night operations
[AGARD-CP-563] p 3042 N95-32486

FLIGHT PATHS

Implementation of a Single-Stage-To-Orbit (SSTO) model for stability and control analysis
p 3059 N95-32432
Low-Level and Nap-of-the-Earth (NOE) night operations
[AGARD-CP-563] p 3042 N95-32486
A tactical navigation and routeing system for low-level flight p 3044 N95-32494

FLIGHT PLANS

Low-Level and Nap-of-the-Earth (NOE) night operations
[AGARD-CP-563] p 3042 N95-32486

FLIGHT SAFETY

Report to the Chairman, Subcommittee on Aviation, Committee on Commerce, Science, and Transportation, US Senate. Aviation safety: Data problems threaten FAA strides on safety analysis system
[GAO/AIMD-95-27] p 3046 N95-32705
Report to the Chairman, Subcommittee on Aviation, Committee on Commerce, Science, and Transportation, US Senate. Aviation Safety: FAA can better prepare general aviation pilots for mountain flying risks
[GAO/RCED-94-15] p 3046 N95-32784

Application of advanced safety technique to ring laser gyro inertial navigation system integration p 3048 N95-33140
The application of Ada and formal methods to a safety critical engine control system p 3094 N95-33142
Evaluating the potential for rotation and loss of flight helmets from inertia and impact loads
| AD-A294041 | p 3170 N95-34489

FLIGHT SIMULATION
The application of helicopter mission simulation to Nap-of-the-Earth operations p 3044 N95-32496
Fixed wing night attack missions: Assessment in a Flight Simulation environment p 3045 N95-32502
Low-order nonlinear dynamic model of IC engine-variable pitch propeller system for general aviation aircraft
| NASA-TM-107006 | p 3050 N95-32916
Altitude cuing effectiveness of terrain texture characteristics in simulated low-altitude flight
| AD-A294369 | p 3056 N95-34362

FLIGHT SIMULATORS
Fixed wing night attack missions: Assessment in a Flight Simulation environment p 3045 N95-32502
Perceptual dimensions of simulated scenes relevant for visual low-altitude flight
| AD-A294385 | p 3056 N95-34344

FLIGHT TESTS
Flight test of a low-altitude helicopter guidance system with obstacle avoidance capability p 3043 N95-32490
Development and flight testing of an Obstacle Avoidance System for US Army helicopters p 3045 N95-32500
An Electronic Workshop on the Performance Seeking Control and Propulsion Controlled Aircraft Results of the F-15 Highly Integrated Digital Electronic Control Flight Research Program
| NASA-TM-104278 | p 3050 N95-33009
An overview of integrated flight-propulsion controls flight research on the NASA F-15 research airplane p 3051 N95-33010
Performance seeking control program overview p 3051 N95-33011
Minimum fuel mode evaluation p 3051 N95-33015
Minimum fan turbine inlet temperature mode evaluation p 3052 N95-33016
Maximum thrust mode evaluation p 3052 N95-33017
Performance seeking control excitation mode p 3052 N95-33019
Flight test of a propulsion controlled aircraft system on the NASA F-15 airplane p 3049 N95-33023
Dynamic ground effects flight test of the NASA F-15 aircraft p 3049 N95-33024
Design challenges encountered in the F-15 PCA flight test program p 3049 N95-33025
Integrated special mission flight management for a flight inspection aircraft p 3049 N95-33145
Balloon-borne radiometer profiler: Field observations
| DE95-011493 | p 3158 N95-33505
Remote sensing of smoke, clouds, and radiation using AVIRIS during SCAR experiments p 3132 N95-33749
Some inadequacies of the current human factors certification process of advanced aircraft technologies p 3176 N95-34785

FLIGHT TRAINING
Altitude cuing effectiveness of terrain texture characteristics in simulated low-altitude flight
| AD-A294369 | p 3056 N95-34362

FLIP-FLOPS
Optical logic implementation in composite biled/bild circuits
| AD-A294160 | p 3105 N95-34758

FLIR DETECTORS
Multispectral image correlation for air-to-ground targeting p 3043 N95-32489
A helmet mounted display for night missions at low altitude p 3045 N95-32503
SIRPH: Steerable infrared picture on helmet mounted display p 3045 N95-32504

FLOATING POINT ARITHMETIC
Bit-level analysis of an SRT divider circuit
| AD-A294842 | p 3105 N95-34565

FLOW DISTRIBUTION
A nonlinear vortex lattice method for unsteady flow with separated vortex
| DLR-FB-94-32 | p 3106 N95-32787
Asymptotic structure of supersonic turbulent boundary layers p 3107 N95-32898
Numerical simulation of supersonic flow using a new analytical bleed boundary condition
| NASA-CR-198368 | p 3054 N95-33208
Water model tests on the Allison T56 series 3 combustion system
| DSTO-TR-0139 | p 3054 N95-33250
Large eddy simulation of turbulent vortices and mixing layers p 3109 N95-33340
A study of supersonic mixing flow field with ramp injector p 3035 N95-34512
Calculation of supersonic combustion in SCRAMJET engines p 3035 N95-34513
Numerical simulation of film cooling effect around axisymmetric body in hypersonic flow field p 3037 N95-34526
Large scale computing and volume visualization p 3041 N95-34556
An LDV investigation of support structure influence on the flow field near the wingtip of a STOVL configuration in hover
| AD-A294126 | p 3042 N95-34750
Subscale study of engine bellmouth inlet vortices in test cell R1D
| AD-A294993 | p 3113 N95-34818

FLOW EQUATIONS
A flux splitting scheme with high-resolution and robustness for discontinuities p 3036 N95-34518

FLOW MEASUREMENT
New advances in physiological measurements during high-G: Technology p 3165 N95-34057

FLOW REGULATORS
An instrument for gravimetric calibration of flow devices with corrosive gases
| DE95-009700 | p 3116 N95-33206

FLOW STABILITY
On the nonlinear stability of a nearby parallel and a non-unidirectional flow p 3112 N95-34284
Stability of steady state solutions for forced Navier-Stokes equations p 3112 N95-34286
Nonlinear stability of unsteady viscous flow
| AD-A294931 | p 3113 N95-34597

FLOW THEORY
On the nonlinear stability of a nearby parallel and a non-unidirectional flow p 3112 N95-34284

FLOW VELOCITY
Foam spread experiments on a water surface
| PB95-211025 | p 3083 N95-32962

FLOW VISUALIZATION
Subscale study of engine bellmouth inlet vortices in test cell R1D
| AD-A294993 | p 3113 N95-34818

FLUENCE
Solar-geophysical data number 607, March 1995. Part 1 (prompt reports). Data for January, February 1995 and late data
| PB95-216388 | p 3248 N95-32963

FLUID BOUNDARIES
Vorticity in shock-accelerated density-stratified interfaces: An analytical and computational study p 3111 N95-33607

FLUID FILMS
Experimental and numerical analysis of controlled impinging liquid jets p 3109 N95-33257

FLUID FILTERS
Gas chromatography/ion mobility spectrometry as a hyphenated technique for improved explosives detection and analysis p 3071 N95-33278

FLUID FLOW
Laminar heat transfer for power-law fluids in thermal entrance region of annular sector ducts p 3108 N95-33255
Low Reynolds number kappa-epsilon and empirical transition models for oscillatory pipe flow and heat transfer
| NASA-TM-109785 | p 3110 N95-33496
The unique radar scattering properties of silicic lava flows and domes p 3141 N95-33811

FLUID INJECTION
Transport phenomena in subsonic and supersonic flows in a duct with mass injection p 3108 N95-32934

FLUID JETS
Experimental and numerical analysis of controlled impinging liquid jets p 3109 N95-33257
Modeling liquid jet atomization processes
| AD-A294888 | p 3112 N95-34572

FLUID MECHANICS
A comparison of interface tracking methods
| DE95-009481 | p 3111 N95-33698

FLUID POWER
Fluid dynamometer having fluid characteristic power absorption adjustment capability
| AD-D017489 | p 3116 N95-34426

FLUORESCENCE
Development of ultrasensitive spectroscopic analysis technology. Development of atomic spectroscopy technology
| DE95-614352 | p 3086 N95-32566
Characterization of microenvironment polarity and solvent accessibility of polysilsesquioxane xerogels by the fluorescent probe technique
| DE95-011874 | p 3062 N95-33835
Ultrafast near-field scanning optical microscopy (NSOM) of emerging display technology media: Solid state electronic structure and dynamics
| AD-A294879 | p 3218 N95-34571

FLUORIDES
A molecular dynamics investigation of the structural characteristics of amorphous and annealed poly (Vinylidene fluoride) and vinylidene fluoride - trifluoroethylene copolymers
| AD-A294116 | p 3086 N95-34502

FLUORINATION
Elemental fluorine based syntheses of pentafluoro phenyl and other aromatic perfluoropolyether polymers
| AD-A294930 | p 3087 N95-34596

FLUORINE
Electron-electron interaction in the ionization of hydrogenlike projectiles by He
| DE95-010822 | p 3208 N95-33374
Elemental fluorine based syntheses of pentafluoro phenyl and other aromatic perfluoropolyether polymers
| AD-A294930 | p 3087 N95-34596
Surface chemistry of diamond single crystals
| AD-A294150 | p 3232 N95-34755

FLUOROCARBONS
Reactions of trifluoroiodomethane on metal surfaces
| DE95-010122 | p 3078 N95-32638

FLUOROHYDROCARBONS
Thermophysical properties of HCFC alternatives
| DE95-009635 | p 3233 N95-32661

FLUX (RATE)
Laser ablation plume thermalization dynamics in background gases studied by time-resolved imaging, spectroscopic, and ion probe diagnostics
| DE95-010277 | p 3118 N95-33246
The CE-QUAL-ICM three-dimensional eutrophication model, release version 1.0
| AD-A294258 | p 3160 N95-34461

FLUX DENSITY
Peak effect and flux pinning in YBa2Cu3O(7-(delta)) single crystals
| DE95-010126 | p 3228 N95-32959
Design rules and reality check for carbon-based ultracapacitors
| DE95-010575 | p 3103 N95-33640

FLUX DIFFERENCE SPLITTING
A multigrid incompressible NS solver p 3036 N95-34517
A flux splitting scheme with high-resolution and robustness for discontinuities p 3036 N95-34518
Role of computational fluid dynamics in aeronautical engineering. Number 12: Formulation and verification of uni-particle upwind schemes for the Euler equations p 3039 N95-34540

FLUX PINNING
Peak effect and flux pinning in YBa2Cu3O(7-(delta)) single crystals
| DE95-010126 | p 3228 N95-32959

FLUX QUANTIZATION
Turbulent heat flux measurements over the Greenland, Norwegian and Barents seas
| AD-A294129 | p 3157 N95-34751

FOAMS
Foam spread experiments on a water surface
| PB95-211025 | p 3083 N95-32962
Glass science tutorial lecture no. 6: The melting of silicate glasses, a review of selected topics
| DE95-010199 | p 3084 N95-33218

FOCAL PLANE DEVICES
Ricor K506B cryocooler performance during the Clementine mission and ground testing
| DE95-010683 | p 3089 N95-32568

FOCUSING
Three-dimensional ground penetrating radar imaging using synthetic aperture time-domain focusing
| DE95-010731 | p 3095 N95-32569
Targets and magnetic elements for pion collection in muon collider drivers
| DE95-010316 | p 3205 N95-32652

FOILS (MATERIALS)
Analysis of LDEF experiment AO187-2 chemical and isotopic measurements of micrometeoroids by secondary ion mass spectrometry
| NASA-CR-198849 | p 3246 N95-32913

FORBIDDEN TRANSITIONS
Overview of rare K decays
| DE95-012081 | p 3208 N95-33850

FORCED VIBRATION
Evaluation of a bridge using simplified element modeling
| DE95-006281 | p 3126 N95-32670

FORESTS
Studies of microwave scattering and canopy architecture for boreal forests
| NASA-CR-199113 | p 3099 N95-33497

Completing below-ground carbon budgets for pastures, recovering forests, and mature forests of Amazonia
| NASA-CR-199129 | p 3143 N95-33498
Studies of microwave scattering and canopy architecture for boreal forests
| NASA-CR-199114 | p 3099 N95-33726
Evaluation of the photochemical reflectance index in AVIRIS imagery p 3131 N95-33747
Vegetation species composition and canopy architecture information expressed in leaf water absorption measured in the 1000 nm and 2200 spectral region by an imaging spectrometer p 3133 N95-33757
AVIRIS spectral trajectories for forested areas of the Gifford Pinchot National Forest p 3135 N95-33766
Estimation of penetration of forest canopies by Interferometric SAR measurements
p 3141 N95-33814
Regional mapping of forest canopy water content and biomass using AIRSAR images over BOREAS study area p 3142 N95-33815

FORGING
The 3D metal forming applications of ALE techniques
| DE95-011745 | p 3080 N95-33653

FORM FACTORS
The (pi)(yields)e(nu)(gamma) decay in chiral perturbation theory
| DE95-619269 | p 3206 N95-32806

FORMALDEHYDE
Selective methane oxidation over promoted oxide catalysts
| DE95-012319 | p 3075 N95-34021

FORMALISM
The non-relativistic charged Bose gas in a magnetic field. Part 1: Formalism
| DE95-619698 | p 3205 N95-32632
Towards a formalism for program generation 1995
| AD-A294941 | p 3183 N95-34604
Analysis of safety requirements in the context of system faults and human errors
| PB95-236105 | p 3171 N95-34658

FORMAT
Exchange, interpretation, and database-search of ion mobility spectra supported by data format JCAMP-DX
p 3070 N95-33274
An interactive environment for the analysis of large Earth observation and model data sets p 3239 N95-34219
Interactive interface for National Center for Atmospheric Research (NCAR) graphics p 3239 N95-34220

FORMING TECHNIQUES
Rigid bodies for metal forming analysis with NIKE3D
| DE95-011740 | p 3182 N95-33652
The 3D metal forming applications of ALE techniques
| DE95-011745 | p 3080 N95-33653

FORMULATIONS
SAR
| AD-A295020 | p 3101 N95-34788

FORTRAN
Interactive interface for National Center for Atmospheric Research (NCAR) graphics p 3239 N95-34220

FORWARD SCATTERING
Comparison of theoretical predictions with field observations for a simple forward scattering sensor
| AD-A294948 | p 3219 N95-34576

FOSSIL FUELS
United Kingdom minerals yearbook, 1994. Statistical data to 1993
| PB95-207841 | p 3155 N95-32599
World mineral statistics, 1988-92. Production: Exports: Imports
| PB95-208096 | p 3155 N95-32601
World mineral production, 1989-93. Preliminary statistics
| PB95-208104 | p 3156 N95-32603

FOSSILS
Introductions of FFV
| PB95-214656 | p 3088 N95-33332
The nature and fate of natural resins in the geosphere 6: Analysis of fossil resins from Axel Heiberg Island Canadian Arctic
| DE95-012212 | p 3154 N95-33394

FOUR-WAVE MIXING
Observation of intraband coherence in the nonlinear optical response of gallium arsenide
| DE95-011281 | p 3227 N95-32600

FOURIER SERIES
A code to compute the action-angle transformation for a particle in an abritrary potential well
| DE95-012554 | p 3098 N95-33336

FOURIER TRANSFORMATION
Conversion of holes into reducing species on surface modified small-particle TiO2
| DE95-008282 | p 3225 N95-32586
Study of liquid crystal spatial light modulator application to Hadamard transform spectrometer: A fast and accurate decoding method
| AD-A293087 | p 3215 N95-32660
Fast approximation of self-similar network traffic
| DE95-011271 | p 3185 N95-32967
Read/write module for high capacity memory disk
| AD-A294946 | p 3178 N95-34745

FRACTALS
Characterization of microgravity effects on bone structure and strength using fractal analysis
p 3165 N95-32419

FRACTURE MECHANICS
A numerical analysis of fracture and high temperature creep characteristics of composites with discontinuous ductile reinforcements
| DE95-010236 | p 3062 N95-32395
Fracture behavior of shallow cracks in full-thickness clad beams from an RPV wall section
| DE95-009175 | p 3126 N95-32684
Investigation of aging effects from high voltage profiles in ceramic phase shifter materials
| AD-A289985 | p 3082 N95-32694
A new approach to fracture of layered fibrous composites: Experiments and analysis
p 3063 N95-33309
Low velocity impact damage in carbon fiber/PEEK composite laminates
| ISBN-0-315-86546-6 | p 3065 N95-33710
Patterns and perspectives in applied fracture mechanics
| DE95-012844 | p 3127 N95-34442
R-curve behavior of whisker-reinforced ceramic composites
| DE95-012873 | p 3087 N95-34798

FRACTURE STRENGTH
Analytical modeling of the effect of crack depth, specimen size, and biaxial stress on the fracture toughness of reactor vessel steels
| DE95-005886 | p 3125 N95-32373
A numerical analysis of fracture and high temperature creep characteristics of composites with discontinuous ductile reinforcements
| DE95-010236 | p 3062 N95-32395
Fracture toughness and tensile behavior of multi-layer laminated metal composite of Al 6090-25 vol % SiCp and Al 5182
| DE95-011421 | p 3062 N95-32602
Fracture behavior of shallow cracks in full-thickness clad beams from an RPV wall section
| DE95-009175 | p 3126 N95-32684
Evaluation of strength properties of developed SiC/C compositionally gradient graphite materials
| DE95-737271 | p 3063 N95-32711
Micromechanics of fiber-reinforced ceramic composites p 3063 N95-32775
The tensile fracture behavior of the weld metal of BIS 812 EMA and Q1N naval construction steels
| DSTO-RR-0021 | p 3078 N95-32926
Fracture toughness assessment of present and future pressure vessel materials based on Charpy impact energy and yield strength
| AD-A294008 | p 3081 N95-34373
Patterns and perspectives in applied fracture mechanics
| DE95-012844 | p 3127 N95-34442
R-curve behavior of whisker-reinforced ceramic composites
| DE95-012873 | p 3087 N95-34798

FRACTURES (MATERIALS)
The tensile fracture behavior of the weld metal of BIS 812 EMA and Q1N naval construction steels
| DSTO-RR-0021 | p 3078 N95-32926
A new approach to fracture of layered fibrous composites: Experiments and analysis
p 3063 N95-33309

FRACTURING
Models for predicting damage evolution in metal matrix composites subjected to cyclic loading
| DE95-007734 | p 3077 N95-32382
Fifth International Conference on Hyperbolic Problems, Theory, Numerics, Applications: Abstracts
| DE95-008173 | p 3194 N95-32389
A numerical analysis of fracture and high temperature creep characteristics of composites with discontinuous ductile reinforcements
| DE95-010236 | p 3062 N95-32395
Strength, ductility, and fracture mode of ternary FeAl alloys
| DE95-010281 | p 3077 N95-32400
Effect of heat treatment at 1,150 C on creep rupture properties of a Fe3Al-based alloy
| DE95-010295 | p 3077 N95-32527
The tensile fracture behavior of the weld metal of BIS 812 EMA and Q1N naval construction steels
| DSTO-RR-0021 | p 3078 N95-32926
A new approach to fracture of layered fibrous composites: Experiments and analysis
p 3063 N95-33309
Enhanced stress projections for error estimation and a singular floating node element for static and dynamic fracture p 3064 N95-33463

FRAGMENTATION
The role of dynamic experimentation for computation analysis
| DE95-007733 | p 3125 N95-32381
Characterizing the fragmentation ring on witness plates p 3056 N95-32426
Test method to measure resistance towards fragmentation by studded tires
| PB95-211017 | p 3121 N95-32612
Proton-induced fragmentation of carbon at energies below 100 MeV p 3161 N95-32720

FREE CONVECTION
Three-dimensional natural convection of a fluid with temperature-dependent viscosity in an enclosure with localized heating
| DE95-002606 | p 3106 N95-32387
Natural convection at microelectrodes
| AD-A294338 | p 3075 N95-34357

FREE ELECTRON LASERS
Heavy ions acceleration in RF wells of 2-frequency electromagnetic field and in the inverted FEL
| DE95-012439 | p 3214 N95-34439

FREE FLOW
Experimental and numerical analysis of controlled impinging liquid jets p 3109 N95-33257
Numerical studies of turbulent free surface flows and unsteady propeller flows
| AD-A294377 | p 3112 N95-34343

FREQUENCIES
Sum frequency generation of dual-wavelength Nd: YAP laser in LiIO3 crystal
| AD-A293094 | p 3117 N95-32472
General limits on the performance of high power radiators
| DE95-010732 | p 3095 N95-32570
Transverse multibunch instabilities for non-rigid bunches
| DE95-012098 | p 3211 N95-32607
A comparison of risk assessment techniques from qualitative to quantitative
| DE95-011430 | p 3197 N95-33220
Temporal dynamics of the multi-frequency spectrum generated by self-phase modulation of two frequencies in single-mode fiber
| DE95-010920 | p 3119 N95-33703

FREQUENCY CONVERTERS
Multiple-beam pulse shaping and preamplification
| DE95-011738 | p 3216 N95-33651

FREQUENCY MODULATION
Studies of microwave scattering and canopy architecture for boreal forests
| NASA-CR-199113 | p 3099 N95-33497

FREQUENCY RANGES
Mathematical modelling in plasma physics
| AD-A294972 | p 3224 N95-34586

FREQUENCY RESPONSE
Frequency response of a TeO2 slow shear wave acousto-optic cell exposed to radiation
| DE95-009588 | p 3226 N95-32589
Seismic response analysis of soil-structure interaction systems in the time domain
| REPT-2212 | p 3091 N95-32992
Development and application of the methods for pilot-aircraft system research to the manual control tasks of modern vehicles p 3094 N95-33139

FRICTION FACTOR
Flow and heat transfer behavior of non-Newtonian fluids in rectangular ducts p 3107 N95-32907

FRONTS (METEOROLOGY)
Diagnosis of frontogenesis of Meiyu front
| AD-A294043 | p 3158 N95-34491

FRUSTRATION
Magnetic excitations in a random exchange system Fe(x)Mn(1-x)TiO3
| DE95-006626 | p 3225 N95-32377

FUEL CELLS
Feasibility survey on international cooperation for high efficiency energy conversion technology in fiscal 1993
| DE95-769804 | p 3148 N95-32546
Design and testing criteria for bipolar plate materials for PEM fuel cell applications
| DE95-010878 | p 3148 N95-32575
Corrosion of separator plate constituents in molten carbonate
| PB95-214490 | p 3149 N95-32813
Encapsulated dry electrolyte composition for time release into a solute
| AD-D017485 | p 3075 N95-34287
Thin-film electrolytes for reduced temperature solid oxide fuel cells
| DE95-011273 | p 3151 N95-34481

FUEL COMBUSTION
Combustion-acoustic stability analysis for premixed gas turbine combustors
[NASA-TM-107024] p 3050 N95-32931
FUEL CONSUMPTION
Minimum fuel mode evaluation p 3051 N95-33015
FUEL INJECTION
Pop tests of storable biopropellant liquid apogee engine
[NAL-TR-1253] p 3060 N95-32755
The effects of high ambient density on diesel spray penetration and spread
[DE95-010761] p 3124 N95-33701
FUEL PRODUCTION
Catalytic conversion of light alkanes: Proof of concept stage
[DE95-012318] p 3076 N95-34810
FUEL SYSTEMS
Alternative-fuels technology: Natural gas vehicles as a way to curb urban air pollution
[DE95-012216] p 3088 N95-33395
FUELS
The 17th Symposium on Biotechnology for Fuels and Chemicals
[DE95-004054] p 3150 N95-33225
FULL SCALE TESTS
Full-scale hingeless rotor performance and loads
[NASA-TM-110356] p 3048 N95-32699
FULLERENES
Feasibility of fullerene thin films for high-speed all-optical switching
[DE95-011735] p 3085 N95-33409
FUNCTIONAL DESIGN SPECIFICATIONS
Functional requirements analysis and human machine interface specifications for handheld metal detector wands
[DE95-009845] p 3167 N95-32535
A procedural framework for designing linear orienting devices p 3181 N95-33325
FURNACES
Glass science tutorial: Lecture no. 4, commercial glass melting and associated air emission issues
[DE95-007818] p 3082 N95-32384
Numerical simulation of heat and mass transport during space crystal growth with MEPHISTO
[NASA-TM-107015] p 3089 N95-32718
Study on turbulent fluctuations in diffusion flames using laser induced fluorescence
[PB95-214425] p 3068 N95-32812
FUSION REACTORS
Development and trial manufacturing of 1/2-scale partial mock-up of blanket box structure for fusion experimental reactor
[DE95-737184] p 3219 N95-32408
Design concept of a cryogenic distillation column cascade for a ITER scale fusion reactor
[DE95-737185] p 3220 N95-32409
Transport studies of tokamak plasmas in JT-60 device
[DE95-737227] p 3220 N95-32417
Irradiation experiments of low copper A533B steels for reactor pressure vessel tested in JMTR
[DE95-737266] p 3077 N95-32531
Irradiation tests of critical components for remote handling in gamma radiation environment
[DE95-737223] p 3221 N95-32565
Optimized profiles for improved confinement and stability in the DIII-D tokamak
[DE95-009606] p 3222 N95-32756
Development of tokamak experiment technology: A study on the nuclear fusion reactor
[DE95-614255] p 3223 N95-33619
FUZZY SYSTEMS
Monitoring of the cutting operations using fuzzy logic p 3189 N95-32999
An alternative reasoning method p 3189 N95-33001
High-tech controls for energy and environment
[DE95-004011] p 3191 N95-33060

G

GALACTIC BULGE
RR lyrae variable stars in the CCD/Transit instrument survey
[AD-A294138] p 3246 N95-34753
GALACTIC CLUSTERS
Compton Observatory observations of clusters of galaxies and extragalactic radio sources
[NASA-CR-189431] p 3246 N95-33261
GALACTIC EVOLUTION
Beryllium and Boron abundances in population II stars
[NASA-CR-189434] p 3247 N95-33262
GALAXIES
Sinuous oscillations and steady warps of polytropic disks
[DE95-013473] p 3247 N95-34216
RR lyrae variable stars in the CCD/Transit instrument survey
[AD-A294138] p 3246 N95-34753
GALERKIN METHOD
High-order Taylor-Galerkin and adaptive hp-methods for hyperbolic systems with application to structural acoustics p 3200 N95-33719
Modeling seismic wave propagation in heterogeneous materials using finite elements p 3156 N95-34283
GALLIUM
Crystalline-as-deposited CaGa2S4: Ce via low-temperature metal-organic chemical vapor deposition
[DE95-010883] p 3229 N95-33401
GALLIUM ANTIMONIDES
Electron and hole transport in compound semiconductors
[AD-A295003] p 3233 N95-34822
GALLIUM ARSENIDE LASERS
Successful development of first-generation laser device; marking China's optoelectronic technology at world class level
[AD-A294206] p 3217 N95-34305
GALLIUM ARSENIDES
Laser based obstacle warning sensors for helicopters p 3045 N95-32499
Observation of intraband coherence in the nonlinear optical response of gallium arsenide
[DE95-011281] p 3227 N95-32600
High power CO2 laser windows and reflection reducing coatings
[AD-A294217] p 3119 N95-34308
Monolithic diode arrays for quasioptical millimeter wave beam steering
[AD-A294256] p 3100 N95-34460
Low temperature growth of thin films by high kinetic energy supersonic molecular beams
[AD-A294516] p 3086 N95-34476
Fabrication of optical channel waveguides in the GaAs/AlGaAs system by MeV ion beam bombardment
[DE95-008973] p 3218 N95-34480
Fundamental surface chemistry of GaAs OMVPE
[DE95-011606] p 3231 N95-34486
Si-device-related interface research
[AD-A293587] p 3076 N95-34615
The growth of ultrathin epitaxial intermetallic films
[AD-A295037] p 3232 N95-34795
Use of D2 to elucidate OMVPE growth mechanisms
[AD-A294999] p 3233 N95-34820
GALLIUM NITRIDES
High rate dry etching of GaN, AlN and InN in ECR Cl2/CH4/H2/Ar plasmas
[DE95-011872] p 3223 N95-33412
GALLIUM PHOSPHIDES
A study of luminescence and absorption spectra of GaP
[DE95-614122] p 3202 N95-32524
GAMMA RAY ASTRONOMY
Gamma ray imaging of the Crab and Vale regions with the UCR double-Compton telescope p 3245 N95-32837
Time correlations between low and high energy gamma rays from discrete sources
[NASA-CR-199214] p 3248 N95-33916
GAMMA RAY OBSERVATORY
Gamma ray imaging of the Crab and Vale regions with the UCR double-Compton telescope p 3245 N95-32837
GRO: Studies of high energy pulsars with EGRET
[NASA-CR-199130] p 3248 N95-33499
GAMMA RAY SPECTRA
GRO: Studies of high energy pulsars with EGRET
[NASA-CR-199130] p 3248 N95-33499
GAMMA RAY TELESCOPES
Gamma ray imaging of the Crab and Vale regions with the UCR double-Compton telescope p 3245 N95-32837
GAMMA RAYS
Irradiation tests of critical components for remote handling in gamma radiation environment
[DE95-737223] p 3221 N95-32565
Compton Observatory observations of clusters of galaxies and extragalactic radio sources
[NASA-CR-189431] p 3246 N95-33261
CDF results on Z(gamma) production
[DE95-011500] p 3213 N95-33406
Time correlations between low and high energy gamma rays from discrete sources
[NASA-CR-199214] p 3248 N95-33916
GAS CHROMATOGRAPHY
Design concept of a cryogenic distillation column cascade for a ITER scale fusion reactor
[DE95-737185] p 3220 N95-32409
Analysis of samples for the first (1994) OPCW round robin interlaboratory comparison test
[PB95-210324] p 3068 N95-33243
The use of ion mobility spectrometry and gas chromatography/mass spectrometry for the detection of illicit drugs on clandestine records p 3070 N95-33276
Hand-portable gas chromatography-ion mobility spectrometer for the determination of the freshness of fish p 3071 N95-33277
Gas chromatography/ion mobility spectrometry as a hyphenated technique for improved explosives detection and analysis p 3071 N95-33278
Direct analysis of organic priority pollutants by IMS p 3071 N95-33280
Data collection in IMS: It's not as easy as it looks p 3072 N95-33286
Geochemical, genetic, and physiological control of pollutant biodegradation
[AD-A294902] p 3155 N95-34591
GAS DENSITY
The effects of high ambient density on diesel spray penetration and spread
[DE95-010761] p 3124 N95-33701
Numerical simulation of interaction between shock wave and density interface p 3039 N95-34543
GAS DETECTORS
Alternative catalyst and exhaust gas sensor work at Argonne National Laboratory
[DE95-007138] p 3152 N95-32553
GAS DISSOCIATION
Practical improvement of MS-X alpha molecular orbital calculation as applied to dissociation process of CO molecule
[REPT-2206] p 3090 N95-32986
GAS DYNAMICS
PINCA: A scalable parallel program for compressible gas dynamics with nonequilibrium chemistry
[DE95-010581] p 3106 N95-32818
Gasdynamic model of turbulent combustion in an explosion
[DE95-010267] p 3074 N95-33627
GAS EXCHANGE
Modeling soil climate controls on the exchange of trace gases between the terrestrial biosphere and the atmosphere p 3153 N95-33337
GAS EXPANSION
Analysis of evaporation in laser welding
[REPT-2207] p 3090 N95-32987
GAS FLOW
The effect of labyrinth seals on the dynamics of turbomachinery p 3122 N95-32752
An instrument for gravimetric calibration of flow devices with corrosive gases
[DE95-009700] p 3116 N95-33206
Gasdynamic model of turbulent combustion in an explosion
[DE95-010267] p 3074 N95-33627
DSMC method applied for reacting gas flows p 3035 N95-34509
GAS IONIZATION
CDW-EIS calculation of longitudinal momentum distribution in single ionization of helium by Ni(24+) ions
[DE95-010816] p 3207 N95-33241
Determination of Benzene, Toluene, and Xylene by means of an ion mobility spectrometer device using photoionization p 3069 N95-33269
Velocity dependence of ionization and excitation of hydrogen molecules by fast proton impact
[DE95-010818] p 3207 N95-33370
Electron-electron interaction in the ionization of hydrogenlike projectiles by He
[DE95-010822] p 3208 N95-33374
Tokamak ETE circuits: Analysis and specifications
[INPE-5573-PRP/182] p 3224 N95-33873
Atoms in strong fields
[AD-A294589] p 3209 N95-34423
GAS TRANSPORT
Zeolite membranes for gas separations
[DE95-012984] p 3068 N95-33224
GAS TURBINE ENGINES
Combustion-acoustic stability analysis for premixed gas turbine combustors
[NASA-TM-107024] p 3050 N95-32931
The application of Ada and formal methods to a safety critical engine control system p 3094 N95-33142
GAS TURBINES
Static pressure drop by swirling flow of an internal cooling air system through a turbine shaft p 3042 N95-34560
Subscale study of engine bellmouth inlet vortices in test cell R1D
[AD-A294993] p 3113 N95-34818

GAS-ION INTERACTIONS
The pinhole interface for IMS/MS
p 3070 N95-33275
GAS-SOLID INTERACTIONS
Numerical studies of turbulent free surface flows and unsteady propeller flows
[AD-A294377] p 3112 N95-34343
GASKETS
Split gasket attachment method statement of government interest
[AD-D017443] p 3123 N95-32924
GASOLINE
Gasoline from natural gas by sulfur processing
[DE95-010651] p 3087 N95-32563
Determination of Benzene, Toluene, and Xylene by means of an ion mobility spectrometer device using photoionization p 3069 N95-33269
Introductions of FFV
[PB95-214656] p 3088 N95-33332
GATES (CIRCUITS)
Novel field effect transistors for low power electronics
[AD-A294221] p 3105 N95-34458
Fabrication technology and measurement of coupled quantum dot devices
[AD-A294853] p 3231 N95-34569
Optical logic implementation in composite biled/bild circuits
[AD-A294160] p 3105 N95-34758
GAUGE INVARIANCE
The interrelation of a Z(3) gauge theory on flat lattices and a spin-1 BEG model
[DE95-623634] p 3227 N95-32631
Virtual effects of physics beyond the standard model
[DE95-012499] p 3207 N95-33201
GAUGE THEORY
The interrelation of a Z(3) gauge theory on flat lattices and a spin-1 BEG model
[DE95-623634] p 3227 N95-32631
GEAR TEETH
Experimental and analytical assessment of the thermal behavior of spiral bevel gears
[NASA-TM-107009] p 3123 N95-33179
Bending strength model for internal spur gear teeth
[NASA-TM-107012] p 3124 N95-33908
GEARS
Experimental and analytical assessment of the thermal behavior of spiral bevel gears
[NASA-TM-107009] p 3123 N95-33179
Bending strength model for internal spur gear teeth
[NASA-TM-107012] p 3124 N95-33908
GELLED PROPELLANTS
Metallized gelled propellants: Oxygen/RP-1/aluminum rocket combustion experiments
[NASA-TM-107025] p 3088 N95-33876
GELS
Plasma mediated ablation of biological tissues with ultrashort laser pulses
[DE95-011748] p 3164 N95-33654
GENE EXPRESSION
Toxin-mediated transfer and expression of genes in nerve cells
[AD-A290501] p 3164 N95-33200
GENERAL AVIATION AIRCRAFT
Report to the Chairman, Subcommittee on Aviation, Committee on Commerce, Science, and Transportation, US Senate. Aviation Safety: FAA can better prepare general aviation pilots for mountain flying risks
[GAO/RCED-94-15] p 3046 N95-32784
Report to the Chairman, Subcommittee on Transportation and Related Agencies, Committee on Appropriations, US Senate. Airport Improvement Program: Reliever airport set-aside funds could be redirected
[GAO/RCED-94-226] p 3055 N95-32786
Low-order nonlinear dynamic model of IC engine-variable pitch propeller system for general aviation aircraft
[NASA-TM-107006] p 3050 N95-32916
GENERAL OVERVIEWS
A decade of neural networks: Practical applications and prospects
[NASA-CR-198867] p 3188 N95-32659
Review of combustion-acoustic instabilities
[NASA-TM-107020] p 3108 N95-32930
Performance seeking control (PSC) for the F-15 highly integrated digital electronic control (HIDEC) aircraft p 3053 N95-33020
GPS-based navigation for space applications p 3058 N95-33144
GENES
Toxin-mediated transfer and expression of genes in nerve cells
[AD-A290501] p 3164 N95-33200
GENETIC ALGORITHMS
Genetic algorithms as global random search methods
[NASA-CR-199088] p 3188 N95-32767
Genetic algorithm based input selection for a neural network function approximator with applications to SSME health monitoring
[NASA-CR-199089] p 3188 N95-32768
On the virtues of parameterized uniform crossover
[AD-A293985] p 3182 N95-34456
Adaptive strategy selection for concept learning
[AD-A294086] p 3193 N95-34473
Conditions for implicit parallelism
[AD-A294110] p 3193 N95-34497
Is the genetic algorithm a cooperative learner?
[AD-A294112] p 3193 N95-34499
Explanations of empirically derived reactive plans
[AD-A294114] p 3193 N95-34501
GENETIC ENGINEERING
On the virtues of parameterized uniform crossover
[AD-A293985] p 3182 N95-34456
GENETICS
Geochemical, genetic, and physiological control of pollutant biodegradation
[AD-A294902] p 3155 N95-34591
GEOCENTRIC COORDINATES
An improved algorithm for computing altitude dependent Corrected GeoMagnetic coordinates
[AD-A293967] p 3144 N95-34454
GEOCHEMISTRY
Users' manual for LEHGC: A Lagrangian-Eulerian finite-element model of HydroGeoChemical transport through saturated-unsaturated media. Version 1.0
[DE95-010513] p 3179 N95-32543
The nature and fate of natural resins in the geosphere 6: Analysis of fossil resins from Axel Heiberg Island Canadian Arctic
[DE95-012212] p 3154 N95-33394
Geochemical, genetic, and physiological control of pollutant biodegradation
[AD-A294902] p 3155 N95-34591
GEOGRAPHIC INFORMATION SYSTEMS
Incorporating bibliographic information into a spatial data query system for the Savannah River Site
[DE95-010965] p 3238 N95-33402
Remotely sensed indicators of habitat heterogeneity and biological diversity: A preliminary report p 3140 N95-33806
Geographic information system for fusion and analysis of high-resolution remote sensing and ground data p 3240 N95-34224
GEOLOGICAL SURVEYS
Quantitative remote sensing of ammonium minerals, Cedar Mountains, Esmeralda County, Nevada p 3128 N95-33734
Mapping minerals, amorphous materials, environmental materials, vegetation, water, ice and snow, and other materials: The USGS tricorder algorithm p 3130 N95-33742
Discrimination of alkalinity in granitoid Rocks: A potential TIMS application p 3138 N95-33798
GEOLOGY
AVIRIS user's guide p 3117 N95-33759
GEOMAGNETISM
An improved algorithm for computing altitude dependent Corrected GeoMagnetic coordinates
[AD-A293967] p 3144 N95-34454
GEOMETRIC ACCURACY
Accurate estimation of sigma(exp 0) using AIRSAR data p 3139 N95-33805
GEOMETRICAL OPTICS
Airborne passive polarimetric measurements of sea surface anisotropy at 92 GHz
[NASA-CR-197288] p 3143 N95-32823
GEOMORPHOLOGY
Analyses of TIMS and AVIRIS data, integrated with field and laboratory spectra, for lithological and mineralogical interpretation of Vulcano Island, Italy p 3137 N95-33790
GEOPHYSICS
Integration of AIRSAR and AVIRIS data for Trail Canyon alluvial fan, Death Valley, California p 3134 N95-33760
GEOSYNCHRONOUS ORBITS
Advanced propulsion for geostationary orbit insertion and north-south station keeping
[NASA-TM-107018] p 3060 N95-32917
GERMANIUM
Impact-parameter dependent L-K vacancy-transfer in collisions of Ni(23+) with Ge solid targets
[DE95-010821] p 3228 N95-33373
GERMANIUM ALLOYS
Fabrication of improved SiGe alloys for an 18-couple module test
[DE95-010238] p 3060 N95-32396
GERMANIUM COMPOUNDS
Efficient pockel's modulators in optical fibers
[AD-A294009] p 3217 N95-34374
GLASS
Glass science tutorial: Lecture no. 4, commercial glass melting and associated air emission issues
[DE95-007818] p 3082 N95-32384
Measurement of gain saturation on Nd: Doped phosphate laser glasses
[REPT-2210] p 3090 N95-32990
Glass science tutorial lecture no. 6: The melting of silicate glasses, a review of selected topics
[DE95-010199] p 3084 N95-33218
Interfacial composition analysis of silicon nitride whisker reinforced oxynitride glass systems
[DE95-012895] p 3085 N95-33635
Quantum cylinder fiber light amplifier
[AD-A294197] p 3217 N95-34300
GLASS FIBER REINFORCED PLASTICS
Response and failure of thick composite rings subjected to uniform external hydrostatic pressure or radial contraction p 3064 N95-33326
GLASS FIBERS
Fatigue damage estimate comparisons for northern European and US wind farm loading environments
[DE95-011061] p 3150 N95-33706
Efficient pockel's modulators in optical fibers
[AD-A294009] p 3217 N95-34374
GLASS LASERS
Measurement of gain saturation on Nd: Doped phosphate laser glasses
[REPT-2210] p 3090 N95-32990
Multiple-beam pulse shaping and preamplification
[DE95-011738] p 3216 N95-33651
GLIDE PATHS
Human piloting factors in the design of control laws for precision landing p 3167 N95-33605
GLOBAL POSITIONING SYSTEM
A tactical navigation and routeing system for low-level flight p 3044 N95-32494
Effects of the specific military aspects of satellite navigation on the civil use of GPS/GLONASS p 3048 N95-33134
GPS-based navigation for space applications p 3058 N95-33144
GPS-Squitter interference analysis
[AD-A293690] p 3047 N95-33480
GLOBAL TRACKING NETWORK
INMARSAT TT&C and communications network and the Beijing INMARSAT Station
[AD-A294163] p 3100 N95-34760
GLONASS
Effects of the specific military aspects of satellite navigation on the civil use of GPS/GLONASS p 3048 N95-33134
GLUONS
NJL Model with nonperturbative dependence on gluon condensate
[DE95-623677] p 3233 N95-32405
Wee partons in large nuclei: From virtual dream to hard reality
[DE95-012168] p 3208 N95-33854
Analytic approach to small x structure functions
[PB95-236030] p 3214 N95-34653
GOGGLES
The ANVIS head-up display: An analysis of its application to naval helicopters
[AD-A294342] p 3170 N95-34358
A comparison of monocular, biocular, and binocular night vision goggles for traversing off-road terrain on foot
[AD-A294018] p 3170 N95-34376
Animation within a multimedia training system for night vision goggles
[AD-A294095] p 3170 N95-34475
Developing multimedia instructional systems: An example application for training in night vision goggles
[AD-A294521] p 3235 N95-34479
GOLD COATINGS
Characterization of DuPont 9015, aqueous processable dry film photoresist for printed wiring boards
[DE95-011239] p 3103 N95-33864
GOVERNMENT PROCUREMENT
Report to Congressional Committees. B-2 bomber: Cost to complete 20 aircraft is uncertain
[GAO/NSIAD-94-217] p 3033 N95-32782
Army aviation: Modernization strategy needs to be reassessed. Report to Congressional requestors
[GAO/NSIAD-95-9] p 3033 N95-32783
Metric conversion: Future progress depends upon private sector and public support. Report to Congressional requesters
[GAO/RCED-94-23] p 3089 N95-32785
Report to the Honorable William V. Roth, Jr., US Senate. Naval aviation: F/A-18 E/F acquisition strategy
[GAO/NSIAD-94-194] p 3197 N95-32886

Annual report to the Chairman, House and Senate Committees on Appropriations. Status of open recommendations: Improving operations of federal departments and agencies
[GAO/OP-94-1] p 3236 N95-32887
Budget estimates: Fiscal year 1994. Volume 2: Construction of facilities
[NASA-TM-110816] p 3245 N95-33081
Comanche helicopter: Testing needs to be completed prior to production decisions
[AD-A294408] p 3049 N95-34422

GOVERNMENT/INDUSTRY RELATIONS
Metric conversion: Future progress depends upon private sector and public support. Report to Congressional requesters
[GAO/RCED-94-23] p 3089 N95-32785
A layered approach to technology transfer of AVIRIS between Earth Search Sciences, Inc. and the Idaho National Engineering Laboratory p 3117 N95-33746
Report to the Ranking Minority Member, Committee on Government Operations, House of Representatives. Paperwork reduction: Reported burden hour increases reflect new estimates, not actual changes
[GAO/PEMD-94-3] p 3236 N95-33907

GRAIN BOUNDARIES
YBa2Cu3O(7-x) 45 deg (001) tilt grain boundaries induced by controlled low-energy sputtering of MgO substrates: Transport properties and atomic-scale structure
[DE95-005826] p 3228 N95-32810

GRAIN SIZE
A study of the effect of grain size on the ballistic performance of silicon carbide
[DE95-011724] p 3126 N95-33068
Improving alpine-region spectral unmixing with optimal-fit snow endmembers p 3135 N95-33764

GRAND CANYON (AZ)
A conflict of water and fire: Remote sensing imagery of the Uinkaret Volcanic Field, Grand Canyon, Arizona p 3117 N95-33795

GRANULAR MATERIALS
Lightweight alumina refractory aggregate. Phase 2: Pilot scale development
[DE95-012154] p 3083 N95-33079

GRAPH THEORY
Approaches to implementing deterministic models in a probabilistic framework
[DE95-009483] p 3197 N95-32391

GRAPHICAL USER INTERFACE
X-Antenna: A graphical interface for antenna analysis codes
[NASA-CR-199212] p 3095 N95-32674
Off-line programming using commerical CAD systems, and design criteria for manipulators with inherent accuracy p 3180 N95-32937
Incorporating bibliographic information into a spatial data query system for the Savannah River Site
[DE95-010865] p 3238 N95-33402
Interactive interface for National Center for Atmospheric Research (NCAR) graphics p 3239 N95-34220
A land-surface testbed for EOSDIS p 3158 N95-34223
Experimenter's laboratory for visualized interactive science p 3184 N95-34228
Focus of attention in decision support systems
[AD-A294037] p 3236 N95-34487

GRAPHITE
Recent results from the D3-D tokamak and implications for future devices
[DE95-009605] p 3222 N95-32592
Integral cesium reservoir: Design and transient operation
[DE95-010152] p 3211 N95-32647
Evaluation of strength properties of developed SiC/C compositionally gradient graphite materials
[DE95-737271] p 3063 N95-32711

GRAPHS (CHARTS)
Grayling 2 information base for generation of synthetic thermal infrared scenes
[AD-A294956] p 3100 N95-34578

GRASSES
Canopy reflectance modelling of semiarid vegetation
[NASA-CR-199117] p 3142 N95-32676

GRASSLANDS
Vegetation species composition and canopy architecture information expressed in leaf water absorption measured in the 1000 nm and 2200 spectral region by an imaging spectrometer p 3133 N95-33757
Use of AIRSAR to identify woody shrub invasion and other indicators of desertification in the Jornada LTER p 3141 N95-33810

GRATINGS (SPECTRA)
Conference proceedings of mathematical methods in electromagnetic theory
[AD-A291165] p 3097 N95-32797
Radiative interactions with micromachined surfaces: Spectral polarized emittance
[DE95-011455] p 3097 N95-33061
Pulsed tunable narrow-bandwidth dye laser, with hollow circular waveguide in cavity
[AD-A294060] p 3120 N95-34469

GRAVIMETERS
Navigational technology of dual usage p 3048 N95-33131

GRAVITATION
Cosmological consequences of topological and geometric phenomena in field theories p 3234 N95-33313
Sinuous oscillations and steady warps of polytropic disks
[DE95-013473] p 3247 N95-34216

GRAVITATIONAL EFFECTS
Characterization of microgravity effects on bone structure and strength using fractal analysis p 3165 N95-32419
The role of the vestibular system in manual target localization p 3166 N95-32422
Effects of gravity and light on plant growth and performance in normal and reduced gravity p 3163 N95-32901
A fundamental study of smoldering with emphasis on experimental design for zero-G
[NASA-CR-198378] p 3089 N95-32929

GRAVITATIONAL FIELDS
Cosmological consequences of topological and geometric phenomena in field theories p 3234 N95-33313
Sinuous oscillations and steady warps of polytropic disks
[DE95-013473] p 3247 N95-34216

GRAVITATIONAL PHYSIOLOGY
Effects of gravity and light on plant growth and performance in normal and reduced gravity p 3163 N95-32901
Current Concepts on G-Protection Research and Development
[AGARD-LS-202] p 3168 N95-34050
G-protection basis/acceleration physiology p 3168 N95-34051
Negative to positive Gz acceleration transition p 3165 N95-34052
Methods for measuring physiological responses and protection in man exposed to high +G(z) p 3166 N95-34058

GRAVITROPISM
Effects of gravity and light on plant growth and performance in normal and reduced gravity p 3163 N95-32901

GRAVITY WAVES
Historical detection of atmospheric impacts by large bolides using acoustic-gravity waves
[DE95-010864] p 3246 N95-33211
An experimental study of collective sea state modes of deep water surface gravity waves
[AD-A294007] p 3160 N95-34372

GREEN'S FUNCTIONS
Penetrable wedge analysis
[AD-A294276] p 3234 N95-34464

GREENHOUSE EFFECT
Technical innovation for reducing emissions of greenhouse effect gas and survey of effects of changes of industrial structures
[DE95-769808] p 3151 N95-32547
Abstracts of oral and poster sessions
[DE95-011951] p 3154 N95-33413

GREENLAND
Turbulent heat flux measurements over the Greenland, Norwegian and Barents seas
[AD-A294129] p 3157 N95-34751

GRID GENERATION (MATHEMATICS)
Simulation of patch and slot antennas using FEM with prismatic elements and investigations of artificial absorber mesh termination schemes
[NASA-CR-198974] p 3097 N95-32822
Enhanced stress projections for error estimation and a singular floating node element for static and dynamic fracture p 3064 N95-33463
A unified multigrid solver for the Navier-Stokes equations on mixed element meshes
[NASA-CR-198183] p 3196 N95-33500
Gasdynamic model of turbulent combustion in an explosion
[DE95-010267] p 3074 N95-33627
The Grid Analysis and Display System (GRADS): A practical tool for Earth science visualization p 3241 N95-34231
Adaptive grid method using elliptic equation for compressible flows p 3035 N95-34515
Grid generation around airfoil with a flap using boundary element method p 3041 N95-34552

GRINDING (MATERIAL REMOVAL)
High-speed, low-damage grinding of advanced ceramics, phase 1
[DE95-011241] p 3085 N95-33425

GROOVES
Application of grating polarizer to 106.4GHz ECH system on Heliotron-E
[NIFS-334] p 3225 N95-34624

GROUND BASED CONTROL
Implementation of a Single-Stage-To-Orbit (SSTO) model for stability and control analysis p 3059 N95-32432
Single event and TREE latchup mitigation for a star tracker sensor: An innovative approach to system level latchup mitigation
[DE95-010331] p 3059 N95-32593

GROUND EFFECT (AERODYNAMICS)
Dynamic ground effects flight test of the NASA F-15 aircraft p 3049 N95-33024
Numerical simulation of two-dimensional PAR-WIG p 3040 N95-34548

GROUND OPERATIONAL SUPPORT SYSTEM
An integrated system for air to ground operations p 3044 N95-32498

GROUND STATE
Progress towards antihydrogen production by the reaction of cold antiprotons with positronium atoms
[DE95-007850] p 3204 N95-32584
A quantum Monte Carlo study of the high-pressure phases of solid hydrogen p 3074 N95-33469

GROUND STATIONS
Identification of critical substorm-expansion-phase phenomena: Problems addressable with GEM observations
[ATR-94(7270)-1] p 3158 N95-33259

GROUND TESTS
Ricor K506B cryocooler performance during the Clementine mission and ground testing
[DE95-010683] p 3089 N95-32568
Propulsion Controlled Aircraft design and development p 3053 N95-33022

GROUND TRUTH
Geographic information system for fusion and analysis of high-resolution remote sensing and ground data p 3240 N95-34224

GROUND WATER
Lithogenic and cosmogenic tracers in catchment hydrology
[DE95-011523] p 3143 N95-33407

GROUND WAVE PROPAGATION
DETVAg-90: Use of GTD for wave propagation over earth
[PB95-211447] p 3098 N95-33231

GROUND-AIR-GROUND COMMUNICATION
OPEX: Second Workshop of the OLYMPUS propagation experimenters. Volume 1: Reference book on attenuation measurement and prediction
[ESA-WPP-083-VOL-1] p 3096 N95-32747

GUIDANCE (MOTION)
Dual use: Opportunities, payoffs, and challenges p 3091 N95-33127

GUIDANCE SENSORS
Dual Usage in Military and Commercial Technology in Guidance and Control
[AGARD-CP-556] p 3091 N95-33126
Dual use: Opportunities, payoffs, and challenges p 3091 N95-33127
Dual-use micromechanical inertial sensors p 3092 N95-33132
The DLR research programme on an integrated multi sensor system for surface movement guidance and control p 3048 N95-33135

GULF STREAM
Polarization and wavelength diversities of Gulf Stream fronts imaged by AIRSAR p 3140 N95-33807

GYROSCOPES
Commercial usage of Navy components developed and manufactured by CRI Delfin p 3092 N95-33129
Dual-use micromechanical inertial sensors p 3092 N95-33132

H

H-INFINITY CONTROL
Popov theory based approach to digital H(infinity)-control with measurement-feedback for Pritchard-Salamon systems
[PB95-218111] p 3192 N95-33399

HABITATS
Remotely sensed indicators of habitat heterogeneity and biological diversity: A preliminary report p 3140 N95-33806

HADRONS
Chiral restoration in hot and/or dense matter
[DE95-012176] p 3204 N95-32621

Strangeness from hadronic processes
[DE95-010311] p 3205 N95-32651
Hadron distributions at higher rapidity using the BRAHMS forward spectrometer
[DE95-008861] p 3207 N95-33203
QCD and hadron structure
[DE95-012173] p 3209 N95-33855

HAFNIUM COMPOUNDS
TEM investigation on the low temperature phase of HfV2
[DE95-009500] p 3225 N95-32532

HALL EFFECT
Development of improved p-type Si-20 at. %Ge by addition of fullerite
[DE95-010230] p 3066 N95-32394
The 8th Winterschool on New Developments in Solid State Physics
[AD-A290163] p 3227 N95-32677
Electronic processes in heterostructures, strained-layer materials, and laterally patterned structures
[AD-A294970] p 3235 N95-34585

HALOS
Status of the large-scale dark-matter axion search
[DE95-008828] p 3246 N95-32597

HAMILTONIAN FUNCTIONS
The non-relativistic charged Bose gas in a magnetic field. Part 1: Formalism
[DE95-619698] p 3205 N95-32632
Solvent effects on the electronic spectrum of R hardt's dye
[AD-A293667] p 3067 N95-32804
The (pi)(yields)e(nu)(gamma) decay in chiral perturbation theory
[DE95-619269] p 3206 N95-32806
A code to compute the action-angle transformation for a particle in an arbitrary potential well
[DE95-012554] p 3098 N95-33336

HANDBOOKS
NASA directives master list and index
[NHB-1410.13O] p 3238 N95-33249

HARDENING (SYSTEMS)
Design and analysis of transient nonlinear coupled systems p 3199 N95-33292

HARDNESS TESTS
Irradiation experiments of low copper A533B steels for reactor pressure vessel tested in JMTR
[DE95-737266] p 3077 N95-32531

HARMONIC OSCILLATORS
Study of the trapped modes at the vacuum ports
[DE95-010570] p 3203 N95-32544

HAZARDS
The concept of the space system based on the Rocket launch vehicle of light-weight class for direct sounding of large-scale natural hazards p 3057 N95-33128
OH-58 pilot display unit (PDU) simulated crash tests
[AD-A294049] p 3170 N95-34378
General procedure for clothing evaluations relative to heat stress
[AD-A294953] p 3171 N95-34577

HEAD-UP DISPLAYS
An integrated system for air to ground operations p 3044 N95-32498
The ANVIS head-up display: An analysis of its application to naval helicopters
[AD-A294342] p 3170 N95-34358
The effects of display location and dimensionality on taxiway navigation
[AD-A294878] p 3047 N95-34570

HEALTH
Chemical substances lists: A guide to the lists used in the Swedish Sunset Project. Supplement to report 13/94. Selecting multiproblem chemicals for risk reduction. A presentation of the Swedish Sunset Project
[PB95-211272] p 3073 N95-33328
General procedure for clothing evaluations relative to heat stress
[AD-A294953] p 3171 N95-34577

HEART DISEASES
Shuttle to Space Station. Heart assist implant. Hubble update. X-30 mock-up
[NASA-TM-110837] p 3056 N95-33167

HEAT EXCHANGERS
Numerical thermal analyses of heat exchangers for the stirling engine application
[NASA-CR-199120] p 3110 N95-33398

HEAT FLUX
Laminar heat transfer for power-law fluids in thermal entrance region of annular sector ducts p 3108 N95-33255
Design and analysis of transient nonlinear coupled systems p 3199 N95-33292
Numerical thermal analyses of heat exchangers for the stirling engine application
[NASA-CR-199120] p 3110 N95-33398
Low Reynolds number kappa-epsilon and empirical transition models for oscillatory pipe flow and heat transfer
[NASA-TM-109785] p 3110 N95-33496
Modeling and simulation of pulsed laser annealing and ablation of solid materials
[DE95-012888] p 3119 N95-34466
Turbulent heat flux measurements over the Greenland, Norwegian and Barents seas
[AD-A294129] p 3157 N95-34751

HEAT MEASUREMENT
First NPL Calorimetry Workshop
[PB95-236063] p 3235 N95-34654

HEAT PIPES
Baseline experimental investigation of an electrohydrodynamically assisted heat pipe p 3113 N95-32427

HEAT RADIATORS
Thermal control technology of communications satellite
[AD-A294249] p 3059 N95-34493

HEAT RESISTANT ALLOYS
Allison engine testing CMSX-4(reg sign) single crystal turbine blades and vanes
[DE95-010308] p 3050 N95-32636

HEAT SINKS
Design and operation of a thermionic converter in air
[DE95-010151] p 3149 N95-32645

HEAT TOLERANCE
Tri-service perspectives on microclimate cooling of protective clothing in the heat
[AD-A294005] p 3170 N95-34370
A prototype computer program that integrates predictive models and medical handbooks for altitude, cold exposure, and heat stress
[AD-A294006] p 3182 N95-34371
General procedure for clothing evaluations relative to heat stress
[AD-A294953] p 3171 N95-34577

HEAT TRANSFER
Baseline experimental investigation of an electrohydrodynamically assisted heat pipe p 3113 N95-32427
Numerical simulation of heat and mass transport during space crystal growth with MEPHISTO
[NASA-TM-107015] p 3089 N95-32718
Study on turbulent fluctuations in diffusion flames using laser induced fluorescence
[PB95-214425] p 3068 N95-32812
Flow and heat transfer behavior of non-Newtonian fluids in rectangular ducts p 3107 N95-32907
Review of combustion-acoustic instabilities
[NASA-TM-107020] p 3108 N95-32930
Enhancement of pool boiling heat transfer to lithium bromide aqueous solution
[REPT-2211] p 3091 N95-32991
Experimental and analytical assessment of the thermal behavior of spiral bevel gears
[NASA-TM-107009] p 3123 N95-33179
Experimental and numerical analysis of controlled impinging liquid jets p 3109 N95-33257
Ignition and combustion of cellulosic dust particles p 3073 N95-33308
Numerical thermal analyses of heat exchangers for the stirling engine application
[NASA-CR-199120] p 3110 N95-33398
Low Reynolds number kappa-epsilon and empirical transition models for oscillatory pipe flow and heat transfer
[NASA-TM-109785] p 3110 N95-33496
An application of mechanical leverage to microactuation
[DE95-011883] p 3124 N95-33836
Evaluation of conductive, radiative, chemical, and convective heat transfer in complex systems using a fast-running, implicit, lumped-capacitance formulation
[DE95-011889] p 3111 N95-33837
Numerical study on stabilization of a diffusion flame over a flat plate p 3035 N95-34510
The effect of buoyancy on flow and heat transfer in curved pipes p 3037 N95-34528
First NPL Calorimetry Workshop
[PB95-236063] p 3235 N95-34654
Review of the research activities of the Energy Research Unit in 1994
[PB95-235008] p 3151 N95-34656

HEAT TRANSFER COEFFICIENTS
Analysis of a HTSC current lead under nonlinear heat transfer conditions
[DE95-009420] p 3102 N95-32714

HEAT TREATMENT
Effect of heat treatment at 1,150 C on creep rupture properties of a Fe3Al-based alloy
[DE95-010295] p 3077 N95-32527
Effect of lead content on Bi-2223 formation by a two-powder process
[DE95-009889] p 3079 N95-33215

HEATING
Three-dimensional natural convection of a fluid with temperature-dependent viscosity in an enclosure with localized heating
[DE95-002606] p 3106 N95-32387
Mechanism(s) for the suppression of the switchable polarization in PZT and BaTiO3
[DE95-009589] p 3226 N95-32590
Thermocapillary flow with evaporation and condensation and its effect on liquid retention in low-g fluid acquisition devices p 3109 N95-33256

HEATING EQUIPMENT
Enhancement of pool boiling heat transfer to lithium bromide aqueous solution
[REPT-2211] p 3091 N95-32991

HEAVY IONS
Estimation of collective instabilities in RHIC
[DE95-011347] p 3211 N95-32485
Damage formation in silicon irradiated by heavy ions with energy more than 1 MeV/a.m.u.
[DE95-623968] p 3204 N95-32610
About the mechanism of heavy ion radiation influence on the metals at high temperature
[DE95-620943] p 3078 N95-32626
Efficiency of modified UA1 jet reconstruction algorithm in PP, PA and AA collisions at STAR
[DE95-009918] p 3212 N95-32665
Minutes of the 12th Joint NASA/DARA-DLR Life Sciences Program Working Group Meeting
[NASA-TM-110655] p 3161 N95-32719
Dosimetry of heavy ions by use of CCD detectors p 3161 N95-32721
Inactivation, DNA double strand break induction and their rejoining in bacterial cells irradiated with heavy ions p 3161 N95-32724
DNA-DSB in CHO-K1 cells induced by heavy-ions: Break rejoining and residual damage (GSI) p 3162 N95-32725
Mutation induction in bacteria after heavy ion irradiation p 3162 N95-32727
Heavy ion induced mutations in mammalian cells: Cross sections and molecular analysis p 3162 N95-32728
Heavy ion action on single cells: Cellular inactivation capability of single accelerated heavy ions p 3162 N95-32729
Cosmic heavy ion tracks in mesoscopic biological test objects p 3163 N95-32730
X-ray-provoked non-Mendelian transgenerational oncodeterminants p 3163 N95-32731
Light particle emission in heavy ion reactions
[DE95-010727] p 3206 N95-32965
Heavy ions acceleration in RF wells of 2-frequency electromagnetic field and in the inverted FEL
[DE95-012439] p 3214 N95-34439

HELICOPTERS
Flight test of a low-altitude helicopter guidance system with obstacle avoidance capability p 3043 N95-32490
Helicopter HF communications using the NVIS mode p 3043 N95-32491
Tactical low-level helicopter communications p 3043 N95-32492
The application of helicopter mission simulation to Nap-of-the-Earth operations p 3044 N95-32496
Development and flight testing of an Obstacle Avoidance System for US Army helicopters p 3045 N95-32500
The Anglo-French Compact Laser Radar demonstrator programme p 3045 N95-32501
The ANVIS head-up display: An analysis of its application to naval helicopters
[AD-A294342] p 3170 N95-34358
Evaluating the potential for rotation and loss of flight helmets from inertia and impact loads
[AD-A294041] p 3170 N95-34489
Direct analysis of transonic rotor noise with CFD technique p 3040 N95-34549

HELIOTRONS
Application of grating polarizer to 106.4GHz ECH system on Heliotron-E
[NIFS-334] p 3225 N95-34624

HELIUM
The fully correlated two-electron problem on a numerical lattice
[DE95-010280] p 3205 N95-32650
Electron-electron interaction in the ionization of hydrogenlike projectiles by He
[DE95-010822] p 3208 N95-33374
Density, heat capacity, viscosity, and thermal conductivity of mixtures of CO2, He, H2, H2O, N2, and O2
[AD-A288731] p 3076 N95-34814

HELIUM ATOMS
The fully correlated two-electron problem on a numerical lattice
[DE95-010280] p 3205 N95-32650
HELIUM COMPOUNDS
The mean lifetimes of the 2p(sigma) lowest bound state of HeH(2+) and its isotopes
[DE95-010812] p 3206 N95-32966
HELIUM IONS
State-selective single electron capture cross sections in He(exp 2+) + Li(2s) and Li(*)(2p) collisions
[DE95-010819] p 3207 N95-33371
Mean lifetime measurements of (3)He(4)He2+
[DE95-010813] p 3209 N95-34355
HELIUM ISOTOPES
Transverse acoustic properties of the B-phase of superfluid helium three p 3074 N95-33414
HELIUM PLASMA
Recent results from the D3-D tokamak and implications for future devices
[DE95-009605] p 3222 N95-32592
HELMET MOUNTED DISPLAYS
Flight test of a low-altitude helicopter guidance system with obstacle avoidance capability p 3043 N95-32490
An integrated system for air to ground operations p 3044 N95-32498
A helmet mounted display for night missions at low altitude p 3045 N95-32503
SIRPH: Steerable infrared picture on helmet mounted display p 3045 N95-32504
Covert Night/Day Operations for Rotorcraft (CONDOR) programme p 3046 N95-32505
HELMETS
OH-58 pilot display unit (PDU) simulated crash tests
[AD-A294049] p 3170 N95-34378
Evaluating the potential for rotation and loss of flight helmets from inertia and impact loads
[AD-A294041] p 3170 N95-34489
HEMODYNAMIC RESPONSES
Noninvasive determination of Cardiac Output
[PB95-208310] p 3164 N95-32611
HETERODYNING
Laser based obstacle warning sensors for helicopters p 3045 N95-32499
HETEROGENEITY
Spin counting in dipolar coupled spin 1/2 systems by multiple quantum NMR spectroscopy in solids: Development of a single quantum propagator and its application to heterogeneous catalysis
[DE95-010246] p 3066 N95-32540
Glass science tutorial lecture no. 6: The melting of silicate glasses, a review of selected topics
[DE95-010199] p 3084 N95-33218
Validating spatial structure in canopy water content using geostatistics p 3135 N95-33768
Experiences using DCE and CORBA to build tools for creating highly-available distributed systems
[AD-A294973] p 3187 N95-34587
HETEROJUNCTIONS
A reconfigurable optoelectronic interconnect technology for multi-processor networks
[DE95-011895] p 3186 N95-33838
HEURISTIC METHODS
Proceedings: High performance functional computing
[DE95-010736] p 3186 N95-33643
Is the genetic algorithm a cooperative learner?
[AD-A294112] p 3193 N95-34499
Explanations of empirically derived reactive plans
[AD-A294114] p 3193 N95-34501
Control of initialization bias in queueing simulations using queueing approximations
[AD-A294121] p 3194 N95-34742
HIERARCHIES
HINT: A new way to measure computer speed
[DE95-010245] p 3177 N95-32398
HIGH ACCELERATION
G-protection basis/acceleration physiology p 3168 N95-34051
Negative to positive Gz acceleration transition p 3165 N95-34052
Selection and special physiological training of flying personnel to high +G(z)-maneuverable flights-main concept p 3166 N95-34053
Positive pressure breathing for G protection (PBG) p 3168 N95-34055
Increase of High-sustained +G(z) tolerance at the expense of pilot's working posture change p 3165 N95-34056
Methods for measuring physiological responses and protection in man exposed to high +G(z) p 3166 N95-34058
G-protection capabilities and current G-protection issues p 3169 N95-34060
HIGH ALTITUDE
Unitized Regenerative Fuel Cells for solar rechargeable aircraft and zero emission vehicles
[DE95-010684] p 3150 N95-33642
ABLEX: High altitude laser propagation experiment
[AD-A294914] p 3120 N95-34592
HIGH CURRENT
Transverse multibunch instabilities for non-rigid bunches
[DE95-012098] p 3211 N95-32607
HIGH ENERGY ELECTRONS
The growth of ultrathin epitaxial intermetallic films
[AD-A295037] p 3232 N95-34795
HIGH ENERGY INTERACTIONS
Charm decays and high energy photoproduction
[DE95-010165] p 3201 N95-32393
High energy collisions involving multiply charged ions
[DE95-010912] p 3206 N95-32763
Top quark signatures in extended color theories
[DE95-007099] p 3234 N95-33202
A map for the thick beam-beam interaction
[DE95-012561] p 3213 N95-33385
Collaborating over the Web: Libraries and laboratories or the Librarian and the Webmaster
[DE95-010572] p 3186 N95-33639
Proceedings of the School for Young High Energy Physicists
[PB95-234993] p 3235 N95-34652
HIGH FREQUENCIES
Development and application of the methods for pilot-aircraft system research to the manual control tasks of modern vehicles p 3094 N95-33139
FH and DS spread-spectrum systems in interference-limited HF channels: A comparison
[PB95-211439] p 3098 N95-33230
HIGH GRAVITY ENVIRONMENTS
Current Concepts on G-Protection Research and Development
[AGARD-LS-202] p 3168 N95-34050
HIGH LEVEL LANGUAGES
A distributed Clips implementation: dClips p 3243 N95-34243
HIGH POWER LASERS
Control of the laser beam irradiation intensity distribution using aspherical multi lens array and edge-shaped plates
[REPT-2209] p 3090 N95-32989
High power CO2 laser windows and reflection reducing coatings
[AD-A294217] p 3119 N95-34308
Extreme broadening of stimulated Raman scattered light from high intensity laser plasma interactions
[AD-A294165] p 3120 N95-34761
HIGH PRESSURE
Application of deformable templates for recognizing tracks detected with High Pressure Drift Tubes
[DE95-621870] p 3188 N95-32627
Fundamental studies of gas phase ionic reactions by ion mobility spectrometry p 3069 N95-33268
A quantum Monte Carlo study of the high-pressure phases of solid hydrogen p 3074 N95-33469
HIGH RESOLUTION
Visualization methods for high-resolution, transient, 3-D, finite element situations
[DE95-009479] p 3179 N95-32390
Three-dimensional ground penetrating radar imaging using synthetic aperture time-domain focusing
[DE95-010731] p 3095 N95-32569
High-resolution TeO2 acousto-optical deflector for millimeter-wave spectrometer
[AD-A293054] p 3215 N95-32701
Comparison of lead zirconate titanate thin films on ruthenium oxide and platinum electrodes
[DE95-617597] p 3082 N95-32710
MODTRAN3: An update and recent validations against airborne high resolution interferometer measurements p 3128 N95-33732
An algorithm for chlorophyll using first difference transformations of AVIRIS reflectance spectra p 3134 N95-33763
Geographic information system for fusion and analysis of high-resolution remote sensing and ground data p 3240 N95-34224
HIGH REYNOLDS NUMBER
Asymptotic structure of supersonic turbulent boundary layers p 3107 N95-32898
The effect of interaction on boundary-layer separation and breakdown p 3109 N95-33310
HIGH SPEED
Feasibility of fullerene thin films for high-speed all-optical switching
[DE95-011735] p 3085 N95-33409
Photonic band gap structures on polymer materials for microstructure waveguides and high-speed interconnects
[AD-A294119] p 3218 N95-34504
Protocol engineering for broadband networks
[AD-A294969] p 3186 N95-34584
HIGH STRENGTH
Metallic laminates for engine applications
[DE95-010259] p 3062 N95-32399
Fatigue properties for the Al-Li alloy 2090, part 3
[PB95-214532] p 3078 N95-32614
HIGH STRENGTH ALLOYS
Fracture toughness assessment of present and future pressure vessel materials based on Charpy impact energy and yield strength
[AD-A294008] p 3081 N95-34373
HIGH TEMPERATURE
A numerical analysis of fracture and high temperature creep characteristics of composites with discontinuous ductile reinforcements
[DE95-010236] p 3062 N95-32395
About the mechanism of heavy ion radiation influence on the metals at high temperature
[DE95-620943] p 3078 N95-32626
The growth of ultrathin epitaxial intermetallic films
[AD-A295037] p 3232 N95-34795
HIGH TEMPERATURE ENVIRONMENTS
Static pressure drop by swirling flow of an internal cooling air system through a turbine shaft p 3042 N95-34560
HIGH TEMPERATURE GAS COOLED REACTORS
Evaluation of strength properties of developed SiC/C compositionally gradient graphite materials
[DE95-737271] p 3063 N95-32711
HIGH TEMPERATURE LUBRICANTS
Evaluation of high-temperature lubricant under cyclic operating conditions
[AD-A294444] p 3086 N95-34494
HIGH TEMPERATURE PLASMAS
Stability analysis of external kink mode for ITER L-mode profile plasmas
[DE95737207] p 3220 N95-32410
Transport studies of tokamak plasmas in JT-60 device
[DE95-737227] p 3220 N95-32417
Experimental study of the processes in the expander of the axisymmetric mirror device
[DE95-009846] p 3221 N95-32536
Studies of impurity mode and ITG mode in toroidal plasmas
[DE95-012134] p 3223 N95-33391
HIGH TEMPERATURE SUPERCONDUCTORS
Materials sciences programs: Fiscal year 1994
[DE95-011248] p 3211 N95-32483
Analysis of a HTSC current lead under nonlinear heat transfer conditions
[DE95-009420] p 3102 N95-32714
Effect of the colony microstructure on transport critical current of high-J(c) Tl-1223 thick films
[DE95-013049] p 3230 N95-34213
Formation of artificially-layered high-temperature superconductors using pulsed-laser deposition
[DE95-012884] p 3231 N95-34465
HIGHLY MANEUVERABLE AIRCRAFT
Nonlinear adaptive control of highly maneuverable high performance aircraft p 3192 N95-33712
HIGHWAYS
Sub-pixel localization of highways in AVIRIS images p 3135 N95-33767
HILBERT SPACE
Sum of fractional derivatives and m-accretive operators
[PB95-215307] p 3195 N95-32893
HISTOGRAMS
A preliminary evaluation of histogram-based binarization algorithms
[DE95-009886] p 3179 N95-32470
ENGIN mini-manual. Version 1.5
[PB95-218095] p 3206 N95-32814
HISTORIES
Historical detection of atmospheric impacts by large bolides using acoustic-gravity waves
[DE95-010864] p 3246 N95-33211
Twenty-five years of progress. Part 1: Birth of NASA. Part 2: The Moon-a goal
[NASA-TM-110819] p 3253 N95-33384
HOLDERS
The effect of sample holder material on ion mobility spectrometry reproducibility p 3071 N95-33282
HOLE BURNING
Spin counting in dipolar coupled spin 1/2 systems by multiple quantum NMR spectroscopy in solids: Development of a single quantum propagator and its application to heterogeneous catalysis
[DE95-010246] p 3066 N95-32540
HOLES (ELECTRON DEFICIENCIES)
Impact-parameter dependent L-K vacancy-transfer in collisions of Ni(23+) with Ge solid targets
[DE95-010821] p 3228 N95-33373

HOLLOW CATHODES
Life test of a xenon hollow cathode for a space plasma contractor
| NASA-CR-195403 | p 3061 N95-33926
HOLOGRAPHY
Development and flight testing of an Obstacle Avoidance System for US Army helicopters p 3045 N95-32500
SIRPH: Steerable infrared picture on helmet mounted display p 3045 N95-32504
Applied Information Systems Research Program (AISRP) Workshop 3 meeting proceedings
| NASA-CR-199103 | p 3239 N95-34218
Multi-layer holographic bifurcative neural network system for real-time adaptive EOS data analysis
p 3148 N95-34233
Read/write module for high capacity memory disk
| AD-A294946 | p 3178 N95-34745
HOMEOSTASIS
Noninvasive determination of Cardiac Output
| PB95-208310 | p 3164 N95-32611
HOMING
Ice-ocean four dimensional structure and dynamics
| AD-A294017 | p 3160 N95-34375
HOMING DEVICES
Multispectral image correlation for air-to-ground targeting p 3043 N95-32489
HOMOGENEOUS TURBULENCE
Direct numerical simulation of compressible isotropic turbulence p 3037 N95-34523
Direct numerical simulation of incompressible homogeneous isotropic turbulence using compressible Navier-Stokes equations p 3037 N95-34529
Direct numerical simulation of incompressible homogeneous isotropic turbulence using NWT
p 3038 N95-34530
HOMOGENIZING
Glass science tutorial lecture no. 6: The melting of silicate glasses, a review of selected topics
| DE95-010199 | p 3084 N95-33218
HOMOTOPY THEORY
Theory and application of homotopy techniques in nonlinear programming and control systems
| AD-A294934 | p 3193 N95-34600
HOT ISOSTATIC PRESSING
Fabrication of improved SiGe alloys for an 18-couple module test
| DE95-010238 | p 3060 N95-32396
Development and trial manufacturing of 1/2-scale partial mock-up of blanket box structure for fusion experimental reactor
| DE95-737184 | p 3219 N95-32408
HOT PRESSING
Development of improved p-type Si-20 at. %Ge by addition of fullerite
| DE95-010230 | p 3066 N95-32394
Fabrication of improved SiGe alloys for an 18-couple module test
| DE95-010238 | p 3060 N95-32396
HOUSINGS
Device for dampening vibratory motion
| AD-D017490 | p 3127 N95-34427
HOVERING
An LDV investigation of support structure influence on the flow field near the wingtip of a STOVL configuration in hover
| AD-A294126 | p 3042 N95-34750
HTPB PROPELLANTS
Fundamental phenomena on fuel decomposition and boundary-layer combustion processes with applications to hybrid rocket motors
| NASA-CR-199126 | p 3061 N95-32932
HUBBLE SPACE TELESCOPE
Shuttle to Space Station. Heart assist implant. Hubble update. X-30 mock-up
| NASA-TM-110837 | p 3056 N95-33167
HUMAN BEHAVIOR
Locus of control and coping style as stress moderators in achievement oriented individuals
| AD-A294275 | p 3166 N95-34463
HUMAN BODY
A novel approach to the problem of highly-sensitive regular analysis for man-made plutonium in environment and human body
| DE95-620764 | p 3164 N95-32666
HUMAN CENTRIFUGES
Selection and special physiological training of flying personnel to high + G(z)-maneuverable flights-main concept p 3166 N95-34053
Methods for measuring physiological responses and protection in man exposed to high + G(z)
p 3166 N95-34058
Selection and training of MiG-29 and future fighter pilots p 3166 N95-34059
HUMAN FACTORS ENGINEERING
The application of helicopter mission simulation to Nap-of-the-Earth operations p 3044 N95-32496
An integrated system for air to ground operations
p 3044 N95-32498
A helmet mounted display for night missions at low altitude p 3045 N95-32503
SIRPH: Steerable infrared picture on helmet mounted display p 3045 N95-32504
Covert Night/Day Operations for Rotorcraft (CONDOR) programme p 3046 N95-32505
Functional requirements analysis and human machine interface specifications for handheld metal detector wands
| DE95-009845 | p 3167 N95-32535
Stimulus-response compatibility
| PB95-214722 | p 3167 N95-33237
Human piloting factors in the design of control laws for precision landing p 3167 N95-33605
Increase of High-sustained + G(z) tolerance at the expense of pilot's working posture change
p 3165 N95-34056
Current issues in the design and information content of instrument approach charts
| AD-A294752 | p 3047 N95-34562
Analysis of safety requirements in the context of system faults and human errors
| PB95-236105 | p 3171 N95-34658
Human Factors Certification of Advanced Aviation Technologies
| NASA-CR-199009 | p 3171 N95-34764
On the use of the systems approach to certify advanced aviation technologies p 3171 N95-34765
A rose by any other name: Certification seen as process rather than content p 3047 N95-34766
A psychologist's view of validating aviation systems
p 3172 N95-34767
Certification of tactics and strategies in aviation
p 3172 N95-34768
Human factors certification: A useful concept?
p 3173 N95-34769
Human factors certification in the development of future air traffic control systems p 3048 N95-34770
Quality assurance and risk management: Perspectives on Human Factors Certification of Advanced Aviation Systems p 3048 N95-34771
Certify for success: A methodology for human-centered certification of advanced aviation systems
p 3173 N95-34773
Certification of training p 3166 N95-34774
Presentation of a Swedish study program concerning recruitment, selection and training of student air traffic controllers: The MRU project phase 1
p 3167 N95-34775
Does human cognition allow Human Factors (HF) certification of advanced aircrew systems?
p 3174 N95-34776
Practical guidelines for workload assessment
p 3174 N95-34777
Is there a role for a test controller in the development of new ATC equipment? p 3174 N95-34778
Towards a framework of human factors certification of complex human-machine systems p 3175 N95-34779
The successful management of programs for human factors certification of advanced aviation technologies
p 3175 N95-34780
Evaluation in context: ATC automation in the field
p 3175 N95-34781
Integrating human factors knowledge into certification: The point of view of the Internatioanal Civil Aviation Organization (ICAO) p 3175 N95-34782
Improving air traffic control: Proving new tools or approving the joint human-machine system?
p 3176 N95-34783
Certification for civil flight decks and the human-computer interface p 3176 N95-34784
Some inadequacies of the current human factors certification process of advanced aircraft technologies
p 3176 N95-34785
Advanced automated glass cockpit certification: Being wary of human factors p 3176 N95-34786
Beware of agents when flying aircraft: Basic principles behind a generic methodology for the evaluation and certification of advanced aviation systems
p 3176 N95-34787
HUMAN PERFORMANCE
A comparison of monocular, biocular, and binocular night vision goggles for traversing off-road terrain on foot
| AD-A294018 | p 3170 N95-34376
Analysis of safety requirements in the context of system faults and human errors
| PB95-236105 | p 3171 N95-34658
Quality assurance and risk management: Perspectives on Human Factors Certification of Advanced Aviation Systems p 3048 N95-34771
Practical guidelines for workload assessment
p 3174 N95-34777
HUMAN REACTIONS
The preservation of human surrogates for biomechanical studies p 3167 N95-33312
HUMAN RESOURCES
European Space Agency 1994 annual report
p 3252 N95-32805
Budget estimates: Fiscal year 1994. Volume 3: Research and program management
| NASA-TM-110817 | p 3245 N95-33082
HUMAN-COMPUTER INTERFACE
Functional requirements analysis and human machine interface specifications for handheld metal detector wands
| DE95-009845 | p 3167 N95-32535
Tracking a turbulent spot in an immersive environment
| NASA-CR-198179 | p 3180 N95-32834
An efficient inference engine for interactive fault diagnosis in a helpdesk application
p 3189 N95-33000
Stimulus-response compatibility
| PB95-214722 | p 3167 N95-33237
Experimenter's laboratory for visualized interactive science p 3184 N95-34228
Analysis of safety requirements in the context of system faults and human errors
| PB95-236105 | p 3171 N95-34658
Certification for civil flight decks and the human-computer interface p 3176 N95-34784
HUMIDITY
Turbulent heat flux measurements over the Greenland, Norwegian and Barents seas
| AD-A294129 | p 3157 N95-34751
HUYGENS PRINCIPLE
Underwater acoustic field extrapolation: Theory and sensitivity analysis
| AD-A294925 | p 3201 N95-34595
HYBRID CIRCUITS
Optical logic implementation in composite biled/bild circuits
| AD-A294160 | p 3105 N95-34758
HYBRID PROPELLANT ROCKET ENGINES
Fundamental phenomena on fuel decomposition and boundary-layer combustion processes with applications to hybrid rocket motors
| NASA-CR-199126 | p 3061 N95-32932
HYBRID PROPULSION
Fundamental phenomena on fuel decomposition and boundary-layer combustion processes with applications to hybrid rocket motors
| NASA-CR-199126 | p 3061 N95-32932
HYDRAZINE ENGINES
Pop tests of storable biopropellant liquid apogee engine
| NAL-TR-1253 | p 3060 N95-32755
HYDRIDES
Microstructural studies of hydrogen damage in metastable stainless steels p 3080 N95-33774
Fundamental surface chemistry of GaAs OMVPE
| DE95-011606 | p 3231 N95-34486
HYDROCARBON FUELS
Metallized gelled propellants: Oxygen/RP-1/aluminum rocket combustion experiments
| NASA-TM-107025 | p 3088 N95-33876
HYDROCARBONS
Alternative catalyst and exhaust gas sensor work at Argonne National Laboratory
| DE95-007138 | p 3152 N95-32553
Selective methane oxidation over promoted oxide catalysts
| DE95-012319 | p 3075 N95-34021
Elemental fluorine based syntheses of pentafluoro phenyl and other aromatic perfluoropolyether polymers
| AD-A294930 | p 3087 N95-34596
The relationship of chemical structure to supercritical-fluid solubility and to cosolvent-modifier properties: A literature review
| AD-A294933 | p 3076 N95-34599
HYDRODYNAMICS
Summary report for ITER Task No. T226B: Evaluation of ITER disruption erosion
| DE95-010402 | p 3219 N95-32401
On the feasibility of using smoothed particle hydrodynamics for underwater explosion calculations
| DE95-008799 | p 3106 N95-32587
Cooling tower and plume modeling for satellite remote sensing applications
| DE95-012000 | p 3143 N95-33849
Consistent finite-volume discretization of hydrodynamic conservation laws for unstructured grids
| DE95-011730 | p 3112 N95-34437
HYDROFOILS
Numerical studies of turbulent free surface flows and unsteady propeller flows
| AD-A294377 | p 3112 N95-34343

HYDROGEN
Unexpected matching insensitivity in DTL of GTA accelerator
[DE95-011964] p 3211 N95-32416
Hydrogen formation in metals and alloys during fusion reactor operation
[DE95-737224] p 3202 N95-32529
Design and testing criteria for bipolar plate materials for PEM fuel cell applications
[DE95-010878] p 3148 N95-32575
N-15 hydrogen profiling of IC metallizations
[DE95-011052] p 3102 N95-32708
Determination of Benzene, Toluene, and Xylene by means of an ion mobility spectrometer device using photoionization p 3069 N95-33269
Velocity dependence of ionization and excitation of hydrogen molecules by fast proton impact
[DE95-010818] p 3207 N95-33370
Indirect measurements of hydrogen: The deficit method for a many-component system
[DE95-010993] p 3208 N95-33623
Theory and application of homotopy techniques in nonlinear programming and control systems
[AD-A294934] p 3193 N95-34600
Density, heat capacity, viscosity, and thermal conductivity of mixtures of CO2, He, H2, H2O, N2, and O2
[AD-A288731] p 3076 N95-34814

HYDROGEN ATOMS
Thermal rearrangement of oxygen-containing (omicron)-allyltoluene derivatives
[DE95-010124] p 3067 N95-32641

HYDROGEN BONDS
Industrial products based upon processible conductive polyaniline
[AD-A294985] p 3087 N95-34817

HYDROGEN COMPOUNDS
The mean lifetimes of the 2p(sigma) lowest bound state of HeH(2+) and its isotopes
[DE95-010812] p 3206 N95-32966

HYDROGEN EMBRITTLEMENT
Hydrogen formation in metals and alloys during fusion reactor operation
[DE95-737224] p 3202 N95-32529
An experimental and numerical analysis of hydrogen assisted cracking and weldability test methodology p 3079 N95-32936
Microstructural studies of hydrogen damage in metastable stainless steels p 3080 N95-33774

HYDROGEN IONS
The effects of H(+) implants on YBa2Cu3O7 superconducting materials
[DE95-614466] p 3227 N95-32698

HYDROGEN ISOTOPES
Design concept of a cryogenic distillation column cascade for a ITER scale fusion reactor
[DE95-737185] p 3220 N95-32409
Microstructural studies of hydrogen damage in metastable stainless steels p 3080 N95-33774

HYDROGEOLOGY
Users' manual for LEHGC: A Lagrangian-Eulerian finite-element model of HydroGeoChemical transport through saturated-unsaturated media. Version 1.0
[DE95-010513] p 3179 N95-32543

HYDROLOGICAL CYCLE
Analyses and forecasts with LAWS winds
[NASA-CR-199134] p 3157 N95-32933
Movement of water vapor in the atmosphere measured by an imaging spectrometer at Rogers Dry Lake, CA p 3132 N95-33753

HYDROLOGY
Lithogenic and cosmogenic tracers in catchment hydrology
[DE95-011523] p 3143 N95-33407
AVIRIS user's guide p 3117 N95-33759

HYDROLOGY MODELS
Improving alpine-region spectral unmixing with optimal-fit snow endmembers p 3135 N95-33764

HYDROLYSIS
A novel approach to increasing cocaine detection confidence utilizing ion mobility spectrometry p 3072 N95-33283

HYDROMETEORS
OPEX Second Workshop of the OLYMPUS Propagation Experimenters. Volume 2: Reference book on depolarisation
[ESA-WPP-083-VOL-2] p 3096 N95-32748

HYDROSTATIC PRESSURE
Response and failure of thick composite rings subjected to uniform external hydrostatic pressure or radial contraction p 3064 N95-33326

HYDROXYL COMPOUNDS
Polymerization of epsilon-caprolactone in the presence of Oh- or COOh-groups containing initiators. Copolymers of lactide with epsilon-caprolactone: Synthesis, characterization and processing
[PB95-208211] p 3084 N95-33227

HYPERBOLIC DIFFERENTIAL EQUATIONS
High-order Taylor-Galerkin and adaptive hp-methods for hyperbolic systems with application to structural acoustics p 3200 N95-33719

HYPERFINE STRUCTURE
Faddeev calculations of p(mu)+p collisions: Effect of hyperfine splitting on the cross sections
[DE95-007838] p 3203 N95-32583

HYPERSONIC BOUNDARY LAYER
The effect of interaction on boundary-layer separation and breakdown p 3109 N95-33310
Studies of hypersonic boundary layer behavior
[AD-A294137] p 3113 N95-34752

HYPERSONIC FLIGHT
Application of CFD techique for HYFLEX aerodynamic design p 3039 N95-34542

HYPERSONIC FLOW
PINCA: A scalable parallel program for compressible gas dynamics with nonequilibrium chemistry
[DE95-010581] p 3106 N95-32818
A variation of the Riemann Problem solution and its application to implicit Godunov's scheme p 3036 N95-34516
Hypersonic CFD analysis for the aerothermodynamic design of HOPE p 3036 N95-34520
Numerical simulation of film cooling effect around axisymmetric body in hypersonic flow field p 3037 N95-34526

HYPERSONIC SPEED
Implementation of a Single-Stage-To-Orbit (SSTO) model for stability and control analysis p 3059 N95-32432
Studies of hypersonic boundary layer behavior
[AD-A294137] p 3113 N95-34752

HYPERSONIC VEHICLES
Application of CFD techique for HYFLEX aerodynamic design p 3039 N95-34542

HYPERSONICS
Special publication of National Aerospace Laboratory
[NAL-SP-27] p 3034 N95-34505

HYPERTEXT
Incorporating bibliographic information into a spatial data query system for the Savannah River Site
[DE95-010965] p 3238 N95-33402

HYPERVELOCITY FLOW
Numerical simulation of high enthalpy shock tunnel p 3035 N95-34514

HYPERVELOCITY IMPACT
Simulation of hypervelocity impact on massively parallel supercomputer
[DE95-007735] p 3184 N95-32383
Characterizing the fragmentation ring on witness plates p 3056 N95-32426
Analysis of LDEF experiment AO187-2 chemical and isotopic measurements of micrometeoroids by secondary ion mass spectrometry
[NASA-CR-198849] p 3246 N95-32913

HYPERVELOCITY WIND TUNNELS
Numerical simulation of high enthalpy shock tunnel p 3035 N95-34514

HYPOTHESES
Evaluation of the photochemical reflectance index in AVIRIS imagery p 3131 N95-33747

HYPOXIA
A prototype computer program that integrates predictive models and medical handbooks for altitude, cold exposure, and heat stress
[AD-A294006] p 3182 N95-34371

HYSTERESIS
Measurement and modelling of structure sensitive magnetic properties of material
[DE95-010128] p 3080 N95-33699

I

IBM COMPUTERS
Proceedings of the REXX symposium for developers and users
[DE95-010668] p 3185 N95-32820

ICE
The mini-CIDEX GC/IMS: Analysis of cometary ice and dust p 3069 N95-33270
Mapping minerals, amorphous materials, environmental materials, vegetation, water, ice and snow, and other materials: The USGS tricorder algorithm p 3130 N95-33742

IDAHO
Mineralogic variations in fluvial sediments contaminated by mine tailings as determined from AVIRIS data, Coeur D'Alene River Valley, Idaho p 3131 N95-33745
A layered approach to technology transfer of AVIRIS between Earth Search Sciences, Inc. and the Idaho National Engineering Laboratory p 3117 N95-33746

IDENTIFYING
Automatic script identification from images using cluster-based templates
[DE95-006339] p 3181 N95-33154

IGNEOUS ROCKS
Quantitative remote sensing of ammonium minerals, Cedar Mountains, Esmeralda County, Nevada p 3128 N95-33734

IGNITION
Ignition and early soot formation in a DI diesel engine using multiple 2-D imaging diagnostics
[DE95-010692] p 3122 N95-32863
Ignition and combustion of cellulosic dust particles p 3073 N95-33308
DSMC method applied for reacting gas flows p 3035 N95-34509
Investigation of starting and ignition transients in the thermally choked ram accelerator p 3054 N95-34805

ILLUMINATING
Mechanism(s) for the suppression of the switchable polarization in PZT and BaTiO3
[DE95-009589] p 3226 N95-32590
Effects of gravity and light on plant growth and performance in normal and reduced gravity p 3163 N95-32901

IMAGE ANALYSIS
Image analysis used to count and measure etched tracks from ionizing radiation p 3210 N95-32424
The RDB: A parallel, spatial database for the IES/BTI system
[DE95-009425] p 3179 N95-32715
A general solution to object matching problems by using the multiresolution approximation p 3189 N95-33002
Studies of microwave scattering and canopy architecture for boreal forests
[NASA-CR-199114] p 3099 N95-33726
Aerolian erosion, transport, and deposition of volcaniclastic sands among the shifting sand dunes, Christmas Lake Valley, Oregon: TIMS image analysis p 3137 N95-33793
Bayes classification of interferometric TOPSAR data p 3140 N95-33808
A document analysis system p 3244 N95-34804

IMAGE CLASSIFICATION
Bayes classification of interferometric TOPSAR data p 3140 N95-33808
Terrain classification using circular polarimetric features p 3140 N95-33809

IMAGE CONVERTERS
Automatic script identification from images using cluster-based templates
[DE95-006339] p 3181 N95-33154

IMAGE CORRELATORS
Multispectral image correlation for air-to-ground targeting p 3043 N95-32489

IMAGE ENHANCEMENT
Aerolian erosion, transport, and deposition of volcaniclastic sands among the shifting sand dunes, Christmas Lake Valley, Oregon: TIMS image analysis p 3137 N95-33793

IMAGE PROCESSING
A preliminary evaluation of histogram-based binarization algorithms
[DE95-009886] p 3179 N95-32470
Prediction of OCR accuracy using simple image features
[DE95-009887] p 3236 N95-32471
Development and flight testing of an Obstacle Avoidance System for US Army helicopters p 3045 N95-32500
Canopy reflectance modelling of semiarid vegetation
[NASA-CR-199117] p 3142 N95-32676
Basis Image Processor Pr5210: Correlator technical description
[PB95-222485] p 3185 N95-32815
The 1994 laboratory calibration of TIMS p 3117 N95-33796
Geographic information system for fusion and analysis of high-resolution remote sensing and ground data p 3240 N95-34224
Topography from shading and stereo p 3241 N95-34229
SAVS: A Space Analysis and Visualization System p 3242 N95-34238
Triple invariant optical pattern recognition using circular harmonic synthetic filters
[AD-A294253] p 3217 N95-34459
Hardware implementation of a desktop supercomputer for high performance image processing
[AD-A294272] p 3178 N95-34462

A document analysis system p 3244 N95-34804

IMAGE RECONSTRUCTION

Three-dimensional ground penetrating radar imaging using synthetic aperture time-domain focusing
[DE95-010731] p 3095 N95-32569

IMAGE RESOLUTION

Combined hyperspatial and hyperspectral imaging spectrometer concept p 3129 N95-33738

Aerolian erosion, transport, and deposition of volcaniclastic sands among the shifting sand dunes, Christmas Lake Valley, Oregon: TIMS image analysis p 3137 N95-33793

The 1994 laboratory calibration of TIMS p 3117 N95-33796

IMAGERY

Characteristics of the HYDICE sensor p 3116 N95-33733

Topography from shading and stereo p 3241 N95-34229

IMAGES

The composite classification problem in optical information processing p 3244 N95-32430

SeaWiFS technical report series. Volume 15: The simulated SesWiFS data set, version 2
[NASA-TM-104566-VOL-15] p 3158 N95-32545

Identification of terrain imagery with unstable reflectivity p 3093 N95-33138

Wavelet analysis of atmospheric turbulence structures: What can we gain from this new technique?
[DE95-011955] p 3156 N95-33847

IMAGING RADAR

On the potential of long wavelength imaging radars for mapping vegetation types and woody biomass in tropical rain forests p 3141 N95-33812

IMAGING SPECTROMETERS

Summaries of the Fifth Annual JPL Airborne Earth Science Workshop. Volume 1: AVIRIS Workshop
[NASA-CR-198922] p 3128 N95-33730

High spectral resolution remote sensing of canopy chemistry p 3128 N95-33731

Quantitative remote sensing of ammonium minerals, Cedar Mountains, Esmeralda County, Nevada p 3128 N95-33734

CNR LARA project, Italy: Airborne laboratory for environmental research p 3129 N95-33735

Combined hyperspatial and hyperspectral imaging spectrometer concept p 3129 N95-33738

Airborne Visible/Infrared Imaging Spectrometer (AVIRIS) onboard calibration system p 3116 N95-33739

New calibration techniques for the Airborne Visible/Infrared Imaging Spectrometer (AVIRIS) p 3116 N95-33740

Initial vegetation species and senescience/stress indicator mapping in the San Luis Valley, Colorado using imaging spectrometer data p 3130 N95-33741

Calibration to surface reflectance of terrestrial imaging spectrometry data: Comparison of methods p 3130 N95-33743

Determination of the in-flight spectral calibration of AVIRIS using atmospheric absorption features p 3117 N95-33751

An improved spectral calibration requirement for AVIRIS p 3117 N95-33752

Movement of water vapor in the atmosphere measured by an imaging spectrometer at Rogers Dry Lake, CA p 3132 N95-33753

In-flight radiometric calibration of AVIRIS in 1994 p 3117 N95-33754

Measurement of atmospheric water vapor, leaf liquid water and reflectance with AVIRIS in the Boreal Ecosystem-Atmosphere Study: Initial results p 3133 N95-33755

Measurement of the spectral absorption of liquid water in melting snow with an imaging spectrometer p 3133 N95-33756

Vegetation species composition and canopy architecture information expressed in leaf water absorption measured in the 1000 nm and 2200 spectral region by an imaging spectrometer p 3133 N95-33757

AVIRIS user's guide p 3117 N95-33759

Aircraft scanner data availability via the version 0 Information Management System p 3134 N95-33762

Airborne Visible/Infrared Imaging Spectrometer (AVIRIS): Sensor improvements for 1994 and 1995 p 3117 N95-33769

Extraction of ozone and chlorophyll-A distribution from AVIRIS data p 3136 N95-33770

Summaries of the Fifth Annual JPL Airborne Earth Science Workshop. Volume 2: TIMS Workshop
[NASA-CR-198923] p 3136 N95-33789

IMAGING TECHNIQUES

An original numerical method for autonomous navigation p 3044 N95-32495

Ricor K506B cryocooler performance during the Clementine mission and ground testing
[DE95-010683] p 3089 N95-32568

Three-dimensional ground penetrating radar imaging using synthetic aperture time-domain focusing
[DE95-010731] p 3095 N95-32569

Dosimetry of heavy ions by use of CCD detectors p 3161 N95-32721

Gamma ray imaging of the Crab and Vale regions with the UCR double-Compton telescope p 3245 N95-32837

Ignition and early soot formation in a DI diesel engine using multiple 2-D imaging diagnostics
[DE95-010692] p 3122 N95-32863

Energy and Technology Review
[DE95-011686] p 3223 N95-33066

Thermographic imaging for high-temperature composite materials: A defect detection study
[NASA-TM-106950] p 3125 N95-33209

Laser ablation plume thermalization dynamics in background gases studied by time-resolved imaging, spectroscopic, and ion probe diagnostics
[DE95-010277] p 3118 N95-33246

Printability of substrate and absorber defects on extreme ultraviolet lithographic masks
[DE95-010916] p 3084 N95-33247

High-resolution magnetic imaging and investigations of thin-film magnetism with spin-polarized electron, ion and atom probes
[DE95-012190] p 3074 N95-33392

Characteristics of the HYDICE sensor p 3116 N95-33733

CNR LARA project, Italy: Airborne laboratory for environmental research p 3129 N95-33735

Mapping target signatures via partial unmixing of AVIRIS data p 3129 N95-33737

Mapping minerals, amorphous materials, environmental materials, vegetation, water, ice and snow, and other materials: The USGS tricorder algorithm p 3130 N95-33742

Calibration to surface reflectance of terrestrial imaging spectrometry data: Comparison of methods p 3130 N95-33743

Remote mineral mapping using AVIRIS data at Summitville, Colorado and the adjacent San Juan Mountains p 3134 N95-33761

Using foreground/background analysis to determine leaf and canopy chemistry p 3135 N95-33765

Measuring soil moisture with imaging radars p 3139 N95-33803

On the potential of long wavelength imaging radars for mapping vegetation types and woody biomass in tropical rain forests p 3141 N95-33812

An interactive environment for the analysis of large Earth observation and model data sets p 3239 N95-34219

Advanced data visualization and sensor fusion: Conversion of techniques from medical imaging to Earth science p 3242 N95-34236

The ANVIS head-up display: An analysis of its application to naval helicopters
[AD-A294342] p 3170 N95-34358

A real-time single-camera, stereoscopic video device
[AD-A294105] p 3116 N95-34496

Ultrafast near-field scanning optical microscopy (NSOM) of emerging display technology media: Solid state electronic structure and dynamics
[AD-A294879] p 3218 N95-34571

SAR
[AD-A295020] p 3101 N95-34788

IMMUNE SYSTEMS

Immunological protection against botulinum neurotoxin by a synthetic vaccine
[AD-A294146] p 3165 N95-34754

IMMUNITY

Immunological protection against botulinum neurotoxin by a synthetic vaccine
[AD-A294146] p 3165 N95-34754

IMMUNOLOGY

Immunological protection against botulinum neurotoxin by a synthetic vaccine
[AD-A294146] p 3165 N95-34754

IMPACT DAMAGE

Study of the space environmental effects on spacecraft engineering materials
[NASA-CR-199090] p 3066 N95-32581

Low velocity impact damage in carbon fiber/PEEK composite laminates
[ISBN-0-315-86546-6] p 3065 N95-33710

IMPACT LOADS

Application of impact dampers in vibration control of flexible structures p 3127 N95-32420

Influence of non classical friction on the rubbing and impact behavior of rotor dynamic systems p 3122 N95-32906

Evaluating the potential for rotation and loss of flight helmets from inertia and impact loads
[AD-A294041] p 3170 N95-34489

IMPACT STRENGTH

Fracture toughness assessment of present and future pressure vessel materials based on Charpy impact energy and yield strength
[AD-A294008] p 3081 N95-34373

IMPACT TESTS

Characterizing the fragmentation ring on witness plates p 3056 N95-32426

A study of the effect of grain size on the ballistic performance of silicon carbide
[DE95-011724] p 3126 N95-33068

Evaluation of a retrofit OH-58 pilot's seat to prevent back injury
[AD-A294895] p 3171 N95-34574

IMPEDANCE

Impedance study for the PEP-2 B-factory
[DE95-010569] p 3203 N95-32567

General limits on the performance of high power radiators
[DE95-010732] p 3095 N95-32570

Summary of the impedance working group
[DE95-012095] p 3211 N95-32606

IMPINGEMENT

Analysis of LDEF experiment AO187-2 chemical and isotopic measurements of micrometeoroids by secondary ion mass spectrometry
[NASA-CR-198849] p 3246 N95-32913

Experimental and numerical analysis of controlled impinging liquid jets p 3109 N95-33257

IMPLANTATION

High resistivity InAlN by nitrogen or oxygen implantation
[DE95-011023] p 3226 N95-32594

IMPROVEMENT

Airborne Visible/Infrared Imaging Spectrometer (AVIRIS): Sensor improvements for 1994 and 1995 p 3117 N95-33769

IMPULSES

Experimental investigation of impulse radar for mitigation of effects of radar absorbing materials
[AD-A294166] p 3100 N95-34762

IMPURITIES

Study of impurity concentrations by VUV spectroscopy on HL-1
[DE95-614186] p 3221 N95-32562

Spontaneous dewetting of a perfluoropolyether
[NASA-TM-106964] p 3083 N95-32919

Studies of impurity mode and ITG mode in toroidal plasmas
[DE95-012134] p 3223 N95-33391

IN-FLIGHT MONITORING

High accuracy in-flight wavelength calibration of imaging spectrometry data p 3132 N95-33750

INCLUSIONS

Inclusion models of tensile fracture in fiber-reinforced brittle-matrix composites p 3065 N95-33721

INCOHERENT SCATTER RADAR

Mid-latitude ionospheric plasma drift: A comparison of digital ionosonde and incoherent scatter radar measurements at Millstone Hill p 3222 N95-32838

INCOMPRESSIBLE FLOW

Unified approach for incompressible flows p 3113 N95-32425

Parallel finite element methods and iterative solution techniques for viscous incompressible flows p 3108 N95-33031

The effect of interaction on boundary-layer separation and breakdown p 3109 N95-33310

Numerical thermal analyses of heat exchangers for the stirling engine application
[NASA-CR-199120] p 3110 N95-33398

A comparison of interface tracking methods
[DE95-009481] p 3111 N95-33698

Direct and large eddy simulations of three dimensional round turbulent jets p 3111 N95-33709

Analysis and finite element approximation of an optimal shape control problem for the steady-state Navier-Stokes equations p 3112 N95-34285

Adaptive grid method using elliptic equation for compressible flows p 3035 N95-34515

A multigrid incompressible NS solver p 3036 N95-34517

Direct numerical simulation of incompressible homogeneous isotropic turbulence using compressible Navier-Stokes equations p 3037 N95-34529

Elementary benchmarks of the NWT computer system and program performance p 3038 N95-34532

Numerical simulations of dynamic stall phenomena in low speed flows p 3040 N95-34546

Parallel computation for two dimensional incompressible flow on array of transputers p 3042 N95-34558

Nonlinear stability of unsteady viscous flow
[AD-A294931] p 3113 N95-34597

INCONEL (TRADEMARK)
Characterizing the fragmentation ring on witness plates p 3056 N95-32426
Fracture toughness assessment of present and future pressure vessel materials based on Charpy impact energy and yield strength
[AD-A294008] p 3081 N95-34373

INDEXES (DOCUMENTATION)
AGARD index of publications: 1992-1994
[AGARD-INDEX-92-94] p 3237 N95-33198
NASA directives master list and index
[NHB-1410.13O] p 3238 N95-33249
Bibliography on cold regions science and technology: Volume 48, part 2
[AD-A293993] p 3243 N95-34421

INDIUM
High rate dry etching of GaN, AlN and InN in ECR Cl2/CH4/H2/Ar plasmas
[DE95-011872] p 3223 N95-33412
Indium mono-ion oscillator
[AD-A293736] p 3104 N95-34451

INDUCTORS
Improved L-C resonant decay technique for Q measurement of quasilinear power inductors: New results for MPP and ferrite powdered cores
[NASA-CR-198373] p 3103 N95-33874

INELASTIC SCATTERING
Magnetic excitations in a random exchange system Fe(x)Mn(1-x)TiO3
[DE95-006626] p 3225 N95-32377
The Q(2)-dependence of the Gross-Llewellyn Smith sum rule and of the parton distributions
[DE95-623678] p 3202 N95-32406
A Study of the A dependence of the deep inelastic scattering of leptons and implications for understanding of the EMC effect
[DE95-613711] p 3206 N95-32796
Analytic approach to small x structure functions
[PB95-236030] p 3214 N95-34653

INELASTIC STRESS
Inelastic response spectra of a system with bilinear restoring characteristics: Effect of plastic-stiffness ratio
[REPT-2213] p 3091 N95-32993

INEQUALITIES
Lieb-thirring constants L(sub gamma,1) for gamma greater than or equal to 1/2
[PB95-212171] p 3196 N95-33234

INERTIAL CONFINEMENT FUSION
COBRA accelerator for Sandia ICF diode research at Cornell University
[DE95-011018] p 3101 N95-32578
Control of the laser beam irradiation intensity distribution using aspherical multi lens array and edge-shaped plates
[REPT-2209] p 3090 N95-32989
Absolute wavefront measurements of high-energy laser beams in the Beamlet Demonstration Project for the National Ignition Facility
[DE95-012224] p 3118 N95-33378
Inertial confinement fusion target component fabrication and technology development support
[DE95-011655] p 3224 N95-34436

INERTIAL NAVIGATION
An original numerical method for autonomous navigation p 3044 N95-32495
Navigational technology of dual usage p 3048 N95-33131
Dual-use micromechanical inertial sensors p 3092 N95-33132
Application of advanced safety technique to ring laser gyro inertial navigation system integration p 3048 N95-33140

INFECTIOUS DISEASES
The preservation of human surrogates for biomechanical studies p 3167 N95-33312

INFERENCE
An efficient inference engine for interactive fault diagnosis in a helpdesk application p 3189 N95-33000

INFILTRATION
Interfacial reactions during the liquid infiltration of titanium matrix composites p 3081 N95-34252

INFORMATION
Report to the Ranking Minority Member, Committee on Government Operations, House of Representatives. Paperwork reduction: Reported burden hour increases reflect new estimates, not actual changes
[GAO/PEMD-94-3] p 3236 N95-33907

INFORMATION DISSEMINATION
Annual report to Congress 1994: Energy Information Administration
[DE95-011240] p 3237 N95-32482
NASA/DOD Aerospace Knowledge Diffusion Research Project. Paper 50: From student to entry-level professional: Examining the role of language and written communications in the reacculturation of aerospace engineering students
[NASA-TM-110834] p 3237 N95-32883
NASA wide electronic publishing system: Electronic printing and duplicating. Stage 3 evaluation report
[NASA-TM-104620] p 3237 N95-32922
Clearing-house mechanism to promote and facilitate technical and scientific cooperation under the UN Convention on Biological Diversity
[PB95-214557] p 3163 N95-33236
Exchange, interpretation, and database-search of ion mobility spectra supported by data format JCAMP-DX p 3070 N95-33274
Collaborating over the Web: Libraries and laboratories or the Librarian and the Webmaster
[DE95-010572] p 3186 N95-33639
Representing incomplete knowledge in relational databases p 3238 N95-33722
Evaluation of the photochemical reflectance index in AVIRIS imagery p 3131 N95-33747
NASA/DOD Aerospace Knowledge Diffusion Research Project. Report 33: The technical communications practices of US aerospace engineers and scientists: Results of the phase 1 AIAA mail survey
[NASA-TM-110180] p 3239 N95-34217

INFORMATION MANAGEMENT
Exchange, interpretation, and database-search of ion mobility spectra supported by data format JCAMP-DX p 3070 N95-33274
Aircraft scanner data availability via the version 0 Information Management System p 3134 N95-33762
Report to the Ranking Minority Member, Committee on Government Operations, House of Representatives. Paperwork reduction: Reported burden hour increases reflect new estimates, not actual changes
[GAO/PEMD-94-3] p 3236 N95-33907

INFORMATION RETRIEVAL
Evaluated nuclear structure data file
[DE95-011343] p 3202 N95-32484
Incorporating bibliographic information into a spatial data query system for the Savannah River Site
[DE95-010965] p 3238 N95-33402

INFORMATION SYSTEMS
The RHIC transfer line cable database
[DE95-011560] p 3236 N95-32412
Annual report to Congress 1994: Energy Information Administration
[DE95-011240] p 3237 N95-32482
Formalization and representation of a product-driven approach to method assembly for situational systems development
[PB95-215190] p 3237 N95-33238
Carbon Dioxide Information Analysis Center and World Data Center: A for Atmospheric trace gases
[DE95-011769] p 3154 N95-33655
Representing incomplete knowledge in relational databases p 3238 N95-33722
Aircraft scanner data availability via the version 0 Information Management System p 3134 N95-33762
Applied Information Systems Research Program (AISRP) Workshop 3 meeting proceedings
[NASA-CR-199103] p 3239 N95-34218
Managing technological change in a military treatment facility: A case study of medical diagnostic imaging support (MDIS) system
[AD-A294894] p 3165 N95-34573
Grayling 2 information base for generation of synthetic thermal infrared scenes
[AD-A294956] p 3100 N95-34578
A curriculum for strategy in the information age: Chaos in a new era
[AD-A295036] p 3244 N95-34794

INFORMATION THEORY
Representing incomplete knowledge in relational databases p 3238 N95-33722

INFORMATION TRANSFER
National Aeronautics and Space Administration (NASA)/American Society for Engineering Education (ASEE) Summer Faculty Fellowship Program, 1994, volume 1
[NASA-CR-188410] p 3248 N95-32418
NASA/DOD Aerospace Knowledge Diffusion Research Project. Paper 50: From student to entry-level professional: Examining the role of language and written communications in the reacculturation of aerospace engineering students
[NASA-TM-110834] p 3237 N95-32883
Exchange, interpretation, and database-search of ion mobility spectra supported by data format JCAMP-DX p 3070 N95-33274
Recoverable distributed shared memory under sequential and relaxed consistency
[AD-A293966] p 3178 N95-34453

INFRARED ASTRONOMY SATELLITE
Infrared detection of chemical corrosion on metal surface
[AD-A295000] p 3081 N95-34821

INFRARED DETECTORS
An integrated system for air to ground operations p 3044 N95-32498
Ricor K506B cryocooler performance during the Clementine mission and ground testing
[DE95-010683] p 3089 N95-32568
Advanced far infrared detector and double donor studies in Ge
[DE95-011261] p 3247 N95-33625
Infrared detection of chemical corrosion on metal surface
[AD-A295000] p 3081 N95-34821

INFRARED IMAGERY
Night attack p 3042 N95-32487
A helmet mounted display for night missions at low altitude p 3045 N95-32503
SIRPH: Steerable infrared picture on helmet mounted display p 3045 N95-32504
Summaries of the Fifth Annual JPL Airborne Earth Science Workshop. Volume 1: AVIRIS Workshop
[NASA-CR-198922] p 3128 N95-33730
CNR LARA project, Italy: Airborne laboratory for environmental research p 3129 N95-33735
Calibration to surface reflectance of terrestrial imaging spectrometry data: Comparison of methods p 3130 N95-33743
Evaluation of the photochemical reflectance index in AVIRIS imagery p 3131 N95-33747
Correction of thin cirrus effects in AVIRIS images using the sensitive 1.375-micron cirrus detecting channel p 3131 N95-33748
Remote sensing of smoke, clouds, and radiation using AVIRIS during SCAR experiments p 3132 N95-33749
Aircraft scanner data availability via the version 0 Information Management System p 3134 N95-33762
AVIRIS spectral trajectories for forested areas of the Gifford Pinchot National Forest p 3135 N95-33766
Sub-pixel localization of highways in AVIRIS images p 3135 N95-33767
Validating spatial structure in canopy water content using geostatistics p 3135 N95-33768
Airborne Visible/Infrared Imaging Spectrometer (AVIRIS): Sensor improvements for 1994 and 1995 p 3117 N95-33769
Preliminary study of Kelso Dunes using AVIRIS, TM, and AIRSAR p 3136 N95-33773
Summaries of the Fifth Annual JPL Airborne Earth Science Workshop. Volume 2: TIMS Workshop
[NASA-CR-198923] p 3136 N95-33789
Analyses of TIMS and AVIRIS data, integrated with field and laboratory spectra, for lithological and mineralogical interpretation of Vulcano Island, Italy p 3137 N95-33790
Urban remote sensing applications: TIMS observations of the City of Scottsdale p 3137 N95-33791
For geological investigations with airborne thermal infrared multispectral images: Transfer of calibration from laboratory spectrometer to TIMS as alternative for removing atmospheric effects p 3137 N95-33792
Aerolian erosion, transport, and deposition of volcaniclastic sands among the shifting sand dunes, Christmas Lake Valley, Oregon: TIMS image analysis p 3137 N95-33793
A conflict of water and fire: Remote sensing imagery of the Uinkaret Volcanic Field, Grand Canyon, Arizona p 3117 N95-33795

INFRARED INSPECTION
Thermographic imaging for high-temperature composite materials: A defect detection study
[NASA-TM-106950] p 3125 N95-33209

INFRARED INSTRUMENTS
HeliRadar: A rotating antenna synthetic aperture radar for helicopter allweather operations p 3093 N95-33137
A 30-pair thin film thermoelectric pile
[AD-A294058] p 3151 N95-34468

INFRARED LASERS
Interfacial reactions during the liquid infiltration of titanium matrix composites p 3081 N95-34252

INFRARED RADAR
SIRPH: Steerable infrared picture on helmet mounted display p 3045 N95-32504

INFRARED RADIATION
Ricor K506B cryocooler performance during the Clementine mission and ground testing
[DE95-010683] p 3089 N95-32568
The growth and optimization of InPSb/InGaAs/InAsSb strained-layer superlattice emitters by metal organic chemical vapor deposition
[DE95-011057] p 3226 N95-32595

Land surface temperature measurements from EOS MODIS data
[NASA-CR-199082] p 3142 N95-32717
Growth and characterization of heterostructures and infrared emitters with compressed InAsSb layers
[DE95-009828] p 3228 N95-33213
Correction of thin cirrus effects in AVIRIS images using the sensitive 1.375-micron cirrus detecting channel
p 3131 N95-33748
A 30-pair thin film thermoelectric pile
[AD-A294058] p 3151 N95-34468
Grayling 2 information base for generation of synthetic thermal infrared scenes
[AD-A294956] p 3100 N95-34578

INFRARED REFLECTION
Infrared detection of chemical corrosion on metal surface
[AD-A295000] p 3081 N95-34821

INFRARED SCANNERS
Summaries of the Fifth Annual JPL Airborne Earth Science Workshop. Volume 2: TIMS Workshop
[NASA-CR-198923] p 3136 N95-33789
For geological investigations with airborne thermal infrared multispectral images: Transfer of calibration from laboratory spectrometer to TIMS as alternative for removing atmospheric effects p 3137 N95-33792
The 1994 laboratory calibration of TIMS
p 3117 N95-33796
The 1994 TIMS airborne calibration experiment: Castaic Lake, California p 3117 N95-33797
TIMS observations of surface emissivity in HAPEX-Sahel p 3139 N95-33799
A field- and laboratory-based quantitative analysis of alluvium: Relating analytical results to TIMS data
p 3139 N95-33800

INFRARED SIGNATURES
Grayling 2 information base for generation of synthetic thermal infrared scenes
[AD-A294956] p 3100 N95-34578

INFRARED SPECTRA
CADIR: A model for generating infrarad images
[PB95-222956] p 3215 N95-33239
Exchange, interpretation, and database-search of ion mobility spectra supported by data format JCAMP-DX
p 3070 N95-33274
High spectral resolution remote sensing of canopy chemistry p 3128 N95-33731
High accuracy in-flight wavelength calibration of imaging spectrometry data p 3132 N95-33750
AVIRIS spectral trajectories for forested areas of the Gifford Pinchot National Forest p 3135 N95-33766
Sub-pixel localization of highways in AVIRIS images
p 3135 N95-33767
Validating spatial structure in canopy water content using geostatistics p 3135 N95-33768
TIMS observations of surface emissivity in HAPEX-Sahel p 3139 N95-33799
Infrared detection of chemical corrosion on metal surface
[AD-A295000] p 3081 N95-34821

INFRARED SPECTROMETERS
Detection of emission sources using passive-remote Fourier Transform Infrared spectroscopy
[DE95-009920] p 3067 N95-32671
Summaries of the Fifth Annual JPL Airborne Earth Science Workshop. Volume 1: AVIRIS Workshop
[NASA-CR-198922] p 3128 N95-33730
High spectral resolution remote sensing of canopy chemistry p 3128 N95-33731
Quantitative remote sensing of ammonium minerals, Cedar Mountains, Esmeralda County, Nevada
p 3128 N95-33734
Using dark current data to estimate AVIRIS noise covariance and improve spectral analyses
p 3129 N95-33736
Mapping target signatures via partial unmixing of AVIRIS data p 3129 N95-33737
Airborne Visible/Infrared Imaging Spectrometer (AVIRIS) onboard calibration system
p 3116 N95-33739
New calibration techniques for the Airborne Visible/Infrared Imaging Spectrometer (AVIRIS)
p 3116 N95-33740
Initial vegetation species and senescience/stress indicator mapping in the San Luis Valley, Colorado using imaging spectrometer data p 3130 N95-33741
A layered approach to technology transfer of AVIRIS between Earth Search Sciences, Inc. and the Idaho National Engineering Laboratory p 3117 N95-33746
Determination of the in-flight spectral calibration of AVIRIS using atmospheric absorption features
p 3117 N95-33751
An improved spectral calibration requirement for AVIRIS p 3117 N95-33752
Movement of water vapor in the atmosphere measured by an imaging spectrometer at Rogers Dry Lake, CA
p 3132 N95-33753
In-flight radiometric calibration of AVIRIS in 1994
p 3117 N95-33754
Measurement of atmospheric water vapor, leaf liquid water and reflectance with AVIRIS in the Boreal Ecosystem-Atmosphere Study: Initial results
p 3133 N95-33755
Measurement of the spectral absorption of liquid water in melting snow with an imaging spectrometer
p 3133 N95-33756
Vegetation species composition and canopy architecture information expressed in leaf water absorption measured in the 1000 nm and 2200 spectral region by an imaging spectrometer p 3133 N95-33757
AVIRIS user's guide p 3117 N95-33759
Integration of AIRSAR and AVIRIS data for Trail Canyon alluvial fan, Death Valley, California
p 3134 N95-33760
Remote mineral mapping using AVIRIS data at Summitville, Colorado and the adjacent San Juan Mountains p 3134 N95-33761
An algorithm for chlorophyll using first difference transformations of AVIRIS reflectance spectra
p 3134 N95-33763
Airborne Visible/Infrared Imaging Spectrometer (AVIRIS): Sensor improvements for 1994 and 1995
p 3117 N95-33769
The JPL Field Emission Spectrometer
p 3117 N95-33794

INFRARED SPECTROSCOPY
Detection of emission sources using passive-remote Fourier Transform Infrared spectroscopy
[DE95-009920] p 3067 N95-32671
Discrimination of alkalinity in granitoid Rocks: A potential TIMS application p 3138 N95-33798

INFRARED TELESCOPES
SOFIA: Aft cavities wind tunnel test
[NASA-TM-110673] p 3033 N95-32682
SOFIA 2 model telescope wind tunnel test report
[NASA-TM-110668] p 3033 N95-32764
Study of a large optical/infrared telescope scheme
[AD-A294042] p 3218 N95-34490

INFRARED TRACKING
Night attack p 3042 N95-32487
Multispectral image correlation for air-to-ground targeting p 3043 N95-32489

INJECTION MOLDING
Apparatus for injection molding high-viscosity materials
[AD-D017471] p 3065 N95-34448

INJECTORS
Pop tests of storable biopropellant liquid apogee engine
[NAL-TR-1253] p 3060 N95-32755
The development of some kinds of LRE injectors
[AD-A294199] p 3061 N95-34302
A study of supersonic mixing flow field with ramp injector p 3035 N95-34512

INJURIES
OH-58 pilot display unit (PDU) simulated crash tests
[AD-A294049] p 3170 N95-34378

INLET TEMPERATURE
Minimum fan turbine inlet temperature mode evaluation p 3052 N95-33016

INMARSAT SATELLITES
INMARSAT TT&C and communications network and the Beijing INMARSAT Station
[AD-A294163] p 3100 N95-34760

INSERTS
Method of installing a metallic threaded insert in a composite/rubber panel
[AD-D017522] p 3065 N95-34620

INSOLATION
Investigation research on introducing new energy technology, promoting its practical application, and providing its instruction
[DE95-769801] p 3148 N95-32403

INSPECTION
Report to the Chairman, Subcommittee on Aviation, Committee on Commerce, Science, and Transportation, US Senate. Aviation safety: Data problems threaten FAA strides on safety analysis system
[GAO/AIMD-95-27] p 3046 N95-32705
Expert systems and artificial intelligence applications in engineering design and inspection p 3190 N95-33008
Integrated special mission flight management for a flight inspection aircraft p 3049 N95-33145

INSTALLING
Solid-state data recorder, next development and use
p 3094 N95-33143

INSTANTONS
The computation of electron transfer rates: The nonadiabatic instanton solution
[AD-A294523] p 3209 N95-34350

INSTRUMENT APPROACH
Current issues in the design and information content of instrument approach charts
[AD-A294752] p 3047 N95-34562
Resource document for the design of electronic instrument approach procedure displays
[AD-A295108] p 3047 N95-34797

INSTRUMENT LANDING SYSTEMS
Current issues in the design and information content of instrument approach charts
[AD-A294752] p 3047 N95-34562

INSTRUMENT ORIENTATION
SeaWiFS technical report series. Volume 22: Prelaunch acceptance report for the SeaWFS radiometer
[NASA-TM-104566-VOL-22] p 3159 N95-32672

INSTRUMENTS
Third International Workshop on Ion Mobility Spectrometry
[NASA-CP-3301] p 3069 N95-33265

INSULATION
The next generation of automobile emissions reduction: Innovative control of off-cycle emissions
[DE95-004057] p 3153 N95-32809

INSULATORS
Performance of partially fluorinated polyimide insulation for aerospace applications
[NASA-CR-198372] p 3060 N95-32673

INTEGRAL EQUATIONS
A posteriori pointwise error estimates for the boundary element method
[DE95-008099] p 3194 N95-32388
Sum of fractional derivatives and m-accretive operators
[PB95-215307] p 3195 N95-32893
Computational electromagnetics and parallel dense matrix computations
[DE95-012286] p 3099 N95-33379
Unified model of the RF plasma sheath
[DE95-012114] p 3224 N95-33851
Penetrable wedge analysis
[AD-A294276] p 3234 N95-34464

INTEGRALS
Associative integral formulas and deformations of Yangians
[PB95-212189] p 3195 N95-32889

INTEGRATED CIRCUITS
N-15 hydrogen profiling of IC metallizations
[DE95-011052] p 3102 N95-32708
A reconfigurable optoelectronic interconnect technology for multi-processor networks
[DE95-011895] p 3186 N95-33838
Self stressing test structure cells
[AD-A294386] p 3104 N95-34345
Novel field effect transistors for low power electronics
[AD-A294221] p 3105 N95-34458
Development of thin film diamond based integrated circuit technology
[AD-A294519] p 3231 N95-34478
Fabrication technology and measurement of coupled quantum dot devices
[AD-A294853] p 3231 N95-34569

INTEGRATED LIBRARY SYSTEMS
An interactive environment for the analysis of large Earth observation and model data sets p 3239 N95-34219
Interactive interface for National Center for Atmospheric Research (NCAR) graphics p 3239 N95-34220
System of experts for intelligent data management (SEIDAM) p 3240 N95-34226
Knowledge-based assistance for science visualization and analysis using large distributed databases
p 3241 N95-34227
Experimenter's laboratory for visualized interactive science p 3184 N95-34228
VIEWCACHE: An incremental pointer-based access method for autonomous interoperable databases
p 3242 N95-34235
SAVS: A Space Analysis and Visualization System
p 3242 N95-34238
A distributed analysis and visualization system for model and observational data p 3243 N95-34240
DataHub: Science data management in support of interactive exploratory analysis p 3243 N95-34241

INTEGRATED OPTICS
Integration of diffractive lenses with addressable vertical-cavity laser arrays
[DE95-009850] p 3118 N95-32663
Optical pulse generation using fiber lasers and integrated optics
[DE95-011517] p 3216 N95-33506
The 11th Annual Review of Progress in Applied Computational Electromagnetics, volume 2
[AD-A294851] p 3100 N95-34567

INTEGRATORS
A digital boxcar integrator for IMS spectra
p 3072 N95-33288

INTERACTIONAL AERODYNAMICS
Numerical analysis around the whole SST configuration p 3039 N95-34541
INTERFACES
The pinhole interface for IMS/MS p 3070 N95-33275
Towards friendlier user interfaces for expert systems [AD-A294056] p 3192 N95-34467
Metal-ceramic interfaces: Overlayer-induced reconstruction and magnetism of 4d transition-metal monolayers
[DE95-011543] p 3075 N95-34483
INTERFACIAL TENSION
Inclusion models of tensile fracture in fiber-reinforced brittle-matrix composites p 3065 N95-33721
INTERFEROMETERS
Laser-based ultrasonics by dual-probe interferometer detection and narrow-band ultrasound generation p 3118 N95-33464
MODTRAN3: An update and recent validations against airborne high resolution interferometer measurements p 3128 N95-33732
The JPL Field Emission Spectrometer p 3117 N95-33794
INTERFEROMETRY
X-ray standing wave interferometry-optics at 1 angstrom with applications to surface and material sciences
[DE95-009688] p 3215 N95-32662
Mid-latitude ionospheric plasma drift: A comparison of digital ionosonde and incoherent scatter radar measurements at Millstone Hill p 3222 N95-32838
Feasibility of fullerene thin films for high-speed all-optical switching
[DE95-011735] p 3085 N95-33409
Bayes classification of interferometric TOPSAR data p 3140 N95-33808
Estimation of penetration of forest canopies by Interferometric SAR measurements p 3141 N95-33814
INTERGRANULAR CORROSION
Irradiation-assisted stress corrosion cracking considerations at temperatures below 288 C
[DE95-008940] p 3077 N95-32555
INTERIOR BALLISTICS
Investigation of starting and ignition transients in the thermally choked ram accelerator p 3054 N95-34805
INTERLAMINAR STRESS
Interlaminar stress analysis of dropped-ply laminated plates and shells by a mixed method p 3064 N95-33327
INTERLAYERS
Diamond multilayer multichip module substrate
[AD-D017468] p 3104 N95-34445
INTERMETALLICS
TEM investigation on the low temperature phase of HIV2
[DE95-009500] p 3225 N95-32532
Intermetallic compound layer growth kinetics in non-lead bearing solders
[DE95-009595] p 3078 N95-32591
Effect of phase transformations on the mechanical properties of a multiphase alloy based on NiAl + Fe
[DE95-010119] p 3079 N95-33217
Theoretical dynamical studies of metal clusters and cluster-ligand systems
[DE95-012461] p 3228 N95-33382
The growth of ultrathin epitaxial intermetallic films
[AD-A295037] p 3232 N95-34795
INTERMOLECULAR FORCES
Lattice Polymer Automata
[DE95-011980] p 3062 N95-33848
INTERNAL COMBUSTION ENGINES
The next generation of automobile emissions reduction: Innovative control of off-cycle emissions
[DE95-004057] p 3153 N95-32809
Low-order nonlinear dynamic model of IC engine-variable pitch propeller system for general aviation aircraft
[NASA-TM-107006] p 3050 N95-32916
INTERNAL ENERGY
DSMC method applied for reacting gas flows p 3035 N95-34509
INTERNAL PRESSURE
Cylindrical shell buckling through strain hardening
[DE95-009545] p 3125 N95-32392
INTERNATIONAL COOPERATION
Feasibility survey on international cooperation for high efficiency energy conversion technology in fiscal 1993
[DE95-769804] p 3148 N95-32546
Minutes of the 12th Joint NASA/DARA-DLR Life Sciences Program Working Group Meeting
[NASA-TM-110655] p 3161 N95-32719
European Space Agency 1994 annual report p 3252 N95-32805
Some results of international cooperation in military to commercial conversion of laser gyro technology p 3092 N95-33130
INTERNATIONAL SPACE STATION
Space Station: Estimated total US funding requirements. Report to Congressional Requesters
[GAO/NSIAD-95-163] p 3058 N95-32884
Logistics Operations Management Center: Maintenance Support Baseline (LOMC-MSB)
[NASA-TM-110624] p 3245 N95-33489
INTERNATIONAL SYSTEM OF UNITS
Metric conversion: Future progress depends upon private sector and public support. Report to Congressional requesters
[GAO/RCED-94-23] p 3089 N95-32785
INTERNATIONAL TRADE
World mineral statistics, 1988-92. Production: Exports: Imports
[PB95-208096] p 3155 N95-32601
INTERNETS
Security and privacy in the NII
[AD-A293475] p 3244 N95-34816
INTERPLANETARY DUST
Analysis of LDEF experiment AO187-2 chemical and isotopic measurements of micrometeoroids by secondary ion mass spectrometry
[NASA-CR-198849] p 3246 N95-32913
INTERPOLATION
High accuracy in-flight wavelength calibration of imaging spectrometry data p 3132 N95-33750
INTERPROCESSOR COMMUNICATION
Distributed shared memory for new generation networks
[AD-A293722] p 3185 N95-32580
INTERSTITIALS
Synthesis of potential new Zintl phases
[DE95-010123] p 3227 N95-32640
INVARIANCE
Overview of rare K decays
[DE95-012081] p 3208 N95-33850
INVENTORY CONTROLS
NASA-Wide Fastener Technical Interchange Meeting
[NASA-CP-3308] p 3123 N95-33199
INVERSE SCATTERING
The method of integration of the nonlinear Schroedinger equation with a source
[DE95-623601] p 3195 N95-32479
Transparent potential perturbations on lattices and in the periodical structures. Elements of the Qualitative Theory of Wave Motion Over the Channels
[DE95-623602] p 3225 N95-32480
Inversion of electron-water elastic scattering data
[DE95-619323] p 3204 N95-32623
INVERSIONS
Inversion of electron-water elastic scattering data
[DE95-619323] p 3204 N95-32623
INVISCID FLOW
The effect of interaction on boundary-layer separation and breakdown p 3109 N95-33310
Direct and large eddy simulations of three dimensional round turbulent jets p 3111 N95-33709
Numerical solutions of inviscid and viscous flows about airfoils by TVD method p 3036 N95-34521
Program developing environment and a CFD application on the Cray T3D p 3038 N95-34535
Numerical analysis around the whole SST configuration p 3039 N95-34541
Numerical simulation of two-dimensional compressible inviscid flow on unstructured grid system p 3041 N95-34557
Modeling liquid jet atomization processes
[AD-A294888] p 3112 N95-34572
IODIDES
Charge-transfer gap closure in transition-metal halides under pressure
[DE95-011268] p 3230 N95-33865
ION ACCELERATORS
Heavy ions acceleration in RF wells of 2-frequency electromagnetic field and in the inverted FEL
[DE95-012439] p 3214 N95-34439
ION BEAMS
Crystalline beam properties as predicted for the storage rings ASTRID and TSR
[DE95-011557] p 3210 N95-32411
Unexpected matching insensitivity in DTL of GTA accelerator
[DE95-011984] p 3211 N95-32416
Estimation of collective instabilities in RHIC
[DE95-011347] p 3211 N95-32485
In situ ion-beam analysis and modification of sol-gel zirconia thin films
[DE95-010994] p 3203 N95-32577
COBRA accelerator for Sandia ICF diode research at Cornell University
[DE95-011018] p 3101 N95-32578
Low-energy Ion-Beam Deposition apparatus equipped with surface analysis system
[DE95-737272] p 3212 N95-32712
YBa2Cu3O(7-x) 45 deg (001) tilt grain boundaries induced by controlled low-energy sputtering of MgO substrates: Transport properties and atomic-scale structure
[DE95-005826] p 3228 N95-32810
Observation of KLM dielectronic recombination resonances in highly charged uranium ions
[DE95-010266] p 3207 N95-33219
Measurements of cross sections and resonance structures following electron-impact excitation/ionization of Na-like Kr and Xe
[DE95-011731] p 3230 N95-34438
Fabrication of optical channel waveguides in the GaAs/AlGaAs system by MeV ion beam bombardment
[DE95-008973] p 3218 N95-34480
ION CHARGE
Proton affinity determinations and proton-bound dimer structure indications in C2 to C15, (alpha),(omega)-alkyldiamines p 3069 N95-33266
ION CURRENTS
Single Langmuir probe characteristic in a magnetized plasma at the TEXT tokamak
[DE95-012144] p 3224 N95-33853
ION ENGINES
Advanced propulsion for geostationary orbit insertion and north-south station keeping
[NASA-TM-107018] p 3060 N95-32917
ION EXCHANGE RESINS
Testing of a carpet catalyst
[PB95-208492] p 3068 N95-33242
ION EXCHANGING
Analysis of samples for the first (1994) OPCW round robin interlaboratory comparison test
[PB95-210324] p 3068 N95-33243
ION EXTRACTION
Direct analysis of organic priority pollutants by IMS p 3071 N95-33280
ION IMPACT
Impact-parameter dependent L-K vacancy-transfer in collisions of Ni(23+) with Ge solid targets
[DE95-010821] p 3228 N95-33373
ION IMPLANTATION
The effects of H(+) implants on YBa2Cu3O7 superconducting materials
[DE95-614466] p 3227 N95-32698
The effects of ion implantation on the tribology of perfluoropolyether-lubricated 440C stainless steel couples
[NASA-TM-106965] p 3083 N95-32918
A background subtraction routine for enhancing energy-filtered plasmon images of MgAl2O4 implanted with Al(+) and Mg(+) ions
[DE95-012850] p 3074 N95-33629
Laser induced diffusion of ion-implanted bismuth in fused silica
[DE95-012869] p 3230 N95-34443
ION IRRADIATION
Smoothing during ion-assisted growth by transient ion beam-induced defects
[DE95-011021] p 3225 N95-32579
Inactivation, DNA double strand break induction and their rejoining in bacterial cells irradiated with heavy ions p 3161 N95-32724
DNA-DSB in CHO-K1 cells induced by heavy-ions: Break rejoining and residual damage (GSI) p 3162 N95-32725
Chromosomal damage observed in first postirradiation metaphases of repair-proficient and -deficient cell lines p 3162 N95-32726
Mutation induction in bacteria after heavy ion irradiation p 3162 N95-32727
Heavy ion induced mutations in mammalian cells: Cross sections and molecular analysis p 3162 N95-32728
Ion assisted deposition of ZnS and MgF2
[AD-A294759] p 3086 N95-34563
ION MOBILITY SPECTROSCOPY
Third International Workshop on Ion Mobility Spectrometry
[NASA-CP-3301] p 3069 N95-33265
The effects of CO2 on the negative reactant ions of IMS p 3069 N95-33267
Fundamental studies of gas phase ionic reactions by ion mobility spectrometry p 3069 N95-33268
Determination of Benzene, Toluene, and Xylene by means of an ion mobility spectrometer device using photoionization p 3069 N95-33269
Engineering approaches and compromises in the design of small ion mobility spectrometers p 3070 N95-33271
Application of Ni-63 photo and corona discharge ionization for the analysis of chemical warfare agents and toxic wastes p 3070 N95-33272

IMS R and D program at Canada customs
p 3070 N95-33273
Exchange, interpretation, and database-search of ion mobility spectra supported by data format JCAMP-DX
p 3070 N95-33274
The pinhole interface for IMS/MS
p 3070 N95-33275
The use of ion mobility spectrometry and gas chromatography/mass spectrometry for the detection of illicit drugs on clandestine records p 3070 N95-33276
Hand-portable gas chromatography-ion mobility spectrometer for the determination of the freshness of fish p 3071 N95-33277
Gas chromatography/ion mobility spectrometry as a hyphenated technique for improved explosives detection and analysis p 3071 N95-33278
Environment applications for ion mobility spectrometry
p 3071 N95-33279
Direct analysis of organic priority pollutants by IMS
p 3071 N95-33280
An ammonia monitor for the water industry
p 3071 N95-33281
The effect of sample holder material on ion mobility spectrometry reproducibility p 3071 N95-33282
A novel approach to increasing cocaine detection confidence utilizing ion mobility spectrometry
p 3072 N95-33283
Application of the ionscan for the detection of methamphetamine and ephedrine in abondoned clandestine laboratories p 3072 N95-33284
Application of Ion Mobility Spectrometry (IMS) in forensic chemistry and toxicology with focus on biological matrices p 3072 N95-33285
Data collection in IMS: It's not as easy as it looks
p 3072 N95-33286
IMS software developments for the detection of chemical warfare agent p 3072 N95-33287
A digital boxcar integrator for IMS spectra
p 3072 N95-33288
Signal processing for ION mobility spectrometers
p 3073 N95-33289
Quantitative analysis of volatile organic compounds using ion mobility spectra and cascade correlation neural networks p 3073 N95-33290
FTP-Server for exchange, interpretation, and database-search of ion mobility spectra, literature, preprints and software p 3073 N95-33291

ION PROBES

Laser ablation plume thermalization dynamics in background gases studied by time-resolved imaging, spectroscopic, and ion probe diagnostics
[DE95-010277] p 3118 N95-33246
High-resolution magnetic imaging and investigations of thin-film magnetism with spin-polarized electron, ion and atom probes
[DE95-012190] p 3074 N95-33392

ION SOURCES

High-resolution magnetic imaging and investigations of thin-film magnetism with spin-polarized electron, ion and atom probes
[DE95-012190] p 3074 N95-33392

ION STORAGE

Crystalline beam properties as predicted for the storage rings ASTRID and TSR
[DE95-011557] p 3210 N95-32411

ION TEMPERATURE

Studies of impurity mode and ITG mode in toroidal plasmas
[DE95-012134] p 3223 N95-33391

ION TRAPS (INSTRUMENTATION)

The uses of Electron Beam Ion Traps in the study of highly charged ions
[DE95-011537] p 3212 N95-33064

IONIC COLLISIONS

Estimation of collective instabilities in RHIC
[DE95-011347] p 3211 N95-32485
Low energy collisions involving multiply charged ions
[DE95-010911] p 3203 N95-32564
Efficiency of modified UA1 jet reconstruction algorithm in PP, PA and AA collisions at STAR
[DE95-009918] p 3212 N95-32665
High energy collisions involving multiply charged ions
[DE95-010912] p 3206 N95-32763
CDW-EIS calculation of longitudinal momentum distribution in single ionization of helium by Ni(24+) ions
[DE95-010816] p 3207 N95-33241
Velocity dependence of ionization and excitation of hydrogen molecules by fast proton impact
[DE95-010818] p 3207 N95-33370
State-selective single electron capture cross sections in He(exp 2+) + Li(2s) and Li(*)(2p) collisions
[DE95-010819] p 3207 N95-33371
An ion-ion collisions system at KSU
[DE95-010820] p 3208 N95-33372
Impact-parameter dependent L-K vacancy-transfer in collisions of Ni(23+) with Ge solid targets
[DE95-010821] p 3228 N95-33373
Electron-electron interaction in the ionization of hydrogenlike projectiles by He
[DE95-010822] p 3208 N95-33374
Measurements of cross sections and resonance structures following electron-impact excitation/ionization of Na-like Kr and Xe
[DE95-011731] p 3230 N95-34438

IONIC DIFFUSION

Laser induced diffusion of ion-implanted bismuth in fused silica
[DE95-012869] p 3230 N95-34443

IONIC MOBILITY

The pinhole interface for IMS/MS
p 3070 N95-33275
FTP-Server for exchange, interpretation, and database-search of ion mobility spectra, literature, preprints and software p 3073 N95-33291

IONIC REACTIONS

Fundamental studies of gas phase ionic reactions by ion mobility spectrometry p 3069 N95-33268

IONIC WAVES

Bernstein-Green-Kruskal wave. 2: The interaction with the Langmuir wave. Stochastic phenomena
[DE95-614202] p 3220 N95-32507
Conversion of the Bernstein-Green-Kruskal wave on the density perturbation, part 1
[DE95-614203] p 3220 N95-32508
Conversion of the Bernstein-Green-Kruskal wave on the density perturbation, part 3
[DE95-614205] p 3221 N95-32509
Conversion of the Bernstein-Green-Kruskal wave on the density perturbation, part 4
[DE95-614206] p 3221 N95-32510

IONIZATION

Radial electric field measurement in a tokamak by the injection of a pulsed neutral beam
[DE95-614176] p 3221 N95-32561
Low energy collisions involving multiply charged ions
[DE95-010911] p 3203 N95-32564
A possible ionization cooling experiment at the AGS
[DE95-010317] p 3205 N95-32654
Advanced far infrared detector and double donor studies in Ge
[DE95-011261] p 3247 N95-33625
Measurements of cross sections and resonance structures following electron-impact excitation/ionization of Na-like Kr and Xe
[DE95-011731] p 3230 N95-34438
International Meeting on Muon Science
[PB95-236014] p 3209 N95-34657

IONIZATION CROSS SECTIONS

Measurements of cross sections and resonance structures following electron-impact excitation/ionization of Na-like Kr and Xe
[DE95-011731] p 3230 N95-34438

IONIZED GASES

Tokamak ETE circuits: Analysis and specifications
[INPE-5573-PRP/182] p 3224 N95-33873

IONIZING RADIATION

Image analysis used to count and measure etched tracks from ionizing radiation p 3210 N95-32424
DNA-DSB in CHO-K1 cells induced by heavy-ions: Break rejoining and residual damage (GSI)
p 3162 N95-32725
Heavy ion induced mutations in mammalian cells: Cross sections and molecular analysis p 3162 N95-32728
X-ray-provoked non-Mendelian transgenerational oncodeterminants p 3163 N95-32731

IONOSONDES

Mid-latitude ionospheric plasma drift: A comparison of digital ionosonde and incoherent scatter radar measurements at Millstone Hill p 3222 N95-32838

IONOSPHERIC DRIFT

Mid-latitude ionospheric plasma drift: A comparison of digital ionosonde and incoherent scatter radar measurements at Millstone Hill p 3222 N95-32838

IONS

Low energy collisions involving multiply charged ions
[DE95-010911] p 3203 N95-32564
Damage formation in silicon irradiated by heavy ions with energy more than 1 MeV/a.m.u.
[DE95-623968] p 3204 N95-32610
The structure of ion track in Solids produced by ions with high level inelastic energy losses
[DE95-620942] p 3205 N95-32625
Estimation of spatially restricted LET using track structure models p 3161 N95-32722
The uses of Electron Beam Ion Traps in the study of highly charged ions
[DE95-011537] p 3212 N95-33064
The pinhole interface for IMS/MS
p 3070 N95-33275
Emittance and energy control in the NLC main linacs
[DE95-012556] p 3213 N95-33338
Unified model of the RF plasma sheath
[DE95-012114] p 3224 N95-33851
Tokamak ETE circuits: Analysis and specifications
[INPE-5573-PRP/182] p 3224 N95-33873
Measurements of cross sections and resonance structures following electron-impact excitation/ionization of Na-like Kr and Xe
[DE95-011731] p 3230 N95-34438

IRIDIUM

Growth and structure of MBE-Deposited iridium silicide
[AD-A295033] p 3232 N95-34792

IRON

Strength, ductility, and fracture mode of ternary FeAl alloys
[DE95-010281] p 3077 N95-32400
Technical innovation for reducing emissions of greenhouse effect gas and survey of effects of changes of industrial structures
[DE95-769808] p 3151 N95-32547

IRON ALLOYS

Effect of heat treatment at 1,150 C on creep rupture properties of a Fe3Al-based alloy
[DE95-010295] p 3077 N95-32527
Static displacements of atoms in crystalline metallic solid solutions
[DE95-012893] p 3233 N95-34802

IRON COMPOUNDS

Natural convection at microelectrodes
[AD-A294338] p 3075 N95-34357

IRRADIANCE

Impact of differences in the solar irradiance spectrum on surface reflectance retrieval with different radiative transfer codes p 3136 N95-33771
DataHub sponsored analysis p 3243 N95-34242
Photobiology and optical properties of planktonic and sea ice microalgae in the high arctic
[AD-A294002] p 3160 N95-34457

IRRADIATION

Irradiation experiments of low copper A533B steels for reactor pressure vessel tested in JMTR
[DE95-737266] p 3077 N95-32531
Irradiation-assisted stress corrosion cracking considerations at temperatures below 288 C
[DE95-008940] p 3077 N95-32555
Irradiation tests of critical components for remote handling in gamma radiation environment
[DE95-737223] p 3221 N95-32565
Behavior of structural and target materials irradiated in spallation neutron environments
[DE95-010879] p 3203 N95-32576
Damage formation in silicon irradiated by heavy ions with energy more than 1 MeV/a.m.u.
[DE95-623968] p 3204 N95-32610
About the mechanism of heavy ion radiation influence on the metals at high temperature
[DE95-620943] p 3078 N95-32626
Analysis of radiation damages of electronic circuits by separate irradiation of their components with a collimated charged particle beam
[DE95-621946] p 3102 N95-32629
A novel approach to the problem of highly-sensitive regular analysis for man-made plutonium in environment and human body
[DE95-620764] p 3164 N95-32666
Low-energy Ion-Beam Deposition apparatus equipped with surface analysis system
[DE95-737272] p 3212 N95-32712
Minutes of the 12th Joint NASA/DARA-DLR Life Sciences Program Working Group Meeting
[NASA-TM-110655] p 3161 N95-32719
Control of the laser beam irradiation intensity distribution using aspherical multi lens array and edge-shaped plates
[REPT-2209] p 3090 N95-32989
Indirect measurements of hydrogen: The deficit method for a many-component system
[DE95-010993] p 3208 N95-33623
A background subtraction routine for enhancing energy-filtered plasmon images of MgAl2O4 implanted with Al(+) and Mg(+) ions
[DE95-012850] p 3074 N95-33629
Method of forming thin films on substrates at low temperatures
[AD-D017470] p 3086 N95-34447

IRRITATION

Environmental evaluation of lactates as cleaning agents
[PB95-214854] p 3067 N95-32615

ISENTROPIC PROCESSES

Consistent finite-volume discretization of hydrodynamic conservation laws for unstructured grids
[DE95-011730] p 3112 N95-34437

ISIS SATELLITES
ENGIN mini-manual. Version 1.5
[PB95-218095] p 3206 N95-32814
ISOELECTRONIC SEQUENCE
An ion-ion collisions system at KSU
[DE95-010820] p 3208 N95-33372
ISOLATION
High resistivity InAlN by nitrogen or oxygen implantation
[DE95-011023] p 3226 N95-32594
ISOMERS
Elemental fluorine based syntheses of pentafluoro phenyl and other aromatic perfluoropolyether polymers
[AD-A294930] p 3087 N95-34596
ISOTOPE SEPARATION
Design concept of a cryogenic distillation column cascade for a ITER scale fusion reactor
[DE95-737185] p 3220 N95-32409
ISOTOPIC LABELING
Analysis of LDEF experiment AO187-2 chemical and isotopic measurements of micrometeoroids by secondary ion mass spectrometry
[NASA-CR-198849] p 3246 N95-32913
Lithogenic and cosmogenic tracers in catchment hydrology
[DE95-011523] p 3143 N95-33407
ISOTROPIC MEDIA
Modeling seismic wave propagation in heterogeneous materials using finite elements p 3156 N95-34283
ISOTROPIC TURBULENCE
Special publication of National Aerospace Laboratory
[NAL-SP-27] p 3034 N95-34505
Direct numerical simulation of compressible isotropic turbulence p 3037 N95-34523
Direct numerical simulation of incompressible homogeneous isotropic turbulence using compressible Navier-Stokes equations p 3037 N95-34529
Direct numerical simulation of incompressible homogeneous isotropic turbulence using NWT p 3038 N95-34530
ITERATION
Design and analysis of transient nonlinear coupled systems p 3199 N95-33292
ITERATIVE SOLUTION
Parallel finite element methods and iterative solution techniques for viscous incompressible flows p 3108 N95-33031
Krylov methods for compressible flows
[NASA-CR-198176] p 3196 N95-33727
QMR methods in computational fluid dynamics
[DE95-012889] p 3113 N95-34800

J

JACOBI INTEGRAL
Solving stiff chemistry problems with FIDAP
[DE95-011053] p 3067 N95-32709
JAMMING
Space-time adaptive processing for airborne radar
[AD-A293032] p 3098 N95-33152
JAPAN
Technology Reports of the Osaka University, vol. 45, nos. 2205-2216 p 3090 N95-32984
JET AIRCRAFT NOISE
Computation of noise radiation from turbofans: A parametric study
[NASA-CR-198359] p 3200 N95-32836
JET ENGINES
Influence of backup bearings and support structure dynamics on the behavior of rotors with active supports
[NASA-CR-199080] p 3121 N95-32689
Steady-state dynamic behavior of an auxiliary bearing supported rotor system p 3121 N95-32690
Dynamic behavior of a magnetic bearing supported jet engine rotor with auxiliary bearings p 3122 N95-32691
JET FLOW
Modeling liquid jet atomization processes
[AD-A294888] p 3112 N95-34572
JET IMPINGEMENT
Pop tests of storable biopropellant liquid apogee engine
[NAL-TR-1253] p 3060 N95-32755
JET THRUST
Maximum thrust mode evaluation p 3052 N95-33017
Rapid deceleration mode evaluation p 3052 N95-33018
Background and principles of throttles-only flight control p 3053 N95-33021
JOINTS (JUNCTIONS)
The effects of H(+) implants on YBa2Cu3O7 superconducting materials
[DE95-614466] p 3227 N95-32698
JOSEPHSON JUNCTIONS
Low-energy response of superconducting tunnel junction x-ray spectrometers
[DE95-011733] p 3230 N95-33650
Properties of high-T(sub c) Josephson junctions with Y(0.7)Ca(0.3)Ba2Cu3O(7-delta) barrier layers
[AD-A294852] p 3231 N95-34568
JUNCTION TRANSISTORS
Operational amplifier using bipolar junction transistors in silicon-on-sapphire
[AD-D017421] p 3105 N95-34618

K

K-EPSILON TURBULENCE MODEL
Low Reynolds number kappa-epsilon and empirical transition models for oscillatory pipe flow and heat transfer
[NASA-TM-109785] p 3110 N95-33496
KALMAN FILTERS
Training neural networks using sequential extended Kalman filtering
[DE95-007874] p 3187 N95-32386
Track finding and fitting in the H1 forward track detector
[PB95-234985] p 3214 N95-34651
KAONS
Search for N(sub (phi))(1960) baryon
[DE95-619290] p 3205 N95-32703
Study of the p + N yields (Sigma(0)K(+)) + N reaction at E(sub p) 70 GeV
[DE95-619273] p 3207 N95-33171
Overview of rare K decays
[DE95-012081] p 3208 N95-33850
KELVIN-HELMHOLTZ INSTABILITY
Direct and large eddy simulations of three dimensional round turbulent jets p 3111 N95-33709
KERNEL FUNCTIONS
Sum of fractional derivatives and m-accretive operators
[PB95-215307] p 3195 N95-32893
Function approximation using adaptive and overlapping intervals
[DE95-010865] p 3191 N95-33212
Penetrable wedge analysis
[AD-A294276] p 3234 N95-34464
KERR EFFECTS
Unusual behavior in the magnetic anisotropy of ultra-thin Co sandwiches: The role of Au underlayers
[DE95-010612] p 3229 N95-33641
KINETIC ENERGY
Low temperature growth of thin films by high kinetic energy supersonic molecular beams
[AD-A294516] p 3086 N95-34476
KINETIC THEORY
Bogolyubov lectures
[DE95-620495] p 3197 N95-32624
KINETICS
Intermetallic compound layer growth kinetics in non-lead bearing solders
[DE95-009595] p 3078 N95-32591
KNOWLEDGE
Conceptual understanding and stability, and knowledge shields for fending off conceptual change
[AD-A293555] p 3166 N95-34609
KNOWLEDGE BASED SYSTEMS
Incorporating distributed problem solving technique into a case-based system p 3188 N95-32997
Knowledge-based system for metallurgical grade design p 3189 N95-32998
An alternative reasoning method p 3189 N95-33001
Representing incomplete knowledge in relational databases p 3238 N95-33722
Improving the comprehensibility, accuracy, and generality of reactive plans
[AD-A294104] p 3193 N95-34495
Is the genetic algorithm a cooperative learner?
[AD-A294112] p 3193 N95-34499
KNOWLEDGE BASES (ARTIFICIAL INTELLIGENCE)
A relational metric, its application to domain analysis, and an example analysis and model of a remote sensing domain
[NASA-TM-110358] p 3198 N95-33875
Applied Information Systems Research Program (AISRP) Workshop 3 meeting proceedings
[NASA-CR-199103] p 3239 N95-34218
Knowledge-based assistance for science visualization and analysis using large distributed databases p 3241 N95-34227
KNOWLEDGE REPRESENTATION
An efficient inference engine for interactive fault diagnosis in a helpdesk application p 3189 N95-33000
A general solution to object matching problems by using the multiresolution approximation p 3189 N95-33002
KRIGING
Validating spatial structure in canopy water content using geostatistics p 3135 N95-33768

L

LABORATORIES
The development and application of massively parallel solid mechanics codes
[DE95-006307] p 3184 N95-32374
COBRA accelerator for Sandia ICF diode research at Cornell University
[DE95-011018] p 3101 N95-32578
Analysis of samples for the first (1994) OPCW round robin interlaboratory comparison test
[PB95-210324] p 3068 N95-33243
A layered approach to technology transfer of AVIRIS between Earth Search Sciences, Inc. and the Idaho National Engineering Laboratory p 3117 N95-33746
LABYRINTH SEALS
The effect of labyrinth seals on the dynamics of turbomachinery p 3122 N95-32752
LACTATES
Environmental evaluation of lactates as cleaning agents
[PB95-214854] p 3067 N95-32615
LACTIC ACID
Environmental evaluation of lactates as cleaning agents
[PB95-214854] p 3067 N95-32615
LAGRANGIAN FUNCTION
Users' manual for LEHGC: A Lagrangian-Eulerian finite-element model of HydroGeoChemical transport through saturated-unsaturated media. Version 1.0
[DE95-010513] p 3179 N95-32543
On the feasibility of using smoothed particle hydrodynamics for underwater explosion calculations
[DE95-008799] p 3106 N95-32587
Rigid bodies for metal forming analysis with NIKE3D
[DE95-011740] p 3182 N95-33652
QCD and hadron structure
[DE95-012173] p 3209 N95-33855
LAKES
Mineralogic variations in fluvial sediments contaminated by mine tailings as determined from AVIRIS data, Coeur D'Alene River Valley, Idaho p 3131 N95-33745
LAMB WAVES
Laser-based ultrasonics by dual-probe interferometer detection and narrow-band ultrasound generation p 3118 N95-33464
LAMINAR BOUNDARY LAYER
Boundary layer transition studies
[NASA-CR-198983] p 3106 N95-32454
Dependency of a boundary layer flow on computational grids p 3040 N95-34550
LAMINAR FLOW
Boundary layer transition studies
[NASA-CR-198983] p 3106 N95-32454
Flow and heat transfer behavior of non-Newtonian fluids in rectangular ducts p 3107 N95-32907
Numerical thermal analyses of heat exchangers for the stirling engine application
[NASA-CR-199120] p 3110 N95-33398
The effect of buoyancy on flow and heat transfer in curved pipes p 3037 N95-34528
Flow and heat transfer in rotating curved pipes p 3040 N95-34545
LAMINAR HEAT TRANSFER
Laminar heat transfer for power-law fluids in thermal entrance region of annular sector ducts p 3108 N95-33255
LAMINATES
Metallic laminates for engine applications
[DE95-010259] p 3062 N95-32399
Fracture toughness and tensile behavior of multi-layer laminated metal composite of Al 6090-25 vol % SiCp and Al 5182
[DE95-011421] p 3062 N95-32602
Micromechanics of fiber-reinforced ceramic composites p 3063 N95-32775
Development of a composite tailoring procedure for airplane wing
[NASA-CR-199081] p 3048 N95-32928
A new approach to fracture of layered fibrous composites: Experiments and analysis p 3063 N95-33309
Interlaminar stress analysis of dropped-ply laminated plates and shells by a mixed method p 3064 N95-33327
Low velocity impact damage in carbon fiber/PEEK composite laminates
[ISBN-0-315-86546-6] p 3065 N95-33710

LAND ICE
Bibliography on cold regions science and technology: Volume 48, part 1
| AD-A293988 | p 3243 N95-34420
Bibliography on cold regions science and technology: Volume 48, part 2
| AD-A293993 | p 3243 N95-34421
LAND MANAGEMENT
AVIRIS user's guide p 3117 N95-33759
LAND SURFACE TEMPERATURE
Land surface temperature measurements from EOS MODIS data
| NASA-CR-199082 | p 3142 N95-32717
LAND USE
Urban remote sensing applications: TIMS observations of the City of Scottsdale p 3137 N95-33791
LANDAU-GINZBURG EQUATIONS
Turbulence and spatio-temporal chaos
| DE95-012912 | p 3068 N95-33223
LANDING AIDS
An approach to sensor data fusion for flying and landing aid purpose p 3043 N95-32488
LANDING GEAR
Machinability study of Aermet 100
| DE95-011532 | p 3084 N95-33408
LANGUAGE PROGRAMMING
The application of Ada and formal methods to a safety critical engine control system p 3094 N95-33142
A distributed Clips implementation: dClips p 3243 N95-34243
LANGUAGES
Scanners, optical character readers, Cyrillic alphabet and Russian translations p 3194 N95-32433
LASER ABLATION
Laser ablation plume thermalization dynamics in background gases studied by time-resolved imaging, spectroscopic, and ion probe diagnostics
| DE95-010277 | p 3118 N95-33246
Analysis of metallic fuels by laser ablation
| DE95-012465 | p 3075 N95-34440
Modeling and simulation of pulsed laser annealing and ablation of solid materials
| DE95-012888 | p 3119 N95-34466
Highly doped p-ZnTe films and quantum well structures grown by nonequilibrium pulsed laser ablation
| DE95-012885 | p 3232 N95-34799
LASER ANNEALING
Laser induced diffusion of ion-implanted bismuth in fused silica
| DE95-012869 | p 3230 N95-34443
Modeling and simulation of pulsed laser annealing and ablation of solid materials
| DE95-012888 | p 3119 N95-34466
LASER APPLICATIONS
Some results of international cooperation in military to commercial conversion of laser gyro technology p 3092 N95-33130
Laser gyroscopy tendencies and their analysis of development in Ukraine p 3092 N95-33133
LASER ARRAYS
Integration of diffractive lenses with addressable vertical-cavity laser arrays
| DE95-009850 | p 3118 N95-32663
LASER BEAMS
Analysis of evaporation in laser welding
| REPT-2207 | p 3090 N95-32987
Control of the laser beam irradiation intensity distribution using aspherical multi lens array and edge-shaped plates
| REPT-2209 | p 3090 N95-32989
Absolute wavefront measurements of high-energy laser beams in the Beamlet Demonstration Project for the National Ignition Facility
| DE95-012224 | p 3118 N95-33378
Acoustic-optic sound velocity profiler
| AD-D017487 | p 3201 N95-34289
TiO2/SiO2 and ZrO2/SiO2 multilayer media film optical loss and laser damage study
| AD-A294192 | p 3217 N95-34298
Using photothermal deflection techniques for studying the attenuations of guided waves propagated in optical thin films
| AD-A294203 | p 3217 N95-34303
A multi-wavelength dye laser system
| AD-A294068 | p 3119 N95-34380
The development of the automatic target recognition system for the UGV/RSTA LADAR
| AD-A294090 | p 3100 N95-34474
ABLEX: High altitude laser propagation experiment
| AD-A294914 | p 3120 N95-34592
Method and apparatus for locking laser wavelength to an atomic transition
| AD-D017425 | p 3120 N95-34619
Laser beaming demonstrations at the Starfire Optical Range
| DE95-007747 | p 3120 N95-34811
LASER CAVITIES
Pulsed tunable narrow-bandwidth dye laser, with hollow circular waveguide in cavity
| AD-A294060 | p 3120 N95-34469
LASER DAMAGE
Influence of CO2 continuous laser preprocessed substrates on optical thin film damage thresholds
| AD-A294190 | p 3217 N95-34297
TiO2/SiO2 and ZrO2/SiO2 multilayer media film optical loss and laser damage study
| AD-A294192 | p 3217 N95-34298
Development of 1.06 micron high efficiency antireflective coating
| AD-A294161 | p 3219 N95-34759
LASER DOPPLER VELOCIMETERS
A dual, parallel cavity Fabry-Perot interferometer
| DE95-010796 | p 3115 N95-32900
LASER FUSION
Measurement of laser wavefront using Shack Hartmann method with new lens array
| REPT-2208 | p 3090 N95-32988
Control of the laser beam irradiation intensity distribution using aspherical multi lens array and edge-shaped plates
| REPT-2209 | p 3090 N95-32989
LASER GUIDANCE
Development and flight testing of an Obstacle Avoidance System for US Army helicopters p 3045 N95-32500
LASER GYROSCOPES
Some results of international cooperation in military to commercial conversion of laser gyro technology p 3092 N95-33130
Laser gyroscopy tendencies and their analysis of development in Ukraine p 3092 N95-33133
Application of advanced safety technique to ring laser gyro inertial navigation system integration p 3048 N95-33140
LASER INDUCED FLUORESCENCE
Study on turbulent fluctuations in diffusion flames using laser induced fluorescence
| PB95-214425 | p 3068 N95-32812
LASER INTERFEROMETRY
Laser-based ultrasonics by dual-probe interferometer detection and narrow-band ultrasound generation p 3118 N95-33464
In situ surface roughness measurement during PECVD diamond film growth
| DE95-013411 | p 3230 N95-34215
LASER MATERIALS
Measurement of gain saturation on Nd: Doped phosphate laser glasses
| REPT-2210 | p 3090 N95-32990
LASER MODE LOCKING
Laser gyroscopy tendencies and their analysis of development in Ukraine p 3092 N95-33133
Method and apparatus for locking laser wavelength to an atomic transition
| AD-D017425 | p 3120 N95-34619
LASER MODES
Bifurcation analysis of multimode instabilities in class B lasers p 3119 N95-33470
LASER OUTPUTS
Laser gyroscopy tendencies and their analysis of development in Ukraine p 3092 N95-33133
Plasma mediated ablation of biological tissues with ultrashort laser pulses
| DE95-011748 | p 3164 N95-33654
Pulsed tunable narrow-bandwidth dye laser, with hollow circular waveguide in cavity
| AD-A294060 | p 3120 N95-34469
Method and apparatus for locking laser wavelength to an atomic transition
| AD-D017425 | p 3120 N95-34619
Development of 1.06 micron high efficiency antireflective coating
| AD-A294161 | p 3219 N95-34759
LASER PLASMA INTERACTIONS
Extreme broadening of stimulated Raman scattered light from high intensity laser plasma interactions
| AD-A294165 | p 3120 N95-34761
LASER PLASMAS
Analysis of metallic fuels by laser ablation
| DE95-012465 | p 3075 N95-34440
LASER PUMPING
Optical pulse generation using fiber lasers and integrated optics
| DE95-011517 | p 3216 N95-33506
LASER SPECTROSCOPY
Development of a prototype lignin concentration sensor
| DE95-010951 | p 3074 N95-33705
Iron Boltzmann factor LIDAR: Proposed new remote-sensing technique for mesospheric temperature
| AD-A293568 | p 3157 N95-34613
LASER STABILITY
Bifurcation analysis of multimode instabilities in class B lasers p 3119 N95-33470
Method and apparatus for locking laser wavelength to an atomic transition
| AD-D017425 | p 3120 N95-34619
LASER TARGETS
Multispectral image correlation for air-to-ground targeting p 3043 N95-32489
Measurement of laser wavefront using Shack Hartmann method with new lens array
| REPT-2208 | p 3090 N95-32988
Inertial confinement fusion target component fabrication and technology development support
| DE95-011655 | p 3224 N95-34436
LASER WELDING
The effect of travel speed on thermal response in CO2 laser welding of small electronic components
| DE95-006314 | p 3118 N95-32683
Analysis of evaporation in laser welding
| REPT-2207 | p 3090 N95-32987
The choice: Welding with CO2 or Nd:YAG lasers
| DE95-011825 | p 3124 N95-33834
LASER WINDOWS
High power CO2 laser windows and reflection reducing coatings
| AD-A294217 | p 3119 N95-34308
LASERS
Development of ultrasensitive spectroscopic analysis technology. Development of atomic spectroscopy technology
| DE95-614352 | p 3066 N95-32566
Measurement of laser wavefront using Shack Hartmann method with new lens array
| REPT-2208 | p 3090 N95-32988
Indium mono-ion oscillator
| AD-A293736 | p 3104 N95-34451
ABLEX: High altitude laser propagation experiment
| AD-A294914 | p 3120 N95-34592
LASING
The 8th Winterschool on New Developments in Solid State Physics
| AD-A290163 | p 3227 N95-32677
LATCH-UP
Single event and TREE latchup mitigation for a star tracker sensor: An innovative approach to system level latchup mitigation
| DE95-010331 | p 3059 N95-32593
LATITUDE
Investigation research on introducing new energy technology, promoting its practical application, and providing its instruction
| DE95-769801 | p 3148 N95-32403
LATTICE PARAMETERS
Strength, ductility, and fracture mode of ternary FeAl alloys
| DE95-010281 | p 3077 N95-32400
Static displacements of atoms in crystalline metallic solid solutions
| DE95-012893 | p 3233 N95-34802
LATTICE VIBRATIONS
Lattice Polymer Automata
| DE95-011980 | p 3062 N95-33848
LAUNCH VEHICLES
The concept of the space system based on the Rocket launch vehicle of light-weight class for direct sounding of large-scale natural hazards p 3057 N95-33128
LAVA
The unique radar scattering properties of silicic lava flows and domes p 3141 N95-33811
LAWS
Globally stable feedback laws for near-minimum-fuel and near-minimum-time pointing maneuvers for a landmark-tracking spacecraft
| DE95-009867 | p 3191 N95-33214
LAYOUTS
Hardware implementation of a desktop supercomputer for high performance image processing
| AD-A294272 | p 3178 N95-34462
LEAD (METAL)
Conversion of holes into reducing species on surface modified small-particle TiO2
| DE95-008282 | p 3225 N95-32586
LEAD OXIDES
Effect of lead content on Bi-2223 formation by a two-powder process
| DE95-009889 | p 3079 N95-33215
LEAD ZIRCONATE TITANATES
Epitaxial Pb(Zr(x)Ti(1-x))O3/SrRuO3 (x = 0, 0.35, 0.65) multilayer thin films on SrTiO3(100) and MgO(100) prepared by MOCVD and RF sputtering
| DE95-008288 | p 3226 N95-32598
Comparison of lead zirconate titanate thin films on ruthenium oxide and platinum electrodes
| DE95-617597 | p 3082 N95-32710

LEADING EDGE SWEEP
Sidewall-effect of the wind tunnel on the estimation of the aerodynamic characteristics of a delta wing
p 3037 N95-34525
LEADING EDGES
A nonlinear vortex lattice method for unsteady flow with separated vortex
|DLR-FB-94-32| p 3106 N95-32787
Calculation for aerodynamic characteristics on delta wing with leading-edge separated vortex effect using boundary element method p 3037 N95-34524
Nonlinear stability of unsteady viscous flow
|AD-A294931| p 3113 N95-34597
LEAKAGE
Actively controlled shaft seals for aerospace applications
|NASA-CR-4678| p 3061 N95-33156
LEARNING
Event-related potentials and electroencephalograms in adaptive operator training: Rationale and annotated bibliography
|AD-A294337| p 3166 N95-34356
Animation within a multimedia training system for night vision goggles
|AD-A294095| p 3170 N95-34475
Conceptual understanding and stability, and knowledge shields for fending off conceptual change
|AD-A293555| p 3166 N95-34609
LEAST SQUARES METHOD
High accuracy in-flight wavelength calibration of imaging spectrometry data p 3132 N95-33750
LEAVES
Measurement of atmospheric water vapor, leaf liquid water and reflectance with AVIRIS in the Boreal Ecosystem-Atmosphere Study: Initial results
p 3133 N95-33755
Vegetation species composition and canopy architecture information expressed in leaf water absorption measured in the 1000 nm and 2200 spectral region by an imaging spectrometer p 3133 N95-33757
LECTURES
Glass science tutorial: Lecture no. 4, commercial glass melting and associated air emission issues
|DE95-007818| p 3082 N95-32384
Bogolyubov lectures
|DE95-620495| p 3197 N95-32624
LENSES
Integration of diffractive lenses with addressable vertical-cavity laser arrays
|DE95-009850| p 3118 N95-32663
Measurement of laser wavefront using Shack Hartmann method with new lens array
|REPT-2208| p 3090 N95-32988
Control of the laser beam irradiation intensity distribution using aspherical multi lens array and edge-shaped plates
|REPT-2209| p 3090 N95-32989
A real-time single-camera, stereoscopic video device
|AD-A294105| p 3116 N95-34496
LEPTONS
A Study of the A dependence of the deep inelastic scattering of leptons and implications for understanding of the EMC effect
|DE95-613711| p 3206 N95-32796
Remarks on the KARMEN anomaly
|PB95-234977| p 3209 N95-34650
LESIONS
Heavy ion induced DNA-DSB in yeast and mammalian cells p 3161 N95-32723
DNA-DSB in CHO-K1 cells induced by heavy-ions: Break rejoining and residual damage (GSI)
p 3162 N95-32725
Mutation induction in bacteria after heavy ion irradiation p 3162 N95-32727
Ultrashort pulse laser effects in the primate eye
|AD-A295024| p 3164 N95-34789
LIBRARIES
Collaborating over the Web: Libraries and laboratories or the Librarian and the Webmaster
|DE95-010572| p 3186 N95-33639
The design of scalable software libraries for distributed memory concurrent computers
|DE95-012891| p 3244 N95-34801
LIE GROUPS
Associative integral formulas and deformations of Yangians
|PB95-212189| p 3195 N95-32889
LIFE (DURABILITY)
The mean lifetimes of the 2p(sigma) lowest bound state of HeH(2+) and its isotopes
|DE95-010812| p 3206 N95-32966
LIFE CYCLE COSTS
Application of fuzzy technology to risk-based design and decision problems
|DE95-006815| p 3178 N95-32378
LIFE SCIENCES
STS-42 mission highlights resource tape. Part 1 of 2
|NASA-TM-110838| p 3058 N95-34280
STS-42 mission highlights resource tape. Part 2 of 2
|NASA-TM-110840| p 3058 N95-34281
LIFE SPAN
Angular dependence of magnetic properties of steels under uniaxial stress
|DE95-010189| p 3078 N95-32648
LIFT
Analysis and design methodology for chordwise deformable wings p 3049 N95-33311
Numerical simulations of dynamic stall phenomena in low speed flows p 3040 N95-34546
Numerical simulation of two-dimensional PAR-WIG p 3040 N95-34548
LIFT DRAG RATIO
Numerical analysis around the whole SST configuration p 3039 N95-34541
LIGANDS
Theoretical dynamical studies of metal clusters and cluster-ligand systems
|DE95-012461| p 3228 N95-33382
LIGHT AMPLIFIERS
Quantum cylinder fiber light amplifier
|AD-A294197| p 3217 N95-34300
LIGHT BEAMS
Propagation of spatial solitons generated by Gaussian beams in a non-linear Kerr medium
|IFTR-9/1995| p 3206 N95-32921
Photonic band gap structures on polymer materials for microstructure waveguides and high-speed interconnects
|AD-A294119| p 3218 N95-34504
Development of 1.06 micron high efficiency antireflective coating
|AD-A294161| p 3219 N95-34759
LIGHT EMISSION
Light particle emission in heavy ion reactions
|DE95-010727| p 3206 N95-32965
Analysis of evaporation in laser welding
|REPT-2207| p 3090 N95-32987
LIGHT EMITTING DIODES
Optical logic implementation in composite biled/bild circuits
|AD-A294160| p 3105 N95-34758
LIGHT HELICOPTERS
Army aviation: Modernization strategy needs to be reassessed. Report to Congressional requestors
|GAO/NSIAD-95-9| p 3033 N95-32783
LIGHT IONS
COBRA accelerator for Sandia ICF diode research at Cornell University
|DE95-011018| p 3101 N95-32578
Mutation induction in bacteria after heavy ion irradiation p 3162 N95-32727
LIGHT MODULATION
Study of liquid crystal spatial light modulator application to Hadamard transform spectrometer: A fast and accurate decoding method
|AD-A293087| p 3215 N95-32660
Applications of organic and polymer nonlinear optical materials in optics computations
|AD-A293088| p 3215 N95-32957
Efficient pockel's modulators in optical fibers
|AD-A294009| p 3217 N95-34374
LIGHT MODULATORS
Applied research on liquid crystal spatial modulators in Hadamard transform spectrometers. Quick and accurate decoding methods
|AD-A294152| p 3219 N95-34756
LIGHT SCATTERING
Analysis of evaporation in laser welding
|REPT-2207| p 3090 N95-32987
Using optical interference methods to measure acousto-optical device thermal effects
|AD-A294219| p 3217 N95-34309
Atmospheric attenuation properties associated with CO2 laser radiation spectra
|AD-A294061| p 3120 N95-34470
Effect of propagation attenuation of thin film waveguide on optical thin film losses
|AD-A294064| p 3218 N95-34471
Comparison of theoretical predictions with field observations for a simple forward scattering sensor
|AD-A294948| p 3219 N95-34576
LIGHT SOURCES
Environmental chamber studies of atmospheric reactivities of volatile organic compounds: Effects of varying chamber and light source
|DE95-009225| p 3152 N95-32686
LIGHT TRANSMISSION
Method for making fiber-optic bundle collimator assembly
|AD-D017486| p 3216 N95-34288
Acoustic-optic sound velocity profiler
|AD-D017487| p 3201 N95-34289
LIGHTING EQUIPMENT
Altitude cuing effectiveness of terrain texture characteristics in simulated low-altitude flight
|AD-A294369| p 3056 N95-34362
LIGNIN
Development of a prototype lignin concentration sensor
|DE95-010951| p 3074 N95-33705
Prospect redux p 3133 N95-33758
LIMNOLOGY
AVIRIS user's guide p 3117 N95-33759
LINE SPECTRA
A study of luminescence and absorption spectra of GaP
|DE95-614122| p 3202 N95-32524
GRO: Studies of high energy pulsars with EGRET
|NASA-CR-199130| p 3248 N95-33499
Atmospheric attenuation properties associated with CO2 laser radiation spectra
|AD-A294061| p 3120 N95-34470
LINEAR ACCELERATORS
Linear orbit parameters for the exact equations of motion
|DE95-011567| p 3210 N95-32414
Unexpected matching insensitivity in DTL of GTA accelerator
|DE95-011984| p 3211 N95-32416
Emittance growth due to decoherence and wakefields
|DE95-012495| p 3213 N95-33376
LINEAR ENERGY TRANSFER (LET)
Estimation of spatially restricted LET using track structure models p 3161 N95-32722
LINEAR PROGRAMMING
A methodology for evaluating air pollution strategies to improve the air quality in Mexico City
|DE95-010874| p 3152 N95-32573
Spectrum allocation strategies for communication networks
|AD-A294936| p 3100 N95-34601
LINEAR QUADRATIC GAUSSIAN CONTROL
A stochastic adaptive control application to flight systems p 3055 N95-34806
LINEAR SYSTEMS
Beam-based magnetic alignment of the final focus test beam
|DE95-012096| p 3212 N95-32657
Rigid bodies for metal forming analysis with NIKE3D
|DE95-011740| p 3182 N95-33652
High-order Taylor-Galerkin and adaptive hp-methods for hyperbolic systems with application to structural acoustics p 3200 N95-33719
A variation of the Riemann Problem solution and its application to implicit Godunov's scheme
p 3036 N95-34516
LININGS
Summary of the impedance working group
|DE95-012095| p 3211 N95-32606
Water model tests on the Allison T56 series 3 combustion system
|DSTO-TR-0139| p 3054 N95-33250
LIQUEFIED NATURAL GAS
Catalytic conversion of light alkanes: Proof of concept stage
|DE95-012318| p 3076 N95-34810
LIQUID ATOMIZATION
Modeling liquid jet atomization processes
|AD-A294888| p 3112 N95-34572
LIQUID CHROMATOGRAPHY
Direct analysis of organic priority pollutants by IMS
p 3071 N95-33280
LIQUID COOLING
Tri-service perspectives on microclimate cooling of protective clothing in the heat
|AD-A294005| p 3170 N95-34370
LIQUID CRYSTALS
Molecular engineering of liquid crystalline polymers by Living polymerization 30. Synthesis and Living cationic polymerization of (2R, 3S)-2-Fluoro-3-methylpentyl 4'-(8-Vinyloxyoctyloxy) Biphenyl-4-carboxylate and its copolymerization with (2R, 3S)-2-Fluoro-3-methylpentyl 4'-(11 Vinyloxyundecanyloxyloxy) biphenyl-4-carboxylate --- carboxylate and its copolymerization with (2R, 3S)-2-Fluoro-3-methylpentyl 4-(11-Vinyloxyundecanyloxy) biphenyl-4-Carboxylate
|AD-A293115| p 3082 N95-32552
Study of liquid crystal spatial light modulator application to Hadamard transform spectrometer: A fast and accurate decoding method
|AD-A293087| p 3215 N95-32660
Applications of organic and polymer nonlinear optical materials in optics computations
|AD-A293088| p 3215 N95-32957
From liquid crystal polymers containing crown ethers to tapered building blocks containing crown ethers which self-assemble into tubular supermolecules
|AD-A294359| p 3086 N95-34361

Applied research on liquid crystal spatial modulators in Hadamard transform spectrometers. Quick and accurate decoding methods
|AD-A294152| p 3219 N95-34756

LIQUID FUELS
Gasoline from natural gas by sulfur processing
|DE95-010651| p 3087 N95-32563

LIQUID HELIUM
Transverse acoustic properties of the B-phase of superfluid helium three p 3074 N95-33414

LIQUID HYDROGEN
Compression mass gauge testing in a liquid hydrogen dewar
|NASA-CR-198366| p 3115 N95-32687

LIQUID INJECTION
Interfacial reactions during the liquid infiltration of titanium matrix composites p 3081 N95-34252
Modeling liquid jet atomization processes
|AD-A294888| p 3112 N95-34572

LIQUID LASERS
A multi-wavelength dye laser system
|AD-A294068| p 3119 N95-34380

LIQUID PHASES
Phase equilibria and phase diagrams in carbide systems
|PB95-211348| p 3068 N95-33229
Supercritical crystallization: The RESs-process and the GAS-process
|PB95-214482| p 3228 N95-33235
From liquid crystal polymers containing crown ethers to tapered building blocks containing crown ethers which self-assemble into tubular supermolecules
|AD-A294359| p 3086 N95-34361

LIQUID PROPELLANT ROCKET ENGINES
The development of some kinds of LRE injectors
|AD-A294199| p 3061 N95-34302

LIQUID ROCKET PROPELLANTS
Metallized gelled propellants: Oxygen/RP-1/aluminum rocket combustion experiments
|NASA-TM-107025| p 3088 N95-33876

LIQUID SURFACES
Experimental and numerical analysis of controlled impinging liquid jets p 3109 N95-33257
Modeling liquid jet atomization processes
|AD-A294888| p 3112 N95-34572

LIQUID-GAS MIXTURES
An experimental and analytical investigation into the performance of centrifugal pumps operating with air-water mixtures p 3123 N95-33323

LIQUID-SOLID INTERFACES
Numerical simulation of heat and mass transport during space crystal growth with MEPHISTO
|NASA-TM-107015| p 3089 N95-32718

LIQUID-VAPOR EQUILIBRIUM
Thermophysical properties of HCFC alternatives
|DE95-009635| p 3233 N95-32661

LIQUID-VAPOR INTERFACES
Thermocapillary flow with evaporation and condensation and its effect on liquid retention in low-g fluid acquisition devices p 3109 N95-33256

LITHIUM
State-selective single electron capture cross sections in He(exp 2+)_+ Li(2s) and Li(*)(2p) collisions
|DE95-010819| p 3207 N95-33371
Thin-film rechargeable lithium batteries
|DE95-008975| p 3103 N95-33697
High rate rechargeable lithium cells employing lithium ion conducting solid electrolytes
|AD-A294390| p 3104 N95-34347

LITHIUM ALLOYS
Fatigue properties for the Al-Li alloy 2090, part 3
|PB95-214532| p 3078 N95-32614
High rate rechargeable lithium cells employing lithium ion conducting solid electrolytes
|AD-A294390| p 3104 N95-34347

LITHIUM COMPOUNDS
Enhancement of pool boiling heat transfer to lithium bromide aqueous solution
|REPT-2211| p 3091 N95-32991

LITHIUM NIOBATES
Optical properties of lithium niobate waveguides, and prism coupling for optimizing waveguide fabrication
|AD-A294111| p 3218 N95-34498

LITHIUM SULFUR BATTERIES
Lessons learned in acquiring new regulations for shipping advanced electric vehicle batteries
|DE95-009908| p 3102 N95-32956

LITHOGRAPHY
Fabrication technology and measurement of coupled quantum dot devices
|AD-A294853| p 3231 N95-34569

LITHOLOGY
A field- and laboratory-based quantitative analysis of alluvium: Relating analytical results to TIMS data p 3139 N95-33800
Lithologic controls on AIRSAR signatures of bedrock and alluvium, at Lunar Crater, Nevada p 3141 N95-33813

LITHOSPHERE
The nature and fate of natural resins in the geosphere 6: Analysis of fossil resins from Axel Heiberg Island Canadian Arctic
|DE95-012212| p 3154 N95-33394

LOADS (FORCES)
Modeling of DC spacecraft power systems p 3062 N95-32423
Bicycle ergometer instrumentation to determine muscle and bone forces during exercise p 3176 N95-32428
Semi-analytic computation of the driven fields in right circular cylindrical microwave applicators
|DE95-010875| p 3203 N95-32574
Motion and force control of coordinated robots
|ISBN-0-315-86323-4| p 3191 N95-33307

LOCAL AREA NETWORKS
Congestion control over ATM local area networks
|DE95-010343| p 3184 N95-32558
Fast approximation of self-similar network traffic
|DE95-011271| p 3185 N95-32967

LOGIC CIRCUITS
Bit-level analysis of an SRT divider circuit
|AD-A294842| p 3105 N95-34565

LOGIC PROGRAMMING
A declarative debugger for a logical-functional language p 3183 N95-33007

LOGISTICS
Report to Congressional Committees. B-1B bomber: Evaluation of Air Force report on B-1B operational readiness assessment
|GAO/NSIAD-95-151| p 3197 N95-32758

LOGISTICS MANAGEMENT
Logistics Operations Management Center: Maintenance Support Baseline (LOMC-MSB)
|NASA-TM-110624| p 3245 N95-33489

LONG DURATION EXPOSURE FACILITY
Analysis of LDEF experiment AO187-2 chemical and isotopic measurements of micrometeoroids by secondary ion mass spectrometry
|NASA-CR-198849| p 3246 N95-32913

LONG DURATION SPACE FLIGHT
Characterization of microgravity effects on bone structure and strength using fractal analysis p 3165 N95-32419

LONGITUDE MEASUREMENT
CDW-EIS calculation of longitudinal momentum distribution in single ionization of helium by Ni(24+) ions
|DE95-010816| p 3207 N95-33241

LONGITUDINAL STABILITY
A code to compute the action-angle transformation for a particle in an abritrary potential well
|DE95-012554| p 3098 N95-33336

LOOP TRANSFER RECOVERY
A robust control system for exact trajectory tracking p 3192 N95-33714

LOOPS
Reducing cache misses in numerical applications using data relocation and prefetching
|AD-A293978| p 3182 N95-34455

LORENTZ TRANSFORMATIONS
The Problem 4/3 as a consequence of contracted length non-covariance
|DE95-623628| p 3207 N95-33226
Boundary and lens rigidity of Lorentzian surfaces
|PB95-212163| p 3196 N95-33233

LOSSES
Off-training-set error for the Gibbs and the Bayes optimal generalizers
|DE95-006344| p 3187 N95-32375

LOW ALTITUDE
Low-Level and Nap-of-the-Earth (NOE) night operations
|AGARD-CP-563| p 3042 N95-32486
Flight test of a low-altitude helicopter guidance system with obstacle avoidance capability p 3043 N95-32490
Helicopter HF communications using the NVIS mode p 3043 N95-32491
Tactical low-level helicopter communications p 3043 N95-32492
A helmet mounted display for night missions at low altitude p 3045 N95-32503
Perceptual dimensions of simulated scenes relevant for visual low-altitude flight
|AD-A294385| p 3056 N95-34344

LOW ASPECT RATIO WINGS
A nonlinear vortex lattice method for unsteady flow with separated vortex
|DLR-FB-94-32| p 3106 N95-32787

LOW CONCENTRATIONS
Solving widespread low-concentration VOC air pollution problems: Gas-phase photocatalytic oxidation answers the needs of many small businesses
|DE95-004059| p 3152 N95-32668

LOW EARTH ORBITS
Operation of the computer model for microenvironment atomic oxygen exposure
|NASA-CR-198190| p 3059 N95-33264

LOW MOLECULAR WEIGHTS
Geochemical, genetic, and physiological control of pollutant biodegradation
|AD-A294902| p 3155 N95-34591

LOW PRESSURE
Laser ablation plume thermalization dynamics in background gases studied by time-resolved imaging, spectroscopic, and ion probe diagnostics
|DE95-010277| p 3118 N95-33246

LOW REYNOLDS NUMBER
Low Reynolds number kappa-epsilon and empirical transition models for oscillatory pipe flow and heat transfer
|NASA-TM-109785| p 3110 N95-33496

LOW TEMPERATURE
TEM investigation on the low temperature phase of HfV2
|DE95-009500| p 3225 N95-32532
Design and operation of a thermionic converter in air
|DE95-010151| p 3149 N95-32645
The tensile fracture behavior of the weld metal of BIS 812 EMA and Q1N naval construction steels
|DSTO-RR-0021| p 3078 N95-32926
Method of forming thin films on substrates at low temperatures
|AD-D017470| p 3086 N95-34447
The growth of ultrathin epitaxial intermetallic films
|AD-A295037| p 3232 N95-34795
Use of D2 to elucidate OMVPE growth mechanisms
|AD-A294999| p 3233 N95-34820

LOW TEMPERATURE ENVIRONMENTS
Bibliography on cold regions science and technology: Volume 48, part 1
|AD-A293988| p 3243 N95-34420
Bibliography on cold regions science and technology: Volume 48, part 2
|AD-A293993| p 3243 N95-34421

LOW VISIBILITY
The effects of display location and dimensionality on taxiway navigation
|AD-A294878| p 3047 N95-34570

LUBRICANT TESTS
Evaluation of high-temperature lubricant under cyclic operating conditions
|AD-A294444| p 3086 N95-34494

LUBRICANTS
Spontaneous dewetting of a perfluoropolyether
|NASA-TM-106964| p 3083 N95-32919

LUMINESCENCE
A study of luminescence and absorption spectra of GaP
|DE95-614122| p 3202 N95-32524
Size, shape, and crystallinity of luminescent structures in oxidized Si nanoclusters and H-passivated porous Si
|DE95-012322| p 3229 N95-33628

LUMINOSITY
CDF results on Z(gamma) production
|DE95-011500| p 3213 N95-33406

LUMINOUS INTENSITY
Extreme broadening of stimulated Raman scattered light from high intensity laser plasma interactions
|AD-A294165| p 3120 N95-34761

LUNAR EXPLORATION
ESA Bulletin, Number 82 p 3252 N95-32538

LUNAR SOIL
Image analysis used to count and measure etched tracks from ionizing radiation p 3210 N95-32424

LYRA CONSTELLATION
RR lyrae variable stars in the CCD/Transit instrument survey
|AD-A294138| p 3246 N95-34753

M

MACH NUMBER
Asymptotic structure of supersonic turbulent boundary layers p 3107 N95-32898
Very large eddy simulations of spatially evolving supersonic turbulent shear layers p 3110 N95-33606

MACHINE LEARNING
Numerical solution of differential equations by artificial neural networks p 3194 N95-32434
A choice of input variables for a multilayer perceptron
|DE95-623573| p 3187 N95-32476
On bootstrapping local search with trail-markers
|DE95-009835| p 3187 N95-32533
Training and recognition of Cantonese phonemes by backpropagation through time p 3188 N95-32996
Induction of dependency structures from data and its application to ozone prediction p 3190 N95-33003

Self-organizing neural network and its applications to vision-guided robot motion coordination
p 3191 N95-33324
Adaptive strategy selection for concept learning
[AD-A294086] p 3193 N95-34473
Improving the comprehensibility, accuracy, and generality of reactive plans
[AD-A294104] p 3193 N95-34495
Is the genetic algorithm a cooperative learner?
[AD-A294112] p 3193 N95-34499
Explanations of empirically derived reactive plans
[AD-A294114] p 3193 N95-34501
Everyday believability
[AD-A294938] p 3193 N95-34602
A model of long term learning: Integration of knowledge acquisition and knowledge compilation
[AD-A294123] p 3235 N95-34743

MACHINE TOOLS
Numerical analysis of the ultraprecision machining of copper
[DE95-007857] p 3089 N95-32585
Open architecture CNC system
[DE95-009485] p 3177 N95-32955

MACHINE TRANSLATION
Scanners, optical character readers, Cyrillic alphabet and Russian translations p 3194 N95-32433

MACHINING
Numerical analysis of the ultraprecision machining of copper
[DE95-007857] p 3089 N95-32585
Monitoring of the cutting operations using fuzzy logic
p 3189 N95-32999

MAGMA
Three-dimensional natural convection of a fluid with temperature-dependent viscosity in an enclosure with localized heating
[DE95-002606] p 3106 N95-32387

MAGNESIUM
A background subtraction routine for enhancing energy-filtered plasmon images of MgAl2O4 implanted with Al(+) and Mg(+) ions
[DE95-012850] p 3074 N95-33629

MAGNESIUM COMPOUNDS
A background subtraction routine for enhancing energy-filtered plasmon images of MgAl2O4 implanted with Al(+) and Mg(+) ions
[DE95-012850] p 3074 N95-33629

MAGNESIUM FLUORIDES
Ion assisted deposition of ZnS and MgF2
[AD-A294759] p 3086 N95-34563

MAGNESIUM OXIDES
YBa2Cu3O(7-x) 45 deg (001) tilt grain boundaries induced by controlled low-energy sputtering of MgO substrates: Transport properties and atomic-scale structure
[DE95-005826] p 3228 N95-32810
Epitaxial Pb(Zr(0.40)Ti(0.60))O3/SrRuO3 and PbTiO3/SrRuO3 multilayer thin films prepared by MOCVD and RF sputtering
[DE95-007146] p 3229 N95-33636

MAGNETIC BEARINGS
Influence of backup bearings and support structure dynamics on the behavior of rotors with active supports
[NASA-CR-199080] p 3121 N95-32689
Dynamic behavior of a magnetic bearing supported jet engine rotor with auxiliary bearings
p 3122 N95-32691
Dynamic modelling and response characteristics of a magnetic bearing rotor system with auxiliary bearings
p 3122 N95-32692
Synchronous dynamics of a coupled shaft/bearing/housing system with auxiliary support from a clearance bearing: Analysis and experiment
p 3122 N95-32693

MAGNETIC CORES
Improved L-C resonant decay technique for Q measurement of quasilinear power inductors: New results for MPP and ferrite powdered cores
[NASA-CR-198373] p 3103 N95-33874

MAGNETIC DIPOLES
Quench antenna and fast-motion investigations during training of a 7T dipole magnet
[DE95-012371] p 3103 N95-33080
Ramp-rate sensitivity of SSC dipole magnet prototypes
[DE95-011162] p 3214 N95-33720

MAGNETIC EFFECTS
Observation of intraband coherence in the nonlinear optical response of gallium arsenide
[DE95-011281] p 3227 N95-32600
Identification of critical substorm-expansion-phase phenomena: Problems addressable with GEM observations
[ATR-94(7270)-1] p 3158 N95-33259

MAGNETIC FIELDS
Anisotropic magnetization of HoNi2B2C
[DE95-010239] p 3198 N95-32397
Status of the large-scale dark-matter axion search
[DE95-008828] p 3246 N95-32597
Observation of intraband coherence in the nonlinear optical response of gallium arsenide
[DE95-011281] p 3227 N95-32600
The non-relativistic charged Bose gas in a magnetic field. Part 1: Formalism
[DE95-619698] p 3205 N95-32632
Angular dependence of magnetic properties of steels under uniaxial stress
[DE95-010189] p 3078 N95-32648
Peak effect and flux pinning in YBa2Cu3O(7-(delta)) single crystals
[DE95-010126] p 3228 N95-32959
The effect of collisionality and diamagnetism on the plasma dynamo
[DE95-012409] p 3223 N95-33221
A final-focus magnet for PEP-2
[DE95-012372] p 3214 N95-33504
Device for dampening vibratory motion
[AD-D017490] p 3127 N95-34427
Quantum transport
[AD-A294977] p 3235 N95-34589

MAGNETIC FILMS
High-resolution magnetic imaging and investigations of thin-film magnetism with spin-polarized electron, ion and atom probes
[DE95-012190] p 3074 N95-33392

MAGNETIC FLUX
Transport studies of tokamak plasmas in JT-60 device
[DE95-737227] p 3220 N95-32417
Peak effect and flux pinning in YBa2Cu3O(7-(delta)) single crystals
[DE95-010126] p 3228 N95-32959
Channel equalized DC squid flux-locked loop
[AD-D017469] p 3104 N95-34446

MAGNETIC MATERIALS
Improved L-C resonant decay technique for Q measurement of quasilinear power inductors: New results for MPP and ferrite powdered cores
[NASA-CR-198373] p 3103 N95-33874

MAGNETIC MEASUREMENT
Measurement and modelling of structure sensitive magnetic properties of material
[DE95-010128] p 3080 N95-33699
Improved L-C resonant decay technique for Q measurement of quasilinear power inductors: New results for MPP and ferrite powdered cores
[NASA-CR-198373] p 3103 N95-33874

MAGNETIC MIRRORS
Experimental study of the processes in the expander of the axisymmetric mirror device
[DE95-009846] p 3221 N95-32536
On the paraxial equilibrium of the finite (beta) plasma in open magnetic configurations
[DE95-614170] p 3221 N95-32560

MAGNETIC MOMENTS
Metal-ceramic interfaces: Overlayer-induced reconstruction and magnetism of 4d transition-metal monolayers
[DE95-011543] p 3075 N95-34483

MAGNETIC PROPERTIES
Angular dependence of magnetic properties of steels under uniaxial stress
[DE95-010189] p 3078 N95-32648
Perpendicular magnetic behavior of ultra-thin Co sandwiches
[DE95-010611] p 3083 N95-32819
Measurement and modelling of structure sensitive magnetic properties of material
[DE95-010128] p 3080 N95-33699

MAGNETIC RELAXATION
International Meeting on Muon Science
[PB95-236014] p 3209 N95-34657

MAGNETIC STORMS
Identification of critical substorm-expansion-phase phenomena: Problems addressable with GEM observations
[ATR-94(7270)-1] p 3158 N95-33259

MAGNETIZATION
Anisotropic magnetization of HoNi2B2C
[DE95-010239] p 3198 N95-32397

MAGNETO-OPTICS
Theory of magneto-optics and circular magnetic x-ray dichroism
[DE95-010129] p 3080 N95-33700

MAGNETOHYDRODYNAMIC FLOW
Experimental study of the processes in the expander of the axisymmetric mirror device
[DE95-009846] p 3221 N95-32536
High beta and second stability region transport and stability analysis
[DE95-011298] p 3225 N95-34812

MAGNETOHYDRODYNAMIC STABILITY
Stability analysis of external kink mode for ITER L-mode profile plasmas
[DE95-737207] p 3220 N95-32410
Optimized profiles for improved confinement and stability in the DIII-D tokamak
[DE95-009606] p 3222 N95-32756
HF-stabilization of plasma with sharp boundary
[DE95-614207] p 3222 N95-32770
High beta and second stability region transport and stability analysis
[DE95-011298] p 3225 N95-34812

MAGNETOHYDRODYNAMIC WAVES
More on core-localized toroidal Alfven eigenmodes
[DE95-010857] p 3224 N95-33696

MAGNETOHYDRODYNAMICS
On the paraxial equilibrium of the finite (beta) plasma in open magnetic configurations
[DE95-614170] p 3221 N95-32560
The effect of collisionality and diamagnetism on the plasma dynamo
[DE95-012409] p 3223 N95-33221
Application of grating polarizer to 106.4GHz ECH system on Heliotron-E
[NIFS-334] p 3225 N95-34624
High beta and second stability region transport and stability analysis
[DE95-011298] p 3225 N95-34812

MAGNETORESISTIVITY
Quantum transport
[AD-A294977] p 3235 N95-34589

MAGNETOSTATICS
Computational electromagnetics and parallel dense matrix computations
[DE95-012286] p 3099 N95-33379

MAGNETOSTRICTION
Magnetostriction and thermal expansion of the Kondo semiconductor Ce3Bi4Pt3
[DE95-011975] p 3229 N95-33386

MAGNETS
Beam-based magnetic alignment of the final focus test beam
[DE95-012096] p 3212 N95-32657

MAGNONS
Magnetic excitations in a random exchange system Fe(x)Mn(1-x)TiO3
[DE95-006626] p 3225 N95-32377

MAINTAINABILITY
Report to Congressional Committees. B-1B bomber: Evaluation of Air Force report on B-1B operational readiness assessment
[GAO/NSIAD-95-151] p 3197 N95-32758

MAINTENANCE
Budget estimates: Fiscal year 1994. Volume 2: Construction of facilities
[NASA-TM-110816] p 3245 N95-33081
Logistics Operations Management Center: Maintenance Support Baseline (LOMC-MSB)
[NASA-TM-110624] p 3245 N95-33489

MAINTENANCE TRAINING
The virtual sailor: Synthetic humans for virtual environments
[AD-A293560] p 3166 N95-34610

MAMMALS
Heavy ion induced DNA-DSB in yeast and mammalian cells p 3161 N95-32723
DNA-DSB in CHO-K1 cells induced by heavy-ions: Break rejoining and residual damage (GSI)
p 3162 N95-32725
Chromosomal damage observed in first postirradiation metaphases of repair-proficient and -deficient cell lines
p 3162 N95-32726
Heavy ion induced mutations in mammalian cells: Cross sections and molecular analysis p 3162 N95-32728

MAN MACHINE SYSTEMS
The application of helicopter mission simulation to Nap-of-the-Earth operations p 3044 N95-32496
An integrated system for air to ground operations
p 3044 N95-32498
Functional requirements analysis and human machine interface specifications for handheld metal detector wands
[DE95-009845] p 3167 N95-32535
Open architecture CNC system
[DE95-009485] p 3177 N95-32955
Stimulus-response compatibility
[PB95-214722] p 3167 N95-33237
Human piloting factors in the design of control laws for precision landing p 3167 N95-33605
Human Factors Certification of Advanced Aviation Technologies
[NASA-CR-199009] p 3171 N95-34764
On the use of the systems approach to certify advanced aviation technologies p 3171 N95-34765
A rose by any other name: Certification seen as process rather than content p 3047 N95-34766

A psychologist's view of validating aviation systems
p 3172 N95-34767
Certification of tactics and strategies in aviation
p 3172 N95-34768
Human factors certification in the development of future air traffic control systems p 3048 N95-34770
Quality assurance and risk management: Perspectives on Human Factors Certification of Advanced Aviation Systems p 3048 N95-34771
User type certification for advanced flight control systems p 3055 N95-34772
Certify for success: A methodology for human-centered certification of advanced aviation systems
p 3173 N95-34773
Does human cognition allow Human Factors (HF) certification of advanced aircrew systems?
p 3174 N95-34776
Towards a framework of human factors certification of complex human-machine systems p 3175 N95-34779
The successful management of programs for human factors certification of advanced aviation technologies
p 3175 N95-34780
Integrating human factors knowledge into certification: The point of view of the Internatioanal Civil Aviation Organization (ICAO) p 3175 N95-34782
Improving air traffic control: Proving new tools or approving the joint human-machine system?
p 3176 N95-34783
Some inadequacies of the current human factors certification process of advanced aircraft technologies
p 3176 N95-34785
Advanced automated glass cockpit certification: Being wary of human factors p 3176 N95-34786
Beware of agents when flying aircraft: Basic principles behind a generic methodology for the evaluation and certification of advanced aviation systems
p 3176 N95-34787

MANAGEMENT
The background and theory of integrated risk management p 3236 N95-32431

MANAGEMENT INFORMATION SYSTEMS
A Spatial Analysis and Modeling System (SAMS) for environment management p 3243 N95-34239

MANAGEMENT METHODS
Issues in NASA program and project management
|NASA-SP-6101(09)| p 3236 N95-34354
The successful management of programs for human factors certification of advanced aviation technologies
p 3175 N95-34780

MANAGEMENT PLANNING
Logistics Operations Management Center: Maintenance Support Baseline (LOMC-MSB)
|NASA-TM-110624| p 3245 N95-33489

MANAGEMENT SYSTEMS
NASA directives master list and index
|NHB-1410.13O| p 3238 N95-33249
Aircraft scanner data availability via the version 0 Information Management System p 3134 N95-33762

MANIFOLDS (MATHEMATICS)
Boundary and lens rigidity of Lorentzian surfaces
|PB95-212163| p 3196 N95-33233

MANIPULATORS
Off-line programming using commerical CAD systems, and design criteria for manipulators with inherent accuracy p 3180 N95-32937
Design and implementation of a two-axis micromanipulator to enhance the gripper positional accuracy of a single flexible link p 3123 N95-33252
Adaptive differential visual feedback for uncalibrated hand-eye coordination and motor control
|AD-A293607| p 3171 N95-34616
Trajectory planning and control of kinematically redundant robotic manipulators p 3194 N95-34807

MANOMETERS
Noninvasive determination of Cardiac Output
|PB95-208310| p 3164 N95-32611

MANPOWER
Budget estimates: Fiscal year 1994. Volume 3: Research and program management
|NASA-TM-110817| p 3245 N95-33082

MANUAL CONTROL
The role of the vestibular system in manual target localization p 3166 N95-32422
Development and application of the methods for pilot-aircraft system research to the manual control tasks of modern vehicles p 3094 N95-33139

MANUALS
Glass science tutorial: Lecture no. 4, commercial glass melting and associated air emission issues
|DE95-007818| p 3082 N95-32384
Operations manual for a compact electromechanical fatigue testing machine
|DSTO-GD-0036| p 3115 N95-32927

MANUFACTURING
Photovoltaic Manufacturing Technology (PVMaT)
|DE95-004093| p 3149 N95-33153
Stochastic network processes
|AD-A294939| p 3187 N95-34603

MANY BODY PROBLEM
Double-strangeness five-body system
|DE95-737277| p 3202 N95-32404

MARINE BIOLOGY
DataHub sponsored analysis p 3243 N95-34242

MARINE CHEMISTRY
The CE-QUAL-ICM three-dimensional eutrophication model, release version 1.0
|AD-A294258| p 3160 N95-34461

MARINE ENVIRONMENTS
A low diffraction beam technique for scanning in the shallow ocean
|DE95-011742| p 3159 N95-33410

MARINE TECHNOLOGY
Recent developments in maritime technology research institute acousto-optical technology research
|AD-A294215| p 3217 N95-34307

MARKET RESEARCH
Read/write module for high capacity memory disk
|AD-A294946| p 3178 N95-34745

MARTENSITIC TRANSFORMATION
Micromechanics of composites with shape memory alloy fibers in uniform thermal fields
|NASA-TM-107011| p 3063 N95-33210
Effect of phase transformations on the mechanical properties of a multiphase alloy based on NiAl + Fe
|DE95-010119| p 3079 N95-33217

MASERS
Predicted operating conditions for maintaining mode purity in the 1MW 200 GHz FOM Free Electron Maser
|DE95-010795| p 3117 N95-32571

MASKS
Printability of substrate and absorber defects on extreme ultraviolet lithographic masks
|DE95-010916| p 3084 N95-33247

MASS
Compression mass gauge testing in a liquid hydrogen dewar
|NASA-CR-198366| p 3115 N95-32687

MASS DISTRIBUTION
Intrinsic charm contribution to double quarkonium hadroproduction
|DE95-012170| p 3204 N95-32617
RR lyrae variable stars in the CCD/Transit instrument survey
|AD-A294138| p 3246 N95-34753

MASS FLOW RATE
An instrument for gravimetric calibration of flow devices with corrosive gases
|DE95-009700| p 3116 N95-33206

MASS SPECTRA
Search for N(sub (phi))(1960) baryon
|DE95-619290| p 3205 N95-32703
Study of the p + N yields (Sigma(0)K(+)) + N reaction at E(sub p) 70 GeV
|DE95-619273| p 3207 N95-33171
The nature and fate of natural resins in the geosphere 6: Analysis of fossil resins from Axel Heiberg Island Canadian Arctic
|DE95-012212| p 3154 N95-33394
CDF results on Z(gamma) production
|DE95-011500| p 3213 N95-33406

MASS SPECTROMETERS
Hadron distributions at higher rapidity using the BRAHMS forward spectrometer
|DE95-008861| p 3207 N95-33203
Determination of Benzene, Toluene, and Xylene by means of an ion mobility spectrometer device using photoionization p 3069 N95-33269

MASS SPECTROSCOPY
Analysis of samples for the first (1994) OPCW round robin interlaboratory comparison test
|PB95-210324| p 3068 N95-33243
The pinhole interface for IMS/MS
p 3070 N95-33275
The use of ion mobility spectrometry and gas chromatography/mass spectrometry for the detection of illicit drugs on clandestine records p 3070 N95-33276
High resolution electrospray mass spectrometry with a magnetic sector instrument: Accurate mass measurement and peptide sequencing
|AD-A293564| p 3076 N95-34611

MASS TRANSFER
Numerical simulation of heat and mass transport during space crystal growth with MEPHISTO
|NASA-TM-107015| p 3089 N95-32718
The CE-QUAL-ICM three-dimensional eutrophication model, release version 1.0
|AD-A294258| p 3160 N95-34461

MASSIVELY PARALLEL PROCESSORS
The development and application of massively parallel solid mechanics codes
|DE95-006307| p 3184 N95-32374
Simulation of hypervelocity impact on massively parallel supercomputer
|DE95-007735| p 3184 N95-32383
Visualization methods for high-resolution, transient, 3-D, finite element situations
|DE95-009479| p 3179 N95-32390
The future of finite element applications on massively parallel supercomputers
|DE95-011659| p 3184 N95-32415
PINCA: A scalable parallel program for compressible gas dynamics with nonequilibrium chemistry
|DE95-010581| p 3106 N95-32818
Computational electromagnetics and parallel dense matrix computations
|DE95-012286| p 3099 N95-33379
Parallel molecular dynamics: Communication requirements for massively parallel machines
|DE95-012948| p 3209 N95-34212
Highly parallel computer AP1000: Architecture and basic software p 3038 N95-34534
Program developing environment and a CFD application on the Cray T3D p 3038 N95-34535

MATCHED FILTERS
The composite classification problem in optical information processing p 3244 N95-32430
Triple invariant optical pattern recognition using circular harmonic synthetic filters
|AD-A294253| p 3217 N95-34459

MATERIALS SCIENCE
Metallurgical and Materials Transactions, volume 25A, no. 9
|AD-A293622| p 3077 N95-32474

MATERIALS TESTS
Microstructural studies of hydrogen damage in metastable stainless steels p 3080 N95-33774

MATHEMATICAL LOGIC
Automated support for software engineering
|AD-A294965| p 3182 N95-34582

MATHEMATICAL MODELS
Analytical modeling of the effect of crack depth, specimen size, and biaxial stress on the fracture toughness of reactor vessel steels
|DE95-005886| p 3125 N95-32373
Models for predicting damage evolution in metal matrix composites subjected to cyclic loading
|DE95-007734| p 3077 N95-32382
Summary report for ITER Task No. T226B: Evaluation of ITER disruption erosion
|DE95-010402| p 3219 N95-32401
Certification of a hybrid parameter model of the fully flexible Shuttle Remote Manipulator System
p 3125 N95-32421
Tactical low-level helicopter communications
p 3043 N95-32492
A highly reliable, high performance open avionics architecture for real time Nap-of-the-Earth operations
p 3044 N95-32497
Comparison of the Wang and Wachsmuth models for (pi) production with measurements at 12 GeV/c
|DE95-010417| p 3203 N95-32542
Users' manual for LEHGC: A Lagrangian-Eulerian finite-element model of HydroGeoChemical transport through saturated-unsaturated media. Version 1.0
|DE95-010513| p 3179 N95-32543
Techniques for the determination of local dynamic pressure and angle of attack on a horizontal axis wind turbine
|DE95-009204| p 3149 N95-32685
Numerical simulation of heat and mass transport during space crystal growth with MEPHISTO
|NASA-TM-107015| p 3089 N95-32718
Micromechanics of fiber-reinforced ceramic composites p 3063 N95-32775
Seismic response analysis of soil-structure interaction systems in the time domain
|REPT-2212| p 3091 N95-32992
Conceptual, causal and numerical modelling and analysis of physical systems p 3190 N95-33006
PSC algorithm description p 3051 N95-33013
Identification of terrain imagery with unstable reflectivity p 3093 N95-33138
Mathematical methods applied to biotechnical processes
|PB95-212114| p 3163 N95-33232
Thermocapillary flow with evaporation and condensation and its effect on liquid retention in low-g fluid acquisition devices p 3109 N95-33256
Quantitative analysis of volatile organic compounds using ion mobility spectra and cascade correlation neural networks p 3073 N95-33290
An experimental and analytical investigation into the performance of centrifugal pumps operating with air-water mixtures p 3123 N95-33323

Low Reynolds number kappa-epsilon and empirical transition models for oscillatory pipe flow and heat transfer
[NASA-TM-109785] p 3110 N95-33496
Gasdynamic model of turbulent combustion in an explosion
[DE95-010267] p 3074 N95-33627
Inclusion models of tensile fracture in fiber-reinforced brittle-matrix composites p 3065 N95-33721
Estimation of penetration of forest canopies by Interferometric SAR measurements p 3141 N95-33814
Application of IEM model on soil moisture and surface roughness estimation p 3142 N95-33816
An application of mechanical leverage to microactuation
[DE95-011883] p 3124 N95-33836
A relational metric, its application to domain analysis, and an example analysis and model of a remote sensing domain
[NASA-TM-110358] p 3198 N95-33875
Bending strength model for internal spur gear teeth
[NASA-TM-107012] p 3124 N95-33908
Discrete modeling of optical pulse propagation in nonlinear media
[DE95-011515] p 3216 N95-34020
Parallel molecular dynamics: Communication requirements for massively parallel machines
[DE95-012948] p 3209 N95-34212
A Spatial Analysis and Modeling System (SAMS) for environment management p 3243 N95-34239
A distributed analysis and visualization system for model and observational data p 3243 N95-34240
The beam envelope equation-systematic solution for a periodic quadrupole lattice with space charge
[DE95-012761] p 3199 N95-34269
Parallel solution of large-scale nonlinear optimization
[AD-A294372] p 3186 N95-34340
Proceedings of the ONR/NRL workshop on modeling the dispersion of nuclear contaminants in the arctic seas
[AD-A294373] p 3159 N95-34341
DSMC method applied for reacting gas flows p 3035 N95-34509
Numerical study on stabilization of a diffusion flame over a flat plate p 3035 N95-34510
Calculation of supersonic combustion in SCRAMJET engines p 3035 N95-34513
High speed variability in x-ray binary systems
[AD-A294634] p 3247 N95-34561
Grayling 2 information base for generation of synthetic thermal infrared scenes
[AD-A294956] p 3100 N95-34578
Mathematical modelling in plasma physics
[AD-A294972] p 3224 N95-34586
Laboratory and numerical modeling of topographic effects on time-dependent ocean currents
[AD-A294920] p 3160 N95-34594
Underwater acoustic field extrapolation: Theory and sensitivity analysis
[AD-A294925] p 3201 N95-34595
Numerical and symbolic algorithms for application specific signal processing
[AD-A294125] p 3100 N95-34749
The development of a distributed computing environment for the design and modeling of plasma spectroscopy experiments
[DE95-011725] p 3183 N95-34813
Environment and circuit model for capacitor-based rail guns
[AD-A293455] p 3057 N95-34815

MATHEMATICAL PROGRAMMING
Penetrable wedge analysis
[AD-A294276] p 3234 N95-34464
Numerical and symbolic algorithms for application specific signal processing
[AD-A294125] p 3100 N95-34749

MATRICES
Differencing the diffusion equation on unstructured meshes in 2-D
[DE95-010410] p 3195 N95-32559

MATRICES (MATHEMATICS)
Calculations of spatial higher modes without deflation procedure
[REPT-2205] p 3090 N95-32985
Terrain classification using circular polarimetric features p 3140 N95-33809

MATRIX MATERIALS
Acoustic attenuation and vibration damping materials
[AD-D017465] p 3201 N95-34444

MATTER (PHYSICS)
Prospect redux p 3133 N95-33758

MAXIMUM LIKELIHOOD ESTIMATES
Gamma ray imaging of the Crab and Vale regions with the UCR double-Compton telescope p 3245 N95-32837

MAXIMUM PRINCIPLE
Maximum principle for subsolutions of degenerate elliptic operators
[DE95-613373] p 3195 N95-32523

MAXWELL EQUATION
Discrete modeling of optical pulse propagation in nonlinear media
[DE95-011515] p 3216 N95-34020
Efficient time domain solutions of Maxwell's equations for aerospace systems
[AD-A294019] p 3196 N95-34377

MEASURE AND INTEGRATION
The 3D metal forming applications of ALE techniques
[DE95-011745] p 3080 N95-33653

MEASURING INSTRUMENTS
The interrelation of a Z(3) gauge theory on flat lattices and a spin-1 BEG model
[DE95-623634] p 3227 N95-32631
The non-relativistic charged Bose gas in a magnetic field. Part 1: Formalism
[DE95-619698] p 3205 N95-32632
Zero modes of Gauss constraint in gaugeless reduction of Yang-Mills theory
[DE95-623676] p 3234 N95-32667
Compression mass gauge testing in a liquid hydrogen dewar
[NASA-CR-198366] p 3115 N95-32687

MECHANICAL MEASUREMENT
Compression mass gauge testing in a liquid hydrogen dewar
[NASA-CR-198366] p 3115 N95-32687

MECHANICAL PROPERTIES
Fatigue properties for the Al-Li alloy 2090, part 3
[PB95-214532] p 3078 N95-32614
Effect of phase transformations on the mechanical properties of a multiphase alloy based on NiAl + Fe
[DE95-010119] p 3079 N95-33217
Ion assisted deposition of ZnS and MgF2
[AD-A294759] p 3086 N95-34563

MEDICAL SCIENCE
Advanced data visualization and sensor fusion: Conversion of techniques from medical imaging to Earth science p 3242 N95-34236

MEDICAL SERVICES
Managing technological change in a military treatment facility: A case study of medical diagnostic imaging support (MDIS) system
[AD-A294894] p 3165 N95-34573

MELTING
Glass science tutorial: Lecture no. 4, commercial glass melting and associated air emission issues
[DE95-007818] p 3082 N95-32384
Solar cell array design method for preventing power reduction due to module output fluctuation
[DE95-769745] p 3148 N95-32402
Optimization of a melting layer model in the radar backscatter, attenuation, and phase shift calculations at centimeter and millimeter wavelengths
[PB95-207189] p 3155 N95-32455
Glass science tutorial lecture no. 6: The melting of silicate glasses, a review of selected topics
[DE95-010199] p 3084 N95-33218
The interaction of vortices with twin boundaries
[DE95-012079] p 3110 N95-33389
Measurement of the spectral absorption of liquid water in melting snow with an imaging spectrometer p 3133 N95-33756

MELTS (CRYSTAL GROWTH)
Numerical simulation of heat and mass transport during space crystal growth with MEPHISTO
[NASA-TM-107015] p 3089 N95-32718

MEMBRANES
Design and testing criteria for bipolar plate materials for PEM fuel cell applications
[DE95-010876] p 3148 N95-32575
Environmental evaluation of lactates as cleaning agents
[PB95-214854] p 3067 N95-32615
Zeolite membranes for gas separations
[DE95-012984] p 3068 N95-33224
Fundamental studies of the mechanism of catalytic reactions with catalysts effective in the gasification of carbon solids and the oxidative coupling of methane
[DE95-012759] p 3075 N95-34268

MEMORY (COMPUTERS)
The development and application of massively parallel solid mechanics codes
[DE95-006307] p 3184 N95-32374
Distributed shared memory for new generation networks
[AD-A293722] p 3185 N95-32580
An object-oriented decomposition of the adaptive-hp finite element method
[DE95-012142] p 3186 N95-33852
Recoverable distributed shared memory under sequential and relaxed consistency
[AD-A293966] p 3178 N95-34453
Three-dimensional recognition via two-stage associative memory
[AD-A293567] p 3183 N95-34612

MENISCI
Thermocapillary flow with evaporation and condensation and its effect on liquid retention in low-g fluid acquisition devices p 3109 N95-33256

MENTAL PERFORMANCE
Event-related potentials and electroencephalograms in adaptive operator training: Rationale and annotated bibliography
[AD-A294337] p 3166 N95-34356
Conceptual understanding and stability, and knowledge shields for fending off conceptual change
[AD-A293555] p 3166 N95-34609
Resource document for the design of electronic instrument approach procedure displays
[AD-A295108] p 3047 N95-34797

MERCURY CADMIUM TELLURIDES
Ricor K506B cryocooler performance during the Clementine mission and ground testing
[DE95-010683] p 3089 N95-32568
The JPL Field Emission Spectrometer p 3117 N95-33794

MESH
The linear elastic biaxial response of plain-woven meshes p 3064 N95-33468

MESONS
Production asymmetries in x(sub f) and P(sup 2)(sub t) for D(sup + /-) mesons
[DE95-007207] p 3201 N95-32379
Scaling law for the Upsilon(4S) yields bar-BB and psi(3770) yields bar-DD decay constants from effective sum rules
[DE95-620538] p 3203 N95-32554
Intrinsic charm contribution to double quarkonium hadroproduction
[DE95-012170] p 3204 N95-32617
QCD mechanisms for double quarkonium and open heavy meson hadroproduction
[DE95-012171] p 3204 N95-32619
Four heavy quark and bound state production in the e(+)e(-) yields Q + (bar-Q' + Q' + bar-Q and e(+)e(-) yields (Q(bar-Q')) + Q' + bar-Q processes in Z(sup 0)-boson pole
[DE95-620533] p 3205 N95-32704
Virtual effects of physics beyond the standard model
[DE95-012499] p 3207 N95-33201
Searching for new physics with charm
[DE95-012498] p 3207 N95-33245
Probing new physics in B Penguins
[DE95-012494] p 3208 N95-33375
A final-focus magnet for PEP-2
[DE95-012372] p 3214 N95-33504

MESOSPHERE
Iron Boltzmann factor LIDAR: Proposed new remote-sensing technique for mesospheric temperature
[AD-A293568] p 3157 N95-34613

MESSAGE PROCESSING
Simulation of a connectionless server for b-ISDN
[PB95-215091] p 3097 N95-32892
A distributed Clips implementation: dClips p 3243 N95-34243
Recoverable distributed shared memory under sequential and relaxed consistency
[AD-A293966] p 3178 N95-34453

MESSAGES
Message based event specification for debugging nondeterministic parallel programs
[DE95-006169] p 3179 N95-32669

METAL BONDING
Tests of adhesives used for plate bonding of ATLAS tile-cal hadron calorimeter
[DE95-009917] p 3082 N95-32664
Synchrotron radiation studies of local structure and bonding in transition metal aluminides and rare earth transition metal magnetic nitrides
[DE95-011579] p 3079 N95-33065

METAL CLUSTERS
Theoretical dynamical studies of metal clusters and cluster-ligand systems
[DE95-012461] p 3228 N95-33382

METAL COATINGS
Coating power RF components with TiN
[DE95-010357] p 3082 N95-32541
CRADA with United Solar Technologies and Pacific Northwest Laboratory (PNL-021): Thin film materialsfor low-cost high performance solar concentrators
[DE95-010423] p 3150 N95-33400
TiO2/SiO2 and ZrO2/SiO2 multilayer media film optical loss and laser damage study
[AD-A294192] p 3217 N95-34298

Spray coating of metals. Proof of concept: Phase 2
[AD-A294393] p 3081 N95-34348
METAL CRYSTALS
Numerical analysis of the ultraprecision machining of copper
[DE95-007857] p 3089 N95-32585
Numerical simulation of heat and mass transport during space crystal growth with MEPHISTO
[NASA-TM-107015] p 3089 N95-32718
METAL FATIGUE
Nitrate stress corrosion crack growth rate in plain carbon steels
[DE95-011689] p 3079 N95-32958
Microstructural studies of hydrogen damage in metastable stainless steels p 3080 N95-33774
METAL FIBERS
Wear resistant composite structure of vitreous carbon containing convoluted fibers
[DE95-011463] p 3063 N95-33062
Micromechanics of composites with shape memory alloy fibers in uniform thermal fields
[NASA-TM-107011] p 3063 N95-33210
METAL FILMS
Low-energy response of superconducting tunnel junction x-ray spectrometers
[DE95-011733] p 3230 N95-33650
METAL FOILS
Electron beam joining of structural ceramics
[DE95-012521] p 3085 N95-34022
METAL FUELS
Analysis of metallic fuels by laser ablation
[DE95-012465] p 3075 N95-34440
METAL HALIDES
Charge-transfer gap closure in transition-metal halides under pressure
[DE95-011268] p 3230 N95-33865
METAL IONS
Alternative catalyst and exhaust gas sensor work at Argonne National Laboratory
[DE95-007138] p 3152 N95-32553
Conversion of holes into reducing species on surface modified small-particle TiO2
[DE95-008282] p 3225 N95-32586
Impact-parameter dependent L-K vacancy-transfer in collisions of Ni(23+) with Ge solid targets
[DE95-010821] p 3228 N95-33373
A background subtraction routine for enhancing energy-filtered plasmon images of MgAl2O4 implanted with Al(+) and Mg(+) ions
[DE95-012850] p 3074 N95-33629
High rate rechargeable lithium cells employing lithium ion conducting solid electrolytes
[AD-A294390] p 3104 N95-34347
METAL MATRIX COMPOSITES
Models for predicting damage evolution in metal matrix composites subjected to cyclic loading
[DE95-007734] p 3077 N95-32382
Metallic laminates for engine applications
[DE95-010259] p 3062 N95-32399
Metallurgical and Materials Transactions, volume 25A, no. 9
[AD-A293622] p 3077 N95-32474
Fracture toughness and tensile behavior of multi-layer laminated metal composite of Al 6090-25 vol % SiCp and Al 5182
[DE95-011421] p 3062 N95-32602
Low strain behaviour of a particulate reinforced aluminum alloy
[ISBN-0-315-84906-1] p 3078 N95-32935
Copper-diamond composite substrates for electronic components
[DE95-011520] p 3079 N95-33063
Stress relaxation in discontinuously reinforced composites
[DE95-010928] p 3064 N95-33704
Interfacial reactions during the liquid infiltration of titanium matrix composites p 3081 N95-34252
METAL NITRIDES
Synchrotron radiation studies of local structure and bonding in transition metal aluminides and rare earth transition metal magnetic nitrides
[DE95-011579] p 3079 N95-33065
METAL PROPELLANTS
Metallized gelled propellants: Oxygen/RP-1/aluminum rocket combustion experiments
[NASA-TM-107025] p 3088 N95-33876
METAL SURFACES
About the mechanism of heavy ion radiation influence on the metals at high temperature
[DE95-620943] p 3078 N95-32626
Reactions of trifluoroiodomethane on metal surfaces
[DE95-010122] p 3078 N95-32638
Spontaneous dewetting of a perfluoropolyether
[NASA-TM-106964] p 3083 N95-32919
Optical anisotropy of (110) surfaces of Ag and Cu
[DE95-010130] p 3229 N95-33637
Infrared detection of chemical corrosion on metal surface
[AD-A295000] p 3081 N95-34821
METAL WORKING
HOTQUA: An expert system prototype for quality monitoring in a rolling mill p 3190 N95-33004
Rigid bodies for metal forming analysis with NIKE3D
[DE95-011740] p 3182 N95-33652
The 3D metal forming applications of ALE techniques
[DE95-011745] p 3080 N95-33653
METAL-GAS SYSTEMS
Hydrogen formation in metals and alloys during fusion reactor operation
[DE95-737224] p 3202 N95-32529
METALLIC HYDROGEN
A quantum Monte Carlo study of the high-pressure phases of solid hydrogen p 3074 N95-33469
METALLICITY
Beryllium and Boron abundances in population II stars
[NASA-CR-189434] p 3247 N95-33262
METALLIZING
N-15 hydrogen profiling of IC metallizations
[DE95-011052] p 3102 N95-32708
Analysis of LDEF experiment AO187-2 chemical and isotopic measurements of micrometeoroids by secondary ion mass spectrometry
[NASA-CR-198849] p 3246 N95-32913
METALLURGY
Metallurgical and Materials Transactions, volume 25A, no. 9
[AD-A293622] p 3077 N95-32474
Knowledge-based system for metallurgical grade design p 3189 N95-32998
METALORGANIC CHEMICAL VAPOR DEPOSITION
The growth and optimization of InPSb/InGaAs/InAsSb strained-layer superlattice emitters by metal organic chemical vapor deposition
[DE95-011057] p 3226 N95-32595
Epitaxial Pb(Zr(x)Ti(1-x))O3/SrRuO3 (x = 0, 0.35, 0.65) multilayer thin films on SrTiO3(100) and MgO(100) prepared by MOCVD and RF sputtering
[DE95-008288] p 3226 N95-32598
Crystalline-as-deposited CaGa2S4: Ce via low-temperature metal-organic chemical vapor deposition
[DE95-010883] p 3229 N95-33401
Epitaxial Pb(Zr(0.40)Ti(0.60))O3/SrRuO3 and PbTiO3/SrRuO3 multilayer thin films prepared by MOCVD and RF sputtering
[DE95-007146] p 3229 N95-33636
METALS
Ductile damage model with void coalescence
[DE95-007855] p 3125 N95-32385
Materials sciences programs: Fiscal year 1994
[DE95-011248] p 3211 N95-32483
United Kingdom minerals yearbook, 1994. Statistical data to 1993
[PB95-207841] p 3155 N95-32599
World mineral statistics, 1988-92. Production: Exports: Imports
[PB95-208096] p 3155 N95-32601
World mineral production, 1989-93. Preliminary statistics
[PB95-208104] p 3156 N95-32603
About the mechanism of heavy ion radiation influence on the metals at high temperature
[DE95-620943] p 3078 N95-32626
Corrosion of separator plate constituents in molten carbonate
[PB95-214490] p 3149 N95-32813
Perpendicular magnetic behavior of ultra-thin Co sandwiches
[DE95-010611] p 3083 N95-32819
Phase equilibria and phase diagrams in carbide systems
[PB95-211348] p 3068 N95-33229
A novel approach to increasing cocaine detection confidence utilizing ion mobility spectrometry p 3072 N95-33283
Spray coating of metals. Proof of concept: Phase 2
[AD-A294393] p 3081 N95-34348
METASTABLE ATOMS
High-resolution magnetic imaging and investigations of thin-film magnetism with spin-polarized electron, ion and atom probes
[DE95-012190] p 3074 N95-33392
METEOROLOGICAL INSTRUMENTS
A tactical present weather sensor for Air Force applications
[AD-A294900] p 3158 N95-34575
METEOROLOGICAL PARAMETERS
OPEX Second Workshop of the OLYMPUS Propagation Experimenters. Volume 3: Reference book on radiometry and meteorological measurements
[ESA-WPP-083-VOL-3] p 3096 N95-32749
METEOROLOGICAL RADAR
OPEX Second Workshop of the OLYMPUS Propagation Experimenters. Volume 4: Reference book on radar
[ESA-WPP-083-VOL-4] p 3096 N95-32750
METEOROLOGICAL SATELLITES
Twenty-five years of progress. Part 1: Birth of NASA. Part 2: The Moon-a goal
[NASA-TM-110819] p 3253 N95-33384
A land-surface testbed for EOSDIS p 3158 N95-34223
METEOROLOGICAL SERVICES
Weather Forecasting: Systems architecture needed for National Weather Service modernization. Report to Congressional requesters
[GAO/AIMD-94-28] p 3157 N95-32760
METHAMPHETAMINE
Application of the ionscan for the detection of methamphetamine and ephedrine in abondoned clandestine laboratories p 3072 N95-33284
METHANE
Zeolite membranes for gas separations
[DE95-012984] p 3068 N95-33224
Multiscale characteristics and modeling of atmospheric methane p 3154 N95-33339
Selective methane oxidation over promoted oxide catalysts
[DE95-012319] p 3075 N95-34021
Fundamental studies of the mechanism of catalytic reactions with catalysts effective in the gasification of carbon solids and the oxidative coupling of methane
[DE95-012759] p 3075 N95-34268
METHOD OF MOMENTS
The 11th Annual Review of Progress in Applied Computational Electromagnetics, volume 2
[AD-A294851] p 3100 N95-34567
METHODOLOGY
Ice-ocean four dimensional structure and dynamics
[AD-A294017] p 3160 N95-34375
METHYL ALCOHOL
Application of the ionscan for the detection of methamphetamine and ephedrine in abondoned clandestine laboratories p 3072 N95-33284
Selective methane oxidation over promoted oxide catalysts
[DE95-012319] p 3075 N95-34021
METHYL COMPOUNDS
The effects of CO2 on the negative reactant ions of IMS p 3069 N95-33267
METRIC SPACE
A relational metric, its application to domain analysis, and an example analysis and model of a remote sensing domain
[NASA-TM-110358] p 3198 N95-33875
METRICATION
Metric conversion: Future progress depends upon private sector and public support. Report to Congressional requesters
[GAO/RCED-94-23] p 3089 N95-32785
MICROBIOLOGY
Geochemical, genetic, and physiological control of pollutant biodegradation
[AD-A294902] p 3155 N95-34591
MICROCLIMATOLOGY
Tri-service perspectives on microclimate cooling of protective clothing in the heat
[AD-A294005] p 3170 N95-34370
MICROCRACKS
Inclusion models of tensile fracture in fiber-reinforced brittle-matrix composites p 3065 N95-33721
MICROELECTRONICS
Numerical analysis of the ultraprecision machining of copper
[DE95-007857] p 3089 N95-32585
Copper-diamond composite substrates for electronic components
[DE95-011520] p 3079 N95-33063
Design and implementation of a two-axis micromanipulator to enhance the gripper positional accuracy of a single flexible link p 3123 N95-33252
MICROGRAVITY
Characterization of microgravity effects on bone structure and strength using fractal analysis p 3165 N95-32419
Application of impact dampers in vibration control of flexible structures p 3127 N95-32420
Bicycle ergometer instrumentation to determine muscle and bone forces during exercise p 3176 N95-32426
Compression mass gauge testing in a liquid hydrogen dewar
[NASA-CR-198366] p 3115 N95-32687
Numerical simulation of heat and mass transport during space crystal growth with MEPHISTO
[NASA-TM-107015] p 3089 N95-32718
Effects of gravity and light on plant growth and performance in normal and reduced gravity p 3163 N95-32901

A fundamental study of smoldering with emphasis on experimental design for zero-G
[NASA-CR-196378] p 3089 N95-32929
Thermocapillary flow with evaporation and condensation and its effect on liquid retention in low-g fluid acquisition devices p 3109 N95-33256
STS-42 mission highlights resource tape. Part 1 of 2
[NASA-TM-110838] p 3058 N95-34280
STS-42 mission highlights resource tape. Part 2 of 2
[NASA-TM-110840] p 3058 N95-34281

MICROMECHANICS
Irradiation-assisted stress corrosion cracking considerations at temperatures below 288 C
[DE95-008940] p 3077 N95-32555
Micromechanics of fiber-reinforced ceramic composites p 3063 N95-32775
Dual-use micromechanical inertial sensors p 3092 N95-33132
Micromechanics of composites with shape memory alloy fibers in uniform thermal fields
[NASA-TM-107011] p 3063 N95-33210
An application of mechanical leverage to microactuation
[DE95-011883] p 3124 N95-33836

MICROMETEOROIDS
Analysis of LDEF experiment AO187-2 chemical and isotopic measurements of micrometeoroids by secondary ion mass spectrometry
[NASA-CR-198849] p 3246 N95-32913

MICROORGANISMS
Mathematical methods applied to biotechnical processes
[PB95-212114] p 3163 N95-33232

MICROPROCESSORS
Formal verification of an avionics microprocessor
[NASA-CR-4682] p 3181 N95-33396
Construction of a connectionist network supercomputer
[AD-A294198] p 3177 N95-34301

MICROSCOPY
Plasma mediated ablation of biological tissues with ultrashort laser pulses
[DE95-011748] p 3164 N95-33654
Ultrafast near-field scanning optical microscopy (NSOM) of emerging display technology media: Solid state electronic structure and dynamics
[AD-A294879] p 3218 N95-34571

MICROSTRUCTURE
Image analysis used to count and measure etched tracks from ionizing radiation p 3210 N95-32424
Effect of heat treatment at 1,150 C on creep rupture properties of a Fe3Al-based alloy
[DE95-010295] p 3077 N95-32527
Spin counting in dipolar coupled spin 1/2 systems by multiple quantum NMR spectroscopy in solids: Development of a single quantum propagator and its application to heterogeneous catalysis
[DE95-010246] p 3066 N95-32540
The effects of H(+) implants on YBa2Cu3O7 superconducting materials
[DE95-614466] p 3227 N95-32698
Comparison of lead zirconate titanate thin films on ruthenium oxide and platinum electrodes
[DE95-617597] p 3082 N95-32710
Structural influences on the work hardening behavior of aluminum
[DE95-011262] p 3080 N95-33626
Epitaxial Pb(Zr(0.40)Ti(0.60))O3/SrRuO3 and PbTiO3/SrRuO3 multilayer thin films prepared by MOCVD and RF sputtering
[DE95-007146] p 3229 N95-33636
Measurement and modelling of structure sensitive magnetic properties of material
[DE95-010128] p 3080 N95-33699
Microstructural studies of hydrogen damage in metastable stainless steels p 3080 N95-33774
Effect of the colony microstructure on transport critical current of high-Jc) Tl-1223 thick films
[DE95-013049] p 3230 N95-34213
Photonic band gap structures on polymer materials for microstructure waveguides and high-speed interconnects
[AD-A294119] p 3218 N95-34504

MICROWAVE CIRCUITS
A 75 watt, 59 to 64 GHz space TWT
[NASA-CR-195450] p 3104 N95-33915

MICROWAVE EQUIPMENT
Activities of the Division of Microwave Technology
[PB95-214524] p 3095 N95-32613
Anechoic chamber upgrade
[AD-A294375] p 3056 N95-34342

MICROWAVE FREQUENCIES
Predicted operating conditions for maintaining mode purity in the 1MW 200 GHz FOM Free Electron Maser
[DE95-010795] p 3117 N95-32571
Integration of AIRSAR and AVIRIS data for Trail Canyon alluvial fan, Death Valley, California p 3134 N95-33760

MICROWAVE IMAGERY
Use of AIRSAR to identify woody shrub invasion and other indicators of desertification in the Jornada LTER p 3141 N95-33810

MICROWAVE LANDING SYSTEMS
The DLR research programme on an integrated multi sensor system for surface movement guidance and control p 3048 N95-33135

MICROWAVE OSCILLATORS
High efficiency vacuum and plasma filled backward wave oscillators: A critical evaluation
[AD-A294963] p 3105 N95-34581

MICROWAVE SCATTERING
Studies of microwave scattering and canopy architecture for boreal forests
[NASA-CR-199113] p 3099 N95-33497
Studies of microwave scattering and canopy architecture for boreal forests
[NASA-CR-199114] p 3099 N95-33726

MICROWAVE SPECTRA
Microwave nondestructive evaluation: State-of-the-Art review
[AD-A294388] p 3125 N95-34346

MICROWAVES
Semi-analytic computation of the driven fields in right circular cylindrical microwave applicators
[DE95-010875] p 3203 N95-32574
Status of the large-scale dark-matter axion search
[DE95-008828] p 3246 N95-32597
Microwave nondestructive evaluation: State-of-the-Art review
[AD-A294388] p 3125 N95-34346
Method of forming thin films on substrates at low temperatures
[AD-D017470] p 3086 N95-34447
Structure and dynamics of excited atoms
[AD-A294997] p 3209 N95-34819

MIDLATITUDE ATMOSPHERE
Analyses and forecasts with LAWS winds
[NASA-CR-199134] p 3157 N95-32933

MIE SCATTERING
Optimization of a melting layer model in the radar backscatter, attenuation, and phase shift calculations at centimeter and millimeter wavelengths
[PB95-207189] p 3155 N95-32455

MILITARY AIR FACILITIES
Report to the Chairman, Subcommittee on Transportation and Related Agencies, Committee on Appropriations, US Senate. Airport Improvement Program: The Military Airport Program has not achieved intended impact
[GAO/RCED-94-209] p 3056 N95-32888

MILITARY HELICOPTERS
Covert Night/Day Operations for Rotorcraft (CONDOR) programme p 3046 N95-32505
Army aviation: Modernization strategy needs to be reassessed. Report to Congressional requestors
[GAO/NSIAD-95-9] p 3033 N95-32783
HeliRadar: A rotating antenna synthetic aperture radar for helicopter allweather operations p 3093 N95-33137
Comanche helicopter: Testing needs to be completed prior to production decisions
[AD-A294408] p 3049 N95-34422

MILITARY OPERATIONS
Covert Night/Day Operations for Rotorcraft (CONDOR) programme p 3046 N95-32505
Report to Congressional Committees. B-1B bomber: Evaluation of Air Force report on B-1B operational readiness assessment
[GAO/NSIAD-95-151] p 3197 N95-32758
Report to Congressional Committees. Air Force fighters: More reliance on reserves increases the need to know their capabilities
[GAO/NSIAD-94-86] p 3197 N95-32807
Some results of international cooperation in military to commercial conversion of laser gyro technology p 3092 N95-33130
Effects of the specific military aspects of satellite navigation on the civil use of GPS/GLONASS p 3048 N95-33134
Proposed incorporation of mission-oriented flying qualities into MIL-STD-1797A
[AD-A294211] p 3055 N95-34306
Managing technological change in a military treatment facility: A case study of medical diagnostic imaging support (MDIS) system
[AD-A294894] p 3165 N95-34573

MILITARY TECHNOLOGY
Dual Usage in Military and Commercial Technology in Guidance and Control
[AGARD-CP-556] p 3091 N95-33126
Navigational technology of dual usage p 3048 N95-33131
The DLR research programme on an integrated multi sensor system for surface movement guidance and control p 3048 N95-33135
HeliRadar: A rotating antenna synthetic aperture radar for helicopter allweather operations p 3093 N95-33137
Application of advanced safety technique to ring laser gyro inertial navigation system integration p 3048 N95-33140
GPS-based navigation for space applications p 3058 N95-33144
Tri-service perspectives on microclimate cooling of protective clothing in the heat
[AD-A294005] p 3170 N95-34370
An investigation of the chemistry of citric acid in military soldering applications
[AD-A295042] p 3105 N95-34796

MILITARY VEHICLES
The development of the automatic target recognition system for the UGV/RSTA LADAR
[AD-A294090] p 3100 N95-34474

MILLIMETER WAVES
High-resolution TeO2 acousto-optical deflector for millimeter-wave spectrometer
[AD-A293054] p 3215 N95-32701
Conference proceedings of mathematical methods in electromagnetic theory
[AD-A291165] p 3097 N95-32797
Monolithic diode arrays for quasioptical millimeter wave beam steering
[AD-A294256] p 3100 N95-34460

MIMD (COMPUTERS)
Elementary benchmarks of the NWT computer system and program performance p 3038 N95-34532

MINERAL DEPOSITS
Mapping minerals, amorphous materials, environmental materials, vegetation, water, ice and snow, and other materials: The USGS tricorder algorithm p 3130 N95-33742
Remote mineral mapping using AVIRIS data at Summitville, Colorado and the adjacent San Juan Mountains p 3134 N95-33761

MINERAL EXPLORATION
Discrimination of alkalinity in granitoid Rocks: A potential TIMS application p 3138 N95-33798

MINERALOGY
Mineralogic variations in fluvial sediments contaminated by mine tailings as determined from AVIRIS data, Coeur D'Alene River Valley, Idaho p 3131 N95-33745
Integration of AIRSAR and AVIRIS data for Trail Canyon alluvial fan, Death Valley, California p 3134 N95-33760
Preliminary study of Kelso Dunes using AVIRIS, TM, and AIRSAR p 3136 N95-33773
Discrimination of alkalinity in granitoid Rocks: A potential TIMS application p 3138 N95-33798

MINERALS
United Kingdom minerals yearbook, 1994. Statistical data to 1993
[PB95-207841] p 3155 N95-32599
World mineral statistics, 1988-92. Production: Exports: Imports
[PB95-208096] p 3155 N95-32601
World mineral production, 1989-93. Preliminary statistics
[PB95-208104] p 3156 N95-32603
Quantitative remote sensing of ammonium minerals, Cedar Mountains, Esmeralda County, Nevada p 3128 N95-33734
Spectral identification of minerals using imaging spectrometry data: Evaluating the effects of signal to noise and spectral resolution using the tricorder algorithm p 3136 N95-33772

MINIATURIZATION
Engineering approaches and compromises in the design of small ion mobility spectrometers p 3070 N95-33271

MINING
United Kingdom minerals yearbook, 1994. Statistical data to 1993
[PB95-207841] p 3155 N95-32599
World mineral statistics, 1988-92. Production: Exports: Imports
[PB95-208096] p 3155 N95-32601
World mineral production, 1989-93. Preliminary statistics
[PB95-208104] p 3156 N95-32603
Mineralogic variations in fluvial sediments contaminated by mine tailings as determined from AVIRIS data, Coeur D'Alene River Valley, Idaho p 3131 N95-33745

MIRRORS
Measurement of laser wavefront using Shack Hartmann method with new lens array
[REPT-2208] p 3090 N95-32988

Laser gyroscopy tendencies and their analysis of development in Ukraine p 3092 N95-33133

MISSILE RANGES
Frequency response of a TeO2 slow shear wave acousto-optic cell exposed to radiation
[DE95-009588] p 3226 N95-32589

MISSION PLANNING
Low-Level and Nap-of-the-Earth (NOE) night operations
[AGARD-CP-563] p 3042 N95-32486

MIXING LAYERS (FLUIDS)
Large eddy simulation of turbulent vortices and mixing layers p 3109 N95-33340
Solitary wave solution for mixing-layer turbulence p 3036 N95-34522

MODAL RESPONSE
Modal identification and its applications to damage detection in vibrating structures p 3126 N95-32920

MODEL REFERENCE ADAPTIVE CONTROL
Trajectory planning and control of kinematically redundant robotic manipulators p 3194 N95-34807

MODELS
Modeling of DC spacecraft power systems p 3062 N95-32423
Evaluation of a bridge using simplified element modeling
[DE95-006281] p 3126 N95-32670
Fast approximation of self-similar network traffic
[DE95-011271] p 3185 N95-32967

MODULATION
Temporal dynamics of the multi-frequency spectrum generated by self-phase modulation of two frequencies in single-mode fiber
[DE95-010920] p 3119 N95-33703

MODULATION TRANSFER FUNCTION
Characteristics of the HYDICE sensor p 3116 N95-33733

MODULATORS
Study of liquid crystal spatial light modulator application to Hadamard transform spectrometer: A fast and accurate decoding method
[AD-A293087] p 3215 N95-32660

MODULES
Solar cell array design method for preventing power reduction due to module output fluctuation
[DE95-769745] p 3148 N95-32402
Device physics of thin-film polycrystalline cells and modules
[DE95-009209] p 3149 N95-32817
Photonic band gap structures on polymer materials for microstructure waveguides and high-speed interconnects
[AD-A294119] p 3218 N95-34504

MOISTURE CONTENT
Investigation of water droplet trajectories within the NASA icing research tunnel
[NASA-TM-107023] p 3034 N95-32769
Vegetation species composition and canopy architecture information expressed in leaf water absorption measured in the 1000 nm and 2200 spectral region by an imaging spectrometer p 3133 N95-33757
Validating spatial structure in canopy water content using geostatistics p 3135 N95-33768
Regional mapping of forest canopy water content and biomass using AIRSAR images over BOREAS study area p 3142 N95-33815
Application of IEM model on soil moisture and surface roughness estimation p 3142 N95-33816
Cooling tower and plume modeling for satellite remote sensing applications
[DE95-012000] p 3143 N95-33849

MOLDING MATERIALS
Apparatus for injection molding high-viscosity materials
[AD-D017471] p 3065 N95-34448

MOLECULAR BEAM EPITAXY
Perpendicular magnetic behavior of ultra-thin Co sandwiches
[DE95-010611] p 3083 N95-32619
Unusual behavior in the magnetic anisotropy of ultra-thin Co sandwiches: The role of Au underlayers
[DE95-010612] p 3229 N95-33641
Low temperature growth of thin films by high kinetic energy supersonic molecular beams
[AD-A294516] p 3086 N95-34476
Fundamental surface chemistry of GaAs OMVPE
[DE95-011606] p 3231 N95-34486
Multilayer optics for soft x-rays
[AD-A295030] p 3219 N95-34791
Growth and structure of MBE-Deposited iridium silicide
[AD-A295033] p 3232 N95-34792

MOLECULAR BEAMS
Growth and structure of MBE-Deposited iridium silicide
[AD-A295033] p 3232 N95-34792

MOLECULAR BIOLOGY
Minutes of the 12th Joint NASA/DARA-DLR Life Sciences Program Working Group Meeting
[NASA-TM-110655] p 3161 N95-32719
Heavy ion induced DNA-DSB in yeast and mammalian cells p 3161 N95-32723
Geochemical, genetic, and physiological control of pollutant biodegradation
[AD-A294902] p 3155 N95-34591

MOLECULAR CLOUDS
Reduction and analysis of seasons 15 and 16 (1991 - 1992) Pioneer Venus radio occulation data and correlative studies with observations of the near infrared emission of Venus
[NASA-CR-199071] p 3247 N95-32700
Formation of high density cores in molecular cloud p 3041 N95-34553

MOLECULAR COLLISIONS
Velocity dependence of ionization and excitation of hydrogen molecules by fast proton impact
[DE95-010818] p 3207 N95-33370

MOLECULAR DYNAMICS
Visualization of parallel molecular dynamics simulation on a remote visualization platform
[DE95-007806] p 3185 N95-32582
Lattice Polymer Automata
[DE95-011980] p 3062 N95-33848
Parallel molecular dynamics: Communication requirements for massively parallel machines
[DE95-012948] p 3209 N95-34212
A molecular dynamics investigation of the structural characteristics of amorphous and annealed poly (Vinylidene fluoride) and vinylidene fluoride - trifluoroethylene copolymers
[AD-A294116] p 3086 N95-34502
Molecular motion of phosphazene-bound NLO chromophores
[AD-A293526] p 3087 N95-34649

MOLECULAR EXCITATION
Practical improvement of MS-X alpha molecular orbital calculation as applied to dissociation process of CO molecule
[REPT-2206] p 3090 N95-32986
Velocity dependence of ionization and excitation of hydrogen molecules by fast proton impact
[DE95-010818] p 3207 N95-33370

MOLECULAR GASES
Velocity dependence of ionization and excitation of hydrogen molecules by fast proton impact
[DE95-010818] p 3207 N95-33370

MOLECULAR IONS
The mean lifetimes of the 2p(sigma) lowest bound state of HeH(2+) and its isotopes
[DE95-010812] p 3206 N95-32966
Mean lifetime measurements of (3)He(4)He2+
[DE95-010813] p 3209 N95-34355

MOLECULAR ORBITALS
Practical improvement of MS-X alpha molecular orbital calculation as applied to dissociation process of CO molecule
[REPT-2206] p 3090 N95-32986
Impact-parameter dependent L-K vacancy-transfer in collisions of Ni(23+) with Ge solid targets
[DE95-010821] p 3228 N95-33373

MOLECULAR PHYSICS
Heavy ion induced mutations in mammalian cells: Cross sections and molecular analysis p 3162 N95-32728

MOLECULAR ROTATION
Stimulated rotational Raman scattering of N2 in the atmosphere
[AD-A294195] p 3157 N95-34299

MOLECULAR SPECTRA
Molecular motion of phosphazene-bound NLO chromophores
[AD-A293526] p 3087 N95-34649

MOLECULAR STRUCTURE
Visualization of parallel molecular dynamics simulation on a remote visualization platform
[DE95-007806] p 3185 N95-32582
Polymerization of epsilon-caprolactone in the presence of Oh- or COOh-groups containing initiators. Copolymers of lactide with epsilon-caprolactone: Synthesis, characterization and processing
[PB95-208211] p 3084 N95-33227
DMTA studies of branching distribution in polyethylene
[PB95-208237] p 3084 N95-33228
Proton affinity determinations and proton-bound dimer structure indications in C2 to C15, (alpha),(omega)-alkyldiamines p 3069 N95-33266
Parallel molecular dynamics: Communication requirements for massively parallel machines
[DE95-012948] p 3209 N95-34212
Parallel solution of large-scale nonlinear optimization
[AD-A294372] p 3186 N95-34340
Synthesis and characterization of a series of organoindium-phosphides including molecular structures of ((Me3CCH2)2InPEt2)2 and ((Me3CCH2)2InP(H)(C6H11))3
[AD-A293965] p 3086 N95-34452
Ultrafast near-field scanning optical microscopy (NSOM) of emerging display technology media: Solid state electronic structure and dynamics
[AD-A294879] p 3218 N95-34571
Industrial products based upon processible conductive polyaniline
[AD-A294985] p 3087 N95-34817

MOLECULAR WEIGHT
High resolution electrospray mass spectrometry with a magnetic sector instrument: Accurate mass measurement and peptide sequencing
[AD-A293564] p 3076 N95-34611

MOLECULES
Thermal rearrangement of oxygen-containing (omicron)-allyltoluene derivatives
[DE95-010124] p 3067 N95-32641
Theoretical dynamical studies of metal clusters and cluster-ligand systems
[DE95-012461] p 3228 N95-33382
Elemental fluorine based syntheses of pentafluoro phenyl and other aromatic perfluoropolyether polymers
[AD-A294930] p 3087 N95-34596

MOLYBDENUM
Combining the QMR method with first principles electronic structure codes
[DE95-009927] p 3228 N95-33240

MOMENTUM
Comparison of the Wang and Wachsmuth models for (pi) production with measurements at 12 GeV/c
[DE95-010417] p 3203 N95-32542
Intrinsic charm contribution to double quarkonium hadroproduction
[DE95-012170] p 3204 N95-32617
QCD mechanisms for double quarkonium and open heavy meson hadroproduction
[DE95-012171] p 3204 N95-32619
The Problem 4/3 as a consequence of contracted length non-covariance
[DE95-623628] p 3207 N95-33226
CDW-EIS calculation of longitudinal momentum distribution in single ionization of helium by Ni(24+) ions
[DE95-010816] p 3207 N95-33241

MOMENTUM THEORY
Unified approach for incompressible flows p 3113 N95-32425

MOMENTUM TRANSFER
Spin effects in high energy photon-hadron scattering in QCD
[DE95-623679] p 3234 N95-32961

MONITORS
Summary of the impedance working group
[DE95-012095] p 3211 N95-32606

MONOMERS
Proton affinity determinations and proton-bound dimer structure indications in C2 to C15, (alpha),(omega)-alkyldiamines p 3069 N95-33266

MONSOONS
Intra-annual and inter-annual rainfall variability over East Asia, Southeast Asia, and South Asia
[AD-A294156] p 3158 N95-34757

MONTE CARLO METHOD
Approaches to implementing deterministic models in a probabilistic framework
[DE95-009483] p 3197 N95-32391
Airborne passive polarimetric measurements of sea surface anisotropy at 92 GHz
[NASA-CR-197288] p 3143 N95-32823
Ocean observations with EOS/MODIS: Algorithm development and post launch studies
[NASA-CR-198928] p 3143 N95-32914
Light particle emission in heavy ion reactions
[DE95-010727] p 3206 N95-32965
A quantum Monte Carlo study of the high-pressure phases of solid hydrogen p 3074 N95-33469
Estimation of penetration of forest canopies by interferometric SAR measurements p 3141 N95-33814
Lattice Polymer Automata
[DE95-011980] p 3062 N95-33848
Certification of MCNP Version 4A for WHC computer platforms, revision 7
[DE95-011545] p 3178 N95-34484
Track finding and fitting in the H1 forward track detector
[PB95-234985] p 3214 N95-34651
Electron and hole transport in compound semiconductors
[AD-A295003] p 3233 N95-34822

MORPHOLOGY
Smoothing during ion-assisted growth by transient ion beam-induced defects
[DE95-011021] p 3225 N95-32579
High rate dry etching of GaN, AlN and InN in ECR Cl2/CH4/H2/Ar plasmas
[DE95-011872] p 3223 N95-33412
Structural influences on the work hardening behavior of aluminum
[DE95-011262] p 3080 N95-33626
Stress relaxation in discontinuously reinforced composites
[DE95-010928] p 3064 N95-33704
Integration of AIRSAR and AVIRIS data for Trail Canyon alluvial fan, Death Valley, California
p 3134 N95-33760
Preliminary study of Kelso Dunes using AVIRIS, TM, and AIRSAR p 3136 N95-33773
In situ surface roughness measurement during PECVD diamond film growth
[DE95-013411] p 3230 N95-34215
MOTION STABILITY
Motion and force control of coordinated robots
[ISBN-0-315-86323-4] p 3191 N95-33307
MOTIVATION
Locus of control and coping style as stress moderators in achievement oriented individuals
[AD-A294275] p 3166 N95-34463
MOUNTAINS
Report to the Chairman, Subcommittee on Aviation, Committee on Commerce, Science, and Transportation, US Senate. Aviation Safety: FAA can better prepare general aviation pilots for mountain flying risks
[GAO/RCED-94-15] p 3046 N95-32784
MULTIBLOCK GRIDS
Parallel computation of transonic flows about an aircraft configuration using multi-block structured grids
p 3039 N95-34537
A large scale 3D Navier-Stokes analysis using NAL-NWT p 3039 N95-34539
MULTIDISCIPLINARY RESEARCH
A distributed system for visualizing and analyzing multivariate and multidisciplinary data
p 3241 N95-34230
MULTIGRID METHODS
A unified multigrid solver for the Navier-Stokes equations on mixed element meshes
[NASA-CR-198183] p 3196 N95-33500
A multigrid incompressible NS solver
p 3036 N95-34517
A simulation of damping process of pendulum motion due to aerodynamic forces p 3041 N95-34551
MULTIMEDIA
Incorporating bibliographic information into a spatial data query system for the Savannah River Site
[DE95-010965] p 3238 N95-33402
Animation within a multimedia training system for night vision goggles
[AD-A294095] p 3170 N95-34475
Developing multimedia instructional systems: An example application for training in night vision goggles
[AD-A294521] p 3235 N95-34479
Protocol engineering for broadband networks
[AD-A294969] p 3186 N95-34584
MULTIPATH TRANSMISSION
Tactical low-level helicopter communications
p 3043 N95-32492
MULTIPHOTON ABSORPTION
Structure and dynamics of excited atoms
[AD-A294997] p 3209 N95-34819
MULTIPOLES
Ramp-rate sensitivity of SSC dipole magnet prototypes
[DE95-011162] p 3214 N95-33720
MULTIPROCESSING (COMPUTERS)
A reconfigurable optoelectronic interconnect technology for multi-processor networks
[DE95-011895] p 3186 N95-33838
MULTISENSOR APPLICATIONS
Dual Usage in Military and Commercial Technology in Guidance and Control
[AGARD-CP-556] p 3091 N95-33126
Dual use: Opportunities, payoffs, and challenges
p 3091 N95-33127
Low-level data fusion for landing runways detection
p 3048 N95-33136
Geographic information system for fusion and analysis of high-resolution remote sensing and ground data
p 3240 N95-34224
Advanced data visualization and sensor fusion: Conversion of techniques from medical imaging to Earth science p 3242 N95-34236
Optimization problems in multitarget/multisensor tracking
[AD-A294978] p 3100 N95-34590
MULTISENSOR FUSION
An approach to sensor data fusion for flying and landing aid purpose p 3043 N95-32488
The DLR research programme on an integrated multi sensor system for surface movement guidance and control p 3048 N95-33135
Low-level data fusion for landing runways detection
p 3048 N95-33136
Geographic information system for fusion and analysis of high-resolution remote sensing and ground data
p 3240 N95-34224
Advanced data visualization and sensor fusion: Conversion of techniques from medical imaging to Earth science p 3242 N95-34236
MULTISPECTRAL BAND SCANNERS
For geological investigations with airborne thermal infrared multispectral images: Transfer of calibration from laboratory spectrometer to TIMS as alternative for removing atmospheric effects p 3137 N95-33792
A conflict of water and fire: Remote sensing imagery of the Uinkaret Volcanic Field, Grand Canyon, Arizona
p 3117 N95-33795
The 1994 laboratory calibration of TIMS
p 3117 N95-33796
The 1994 TIMS airborne calibration experiment: Castaic Lake, California p 3117 N95-33797
TIMS observations of surface emissivity in HAPEX-Sahel p 3139 N95-33799
A field- and laboratory-based quantitative analysis of alluvium: Relating analytical results to TIMS data
p 3139 N95-33800
MULTISPECTRAL RADAR
The Anglo-French Compact Laser Radar demonstrator programme p 3045 N95-32501
MULTIVARIATE STATISTICAL ANALYSIS
Causal correlation of foliar biochemical concentrations with AVIRIS spectra using forced entry linear regression
p 3130 N95-33744
Multivariate statistical analysis software technologies for astrophysical research involving large data bases
p 3240 N95-34222
A distributed system for visualizing and analyzing multivariate and multidisciplinary data
p 3241 N95-34230
MUON SPIN ROTATION
International Meeting on Muon Science
[PB95-236014] p 3209 N95-34657
MUONIUM
International Meeting on Muon Science
[PB95-236014] p 3209 N95-34657
MUONS
Charm decays and high energy photoproduction
[DE95-010165] p 3201 N95-32393
Application of deformable templates for recognizing tracks detected with High Pressure Drift Tubes
[DE95-621870] p 3188 N95-32627
Targets and magnetic elements for pion collection in muon collider drivers
[DE95-010316] p 3205 N95-32652
Light particle emission in heavy ion reactions
[DE95-010727] p 3206 N95-32965
International Meeting on Muon Science
[PB95-236014] p 3209 N95-34657
MUSCLES
Characterization of microgravity effects on bone structure and strength using fractal analysis
p 3165 N95-32419
Bicycle ergometer instrumentation to determine muscle and bone forces during exercise p 3176 N95-32428
MUSCULOSKELETAL SYSTEM
Bicycle ergometer instrumentation to determine muscle and bone forces during exercise p 3176 N95-32428
MUTATIONS
Mutation induction in bacteria after heavy ion irradiation p 3162 N95-32727
Heavy ion induced mutations in mammalian cells: Cross sections and molecular analysis p 3162 N95-32728
MYLAR (TRADEMARK)
Cathode readout with stripped resistive drift tubes
[DE95-621871] p 3102 N95-32628

N

NACELLES
Drag measurements of an axisymmetric nacelle mounted on a flat plate at supersonic speeds
[NASA-TM-4660] p 3034 N95-32821
Fan noise prediction assessment
[NASA-CR-195051] p 3200 N95-33831
NAP-OF-THE-EARTH NAVIGATION
Low-Level and Nap-of-the-Earth (NOE) night operations
[AGARD-CP-563] p 3042 N95-32486
Night attack p 3042 N95-32487
The application of helicopter mission simulation to Nap-of-the-Earth operations p 3044 N95-32496
A highly reliable, high performance open avionics architecture for real time Nap-of-the-Earth operations
p 3044 N95-32497
Laser based obstacle warning sensors for helicopters
p 3045 N95-32499
Covert Night/Day Operations for Rotorcraft (CONDOR) programme p 3046 N95-32505
NAPHTHALENE
Geochemical, genetic, and physiological control of pollutant biodegradation
[AD-A294902] p 3155 N95-34591
NARCOTICS
IMS R and D program at Canada customs
p 3070 N95-33273
The effect of sample holder material on ion mobility spectrometry reproducibility p 3071 N95-33282
A novel approach to increasing cocaine detection confidence utilizing ion mobility spectrometry
p 3072 N95-33283
NARROWBAND
Pulsed tunable narrow-bandwidth dye laser, with hollow circular waveguide in cavity
[AD-A294060] p 3120 N95-34469
NASA PROGRAMS
Minutes of the 12th Joint NASA/DARA-DLR Life Sciences Program Working Group Meeting
[NASA-TM-110655] p 3161 N95-32719
Budget estimates: Fiscal year 1994. Volume 1: Agency summary
[NASA-TM-110815] p 3244 N95-33069
Budget estimates: Fiscal year 1994. Volume 2: Construction of facilities
[NASA-TM-110816] p 3245 N95-33081
Budget estimates: Fiscal year 1994. Volume 3: Research and program management
[NASA-TM-110817] p 3245 N95-33082
NASA-Wide Fastener Technical Interchange Meeting
[NASA-CP-3308] p 3123 N95-33199
NASA directives master list and index
[NHB-1410.13O] p 3238 N95-33249
A layered approach to technology transfer of AVIRIS between Earth Search Sciences, Inc. and the Idaho National Engineering Laboratory p 3117 N95-33746
NASA/DOD Aerospace Knowledge Diffusion Research Project. Report 33: The technical communications practices of US aerospace engineers and scientists: Results of the phase 1 AIAA mail survey
[NASA-TM-110180] p 3239 N95-34217
Issues in NASA program and project management
[NASA-SP-6101(09)] p 3236 N95-34354
NASA SPACE PROGRAMS
Space Station: Estimated total US funding requirements. Report to Congressional Requesters
[GAO/NSIAD-95-163] p 3058 N95-32884
Twenty-five years of progress. Part 1: Birth of NASA. Part 2: The Moon-a goal
[NASA-TM-110819] p 3253 N95-33384
The Space Shuttle: America's team reaching for the future
[NASA-CR-199222] p 3058 N95-33728
NATIONS
World mineral statistics, 1988-92. Production: Exports: Imports
[PB95-208096] p 3155 N95-32601
World mineral production, 1989-93. Preliminary statistics
[PB95-208104] p 3156 N95-32603
NATURAL GAS
Gasoline from natural gas by sulfur processing
[DE95-010651] p 3087 N95-32563
Alternative-fuels technology: Natural gas vehicles as a way to curb urban air pollution
[DE95-012216] p 3088 N95-33395
NATURAL LANGUAGE (COMPUTERS)
Towards friendlier user interfaces for expert systems
[AD-A294056] p 3192 N95-34467
Focus of attention in decision support systems
[AD-A294037] p 3236 N95-34487
NAVIER-STOKES EQUATION
Large-eddy simulation of the development of stably-stratified atmospheric boundary layers over cool flat surfaces
[DE95-009574] p 3156 N95-32697
PINCA: A scalable parallel program for compressible gas dynamics with nonequilibrium chemistry
[DE95-010581] p 3106 N95-32818
Application of vorticity transport analysis to the development of physically accurate turbulence models
p 3107 N95-32905
Turbulence models in the Navier-Stokes simulation of airfoil stall
[TRITA-NA-9312] p 3108 N95-33059

A unified multigrid solver for the Navier-Stokes equations on mixed element meshes
[NASA-CR-198183] p 3196 N95-33500
Analysis and finite element approximation of an optimal shape control problem for the steady-state Navier-Stokes equations p 3112 N95-34285
Stability of steady state solutions for forced Navier-Stokes equations p 3112 N95-34286
Numerical studies of turbulent free surface flows and unsteady propeller flows
[AD-A294377] p 3112 N95-34343
Numerical study on stabilization of a diffusion flame over a flat plate p 3035 N95-34510
Calculation of supersonic combustion in SCRAMJET engines p 3035 N95-34513
A multigrid incompressible NS solver p 3036 N95-34517
A flux splitting scheme with high-resolution and robustness for discontinuities p 3036 N95-34518
Hypersonic CFD analysis for the aerothermodynamic design of HOPE p 3036 N95-34520
Numerical solutions of inviscid and viscous flows about airfoils by TVD method p 3036 N95-34521
Solitary wave solution for mixing-layer turbulence p 3036 N95-34522
Numerical simulation of film cooling effect around axisymmetric body in hypersonic flow field p 3037 N95-34526
Direct numerical simulation of incompressible homogeneous isotropic turbulence using compressible Navier-Stokes equations p 3037 N95-34529
Direct numerical simulation of incompressible homogeneous isotropic turbulence using NWT p 3038 N95-34530
Effect of schemes on numerical simulations of shock wave reflection p 3038 N95-34531
Performance evaluation of the NWT with incompressible NS code p 3038 N95-34533
Parallel computation of transonic flows about an aircraft configuration using multi-block structured grids p 3039 N95-34537
Vector-parallel simulations of transonic wind tunnel flows about a fully configured model of aircraft p 3039 N95-34538
A large scale 3D Navier-Stokes analysis using NAL-NWT p 3039 N95-34539
Computations of low speed flow about space-plane p 3040 N95-34544
Numerical simulations of dynamic stall phenomena in low speed flows p 3040 N95-34546
Numerical simulation of unsteady viscous flow around an airfoil with oscillating spoiler p 3040 N95-34547
Dependency of a boundary layer flow on computational grids p 3040 N95-34550
A simulation of damping process of pendulum motion due to aerodynamic forces p 3041 N95-34551
Parallel computation for two dimensional incompressible flow on array of transputers p 3042 N95-34558

NAVIGATION
SeaWiFS technical report series. Volume 15: The simulated SesWiFS data set, version 2
[NASA-TM-104566-VOL-15] p 3158 N95-32545
Dual Usage in Military and Commercial Technology in Guidance and Control
[AGARD-CP-556] p 3091 N95-33126
Dual use: Opportunities, payoffs, and challenges p 3091 N95-33127

NAVIGATION AIDS
An approach to sensor data fusion for flying and landing aid purpose p 3043 N95-32488
Laser based obstacle warning sensors for helicopters p 3045 N95-32499
Fixed wing night attack missions: Assessment in a Flight Simulation environment p 3045 N95-32502
A helmet mounted display for night missions at low altitude p 3045 N95-32503
SIRPH: Steerable infrared picture on helmet mounted display p 3045 N95-32504
Effects of the specific military aspects of satellite navigation on the civil use of GPS/GLONASS p 3048 N95-33134
Current issues in the design and information content of instrument approach charts
[AD-A294752] p 3047 N95-34562

NAVIGATION INSTRUMENTS
An approach to sensor data fusion for flying and landing aid purpose p 3043 N95-32488
Low-level data fusion for landing runways detection p 3048 N95-33136

NAVY
Commercial usage of Navy components developed and manufactured by CRI Delfin p 3092 N95-33129

NEAR FIELDS
Propagation of spatial solitons generated by Gaussian beams in a non-linear Kerr medium
[IFTR-9/1995] p 3206 N95-32921

NEAR INFRARED RADIATION
Reduction and analysis of seasons 15 and 16 (1991 - 1992) Pioneer Venus radio occulation data and correlative studies with observations of the near infrared emission of Venus
[NASA-CR-199071] p 3247 N95-32700
High spectral resolution remote sensing of canopy chemistry p 3128 N95-33731

NEGATIVE IONS
The effects of CO2 on the negative reactant ions of IMS p 3069 N95-33267

NEODYMIUM
Measurement of gain saturation on Nd: Doped phosphate laser glasses
[REPT-2210] p 3090 N95-32990

NEODYMIUM LASERS
Sum frequency generation of dual-wavelength Nd: YAP laser in LiIO3 crystal
[AD-A293094] p 3117 N95-32472

NETWORK ANALYSIS
Bit-level analysis of an SRT divider circuit
[AD-A294842] p 3105 N95-34565

NETWORK SYNTHESIS
Multiobjective optimization of hybrid regenerative life support technologies. Topic D: Technology Assessment
[NASA-CR-199125] p 3167 N95-32688

NEURAL NETS
Training neural networks using sequential extended Kalman filtering
[DE95-007874] p 3187 N95-32386
Numerical solution of differential equations by artificial neural networks p 3194 N95-32434
A choice of input variables for a multilayer perceptron
[DE95-623573] p 3187 N95-32476
A decade of neural networks: Practical applications and prospects
[NASA-CR-198867] p 3188 N95-32659
Genetic algorithm based input selection for a neural network function approximator with applications to SSME health monitoring
[NASA-CR-199089] p 3188 N95-32768
Training and recognition of Cantonese onemes by backpropagation through time p 3180 N95-32996
High-tech controls for energy and environment
[DE95-004011] p 3191 N95-33060
IMS R and D program at Canada customs p 3070 N95-33273
Signal processing for ION mobility spectrometers p 3073 N95-33289
Quantitative analysis of volatile organic compounds using ion mobility spectra and cascade correlation neural networks p 3073 N95-33290
Self-organizing neural network and its applications to vision-guided robot motion coordination p 3191 N95-33324
Applied Information Systems Research Program (AISRP) Workshop 3 meeting proceedings
[NASA-CR-199103] p 3239 N95-34218
Multi-layer holographic bifurcative neural network system for real-time adaptive EOS data analysis p 3148 N95-34233
DataHub sponsored analysis p 3243 N95-34242
Construction of a connectionist network supercomputer
[AD-A294198] p 3177 N95-34301
Hardware implementation of a desktop supercomputer for high performance image processing
[AD-A294272] p 3178 N95-34462
Hybrid pyramid/neural network vision system
[AD-A294919] p 3193 N95-34593

NEURONS
Toxin-mediated transfer and expression of genes in nerve cells
[AD-A290501] p 3164 N95-33200

NEUROPHYSIOLOGY
Toxin-mediated transfer and expression of genes in nerve cells
[AD-A290501] p 3164 N95-33200

NEUTRAL ATMOSPHERES
Reduction and analysis of seasons 15 and 16 (1991 - 1992) Pioneer Venus radio occulation data and correlative studies with observations of the near infrared emission of Venus
[NASA-CR-199071] p 3247 N95-32700

NEUTRAL BEAMS
Transport studies of tokamak plasmas in JT-60 device
[DE95-737227] p 3220 N95-32417
Radial electric field measurement in a tokamak by the injection of a pulsed neutral beam
[DE95-614176] p 3221 N95-32561

NEUTRAL PARTICLES
Search for N(sub (phi))(1960) baryon
[DE95-619290] p 3205 N95-32703
Study of the p + N yields (Sigma(0)K(+)) + N reaction at E(sub p) 70 GeV
[DE95-619273] p 3207 N95-33171
Tokamak ETE circuits: Analysis and specifications
[INPE-5573-PRP/182] p 3224 N95-33873
Certification of MCNP Version 4A for WHC computer platforms, revision 7
[DE95-011546] p 3178 N95-34484

NEUTRINOS
Remarks on the KARMEN anomaly
[PB95-234977] p 3209 N95-34650
International Meeting on Muon Science
[PB95-236014] p 3209 N95-34657

NEUTRON DIFFRACTION
ENGIN mini-manual. Version 1.5
[PB95-218095] p 3206 N95-32814

NEUTRON SCATTERING
Magnetic excitations in a random exchange system Fe(x)Mn(1-x)TiO3
[DE95-006626] p 3225 N95-32377
ENGIN mini-manual. Version 1.5
[PB95-218095] p 3206 N95-32814

NEUTRON SOURCES
Behavior of structural and target materials irradiated in spallation neutron environments
[DE95-010879] p 3203 N95-32576

NEUTRONS
Physics of the CEM92M Code
[DE95-623579] p 3202 N95-32477
Behavior of structural and target materials irradiated in spallation neutron environments
[DE95-010879] p 3203 N95-32576
Calculations of spatial higher modes without deflation procedure
[REPT-2205] p 3090 N95-32985
Certification of MCNP Version 4A for WHC computer platforms, revision 7
[DE95-011546] p 3178 N95-34484

NEWTON METHODS
Krylov methods for compressible flows
[NASA-CR-198176] p 3196 N95-33727

NEWTON-RAPHSON METHOD
Design and analysis of transient nonlinear coupled systems p 3199 N95-33292

NICKEL
Reactions of trifluoroiodomethane on metal surfaces
[DE95-010122] p 3078 N95-32638
Impact-parameter dependent L-K vacancy-transfer in collisions of Ni(23+) with Ge solid targets
[DE95-010821] p 3228 N95-33373

NICKEL ALLOYS
Static displacements of atoms in crystalline metallic solid solutions
[DE95-012893] p 3233 N95-34802

NICKEL ISOTOPES
Application of Ni-63 photo and corona discharge ionization for the analysis of chemical warfare agents and toxic wastes p 3070 N95-33272

NIGHT
Low-Level and Nap-of-the-Earth (NOE) night operations
[AGARD-CP-563] p 3042 N95-32486
Night attack p 3042 N95-32487
An approach to sensor data fusion for flying and landing aid purpose p 3043 N95-32488

NIGHT VISION
Night attack p 3042 N95-32487
Multispectral image correlation for air-to-ground targeting p 3043 N95-32489
Laser based obstacle warning sensors for helicopters p 3045 N95-32499
Fixed wing night attack missions: Assessment in a Flight Simulation environment p 3045 N95-32502
A helmet mounted display for night missions at low altitude p 3045 N95-32503
SIRPH: Steerable infrared picture on helmet mounted display p 3045 N95-32504
The ANVIS head-up display: An analysis of its application to naval helicopters
[AD-A294342] p 3170 N95-34358
A comparison of monocular, biocular, and binocular night vision goggles for traversing off-road terrain on foot
[AD-A294018] p 3170 N95-34376
Animation within a multimedia training system for night vision goggles
[AD-A294095] p 3170 N95-34475
Developing multimedia instructional systems: An example application for training in night vision goggles
[AD-A294521] p 3235 N95-34479

NITRATES
Nitrate stress corrosion crack growth rate in plain carbon steels
[DE95-011689] p 3079 N95-32958

NITRIDES
High rate dry etching of GaN, AlN and InN in ECR Cl2/CH4/H2/Ar plasmas
[DE95-011872] p 3223 N95-33412

NITROGEN
High resistivity InAlN by nitrogen or oxygen implantation
[DE95-011023] p 3226 N95-32594
Zeolite membranes for gas separations
[DE95-012984] p 3068 N95-33224
Stimulated rotational Raman scattering of N2 in the atmosphere
[AD-A294195] p 3157 N95-34299
Density, heat capacity, viscosity, and thermal conductivity of mixtures of CO2, He, H2, H2O, N2, and O2
[AD-A288731] p 3076 N95-34814

NITROGEN 15
N-15 hydrogen profiling of IC metallizations
[DE95-011052] p 3102 N95-32708

NOBLE METALS
Alternative catalyst and exhaust gas sensor work at Argonne National Laboratory
[DE95-007138] p 3152 N95-32553

NOISE INTENSITY
Using dark current data to estimate AVIRIS noise covariance and improve spectral analyses
p 3129 N95-33736
Speaker identification using the two-dimensional cepstrum transform
[AD-A294204] p 3099 N95-34304

NOISE POLLUTION
Pollution in Norway
[PB95-214565] p 3153 N95-33331

NOISE PREDICTION (AIRCRAFT)
Computation of noise radiation from turbofans: A parametric study
[NASA-CR-198359] p 3200 N95-32836
Fan noise prediction assessment
[NASA-CR-195051] p 3200 N95-33831

NOISE REDUCTION
Signal processing for ION mobility spectrometers
p 3073 N95-33289
Active noise control in finite length waveguides
p 3098 N95-33322

NONADIABATIC CONDITIONS
The computation of electron transfer rates: The nonadiabatic instanton solution
[AD-A294523] p 3209 N95-34350

NONAQUEOUS ELECTROLYTES
Design rules and reality check for carbon-based ultracapacitors
[DE95-010575] p 3103 N95-33640

NONDESTRUCTIVE TESTS
Angular dependence of magnetic properties of steels under uniaxial stress
[DE95-010189] p 3078 N95-32648
Photovoltaic Manufacturing Technology (PVMaT)
[DE95-004093] p 3149 N95-33153
Thermographic imaging for high-temperature composite materials: A defect detection study
[NASA-TM-106950] p 3125 N95-33209
Measurement and modelling of structure sensitive magnetic properties of material
[DE95-010128] p 3080 N95-33699
Microwave nondestructive evaluation: State-of-the-Art review
[AD-A294388] p 3125 N95-34346
Efficient pockel's modulators in optical fibers
[AD-A294009] p 3217 N95-34374

NONEQUILIBRIUM PLASMAS
On the paraxial equilibrium of the finite (beta) plasma in open magnetic configurations
[DE95-614170] p 3221 N95-32560

NONHOLONOMIC EQUATIONS
Nonholonomic control of coupled spatial multibody systems p 3192 N95-33604

NONINTRUSIVE MEASUREMENT
New advances in physiological measurements during high-G: Technology p 3165 N95-34057

NONISENTROPICITY
Stability of steady state solutions for forced Navier-Stokes equations p 3112 N95-34286

NONLINEAR EQUATIONS
The method of integration of the nonlinear Schroedinger equation with a source
[DE95-623601] p 3195 N95-32479
Operational equations for three-dimensional data
[DE95-011332] p 3198 N95-33248

NONLINEAR FEEDBACK
Nonlinear adaptive control of highly maneuverable high performance aircraft p 3192 N95-33712

NONLINEAR OPTICS
Propagation of spatial solitons generated by Gaussian beams in a non-linear Kerr medium
[IFTR-9/1995] p 3206 N95-32921
Applications of organic and polymer nonlinear optical materials in optics computations
[AD-A293088] p 3215 N95-32957
Effects of enhanced chromatic nonlinearity during the AGS gamma(t)-jump
[DE95-011703] p 3212 N95-33067
Phase control and measurement of ultrashort optical pulses
[DE95-011746] p 3216 N95-33411
Discrete modeling of optical pulse propagation in nonlinear media
[DE95-011515] p 3216 N95-34020
England develops world's fastest optic switch breakthrough in high-speed communications
[AD-A294038] p 3105 N95-34488

NONLINEAR PROGRAMMING
Some issues in nonlinear programming algorithms for problems with simulation constraints
[AD-A294932] p 3182 N95-34598
Theory and application of homotopy techniques in nonlinear programming and control systems
[AD-A294934] p 3193 N95-34600

NONLINEAR SYSTEMS
Laser gyroscopy tendencies and their analysis of development in Ukraine p 3092 N95-33133
Design and analysis of transient nonlinear coupled systems p 3199 N95-33292
Parallel solution of large-scale nonlinear optimization
[AD-A294372] p 3186 N95-34340

NONLINEARITY
Observation of intraband coherence in the nonlinear optical response of gallium arsenide
[DE95-011281] p 3227 N95-32600
Chiral restoration in hot and/or dense matter
[DE95-012176] p 3204 N95-32621
Function approximation using adaptive and overlapping intervals
[DE95-010865] p 3191 N95-33212
Globally stable feedback laws for near-minimum-fuel and near-minimum-time pointing maneuvers for a landmark-tracking spacecraft
[DE95-009867] p 3191 N95-33214
A new approach to fracture of layered fibrous composites: Experiments and analysis
p 3063 N95-33309
Nonlinear analyses of storage ring lattices using one-turn maps
[DE95-012515] p 3213 N95-33335
Studies of impurity mode and ITG mode in toroidal plasmas
[DE95-012134] p 3223 N95-33391
Multiple-beam pulse shaping and preamplification
[DE95-011738] p 3216 N95-33651
Rigid bodies for metal forming analysis with NIKE3D
[DE95-011740] p 3182 N95-33652
Evaluation of conductive, radiative, chemical, and convective heat transfer in complex systems using a fast-running, implicit, lumped-capacitance formulation
[DE95-011889] p 3111 N95-33837
Discrete modeling of optical pulse propagation in nonlinear media
[DE95-011515] p 3216 N95-34020
Efficient pockel's modulators in optical fibers
[AD-A294009] p 3217 N95-34374
Atoms in strong fields
[AD-A294589] p 3209 N95-34423
Nonlinear stability of unsteady viscous flow
[AD-A294931] p 3113 N95-34597
Extreme broadening of stimulated Raman scattered light from high intensity laser plasma interactions
[AD-A294165] p 3120 N95-34761

NONNEWTONIAN FLOW
Flow and heat transfer behavior of non-Newtonian fluids in rectangular ducts p 3107 N95-32907

NONUNIFORM FLOW
Advanced boundary element methods in aeroacoustics and elastodynamics p 3200 N95-33694

NONUNIFORMITY
Off-training-set error for the Gibbs and the Bayes optimal generalizers
[DE95-006344] p 3187 N95-32375

NORADRENALINE
Measurement and regulation of central noradrenergic receptors
[AD-A294065] p 3165 N95-34472

NOREPINEPHRINE
Measurement and regulation of central noradrenergic receptors
[AD-A294065] p 3165 N95-34472

NORMAL DENSITY FUNCTIONS
Is the genetic algorithm a cooperative learner?
[AD-A294112] p 3193 N95-34499

NORTH ATLANTIC TREATY ORGANIZATION (NATO)
AGARD index of publications: 1992-1994
[AGARD-INDEX-92-94] p 3237 N95-33198

NORWAY
Analysis of samples for the first (1994) OPCW round robin interlaboratory comparison test
[PB95-210324] p 3068 N95-33243
Pollution in Norway
[PB95-214565] p 3153 N95-33331

NOZZLE FLOW
Foam spread experiments on a water surface
[PB95-211025] p 3083 N95-32962
The development of some kinds of LRE injectors
[AD-A294199] p 3061 N95-34302

NUCLEAR DEFORMATION
A Study of the A dependence of the deep inelastic scattering of leptons and implications for understanding of the EMC effect
[DE95-613711] p 3206 N95-32796

NUCLEAR FUELS
Analysis of metallic fuels by laser ablation
[DE95-012465] p 3075 N95-34440

NUCLEAR FUSION
Development of tokamak experiment technology: A study on the nuclear fusion reactor
[DE95-614255] p 3223 N95-33619

NUCLEAR INTERACTIONS
On application of wavelet analysis to separation of secondary particles from nucleus-nucleus interactions
[DE95-623572] p 3205 N95-32630

NUCLEAR MAGNETIC RESONANCE
NQR-NMR studies of higher alcohol synthesis Cu-Co catalysts
[DE95-010524] p 3066 N95-32557
Synthesis and characterization of a series of organoindium-phosphides including molecular structures of ((Me3CCH2)2InPEt2)2 and ((Me3CCH2)2InP(H)(C6H11))3
[AD-A293965] p 3086 N95-34452

NUCLEAR PARTICLES
Proton-induced fragmentation of carbon at energies below 100 MeV p 3161 N95-32720

NUCLEAR POWER PLANTS
Energy and Technology Review
[DE95-011686] p 3223 N95-33066

NUCLEAR QUADRUPOLE RESONANCE
NQR-NMR studies of higher alcohol synthesis Cu-Co catalysts
[DE95-010524] p 3066 N95-32557

NUCLEAR RADIATION
Single event and TREE latchup mitigation for a star tracker sensor: An innovative approach to system level latchup mitigation
[DE95-010331] p 3059 N95-32593

NUCLEAR REACTIONS
Physics of the CEM92M Code
[DE95-623579] p 3202 N95-32477
N-15 hydrogen profiling of IC metallizations
[DE95-011052] p 3102 N95-32708
Technical support in the area of theoretical support of nuclear preequilibrium
[DE95-011617] p 3212 N95-32960

NUCLEAR STRUCTURE
Evaluated nuclear structure data file
[DE95-011343] p 3202 N95-32484
QCD and hadron structure
[DE95-012173] p 3209 N95-33855

NUCLEATE BOILING
Enhancement of pool boiling heat transfer to lithium bromide aqueous solution
[REPT-2211] p 3091 N95-32991

NUCLEATION
Modeling and simulation of pulsed laser annealing and ablation of solid materials
[DE95-012888] p 3119 N95-34466
Nucleation, propagation, electronic levels and elimination of misfit dislocations in 3-5 semiconductor interfaces
[DE95-011595] p 3231 N95-34485

NUCLEI (NUCLEAR PHYSICS)
Proton-induced fragmentation of carbon at energies below 100 MeV p 3161 N95-32720

NUCLEON-NUCLEON INTERACTIONS
Strangeness from hadronic processes
[DE95-010311] p 3205 N95-32651

NUCLEONS
Strangeness from hadronic processes
[DE95-010311] p 3205 N95-32651
A Study of the A dependence of the deep inelastic scattering of leptons and implications for understanding of the EMC effect
[DE95-613711] p 3206 N95-32796
Study of the p + N yields (Sigma(0)K(+)) + N reaction at E(sub p) 70 GeV
[DE95-619273] p 3207 N95-33171

NUCLIDES
Evaluated nuclear structure data file
[DE95-011343] p 3202 N95-32484

NUMERICAL ANALYSIS
A numerical analysis of fracture and high temperature creep characteristics of composites with discontinuous ductile reinforcements
[DE95-010236] p 3062 N95-32395

An original numerical method for autonomous navigation p 3044 N95-32495
Numerical analysis of the ultraprecision machining of copper
[DE95-007857] p 3089 N95-32585
Penetrable wedge analysis
[AD-A294276] p 3234 N95-34464

NUMERICAL CONTROL
Off-line programming using commerical CAD systems, and design criteria for manipulators with inherent accuracy p 3180 N95-32937
Open architecture CNC system
[DE95-009485] p 3177 N95-32955

NUMERICAL FLOW VISUALIZATION
Tracking a turbulent spot in an immersive environment
[NASA-CR-198179] p 3180 N95-32834
Large scale computing and volume visualization p 3041 N95-34556

NUSSELT NUMBER
Flow and heat transfer behavior of non-Newtonian fluids in rectangular ducts p 3107 N95-32907

NUTRIENTS
The CE-QUAL-ICM three-dimensional eutrophication model, release version 1.0
[AD-A294258] p 3160 N95-34461

O

OBJECT-ORIENTED PROGRAMMING
Proceedings of the REXX symposium for developers and users
[DE95-010668] p 3185 N95-32820
A relational metric, its application to domain analysis, and an example analysis and model of a remote sensing domain
[NASA-TM-110358] p 3198 N95-33875

OBLIQUE SHOCK WAVES
Numerical simulation of supersonic flow using a new analytical bleed boundary condition
[NASA-CR-198368] p 3054 N95-33208
Vorticity in shock-accelerated density-stratified interfaces: An analytical and computational study p 3111 N95-33607
Effect of schemes on numerical simulations of shock wave reflection p 3038 N95-34531
Numerical simulation of interaction between shock wave and density interface p 3039 N95-34543

OBSERVABILITY (SYSTEMS)
The method of model-based reasoning and application of an intelligent adaptive observer on the integrated process p 3190 N95-33005

OBSERVATION
The structure of ion track in Solids produced by ions with high level inelastic energy losses
[DE95-620942] p 3205 N95-32625

OBSTACLE AVOIDANCE
Flight test of a low-altitude helicopter guidance system with obstacle avoidance capability p 3043 N95-32490
A tactical navigation and routeing system for low-level flight p 3044 N95-32494
Development and flight testing of an Obstacle Avoidance System for US Army helicopters p 3045 N95-32500

OCCUPATION
Aerospace physiology AFSC 4M0X1
[AD-A294839] p 3165 N95-34564

OCEAN COLOR SCANNER
SeaWiFS technical report series. Volume 22: Prelaunch acceptance report for the SeaWFS radiometer
[NASA-TM-104566-VOL-22] p 3159 N95-32672
Ocean observations with EOS/MODIS: Algorithm development and post launch studies
[NASA-CR-198928] p 3143 N95-32914

OCEAN CURRENTS
Laboratory and numerical modeling of topographic effects on time-dependent ocean currents
[AD-A294920] p 3160 N95-34594

OCEAN DATA ACQUISITIONS SYSTEMS
Ice-ocean four dimensional structure and dynamics
[AD-A294017] p 3160 N95-34375

OCEAN DYNAMICS
Airborne passive polarimetric measurements of sea surface anisotropy at 92 GHz
[NASA-CR-197288] p 3143 N95-32823
Ice-ocean four dimensional structure and dynamics
[AD-A294017] p 3160 N95-34375

OCEAN MODELS
Airborne passive polarimetric measurements of sea surface anisotropy at 92 GHz
[NASA-CR-197288] p 3143 N95-32823
Proceedings of the ONR/NRL workshop on modeling the dispersion of nuclear contaminants in the arctic seas
[AD-A294373] p 3159 N95-34341

OCEAN SURFACE
Airborne passive polarimetric measurements of sea surface anisotropy at 92 GHz
[NASA-CR-197288] p 3143 N95-32823
Ocean observations with EOS/MODIS: Algorithm development and post launch studies
[NASA-CR-198928] p 3143 N95-32914
A low diffraction beam technique for scanning in the shallow ocean
[DE95-011742] p 3159 N95-33410
An experimental study of collective sea state modes of deep water surface gravity waves
[AD-A294007] p 3160 N95-34372

OCEANOGRAPHY
SeaWiFS technical report series. Volume 15: The simulated SesWiFS data set, version 2
[NASA-TM-104566-VOL-15] p 3158 N95-32545
SeaWiFS technical report series. Volume 22: Prelaunch acceptance report for the SeaWFS radiometer
[NASA-TM-104566-VOL-22] p 3159 N95-32672
SeaWiFS technical report series. Volume 31: Stray light in the SeaWiFS radiometer
[NASA-TM-104566-VOL-31] p 3159 N95-32833
A low diffraction beam technique for scanning in the shallow ocean
[DE95-011742] p 3159 N95-33410
AVIRIS user's guide p 3117 N95-33759

OCEANS
SeaWiFS technical report series. Volume 15: The simulated SesWiFS data set, version 2
[NASA-TM-104566-VOL-15] p 3158 N95-32545
SeaWiFS technical report series. Volume 31: Stray light in the SeaWiFS radiometer
[NASA-TM-104566-VOL-31] p 3159 N95-32833
DataHub sponsored analysis p 3243 N95-34242

OFFSHORE PLATFORMS
Ice-ocean four dimensional structure and dynamics
[AD-A294017] p 3160 N95-34375

OH-58 HELICOPTER
OH-58 pilot display unit (PDU) simulated crash tests
[AD-A294049] p 3170 N95-34378
Evaluation of a retrofit OH-58 pilot's seat to prevent back injury
[AD-A294895] p 3171 N95-34574

OILS
Evaluation of high-temperature lubricant under cyclic operating conditions
[AD-A294444] p 3086 N95-34494

ON-LINE SYSTEMS
Evaluated nuclear structure data file
[DE95-011343] p 3202 N95-32484
Development of a prototype lignin concentration sensor
[DE95-010951] p 3074 N95-33705
Interactive interface for National Center for Atmospheric Research (NCAR) graphics p 3239 N95-34220
A land-surface testbed for EOSDIS p 3158 N95-34223
VIEWCACHE: An incremental pointer-based access method for autonomous interoperable databases p 3242 N95-34235

ONBOARD DATA PROCESSING
Determination of the in-flight spectral calibration of AVIRIS using atmospheric absorption features p 3117 N95-33751

ONE DIMENSIONAL FLOW
Stability of steady state solutions for forced Navier-Stokes equations p 3112 N95-34286

OPERATING COSTS
The choice: Welding with CO2 or Nd:YAG lasers
[DE95-011825] p 3124 N95-33834

OPERATING SYSTEMS (COMPUTERS)
Experimenter's laboratory for visualized interactive science p 3184 N95-34228
Everyday believability
[AD-A294938] p 3193 N95-34602

OPERATING TEMPERATURE
Thin-film electrolytes for reduced temperature solid oxide fuel cells
[DE95-011273] p 3151 N95-34481

OPERATIONAL AMPLIFIERS
Operational amplifier using bipolar junction transistors in silicon-on-sapphire
[AD-D017421] p 3105 N95-34618

OPERATORS (MATHEMATICS)
Maximum principle for subsolutions of degenerate elliptic operators
[DE95-613373] p 3195 N95-32523
Counterexample to the lieb-thirring conjecture concerning the moments of the eigenvalues of the Schroedinger operator
[PB95-212197] p 3195 N95-32890
Lieb-thirring constants L(sub gamma,1) for gamma greater than or equal to 1/2
[PB95-212171] p 3196 N95-33234

OPERATORS (PERSONNEL)
Event-related potentials and electroencephalograms in adaptive operator training: Rationale and annotated bibliography
[AD-A294337] p 3166 N95-34356

OPTICAL BISTABILITY
Applications of organic and polymer nonlinear optical materials in optics computations
[AD-A293088] p 3215 N95-32957

OPTICAL COMMUNICATION
Successful development of first-generation laser device; marking China's optoelectronic technology at world class level
[AD-A294206] p 3217 N95-34305
Laser beaming demonstrations at the Starfire Optical Range
[DE95-007747] p 3120 N95-34811

OPTICAL COMPUTERS
Programmable real-time optoelectronic hybrid threshold logic processors
[AD-A294067] p 3104 N95-34379
Accuracy enhancement in optical computing
[AD-A294958] p 3219 N95-34579

OPTICAL CORRELATORS
The composite classification problem in optical information processing p 3244 N95-32430
Triple invariant optical pattern recognition using circular harmonic synthetic filters
[AD-A294253] p 3217 N95-34459

OPTICAL COUPLING
Integration of diffractive lenses with addressable vertical-cavity laser arrays
[DE95-009850] p 3118 N95-32663

OPTICAL DATA PROCESSING
The composite classification problem in optical information processing p 3244 N95-32430
Frequency response of a TeO2 slow shear wave acousto-optic cell exposed to radiation
[DE95-009588] p 3226 N95-32589
Multi-layer holographic bifurcative neural network system for real-time adaptive EOS data analysis p 3148 N95-34233
Development of an expert data reduction assistant p 3242 N95-34234
DataHub: Science data management in support of interactive exploratory analysis p 3243 N95-34241
DataHub sponsored analysis p 3243 N95-34242
Programmable real-time optoelectronic hybrid threshold logic processors
[AD-A294067] p 3104 N95-34379
Triple invariant optical pattern recognition using circular harmonic synthetic filters
[AD-A294253] p 3217 N95-34459
Accuracy enhancement in optical computing
[AD-A294958] p 3219 N95-34579
Optical logic implementation in composite biled/bild circuits
[AD-A294160] p 3105 N95-34758

OPTICAL DISKS
High performance compression of science data p 3242 N95-34237
Read/write module for high capacity memory disk
[AD-A294946] p 3178 N95-34745

OPTICAL EQUIPMENT
England develops world's fastest optic switch breakthrough in high-speed communications
[AD-A294038] p 3105 N95-34488
Study of a large optical/infrared telescope scheme
[AD-A294042] p 3218 N95-34490

OPTICAL FIBERS
A fiber-optic connector
[AD-D017424] p 3215 N95-32923
Optical pulse generation using fiber lasers and integrated optics
[DE95-011517] p 3216 N95-33506
Temporal dynamics of the multi-frequency spectrum generated by self-phase modulation of two frequencies in single-mode fiber
[DE95-010920] p 3119 N95-33703
The development of a large-area chemical sensor: A new platform for selective coatings
[DE95-011489] p 3075 N95-33832
Method for making fiber-optic bundle collimator assembly
[AD-D017486] p 3216 N95-34288
Efficient pockel's modulators in optical fibers
[AD-A294009] p 3217 N95-34374

OPTICAL FILTERS
The composite classification problem in optical information processing p 3244 N95-32430
Triple invariant optical pattern recognition using circular harmonic synthetic filters
[AD-A294253] p 3217 N95-34459

OPTICAL MATERIALS
Applications of organic and polymer nonlinear optical materials in optics computations
[AD-A293088] p 3215 N95-32957
Measurement of laser wavefront using Shack Hartmann method with new lens array
[REPT-2208] p 3090 N95-32988
Effect of propagation attenuation of thin film waveguide on optical thin film losses
[AD-A294064] p 3218 N95-34471

OPTICAL MEASUREMENT
Absolute wavefront measurements of high-energy laser beams in the Beamlet Demonstration Project for the National Ignition Facility
[DE95-012224] p 3118 N95-33378
Phase control and measurement of ultrashort optical pulses
[DE95-011746] p 3216 N95-33411
Using optical interference methods to measure acousto-optical device thermal effects
[AD-A294219] p 3217 N95-34309

OPTICAL MEASURING INSTRUMENTS
Dosimetry of heavy ions by use of CCD detectors p 3161 N95-32721
Measurement of laser wavefront using Shack Hartmann method with new lens array
[REPT-2208] p 3090 N95-32988
HeliRadar: A rotating antenna synthetic aperture radar for helicopter allweather operations p 3093 N95-33137
The development of a large-area chemical sensor: A new platform for selective coatings
[DE95-011489] p 3075 N95-33832
Acoustic-optic sound velocity profiler
[AD-D017487] p 3201 N95-34289

OPTICAL MICROSCOPES
Ultrafast near-field scanning optical microscopy (NSOM) of emerging display technology media: Solid state electronic structure and dynamics
[AD-A294879] p 3218 N95-34571

OPTICAL POLARIZATION
Terrain classification using circular polarimetric features p 3140 N95-33809

OPTICAL PROPERTIES
Prospect redux p 3133 N95-33758
Photobiology and optical properties of planktonic and sea ice microalgae in the high arctic
[AD-A294002] p 3160 N95-34457
Optical properties of lithium niobate waveguides, and prism coupling for optimizing waveguide fabrication
[AD-A294111] p 3218 N95-34498
Ion assisted deposition of ZnS and MgF2
[AD-A294759] p 3086 N95-34563
Development of 1.06 micron high efficiency antireflective coating
[AD-A294161] p 3219 N95-34759

OPTICAL RADAR
Flight test of a low-altitude helicopter guidance system with obstacle avoidance capability p 3043 N95-32490
Laser based obstacle warning sensors for helicopters p 3045 N95-32499
Development and flight testing of an Obstacle Avoidance System for US Army helicopters p 3045 N95-32500
The Anglo-French Compact Laser Radar demonstrator programme p 3045 N95-32501
Development of High Spectral Resolution Lidar (HSRL) technology
[DE95-011906] p 3099 N95-33839
The development of the automatic target recognition system for the UGV/RSTA LADAR
[AD-A294090] p 3100 N95-34474
Iron Boltzmann factor LIDAR: Proposed new remote-sensing technique for mesosphenic temperature
[AD-A293568] p 3157 N95-34613

OPTICAL REFLECTION
Damage formation in silicon irradiated by heavy ions with energy more than 1 MeV/a.m.u.
[DE95-623968] p 3204 N95-32610
Using photothermal deflection techniques for studying the attenuations of guided waves propagated in optical thin films
[AD-A294203] p 3217 N95-34303

OPTICAL SCANNERS
A preliminary evaluation of histogram-based binarization algorithms
[DE95-009886] p 3179 N95-32470
Prediction of OCR accuracy using simple image features
[DE95-009887] p 3236 N95-32471
Ultrafast near-field scanning optical microscopy (NSOM) of emerging display technology media: Solid state electronic structure and dynamics
[AD-A294879] p 3218 N95-34571

OPTICAL SWITCHING
England develops world's fastest optic switch breakthrough in high-speed communications
[AD-A294038] p 3105 N95-34488

OPTICAL THICKNESS
Ocean observations with EOS/MODIS: Algorithm development and post launch studies
[NASA-CR-198928] p 3143 N95-32914

OPTICAL TRACKING
Night attack p 3042 N95-32487

OPTICAL WAVEGUIDES
Conference proceedings of mathematical methods in electromagnetic theory
[AD-A291165] p 3097 N95-32797
Propagation of spatial solitons generated by Gaussian beams in a non-linear Kerr medium
[IFTR-9/1995] p 3206 N95-32921
A fiber-optic connector
[AD-D017424] p 3215 N95-32923
Applications of organic and polymer nonlinear optical materials in optics computations
[AD-A293088] p 3215 N95-32957
Using photothermal deflection techniques for studying the attenuations of guided waves propagated in optical thin films
[AD-A294203] p 3217 N95-34303
Effect of propagation attenuation of thin film waveguide on optical thin film losses
[AD-A294064] p 3218 N95-34471
Fabrication of optical channel waveguides in the GaAs/AlGaAs system by MeV ion beam bombardment
[DE95-008973] p 3218 N95-34480
Photonic band gap structures on polymer materials for microstructure waveguides and high-speed interconnects
[AD-A294119] p 3218 N95-34504

OPTIMAL CONTROL
A methodology for evaluating air pollution strategies to improve the air quality in Mexico City
[DE95-010874] p 3152 N95-32573
HOTQUA: An expert system prototype for quality monitoring in a rolling mill p 3190 N95-33004
The method of model-based reasoning and application of an intelligent adaptive observer on the integrated process p 3190 N95-33005
An Electronic Workshop on the Performance Seeking Control and Propulsion Controlled Aircraft Results of the F-15 Highly Integrated Digital Electronic Control Flight Research Program
[NASA-TM-104278] p 3050 N95-33009
An overview of integrated flight-propulsion controls flight research on the NASA F-15 research airplane p 3051 N95-33010
Performance seeking control program overview p 3051 N95-33011
PSC algorithm description p 3051 N95-33013
Performance seeking control excitation mode p 3052 N95-33019
Performance seeking control (PSC) for the F-15 highly integrated digital electronic control (HIDEC) aircraft p 3053 N95-33020
Motion and force control of coordinated robots
[ISBN-0-315-86323-4] p 3191 N95-33307
Analysis and finite element approximation of an optimal shape control problem for the steady-state Navier-Stokes equations p 3112 N95-34285

OPTIMIZATION
Three-dimensional aerodynamic shape optimization using discrete sensitivity analysis p 3048 N95-32904

ORBIT INSERTION
Advanced propulsion for geostationary orbit insertion and north-south station keeping
[NASA-TM-107018] p 3060 N95-32917

ORBITALS
Linear orbit parameters for the exact equations of motion
[DE95-011567] p 3210 N95-32414

ORDER-DISORDER TRANSFORMATIONS
Quantum transport
[AD-A294977] p 3235 N95-34589

ORGANIC COMPOUNDS
Solving widespread low-concentration VOC air pollution problems: Gas-phase photocatalytic oxidation answers the needs of many small businesses
[DE95-004059] p 3152 N95-32668
Environmental chamber studies of atmospheric reactivities of volatile organic compounds: Effects of varying chamber and light source
[DE95-009225] p 3152 N95-32686
Supercritical crystallization: The RESs-process and the GAS-process
[PB95-214482] p 3228 N95-33235
Quantitative analysis of volatile organic compounds using ion mobility spectra and cascade correlation neural networks p 3073 N95-33290
Zero discharge organic coatings: Powder paint - UV curable paint - E-coat
[AD-A293573] p 3087 N95-34614

ORGANIC MATERIALS
Characterization of microenvironment polarity and solvent accessibility of polysilsesquioxane xerogels by the fluorescent probe technique
[DE95-011874] p 3062 N95-33835

ORGANIC SEMICONDUCTORS
Applications of organic and polymer nonlinear optical materials in optics computations
[AD-A293088] p 3215 N95-32957

ORGANIZATIONS
Solving widespread low-concentration VOC air pollution problems: Gas-phase photocatalytic oxidation answers the needs of many small businesses
[DE95-004059] p 3152 N95-32668

ORGANOMETALLIC COMPOUNDS
Theoretical dynamical studies of metal clusters and cluster-ligand systems
[DE95-012461] p 3228 N95-33382
Fundamental surface chemistry of GaAs OMVPE
[DE95-011606] p 3231 N95-34486
Use of D2 to elucidate OMVPE growth mechanisms
[AD-A294999] p 3233 N95-34820

ORIFICE FLOW
Modeling liquid jet atomization processes
[AD-A294888] p 3112 N95-34572

ORR-SOMMERFELD EQUATIONS
On the nonlinear stability of a nearby parallel and a non-unidirectional flow p 3112 N95-34284

OSCILLATING FLOW
Numerical thermal analyses of heat exchangers for the stirling engine application
[NASA-CR-199120] p 3110 N95-33398

OSCILLATIONS
Low Reynolds number kappa-epsilon and empirical transition models for oscillatory pipe flow and heat transfer
[NASA-TM-109785] p 3110 N95-33496
Remarks on the KARMEN anomaly
[PB95-234977] p 3209 N95-34650

OSCILLATORS
Multiple-beam pulse shaping and preamplification
[DE95-011738] p 3216 N95-33651
Temporal dynamics of the multi-frequency spectrum generated by self-phase modulation of two frequencies in single-mode fiber
[DE95-010920] p 3119 N95-33703
Indium mono-ion oscillator
[AD-A293736] p 3104 N95-34451
A simulation of damping process of pendulum motion due to aerodynamic forces p 3041 N95-34551

OVARIES
Chromosomal damage observed in first postirradiation metaphases of repair-proficient and -deficient cell lines p 3162 N95-32726

OXIDATION
Solving widespread low-concentration VOC air pollution problems: Gas-phase photocatalytic oxidation answers the needs of many small businesses
[DE95-004059] p 3152 N95-32668
Thermo-chemical ablation of heat shields under Earth reentry conditions p 3059 N95-32903
The oxidation of energetic materials in supercritical water
[DE95-010888] p 3088 N95-33702
Selective methane oxidation over promoted oxide catalysts
[DE95-012319] p 3075 N95-34021
Fundamental studies of the mechanism of catalytic reactions with catalysts effective in the gasification of carbon solids and the oxidative coupling of methane
[DE95-012759] p 3075 N95-34268

OXIDATION-REDUCTION REACTIONS
Natural convection at microelectrodes
[AD-A294338] p 3075 N95-34357

OXIDE FILMS
Influence of processing variables on the structure and properties of ZnO films
[DE95-011494] p 3084 N95-33405
Novel ferroelectric heterostructures for high-density DRAMS
[AD-A294517] p 3199 N95-34477

OXIDES
High-resolution TeO2 acousto-optical deflector for millimeter-wave spectrometer
[AD-A293054] p 3215 N95-32701
Comparison of lead zirconate titanate thin films on ruthenium oxide and platinum electrodes
[DE95-617597] p 3082 N95-32710
Thin-film electrolytes for reduced temperature solid oxide fuel cells
[DE95-011273] p 3151 N95-34481

OXYGEN
High resistivity InAlN by nitrogen or oxygen implantation
[DE95-011023] p 3226 N95-32594
Proton-induced fragmentation of carbon at energies below 100 MeV p 3161 N95-32720
Unitized Regenerative Fuel Cells for solar rechargeable aircraft and zero emission vehicles
[DE95-010684] p 3150 N95-33642
Metallized gelled propellants: Oxygen/RP-1/aluminum rocket combustion experiments
[NASA-TM-107025] p 3088 N95-33876
OXYGEN ATOMS
Operation of the computer model for microenvironment atomic oxygen exposure
[NASA-CR-198190] p 3059 N95-33264
OXYGEN IONS
Electron-electron interaction in the ionization of hydrogenlike projectiles by He
[DE95-010822] p 3208 N95-33374
Fabrication of optical channel waveguides in the GaAs/AlGaAs system by MeV ion beam bombardment
[DE95-008973] p 3218 N95-34480
OXYGEN MASKS
Positive pressure breathing for G protection (PBG) p 3168 N95-34055
OXYNITRIDES
Interfacial composition analysis of silicon nitride whisker reinforced oxynitride glass systems
[DE95-012895] p 3085 N95-33635
OZONE
Environmental chamber studies of atmospheric reactivities of volatile organic compounds: Effects of varying chamber and light source
[DE95-009225] p 3152 N95-32686
Induction of dependency structures from data and its application to ozone prediction p 3190 N95-33003
Extraction of ozone and chlorophyll-A distribution from AVIRIS data p 3136 N95-33770

P

P BAND
Polarization and wavelength diversities of Gulf Stream fronts imaged by AIRSAR p 3140 N95-33807
P-TYPE SEMICONDUCTORS
Development of silicon drift detectors for strangeness measurements
[DE95-012366] p 3208 N95-33380
PACIFIC NORTHWEST (US)
AVIRIS spectral trajectories for forested areas of the Gifford Pinchot National Forest p 3135 N95-33766
PACKETS (COMMUNICATION)
Simulation of a connectionless server for b-ISDN
[PB95-215091] p 3097 N95-32892
Stochastic network processes
[AD-A294939] p 3187 N95-34603
PACKING DENSITY
Ion assisted deposition of ZnS and MgF2
[AD-A294759] p 3086 N95-34563
PAINTS
Zero discharge organic coatings: Powder paint - UV curable paint - E-coat
[AD-A293573] p 3087 N95-34614
PAIR PRODUCTION
QCD mechanisms for double quarkonium and open heavy meson hadroproduction
[DE95-012171] p 3204 N95-32619
Top quark signatures in extended color theories
[DE95-007099] p 3234 N95-33202
Nonequilibrium problems in Quantum Field Theory and Schwinger's closed time path formalism
[DE95-012056] p 3234 N95-33388
PALLADIUM
Metal-ceramic interfaces: Overlayer-induced reconstruction and magnetism of 4d transition-metal monolayers
[DE95-011543] p 3075 N95-34483
PARABOLAS
Nonlinear stability of unsteady viscous flow
[AD-A294931] p 3113 N95-34597
PARACHUTES
Energy absorption device for shock loading
[AD-D017476] p 3124 N95-34449
PARALLEL COMPUTERS
The development and application of massively parallel solid mechanics codes
[DE95-006307] p 3184 N95-32374
Proceedings: High performance functional computing
[DE95-010736] p 3186 N95-33643
Direct numerical simulation of incompressible homogeneous isotropic turbulence using NWT p 3038 N95-34530
High order accuracy computational methods in aerodynamics using parallel architectures
[AD-A294167] p 3042 N95-34763
SAR
[AD-A295020] p 3101 N95-34788
PARALLEL FLOW
On the nonlinear stability of a nearby parallel and a non-unidirectional flow p 3112 N95-34284
DSMC method applied for reacting gas flows p 3035 N95-34509
PARALLEL PROCESSING (COMPUTERS)
The development and application of massively parallel solid mechanics codes
[DE95-006307] p 3184 N95-32374
Simulation of hypervelocity impact on massively parallel supercomputer
[DE95-007735] p 3184 N95-32383
Visualization methods for high-resolution, transient, 3-D, finite element situations
[DE95-009479] p 3179 N95-32390
The future of finite element applications on massively parallel supercomputers
[DE95-011659] p 3184 N95-32415
Visualization of parallel molecular dynamics simulation on a remote visualization platform
[DE95-007806] p 3185 N95-32582
Message based event specification for debugging nondeterministic parallel programs
[DE95-006169] p 3179 N95-32669
The RDB: A parallel, spatial database for the IES/BTI system
[DE95-009425] p 3179 N95-32715
Basis Image Processor Pr5210: Correlator technical description
[PB95-222485] p 3185 N95-32815
PINCA: A scalable parallel program for compressible gas dynamics with nonequilibrium chemistry
[DE95-010581] p 3106 N95-32818
Parallel finite element methods and iterative solution techniques for viscous incompressible flows p 3108 N95-33031
Computational electromagnetics and parallel dense matrix computations
[DE95-012286] p 3099 N95-33379
Cost-effective data-parallel load balancing
[DE95-010985] p 3186 N95-33403
Proceedings: High performance functional computing
[DE95-010736] p 3186 N95-33643
Parallel molecular dynamics: Communication requirements for massively parallel machines
[DE95-012948] p 3209 N95-34212
Parallel solution of large-scale nonlinear optimization
[AD-A294372] p 3186 N95-34340
Efficient time domain solutions of Maxwell's equations for aerospace systems
[AD-A294019] p 3196 N95-34377
Recoverable distributed shared memory under sequential and relaxed consistency
[AD-A293966] p 3178 N95-34453
Conditions for implicit parallelism
[AD-A294110] p 3193 N95-34497
Highly parallel computer AP1000: Architecture and basic software p 3038 N95-34534
An unsteady simulation of a centrifugal compressor stage using the NWT p 3038 N95-34536
Parallel computation of transonic flows about an aircraft configuration using multi-block structured grids p 3039 N95-34537
Vector-parallel simulations of transonic wind tunnel flows about a fully configured model of aircraft p 3039 N95-34538
A large scale 3D Navier-Stokes analysis using NAL-NWT p 3039 N95-34539
Computations of low speed flow about space-plane p 3040 N95-34544
Parallel computation for two dimensional incompressible flow on array of transputers p 3042 N95-34558
The 11th Annual Review of Progress in Applied Computational Electromagnetics, volume 2
[AD-A294851] p 3100 N95-34567
High order accuracy computational methods in aerodynamics using parallel architectures
[AD-A294167] p 3042 N95-34763
The design of scalable software libraries for distributed memory concurrent computers
[DE95-012891] p 3244 N95-34801
PARALLEL PROGRAMMING
HINT: A new way to measure computer speed
[DE95-010245] p 3177 N95-32398
A distributed Clips implementation: dClips p 3243 N95-34243
PARAMETER IDENTIFICATION
Mathematical methods applied to biotechnical processes
[PB95-212114] p 3163 N95-33232
Identification of flexible structures under closed loop control p 3192 N95-33713
PARAMETERIZATION
Genetic algorithm based input selection for a neural network function approximator with applications to SSME health monitoring
[NASA-CR-199089] p 3188 N95-32768
PARSING ALGORITHMS
Incorporating bibliographic information into a spatial data query system for the Savannah River Site
[DE95-010965] p 3238 N95-33402
PARTIAL DIFFERENTIAL EQUATIONS
Numerical solution of differential equations by artificial neural networks p 3194 N95-32434
Turbulence and spatio-temporal chaos
[DE95-012912] p 3068 N95-33223
Bifurcation analysis of multimode instabilities in class B lasers p 3119 N95-33470
Some issues in nonlinear programming algorithms for problems with simulation constraints
[AD-A294932] p 3182 N95-34598
PARTICLE ACCELERATION
Heavy ions acceleration in RF wells of 2-frequency electromagnetic field and in the inverted FEL
[DE95-012439] p 3214 N95-34439
PARTICLE ACCELERATOR TARGETS
Impact-parameter dependent L-K vacancy-transfer in collisions of Ni(23+) with Ge solid targets
[DE95-010821] p 3228 N95-33373
PARTICLE ACCELERATORS
Coating power RF components with TiN
[DE95-010357] p 3082 N95-32541
Beam dynamics group summary
[DE95-008885] p 3213 N95-33204
An ion-ion collisions system at KSU
[DE95-010820] p 3208 N95-33372
PARTICLE BEAMS
The effect and correction of coupling generated by the RHIC triplet quadrupoles
[DE95-011562] p 3210 N95-32413
Linear orbit parameters for the exact equations of motion
[DE95-011567] p 3210 N95-32414
Analysis of radiation damages of electronic circuits by separate irradiation of their components with a collimated charged particle beam
[DE95-621946] p 3102 N95-32629
Beam dynamics group summary
[DE95-008865] p 3213 N95-33204
The beam envelope equation-systematic solution for a periodic quadrupole lattice with space charge
[DE95-012761] p 3199 N95-34269
PARTICLE COLLISIONS
Proton-induced fragmentation of carbon at energies below 100 MeV p 3161 N95-32720
Proton affinity determinations and proton-bound dimer structure indications in C2 to C15, (alpha),(omega)-alkyldiamines p 3069 N95-33266
Emittance growth due to decoherence and wakefields
[DE95-012495] p 3213 N95-33376
PARTICLE DECAY
Double-strangeness five-body system
[DE95-737277] p 3202 N95-32404
Vacuum polarization correction to the positronium decay rate
[DE95-614164] p 3202 N95-32481
Scaling law for the Upsilon(4S) yields bar-BB and psi(3770) yields bar-DD decay constants from effective sum rules
[DE95-620538] p 3203 N95-32554
Virtual effects of physics beyond the standard model
[DE95-012499] p 3207 N95-33201
Searching for new physics with charm
[DE95-012498] p 3207 N95-33245
Probing new physics in B Penguins
[DE95-012494] p 3208 N95-33375
Overview of rare K decays
[DE95-012081] p 3208 N95-33850
Remarks on the KARMEN anomaly
[PB95-234977] p 3209 N95-34650
PARTICLE DIFFUSION
Calculations of spatial higher modes without deflation procedure
[REPT-2205] p 3090 N95-32985
PARTICLE EMISSION
Light particle emission in heavy ion reactions
[DE95-010727] p 3206 N95-32965
PARTICLE INTERACTIONS
High energy collisions involving multiply charged ions
[DE95-010912] p 3206 N95-32763
Electron-electron interaction in the ionization of hydrogenlike projectiles by He
[DE95-010822] p 3208 N95-33374
Lithogenic and cosmogenic tracers in catchment hydrology
[DE95-011523] p 3143 N95-33407

PARTICLE MASS
Study of the p + N yields (Sigma(0)K(+)) + N reaction at E(sub p) 70 GeV
[DE95-619273] p 3207 N95-33171
PARTICLE PRODUCTION
Comparison of the Wang and Wachsmuth models for (pi) production with measurements at 12 GeV/c
[DE95-010417] p 3203 N95-32542
Search for N(sub (phi))(1960) baryon
[DE95-619290] p 3205 N95-32703
Four heavy quark and bound state production in the e(+)e(-) yields Q + (bar-Q' + Q' + bar-Q and e(+)e(-) yields (Q(bar-Q')) + Q' + bar-Q processes in Z(sup 0)-boson pole
[DE95-620533] p 3205 N95-32704
Hadron distributions at higher rapidity using the BRAHMS forward spectrometer
[DE95-C08861] p 3207 N95-33203
CDF results on Z(gamma) production
[DE95-011500] p 3213 N95-33406
PARTICLE SIZE DISTRIBUTION
Investigation of water droplet trajectories within the NASA icing research tunnel
[NASA-TM-107023] p 3034 N95-32769
PARTICLE SPIN
Spin counting in dipolar coupled spin 1/2 systems by multiple quantum NMR spectroscopy in solids: Development of a single quantum propagator and its application to heterogeneous catalysis
[DE95-010246] p 3066 N95-32540
Spin effects in high energy photon-hadron scattering in QCD
[DE95-623679] p 3234 N95-32961
PARTICLE THEORY
Virtual effects of physics beyond the standard model
[DE95-012499] p 3207 N95-33201
Top quark signatures in extended color theories
[DE95-007099] p 3234 N95-33202
PARTICLE TRACKS
Dosimetry of heavy ions by use of CCD detectors
p 3161 N95-32721
Estimation of spatially restricted LET using track structure models p 3161 N95-32722
Cosmic heavy ion tracks in mesoscopic biological test objects p 3163 N95-32730
Track finding and fitting in the H1 forward track detector
[PB95-234985] p 3214 N95-34651
PARTICLE TRAJECTORIES
Cosmic heavy ion tracks in mesoscopic biological test objects p 3163 N95-32730
Investigation of water droplet trajectories within the NASA icing research tunnel
[NASA-TM-107023] p 3034 N95-32769
A map for the thick beam-beam interaction
[DE95-012561] p 3213 N95-33385
PARTICULATE REINFORCED COMPOSITES
Low strain behaviour of a particulate reinforced aluminum alloy
[ISBN-0-315-84906-1] p 3078 N95-32935
PARTICULATE SAMPLING
Analysis of metallic fuels by laser ablation
[DE95-012465] p 3075 N95-34440
PARTICULATES
Fracture toughness and tensile behavior of multi-layer laminated metal composite of Al 6090-25 vol % SiCp and Al 5182
[DE95-011421] p 3062 N95-32602
Photobiology and optical properties of planktonic and sea ice microalgae in the high arctic
[AD-A294002] p 3160 N95-34457
PARTONS
The Q(2)-dependence of the Gross-Llewellyn Smith sum rule and of the parton distributions
[DE95-623678] p 3202 N95-32406
Wee partons in large nuclei: From virtual dream to hard reality
[DE95-012168] p 3208 N95-33854
PATTERN RECOGNITION
The composite classification problem in optical information processing p 3244 N95-32430
A choice of input variables for a multilayer perceptron
[DE95-623573] p 3187 N95-32476
A general solution to object matching problems by using the multiresolution approximation p 3189 N95-33002
Identification of terrain imagery with unstable reflectivity p 3093 N95-33138
Automatic script identification from images using cluster-based templates
[DE95-006339] p 3181 N95-33154
Function approximation using adaptive and overlapping intervals
[DE95-010865] p 3191 N95-33212
Triple invariant optical pattern recognition using circular harmonic synthetic filters
[AD-A294253] p 3217 N95-34459
The development of the automatic target recognition system for the UGV/RSTA LADAR
[AD-A294090] p 3100 N95-34474
Everyday believability
[AD-A294938] p 3193 N95-34602
Three-dimensional recognition via two-stage associative memory
[AD-A293567] p 3183 N95-34612
Track finding and fitting in the H1 forward track detector
[PB95-234985] p 3214 N95-34651
PATTERN REGISTRATION
Identification of terrain imagery with unstable reflectivity p 3093 N95-33138
PECLET NUMBER
Flow and heat transfer behavior of non-Newtonian fluids in rectangular ducts p 3107 N95-32907
PEEK
Low velocity impact damage in carbon fiber/PEEK composite laminates
[ISBN-0-315-86546-6] p 3085 N95-33710
PELLETS
Lightweight alumina refractory aggregate. Phase 2: Pilot scale development
[DE95-012154] p 3083 N95-33079
PENETRATION
The effects of high ambient density on diesel spray penetration and spread
[DE95-010761] p 3124 N95-33701
Estimation of penetration of forest canopies by interferometric SAR measurements
p 3141 N95-33814
PEPTIDES
High resolution electrospray mass spectrometry with a magnetic sector instrument: Accurate mass measurement and peptide sequencing
[AD-A293564] p 3076 N95-34611
PERFORMANCE PREDICTION
HYBRID2: A versatile model of the performance of hybrid power systems
[DE95-004062] p 3148 N95-32551
Characteristics of the HYDICE sensor
p 3116 N95-33733
Tri-service perspectives on microclimate cooling of protective clothing in the heat
[AD-A294005] p 3170 N95-34370
A prototype computer program that integrates predictive models and medical handbooks for altitude, cold exposure, and heat stress
[AD-A294006] p 3182 N95-34371
Locus of control and coping style as stress moderators in achievement oriented individuals
[AD-A294275] p 3166 N95-34463
PERFORMANCE TESTS
Frequency response of a TeO2 slow shear wave acousto-optic cell exposed to radiation
[DE95-009588] p 3226 N95-32589
Direct analysis of organic priority pollutants by IMS
p 3071 N95-33280
Balloon-borne radiometer profiler: Field observations
[DE95-011493] p 3158 N95-33505
Optical pulse generation using fiber lasers and integrated optics
[DE95-011517] p 3216 N95-33506
Development of a prototype lignin concentration sensor
[DE95-010951] p 3074 N95-33705
Studies of microwave scattering and canopy architecture for boreal forests
[NASA-CR-199114] p 3099 N95-33726
Quantum cylinder fiber light amplifier
[AD-A294197] p 3217 N95-34300
Ice-ocean four dimensional structure and dynamics
[AD-A294017] p 3160 N95-34375
A comparison of monocular, biocular, and binocular night vision goggles for traversing off-road terrain on foot
[AD-A294018] p 3170 N95-34376
Performance evaluation of the NWT with incompressible NS code p 3038 N95-34533
A tactical present weather sensor for Air Force applications
[AD-A294900] p 3158 N95-34575
Range graphics benchmark
[AD-A293541] p 3057 N95-34606
PERMEABILITY
Design and testing criteria for bipolar plate materials for PEM fuel cell applications
[DE95-010878] p 3148 N95-32575
PEROVSKITES
Novel ferroelectric heterostructures for high-density DRAMS
[AD-A294517] p 3199 N95-34477
PERSONAL COMPUTERS
Noninvasive determination of Cardiac Output
[PB95-208310] p 3164 N95-32611
PERSONNEL
Charm decays and high energy photoproduction
[DE95-010165] p 3201 N95-32393
Thermal rearrangement of oxygen-containing (omicron)-allyltoluene derivatives
[DE95-010124] p 3067 N95-32641
The virtual sailor: Synthetic humans for virtual environments
[AD-A293560] p 3166 N95-34610
PERSONNEL DEVELOPMENT
Aerospace physiology AFSC 4M0X1
[AD-A294839] p 3165 N95-34564
PERSONNEL MANAGEMENT
Budget estimates: Fiscal year 1994. Volume 3: Research and program management
[NASA-TM-110817] p 3245 N95-33082
NASA directives master list and index
[NHB-1410.13O] p 3238 N95-33249
PERTURBATION
Transparent potential perturbations on lattices and in the periodical structures. Elements of the Qualitative Theory of Wave Motion Over the Channels
[DE95-623602] p 3225 N95-32480
Performance seeking control excitation mode
p 3052 N95-33019
PERTURBATION THEORY
Zero modes of Gauss constraint in gaugeless reduction of Yang-Mills theory
[DE95-623676] p 3234 N95-32667
Four heavy quark and bound state production in the e(+)e(-) yields Q + (bar-Q' + Q' + bar-Q and e(+)e(-) yields (Q(bar-Q')) + Q' + bar-Q processes in Z(sup 0)-boson pole
[DE95-620533] p 3205 N95-32704
The (pi)(yields)e(nu)(gamma) decay in chiral perturbation theory
[DE95-619269] p 3206 N95-32806
PETN
Gas chromatography/ion mobility spectrometry as a hyphenated technique for improved explosives detection and analysis p 3071 N95-33278
PETROLOGY
Quantitative remote sensing of ammonium minerals, Cedar Mountains, Esmeralda County, Nevada
p 3128 N95-33734
PH
Synthesis and characterization of a series of organoindium-phosphides including molecular structures of ((Me3CCH2)2InPEt2)2 and ((Me3CCH2)2InP(H)(C6H11))3
[AD-A293965] p 3086 N95-34452
PHASE CONTROL
Phase control and measurement of ultrashort optical pulses
[DE95-011746] p 3216 N95-33411
PHASE DIAGRAMS
Phase equilibria and phase diagrams in carbide systems
[PB95-211348] p 3068 N95-33229
A quantum Monte Carlo study of the high-pressure phases of solid hydrogen p 3074 N95-33469
PHASE ERROR
The effect of phase advance errors between interaction points on beam halos
[DE95-012559] p 3214 N95-34023
PHASE SEPARATION (MATERIALS)
Dividing annular/two-phase flow in horizontal T-junctions
[ISBN-0-315-84910-X] p 3057 N95-33030
PHASE SHIFT
An experimental study of collective sea state modes of deep water surface gravity waves
[AD-A294007] p 3160 N95-34372
Vertical velocity ambiguity resolution method
[AD-D017481] p 3201 N95-34424
Monolithic diode arrays for quasioptical millimeter wave beam steering
[AD-A294256] p 3100 N95-34460
PHASE TRANSFORMATIONS
Metallurgical and Materials Transactions, volume 25A, no. 9
[AD-A293622] p 3077 N95-32474
The interrelation of a Z(3) gauge theory on flat lattices and a spin-1 BEG model
[DE95-623634] p 3227 N95-32631
Effect of phase transformations on the mechanical properties of a multiphase alloy based on NiAl+Fe
[DE95-010119] p 3079 N95-33217
Microstructural studies of hydrogen damage in metastable stainless steels p 3080 N95-33774
From liquid crystal polymers containing crown ethers to tapered building blocks containing crown ethers which self-assemble into tubular supermolecules
[AD-A294359] p 3086 N95-34361

Modeling and simulation of pulsed laser annealing and ablation of solid materials
[DE95-012888] p 3119 N95-34466

PHASE VELOCITY
Structural wave propagation and sound radiation study through time and spatial processing
p 3200 N95-33251
Experimental investigation of the separation of texture and residual stress induced anisotropy via oblique incidence acoustoelasticity p 3126 N95-33253

PHASED ARRAYS
Monolithic diode arrays for quasioptical millimeter wave beam steering
[AD-A294256] p 3100 N95-34460
Study of a large optical/infrared telescope scheme
[AD-A294042] p 3218 N95-34490

PHENOMENOLOGY
The structure of ion track in Solids produced by ions with high level inelastic energy losses
[DE95-620942] p 3205 N95-32625

PHENYLS
Elemental fluorine based syntheses of pentafluoro phenyl and other aromatic perfluoropolyether polymers
[AD-A294930] p 3087 N95-34596

PHILIPPINES
Raingauge network optimization and GIS: A case study of the Mananga basin. Communications of the Sanitary Engineering and Water Management Division
[PB95-214284] p 3157 N95-32891

PHONEMES
Training and recognition of Cantonese phonemes by backpropagation through time p 3188 N95-32996

PHOSPHATES
Measurement of gain saturation on Nd: Doped phosphate laser glasses
[REPT-2210] p 3090 N95-32990

PHOSPHAZENE
Molecular motion of phosphazene-bound NLO chromophores
[AD-A293526] p 3087 N95-34649

PHOSPHORIC ACID FUEL CELLS
Feasibility survey on international cooperation for high efficiency energy conversion technology in fiscal 1993
[DE95-769804] p 3148 N95-32546

PHOSPHORUS
Thin-film rechargeable lithium batteries
[DE95-008975] p 3103 N95-33697

PHOTOCHEMICAL OXIDANTS
Environmental chamber studies of atmospheric reactivities of volatile organic compounds: Effects of varying chamber and light source
[DE95-009225] p 3152 N95-32686

PHOTOCHEMICAL REACTIONS
Environmental chamber studies of atmospheric reactivities of volatile organic compounds: Effects of varying chamber and light source
[DE95-009225] p 3152 N95-32686
The 3rd international conference on solar energy storage and applied photochemistry
[AD-A294343] p 3150 N95-34359
The international conference on solar energy storage and applied photochemistry
[AD-A294347] p 3150 N95-34360
Surface chemistry of diamond single crystals
[AD-A294150] p 3232 N95-34755

PHOTOELECTRIC EMISSION
Photoemission study of some novel materials: Rare earth/transition metal interface, Ba*(0.6)*K*(0.4)*BiO3* and AlPdMn
[DE95-010125] p 3227 N95-32643

PHOTOIONIZATION
Development of ultrasensitive spectroscopic analysis technology. Development of atomic spectroscopy technology
[DE95-614352] p 3066 N95-32566
Determination of Benzene, Toluene, and Xylene by means of an ion mobility spectrometer device using photoionization p 3069 N95-33269
Structure and dynamics of excited atoms
[AD-A294997] p 3209 N95-34819

PHOTONS
Photon echoes from the absorption continuum of a semiconductor
[DE95-011274] p 3101 N95-32596
Status of the large-scale dark-matter axion search
[DE95-008828] p 3246 N95-32597
Spin effects in high energy photon-hadron scattering in QCD
[DE95-623679] p 3234 N95-32961
Lattice Polymer Automata
[DE95-011980] p 3062 N95-33848
Certification of MCNP Version 4A for WHC computer platforms, revision 7
[DE95-011546] p 3178 N95-34484

PHOTOPRODUCTION
Charm decays and high energy photoproduction
[DE95-010165] p 3201 N95-32393

PHOTOSYNTHESIS
Evaluation of the photochemical reflectance index in AVIRIS imagery p 3131 N95-33747
Prospect redux p 3133 N95-33758
The international conference on solar energy storage and applied photochemistry
[AD-A294347] p 3150 N95-34360

PHOTOTRANSISTORS
A reconfigurable optoelectronic interconnect technology for multi-processor networks
[DE95-011895] p 3186 N95-33838

PHOTOTROPISM
Effects of gravity and light on plant growth and performance in normal and reduced gravity
p 3163 N95-32901

PHOTOVOLTAIC CONVERSION
HYBRID2: A versatile model of the performance of hybrid power systems
[DE95-004062] p 3148 N95-32551

PHYSICAL CHEMISTRY
Analysis of samples for the first (1994) OPCW round robin interlaboratory comparison test
[PB95-210324] p 3068 N95-33243

PHYSICAL EXERCISE
Application of fuzzy technology to risk-based design and decision problems
[DE95-006815] p 3178 N95-32378
Bicycle ergometer instrumentation to determine muscle and bone forces during exercise p 3176 N95-32428
Selection and special physiological training of flying personnel to high +G(z)-maneuverable flights-main concept p 3166 N95-34053

PHYSICAL OPTICS
Photonic band gap structures on polymer materials for microstructure waveguides and high-speed interconnects
[AD-A294119] p 3218 N95-34504

PHYSICAL PROPERTIES
Sensitizing substances
[PB95-211256] p 3074 N95-33634
Growth and structure of MBE-Deposited iridium silicide
[AD-A295033] p 3232 N95-34792

PHYSIOLOGICAL EFFECTS
Negative to positive Gz acceleration transition
p 3165 N95-34052
Anti-G suits p 3168 N95-34054

PHYSIOLOGICAL RESPONSES
Methods for measuring physiological responses and protection in man exposed to high +G(z)
p 3166 N95-34058
A prototype computer program that integrates predictive models and medical handbooks for altitude, cold exposure, and heat stress
[AD-A294006] p 3182 N95-34371
Immunological protection against botulinum neurotoxin by a synthetic vaccine
[AD-A294146] p 3165 N95-34754

PHYSIOLOGICAL TESTS
Selection and special physiological training of flying personnel to high +G(z)-maneuverable flights-main concept p 3166 N95-34053
New advances in physiological measurements during high-G: Technology p 3165 N95-34057
Methods for measuring physiological responses and protection in man exposed to high +G(z)
p 3166 N95-34058
G-protection capabilities and current G-protection issues p 3169 N95-34060
Aerospace physiology AFSC 4M0X1
[AD-A294839] p 3165 N95-34564
General procedure for clothing evaluations relative to heat stress
[AD-A294953] p 3171 N95-34577

PHYSIOLOGY
Event-related potentials and electroencephalograms in adaptive operator training: Rationale and annotated bibliography
[AD-A294337] p 3166 N95-34356
General procedure for clothing evaluations relative to heat stress
[AD-A294953] p 3171 N95-34577
Geochemical, genetic, and physiological control of pollutant biodegradation
[AD-A294902] p 3155 N95-34591

PHYTOPLANKTON
DataHub sponsored analysis p 3243 N95-34242
The CE-QUAL-ICM three-dimensional eutrophication model, release version 1.0
[AD-A294258] p 3160 N95-34461

PILOT PERFORMANCE
Development and application of the methods for pilot-aircraft system research to the manual control tasks of modern vehicles p 3094 N95-33139
The effects of display location and dimensionality on taxiway navigation
[AD-A294878] p 3047 N95-34570
Human Factors Certification of Advanced Aviation Technologies
[NASA-CR-199009] p 3171 N95-34784
A rose by any other name: Certification seen as process rather than content p 3047 N95-34766
A psychologist's view of validating aviation systems
p 3172 N95-34767
Certification of tactics and strategies in aviation
p 3172 N95-34768
Advanced automated glass cockpit certification: Being wary of human factors p 3176 N95-34786
Beware of agents when flying aircraft: Basic principles behind a generic methodology for the evaluation and certification of advanced aviation systems
p 3176 N95-34787

PILOT SELECTION
Selection and special physiological training of flying personnel to high +G(z)-maneuverable flights-main concept p 3166 N95-34053
Selection and training of MiG-29 and future fighter pilots p 3166 N95-34059

PILOT TRAINING
Selection and special physiological training of flying personnel to high +G(z)-maneuverable flights-main concept p 3166 N95-34053
Selection and training of MiG-29 and future fighter pilots p 3166 N95-34059
Certification of training p 3166 N95-34774

PINHOLES
The pinhole interface for IMS/MS
p 3070 N95-33275

PINNING
The interaction of vortices with twin boundaries
[DE95-012079] p 3110 N95-33389

PIONS
Comparison of the Wang and Wachsmuth models for (pi) production with measurements at 12 GeV/c
[DE95-010417] p 3203 N95-32542
Strangeness from hadronic processes
[DE95-010311] p 3205 N95-32651
Targets and magnetic elements for pion collection in muon collider drivers
[DE95-010316] p 3205 N95-32652

PIPE FLOW
Dividing annular/two-phase flow in horizontal T-junctions
[ISBN-0-315-84910-X] p 3057 N95-33030
Low Reynolds number kappa-epsilon and empirical transition models for oscillatory pipe flow and heat transfer
[NASA-TM-109785] p 3110 N95-33496

PIPELINES
Design of deepwater pipelines
[PB95-215109] p 3095 N95-33244

PIPES (TUBES)
The effect of buoyancy on flow and heat transfer in curved pipes p 3037 N95-34528
Flow and heat transfer in rotating curved pipes
p 3040 N95-34545

PITCHING MOMENTS
SOFIA 2 model telescope wind tunnel test report
[NASA-TM-110668] p 3033 N95-32764

PIXELS
Sub-pixel localization of highways in AVIRIS images
p 3135 N95-33767
Validating spatial structure in canopy water content using geostatistics p 3135 N95-33768
Extraction of ozone and chlorophyll-A distribution from AVIRIS data p 3136 N95-33770

PLANE WAVES
Application of grating polarizer to 106.4GHz ECH system on Heliotron-E
[NIFS-334] p 3225 N95-34824

PLANETARY ATMOSPHERES
Nonlinear symmetric stability of planetary atmospheres
[DE95-012133] p 3248 N95-33390
Construction of an advanced software tool for planetary atmospheric modeling p 3184 N95-34225
Planetary data analysis and display system: A version of PC-McIDAS p 3241 N95-34232

PLANETARY MAPPING
Topography from shading and stereo
p 3241 N95-34229

PLANETARY NEBULAE
The mini-CIDEX GC/IMS: Analysis of cometary ice and dust p 3069 N95-33270

PLANKTON
Photobiology and optical properties of planktonic and sea ice microalgae in the high arctic
[AD-A294002] p 3160 N95-34457

PLASMA CHEMISTRY
High rate dry etching of GaN, AlN and InN in ECR Cl2/CH4/H2/Ar plasmas
|DE95-011872| p 3223 N95-33412
PLASMA COMPOSITION
Study of impurity concentrations by VUV spectroscopy on HL-1
|DE95-614186| p 3221 N95-32562
PLASMA CONTROL
Experimental study of the processes in the expander of the axisymmetric mirror device
|DE95-009846| p 3221 N95-32536
On the paraxial equilibrium of the finite (beta) plasma in open magnetic configurations
|DE95-614170| p 3221 N95-32560
Optimized profiles for improved confinement and stability in the DIII-D tokamak
|DE95-009606| p 3222 N95-32756
Development of tokamak experiment technology: A study on the nuclear fusion reactor
|DE95-614255| p 3223 N95-33619
PLASMA DENSITY
Conversion of the Bernstein-Green-Kruskal wave on the density perturbation, part 1
|DE95-614203| p 3220 N95-32508
Conversion of the Bernstein-Green-Kruskal wave on the density perturbation, part 3
|DE95-614205| p 3221 N95-32509
Conversion of the Bernstein-Green-Kruskal wave on the density perturbation, part 4
|DE95-614206| p 3221 N95-32510
Recent results from the D3-D tokamak and implications for future devices
|DE95-009605| p 3222 N95-32592
PLASMA DIAGNOSTICS
Radial electric field measurement in a tokamak by the injection of a pulsed neutral beam
|DE95-614176| p 3221 N95-32561
Energy and Technology Review
|DE95-011686| p 3223 N95-33066
Laser ablation plume thermalization dynamics in background gases studied by time-resolved imaging, spectroscopic, and ion probe diagnostics
|DE95-010277| p 3118 N95-33246
The development of a distributed computing environment for the design and modeling of plasma spectroscopy experiments
|DE95-011725| p 3183 N95-34813
PLASMA DRIFT
Optimized profiles for improved confinement and stability in the DIII-D tokamak
|DE95-009606| p 3222 N95-32756
Mid-latitude ionospheric plasma drift: A comparison of digital ionosonde and incoherent scatter radar measurements at Millstone Hill p 3222 N95-32838
PLASMA DYNAMICS
Analysis of evaporation in laser welding
|REPT-2207| p 3090 N95-32987
PLASMA EQUILIBRIUM
High beta and second stability region transport and stability analysis
|DE95-011298| p 3225 N95-34812
PLASMA FREQUENCIES
Mathematical modelling in plasma physics
|AD-A294972| p 3224 N95-34586
PLASMA HEATING
Transport studies of tokamak plasmas in JT-60 device
|DE95-737227| p 3220 N95-32417
Predicted operating conditions for maintaining mode purity in the 1MW 200 GHz FOM Free Electron Maser
|DE95-010795| p 3117 N95-32571
Application of grating polarizer to 106.4GHz ECH system on Heliotron-E
|NIFS-334| p 3225 N95-34624
PLASMA OSCILLATIONS
HF-stabilization of plasma with sharp boundary
|DE95-614207| p 3222 N95-32770
PLASMA PHYSICS
Tokamak ETE circuits: Analysis and specifications
|INPE-5573-PRP/182| p 3224 N95-33873
Mathematical modelling in plasma physics
|AD-A294972| p 3224 N95-34586
PLASMA PRESSURE
Recent results from the D3-D tokamak and implications for future devices
|DE95-009605| p 3222 N95-32592
PLASMA RADIATION
Tokamak ETE circuits: Analysis and specifications
|INPE-5573-PRP/182| p 3224 N95-33873
PLASMA SHEATHS
Unified model of the RF plasma sheath
|DE95-012114| p 3224 N95-33851
PLASMA WAVES
Bernstein-Green-Kruskal wave. 2: The interaction with the Langmuir wave. Stochastic phenomena
|DE95-614202| p 3220 N95-32507
Conversion of the Bernstein-Green-Kruskal wave on the density perturbation, part 1
|DE95-614203| p 3220 N95-32508
Conversion of the Bernstein-Green-Kruskal wave on the density perturbation, part 3
|DE95-614205| p 3221 N95-32509
Conversion of the Bernstein-Green-Kruskal wave on the density perturbation, part 4
|DE95-614206| p 3221 N95-32510
HF-stabilization of plasma with sharp boundary
|DE95-614207| p 3222 N95-32770
High efficiency vacuum and plasma filled backward wave oscillators: A critical evaluation
|AD-A294963| p 3105 N95-34581
PLASMAS (PHYSICS)
COBRA accelerator for Sandia ICF diode research at Cornell University
|DE95-011018| p 3101 N95-32578
Fusion Safety Program annual report, fiscal year 1994
|DE95-008872| p 3221 N95-32588
Recent results from the D3-D tokamak and implications for future devices
|DE95-009605| p 3222 N95-32592
TRAP: Tokamak Refueling by Accelerated Plasmoids
|DE95-009925| p 3223 N95-33216
The effect of collisionality and diamagnetism on the plasma dynamo
|DE95-012409| p 3223 N95-33221
Laser ablation plume thermalization dynamics in background gases studied by time-resolved imaging, spectroscopic, and ion probe diagnostics
|DE95-010277| p 3118 N95-33246
Plasma mediated ablation of biological tissues with ultrashort laser pulses
|DE95-011748| p 3164 N95-33654
More on core-localized toroidal Alfven eigenmodes
|DE95-010857| p 3224 N95-33696
Single Langmuir probe characteristic in a magnetized plasma at the TEXT tokamak
|DE95-012144| p 3224 N95-33853
Extreme broadening of stimulated Raman scattered light from high intensity laser plasma interactions
|AD-A294165| p 3120 N95-34761
The development of a distributed computing environment for the design and modeling of plasma spectroscopy experiments
|DE95-011725| p 3183 N95-34813
PLASMONS
A background subtraction routine for enhancing energy-filtered plasmon images of MgAl2O4 implanted with Al(+) and Mg(+) ions
|DE95-012850| p 3074 N95-33629
PLASTIC COATINGS
Encapsulated dry electrolyte composition for time release into a solute
|AD-D017485| p 3075 N95-34287
PLASTIC DEFORMATION
Low strain behaviour of a particulate reinforced aluminum alloy
|ISBN-0-315-84906-1| p 3078 N95-32935
PLASTIC PROPERTIES
Inelastic response spectra of a system with bilinear restoring characteristics: Effect of plastic-stiffness ratio
|REPT-2213| p 3091 N95-32993
Development of local shear bands and orientation gradients in fcc polycrystals
|DE95-012072| p 3231 N95-34450
PLASTICS
Measurement of laser wavefront using Shack Hartmann method with new lens array
|REPT-2208| p 3090 N95-32988
PLATES (STRUCTURAL MEMBERS)
Corrosion of separator plate constituents in molten carbonate
|PB95-214490| p 3149 N95-32813
PLATINUM
Comparison of lead zirconate titanate thin films on ruthenium oxide and platinum electrodes
|DE95-617597| p 3082 N95-32710
PLATINUM COMPOUNDS
Magnetostriction and thermal expansion of the Kondo semiconductor Ce3Bi4Pt3
|DE95-011975| p 3229 N95-33386
PLUMES
Detection of emission sources using passive-remote Fourier Transform Infrared spectroscopy
|DE95-009920| p 3067 N95-32671
Laser ablation plume thermalization dynamics in background gases studied by time-resolved imaging, spectroscopic, and ion probe diagnostics
|DE95-010277| p 3118 N95-33246
Cooling tower and plume modeling for satellite remote sensing applications
|DE95-012000| p 3143 N95-33849
PLUNGERS
Device for dampening vibratory motion
|AD-D017490| p 3127 N95-34427
PLUTONIUM ISOTOPES
A novel approach to the problem of highly-sensitive regular analysis for man-made plutonium in environment and human body
|DE95-620764| p 3164 N95-32666
PLUTONIUM 239
A novel approach to the problem of highly-sensitive regular analysis for man-made plutonium in environment and human body
|DE95-620764| p 3164 N95-32666
PLY ORIENTATION
Micromechanics of fiber-reinforced ceramic composites p 3063 N95-32775
POINT DEFECTS
Smoothing during ion-assisted growth by transient ion beam-induced defects
|DE95-011021| p 3225 N95-32579
Peak effect and flux pinning in YBa2Cu3O(7-(delta)) single crystals
|DE95-010126| p 3228 N95-32959
POINT SOURCES
Time correlations between low and high energy gamma rays from discrete sources
|NASA-CR-199214| p 3248 N95-33916
POISSON EQUATION
Unified model of the RF plasma sheath
|DE95-012114| p 3224 N95-33851
Upwind schemes for the two-dimensional Euler equations p 3042 N95-34559
POISSON RATIO
Poisson's ratio for tetragonal crystals
|AD-A293544| p 3232 N95-34607
Poisson's ratio for cubic crystals
|AD-A293549| p 3232 N95-34608
POLARIMETRY
Airborne passive polarimetric measurements of sea surface anisotropy at 92 GHz
|NASA-CR-197288| p 3143 N95-32823
Polarization and wavelength diversities of Gulf Stream fronts imaged by AIRSAR p 3140 N95-33807
Terrain classification using circular polarimetric features p 3140 N95-33809
Use of AIRSAR to identify woody shrub invasion and other indicators of desertification in the Jornada LTER p 3141 N95-33810
POLARITY
Solvent effects on the electronic spectrum of R hardt's dye
|AD-A293667| p 3067 N95-32804
Characterization of microenvironment polarity and solvent accessibility of polysilsesquioxane xerogels by the fluorescent probe technique
|DE95-011874| p 3062 N95-33835
POLARIZATION (SPIN ALIGNMENT)
Vacuum polarization correction to the positronium decay rate
|DE95-614164| p 3202 N95-32481
POLARIZATION (WAVES)
Application of grating polarizer to 106.4GHz ECH system on Heliotron-E
|NIFS-334| p 3225 N95-34624
POLARIZATION CHARACTERISTICS
Isgur-Wise function and polarization characteristics of Lambda(sub b)-baryon
|DE95-623696| p 3202 N95-32407
POLARIZED LIGHT
Method and apparatus for locking laser wavelength to an atomic transition
|AD-D017425| p 3120 N95-34619
POLARIZED RADIATION
Radiative interactions with micromachined surfaces: Spectral polarized emittance
|DE95-011455| p 3097 N95-33061
POLARIZERS
Application of grating polarizer to 106.4GHz ECH system on Heliotron-E
|NIFS-334| p 3225 N95-34624
POLLUTION CONTROL
An electronic design guideline for incorporating pollution prevention into US Department of Energy design projects
|DE95-008935| p 3151 N95-32475
A methodology for evaluating air pollution strategies to improve the air quality in Mexico City
|DE95-010874| p 3152 N95-32573
Chemical substances lists: A guide to the lists used in the Swedish Sunset Project. Supplement to report 13/94. Selecting multiproblem chemicals for risk reduction. A presentation of the Swedish Sunset Project
|PB95-211272| p 3073 N95-33328

Phthalic acid esters used as plastic additives. Volume 1: Ecotoxicological risk assessment. Volume 2: Comparisons of toxicological effects
| PB95-211280 | p 3084 N95-33329

Pollution in Norway
| PB95-214565 | p 3153 N95-33331

Introductions of FFV
| PB95-214656 | p 3088 N95-33332

POLLUTION MONITORING

Winter season air pollution in El Paso-Ciudad Juarez. A review of air pollution studies in an international airshed
| DE95-009083 | p 3152 N95-32556

Detection of emission sources using passive-remote Fourier Transform Infrared spectroscopy
| DE95-009920 | p 3067 N95-32671

Field Raman spectrograph for environmental analysis
| DE95-007969 | p 3153 N95-32816

An ammonia monitor for the water industry
p 3071 N95-33281

ABCASH plotting program users guide
| DE95-011652 | p 3155 N95-34435

POLLUTION TRANSPORT

Multimedia Environmental Pollutant Assessment System (MEPAS(trademark)): Exposure pathway and human health impact assessment models
| DE95-012763 | p 3155 N95-34441

POLYCHLORINATED BIPHENYLS

Environment applications for ion mobility spectrometry
p 3071 N95-33279

POLYCRYSTALS

Device physics of thin-film polycrystalline cells and modules
| DE95-009209 | p 3149 N95-32817

Effect of the colony microstructure on transport critical current of high-J(c) Tl-1223 thick films
| DE95-013049 | p 3230 N95-34213

Development of local shear bands and orientation gradients in fcc polycrystals
| DE95-012072 | p 3231 N95-34450

POLYCYCLIC AROMATIC HYDROCARBONS

Geochemical, genetic, and physiological control of pollutant biodegradation
| AD-A294902 | p 3155 N95-34591

POLYESTER RESINS

Adhesion of novel high-performance polymers to carbon fibers: Fiber surface treatment, characterization, and microbond single fiber pull-out test p 3085 N95-34282

POLYESTERS

Polymerization of epsilon-caprolactone in the presence of Oh- or COOh-groups containing initiators. Copolymers of lactide with epsilon-caprolactone: Synthesis, characterization and processing
| PB95-208211 | p 3084 N95-33227

POLYETHYLENES

DMTA studies of branching distribution in polyethylene
| PB95-208237 | p 3084 N95-33228

POLYGONS

Differencing the diffusion equation on unstructured meshes in 2-D
| DE95-010410 | p 3195 N95-32559

POLYIMIDES

Performance of partially fluorinated polyimide insulation for aerospace applications
| NASA-CR-198372 | p 3060 N95-32673

POLYMERIC FILMS

The effects of ion implantation on the tribology of perfluoropolyether-lubricated 440C stainless steel couples
| NASA-TM-106965 | p 3083 N95-32918

Spontaneous dewetting of a perfluoropolyether
| NASA-TM-106964 | p 3083 N95-32919

CRADA with United Solar Technologies and Pacific Northwest Laboratory (PNL-021): Thin film materialsfor low-cost high performance solar concentrators
| DE95-010423 | p 3150 N95-33400

Encapsulated dry electrolyte composition for time release into a solute
| AD-D017485 | p 3075 N95-34287

POLYMERIZATION

Spin counting in dipolar coupled spin 1/2 systems by multiple quantum NMR spectroscopy in solids: Development of a single quantum propagator and its application to heterogeneous catalysis
| DE95-010246 | p 3066 N95-32540

Molecular engineering of liquid crystalline polymers by Living polymerization 30. Synthesis and Living cationic polymerization of (2R, 3S)-2-Fluoro-3-methylpentyl 4'-(8-Vinyloxyoctyloxy) Biphenyl-4-carboxylate and its copolymerization with (2R, 3S)-2-Fluoro-3-methylpentyl 4'-(11 Vinyloxyundecanyloxyloxy) biphenyl-4-carboxylate --- carboxylate and its copolymerization with (2R, 3S)-2-Fluoro-3-methylpentyl 4-(11-Vinyloxyundecanyloxy) biphenyi-4-Carboxylate
| AD-A293115 | p 3082 N95-32552

Polymerization of epsilon-caprolactone in the presence of Oh- or COOh-groups containing initiators. Copolymers of lactide with epsilon-caprolactone: Synthesis, characterization and processing
| PB95-208211 | p 3084 N95-33227

POLYMERS

From liquid crystal polymers containing crown ethers to tapered building blocks containing crown ethers which self-assemble into tubular supermolecules
| AD-A294359 | p 3086 N95-34361

Molecular motion of phosphazene-bound NLO chromophores
| AD-A293526 | p 3087 N95-34649

Industrial products based upon processible conductive polyaniline
| AD-A294985 | p 3087 N95-34817

POLYNOMIALS

Tracing a planar algebraic curve
| DE95-613375 | p 3195 N95-33058

Operational equations for three-dimensional data
| DE95-011332 | p 3196 N95-33248

An object-oriented decomposition of the adaptive-hp finite element method
| DE95-012142 | p 3186 N95-33852

POLYPHENYLS

Environment applications for ion mobility spectrometry
p 3071 N95-33279

POLYTROPIC PROCESSES

Sinuous oscillations and steady warps of polytropic disks
| DE95-013473 | p 3247 N95-34216

POLYURETHANE FOAM

A fundamental study of smoldering with emphasis on experimental design for zero-G
| NASA-CR-198378 | p 3089 N95-32929

PONDS

Mineralogic variations in fluvial sediments contaminated by mine tailings as determined from AVIRIS data, Coeur D'Alene River Valley, Idaho p 3131 N95-33745

PONTRYAGIN PRINCIPLE

Trajectory planning and control of kinematically redundant robotic manipulators p 3194 N95-34807

POPULATIONS

Heavy ion action on single cells: Cellular inactivation capability of single accelerated heavy ions
p 3162 N95-32729

Remotely sensed indicators of habitat heterogeneity and biological diversity: A preliminary report
p 3140 N95-33806

POROSITY

Size, shape, and crystallinity of luminescent structures in oxidized Si nanoclusters and H-passivated porous Si
| DE95-012322 | p 3229 N95-33628

Design rules and reality check for carbon-based ultracapacitors
| DE95-010575 | p 3103 N95-33640

POROUS MATERIALS

Investigation on deflagration to detonation transition in porous energetic materials
| DE95-011638 | p 3088 N95-32605

Characterization of microenvironment polarity and solvent accessibility of polysilsesquioxane xerogels by the fluorescent probe technique
| DE95-011874 | p 3062 N95-33835

PORTABLE EQUIPMENT

Functional requirements analysis and human machine interface specifications for handheld metal detector wands
| DE95-009845 | p 3167 N95-32535

Engineering approaches and compromises in the design of small ion mobility spectrometers
p 3070 N95-33271

Hand-portable gas chromatography-ion mobility spectrometer for the determination of the freshness of fish p 3071 N95-33277

A tactical present weather sensor for Air Force applications
| AD-A294900 | p 3158 N95-34575

POSITION (LOCATION)

HYBRID2: A versatile model of the performance of hybrid power systems
| DE95-004062 | p 3148 N95-32551

Recent results from the D3-D tokamak and implications for future devices
| DE95-009605 | p 3222 N95-32592

Printability of substrate and absorber defects on extreme ultraviolet lithographic masks
| DE95-010916 | p 3084 N95-33247

Sub-pixel localization of highways in AVIRIS images
p 3135 N95-33767

POSITION SENSING

Design and implementation of a two-axis micromanipulator to enhance the gripper positional accuracy of a single flexible link p 3123 N95-33252

POSITRON ANNIHILATION

Scaling law for the Upsilon(4S) yields bar-BB and psi(3770) yields bar-DD decay constants from effective sum rules
| DE95-620538 | p 3203 N95-32554

Four heavy quark and bound state production in the e(+)e(-) yields Q + (bar-Q' + Q' + bar-Q and e(+)e(-) yields (Q(bar-Q')) + Q' + bar-Q processes in Z(sup 0)-boson pole
| DE95-620533 | p 3205 N95-32704

POSITRONIUM

Vacuum polarization correction to the positronium decay rate
| DE95-614164 | p 3202 N95-32481

Progress towards antihydrogen production by the reaction of cold antiprotons with positronium atoms
| DE95-007850 | p 3204 N95-32584

POSTFLIGHT ANALYSIS

FORTRAN program for analyzing ground-based radar data: Usage and derivations, version 6.2
| NASA-TP-3430 | p 3181 N95-33193

POTASSIUM CHLORIDES

High power CO2 laser windows and reflection reducing coatings
| AD-A294217 | p 3119 N95-34308

POTENTIAL ENERGY

Active noise control in finite length waveguides
p 3098 N95-33322

POWER AMPLIFIERS

Multiple-beam pulse shaping and preamplification
| DE95-011738 | p 3216 N95-33651

POWER BEAMING

Laser beaming demonstrations at the Starfire Optical Range
| DE95-007747 | p 3120 N95-34811

POWER CONVERTERS

Integral cesium reservoir: Design and transient operation
| DE95-010152 | p 3211 N95-32647

POWER LINES

The RHIC transfer line cable database
| DE95-011560 | p 3236 N95-32412

POWER TRANSMISSION

Fluid dynamometer having fluid characteristic power absorption adjustment capability
| AD-D017489 | p 3116 N95-34426

POWERED MODELS

An LDV investigation of support structure influence on the flow field near the wingtip of a STOVL configuration in hover
| AD-A294126 | p 3042 N95-34750

PREAMPLIFIERS

Channel equalized DC squid flux-locked loop
| AD-D017469 | p 3104 N95-34446

PRECAMBRIAN PERIOD

Discrimination of alkalinity in granitoid Rocks: A potential TIMS application p 3138 N95-33798

PRECIPITATION (METEOROLOGY)

OPEX Second Workshop of the OLYMPUS Propagation Experimenters. Volume 4: Reference book on radar
| ESA-WPP-083-VOL-4 | p 3096 N95-32750

A tactical present weather sensor for Air Force applications
| AD-A294900 | p 3158 N95-34575

PRECIPITATION PARTICLE MEASUREMENT

A tactical present weather sensor for Air Force applications
| AD-A294900 | p 3158 N95-34575

PRECISION

Advanced precision expendable pattern casting technology
| DE95-012200 | p 3095 N95-33393

Optical properties of lithium niobate waveguides, and prism coupling for optimizing waveguide fabrication
| AD-A294111 | p 3218 N95-34498

PREDICTION ANALYSIS TECHNIQUES

A note on separation prediction of two-dimensional turbulent boundary layer
| REPT-2216 | p 3091 N95-32994

PREDICTIONS

The role of dynamic experimentation for computation analysis
| DE95-007733 | p 3125 N95-32381

Environmental chamber studies of atmospheric reactivities of volatile organic compounds: Effects of varying chamber and light source
| DE95-009225 | p 3152 N95-32686

PREMIXED FLAMES

Combustion-acoustic stability analysis for premixed gas turbine combustors
| NASA-TM-107024 | p 3050 N95-32931

PRESERVING

The preservation of human surrogates for biomechanical studies p 3167 N95-33312

PRESSES
Fracture toughness and tensile behavior of multi-layer laminated metal composite of Al 6090-25 vol % SiCp and Al 5182
[DE95-011421] p 3062 N95-32602
PRESSURE BREATHING
Positive pressure breathing for G protection (PBG) p 3168 N95-34055
PRESSURE DEPENDENCE
Charge-transfer gap closure in transition-metal halides under pressure
[DE95-011258] p 3230 N95-33865
PRESSURE DROP
Static pressure drop by swirling flow of an internal cooling air system through a turbine shaft p 3042 N95-34560
PRESSURE EFFECTS
Fundamental studies of gas phase ionic reactions by ion mobility spectrometry p 3069 N95-33268
Response and failure of thick composite rings subjected to uniform external hydrostatic pressure or radial contraction p 3064 N95-33326
PRESSURE GRADIENTS
Subscale study of engine bellmouth inlet vortices in test cell R1D
[AD-A294993] p 3113 N95-34818
PRESSURE MEASUREMENT
New advances in physiological measurements during high-G: Technology p 3165 N95-34057
Subscale study of engine bellmouth inlet vortices in test cell R1D
[AD-A294993] p 3113 N95-34818
PRESSURE OSCILLATIONS
Sinuous oscillations and steady warps of polytropic disks
[DE95-013473] p 3247 N95-34216
PRESSURE PULSES
Bolt preload selection for pulsed-loaded vessel closures
[DE95-006346] p 3121 N95-32376
Pop tests of storable biopropellant liquid apogee engine
[NAL-TR-1253] p 3060 N95-32755
PRESSURE SUITS
Anti-G suits p 3168 N95-34054
PRESSURE VESSELS
Irradiation experiments of low copper A533B steels for reactor pressure vessel tested in JMTR
[DE95-737266] p 3077 N95-32531
Fracture toughness assesament of present and future pressure vessel materials based on Charpy impact energy and yield strength
[AD-A294006] p 3081 N95-34373
Patterns and perspectives in applied fracture mechanics
[DE95-012844] p 3127 N95-34442
PRESSURIZING
Anti-G suits p 3168 N95-34054
PRESTRESSING
Bolt preload selection for pulsed-loaded vessel closures
[DE95-006346] p 3121 N95-32376
PRETREATMENT
Influence of CO2 continuous laser preprocessed substrates on optical thin film damage thresholds
[AD-A294190] p 3217 N95-34297
PRIMATES
Ultrashort pulse laser effects in the primate eye
[AD-A295024] p 3164 N95-34789
PRINTED CIRCUITS
Characterization of DuPont 9015, aqueous processable dry film photoresist for printed wiring boards
[DE95-011239] p 3103 N95-33864
PRINTING
NASA wide electronic publishing system: Electronic printing and duplicating. Stage 3 evaluation report
[NASA-TM-104620] p 3237 N95-32922
PRIORITIES
Direct analysis of organic priority pollutants by IMS p 3071 N95-33280
PRISMS
Operational equations for three-dimensional data
[DE95-011332] p 3196 N95-33248
Optical properties of lithium niobate waveguides, and prism coupling for optimizing waveguide fabrication
[AD-A294111] p 3218 N95-34498
PROBABILITY DISTRIBUTION FUNCTIONS
Genetic algorithms as global random search methods
[NASA-CR-199088] p 3188 N95-32767
PROBABILITY THEORY
Off-training-set error for the Gibbs and the Bayes optimal generalizers
[DE95-006344] p 3187 N95-32375
Angular dependance of magnetic properties of steels under uniaxial stress
[DE95-010189] p 3078 N95-32648
Intra-annual and inter-annual rainfall variability over East Asia, Southeast Asia, and South Asia
[AD-A294156] p 3158 N95-34757
PROBLEM SOLVING
Solving stiff chemistry problems with FIDAP
[DE95-011053] p 3067 N95-32709
Incorporating distributed problem solving technique into a case-based system p 3188 N95-32997
Multivariate statistical analysis software technologies for astrophysical research involving large data bases p 3240 N95-34222
Improving the comprehensibility, accuracy, and generality of reactive plans
[AD-A294104] p 3193 N95-34495
Conditions for implicit parallelism
[AD-A294110] p 3193 N95-34497
Explanations of empirically derived reactive plans
[AD-A294114] p 3193 N95-34501
Optimization problems in multitarget/multisensor tracking
[AD-A294978] p 3100 N95-34590
Hybrid pyramid/neural network vision system
[AD-A294919] p 3193 N95-34593
Spectrum allocation strategies for communication networks
[AD-A294936] p 3100 N95-34601
PROCEDURES
Glass science tutorial: Lecture no. 4, commercial glass melting and associated air emission issues
[DE95-007818] p 3082 N95-32384
NASA/DOD Aerospace Knowledge Diffusion Research Project. Report 33: The technical communications practices of US aerospace engineers and scientists: Results of the phase 1 AIAA mail survey
[NASA-TM-110180] p 3239 N95-34217
PROCESS CONTROL (INDUSTRY)
Monitoring of the cutting operations using fuzzy logic p 3189 N95-32999
HOTQUA: An expert system prototype for quality monitoring in a rolling mill p 3190 N95-33004
The method of model-based reasoning and application of an intelligent adaptive observer on the integrated process p 3190 N95-33005
High-tech controls for energy and environment
[DE95-004011] p 3191 N95-33060
PROCUREMENT MANAGEMENT
Report to the Honorable William V. Roth, Jr., US Senate. Naval aviation: F/A-18 E/F acquisition strategy
[GAO/NSIAD-94-194] p 3197 N95-32886
Annual report to the Chairman, House and Senate Committees on Appropriations. Status of open recommendations: Improving operations of federal departments and agencies
[GAO/OP-94-1] p 3236 N95-32887
NASA directives master list and index
[NHB-1410.13O] p 3238 N95-33249
PRODUCT DEVELOPMENT
Development and flight testing of an Obstacle Avoidance System for US Army helicopters p 3045 N95-32500
PRODUCTION
Lightweight alumina refractory aggregate. Phase 2: Pilot scale development
[DE95-012154] p 3083 N95-33079
PRODUCTIVITY
DataHub sponsored analysis p 3243 N95-34242
PROGENY
Conditions for implicit parallelism
[AD-A294110] p 3193 N95-34497
PROGRAM VERIFICATION (COMPUTERS)
Message based event specification for debugging nondeterministic parallel programs
[DE95-006169] p 3179 N95-32669
Land surface temperature measurements from EOS MODIS data
[NASA-CR-199082] p 3142 N95-32717
A declarative debugger for a logical-functional language p 3183 N95-33007
Formal verification of an avionics microprocessor
[NASA-CR-4682] p 3181 N95-33396
Verification of turbine cascade flow with tip clearance p 3035 N95-34511
PROGRAMMING ENVIRONMENTS
Off-line programming using commerical CAD systems, and design criteria for manipulators with inherent accuracy p 3180 N95-32937
A distributed Clips implementation: dClips p 3243 N95-34243
Program developing environment and a CFD application on the Cray T3D p 3038 N95-34535
PROGRAMMING LANGUAGES
Proceedings: High performance functional computing
[DE95-010736] p 3186 N95-33643
PROJECT MANAGEMENT
Space Station: Estimated total US funding requirements. Report to Congressional Requesters
[GAO/NSIAD-95-163] p 3058 N95-32884
Budget estimates: Fiscal year 1994. Volume 3: Research and program management
[NASA-TM-110817] p 3245 N95-33082
NASA directives master list and index
[NHB-1410.13O] p 3238 N95-33249
Issues in NASA program and project management
[NASA-SP-6101(09)] p 3236 N95-34354
PROJECTILES
Intrinsic charm contribution to double quarkonium hadroproduction
[DE95-012170] p 3204 N95-32617
QCD mechanisms for double quarkonium and open heavy meson hadroproduction
[DE95-012171] p 3204 N95-32619
Electron-electron interaction in the ionization of hydrogenlike projectiles by He
[DE95-010822] p 3208 N95-33374
PROLOG (PROGRAMMING LANGUAGE)
A declarative debugger for a logical-functional language p 3183 N95-33007
PROPAGATION MODES
Helicopter HF communications using the NVIS mode p 3043 N95-32491
Calculations of spatial higher modes without deflation procedure
[REPT-2205] p 3090 N95-32985
PROPAGATION VELOCITY
Quench propagation velocity for highly stabilized conductors
[DE95-011040] p 3103 N95-33404
Laser-based ultrasonics by dual-probe interferometer detection and narrow-band ultrasound generation p 3118 N95-33484
Implications of early stages in the growth of stress corrosion cracking on component reliability
[DE95-011498] p 3127 N95-33833
PROPELLANT ADDITIVES
Metallized gelled propellants: Oxygen/RP-1/aluminum rocket combustion experiments
[NASA-TM-107025] p 3088 N95-33876
PROPELLANT COMBUSTION
Pop tests of storable biopropellant liquid apogee engine
[NAL-TR-1253] p 3060 N95-32755
Fundamental phenomena on fuel decomposition and boundary-layer combustion processes with applications to hybrid rocket motors
[NASA-CR-199126] p 3061 N95-32932
Metallized gelled propellants: Oxygen/RP-1/aluminum rocket combustion experiments
[NASA-TM-107025] p 3088 N95-33876
PROPELLANT DECOMPOSITION
Fundamental phenomena on fuel decomposition and boundary-layer combustion processes with applications to hybrid rocket motors
[NASA-CR-199126] p 3061 N95-32932
PROPELLANT GRAINS
Observations of surface structure and regression behavior of solid propellant strands burning under narrow gap conditions p 3088 N95-33254
PROPELLANT SPRAYS
Modeling liquid jet atomization processes
[AD-A294888] p 3112 N95-34572
PROPELLANTS
The oxidation of energetic materials in supercritical water
[DE95-010888] p 3088 N95-33702
PROPELLERS
Numerical studies of turbulent free surface flows and unsteady propeller flows
[AD-A294377] p 3112 N95-34343
PROPOSALS
Air force office of scientific research. Research proposal
[AD-A293401] p 3252 N95-32473
PROPULSION SYSTEM PERFORMANCE
Low-order nonlinear dynamic model of IC engine-variable pitch propeller system for general aviation aircraft
[NASA-TM-107006] p 3050 N95-32916
PSC algorithm description p 3051 N95-33013
Performance seeking control (PSC) for the F-15 highly integrated digital electronic control (HIDEC) aircraft p 3053 N95-33020
SSME Post Test Diagnostic System: Systems Section
[NASA-CR-198375] p 3061 N95-34625
Subscale study of engine bellmouth inlet vortices in test cell R1D
[AD-A294993] p 3113 N95-34818
PROPULSIVE EFFICIENCY
Metallized gelled propellants: Oxygen/RP-1/aluminum rocket combustion experiments
[NASA-TM-107025] p 3088 N95-33876
PROTECTION
D3-D power supply, design, and development
[DE95-009603] p 3222 N95-32656

Immunological protection against botulinum neurotoxin by a synthetic vaccine
[AD-A294146] p 3165 N95-34754
PROTECTIVE CLOTHING
Tri-service perspectives on microclimate cooling of protective clothing in the heat
[AD-A294005] p 3170 N95-34370
PROTECTIVE COATINGS
Coating power RF components with TiN
[DE95-010357] p 3082 N95-32541
CRADA with United Solar Technologies and Pacific Northwest Laboratory (PNL-021): Thin film materialsfor low-cost high performance solar concentrators
[DE95-010423] p 3150 N95-33400
PROTEINS
Prospect redux p 3133 N95-33758
PROTOCOL (COMPUTERS)
Congestion control over ATM local area networks
[DE95-010343] p 3184 N95-32558
Distributed shared memory for new generation networks
[AD-A293722] p 3185 N95-32580
Exchange, interpretation, and database-search of ion mobility spectra supported by data format JCAMP-DX p 3070 N95-33274
Performance analysis of combined concurrency control and commit protocols in distributed database systems p 3238 N95-33711
Protocol engineering for broadband networks
[AD-A294969] p 3186 N95-34584
PROTON BEAMS
Search for N(sub (phi))(1960) baryon
[DE95-619290] p 3205 N95-32703
Study of the p + N yields (Sigma(0)K(+)) + N reaction at E(sub p) 70 GeV
[DE95-619273] p 3207 N95-33171
PROTON IMPACT
Velocity dependence of ionization and excitation of hydrogen molecules by fast proton impact
[DE95-010818] p 3207 N95-33370
PROTON IRRADIATION
Peak effect and flux pinning in YBa2Cu3O(7-(delta)) single crystals
[DE95-010126] p 3228 N95-32959
PROTON-PROTON REACTIONS
Comparison of the Wang and Wachsmuth models for (pi) production with measurements at 12 GeV/c
[DE95-010417] p 3203 N95-32542
Efficiency of modified UA1 jet reconstruction algorithm in PP, PA and AA collisions at STAR
[DE95-009918] p 3212 N95-32665
PROTONS
Design and testing criteria for bipolar plate materials for PEM fuel cell applications
[DE95-010878] p 3148 N95-32575
Progress towards antihydrogen production by the reaction of cold antiprotons with positronium atoms
[DE95-007850] p 3204 N95-32584
Proton-induced fragmentation of carbon at energies below 100 MeV p 3161 N95-32720
Dosimetry of heavy ions by use of CCD detectors p 3161 N95-32721
Proton affinity determinations and proton-bound dimer structure indications in C2 to C15, (alpha),(omega)-alkyldiamines p 3069 N95-33266
Velocity dependence of ionization and excitation of hydrogen molecules by fast proton impact
[DE95-010818] p 3207 N95-33370
PROTOTYPES
Fast feedback for linear colliders
[DE95-012099] p 3211 N95-32608
Cathode readout with stripped resistive drift tubes
[DE95-621871] p 3102 N95-32628
Development of a prototype lignin concentration sensor
[DE95-010951] p 3074 N95-33705
PSYCHOPHYSIOLOGY
Stimulus-response compatibility
[PB95-214722] p 3167 N95-33237
PUBLIC HEALTH
Multimedia Environmental Pollutant Assessment System (MEPAS(trademark)): Exposure pathway and human health impact assessment models
[DE95-012763] p 3155 N95-34441
PUBLIC RELATIONS
Metric conversion: Future progress depends upon private sector and public support. Report to Congressional requesters
[GAO/RCED-94-23] p 3089 N95-32785
PULSAR MAGNETOSPHERES
GRO: Studies of high energy pulsars with EGRET
[NASA-CR-199130] p 3248 N95-33499
PULSARS
Gamma ray imaging of the Crab and Vale regions with the UCR double-Compton telescope p 3245 N95-32837
GRO: Studies of high energy pulsars with EGRET
[NASA-CR-199130] p 3248 N95-33499
PULSE COMMUNICATION
Tactical low-level helicopter communications p 3043 N95-32492
Successful development of first-generation laser device; marking China's optoelectronic technology at world class level
[AD-A294206] p 3217 N95-34305
PULSE DURATION
General limits on the performance of high power radiators
[DE95-010732] p 3095 N95-32570
Development of 1.06 micron high efficiency antireflective coating
[AD-A294161] p 3219 N95-34759
Ultrashort pulse laser effects in the primate eye
[AD-A295024] p 3164 N95-34789
PULSE GENERATORS
Optical pulse generation using fiber lasers and integrated optics
[DE95-011517] p 3216 N95-33506
PULSE TIME MODULATION
Vertical velocity ambiguity resolution method
[AD-D017481] p 3201 N95-34424
PULSED LASER DEPOSITION
Laser ablation plume thermalization dynamics in background gases studied by time-resolved imaging, spectroscopic, and ion probe diagnostics
[DE95-010277] p 3118 N95-33246
Influence of processing variables on the structure and properties of ZnO films
[DE95-011494] p 3084 N95-33405
Formation of artificially-layered high-temperature superconductors using pulsed-laser deposition
[DE95-012884] p 3231 N95-34465
Novel ferroelectric heterostructures for high-density DRAMS
[AD-A294517] p 3199 N95-34477
Highly doped p-ZnTe films and quantum well structures grown by nonequilibrium pulsed laser ablation
[DE95-012885] p 3232 N95-34799
PULSED LASERS
Sum frequency generation of dual-wavelength Nd: YAP laser in LiIO3 crystal
[AD-A293094] p 3117 N95-32472
New advances in 1341.4 nm Nd:YAP lasers
[AD-A293070] p 3118 N95-32702
Plasma mediated ablation of biological tissues with ultrashort laser pulses
[DE95-011748] p 3164 N95-33654
Successful development of first-generation laser device; marking China's optoelectronic technology at world class level
[AD-A294206] p 3217 N95-34305
Formation of artificially-layered high-temperature superconductors using pulsed-laser deposition
[DE95-012884] p 3231 N95-34465
Modeling and simulation of pulsed laser annealing and ablation of solid materials
[DE95-012888] p 3119 N95-34466
Pulsed tunable narrow-bandwidth dye laser, with hollow circular waveguide in cavity
[AD-A294060] p 3120 N95-34469
England develops world's fastest optic switch breakthrough in high-speed communications
[AD-A294038] p 3105 N95-34488
Ultrashort pulse laser effects in the primate eye
[AD-A295024] p 3164 N95-34789
Highly doped p-ZnTe films and quantum well structures grown by nonequilibrium pulsed laser ablation
[DE95-012885] p 3232 N95-34799
PULSED RADIATION
New advances in 1341.4 nm Nd:YAP lasers
[AD-A293070] p 3118 N95-32702
Discrete modeling of optical pulse propagation in nonlinear media
[DE95-011515] p 3216 N95-34020
Method of forming thin films on substrates at low temperatures
[AD-D017470] p 3086 N95-34447
PUMP IMPELLERS
An experimental and analytical investigation into the performance of centrifugal pumps operating with air-water mixtures p 3123 N95-33323
PURITY
Predicted operating conditions for maintaining mode purity in the 1MW 200 GHz FOM Free Electron Maser
[DE95-010795] p 3117 N95-32571
PYROLYSIS
A novel approach to increasing cocaine detection confidence utilizing ion mobility spectrometry p 3072 N95-33283
Use of D2 to elucidate OMVPE growth mechanisms
[AD-A294999] p 3233 N95-34820
PYROTECHNICS
The oxidation of energetic materials in supercritical water
[DE95-010888] p 3088 N95-33702

Q

Q FACTORS
Status of the large-scale dark-matter axion search
[DE95-008828] p 3246 N95-32597
Improved L-C resonant decay technique for Q measurement of quasilinear power inductors: New results for MPP and ferrite powdered cores
[NASA-CR-198373] p 3103 N95-33874
Q SWITCHED LASERS
Optical pulse generation using fiber lasers and integrated optics
[DE95-011517] p 3216 N95-33506
Temporal dynamics of the multi-frequency spectrum generated by self-phase modulation of two frequencies in single-mode fiber
[DE95-010920] p 3119 N95-33703
QUADRUPOLES
The effect and correction of coupling generated by the RHIC triplet quadrupoles
[DE95-011562] p 3210 N95-32413
Beam-based magnetic alignment of the final focus test beam
[DE95-012096] p 3212 N95-32657
Beam-based optical tuning of the Final Focus Test Beam
[DE95-012097] p 3215 N95-32658
A final-focus magnet for PEP-2
[DE95-012372] p 3214 N95-33504
The beam envelope equation-systematic solution for a periodic quadrupole lattice with space charge
[DE95-012761] p 3199 N95-34269
QUALITY
Prediction of OCR accuracy using simple image features
[DE95-009887] p 3236 N95-32471
QUALITY CONTROL
HOTQUA: An expert system prototype for quality monitoring in a rolling mill p 3190 N95-33004
NASA-Wide Fastener Technical Interchange Meeting
[NASA-CP-3308] p 3123 N95-33199
Analysis of samples for the first (1994) OPCW round robin interlaboratory comparison test
[PB95-210324] p 3068 N95-33243
Quality assurance and risk management: Perspectives on Human Factors Certification of Advanced Aviation Systems p 3048 N95-34771
QUANTITATIVE ANALYSIS
Development of ultrasensitive spectroscopic analysis technology. Development of atomic spectroscopy technology
[DE95-614352] p 3066 N95-32566
Application of Ion Mobility Spectrometry (IMS) in forensic chemistry and toxicology with focus on biological matrices p 3072 N95-33285
Quantitative analysis of volatile organic compounds using ion mobility spectra and cascade correlation neural networks p 3073 N95-33290
Analysis of metallic fuels by laser ablation
[DE95-012465] p 3075 N95-34440
QUANTUM AMPLIFIERS
Quantum cylinder fiber light amplifier
[AD-A294197] p 3217 N95-34300
QUANTUM CHEMISTRY
A quantum Monte Carlo study of the high-pressure phases of solid hydrogen p 3074 N95-33469
The computation of electron transfer rates: The nonadiabatic instanton solution
[AD-A294523] p 3209 N95-34350
QUANTUM CHROMODYNAMICS
QCD mechanisms for double quarkonium and open heavy meson hadroproduction
[DE95-012171] p 3204 N95-32619
Chiral restoration in hot and/or dense matter
[DE95-012176] p 3204 N95-32621
Four heavy quark and bound state production in the e(+)e(-) yields Q + (bar-Q' + Q' + bar-Q and e(+)e(-) yields (Q(bar-Q')) + Q' + bar-Q processes in Z(sup 0)-boson pole
[DE95-620533] p 3205 N95-32704
Spin effects in high energy photon-hadron scattering in QCD
[DE95-623679] p 3234 N95-32961
Top quark signatures in extended color theories
[DE95-007099] p 3234 N95-33202
QCD and hadron structure
[DE95-012173] p 3209 N95-33855
Proceedings of the School for Young High Energy Physicists
[PB95-234993] p 3235 N95-34652

QUANTUM COUNTERS
Spin counting in dipolar coupled spin 1/2 systems by multiple quantum NMR spectroscopy in solids: Development of a single quantum propagator and its application to heterogeneous catalysis
[DE95-010246] p 3066 N95-32540
QUANTUM ELECTRODYNAMICS
Vacuum polarization correction to the positronium decay rate
[DE95-614164] p 3202 N95-32481
Proceedings of the School for Young High Energy Physicists
[PB95-234993] p 3235 N95-34652
QUANTUM ELECTRONICS
Fabrication technology and measurement of coupled quantum dot devices
[AD-A294853] p 3231 N95-34569
Electronic processes in heterostructures, strained-layer materials, and laterally patterned structures
[AD-A294970] p 3235 N95-34585
QUANTUM MECHANICS
General-covariant Quantum Mechanics of Dirac particle in curved space-times
[DE95-623600] p 3233 N95-32478
Spin counting in dipolar coupled spin 1/2 systems by multiple quantum NMR spectroscopy in solids: Development of a single quantum propagator and its application to heterogeneous catalysis
[DE95-010246] p 3066 N95-32540
Quantum mechanical capacitance in a scanning tunneling microscope
[DE95-011272] p 3230 N95-33880
Atoms in strong fields
[AD-A294589] p 3209 N95-34423
QUANTUM THEORY
General-covariant Quantum Mechanics of Dirac particle in curved space-times
[DE95-623600] p 3233 N95-32478
Campbell-Hausdorff formula and algebras with operator
[DE95-623635] p 3195 N95-32609
Nonequilibrium problems in Quantum Field Theory and Schwinger's closed time path formalism
[DE95-012056] p 3234 N95-33388
Theory of magneto-optics and circular magnetic x-ray dichroism
[DE95-010129] p 3080 N95-33700
Electronic processes in heterostructures, strained-layer materials, and laterally patterned structures
[AD-A294970] p 3235 N95-34585
Proceedings of the School for Young High Energy Physicists
[PB95-234993] p 3235 N95-34652
QUANTUM WELL LASERS
Successful development of first-generation laser device; marking China's optoelectronic technology at world class level
[AD-A294206] p 3217 N95-34305
QUANTUM WELLS
The 8th Winterschool on New Developments in Solid State Physics
[AD-A290163] p 3227 N95-32677
Growth and characterization of heterostructures and infrared emitters with compressed InAsSb layers
[DE95-009828] p 3228 N95-33213
Fabrication of optical channel waveguides in the GaAs/AlGaAs system by MeV ion beam bombardment
[DE95-008973] p 3218 N95-34480
Multilayer thermoelectric films: A strategy for the enhancement of ZT
[DE95-011535] p 3081 N95-34482
Highly doped p-ZnTe films and quantum well structures grown by nonequilibrium pulsed laser ablation
[DE95-012885] p 3232 N95-34799
QUARK MODELS
Isgur-Wise function and polarization characteristics of Lambda(sub b)-baryon
[DE95-623696] p 3202 N95-32407
QUARKS
Scaling law for the Upsilon(4S) yields bar-BB and psi(3770) yields bar-DD decay constants from effective sum rules
[DE95-620538] p 3203 N95-32554
Intrinsic charm contribution to double quarkonium hadroproduction
[DE95-012170] p 3204 N95-32617
Four heavy quark and bound state production in the e(+)e(-) yields Q + (bar-Q' + Q' + bar-Q and e(+)e(-) yields (Q(bar-Q')) + Q' + bar-Q processes in Z(sup 0)-boson pole
[DE95-620533] p 3205 N95-32704
Spin effects in high energy photon-hadron scattering in QCD
[DE95-623679] p 3234 N95-32961
Top quark signatures in extended color theories
[DE95-007099] p 3234 N95-33202
Searching for new physics with charm
[DE95-012498] p 3207 N95-33245
Development of silicon drift detectors for strangeness measurements
[DE95-012366] p 3208 N95-33380
QUARTZ
Solubility behavior of quartz and corundum in supercritical water: A quantitative thermodynamic interpretation
[DE95-012294] p 3234 N95-34211
QUARTZ CRYSTALS
Infrared detection of chemical corrosion on metal surface
[AD-A295000] p 3081 N95-34821
QUATERNARY ALLOYS
Phase equilibria and phase diagrams in carbide systems
[PB95-211348] p 3068 N95-33229
QUENCHING (COOLING)
Quench antenna and fast-motion investigations during training of a 7T dipole magnet
[DE95-012371] p 3103 N95-33080
QUERY LANGUAGES
Incorporating bibliographic information into a spatial data query system for the Savannah River Site
[DE95-010965] p 3238 N95-33402
QUEUEING THEORY
Control of initialization bias in queueing simulations using queueing approximations
[AD-A294121] p 3194 N95-34742

R

RACKS (FRAMES)
A study of space-rated connectors using a robot end-effector
[NASA-CR-199116] p 3121 N95-32675
RADAR ANTENNAS
HeliRadar: A rotating antenna synthetic aperture radar for helicopter allweather operations
p 3093 N95-33137
RADAR ATTENUATION
Optimization of a melting layer model in the radar backscatter, attenuation, and phase shift calculations at centimeter and millimeter wavelengths
[PB95-207189] p 3155 N95-32455
RADAR BEACONS
GPS-Squitter interference analysis
[AD-A293690] p 3047 N95-33480
RADAR CROSS SECTIONS
Efficient time domain solutions of Maxwell's equations for aerospace systems
[AD-A294019] p 3196 N95-34377
RADAR DATA
Three-dimensional ground penetrating radar imaging using synthetic aperture time-domain focusing
[DE95-010731] p 3095 N95-32569
FORTRAN program for analyzing ground-based radar data: Usage and derivations, version 6.2
[NASA-TP-3430] p 3181 N95-33193
Integration of AIRSAR and AVIRIS data for Trail Canyon alluvial fan, Death Valley, California
p 3134 N95-33760
New observations of Bolivian wind streaks by JPL Airborne SAR: Preliminary results p 3139 N95-33802
Measuring soil moisture with imaging radars
p 3139 N95-33803
Use of TOPSAR digital elevation data to determine the 3-dimensional shape of an alluvial fan
p 3139 N95-33804
Accurate estimation of sigma(exp 0) using AIRSAR data p 3139 N95-33805
Remotely sensed indicators of habitat heterogeneity and biological diversity: A preliminary report
p 3140 N95-33806
Bayes classification of interferometric TOPSAR data
p 3140 N95-33808
Use of AIRSAR to identify woody shrub invasion and other indicators of desertification in the Jornada LTER
p 3141 N95-33810
The unique radar scattering properties of silicic lava flows and domes p 3141 N95-33811
On the potential of long wavelength imaging radars for mapping vegetation types and woody biomass in tropical rain forests p 3141 N95-33812
Lithologic controls on AIRSAR signatures of bedrock and alluvium, at Lunar Crater, Nevada
p 3141 N95-33813
Application of IEM model on soil moisture and surface roughness estimation p 3142 N95-33816
RADAR DETECTION
Laser based obstacle warning sensors for helicopters
p 3045 N95-32499
Covert Night/Day Operations for Rotorcraft (CONDOR) programme p 3046 N95-32505
Space-time adaptive processing for airborne radar
[AD-A293032] p 3098 N95-33152
RADAR EQUIPMENT
GPS-Squitter interference analysis
[AD-A293690] p 3047 N95-33480
RADAR FILTERS
Space-time adaptive processing for airborne radar
[AD-A293032] p 3098 N95-33152
RADAR IMAGERY
RASSP benchmark 1 technical description. Revision 1
[AD-A293030] p 3096 N95-32773
Development of an L-, C-, and X-band radar for backscattering studies over vegetation
[NASA-CR-199112] p 3097 N95-33033
Identification of terrain imagery with unstable reflectivity p 3093 N95-33138
Studies of microwave scattering and canopy architecture for boreal forests
[NASA-CR-199114] p 3099 N95-33726
New observations of Bolivian wind streaks by JPL Airborne SAR: Preliminary results p 3139 N95-33802
Measuring soil moisture with imaging radars
p 3139 N95-33803
Polarization and wavelength diversities of Gulf Stream fronts imaged by AIRSAR p 3140 N95-33807
Bayes classification of interferometric TOPSAR data
p 3140 N95-33808
Regional mapping of forest canopy water content and biomass using AIRSAR images over BOREAS study area p 3142 N95-33815
Application of IEM model on soil moisture and surface roughness estimation p 3142 N95-33816
The development of the automatic target recognition system for the UGV/RSTA LADAR
[AD-A294090] p 3100 N95-34474
SAR
[AD-A295020] p 3101 N95-34788
RADAR MEASUREMENT
Mid-latitude ionospheric plasma drift: A comparison of digital ionosonde and incoherent scatter radar measurements at Millstone Hill p 3222 N95-32838
Iron Boltzmann factor LIDAR: Proposed new remote-sensing technique for mesospheric temperature
[AD-A293568] p 3157 N95-34613
RADAR SCATTERING
Development of an L-, C-, and X-band radar for backscattering studies over vegetation
[NASA-CR-199112] p 3097 N95-33033
Accurate estimation of sigma(exp 0) using AIRSAR data p 3139 N95-33805
Remotely sensed indicators of habitat heterogeneity and biological diversity: A preliminary report
p 3140 N95-33806
Terrain classification using circular polarimetric features p 3140 N95-33809
The unique radar scattering properties of silicic lava flows and domes p 3141 N95-33811
Lithologic controls on AIRSAR signatures of bedrock and alluvium, at Lunar Crater, Nevada
p 3141 N95-33813
Estimation of penetration of forest canopies by Interferometric SAR measurements
p 3141 N95-33814
Regional mapping of forest canopy water content and biomass using AIRSAR images over BOREAS study area p 3142 N95-33815
RADAR SIGNATURES
Lithologic controls on AIRSAR signatures of bedrock and alluvium, at Lunar Crater, Nevada
p 3141 N95-33813
RADAR TARGETS
The Anglo-French Compact Laser Radar demonstrator programme p 3045 N95-32501
RADAR TRACKING
FORTRAN program for analyzing ground-based radar data: Usage and derivations, version 6.2
[NASA-TP-3430] p 3181 N95-33193
The unique radar scattering properties of silicic lava flows and domes p 3141 N95-33811
RADARSAT
Geographic information system for fusion and analysis of high-resolution remote sensing and ground data
p 3240 N95-34224
RADIANCE
Ocean observations with EOS/MODIS: Algorithm development and post launch studies
[NASA-CR-198928] p 3143 N95-32914
MODTRAN3: An update and recent validations against airborne high resolution interferometer measurements
p 3128 N95-33732
Using dark current data to estimate AVIRIS noise covariance and improve spectral analyses
p 3129 N95-33736
Determination of the in-flight spectral calibration of AVIRIS using atmospheric absorption features
p 3117 N95-33751

An improved spectral calibration requirement for AVIRIS p 3117 N95-33752
Movement of water vapor in the atmosphere measured by an imaging spectrometer at Rogers Dry Lake, CA p 3132 N95-33753
In-flight radiometric calibration of AVIRIS in 1994 p 3117 N95-33754
Grayling 2 information base for generation of synthetic thermal infrared scenes
| AD-A294956 | p 3100 N95-34578

RADIATION ABSORPTION
Causal correlation of foliar biochemical concentrations with AVIRIS spectra using forced entry linear regression p 3130 N95-33744
Effect of propagation attenuation of thin film waveguide on optical thin film losses
| AD-A294064 | p 3218 N95-34471

RADIATION CHEMISTRY
Low-energy Ion-Beam Deposition apparatus equipped with surface analysis system
| DE95-737272 | p 3212 N95-32712

RADIATION COUNTERS
Shuttle Potential and Return Electron Experiment (SPREE) electrostatic analyzer (ESA) calibration report
| AD-A293026 | p 3057 N95-32772
Light particle emission in heavy ion reactions
| DE95-010727 | p 3206 N95-32965
A final-focus magnet for PEP-2
| DE95-012372 | p 3214 N95-33504

RADIATION DAMAGE
Study of the space environmental effects on spacecraft engineering materials
| NASA-CR-199090 | p 3066 N95-32581
Analysis of radiation damages of electronic circuits by separate irradiation of their components with a collimated charged particle beam
| DE95-621946 | p 3202 N95-32629
Minutes of the 12th Joint NASA/DARA-DLR Life Sciences Program Working Group Meeting
| NASA-TM-110655 | p 3161 N95-32719
Heavy ion induced DNA-DSB in yeast and mammalian cells p 3161 N95-32723
Inactivation, DNA double strand break induction and their rejoining in bacterial cells irradiated with heavy ions p 3161 N95-32724
DNA-DSB in CHO-K1 cells induced by heavy-ions: Break rejoining and residual damage (GSI) p 3162 N95-32725
Chromosomal damage observed in first postirradiation metaphases of repair-proficient and -deficient cell lines p 3162 N95-32726
Mutation induction in bacteria after heavy ion irradiation p 3162 N95-32727
Heavy ion induced mutations in mammalian cells: Cross sections and molecular analysis p 3162 N95-32728
Heavy ion action on single cells: Cellular inactivation capability of single accelerated heavy ions p 3162 N95-32729
Cosmic heavy ion tracks in mesoscopic biological test objects p 3163 N95-32730
X-ray-provoked non-Mendelian transgenerational oncodeterminants p 3163 N95-32731

RADIATION DETECTORS
Dosimetry of heavy ions by use of CCD detectors p 3161 N95-32721

RADIATION DISTRIBUTION
Advanced boundary element methods in aeroacoustics and elastodynamics p 3200 N95-33694

RADIATION DOSAGE
Irradiation experiments of low copper A533B steels for reactor pressure vessel tested in JMTR
| DE95-737266 | p 3077 N95-32531
Cosmic heavy ion tracks in mesoscopic biological test objects p 3163 N95-32730

RADIATION EFFECTS
Irradiation-assisted stress corrosion cracking considerations at temperatures below 288 C
| DE95-008940 | p 3077 N95-32555
Irradiation tests of critical components for remote handling in gamma radiation environment
| DE95-737223 | p 3221 N95-32565
Study of the space environmental effects on spacecraft engineering materials
| NASA-CR-199090 | p 3066 N95-32581
Frequency response of a TeO2 slow shear wave acousto-optic cell exposed to radiation
| DE95-009588 | p 3226 N95-32589
Proton-induced fragmentation of carbon at energies below 100 MeV p 3161 N95-32720
Heavy ion induced DNA-DSB in yeast and mammalian cells p 3161 N95-32723
Inactivation, DNA double strand break induction and their rejoining in bacterial cells irradiated with heavy ions p 3161 N95-32724
DNA-DSB in CHO-K1 cells induced by heavy-ions: Break rejoining and residual damage (GSI) p 3162 N95-32725
Mutation induction in bacteria after heavy ion irradiation p 3162 N95-32727
Heavy ion induced mutations in mammalian cells: Cross sections and molecular analysis p 3162 N95-32728
Heavy ion action on single cells: Cellular inactivation capability of single accelerated heavy ions p 3162 N95-32729
Cosmic heavy ion tracks in mesoscopic biological test objects p 3163 N95-32730
X-ray-provoked non-Mendelian transgenerational oncodeterminants p 3163 N95-32731

RADIATION MEASUREMENT
Radiative interactions with micromachined surfaces: Spectral polarized emittance
| DE95-011455 | p 3097 N95-33061

RADIATION SHIELDING
Hydrogen formation in metals and alloys during fusion reactor operation
| DE95-737224 | p 3202 N95-32529

RADIATION THERAPY
First NPL Calorimetry Workshop
| PB95-236063 | p 3235 N95-34654

RADIATION TOLERANCE
Chromosomal damage observed in first postirradiation metaphases of repair-proficient and -deficient cell lines p 3162 N95-32726

RADIATION TRANSPORT
Summary report for ITER Task No. T226B: Evaluation of ITER disruption erosion
| DE95-010402 | p 3219 N95-32401

RADIATIVE TRANSFER
Ocean observations with EOS/MODIS: Algorithm development and post launch studies
| NASA-CR-198928 | p 3143 N95-32914
Comparison of seasonal and zonal patterns of the direct and indirect radiative forcing of climate by aerosols
| DE95-010896 | p 3153 N95-33192
Balloon-borne radiometer profiler: Field observations
| DE95-011493 | p 3158 N95-33505
MODTRAN3: An update and recent validations against airborne high resolution interferometer measurements p 3128 N95-33732
Impact of differences in the solar irradiance spectrum on surface reflectance retrieval with different radiative transfer codes p 3136 N95-33771
Enhanced shortwave cloud radiative forcing due to anthropogenic aerosols
| DE95-013319 | p 3156 N95-34214
Photobiology and optical properties of planktonic and sea ice microalgae in the high arctic
| AD-A294002 | p 3160 N95-34457

RADICALS
Use of D2 to elucidate OMVPE growth mechanisms
| AD-A294999 | p 3233 N95-34820

RADIO ATTENUATION
DETVAg-90: Use of GTD for wave propagation over earth
| PB95-211447 | p 3098 N95-33231

RADIO COMMUNICATION
Helicopter HF communications using the NVIS mode p 3043 N95-32491
Tactical low-level helicopter communications p 3043 N95-32492

RADIO EMISSION
Compton Observatory observations of clusters of galaxies and extragalactic radio sources
| NASA-CR-189431 | p 3246 N95-33261

RADIO EQUIPMENT
Coating power RF components with TiN
| DE95-010357 | p 3082 N95-32541

RADIO FREQUENCIES
Tactical low-level helicopter communications p 3043 N95-32492
Coating power RF components with TiN
| DE95-010357 | p 3082 N95-32541
Emittance and energy control in the NLC main linacs
| DE95-012556 | p 3213 N95-33338
Epitaxial Pb(Zr(0.40)Ti(0.60))O3/SrRuO3 and PbTiO3/SrRuO3 multilayer thin films prepared by MOCVD and RF sputtering
| DE95-007146 | p 3229 N95-33636
Unified model of the RF plasma sheath
| DE95-012114 | p 3224 N95-33851
Mathematical modelling in plasma physics
| AD-A294972 | p 3224 N95-34586

RADIO FREQUENCY INTERFERENCE
Space-time adaptive processing for airborne radar
| AD-A293032 | p 3098 N95-33152

RADIO OCCULTATION
Reduction and analysis of seasons 15 and 16 (1991 - 1992) Pioneer Venus radio occulation data and correlative studies with observations of the near infrared emission of Venus
| NASA-CR-199071 | p 3247 N95-32700

RADIO RECEIVERS
Anechoic chamber upgrade
| AD-A294375 | p 3056 N95-34342

RADIO TRANSMISSION
DETVAg-90: Use of GTD for wave propagation over earth
| PB95-211447 | p 3098 N95-33231

RADIO WAVES
DETVAg-90: Use of GTD for wave propagation over earth
| PB95-211447 | p 3098 N95-33231

RADIOACTIVE CONTAMINANTS
Proceedings of the ONR/NRL workshop on modeling the dispersion of nuclear contaminants in the arctic seas
| AD-A294373 | p 3159 N95-34341
Multimedia Environmental Pollutant Assessment System (MEPAS(trademark)): Exposure pathway and human health impact assessment models
| DE95-012763 | p 3155 N95-34441

RADIOACTIVE DECAY
Evaluated nuclear structure data file
| DE95-011343 | p 3202 N95-32484

RADIOACTIVE ISOTOPES
Application of Ni-63 photo and corona discharge ionization for the analysis of chemical warfare agents and toxic wastes p 3070 N95-33272
Proceedings of the ONR/NRL workshop on modeling the dispersion of nuclear contaminants in the arctic seas
| AD-A294373 | p 3159 N95-34341

RADIOACTIVE WASTES
Users' manual for LEHGC: A Lagrangian-Eulerian finite-element model of HydroGeoChemical transport through saturated-unsaturated media. Version 1.0
| DE95-010513 | p 3179 N95-32543
Glass science tutorial lecture no. 6: The melting of silicate glasses, a review of selected topics
| DE95-010199 | p 3084 N95-33218
Proceedings of the ONR/NRL workshop on modeling the dispersion of nuclear contaminants in the arctic seas
| AD-A294373 | p 3159 N95-34341

RADIOACTIVITY
ABCASH plotting program users guide
| DE95-011652 | p 3155 N95-34435

RADIOBIOLOGY
Proton-induced fragmentation of carbon at energies below 100 MeV p 3161 N95-32720
Cosmic heavy ion tracks in mesoscopic biological test objects p 3163 N95-32730
First NPL Calorimetry Workshop
| PB95-236063 | p 3235 N95-34654

RADIOISOTOPE BATTERIES
Fabrication of improved SiGe alloys for an 18-couple module test
| DE95-010238 | p 3060 N95-32396

RADIOLOGY
Managing technological change in a military treatment facility: A case study of medical diagnostic imaging support (MDIS) system
| AD-A294894 | p 3165 N95-34573

RADIOMETERS
SeaWiFS technical report series. Volume 22: Prelaunch acceptance report for the SeaWFS radiometer
| NASA-TM-104566-VOL-22 | p 3159 N95-32672
OPEX Second Workshop of the OLYMPUS Propagation Experimenters. Volume 3: Reference book on radiometry and meteorological measurements
| ESA-WPP-083-VOL-3 | p 3096 N95-32749
SeaWiFS technical report series. Volume 31: Stray light in the SeaWiFS radiometer
| NASA-TM-104566-VOL-31 | p 3159 N95-32833
Low-level data fusion for landing runways detection p 3048 N95-33136
CADIR: A model for generating infrarad images
| PB95-222956 | p 3215 N95-33239
Balloon-borne radiometer profiler: Field observations
| DE95-011493 | p 3158 N95-33505

RAIL TRANSPORTATION
Navigational technology of dual usage p 3048 N95-33131
Numerical simulation of aerodynamic problems in high speed railways, part 2 p 3041 N95-34554

RAILGUN ACCELERATORS
Environment and circuit model for capacitor-based rail guns
| AD-A293455 | p 3057 N95-34815

RAIN
Raingauge network optimization and GIS: A case study of the Mananga basin. Communications of the Sanitary Engineering and Water Management Division
| PB95-214284 | p 3157 N95-32891

Intra-annual and inter-annual rainfall variability over East Asia, Southeast Asia, and South Asia
[AD-A294156] p 3158 N95-34757

RAIN FORESTS
On the potential of long wavelength imaging radars for mapping vegetation types and woody biomass in tropical rain forests p 3141 N95-33812

RAM ACCELERATORS
Investigation of starting and ignition transients in the thermally choked ram accelerator p 3054 N95-34805

RAMAN SPECTRA
Stimulated rotational Raman scattering of N2 in the atmosphere
[AD-A294195] p 3157 N95-34299

RAMAN SPECTROSCOPY
Field Raman spectrograph for environmental analysis
[DE95-007969] p 3153 N95-32816
The development of a large-area chemical sensor: A new platform for selective coatings
[DE95-011489] p 3075 N95-33832

RANDOM ACCESS MEMORY
Arbitrary waveform generator
[AD-D017451] p 3097 N95-32925
Novel ferroelectric heterostructures for high-density DRAMS
[AD-A294517] p 3199 N95-34477

RANDOM NOISE
Modeling and inference with fractional Brownian motion and fractional Gaussian noise p 3199 N95-33415

RANDOM SAMPLING
Genetic algorithms as global random search methods
[NASA-CR-199088] p 3188 N95-32767

RANDOM VARIABLES
Control of initialization bias in queueing simulations using queueing approximations
[AD-A294121] p 3194 N95-34742

RATINGS
D3-D power supply, design, and development
[DE95-009603] p 3222 N95-32656
Range graphics benchmark
[AD-A293541] p 3057 N95-34606

RATIOS
Fracture toughness and tensile behavior of multi-layer laminated metal composite of Al 6090-25 vol % SiCp and Al 5182
[DE95-011421] p 3062 N95-32602

RAY TRACING
Optimum Routeing: Analytical constraint of search space p 3044 N95-32493
Operation of the computer model for microenvironment solar exposure
[NASA-CR-198189] p 3059 N95-33890

RAYLEIGH SCATTERING
Studies of hypersonic boundary layer behavior
[AD-A294137] p 3113 N95-34752

RDX
Gas chromatography/ion mobility spectrometry as a hyphenated technique for improved explosives detection and analysis p 3071 N95-33278

REACTING FLOW
Thermo-chemical ablation of heat shields under Earth reentry conditions p 3059 N95-32903
A flux splitting scheme with high-resolution and robustness for discontinuities p 3036 N95-34518

REACTION KINETICS
Environmental chamber studies of atmospheric reactivities of volatile organic compounds: Effects of varying chamber and light source
[DE95-009225] p 3152 N95-32686
Solving stiff chemistry problems with FIDAP
[DE95-011053] p 3067 N95-32709
Combustion-acoustic stability analysis for premixed gas turbine combustors
[NASA-TM-107024] p 3050 N95-32931
Effect of lead content on Bi-2223 formation by a two-powder process
[DE95-009889] p 3079 N95-33215
Testing of a carpet catalyst
[PB95-208492] p 3068 N95-33242
Fundamental studies of gas phase ionic reactions by ion mobility spectrometry p 3069 N95-33268
Design and analysis of transient nonlinear coupled systems p 3199 N95-33292
Interfacial reactions during the liquid infiltration of titanium matrix composites p 3081 N95-34252
Fundamental studies of the mechanism of catalytic reactions with catalysts effective in the gasification of carbon solids and the oxidative coupling of methane
[DE95-012759] p 3075 N95-34268

REACTION TIME
A 30-pair thin film thermoelectric pile
[AD-A294058] p 3151 N95-34468

REACTION WHEELS
Globally stable feedback laws for near-minimum-fuel and near-minimum-time pointing maneuvers for a landmark-tracking spacecraft
[DE95-009867] p 3191 N95-33214

REACTIVITY
Influence of processing variables on the structure and properties of ZnO films
[DE95-011494] p 3084 N95-33405
Improving the comprehensibility, accuracy, and generality of reactive plans
[AD-A294104] p 3193 N95-34495
Explanations of empirically derived reactive plans
[AD-A294114] p 3193 N95-34501

REACTOR CORES
Irradiation tests of critical components for remote handling in gamma radiation environment
[DE95-737223] p 3221 N95-32565

REACTOR DESIGN
Development and trial manufacturing of 1/2-scale partial mock-up of blanket box structure for fusion experimental reactor
[DE95-737184] p 3219 N95-32408

REACTOR MATERIALS
Irradiation experiments of low copper A533B steels for reactor pressure vessel tested in JMTR
[DE95-737266] p 3077 N95-32531
Evaluation of strength properties of developed SiC/C compositionally gradient graphite materials
[DE95-737271] p 3063 N95-32711
A background subtraction routine for enhancing energy-filtered plasmon images of MgAl2O4 implanted with Al(+) and Mg(+) ions
[DE95-012850] p 3074 N95-33629

READOUT
Cathode readout with stripped resistive drift tubes
[DE95-621871] p 3102 N95-32628

REAL GASES
Numerical simulation of high enthalpy shock tunnel p 3035 N95-34514

REAL TIME OPERATION
A highly reliable, high performance open avionics architecture for real time Nap-of-the-Earth operations p 3044 N95-32497
The application of Ada and formal methods to a safety critical engine control system p 3094 N95-33142
Multi-layer holographic bifurcative neural network system for real-time adaptive EOS data analysis p 3148 N95-34233
Programmable real-time optoelectronic hybrid threshold logic processors
[AD-A294067] p 3104 N95-34379
The development of the automatic target recognition system for the UGV/RSTA LADAR
[AD-A294090] p 3100 N95-34474
A real-time single-camera, stereoscopic video device
[AD-A294105] p 3116 N95-34496
Image compression scheme for network transmission
[AD-A294959] p 3182 N95-34580
Optimization problems in multitarget/multisensor tracking
[AD-A294978] p 3100 N95-34590
Infrared detection of chemical corrosion on metal surface
[AD-A295000] p 3081 N95-34821

RECOIL IONS
CDW-EIS calculation of longitudinal momentum distribution in single ionization of helium by Ni(24+) ions
[DE95-010816] p 3207 N95-33241
Electron-electron interaction in the ionization of hydrogenlike projectiles by He
[DE95-010822] p 3208 N95-33374

RECOMMENDATIONS
Annual report to the Chairman, House and Senate Committees on Appropriations. Status of open recommendations: Improving operations of federal departments and agencies
[GAO/OP-94-1] p 3236 N95-32887

RECONNAISSANCE
Night attack p 3042 N95-32487
The development of the automatic target recognition system for the UGV/RSTA LADAR
[AD-A294090] p 3100 N95-34474

RECRYSTALLIZATION
Structural influences on the work hardening behavior of aluminum
[DE95-011262] p 3080 N95-33626
Development of local shear bands and orientation gradients in fcc polycrystals
[DE95-012072] p 3231 N95-34450

RECTANGLES
Hybrid pyramid/neural network vision system
[AD-A294919] p 3193 N95-34593

RECTANGULAR WAVEGUIDES
Active noise control in finite length waveguides p 3098 N95-33322

RECYCLING
Technical innovation for reducing emissions of greenhouse effect gas and survey of effects of changes of industrial structures
[DE95-769808] p 3151 N95-32547

REDUNDANCY
Trajectory planning and control of kinematically redundant robotic manipulators p 3194 N95-34807

REDUNDANT COMPONENTS
Influence of backup bearings and support structure dynamics on the behavior of rotors with active supports
[NASA-CR-199080] p 3121 N95-32689
Steady-state dynamic behavior of an auxiliary bearing supported rotor system p 3121 N95-32690
Dynamic behavior of a magnetic bearing supported jet engine rotor with auxiliary bearings p 3122 N95-32691
Dynamic modelling and response characteristics of a magnetic bearing rotor system with auxiliary bearings p 3122 N95-32692
Synchronous dynamics of a coupled shaft/bearing/housing system with auxiliary support from a clearance bearing: Analysis and experiment p 3122 N95-32693

REENTRY SHIELDING
Thermo-chemical ablation of heat shields under Earth reentry conditions p 3059 N95-32903

REENTRY VEHICLES
Numerical simulation of high enthalpy shock tunnel p 3035 N95-34514

REFINING
The method of model-based reasoning and application of an intelligent adaptive observer on the integrated process p 3190 N95-33005
Glass science tutorial lecture no. 6: The melting of silicate glasses, a review of selected topics
[DE95-010199] p 3084 N95-33218

REFLECTANCE
Conversion of holes into reducing species on surface modified small-particle TiO2
[DE95-008282] p 3225 N95-32586
Damage formation in silicon irradiated by heavy ions with energy more than 1 MeV/a.m.u.
[DE95-623968] p 3204 N95-32610
Identification of terrain imagery with unstable reflectivity p 3093 N95-33138
CRADA with United Solar Technologies and Pacific Northwest Laboratory (PNL-021): Thin film materialsfor low-cost high performance solar concentrators
[DE95-010423] p 3150 N95-33400
An algorithm for chlorophyll using first difference transformations of AVIRIS reflectance spectra p 3134 N95-33763
In situ surface roughness measurement during PECVD diamond film growth
[DE95-013411] p 3230 N95-34215

REFLECTED WAVES
Application of grating polarizer to 106.4GHz ECH system on Heliotron-E
[NIFS-334] p 3225 N95-34624

REFLECTION
Operation of the computer model for microenvironment solar exposure
[NASA-CR-198189] p 3059 N95-33890

REFRACTIVITY
Using optical interference methods to measure acousto-optical device thermal effects
[AD-A294219] p 3217 N95-34309
Effect of propagation attenuation of thin film waveguide on optical thin film losses
[AD-A294064] p 3218 N95-34471
Optical properties of lithium niobate waveguides, and prism coupling for optimizing waveguide fabrication
[AD-A294111] p 3218 N95-34498

REFRACTORY MATERIALS
Lightweight alumina refractory aggregate. Phase 2: Pilot scale development
[DE95-012154] p 3083 N95-33079

REFRACTORY METALS
Metallurgical and Materials Transactions, volume 25A, no. 9
[AD-A293622] p 3077 N95-32474
Electron beam joining of structural ceramics
[DE95-012521] p 3085 N95-34022

REFRIGERANTS
Thermophysical properties of HCFC alternatives
[DE95-009635] p 3233 N95-32661

REFUELING
TRAP: Tokamak Refueling by Accelerated Plasmoids
[DE95-009925] p 3223 N95-33216

REGENERATION (ENGINEERING)
Multiobjective optimization of hybrid regenerative life support technologies. Topic D: Technology Assessment
[NASA-CR-199125] p 3167 N95-32688

REGENERATIVE FUEL CELLS
Unitized Regenerative Fuel Cells for solar rechargeable aircraft and zero emission vehicles
[DE95-010684] p 3150 N95-33642
REGENERATORS
Numerical thermal analyses of heat exchangers for the stirling engine application
[NASA-CR-199120] p 3110 N95-33398
REGRESSION ANALYSIS
Using foreground/background analysis to determine leaf and canopy chemistry p 3135 N95-33765
Locus of control and coping style as stress moderators in achievement oriented individuals
[AD-A294275] p 3166 N95-34463
REGRESSION COEFFICIENTS
Locus of control and coping style as stress moderators in achievement oriented individuals
[AD-A294275] p 3166 N95-34463
REGULATIONS
Solving widespread low-concentration VOC air pollution problems: Gas-phase photocatalytic oxidation answers the needs of many small businesses
[DE95-004059] p 3152 N95-32668
Lessons learned in acquiring new regulations for shipping advanced electric vehicle batteries
[DE95-009908] p 3102 N95-32956
Report to the Ranking Minority Member, Committee on Government Operations, House of Representatives. Paperwork reduction: Reported burden hour increases reflect new estimates, not actual changes
[GAO/PEMD-94-3] p 3236 N95-33907
REGULATORS
Solving widespread low-concentration VOC air pollution problems: Gas-phase photocatalytic oxidation answers the needs of many small businesses
[DE95-004059] p 3152 N95-32668
REINFORCING FIBERS
Inclusion models of tensile fracture in fiber-reinforced brittle-matrix composites p 3065 N95-33721
Fiber coatings for brittle matrix composites p 3065 N95-34808
RELATIVISTIC EFFECTS
Cosmological consequences of topological and geometric phenomena in field theories p 3234 N95-33313
RELATIVITY
Fifth International Conference on Hyperbolic Problems, Theory, Numerics, Applications: Abstracts
[DE95-008173] p 3194 N95-32389
Cosmological consequences of topological and geometric phenomena in field theories p 3234 N95-33313
RELAXATION (MECHANICS)
DMTA studies of branching distribution in polyethylene
[PB95-208237] p 3084 N95-33228
RELIABILITY
Intermetallic compound layer growth kinetics in non-lead bearing solders
[DE95-009595] p 3078 N95-32591
D3-D power supply, design, and development
[DE95-009603] p 3222 N95-32656
The effect of sample holder material on ion mobility spectrometry reproducibility p 3071 N95-33282
Read/write module for high capacity memory disk
[AD-A294946] p 3178 N95-34745
RELIEF MAPS
Flight test of a low-altitude helicopter guidance system with obstacle avoidance capability p 3043 N95-32490
RELOCATION
Reducing cache misses in numerical applications using data relocation and prefetching
[AD-A293978] p 3182 N95-34455
REMOTE HANDLING
Irradiation tests of critical components for remote handling in gamma radiation environment
[DE95-737223] p 3221 N95-32565
REMOTE MANIPULATOR SYSTEM
Certification of a hybrid parameter model of the fully flexible Shuttle Remote Manipulator System p 3125 N95-32421
REMOTE SENSING
Laser based obstacle warning sensors for helicopters p 3045 N95-32499
SeaWiFS technical report series. Volume 22: Prelaunch acceptance report for the SeaWFS radiometer
[NASA-TM-104566-VOL-22] p 3159 N95-32672
Airborne passive polarimetric measurements of sea surface anisotropy at 92 GHz
[NASA-CR-197288] p 3143 N95-32823
Development of an L-, C-, and X-band radar for backscattering studies over vegetation
[NASA-CR-199112] p 3097 N95-33033
Low-level data fusion for landing runways detection p 3048 N95-33136
Studies of microwave scattering and canopy architecture for boreal forests
[NASA-CR-199113] p 3099 N95-33497
High spectral resolution remote sensing of canopy chemistry p 3128 N95-33731
Quantitative remote sensing of ammonium minerals, Cedar Mountains, Esmeralda County, Nevada p 3128 N95-33734
CNR LARA project, Italy: Airborne laboratory for environmental research p 3129 N95-33735
Causal correlation of foliar biochemical concentrations with AVIRIS spectra using forced entry linear regression p 3130 N95-33744
Mineralogic variations in fluvial sediments contaminated by mine tailings as determined from AVIRIS data, Coeur D'Alene River Valley, Idaho p 3131 N95-33745
Correction of thin cirrus effects in AVIRIS images using the sensitive 1.375-micron cirrus detecting channel p 3131 N95-33748
Remote sensing of smoke, clouds, and radiation using AVIRIS during SCAR experiments p 3132 N95-33749
High accuracy in-flight wavelength calibration of imaging spectrometry data p 3132 N95-33750
Integration of AIRSAR and AVIRIS data for Trail Canyon alluvial fan, Death Valley, California p 3134 N95-33760
An algorithm for chlorophyll using first difference transformations of AVIRIS reflectance spectra p 3134 N95-33763
AVIRIS spectral trajectories for forested areas of the Gifford Pinchot National Forest p 3135 N95-33766
Sub-pixel localization of highways in AVIRIS images p 3135 N95-33767
Validating spatial structure in canopy water content using geostatistics p 3135 N95-33768
Airborne Visible/Infrared Imaging Spectrometer (AVIRIS): Sensor improvements for 1994 and 1995 p 3117 N95-33769
Preliminary study of Kelso Dunes using AVIRIS, TM, and AIRSAR p 3136 N95-33773
Summaries of the Fifth Annual JPL Airborne Earth Science Workshop. Volume 2: TIMS Workshop
[NASA-CR-198923] p 3136 N95-33789
Analyses of TIMS and AVIRIS data, integrated with field and laboratory spectra, for lithological and mineralogical interpretation of Vulcano Island, Italy p 3137 N95-33790
Urban remote sensing applications: TIMS observations of the City of Scottsdale p 3137 N95-33791
Aerolian erosion, transport, and deposition of volcaniclastic sands among the shifting sand dunes, Christmas Lake Valley, Oregon: TIMS image analysis p 3137 N95-33793
A conflict of water and fire: Remote sensing imagery of the Uinkaret Volcanic Field, Grand Canyon, Arizona p 3117 N95-33795
Summaries of the Fifth Annual JPL Airborne Earth Science Workshop. Volume 3: AIRSAR Workshop
[NASA-CR-198924] p 3139 N95-33801
Remotely sensed indicators of habitat heterogeneity and biological diversity: A preliminary report p 3140 N95-33806
Use of AIRSAR to identify woody shrub invasion and other indicators of desertification in the Jornada LTER p 3141 N95-33810
A relational metric, its application to domain analysis, and an example analysis and model of a remote sensing domain
[NASA-TM-110358] p 3198 N95-33875
Applied Information Systems Research Program (AISRP) Workshop 3 meeting proceedings
[NASA-CR-199103] p 3239 N95-34218
Geographic information system for fusion and analysis of high-resolution remote sensing and ground data p 3240 N95-34224
Advanced data visualization and sensor fusion: Conversion of techniques from medical imaging to Earth science p 3242 N95-34236
A Spatial Analysis and Modeling System (SAMS) for environment management p 3243 N95-34239
REMOTE SENSORS
An ammonia monitor for the water industry p 3071 N95-33281
New calibration techniques for the Airborne Visible/Infrared Imaging Spectrometer (AVIRIS) p 3116 N95-33740
REMOTELY PILOTED VEHICLES
Fracture behavior of shallow cracks in full-thickness clad beams from an RPV wall section
[DE95-009175] p 3126 N95-32684
REPLACING
D3-D power supply, design, and development
[DE95-009603] p 3222 N95-32656
Proposed incorporation of mission-oriented flying qualities into MIL-STD-1797A
[AD-A294211] p 3055 N95-34306
REPORTS
Technology Reports of the Osaka University, vol. 45, nos. 2205-2216 p 3090 N95-32984
NASA/DOD Aerospace Knowledge Diffusion Research Project. Report 33: The technical communications practices of US aerospace engineers and scientists: Results of the phase 1 AIAA mail survey
[NASA-TM-110180] p 3239 N95-34217
REPRODUCTION (COPYING)
NASA wide electronic publishing system: Electronic printing and duplicating. Stage 3 evaluation report
[NASA-TM-104620] p 3237 N95-32922
Reducing cache misses in numerical applications using data relocation and prefetching
[AD-A293978] p 3182 N95-34455
Is the genetic algorithm a cooperative learner?
[AD-A294112] p 3193 N95-34499
RESEARCH
National Aeronautics and Space Administration (NASA)/American Society for Engineering Education (ASEE) Summer Faculty Fellowship Program, 1994, volume 1
[NASA-CR-188410] p 3248 N95-32418
RESEARCH AIRCRAFT
An Electronic Workshop on the Performance Seeking Control and Propulsion Controlled Aircraft Results of the F-15 Highly Integrated Digital Electronic Control Flight Research Program
[NASA-TM-104278] p 3050 N95-33009
An overview of integrated flight-propulsion controls flight research on the NASA F-15 research airplane p 3051 N95-33010
Performance seeking control program overview p 3051 N95-33011
F-15 propulsion system p 3051 N95-33012
PSC algorithm description p 3051 N95-33013
PSC implementation and integration p 3051 N95-33014
Minimum fuel mode evaluation p 3051 N95-33015
Minimum fan turbine inlet temperature mode evaluation p 3052 N95-33016
Maximum thrust mode evaluation p 3052 N95-33017
Performance seeking control excitation mode p 3052 N95-33019
Performance seeking control (PSC) for the F-15 highly integrated digital electronic control (HIDEC) aircraft p 3053 N95-33020
Design challenges encountered in the F-15 PCA flight test program p 3049 N95-33025
RESEARCH AND DEVELOPMENT
Air force office of scientific research. Research proposal
[AD-A293401] p 3252 N95-32473
Research and technology 1994: Annual report of the Marshall Space Flight Center
[NASA-TM-108470] p 3252 N95-33042
Budget estimates: Fiscal year 1994. Volume 1: Agency summary
[NASA-TM-110815] p 3244 N95-33069
Third International Workshop on Ion Mobility Spectrometry
[NASA-CP-3301] p 3069 N95-33265
IMS R and D program at Canada customs p 3070 N95-33273
Bibliography on cold regions science and technology: Volume 48, part 1
[AD-A293988] p 3243 N95-34420
Evaluation in context: ATC automation in the field p 3175 N95-34781
RESEARCH FACILITIES
Materials sciences programs: Fiscal year 1994
[DE95-011248] p 3211 N95-32483
Budget estimates: Fiscal year 1994. Volume 2: Construction of facilities
[NASA-TM-110816] p 3245 N95-33081
An ion-ion collisions system at KSU
[DE95-010820] p 3208 N95-33372
The Space Shuttle: America's team reaching for the future
[NASA-CR-199222] p 3058 N95-33728
International Meeting on Muon Science
[PB95-236014] p 3209 N95-34657
RESEARCH MANAGEMENT
Aviation security: Development of new security technology has not met expectations. Report to Congressional requesters
[GAO/RCED-94-142] p 3046 N95-32885
RESEARCH PROJECTS
National Aeronautics and Space Administration (NASA)/American Society for Engineering Education (ASEE) Summer Faculty Fellowship Program, 1994, volume 1
[NASA-CR-188410] p 3248 N95-32418
Materials sciences programs: Fiscal year 1994
[DE95-011248] p 3211 N95-32483

The Anglo-French Compact Laser Radar demonstrator programme p 3045 N95-32501
Covert Night/Day Operations for Rotorcraft (CONDOR) programme p 3046 N95-32505
The DLR research programme on an integrated multi sensor system for surface movement guidance and control p 3048 N95-33135
Third International Workshop on Ion Mobility Spectrometry
|NASA-CP-3301| p 3069 N95-33265
Review of the research activities of the Energy Research Unit in 1994
|PB95-235008| p 3151 N95-34656

RESERVOIRS
Design and operation of a thermionic converter in air
|DE95-010151| p 3149 N95-32645
Integral cesium reservoir: Design and transient operation
|DE95-010152| p 3211 N95-32647
Numerical thermal analyses of heat exchangers for the stirling engine application
|NASA-CR-199120| p 3110 N95-33398

RESIDUAL STRESS
Models for predicting damage evolution in metal matrix composites subjected to cyclic loading
|DE95-007734| p 3077 N95-32382
Experimental investigation of the separation of texture and residual stress induced anisotropy via oblique incidence acoustoelasticity p 3126 N95-33253
Stress relaxation in discontinuously reinforced composites
|DE95-010928| p 3064 N95-33704

RESIDUES
Gas chromatography/ion mobility spectrometry as a hyphenated technique for improved explosives detection and analysis p 3071 N95-33278
Application of the ionscan for the detection of methamphetamine and ephedrine in abondoned clandestine laboratories p 3072 N95-33284
An investigation of the chemistry of citric acid in military soldering applications
|AD-A295042| p 3105 N95-34796

RESIN MATRIX COMPOSITES
Wear resistant composite structure of vitreous carbon containing convoluted fibers
|DE95-011463| p 3063 N95-33062
Low velocity impact damage in carbon fiber/PEEK composite laminates
|ISBN-0-315-86546-6| p 3065 N95-33710

RESINS
The nature and fate of natural resins in the geosphere 6: Analysis of fossil resins from Axel Heiberg Island Canadian Arctic
|DE95-012212| p 3154 N95-33394

RESOLUTION
Zero modes of Gauss constraint in gaugeless reduction of Yang-Mills theory
|DE95-623676| p 3234 N95-32667
Signal processing for ION mobility spectrometers p 3073 N95-33289

RESONANCE
Doppleron resonances in the diffraction of atoms by an evanescent field
|DE95-619190| p 3204 N95-32622
Observation of KLM dielectronic recombination resonances in highly charged uranium ions
|DE95-010266| p 3207 N95-33219
Nonlinear analyses of storage ring lattices using one-turn maps
|DE95-012515| p 3213 N95-33335
The effect of phase advance errors between interaction points on beam halos
|DE95-012559| p 3214 N95-34023
Studies of halo distributions under beam-beam interaction
|DE95-012560| p 3214 N95-34024
Measurements of cross sections and resonance structures following electron-impact excitation/ionization of Na-like Kr and Xe
|DE95-011731| p 3230 N95-34438
Quantum transport
|AD-A294977| p 3235 N95-34589
RR lyrae variable stars in the CCD/Transit instrument survey
|AD-A294138| p 3246 N95-34753

RESONANCE FLUORESCENCE
Iron Boltzmann factor LIDAR: Proposed new remote-sensing technique for mesospheric temperature
|AD-A293568| p 3157 N95-34613

RESONANT FREQUENCIES
Minimum wakefield achievable by waveguide damped cavity
|DE95-012100| p 3095 N95-32616

RESONANT VIBRATION
Improved L-C resonant decay technique for Q measurement of quasilinear power inductors: New results for MPP and ferrite powdered cores
|NASA-CR-198373| p 3103 N95-33874
Acoustic attenuation and vibration damping materials
|AD-D017465| p 3201 N95-34444

RESONATORS
Laser gyroscopy tendencies and their analysis of development in Ukraine p 3092 N95-33133

RESOURCES MANAGEMENT
Raingauge network optimization and GIS: A case study of the Mananga basin. Communications of the Sanitary Engineering and Water Management Division
|PB95-214284| p 3157 N95-32891
Clearing-house mechanism to promote and facilitate technical and scientific cooperation under the UN Convention on Biological Diversity
|PB95-214557| p 3163 N95-33236

RESPIRATION
Noninvesive determination of Cardiac Output
|PB95-208310| p 3164 N95-32611
Sensitizing substances
|PB95-211256| p 3074 N95-33634
Prospect redux p 3133 N95-33758

RESPONSES
Stimulus-response compatibility
|PB95-214722| p 3167 N95-33237

RESTORATION
Chiral restoration in hot and/or dense matter
|DE95-012176| p 3204 N95-32621

RETAINING
Thermocapillary flow with evaporation and condensation and its effect on liquid retention in low-g fluid acquisition devices p 3109 N95-33256

RETARDING
Quantum transport
|AD-A294977| p 3235 N95-34589

RETINA
Ultrashort pulse laser effects in the primate eye
|AD-A295024| p 3164 N95-34789

RETRACTABLE EQUIPMENT
The 1994 TIMS airborne calibration experiment: Castaic Lake, California p 3117 N95-33797

RETROFITTING
Evaluation of a retrofit OH-58 pilot's seat to prevent back injury
|AD-A294895| p 3171 N95-34574

REVERSING
Smoothing during ion-assisted growth by transient ion beam-induced defects
|DE95-011021| p 3225 N95-32579

REYNOLDS EQUATION
Numerical studies of turbulent free surface flows and unsteady propeller flows
|AD-A294377| p 3112 N95-34343

REYNOLDS NUMBER
Flow and heat transfer behavior of non-Newtonian fluids in rectangular ducts p 3107 N95-32907

RHODIUM
Metal-ceramic interfaces: Overlayer-induced reconstruction and magnetism of 4d transition-metal monolayers
|DE95-011543| p 3075 N95-34483

RIGID ROTORS
Full-scale hingeless rotor performance and loads
|NASA-TM-110356| p 3048 N95-32699

RIGID STRUCTURES
Nonholonomic control of coupled spatial multibody systems p 3192 N95-33604
Rigid bodies for metal forming analysis with NIKE3D
|DE95-011740| p 3182 N95-33652

RING LASERS
Laser gyroscopy tendencies and their analysis of development in Ukraine p 3092 N95-33133
Application of advanced safety technique to ring laser gyro inertial navigation system integration p 3048 N95-33140

RING STRUCTURES
Response and failure of thick composite rings subjected to uniform external hydrostatic pressure or radial contraction p 3064 N95-33326

RISK
Approaches to implementing deterministic models in a probabilistic framework
|DE95-009483| p 3197 N95-32391
The background and theory of integrated risk management p 3236 N95-32431
X-ray-provoked non-Mendelian transgenerational oncodeterminants p 3163 N95-32731
A comparison of risk assessment techniques from qualitative to quantitative
|DE95-011430| p 3197 N95-33220
Chemical substances lists: A guide to the lists used in the Swedish Sunset Project. Supplement to report 13/94. Selecting multiproblem chemicals for risk reduction. A presentation of the Swedish Sunset Project
|PB95-211272| p 3073 N95-33328
Phthalic acid esters used as plastic additives. Volume 1: Ecotoxicological risk assessment. Volume 2: Comparisons of toxicological effects
|PB95-211280| p 3084 N95-33329
Risk assessment of polybrominated diphenyl ethers
|PB95-211306| p 3073 N95-33330

RIVERS
Raingauge network optimization and GIS: A case study of the Mananga basin. Communications of the Sanitary Engineering and Water Management Division
|PB95-214284| p 3157 N95-32891
Mineralogic variations in fluvial sediments contaminated by mine tailings as determined from AVIRIS data, Coeur D'Alene River Valley, Idaho p 3131 N95-33745
Intra-annual and inter-annual rainfall variability over East Asia, Southeast Asia, and South Asia
|AD-A294156| p 3158 N95-34757

ROBOT ARMS
Design and implementation of a two-axis micromanipulator to enhance the gripper positional accuracy of a single flexible link p 3123 N95-33252
Trajectory planning and control of kinematically redundant robotic manipulators p 3194 N95-34807

ROBOT CONTROL
Off-line programming using commerical CAD systems, and design criteria for manipulators with inherent accuracy p 3180 N95-32937
Design and implementation of a two-axis micromanipulator to enhance the gripper positional accuracy of a single flexible link p 3123 N95-33252
Motion and force control of coordinated robots
|ISBN-0-315-86323-4| p 3191 N95-33307
Self-organizing neural network and its applications to vision-guided robot motion coordination p 3191 N95-33324
Adaptive differential visual feedback for uncalibrated hand-eye coordination and motor control
|AD-A293607| p 3171 N95-34616
Trajectory planning and control of kinematically redundant robotic manipulators p 3194 N95-34807

ROBOT DYNAMICS
Self-organizing neural network and its applications to vision-guided robot motion coordination p 3191 N95-33324

ROBOT SENSORS
Adaptive differential visual feedback for uncalibrated hand-eye coordination and motor control
|AD-A293607| p 3171 N95-34616

ROBOTICS
On bootstrapping local search with trail-markers
|DE95-009835| p 3187 N95-32533
A study of space-rated connectors using a robot end-effector
|NASA-CR-199116| p 3121 N95-32675
Off-line programming using commerical CAD systems, and design criteria for manipulators with inherent accuracy p 3180 N95-32937

ROBOTS
On bootstrapping local search with trail-markers
|DE95-009835| p 3187 N95-32533
A study of space-rated connectors using a robot end-effector
|NASA-CR-199116| p 3121 N95-32675
Design and implementation of a two-axis micromanipulator to enhance the gripper positional accuracy of a single flexible link p 3123 N95-33252
Motion and force control of coordinated robots
|ISBN-0-315-86323-4| p 3191 N95-33307

ROBUSTNESS (MATHEMATICS)
Intervals in evolutionary algorithms for global optimization
|DE95-010866| p 3179 N95-32572
A robust control system for exact trajectory tracking p 3192 N95-33714

ROCK MECHANICS
Users' manual for LEHGC: A Lagrangian-Eulerian finite-element model of HydroGeoChemical transport through saturated-unsaturated media. Version 1.0
|DE95-010513| p 3179 N95-32543

ROCKET ENGINE DESIGN
Design of ETO propulsion turbine using CFD analyses
|NASA-CR-199085| p 3123 N95-32915

ROCKET FIRING
Fundamental phenomena on fuel decomposition and boundary-layer combustion processes with applications to hybrid rocket motors
|NASA-CR-199126| p 3061 N95-32932

ROCKS
Discrimination of alkalinity in granitoid Rocks: A potential TIMS application p 3138 N95-33798

ROLLER BEARINGS
Influence of backup bearings and support structure dynamics on the behavior of rotors with active supports
|NASA-CR-199080| p 3121 N95-32689
Dynamic behavior of a magnetic bearing supported jet engine rotor with auxiliary bearings
p 3122 N95-32691
Dynamic modelling and response characteristics of a magnetic bearing rotor system with auxiliary bearings
p 3122 N95-32692
Synchronous dynamics of a coupled shaft/bearing/housing system with auxiliary support from a clearance bearing: Analysis and experiment
p 3122 N95-32693
ROOM TEMPERATURE
Development of improved p-type Si-20 at. %Ge by addition of fullerite
|DE95-010230| p 3066 N95-32394
A study of luminescence and absorption spectra of GaP
|DE95-614122| p 3202 N95-32524
ROTARY STABILITY
The effect of labyrinth seals on the dynamics of turbomachinery p 3122 N95-32752
Influence of non classical friction on the rubbing and impact behavior of rotor dynamic systems
p 3122 N95-32906
ROTARY WING AIRCRAFT
Low-Level and Nap-of-the-Earth (NOE) night operations
|AGARD-CP-563| p 3042 N95-32486
Covert Night/Day Operations for Rotorcraft (CONDOR) programme p 3046 N95-32505
Transmittance characteristics of US Army rotary-wing aircraft transparencies
|AD-A295035| p 3049 N95-34793
ROTATING DISKS
Experimental and numerical analysis of controlled impinging liquid jets p 3109 N95-33257
ROTATING SHAFTS
Synchronous dynamics of a coupled shaft/bearing/housing system with auxiliary support from a clearance bearing: Analysis and experiment
p 3122 N95-32693
Full-scale hingeless rotor performance and loads
|NASA-TM-110356| p 3048 N95-32699
Actively controlled shaft seals for aerospace applications
|NASA-CR-4678| p 3061 N95-33156
Fluid dynamometer having fluid characteristic power absorption adjustment capability
|AD-D017489| p 3116 N95-34426
ROTATION
Sinuous oscillations and steady warps of polytropic disks
|DE95-013473| p 3247 N95-34216
Flow and heat transfer in rotating curved pipes
p 3040 N95-34545
ROTOR AERODYNAMICS
Full-scale hingeless rotor performance and loads
|NASA-TM-110356| p 3048 N95-32699
Direct analysis of transonic rotor noise with CFD technique p 3040 N95-34549
ROTOR BLADES
Full-scale hingeless rotor performance and loads
|NASA-TM-110356| p 3048 N95-32699
ROTOR DYNAMICS
Influence of backup bearings and support structure dynamics on the behavior of rotors with active supports
|NASA-CR-199080| p 3121 N95-32689
Steady-state dynamic behavior of an auxiliary bearing supported rotor system p 3121 N95-32690
Dynamic behavior of a magnetic bearing supported jet engine rotor with auxiliary bearings
p 3122 N95-32691
Dynamic modelling and response characteristics of a magnetic bearing rotor system with auxiliary bearings
p 3122 N95-32692
Synchronous dynamics of a coupled shaft/bearing/housing system with auxiliary support from a clearance bearing: Analysis and experiment
p 3122 N95-32693
The effect of labyrinth seals on the dynamics of turbomachinery p 3122 N95-32752
Influence of non classical friction on the rubbing and impact behavior of rotor dynamic systems
p 3122 N95-32906
ROTORS
Influence of backup bearings and support structure dynamics on the behavior of rotors with active supports
|NASA-CR-199080| p 3121 N95-32689
Steady-state dynamic behavior of an auxiliary bearing supported rotor system p 3121 N95-32690
Dynamic behavior of a magnetic bearing supported jet engine rotor with auxiliary bearings
p 3122 N95-32691
Dynamic modelling and response characteristics of a magnetic bearing rotor system with auxiliary bearings
p 3122 N95-32692
Synchronous dynamics of a coupled shaft/bearing/housing system with auxiliary support from a clearance bearing: Analysis and experiment
p 3122 N95-32693
ROUTES
Optimum Routeing: Analytical constraint of search space p 3044 N95-32493
RUBBER
Method of installing a metallic threaded insert in a composite/rubber panel
|AD-D017522| p 3065 N95-34620
RUBY LASERS
Laser beaming demonstrations at the Starfire Optical Range
|DE95-007747| p 3120 N95-34811
RUNGE-KUTTA METHOD
A multigrid incompressible NS solver
p 3036 N95-34517
Direct numerical simulation of incompressible homogeneous isotropic turbulence using compressible Navier-Stokes equations p 3037 N95-34529
Effect of schemes on numerical simulations of shock wave reflection p 3038 N95-34531
Numerical simulation of two-dimensional compressible inviscid flow on unstructured grid system
p 3041 N95-34557
Parallel computation for two dimensional incompressible flow on array of transputers p 3042 N95-34558
RUNWAYS
Low-level data fusion for landing runways detection
p 3048 N95-33136
RUTHENIUM
Comparison of lead zirconate titanate thin films on ruthenium oxide and platinum electrodes
|DE95-617597| p 3082 N95-32710
Metal-ceramic interfaces: Overlayer-induced reconstruction and magnetism of 4d transition-metal monolayers
|DE95-011543| p 3075 N95-34483

S

S WAVES
Faddeev calculations of p(mu)+p collisions: Effect of hyperfine splitting on the cross sections
|DE95-007838| p 3203 N95-32583
Frequency response of a TeO2 slow shear wave acousto-optic cell exposed to radiation
|DE95-009588| p 3226 N95-32589
SAFETY
Fusion Safety Program annual report, fiscal year 1994
|DE95-008872| p 3221 N95-32588
Analysis of safety requirements in the context of system faults and human errors
|PB95-236105| p 3171 N95-34658
SAFETY DEVICES
Aviation security: Development of new security technology has not met expectations. Report to Congressional requesters
|GAO/RCED-94-142| p 3046 N95-32885
SALICYLATES
The effects of CO2 on the negative reactant ions of IMS p 3069 N95-33267
SAMPLING
Off-training-set error for the Gibbs and the Bayes optimal generalizers
|DE95-006344| p 3187 N95-32375
The effect of sample holder material on ion mobility spectrometry reproducibility p 3071 N95-33282
SAN JUAN MOUNTAINS (CO)
Remote mineral mapping using AVIRIS data at Summitville, Colorado and the adjacent San Juan Mountains p 3134 N95-33761
SANDS
Preliminary study of Kelso Dunes using AVIRIS, TM, and AIRSAR p 3136 N95-33773
SANDWICH STRUCTURES
Perpendicular magnetic behavior of ultra-thin Co sandwiches
|DE95-010611| p 3083 N95-32819
Unusual behavior in the magnetic anisotropy of ultra-thin Co sandwiches: The role of Au underlayers
|DE95-010612| p 3229 N95-33641
SAPPHIRE
Fiber coatings for brittle matrix composites
p 3065 N95-34808
SATELLITE COMMUNICATION
OPEX: Second Workshop of the OLYMPUS propagation experimenters. Volume 1: Reference book on attenuation measurement and prediction
|ESA-WPP-083-VOL-1| p 3096 N95-32747
OPEX Second Workshop of the OLYMPUS Propagation Experimenters. Volume 2: Reference book on depolarisation
|ESA-WPP-083-VOL-2| p 3096 N95-32748
OPEX Second Workshop of the OLYMPUS Propagation Experimenters. Volume 3: Reference book on radiometry and meteorological measurements
|ESA-WPP-083-VOL-3| p 3096 N95-32749
OPEX Second Workshop of the OLYMPUS Propagation Experimenters. Volume 4: Reference book on radar
|ESA-WPP-083-VOL-4| p 3096 N95-32750
A 75 watt, 59 to 64 GHz space TWT
|NASA-CR-195450| p 3104 N95-33915
SATELLITE CONTROL
INMARSAT TT&C and communications network and the Beijing INMARSAT Station
|AD-A294163| p 3100 N95-34760
SATELLITE DESIGN
Development of a composite satellite structure for FORTE
|DE95-009416| p 3058 N95-32713
Thermal control technology of communications satellite
|AD-A294249| p 3059 N95-34493
SATELLITE IMAGERY
Multispectral image correlation for air-to-ground targeting p 3043 N95-32489
Canopy reflectance modelling of semiarid vegetation
|NASA-CR-199117| p 3142 N95-32676
Correction of thin cirrus effects in AVIRIS images using the sensitive 1.375-micron cirrus detecting channel
p 3131 N95-33748
An interactive environment for the analysis of large Earth observation and model data sets p 3239 N95-34219
A land-surface testbed for EOSDIS
p 3158 N95-34223
A distributed analysis and visualization system for model and observational data p 3243 N95-34240
DataHub sponsored analysis p 3243 N95-34242
SATELLITE NAVIGATION SYSTEMS
Effects of the specific military aspects of satellite navigation on the civil use of GPS/GLONASS
p 3048 N95-33134
SATELLITE OBSERVATION
Cooling tower and plume modeling for satellite remote sensing applications
|DE95-012000| p 3143 N95-33849
SATELLITE SURFACES
Operation of the computer model for microenvironment atomic oxygen exposure
|NASA-CR-198190| p 3059 N95-33264
Operation of the computer model for microenvironment solar exposure
|NASA-CR-198189| p 3059 N95-33890
SATELLITE TEMPERATURE
Thermal design of returnable satellites
|AD-A294113| p 3059 N95-34500
SATELLITE TRACKING
INMARSAT TT&C and communications network and the Beijing INMARSAT Station
|AD-A294163| p 3100 N95-34760
SATURATION
Measurement of gain saturation on Nd: Doped phosphate laser glasses
|REPT-2210| p 3090 N95-32990
SCALARS
Chiral restoration in hot and/or dense matter
|DE95-012176| p 3204 N95-32621
Construction and analysis of difference approximation for scalar conservation laws and its consistency with entropy condition using Boltzmann-like approach
p 3036 N95-34519
SCALE MODELS
Subscale study of engine bellmouth inlet vortices in test cell R1D
|AD-A294993| p 3113 N95-34818
SCALING LAWS
Scaling law for the Upsilon(4S) yields bar-BB and psi(3770) yields bar-DD decay constants from effective sum rules
|DE95-620538| p 3203 N95-32554
SCANNING
A low diffraction beam technique for scanning in the shallow ocean
|DE95-011742| p 3159 N95-33410
SCANNING ELECTRON MICROSCOPY
Interfacial composition analysis of silicon nitride whisker reinforced oxynitride glass systems
|DE95-012895| p 3085 N95-33635
SCANNING TUNNELING MICROSCOPY
The structure of ion track in Solids produced by ions with high level inelastic energy losses
|DE95-620842| p 3205 N95-32625
Quantum mechanical capacitance in a scanning tunneling microscope
|DE95-011272| p 3230 N95-33880

SCATTERING
The 8th Winterschool on New Developments in Solid State Physics
[AD-A290163] p 3227 N95-32677
Theory of magneto-optics and circular magnetic x-ray dichroism
[DE95-010129] p 3080 N95-33700
Comparison of theoretical predictions with field observations for a simple forward scattering sensor
[AD-A294948] p 3219 N95-34576
Extreme broadening of stimulated Raman scattered light from high intensity laser plasma interactions
[AD-A294165] p 3120 N95-34761

SCATTERING CROSS SECTIONS
Physics of the CEM92M Code
[DE95-623579] p 3202 N95-32477
Inversion of electron-water elastic scattering data
[DE95-619323] p 3204 N95-32623

SCATTERING FUNCTIONS
Comparison of theoretical predictions with field observations for a simple forward scattering sensor
[AD-A294948] p 3219 N95-34576

SCHEDULING
Cost-effective data-parallel load balancing
[DE95-010985] p 3186 N95-33403

SCHOTTKY DIODES
Monolithic diode arrays for quasioptical millimeter wave beam steering
[AD-A294256] p 3100 N95-34460
Development of thin film diamond based integrated circuit technology
[AD-A294519] p 3231 N95-34478
Growth and structure of MBE-Deposited iridium silicide
[AD-A295033] p 3232 N95-34792

SCHROEDINGER EQUATION
The method of integration of the nonlinear Schroedinger equation with a source
[DE95-623601] p 3195 N95-32479
Transparent potential perturbations on lattices and in the periodical structures. Elements of the Qualitative Theory of Wave Motion Over the Channels
[DE95-623602] p 3225 N95-32480
The fully correlated two-electron problem on a numerical lattice
[DE95-010280] p 3205 N95-32650
Counterexample to the lieb-thirring conjecture concerning the moments of the eigenvalues of the Schroedinger operator
[PB95-212197] p 3195 N95-32890
Lieb-thirring constants L(sub gamma,1) for gamma greater than or equal to 1/2
[PB95-212171] p 3196 N95-33234

SCIENTIFIC VISUALIZATION
Visualization methods for high-resolution, transient, 3-D, finite element situations
[DE95-009479] p 3179 N95-32390
Off-line programming using commerical CAD systems, and design criteria for manipulators with inherent accuracy p 3180 N95-32937
Applied Information Systems Research Program (AISRP) Workshop 3 meeting proceedings
[NASA-CR-199103] p 3239 N95-34218
Construction of an advanced software tool for planetary atmospheric modeling p 3184 N95-34225
Knowledge-based assistance for science visualization and analysis using large distributed databases p 3241 N95-34227
Experimenter's laboratory for visualized interactive science p 3184 N95-34228
A distributed system for visualizing and analyzing multivariate and multidisciplinary data p 3241 N95-34230
The Grid Analysis and Display System (GRADS): A practical tool for Earth science visualization p 3241 N95-34231
Advanced data visualization and sensor fusion: Conversion of techniques from medical imaging to Earth science p 3242 N95-34236
SAVS: A Space Analysis and Visualization System p 3242 N95-34238
A Spatial Analysis and Modeling System (SAMS) for environment management p 3243 N95-34239
A distributed analysis and visualization system for model and observational data p 3243 N95-34240
DataHub: Science data management in support of interactive exploratory analysis p 3243 N95-34241
Range graphics benchmark
[AD-A293541] p 3057 N95-34606

SCINTILLATION
ABLEX: High altitude laser propagation experiment
[AD-A294914] p 3120 N95-34592

SCINTILLATION COUNTERS
Efficiency of modified UA1 jet reconstruction algorithm in PP, PA and AA collisions at STAR
[DE95-009918] p 3212 N95-32665

SEA ICE
Ice-ocean four dimensional structure and dynamics
[AD-A294017] p 3160 N95-34375
Bibliography on cold regions science and technology: Volume 48, part 1
[AD-A293988] p 3243 N95-34420
Bibliography on cold regions science and technology: Volume 48, part 2
[AD-A293993] p 3243 N95-34421
Photobiology and optical properties of planktonic and sea ice microalgae in the high arctic
[AD-A294002] p 3160 N95-34457

SEA STATES
An experimental study of collective sea state modes of deep water surface gravity waves
[AD-A294007] p 3160 N95-34372

SEA SURFACE TEMPERATURE
DataHub sponsored analysis p 3243 N95-34242
Turbulent heat flux measurements over the Greenland, Norwegian and Barents seas
[AD-A294129] p 3157 N95-34751

SEALING
Split gasket attachment method statement of government interest
[AD-D017443] p 3123 N95-32924

SEALS (STOPPERS)
Actively controlled shaft seals for aerospace applications
[NASA-CR-4678] p 3061 N95-33156

SEAPLANES
Sea wave parameters, small altitudes and distances measurers design for movement control systems of ships, wing-in-surface effect crafts and seaplanes p 3094 N95-33141

SEARCHING
Optimum Routeing: Analytical constraint of search space p 3044 N95-32493
Genetic algorithms as global random search methods
[NASA-CR-199088] p 3188 N95-32767

SEATS
Increase of High-sustained +G(z) tolerance at the expense of pilot's working posture change p 3165 N95-34056
Evaluation of a retrofit OH-58 pilot's seat to prevent back injury
[AD-A294895] p 3171 N95-34574

SECONDARY FLOW
Flow and heat transfer behavior of non-Newtonian fluids in rectangular ducts p 3107 N95-32907
Design of secondary flow control cascade using numerical simulation p 3034 N95-34507
The effect of buoyancy on flow and heat transfer in curved pipes p 3037 N95-34528

SECONDARY ION MASS SPECTROMETRY
Analysis of LDEF experiment AO187-2 chemical and isotopic measurements of micrometeoroids by secondary ion mass spectrometry
[NASA-CR-198849] p 3246 N95-32913

SEDIMENTS
The nature and fate of natural resins in the geosphere 6: Analysis of fossil resins from Axel Heiberg Island Canadian Arctic
[DE95-012212] p 3154 N95-33394
Mineralogic variations in fluvial sediments contaminated by mine tailings as determined from AVIRIS data, Coeur D'Alene River Valley, Idaho p 3131 N95-33745
A conflict of water and fire: Remote sensing imagery of the Uinkaret Volcanic Field, Grand Canyon, Arizona p 3117 N95-33795
The CE-QUAL-ICM three-dimensional eutrophication model, release version 1.0
[AD-A294258] p 3160 N95-34461
Underwater acoustic field extrapolation: Theory and sensitivity analysis
[AD-A294925] p 3201 N95-34595

SEEBECK EFFECT
Development of improved p-type Si-20 at. %Ge by addition of fullerite
[DE95-010230] p 3066 N95-32394

SEGMENTS
Production asymmetries in x(sub f) and P(sup 2)(sub t) for D(sup +/-) mesons
[DE95-007207] p 3201 N95-32379

SEISMIC WAVES
Seismic response analysis of soil-structure interaction systems in the time domain
[REPT-2212] p 3091 N95-32992
Modeling seismic wave propagation in heterogeneous materials using finite elements p 3156 N95-34283

SEISMOLOGY
Seismic response analysis of soil-structure interaction systems in the time domain
[REPT-2212] p 3091 N95-32992
Modeling seismic wave propagation in heterogeneous materials using finite elements p 3156 N95-34283

SELECTION
The choice: Welding with CO2 or Nd:YAG lasers
[DE95-011825] p 3124 N95-33834
Presentation of a Swedish study program concerning recruitment, selection and training of student air traffic controllers: The MRU project phase 1 p 3167 N95-34775

SELECTORS
Crosspoint analog data selector
[AD-D017482] p 3104 N95-34425

SELENIUM
Advanced far infrared detector and double donor studies in Ge
[DE95-011261] p 3247 N95-33625

SELF FOCUSING
Propagation of spatial solitons generated by Gaussian beams in a non-linear Kerr medium
[IFTR-9/1995] p 3206 N95-32921

SELF LUBRICATING MATERIALS
Wear resistant composite structure of vitreous carbon containing convoluted fibers
[DE95-011463] p 3063 N95-33062

SEMANTICS
Sleep sets method for partial order verification of concurrent systems
[PB95-236121] p 3183 N95-34655

SEMICONDUCTOR DEVICES
Applications of organic and polymer nonlinear optical materials in optics computations
[AD-A293088] p 3215 N95-32957
Discrete modeling of optical pulse propagation in nonlinear media
[DE95-011515] p 3216 N95-34020
Fabrication technology and measurement of coupled quantum dot devices
[AD-A294853] p 3231 N95-34569

SEMICONDUCTOR JUNCTIONS
Quantum mechanical capacitance in a scanning tunneling microscope
[DE95-011272] p 3230 N95-33880

SEMICONDUCTOR LASERS
Read/write module for high capacity memory disk
[AD-A294946] p 3178 N95-34745
Optical logic implementation in composite biled/bild circuits
[AD-A294160] p 3105 N95-34758

SEMICONDUCTORS (MATERIALS)
Materials sciences programs: Fiscal year 1994
[DE95-011248] p 3211 N95-32483
A study of luminescence and absorption spectra of GaP
[DE95-614122] p 3202 N95-32524
Photon echoes from the absorption continuum of a semiconductor
[DE95-011274] p 3101 N95-32596
Observation of intraband coherence in the nonlinear optical response of gallium arsenide
[DE95-011281] p 3227 N95-32600
Magnetostriction and thermal expansion of the Kondo semiconductor Ce3Bi4Pt3
[DE95-011975] p 3229 N95-33386
Development of environmentally conscious cleaning process for leadless chip carrier assemblies
[DE95-010186] p 3154 N95-33638
Quantum cylinder fiber light amplifier
[AD-A294197] p 3217 N95-34300
Low temperature growth of thin films by high kinetic energy supersonic molecular beams
[AD-A294516] p 3086 N95-34476
Fabrication of optical channel waveguides in the GaAs/AlGaAs system by MeV ion beam bombardment
[DE95-008973] p 3218 N95-34480
Nucleation, propagation, electronic levels and elimination of misfit dislocations in 3-5 semiconductor interfaces
[DE95-011595] p 3231 N95-34485
Fundamental surface chemistry of GaAs OMVPE
[DE95-011606] p 3231 N95-34486
Si-device-related interface research
[AD-A293587] p 3076 N95-34615
International Meeting on Muon Science
[PB95-236014] p 3209 N95-34657
Electron and hole transport in compound semiconductors
[AD-A295003] p 3233 N95-34822

SENSITIVITY
Solvent effects on the electronic spectrum of R hardt's dye
[AD-A293667] p 3067 N95-32804
Design and analysis of transient nonlinear coupled systems p 3199 N95-33292
Measurement and modelling of structure sensitive magnetic properties of material
[DE95-010128] p 3080 N95-33699

Correction of thin cirrus effects in AVIRIS images using the sensitive 1.375-micron cirrus detecting channel
p 3131 N95-33748
Read/write module for high capacity memory disk
[AD-A294946] p 3178 N95-34745

SENSITIZING
Sensitizing substances
[PB95-211256] p 3074 N95-33634

SENSORIMOTOR PERFORMANCE
The role of the vestibular system in manual target localization p 3166 N95-32422
The virtual sailor: Synthetic humans for virtual environments
[AD-A293560] p 3166 N95-34610

SENSORS
Airborne Visible/Infrared Imaging Spectrometer (AVIRIS): Sensor improvements for 1994 and 1995
p 3117 N95-33769

SENSORY PERCEPTION
The role of the vestibular system in manual target localization p 3166 N95-32422

SEPARATED FLOW
Boundary layer transition studies
[NASA-CR-198983] p 3106 N95-32454
A nonlinear vortex lattice method for unsteady flow with separated vortex
[DLR-FB-94-32] p 3106 N95-32787
Calculation for aerodynamic characteristics on delta wing with leading-edge separated vortex effect using boundary element method p 3037 N95-34524
Numerical simulations of dynamic stall phenomena in low speed flows p 3040 N95-34546

SEQUENCING
High resolution electrospray mass spectrometry with a magnetic sector instrument: Accurate mass measurement and peptide sequencing
[AD-A293564] p 3076 N95-34611

SERVICE LIFE
Application of fuzzy technology to risk-based design and decision problems
[DE95-006815] p 3178 N95-32378
Thermal control technology of communications satellite
[AD-A294249] p 3059 N95-34493

SEWAGE TREATMENT
An ammonia monitor for the water industry
p 3071 N95-33281

SHADES
Topography from shading and stereo
p 3241 N95-34229

SHAFTS (MACHINE ELEMENTS)
Static pressure drop by swirling flow of an internal cooling air system through a turbine shaft p 3042 N95-34560

SHAKERS
Operations manual for a compact electromechanical fatigue testing machine
[DSTO-GD-0036] p 3115 N95-32927

SHAPE CONTROL
Analysis and finite element approximation of an optimal shape control problem for the steady-state Navier-Stokes equations p 3112 N95-34285

SHAPE MEMORY ALLOYS
Micromechanics of composites with shape memory alloy fibers in uniform thermal fields
[NASA-TM-107011] p 3063 N95-33210
Effect of phase transformations on the mechanical properties of a multiphase alloy based on NiAl + Fe
[DE95-010119] p 3079 N95-33217

SHAPES
Size, shape, and crystallinity of luminescent structures in oxidized Si nanoclusters and H-passivated porous Si
[DE95-012322] p 3229 N95-33628
Multiple-beam pulse shaping and preamplification
[DE95-011738] p 3216 N95-33651
Non-smooth optimization algorithms, system theory and software tools
[AD-A294944] p 3183 N95-34605

SHEAR FLOW
Very large eddy simulations of spatially evolving supersonic turbulent shear layers p 3110 N95-33606
DSMC method applied for reacting gas flows
p 3035 N95-34509

SHEAR LAYERS
Large eddy simulation of turbulent vortices and mixing layers p 3109 N95-33340
Very large eddy simulations of spatially evolving supersonic turbulent shear layers p 3110 N95-33606

SHEAR STRENGTH
Electron beam joining of structural ceramics
[DE95-012521] p 3085 N95-34022

SHEAR STRESS
Shock properties of high-strength ceramics
[DE95-007731] p 3082 N95-32380
Ductile damage model with void coalescence
[DE95-007855] p 3125 N95-32385
Tests of adhesives used for plate bonding of ATLAS tile-cal hadron calorimeter
[DE95-009917] p 3082 N95-32664
The linear elastic biaxial response of plain-woven meshes p 3064 N95-33468

SHEATHS
Mathematical modelling in plasma physics
[AD-A294972] p 3224 N95-34586

SHIELDING
Analysis of evaporation in laser welding
[REPT-2207] p 3090 N95-32987

SHOCK ABSORBERS
Energy absorption device for shock loading
[AD-D017476] p 3124 N95-34449

SHOCK FRONTS
Shock properties of high-strength ceramics
[DE95-007731] p 3082 N95-32380

SHOCK LOADS
Shock properties of high-strength ceramics
[DE95-007731] p 3082 N95-32380

SHOCK TUNNELS
Numerical simulation of high enthalpy shock tunnel
p 3035 N95-34514

SHOCK WAVE INTERACTION
Fifth International Conference on Hyperbolic Problems, Theory, Numerics, Applications: Abstracts
[DE95-008173] p 3194 N95-32389
Seismic response analysis of soil-structure interaction systems in the time domain
[REPT-2212] p 3091 N95-32992
Numerical simulation of supersonic flow using a new analytical bleed boundary condition
[NASA-CR-198368] p 3054 N95-33208
Vorticity in shock-accelerated density-stratified interfaces: An analytical and computational study
p 3111 N95-33607
Numerical simulation of interaction between shock wave and density interface p 3039 N95-34543
Studies of hypersonic boundary layer behavior
[AD-A294137] p 3113 N95-34752

SHOCK WAVE PROPAGATION
Structure of weak shock waves in bubbly liquid
p 3037 N95-34527
Numerical simulation of interaction between shock wave and density interface p 3039 N95-34543

SHOCK WAVES
Shock properties of high-strength ceramics
[DE95-007731] p 3082 N95-32380
The role of dynamic experimentation for computation analysis
[DE95-007733] p 3125 N95-32381
Simulation of hypervelocity impact on massively parallel supercomputer
[DE95-007735] p 3184 N95-32383
Near-limit drop deformation and secondary breakup
p 3107 N95-32902
Historical detection of atmospheric impacts by large bolides using acoustic-gravity waves
[DE95-010864] p 3246 N95-33211
Energy absorption device for shock loading
[AD-D017476] p 3124 N95-34449
A study of supersonic mixing flow field with ramp injector p 3035 N95-34512
Structure of weak shock waves in bubbly liquid
p 3037 N95-34527

SHORT WAVE RADIATION
Comparison of seasonal and zonal patterns of the direct and indirect radiative forcing of climate by aerosols
[DE95-010896] p 3153 N95-33192

SHUTTLE IMAGING RADAR
Geographic information system for fusion and analysis of high-resolution remote sensing and ground data
p 3240 N95-34224

SIGNAL ANALYSIS
Signal processing for ION mobility spectrometers
p 3073 N95-33289

SIGNAL ANALYZERS
RASSP benchmark 1 technical description. Revision 1
[AD-A293030] p 3096 N95-32773

SIGNAL DETECTION
A digital boxcar integrator for IMS spectra
p 3072 N95-33288

SIGNAL DETECTORS
Vertical velocity ambiguity resolution method
[AD-D017481] p 3201 N95-34424

SIGNAL GENERATORS
Arbitrary waveform generator
[AD-D017451] p 3097 N95-32925
Laser-based ultrasonics by dual-probe interferometer detection and narrow-band ultrasound generation
p 3118 N95-33464

SIGNAL MEASUREMENT
A 30-pair thin film thermoelectric pile
[AD-A294058] p 3151 N95-34468

SIGNAL PROCESSING
Frequency response of a TeO2 slow shear wave acousto-optic cell exposed to radiation
[DE95-009588] p 3226 N95-32589
RASSP benchmark 1 technical description. Revision 1
[AD-A293030] p 3096 N95-32773
Third International Workshop on Ion Mobility Spectrometry
[NASA-CP-3301] p 3069 N95-33265
Signal processing for ION mobility spectrometers
p 3073 N95-33289
Parallel solution of large-scale nonlinear optimization
[AD-A294372] p 3186 N95-34340
Vertical velocity ambiguity resolution method
[AD-D017481] p 3201 N95-34424
Channel equalized DC squid flux-locked loop
[AD-D017469] p 3104 N95-34446
Space probe data processing
[AD-A294124] p 3058 N95-34744
Numerical and symbolic algorithms for application specific signal processing
[AD-A294125] p 3100 N95-34749

SIGNAL TO NOISE RATIOS
Spectral identification of minerals using imaging spectrometry data: Evaluating the effects of signal to noise and spectral resolution using the tricorder algorithm
p 3136 N95-33772
Triple invariant optical pattern recognition using circular harmonic synthetic filters
[AD-A294253] p 3217 N95-34459
Applied research on liquid crystal spatial modulators in Hadamard transform spectrometers. Quick and accurate decoding methods
[AD-A294152] p 3219 N95-34756

SIGNATURE ANALYSIS
Mapping target signatures via partial unmixing of AVIRIS data p 3129 N95-33737

SIGNATURES
Grayling 2 information base for generation of synthetic thermal infrared scenes
[AD-A294956] p 3100 N95-34578

SILICA GEL
Characterization of microenvironment polarity and solvent accessibility of polysilsesquioxane xerogels by the fluorescent probe technique
[DE95-011874] p 3062 N95-33835

SILICA GLASS
Efficient pockel's modulators in optical fibers
[AD-A294009] p 3217 N95-34374
Laser induced diffusion of ion-implanted bismuth in fused silica
[DE95-012869] p 3230 N95-34443

SILICATES
Glass science tutorial lecture no. 6: The melting of silicate glasses, a review of selected topics
[DE95-010199] p 3084 N95-33218

SILICIDES
Growth and structure of MBE-Deposited iridium silicide
[AD-A295033] p 3232 N95-34792

SILICON
Damage formation in silicon irradiated by heavy ions with energy more than 1 MeV/a.m.u.
[DE95-623968] p 3204 N95-32610
Proton-induced fragmentation of carbon at energies below 100 MeV p 3161 N95-32720
Radiative interactions with micromachined surfaces: Spectral polarized emittance
[DE95-011455] p 3097 N95-33061
Dual-use micromechanical inertial sensors
p 3092 N95-33132
Development of silicon drift detectors for strangeness measurements
[DE95-012366] p 3208 N95-33380
Size, shape, and crystallinity of luminescent structures in oxidized Si nanoclusters and H-passivated porous Si
[DE95-012322] p 3229 N95-33628
In situ surface roughness measurement during PECVD diamond film growth
[DE95-013411] p 3230 N95-34215
Si-device-related interface research
[AD-A293587] p 3076 N95-34615
International Meeting on Muon Science
[PB95-236014] p 3209 N95-34657

SILICON ALLOYS
Fabrication of improved SiGe alloys for an 18-couple module test
[DE95-010238] p 3060 N95-32396

SILICON CARBIDES
Evaluation of strength properties of developed SiC/C compositionally gradient graphite materials
[DE95-737271] p 3063 N95-32711
Low strain behaviour of a particulate reinforced aluminum alloy
[ISBN-0-315-84906-1] p 3078 N95-32935

A study of the effect of grain size on the ballistic performance of silicon carbide
[DE95-011724] p 3126 N95-33068
Stress relaxation in discontinuously reinforced composites
[DE95-010928] p 3064 N95-33704
SILICON DIOXIDE
Zeolite membranes for gas separations
[DE95-012984] p 3068 N95-33224
Influence of processing variables on the structure and properties of ZnO films
[DE95-011494] p 3084 N95-33405
Characterization of microenvironment polarity and solvent accessibility of polysilsesquioxane xerogels by the fluorescent probe technique
[DE95-011874] p 3062 N95-33835
Development of 1.06 micron high efficiency antireflective coating
[AD-A294161] p 3219 N95-34759
SILICON NITRIDES
High-speed, low-damage grinding of advanced ceramics, phase 1
[DE95-011241] p 3085 N95-33425
Interfacial composition analysis of silicon nitride whisker reinforced oxynitride glass systems
[DE95-012895] p 3085 N95-33635
Electron beam joining of structural ceramics
[DE95-012521] p 3085 N95-34022
SILICON OXIDES
TiO2/SiO2 and ZrO2/SiO2 multilayer media film optical loss and laser damage study
[AD-A294192] p 3217 N95-34298
SILVER
Optical anisotropy of (110) surfaces of Ag and Cu
[DE95-010130] p 3229 N95-33637
SIMD (COMPUTERS)
Elementary benchmarks of the NWT computer system and program performance p 3038 N95-34532
SIMULATED ANNEALING
Intervals in evolutionary algorithms for global optimization
[DE95-010866] p 3179 N95-32572
SIMULATION
Simulation of hypervelocity impact on massively parallel supercomputer
[DE95-007735] p 3184 N95-32383
Charm decays and high energy photoproduction
[DE95-010165] p 3201 N95-32393
Modeling of DC spacecraft power systems p 3062 N95-32423
SeaWiFS technical report series. Volume 15: The simulated SesWiFS data set, version 2
[NASA-TM-104566-VOL-15] p 3158 N95-32545
Large-eddy simulation of the development of stably-stratified atmospheric boundary layers over cool flat surfaces
[DE95-009574] p 3156 N95-32697
Evaluation of conductive, radiative, chemical, and convective heat transfer in complex systems using a fast-running, implicit, lumped-capacitance formulation
[DE95-011889] p 3111 N95-33837
Lattice Polymer Automata
[DE95-011980] p 3062 N95-33848
Numerical simulation of high enthalpy shock tunnel p 3035 N95-34514
An unsteady simulation of a centrifugal compressor stage using the NWT p 3038 N95-34536
Vector-parallel simulations of transonic wind tunnel flows about a fully configured model of aircraft p 3039 N95-34538
A simulation of damping process of pendulum motion due to aerodynamic forces p 3041 N95-34551
Formation of high density cores in molecular cloud p 3041 N95-34553
Some issues in nonlinear programming algorithms for problems with simulation constraints
[AD-A294932] p 3182 N95-34598
SIMULATORS
Electron and hole transport in compound semiconductors
[AD-A295003] p 3233 N95-34822
SINGLE CRYSTALS
Anisotropic magnetization of HoNi2B2C
[DE95-010239] p 3198 N95-32397
Numerical analysis of the ultraprecision machining of copper
[DE95-007857] p 3089 N95-32585
The structure of ion track in Solids produced by ions with high level inelastic energy losses
[DE95-620942] p 3205 N95-32625
Peak effect and flux pinning in YBa2Cu3O(7-(delta)) single crystals
[DE95-010126] p 3228 N95-32959
Development of thin film diamond based integrated circuit technology
[AD-A294519] p 3231 N95-34478
Growth of GaN single-crystal boules
[AD-A294976] p 3232 N95-34588
Surface chemistry of diamond single crystals
[AD-A294150] p 3232 N95-34755
Multilayer optics for soft x-rays
[AD-A295030] p 3219 N95-34791
SINGLE ENGINE AIRCRAFT
Low-order nonlinear dynamic model of IC engine-variable pitch propeller system for general aviation aircraft
[NASA-TM-107006] p 3050 N95-32916
SINGLE STAGE TO ORBIT VEHICLES
Implementation of a Single-Stage-To-Orbit (SSTO) model for stability and control analysis p 3059 N95-32432
SINGULAR INTEGRAL EQUATIONS
A posteriori pointwise error estimates for the boundary element method
[DE95-008099] p 3194 N95-32388
SIS (SUPERCONDUCTORS)
Properties of high-T(sub c) Josephson junctions with Y(0.7)Ca(0.3)Ba2Cu3O(7-delta) barrier layers
[AD-A294852] p 3231 N95-34568
SISO (CONTROL SYSTEMS)
An alternative reasoning method p 3189 N95-33001
SITE SELECTION
Aerospace Guidance and Metrology Center: Cost growth and other factors affect closure and privatization. Report to Congressional requesters
[GAO/NSIAD-95-60] p 3235 N95-32706
SITTING POSITION
Increase of High-sustained +G(z) tolerance at the expense of pilot's working posture change p 3165 N95-34056
SIZE DISTRIBUTION
Improving alpine-region spectral unmixing with optimal-fit snow endmembers p 3135 N95-33764
Cooling tower and plume modeling for satellite remote sensing applications
[DE95-012000] p 3143 N95-33849
SLENDER BODIES
Calculation for aerodynamic characteristics on delta wing with leading-edge separated vortex effect using boundary element method p 3037 N95-34524
SLENDER WINGS
Analysis and design methodology for chordwise deformable wings p 3049 N95-33311
SLIDING FRICTION
Influence of non classical friction on the rubbing and impact behavior of rotor dynamic systems p 3122 N95-32906
The effects of ion implantation on the tribology of perfluoropolyether-lubricated 440C stainless steel couples
[NASA-TM-106965] p 3083 N95-32918
Fiber coatings for brittle matrix composites p 3065 N95-34808
SLOPES
A conflict of water and fire: Remote sensing imagery of the Uinkaret Volcanic Field, Grand Canyon, Arizona p 3117 N95-33795
Comparison of theoretical predictions with field observations for a simple forward scattering sensor
[AD-A294948] p 3219 N95-34576
Everyday believability
[AD-A294938] p 3193 N95-34602
SLOT ANTENNAS
Simulation of patch and slot antennas using FEM with prismatic elements and investigations of artificial absorber mesh termination schemes
[NASA-CR-198974] p 3097 N95-32822
SLOTS
Study of the trapped modes at the vacuum ports
[DE95-010570] p 3203 N95-32544
Split gasket attachment method statement of government interest
[AD-D017443] p 3123 N95-32924
SMOKE
Remote sensing of smoke, clouds, and radiation using AVIRIS during SCAR experiments p 3132 N95-33749
Corrosion of fire-damaged aircraft
[AD-A294968] p 3049 N95-34583
SMOOTHING
Smoothing during ion-assisted growth by transient ion beam-induced defects
[DE95-011021] p 3225 N95-32579
SNAKES
COBRA accelerator for Sandia ICF diode research at Cornell University
[DE95-011018] p 3101 N95-32578
SNOW
Optimization of a melting layer model in the radar backscatter, attenuation, and phase shift calculations at centimeter and millimeter wavelengths
[PB95-207189] p 3155 N95-32455
Mapping minerals, amorphous materials, environmental materials, vegetation, water, ice and snow, and other materials: The USGS tricorder algorithm p 3130 N95-33742
Improving alpine-region spectral unmixing with optimal-fit snow endmembers p 3135 N95-33764
SNOW COVER
Measurement of the spectral absorption of liquid water in melting snow with an imaging spectrometer p 3133 N95-33756
Improving alpine-region spectral unmixing with optimal-fit snow endmembers p 3135 N95-33764
SODIUM
Doppleron resonances in the diffraction of atoms by an evanescent field
[DE95-619190] p 3204 N95-32622
SODIUM SULFUR BATTERIES
Lessons learned in acquiring new regulations for shipping advanced electric vehicle batteries
[DE95-009908] p 3102 N95-32956
SOFIA (AIRBORNE OBSERVATORY)
SOFIA: Aft cavities wind tunnel test
[NASA-TM-110673] p 3033 N95-32682
SOFIA 2 model telescope wind tunnel test report
[NASA-TM-110668] p 3033 N95-32764
SOFTWARE DEVELOPMENT TOOLS
Development of a tool-set for simultaneous, multi-site observations of astronomical objects p 3239 N95-34221
Construction of an advanced software tool for planetary atmospheric modeling p 3184 N95-34225
The Grid Analysis and Display System (GRADS): A practical tool for Earth science visualization p 3241 N95-34231
Development of an expert data reduction assistant p 3242 N95-34234
High performance compression of science data p 3242 N95-34237
SOFTWARE ENGINEERING
Formalization and representation of a product-driven approach to method assembly for situational systems development
[PB95-215190] p 3237 N95-33238
Third International Workshop on Ion Mobility Spectrometry
[NASA-CP-3301] p 3069 N95-33265
IMS software developments for the detection of chemical warfare agent p 3072 N95-33287
Applied Information Systems Research Program (AISRP) Workshop 3 meeting proceedings
[NASA-CR-199103] p 3239 N95-34218
An interactive environment for the analysis of large Earth observation and model data sets p 3239 N95-34219
Development of a tool-set for simultaneous, multi-site observations of astronomical objects p 3239 N95-34221
Multivariate statistical analysis software technologies for astrophysical research involving large data bases p 3240 N95-34222
Construction of an advanced software tool for planetary atmospheric modeling p 3184 N95-34225
A distributed analysis and visualization system for model and observational data p 3243 N95-34240
Construction of a connectionist network supercomputer
[AD-A294198] p 3177 N95-34301
Anechoic chamber upgrade
[AD-A294375] p 3056 N95-34342
Automated support for software engineering
[AD-A294965] p 3182 N95-34582
Experiences using DCE and CORBA to build tools for creating highly-available distributed systems
[AD-A294973] p 3187 N95-34587
The design of scalable software libraries for distributed memory concurrent computers
[DE95-012891] p 3244 N95-34801
SOIL MAPPING
Completing below-ground carbon budgets for pastures, recovering forests, and mature forests of Amazonia
[NASA-CR-199129] p 3143 N95-33498
SOIL MECHANICS
Seismic response analysis of soil-structure interaction systems in the time domain
[REPT-2212] p 3091 N95-32992
SOIL MOISTURE
Modeling soil climate controls on the exchange of trace gases between the terrestrial biosphere and the atmosphere p 3153 N95-33337
Completing below-ground carbon budgets for pastures, recovering forests, and mature forests of Amazonia
[NASA-CR-199129] p 3143 N95-33498
Measuring soil moisture with imaging radars p 3139 N95-33803
Application of IEM model on soil moisture and surface roughness estimation p 3142 N95-33816

SOIL SAMPLING
Analysis of samples for the first (1994) OPCW round robin interlaboratory comparison test
[PB95-210324] p 3068 N95-33243
Completing below-ground carbon budgets for pastures, recovering forests, and mature forests of Amazonia
[NASA-CR-199129] p 3143 N95-33498
SOILS
A novel approach to the problem of highly-sensitive regular analysis for man-made plutonium in environment and human body
[DE95-620764] p 3164 N95-32666
Modeling soil climate controls on the exchange of trace gases between the terrestrial biosphere and the atmosphere p 3153 N95-33337
Lithogenic and cosmogenic tracers in catchment hydrology
[DE95-011523] p 3143 N95-33407
Completing below-ground carbon budgets for pastures, recovering forests, and mature forests of Amazonia
[NASA-CR-199129] p 3143 N95-33498
Initial vegetation species and senescience/stress indicator mapping in the San Luis Valley, Colorado using imaging spectrometer data p 3130 N95-33741
SOL-GEL PROCESSES
In situ ion-beam analysis and modification of sol-gel zirconia thin films
[DE95-010994] p 3203 N95-32577
Indirect measurements of hydrogen: The deficit method for a many-component system
[DE95-010993] p 3208 N95-33623
Thin-film electrolytes for reduced temperature solid oxide fuel cells
[DE95-011273] p 3151 N95-34481
SOLAR ARRAYS
Solar cell array design method for preventing power reduction due to module output fluctuation
[DE95-769745] p 3148 N95-32402
SOLAR CELLS
Solar cell array design method for preventing power reduction due to module output fluctuation
[DE95-769745] p 3148 N95-32402
Investigation research on introducing new energy technology, promoting its practical application, and providing its instruction
[DE95-769801] p 3148 N95-32403
Device physics of thin-film polycrystalline cells and modules
[DE95-009209] p 3149 N95-32817
Thin-film rechargeable lithium batteries
[DE95-008975] p 3103 N95-33697
The international conference on solar energy storage and applied photochemistry
[AD-A294347] p 3150 N95-34360
SOLAR COLLECTORS
CRADA with United Solar Technologies and Pacific Northwest Laboratory (PNL-021): Thin film materialsfor low-cost high performance solar concentrators
[DE95-010423] p 3150 N95-33400
SOLAR CONSTANT
MODTRAN3: An update and recent validations against airborne high resolution interferometer measurements p 3128 N95-33732
SOLAR ELECTRIC PROPULSION
Advanced propulsion for geostationary orbit insertion and north-south station keeping
[NASA-TM-107018] p 3060 N95-32917
SOLAR ENERGY
Prospect redux p 3133 N95-33758
The 3rd international conference on solar energy storage and applied photochemistry
[AD-A294343] p 3150 N95-34359
The international conference on solar energy storage and applied photochemistry
[AD-A294347] p 3150 N95-34360
SOLAR ENERGY CONVERSION
CRADA with United Solar Technologies and Pacific Northwest Laboratory (PNL-021): Thin film materialsfor low-cost high performance solar concentrators
[DE95-010423] p 3150 N95-33400
SOLAR FLARES
Solar-geophysical data number 607, March 1995. Part 1 (prompt reports). Data for January, February 1995 and late data
[PB95-216388] p 3248 N95-32963
Solar-geophysical data number 607, March 1995: Part 2 (comprehensive reports). Data for September 1994 and miscellaneous
[PB95-216800] p 3248 N95-32964
SOLAR FLUX
Solar-geophysical data number 607, March 1995: Part 2 (comprehensive reports). Data for September 1994 and miscellaneous
[PB95-216800] p 3248 N95-32964
SOLAR MAGNETIC FIELD
Solar-geophysical data number 607, March 1995. Part 1 (prompt reports). Data for January, February 1995 and late data
[PB95-216388] p 3248 N95-32963
SOLAR PHYSICS
Solar-geophysical data number 607, March 1995. Part 1 (prompt reports). Data for January, February 1995 and late data
[PB95-216388] p 3248 N95-32963
Solar-geophysical data number 607, March 1995: Part 2 (comprehensive reports). Data for September 1994 and miscellaneous
[PB95-216800] p 3248 N95-32964
SOLAR PROMINENCES
Solar-geophysical data number 607, March 1995. Part 1 (prompt reports). Data for January, February 1995 and late data
[PB95-216388] p 3248 N95-32963
Solar-geophysical data number 607, March 1995: Part 2 (comprehensive reports). Data for September 1994 and miscellaneous
[PB95-216800] p 3248 N95-32964
SOLAR RADIATION
Remote sensing of smoke, clouds, and radiation using AVIRIS during SCAR experiments p 3132 N95-33749
Impact of differences in the solar irradiance spectrum on surface reflectance retrieval with different radiative transfer codes p 3136 N95-33771
Operation of the computer model for microenvironment solar exposure
[NASA-CR-198189] p 3059 N95-33890
SOLAR RADIO BURSTS
Solar-geophysical data number 607, March 1995. Part 1 (prompt reports). Data for January, February 1995 and late data
[PB95-216388] p 3248 N95-32963
Solar-geophysical data number 607, March 1995: Part 2 (comprehensive reports). Data for September 1994 and miscellaneous
[PB95-216800] p 3248 N95-32964
SOLAR SPECTRA
Impact of differences in the solar irradiance spectrum on surface reflectance retrieval with different radiative transfer codes p 3136 N95-33771
SOLAR WIND
Solar-geophysical data number 607, March 1995. Part 1 (prompt reports). Data for January, February 1995 and late data
[PB95-216388] p 3248 N95-32963
Solar-geophysical data number 607, March 1995: Part 2 (comprehensive reports). Data for September 1994 and miscellaneous
[PB95-216800] p 3248 N95-32964
SOLDERING
An investigation of the chemistry of citric acid in military soldering applications
[AD-A295042] p 3105 N95-34796
SOLDERS
Intermetallic compound layer growth kinetics in non-lead bearing solders
[DE95-009595] p 3078 N95-32591
SOLID CRYOGENS
A quantum Monte Carlo study of the high-pressure phases of solid hydrogen p 3074 N95-33469
SOLID ELECTROLYTES
Encapsulated dry electrolyte composition for time release into a solute
[AD-D017485] p 3075 N95-34287
High rate rechargeable lithium cells employing lithium ion conducting solid electrolytes
[AD-A294390] p 3104 N95-34347
Thin-film electrolytes for reduced temperature solid oxide fuel cells
[DE95-011273] p 3151 N95-34481
SOLID MECHANICS
The development and application of massively parallel solid mechanics codes
[DE95-006307] p 3184 N95-32374
SOLID PHASES
TEM investigation on the low temperature phase of HfV2
[DE95-009500] p 3225 N95-32532
SOLID PROPELLANT COMBUSTION
Observations of surface structure and regression behavior of solid propellant strands burning under narrow gap conditions p 3088 N95-33254
SOLID PROPELLANTS
Observations of surface structure and regression behavior of solid propellant strands burning under narrow gap conditions p 3088 N95-33254
SOLID SOLUTIONS
Thermoelectric material development
[DE95-007800] p 3149 N95-32811
Static displacements of atoms in crystalline metallic solid solutions
[DE95-012893] p 3233 N95-34802
SOLID STATE
Intermetallic compound layer growth kinetics in non-lead bearing solders
[DE95-009595] p 3078 N95-32591
Solid-state data recorder, next development and use p 3094 N95-33143
The interaction of vortices with twin boundaries
[DE95-012079] p 3110 N95-33389
Aircraft scanner data availability via the version 0 Information Management System p 3134 N95-33762
SOLID STATE DEVICES
A novel approach to the problem of highly-sensitive regular analysis for man-made plutonium in environment and human body
[DE95-620764] p 3164 N95-32666
SOLID STATE LASERS
Development and flight testing of an Obstacle Avoidance System for US Army helicopters p 3045 N95-32500
SOLID STATE PHYSICS
The 8th Winterschool on New Developments in Solid State Physics
[AD-A290163] p 3227 N95-32677
Molecular motion of phosphazene-bound NLO chromophores
[AD-A293526] p 3087 N95-34649
Industrial products based upon processible conductive polyaniline
[AD-A294985] p 3087 N95-34817
SOLID-SOLID INTERFACES
Interfacial reactions during the liquid infiltration of titanium matrix composites p 3081 N95-34252
SOLIDS
Shock properties of high-strength ceramics
[DE95-007731] p 3082 N95-32380
Spin counting in dipolar coupled spin 1/2 systems by multiple quantum NMR spectroscopy in solids: Development of a single quantum propagator and its application to heterogeneous catalysis
[DE95-010246] p 3066 N95-32540
The structure of ion track in Solids produced by ions with high level inelastic energy losses
[DE95-620942] p 3205 N95-32625
Modeling and simulation of pulsed laser annealing and ablation of solid materials
[DE95-012888] p 3119 N95-34466
SOLITARY WAVES
Propagation of spatial solitons generated by Gaussian beams in a non-linear Kerr medium
[IFTR-9/1995] p 3206 N95-32921
Solitary wave solution for mixing-layer turbulence p 3036 N95-34522
Turbulent solitary wave propagating through wall Boundary Layer p 3041 N95-34555
SOLSTICES
Solar-geophysical data number 607, March 1995: Part 2 (comprehensive reports). Data for September 1994 and miscellaneous
[PB95-216800] p 3248 N95-32964
SOLUBILITY
Effect of lead content on Bi-2223 formation by a two-powder process
[DE95-009889] p 3079 N95-33215
Supercritical crystallization: The RESs-process and the GAS-process
[PB95-214482] p 3226 N95-33235
Solubility behavior of quartz and corundum in supercritical water: A quantitative thermodynamic interpretation
[DE95-012294] p 3234 N95-34211
The relationship of chemical structure to supercritical-fluid solubility and to cosolvent-modifier properties: A literature review
[AD-A294933] p 3076 N95-34599
SOLUTES
Lithogenic and cosmogenic tracers in catchment hydrology
[DE95-011523] p 3143 N95-33407
The relationship of chemical structure to supercritical-fluid solubility and to cosolvent-modifier properties: A literature review
[AD-A294933] p 3076 N95-34599
SOLVATION
Industrial products based upon processible conductive polyaniline
[AD-A294985] p 3087 N95-34817
SOLVENTS
Environmental evaluation of lactates as cleaning agents
[PB95-214854] p 3067 N95-32615
Solvent effects on the electronic spectrum of R hardt's dye
[AD-A293667] p 3067 N95-32604

Characterization of microenvironment polarity and solvent accessibility of polysilsesquioxane xerogels by the fluorescent probe technique
[DE95-011874] p 3062 N95-33835
The relationship of chemical structure to supercritical-fluid solubility and to cosolvent-modifier properties: A literature review
[AD-A294933] p 3076 N95-34599
Industrial products based upon processible conductive polyaniline
[AD-A294985] p 3087 N95-34817

SOOT
Ignition and early soot formation in a DI diesel engine using multiple 2-D imaging diagnostics
[DE95-010692] p 3122 N95-32863

SOS (SEMICONDUCTORS)
Operational amplifier using bipolar junction transistors in silicon-on-sapphire
[AD-D017421] p 3105 N95-34618

SOUND DETECTING AND RANGING
Vertical velocity ambiguity resolution method
[AD-D017481] p 3201 N95-34424

SOUND FIELDS
Underwater acoustic field extrapolation: Theory and sensitivity analysis
[AD-A294925] p 3201 N95-34595

SOUND PRESSURE
Active noise control in finite length waveguides
p 3098 N95-33322

SOUND PROPAGATION
Structural wave propagation and sound radiation study through time and spatial processing
p 3200 N95-33251
Acoustic-optic sound velocity profiler
[AD-D017487] p 3201 N95-34289

SOUND TRANSDUCERS
Plasma mediated ablation of biological tissues with ultrashort laser pulses
[DE95-011748] p 3164 N95-33654

SOUND TRANSMISSION
Acoustic-optic sound velocity profiler
[AD-D017487] p 3201 N95-34289
Vertical velocity ambiguity resolution method
[AD-D017481] p 3201 N95-34424
Penetrable wedge analysis
[AD-A294276] p 3234 N95-34464

SOUND WAVES
High-resolution TeO2 acousto-optical deflector for millimeter-wave spectrometer
[AD-A293054] p 3215 N95-32701
Historical detection of atmospheric impacts by large bolides using acoustic-gravity waves
[DE95-010864] p 3246 N95-33211
Structural wave propagation and sound radiation study through time and spatial processing
p 3200 N95-33251
Acoustic-optic sound velocity profiler
[AD-D017487] p 3201 N95-34289
Recent developments in maritime technology research institute acousto-optical technology research
[AD-A294215] p 3217 N95-34307

SPACE CHARGE
The beam envelope equation-systematic solution for a periodic quadrupole lattice with space charge
[DE95-012761] p 3199 N95-34269

SPACE COOLING (BUILDINGS)
Technical innovation for reducing emissions of greenhouse effect gas and survey of effects of changes of industrial structures
[DE95-769808] p 3151 N95-32547

SPACE DEBRIS
Analysis of LDEF experiment AO187-2 chemical and isotopic measurements of micrometeoroids by secondary ion mass spectrometry
[NASA-CR-198849] p 3246 N95-32913

SPACE EXPLORATION
Budget estimates: Fiscal year 1994. Volume 1: Agency summary
[NASA-TM-110815] p 3244 N95-33069

SPACE FLIGHT
The role of the vestibular system in manual target localization p 3166 N95-32422
Twenty-five years of progress. Part 1: Birth of NASA. Part 2: The Moon-a goal
[NASA-TM-110819] p 3253 N95-33384

SPACE HEATING (BUILDINGS)
Technical innovation for reducing emissions of greenhouse effect gas and survey of effects of changes of industrial structures
[DE95-769808] p 3151 N95-32547

SPACE MISSIONS
GPS-based navigation for space applications
p 3058 N95-33144

SPACE NAVIGATION
GPS-based navigation for space applications
p 3058 N95-33144

SPACE PLASMAS
Shuttle Potential and Return Electron Experiment (SPREE) electrostatic analyzer (ESA) calibration report
[AD-A293026] p 3057 N95-32772
Life test of a xenon hollow cathode for a space plasma contractor
[NASA-CR-195403] p 3061 N95-33926

SPACE PLATFORMS
Prospect redux p 3133 N95-33758

SPACE PROBES
Space probe data processing
[AD-A294124] p 3058 N95-34744

SPACE PROCESSING
A study of space-rated connectors using a robot end-effector
[NASA-CR-199116] p 3121 N95-32675

SPACE PROGRAMS
Baseline experimental investigation of an electrohydrodynamically assisted heat pipe
p 3113 N95-32427

SPACE SHUTTLE MAIN ENGINE
Genetic algorithm based input selection for a neural network function approximator with applications to SSME health monitoring
[NASA-CR-199089] p 3188 N95-32768
SSME Post Test Diagnostic System: Systems Section
[NASA-CR-198375] p 3061 N95-34625

SPACE SHUTTLES
Certification of a hybrid parameter model of the fully flexible Shuttle Remote Manipulator System
p 3125 N95-32421
Liftoff to learning: Assignment space
[NASA-TM-110820] p 3057 N95-32539
The Space Shuttle: America's team reaching for the future
[NASA-CR-199222] p 3058 N95-33728
STS-42 mission highlights resource tape. Part 1 of 2
[NASA-TM-110838] p 3058 N95-34280

SPACE STATION FREEDOM
Shuttle to Space Station. Heart assist implant. Hubble update. X-30 mock-up
[NASA-TM-110837] p 3056 N95-33167

SPACE STATIONS
Validation of space/ground antenna control algorithms using a computer-aided design tool
p 3183 N95-32429
Multiobjective optimization of hybrid regenerative life support technologies. Topic D: Technology Assessment
[NASA-CR-199125] p 3167 N95-32688
Life test of a xenon hollow cathode for a space plasma contractor
[NASA-CR-195403] p 3061 N95-33926

SPACE TRANSPORTATION
Research and technology 1994: Annual report of the Marshall Space Flight Center
[NASA-TM-108470] p 3252 N95-33042

SPACE TRANSPORTATION SYSTEM
STS-42 mission highlights resource tape. Part 1 of 2
[NASA-TM-110838] p 3058 N95-34280
STS-42 mission highlights resource tape. Part 2 of 2
[NASA-TM-110840] p 3058 N95-34281

SPACE-TIME FUNCTIONS
General-covariant Quantum Mechanics of Dirac particle in curved space-times
[DE95-623600] p 3233 N95-32478

SPACEBORNE ASTRONOMY
Development of a tool-set for simultaneous, multi-site observations of astronomical objects
p 3239 N95-34221

SPACEBORNE EXPERIMENTS
Cosmic heavy ion tracks in mesoscopic biological test objects p 3163 N95-32730
Effects of gravity and light on plant growth and performance in normal and reduced gravity
p 3163 N95-32901

SPACECRAFT CHARGING
Life test of a xenon hollow cathode for a space plasma contractor
[NASA-CR-195403] p 3061 N95-33926

SPACECRAFT CONSTRUCTION MATERIALS
Study of the space environmental effects on spacecraft engineering materials
[NASA-CR-199090] p 3066 N95-32581

SPACECRAFT DESIGN
Study of the space environmental effects on spacecraft engineering materials
[NASA-CR-199090] p 3066 N95-32581

SPACECRAFT GLOW
Life test of a xenon hollow cathode for a space plasma contractor
[NASA-CR-195403] p 3061 N95-33926

SPACECRAFT LUBRICATION
The effects of ion implantation on the tribology of perfluoropolyether-lubricated 440C stainless steel couples
[NASA-TM-106965] p 3083 N95-32918
Spontaneous dewetting of a perfluoropolyether
[NASA-TM-106964] p 3083 N95-32919

SPACECRAFT MANEUVERS
Globally stable feedback laws for near-minimum-fuel and near-minimum-time pointing maneuvers for a landmark-tracking spacecraft
[DE95-009867] p 3191 N95-33214

SPACECRAFT POWER SUPPLIES
Modeling of DC spacecraft power systems
p 3062 N95-32423

SPACECRAFT PROPULSION
Pop tests of storable biopropellant liquid apogee engine
[NAL-TR-1253] p 3060 N95-32755
Design of ETO propulsion turbine using CFD analyses
[NASA-CR-199085] p 3123 N95-32915

SPACECRAFT REENTRY
Thermo-chemical ablation of heat shields under Earth reentry conditions p 3059 N95-32903

SPACECRAFT STABILITY
Implementation of a Single-Stage-To-Orbit (SSTO) model for stability and control analysis
p 3059 N95-32432

SPACECRAFT STRUCTURES
Development of a composite satellite structure for FORTE
[DE95-009416] p 3058 N95-32713
A three-dimensional nonlinear Timoshenko beam based on the core-congruential formulation
[NASA-CR-199042] p 3180 N95-32765

SPACECREWS
STS-42 mission highlights resource tape. Part 2 of 2
[NASA-TM-110840] p 3058 N95-34281

SPACELAB
STS-42 mission highlights resource tape. Part 2 of 2
[NASA-TM-110840] p 3058 N95-34281

SPALLATION
Ductile damage model with void coalescence
[DE95-007855] p 3125 N95-32385
Behavior of structural and target materials irradiated in spallation neutron environments
[DE95-010879] p 3203 N95-32576

SPATIAL DISTRIBUTION
Estimation of spatially restricted LET using track structure models p 3161 N95-32722
Validating spatial structure in canopy water content using geostatistics p 3135 N95-33768

SPATIAL RESOLUTION
A Spatial Analysis and Modeling System (SAMS) for environment management p 3243 N95-34239

SPECIFIC HEAT
Anisotropic magnetization of HoNi2B2C
[DE95-010239] p 3198 N95-32397
Density, heat capacity, viscosity, and thermal conductivity of mixtures of CO2, He, H2, H2O, N2, and O2
[AD-A288731] p 3076 N95-34814

SPECIFIC IMPULSE
Metallized gelled propellants: Oxygen/RP-1/aluminum rocket combustion experiments
[NASA-TM-107025] p 3088 N95-33876

SPECIFICATIONS
The PEP-2 project-wide database
[DE95-012512] p 3213 N95-33333
Experiences using DCE and CORBA to build tools for creating highly-available distributed systems
[AD-A294973] p 3187 N95-34587

SPECIMEN GEOMETRY
Patterns and perspectives in applied fracture mechanics
[DE95-012844] p 3127 N95-34442

SPECTRA
Temporal dynamics of the multi-frequency spectrum generated by self-phase modulation of two frequencies in single-mode fiber
[DE95-010920] p 3119 N95-33703
Characteristics of the HYDICE sensor
p 3116 N95-33733
Improving alpine-region spectral unmixing with optimal-fit snow endmembers p 3135 N95-33764
Development of High Spectral Resolution Lidar (HSRL) technology
[DE95-011906] p 3099 N95-33839
Synthesis and characterization of a series of organoindium-phosphides including molecular structures of ((Me3CCH2)2InPEt2)2 and ((Me3CCH2)2InP(H)(C6H11))3
[AD-A293965] p 3086 N95-34452
Spectrum allocation strategies for communication networks
[AD-A294936] p 3100 N95-34601
High order accuracy computational methods in aerodynamics using parallel architectures
[AD-A294167] p 3042 N95-34763

Transmittance characteristics of US Army rotary-wing aircraft transparencies
[AD-A295035] p 3049 N95-34793

SPECTRAL BANDS
Preliminary study of Kelso Dunes using AVIRIS, TM, and AIRSAR p 3136 N95-33773

SPECTRAL CORRELATION
Inelastic response spectra of a system with bilinear restoring characteristics: Effect of plastic-stiffness ratio
[REPT-2213] p 3091 N95-32993

SPECTRAL EMISSION
Land surface temperature measurements from EOS MODIS data
[NASA-CR-199082] p 3142 N95-32717
Radiative interactions with micromachined surfaces: Spectral polarized emittance
[DE95-011455] p 3097 N95-33061

SPECTRAL REFLECTANCE
Canopy reflectance modelling of semiarid vegetation
[NASA-CR-199117] p 3142 N95-32676
Land surface temperature measurements from EOS MODIS data
[NASA-CR-199082] p 3142 N95-32717
Initial vegetation species and senescience/stress indicator mapping in the San Luis Valley, Colorado using imaging spectrometer data p 3130 N95-33741
Calibration to surface reflectance of terrestrial imaging spectrometry data: Comparison of methods p 3130 N95-33743
Causal correlation of foliar biochemical concentrations with AVIRIS spectra using forced entry linear regression p 3130 N95-33744
Mineralogic variations in fluvial sediments contaminated by mine tailings as determined from AVIRIS data, Coeur D'Alene River Valley, Idaho p 3131 N95-33745
Evaluation of the photochemical reflectance index in AVIRIS imagery p 3131 N95-33747
Correction of thin cirrus effects in AVIRIS images using the sensitive 1.375-micron cirrus detecting channel p 3131 N95-33748
Remote sensing of smoke, clouds, and radiation using AVIRIS during SCAR experiments p 3132 N95-33749
High accuracy in-flight wavelength calibration of imaging spectrometry data p 3132 N95-33750
Measurement of atmospheric water vapor, leaf liquid water and reflectance with AVIRIS in the Boreal Ecosystem-Atmosphere Study: Initial results p 3133 N95-33755
Vegetation species composition and canopy architecture information expressed in leaf water absorption measured in the 1000 nm and 2200 spectral region by an imaging spectrometer p 3133 N95-33757
Impact of differences in the solar irradiance spectrum on surface reflectance retrieval with different radiative transfer codes p 3136 N95-33771
Enhanced shortwave cloud radiative forcing due to anthropogenic aerosols
[DE95-013319] p 3156 N95-34214

SPECTRAL RESOLUTION
High spectral resolution remote sensing of canopy chemistry p 3128 N95-33731
Spectral identification of minerals using imaging spectrometry data: Evaluating the effects of signal to noise and spectral resolution using the tricorder algorithm p 3136 N95-33772
The 1994 laboratory calibration of TIMS p 3117 N95-33796
Development of High Spectral Resolution Lidar (HSRL) technology
[DE95-011906] p 3099 N95-33839

SPECTRAL SIGNATURES
Hand-portable gas chromatography-ion mobility spectrometer for the determination of the freshness of fish p 3071 N95-33277

SPECTROGRAPHS
Field Raman spectrograph for environmental analysis
[DE95-007969] p 3153 N95-32816

SPECTROMETERS
Development of ultrasensitive spectroscopic analysis technology. Development of atomic spectroscopy technology
[DE95-614352] p 3066 N95-32566
In situ ion-beam analysis and modification of sol-gel zirconia thin films
[DE95-010994] p 3203 N95-32577
Application of deformable templates for recognizing tracks detected with High Pressure Drift Tubes
[DE95-621870] p 3188 N95-32627
Study of liquid crystal spatial light modulator application to Hadamard transform spectrometer: A fast and accurate decoding method
[AD-A293087] p 3215 N95-32660
Low-energy response of superconducting tunnel junction x-ray spectrometers
[DE95-011733] p 3230 N95-33650
Applied research on liquid crystal spatial modulators in Hadamard transform spectrometers. Quick and accurate decoding methods
[AD-A294152] p 3219 N95-34756

SPECTROPHOTOMETRY
Development of environmentally conscious cleaning process for leadless chip carrier assemblies
[DE95-010186] p 3154 N95-33638

SPECTRORADIOMETERS
AVIRIS user's guide p 3117 N95-33759
An algorithm for chlorophyll using first difference transformations of AVIRIS reflectance spectra p 3134 N95-33763

SPECTROSCOPIC ANALYSIS
Development of ultrasensitive spectroscopic analysis technology. Development of atomic spectroscopy technology
[DE95-614352] p 3066 N95-32566
Beryllium and Boron abundances in population II stars
[NASA-CR-189434] p 3247 N95-33262
Environment applications for ion mobility spectrometry p 3071 N95-33279
High resolution electrospray mass spectrometry with a magnetic sector instrument: Accurate mass measurement and peptide sequencing
[AD-A293564] p 3076 N95-34611

SPECTROSCOPY
Study of impurity concentrations by VUV spectroscopy on HL-1
[DE95-614186] p 3221 N95-32562
Development of ultrasensitive spectroscopic analysis technology. Development of atomic spectroscopy technology
[DE95-614352] p 3066 N95-32566
Photoemission study of some novel materials: Rare earth/transition metal interface, Ba*(0.6)*K*(0.4)*BiO3* and AlPdMn
[DE95-010125] p 3227 N95-32643
High-resolution magnetic imaging and investigations of thin-film magnetism with spin-polarized electron, ion and atom probes
[DE95-012190] p 3074 N95-33392
Optical anisotropy of (110) surfaces of Ag and Cu
[DE95-010130] p 3229 N95-33637
The development of a distributed computing environment for the design and modeling of plasma spectroscopy experiments
[DE95-011725] p 3183 N95-34813

SPECTRUM ANALYSIS
High spectral resolution remote sensing of canopy chemistry p 3128 N95-33731
Using dark current data to estimate AVIRIS noise covariance and improve spectral analyses p 3129 N95-33736
Mapping minerals, amorphous materials, environmental materials, vegetation, water, ice and snow, and other materials: The USGS tricorder algorithm p 3130 N95-33742
Calibration to surface reflectance of terrestrial imaging spectrometry data: Comparison of methods p 3130 N95-33743
Using foreground/background analysis to determine leaf and canopy chemistry p 3135 N95-33765
AVIRIS spectral trajectories for forested areas of the Gifford Pinchot National Forest p 3135 N95-33766
Spectral identification of minerals using imaging spectrometry data: Evaluating the effects of signal to noise and spectral resolution using the tricorder algorithm p 3136 N95-33772

SPEECH RECOGNITION
Training and recognition of Cantonese phonemes by backpropagation through time p 3188 N95-32996
Speaker identification using the two-dimensional cepstrum transform
[AD-A294204] p 3099 N95-34304

SPEED REGULATORS
Wind turbine trailing edge aerodynamic brakes
[DE95-004061] p 3033 N95-32548

SPHERES
Stress relaxation in discontinuously reinforced composites
[DE95-010928] p 3064 N95-33704
Comparison of theoretical predictions with field observations for a simple forward scattering sensor
[AD-A294948] p 3219 N95-34576

SPHERICAL HARMONICS
An improved algorithm for computing altitude dependent Corrected GeoMagnetic coordinates
[AD-A293967] p 3144 N95-34454

SPIN
The interrelation of a Z(3) gauge theory on flat lattices and a spin-1 BEG model
[DE95-623634] p 3227 N95-32631

SPIN-SPIN COUPLING
Spin counting in dipolar coupled spin 1/2 systems by multiple quantum NMR spectroscopy in solids: Development of a single quantum propagator and its application to heterogeneous catalysis
[DE95-010246] p 3066 N95-32540

SPLINE FUNCTIONS
A code to compute the action-angle transformation for a particle in an abritrary potential well
[DE95-012554] p 3098 N95-33336
Cubic-B-spline boundary elements for two-dimensional and axisymmetric elastostatics p 3127 N95-33695

SPOILERS
Numerical simulation of unsteady viscous flow around an airfoil with oscillating spoiler p 3040 N95-34547

SPRAYERS
The effects of high ambient density on diesel spray penetration and spread
[DE95-010761] p 3124 N95-33701

SPREAD SPECTRUM TRANSMISSION
FH and DS spread-spectrum systems in interference-limited HF channels: A comparison
[PB95-211439] p 3098 N95-33230

SPREADING
Foam spread experiments on a water surface
[PB95-211025] p 3083 N95-32962

SPUTTERING
Epitaxial Pb(Zr(x)Ti(1-x))O3/SrRuO3 ($x \simeq 0, 0.35, 0.65$) multilayer thin films on SrTiO3(100) and MgO(100) prepared by MOCVD and RF sputtering
[DE95-008288] p 3226 N95-32598
YBa2Cu3O(7-x) 45 deg (001) tilt grain boundaries induced by controlled low-energy sputtering of MgO substrates: Transport properties and atomic-scale structure
[DE95-005826] p 3228 N95-32810
Influence of processing variables on the structure and properties of ZnO films
[DE95-011494] p 3084 N95-33405
Epitaxial Pb(Zr(0.40)Ti(0.60))O3/SrRuO3 and PbTiO3/SrRuO3 multilayer thin films prepared by MOCVD and RF sputtering
[DE95-007146] p 3229 N95-33636
Multilayer thermoelectric films: A strategy for the enhancement of ZT
[DE95-011535] p 3081 N95-34482

SQUEEZED STATES (QUANTUM THEORY)
Probe transparency in a two-level medium embedded by a squeezed vacuum
[DE95-614123] p 3198 N95-32525

STABILITY
Estimation of collective instabilities in RHIC
[DE95-011347] p 3211 N95-32485
Transverse multibunch instabilities for non-rigid bunches
[DE95-012098] p 3211 N95-32607
Synthesis of potential new Zintl phases
[DE95-010123] p 3227 N95-32640
Globally stable feedback laws for near-minimum-fuel and near-minimum-time pointing maneuvers for a landmark-tracking spacecraft
[DE95-009867] p 3191 N95-33214
Nonlinear symmetric stability of planetary atmospheres
[DE95-012133] p 3248 N95-33390
Influence of processing variables on the structure and properties of ZnO films
[DE95-011494] p 3084 N95-33405
Nonlinear stability of unsteady viscous flow
[AD-A294931] p 3113 N95-34597

STABILITY TESTS
Stability analysis of external kink mode for ITER L-mode profile plasmas
[DE95-737207] p 3220 N95-32410
Implementation of a Single-Stage-To-Orbit (SSTO) model for stability and control analysis p 3059 N95-32432

STABILIZATION
Fast feedback for linear colliders
[DE95-012099] p 3211 N95-32608
Method and apparatus for locking laser wavelength to an atomic transition
[AD-D017425] p 3120 N95-34619

STABILIZED PLATFORMS
Balloon-borne radiometer profiler: Field observations
[DE95-011493] p 3158 N95-33505

STABILIZERS (AGENTS)
Quench propagation velocity for highly stabilized conductors
[DE95-011040] p 3103 N95-33404

STAINLESS STEELS
Cylindrical shell buckling through strain hardening
[DE95-009545] p 3125 N95-32392

Development and trial manufacturing of 1/2-scale partial mock-up of blanket box structure for fusion experimental reactor
[DE95-737184] p 3219 N95-32408
Irradiation-assisted stress corrosion cracking considerations at temperatures below 288 C
[DE95-008940] p 3077 N95-32555
About the mechanism of heavy ion radiation influence on the metals at high temperature
[DE95-620943] p 3078 N95-32626
The effects of ion implantation on the tribology of perfluoropolyether-lubricated 440C stainless steel couples
[NASA-TM-106965] p 3083 N95-32918
Implications of early stages in the growth of stress corrosion cracking on component reliability
[DE95-011498] p 3127 N95-33833
Fracture toughness assessment of present and future pressure vessel materials based on Charpy impact energy and yield strength
[AD-A294008] p 3081 N95-34373

STANDARD MODEL (PARTICLE PHYSICS)
Searching for new physics with charm
[DE95-012498] p 3207 N95-33245
Overview of rare K decays
[DE95-012081] p 3208 N95-33850

STANDARDS
Proposed incorporation of mission-oriented flying qualities into MIL-STD-1797A
[AD-A294211] p 3055 N95-34306
Experiences using DCE and CORBA to build tools for creating highly-available distributed systems
[AD-A294973] p 3187 N95-34587

STAR TRACKERS
Single event and TREE latchup mitigation for a star tracker sensor: An innovative approach to system level latchup mitigation
[DE95-010331] p 3059 N95-32593

STARTING
Investigation of starting and ignition transients in the thermally choked ram accelerator p 3054 N95-34805

STATIC FIRING
Fundamental phenomena on fuel decomposition and boundary-layer combustion processes with applications to hybrid rocket motors
[NASA-CR-199126] p 3061 N95-32932

STATIC PRESSURE
Static pressure drop by swirling flow of an internal cooling air system through a turbine shaft p 3042 N95-34560

STATIONKEEPING
Advanced propulsion for geostationary orbit insertion and north-south station keeping
[NASA-TM-107018] p 3060 N95-32917

STATISTICAL ANALYSIS
A posteriori pointwise error estimates for the boundary element method
[DE95-008099] p 3194 N95-32388
Comparison of the Wang and Wachsmuth models for (pi) production with measurements at 12 GeV/c
[DE95-010417] p 3203 N95-32542
Using foreground/background analysis to determine leaf and canopy chemistry p 3135 N95-33765
Validating spatial structure in canopy water content using geostatistics p 3135 N95-33768
Branch and bound methods for search problems
[AD-A294522] p 3182 N95-34349
Solitary wave solution for mixing-layer turbulence p 3036 N95-34522
Hybrid pyramid/neural network vision system
[AD-A294919] p 3193 N95-34593
Control of initialization bias in queueing simulations using queueing approximations
[AD-A294121] p 3194 N95-34742

STATISTICAL MECHANICS
Bogolyubov lectures
[DE95-620495] p 3197 N95-32624

STATISTICAL WEATHER FORECASTING
Induction of dependency structures from data and its application to ozone prediction p 3190 N95-33003

STEADY FLOW
Flow and heat transfer behavior of non-Newtonian fluids in rectangular ducts p 3107 N95-32907
Structure of weak shock waves in bubbly liquid p 3037 N95-34527

STEADY STATE
Steady-state dynamic behavior of an auxiliary bearing supported rotor system p 3121 N95-32690
Stability of steady state solutions for forced Navier-Stokes equations p 3112 N95-34286
Natural convection at microelectrodes
[AD-A294336] p 3075 N95-34357
Subscale study of engine bellmouth inlet vortices in test cell R1D
[AD-A294993] p 3113 N95-34818

STEAM FLOW
Dividing annular/two-phase flow in horizontal T-junctions
[ISBN-0-315-84910-X] p 3057 N95-33030

STEEL STRUCTURES
Angular dependence of magnetic properties of steels under uniaxial stress
[DE95-010189] p 3078 N95-32648

STEELS
Analytical modeling of the effect of crack depth, specimen size, and biaxial stress on the fracture toughness of reactor vessel steels
[DE95-005886] p 3125 N95-32373
Irradiation experiments of low copper A533B steels for reactor pressure vessel tested in JMTR
[DE95-737266] p 3077 N95-32531
Technical innovation for reducing emissions of greenhouse effect gas and survey of effects of changes of industrial structures
[DE95-769808] p 3151 N95-32547
Angular dependence of magnetic properties of steels under uniaxial stress
[DE95-010189] p 3078 N95-32648
The tensile fracture behavior of the weld metal of BIS 812 EMA and Q1N naval construction steels
[DSTO-RR-0021] p 3078 N95-32926
Knowledge-based system for metallurgical grade design p 3189 N95-32998
HOTQUA: An expert system prototype for quality monitoring in a rolling mill p 3190 N95-33004

STEERABLE ANTENNAS
Monolithic diode arrays for quasioptical millimeter wave beam steering
[AD-A294256] p 3100 N95-34460

STELLAR ENVELOPES
ROSAT survey of emission from Be stars
[NASA-CR-199086] p 3245 N95-32835

STELLAR FLARES
ROSAT survey of emission from Be stars
[NASA-CR-199086] p 3245 N95-32835

STELLAR LUMINOSITY
ROSAT survey of emission from Be stars
[NASA-CR-199086] p 3245 N95-32835

STELLAR MASS EJECTION
Solar-geophysical data number 607, March 1995. Part 1 (prompt reports). Data for January, February 1995 and late data
[PB95-216388] p 3248 N95-32963
Solar-geophysical data number 607, March 1995: Part 2 (comprehensive reports). Data for September 1994 and miscellaneous
[PB95-216800] p 3248 N95-32964

STELLAR PHYSICS
GRO: Studies of high energy pulsars with EGRET
[NASA-CR-199130] p 3248 N95-33499

STELLAR TEMPERATURE
ROSAT survey of emission from Be stars
[NASA-CR-199086] p 3245 N95-32835

STIFFENING
Acoustic attenuation and vibration damping materials
[AD-D017465] p 3201 N95-34444

STIFFNESS
Solving stiff chemistry problems with FIDAP
[DE95-011053] p 3067 N95-32709
Inelastic response spectra of a system with bilinear restoring characteristics: Effect of plastic-stiffness ratio
[REPT-2213] p 3091 N95-32993

STIMULI
Stimulus-response compatibility
[PB95-214722] p 3167 N95-33237

STIRLING CYCLE
Ricor K506B cryocooler performance during the Clementine mission and ground testing
[DE95-010683] p 3089 N95-32568

STIRLING ENGINES
Numerical thermal analyses of heat exchangers for the stirling engine application
[NASA-CR-199120] p 3110 N95-33398

STOCHASTIC PROCESSES
Bernstein-Green-Kruskal wave. 2: The interaction with the Langmuir wave. Stochastic phenomena
[DE95-614202] p 3220 N95-32507
Conversion of the Bernstein-Green-Kruskal wave on the density perturbation, part 4
[DE95-614206] p 3221 N95-32510
Turbulence and spatio-temporal chaos
[DE95-012912] p 3068 N95-33223
Modeling and inference with fractional Brownian motion and fractional Gaussian noise p 3199 N95-33415
Stochastic network processes
[AD-A294939] p 3187 N95-34603
Control of initialization bias in queueing simulations using queueing approximations
[AD-A294121] p 3194 N95-34742
Uncertainty analysis using stochastic finite elements p 3196 N95-34803
A stochastic adaptive control application to flight systems p 3055 N95-34806

STOICHIOMETRY
Intermetallic compound layer growth kinetics in non-lead bearing solders
[DE95-009595] p 3078 N95-32591

STORAGE RINGS (PARTICLE ACCELERATORS)
Crystalline beam properties as predicted for the storage rings ASTRID and TSR
[DE95-011557] p 3210 N95-32411
Study of the trapped modes at the vacuum ports
[DE95-010570] p 3203 N95-32544
Impedance study for the PEP-2 B-factory
[DE95-010569] p 3203 N95-32567
VHS-tape system for general purpose computer. For next generation mass storage system
[DE95-737268] p 3177 N95-32757
Nonlinear analyses of storage ring lattices using one-turn maps
[DE95-012515] p 3213 N95-33335
Emittance growth due to decoherence and wakefields
[DE95-012495] p 3213 N95-33376
Injection envelope matching in storage rings
[DE95-012496] p 3213 N95-33377
A map for the thick beam-beam interaction
[DE95-012561] p 3213 N95-33385
A final-focus magnet for PEP-2
[DE95-012372] p 3214 N95-33504
Track finding and fitting in the H1 forward track detector
[PB95-234985] p 3214 N95-34651
Analytic approach to small x structure functions
[PB95-236030] p 3214 N95-34653

STRAIN HARDENING
Cylindrical shell buckling through strain hardening
[DE95-009545] p 3125 N95-32392
Low strain behaviour of a particulate reinforced aluminum alloy
[ISBN-0-315-84906-1] p 3078 N95-32935
Structural influences on the work hardening behavior of aluminum
[DE95-011262] p 3080 N95-33626

STRAIN MEASUREMENT
A fiber optic strain measurement and quench localization for use in superconducting accelerator dipole magnets
[DE95-012370] p 3215 N95-33381

STRAIN RATE
Low strain behaviour of a particulate reinforced aluminum alloy
[ISBN-0-315-84906-1] p 3078 N95-32935

STRANDS
Inactivation, DNA double strand break induction and their rejoining in bacterial cells irradiated with heavy ions p 3161 N95-32724
DNA-DSB in CHO-K1 cells induced by heavy-ions: Break rejoining and residual damage (GSI) p 3162 N95-32725
Chromosomal damage observed in first postirradiation metaphases of repair-proficient and -deficient cell lines p 3162 N95-32726

STRANGENESS
Double-strangeness five-body system
[DE95-737277] p 3202 N95-32404
Strangeness from hadronic processes
[DE95-010311] p 3205 N95-32651
Development of silicon drift detectors for strangeness measurements
[DE95-012366] p 3208 N95-33380

STRATEGY
A curriculum for strategy in the information age: Chaos in a new era
[AD-A295036] p 3244 N95-34794

STRATIFIED FLOW
Vorticity in shock-accelerated density-stratified interfaces: An analytical and computational study p 3111 N95-33607

STRATOSPHERE
Ocean observations with EOS/MODIS: Algorithm development and post launch studies
[NASA-CR-198928] p 3143 N95-32914

STRESS (PHYSIOLOGY)
Locus of control and coping style as stress moderators in achievement oriented individuals
[AD-A294275] p 3166 N95-34463
Measurement and regulation of central noradrenergic receptors
[AD-A294065] p 3165 N95-34472

STRESS ANALYSIS
Micromechanics of composites with shape memory alloy fibers in uniform thermal fields
[NASA-TM-107011] p 3063 N95-33210
Design of deepwater pipelines
[PB95-215109] p 3095 N95-33244
Interlaminar stress analysis of dropped-ply laminated plates and shells by a mixed method p 3064 N95-33327

Enhanced stress projections for error estimation and a singular floating node element for static and dynamic fracture p 3064 N95-33463
The linear elastic biaxial response of plain-woven meshes p 3064 N95-33468
Bending strength model for internal spur gear teeth [NASA-TM-107012] p 3124 N95-33908

STRESS CORROSION CRACKING
Irradiation-assisted stress corrosion cracking considerations at temperatures below 288 C [DE95-008940] p 3077 N95-32555
Nitrate stress corrosion crack growth rate in plain carbon steels [DE95-011689] p 3079 N95-32958
Implications of early stages in the growth of stress corrosion cracking on component reliability [DE95-011498] p 3127 N95-33833

STRESS DISTRIBUTION
Angular dependence of magnetic properties of steels under uniaxial stress [DE95-010189] p 3078 N95-32648
Interlaminar stress analysis of dropped-ply laminated plates and shells by a mixed method p 3064 N95-33327
Plasma mediated ablation of biological tissues with ultrashort laser pulses [DE95-011748] p 3164 N95-33654

STRESS INTENSITY FACTORS
N-15 hydrogen profiling of IC metallizations [DE95-011052] p 3102 N95-32708

STRESS PROPAGATION
High-order Taylor-Galerkin and adaptive hp-methods for hyperbolic systems with application to structural acoustics p 3200 N95-33719

STRESS RELAXATION
Stress relaxation in discontinuously reinforced composites [DE95-010928] p 3064 N95-33704

STRESS-STRAIN RELATIONSHIPS
Cylindrical shell buckling through strain hardening [DE95-009545] p 3125 N95-32392
Micromechanics of fiber-reinforced ceramic composites p 3063 N95-32775
Design and analysis of transient nonlinear coupled systems p 3199 N95-33292
A new approach to fracture of layered fibrous composites: Experiments and analysis p 3063 N95-33309

STRETCHERS
Phase control and measurement of ultrashort optical pulses [DE95-011746] p 3216 N95-33411

STRINGS
On the virtues of parameterized uniform crossover [AD-A293985] p 3182 N95-34456

STRONTIUM COMPOUNDS
Formation of artificially-layered high-temperature superconductors using pulsed-laser deposition [DE95-012884] p 3231 N95-34465

STRONTIUM TITANATES
Epitaxial Pb(Zr(x)Ti(1-x))O3/SrRuO3 (x = 0, 0.35, 0.65) multilayer thin films on SrTiO3(100) and MgO(100) prepared by MOCVD and RF sputtering [DE95-008288] p 3226 N95-32598

STRUCTURAL ANALYSIS
Application of impact dampers in vibration control of flexible structures p 3127 N95-32420
A three-dimensional nonlinear Timoshenko beam based on the core-congruential formulation [NASA-CR-199042] p 3180 N95-32765
Cubic-B-spline boundary elements for two-dimensional and axisymmetric elastostatics p 3127 N95-33695
High-order Taylor-Galerkin and adaptive hp-methods for hyperbolic systems with application to structural acoustics p 3200 N95-33719
Wavelet analysis of atmospheric turbulence structures: What can we gain from this new technique? [DE95-011955] p 3156 N95-33847

STRUCTURAL BASINS
Raingauge network optimization and GIS: A case study of the Mananga basin. Communications of the Sanitary Engineering and Water Management Division [PB95-214284] p 3157 N95-32891

STRUCTURAL DESIGN
Analysis and design methodology for chordwise deformable wings p 3049 N95-33311
A molecular dynamics investigation of the structural characteristics of amorphous and annealed poly (Vinylidene fluoride) and vinylidene fluoride - trifluoroethylene copolymers [AD-A294116] p 3086 N95-34502

STRUCTURAL DESIGN CRITERIA
Design of deepwater pipelines [PB95-215109] p 3095 N95-33244
Engineering approaches and compromises in the design of small ion mobility spectrometers p 3070 N95-33271

STRUCTURAL VIBRATION
Synchronous dynamics of a coupled shaft/bearing/housing system with auxiliary support from a clearance bearing: Analysis and experiment p 3122 N95-32693
Modal identification and its applications to damage detection in vibrating structures p 3126 N95-32920
Structural wave propagation and sound radiation study through time and spatial processing p 3200 N95-33251

STRUCTURED GRIDS (MATHEMATICS)
Parallel computation of transonic flows about an aircraft configuration using multi-block structured grids p 3039 N95-34537
A large scale 3D Navier-Stokes analysis using NAL-NWT p 3039 N95-34539
Parallel computation for two dimensional incompressible flow on array of transputers p 3042 N95-34558

STRUCTURED PROGRAMMING
A declarative debugger for a logical-functional language p 3183 N95-33007

STUDENTS
Liftoff to learning: Assignment space [NASA-TM-110820] p 3057 N95-32539

SUBLIMATION
Thermo-chemical ablation of heat shields under Earth reentry conditions p 3059 N95-32903

SUBMILLIMETER WAVES
Electronic processes in heterostructures, strained-layer materials, and laterally patterned structures [AD-A294970] p 3235 N95-34585

SUBROUTINES
Interactive interface for National Center for Atmospheric Research (NCAR) graphics p 3239 N95-34220

SUBSONIC FLOW
Transport phenomena in subsonic and supersonic flows in a duct with mass injection p 3108 N95-32934
Computations of low speed flow about space-plane p 3040 N95-34544

SUBSONIC SPEED
Minimum fuel mode evaluation p 3051 N95-33015

SUBSTITUTES
Alternative-fuels technology: Natural gas vehicles as a way to curb urban air pollution [DE95-012216] p 3088 N95-33395

SUBSTRATES
Numerical analysis of the ultraprecision machining of copper [DE95-007857] p 3089 N95-32585
YBa2Cu3O(7-x) 45 deg (001) tilt grain boundaries induced by controlled low-energy sputtering of MgO substrates: Transport properties and atomic-scale structure [DE95-005826] p 3228 N95-32810
Copper-diamond composite substrates for electronic components [DE95-011520] p 3079 N95-33063
Printability of substrate and absorber defects on extreme ultraviolet lithographic masks [DE95-010916] p 3084 N95-33247
Effect of the colony microstructure on transport critical current of high-J(c) Tl-1223 thick films [DE95-013049] p 3230 N95-34213
Influence of CO2 continuous laser preprocessed substrates on optical thin film damage thresholds [AD-A294190] p 3217 N95-34297
Diamond multilayer multichip module substrate [AD-D017468] p 3104 N95-34445
Method of forming thin films on substrates at low temperatures [AD-D017470] p 3086 N95-34447
Growth of GaN single-crystal boules [AD-A294976] p 3232 N95-34586

SUCTION
Boundary layer transition studies [NASA-CR-198983] p 3106 N95-32454

SULFATES
Remote sensing of smoke, clouds, and radiation using AVIRIS during SCAR experiments p 3132 N95-33749

SULFUR COMPOUNDS
Gasoline from natural gas by sulfur processing [DE95-010651] p 3087 N95-32563

SULFURIC ACID
Reduction and analysis of seasons 15 and 16 (1991 - 1992) Pioneer Venus radio occulation data and correlative studies with observations of the near infrared emission of Venus [NASA-CR-199071] p 3247 N95-32700

SUM RULES
The Q(2)-dependence of the Gross-Llewellyn Smith sum rule and of the parton distributions [DE95-623678] p 3202 N95-32406
Scaling law for the Upsilon(4S) yields bar-BB and psi(3770) yields bar-DD decay constants from effective sum rules [DE95-620538] p 3203 N95-32554

SUN
Solar-geophysical data number 607, March 1995. Part 1 (prompt reports). Data for January, February 1995 and late data [PB95-216388] p 3248 N95-32963

SUNSET
Chemical substances lists: A guide to the lists used in the Swedish Sunset Project. Supplement to report 13/94. Selecting multiproblem chemicals for risk reduction. A presentation of the Swedish Sunset Project [PB95-211272] p 3073 N95-33328

SUPERCHARGERS
Unitized Regenerative Fuel Cells for solar rechargeable aircraft and zero emission vehicles [DE95-010684] p 3150 N95-33642

SUPERCOMPUTERS
Simulation of hypervelocity impact on massively parallel supercomputer [DE95-007735] p 3184 N95-32383
HINT: A new way to measure computer speed [DE95-010245] p 3177 N95-32398
The future of finite element applications on massively parallel supercomputers [DE95-011659] p 3184 N95-32415
High performance systems [DE95-009523] p 3185 N95-32771
Construction of a connectionist network supercomputer [AD-A294198] p 3177 N95-34301
Hardware implementation of a desktop supercomputer for high performance image processing [AD-A294272] p 3178 N95-34462
Optical interconnects for 3D computer architectures [AD-A294118] p 3178 N95-34503

SUPERCONDUCTING FILMS
The effects of H(+) implants on YBa2Cu3O7 superconducting materials [DE95-614466] p 3227 N95-32698
Formation of artificially-layered high-temperature superconductors using pulsed-laser deposition [DE95-012884] p 3231 N95-34465

SUPERCONDUCTING MAGNETS
Analysis of a HTSC current lead under nonlinear heat transfer conditions [DE95-009420] p 3102 N95-32714
Quench antenna and fast-motion investigations during training of a 7T dipole magnet [DE95-012371] p 3103 N95-33080
A final-focus magnet for PEP-2 [DE95-012372] p 3214 N95-33504
Ramp-rate sensitivity of SSC dipole magnet prototypes [DE95-011162] p 3214 N95-33720

SUPERCONDUCTING SUPER COLLIDER
Ramp-rate sensitivity of SSC dipole magnet prototypes [DE95-011162] p 3214 N95-33720

SUPERCONDUCTIVITY
Summary of the impedance working group [DE95-012095] p 3211 N95-32606
Photoemission study of some novel materials: Rare earth/transition metal interface, Ba*(0.6)*K*(0.4)*BiO3* and AlPdMn [DE95-010125] p 3227 N95-32643
Quench propagation velocity for highly stabilized conductors [DE95-011040] p 3103 N95-33404
Low-energy response of superconducting tunnel junction x-ray spectrometers [DE95-011733] p 3230 N95-33650

SUPERCONDUCTORS (MATERIALS)
Background meeting and technology demonstration: Chromium electroplating of superconductor strand [DE95-011736] p 3068 N95-33070
Quench propagation velocity for highly stabilized conductors [DE95-011040] p 3103 N95-33404
Channel equalized DC squid flux-locked loop [AD-D017469] p 3104 N95-34446

SUPERCRITICAL FLOW
Supercritical crystallization: The RESs-process and the GAS-process [PB95-214482] p 3228 N95-33235

SUPERCRITICAL FLUIDS
Supercritical crystallization: The RESs-process and the GAS-process [PB95-214482] p 3228 N95-33235
The oxidation of energetic materials in supercritical water [DE95-010888] p 3088 N95-33702

Solubility behavior of quartz and corundum in supercritical water: A quantitative thermodynamic interpretation
[DE95-012294] p 3234 N95-34211
The relationship of chemical structure to supercritical-fluid solubility and to cosolvent-modifier properties: A literature review
[AD-A294933] p 3076 N95-34599

SUPERFLUIDITY
Transverse acoustic properties of the B-phase of superfluid helium three p 3074 N95-33414

SUPERGIANT STARS
Beryllium and Boron abundances in population II stars
[NASA-CR-189434] p 3247 N95-33262

SUPERHIGH FREQUENCIES
Development of an L-, C-, and X-band radar for backscattering studies over vegetation
[NASA-CR-199112] p 3097 N95-33033

SUPERLATTICES
The growth and optimization of InPSb/InGaAs/InAsSb strained-layer superlattice emitters by metal organic chemical vapor deposition
[DE95-011057] p 3226 N95-32595
Growth and characterization of heterostructures and infrared emitters with compressed InAsSb layers
[DE95-009826] p 3228 N95-33213
Formation of artificially-layered high-temperature superconductors using pulsed-laser deposition
[DE95-012884] p 3231 N95-34465

SUPERSONIC BOUNDARY LAYERS
Asymptotic structure of supersonic turbulent boundary layers p 3107 N95-32898
Numerical simulation of supersonic flow using a new analytical bleed boundary condition
[NASA-CR-198368] p 3054 N95-33208

SUPERSONIC COMBUSTION
Calculation of supersonic combustion in SCRAMJET engines p 3035 N95-34513

SUPERSONIC COMBUSTION RAMJET ENGINES
Calculation of supersonic combustion in SCRAMJET engines p 3035 N95-34513

SUPERSONIC FLOW
Transport phenomena in subsonic and supersonic flows in a duct with mass injection p 3108 N95-32934
Numerical simulation of supersonic flow using a new analytical bleed boundary condition
[NASA-CR-198368] p 3054 N95-33208
Very large eddy simulations of spatially evolving supersonic turbulent shear layers p 3110 N95-33606
DSMC method applied for reacting gas flows p 3035 N95-34509
A study of supersonic mixing flow field with ramp injector p 3035 N95-34512
Calculation of supersonic combustion in SCRAMJET engines p 3035 N95-34513
Dependency of a boundary layer flow on computational grids p 3040 N95-34550

SUPERSONIC INLETS
Drag measurements of an axisymmetric nacelle mounted on a flat plate at supersonic speeds
[NASA-TM-4660] p 3034 N95-32821
Numerical simulation of supersonic flow using a new analytical bleed boundary condition
[NASA-CR-198368] p 3054 N95-33208

SUPERSONIC SPEED
Drag measurements of an axisymmetric nacelle mounted on a flat plate at supersonic speeds
[NASA-TM-4660] p 3034 N95-32821
Minimum fuel mode evaluation p 3051 N95-33015
Rapid deceleration mode evaluation p 3052 N95-33018
Studies of hypersonic boundary layer behavior
[AD-A294137] p 3113 N95-34752

SUPERSONIC TRANSPORTS
Drag measurements of an axisymmetric nacelle mounted on a flat plate at supersonic speeds
[NASA-TM-4660] p 3034 N95-32821
Numerical analysis around the whole SST configuration p 3039 N95-34541

SUPERSYMMETRY
Virtual effects of physics beyond the standard model
[DE95-012499] p 3207 N95-33201

SUPINE POSITION
G-protection basis/acceleration physiology p 3168 N95-34051
Increase of High-sustained +G(z) tolerance at the expense of pilot's working posture change p 3165 N95-34056

SUPPLYING
Stochastic network processes
[AD-A294939] p 3187 N95-34603

SUPPORT SYSTEMS
Focus of attention in decision support systems
[AD-A294037] p 3236 N95-34487
Space probe data processing
[AD-A294124] p 3058 N95-34744

SURFACE COOLING
Large-eddy simulation of the development of stably-stratified atmospheric boundary layers over cool flat surfaces
[DE95-009574] p 3156 N95-32697

SURFACE DEFECTS
Thermographic imaging for high-temperature composite materials: A defect detection study
[NASA-TM-106950] p 3125 N95-33209

SURFACE EMITTING LASERS
Integration of diffractive lenses with addressable vertical-cavity laser arrays
[DE95-009850] p 3118 N95-32663
A reconfigurable optoelectronic interconnect technology for multi-processor networks
[DE95-011895] p 3186 N95-33838

SURFACE FINISHING
CRADA with United Solar Technologies and Pacific Northwest Laboratory (PNL-021): Thin film materialsfor low-cost high performance solar concentrators
[DE95-010423] p 3150 N95-33400
High-speed, low-damage grinding of advanced ceramics, phase 1
[DE95-011241] p 3085 N95-33425
Spray coating of metals. Proof of concept: Phase 2
[AD-A294393] p 3081 N95-34348

SURFACE IONIZATION
Application of Ni-63 photo and corona discharge ionization for the analysis of chemical warfare agents and toxic wastes p 3070 N95-33272

SURFACE NAVIGATION
The effects of display location and dimensionality on taxiway navigation
[AD-A294878] p 3047 N95-34570

SURFACE PROPERTIES
Solving stiff chemistry problems with FIDAP
[DE95-011053] p 3067 N95-32709
Low-energy Ion-Beam Deposition apparatus equipped with surface analysis system
[DE95-737272] p 3212 N95-32712
The use of ion mobility spectrometry and gas chromatography/mass spectrometry for the detection of illicit drugs on clandestine records p 3070 N95-33276
Calibration to surface reflectance of terrestrial imaging spectrometry data: Comparison of methods p 3130 N95-33743
A field- and laboratory-based quantitative analysis of alluvium: Relating analytical results to TIMS data p 3139 N95-33800
Fundamental surface chemistry of GaAs OMVPE
[DE95-011606] p 3231 N95-34486

SURFACE REACTIONS
Solving stiff chemistry problems with FIDAP
[DE95-011053] p 3067 N95-32709
Foam spread experiments on a water surface
[PB95-211025] p 3083 N95-32962
Interfacial reactions during the liquid infiltration of titanium matrix composites p 3081 N95-34252
Fundamental surface chemistry of GaAs OMVPE
[DE95-011606] p 3231 N95-34486
Surface chemistry of diamond single crystals
[AD-A294150] p 3232 N95-34755

SURFACE ROUGHNESS
Ocean observations with EOS/MODIS: Algorithm development and post launch studies
[NASA-CR-198928] p 3143 N95-32914
Monitoring of the cutting operations using fuzzy logic p 3189 N95-32999
High-speed, low-damage grinding of advanced ceramics, phase 1
[DE95-011241] p 3085 N95-33425
Measuring soil moisture with imaging radars p 3139 N95-33803
Application of IEM model on soil moisture and surface roughness estimation p 3142 N95-33816
In situ surface roughness measurement during PECVD diamond film growth
[DE95-013411] p 3230 N95-34215
Infrared detection of chemical corrosion on metal surface
[AD-A295000] p 3081 N95-34821

SURFACE ROUGHNESS EFFECTS
Effect of propagation attenuation of thin film waveguide on optical thin film losses
[AD-A294064] p 3218 N95-34471

SURFACE TEMPERATURE
Modeling soil climate controls on the exchange of trace gases between the terrestrial biosphere and the atmosphere p 3153 N95-33337
Urban remote sensing applications: TIMS observations of the City of Scottsdale p 3137 N95-33791

SURFACE TREATMENT
Tests of adhesives used for plate bonding of ATLAS tile-cal hadron calorimeter
[DE95-009917] p 3082 N95-32664
Adhesion of novel high-performance polymers to carbon fibers: Fiber surface treatment, characterization, and microbond single fiber pull-out test p 3085 N95-34282

SURFACE VEHICLES
Vertical velocity ambiguity resolution method
[AD-D017481] p 3201 N95-34424

SURFACE WAVES
Sea wave parameters, small altitudes and distances measurers design for movement control systems of ships, wing-in-surface effect crafts and seaplanes p 3094 N95-33141
Laser-based ultrasonics by dual-probe interferometer detection and narrow-band ultrasound generation p 3118 N95-33464
Numerical studies of turbulent free surface flows and unsteady propeller flows
[AD-A294377] p 3112 N95-34343
An experimental study of collective sea state modes of deep water surface gravity waves
[AD-A294007] p 3160 N95-34372

SURVEILLANCE
GPS-Squitter interference analysis
[AD-A293690] p 3047 N95-33480

SURVEYS
Feasibility survey on international cooperation for high efficiency energy conversion technology in fiscal 1993
[DE95-769804] p 3148 N95-32546
Technical innovation for reducing emissions of greenhouse effect gas and survey of effects of changes of industrial structures
[DE95-769808] p 3151 N95-32547
A survey of parametrized variational principles and applications to computational mechanics
[NASA-CR-199041] p 3180 N95-32766
A comparison of risk assessment techniques from qualitative to quantitative
[DE95-011430] p 3197 N95-33220
Chemical substances lists: A guide to the lists used in the Swedish Sunset Project. Supplement to report 13/94. Selecting multiproblem chemicals for risk reduction. A presentation of the Swedish Sunset Project
[PB95-211272] p 3073 N95-33328
The PEP-2 project-wide database
[DE95-012512] p 3213 N95-33333
Aerospace physiology AFSC 4M0X1
[AD-A294839] p 3165 N95-34564
RR lyrae variable stars in the CCD/Transit instrument survey
[AD-A294138] p 3246 N95-34753
Transmittance characteristics of US Army rotary-wing aircraft transparencies
[AD-A295035] p 3049 N95-34793

SWEDEN
Presentation of a Swedish study program concerning recruitment, selection and training of student air traffic controllers: The MRU project phase 1 p 3167 N95-34775

SWEPT WINGS
A large scale 3D Navier-Stokes analysis using NAL-NWT p 3039 N95-34539

SWIRLING
Static pressure drop by swirling flow of an internal cooling air system through a turbine shaft p 3042 N95-34560

SWITCHES
A reconfigurable optoelectronic interconnect technology for multi-processor networks
[DE95-011895] p 3186 N95-33838
Protocol engineering for broadband networks
[AD-A294969] p 3186 N95-34584

SWITCHING
Modeling of DC spacecraft power systems p 3062 N95-32423
Mechanism(s) for the suppression of the switchable polarization in PZT and BaTiO3
[DE95-009589] p 3226 N95-32590
Feasibility of fullerene thin films for high-speed all-optical switching
[DE95-011735] p 3085 N95-33409
Image compression scheme for network transmission
[AD-A294959] p 3182 N95-34580

SWITCHING CIRCUITS
Tokamak ETE circuits: Analysis and specifications
[INPE-5573-PRP/182] p 3224 N95-33873
Improved L-C resonant decay technique for Q measurement of quasilinear power inductors: New results for MPP and ferrite powdered cores
[NASA-CR-198373] p 3103 N95-33874

SYMBOLS
Scanners, optical character readers, Cyrillic alphabet and Russian translations p 3194 N95-32433
Allison engine testing CMSX-4(reg sign) single crystal turbine blades and vanes
[DE95-010308] p 3050 N95-32636

SYMMETRY
Experimental study of the processes in the expander of the axisymmetric mirror device
[DE95-009846] p 3221 N95-32536
Chiral restoration in hot and/or dense matter
[DE95-012176] p 3204 N95-32621
Zero modes of Gauss constraint in gaugeless reduction of Yang-Mills theory
[DE95-623676] p 3234 N95-32667
The (pi)(yields)e(nu)(gamma) decay in chiral perturbation theory
[DE95-619269] p 3206 N95-32806
SYNCHRONISM
Congestion control over ATM local area networks
[DE95-010343] p 3184 N95-32558
The effect of travel speed on thermal response in CO2 laser welding of small electronic components
[DE95-006314] p 3118 N95-32683
SYNCHRONOUS SATELLITES
Thermal control technology of communications satellite
[AD-A294249] p 3059 N95-34493
SYNCHROTRON RADIATION
Photoemission study of some novel materials: Rare earth/transition metal interface, Ba*(0.6)*K*(0.4)*BiO3* and AlPdMn
[DE95-010125] p 3227 N95-32643
Synchrotron radiation studies of local structure and bonding in transition metal aluminides and rare earth transition metal magnetic nitrides
[DE95-011579] p 3079 N95-33065
Effects of enhanced chromatic nonlinearity during the AGS gamma(t)-jump
[DE95-011703] p 3212 N95-33067
Compton Observatory observations of clusters of galaxies and extragalactic radio sources
[NASA-CR-189431] p 3246 N95-33261
Injection envelope matching in storage rings
[DE95-012496] p 3213 N95-33377
SYNCHROTRONS
Effects of enhanced chromatic nonlinearity during the AGS gamma(t)-jump
[DE95-011703] p 3212 N95-33067
SYNTHESIS (CHEMISTRY)
Spin counting in dipolar coupled spin 1/2 systems by multiple quantum NMR spectroscopy in solids: Development of a single quantum propagator and its application to heterogeneous catalysis
[DE95-010246] p 3066 N95-32540
NQR-NMR studies of higher alcohol synthesis Cu-Co catalysts
[DE95-010524] p 3066 N95-32557
Formation of artificially-layered high-temperature superconductors using pulsed-laser deposition
[DE95-012884] p 3231 N95-34465
SYNTHETIC APERTURE RADAR
RASSP benchmark 1 technical description. Revision 1
[AD-A293030] p 3096 N95-32773
HeliRadar: A rotating antenna synthetic aperture radar for helicopter allweather operations
p 3093 N95-33137
Identification of terrain imagery with unstable reflectivity p 3093 N95-33138
Studies of microwave scattering and canopy architecture for boreal forests
[NASA-CR-199113] p 3099 N95-33497
Studies of microwave scattering and canopy architecture for boreal forests
[NASA-CR-199114] p 3099 N95-33726
Summaries of the Fifth Annual JPL Airborne Earth Science Workshop. Volume 3: AIRSAR Workshop
[NASA-CR-198924] p 3139 N95-33801
New observations of Bolivian wind streaks by JPL Airborne SAR: Preliminary results p 3139 N95-33802
Use of TOPSAR digital elevation data to determine the 3-dimensional shape of an alluvial fan
p 3139 N95-33804
Accurate estimation of sigma(exp 0) using AIRSAR data p 3139 N95-33805
Remotely sensed indicators of habitat heterogeneity and biological diversity: A preliminary report
p 3140 N95-33806
Polarization and wavelength diversities of Gulf Stream fronts imaged by AIRSAR p 3140 N95-33807
Use of AIRSAR to identify woody shrub invasion and other indicators of desertification in the Jornada LTER
p 3141 N95-33810
The unique radar scattering properties of silicic lava flows and domes p 3141 N95-33811
On the potential of long wavelength imaging radars for mapping vegetation types and woody biomass in tropical rain forests p 3141 N95-33812
Lithologic controls on AIRSAR signatures of bedrock and alluvium, at Lunar Crater, Nevada
p 3141 N95-33813
Estimation of penetration of forest canopies by Interferometric SAR measurements
p 3141 N95-33814
Regional mapping of forest canopy water content and biomass using AIRSAR images over BOREAS study area p 3142 N95-33815
Application of IEM model on soil moisture and surface roughness estimation p 3142 N95-33816
Geographic information system for fusion and analysis of high-resolution remote sensing and ground data
p 3240 N95-34224
SAR
[AD-A295020] p 3101 N95-34788
SYNTHETIC APERTURES
Three-dimensional ground penetrating radar imaging using synthetic aperture time-domain focusing
[DE95-010731] p 3095 N95-32569
SYSTEMS ANALYSIS
Adaptive strategy selection for concept learning
[AD-A294086] p 3193 N95-34473
Conditions for implicit parallelism
[AD-A294110] p 3193 N95-34497
Explanations of empirically derived reactive plans
[AD-A294114] p 3193 N95-34501
Non-smooth optimization algorithms, system theory and software tools
[AD-A294944] p 3183 N95-34605
SSME Post Test Diagnostic System: Systems Section
[NASA-CR-198375] p 3061 N95-34625
Sleep sets method for partial order verification of concurrent systems
[PB95-236121] p 3183 N95-34655
Analysis of safety requirements in the context of system faults and human errors
[PB95-236105] p 3171 N95-34658
Numerical and symbolic algorithms for application specific signal processing
[AD-A294125] p 3100 N95-34749
INMARSAT TT&C and communications network and the Beijing INMARSAT Station
[AD-A294163] p 3100 N95-34760
Certify for success: A methodology for human-centered certification of advanced aviation systems
p 3173 N95-34773
Uncertainty analysis using stochastic finite elements
p 3196 N95-34803
SYSTEMS ENGINEERING
Application of fuzzy technology to risk-based design and decision problems
[DE95-006815] p 3178 N95-32378
Formalization and representation of a product-driven approach to method assembly for situational systems development
[PB95-215190] p 3237 N95-33238
Aircraft scanner data availability via the version 0 Information Management System p 3134 N95-33762
Development of a tool-set for simultaneous, multi-site observations of astronomical objects
p 3239 N95-34221
Topography from shading and stereo
p 3241 N95-34229
Planetary data analysis and display system: A version of PC-MCIDAS p 3241 N95-34232
Construction of a connectionist network supercomputer
[AD-A294198] p 3177 N95-34301
Automated support for software engineering
[AD-A294965] p 3182 N95-34582
Experiences using DCE and CORBA to build tools for creating highly-available distributed systems
[AD-A294973] p 3187 N95-34587
Human factors certification in the development of future air traffic control systems p 3048 N95-34770
Quality assurance and risk management: Perspectives on Human Factors Certification of Advanced Aviation Systems p 3048 N95-34771
SYSTEMS HEALTH MONITORING
Genetic algorithm based input selection for a neural network function approximator with applications to SSME health monitoring
[NASA-CR-199089] p 3188 N95-32768
SSME Post Test Diagnostic System: Systems Section
[NASA-CR-198375] p 3061 N95-34625
SYSTEMS INTEGRATION
The application of helicopter mission simulation to Nap-of-the-Earth operations p 3044 N95-32496
An integrated system for air to ground operations
p 3044 N95-32498
A helmet mounted display for night missions at low altitude p 3045 N95-32503
PSC implementation and integration
p 3051 N95-33014
The DLR research programme on an integrated multi sensor system for surface movement guidance and control p 3048 N95-33135
Application of advanced safety technique to ring laser gyro inertial navigation system integration
p 3048 N95-33140
Integrated special mission flight management for a flight inspection aircraft p 3049 N95-33145
Gas chromatography/ion mobility spectrometry as a hyphenated technique for improved explosives detection and analysis p 3071 N95-33278
Data collection in IMS: It's not as easy as it looks
p 3072 N95-33286
Topography from shading and stereo
p 3241 N95-34229
A distributed system for visualizing and analyzing multivariate and multidisciplinary data
p 3241 N95-34230
VIEWCACHE: An incremental pointer-based access method for autonomous interoperable databases
p 3242 N95-34235
SAVS: A Space Analysis and Visualization System
p 3242 N95-34238
A Spatial Analysis and Modeling System (SAMS) for environment management p 3243 N95-34239
SYSTEMS MANAGEMENT
System of experts for intelligent data management (SEIDAM) p 3240 N95-34226

T

T-56 ENGINE
Water model tests on the Allison T56 series 3 combustion system
[DSTO-TR-0139] p 3054 N95-33250
TACHOMETERS
Solid-state data recorder, next development and use
p 3094 N95-33143
TACTICS
Helicopter HF communications using the NVIS mode
p 3043 N95-32491
Tactical low-level helicopter communications
p 3043 N95-32492
A tactical navigation and routeing system for low-level flight p 3044 N95-32494
TAKEOFF
An LDV investigation of support structure influence on the flow field near the wingtip of a STOVL configuration in hover
[AD-A294126] p 3042 N95-34750
TARGET ACQUISITION
The development of the automatic target recognition system for the UGV/RSTA LADAR
[AD-A294090] p 3100 N95-34474
TARGET RECOGNITION
Mapping target signatures via partial unmixing of AVIRIS data p 3129 N95-33737
Branch and bound methods for search problems
[AD-A294522] p 3182 N95-34349
The development of the automatic target recognition system for the UGV/RSTA LADAR
[AD-A294090] p 3100 N95-34474
TARGETS
Production asymmetries in x(sub f) and P(sup 2)(sub t) for D(sup +/-) mesons
[DE95-007207] p 3201 N95-32379
Behavior of structural and target materials irradiated in spallation neutron environments
[DE95-010879] p 3203 N95-32576
Targets and magnetic elements for pion collection in muon collider drivers
[DE95-010316] p 3205 N95-32652
Branch and bound methods for search problems
[AD-A294522] p 3182 N95-34349
Experimental investigation of impulse radar for mitigation of effects of radar absorbing materials
[AD-A294166] p 3100 N95-34762
TASKS
Development and application of the methods for pilot-aircraft system research to the manual control tasks of modern vehicles p 3094 N95-33139
Resource document for the design of electronic instrument approach procedure displays
[AD-A295108] p 3047 N95-34797
TAXIING
The effects of display location and dimensionality on taxiway navigation
[AD-A294878] p 3047 N95-34570
TEARING MODES (PLASMAS)
Transport studies of tokamak plasmas in JT-60 device
[DE95-737227] p 3220 N95-32417
TECHNOLOGICAL FORECASTING
Navigational technology of dual usage
p 3048 N95-33131
Solid-state data recorder, next development and use
p 3094 N95-33143

TECHNOLOGY ASSESSMENT
Fixed wing night attack missions: Assessment in a Flight Simulation environment p 3045 N95-32502
A decade of neural networks: Practical applications and prospects
[NASA-CR-198867] p 3188 N95-32659
Research and technology 1994: Annual report of the Marshall Space Flight Center
[NASA-TM-108470] p 3252 N95-33042
Dual use: Opportunities, payoffs, and challenges p 3091 N95-33127
The concept of the space system based on the Rocket launch vehicle of light-weight class for direct sounding of large-scale natural hazards p 3057 N95-33128
Dual-use micromechanical inertial sensors p 3092 N95-33132
Laser gyroscopy tendencies and their analysis of development in Ukraine p 3092 N95-33133
Effects of the specific military aspects of satellite navigation on the civil use of GPS/GLONASS p 3048 N95-33134
HeliRadar: A rotating antenna synthetic aperture radar for helicopter allweather operations p 3093 N95-33137
The effect of sample holder material on ion mobility spectrometry reproducibility p 3071 N95-33282
Data collection in IMS: It's not as easy as it looks p 3072 N95-33286

TECHNOLOGY TRANSFER
Research and technology 1994: Annual report of the Marshall Space Flight Center
[NASA-TM-108470] p 3252 N95-33042
The concept of the space system based on the Rocket launch vehicle of light-weight class for direct sounding of large-scale natural hazards p 3057 N95-33128
Commercial usage of Navy components developed and manufactured by CRI Delfin p 3092 N95-33129
Some results of international cooperation in military to commercial conversion of laser gyro technology p 3092 N95-33130
Navigational technology of dual usage p 3048 N95-33131
Dual-use micromechanical inertial sensors p 3092 N95-33132
Effects of the specific military aspects of satellite navigation on the civil use of GPS/GLONASS p 3048 N95-33134
A layered approach to technology transfer of AVIRIS between Earth Search Sciences, Inc. and the Idaho National Engineering Laboratory p 3117 N95-33746
Advanced data visualization and sensor fusion: Conversion of techniques from medical imaging to Earth science p 3242 N95-34236
Recent developments in maritime technology research institute acousto-optical technology research
[AD-A294215] p 3217 N95-34307

TECHNOLOGY UTILIZATION
Activities of the Division of Microwave Technology
[PB95-214524] p 3095 N95-32613
A decade of neural networks: Practical applications and prospects
[NASA-CR-198867] p 3188 N95-32659
Development of a composite satellite structure for FORTE
[DE95-009416] p 3058 N95-32713
Industrial and Engineering Applications of Artificial Intelligence and Expert Systems: Invited and additional papers
[DSTO-GD-0051] p 3188 N95-32995
Expert systems and artificial intelligence applications in engineering design and inspection p 3190 N95-33008
Dual use: Opportunities, payoffs, and challenges p 3091 N95-33127
Commercial usage of Navy components developed and manufactured by CRI Delfin p 3092 N95-33129
Some results of international cooperation in military to commercial conversion of laser gyro technology p 3092 N95-33130
Navigational technology of dual usage p 3048 N95-33131
Dual-use micromechanical inertial sensors p 3092 N95-33132
Laser gyroscopy tendencies and their analysis of development in Ukraine p 3092 N95-33133
The DLR research programme on an integrated multi sensor system for surface movement guidance and control p 3048 N95-33135
Solid-state data recorder, next development and use p 3094 N95-33143
GPS-based navigation for space applications p 3058 N95-33144
Managing technological change in a military treatment facility: A case study of medical diagnostic imaging support (MDIS) system
[AD-A294894] p 3185 N95-34573

TEFLON (TRADEMARK)
Characterizing the fragmentation ring on witness plates p 3056 N95-32426

TELECOMMUNICATION
FH and DS spread-spectrum systems in interference-limited HF channels: A comparison
[PB95-211439] p 3098 N95-33230
Spectrum allocation strategies for communication networks
[AD-A294936] p 3100 N95-34601
Stochastic network processes
[AD-A294939] p 3187 N95-34603
Design and analysis of lossless and lossy data compression methods with applications to communication and caching
[AD-A295025] p 3101 N95-34790

TELEMETRY
Space probe data processing
[AD-A294124] p 3058 N95-34744
INMARSAT TT&C and communications network and the Beijing INMARSAT Station
[AD-A294163] p 3100 N95-34760

TELEPHONES
Stochastic network processes
[AD-A294939] p 3187 N95-34603

TELESCOPES
Development of a tool-set for simultaneous, multi-site observations of astronomical objects p 3239 N95-34221

TELEVISION SYSTEMS
A real-time single-camera, stereoscopic video device
[AD-A294105] p 3116 N95-34496

TELLURIUM COMPOUNDS
High-resolution TeO2 acousto-optical deflector for millimeter-wave spectrometer
[AD-A293054] p 3215 N95-32701

TEMPERATE REGIONS
Mid-latitude ionospheric plasma drift: A comparison of digital ionosonde and incoherent scatter radar measurements at Millstone Hill p 3222 N95-32838

TEMPERATURE CONTROL
Baseline experimental investigation of an electrohydrodynamically assisted heat pipe p 3113 N95-32427
Design and testing criteria for bipolar plate materials for PEM fuel cell applications
[DE95-010878] p 3148 N95-32575
Minimum fan turbine iniet temperature mode evaluation p 3052 N95-33016
Method of forming thin films on substrates at low temperatures
[AD-D017470] p 3086 N95-34447
Thermal control technology of communications satellite
[AD-A294249] p 3059 N95-34493
Thermal design of returnable satellites
[AD-A294113] p 3059 N95-34500

TEMPERATURE DEPENDENCE
Three-dimensional natural convection of a fluid with temperature-dependent viscosity in an enclosure with localized heating
[DE95-002606] p 3106 N95-32387
Anisotropic magnetization of HoNi2B2C
[DE95-010239] p 3198 N95-32397
Irradiation-assisted stress corrosion cracking considerations at temperatures below 288 C
[DE95-008940] p 3077 N95-32555
Analysis of a HTSC current lead under nonlinear heat transfer conditions
[DE95-009420] p 3102 N95-32714
Design and analysis of transient nonlinear coupled systems p 3199 N95-33292
Magnetostriction and thermal expansion of the Kondo semiconductor Ce3Bi4Pt3
[DE95-011975] p 3229 N95-33386
Properties of high-T(sub c) Josephson junctions with Y(0.7)Ca(0.3)Ba2Cu3O(7-delta) barrier layers
[AD-A294852] p 3231 N95-34568

TEMPERATURE DISTRIBUTION
Transport phenomena in subsonic and supersonic flows in a duct with mass injection p 3108 N95-32934

TEMPERATURE EFFECTS
Effect of heat treatment at 1,150 C on creep rupture properties of a Fe3Al-based alloy
[DE95-010295] p 3077 N95-32527
The effect of travel speed on thermal response in CO2 laser welding of small electronic components
[DE95-006314] p 3118 N95-32683
The tensile fracture behavior of the weld metal of BIS 812 EMA and Q1N naval construction steels
[DSTO-RR-0021] p 3078 N95-32926
Micromechanics of composites with shape memory alloy fibers in uniform thermal fields
[NASA-TM-107011] p 3063 N95-33210
Thermocapillary flow with evaporation and condensation and its effect on liquid retention in low-g fluid acquisition devices p 3109 N95-33256
Experimental and numerical analysis of controlled impinging liquid jets p 3109 N95-33257
Using optical interference methods to measure acousto-optical device thermal effects
[AD-A294219] p 3217 N95-34309
Fracture toughness assessment of present and future pressure vessel materials based on Charpy impact energy and yield strength
[AD-A294008] p 3081 N95-34373

TEMPERATURE MEASUREMENT
Land surface temperature measurements from EOS MODIS data
[NASA-CR-199082] p 3142 N95-32717
Iron Boltzmann factor LIDAR: Proposed new remote-sensing technique for mesospheric temperature
[AD-A293568] p 3157 N95-34613

TEMPERATURE MEASURING INSTRUMENTS
A 30-pair thin film thermoelectric pile
[AD-A294058] p 3151 N95-34468

TEMPLATES
Application of deformable templates for recognizing tracks detected with High Pressure Drift Tubes
[DE95-621870] p 3188 N95-32627
Automatic script identification from images using cluster-based templates
[DE95-006339] p 3181 N95-33154

TEMPORAL DISTRIBUTION
Training and recognition of Cantonese phonemes by backpropagation through time p 3188 N95-32996
Time correlations between low and high energy gamma rays from discrete sources
[NASA-CR-199214] p 3248 N95-33916

TEMPORAL RESOLUTION
A dual, parallel cavity Fabry-Perot interferometer
[DE95-010796] p 3115 N95-32900

TENSILE DEFORMATION
Structural influences on the work hardening behavior of aluminum
[DE95-011262] p 3080 N95-33626
Inclusion models of tensile fracture in fiber-reinforced brittle-matrix composites p 3065 N95-33721

TENSILE STRENGTH
The tensile fracture behavior of the weld metal of BIS 812 EMA and Q1N naval construction steels
[DSTO-RR-0021] p 3078 N95-32926
Adhesion of novel high-performance polymers to carbon fibers: Fiber surface treatment, characterization, and microbond single fiber pull-out test p 3085 N95-34282

TENSILE STRESS
The linear elastic biaxial response of plain-woven meshes p 3064 N95-33468

TENSILE TESTS
Tests of adhesives used for plate bonding of ATLAS tile-cal hadron calorimeter
[DE95-009917] p 3082 N95-32664
The tensile fracture behavior of the weld metal of BIS 812 EMA and Q1N naval construction steels
[DSTO-RR-0021] p 3078 N95-32926

TENSORS
The non-relativistic charged Bose gas in a magnetic field. Part 1: Formalism
[DE95-619698] p 3205 N95-32632

TERMINOLOGY
An empirical investigation of the semantic warrants exercised in thesaurus construction
[ISBN-0-315-86393-5] p 3238 N95-33334

TERNARY ALLOYS
Strength, ductility, and fracture mode of ternary FeAl alloys
[DE95-010281] p 3077 N95-32400

TERRAIN
Identification of terrain imagery with unstable reflectivity p 3093 N95-33138
Bayes classification of interferometric TOPSAR data p 3140 N95-33808
Terrain classification using circular polarimetric features p 3140 N95-33809
Perceptual dimensions of simulated scenes relevant for visual low-altitude flight
[AD-A294385] p 3056 N95-34344
Altitude cuing effectiveness of terrain texture characteristics in simulated low-altitude flight
[AD-A294369] p 3056 N95-34362
A comparison of monocular, biocular, and binocular night vision goggles for traversing off-road terrain on foot
[AD-A294018] p 3170 N95-34376

TERRAIN ANALYSIS
Bayes classification of interferometric TOPSAR data p 3140 N95-33808
Terrain classification using circular polarimetric features p 3140 N95-33809

TERRAIN FOLLOWING
Flight test of a low-altitude helicopter guidance system with obstacle avoidance capability p 3043 N95-32490
A tactical navigation and routeing system for low-level flight p 3044 N95-32494
A highly reliable, high performance open avionics architecture for real time Nap-of-the-Earth operations p 3044 N95-32497
An integrated system for air to ground operations p 3044 N95-32498
TEST CHAMBERS
Environmental chamber studies of atmospheric reactivities of volatile organic compounds: Effects of varying chamber and light source
[DE95-009225] p 3152 N95-32686
TEST FACILITIES
COBRA accelerator for Sandia ICF diode research at Cornell University
[DE95-011018] p 3101 N95-32578
TETHERED BALLOONS
Balloon-borne radiometer profiler: Field observations
[DE95-011493] p 3158 N95-33505
TETHERED SATELLITES
Shuttle Potential and Return Electron Experiment (SPREE) electrostatic analyzer (ESA) calibration report
[AD-A293026] p 3057 N95-32772
TETRAGONS
Poisson's ratio for tetragonal crystals
[AD-A293544] p 3232 N95-34607
TEXTILES
General procedure for clothing evaluations relative to heat stress
[AD-A294953] p 3171 N95-34577
TEXTS
Single Langmuir probe characteristic in a magnetized plasma at the TEXT tokamak
[DE95-012144] p 3224 N95-33853
Design and analysis of lossless and lossy data compression methods with applications to communication and caching
[AD-A295025] p 3101 N95-34790
TEXTURES
Experimental investigation of the separation of texture and residual stress induced anisotropy via oblique incidence acoustoelasticity p 3126 N95-33253
Perceptual dimensions of simulated scenes relevant for visual low-altitude flight
[AD-A294385] p 3056 N95-34344
Altitude cuing effectiveness of terrain texture characteristics in simulated low-altitude flight
[AD-A294369] p 3056 N95-34362
THALLIUM COMPOUNDS
Effect of the colony microstructure on transport critical current of high-J(c) Tl-1223 thick films
[DE95-013049] p 3230 N95-34213
THEMATIC MAPPING
Mapping minerals, amorphous materials, environmental materials, vegetation, water, ice and snow, and other materials: The USGS tricorder algorithm p 3130 N95-33742
Remote mineral mapping using AVIRIS data at Summitville, Colorado and the adjacent San Juan Mountains p 3134 N95-33761
Analyses of TIMS and AVIRIS data, integrated with field and laboratory spectra, for lithological and mineralogical interpretation of Vulcano Island, Italy p 3137 N95-33790
Aerolian erosion, transport, and deposition of volcaniclastic sands among the shifting sand dunes, Christmas Lake Valley, Oregon: TIMS image analysis p 3137 N95-33793
A conflict of water and fire: Remote sensing imagery of the Uinkaret Volcanic Field, Grand Canyon, Arizona p 3117 N95-33795
On the potential of long wavelength imaging radars for mapping vegetation types and woody biomass in tropical rain forests p 3141 N95-33812
Regional mapping of forest canopy water content and biomass using AIRSAR images over BOREAS study area p 3142 N95-33815
THEOREMS
Theory and application of homotopy techniques in nonlinear programming and control systems
[AD-A294934] p 3193 N95-34600
THEORETICAL PHYSICS
Calculations of spatial higher modes without deflation procedure
[REPT-2205] p 3090 N95-32985
Practical improvement of MS-X alpha molecular orbital calculation as applied to dissociation process of CO molecule
[REPT-2206] p 3090 N95-32986
Virtual effects of physics beyond the standard model
[DE95-012499] p 3207 N95-33201
CDW-EIS calculation of longitudinal momentum distribution in single ionization of helium by Ni(24+) ions
[DE95-010816] p 3207 N95-33241
THERMAL ANALYSIS
Experimental and analytical assessment of the thermal behavior of spiral bevel gears
[NASA-TM-107009] p 3123 N95-33179
Numerical thermal analyses of heat exchangers for the stirling engine application
[NASA-CR-199120] p 3110 N95-33398
THERMAL CONDUCTIVITY
Development of improved p-type Si-20 at. %Ge by addition of fullerite
[DE95-010230] p 3066 N95-32394
Thermoelectric material development
[DE95-007890] p 3149 N95-32811
Copper-diamond composite substrates for electronic components
[DE95-011520] p 3079 N95-33063
Using photothermal deflection techniques for studying the attenuations of guided waves propagated in optical thin films
[AD-A294203] p 3217 N95-34303
Using optical interference methods to measure acousto-optical device thermal effects
[AD-A294219] p 3217 N95-34309
Density, heat capacity, viscosity, and thermal conductivity of mixtures of CO2, He, H2, H2O, N2, and O2
[AD-A288731] p 3076 N95-34814
THERMAL CYCLING TESTS
The next generation of automobile emissions reduction: Innovative control of off-cycle emissions
[DE95-004057] p 3153 N95-32809
THERMAL DECOMPOSITION
Microstructural studies of hydrogen damage in metastable stainless steels p 3080 N95-33774
THERMAL EMISSION
Radiative interactions with micromachined surfaces: Spectral polarized emittance
[DE95-011455] p 3097 N95-33061
The 1994 TIMS airborne calibration experiment: Castaic Lake, California p 3117 N95-33797
Discrimination of alkalinity in granitoid Rocks: A potential TIMS application p 3138 N95-33798
A field- and laboratory-based quantitative analysis of alluvium: Relating analytical results to TIMS data p 3139 N95-33800
Thermal design of returnable satellites
[AD-A294113] p 3059 N95-34500
THERMAL ENERGY
Summary report for ITER Task No. T226B: Evaluation of ITER disruption erosion
[DE95-010402] p 3219 N95-32401
THERMAL EXPANSION
Magnetostriction and thermal expansion of the Kondo semiconductor Ce3Bi4Pt3
[DE95-011975] p 3229 N95-33386
THERMAL MAPPING
Summaries of the Fifth Annual JPL Airborne Earth Science Workshop. Volume 2: TIMS Workshop
[NASA-CR-198923] p 3136 N95-33789
Urban remote sensing applications: TIMS observations of the City of Scottsdale p 3137 N95-33791
For geological investigations with airborne thermal infrared multispectral images: Transfer of calibration from laboratory spectrometer to TIMS as alternative for removing atmospheric effects p 3137 N95-33792
The 1994 laboratory calibration of TIMS p 3117 N95-33796
Discrimination of alkalinity in granitoid Rocks: A potential TIMS application p 3138 N95-33798
A field- and laboratory-based quantitative analysis of alluvium: Relating analytical results to TIMS data p 3139 N95-33800
THERMAL NEUTRONS
A novel approach to the problem of highly-sensitive regular analysis for man-made plutonium in environment and human body
[DE95-620764] p 3164 N95-32666
THERMAL RADIATION
Radiative interactions with micromachined surfaces: Spectral polarized emittance
[DE95-011455] p 3097 N95-33061
THERMAL RESISTANCE
Copper-diamond composite substrates for electronic components
[DE95-011520] p 3079 N95-33063
A 30-pair thin film thermoelectric pile
[AD-A294058] p 3151 N95-34468
THERMAL STRESSES
Models for predicting damage evolution in metal matrix composites subjected to cyclic loading
[DE95-007734] p 3077 N95-32382
The effect of travel speed on thermal response in CO2 laser welding of small electronic components
[DE95-006314] p 3118 N95-32683
Stress relaxation in discontinuously reinforced composites
[DE95-010928] p 3064 N95-33704
Using optical interference methods to measure acousto-optical device thermal effects
[AD-A294219] p 3217 N95-34309
THERMIONIC CONVERTERS
Design and operation of a thermionic converter in air
[DE95-010151] p 3149 N95-32645
Integral cesium reservoir: Design and transient operation
[DE95-010152] p 3211 N95-32647
THERMODYNAMIC PROPERTIES
Thermal design of returnable satellites
[AD-A294113] p 3059 N95-34500
Density, heat capacity, viscosity, and thermal conductivity of mixtures of CO2, He, H2, H2O, N2, and O2
[AD-A288731] p 3076 N95-34814
THERMODYNAMICS
Models for predicting damage evolution in metal matrix composites subjected to cyclic loading
[DE95-007734] p 3077 N95-32382
Phase equilibria and phase diagrams in carbide systems
[PB95-211348] p 3068 N95-33229
Solubility behavior of quartz and corundum in supercritical water: A quantitative thermodynamic interpretation
[DE95-012294] p 3234 N95-34211
THERMOELECTRIC GENERATORS
Fabrication of improved SiGe alloys for an 18-couple module test
[DE95-010238] p 3060 N95-32396
Thermoelectric material development
[DE95-007890] p 3149 N95-32811
THERMOELECTRIC MATERIALS
Thermoelectric material development
[DE95-007890] p 3149 N95-32811
Multilayer thermoelectric films: A strategy for the enhancement of ZT
[DE95-011535] p 3081 N95-34482
THERMOELECTRICITY
A 30-pair thin film thermoelectric pile
[AD-A294058] p 3151 N95-34468
Multilayer thermoelectric films: A strategy for the enhancement of ZT
[DE95-011535] p 3081 N95-34482
THERMOGRAPHY
Thermographic imaging for high-temperature composite materials: A defect detection study
[NASA-TM-106950] p 3125 N95-33209
THERMOPHOTOVOLTAIC CONVERSION
A thermophotovoltaic generator for use in a lightweight electric car: Year 1 progress report
[DE95-011355] p 3102 N95-32968
THERMOPHYSICAL PROPERTIES
Thermophysical properties of HCFC alternatives
[DE95-009635] p 3233 N95-32661
THERMOPLASTIC RESINS
Adhesion of novel high-performance polymers to carbon fibers: Fiber surface treatment, characterization, and microbond single fiber pull-out test p 3085 N95-34282
THESAURI
An empirical investigation of the semantic warrants exercised in thesaurus construction
[ISBN-0-315-86393-5] p 3238 N95-33334
THICK FILMS
Effect of the colony microstructure on transport critical current of high-J(c) Tl-1223 thick films
[DE95-013049] p 3230 N95-34213
THIN FILMS
Coating power RF components with TiN
[DE95-010357] p 3082 N95-32541
In situ ion-beam analysis and modification of sol-gel zirconia thin films
[DE95-010994] p 3203 N95-32577
Epitaxial Pb(Zr(x)Ti(1-x))O3/SrRuO3 (x = 0, 0.35, 0.65) multilayer thin films on SrTiO3(100) and MgO(100) prepared by MOCVD and RF sputtering
[DE95-008288] p 3226 N95-32598
Comparison of lead zirconate titanate thin films on ruthenium oxide and platinum electrodes
[DE95-617597] p 3082 N95-32710
Low-energy Ion-Beam Deposition apparatus equipped with surface analysis system
[DE95-737272] p 3212 N95-32712
YBa2Cu3O(7-x) 45 deg (001) tilt grain boundaries induced by controlled low-energy sputtering of MgO substrates: Transport properties and atomic-scale structure
[DE95-005826] p 3228 N95-32810

Device physics of thin-film polycrystalline cells and modules
[DE95-009209] p 3149 N95-32817
Perpendicular magnetic behavior of ultra-thin Co sandwiches
[DE95-010611] p 3083 N95-32819
The effects of ion implantation on the tribology of perfluoropolyether-lubricated 440C stainless steel couples
[NASA-TM-106965] p 3083 N95-32918
Experimental and numerical analysis of controlled impinging liquid jets p 3109 N95-33257
High-resolution magnetic imaging and investigations of thin-film magnetism with spin-polarized electron, ion and atom probes
[DE95-012190] p 3074 N95-33392
CRADA with United Solar Technologies and Pacific Northwest Laboratory (PNL-021): Thin film materialsfor low-cost high performance solar concentrators
[DE95-010423] p 3150 N95-33400
Feasibility of fullerene thin films for high-speed all-optical switching
[DE95-011735] p 3085 N95-33409
Indirect measurements of hydrogen: The deficit method for a many-component system
[DE95-010993] p 3208 N95-33623
Epitaxial Pb(Zr(0.40)Ti(0.60))O3/SrRuO3 and PbTiO3/SrRuO3 multilayer thin films prepared by MOCVD and RF sputtering
[DE95-007146] p 3229 N95-33636
Optical anisotropy of (110) surfaces of Ag and Cu
[DE95-010130] p 3229 N95-33637
Low-energy response of superconducting tunnel junction x-ray spectrometers
[DE95-011733] p 3230 N95-33650
Thin-film rechargeable lithium batteries
[DE95-008975] p 3103 N95-33697
Characterization of DuPont 9015, aqueous processable dry film photoresist for printed wiring boards
[DE95-011239] p 3103 N95-33864
In situ surface roughness measurement during PECVD diamond film growth
[DE95-013411] p 3230 N95-34215
Influence of CO2 continuous laser preprocessed substrates on optical thin film damage thresholds
[AD-A294190] p 3217 N95-34297
TiO2/SiO2 and ZrO2/SiO2 multilayer media film optical loss and laser damage study
[AD-A294192] p 3217 N95-34298
Using photothermal deflection techniques for studying the attenuations of guided waves propagated in optical thin films
[AD-A294203] p 3217 N95-34303
Recent developments in maritime technology research institute acousto-optical technology research
[AD-A294215] p 3217 N95-34307
Method of forming thin films on substrates at low temperatures
[AD-D017470] p 3086 N95-34447
Formation of artificially-layered high-temperature superconductors using pulsed-laser deposition
[DE95-012884] p 3231 N95-34465
A 30-pair thin film thermoelectric pile
[AD-A294058] p 3151 N95-34468
Effect of propagation attenuation of thin film waveguide on optical thin film losses
[AD-A294064] p 3218 N95-34471
Low temperature growth of thin films by high kinetic energy supersonic molecular beams
[AD-A294516] p 3086 N95-34476
Novel ferroelectric heterostructures for high-density DRAMS
[AD-A294517] p 3199 N95-34477
Development of thin film diamond based integrated circuit technology
[AD-A294519] p 3231 N95-34478
Thin-film electrolytes for reduced temperature solid oxide fuel cells
[DE95-011273] p 3151 N95-34481
Multilayer thermoelectric films: A strategy for the enhancement of ZT
[DE95-011535] p 3081 N95-34482
Ion assisted deposition of ZnS and MgF2
[AD-A294759] p 3086 N95-34563
Multilayer optics for soft x-rays
[AD-A295030] p 3219 N95-34791
The growth of ultrathin epitaxial intermetallic films
[AD-A295037] p 3232 N95-34795

THIN LAYER CHROMATOGRAPHY
Application of Ion Mobility Spectrometry (IMS) in forensic chemistry and toxicology with focus on biological matrices p 3072 N95-33285

THREADS
Method of installing a metallic threaded insert in a composite/rubber panel
[AD-D017522] p 3065 N95-34620

THREE DIMENSIONAL BODIES
Use of TOPSAR digital elevation data to determine the 3-dimensional shape of an alluvial fan p 3139 N95-33804
Three-dimensional recognition via two-stage associative memory
[AD-A293567] p 3183 N95-34612

THREE DIMENSIONAL FLOW
The effect of labyrinth seals on the dynamics of turbomachinery p 3122 N95-32752
Investigation of water droplet trajectories within the NASA icing research tunnel
[NASA-TM-107023] p 3034 N95-32769
Three-dimensional aerodynamic shape optimization using discrete sensitivity analysis p 3048 N95-32904
Direct and large eddy simulations of three dimensional round turbulent jets p 3111 N95-33709
Design of secondary flow control cascade using numerical simulation p 3034 N95-34507
A study on the convergence of a 3-D Euler code for cascade flow calculations p 3034 N95-34508
Program developing environment and a CFD application on the Cray T3D p 3038 N95-34535

THREE DIMENSIONAL MODELS
Visualization methods for high-resolution, transient, 3-D, finite element situations
[DE95-009479] p 3179 N95-32390
The CE-QUAL-ICM three-dimensional eutrophication model, release version 1.0
[AD-A294258] p 3160 N95-34461
An unsteady simulation of a centrifugal compressor stage using the NWT p 3038 N95-34536
A large scale 3D Navier-Stokes analysis using NAL-NWT p 3039 N95-34539
Formation of high density cores in molecular cloud p 3041 N95-34553

THRESHOLD CURRENTS
Influence of CO2 continuous laser preprocessed substrates on optical thin film damage thresholds
[AD-A294190] p 3217 N95-34297

THRESHOLD LOGIC
Programmable real-time optoelectronic hybrid threshold logic processors
[AD-A294067] p 3104 N95-34379

THRUST CONTROL
An Electronic Workshop on the Performance Seeking Control and Propulsion Controlled Aircraft Results of the F-15 Highly Integrated Digital Electronic Control Flight Research Program
[NASA-TM-104278] p 3050 N95-33009
An overview of integrated flight-propulsion controls flight research on the NASA F-15 research airplane p 3051 N95-33010
Performance seeking control program overview p 3051 N95-33011
PSC algorithm description p 3051 N95-33013
Maximum thrust mode evaluation p 3052 N95-33017
Rapid deceleration mode evaluation p 3052 N95-33018
Background and principles of throttles-only flight control p 3053 N95-33021
Propulsion Controlled Aircraft design and development p 3053 N95-33022
Flight test of a propulsion controlled aircraft system on the NASA F-15 airplane p 3049 N95-33023
Design challenges encountered in the F-15 PCA flight test program p 3049 N95-33025

TILES
Unusual behavior in the magnetic anisotropy of ultra-thin Co sandwiches: The role of Au underlayers
[DE95-010612] p 3229 N95-33641

TIME CONSTANT
A 30-pair thin film thermoelectric pile
[AD-A294058] p 3151 N95-34468

TIME DEPENDENCE
The fully correlated two-electron problem on a numerical lattice
[DE95-010280] p 3205 N95-32650
Zero modes of Gauss constraint in gaugeless reduction of Yang-Mills theory
[DE95-623676] p 3234 N95-32667
Observations of surface structure and regression behavior of solid propellant strands burning under narrow gap conditions p 3088 N95-33254
Nonequilibrium problems in Quantum Field Theory and Schwinger's closed time path formalism
[DE95-012056] p 3234 N95-33388
Unified model of the RF plasma sheath
[DE95-012114] p 3224 N95-33851
Laboratory and numerical modeling of topographic effects on time-dependent ocean currents
[AD-A294920] p 3160 N95-34594
Remarks on the KARMEN anomaly
[PB95-234977] p 3209 N95-34650
QMR methods in computational fluid dynamics
[DE95-012889] p 3113 N95-34800

TIME RESPONSE
Seismic response analysis of soil-structure interaction systems in the time domain
[REPT-2212] p 3091 N95-32992
Vertical velocity ambiguity resolution method
[AD-D017481] p 3201 N95-34424

TIME SERIES ANALYSIS
Penetrable wedge analysis
[AD-A294276] p 3234 N95-34464
High speed variability in x-ray binary systems
[AD-A294634] p 3247 N95-34561

TIME SHARING
Distributed shared memory for new generation networks
[AD-A293722] p 3185 N95-32580

TIMOSHENKO BEAMS
A three-dimensional nonlinear Timoshenko beam based on the core-congruential formulation
[NASA-CR-199042] p 3180 N95-32765

TIRES
Test method to measure resistance towards fragmentation by studded tires
[PB95-211017] p 3121 N95-32612

TISSUES (BIOLOGY)
A novel approach to the problem of highly-sensitive regular analysis for man-made plutonium in environment and human body
[DE95-620764] p 3164 N95-32666
The preservation of human surrogates for biomechanical studies p 3167 N95-33312
Plasma mediated ablation of biological tissues with ultrashort laser pulses
[DE95-011748] p 3164 N95-33654

TITANIUM ALLOYS
Interfacial reactions during the liquid infiltration of titanium matrix composites p 3081 N95-34252

TITANIUM NITRIDES
Coating power RF components with TiN
[DE95-010357] p 3082 N95-32541

TITANIUM OXIDES
Conversion of holes into reducing species on surface modified small-particle TiO2
[DE95-008282] p 3225 N95-32586
TiO2/SiO2 and ZrO2/SiO2 multilayer media film optical loss and laser damage study
[AD-A294192] p 3217 N95-34298

TOKAMAK DEVICES
Summary report for ITER Task No. T226B: Evaluation of ITER disruption erosion
[DE95-010402] p 3219 N95-32401
Development and trial manufacturing of 1/2-scale partial mock-up of blanket box structure for fusion experimental reactor
[DE95-737184] p 3219 N95-32408
Design concept of a cryogenic distillation column cascade for a ITER scale fusion reactor
[DE95-737185] p 3220 N95-32409
Stability analysis of external kink mode for ITER L-mode profile plasmas
[DE95-737207] p 3220 N95-32410
Transport studies of tokamak plasmas in JT-60 device
[DE95-737227] p 3220 N95-32417
Experimental study of the processes in the expander of the axisymmetric mirror device
[DE95-009846] p 3221 N95-32536
Radial electric field measurement in a tokamak by the injection of a pulsed neutral beam
[DE95-614176] p 3221 N95-32561
Study of impurity concentrations by VUV spectroscopy on HL-1
[DE95-614186] p 3221 N95-32562
Irradiation tests of critical components for remote handling in gamma radiation environment
[DE95-737223] p 3221 N95-32565
Recent results from the D3-D tokamak and implications for future devices
[DE95-009605] p 3222 N95-32592
D3-D power supply, design, and development
[DE95-009603] p 3222 N95-32656
Optimized profiles for improved confinement and stability in the DIII-D tokamak
[DE95-009606] p 3222 N95-32756
TRAP: Tokamak Refueling by Accelerated Plasmoids
[DE95-009825] p 3223 N95-33216
Studies of impurity mode and ITG mode in toroidal plasmas
[DE95-012134] p 3223 N95-33391
Development of tokamak experiment technology: A study on the nuclear fusion reactor
[DE95-614255] p 3223 N95-33619
More on core-localized toroidal Alfven eigenmodes
[DE95-010857] p 3224 N95-33696

Single Langmuir probe characteristic in a magnetized plasma at the TEXT tokamak
[DE95-012144] p 3224 N95-33853
Tokamak ETE circuits: Analysis and specifications
[INPE-5573-PRP/182] p 3224 N95-33873
High beta and second stability region transport and stability analysis
[DE95-011298] p 3225 N95-34812

TOLUENE
Determination of Benzene, Toluene, and Xylene by means of an ion mobility spectrometer device using photoionization p 3069 N95-33269

TOPOGRAPHY
Use of TOPSAR digital elevation data to determine the 3-dimensional shape of an alluvial fan p 3139 N95-33804
Topography from shading and stereo p 3241 N95-34229
Laboratory and numerical modeling of topographic effects on time-dependent ocean currents
[AD-A294920] p 3160 N95-34594

TOPOLOGY
Cosmological consequences of topological and geometric phenomena in field theories p 3234 N95-33313
A comparison of interface tracking methods
[DE95-009481] p 3111 N95-33698

TOROIDAL PLASMAS
Studies of impurity mode and ITG mode in toroidal plasmas
[DE95-012134] p 3223 N95-33391
Tokamak ETE circuits: Analysis and specifications
[INPE-5573-PRP/182] p 3224 N95-33873

TORQUERS
Commercial usage of Navy components developed and manufactured by CRI Delfin p 3092 N95-33129

TOUGHNESS
Metallic laminates for engine applications
[DE95-010259] p 3062 N95-32399
Fracture toughness assessment of present and future pressure vessel materials based on Charpy impact energy and yield strength
[AD-A294008] p 3081 N95-34373

TOWERS
Cooling tower and plume modeling for satellite remote sensing applications
[DE95-012000] p 3143 N95-33849

TOXIC HAZARDS
Users' manual for LEHGC: A Lagrangian-Eulerian finite-element model of HydroGeoChemical transport through saturated-unsaturated media. Version 1.0
[DE95-010513] p 3179 N95-32543
Detection of emission sources using passive-remote Fourier Transform Infrared spectroscopy
[DE95-009920] p 3067 N95-32671
Multimedia Environmental Pollutant Assessment System (MEPAS(trademark)): Exposure pathway and human health impact assessment models
[DE95-012763] p 3155 N95-34441

TOXICOLOGY
Application of Ion Mobility Spectrometry (IMS) in forensic chemistry and toxicology with focus on biological matrices p 3072 N95-33285

TOXINS AND ANTITOXINS
High resolution electrospray mass spectrometry with a magnetic sector instrument: Accurate mass measurement and peptide sequencing
[AD-A293564] p 3076 N95-34611
Immunological protection against botulinum neurotoxin by a synthetic vaccine
[AD-A294146] p 3165 N95-34754

TRACE CONTAMINANTS
The use of ion mobility spectrometry and gas chromatography/mass spectrometry for the detection of illicit drugs on clandestine records p 3070 N95-33276

TRACE ELEMENTS
Application of Ni-63 photo and corona discharge ionization for the analysis of chemical warfare agents and toxic wastes p 3070 N95-33272
Direct analysis of organic priority pollutants by IMS p 3071 N95-33280
Modeling soil climate controls on the exchange of trace gases between the terrestrial biosphere and the atmosphere p 3153 N95-33337
Remote sensing of smoke, clouds, and radiation using AVIRIS during SCAR experiments p 3132 N95-33749

TRACKING PROBLEM
A robust control system for exact trajectory tracking p 3192 N95-33714

TRADEOFFS
The application of helicopter mission simulation to Nap-of-the-Earth operations p 3044 N95-32496

TRAILING EDGES
Wind turbine trailing edge aerodynamic brakes
[DE95-004061] p 3033 N95-32548

TRAINING ANALYSIS
Aerospace physiology AFSC 4M0X1
[AD-A294839] p 3165 N95-34564

TRAINING SIMULATORS
Selection and special physiological training of flying personnel to high +G(z)-maneuverable flights-main concept p 3166 N95-34053

TRAJECTORIES
A tactical navigation and routeing system for low-level flight p 3044 N95-32494
Globally stable feedback laws for near-minimum-fuel and near-minimum-time pointing maneuvers for a landmark-tracking spacecraft
[DE95-009867] p 3191 N95-33214
Emittance and energy control in the NLC main linacs
[DE95-012556] p 3213 N95-33338

TRAJECTORY CONTROL
A robust control system for exact trajectory tracking p 3192 N95-33714

TRAJECTORY OPTIMIZATION
Advanced propulsion for geostationary orbit insertion and north-south station keeping
[NASA-TM-107018] p 3060 N95-32917
Trajectory planning and control of kinematically redundant robotic manipulators p 3194 N95-34807

TRAJECTORY PLANNING
On bootstrapping local search with trail-markers
[DE95-009835] p 3187 N95-32533
Off-line programming using commerical CAD systems, and design criteria for manipulators with inherent accuracy p 3180 N95-32937
Adaptive differential visual feedback for uncalibrated hand-eye coordination and motor control
[AD-A293607] p 3171 N95-34616
Trajectory planning and control of kinematically redundant robotic manipulators p 3194 N95-34807

TRANSFER OF TRAINING
Event-related potentials and electroencephalograms in adaptive operator training: Rationale and annotated bibliography
[AD-A294337] p 3166 N95-34356

TRANSFER ORBITS
Advanced propulsion for geostationary orbit insertion and north-south station keeping
[NASA-TM-107018] p 3060 N95-32917

TRANSITION METALS
Strength, ductility, and fracture mode of ternary FeAl alloys
[DE95-010281] p 3077 N95-32400
Synthesis of potential new Zintl phases
[DE95-010123] p 3227 N95-32640
Photoemission study of some novel materials: Rare earth/transition metal interface, Ba*(0.6)*K*(0.4)*BiO3* and AlPdMn
[DE95-010125] p 3227 N95-32643
Synchrotron radiation studies of local structure and bonding in transition metal aluminides and rare earth transition metal magnetic nitrides
[DE95-011579] p 3079 N95-33065
Theory of magneto-optics and circular magnetic x-ray dichroism
[DE95-010129] p 3080 N95-33700
Charge-transfer gap closure in transition-metal halides under pressure
[DE95-011268] p 3230 N95-33865
Metal-ceramic interfaces: Overlayer-induced reconstruction and magnetism of 4d transition-metal monolayers
[DE95-011543] p 3075 N95-34483

TRANSITION TEMPERATURE
Anisotropic magnetization of HoNi2B2C
[DE95-010239] p 3198 N95-32397
Effect of phase transformations on the mechanical properties of a multiphase alloy based on NiAl+Fe
[DE95-010119] p 3079 N95-33217
Quench propagation velocity for highly stabilized conductors
[DE95-011040] p 3103 N95-33404

TRANSMISSION ELECTRON MICROSCOPY
TEM investigation on the low temperature phase of HfV2
[DE95-009500] p 3225 N95-32532
Comparison of lead zirconate titanate thin films on ruthenium oxide and platinum electrodes
[DE95-617597] p 3082 N95-32710
Interfacial composition analysis of silicon nitride whisker reinforced oxynitride glass systems
[DE95-012895] p 3085 N95-33635
Epitaxial Pb(Zr(0.40)Ti(0.60))O3/SrRuO3 and PbTiO3/SrRuO3 multilayer thin films prepared by MOCVD and RF sputtering
[DE95-007146] p 3229 N95-33636

TRANSMISSION LOSS
DETVAg-90: Use of GTD for wave propagation over earth
[PB95-211447] p 3098 N95-33231
Improved L-C resonant decay technique for Q measurement of quasilinear power inductors: New results for MPP and ferrite powdered cores
[NASA-CR-198373] p 3103 N95-33874

TRANSMISSIONS (MACHINE ELEMENTS)
Experimental and analytical assessment of the thermal behavior of spiral bevel gears
[NASA-TM-107009] p 3123 N95-33179

TRANSMITTANCE
Transmittance characteristics of US Army rotary-wing aircraft transparencies
[AD-A295035] p 3049 N95-34793

TRANSMITTER RECEIVERS
A reconfigurable optoelectronic interconnect technology for multi-processor networks
[DE95-011895] p 3186 N95-33838

TRANSONIC FLOW
Numerical solutions of inviscid and viscous flows about airfoils by TVD method p 3036 N95-34521
Parallel computation of transonic flows about an aircraft configuration using multi-block structured grids p 3039 N95-34537
Vector-parallel simulations of transonic wind tunnel flows about a fully configured model of aircraft p 3039 N95-34538

TRANSONIC SPEED
Direct analysis of transonic rotor noise with CFD technique p 3040 N95-34549
Numerical simulation of two-dimensional compressible inviscid flow on unstructured grid system p 3041 N95-34557

TRANSONIC WIND TUNNELS
Vector-parallel simulations of transonic wind tunnel flows about a fully configured model of aircraft p 3039 N95-34538

TRANSPARENCE
Transparent potential perturbations on lattices and in the periodical structures. Elements of the Qualitative Theory of Wave Motion Over the Channels
[DE95-623602] p 3225 N95-32480

TRANSPORT AIRCRAFT
Certification for civil flight decks and the human-computer interface p 3176 N95-34784
Some inadequacies of the current human factors certification process of advanced aircraft technologies p 3176 N95-34785

TRANSPORT PROPERTIES
Unexpected matching insensitivity in DTL of GTA accelerator
[DE95-011984] p 3211 N95-32416
YBa2Cu3O(7-x) 45 deg (001) tilt grain boundaries induced by controlled low-energy sputtering of MgO substrates: Transport properties and atomic-scale structure
[DE95-005826] p 3228 N95-32810
Transport phenomena in subsonic and supersonic flows in a duct with mass injection p 3108 N95-32934
Certification of MCNP Version 4A for WHC computer platforms, revision 7
[DE95-011546] p 3178 N95-34484
Electron and hole transport in compound semiconductors
[AD-A295003] p 3233 N95-34822

TRANSPORT THEORY
Transport studies of tokamak plasmas in JT-60 device
[DE95-737227] p 3220 N95-32417
Users' manual for LEHGC: A Lagrangian-Eulerian finite-element model of HydroGeoChemical transport through saturated-unsaturated media. Version 1.0
[DE95-010513] p 3179 N95-32543
Study of the trapped modes at the vacuum ports
[DE95-010570] p 3203 N95-32544
Application of vorticity transport analysis to the development of physically accurate turbulence models p 3107 N95-32905

TRANSPORT VEHICLES
Solid-state data recorder; next development and use p 3094 N95-33143

TRANSPORTATION
Lessons learned in acquiring new regulations for shipping advanced electric vehicle batteries
[DE95-009908] p 3102 N95-32956

TRANSPUTERS
Parallel computation for two dimensional incompressible flow on array of transputers p 3042 N95-34558

TRANSVERSE OSCILLATION
The effect of labyrinth seals on the dynamics of turbomachinery p 3122 N95-32752

TRANSVERSE WAVES
Transverse acoustic properties of the B-phase of superfluid helium three p 3074 N95-33414

TRAPPED PARTICLES
Study of the trapped modes at the vacuum ports
[DE95-010570] p 3203 N95-32544

The uses of Electron Beam Ion Traps in the study of highly charged ions
[DE95-011537] p 3212 N95-33064

TRAPPING
Direct analysis of organic priority pollutants by IMS
p 3071 N95-33260

TRAVELING WAVE TUBES
A 75 watt, 59 to 64 GHz space TWT
[NASA-CR-195450] p 3104 N95-33915

TRAVELING WAVES
Bifurcation analysis of multimode instabilities in class B lasers p 3119 N95-33470

TRIANGLES
CADIR: A model for generating infrarad images
[PB95-222956] p 3215 N95-33239

TRIANGULATION
On the Minimum Weight Steiner Triangular Tiling Problem
[DE95-009482] p 3180 N95-32716

TRIBOLOGY
The effects of ion implantation on the tribology of perfluoropolyether-lubricated 440C stainless steel couples
[NASA-TM-106965] p 3083 N95-32918
Surface chemistry of diamond single crystals
[AD-A294150] p 3232 N95-34755

TRITIUM
Fusion Safety Program annual report, fiscal year 1994
[DE95-008872] p 3221 N95-32588
Energy and Technology Review
[DE95-011686] p 3223 N95-33066
Inertial confinement fusion target component fabrication and technology development support
[DE95-011655] p 3224 N95-34436

TROPICAL REGIONS
Evaluation of the photochemical reflectance index in AVIRIS imagery p 3131 N95-33747
On the potential of long wavelength imaging radars for mapping vegetation types and woody biomass in tropical rain forests p 3141 N95-33812

TROPOSPHERE
Comparison of seasonal and zonal patterns of the direct and indirect radiative forcing of climate by aerosols
[DE95-010896] p 3153 N95-33192
Enhanced shortwave cloud radiative forcing due to anthropogenic aerosols
[DE95-013319] p 3156 N95-34214

TUNABLE LASERS
Pulsed tunable narrow-bandwidth dye laser, with hollow circular waveguide in cavity
[AD-A294060] p 3120 N95-34469

TUNING
Beam-based magnetic alignment of the final focus test beam
[DE95-012096] p 3212 N95-32657
Beam-based optical tuning of the Final Focus Test Beam
[DE95-012097] p 3215 N95-32658
Conforming tuning coupler for flextensional transducers
[AD-D017285] p 3105 N95-34617

TUNNEL JUNCTIONS
Low-energy response of superconducting tunnel junction x-ray spectrometers
[DE95-011733] p 3230 N95-33650
Quantum mechanical capacitance in a scanning tunneling microscope
[DE95-011272] p 3230 N95-33880

TUNNELS
The 8th Winterschool on New Developments in Solid State Physics
[AD-A290163] p 3227 N95-32677

TURBINE BLADES
Allison engine testing CMSX-4(reg sign) single crystal turbine blades and vanes
[DE95-010308] p 3050 N95-32636
Design of ETO propulsion turbine using CFD analyses
[NASA-CR-199085] p 3123 N95-32915

TURBINE PUMPS
Design of ETO propulsion turbine using CFD analyses
[NASA-CR-199085] p 3123 N95-32915

TURBINES
Allison engine testing CMSX-4(reg sign) single crystal turbine blades and vanes
[DE95-010308] p 3050 N95-32636
Fatigue damage estimate comparisons for northern European and US wind farm loading environments
[DE95-011061] p 3150 N95-33706
Verification of turbine cascade flow with tip clearance
p 3035 N95-34511

TURBOFAN ENGINES
Computation of noise radiation from turbofans: A parametric study
[NASA-CR-198359] p 3200 N95-32836
An Electronic Workshop on the Performance Seeking Control and Propulsion Controlled Aircraft Results of the F-15 Highly Integrated Digital Electronic Control Flight Research Program
[NASA-TM-104278] p 3050 N95-33009
An overview of integrated flight-propulsion controls flight research on the NASA F-15 research airplane
p 3051 N95-33010
F-15 propulsion system p 3051 N95-33012

TURBOFANS
Computation of noise radiation from turbofans: A parametric study
[NASA-CR-198359] p 3200 N95-32836

TURBOGENERATORS
Integral cesium reservoir: Design and transient operation
[DE95-010152] p 3211 N95-32647

TURBOJET ENGINE CONTROL
An Electronic Workshop on the Performance Seeking Control and Propulsion Controlled Aircraft Results of the F-15 Highly Integrated Digital Electronic Control Flight Research Program
[NASA-TM-104278] p 3050 N95-33009
An overview of integrated flight-propulsion controls flight research on the NASA F-15 research airplane
p 3051 N95-33010
Performance seeking control program overview
p 3051 N95-33011
PSC algorithm description p 3051 N95-33013
Minimum fuel mode evaluation p 3051 N95-33015
Minimum fan turbine inlet temperature mode evaluation p 3052 N95-33016
Maximum thrust mode evaluation
p 3052 N95-33017
Rapid deceleration mode evaluation
p 3052 N95-33018
Performance seeking control excitation mode
p 3052 N95-33019
Performance seeking control (PSC) for the F-15 highly integrated digital electronic control (HIDEC) aircraft
p 3053 N95-33020
Propulsion Controlled Aircraft design and development
p 3053 N95-33022

TURBOMACHINERY
The effect of labyrinth seals on the dynamics of turbomachinery p 3122 N95-32752

TURBULENCE
Study on turbulent fluctuations in diffusion flames using laser induced fluorescence
[PB95-214425] p 3068 N95-32812
Application of vorticity transport analysis to the development of physically accurate turbulence models
p 3107 N95-32905
Turbulence and spatio-temporal chaos
[DE95-012912] p 3068 N95-33223
Very large eddy simulations of spatially evolving supersonic turbulent shear layers p 3110 N95-33606
Wavelet analysis of atmospheric turbulence structures: What can we gain from this new technique?
[DE95-011955] p 3156 N95-33847
An experimental study of collective sea state modes of deep water surface gravity waves
[AD-A294007] p 3160 N95-34372
Solitary wave solution for mixing-layer turbulence
p 3036 N95-34522
Formation of high density cores in molecular cloud
p 3041 N95-34553
Turbulent solitary wave propagating through wall Boundary Layer p 3041 N95-34555
ABLEX: High altitude laser propagation experiment
[AD-A294914] p 3120 N95-34592

TURBULENCE MODELS
Asymptotic structure of supersonic turbulent boundary layers p 3107 N95-32898
Application of vorticity transport analysis to the development of physically accurate turbulence models
p 3107 N95-32905
Turbulence models in the Navier-Stokes simulation of airfoil stall
[TRITA-NA-9312] p 3108 N95-33059
Large eddy simulation of turbulent vortices and mixing layers p 3109 N95-33340
Numerical studies of turbulent free surface flows and unsteady propeller flows
[AD-A294377] p 3112 N95-34343
A multigrid incompressible NS solver
p 3036 N95-34517
Direct numerical simulation of compressible isotropic turbulence p 3037 N95-34523
Numerical simulation of unsteady viscous flow around an airfoil with oscillating spoiler p 3040 N95-34547

TURBULENT BOUNDARY LAYER
Boundary layer transition studies
[NASA-CR-198983] p 3106 N95-32454
Asymptotic structure of supersonic turbulent boundary layers p 3107 N95-32898
A note on separation prediction of two-dimensional turbulent boundary layer
[REPT-2216] p 3091 N95-32994
Dependency of a boundary layer flow on computational grids p 3040 N95-34550
Turbulent solitary wave propagating through wall Boundary Layer p 3041 N95-34555
Studies of hypersonic boundary layer behavior
[AD-A294137] p 3113 N95-34752

TURBULENT COMBUSTION
Gasdynamic model of turbulent combustion in an explosion
[DE95-010267] p 3074 N95-33627

TURBULENT FLOW
Study on turbulent fluctuations in diffusion flames using laser induced fluorescence
[PB95-214425] p 3068 N95-32812
Tracking a turbulent spot in an immersive environment
[NASA-CR-198179] p 3180 N95-32834
Asymptotic structure of supersonic turbulent boundary layers p 3107 N95-32898
Application of vorticity transport analysis to the development of physically accurate turbulence models
p 3107 N95-32905
A note on separation prediction of two-dimensional turbulent boundary layer
[REPT-2216] p 3091 N95-32994
Large eddy simulation of turbulent vortices and mixing layers p 3109 N95-33340
Direct and large eddy simulations of three dimensional round turbulent jets p 3111 N95-33709
Numerical studies of turbulent free surface flows and unsteady propeller flows
[AD-A294377] p 3112 N95-34343
Direct numerical simulation of compressible isotropic turbulence p 3037 N95-34523

TURBULENT HEAT TRANSFER
Turbulent heat flux measurements over the Greenland, Norwegian and Barents seas
[AD-A294129] p 3157 N95-34751

TURBULENT JETS
Direct and large eddy simulations of three dimensional round turbulent jets p 3111 N95-33709

TURBULENT MIXING
Large eddy simulation of turbulent vortices and mixing layers p 3109 N95-33340
Very large eddy simulations of spatially evolving supersonic turbulent shear layers p 3110 N95-33606
Gasdynamic model of turbulent combustion in an explosion
[DE95-010267] p 3074 N95-33627
A study of supersonic mixing flow field with ramp injector p 3035 N95-34512

TVD SCHEMES
Unified approach for incompressible flows
p 3113 N95-32425
Verification of turbine cascade flow with tip clearance
p 3035 N95-34511
A variation of the Riemann Problem solution and its application to implicit Godunov's scheme
p 3036 N95-34516
A flux splitting scheme with high-resolution and robustness for discontinuities p 3036 N95-34518
Hypersonic CFD analysis for the aerothermodynamic design of HOPE p 3036 N95-34520
Numerical solutions of inviscid and viscous flows about airfoils by TVD method p 3036 N95-34521
Numerical simulation of film cooling effect around axisymmetric body in hypersonic flow field
p 3037 N95-34526
Effect of schemes on numerical simulations of shock wave reflection p 3038 N95-34531
Program developing environment and a CFD application on the Cray T3D p 3038 N95-34535
Vector-parallel simulations of transonic wind tunnel flows about a fully configured model of aircraft
p 3039 N95-34538
Numerical simulation of interaction between shock wave and density interface p 3039 N95-34543
Numerical simulation of unsteady viscous flow around an airfoil with oscillating spoiler p 3040 N95-34547
Direct analysis of transonic rotor noise with CFD technique p 3040 N95-34549

TWO DIMENSIONAL BOUNDARY LAYER
Asymptotic structure of supersonic turbulent boundary layers p 3107 N95-32898
A note on separation prediction of two-dimensional turbulent boundary layer
[REPT-2216] p 3091 N95-32994

TWO DIMENSIONAL FLOW
A note on separation prediction of two-dimensional turbulent boundary layer
[REPT-2216] p 3091 N95-32994
Parallel finite element methods and iterative solution techniques for viscous incompressible flows
p 3108 N95-33031

Analysis and finite element approximation of an optimal shape control problem for the steady-state Navier-Stokes equations p 3112 N95-34285
Numerical simulation of two-dimensional compressible inviscid flow on unstructured grid system p 3041 N95-34557
Parallel computation for two dimensional incompressible flow on array of transputers p 3042 N95-34558

TWO DIMENSIONAL MODELS
Calculations of spatial higher modes without deflation procedure
| REPT-2205 | p 3090 N95-32985
Speaker identification using the two-dimensional cepstrum transform
| AD-A294204 | p 3099 N95-34304
Penetrable wedge analysis
| AD-A294276 | p 3234 N95-34464
Modeling and simulation of pulsed laser annealing and ablation of solid materials
| DE95-012888 | p 3119 N95-34466

TWO PHASE FLOW
Dividing annular/two-phase flow in horizontal T-junctions
| ISBN-0-315-84910-X | p 3057 N95-33030
An experimental and analytical investigation into the performance of centrifugal pumps operating with air-water mixtures p 3123 N95-33323

U

UH-1 HELICOPTER
User acceptability and comfort of the communications earplug (CEP) when used in the UH-1 helicopter
| AD-A294047 | p 3170 N95-34492

UKRAINE
Laser gyroscopy tendencies and their analysis of development in Ukraine p 3092 N95-33133

ULTRAHIGH FREQUENCIES
Helicopter HF communications using the NVIS mode p 3043 N95-32491

ULTRASHORT PULSED LASERS
Phase control and measurement of ultrashort optical pulses
| DE95-011746 | p 3216 N95-33411

ULTRASONIC FLAW DETECTION
Laser-based ultrasonics by dual-probe interferometer detection and narrow-band ultrasound generation p 3118 N95-33464

ULTRASONIC WELDING
Recent developments in maritime technology research institute acousto-optical technology research
| AD-A294215 | p 3217 N95-34307

ULTRAVIOLET RADIATION
Study of the space environmental effects on spacecraft engineering materials
| NASA-CR-199090 | p 3066 N95-32581

ULTRAVIOLET SPECTRA
Beryllium and Boron abundances in population II stars
| NASA-CR-189434 | p 3247 N95-33262

UNDERWATER ACOUSTICS
Underwater acoustic field extrapolation: Theory and sensitivity analysis
| AD-A294925 | p 3201 N95-34595

UNDERWATER EXPLOSIONS
On the feasibility of using smoothed particle hydrodynamics for underwater explosion calculations
| DE95-008799 | p 3106 N95-32587

UNDERWATER STRUCTURES
Design of deepwater pipelines
| PB95-215109 | p 3095 N95-33244

UNDERWATER VEHICLES
Ice-ocean four dimensional structure and dynamics
| AD-A294017 | p 3160 N95-34375
Vertical velocity ambiguity resolution method
| AD-D017481 | p 3201 N95-34424

UNITED KINGDOM
Covert Night/Day Operations for Rotorcraft (CONDOR) programme p 3046 N95-32505
United Kingdom minerals yearbook, 1994. Statistical data to 1993
| PB95-207841 | p 3155 N95-32599

UNITED STATES
Covert Night/Day Operations for Rotorcraft (CONDOR) programme p 3046 N95-32505
HYBRID2: A versatile model of the performance of hybrid power systems
| DE95-004062 | p 3148 N95-32551

UNIVERSITIES
National Aeronautics and Space Administration (NASA)/American Society for Engineering Education (ASEE) Summer Faculty Fellowship Program, 1994, volume 1
| NASA-CR-188410 | p 3248 N95-32418
Technology Reports of the Osaka University, vol. 45, nos. 2205-2216 p 3090 N95-32984

UNIVERSITY PROGRAM
Technology Reports of the Osaka University, vol. 45, nos. 2205-2216 p 3090 N95-32984

UNIX (OPERATING SYSTEM)
xdamp: An IDL(R)-based Data Manipulation Program
| DE95-011242 | p 3181 N95-33624
SAVS: A Space Analysis and Visualization System p 3242 N95-34238

UNSTEADY FLOW
Visualization methods for high-resolution, transient, 3-D, finite element situations
| DE95-009479 | p 3179 N95-32390
A nonlinear vortex lattice method for unsteady flow with separated vortex
| DLR-FB-94-32 | p 3106 N95-32787
Numerical studies of turbulent free surface flows and unsteady propeller flows
| AD-A294377 | p 3112 N95-34343
A study on the convergence of a 3-D Euler code for cascade flow calculations p 3034 N95-34508
Numerical solutions of inviscid and viscous flows about airfoils by TVD method p 3036 N95-34521
Structure of weak shock waves in bubbly liquid p 3037 N95-34527
An unsteady simulation of a centrifugal compressor stage using the NWT p 3038 N95-34536
Numerical simulation of unsteady viscous flow around an airfoil with oscillating spoiler p 3040 N95-34547
Nonlinear stability of unsteady viscous flow
| AD-A294931 | p 3113 N95-34597

UNSTRUCTURED GRIDS (MATHEMATICS)
Visualization methods for high-resolution, transient, 3-D, finite element situations
| DE95-009479 | p 3179 N95-32390
Differencing the diffusion equation on unstructured meshes in 2-D
| DE95-010410 | p 3195 N95-32559
A unified multigrid solver for the Navier-Stokes equations on mixed element meshes
| NASA-CR-198183 | p 3196 N95-33500
An object-oriented decomposition of the adaptive-hp finite element method
| DE95-012142 | p 3186 N95-33852
Efficient time domain solutions of Maxwell's equations for aerospace systems
| AD-A294019 | p 3196 N95-34377
Consistent finite-volume discretization of hydrodynamic conservation laws for unstructured grids
| DE95-011730 | p 3112 N95-34437
Numerical simulation of two-dimensional compressible inviscid flow on unstructured grid system p 3041 N95-34557

UPGRADING
Weather Forecasting: Systems architecture needed for National Weather Service modernization. Report to Congressional requesters
| GAO/AIMD-94-28 | p 3157 N95-32760

URANIUM
A novel approach to the problem of highly-sensitive regular analysis for man-made plutonium in environment and human body
| DE95-620764 | p 3164 N95-32666
Observation of KLM dielectronic recombination resonances in highly charged uranium ions
| DE95-010266 | p 3207 N95-33219

URBAN DEVELOPMENT
Urban remote sensing applications: TIMS observations of the City of Scottsdale p 3137 N95-33791

USER MANUALS (COMPUTER PROGRAMS)
Users' manual for LEHGC: A Lagrangian-Eulerian finite-element model of HydroGeoChemical transport through saturated-unsaturated media. Version 1.0
| DE95-010513 | p 3179 *N95-32543
X-Antenna: A graphical interface for antenna analysis codes
| NASA-CR-199212 | p 3095 N95-32674
OPEX Second Workshop of the OLYMPUS Propagation Experimenters. Volume 5: Reference book on data processing
| ESA-WPP-083-VOL-5 | p 3096 N95-32751
FORTRAN program for analyzing ground-based radar data: Usage and derivations, version 6.2
| NASA-TP-3430 | p 3181 N95-33193
Operation of the computer model for microenvironment atomic oxygen exposure
| NASA-CR-198190 | p 3059 N95-33264
Operation of the computer model for microenvironment solar exposure
| NASA-CR-198189 | p 3059 N95-33890
ABCASH plotting program users guide
| DE95-011652 | p 3155 N95-34435

USER REQUIREMENTS
Parallel molecular dynamics: Communication requirements for massively parallel machines
| DE95-012948 | p 3209 N95-34212
Resource document for the design of electronic instrument approach procedure displays
| AD-A295108 | p 3047 N95-34797

V

V/STOL AIRCRAFT
An LDV investigation of support structure influence on the flow field near the wingtip of a STOVL configuration in hover
| AD-A294126 | p 3042 N95-34750

VACCINES
Immunological protection against botulinum neurotoxin by a synthetic vaccine
| AD-A294146 | p 3165 N95-34754

VACUUM
Fabrication of improved SiGe alloys for an 18-couple module test
| DE95-010238 | p 3060 N95-32396
Vacuum polarization correction to the positronium decay rate
| DE95-614164 | p 3202 N95-32481
Probe transparency in a two-level medium embedded by a squeezed vacuum
| DE95-614123 | p 3198 N95-32525
Study of the trapped modes at the vacuum ports
| DE95-010570 | p 3203 N95-32544
D3-D power supply, design, and development
| DE95-009603 | p 3222 N95-32656
High efficiency vacuum and plasma filled backward wave oscillators: A critical evaluation
| AD-A294963 | p 3105 N95-34581

VACUUM CHAMBERS
Study of the trapped modes at the vacuum ports
| DE95-010570 | p 3203 N95-32544

VACUUM SYSTEMS
Coating power RF components with TiN
| DE95-010357 | p 3082 N95-32541
Efficient pockel's modulators in optical fibers
| AD-A294009 | p 3217 N95-34374

VALLEYS
Intra-annual and inter-annual rainfall variability over East Asia, Southeast Asia, and South Asia
| AD-A294156 | p 3158 N95-34757

VANADIUM COMPOUNDS
TEM investigation on the low temperature phase of HfV2
| DE95-009500 | p 3225 N95-32532

VANES
Allison engine testing CMSX-4(reg sign) single crystal turbine blades and vanes
| DE95-010308 | p 3050 N95-32636

VAPOR DEPOSITION
The growth and optimization of InPSb/InGaAs/InAsSb strained-layer superlattice emitters by metal organic chemical vapor deposition
| DE95-011057 | p 3226 N95-32595
CVD diamond cost analysis update
| AD-A289990 | p 3227 N95-32695
Evaluation of strength properties of developed SiC/C compositionally gradient graphite materials
| DE95-737271 | p 3063 N95-32711
Low-energy Ion-Beam Deposition apparatus equipped with surface analysis system
| DE95-737272 | p 3212 N95-32712
An instrument for gravimetric calibration of flow devices with corrosive gases
| DE95-009700 | p 3116 N95-33206
Development of thin film diamond based integrated circuit technology
| AD-A294519 | p 3231 N95-34478
Thin-film electrolytes for reduced temperature solid oxide fuel cells
| DE95-011273 | p 3151 N95-34481

VAPOR PHASE EPITAXY
Fundamental surface chemistry of GaAs OMVPE
| DE95-011606 | p 3231 N95-34486
Use of D2 to elucidate OMVPE growth mechanisms
| AD-A294999 | p 3233 N95-34820

VAPOR PHASES
Thermal rearrangement of oxygen-containing (omicron)-allyltoluene derivatives
| DE95-010124 | p 3067 N95-32641
Solving widespread low-concentration VOC air pollution problems: Gas-phase photocatalytic oxidation answers the needs of many small businesses
| DE95-004059 | p 3152 N95-32668
Environmental chamber studies of atmospheric reactivities of volatile organic compounds: Effects of varying chamber and light source
| DE95-009225 | p 3152 N95-32686
Fundamental studies of gas phase ionic reactions by ion mobility spectrometry p 3069 N95-33268

Application of Ni-63 photo and corona discharge ionization for the analysis of chemical warfare agents and toxic wastes p 3070 N95-33272

VAPORS

Reduction and analysis of seasons 15 and 16 (1991 - 1992) Pioneer Venus radio occulation data and correlative studies with observations of the near infrared emission of Venus
[NASA-CR-199071] p 3247 N95-32700

Analysis of evaporation in laser welding
[REPT-2207] p 3090 N95-32987

Application of the ionscan for the detection of methamphetamine and ephedrine in abondoned clandestine laboratories p 3072 N95-33284

VARACTOR DIODES

Monolithic diode arrays for quasioptical millimeter wave beam steering
[AD-A294256] p 3100 N95-34460

VARIABILITY

Mineralogic variations in fluvial sediments contaminated by mine tailings as determined from AVIRIS data, Coeur D'Alene River Valley, Idaho p 3131 N95-33745

Intra-annual and inter-annual rainfall variability over East Asia, Southeast Asia, and South Asia
[AD-A294156] p 3158 N95-34757

VARIABLE PITCH PROPELLERS

Low-order nonlinear dynamic model of IC engine-variable pitch propeller system for general aviation aircraft
[NASA-TM-107006] p 3050 N95-32916

VARIABLE STARS

RR lyrae variable stars in the CCD/Transit instrument survey
[AD-A294138] p 3246 N95-34753

VARIATIONAL PRINCIPLES

Optimum Routeing: Analytical constraint of search space p 3044 N95-32493

A survey of parametrized variational principles and applications to computational mechanics
[NASA-CR-199041] p 3180 N95-32766

Interlaminar stress analysis of dropped-ply laminated plates and shells by a mixed method p 3064 N95-33327

VAX COMPUTERS

ENGIN mini-manual. Version 1.5
[PB95-218095] p 3206 N95-32814

VECTOR SPACES

Associative integral formulas and deformations of Yangians
[PB95-212189] p 3195 N95-32889

VEGETATION

Initial vegetation species and senescience/stress indicator mapping in the San Luis Valley, Colorado using imaging spectrometer data p 3130 N95-33741

Mapping minerals, amorphous materials, environmental materials, vegetation, water, ice and snow, and other materials: The USGS tricorder algorithm p 3130 N95-33742

On the potential of long wavelength imaging radars for mapping vegetation types and woody biomass in tropical rain forests p 3141 N95-33812

VEGETATION GROWTH

Effects of gravity and light on plant growth and performance in normal and reduced gravity p 3163 N95-32901

VEGETATIVE INDEX

Evaluation of the photochemical reflectance index in AVIRIS imagery p 3131 N95-33747

VELOCITY

Velocity dependence of ionization and excitation of hydrogen molecules by fast proton impact
[DE95-010818] p 3207 N95-33370

VELOCITY MEASUREMENT

Experimental investigation of the separation of texture and residual stress induced anisotropy via oblique incidence acoustoelasticity p 3126 N95-33253

New advances in physiological measurements during high-G: Technology p 3165 N95-34057

Vertical velocity ambiguity resolution method
[AD-D017481] p 3201 N95-34424

VENUS (PLANET)

Reduction and analysis of seasons 15 and 16 (1991 - 1992) Pioneer Venus radio occulation data and correlative studies with observations of the near infrared emission of Venus
[NASA-CR-199071] p 3247 N95-32700

VENUS ATMOSPHERE

Reduction and analysis of seasons 15 and 16 (1991 - 1992) Pioneer Venus radio occulation data and correlative studies with observations of the near infrared emission of Venus
[NASA-CR-199071] p 3247 N95-32700

VERBAL COMMUNICATION

NASA/DOD Aerospace Knowledge Diffusion Research Project. Paper 50: From student to entry-level professional: Examining the role of language and written communications in the reacculturation of aerospace engineering students
[NASA-TM-110834] p 3237 N95-32683

A relational metric, its application to domain analysis, and an example analysis and model of a remote sensing domain
[NASA-TM-110358] p 3198 N95-33875

VERTEBRAE

Characterization of microgravity effects on bone structure and strength using fractal analysis p 3165 N95-32419

VERTICAL DISTRIBUTION

Photobiology and optical properties of planktonic and sea ice microalgae in the high arctic
[AD-A294002] p 3160 N95-34457

VERY HIGH FREQUENCIES

Helicopter HF communications using the NVIS mode p 3043 N95-32491

VERY LARGE SCALE INTEGRATION

Hardware implementation of a desktop supercomputer for high performance image processing
[AD-A294272] p 3178 N95-34462

Optical logic implementation in composite biled/bild circuits
[AD-A294160] p 3105 N95-34758

VESTIBULES

The role of the vestibular system in manual target localization p 3166 N95-32422

VIBRATION

Application of impact dampers in vibration control of flexible structures p 3127 N95-32420

VIBRATION DAMPING

Application of impact dampers in vibration control of flexible structures p 3127 N95-32420

Device for dampening vibratory motion
[AD-D017490] p 3127 N95-34427

Acoustic attenuation and vibration damping materials
[AD-D017465] p 3201 N95-34444

VIBRATION ISOLATORS

Device for dampening vibratory motion
[AD-D017490] p 3127 N95-34427

VIDEO COMPRESSION

Design and analysis of lossless and lossy data compression methods with applications to communication and caching
[AD-A295025] p 3101 N95-34790

VIDEO TAPES

VHS-tape system for general purpose computer. For next generation mass storage system
[DE95-737268] p 3177 N95-32757

VIEWING

A real-time single-camera, stereoscopic video device
[AD-A294105] p 3116 N95-34496

VINYL POLYMERS

Molecular engineering of liquid crystalline polymers by Living polymerization 30. Synthesis and Living cationic polymerization of (2R, 3S)-2-Fluoro-3-methylpentyl 4'-(8-Vinyloxyoctyloxy) Biphenyl-4-carboxylate and its copolymerization with (2R, 3S)-2-Fluoro-3-methylpentyl 4'-(11 Vinyloxyundecanyloxyloxy) biphenyl-4-carboxylate --- carboxylate and its copolymerization with (2R, 3S)-2-Fluoro-3-methylpentyl 4-(11-Vinyloxyundecanyloxy) biphenyl-4-Carboxylate
[AD-A293115] p 3082 N95-32552

VINYLIDENE

A molecular dynamics investigation of the structural characteristics of amorphous and annealed poly (Vinylidene fluoride) and vinylidene fluoride - trifluoroethylene copolymers
[AD-A294116] p 3086 N95-34502

VIRTUAL REALITY

Tracking a turbulent spot in an immersive environment
[NASA-CR-198179] p 3180 N95-32834

Wee partons in large nuclei: From virtual dream to hard reality
[DE95-012168] p 3208 N95-33854

A relational metric, its application to domain analysis, and an example analysis and model of a remote sensing domain
[NASA-TM-110358] p 3198 N95-33875

The virtual sailor: Synthetic humans for virtual environments
[AD-A293560] p 3166 N95-34610

VISCOPLASTICITY

Models for predicting damage evolution in metal matrix composites subjected to cyclic loading
[DE95-007734] p 3077 N95-32382

VISCOSITY

Three-dimensional natural convection of a fluid with temperature-dependent viscosity in an enclosure with localized heating
[DE95-002606] p 3106 N95-32387

The unique radar scattering properties of silicic lava flows and domes p 3141 N95-33811

Apparatus for injection molding high-viscosity materials
[AD-D017471] p 3065 N95-34448

Density, heat capacity, viscosity, and thermal conductivity of mixtures of CO2, He, H2, H2O, N2, and O2
[AD-A288731] p 3076 N95-34814

VISCOUS FLOW

Parallel finite element methods and iterative solution techniques for viscous incompressible flows p 3108 N95-33031

The effect of interaction on boundary-layer separation and breakdown p 3109 N95-33310

Analysis and finite element approximation of an optimal shape control problem for the steady-state Navier-Stokes equations p 3112 N95-34285

Numerical solutions of inviscid and viscous flows about airfoils by TVD method p 3036 N95-34521

Elementary benchmarks of the NWT computer system and program performance p 3038 N95-34532

Flow and heat transfer in rotating curved pipes p 3040 N95-34545

Numerical simulation of unsteady viscous flow around an airfoil with oscillating spoiler p 3040 N95-34547

Nonlinear stability of unsteady viscous flow
[AD-A294931] p 3113 N95-34597

VISIBILITY

A tactical present weather sensor for Air Force applications
[AD-A294900] p 3158 N95-34575

VISIBLE SPECTRUM

Spectral identification of minerals using imaging spectrometry data: Evaluating the effects of signal to noise and spectral resolution using the tricorder algorithm p 3136 N95-33772

Tokamak ETE circuits: Analysis and specifications
[INPE-5573-PRP/182] p 3224 N95-33873

A 30-pair thin film thermoelectric pile
[AD-A294058] p 3151 N95-34468

VISUAL FLIGHT

Perceptual dimensions of simulated scenes relevant for visual low-altitude flight
[AD-A294385] p 3056 N95-34344

VISUAL PERCEPTION

Perceptual dimensions of simulated scenes relevant for visual low-altitude flight
[AD-A294385] p 3056 N95-34344

A comparison of monocular, biocular, and binocular night vision goggles for traversing off-road terrain on foot
[AD-A294018] p 3170 N95-34376

VITRIFICATION

Glass science tutorial lecture no. 6: The melting of silicate glasses, a review of selected topics
[DE95-010199] p 3084 N95-33218

VOICE COMMUNICATION

Tactical low-level helicopter communications p 3043 N95-32492

Speaker identification using the two-dimensional cepstrum transform
[AD-A294204] p 3099 N95-34304

VOIDS

Ductile damage model with void coalescence
[DE95-007855] p 3125 N95-32385

N-15 hydrogen profiling of IC metallizations
[DE95-011052] p 3102 N95-32708

VOLATILITY

Quantitative analysis of volatile organic compounds using ion mobility spectra and cascade correlation neural networks p 3073 N95-33290

VOLCANOES

Analyses of TIMS and AVIRIS data, integrated with field and laboratory spectra, for lithological and mineralogical interpretation of Vulcano Island, Italy p 3137 N95-33790

VOLCANOLOGY

AVIRIS user's guide p 3117 N95-33759

VOLTAGE CONVERTERS (DC TO DC)

Modeling of DC spacecraft power systems p 3062 N95-32423

VORTEX LATTICE METHOD

A nonlinear vortex lattice method for unsteady flow with separated vortex
[DLR-FB-94-32] p 3106 N95-32787

VORTEX RINGS

Direct and large eddy simulations of three dimensional round turbulent jets p 3111 N95-33709

VORTEX SHEETS

A nonlinear vortex lattice method for unsteady flow with separated vortex
[DLR-FB-94-32] p 3106 N95-32787

Direct and large eddy simulations of three dimensional round turbulent jets p 3111 N95-33709

VORTICES
Tracking a turbulent spot in an immersive environment [NASA-CR-198179] p 3180 N95-32834
Large eddy simulation of turbulent vortices and mixing layers p 3109 N95-33340
The interaction of vortices with twin boundaries [DE95-012079] p 3110 N95-33389
Very large eddy simulations of spatially evolving supersonic turbulent shear layers p 3110 N95-33606
Vorticity in shock-accelerated density-stratified interfaces: An analytical and computational study p 3111 N95-33607
Direct and large eddy simulations of three dimensional round turbulent jets p 3111 N95-33709
Solitary wave solution for mixing-layer turbulence p 3036 N95-34522
Direct numerical simulation of compressible isotropic turbulence p 3037 N95-34523
Calculation for aerodynamic characteristics on delta wing with leading-edge separated vortex effect using boundary element method p 3037 N95-34524
Sidewall-effect of the wind tunnel on the estimation of the aerodynamic characteristics of a delta wing p 3037 N95-34525
Numerical simulation of interaction between shock wave and density interface p 3039 N95-34543
Turbulent solitary wave propagating through wall Boundary Layer p 3041 N95-34555
Subscale study of engine bellmouth inlet vortices in test cell R1D [AD-A294993] p 3113 N95-34818
VORTICITY
Application of vorticity transport analysis to the development of physically accurate turbulence models p 3107 N95-32905
Transport phenomena in subsonic and supersonic flows in a duct with mass injection p 3108 N95-32934
Vorticity in shock-accelerated density-stratified interfaces: An analytical and computational study p 3111 N95-33607
A comparison of interface tracking methods [DE95-009481] p 3111 N95-33698
Parallel computation for two dimensional incompressible flow on array of transputers p 3042 N95-34558

W

WAKES
A code to compute the action-angle transformation for a particle in an abritrary potential well [DE95-012554] p 3098 N95-33336
WALL FLOW
Experimental study of the processes in the expander of the axisymmetric mirror device [DE95-009846] p 3221 N95-32536
WALLS
Design of deepwater pipelines [PB95-215109] p 3095 N95-33244
Sidewall-effect of the wind tunnel on the estimation of the aerodynamic characteristics of a delta wing p 3037 N95-34525
The effect of buoyancy on flow and heat transfer in curved pipes p 3037 N95-34528
Effect of schemes on numerical simulations of shock wave reflection p 3038 N95-34531
WARFARE
Low-Level and Nap-of-the-Earth (NOE) night operations [AGARD-CP-563] p 3042 N95-32486
Night attack p 3042 N95-32487
WARNING SYSTEMS
An integrated system for air to ground operations p 3044 N95-32498
Laser based obstacle warning sensors for helicopters p 3045 N95-32499
Functional requirements analysis and human machine interface specifications for handheld metal detector wands [DE95-009845] p 3167 N95-32535
A 30-pair thin film thermoelectric pile [AD-A294058] p 3151 N95-34468
WASTE TREATMENT
Proceedings of the ONR/NRL workshop on modeling the dispersion of nuclear contaminants in the arctic seas [AD-A294373] p 3159 N95-34341
WASTE WATER
Multiobjective optimization of hybrid regenerative life support technologies. Topic D: Technology Assessment [NASA-CR-199125] p 3167 N95-32688
WATER
Foam spread experiments on a water surface [PB95-211025] p 3083 N95-32962
The oxidation of energetic materials in supercritical water [DE95-010888] p 3088 N95-33702
Mapping minerals, amorphous materials, environmental materials, vegetation, water, ice and snow, and other materials: The USGS tricorder algorithm p 3130 N95-33742
Measurement of the spectral absorption of liquid water in melting snow with an imaging spectrometer p 3133 N95-33756
Solubility behavior of quartz and corundum in supercritical water: A quantitative thermodynamic interpretation [DE95-012294] p 3234 N95-34211
An investigation of the chemistry of citric acid in military soldering applications [AD-A295042] p 3105 N95-34796
Density, heat capacity, viscosity, and thermal conductivity of mixtures of CO2, He, H2, H2O, N2, and O2 [AD-A288731] p 3076 N95-34814
WATER COLOR
SeaWiFS technical report series. Volume 22: Prelaunch acceptance report for the SeaWFS radiometer [NASA-TM-104566-VOL-22] p 3159 N95-32672
WATER FLOW
Dividing annular/two-phase flow in horizontal T-junctions [ISBN-0-315-84910-X] p 3057 N95-33030
WATER POLLUTION
An ammonia monitor for the water industry p 3071 N95-33281
Pollution in Norway [PB95-214565] p 3153 N95-33331
Proceedings of the ONR/NRL workshop on modeling the dispersion of nuclear contaminants in the arctic seas [AD-A294373] p 3159 N95-34341
WATER QUALITY
The CE-QUAL-ICM three-dimensional eutrophication model, release version 1.0 [AD-A294258] p 3160 N95-34461
WATER RECLAMATION
Multiobjective optimization of hybrid regenerative life support technologies. Topic D: Technology Assessment [NASA-CR-199125] p 3167 N95-32688
WATER TREATMENT
Multiobjective optimization of hybrid regenerative life support technologies. Topic D: Technology Assessment [NASA-CR-199125] p 3167 N95-32688
WATER TUNNEL TESTS
Water model tests on the Allison T56 series 3 combustion system [DSTO-TR-0139] p 3054 N95-33250
WATER VAPOR
Analyses and forecasts with LAWS winds [NASA-CR-199134] p 3157 N95-32933
Correction of thin cirrus effects in AVIRIS images using the sensitive 1.375-micron cirrus detecting channel p 3131 N95-33748
Movement of water vapor in the atmosphere measured by an imaging spectrometer at Rogers Dry Lake, CA p 3132 N95-33753
Measurement of atmospheric water vapor, leaf liquid water and reflectance with AVIRIS in the Boreal Ecosystem-Atmosphere Study: Initial results p 3133 N95-33755
Atmospheric attenuation properties associated with CO2 laser radiation spectra [AD-A294061] p 3120 N95-34470
WATER WAVES
Airborne passive polarimetric measurements of sea surface anisotropy at 92 GHz [NASA-CR-197288] p 3143 N95-32823
Sea wave parameters, small altitudes and distances measurers design for movement control systems of ships, wing-in-surface effect crafts and seaplanes p 3094 N95-33141
A low diffraction beam technique for scanning in the shallow ocean [DE95-011742] p 3159 N95-33410
An experimental study of collective sea state modes of deep water surface gravity waves [AD-A294007] p 3160 N95-34372
WAVE ATTENUATION
Laser-based ultrasonics by dual-probe interferometer detection and narrow-band ultrasound generation p 3118 N95-33464
WAVE EXCITATION
Magnetic excitations in a random exchange system Fe(x)Mn(1-x)TiO3 [DE95-006626] p 3225 N95-32377
WAVE FRONTS
Measurement of laser wavefront using Shack Hartmann method with new lens array [REPT-2208] p 3090 N95-32988
Absolute wavefront measurements of high-energy laser beams in the Beamlet Demonstration Project for the National Ignition Facility [DE95-012224] p 3118 N95-33378
WAVE INTERACTION
Bernstein-Green-Kruskal wave. 2: The interaction with the Langmuir wave. Stochastic phenomena [DE95-614202] p 3220 N95-32507
Conversion of the Bernstein-Green-Kruskal wave on the density perturbation, part 1 [DE95-614203] p 3220 N95-32508
Conversion of the Bernstein-Green-Kruskal wave on the density perturbation, part 3 [DE95-614205] p 3221 N95-32509
Conversion of the Bernstein-Green-Kruskal wave on the density perturbation, part 4 [DE95-614206] p 3221 N95-32510
WAVE PROPAGATION
DETVAg-90: Use of GTD for wave propagation over earth [PB95-211447] p 3098 N95-33231
Structural wave propagation and sound radiation study through time and spatial processing p 3200 N95-33251
High-order Taylor-Galerkin and adaptive hp-methods for hyperbolic systems with application to structural acoustics p 3200 N95-33719
Discrete modeling of optical pulse propagation in nonlinear media [DE95-011515] p 3216 N95-34020
Modeling seismic wave propagation in heterogeneous materials using finite elements p 3156 N95-34283
Acoustic-optic sound velocity profiler [AD-D017487] p 3201 N95-34289
Using photothermal deflection techniques for studying the attenuations of guided waves propagated in optical thin films [AD-A294203] p 3217 N95-34303
An experimental study of collective sea state modes of deep water surface gravity waves [AD-A294007] p 3160 N95-34372
WAVE REFLECTION
Effect of schemes on numerical simulations of shock wave reflection p 3038 N95-34531
WAVEFORMS
Arbitrary waveform generator [AD-D017451] p 3097 N95-32925
WAVEGUIDES
Minimum wakefield achievable by waveguide damped cavity [DE95-012100] p 3095 N95-32616
Pulsed tunable narrow-bandwidth dye laser, with hollow circular waveguide in cavity [AD-A294060] p 3120 N95-34469
England develops world's fastest optic switch breakthrough in high-speed communications [AD-A294038] p 3105 N95-34488
Optical properties of lithium niobate waveguides, and prism coupling for optimizing waveguide fabrication [AD-A294111] p 3218 N95-34498
Photonic band gap structures on polymer materials for microstructure waveguides and high-speed interconnects [AD-A294119] p 3218 N95-34504
WAVELENGTHS
High accuracy in-flight wavelength calibration of imaging spectrometry data p 3132 N95-33750
WAVELET ANALYSIS
On application of wavelet analysis to separation of secondary particles from nucleus-nucleus interactions [DE95-623572] p 3205 N95-32630
A general solution to object matching problems by using the multiresolution approximation p 3189 N95-33002
Wavelet analysis of atmospheric turbulence structures: What can we gain from this new technique? [DE95-011955] p 3156 N95-33847
WEAPON SYSTEMS
Application of fuzzy technology to risk-based design and decision problems [DE95-006815] p 3178 N95-32378
Helicopter HF communications using the NVIS mode p 3043 N95-32491
Fixed wing night attack missions: Assessment in a Flight Simulation environment p 3045 N95-32502
A reconfigurable optoelectronic interconnect technology for multi-processor networks [DE95-011895] p 3186 N95-33838
WEAPONS DEVELOPMENT
Report to Congressional Committees. B-2 bomber: Cost to complete 20 aircraft is uncertain [GAO/NSIAD-94-217] p 3033 N95-32782
Report to the Honorable William V. Roth, Jr., US Senate. Naval aviation: F/A-18 E/F acquisition strategy [GAO/NSIAD-94-194] p 3197 N95-32886
WEAR
Test method to measure resistance towards fragmentation by studded tires [PB95-211017] p 3121 N95-32612
Monitoring of the cutting operations using fuzzy logic p 3189 N95-32999

WEAR RESISTANCE
Wear resistant composite structure of vitreous carbon containing convoluted fibers
[DE95-011463] p 3063 N95-33062
WEATHER
Investigation research on introducing new energy technology, promoting its practical application, and providing its instruction
[DE95-769801] p 3148 N95-32403
WEATHER FORECASTING
Weather Forecasting: Systems architecture needed for National Weather Service modernization. Report to Congressional requesters
[GAO/AIMD-94-28] p 3157 N95-32760
WEATHERING
Photovoltaic Manufacturing Technology (PVMaT)
[DE95-004093] p 3149 N95-33153
Lithologic controls on AIRSAR signatures of bedrock and alluvium, at Lunar Crater, Nevada
p 3141 N95-33813
WEDGES
Unusual behavior in the magnetic anisotropy of ultra-thin Co sandwiches: The role of Au underlayers
[DE95-010612] p 3229 N95-33641
Penetrable wedge analysis
[AD-A294276] p 3234 N95-34464
WEIGHT INDICATORS
An instrument for gravimetric calibration of flow devices with corrosive gases
[DE95-009700] p 3116 N95-33206
WEIGHT MEASUREMENT
An instrument for gravimetric calibration of flow devices with corrosive gases
[DE95-009700] p 3116 N95-33206
High resolution electrospray mass spectrometry with a magnetic sector instrument: Accurate mass measurement and peptide sequencing
[AD-A293564] p 3076 N95-34611
WEIGHTING FUNCTIONS
Comparison of theoretical predictions with field observations for a simple forward scattering sensor
[AD-A294948] p 3219 N95-34576
WELD STRENGTH
An experimental and numerical analysis of hydrogen assisted cracking and weldability test methodology
p 3079 N95-32936
Electron beam joining of structural ceramics
[DE95-012521] p 3085 N95-34022
WELD TESTS
An experimental and numerical analysis of hydrogen assisted cracking and weldability test methodology
p 3079 N95-32936
Electron beam joining of structural ceramics
[DE95-012521] p 3085 N95-34022
WELDABILITY
An experimental and numerical analysis of hydrogen assisted cracking and weldability test methodology
p 3079 N95-32936
WELDED JOINTS
The tensile fracture behavior of the weld metal of BIS 812 EMA and Q1N naval construction steels
[DSTO-RR-0021] p 3078 N95-32926
An experimental and numerical analysis of hydrogen assisted cracking and weldability test methodology
p 3079 N95-32936
WELDED STRUCTURES
The development of some kinds of LRE injectors
[AD-A294199] p 3061 N95-34302
WELDING
The effect of travel speed on thermal response in CO2 laser welding of small electronic components
[DE95-006314] p 3118 N95-32683
WETTABILITY
Spontaneous dewetting of a perfluoropolyether
[NASA-TM-106964] p 3083 N95-32919
WHISKER COMPOSITES
Interfacial composition analysis of silicon nitride whisker reinforced oxynitride glass systems
[DE95-012895] p 3085 N95-33635
R-curve behavior of whisker-reinforced ceramic composites
[DE95-012873] p 3087 N95-34798
WIDEBAND COMMUNICATION
FH and DS spread-spectrum systems in interference-limited HF channels: A comparison
[PB95-211439] p 3098 N95-33230
WIND (METEOROLOGY)
Analyses and forecasts with LAWS winds
[NASA-CR-199134] p 3157 N95-32933
WIND EFFECTS
Preliminary study of Kelso Dunes using AVIRIS, TM, and AIRSAR p 3136 N95-33773
The 1994 TIMS airborne calibration experiment: Castaic Lake, California p 3117 N95-33797
An experimental study of collective sea state modes of deep water surface gravity waves
[AD-A294007] p 3160 N95-34372
WIND EROSION
New observations of Bolivian wind streaks by JPL Airborne SAR: Preliminary results p 3139 N95-33802
WIND SHEAR
Human piloting factors in the design of control laws for precision landing p 3167 N95-33605
WIND TUNNEL MODELS
SOFIA 2 model telescope wind tunnel test report
[NASA-TM-110668] p 3033 N95-32764
WIND TUNNEL STABILITY TESTS
Full-scale hingeless rotor performance and loads
[NASA-TM-110356] p 3048 N95-32699
WIND TUNNEL TESTS
Boundary layer transition studies
[NASA-CR-198983] p 3106 N95-32454
SOFIA: Aft cavities wind tunnel test
[NASA-TM-110673] p 3033 N95-32682
SOFIA 2 model telescope wind tunnel test report
[NASA-TM-110668] p 3033 N95-32764
Drag measurements of an axisymmetric nacelle mounted on a flat plate at supersonic speeds
[NASA-TM-4660] p 3034 N95-32821
Numerical simulation of high enthalpy shock tunnel
p 3035 N95-34514
Sidewall-effect of the wind tunnel on the estimation of the aerodynamic characteristics of a delta wing
p 3037 N95-34525
Elementary benchmarks of the NWT computer system and program performance p 3038 N95-34532
WIND TUNNEL WALLS
Investigation of water droplet trajectories within the NASA icing research tunnel
[NASA-TM-107023] p 3034 N95-32769
WIND TUNNELS
Investigation of water droplet trajectories within the NASA icing research tunnel
[NASA-TM-107023] p 3034 N95-32769
Sidewall-effect of the wind tunnel on the estimation of the aerodynamic characteristics of a delta wing
p 3037 N95-34525
Direct numerical simulation of incompressible homogeneous isotropic turbulence using NWT
p 3038 N95-34530
Performance evaluation of the NWT with incompressible NS code p 3038 N95-34533
WIND TURBINES
Wind turbine trailing edge aerodynamic brakes
[DE95-004061] p 3033 N95-32548
HYBRID2: A versatile model of the performance of hybrid power systems
[DE95-004062] p 3148 N95-32551
Techniques for the determination of local dynamic pressure and angle of attack on a horizontal axis wind turbine
[DE95-009204] p 3149 N95-32685
Tomorrow's energy today for cities and countries
[DE95-012464] p 3150 N95-33383
Fatigue damage estimate comparisons for northern European and US wind farm loading environments
[DE95-011061] p 3150 N95-33706
WIND VELOCITY
Fatigue damage estimate comparisons for northern European and US wind farm loading environments
[DE95-011061] p 3150 N95-33706
Turbulent heat flux measurements over the Greenland, Norwegian and Barents seas
[AD-A294129] p 3157 N95-34751
WINDING
A fiber optic strain measurement and quench localization for use in superconducting accelerator dipole magnets
[DE95-012370] p 3215 N95-33381
WINDOWS (APERTURES)
High power CO2 laser windows and reflection reducing coatings
[AD-A294217] p 3119 N95-34308
WINDPOWER UTILIZATION
Tomorrow's energy today for cities and countries
[DE95-012464] p 3150 N95-33383
Fatigue damage estimate comparisons for northern European and US wind farm loading environments
[DE95-011061] p 3150 N95-33706
Review of the research activities of the Energy Research Unit in 1994
[PB95-235008] p 3151 N95-34656
WINDPOWERED GENERATORS
Fatigue damage estimate comparisons for northern European and US wind farm loading environments
[DE95-011061] p 3150 N95-33706
WINDSHIELDS
Transmittance characteristics of US Army rotary-wing aircraft transparencies
[AD-A295035] p 3049 N95-34793
WING CAMBER
Analysis and design methodology for chordwise deformable wings p 3049 N95-33311
WING NACELLE CONFIGURATIONS
Numerical analysis around the whole SST configuration p 3039 N95-34541
WING TIPS
An LDV investigation of support structure influence on the flow field near the wingtip of a STOVL configuration in hover
[AD-A294126] p 3042 N95-34750
WINGS
Development of a composite tailoring procedure for airplane wing
[NASA-CR-199081] p 3048 N95-32928
Numerical simulation of two-dimensional PAR-WIG
p 3040 N95-34548
WINTER
Test method to measure resistance towards fragmentation by studded tires
[PB95-211017] p 3121 N95-32612
WIRE
The RHIC transfer line cable database
[DE95-011560] p 3236 N95-32412
The 8th Winterschool on New Developments in Solid State Physics
[AD-A290163] p 3227 N95-32677
Background meeting and technology demonstration: Chromium electroplating of superconductor strand
[DE95-011736] p 3068 N95-33070
Quantum transport
[AD-A294977] p 3235 N95-34589
WIRE CLOTH
The linear elastic biaxial response of plain-woven meshes p 3064 N95-33468
WIRING
Optical interconnects for 3D computer architectures
[AD-A294118] p 3178 N95-34503
WORDS (LANGUAGE)
Scanners, optical character readers, Cyrillic alphabet and Russian translations p 3194 N95-32433
Synthesis of potential new Zintl phases
[DE95-010123] p 3227 N95-32640
An empirical investigation of the semantic warrants exercised in thesaurus construction
[ISBN-0-315-86393-5] p 3238 N95-33334
WORKING FLUIDS
Laminar heat transfer for power-law fluids in thermal entrance region of annular sector ducts
p 3108 N95-33255
WORKLOADS (PSYCHOPHYSIOLOGY)
Event-related potentials and electroencephalograms in adaptive operator training: Rationale and annotated bibliography
[AD-A294337] p 3166 N95-34356
Practical guidelines for workload assessment
p 3174 N95-34777
WORKSTATIONS
Stimulus-response compatibility
[PB95-214722] p 3167 N95-33237
Planetary data analysis and display system: A version of PC-McIDAS p 3241 N95-34232
Recoverable distributed shared memory under sequential and relaxed consistency
[AD-A293966] p 3178 N95-34453
Range graphics benchmark
[AD-A293541] p 3057 N95-34606
WORLD DATA CENTERS
Carbon Dioxide Information Analysis Center and World Data Center: A for Atmospheric trace gases
[DE95-011769] p 3154 N95-33655
WORLD WIDE WEB
Collaborating over the Web: Libraries and laboratories or the Librarian and the Webmaster
[DE95-010572] p 3186 N95-33639
WOVEN COMPOSITES
The linear elastic biaxial response of plain-woven meshes p 3064 N95-33468

X

X RAY ANALYSIS
X-ray standing wave interferometry-optics at 1 angstrom with applications to surface and material sciences
[DE95-009688] p 3215 N95-32662
X RAY ASTRONOMY
ROSAT survey of emission from Be stars
[NASA-CR-199086] p 3245 N95-32835
High speed variability in x-ray binary systems
[AD-A294634] p 3247 N95-34561
X RAY BINARIES
High speed variability in x-ray binary systems
[AD-A294634] p 3247 N95-34561

X RAY DIFFRACTION
The growth and optimization of InPSb/InGaAs/InAsSb strained-layer superlattice emitters by metal organic chemical vapor deposition
[DE95-011057] p 3226 N95-32595
Influence of processing variables on the structure and properties of ZnO films
[DE95-011494] p 3084 N95-33405
Epitaxial Pb(Zr(0.40)Ti(0.60))O3/SrRuO3 and PbTiO3/SrRuO3 multilayer thin films prepared by MOCVD and RF sputtering
[DE95-007146] p 3229 N95-33636
X RAY LASERS
Energy and Technology Review
[DE95-011686] p 3223 N95-33066
X RAY OPTICS
X-ray standing wave interferometry-optics at 1 angstrom with applications to surface and material sciences
[DE95-009688] p 3215 N95-32662
X RAY SOURCES
High speed variability in x-ray binary systems
[AD-A294634] p 3247 N95-34561
X RAYS
Chromosomal damage observed in first postirradiation metaphases of repair-proficient and -deficient cell lines
p 3162 N95-32726
X-ray-provoked non-Mendelian transgenerational oncodeterminants p 3163 N95-32731
Low-energy response of superconducting tunnel junction x-ray spectrometers
[DE95-011733] p 3230 N95-33650
Theory of magneto-optics and circular magnetic x-ray dichroism
[DE95-010129] p 3080 N95-33700
Multilayer optics for soft x-rays
[AD-A295030] p 3219 N95-34791
X-30 VEHICLE
Shuttle to Space Station. Heart assist implant. Hubble update. X-30 mock-up
[NASA-TM-110837] p 3056 N95-33167
XENON
Life test of a xenon hollow cathode for a space plasma contractor
[NASA-CR-195403] p 3061 N95-33926
XENON 129
About the mechanism of heavy ion radiation influence on the metals at high temperature
[DE95-620943] p 3078 N95-32626
XYLENE
Determination of Benzene, Toluene, and Xylene by means of an ion mobility spectrometer device using photoionization p 3069 N95-33269

Y

YAG LASERS
Laser beaming demonstrations at the Starfire Optical Range
[DE95-007747] p 3120 N95-34811
YANG-MILLS THEORY
Zero modes of Gauss constraint in gaugeless reduction of Yang-Mills theory
[DE95-623676] p 3234 N95-32667
YBCO SUPERCONDUCTORS
The effects of H(+) implants on YBa2Cu3O7 superconducting materials
[DE95-614466] p 3227 N95-32698
Peak effect and flux pinning in YBa2Cu3O(7-(delta)) single crystals
[DE95-010126] p 3228 N95-32959
The interaction of vortices with twin boundaries
[DE95-012079] p 3110 N95-33389
Properties of high-T(sub c) Josephson junctions with Y(0.7)Ca(0.3)Ba2Cu3O(7-delta) barrier layers
[AD-A294852] p 3231 N95-34568
YEAST
Heavy ion induced DNA-DSB in yeast and mammalian cells p 3161 N95-32723
Heavy ion action on single cells: Cellular inactivation capability of single accelerated heavy ions
p 3162 N95-32729
YIELD POINT
Cylindrical shell buckling through strain hardening
[DE95-009545] p 3125 N95-32392
Development of 1.06 micron high efficiency antireflective coating
[AD-A294161] p 3219 N95-34759
YIELD STRENGTH
Fracture toughness and tensile behavior of multi-layer laminated metal composite of Al 6090-25 vol % SiCp and Al 5182
[DE95-011421] p 3062 N95-32602
Fracture toughness assessment of present and future pressure vessel materials based on Charpy impact energy and yield strength
[AD-A294008] p 3081 N95-34373
YTTERBIUM
Optical pulse generation using fiber lasers and integrated optics
[DE95-011517] p 3216 N95-33506
YTTRIA-STABILIZED ZIRCONIA
Thin-film electrolytes for reduced temperature solid oxide fuel cells
[DE95-011273] p 3151 N95-34481
YTTRIUM
Laser ablation plume thermalization dynamics in background gases studied by time-resolved imaging, spectroscopic, and ion probe diagnostics
[DE95-010277] p 3118 N95-33246

Z

ZEEMAN EFFECT
Method and apparatus for locking laser wavelength to an atomic transition
[AD-D017425] p 3120 N95-34619
ZEOLITES
Alternative catalyst and exhaust gas sensor work at Argonne National Laboratory
[DE95-007138] p 3152 N95-32553
Visualization of parallel molecular dynamics simulation on a remote visualization platform
[DE95-007806] p 3185 N95-32582
Zeolite membranes for gas separations
[DE95-012984] p 3088 N95-33224
ZINC OXIDES
Influence of processing variables on the structure and properties of ZnO films
[DE95-011494] p 3084 N95-33405
ZINC SELENIDES
High power CO2 laser windows and reflection reducing coatings
[AD-A294217] p 3119 N95-34308
ZINC SULFIDES
Ion assisted deposition of ZnS and MgF2
[AD-A294759] p 3086 N95-34563
ZINC TELLURIDES
Highly doped p-ZnTe films and quantum well structures grown by nonequilibrium pulsed laser ablation
[DE95-012885] p 3232 N95-34799
ZIRCONIUM OXIDES
In situ ion-beam analysis and modification of sol-gel zirconia thin films
[DE95-010994] p 3203 N95-32577
Indirect measurements of hydrogen: The deficit method for a many-component system
[DE95-010993] p 3208 N95-33623
TiO2/SiO2 and ZrO2/SiO2 multilayer media film optical loss and laser damage study
[AD-A294192] p 3217 N95-34298

Typical Personal Author Index Listing

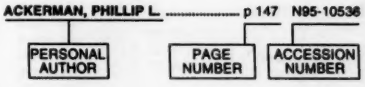

Listings in this index are arranged alphabetically by personal author. The page number helps you locate the citation in the abstract section. The accession number denotes the number by which the citation is identified.

A

ABBOTT, DAVID W. ..... p 3055 N95-34772
ABDEL-MALEK, KARIM ANTOUN p 3180 N95-32937
ABDELWAHAB, S. M. ..... p 3202 N95-32524
ABER, JOHN D. ..... p 3128 N95-33731
ABERNATHY, C. R. ..... p 3226 N95-32594
p 3223 N95-33412
ACHARYA, RAJ S. ..... p 3165 N95-32419
ACKER, JAMES G. ..... p 3159 N95-32672
p 3159 N95-32833
ADAMI, JANS F. ..... p 3166 N95-34609
ADAMS, B. E. ..... p 3154 N95-33638
ADAMS, JOHN B. ..... p 3135 N95-33766
ADAWI, M. A. ..... p 3204 N95-32610
ADLER, D. L. ..... p 3229 N95-33628
ADLER, J. ..... p 3070 N95-33272
ADOLPHSEN, C. ..... p 3211 N95-32608
p 3213 N95-33338
AFANASEV, S. V. ..... p 3205 N95-32630
AFFINITO, J. D. ..... p 3150 N95-33400
AGER, CATHY ..... p 3130 N95-33741
p 3134 N95-33761
AHRENS, JAMES P. ..... p 3186 N95-33403
AHRENS, L. A. ..... p 3212 N95-33067
AISO, HIDEAKI ..... p 3036 N95-34519
AKAISHI, YOSHINORI ..... p 3202 N95-32404
AKL, FRED A. ..... p 3127 N95-32420
AKLUFI, MONTI E. ..... p 3086 N95-34447
ALENCASTRO, RICARDO BICCA DE
p 3067 N95-32804
ALEXANDER, K. B. ..... p 3085 N95-33635
ALEXANDER, WINSER E. ..... p 3189 N95-33002
ALI, MOONIS ..... p 3188 N95-32995
ALI, R. ..... p 3208 N95-33374
ALIABADI, H. ..... p 3207 N95-33370
ALLCOCK, HARRY R. ..... p 3087 N95-34649
ALLEN, D. ..... p 3088 N95-33702
ALLEN, D. H. ..... p 3077 N95-32382
ALLEN, L. J. ..... p 3204 N95-32623
ALLEN, MARK ..... p 3241 N95-34230
ALLEVATO, CAMILLO ..... p 3149 N95-32811
ALLISON, S. ..... p 3211 N95-32608
ALMAGRI, A. F. ..... p 3223 N95-33221
ALTAJSKIJ, M. V. ..... p 3205 N95-32630
ALTEMOS, EDWARD A. ..... p 3102 N95-32956
ALTENBACH, THOMAS J. ..... p 3197 N95-33220
ALZHEIMER, J. M. ..... p 3158 N95-33505
AMALBERTI, RENE ..... p 3176 N95-34786
AMAYA-RASTBURG, B. ..... p 3096 N95-32747
AMES, GREGORY H. ..... p 3215 N95-32923
p 3216 N95-34288
AMIRSOLEYMANI, SHAHRZAD .. p 3238 N95-33711
AMOS, K. ..... p 3204 N95-32623
ANANIKYAN, N. S. ..... p 3227 N95-33631
ANCKER, K. ..... p 3067 N95-32615
ANDERS, A. ..... p 3163 N95-32731
ANDERS, F. ..... p 3163 N95-32731
ANDERSON, A. H. ..... p 3096 N95-32773
ANDERSON, CHARLES ..... p 3089 N95-32585
ANDERSON, DAVID E. ..... p 3101 N95-32578
ANDERSON, DONALD L. ..... p 3137 N95-33791
p 3137 N95-33792
ANDERSON, G. A. ..... p 3158 N95-33505
ANDERSON, G. K. ..... p 3088 N95-33702
ANDERSON, GAIL P. ..... p 3128 N95-33732
ANDERSON, J. C. ..... p 3096 N95-32773
ANDERSON, KEN B. ..... p 3154 N95-33394
ANDERSON, STEVEN W. ..... p 3141 N95-33811
ANDERSSON, GUNNAR ..... p 3098 N95-33230
ANDERSSON, I. ..... p 3068 N95-33229
ANDERSSON, LARS ..... p 3196 N95-33233
ANDO, YASUNORI ..... p 3035 N95-34512
ANDREOLI, G. ..... p 3133 N95-33758
ANIKEEV, A. V. ..... p 3221 N95-32536
ANTOGNAZZA, L. ..... p 3231 N95-34568
ANTONIADIS, DIMITRI A. ..... p 3231 N95-34569
ANTONSEN, T. ..... p 3117 N95-32571
AOKI, YASUSHI ..... p 3212 N95-32712
AOYAMA, TAKASHI ..... p 3040 N95-34549
APEN, ELIZABETH ..... p 3229 N95-33401
APONSO, BIMAL L. ..... p 3055 N95-34306
ARCHULETA, F. L. ..... p 3088 N95-33702
ARNOLD, KATHRYN E. ..... p 3209 N95-34212
ARPAIA, G. ..... p 3045 N95-32502
ARSENAULT, R. J. ..... p 3064 N95-33704
ASHDOWN, A. M. ..... p 3094 N95-33142
ASHLEY, P. R. ..... p 3218 N95-34480
ASO, SHIGERU ..... p 3035 N95-34512
p 3040 N95-34546
ASO, SHIGERU, ... p 3037 N95-34526
ASP, W. ..... p 3095 N95-32613
ATANASSOV, G. A. ..... p 3119 N95-34308
ATASSI, M. Z. ..... p 3165 N95-34754
ATENCIO, J. H. ..... p 3088 N95-33702
ATTAWAY, S. W. ..... p 3106 N95-32587
AUGUST, GERALD ..... p 3043 N95-32492
AUSTIN, PHILIP JOSEPH ..... p 3073 N95-33308
AVALLE, MASSIMO ..... p 3044 N95-32498
AVARA, G. R. ..... p 3115 N95-32900
AZGUI, F. ..... p 3230 N95-33650

B

BABA, KENSUKE ..... p 3091 N95-32992
BACA, G. T. ..... p 3088 N95-33702
BADZIAN, ANDRZEJ ..... p 3231 N95-34478
BAER, T. A. ..... p 3067 N95-32709
BAGINYAN, S. ..... p 3188 N95-32627
BAGRYANSKY, P. A. ..... p 3221 N95-32536
BAHILL, A. T. ..... p 3178 N95-32378
BAI, BURTSITSIG ..... p 3041 N95-34555
BAI, G. R. ..... p 3226 N95-32598
p 3229 N95-33636
BAIK, DAE HYUN ..... p 3066 N95-32566
BAILEY, MICHAEL ..... p 3241 N95-34230
BALATZ, M. YA. ..... p 3205 N95-32703
BALDO, P. M. ..... p 3226 N95-32598
p 3229 N95-33636
BALDWIN, ROD ..... p 3175 N95-34780
BALLARD, JERRELL R., JR. ..... p 3100 N95-34578
BALLARD, WILLIAM P. ..... p 3181 N95-33624
BALLATO, ARTHUR ..... p 3232 N95-34607
p 3232 N95-34608
BALLDIN, ULF I. ..... p 3165 N95-34057
BALLYK, JOHN DAVID ..... p 3057 N95-33030
BALMFORTH, N. J. ..... p 3247 N95-34216
BALOOCH, MEHDI ..... p 3085 N95-33409
BALZAROTTI, G. ..... p 3043 N95-32488
BALZAROTTI, GIORGIO ..... p 3045 N95-32504
BAN, HIROYUKI ..... p 3060 N95-32755
BANDYOPADHYAY, K. ..... p 3125 N95-32392
BANDYOPADHYAY, SUPRIYO .... p 3235 N95-34589
BANE, K. L. F. ..... p 3213 N95-33338
BANKS, DAVID C. ..... p 3180 N95-32834
BANKS, MICHAEL A. ..... p 3086 N95-34452
BANKS, P. ..... p 3101 N95-34788
BANKS, W. ..... p 3167 N95-32535
BANNEROT, RICHARD ..... p 3248 N95-32418
BAOTANG, YANG ..... p 3217 N95-34459
BAPTISTA, J. P. V. POIARES ..... p 3096 N95-32747
p 3096 N95-32750
BAR-AD, S. ..... p 3101 N95-32596
p 3227 N95-32600
BARANOV, S. ..... p 3188 N95-32627
BARB, FLORIN DAN ..... p 3192 N95-33399
BARBALISCIA, F. ..... p 3096 N95-32747
p 3096 N95-32749
BARBARA, PAUL F. ..... p 3218 N95-34571
BARBEE, TROY W., JR. ..... p 3081 N95-34482
BARBOUR, TIM ..... p 3183 N95-33007
BARCLAY, REBECCA O. ..... p 3237 N95-32883
p 3239 N95-34217
BARE, HAROLD F. ..... p 3178 N95-34503
BARFKNECHT, A. T. ..... p 3230 N95-33650
BARGER, V. ..... p 3209 N95-34650
BARHORST, ALAN A. ..... p 3125 N95-32421
BARLOW, TODD ..... p 3047 N95-34797
BARNES, ROBERT A. ..... p 3159 N95-32672
p 3159 N95-32833
BARNES, WILLIAM L. ..... p 3159 N95-32672
BARRAGY, EDWARD JOSEPH ... p 3108 N95-33031
BARRERA-ROLDAN, ADRIAN S. p 3152 N95-32573
BARRY, SUSAN R. ..... p 3166 N95-32422
BASEDOW, R. W. ..... p 3116 N95-33733
BASS, B. R. ..... p 3126 N95-32684
BATE, D. G. ..... p 3155 N95-32599
p 3155 N95-32601
p 3156 N95-32603
BATES, J. B. ..... p 3103 N95-33697
BATTRICK, B. ..... p 3252 N95-32805
BATTRICK, BRUCE ..... p 3252 N95-32538
BAUCOM, K. C. ..... p 3228 N95-33213
BAUER, CHRISTOPHER ..... p 3110 N95-33496
BAUGH, WILLIAM M. ..... p 3128 N95-33734
BAUMBACH, J. I. ..... p 3069 N95-33269
p 3073 N95-33291
BAUMBACK, J. I. ..... p 3070 N95-33274
BEACHLEY, O. T., JR. ..... p 3086 N95-34452
BEASLEY, JAMES O., II ..... p 3070 N95-33276
BEATTY, DAVID A. ..... p 3124 N95-34449
BEAUDOIN, A. J., JR. ..... p 3231 N95-34450
BECHER, G. ..... p 3162 N95-32725
BECHER, P. F. ..... p 3085 N95-33635
p 3087 N95-34798
BECHER, W. ..... p 3162 N95-32729
BEGG, LESTER L. ..... p 3149 N95-32645
p 3211 N95-32647
BEHL, WISHVENDER K. ..... p 3104 N95-34347
BELOUS, YU. P. ..... p 3048 N95-33131
BELOV, A. G. ..... p 3164 N95-32666
BELSHAW, J. ..... p 3096 N95-32747
p 3096 N95-32748
p 3096 N95-32751
BELYAEV, I. M. ..... p 3205 N95-32703
BEN-ITZHAK, I. ..... p 3206 N95-32763
p 3206 N95-32966
p 3207 N95-33370
p 3209 N95-34355
BENDER, EDWARD ..... p 3170 N95-34376
BENJAMIN, ALLAN S. ..... p 3111 N95-33837
BENJEGERDES, R. ..... p 3103 N95-33080
BENNETT, LAWRENCE F. ..... p 3101 N95-32578
BENNETT, W. D. ..... p 3150 N95-33400
BENSCH, H. ..... p 3069 N95-33269
BENT, PAUL H. ..... p 3200 N95-33831
BENTLEY, J. ..... p 3074 N95-33629
BEPPU, GORO ..... p 3036 N95-34521
BERAUN, RICARDO ..... p 3111 N95-33837
BERENDS, EDWIN M. ..... p 3228 N95-33235
BERG, J. SCOTT ..... p 3211 N95-32607
p 3098 N95-33336
BERGER, D. ..... p 3069 N95-33269
BERGER, K. W. ..... p 3084 N95-33247
BERGLUND, LARS ..... p 3215 N95-33239
BERGSTROEM, BENGT ..... p 3167 N95-33237
BERK, H. L. ..... p 3224 N95-33696
BERNHARD, WERNER ..... p 3072 N95-33285
BERNSTEIN, GARY H. ..... p 3235 N95-34589
BERRY, F. C. ..... p 3062 N95-32423
BERRY, RAY A. ..... p 3081 N95-34348
BHALLA, C. P. ..... p 3207 N95-33371
BHARADWAJ, V. ..... p 3215 N95-32658

BHAVNANI, K. H. p 3144 N95-34454
BI, FENGFEI p 3215 N95-32660
BIAN, HUIAN p 3215 N95-32701
BIANCHI, R. p 3129 N95-33735
BICKMORE, TIMOTHY p 3061 N95-34625
BIEFELD, R. M. p 3226 N95-32595
p 3228 N95-33213
BIFANG, ZHOU p 3218 N95-34490
BINER, S. B. p 3062 N95-32395
BING, YI p 3158 N95-34491
BINGHUO, XU p 3217 N95-34309
BINGQUAN, ZHANG p 3219 N95-34756
BIONDO, SAMUEL J. p 3191 N95-33060
BIRKETT, P. R. p 3044 N95-32496
BIRMAN, VICTOR p 3063 N95-33210
BISH, P. p 3103 N95-33080
BISHOP, CHIP p 3125 N95-33209
BLACKBURN, L. D. p 3079 N95-32958
BLACKER, TED D. p 3064 N95-33463
BLANCHAT, T. K. p 3106 N95-32387
BLANDO, LUIS R. p 3236 N95-32471
BLANFORD, GEORGE E. p 3210 N95-32424
BLASKIEWICZ, M. p 3211 N95-32485
BLASKIEWICZ, M. M. p 3212 N95-33067
BLAYLOCK, JAMES p 3048 N95-33140
BLIBECHE, MOUNIR p 3127 N95-33695
BLISS, ERLAN S. p 3118 N95-33378
BLISS, M. p 3075 N95-33832
BLOM, RONALD p 3241 N95-34230
BLOTTNER, F. G. p 3106 N95-32818
BLUMBERG, DAN G. p 3136 N95-33773
p 3139 N95-33802
BLUME, LEO p 3241 N95-34230
BOARDMAN, JOSEPH W. p 3129 N95-33736
p 3129 N95-33737
BOUEN, THOMAS A. p 3154 N95-33655
BODIS, JAMES R. p 3125 N95-33209
BOEHM, A. P. W. p 3186 N95-33643
BOGLIOLO, M. PAOLA p 3137 N95-33790
BONYUSHKINA, A. Y. p 3187 N95-32476
BOOKLESS, W. A. p 3223 N95-33066
BORBA, D. p 3224 N95-33696
BORDON, MICHAEL J. p 3203 N95-32576
BORUE, VADIM p 3112 N95-34343
BORUP, RODNEY L. p 3148 N95-32575
BOSSE, ALBERT BERNARD p 3192 N95-33713
BOTKIN, D. p 3230 N95-33880
BOUHNIX, J. P. p 3206 N95-32966
p 3209 N95-34355
BOURASSA, R. J. p 3059 N95-33264
p 3059 N95-33890
BOWERS, S. M. p 3121 N95-32376
BOWMAN, J. C. p 3248 N95-33390
BOWMAN, KENNETH P. p 3239 N95-34219
BOYD, M. J. p 3043 N95-32489
BOYER, DON L. p 3160 N95-34594
BOYES, JOHN D. p 3101 N95-32578
BRADSHAW, R. F. D. p 3070 N95-33271
BRAEUNING, H. p 3228 N95-33373
BRANDBERG, AKE p 3088 N95-33332
BRANIGAN, ROBERT G. p 3043 N95-32490
p 3045 N95-32500
BRATT, C. p 3078 N95-32614
BREED, CAROL S. p 3141 N95-33810
BRENNAN, J. M. p 3212 N95-33067
BRESHEARS, W. D. p 3088 N95-33702
BRINKKEMPER, SJAAK p 3237 N95-33238
BRIOTTET, XAVIER p 3048 N95-33136
BROATCH, S. A. p 3044 N95-32494
BRODACKI, M. p 3070 N95-33272
BRODSKY, S. J. p 3204 N95-32617
BROKENSHIRE, J. L. p 3071 N95-33281
BROWN, B. W. p 3151 N95-32475
BROWN, C. G. p 3119 N95-33703
BROWN, G. E. p 3204 N95-32621
BROWN, G. L. p 3113 N95-34752
BROWN, NISA N. p 3111 N95-33837
BROWN, PATRICIA A. p 3072 N95-33284
BROWN, W. L. p 3229 N95-33628
BROWNING, D. F. p 3216 N95-33506
BRUCKART, JAMES E. p 3170 N95-34489
BRUEMMER, S. M. p 3077 N95-32555
BRUENER, D. B. p 3059 N95-32593
BRUSSAARD, G. p 3096 N95-32747
p 3096 N95-32749
BRYANT, RANDAL E. p 3105 N95-34565
BUCHELNIKOVA, N. S. p 3220 N95-32507
p 3220 N95-32508
p 3221 N95-32509
p 3221 N95-32510
BUCHOLZ, D. BRUCE p 3228 N95-32810
BUDAI, J. D. p 3231 N95-34465
p 3232 N95-34799
BUDKEWITSCH, PAUL p 3141 N95-33813
BUDNICK, J. I. p 3079 N95-33065
BUECHTEMANN, W. p 3045 N95-32499
BUELOW, S. J. p 3088 N95-33702
BUGROV, V. N. p 3164 N95-32666
BUICK, F. p 3166 N95-34058
BUKASA, BIRGIT p 3175 N95-34779
BUKLANOV, G. V. p 3164 N95-32666
BULLETT, TERENCE WILLIAM p 3222 N95-32838
BUONGIORNO, M. FABRIZIA p 3137 N95-33790
BURAK, DARIUSZ p 3206 N95-32921
BURCH, I. A. p 3078 N95-32926
BURCHAM, FRANK W., JR. p 3051 N95-33010
p 3053 N95-33021
p 3049 N95-33023
p 3049 N95-33025
BURCHETT, S. N. p 3118 N95-32683
BURGREEN, GREGORY WAYNE p 3048 N95-32904
BURICHENKO, A. P. p 3202 N95-32481
BURKE, D. p 3212 N95-32657
p 3215 N95-32658
BURKE, G. J. p 3095 N95-32570
BURKE, IAN p 3129 N95-33738
BURKE, S. p 3214 N95-34651
BURKEN, JOHN p 3049 N95-33025
BURKHARDT, MARTIN p 3231 N95-34569
BURKHART, S. C. p 3216 N95-33506
p 3216 N95-33651
BURKHOLDER, P. S. p 3050 N95-32636
BURNHAM, EDWARD ALONZA, JR. p 3054 N95-34805
BURNS, J. W. p 3168 N95-34051
p 3169 N95-34060
BURRELL, K. H. p 3222 N95-32756
BURRIS, H. R. p 3120 N95-34761
BURSILL, L. A. p 3082 N95-32710
BURTIS, MARVEL D. p 3154 N95-33655
BURTON, DONALD E. p 3112 N95-34437
BURTON, R. A. p 3063 N95-33062
BURTON, R. G. p 3063 N95-33062
BUSHMAN, MARK p 3051 N95-33012
BUTENHOFF, T. J. p 3088 N95-33702
BUTLER, T. A. p 3058 N95-32713
BUTT, AAMIR S. p 3127 N95-32420
BUTTS, R. R. p 3120 N95-34592
BUZBEE, WILLIAM p 3239 N95-34220
BYCHKOV, V. N. p 3102 N95-32628

C

CADWALLADER, LEE C. p 3221 N95-32588
CAI, NING-BIN p 3190 N95-33005
CAILLAT, THIERRY p 3149 N95-32811
CALISH, S. p 3213 N95-33333
CALLAN, C. p 3244 N95-34816
CALN, CLARENCE P. p 3164 N95-34789
CAMERON, CHARLES E. p 3087 N95-34649
CANDY, J. p 3224 N95-33696
CANFIELD, P. C. p 3198 N95-32397
p 3229 N95-33386
CANTALLOUBE, HUBERT p 3044 N95-32495
CAO, JIANSHU p 3209 N95-34350
CAPLAN, M. p 3117 N95-32571
CAPLINGER, MICHAEL p 3241 N95-34229
CAPSONI, C. p 3096 N95-32750
CARANDE, R. p 3140 N95-33808
CARD, CURTIS LEE p 3156 N95-34283
CARLE, GLENN C. p 3069 N95-33270
CARLSON, K. p 3179 N95-32715
CARLSSON, H. p 3067 N95-32615
CARNES, K. D. p 3207 N95-33370
CARR, THOMAS WILLIAM p 3119 N95-33470
CARRABBA, MICHAEL M. p 3153 N95-32816
CARROLL, SEAN MICHAEL p 3234 N95-33313
CARSON, R. F. p 3118 N95-32663
CARTAGENA, ERIC N. p 3105 N95-34618
CARTER, L. L. p 3178 N95-34484
CARTER, T. p 3201 N95-32379
CARTER, W. p 3152 N95-32686
CASATI, GIULIO p 3209 N95-34423
CASPI, S. p 3214 N95-33504
CASSEL, KEVIN WAYNE p 3109 N95-33310
CAVALLI, R. M. p 3129 N95-33735
CEDERWALL, RICHARD T. p 3156 N95-32697
CENTURIONI, D. X. p 3060 N95-32396
CERCO, CARL F. p 3160 N95-34461
CHA, HYUNG KI p 3066 N95-32566
CHABAL, Y. J. p 3229 N95-33628
CHAKOUMAKOS, B. C. p 3231 N95-34465
CHAKRABARTI, SUPRIYA p 3239 N95-34221
CHAMBERLAIN, P. J. p 3155 N95-34441
CHAMPETIER, C. p 3058 N95-33144
CHAN, A. p 3213 N95-33333
CHAN, PAUL p 3243 N95-34239
CHAN, V. p 3222 N95-32756
CHAN, Y. T. p 3123 N95-32915
CHANDRA, M. p 3096 N95-32750
CHANG, L. p 3071 N95-33280
CHANG, ROBERT P. H. p 3228 N95-32810
CHANG, TYNE-HSIEN p 3113 N95-32425
CHANG, YAU-SHEUN p 3049 N95-33311
CHAO, A. p 3203 N95-32567
CHAO, A. W. p 3211 N95-32606
p 3213 N95-33376
CHAO, YUH-JIN p 3125 N95-32373
CHAPMAN, G. R. p 3156 N95-32603
CHAPMAN, S. P. p 3226 N95-32589
CHAR, K. p 3231 N95-34568
CHARLTON, M. p 3204 N95-32584
CHASON, E. p 3225 N95-32579
CHATTOPADHYAY, ADITI p 3048 N95-32928
CHEMLA, D. S. p 3101 N95-32596
p 3227 N95-32600
p 3230 N95-33880
CHEN, ANTHONY L. p 3230 N95-33865
CHEN, C. Y. p 3208 N95-33372
p 3208 N95-33374
CHEN, CHIH-KENG p 3192 N95-33604
CHEN, CHIN-TU p 3242 N95-34236
CHEN, FA LAI p 3195 N95-33058
CHEN, HELEN p 3184 N95-32558
CHEN, M. H. p 3230 N95-34438
CHEN, PANG C. p 3187 N95-32533
CHEN, SHUCHUN p 3080 N95-33774
CHEN, T. p 3213 N95-33335
p 3213 N95-33385
p 3214 N95-34023
p 3214 N95-34024
CHEN, X. J. p 3204 N95-32623
CHEN, YUAN-LIANG A. p 3056 N95-32426
CHEN, Z. p 3206 N95-32966
p 3209 N95-34355
CHEN, ZAI p 3229 N95-33637
CHEN, ZHAO-JUN p 3080 N95-33699
CHENG, JULIAN p 3186 N95-33838
CHENG, SHANG-GUAN p 3119 N95-34380
CHENGHUI, HUANG p 3117 N95-32472
p 3118 N95-32702
CHERNYAVETS, V. V. p 3094 N95-33141
CHETWYND, JAMES H. p 3128 N95-33732
CHHABILDAS, L. C. p 3125 N95-32381
CHIAVERINI, MARTIN J. p 3061 N95-32932
CHICHINADZE, M. V. p 3092 N95-33129
CHIEN, K. Y. p 3074 N95-33627
CHO, B. K. p 3198 N95-32397
CHO, CHAHEE P. p 3127 N95-34427
CHO, SUL p 3192 N95-33712
CHOI, J. p 3244 N95-34801
CHOUDHURY, DEBABANI p 3100 N95-34460
CHOVIT, CHRIS p 3116 N95-33739
p 3116 N95-33740
CHOW, WINSTON CHIH p 3199 N95-33415
CHRIEN, T. G. p 3117 N95-33769
CHRIEN, THOMAS G. p 3116 N95-33739
p 3116 N95-33740
p 3132 N95-33750
p 3117 N95-33796
CHRISTEN, D. K. p 3230 N95-34213
CHRISTENSEN, PHILIP R. p 3137 N95-33791
p 3137 N95-33793
p 3139 N95-33800
CHRISTIE, B. p 3212 N95-32665
CHRISTON, M. A. p 3179 N95-32390
CHRISTON, MARK A. p 3184 N95-32415
CHU, DAVID p 3080 N95-33626
CHU, FUMING p 3225 N95-32532
CHU, HAIQUN p 3215 N95-32701
CHU, K. C. p 3216 N95-33411
CHU, M. S. p 3222 N95-32756
CHU, T. Y. p 3106 N95-32387
CHUBB, S. R. p 3140 N95-33807
CHUBURKOV, Y. T. p 3164 N95-32666
CHUNFEI, LI p 3104 N95-34379
CHUNG, T. p 3096 N95-32747
CHURCH, HUGH W. p 3152 N95-32556
CLARK, RAYMOND F. p 3043 N95-32490
CLARK, ROGER N. p 3130 N95-33741
p 3130 N95-33742
p 3130 N95-33743
p 3134 N95-33761
p 3136 N95-33772
CLARK, THOMAS L. p 3089 N95-32568
CLEIS, RICHARD A. p 3120 N95-34811
CLEMENT, P. p 3195 N95-32893
CLERE, J. M. p 3168 N95-34054
CLINE, CARL F. p 3126 N95-33068
COAKLEY, P. G. p 3059 N95-32593
COBB, HELEN G. p 3193 N95-34499
COBURN, WILLIAM p 3057 N95-34815
COCKE, C. L. p 3203 N95-32564
p 3206 N95-32763
p 3208 N95-33372
p 3208 N95-33374
COE, H. H. p 3124 N95-33908

COEVERING, L. p 3096 N95-32747
COFFEY, HELEN E. p 3248 N95-32963
p 3248 N95-32964
COHEN, J. S. p 3203 N95-32583
COHEN, MARTIN J. p 3072 N95-33288
COHEN, P. I. p 3232 N95-34795
COHN, MARTIN p 3242 N95-34237
COLE, THOMAS p 3160 N95-34461
COLELLA, N. J. p 3059 N95-32593
COLELLA, NICHOLAS J. p 3079 N95-33063
p 3150 N95-33642
COLLINS, DONALD J. p 3241 N95-34227
p 3243 N95-34242
COLLINS, J. P. p 3074 N95-33627
COMPARIN, JEFFREY H. p 3072 N95-33284
CONEL, JAMES E. p 3132 N95-33753
p 3117 N95-33754
p 3133 N95-33755
CONNERS, TIMOTHY R. p 3052 N95-33018
CONNOLLY, GEORGE C. p 3201 N95-34289
CONVERSE, BLAKE L. p 3116 N95-34496
COOK, B. A. p 3066 N95-32394
p 3060 N95-32396
COOKE, DANIEL E. p 3183 N95-34604
COOPER, FRED p 3234 N95-33388
CORBIN, STEPHEN FRANCIS JOSEPH
p 3078 N95-32935
CORCORAN, T. J. p 3043 N95-32489
CORDA, STEPHEN p 3049 N95-33024
CORNWALL, M. p 3101 N95-34788
COUCH, RICHARD p 3080 N95-33653
COULSON, RICHARD L. p 3166 N95-34609
COWAN, WILLIAM p 3120 N95-34811
COWAN,ELIZABETH p 3050 N95-32931
COWEN, DAVID J. p 3238 N95-33402
CRABTREE, G. W. p 3110 N95-33389
CRAFT, DAVID C. p 3226 N95-32589
CRAIG, D. M. p 3226 N95-32589
CRANDALL, JEFF RICHARD p 3167 N95-33312
CRANE, G. p 3213 N95-33333
CRAWFORD, M. HAGEROTT p 3223 N95-33412
CREIGHTON, J. R. p 3231 N95-34486
CRIVELLI, LUIS A. p 3180 N95-32765
CROSS, JOHN H. p 3069 N95-33265
CROWN, DAVID A. p 3141 N95-33811
CSENCSITS, R. p 3226 N95-32598
p 3229 N95-33636
CUDDY, MATTHEW p 3102 N95-32808
CUMMING, C. A. p 3071 N95-33281
CUMMING, IAN G. p 3140 N95-33809
CUNNINGHAM, THOMAS p 3091 N95-33127
CUQLOCK-KNOPP, V. G. p 3170 N95-34376
CURRAN, FRANCIS M. p 3060 N95-32917
CURRAN, PAUL J. p 3130 N95-33744
CURSOLLE, JEAN-PIERRE p 3045 N95-32503
CUSHMAN, ROBERT M. p 3154 N95-33655
CUSHMAN, WILLIAM B. p 3201 N95-34444

D

DAGOSTINO, P. A. p 3076 N95-34611
DAHL, MATTIAS p 3196 N95-33233
DAHLBERG, MARTIN p 3083 N95-32962
DAI, QING p 3081 N95-34821
DALLY, W. p 3101 N95-34788
p 3244 N95-34816
DAMICO, M. p 3096 N95-32750
DAMOHDARAN-KAMAL, S. K. p 3179 N95-32669
DAMOTTANETO, JOAQUIM D. p 3067 N95-32804
DAMRAU, M. p 3228 N95-33373
DANFORTH, P. M. p 3119 N95-33703
DANIELSSON, B. p 3096 N95-32747
DARBY, SHAUNA M. p 3067 N95-32671
DARLING, DOUGLAS p 3108 N95-32930
p 3050 N95-32931
DASILVA, L. B. p 3164 N95-33654
DAVIDSON, ERIC A. p 3143 N95-33498
DAVIDSON, H. L. p 3079 N95-33063
DAVIES, A. N. p 3070 N95-33274
DAVIES, P. G. p 3096 N95-32747
DAVIN, J. M. p 3216 N95-33651
DAVIS, ANTHONY M. p 3234 N95-34464
DAVIS, DENNIS M. p 3071 N95-33277
p 3072 N95-33286
DAVIS, JANET BETH p 3065 N95-34808
DAVIS, JEFFREY E. p 3085 N95-33409
DAVIS, JON p 3104 N95-33915
DAVIS, R. W. p 3059 N95-32593
DAVYDENKO, V. I. p 3221 N95-32561
DAW, E. p 3246 N95-32597
DAWLEY, J. T. p 3079 N95-33215
DAWSON, L. R. p 3228 N95-33213
DAWSON, TERENCE P. p 3130 N95-33744
DEAN, KENNETH A. p 3228 N95-32810
DEBELER, MURIEL p 3189 N95-33000
DEC, JOHN E. p 3122 N95-32863
DEF.P.W.BARBOSA, LUIS FILIPE p 3224 N95-33873
DEGROH, HENRY C., III p 3089 N95-32718
DEHMELT, HANS p 3104 N95-34451
DEJONG, F. J. p 3123 N95-32915
DEJONG, KENNETH A. p 3182 N95-34456
DEJONGHE, LUTGARD C. p 3151 N95-34481
DEKEYSER, VERONIQUE p 3176 N95-34787
DEKONING, WILLEM p 3192 N95-33399
DELANEY, PATRICK J. p 3194 N95-34742
DELBOSCO, EDSON p 3224 N95-33873
DELEMOS, R. p 3171 N95-34658
DELLORCO, P. C. p 3088 N95-33702
DELUCA, J. A. p 3230 N95-34213
DEMIAN, A. p 3228 N95-33373
DEMIRGIAN, JACK C. p 3067 N95-32671
DENG, D. p 3211 N95-32485
DENG, D. P. p 3212 N95-33067
DENNIS, JOHN E., JR. p 3182 N95-34598
DESOUZA, SELMAR p 3151 N95-34481
DESPAIN, A. p 3101 N95-34788
DESU, S. B. p 3082 N95-32710
DEUTCH, B. I. p 3204 N95-32584
DEVRED, A. p 3103 N95-33404
p 3214 N95-33720
DEVRIES, JORRIT ERNST p 3068 N95-32812
DEWITT, D. p 3230 N95-34438
DHAWAN, ATAM P. p 3188 N95-32767
p 3188 N95-32768
DICARLO, CHERYL D. p 3164 N95-34789
DICUS, D. A. p 3234 N95-33202
DIDYK, A. Y. p 3204 N95-32610
p 3205 N95-32625
p 3078 N95-32626
p 3102 N95-32629
DIECKMAN, STEPHEN L. p 3152 N95-32553
DIEP, J. p 3148 N95-34233
DIGHDE, RAJESH MANOHAR p 3079 N95-32936
DIMOS, D. p 3229 N95-33636
DIMOS, DUANE p 3226 N95-32590
DINTELMANN, F. p 3096 N95-32747
p 3096 N95-32748
DIORIO, MARC p 3141 N95-33813
DITILLO, JOHN p 3067 N95-32671
DITZLER, W. R. p 3043 N95-32489
DJORGOVSKI, GEORGE p 3240 N95-34222
DODDI, S. p 3180 N95-32716
DOERNER, R. p 3208 N95-33374
DOLAN, THOMAS J. p 3221 N95-32588
DOLMAN, W. C. p 3094 N95-33142
DON, W. S. p 3042 N95-34763
DONG, J. Q. p 3223 N95-33391
DONG, WEN-BAO p 3190 N95-33005
DONGARRA, J. J. p 3244 N95-34801
DONNELLY, BRIAN p 3070 N95-33276
DORING, H.-R. p 3070 N95-33272
DOROFEEV, V. A. p 3205 N95-32703
DORRIS, S. E. p 3079 N95-33215
DORSEY, J. A. p 3151 N95-32475
DORTOMB, CLAUDE p 3042 N95-32487
DOVBESHKO, ALEXANDER A. p 3092 N95-33133
DOYLE, RICHARD J. p 3241 N95-34227
DOZIER, JEFF p 3133 N95-33756
p 3135 N95-33764
p 3158 N95-34223
DREUTE, J. p 3161 N95-32720
DROBINA, T. P. p 3164 N95-32666
DRUMMOND, CHARLES J. p 3191 N95-33060
DRUYAN, LEONARD M. p 3154 N95-33413
DU, T. C. p 3118 N95-32663
DUBOIS, PASCALE p 3240 N95-34224
DUBOIS, PASCALE C. p 3139 N95-33803
DUDGEON, DAN E. p 3100 N95-34474
DUDNEY, N. J. p 3103 N95-33697
DUFFEY, T. A. p 3121 N95-32376
p 3126 N95-32670
DUHAMEL, T. p 3058 N95-33144
DUNCAN, A. B. p 3113 N95-32427
DUNNING, F. B. p 3074 N95-33392
DUTTA, B. p 3234 N95-33202
DWARKA, PANKAJ RAI p 3112 N95-34284
DYE, ROBERT C. p 3229 N95-33401
DYER, R. B. p 3088 N95-33702
DYSON, F. p 3101 N95-34788
DZERGACH, A. I. p 3214 N95-34439

E

EASTWOOD, M. L. p 3117 N95-33769
EASTWOOD, MIKE p 3116 N95-33739
p 3116 N95-33740
EATON, G. H. p 3209 N95-34657
EDESKUTY, F. J. p 3102 N95-32714
EDGETT, KENNETH S. p 3137 N95-33792
p 3137 N95-33793
EDSON, ROBERT p 3159 N95-34341
EDWARDS, JOHN M. p 3177 N95-32955
EFREMOV, A. V. p 3094 N95-33139
EIBERT, M. p 3045 N95-32499
EIMERL, D. p 3119 N95-33703
EINFELD, WAYNE p 3152 N95-32556
EISENMANN, ERHARD T. p 3103 N95-33640
EJIRI, A. p 3225 N95-34624
EL-SADEK, A. p 3228 N95-33373
ELKS, CARL p 3044 N95-32497
ELLSWORTH, R. W. p 3248 N95-33916
ELNOZAHY, E. N. p 3187 N95-34587
ELORANTA, EDWIN W. p 3099 N95-33839
ELSON, LEE p 3241 N95-34230
ELWELL, JOHN M., JR. p 3092 N95-33132
EME, W. G. p 3183 N95-34813
EMERY, WILLIAM p 3158 N95-34223
ENGEL, BRAD N. p 3083 N95-32819
p 3229 N95-33641
ENGMAN, E. T. p 3142 N95-33816
ENGMAN, TED p 3139 N95-33803
ENOCHS, EDGAR R. p 3042 N95-34750
ENOEDA, MIKIO p 3220 N95-32409
EPPERSON, SEAN T. p 3170 N95-34475
EREKSON, E. J. p 3087 N95-32563
ERICKSON, G. L. p 3050 N95-32636
ERIDON, J. M. p 3050 N95-32636
ERIKSON, J. p 3078 N95-32614
ERTEZA, IREENA A. p 3226 N95-32589
ESAIAS, WAYNE E. p 3159 N95-32672
p 3159 N95-32833
ESCOURROU, P. p 3164 N95-32611
ESER, DURSUN p 3122 N95-32752
ESPEY, CHRISTOPH p 3122 N95-32863
ESPINOZA, BRENT F. p 3229 N95-33401
ESRY, B. D. p 3206 N95-32966
p 3207 N95-33370
EVANS, ALYSON E. p 3048 N95-34770
EVANS, JOSEPH T., JR. p 3226 N95-32590
EVANS, N. D. p 3074 N95-33629
EXARHOS, GREGORY J. p 3084 N95-33405

F

FACIUS, R. p 3163 N95-32730
FADALE, TUSHAR DASHARATH p 3196 N95-34803
FALCO, CHARLES M. p 3083 N95-32819
p 3229 N95-33641
p 3219 N95-34791
p 3232 N95-34792
FALCONER, JOHN p 3068 N95-33224
FAN, ZHENGXIU p 3217 N95-34298
FANG, CHIEN p 3184 N95-32558
FANG, H. E. p 3184 N95-32383
FANG, X. D. p 3189 N95-32998
p 3190 N95-33004
FARMER, JOSEPH C. p 3081 N95-34482
FARR, TOM G. p 3139 N95-33804
FARRAND, W. H. p 3131 N95-33745
FARRAR, C. R. p 3126 N95-32670
FAUST, JESSICA p 3116 N95-33740
FEDOR, CHESTER p 3104 N95-34425
FEDOSEJEVS, G. p 3136 N95-33771
FEIT, M. D. p 3164 N95-33654
FELIPPA, CARLOS A. p 3180 N95-32765
p 3180 N95-32766
FELSTEIN, STEVEN R. p 3087 N95-34614
FELTOVICH, PAUL J. p 3166 N95-34609
FENDRICH, J. p 3110 N95-33389
FENG, X. p 3204 N95-32584
FENG, YU YU p 3195 N95-33058
FENGFEI, BI p 3219 N95-34756
FENNER, DAVID B. p 3199 N95-34477
FEO, JOHN T. p 3186 N95-33643
FERGUSON, JAMES S. p 3117 N95-33746
FERGUSON, JOANNE E. p 3117 N95-33746
FERGUSON, R. E. p 3074 N95-33627
FERNANDEZ-PELLO, CARLOS p 3089 N95-32929
FERNOW, R. C. p 3203 N95-32542
p 3205 N95-32652
p 3205 N95-32654
FERRON, J. R. p 3222 N95-32756
FETTER, L. A. p 3084 N95-33247
FETTEROLF, DEAN D. p 3070 N95-33276
FIELD, RICHARD p 3088 N95-33254
FIELDS, R. p 3171 N95-34658
FIFER, R. A. p 3076 N95-34599
FIGUEROA, FERNANDO p 3176 N95-32428
FILATOV, YU. V. p 3092 N95-33130
FILTER, W. F. p 3102 N95-32708
FIORI, L. p 3043 N95-32488
FIORI, LORENZO p 3045 N95-32504
FIRESTONE, ELAINE R. p 3158 N95-32545
p 3159 N95-32833
FIRESTONE, ELAINE, R. p 3159 N95-32672

FISCHER, JOHN ..... p 3105 N95-34796
FISCHER, P. ..... p 3042 N95-34763
FISHER, A. ..... p 3120 N95-34761
FITZPATRICK, KEVIN C. ..... p 3104 N95-34425
FIUMI, L. ..... p 3129 N95-33735
FIX, BRADLEY L. ..... p 3084 N95-33406
FLAMM, JEFFREY D. ..... p 3034 N95-32621
FLEDDERMANN, CHARLES ..... p 3105 N95-34581
FLEMING, C. ..... p 3163 N95-32731
FLOETTMANN, K. ..... p 3212 N95-32657
FLORO, J. A. ..... p 3225 N95-32579
FLOWERS, GEORGE T. ..... p 3121 N95-32689
p 3121 N95-32690
p 3122 N95-32691
p 3122 N95-32692
p 3122 N95-32693
FLYNN, J. ..... p 3235 N95-34652
FOLLSTAEDT, D. M. ..... p 3228 N95-33213
FORD, R. A. ..... p 3096 N95-32773
FOREMAN, RONALD J. ..... p 3081 N95-34482
FORSEN, K. ..... p 3068 N95-33229
FORSHAW, J. R. ..... p 3214 N95-34653
FORSMAN, KIMMO ..... p 3099 N95-33379
FORSYTH, GRAHAM F. ..... p 3188 N95-32995
FOSTER, C. M. ..... p 3226 N95-32598
p 3229 N95-33636
FOWLER, LAURA D. ..... p 3153 N95-33205
FOX, WARREN L. ..... p 3201 N95-34595
FRAME, EDWIN A. ..... p 3086 N95-34494
FRANCES, D. ..... p 3190 N95-33004
FRANCIONI, J. M. ..... p 3179 N95-32669
FRANK, M. ..... p 3230 N95-33650
FRANKEL, N. E. ..... p 3205 N95-32632
FRANKLIN, JANET ..... p 3142 N95-32676
FRANKLIN, M. S. ..... p 3043 N95-32489
FRASIER, D. J. ..... p 3050 N95-32636
FREE, APRIL M. ..... p 3122 N95-32692
FREEMAN, A. J. ..... p 3075 N95-34483
FREEMAN, ANDREW ..... p 3081 N95-34821
FREEMAN, ANTHONY ..... p 3240 N95-34224
FREIJ, L. ..... p 3084 N95-33329
FREIJ, LARS ..... p 3073 N95-33328
p 3073 N95-33330
p 3074 N95-33634
FREITAG, K. ..... p 3228 N95-33373
FREZET, M. ..... p 3058 N95-33144
FRIEDLAND, PETER ..... p 3184 N95-34225
FRIEDMAN, S. L. ..... p 3229 N95-33628
FROHNE, V. ..... p 3208 N95-33374
FROLKING, STEPHEN EDWARD ..... p 3153 N95-33337
FU, GU PEI ..... p 3086 N95-34563
FU, LEI ..... p 3064 N95-33326
FUCHS, W. KENT ..... p 3178 N95-34453
FUERSCHBACH, P. W. ..... p 3118 N95-32683
FUGATE, ROBERT Q. ..... p 3120 N95-34811
FUJII, KIMIO ..... p 3063 N95-32711
FUJII, KOZO ..... p 3037 N95-34525
FUKUDA, MASAHIRO ..... p 3035 N95-34512
FUNG, KO ..... p 3240 N95-34226
FUNKHOUSER, JEFFREY W. ..... p 3228 N95-32810
FURUKAWA, MASAHIRO ..... p 3091 N95-32991
FURUYA, KAZUYUKI ..... p 3221 N95-32565
FUSSEL, K. ..... p 3162 N95-32726

G

GAHL, JOHN ..... p 3105 N95-34581
GAILLARD, IRENE ..... p 3176 N95-34783
GALLAGHER, THOMAS F. ..... p 3209 N95-34819
GALLARDO, J. C. ..... p 3205 N95-32652
p 3205 N95-32654
GALOTTI, VINCENT ..... p 3175 N95-34782
GAMON, JOHN A. ..... p 3131 N95-33747
GAMWELL, W. R. ..... p 3123 N95-33199
GANCHEV, S. ..... p 3125 N95-34346
GANSHENG, LI ..... p 3118 N95-32702
GANTENBEIN, REX E. ..... p 3183 N95-32429
GAO, BO-CAI ..... p 3131 N95-33748
p 3132 N95-33749
GAO, SHIXIANG ..... p 3107 N95-32907
GAO, WEIGANG ..... p 3156 N95-33847
GAO, XIAOPING ..... p 3075 N95-34357
GARDINER, T. ..... p 3110 N95-33389
GARLAND, DANIEL J. ..... p 3171 N95-34764
GARRETT, PAULA ..... p 3186 N95-33639
GASIEWSKI, A. J. ..... p 3143 N95-32823
GASTIL, MARY ..... p 3134 N95-33763
GATLIN, DONALD H. ..... p 3051 N95-33010
GEBALLE, T. H. ..... p 3231 N95-34568
GELBWACHS, JERRY A. ..... p 3157 N95-34613
GELLER, CLINT B. ..... p 3149 N95-32645
GENESELLI, FRANCESCO ..... p 3137 N95-33790
GEOHEGAN, D. B. ..... p 3232 N95-34799
GEOHEGAN, DAVID B. ..... p 3118 N95-33246
GEORGE, E. P. ..... p 3077 N95-32400
p 3079 N95-33217
GERBER, SCOTT S. ..... p 3103 N95-33874
GERSHENSON, MEIR ..... p 3104 N95-34446
GERTNER, I. ..... p 3206 N95-32966
p 3209 N95-34355
GHANAYEM, OMAR ..... p 3189 N95-33001
GIAM, C. S. ..... p 3071 N95-33280
GIANOULAKIS, S. E. ..... p 3118 N95-32683
GIBELING, H. J. ..... p 3123 N95-32915
GIBERT, JACEK ..... p 3190 N95-33008
GIBSON, RICHARD S. ..... p 3166 N95-34774
GIESE, J. P. ..... p 3203 N95-32564
p 3206 N95-32763
p 3208 N95-33372
p 3208 N95-33374
GILDENBLAT, GENNADY ..... p 3231 N95-34478
GILES, K. ..... p 3069 N95-33268
GILL, PATRICIA A. ..... p 3160 N95-34372
GILLESPIE, ALAN R. ..... p 3135 N95-33766
GILLIS, J. R. ..... p 3059 N95-33264
p 3059 N95-33890
GILPATRICK, J. D. ..... p 3211 N95-32416
GILSON, RICHARD D. ..... p 3055 N95-34772
GLASS, S. J. ..... p 3085 N95-34022
GLAZOV, A. ..... p 3188 N95-32627
GLINSKY, M. E. ..... p 3164 N95-33654
GLOAGUEN, C. ..... p 3096 N95-32750
GLUTSCH, S. ..... p 3101 N95-32596
p 3227 N95-32600
GODDARD, J. W. F. ..... p 3096 N95-32750
GOETZ, ALEXANDER F. H. ..... p 3132 N95-33750
GOETZ, F. H. ..... p 3130 N95-33743
GOGINENI, S. P. ..... p 3099 N95-33497
p 3099 N95-33726
GOLDAMMER, STEVE ..... p 3103 N95-33864
GOLDSTEIN, B. L. ..... p 3095 N95-32674
GOLE, P. ..... p 3096 N95-32751
GOLOSKOKOV, S. V. ..... p 3234 N95-32961
GOLOVKIN, S. V. ..... p 3207 N95-33171
GONG, J. ..... p 3097 N95-32822
GONZALEZ, RICHARD R. ..... p 3171 N95-34577
GOODALL, P. S. ..... p 3075 N95-34440
GOODENOUGH, DAVID G. ..... p 3240 N95-34226
GOODRICH, CHARLES C. ..... p 3242 N95-34238
GOOSMAN, D. R. ..... p 3115 N95-32900
GORDON, DIANA F. ..... p 3193 N95-34473
p 3193 N95-34495
GORDON, HOWARD R. ..... p 3193 N95-34501
GORSKI, JOSEPH JOHN ..... p 3143 N95-32914
GOTTLIEB, DAVID ..... p 3107 N95-32905
GOYAL, A. ..... p 3042 N95-34763
GRABBE, S. R. ..... p 3230 N95-34213
GRADY, CAROL ..... p 3207 N95-33371
GRADY, D. E. ..... p 3245 N95-32835
GRAEFENHAIN, U. ..... p 3082 N95-32380
GRANATA, RICHARD D. ..... p 3072 N95-33287
GRANT, R. ..... p 3087 N95-34614
GRASTATARO, C. I. ..... p 3078 N95-32591
GRATSON, D. ..... p 3058 N95-32713
GRAY, L. J. ..... p 3152 N95-32688
p 3194 N95-32388
GREELEY, RONALD ..... p 3126 N95-33222
p 3136 N95-33773
GREEN, H. JAMES ..... p 3139 N95-33802
GREEN, R. O. ..... p 3148 N95-32551
GREEN, ROBERT O. ..... p 3117 N95-33769
p 3128 N95-33730
p 3129 N95-33737
p 3116 N95-33739
p 3116 N95-33740
p 3130 N95-33743
p 3131 N95-33747
p 3117 N95-33751
p 3117 N95-33752
p 3132 N95-33753
p 3117 N95-33754
p 3133 N95-33755
p 3133 N95-33756
p 3133 N95-33757
p 3117 N95-33759
p 3135 N95-33764
GREENLY, JOHN B. ..... p 3101 N95-32578
GREFENSTETTE, JOHN J. ..... p 3193 N95-34497
p 3193 N95-34501
GREGG, WATSON W. ..... p 3158 N95-32545
GREITZER, F. L. ..... p 3151 N95-32475
GRIFFIN, MAURICE ..... p 3097 N95-32925
GRIMSRUD, E. P. ..... p 3069 N95-33268
GROEGER, H. ..... p 3163 N95-32731
GROMME, T. ..... p 3211 N95-32608
GROPP, WILLIAM ..... p 3099 N95-33379
GROSS, M. E. ..... p 3150 N95-33400
GROSSBERG, P. ..... p 3211 N95-32608
GROSSMAN, T. ..... p 3187 N95-32375
GROVER, KEVIN ..... p 3179 N95-32470
GRUEN, D. M. ..... p 3230 N95-34215
GRUENBAUM, P. E. ..... p 3059 N95-33264
p 3059 N95-33890
GRYK, THOMAS J. ..... p 3216 N95-34288
GUIFANG, YU ..... p 3117 N95-32472
p 3118 N95-32702
GUNTER, D. ..... p 3110 N95-33389
GUOZHEN, ZHAO ..... p 3217 N95-34309
GUPTA, D. ..... p 3125 N95-32392
GURNEY, JOHN O., JR. ..... p 3236 N95-34487
GUSACK, JAMES A. ..... p 3065 N95-34448
GUSTAFSON, JOHN L. ..... p 3177 N95-32398
GUYENNE, DUC ..... p 3252 N95-32538
GUYENNE, T. D. ..... p 3252 N95-32805
GUZMAN, FRANCISCO ..... p 3152 N95-32573
GYLLENHAAL, JOHN C. ..... p 3182 N95-34455

H

HAAB, GRANT E. ..... p 3182 N95-34455
HAAS, FRANZ ..... p 3178 N95-34503
HADLEY, DEAN R. ..... p 3089 N95-32568
HAERING, EDWARD A., JR. ..... p 3181 N95-33193
HAGIGAT, MICHAEL KENT ..... p 3122 N95-32906
HAGLUND, B. O. ..... p 3068 N95-33229
HAGLUND, RUNE ..... p 3167 N95-34775
HAGMANN, C. ..... p 3246 N95-32597
HAGN, GEORGE H. ..... p 3043 N95-32492
HAHN, E. ..... p 3082 N95-32541
HAJEK, PAVEL ..... p 3116 N95-33739
p 3116 N95-33740
p 3117 N95-33754
p 3117 N95-33796
HALBLEIB, J. A. ..... p 3085 N95-34022
HALEY, JOSEPH L., JR. ..... p 3170 N95-34378
p 3170 N95-34489
p 3171 N95-34574
HALL, ERIC B. ..... p 3244 N95-32430
HALLIDAY, I. G. ..... p 3235 N95-34652
HALLIDAY, J. ..... p 3151 N95-34656
HALLING, M. ..... p 3215 N95-32658
HALLY, W. ..... p 3196 N95-34377
HAMADA, T. ..... p 3177 N95-32757
HAMILTON, VICTORIA E. ..... p 3137 N95-33791
p 3139 N95-33800
HAMMEL, CAROL ..... p 3102 N95-32956
HAMMOUD, AHMAD N. ..... p 3060 N95-32673
HAMZA, ALEX V. ..... p 3085 N95-33409
HAN, MING ..... p 3227 N95-32698
HANCOCK, J. R. ..... p 3076 N95-34611
HANDLEY, THOMAS H., JR. ..... p 3241 N95-34227
p 3243 N95-34241
HANDSCHUH, ROBERT F. ..... p 3123 N95-33179
HANGST, J. S. ..... p 3204 N95-32584
HANISCH, ROBERT J. ..... p 3242 N95-34234
HANSEN, CHARLES D. ..... p 3186 N95-33403
HANSEN, D. F. ..... p 3158 N95-34575
HANSEN, ELAINE R. ..... p 3184 N95-34228
HANSMAN, R. J., JR. ..... p 3047 N95-34562
HAPANYENGWI, GILFORD TAERA
p 3238 N95-33722
HARDEN, C. S. ..... p 3069 N95-33266
HARDEN, CHARLES S. ..... p 3071 N95-33277
p 3072 N95-33286
HARDIE, R. WAYNE ..... p 3152 N95-32573
HARDING, DAVID J. ..... p 3141 N95-33814
HARDY, D. A. ..... p 3057 N95-32772
HARLOFF, G. J. ..... p 3054 N95-33208
HARMAN, WILLIAM H., III ..... p 3047 N95-33480
HARMSEN, FRANK ..... p 3237 N95-33238
HARP, JASON ..... p 3227 N95-32640
HARPER, RICHARD E. ..... p 3044 N95-32497
HARRINGA, J. L. ..... p 3066 N95-32394
p 3060 N95-32396
HARRINGTON, PETER DEB. ..... p 3073 N95-33290
HARRIS, K. ..... p 3050 N95-32636
HARRIS, T. D. ..... p 3229 N95-33628
HARRISON, K. ..... p 3045 N95-32501
HARRISON, PETER NEWTON ..... p 3064 N95-33327
HARSANYI, JOSEPH C. ..... p 3131 N95-33745
HART, Q. J. ..... p 3135 N95-33765
HARTING, GEORGE C. ..... p 3061 N95-32932
HARTMAN, S. ..... p 3215 N95-32658
HARTNEY, C. ..... p 3167 N95-32535
HARWOOD, KELLY ..... p 3175 N95-34781
HASHIMOTO, TAKESHI ..... p 3037 N95-34527
HASHIMOTO, TOSHIYUKI ..... p 3219 N95-32408
HASSANEIN, A. ..... p 3219 N95-32401
HATAYAMA, SHIGEKI ..... p 3038 N95-34532
HATTORI, K. ..... p 3223 N95-33221
HAVERLAND, M. ..... p 3049 N95-33145
HAXO, R. S. ..... p 3135 N95-33768
HAYASE, K. ..... p 3223 N95-33221
HAYNES, W. M. ..... p 3233 N95-32661
HAYOT, F. ..... p 3068 N95-33223
HE, JUN ..... p 3107 N95-32898
HE, XIAOCHUN ..... p 3206 N95-32965
HEBER, O. ..... p 3206 N95-32966
p 3209 N95-34355

HECHT, LAURA F. p 3237 N95-32883
HEDBERG, CARL p 3215 N95-33239
HEIDEBRECHT, KATHLEEN B. p 3132 N95-33750
HEIDEBRECHT, KATHY p 3130 N95-33743
HEIFETS, S. p 3203 N95-32544
p 3203 N95-32567
HEIJENK, GEERT p 3097 N95-32892
HEILMANN, J. p 3162 N95-32725
HEIN, C. A. p 3144 N95-34454
HEINEMANN, H. p 3075 N95-34268
HEINRICH, WOLFGANG p 3161 N95-32720
HEISEY, CHERYL LAVONNE p 3085 N95-34282
HEISTER, STEPHEN D. p 3112 N95-34572
HELM, R. p 3212 N95-32657
p 3215 N95-32658
HELMICH, D. R. p 3085 N95-34022
HELMLINGER, MARK p 3117 N95-33754
HELMS, K. L. E. p 3077 N95-32382
HEMBREE, PATRICIA B. p 3081 N95-34348
HENCKEN, K. R. p 3124 N95-33701
HENDERSON, J. A. p 3106 N95-32387
HENDERSON, R. C. W. p 3214 N95-34651
HENDRICKSON, L. p 3211 N95-32608
HENESIAN, M. A. p 3119 N95-33703
HENNESSY, L. W. p 3171 N95-34764
HENRIKSEN, GARY p 3102 N95-32956
HERITAGE, J. P. p 3216 N95-33411
HERMAN, RICHARD G. p 3075 N95-34021
HERNANDEZ, M. A. p 3117 N95-33769
HERRERA-FIERRO, PILAR p 3083 N95-32919
HERRING, J. STEPHEN p 3221 N95-32588
HEWETT, J. L. p 3207 N95-33201
p 3207 N95-33245
p 3208 N95-33375
HEWITT, C. p 3044 N95-32494
HIBBEN, STUART G. p 3243 N95-34420
p 3243 N95-34421
HIERS, ROBERT S., JR. p 3113 N95-34818
HIGASHINO, FUMIO p 3038 N95-34531
HIGHLEY, D. E. p 3155 N95-32599
HILJANEN, M. p 3084 N95-33227
HILL, JOHN p 3243 N95-34239
HILL, NORMAN F. p 3082 N95-32664
HILLER, L. H. p 3230 N95-33650
HILLIER, J. A. p 3155 N95-32599
p 3155 N95-32601
p 3156 N95-32603
HIMEL, T. p 3211 N95-32608
HINO, TAKANORI p 3036 N95-34517
HINTON, M. p 3073 N95-33289
HIRANO, Y. p 3223 N95-33221
HIRATA, NOBUYUKI p 3040 N95-34548
HIRZEBRUCH, S. E. p 3161 N95-32720
HISCOCK, EBEN p 3058 N95-34744
HISKES, R. p 3226 N95-32598
p 3229 N95-33636
HOANG, V. p 3167 N95-32535
HOBAN, FRANCIS T. p 3236 N95-34354
HOCHBERG, JUDITH p 3181 N95-33154
HODGES, R. S. p 3076 N95-34611
HOEHN, ALEXANDER p 3163 N95-32901
HOFFMAN, ALAN L. p 3223 N95-33216
HOFFMAN, EDWARD J. p 3236 N95-34354
HOGG, G. M. p 3045 N95-32501
HOH, ROGER H. p 3055 N95-34306
HOLDER, SANDRA L. p 3045 N95-32500
HOLECZ, FRANCESCO p 3139 N95-33805
HOLLENBERG, LLOYD C. L. p 3204 N95-32622
HOLLEY, W. p 3149 N95-33153
HOLLIDAY, T. L. p 3071 N95-33280
HOLLIDAY, WILLIAM N. p 3238 N95-33402
HOLM, P. p 3098 N95-33231
HOLMAN, ROBERT W. p 3086 N95-34502
HOLMES, ALAN W. p 3159 N95-32833
HOLT, A. R. p 3096 N95-32750
HOLZSCHEITER, M. H. p 3204 N95-32584
HOMER, L. D. p 3076 N95-34814
HONEY, DAVID A. p 3178 N95-34503
HONG, BONG GUEN p 3223 N95-33619
HONJO, MASATSUGU p 3090 N95-32986
HOOK, SIMON p 3139 N95-33799
HOOK, SIMON J. p 3117 N95-33794
p 3117 N95-33797
HOOKER, STANFORD B. p 3158 N95-32545
p 3159 N95-32672
p 3159 N95-32833
HOPKIN, V. DAVID p 3171 N95-34764
HOPKINS, DALE A. p 3063 N95-33210
HOPPE, MARTIN p 3224 N95-34436
HORAK, K. p 3094 N95-33143
HORN, BERTHOLD P. p 3241 N95-34229
HORN, K. M. p 3102 N95-32708
HORNBOSTEL, A. p 3096 N95-32749
p 3096 N95-32750
p 3096 N95-32751
HORNECK, G. p 3162 N95-32727
HORNER, M. HARLAN p 3149 N95-32645
p 3211 N95-32647
HORTON, J. A. p 3077 N95-32400
p 3079 N95-33217
HORTON, W. p 3223 N95-33391
HOSGOOD, B. p 3133 N95-33758
HOSOKAWA, IWAO p 3038 N95-34530
HOUSHMAND, B. p 3140 N95-33808
HOWARD, A. J. p 3228 N95-33213
p 3223 N95-33412
HOWARD, C. D. p 3124 N95-34449
HOWARD, DOUGLAS p 3137 N95-33791
HOWARD, RALPH p 3196 N95-33233
HOWELL, E. H. p 3206 N95-32965
HSIA, RONG PING p 3108 N95-33255
HSIANG, LIEN-PENG p 3107 N95-32902
HSU, A. Y. p 3142 N95-33816
HSUEH, CHUN-HWAY p 3087 N95-34798
HU, CHI-YU p 3203 N95-32583
HU, YAN-RU p 3191 N95-33307
HUANG, JIN p 3118 N95-33464
HUANG, K. S. p 3148 N95-34233
HUBBARD, DAVID C. p 3056 N95-34362
HUBBE, J. M. p 3158 N95-33505
HUBER, A. p 3057 N95-32772
HUENTRUP, G. p 3161 N95-32720
HUGHES, M. H. p 3225 N95-34812
HUGHES, ROBERT S., JR. p 3085 N95-33409
HUMPHRY, DONALD E. p 3069 N95-33270
HUNDLEY, M. F. p 3198 N95-32397
p 3229 N95-33386
HUNG, JOHN Y. p 3127 N95-34427
HUNSUCKER, JOHN L. p 3236 N95-32431
HUNT, H. B., III p 3099 N95-33387
HUNT, J. J. p 3252 N95-32805
HUNTER, J. p 3219 N95-32401
HURTADO, L. D. p 3077 N95-32382
HUTCHINS, JAMES p 3184 N95-32558
HUTCHINSON, N. E. p 3155 N95-32601
HUYSMANS, G. T. A. p 3224 N95-33696
HVELPLUND, P. p 3204 N95-32584
HWANG, CHUL KEW p 3223 N95-33619
HWANG, S. p 3066 N95-32540
HWANG, S. L. p 3085 N95-33635
HWU, WEN-MEI W. p 3182 N95-34455
HYLTON, JAMES O. p 3116 N95-33206

I

IBRAHIM, MOUNIR p 3034 N95-32769
ICE, G. p 3233 N95-34802
IDE, JAMES R. p 3060 N95-32673
IGLESIA, E. p 3075 N95-34268
IIDA, MASANOBU p 3041 N95-34554
IIHARA, SIGEYASU p 3060 N95-32755
IISAKA, JOJI p 3240 N95-34226
IKPEME, S. p 3161 N95-32723
ILA, D. p 3218 N95-34480
IMAMURA, JAMES N. p 3247 N95-34561
IMHOFF, MARC p 3140 N95-33806
IMLAY, S. T. p 3106 N95-32818
IN, SANG RYUL p 3223 N95-33619
INGALLS, STEPHEN A. p 3059 N95-32432
INGWERSEN, PETE p 3101 N95-32578
INOUE, YUTAKA p 3091 N95-32992
p 3091 N95-32993
IONESCU, VLAD p 3192 N95-33399
IROKAWA, YOSHIHIRO p 3090 N95-32986
IRWIN, J. p 3212 N95-32657
p 3215 N95-32658
p 3213 N95-33335
p 3213 N95-33385
p 3214 N95-34023
p 3214 N95-34024
ISAYAMA, A. p 3225 N95-34624
ISHIGAKI, HIROSHI p 3037 N95-34528
p 3040 N95-34545
ISHIGURO, MITSUO p 3039 N95-34542
ISHII, RYUJI p 3037 N95-34527
ISOGAI, KOJI p 3040 N95-34547
ITO, A. p 3225 N95-32377
ITO, RYOZO p 3039 N95-34537
ITOH, KATSUHIRO p 3035 N95-34514
ITON, LENNOX E. p 3152 N95-32553
ITTEN, K. I. p 3136 N95-33770
IVANOV, A. A. p 3221 N95-32536
p 3221 N95-32561
IVANOV, D. YU. p 3202 N95-32481
IVANOV, M. A. p 3202 N95-32407
IVANOV, V. V. p 3187 N95-32476
IVERSON, R. p 3215 N95-32658
IVEY, REBECCA H. p 3049 N95-34793
IWAMIYA, TOSHIYUKI p 3036 N95-34519
IWASA, MASAMICHI p 3041 N95-34552
IZDEBSKI, STANLEY J. p 3065 N95-34620

J

JACHMICH, STEFAN p 3224 N95-33853
JACKSON, ALISTAIR p 3173 N95-34769
JACOBSON, ALLAN S. p 3241 N95-34227
p 3241 N95-34230
JACQUEMOUD, S. p 3133 N95-33758
p 3135 N95-33765
JADAMEC, J. RICHARD p 3071 N95-33282
p 3072 N95-33283
JAEGER, M. p 3228 N95-33373
JAFFRIN, M. p 3164 N95-32611
JAGERSAND, MARTIN p 3171 N95-34616
JAKOBY, R. p 3096 N95-32748
JAMESON, ANTONY p 3034 N95-34506
JANHAELL, S. p 3067 N95-32615
JANSEN, R. W. p 3140 N95-33807
JANSSENS, BOB p 3178 N95-34453
JASKE, ROBERT p 3243 N95-34239
JAVAUX, DENIS p 3176 N95-34787
JAYAPRAKASH, C. p 3068 N95-33223
JEFFERS, LARRY A. p 3074 N95-33705
JELLINEK, J. p 3228 N95-33382
JENKINS, JON M. p 3247 N95-32700
JENSEN, JOHN R. p 3238 N95-33402
JENSEN, MARK p 3078 N95-32638
JEONG, SEUNG HO p 3223 N95-33619
JERNIGAN, J. GARRETT p 3239 N95-34221
JI, H. p 3223 N95-33221
JI, SULING p 3215 N95-32957
JIANG, X. p 3233 N95-34802
JIANGUO, HE p 3100 N95-34762
JIANYING, ZHOU p 3120 N95-34469
JIE, WU p 3104 N95-34379
JIN, JIANHUI p 3215 N95-32701
JINFA, TANG p 3218 N95-34471
p 3086 N95-34563
JITSUNO, TAKAHISA p 3090 N95-32988
p 3090 N95-32989
JIURONG, GUO p 3059 N95-34493
JIWAN, XU p 3059 N95-34500
JOHANSSON, ERIK M. p 3095 N95-32569
JOHANSSON, G. p 3086 N95-34361
JOHANSSON, LOVISA p 3088 N95-33332
JOHNSEN, BJORN A. p 3068 N95-33243
JOHNSON, DAVID K. p 3061 N95-32932
JOHNSON, GORDON G. p 3194 N95-32433
JOHNSON, HOWELL p 3116 N95-33739
p 3116 N95-33740
JOHNSON, HOWELL K. p 3117 N95-33759
JOHNSON, JOSEPH C. p 3157 N95-34751
JOHNSON, K. F. p 3211 N95-32416
JOHNSON, S. G. p 3075 N95-34440
JOHNSON, TERESA L. p 3182 N95-34455
JOHNSTON, D. C. p 3198 N95-32397
JOHNSTON, MARK D. p 3242 N95-34234
JONES, R. H. p 3077 N95-32555
p 3127 N95-33833
JONES, SONJA B. p 3154 N95-33655
JONES, WILLIAM R., JR. p 3083 N95-32918
p 3083 N95-32919
JOUNOUCHI, TADAMASA p 3039 N95-34540
JOURDAN, THOMAS p 3070 N95-33276
JUNKINS, JOHN L. p 3191 N95-33214
JURNS, J. M. p 3115 N95-32687

K

KABANOV, V. S. p 3214 N95-34439
KAHANA, D. E. p 3205 N95-32651
KAHANA, S. H. p 3205 N95-32651
KAHLE, ANNE p 3139 N95-33799
KAHLE, ANNE B. p 3117 N95-33794
KAJI, MASUO p 3091 N95-32991
KAJI, SHOJIRO p 3034 N95-34508
p 3042 N95-34560
KAKUDATE, SATOSHI p 3221 N95-32565
KALAM, A. p 3188 N95-32997
KALINOWSKI, JOSEPH E. p 3149 N95-32645
KAMINSKI, DAVID A. p 3078 N95-32648
KAMP, M VD. p 3096 N95-32748
KANABE, TADASHI p 3090 N95-32990
KANAI, JUNICHI p 3179 N95-32470
p 3236 N95-32471
KANDLER, T. p 3228 N95-33373
KANNAPAREDDY, MOHAN RAJ p 3110 N95-33398
KAPLAN, D. B. p 3209 N95-33855
KARASHIMA, KEIICHI p 3037 N95-34525
KARES, ROBERT J. p 3203 N95-32574
KARJALAINEN, T. p 3084 N95-33227
KARMASIN, V. P. p 3057 N95-33128
KARPAS, Z. p 3069 N95-33266
KARPUSHOV, A. N. p 3221 N95-32561
KARRASK, V. K. p 3057 N95-33128

KARTZ, MICHAEL W. p 3118 N95-33378
KATAEV, A. L. p 3202 N95-32406
KATAYAMA, MASAYUKI p 3037 N95-34526
KAUFMAN, YORMAN J. p 3131 N95-33748
p 3132 N95-33749
KAVARNOS, GEORGE J. p 3086 N95-34502
KAWAMATA, YOSHIHIRO p 3035 N95-34513
KAWAMOTO, MAKOTO p 3037 N95-34529
KAWANO, H. p 3225 N95-32377
KAWECKI, A. p 3096 N95-32750
KAYAR, S. R. p 3076 N95-34814
KAYSER, DETLEF p 3048 N95-33134
KAZANSKY, P. G. p 3217 N95-34374
KEAS, PAUL p 3033 N95-32764
KEENAN, JAMES ANTHONY p 3059 N95-32903
KEENE, MICHAEL L. p 3237 N95-32883
KEENEY, J. A. p 3126 N95-32684
KEHR, E. p 3162 N95-32726
KEKELIDZE, G. D. p 3102 N95-32628
KELLER, J. p 3136 N95-33770
KELLER, RICHARD M. p 3184 N95-34225
KELLER, THOMAS p 3072 N95-33285
KELLERMAN, B. K. p 3225 N95-32579
KELLEY, M. A. p 3226 N95-32589
KELLEY, MICHAEL p 3180 N95-32834
KELLEY, N. D. p 3150 N95-33706
KELLY, PATRICK p 3181 N95-33154
KEMENY, SABRINA p 3188 N95-32659
KENIK, E. A. p 3074 N95-33629
KENNEDY, JOHN M. p 3237 N95-32883
p 3239 N95-34217
KERGUELEN, M. p 3168 N95-34054
KERNS, JOHN A. p 3079 N95-33063
KERNS, LILA p 3181 N95-33154
KETTUNEN, LAURI p 3099 N95-33379
KEY, JAMES F. p 3081 N95-34348
KHARITONOV, Y. P. p 3164 N95-32666
KHEIRANDISH, HAMID REZA p 3036 N95-34521
KHOMENKO, M. N. p 3166 N95-34053
p 3165 N95-34056
KHUDAVERDYAN, O. M. p 3195 N95-32609
KHVEDELIDZE, A. p 3234 N95-32667
KICHER, THOMAS P. p 3123 N95-33179
KIEFER, J. p 3161 N95-32722
p 3161 N95-32723
p 3162 N95-32728
p 3162 N95-32729
p 3163 N95-32731
KIEREIN-YOUNG, KATHRYN S. p 3134 N95-33760
KIKUCHI, AKIHIRO p 3037 N95-34524
KIKUCHI, K. p 3034 N95-34507
KIKUCHI, KATSUHIRO p 3037 N95-34524
KIKUCHI, KAZUO p 3035 N95-34511
KILCOYNE, S. P. p 3118 N95-32663
p 3223 N95-33412
KILGO, A. C. p 3078 N95-32591
KIM, DUCK HYUN p 3066 N95-32566
KIM, HONGCHUL p 3112 N95-34285
KIM, JUNG H. p 3189 N95-33002
KIM, SUNG KYU p 3223 N95-33619
KIMBRELL, S. M. p 3075 N95-34440
KIMBROUGH, J. R. p 3059 N95-32593
KIMURA, TOSHIYA p 3041 N95-34553
KING, CHRISTOPHER N. p 3229 N95-33401
KING, TRUDE V. V. p 3130 N95-33741
p 3134 N95-33761
KINOSHITA, TOSHIHIRO p 3038 N95-34535
KINSLEY, E. p 3226 N95-32589
KINTER, JAMES L., III p 3241 N95-34231
KISELEV, V. V. p 3203 N95-32554
p 3205 N95-32704
KISHIBE, TADAHARU p 3042 N95-34560
KISHIMOTO, TAKUJI p 3039 N95-34539
KITCHEN, JAMES C. p 3219 N95-34576
KIZAKI, MINORU p 3077 N95-32531
KLAVETTER, FLOYD p 3087 N95-34817
KLEIN, KURT p 3048 N95-33135
KLEISS, JAMES A. p 3056 N95-34344
KLEM, J. p 3186 N95-33838
KLEMOLA, KIMMO p 3068 N95-33242
KLEMP, JOSEPH B. p 3184 N95-34228
KLEMP, MARJORIE K. p 3184 N95-34228
KLEPEL, ST. p 3072 N95-33287
KLIER, KAMIL p 3075 N95-34021
KLUEVER, CRAIG A. p 3060 N95-32917
KLYDE, DAVID H. p 3055 N95-34306
KNAPP, D. A. p 3230 N95-34438
KNAPP, DAVID p 3207 N95-33219
KNAPP, DAVID A. p 3212 N95-33064
KNIGHTON, W. B. p 3089 N95-33268
KNILL, E. p 3187 N95-32375
KNOROVSKY, G. A. p 3118 N95-32683
KNUDSEN, H. p 3204 N95-32584
p 3207 N95-33370
KO, K. p 3203 N95-32567
KOBAYASHI, H. p 3148 N95-32402
KOBAYASHI, HIDEYUKI p 3060 N95-32755
KOCENKO, LAWRENCE p 3082 N95-32664
KOCH, STEVEN p 3243 N95-34240
KOCHER, CHRISTOPHER GEORGE p 3064 N95-33468
KOCKS, U. F. p 3231 N95-34450
KODALI, PADMA p 3203 N95-32577
p 3208 N95-33623
KODAMA, H. p 3034 N95-34507
KOELMAN, HARTMUT p 3172 N95-34768
KOHLBERG, IRA p 3057 N95-34815
KOJIRO, DANIEL R. p 3069 N95-33270
KOMACHENKO, Y. Y. p 3206 N95-32806
KONTOTHANASSIS, LEONIDAS I. p 3185 N95-32580
KORNREICH, PHILIPP p 3217 N95-34300
KOST, M. p 3162 N95-32729
KOTELNIKOV, I. A. p 3222 N95-32770
KOTHE, DOUGLAS B. p 3111 N95-33698
KOULAN, HAN p 3151 N95-34468
KOUTNY, M. p 3183 N95-34655
KOVACH, J. A. p 3085 N95-33425
KOWALENKO, VICTOR p 3205 N95-32632
KOZAK, J. p 3094 N95-33143
KOZAK, JERNEJ p 3195 N95-33058
KOZKO, Y. A. p 3093 N95-33138
KOZUBEK, S. p 3162 N95-32727
KRAFT-WEYRATHER, W. p 3162 N95-32726
KRAFT, G. p 3162 N95-32725
p 3162 N95-32726
p 3162 N95-32729
KRAUSS, A. R. p 3230 N95-34215
KRAUTER, K. p 3211 N95-32608
KREITMAIR-STECK, W. p 3093 N95-33137
KRIEGER, B. p 3208 N95-33380
KRILE, THOMAS F. p 3219 N95-34579
KRISHNAMURTHI, VIDHYA p 3207 N95-33370
KROEGER, D. M. p 3230 N95-34213
KROFCHECK, D. p 3208 N95-33380
KROLL, NORMAN M. p 3095 N95-32616
KRUGER, A. A. p 3082 N95-32384
KRUSE, FRED A. p 3128 N95-33734
p 3129 N95-33737
KRUSHELNICK, K. M. p 3120 N95-34761
KRYWINSKI, J. p 3103 N95-33080
KUBISTA, E. p 3096 N95-32750
KUBO, K. p 3213 N95-33338
KUCHNIR, M. p 3082 N95-32541
KUHL, A. L. p 3074 N95-33627
KUMAMOTO, YUICHI p 3040 N95-34546
KUNG, PANG-JEN p 3199 N95-34477
KUNKEE, D. B. p 3143 N95-32823
KUO, KENNETH K. p 3061 N95-32932
KUO, SHYANG-LIN p 3108 N95-32934
KUPIEC, JOHN A. p 3130 N95-33744
KURER, U. p 3136 N95-33770
KURODA, YUKIO p 3060 N95-32755
KUROSAKI, RYUJIRO p 3037 N95-34526
KUROTAKI, TAKUJI p 3037 N95-34526
KURRUS, R. p 3245 N95-33489
KURTZ, S. R. p 3226 N95-32595
p 3228 N95-33213
KUSAKA, KAZUO p 3060 N95-32755
KVITSINSKY, A. p 3203 N95-32583
KWOK, W. K. p 3110 N95-33389

L

LABOV, S. E. p 3230 N95-33650
LACERDA, A. p 3229 N95-33386
LACKMAN, ROBERT L. p 3239 N95-34220
LACOSS, RICHARD T. p 3100 N95-34474
LAGOW, RICHARD J. p 3087 N95-34596
LAGRANGE, DONALD E. p 3124 N95-34449
LAHAYE, R. J. p 3222 N95-32756
LAM, POH-SANG p 3125 N95-32373
LAMPEN, P. H. p 3070 N95-33274
LANCTO, R. p 3082 N95-32694
LANDERS, A. p 3208 N95-33372
LANGE, W. JOSEPH p 3120 N95-34811
LANGNER, C. G. p 3095 N95-33244
LANSKIJ, I. M. p 3221 N95-32560
LAO, L. L. p 3222 N95-32756
LAPTEV, ARI p 3195 N95-32890
LARICCHIA, G. p 3204 N95-32584
LASATER, SALLY W. p 3184 N95-34228
LASSWELL, JAMES W. p 3047 N95-34570
LAVERGNAT, J. p 3096 N95-32749
LAWBAUGH, WILLIAM M. p 3236 N95-34354
LAWEN, JAMES L., JR. p 3122 N95-32693
LAWRENCE, ANDRE p 3070 N95-33273
LAWRENCE, CHARLES p 3121 N95-32690
LAZEEV, B. N. p 3220 N95-32507
p 3220 N95-32508
p 3221 N95-32509
p 3221 N95-32510
LE, CALVIN p 3057 N95-34815
LEAL, JAMES p 3087 N95-34614
LEAR, K. L. p 3118 N95-32663
LEATHERMAN, PHILLIP p 3120 N95-34811
LEBERL, FRANZ p 3240 N95-34224
LECKIE, CHRIS p 3189 N95-33000
LEE, EDWARD P. p 3199 N95-34269
LEE, HOWARD W. H. p 3085 N95-33409
LEE, J. S. p 3140 N95-33807
LEE, JEONGHEE p 3075 N95-34357
LEE, KWANG WON p 3223 N95-33619
LEE, LI p 3200 N95-33694
LEE, R. W. p 3183 N95-34813
LEE, TONG-YEE p 3185 N95-32582
LEE, Y. Y. p 3205 N95-32652
LEGER, ALAIN p 3045 N95-32503
LEHMAN, JILL F. p 3193 N95-34602
LEKSONO, MOELJANTO p 3232 N95-34588
LELAKIS, IOANNIS p 3099 N95-34304
LENT, CRAIG S. p 3235 N95-34589
LENZ, G. p 3162 N95-32729
LEONG, KENG H. p 3124 N95-33834
LEONHARDT, J. W. p 3069 N95-33269
LEPAGE, BEN A. p 3154 N95-33394
LEPPERT, FRANCK p 3045 N95-32503
LEROUX, MARCEL p 3176 N95-34783
LESHCHYSHYN, ANDREW p 3056 N95-34342
LESUER, D. R. p 3062 N95-32399
p 3062 N95-32602
LEUNG, C. H. C. p 3188 N95-32997
LEVINE, DAVID p 3099 N95-33379
LEVINE, LESLIE p 3171 N95-34577
LEVINE, TIMOTHY E. p 3208 N95-33623
LEVINE, TIMOTHY EDGE p 3203 N95-32577
LEVUSH, B. p 3117 N95-32571
LEWAK, D. p 3208 N95-33380
LEWIS, B. B. p 3121 N95-32376
LEWIS, D. KENT p 3159 N95-33410
LI, BAI-LIAN p 3156 N95-33847
LI, CHUNFEI p 3215 N95-32957
p 3105 N95-34758
LI, FANG p 3067 N95-32641
LI, K. C. p 3188 N95-32996
LI, KEHUA p 3221 N95-32562
LI, SHENG p 3105 N95-34488
LI, XIAO-PING p 3210 N95-32411
LI, Y. PHILIP p 3243 N95-34243
LI, Z. p 3226 N95-32598
p 3229 N95-33636
LI, ZHANG p 3158 N95-34491
LIANSHENG, YU p 3217 N95-34307
LIENAU, JEFFREY JAY p 3111 N95-33709
LIETZKE, A. F. p 3103 N95-33080
LIKHODED, A. K. p 3205 N95-32704
LIMAYE, SANJAY S. p 3241 N95-34232
LIMBURG, HELEN p 3104 N95-33915
LIN-LIU, Y. R. p 3222 N95-32756
LIN, C. D. p 3206 N95-32966
p 3207 N95-33241
p 3209 N95-34355
LIN, X. p 3203 N95-32567
LIN, XINTIAN E. p 3095 N95-32616
LINLEY, K. A. p 3155 N95-32599
p 3155 N95-32601
LION, LEONARD W. p 3155 N95-34591
LIOU, MENG-SING p 3036 N95-34518
LIPINSKI, RONALD J. p 3120 N95-34811
LIPPE, R. p 3072 N95-33287
LISTOPADOV, O. A. p 3234 N95-32961
LITTENBERG, LAURENCE p 3208 N95-33850
LITTMAN, DAVID C. p 3124 N95-34449
LIU, C. L. p 3119 N95-34466
LIU, C. T. p 3079 N95-33217
LIU, HUA-KUANG p 3148 N95-34233
LIU, JIAMING p 3158 N95-34757
LIU, MING T. p 3186 N95-34584
LIU, SHUTIAN p 3105 N95-34758
LIU, XU p 3217 N95-34303
LIU, YUSHAN p 3221 N95-32562
LIVINGSTONE, CHARLES E. p 3140 N95-33809
LOCKHART, G. LANCE p 3097 N95-33033
p 3099 N95-33497
p 3099 N95-33726
LOEBRICH, M. p 3161 N95-32723
LOEHMAN, R. E. p 3085 N95-34022
LOFTY, G. J. p 3155 N95-32599
p 3155 N95-32601
p 3156 N95-32603
LONDEN, S. O. p 3195 N95-32893
LONGHURST, GLEN R. p 3221 N95-32588
LOPEZ, AARON A. p 3177 N95-32955
LOUGHIN, S. p 3060 N95-32396
LOUKIACHTCHENKO, V. I. p 3057 N95-33128
LOUKIANOV, D. P. p 3092 N95-33130
LOWNDES, D. H. p 3232 N95-34799
LOY, D. A. p 3062 N95-33835

LU, YEU-CHERNG p 3061 N95-32932
LU, YIN-CHEN p 3186 N95-33838
LUBBEN, D. p 3103 N95-33697
LUCCA, DON p 3089 N95-32585
LUN, A. p 3204 N95-32323
LUNDBERG, GOERAN p 3084 N95-33329
LUO, CHENGLIN p 3227 N95-32698
LUO, CUIXIAN p 3221 N95-32562
LUO, D. p 3152 N95-32686
LUTJENS, S. W. p 3059 N95-32593
LUTTGES, M. W. p 3149 N95-32685
LUXON, J. L. p 3222 N95-32592
LYONS, C. p 3152 N95-32668
LYONS, CAROL E. p 3153 N95-32809
LYONS, JAMES E. p 3076 N95-34810
LYONS, L. R. p 3158 N95-33259
LYSENKO, W. P. p 3211 N95-32416
LYUBOVITSKIJ, V. E. p 3202 N95-32407

M

MA, KUN p 3091 N95-32994
MACCHARLES, CYNTHIA V. p 3238 N95-33402
MACGREGOR, I. p 3213 N95-33333
MACHA, SUSAN M. p 3067 N95-32671
MACKAY, W. W. p 3211 N95-32485
p 3212 N95-33067
MACKENZIE, R. p 3211 N95-32608
MACKEY, HALKARD E., JR. p 3238 N95-33402
MACLEOD, IAIN S. p 3048 N95-34771
p 3174 N95-34776
MADSEN, EUGENE L. p 3155 N95-34591
MAEDA, TATSUO p 3041 N95-34554
MAEJIMA, Y. p 3223 N95-33221
MAES, CARL p 3120 N95-34811
MAGGIORE, CARL J. p 3203 N95-32577
p 3208 N95-33623
MAH, G. R. p 3134 N95-33762
MAHONEY, TIMOTHY I. p 3065 N95-34448
MAINE, TRINDEL A. p 3049 N95-33023
p 3049 N95-33025
MAKER, BRADLEY N. p 3182 N95-33652
MAKOWIECKI, DANIEL p 3079 N95-33063
MALKIN, S. p 3085 N95-33425
MALKINA, I. p 3152 N95-32686
MALLET, C. p 3096 N95-32749
MALLON, C. E. p 3059 N95-32593
MALOAN, J. p 3166 N95-34058
MALONEY, JOHN D. p 3086 N95-34452
MALTBY, JOHN D. p 3105 N95-34617
MAMMINI, B. M. p 3164 N95-33654
MANE, V. p 3211 N95-32485
MANKA, C. p 3120 N95-34761
MANKOFSKY, ALAN p 3242 N95-34238
MANOUSIOUTHAKIS, VASILIOS p 3167 N95-32688
MANSOUR, H. M. M. p 3202 N95-32524
MANWELL, JAMES p 3148 N95-32551
MARATHE, M. V. p 3099 N95-33387
MARCUS, M. A. p 3229 N95-33628
MARI, JORGE p 3163 N95-33232
MARINO, C. M. p 3129 N95-33735
MARKOS, SANDOR p 3189 N95-32999
MARKS, LAURENCE D. p 3228 N95-32810
MARLIERE, CHRISTIAN p 3083 N95-32819
p 3229 N95-33641
MARMORINO, G. O. p 3140 N95-33807
MARONI, VICTOR A. p 3152 N95-32553
MARRERO-SANTOS, Y. p 3077 N95-32527
MARSDEN, PAUL p 3071 N95-33278
MARSH, ELAINE p 3192 N95-34467
p 3236 N95-34487
MARSHALL, HERMAN L. p 3239 N95-34221
MARTELLUCCI, A. p 3096 N95-32748
p 3096 N95-32749
MARTIN, MARY E. p 3128 N95-33731
MARTIN, MICHAEL p 3241 N95-34232
MARTIN, P. M. p 3150 N95-33400
MASAKI, DAISAKU p 3034 N95-34508
MASHNIK, S. G. p 3202 N95-32477
MASSON, MICHEL p 3176 N95-34787
MAST, JEFFREY E. p 3095 N95-32569
MASWADEH, WALEED p 3072 N95-33286
MASWADEH, WALEED M. p 3071 N95-33277
MATAGNE, J. p 3096 N95-32751
MATRAGRANO, M. p 3231 N95-34485
MATSUNO, KENICHI p 3035 N95-34515
MATSUO, YUICHI p 3037 N95-34523
p 3041 N95-34555
MATSUSHIMA, KISA p 3040 N95-34544
MATTOK, CLARE p 3252 N95-32538
MAURICE, JERRY p 3105 N95-34796
MAURINO, DANIEL p 3175 N95-34782
MAVRIPLIS, D. J. p 3196 N95-33500
MAXFIELD, S. J. p 3214 N95-34651
MAYER, JAMES W. p 3203 N95-32577
p 3208 N95-33623
MAZIASZ, P. J. p 3077 N95-32527
MCAFEE, W. J. p 3126 N95-32684
MCCABE, GRANT T. p 3054 N95-33250
MCCALLEN, ROSE p 3080 N95-33653
MCCALLION, K. J. p 3094 N95-33142
MCCAMY, J. W. p 3232 N95-34799
MCCARTHY, KATHRYN A. p 3221 N95-32588
MCCLAIN, CHARLES R. p 3159 N95-32672
MCCLUMPHA, ANDREW J. p 3176 N95-34784
MCDONALD, ROBERT J. p 3104 N95-34446
MCELIECE, ROBERT J. p 3100 N95-34601
MCENTIRE, B. J. p 3170 N95-34378
MCGARITY, J. O. p 3057 N95-32772
MCGLAUN, M. p 3184 N95-32374
MCGOWIN, EVERETTE, III p 3049 N95-34793
MCGREEVY, MICHAEL W. p 3198 N95-33875
MCKAMEY, C. G. p 3077 N95-32527
MCKAY, CHRISTOPHER P. p 3184 N95-34225
MCKNIGHT, J. E. p 3043 N95-32489
MCLEAN, WILLIAM E. p 3049 N95-34793
MCONAGHY, CHARLES F. p 3085 N95-33409
MEADE, ANDREW J., JR. p 3194 N95-32434
MEARS, C. A. p 3230 N95-33650
MECKING, H. p 3231 N95-34450
MEDVEDEV, A. A. p 3057 N95-33128
MEISTER, DOROTHY C. p 3120 N95-34811
MELACK, JOHN p 3134 N95-33763
MELCHERT, F. p 3208 N95-33372
MELENDREZ, DAVID E. p 3137 N95-33791
MELIANKOV, N. A. p 3057 N95-33128
MELNIKOV, V. K. p 3195 N95-32479
MEN'SHOV, IGOR p 3036 N95-34516
MERCADO, AL p 3071 N95-33278
MERGEL, V. p 3208 N95-33374
MERKLE, JOHN G. p 3127 N95-34442
MERKLE, KARL L. p 3228 N95-32810
MERRILL, BRAD J. p 3221 N95-32588
MERRISON, J. P. p 3204 N95-32584
MERRITT, JOHN O. p 3170 N95-34376
MERWIN, LARRY p 3105 N95-34796
MESZAROS, IMRE p 3189 N95-32999
MEYER, CLAUDIA M. p 3188 N95-32768
MEYER, S. p 3213 N95-33333
MEZA, FRANCISCO Q. p 3235 N95-34479
MIAO, F. Q. p 3087 N95-32563
MIAOLING, HUANG p 3117 N95-32472
MICHALERIS, PANAGIOTIS p 3199 N95-33292
MICHEL, T. R. p 3140 N95-33808
MICHEL, THIERRY R. p 3141 N95-33814
MICHELSON, DAVID G. p 3140 N95-33809
MICIC, O. I. p 3225 N95-32586
MIDOLLINI, B. p 3043 N95-32488
MIDOLLINI, BEATRICE p 3045 N95-32504
MIDTLAND, S. p 3153 N95-33331
MIGLIORE, P. G. p 3033 N95-32548
MIKKELSEN, U. p 3207 N95-33370
MILES, R. B. p 3113 N95-34752
MILLER, GLENN E. p 3242 N95-34234
MILLER, L. SCOTT p 3033 N95-32548
MILLER, M. S. p 3149 N95-32685
MILLER, STEPHEN A. p 3120 N95-34619
MILLER, STEVEN P. p 3181 N95-33396
MILNE, ANTHONY p 3140 N95-33806
MINER, DENNIS K. p 3244 N95-34794
MINICHINO, CAMILLA p 3209 N95-34350
MINISCLOU, S. p 3045 N95-32501
MINTS, R. G. p 3103 N95-33404
MINTY, M. p 3211 N95-32608
MINTY, M. G. p 3213 N95-33376
p 3213 N95-33377
MITCHELL, DAVID G. p 3055 N95-34306
MITCHELL, T. E. p 3225 N95-32532
MITLITSKY, FRED p 3150 N95-33642
MIYAJI, KOJI p 3037 N95-34525
MIYAKE, YOSHIAKI p 3035 N95-34511
MIYAMOTO, ISAMU p 3090 N95-32987
MNCLN, SANIL J. p 3165 N95-34472
MOCHALOV, A. V. p 3092 N95-33130
MOCHIZUKI, MUNEKAZU p 3037 N95-34528
MOECKLY, B. H. p 3231 N95-34568
MOK, FAI p 3178 N95-34745
MOLTZ, D. p 3246 N95-32597
MONTENEGRO, E. C. p 3206 N95-32763
p 3208 N95-33374
MOODY, PAUL E. p 3123 N95-32924
MOORE, ELLEN L. p 3100 N95-34460
MOORE, FRED W. p 3237 N95-32922
MOORES, GENEVA F. p 3074 N95-33414
MOORHOUSE, DAVID JOHN p 3167 N95-33605
MORENCY, ROGER L. p 3215 N95-32923
MORGAN, GARTH p 3140 N95-33806
MORI, SEIJI p 3202 N95-32529
MORITA, YOUSUKE p 3221 N95-32565
MORRIS, J. B. p 3076 N95-34599
MORRIS, J. V. p 3214 N95-34651
MOSKOWITZ, BRUCE p 3207 N95-33203
MOTLOCH, CHESTER C. p 3221 N95-32588
MOUNIR, M. p 3202 N95-32524
MOZO, BEN T. p 3170 N95-34492
MUEGGE, ED p 3060 N95-32673
MUELLER, GREGORY P. p 3164 N95-33200
MUELLER, S. ALYSSA p 3166 N95-32422
MULBURY, DOUGLAS S. p 3166 N95-34463
MULLANE, MICHELLE p 3166 N95-34356
MULLINS, CHARLES B. p 3086 N95-34476
MUNGHAM, TONY p 3070 N95-33273
MURATA, YOSHIAKI p 3039 N95-34543
MURPHY, BARBARA A. p 3170 N95-34492
MURPHY, JOHN E. p 3204 N95-32622
MURR, F. p 3096 N95-32749
p 3096 N95-32751
MURTY, A. N. p 3066 N95-32557
MUSICK, H. BRAD p 3141 N95-33810
MYCEK, M. A. p 3101 N95-32596
p 3227 N95-32600
MYERS, BLAKE p 3150 N95-33642
MYERS, ROGER M. p 3060 N95-32917
MYINT, KHIN SWE p 3202 N95-32404
MYKITYSHYN, MARK p 3047 N95-34562

N

NABER, J. D. p 3124 N95-33701
NACHTIGAL, N. M. p 3113 N95-34800
NACHTIGAL, NOEL M. p 3228 N95-33240
NAGAI, SIRO p 3212 N95-32712
NAGASAKI, K. p 3225 N95-34624
NAGASHIMA, TOSHIO p 3035 N95-34509
NAGOURNEY, WARREN p 3104 N95-34451
NAGY, M. p 3233 N95-32405
NAISH, LEE p 3183 N95-33007
NAKAHARA, J. F. p 3060 N95-32396
NAKAI, SADAO p 3090 N95-32988
p 3090 N95-32989
p 3090 N95-32990
NAKAMICHI, JIRO p 3036 N95-34521
NAKAMURA, CASMARA p 3041 N95-34551
NAKAMURA, TAKASHI p 3038 N95-34533
NAKAMURA, YOSHIAKI p 3036 N95-34516
p 3041 N95-34551
NAKAMURA, YOSHIKO p 3037 N95-34526
NAKANO, JUNICHI p 3063 N95-32711
NAKATSUKA, MASAHIRO p 3090 N95-32988
p 3090 N95-32989
p 3090 N95-32990
NALLASAMY, M. p 3200 N95-32836
NANDI, S. p 3234 N95-33202
NARTKER, THOMAS A. p 3236 N95-32471
NASBY, ROBERT D. p 3226 N95-32590
NASH, J. K. p 3183 N95-34813
NASTASI, MICHAEL p 3203 N95-32577
p 3208 N95-33623
NATOLI, VINCENT DOMINIC p 3074 N95-33469
NEBYLOV, A. V. p 3094 N95-33141
NEDAIVODA, A. K. p 3057 N95-33128
NELSON, ERIC M. p 3203 N95-32574
NELSON, RANDAL C. p 3183 N95-34612
p 3171 N95-34616
NELSON, TOMMY R. p 3154 N95-33655
NEPSTAD, DANIEL C. p 3143 N95-33498
NEREM, A. p 3222 N95-32656
NESENYUK, L. P. p 3048 N95-33131
NETEL, H. p 3230 N95-33650
NEUFFER, D. V. p 3205 N95-32652
p 3205 N95-32654
NEUMEIER, J. J. p 3229 N95-33386
NEWMAN, E. H. p 3095 N95-32674
NEWMAN, JAMES C., JR. p 3127 N95-34442
NEWMAN, KIRK E. p 3065 N95-34448
NG, C. p 3203 N95-32567
NG, LAY-KEOW p 3070 N95-33273
NGO, E. p 3082 N95-32694
NGUYEN, CHARLES C. p 3121 N95-32675
NGUYEN, K. B. p 3084 N95-33247
NICHOLAS, JOHN B. p 3185 N95-32582
NICKLOW, R. M. p 3225 N95-32377
NIEDRA, JANIS M. p 3103 N95-33874
NIKI, K. p 3177 N95-32757
NIKITENKO, V. I. p 3110 N95-33389
NIKULIN, M. G. p 3214 N95-34439
NILSSON, CHARLOTTE p 3084 N95-33329
NIMZ, GREGORY J. p 3143 N95-33407
NISHI, NORIAKI p 3090 N95-32989
NISHIDA, HIDETOSHI p 3037 N95-34529
NISHIGORI, TAKEO p 3090 N95-32985
NISSAN, ROBIN p 3105 N95-34796
NISSEN, R. P. p 3084 N95-33247
NOBBS, STEVEN p 3051 N95-33014
NOBBS, STEVEN G. p 3051 N95-33012
p 3051 N95-33013
p 3051 N95-33015
p 3052 N95-33016

	p 3052	N95-33017
	p 3052	N95-33018
NOBLE, RICHARD	p 3068	N95-33224
NOLTING, M.	p 3069	N95-33269
NOMURA, TOSHIYUKI	p 3040	N95-34550
NOOJIN, GARY D.	p 3164	N95-34789
NORTON, D. P.	p 3231	N95-34465
NORWOOD, LAVAN	p 3071	N95-33282
	p 3072	N95-33283
NOVACK, H. IAN	p 3116	N95-33740
NOVGORODSKI, A. V.	p 3092	N95-33129
NOVIKOV, E. A.	p 3102	N95-32628
NOVO, EVLYN	p 3134	N95-33763
NOZAKI, O.	p 3034	N95-34507
NOZAKI, OSAMU	p 3035	N95-34511
NTUEN, CELESTIN	p 3189	N95-33002
NURNBERGER, M.	p 3097	N95-32822

O

OAKES, STEPHEN	p 3190	N95-33008
OBARA, HENJIRO	p 3221	N95-32565
OBARA, TETSURO	p 3039	N95-34543
OBATA, MASANORI	p 3042	N95-34558
OBATA, SHIGEO	p 3035	N95-34509
OBERHARDT, M. R.	p 3057	N95-32772
OBRIEN, SUSAN K.	p 3066	N95-32581
ODA, H.	p 3082	N95-32552
ODAY, M. E.	p 3082	N95-32694
ODONNEL, R.	p 3208	N95-33380
ODONIEC, G.	p 3208	N95-33380
OGASAWARA, KOU	p 3039	N95-34542
OGAWA, M.	p 3177	N95-32757
OGAWA, SATORU	p 3036	N95-34522
	p 3038	N95-34531
	p 3039	N95-34538
	p 3041	N95-34554
OGITSU, T.	p 3103	N95-33404
	p 3214	N95-33720
OGLETREE, D. F.	p 3230	N95-33880
OGLOBLIN, A. V.	p 3094	N95-33139
OH, BYUNG HOON	p 3223	N95-33619
OH, CHOONG KUN	p 3110	N95-33606
OHERN, T. J.	p 3106	N95-32387
OHKAWA, YOSHINAO	p 3221	N95-32565
OHKITA, Y.	p 3034	N95-34507
OHNO, HIDEKI	p 3212	N95-32712
OHYAGI, SHIGEHARU	p 3035	N95-34510
	p 3039	N95-34543
OIDE, K.	p 3212	N95-32657
OIDE, SHIN-ICHI	p 3038	N95-34530
OKA, KIYOSHI	p 3221	N95-32565
OKON, I. M.	p 3048	N95-33131
OKUNO, KENJI	p 3220	N95-32409
OLESON, STEVEN R.	p 3060	N95-32917
OLSEN, CHRISTOPHER S.	p 3247	N95-33625
ONEILL, P. E.	p 3142	N95-33816
ONIZAWA, KUNIO	p 3077	N95-32531
OPPENHEIM, A. K.	p 3074	N95-33627
OPPENHEIM, ALAN V.	p 3100	N95-34749
OPSTAD, AASE M.	p 3068	N95-33243
ORAEVSKY, A. A.	p 3164	N95-33654
OREDSSON, BRITA	p 3074	N95-33634
OREN, RAM	p 3141	N95-33812
ORLANDO, VINCENT A.	p 3047	N95-33480
ORME, JOHN S.	p 3051	N95-33011
	p 3051	N95-33015
	p 3052	N95-33016
	p 3052	N95-33017
	p 3052	N95-33018
	p 3053	N95-33020
ORR, TONY	p 3140	N95-33806
ORSZAG, STEVEN A.	p 3112	N95-34343
ORTGIES, G.	p 3096	N95-32749
OSOSKOV, G.	p 3188	N95-32627
OSSARD, G.	p 3168	N95-34054
OSTAFIN, A. E.	p 3225	N95-32586
OTERO, IVAN	p 3080	N95-33653
OTTENHOFF, H. C.	p 3043	N95-32489
OYEDIRAN, AYO	p 3108	N95-32930
	p 3050	N95-32931
OZDEMIR, T.	p 3097	N95-32822
OZEKI, TAKAHISA	p 3220	N95-32410

P

PAEGLE, JAN	p 3157	N95-32933
PAGNI, PATRICK J.	p 3089	N95-32929
PAINTER, THOMAS H.	p 3135	N95-33764
PALASZEWSKI, BRYAN	p 3088	N95-33876
PALMER, R. B.	p 3205	N95-32652
	p 3205	N95-32654
PALMER, RONALD W.	p 3171	N95-34574
PALMER, TODD S.	p 3195	N95-32559
PAN, GUOQIANG	p 3227	N95-32698
PANDOLF, KENT B.	p 3170	N95-34370
PANETTA, PAUL	p 3228	N95-32959
PANG, Y.	p 3205	N95-32651
PANKOVA, JAQUES I.	p 3232	N95-34588
PAQUETTE, K. L.	p 3164	N95-33654
PARABONI, A.	p 3096	N95-32748
PARIES, JEAN	p 3176	N95-34785
PARK, EUI H.	p 3189	N95-33002
PARK, KIYEON	p 3091	N95-32992
PARK, SEUNG Y.	p 3230	N95-34443
PARKER, DONALD C.	p 3072	N95-33288
PARMETER, J. E.	p 3223	N95-33412
PARTLAN, M.	p 3208	N95-33380
PARZEN, G.	p 3210	N95-32414
PASHNEV, A. I.	p 3225	N95-32480
PATEL, G. D.	p 3214	N95-34651
PATERSON, KURTIS GERHARDT	p 3154	N95-33339
PATIL, RAJENDRA B.	p 3179	N95-32572
	p 3191	N95-33212
PATT, FREDERICK S.	p 3158	N95-32545
PAUL, P. H.	p 3084	N95-33247
PAULINO, G. H.	p 3194	N95-32388
PAULINO, GLAUCIO H.	p 3126	N95-33222
PAWLINA, A.	p 3096	N95-32751
PAXSON, VERN	p 3185	N95-32967
PAYNE, J. L.	p 3106	N95-32818
PEACH, K. J.	p 3235	N95-34652
PEACHEY, NATHANIEL M.	p 3229	N95-33401
PEARSON, A.	p 3083	N95-33079
PEARSON, JOHN	p 3193	N95-34593
PEARTON, S. J.	p 3226	N95-32594
	p 3223	N95-33412
PEASE, D. M.	p 3079	N95-33065
PEATMAN, WILLIAM C.	p 3105	N95-34458
PECARIC, M.	p 3166	N95-34058
PECK, CHARLES C.	p 3188	N95-32767
	p 3188	N95-32768
PEEL, JOHN, III	p 3117	N95-33746
PEERY, J.	p 3184	N95-32374
PEGGS, S.	p 3210	N95-32413
	p 3211	N95-32485
	p 3212	N95-33067
	p 3213	N95-33204
PEIFU, GU	p 3119	N95-34308
PEIQIAN, ZHAO	p 3218	N95-34490
PELIZZARI, CHARLES	p 3242	N95-34236
PELLETIER, E.	p 3218	N95-34471
PELTON, GARRETT A.	p 3193	N95-34602
PENNINGTON, D. M.	p 3119	N95-33703
PERCEC, V.	p 3082	N95-32552
	p 3086	N95-34361
PERELYGIN, V. P.	p 3164	N95-32666
PEREZ-BRITO, JOAQUIN	p 3190	N95-33003
PERKINS, C.	p 3203	N95-32567
PERRY, D. L.	p 3075	N95-34268
PERRY, M. D.	p 3164	N95-33654
PERVUSHIN, V.	p 3234	N95-32667
PESHEKHONOV, V. D.	p 3102	N95-32628
PESHEKHONOV, V. G.	p 3048	N95-33131
PETERS, DEAN	p 3170	N95-34358
PETERSON, A.	p 3244	N95-34816
PETERSON, RANDALL L.	p 3048	N95-32699
PETITT, G. A.	p 3206	N95-32965
PETTI, DAVID A.	p 3221	N95-32588
PHILLIPS, M. W.	p 3225	N95-34812
PHILLIPS, R. G. N.	p 3209	N95-34650
PHILOSOPHOV, S. N.	p 3057	N95-33128
PICRAUX, S. T.	p 3225	N95-32579
PIERCE, J.	p 3152	N95-32686
PIERI, DAVID C.	p 3137	N95-33790
PIETKIEWICZ-KOUTNY, M.	p 3183	N95-34655
PIGNATTI, S.	p 3129	N95-33735
PIKE, GORDON E.	p 3226	N95-32590
PILAR, HERRERA-FIERRO	p 3083	N95-32918
PILAT, F.	p 3210	N95-32413
PILON, PIERRE	p 3070	N95-33273
PINCOSY, P. A.	p 3095	N95-32570
PINEDADEGYVEZ, JOSE	p 3178	N95-34462
PINELLI, THOMAS E.	p 3237	N95-32883
	p 3239	N95-34217
PINZON, J. E.	p 3135	N95-33765
PITZ, M. A.	p 3079	N95-33215
PLAUT, JEFFREY J.	p 3141	N95-33811
PLICHTA, EDWARD J.	p 3104	N95-34347
PLOGER, SCOTT A.	p 3081	N95-34348
PLUMER, E. S.	p 3187	N95-32386
POKER, D. B.	p 3218	N95-34480
POLAK, ELIJAH	p 3183	N95-34605
POON, J. C. H.	p 3188	N95-32996
POORE, AUBREY B.	p 3100	N95-34590
POROD, WOLFGANG	p 3235	N95-34589
POTTER, THOMAS, F.	p 3153	N95-32809
POULSEN, P.	p 3095	N95-32570
POWERS, B. J.	p 3143	N95-33849
POWERS, SHERYLL GOECKE	p 3050	N95-33009
POZZOLI, R.	p 3221	N95-32561
PRAGER, S. C.	p 3223	N95-33221
PRELLER, RUTH H.	p 3159	N95-34341
PRESS, W.	p 3244	N95-34816
PRIEST, ROBERT E.	p 3089	N95-32568
PRIOR, A. R. J.	p 3165	N95-34052
	p 3168	N95-34055
PROBST, R.	p 3092	N95-33130
PROIA, M.	p 3043	N95-32491
PROSS, H.-D.	p 3162	N95-32729
PROVOST, L. R.	p 3076	N95-34611
PURETZKY, A. A.	p 3118	N95-33246
PYHAELAHTI, ANTTI	p 3068	N95-33242

Q

QIJIN, YE	p 3118	N95-32702
QIULIN, SHAO	p 3151	N95-34468
QUANDT, GENE A.	p 3033	N95-32548
QUANMING, QIAO	p 3158	N95-34491
QUARTARONE, JAMES R.	p 3116	N95-34426

R

RADHAKRISHNAN, KRISHNAN	p 3108	N95-32930
	p 3050	N95-32931
RAGHAVAN, SRINI	p 3087	N95-34614
RAGHAVENDRA, C. S.	p 3185	N95-32582
RAIMONDI, P.	p 3212	N95-32657
	p 3215	N95-32658
RAJH, T.	p 3225	N95-32586
RAMAN, RAGHU	p 3089	N95-32718
RAMANATHAN, VEERABHADRAN	p 3242	N95-34236
RAMASWAMY, MYTHILY	p 3195	N95-32523
RAMASWAMY, S.	p 3195	N95-32523
RAMESH, R.	p 3226	N95-32590
RAMSEY, MICHAEL S.	p 3137	N95-33793
	p 3117	N95-33795
RANDALL, DAVID A.	p 3153	N95-33205
RANEY, E. A.	p 3151	N95-32475
RANEY, J. J.	p 3117	N95-33769
RAO, RUIZHONG	p 3120	N95-34470
RAPTIS, A. C.	p 3152	N95-32553
RASH, CLARENCE E.	p 3049	N95-34793
RASMUSSEN, STEEN	p 3062	N95-33848
RATAN, SANTOSH	p 3126	N95-32920
RATAN, V.	p 3187	N95-34587
RATTI, A.	p 3211	N95-32485
RAUBENHEIMER, T.	p 3213	N95-33338
RAVI, R.	p 3099	N95-33387
RAVI, S. S.	p 3099	N95-33387
RAY-CHAUDHURI, A. K.	p 3084	N95-33247
RAYMOND, MARK V.	p 3226	N95-32590
REALMUTO, VINCENT J.	p 3136	N95-33789
	p 3117	N95-33796
	p 3117	N95-33797
REANEY, IAN M.	p 3082	N95-32710
REARDON, MATTHEW J.	p 3182	N95-34371
REAVES, PAT H.	p 3104	N95-34445
REDEKER, A.	p 3049	N95-33145
REED, G. E.	p 3071	N95-33280
REED, JAMES A.	p 3113	N95-34818
REED, K. J.	p 3230	N95-34438
REEHORST, ANDREW	p 3034	N95-32769
REGENSCHEIT, PRISKA	p 3072	N95-33285
REHN, L. E.	p 3226	N95-32598
	p 3229	N95-33636
REJMANKOVA, E.	p 3135	N95-33768
REMENYIK, CARL J.	p 3116	N95-33206
REMER, LORRAINE	p 3132	N95-33749
REUTER, WALTER G.	p 3127	N95-34442
REVELLE, DOUGLAS O.	p 3246	N95-33211
RHEE, YOUNG JOO	p 3066	N95-32566
RHO, M.	p 3204	N95-32621
RHODES, B. J.	p 3071	N95-33290
RHORER, RICHARD	p 3089	N95-32585
RIBERA, JOHN E.	p 3170	N95-34492
RICCIARDI, BERNARD V.	p 3043	N95-32492
RICHARD, JACQUES C.	p 3050	N95-32916
RICHARD, P.	p 3206	N95-32763
	p 3208	N95-33372
RIDER, WILLIAM J.	p 3111	N95-33696
RIEHL, JOHN P.	p 3060	N95-32917
RIENTJES, T. H. M.	p 3157	N95-32891
RIGDON, STEPHEN	p 3071	N95-33282
	p 3072	N95-33283
RIGNOT, ERIC	p 3139	N95-33805
	p 3142	N95-33815
RIGNOT, ERIC J.	p 3141	N95-33812
RILEY, MERLE E.	p 3224	N95-33851
RITCHIE, DAVID J.	p 3186	N95-33639
RITCHIE, ROBERT K.	p 3071	N95-33279
RITTER, S.	p 3162	N95-32726

RIVARD, BENOIT ..... p 3141 N95-33813
ROBERTS, DAR A. ..... p 3131 N95-33747
p 3133 N95-33755
p 3133 N95-33757
p 3135 N95-33764
p 3135 N95-33766
ROBERTS, R. G. ..... p 3235 N95-34652
p 3214 N95-34653
ROBINETT, RUSH D. ..... p 3191 N95-33214
ROBINSON, A. ..... p 3184 N95-32374
ROBINSON, GARY N. ..... p 3081 N95-34821
ROBINSON, JEFFREY A. ..... p 3089 N95-32568
ROBINSON, M. C. ..... p 3149 N95-32685
ROCCO, G. A. ..... p 3096 N95-32773
ROCHON, GILBERT ..... p 3243 N95-34239
ROCKETT, P. ..... p 3219 N95-32401
RODEN, D. W. ..... p 3044 N95-32496
RODLOFF, R. ..... p 3092 N95-33130
RODRIGUEZ, E. ..... p 3140 N95-33808
RODRIGUEZ, ERNESTO ..... p 3141 N95-33814
RODRIGUEZ, V. D. ..... p 3207 N95-33241
ROECHER, H. ..... p 3161 N95-32720
ROGALEV, R. N. ..... p 3206 N95-32806
ROGERS, A. C. ..... p 3115 N95-32687
ROGERS, ROBIN D. ..... p 3086 N95-34452
ROHMAT, TRI AGUNG ..... p 3035 N95-34510
ROME, M. ..... p 3221 N95-32561
RONGLE, LIN ..... p 3100 N95-34760
ROSE, J. ..... p 3211 N95-32485
ROSE, ROBERT ..... p 3058 N95-34744
ROSEMARIN, A. ..... p 3163 N95-33236
ROSEN, J. B. ..... p 3186 N95-34340
ROSENBERG, L. ..... p 3246 N95-32597
ROSENKRANTZ, D. J. ..... p 3099 N95-33387
ROSNER, B. ..... p 3206 N95-32966
p 3209 N95-34355
ROSS, F. M. ..... p 3229 N95-33628
ROTAR, PAUL ..... p 3158 N95-34223
ROTH, DON J. ..... p 3125 N95-33209
ROTHMAYER, A. P. ..... p 3113 N95-34597
ROULEAU, C. M. ..... p 3232 N95-34799
ROUSE, WILLIAM B. ..... p 3173 N95-34773
ROUSSOPOULOS, N. ..... p 3242 N95-34235
ROWELL, C. ..... p 3196 N95-34377
ROWLES, CHRIS ..... p 3189 N95-33000
RUBADEUX, K. L. ..... p 3124 N95-33908
RUBENCHIK, A. M. ..... p 3164 N95-33654
RUBIN, MARK R. ..... p 3243 N95-34241
RUCKER, F. ..... p 3096 N95-32748
p 3096 N95-32749
RUDBERG, BJORN ..... p 3185 N95-32815
RUDERMAN, MALVIN ..... p 3248 N95-33499
RUDISILL, MARIANNE ..... p 3176 N95-34784
RUDOLPH, ANDREAS ..... p 3071 N95-33279
RUFF, STEVEN W. ..... p 3138 N95-33798
RUHUA, SONG ..... p 3157 N95-34299
RUIRONG, ZENG ..... p 3117 N95-32472
p 3118 N95-32702
RUIYING, FAN ..... p 3219 N95-34759
RUIZ-SUAREZ, J. CARLOS ..... p 3190 N95-33003
RUSSELL, P. S. ..... p 3217 N95-34374
RUSSMANN, C. ..... p 3162 N95-32729
RUSTHOI, D. P. ..... p 3211 N95-32416
RUTH, R. D. ..... p 3213 N95-33338
RUTH, RONALD D. ..... p 3211 N95-32607
RYAN, CHRISTINE A. ..... p 3237 N95-32922
RYUTOV, D. D. ..... p 3221 N95-32561

S

SAATCHI, SASAN ..... p 3142 N95-33815
SABELKO, J. J. ..... p 3225 N95-32586
SABOL, DONALD E., JR. ..... p 3135 N95-33766
SAEED, A. ..... p 3171 N95-34658
SAEVBARK, BENGT ..... p 3088 N95-33332
SAFJAN, ANDRZEJ JERZY ..... p 3200 N95-33719
SAHLSTROM, K. E. ..... p 3069 N95-33268
SAHO, N. ..... p 3214 N95-33504
SAITO, SHIGERU ..... p 3040 N95-34549
SAITO, TSUTOMU ..... p 3038 N95-34535
SAJDA, PAUL ..... p 3193 N95-34593
SALANT, RICHARD F. ..... p 3061 N95-33156
SALLADE, GEORGE J. ..... p 3065 N95-34448
SALMERON, M. ..... p 3230 N95-33880
SALMON, J. THADDEUS ..... p 3118 N95-33378
SALONEN, E. ..... p 3096 N95-32749
p 3096 N95-32751
SALTER, J. M. ..... p 3183 N95-34813
SALU, YEHUDA ..... p 3135 N95-33767
SALVI, STEFANO ..... p 3137 N95-33790
SAMTANEY, RAVINDRA ..... p 3111 N95-33607
SAMUELS, JOHN A. ..... p 3229 N95-33401
SANCHEZ, A. D. ..... p 3226 N95-32589
SANDER, O. R. ..... p 3211 N95-32416
SANDERSON, E. W. ..... p 3135 N95-33768
SANFORD, BEVERLY ..... p 3175 N95-34781
SARAVANOS, DIMITRIS A. ..... p 3063 N95-33210
SARFF, J. S. ..... p 3223 N95-33221
SARKAR, S. ..... p 3209 N95-34650
SARMOUK, ABDERREZAK ..... p 3245 N95-32837
SARTURE, C. M. ..... p 3117 N95-33769
SARTURE, CHARLES ..... p 3116 N95-33739
p 3116 N95-33740
SARVER-VERHEY, TIMOTHY R. ..... p 3061 N95-33926
SASS, R. ..... p 3211 N95-32608
SATO, HIROYUKI ..... p 3038 N95-34534
SATO, MASAHIRO ..... p 3060 N95-32755
SATO, SATOSHI ..... p 3219 N95-32408
SATOFUKA, NOBUYUKI ..... p 3035 N95-34515
p 3042 N95-34558
SATOGATA, T. ..... p 3236 N95-32412
p 3212 N95-33067
SAUNDERS, DAVID S. ..... p 3078 N95-32926
SAUNDERS, R. S. ..... p 3241 N95-34232
SAVAGE, MICHAEL ..... p 3124 N95-33908
SAVAGE, RICHARD C. ..... p 3242 N95-34236
SAVELIEV, V. V. ..... p 3093 N95-33138
SAWADA, S. ..... p 3233 N95-32405
SAWAGUCHI, SEIICHI ..... p 3035 N95-34512
SAWKA, MICHAEL N. ..... p 3171 N95-34577
SCANLAN, R. ..... p 3103 N95-33080
SCANLAN, RONALD M. ..... p 3215 N95-33381
SCARABOTTO, E. ..... p 3045 N95-32502
SCHABER, GERALD G. ..... p 3141 N95-33810
SCHAEFER, M. ..... p 3161 N95-32724
SCHAEFER, PETER ..... p 3049 N95-33025
SCHAENZER, GUNTHER ..... p 3048 N95-33134
SCHAEPMAN, M. ..... p 3136 N95-33770
SCHARSTEIN, ROBERT W. ..... p 3234 N95-34464
SCHAUB, HANSPETER ..... p 3191 N95-33214
SCHAUS, CHRISTIAN F. ..... p 3229 N95-33401
SCHKOLNIK, GERARD ..... p 3052 N95-33019
SCHLAEPFER, D. ..... p 3136 N95-33770
SCHLAGEL, T. J. ..... p 3205 N95-32651
SCHMIDT, GEORGE RAYMOND ..... p 3109 N95-33256
SCHMIDT, P. ..... p 3162 N95-32728
SCHMIDT, R. ..... p 3103 N95-33080
SCHMITZ, C. ..... p 3161 N95-32724
SCHMITZ, M. ..... p 3161 N95-32720
SCHMUCK, G. ..... p 3133 N95-33758
SCHMUGGE, THOMAS ..... p 3139 N95-33799
SCHNEIBEL, J. H. ..... p 3077 N95-32400
SCHNEIDER, D. ..... p 3230 N95-34438
SCHNEIDER, E. ..... p 3162 N95-32728
p 3162 N95-32729
p 3163 N95-32731
SCHNEIDER, H. ..... p 3163 N95-32731
SCHNEIDER, R. P. ..... p 3118 N95-32663
SCHOLL, E. H. ..... p 3236 N95-32412
SCHOTT, J. U. ..... p 3161 N95-32721
SCHROEDER, M. A. ..... p 3076 N95-34599
SCHULTZ, DAVID R. ..... p 3205 N95-32650
SCHULZ, CINDY K. ..... p 3210 N95-32424
SCHULZ, M. ..... p 3228 N95-33373
SCHUPPLER, S. ..... p 3229 N95-33628
SCHWARTZ, S. E. ..... p 3153 N95-33192
p 3156 N95-34214
SCOTT, K. A. ..... p 3158 N95-33505
SCOTT, MICHAEL L. ..... p 3185 N95-32580
SEAL, M. R. ..... p 3102 N95-32968
SEEMAN, J. ..... p 3203 N95-32567
SEGAL, M. E. ..... p 3187 N95-34587
SEKOGUCHI, KOTOHIKO ..... p 3091 N95-32991
SEKULIC, D. P. ..... p 3102 N95-32714
SELLIDJ, ABDELKRIM ..... p 3086 N95-34476
SELLIS, TIMOS ..... p 3242 N95-34235
SEMCHUK, P. D. ..... p 3076 N95-34611
SEMERARO, B. D. ..... p 3113 N95-34800
SEMPLE, W. G. ..... p 3044 N95-32493
SENG, LIM ..... p 3182 N95-34580
SENGLAUB, M. E. ..... p 3178 N95-32378
SENGUPTA, L. C. ..... p 3082 N95-32694
SERFOSS, GARY L. ..... p 3056 N95-34362
SERFOZO, RICHARD F. ..... p 3187 N95-34603
SERIN, NADIR ..... p 3061 N95-32932
SESSLER, ANDREW ..... p 3210 N95-32411
SEWALL, NOEL R. ..... p 3089 N95-32568
SHACKELFORD, LINDA ..... p 3165 N95-32419
SHAFRANOV, M. D. ..... p 3102 N95-32628
SHAMANSKY, H. T. ..... p 3095 N95-32674
SHAMILOGLU, EDL ..... p 3105 N95-34581
SHANKAR, VIJAYA ..... p 3196 N95-34377
SHAO, MAXINE ..... p 3069 N95-33270
SHARAPOV, S. ..... p 3224 N95-33696
SHARMA, SHIV K. ..... p 3084 N95-33405
SHARP, RICHARD ..... p 3080 N95-33653
SHARPE, RON ..... p 3190 N95-33008
SHAW, W. J. ..... p 3158 N95-33505
SHCHERBAKOV, R. R. ..... p 3227 N95-32631
SHEA, K. J. ..... p 3062 N95-33835
SHEA, T. J. ..... p 3211 N95-32485
SHEEN, SHU-HAW ..... p 3152 N95-32553
SHELTON, WILLIAM A. ..... p 3228 N95-33240
SHEN, HONGYUAN ..... p 3117 N95-32472
p 3118 N95-32702
SHEPHERD, T. G. ..... p 3248 N95-33390
SHERBY, O. D. ..... p 3062 N95-32602
SHERMAN, MARTIN P. ..... p 3111 N95-33837
SHESTERMANOV, K. ..... p 3212 N95-32665
SHEVLYAGIN, M. V. ..... p 3205 N95-32704
SHI, JIANCHENG ..... p 3142 N95-33816
SHI, N. ..... p 3064 N95-33704
SHIBANUMA, KIYOSHI ..... p 3221 N95-32565
SHIMA, EIJI ..... p 3039 N95-34540
SHIMADA, T. ..... p 3223 N95-33221
SHIMIZU, KUNIHIRO ..... p 3035 N95-34511
SHIMIZU, RYUICHI ..... p 3090 N95-32986
SHIN, JANG SOO ..... p 3066 N95-32566
SHIN, K. K. ..... p 3188 N95-32998
SHINDO, MASAMI ..... p 3083 N95-32711
SHINGAL, R. ..... p 3207 N95-33371
SHINOHARA, M. ..... p 3177 N95-32757
SHIPLEY, D. E. ..... p 3149 N95-32685
SHIRAI, HIROSHI ..... p 3220 N95-32417
SHIRAYAMA, SUSUMU ..... p 3041 N95-34556
SHIVATHAYA, S. S. ..... p 3189 N95-32998
SHIXIAO, YUE ..... p 3157 N95-34299
SHOFF, DONALD B. ..... p 3071 N95-33277
p 3072 N95-33286
SHOGRIN, BRADLEY ..... p 3083 N95-32918
p 3083 N95-32919
SHORE, G. M. ..... p 3235 N95-34652
SHTANKO, S. P. ..... p 3164 N95-32666
SHTEYNGART, S. ..... p 3125 N95-32392
SHU, C. W. ..... p 3042 N95-34783
SHUBERT, W. K. ..... p 3158 N95-34575
SHUL, R. J. ..... p 3223 N95-33412
SHUR, MICHAEL ..... p 3233 N95-34822
SHUTIAN, LIU ..... p 3104 N95-34379
SICKOREZ, DONN G. ..... p 3248 N95-32418
SIDOROV, A. V. ..... p 3202 N95-32406
SIEBERS, D. L. ..... p 3124 N95-33701
SIEGNER, U. ..... p 3101 N95-32596
p 3227 N95-32600
SIEMANN, R. H. ..... p 3214 N95-34023
p 3214 N95-34024
SIKIVIE, P. ..... p 3246 N95-32597
SIKKENGA, S. L. ..... p 3050 N95-32636
SILVER, GARY L. ..... p 3196 N95-33248
SIMMS, D. A. ..... p 3149 N95-32685
SIMONEN, E. P. ..... p 3077 N95-32555
p 3127 N95-33833
SIMS, MICHAEL H. ..... p 3184 N95-34225
SINCLAIR, M. B. ..... p 3229 N95-33636
SINHA, MAHADEVA P. ..... p 3117 N95-33796
SINHA, S. C. ..... p 3122 N95-32691
SIPES, DAWN E. ..... p 3170 N95-34376
SISK, THOMAS ..... p 3140 N95-33806
SITES, J. R. ..... p 3149 N95-32817
SKLOSS, TIMOTHY W. ..... p 3087 N95-34649
SKOELD, Y. A. ..... p 3067 N95-32615
SLAUGHTER, JON M. ..... p 3219 N95-34791
SLINGO, A. ..... p 3156 N95-34214
SLIWA, LAURE ..... p 3048 N95-33136
SLOUGH, JOHN T. ..... p 3223 N95-33216
SLUTTER, W. E. ..... p 3057 N95-32772
SMALL, RONALD L. ..... p 3173 N95-34773
SMALL, W., IV ..... p 3164 N95-33654
SMIRNOV, G. I. ..... p 3206 N95-32796
SMITH, ANDREW E. ..... p 3204 N95-32622
SMITH, ANDREW V. ..... p 3075 N95-34287
SMITH, B. G. ..... p 3058 N95-32713
SMITH, C. ..... p 3124 N95-33836
SMITH, DAVID C. ..... p 3229 N95-33401
SMITH, DAVID L. ..... p 3101 N95-32578
SMITH, DOUGLAS R. ..... p 3182 N95-34582
SMITH, G. E. ..... p 3054 N95-33208
SMITH, GUY A. ..... p 3066 N95-32581
SMITH, HENRY I. ..... p 3231 N95-34569
SMITH, J. L. ..... p 3215 N95-32662
SMITH, JIM ..... p 3105 N95-34796
SMITH, JOE N., JR. ..... p 3149 N95-32645
p 3211 N95-32647
SMITH, JOSHUA R. ..... p 3062 N95-33848
SMITH, M. ..... p 3211 N95-32416
SMITH, M. O. ..... p 3135 N95-33765
SMITH, MILTON O. ..... p 3135 N95-33766
SMITH, P. B. W. ..... p 3069 N95-33266
SMITS, A. J. ..... p 3113 N95-34752
SNELL, QUINN O. ..... p 3177 N95-32398
SNIEGOWSKI, J. J. ..... p 3124 N95-33836
SNYDER, A. PETER ..... p 3071 N95-33277
p 3072 N95-33286
SOETRISNO, M. ..... p 3106 N95-32818
SOLYOM, P. ..... p 3067 N95-32615
SOMMER, WALTER F. ..... p 3203 N95-32576
SONG, KY SEOK ..... p 3066 N95-32566

SONG, SEUNG JAE	p 3063	N95-33309
SONG, WOO SUP	p 3223	N95-33619
SORRELL, F. Y.	p 3160	N95-34375
SOUTHAM, T. H.	p 3046	N95-32505
SPADAFORA, STEPHEN J.	p 3087	N95-34614
SPANGLER, GLENN E.	p 3069	N95-33267
	p 3070	N95-33275
SPARKS, C.	p 3233	N95-34802
SPEARS, WILLIAM M.	p 3182	N95-34456
	p 3193	N95-34473
SPECHT, E. D.	p 3077	N95-32400
	p 3230	N95-34213
SPENCE, CLAY	p 3193	N95-34593
SPENCE, W.	p 3215	N95-32658
SPENCE, W. L.	p 3213	N95-33376
	p 3213	N95-33377
SPIEGEL, E. A.	p 3247	N95-34216
SPINHIRNE, JAMES M.	p 3120	N95-34811
SPINONI, I. M.	p 3045	N95-32502
SPIRE, RAND J.	p 3166	N95-34609
SPONDER, LEOPOLD	p 3115	N95-32927
SQUIRE, DWIGHT V.	p 3084	N95-33408
SREEDHAR, MADHU KUMAR	p 3109	N95-33340
SRIVAS, MANDAYAM, K.	p 3181	N95-33396
SROMOVSKY, L. A.	p 3241	N95-34232
STACH, J.	p 3070	N95-33272
	p 3072	N95-33287
STAENZ, K.	p 3136	N95-33771
STALKER, K. TERRY	p 3226	N95-32589
STARCK, PAUL	p 3084	N95-33228
STAROSELSKY, ILYA	p 3112	N95-34343
STARROCK, V.	p 3072	N95-33287
STAVNES, MARK W.	p 3060	N95-32673
STEIN, EARL S.	p 3172	N95-34767
STEINMETZ, L. L.	p 3115	N95-32900
STELL, JAMES DENNIS	p 3098	N95-33322
STERNBERG, NATALIA	p 3224	N95-34586
STERRETT, JOHN DOUGLAS	p 3123	N95-33323
STETINA, FRAN	p 3243	N95-34239
STEVENS, RICK L.	p 3209	N95-34212
STEVENS, ROBERT	p 3089	N95-32585
STEWART, D. SCOTT	p 3088	N95-32605
STEWART, JAIMEE	p 3166	N95-34356
STEWART, JAMES F.	p 3051	N95-33010
STIELER, B.	p 3092	N95-33130
STIMAC, ROBERT M.	p 3072	N95-33288
STITZEL, J. C.	p 3151	N95-32475
STJOHN, H.	p 3222	N95-32756
STOCKLI, M. P.	p 3208	N95-33372
STOCKS, GEORGE M.	p 3228	N95-33240
STOEFFL, W.	p 3246	N95-32597
STOFAN, ELLEN R.	p 3141	N95-33811
STOLARSKI, DAVID J.	p 3164	N95-34789
STOLIN, A. A.	p 3195	N95-32889
STOLL, U.	p 3162	N95-32728
STONE, ERIC A.	p 3165	N95-34472
STORER, JAMES A.	p 3242	N95-34237
STOSS, FREDERICK W.	p 3154	N95-33655
STOWELL, S.	p 3082	N95-32694
STREIBEL, T.	p 3161	N95-32720
STRELTSOV, V. N.	p 3207	N95-33226
STRENGE, D. L.	p 3155	N95-34441
STRIBULA, CHUCK	p 3048	N95-33140
STRINGFELLOW, GERALD B.	p 3233	N95-34820
STRINGFIELD, RAY M.	p 3203	N95-32574
STUART, B. C.	p 3164	N95-33654
STUBBINS, JAMES F.	p 3203	N95-32576
STULEN, R. H.	p 3084	N95-33247
STUMP, F.	p 3245	N95-33489
STUPAKOV, G.	p 3203	N95-32544
	p 3203	N95-32567
STUPAKOV, G. P.	p 3166	N95-34053
	p 3165	N95-34056
SU, CHIH-WU	p 3071	N95-33282
	p 3072	N95-33283
SUCAR, L. ENRIQUE	p 3190	N95-33003
SUDAN, RAVI N.	p 3101	N95-32578
SUGAWARA, GLEN	p 3097	N95-32925
SULLIVAN, A.	p 3216	N95-33411
SULLIVAN, CORNELIUS W.	p 3160	N95-34457
SULLIVAN, N.	p 3246	N95-32597
SULLIVAN, PATRICK M.	p 3104	N95-34445
SUMMERS, LESLIE J.	p 3081	N95-34482
SUN, E. Y.	p 3085	N95-33635
SUN, MAOCONG	p 3215	N95-32957
SUNDARAM, R.	p 3099	N95-33387
SUTHERLAND, H. J.	p 3150	N95-33706
SUTLIFF, J. A.	p 3230	N95-34213
SUYAMA, TAKAYUKI	p 3091	N95-32991
SUZUKI, MASAHIDE	p 3077	N95-32531
SUZUKI, TOSHIHIRO	p 3042	N95-34558
SUZUKI, Y.	p 3177	N95-32757
SVOBODA, J.	p 3094	N95-33143
SWAIN, S.	p 3198	N95-32525
SWANSIGER, T. G.	p 3083	N95-33079
SWARTS, E. LOWELL	p 3084	N95-33218
SWAYZE, GREGG A.	p 3130	N95-33741
	p 3130	N95-33742
	p 3130	N95-33743
	p 3134	N95-33761
	p 3136	N95-33772
SWEGLE, J. W.	p 3106	N95-32587
SWIHART, DONALD	p 3048	N95-33140
SYN, C. K.	p 3062	N95-32399
	p 3062	N95-32602
SYN, CHOL K.	p 3084	N95-33408
SZAJOWSKI, P. J.	p 3229	N95-33628
SZALAY, TIBOR	p 3189	N95-32999
SZCZUR, MARTI R.	p 3184	N95-34228
SZEGLOWSKI, Z.	p 3164	N95-32666
SZUSZCZEWICZ, EDWARD P.	p 3242	N95-34238

T

TACHIBANA, MASAKAZU	p 3042	N95-34559
TADA, EISUKE	p 3221	N95-32565
TADA, MASAKAZU	p 3090	N95-32990
TADANO, MAKOTO	p 3060	N95-32755
TAGIROV, E. A.	p 3233	N95-32478
TAGUCHI, HIDEYUKI	p 3035	N95-34513
TAGUCHI, KOU	p 3221	N95-32565
TAKAHASHI, MASAHIRO	p 3035	N95-34514
TAKAI, YOSHIZO	p 3090	N95-32986
TAKAKURA, YOKO	p 3038	N95-34531
	p 3039	N95-34538
TAKANASHI, SUSUMU	p 3039	N95-34537
	p 3040	N95-34544
TAKANO, M.	p 3177	N95-32757
TAKATSU, HIDEYUKI	p 3219	N95-32408
	p 3202	N95-32529
TAKEDA, TOSHIKAZU	p 3090	N95-32985
TAKEUCHI, NORI	p 3069	N95-33270
TAL, JACOB	p 3177	N95-32955
TALBOTT, D. V.	p 3197	N95-32391
TAMMARU, IVO	p 3104	N95-33915
TAMURA, A.	p 3034	N95-34507
TAMURA, ATSUHIRO	p 3035	N95-34511
TANAKA, ICHIRO	p 3091	N95-32994
TANIS, JOHN	p 3207	N95-33219
TANNER, D.	p 3246	N95-32597
TAPIA, RICHARD A.	p 3182	N95-34598
TATES, JOHN T., JR.	p 3232	N95-34755
TATTERSALL, ANDREW J.	p 3174	N95-34777
TAUCHER-SCHOLZ, G.	p 3162	N95-32725
TAYLOR-MEYERS, SHARON	p 3087	N95-34649
TAYLOR, C.	p 3103	N95-33080
TAYLOR, C. E.	p 3214	N95-33504
TAYLOR, E. W.	p 3226	N95-32589
TAYLOR, ROBERT M.	p 3048	N95-34771
	p 3174	N95-34776
TAYLOR, S.	p 3073	N95-33289
TAYLOR, T.	p 3218	N95-34480
TAYLOR, T. S.	p 3222	N95-32756
TAYLOR, VALERIE E.	p 3209	N95-34212
TEILLET, P. M.	p 3136	N95-33771
TENENBAUM, P.	p 3212	N95-32657
	p 3215	N95-32658
TENKATE, HERMAN H. J.	p 3215	N95-33381
TENNANT, D. M.	p 3084	N95-33247
TEPIKIAN, S.	p 3210	N95-32413
TERVONEN, J.	p 3096	N95-32751
TESMER, JOSEPH R.	p 3203	N95-32577
	p 3208	N95-33623
THAKOOR, ANIL	p 3188	N95-32659
THAYER, GARY R.	p 3152	N95-32573
THOMAS, GERALD B.	p 3201	N95-34444
THOMAS, M. C.	p 3050	N95-32636
THOMAS, SCOTT KEITH	p 3109	N95-33257
THOMAS, TIMOTHY	p 3181	N95-33154
THOMPSON, DAVID E.	p 3184	N95-34225
THOMPSON, J. D.	p 3229	N95-33386
THOMPSON, K. A.	p 3213	N95-33338
THOMPSON, T. C.	p 3058	N95-32713
THORNE, R. S.	p 3214	N95-34653
THURNAUER, M. C.	p 3225	N95-32586
TICHENOR, D. A.	p 3084	N95-33247
TIDIRIRI, M. D.	p 3196	N95-33727
TIEDE, D. M.	p 3225	N95-32586
TIEU, A. K.	p 3190	N95-33004
TIGHE, R.	p 3246	N95-32597
TILLERY, LAURA S.	p 3165	N95-34573
TING, A.	p 3120	N95-34761
TKACZYK, J. E.	p 3230	N95-34213
TOHAMMAIAN, A.	p 3196	N95-34377
TOKUDA, SHINJI	p 3220	N95-32410
TONKS, D. L.	p 3125	N95-32385
TORAO, YOSHIMI	p 3037	N95-34529
TORCZON, VIRGINIA J.	p 3182	N95-34598
TORCZYNSKI, J. R.	p 3106	N95-32387
	p 3067	N95-32709
TORGERSON, WARREN	p 3170	N95-34376
TORNES, JOHN A.	p 3068	N95-33243
TORRELLAS, JOSEP	p 3182	N95-34455
TORUN, Y.	p 3205	N95-32652
TOTH, CYNTHIA A.	p 3164	N95-34789
TRAN, AN VAN	p 3243	N95-34242
TRAPP, D. J.	p 3079	N95-33215
TRBOJEVIC, D.	p 3210	N95-32413
	p 3212	N95-33067
TREJO, LEONARD J.	p 3166	N95-34356
TRENT, VICTOR S.	p 3122	N95-32692
TROIANO, EDWARD	p 3081	N95-34373
TROYER, G. L.	p 3155	N95-34435
TRUCANO, T. G.	p 3125	N95-32381
TRUMBORE, SUSAN E.	p 3143	N95-33498
TRUONG, C. M.	p 3231	N95-34486
TSAI, WEN-BIN	p 3065	N95-33721
TSUBAKIMOTO, KOJI	p 3090	N95-32989
TSUBOI, NOBUYUKI	p 3041	N95-34557
TSUGE, SHUNICHI	p 3036	N95-34522
	p 3041	N95-34555
TSUI, D. C.	p 3235	N95-34585
TSUKINO, NORIYUKI	p 3090	N95-32990
TSYBOULSKII, G. A.	p 3057	N95-33128
TUCKER, COMPTON J.	p 3135	N95-33766
TUCKER, STEPHENSON	p 3120	N95-34811
TUENGE, RICHARD T.	p 3229	N95-33401
TUEY, RICHARD C.	p 3237	N95-32922
TULI, J. K.	p 3202	N95-32484
TULUPOV, A.	p 3117	N95-32571
TURCHI, C.	p 3152	N95-32668
TURMAN, B. N.	p 3085	N95-34022
TURNBULL, A. D.	p 3222	N95-32756
TURNER, R.	p 3073	N95-33289
TUTTLE, BRUCE A.	p 3226	N95-32590
TYHURST, R. W.	p 3043	N95-32489
TYREE, VANCE C.	p 3104	N95-34345

U

UCHIDA, TAKASHI	p 3039	N95-34541
UGGERHOJ, E.	p 3204	N95-32584
UHRENIUS, B.	p 3068	N95-33229
UKAI, K.	p 3177	N95-32757
ULLRICH, J.	p 3228	N95-33373
UNDERWOOD, JOHN H.	p 3127	N95-34442
UPTON, S.	p 3096	N95-32751
URBANUS, W.	p 3117	N95-32571
URNES, JAMES M., SR.	p 3053	N95-33022
USTIN, S. L.	p 3133	N95-33758
	p 3135	N95-33765
	p 3135	N95-33768
UZELAC, Z.	p 3102	N95-32714

V

VANAYEV, A. P.	p 3094	N95-33141
VANBIBBER, K.	p 3246	N95-32597
VANCE, LARRY	p 3117	N95-33746
VANDAM, J.	p 3224	N95-33696
VANDENBOSCH, JEANNETTE	p 3117	N95-33754
	p 3117	N95-33797
VANDERBEEK, C. J.	p 3110	N95-33389
VANDERBORGH, NICHOLAS E.	p 3148	N95-32575
VANDERSANDE, JAN W.	p 3149	N95-32811
VANDIJK, M. J.	p 3157	N95-32891
VANLEHN, KURT	p 3235	N95-34743
VANOORT, JOHANNES M.	p 3215	N95-33381
VANWONTERGHEM, B. W.	p 3216	N95-33506
	p 3216	N95-33651
VANWONTERGHEM, BRUNO M.	p 3118	N95-33378
VANZYL, JAKOB	p 3139	N95-33801
	p 3139	N95-33803
	p 3142	N95-33815
VARTULI, C. B.	p 3226	N95-32594
	p 3223	N95-33412
VAVILOV, D. V.	p 3207	N95-33171
VAWTER, G. A.	p 3118	N95-32663
VENKATAKRISHNAN, V.	p 3196	N95-33500
VENUGOPALAN, RAJU	p 3208	N95-33854
VERAGUTH, S.	p 3136	N95-33770
VERDEBOUT, J.	p 3133	N95-33758
VERGARA, I.	p 3079	N95-33217
VERLY, JACQUES G.	p 3100	N95-34474
VIANCO, P. T.	p 3078	N95-32591
VIDIECAN, J.	p 3094	N95-33143
VIGIL, MANUEL B.	p 3185	N95-32771
VIGILANTE, GREGORY	p 3081	N95-34373
VIGLIALORO, G.	p 3043	N95-32488
VIJAY, D. P.	p 3082	N95-32710
VIKTOROV, V. A.	p 3207	N95-33171
VIMAN, L.	p 3121	N95-32612
VINOGRADOV, S. V.	p 3214	N95-34439
VISCO, STEVEN J.	p 3151	N95-34481
VITTER, JEFFREY S.	p 3101	N95-34790

VLASKO-VLASOV, V. K. p 3110 N95-33389
VOGT, R. p 3204 N95-32617
p 3204 N95-32619
VOLAKIS, J p 3097 N95-32822
VOLKOV, M. K. p 3233 N95-32405
VONIRMER, A. p 3070 N95-33274
p 3073 N95-33291
VOSSEN, JACK p 3149 N95-32813
VOTH, GREGORY A. p 3209 N95-34350
VUCHIC, BORIS V. p 3228 N95-32810

W

WADA, YASUHIRO p 3036 N95-34518
p 3036 N95-34520
p 3041 N95-34554
WAGENER, R. p 3153 N95-33192
WAGNER, ANDREW V. p 3081 N95-34482
WAGNER, DAN p 3172 N95-34767
WAGNER, ROBERT G. p 3213 N95-33406
WALKER, CONSTANCE KALBACH
p 3212 N95-32960
WALKER, D. W. p 3244 N95-34801
WALKUP, JOHN F. p 3219 N95-34579
WALSH, JOHN E. p 3239 N95-34219
WALTER, KEVIN C. p 3203 N95-32577
p 3208 N95-33623
WALTERS, G. K. p 3074 N95-33392
WALTON, J. T. p 3208 N95-33380
WAN, ZHENGMING p 3142 N95-32717
WANG, GUANGHOU p 3227 N95-32698
WANG, GUOHUA H. p 3055 N95-34806
WANG, HAO p 3065 N95-33710
WANG, J. R. p 3142 N95-33816
WANG, JINXUE p 3128 N95-33732
WANG, JUNBO p 3120 N95-34470
WANG, LI-SHUN p 3151 N95-34481
WANG, MICHAEL p 3218 N95-34504
WANG, MUYIN p 3157 N95-32933
WANG, N. W. p 3208 N95-33380
WANG, QUANMING p 3221 N95-32562
WANG, XIAO p 3035 N95-34510
WANG, XINDONG p 3080 N95-33700
WANG, Y. D. p 3207 N95-33241
WARCZAK, A. p 3228 N95-33373
WARD, JAMES p 3098 N95-33152
WARNER, A. p 3212 N95-33067
WARNER, HAROLD D. p 3056 N95-34362
WARNOCK, ROBERT L. p 3098 N95-33336
WARREN, M. E. p 3118 N95-32663
WARREN, WILLIAM L. p 3226 N95-32590
WARRIER, SUNIL GOVINDA p 3081 N95-34252
WASHBURN, ALAN R. p 3182 N95-34349
WATANABE, SHIGEYA p 3039 N95-34542
WATMUFF, JONATHAN H. p 3106 N95-32454
WATSON, G. P. p 3231 N95-34485
WATSON, LAYNE T. p 3193 N95-34600
WATSON, LLOYD D. p 3081 N95-34348
WAUCHOPE, KENNETH p 3236 N95-34487
WAY, JO BEA p 3240 N95-34224
WEAVER, JOHN H. p 3076 N95-34615
WEAVER, L. D. p 3120 N95-34592
WEBER, CARLOS p 3108 N95-33059
WEEKS, ROBERT A. p 3230 N95-34443
WEI, J. p 3210 N95-32413
p 3211 N95-32485
p 3212 N95-33067
WEI, JIE p 3210 N95-32411
WEI, RUEY-CHANG p 3200 N95-33251
WEI, YONGHUA p 3192 N95-33714
WEI, Z. p 3155 N95-32455
WEIDL, TIMO p 3196 N95-33234
WEINBERGER, P. p 3244 N95-34816
WEINSTEIN, A. p 3213 N95-33333
WEISS, R. p 3211 N95-32416
WEISS, S. p 3230 N95-33880
WEISS, STEVEN p 3056 N95-34342
WELLS, EDWARD A. p 3053 N95-33022
WELP, U. p 3110 N95-33389
WELSCH, H. p 3166 N95-34059
WENDT, J. R. p 3118 N95-32663
WENRICH, MELISSA L. p 3137 N95-33791
p 3139 N95-33800
WENTWORTH, SEAN L. p 3049 N95-34793
WENXIONG, LIN p 3117 N95-32472
p 3118 N95-32702
WERNLUND, ROGER F. p 3072 N95-33288
WESTFIELD, WILLIAM T. p 3049 N95-34583
WESTRUM, RON p 3174 N95-34778
WETTERER, CHARLES J. p 3246 N95-34753
WHEATCRAFT, D. p 3223 N95-33066
WHETSTONE, J. R. p 3050 N95-32636
WHITE, HENRY S. p 3075 N95-34357
WHITE, J. M. p 3225 N95-32579
WHITE, RONALD J. p 3161 N95-32719
WHITE, TIMOTHY R. p 3238 N95-33402
WHITE, W. E. p 3216 N95-33411
WHITEMAN, C. D. p 3158 N95-33505
WHITMAN, PAUL p 3058 N95-34744
WHITMORE, STEPHEN A. p 3181 N95-33193
WICHSLER, M. p 3203 N95-32576
WIEDMANN, MICHAEL H. p 3083 N95-32819
WIENANDS, U. p 3203 N95-32567
WILBAUX, FLORENCE p 3176 N95-34786
WILBUR, PAUL J. p 3083 N95-32918
WILCOX, FLOYD J., JR. p 3034 N95-32821
WILCOX, R. B. p 3216 N95-33506
p 3216 N95-33651
WILEY, J. C. p 3186 N95-33852
WILHELMSON, ROBERT p 3243 N95-34240
WILHELMSON, ROBERT B. p 3239 N95-34219
WILLIAMS, D. J. p 3136 N95-33771
WILLIAMS, J. G. p 3189 N95-32998
WILLIAMS, WARREN p 3057 N95-34815
WILLIAMSON, DON L. p 3083 N95-32918
WILLIS, M. p 3096 N95-32751
WILLS, L. A. p 3226 N95-32598
p 3229 N95-33636
WILSON, BLAKE FLEMING MICHAEL
p 3238 N95-33334
WILSON, JOHN R. p 3047 N95-34766
WINDT, D. L. p 3084 N95-33247
WINJE, ROBERT L. p 3201 N95-34424
WINN, D. R. p 3205 N95-32652
p 3205 N95-32654
WINTER, L. p 3179 N95-32715
WIRTZ, M. M. p 3043 N95-32489
WISE, JOHN A. p 3171 N95-34764
p 3171 N95-34765
WISE, MARK A. p 3171 N95-34765
WOLFRAMM, A. P. p 3093 N95-33137
WOLPERT, D. p 3187 N95-32375
WONG, C. C. p 3106 N95-32818
WONG, J. p 3213 N95-33333
WONG, K. L. p 3206 N95-32763
p 3208 N95-33374
WONG, S. K. p 3188 N95-32997
WOO, WOONTAEK p 3091 N95-32993
WOOD, E. H. p 3166 N95-34058
WOOD, E. L. p 3075 N95-34440
WOOD, R. F. p 3119 N95-34466
WOODWARD, ROBERT H. p 3158 N95-32545
WORKMAN, GARY L. p 3066 N95-32581
WRIGHT, J. S. p 3206 N95-32814
WRIGHT, MELANIE C. p 3047 N95-34797
WROBLESKI, WILLIAM J. p 3211 N95-32647
WRONSKI, W. p 3102 N95-32629
WU, JIE p 3105 N95-34758
WU, RUQIAN p 3075 N95-34483
WU, W. p 3203 N95-32564
p 3206 N95-32763
p 3208 N95-33374
WU, XILIN p 3227 N95-32643
WU, ZHOULING p 3217 N95-34298
WYNNE, KENNETH J. p 3087 N95-34649

X

XIA, S. p 3190 N95-33006
XIA, ZHIYONG CEDRIC p 3063 N95-32775
XIBIN, GUO p 3118 N95-32702
XIE, HUAJUN p 3121 N95-32690
p 3122 N95-32691
XIE, Y. H. p 3229 N95-33628
XINGLI, TANG p 3119 N95-34380
XU, BINGHUO p 3215 N95-32701
XU, DAOPING p 3112 N95-34286
XU, J. p 3125 N95-32392
XU, LIU p 3218 N95-34471
XU, PUNG p 3136 N95-33773
XUEQUN, HU p 3086 N95-34563

Y

YAGI, Y. p 3223 N95-33221
YAKOVCHENKO, S. G. p 3222 N95-32770
YAMADA, YOJI p 3182 N95-34455
YAMAKAWA, MASASHI p 3035 N95-34515
YAMAMOTO, KIYOSHI p 3037 N95-34523
p 3038 N95-34530
YAMAMOTO, YUKIMITSU p 3036 N95-34520
p 3039 N95-34542
YAMANE, TAKASHI p 3038 N95-34536
YAMANE, YOSHIYUKI p 3035 N95-34512
YAMANISHI, TOSHIHIKO p 3220 N95-32409
YAMAZAKI, TETSUO p 3039 N95-34541
YAN, Y. T. p 3213 N95-33335
YANAGIZAWA, MITSUNORI p 3037 N95-34524
p 3041 N95-34552
YANG, AN-JEN p 3191 N95-33324
YANG, GAO p 3217 N95-34297
YANG, GUANGJI p 3158 N95-34757
YANG, KI HO p 3066 N95-32566
YAO, MINWU p 3089 N95-32718
YAO, X. p 3190 N95-33004
YE, ZHENG-YIN p 3106 N95-32787
YEH, G. T. p 3179 N95-32543
YEONG, MENGYIK p 3181 N95-33325
YI, JONG HOON p 3066 N95-32566
YI, SU p 3100 N95-34762
YOKOO, NORIKO p 3221 N95-32565
YOON, BYUNG JOO p 3223 N95-33619
YOON, GEUN YOUNG p 3090 N95-32988
YOON, JAE SUNG p 3223 N95-33619
YOON, SUNG H. p 3189 N95-33002
YOSHIDA, MASAHIRO p 3038 N95-34531
p 3038 N95-34533
p 3040 N95-34547
YOSHIDA, YASUO p 3041 N95-34554
YOSHIOKA, MINAKO p 3036 N95-34520
YOSHIZAWA, H. p 3225 N95-32377
YOST, DOUGLAS M. p 3086 N95-34494
YU, CHENG p 3217 N95-34459
YU, NING p 3203 N95-32577
p 3208 N95-33623
YU, PETER Y. p 3230 N95-33865
YUAN, V. W. p 3211 N95-32416
YUAN, WENLIN p 3221 N95-32562
YUE, SHIXIAO p 3120 N95-34470
YUEMEI, LU p 3219 N95-34759
YUEYING, YU p 3061 N95-34302
YUMING, CHEN p 3086 N95-34563

Z

ZAJFMAN, D. p 3209 N95-34355
ZAKANY, JAMES S. p 3088 N95-33876
ZAKHAREV, B. N. p 3225 N95-32480
ZALEWSKI, E. p 3116 N95-33733
ZAMORA, DIEGO p 3104 N95-33915
ZANEVELD, J. R. p 3219 N95-34576
ZARIKIAN, V. p 3194 N95-32388
ZELENKA, RICHARD E. p 3043 N95-32490
ZELTZER, DAVID L. p 3166 N95-34610
ZEMEL, JAY N. p 3097 N95-33061
ZERNER, MICHAEL C. p 3067 N95-32804
ZHANG, BINGQUAN B. p 3215 N95-32660
ZHANG, M. H. p 3135 N95-33768
ZHANG, SEN p 3048 N95-32928
ZHANG, XIAOYING p 3123 N95-33252
ZHANG, Y. p 3225 N95-32586
ZHANG, YANSI p 3112 N95-34343
ZHANG, YI p 3165 N95-34472
ZHANG, ZIYANG p 3206 N95-32965
ZHAO, GUOZHEN p 3215 N95-32701
ZHAO, MING p 3189 N95-33000
ZHAO, XIANG p 3126 N95-33253
ZHENG, PENG p 3073 N95-33290
ZHENGDONG, ZENG p 3117 N95-32472
ZHENGDONG, ZHENG p 3118 N95-32702
ZHENGGUO, LU p 3120 N95-34469
ZHENGXIU, FAN p 3217 N95-34297
ZHESTKOV, Y. G. p 3205 N95-32630
ZHIJIANG, WANG p 3217 N95-34297
ZHILTSOV, V. E. p 3102 N95-32628
ZHONGLIANG, LU p 3100 N95-34762
ZHOU, JIANGYING p 3244 N95-34804
ZHOU, P. p 3198 N95-32525
ZHOU, YUPING p 3117 N95-32472
p 3118 N95-32702
ZHOU, ZHEN-LEI p 3194 N95-34807
ZHOULING, WU p 3217 N95-34297
ZHU, B. p 3180 N95-32716
ZHU, H. D. p 3062 N95-33835
ZIEMNIAK, S. E. p 3234 N95-34211
ZIMIN, SERGEI p 3202 N95-32529
ZIMMERMAN, R. L. p 3218 N95-34480
ZIMMERMANN, F. p 3213 N95-33338
ZIMMERMANN, H. p 3161 N95-32724
ZIMMERMANN, REINER p 3141 N95-33812
ZINKLE, S. J. p 3074 N95-33629
ZINNER, ERNST p 3246 N95-32913
ZIOLKOWSKI, RICHARD W. p 3216 N95-34020
ZOLOTOREV, M. p 3203 N95-32567
ZOLPER, J. C. p 3226 N95-32594
p 3118 N95-32663
p 3186 N95-33838
ZOUGHI, R. p 3125 N95-34346
ZRELOV, P. V. p 3187 N95-32476
ZSCHACK, P. p 3233 N95-34802
ZUERNDORFER, B. W. p 3096 N95-32773
ZUHR, RAYMOND A. p 3230 N95-34443
ZUIKER, C. D. p 3230 N95-34215
ZUKIN, JANET H. p 3135 N95-33766

ZVARA, I. ..... p 3164 N95-32666
ZWICK, HAROLD ..... p 3129 N95-33738

CORPORATE SOURCE INDEX

Typical Corporate Source Index Listing

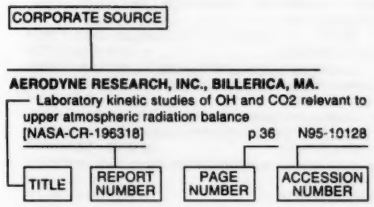

Listings in this index are arranged alphabetically by corporate source. The title of the document provides the user with a brief description of the subject matter. The report number helps to indicate the type of document cited (e.g., NASA report, translation, NASA contractor report). The accession number denotes the number by which the citation is identified. The page number helps you locate the citation in the abstract section. The titles are arranged under each corporate source in ascending accession number order.

A

ACADEMY OF SCIENCES (USSR), NOVOSIBIRSK (USSR).
Vacuum polarization correction to the positronium decay rate
[DE95-614164] p 3202 N95-32481

Bernstein-Green-Kruskal wave. 2: The interaction with the Langmuir wave. Stochastic phenomena
[DE95-614202] p 3220 N95-32507

Conversion of the Bernstein-Green-Kruskal wave on the density perturbation, part 1
[DE95-614203] p 3220 N95-32508

Conversion of the Bernstein-Green-Kruskal wave on the density perturbation, part 3
[DE95-614205] p 3221 N95-32509

Conversion of the Bernstein-Green-Kruskal wave on the density perturbation, part 4
[DE95-614206] p 3221 N95-32510

On the paraxial equilibrium of the finite (beta) plasma in open magnetic configurations
[DE95-614170] p 3221 N95-32560

Radial electric field measurement in a tokamak by the injection of a pulsed neutral beam
[DE95-614176] p 3221 N95-32561

HF-stabilization of plasma with sharp boundary
[DE95-614207] p 3222 N95-32770

ACTION RECHERCHES APPLICATION MATRA IRIT EN INTERFACE HOMME SYSTEME (FRANCE).
Improving air traffic control: Proving new tools or approving the joint human-machine system?
p 3176 N95-34783

ADVANCED DEVICE TECHNOLOGIES, INC., CHARLOTTESVILLE, VA.
Novel field effect transistors for low power electronics
[AD-A294221] p 3105 N95-34458

ADVANCED FUEL RESEARCH, INC., EAST HARTFORD, CT.
Novel ferroelectric heterostructures for high-density DRAMS
[AD-A294517] p 3199 N95-34477

ADVISORY GROUP FOR AEROSPACE RESEARCH AND DEVELOPMENT, NEUILLY-SUR-SEINE (FRANCE).
Low-Level and Nap-of-the-Earth (NOE) night operations
[AGARD-CP-563] p 3042 N95-32486

Dual Usage in Military and Commercial Technology in Guidance and Control
[AGARD-CP-556] p 3091 N95-33126

AGARD index of publications: 1992-1994
[AGARD-INDEX-92-94] p 3237 N95-33198

Current Concepts on G-Protection Research and Development
[AGARD-LS-202] p 3168 N95-34050

AERODATA FLUGMESSTECHNIK G.M.B.H., BRUNSWICK (GERMANY).
Integrated special mission flight management for a flight inspection aircraft p 3049 N95-33145

AERODYNE RESEARCH, INC., BILLERICA, MA.
Infrared detection of chemical corrosion on metal surface
[AD-A295000] p 3081 N95-34821

AEROJET-GENERAL CORP., SACRAMENTO, CA.
SSME Post Test Diagnostic System: Systems Section
[NASA-CR-198375] p 3061 N95-34625

AERONAUTICA MILITARE ITALIANA, ROME.
Fixed wing night attack missions: Assessment in a Flight Simulation environment p 3045 N95-32502

AEROSPACE CORP., EL SEGUNDO, CA.
Identification of critical substorm-expansion-phase phenomena: Problems addressable with GEM observations
[ATR-94(7270)-1] p 3158 N95-33259

A distributed Clips implementation: dClips
p 3243 N95-34243

Iron Boltzmann factor LIDAR: Proposed new remote-sensing technique for mesospheric temperature
[AD-A293568] p 3157 N95-34613

AEROSYSTEMS INTERNATIONAL, YEOVIL (ENGLAND).
Does human cognition allow Human Factors (HF) certification of advanced aircrew systems?
p 3174 N95-34776

AIN SHAMS UNIV., CAIRO (EGYPT).
The 3rd international conference on solar energy storage and applied photochemistry
[AD-A294343] p 3150 N95-34359

The international conference on solar energy storage and applied photochemistry
[AD-A294347] p 3150 N95-34360

AIR-CONDITIONING AND REFRIGERATION TECHNOLOGY INST., INC., ARLINGTON, VA.
Thermophysical properties of HCFC alternatives
[DE95-009635] p 3233 N95-32661

AIR FORCE INST. OF AVIATION AND SPACE MEDICINE, MOSCOW (RUSSIA).
Selection and special physiological training of flying personnel to high +G(z)-maneuverable flights-main concept p 3166 N95-34053

Increase of High-sustained +G(z) tolerance at the expense of pilot's working posture change
p 3165 N95-34056

AIR FORCE INST. OF TECH., WRIGHT-PATTERSON AFB, OH.
Applications of organic and polymer nonlinear optical materials in optics computations
[AD-A293088] p 3215 N95-32957

Triple invariant optical pattern recognition using circular harmonic synthetic filters
[AD-A294253] p 3217 N95-34459

Thermal control technology of communications satellite
[AD-A294249] p 3059 N95-34493

Ion assisted deposition of ZnS and MgF2
[AD-A294759] p 3086 N95-34563

The effects of display location and dimensionality on taxiway navigation
[AD-A294878] p 3047 N95-34570

RR lyrae variable stars in the CCD/Transit instrument survey
[AD-A294138] p 3246 N95-34753

AIR FORCE OCCUPATIONAL MEASUREMENT CENTER, RANDOLPH AFB, TX.
Aerospace physiology AFSC 4M0X1
[AD-A294839] p 3165 N95-34564

AIR FORCE OFFICE OF SCIENTIFIC RESEARCH, BOLLING AFB, WASHINGTON, DC.
Air force office of scientific research. Research proposal
[AD-A293401] p 3252 N95-32473

AIR FORCE SYSTEMS COMMAND, WRIGHT-PATTERSON AFB, OH.
Influence of CO2 continuous laser preprocessed substrates on optical thin film damage thresholds
[AD-A294190] p 3217 N95-34297

TiO2/SiO2 and ZrO2/SiO2 multilayer media film optical loss and laser damage study
[AD-A294192] p 3217 N95-34298

Stimulated rotational Raman scattering of N2 in the atmosphere
[AD-A294195] p 3157 N95-34299

The development of some kinds of LRE injectors
[AD-A294199] p 3061 N95-34302

Using photothermal deflection techniques for studying the attenuations of guided waves propagated in optical thin films
[AD-A294203] p 3217 N95-34303

Successful development of first-generation laser device; marking China's optoelectronic technology at world class level
[AD-A294206] p 3217 N95-34305

Recent developments in maritime technology research institute acousto-optical technology research
[AD-A294215] p 3217 N95-34307

High power CO2 laser windows and reflection reducing coatings
[AD-A294217] p 3119 N95-34308

Using optical interference methods to measure acousto-optical device thermal effects
[AD-A294219] p 3217 N95-34309

Programmable real-time optoelectronic hybrid threshold logic processors
[AD-A294067] p 3104 N95-34379

A multi-wavelength dye laser system
[AD-A294068] p 3119 N95-34380

A 30-pair thin film thermoelectric pile
[AD-A294058] p 3151 N95-34468

Pulsed tunable narrow-bandwidth dye laser, with hollow circular waveguide in cavity
[AD-A294060] p 3120 N95-34469

Atmospheric attenuation properties associated with CO2 laser radiation spectra
[AD-A294061] p 3120 N95-34470

Effect of propagation attenuation of thin film waveguide on optical thin film losses
[AD-A294064] p 3218 N95-34471

England develops world's fastest optic switch breakthrough in high-speed communications
[AD-A294038] p 3105 N95-34488

Study of a large optical/infrared telescope scheme
[AD-A294042] p 3218 N95-34490

Diagnosis of frontogenesis of Meiyu front
[AD-A294043] p 3158 N95-34491

Thermal design of returnable satellites
[AD-A294113] p 3059 N95-34500

Applied research on liquid crystal spatial modulators in Hadamard transform spectrometers. Quick and accurate decoding methods
[AD-A294152] p 3219 N95-34756

Intra-annual and inter-annual rainfall variability over East Asia, Southeast Asia, and South Asia
[AD-A294156] p 3158 N95-34757

Optical logic implementation in composite biled/bild circuits
[AD-A294160] p 3105 N95-34758

Development of 1.06 micron high efficiency antireflective coating
[AD-A294161] p 3219 N95-34759

INMARSAT TT&C and communications network and the Beijing INMARSAT Station
[AD-A294163] p 3100 N95-34760
Experimental investigation of impulse radar for mitigation of effects of radar absorbing materials
[AD-A294166] p 3100 N95-34762

AKRON UNIV., AKRON, OH.
Laminar heat transfer for power-law fluids in thermal entrance region of annular sector ducts
p 3108 N95-33255

ALABAMA UNIV., BIRMINGHAM, AL.
Advanced precision expendable pattern casting technology
[DE95-012200] p 3095 N95-33393

ALABAMA UNIV., HUNTSVILLE, AL.
Study of the space environmental effects on spacecraft engineering materials
[NASA-CR-199090] p 3066 N95-32581
Thermocapillary flow with evaporation and condensation and its effect on liquid retention in low-g fluid acquisition devices p 3109 N95-33256

ALABAMA UNIV., TUSCALOOSA, AL.
Penetrable wedge analysis
[AD-A294276] p 3234 N95-34464

ALENIA AERONAUTICA, TURIN (ITALY).
An integrated system for air to ground operations
p 3044 N95-32498

ALLIED-SIGNAL AEROSPACE CO., KANSAS CITY, MO.
Development of environmentally conscious cleaning process for leadless chip carrier assemblies
[DE95-010186] p 3154 N95-33638
Characterization of DuPont 9015, aqueous processable dry film photoresist for printed wiring boards
[DE95-011239] p 3103 N95-33864

ALLISON ENGINE CO., INDIANAPOLIS, IN.
Allison engine testing CMSX-4(reg sign) single crystal turbine blades and vanes
[DE95-010308] p 3050 N95-32636

ALUMINUM CO. OF AMERICA, ALCOA CENTER, PA.
Lightweight alumina refractory aggregate. Phase 2: Pilot scale development
[DE95-012154] p 3083 N95-33079

AMES LAB., IA.
Development of improved p-type Si-20 at. %Ge by addition of fullerite
[DE95-010230] p 3066 N95-32394
A numerical analysis of fracture and high temperature creep characteristics of composites with discontinuous ductile reinforcements
[DE95-010236] p 3062 N95-32395
Fabrication of improved SiGe alloys for an 18-couple module test
[DE95-010238] p 3060 N95-32396
Anisotropic magnetization of HoNi2B2C
[DE95-010239] p 3198 N95-32397
HINT: A new way to measure computer speed
[DE95-010245] p 3177 N95-32398
Spin counting in dipolar coupled spin 1/2 systems by multiple quantum NMR spectroscopy in solids: Development of a single quantum propagator and its application to heterogeneous catalysis
[DE95-010246] p 3066 N95-32540
Reactions of trifluoroiodomethane on metal surfaces
[DE95-010122] p 3078 N95-32638
Synthesis of potential new Zintl phases
[DE95-010123] p 3227 N95-32640
Thermal rearrangement of oxygen-containing (omicron)-allyl benzene derivatives
[DE95-010124] p 3067 N95-32641
Photoemission study of some novel materials: Rare earth/transition metal interface, Ba*(0.6)*K*(0.4)*BiO3* and AlPdMn
[DE95-010125] p 3227 N95-32643
Angular dependence of magnetic properties of steels under uniaxial stress
[DE95-010189] p 3078 N95-32648
Peak effect and flux pinning in YBa2Cu3O(7-(delta)) single crystals
[DE95-010126] p 3228 N95-32959
Optical anisotropy of (110) surfaces of Ag and Cu
[DE95-010130] p 3229 N95-33637
Measurement and modelling of structure sensitive magnetic properties of material
[DE95-010128] p 3080 N95-33699
Theory of magneto-optics and circular magnetic x-ray dichroism
[DE95-010129] p 3080 N95-33700

ANALYTIC SCIENCES CORP., SAN ANTONIO, TX.
Ultrashort pulse laser effects in the primate eye
[AD-A295024] p 3164 N95-34789

APPLIED RESEARCH CORP., LANDOVER, MD.
ROSAT survey of emission from Be stars
[NASA-CR-199086] p 3245 N95-32835

ARGONNE NATIONAL LAB., IDAHO FALLS, ID.
Analysis of metallic fuels by laser ablation
[DE95-012465] p 3075 N95-34440

ARGONNE NATIONAL LAB., IL.
Summary report for ITER Task No. T226B: Evaluation of ITER disruption erosion
[DE95-010402] p 3219 N95-32401
Alternative catalyst and exhaust gas sensor work at Argonne National Laboratory
[DE95-007136] p 3152 N95-32553
Conversion of holes into reducing species on surface modified small-particle TiO2
[DE95-008282] p 3225 N95-32586
Epitaxial Pb(Zr(x)Ti(1-x))O3/SrRuO3 (x = 0, 0.35, 0.65) multilayer thin films on SrTiO3(100) and MgO(100) prepared by MOCVD and RF sputtering
[DE95-008288] p 3226 N95-32598
Tests of adhesives used for plate bonding of ATLAS tile-cal hadron calorimeter
[DE95-009917] p 3082 N95-32664
Efficiency of modified UA1 jet reconstruction algorithm in PP, PA and AA collisions at STAR
[DE95-009918] p 3212 N95-32665
Detection of emission sources using passive-remote Fourier Transform Infrared spectroscopy
[DE95-009920] p 3067 N95-32671
YBa2Cu3O(7-x) 45 deg (001) tilt grain boundaries induced by controlled low-energy sputtering of MgO substrates: Transport properties and atomic-scale structure
[DE95-005826] p 3228 N95-32810
Lessons learned in acquiring new regulations for shipping advanced electric vehicle batteries
[DE95-009908] p 3102 N95-32956
Effect of lead content on Bi-2223 formation by a two-powder process
[DE95-009889] p 3079 N95-33215
Computational electromagnetics and parallel dense matrix computations
[DE95-012286] p 3099 N95-33379
Theoretical dynamical studies of metal clusters and cluster-ligand systems
[DE95-012461] p 3228 N95-33382
The interaction of vortices with twin boundaries
[DE95-012079] p 3110 N95-33389
The nature and fate of natural resins in the geosphere 6: Analysis of fossil resins from Axel Heiberg Island Canadian Arctic
[DE95-012212] p 3154 N95-33394
Alternative-fuels technology: Natural gas vehicles as a way to curb urban air pollution
[DE95-012216] p 3088 N95-33395
Epitaxial Pb(Zr(0.40)Ti(0.60))O3/SrRuO3 and PbTiO3/SrRuO3 multilayer thin films prepared by MOCVD and RF sputtering
[DE95-007146] p 3229 N95-33636
The choice: Welding with CO2 or Nd:YAG lasers
[DE95-011825] p 3124 N95-33834
Wavelet analysis of atmospheric turbulence structures: What can we gain from this new technique?
[DE95-011955] p 3156 N95-33847
Parallel molecular dynamics: Communication requirements for massively parallel machines
[DE95-012948] p 3209 N95-34212
In situ surface roughness measurement during PECVD diamond film growth
[DE95-013411] p 3230 N95-34215

ARIZONA STATE UNIV., FLAGSTAFF, AZ.
Laboratory and numerical modeling of topographic effects on time-dependent ocean currents
[AD-A294920] p 3160 N95-34594

ARIZONA STATE UNIV., TEMPE, AZ.
Development of a composite tailoring procedure for airplane wing
[NASA-CR-199081] p 3048 N95-32928
Preliminary study of Kelso Dunes using AVIRIS, TM, and AIRSAR p 3136 N95-33773
Urban remote sensing applications: TIMS observations of the City of Scottsdale p 3137 N95-33791
For geological investigations with airborne thermal infrared multispectral images: Transfer of calibration from laboratory spectrometer to TIMS as alternative for removing atmospheric effects p 3137 N95-33792
Aerolian erosion, transport, and deposition of volcaniclastic sands among the shifting sand dunes, Christmas Lake Valley, Oregon: TIMS image analysis p 3137 N95-33793
A conflict of water and fire: Remote sensing imagery of the Uinkaret Volcanic Field, Grand Canyon, Arizona p 3117 N95-33795
Discrimination of alkalinity in granitoid Rocks: A potential TIMS application p 3138 N95-33798
A field- and laboratory-based quantitative analysis of alluvium: Relating analytical results to TIMS data p 3139 N95-33800
New observations of Bolivian wind streaks by JPL Airborne SAR: Preliminary results p 3139 N95-33802

ARIZONA UNIV., TUCSON, AZ.
Perpendicular magnetic behavior of ultra-thin Co sandwiches
[DE95-010611] p 3083 N95-32819
Unusual behavior in the magnetic anisotropy of ultra-thin Co sandwiches: The role of Au underlayers
[DE95-010612] p 3229 N95-33641
Discrete modeling of optical pulse propagation in nonlinear media
[DE95-011515] p 3216 N95-34020
Multilayer optics for soft x-rays
[AD-A295030] p 3219 N95-34791
Growth and structure of MBE-Deposited iridium silicide
[AD-A295033] p 3232 N95-34792

ARMSTRONG LAB., BROOKS AFB, TX.
G-protection basis/acceleration physiology
p 3168 N95-34051

ARMY AEROMEDICAL RESEARCH LAB., FORT RUCKER, AL.
OH-58 pilot display unit (PDU) simulated crash tests
[AD-A294049] p 3170 N95-34378
Evaluating the potential for rotation and loss of flight helmets from inertia and impact loads
[AD-A294041] p 3170 N95-34489
User acceptability and comfort of the communications earplug (CEP) when used in the UH-1 helicopter
[AD-A294047] p 3170 N95-34492
Evaluation of a retrofit OH-58 pilot's seat to prevent back injury
[AD-A294895] p 3171 N95-34574
Transmittance characteristics of US Army rotary-wing aircraft transparencies
[AD-A295035] p 3049 N95-34793

ARMY ARMAMENT RESEARCH, DEVELOPMENT AND ENGINEERING CENTER, PICATINNY ARSENAL, NJ.
Anechoic chamber upgrade
[AD-A294375] p 3056 N95-34342

ARMY ARMAMENT RESEARCH, DEVELOPMENT AND ENGINEERING CENTER, WATERVLIET, NY.
Fracture toughness assessment of present and future pressure vessel materials based on Charpy impact energy and yield strength
[AD-A294008] p 3081 N95-34373

ARMY COLD REGIONS RESEARCH AND ENGINEERING LAB., HANOVER, NH.
Bibliography on cold regions science and technology: Volume 48, part 1
[AD-A293988] p 3243 N95-34420
Bibliography on cold regions science and technology: Volume 48, part 2
[AD-A293993] p 3243 N95-34421

ARMY COMMUNICATIONS-ELECTRONICS COMMAND, FORT MONMOUTH, NJ.
Tactical low-level helicopter communications
p 3043 N95-32492

ARMY ENGINEER WATERWAYS EXPERIMENT STATION, VICKSBURG, MS.
The CE-QUAL-ICM three-dimensional eutrophication model, release version 1.0
[AD-A294258] p 3160 N95-34461
Grayling 2 information base for generation of synthetic thermal infrared scenes
[AD-A294956] p 3100 N95-34578

ARMY MEDICAL RESEARCH AND DEVELOPMENT COMMAND, FORT DETRICK, MD.
Tri-service perspectives on microclimate cooling of protective clothing in the heat
[AD-A294005] p 3170 N95-34370

ARMY NIGHT VISION LAB., FORT BELVOIR, VA.
Development and flight testing of an Obstacle Avoidance System for US Army helicopters p 3045 N95-32500

ARMY RESEARCH AND DEVELOPMENT GROUP (EUROPE), FPO NEW YORK, NY.
Conference proceedings of mathematical methods in electromagnetic theory
[AD-A291165] p 3097 N95-32797

ARMY RESEARCH INST. OF ENVIRONMENTAL MEDICINE, NATICK, MA.
A prototype computer program that integrates predictive models and medical handbooks for altitude, cold exposure, and heat stress
[AD-A294006] p 3182 N95-34371
General procedure for clothing evaluations relative to heat stress
[AD-A294953] p 3171 N95-34577

ARMY RESEARCH LAB., ABERDEEN PROVING GROUND, MD.
A comparison of monocular, biocular, and binocular night vision goggles for traversing off-road terrain on foot
[AD-A294018] p 3170 N95-34376
The relationship of chemical structure to supercritical-fluid solubility and to cosolvent-modifier properties: A literature review
[AD-A294933] p 3076 N95-34599

ARMY RESEARCH LAB., ADELPHI, MD.
Focus of attention in decision support systems
[AD-A294037] p 3236 N95-34487
Environment and circuit model for capacitor-based rail guns
[AD-A293455] p 3057 N95-34815
ARMY RESEARCH LAB., CLEVELAND, OH.
Experimental and analytical assessment of the thermal behavior of spiral bevel gears
[NASA-TM-107009] p 3123 N95-33179
ARMY RESEARCH LAB., FORT MONMOUTH, NJ.
High rate rechargeable lithium cells employing lithium ion conducting solid electrolytes
[AD-A294390] p 3104 N95-34347
Poisson's ratio for tetragonal crystals
[AD-A293544] p 3232 N95-34607
Poisson's ratio for cubic crystals
[AD-A293549] p 3232 N95-34608
ARMY RESEARCH LAB., WATERTOWN, MA.
Investigation of aging effects from high voltage profiles in ceramic phase shifter materials
[AD-A289985] p 3082 N95-32694
ARMY WAR COLL., CARLISLE BARRACKS, PA.
A curriculum for strategy in the information age: Chaos in a new era
[AD-A295036] p 3244 N95-34794
ARNOLD ENGINEERING DEVELOPMENT CENTER, ARNOLD AFS, TN.
Subscale study of engine bellmouth inlet vortices in test cell R1D
[AD-A294993] p 3113 N95-34818
ASTRALUX, INC., BOULDER, CO.
Growth of GaN single-crystal boules
[AD-A294976] p 3232 N95-34588
AUBURN UNIV., AL.
Influence of backup bearings and support structure dynamics on the behavior of rotors with active supports
[NASA-CR-199080] p 3121 N95-32689
Dynamic behavior of a magnetic bearing supported jet engine rotor with auxiliary bearings
p 3122 N95-32691
Dynamic modelling and response characteristics of a magnetic bearing rotor system with auxiliary bearings
p 3122 N95-32692
Synchronous dynamics of a coupled shaft/bearing/housing system with auxiliary support from a clearance bearing: Analysis and experiment
p 3122 N95-32693
An experimental and analytical investigation into the performance of centrifugal pumps operating with air-water mixtures p 3123 N95-33323
AUSTRIAN ROAD SAFETY BOARD (AUSTRIA).
Towards a framework of human factors certification of complex human-machine systems p 3175 N95-34779

B

BABCOCK AND WILCOX CO., ALLIANCE, OH.
Development of a prototype lignin concentration sensor
[DE95-010951] p 3074 N95-33705
BALDWIN INTERNATIONAL SERVICES, HEFFINGEN (LUXEMBOURG).
The successful management of programs for human factors certification of advanced aviation technologies
p 3175 N95-34780
BARRINGER RESEARCH LTD., REXDALE (ONTARIO).
Environment applications for ion mobility spectrometry
p 3071 N95-33275
BATTELLE MEMORIAL INST., COLUMBUS, OH.
Resource document for the design of electronic instrument approach procedure displays
[AD-A295108] p 3047 N95-34797
BAYLOR COLL. OF MEDICINE, HOUSTON, TX.
Immunological protection against botulinum neurotoxin by a synthetic vaccine
[AD-A294146] p 3165 N95-34754
BOEING DEFENSE AND SPACE GROUP, SEATTLE, WA.
Operation of the computer model for microenvironment atomic oxygen exposure
[NASA-CR-198190] p 3059 N95-33264
Operation of the computer model for microenvironment solar exposure
[NASA-CR-198189] p 3059 N95-33890
BOSTON UNIV., BOSTON, MA.
Development of a tool-set for simultaneous, multi-site observations of astronomical objects
p 3239 N95-34221
BRANDEIS UNIV., WALTHAM, MA.
High performance compression of science data
p 3242 N95-34237
BRITISH AEROSPACE AIRCRAFT GROUP, PRESTON (ENGLAND).
Optimum Routeing: Analytical constraint of search space p 3044 N95-32493
BRITISH COLUMBIA UNIV., VANCOUVER (BRITISH COLUMBIA).
Terrain classification using circular polarimetric features p 3140 N95-33809
BROOKHAVEN NATIONAL LAB., UPTON, NY.
Cylindrical shell buckling through strain hardening
[DE95-009545] p 3125 N95-32392
Crystalline beam properties as predicted for the storage rings ASTRID and TSR
[DE95-011557] p 3210 N95-32411
The RHIC transfer line cable database
[DE95-011560] p 3236 N95-32412
The effect and correction of coupling generated by the RHIC triplet quadrupoles
[DE95-011562] p 3210 N95-32413
Linear orbit parameters for the exact equations of motion
[DE95-011567] p 3210 N95-32414
Evaluated nuclear structure data file
[DE95-011343] p 3202 N95-32484
Estimation of collective instabilities in RHIC
[DE95-011347] p 3211 N95-32485
Comparison of the Wang and Wachsmuth models for (pi) production with measurements at 12 GeV/c
[DE95-010417] p 3203 N95-32542
Strangeness from hadronic processes
[DE95-010311] p 3205 N95-32651
Targets and magnetic elements for pion collection in muon collider drivers
[DE95-010316] p 3205 N95-32652
A possible ionization cooling experiment at the AGS
[DE95-010317] p 3205 N95-32654
Effects of enhanced chromatic nonlinearity during the AGS gamma(t)-jump
[DE95-011703] p 3212 N95-33067
Comparison of seasonal and zonal patterns of the direct and indirect radiative forcing of climate by aerosols
[DE95-010896] p 3153 N95-33192
Hadron distributions at higher rapidity using the BRAHMS forward spectrometer
[DE95-008861] p 3207 N95-33203
Beam dynamics group summary
[DE95-008865] p 3213 N95-33204
Overview of rare K decays
[DE95-012081] p 3208 N95-33850
Enhanced shortwave cloud radiative forcing due to anthropogenic aerosols
[DE95-013319] p 3156 N95-34214
BROWN UNIV., PROVIDENCE, RI.
High order accuracy computational methods in aerodynamics using parallel architectures
[AD-A294167] p 3042 N95-34763
BRUNEL TECHNICAL COLL., BRISTOL (ENGLAND).
Application of Ni-63 photo and corona discharge ionization for the analysis of chemical warfare agents and toxic wastes p 3070 N95-33272
IMS software developments for the detection of chemical warfare agent p 3072 N95-33287
BULSTRODE TECHNOLOGY, HEMPSTEAD (ENGLAND).
Engineering approaches and compromises in the design of small ion mobility spectrometers
p 3070 N95-33271
BUREAU DES SYSTEMES D'ARMES, (FRANCE).
Night attack p 3042 N95-32487
BUREAU ENQUETES ACCIDENTS, PARIS (FRANCE).
Some inadequacies of the current human factors certification process of advanced aircraft technologies
p 3176 N95-34785
BURTON TECHNOLOGIES, INC., RALEIGH, NC.
Wear resistant composite structure of vitreous carbon containing convoluted fibers
[DE95-011463] p 3063 N95-33062

C

CALIFORNIA INST. OF TECH., PASADENA, CA.
Multivariate statistical analysis software technologies for astrophysical research involving large data bases
p 3240 N95-34222
Spectrum allocation strategies for communication networks
[AD-A294936] p 3100 N95-34601
CALIFORNIA UNIV., BERKELEY, CA.
A fundamental study of smoldering with emphasis on experimental design for zero-G
[NASA-CR-198378] p 3089 N95-32929
Construction of a connectionist network supercomputer
[AD-A294198] p 3177 N95-34301
Non-smooth optimization algorithms, system theory and software tools
[AD-A294944] p 3183 N95-34605
CALIFORNIA UNIV., BERKELEY. LAWRENCE BERKELEY LAB, CA.
Photon echoes from the absorption continuum of a semiconductor
[DE95-011274] p 3101 N95-32596
Observation of intraband coherence in the nonlinear optical response of gallium arsenide
[DE95-011281] p 3227 N95-32600
Intrinsic charm contribution to double quarkonium hadroproduction
[DE95-012170] p 3204 N95-32617
QCD mechanisms for double quarkonium and open heavy meson hadroproduction
[DE95-012171] p 3204 N95-32619
Fast approximation of self-similar network traffic
[DE95-011271] p 3185 N95-32967
Development of silicon drift detectors for strangeness measurements
[DE95-012366] p 3208 N95-33380
A fiber optic strain measurement and quench localization for use in superconducting accelerator dipole magnets
[DE95-012370] p 3215 N95-33381
A final-focus magnet for PEP-2
[DE95-012372] p 3214 N95-33504
Advanced far infrared detector and double donor studies in Ge
[DE95-011261] p 3247 N95-33625
Structural influences on the work hardening behavior of aluminum
[DE95-011262] p 3080 N95-33626
Size, shape, and crystallinity of luminescent structures in oxidized Si nanoclusters and H-passivated porous Si
[DE95-012322] p 3229 N95-33628
Charge-transfer gap closure in transition-metal halides under pressure
[DE95-011268] p 3230 N95-33865
Quantum mechanical capacitance in a scanning tunneling microscope
[DE95-011272] p 3230 N95-33880
Fundamental studies of the mechanism of catalytic reactions with catalysts effective in the gasification of carbon solids and the oxidative coupling of methane
[DE95-012759] p 3075 N95-34268
The beam envelope equation-systematic solution for a periodic quadrupole lattice with space charge
[DE95-012761] p 3199 N95-34269
Heavy ions acceleration in RF wells of 2-frequency electromagnetic field and in the inverted FEL
[DE95-012439] p 3214 N95-34439
Thin-film electrolytes for reduced temperature solid oxide fuel cells
[DE95-011273] p 3151 N95-34481
CALIFORNIA UNIV., DAVIS, CA.
Analysis and design methodology for chordwise deformable wings p 3049 N95-33311
Direct and large eddy simulations of three dimensional round turbulent jets p 3111 N95-33709
Prospect redux p 3133 N95-33758
Using foreground/background analysis to determine leaf and canopy chemistry p 3135 N95-33765
Validating spatial structure in canopy water content using geostatistics p 3135 N95-33768
CALIFORNIA UNIV., LOS ANGELES, CA.
Multiobjective optimization of hybrid regenerative life support technologies. Topic D: Technology Assessment
[NASA-CR-199125] p 3167 N95-32688
A stochastic adaptive control application to flight systems p 3055 N95-34806
CALIFORNIA UNIV., RIVERSIDE, CA.
Gamma ray imaging of the Crab and Vale regions with the UCR double-Compton telescope
p 3245 N95-32837
CALIFORNIA UNIV., SAN DIEGO, CA.
Minimum wakefield achievable by waveguide damped cavity
[DE95-012100] p 3095 N95-32616
CALIFORNIA UNIV., SANTA BARBARA, CA.
Land surface temperature measurements from EOS MODIS data
[NASA-CR-199082] p 3142 N95-32717
Fiber coatings for brittle matrix composites
p 3065 N95-34808
CAMBRIDGE HYDRODYNAMICS, INC., PRINCETON, NJ.
Numerical studies of turbulent free surface flows and unsteady propeller flows
[AD-A294377] p 3112 N95-34343
CANADA CENTRE FOR REMOTE SENSING, OTTAWA (ONTARIO).
Impact of differences in the solar irradiance spectrum on surface reflectance retrieval with different radiative transfer codes p 3136 N95-33771
Lithologic controls on AIRSAR signatures of bedrock and alluvium, at Lunar Crater, Nevada
p 3141 N95-33813

CANADA CENTRE FOR REMOTE SENSING, VICTORIA (BRITISH COLUMBIA).
System of experts for intelligent data management (SEIDAM) p 3240 N95-34226
CARNEGIE-MELLON UNIV., PITTSBURGH, PA.
Metallurgical and Materials Transactions, volume 25A, no. 9
[AD-A293622] p 3077 N95-32474
Bit-level analysis of an SRT divider circuit
[AD-A294842] p 3105 N95-34565
Experiences using DCE and CORBA to build tools for creating highly-available distributed systems
[AD-A294973] p 3187 N95-34587
Everyday believability
[AD-A294938] p 3193 N95-34602
CASE WESTERN RESERVE UNIV., CLEVELAND, OH.
Molecular engineering of liquid crystalline polymers by Living polymerization 30. Synthesis and Living cationic polymerization of (2R, 3S)-2-Fluoro-3-methylpentyl 4'-(8-Vinyloxyoctyloxy) Biphenyl-4-carboxylate and its copolymerization with (2R, 3S)-2-Fluoro-3-methylpentyl 4'-(11 Vinyloxyundecanyloxyloxy) biphenyl-4-carboxylate
[AD-A293115] p 3082 N95-32552
Influence of non classical friction on the rubbing and impact behavior of rotor dynamic systems
p 3122 N95-32906
Nonholonomic control of coupled spatial multibody systems p 3192 N95-33604
From liquid crystal polymers containing crown ethers to tapered building blocks containing crown ethers which self-assemble into tubular supermolecules
[AD-A294359] p 3086 N95-34361
CATHOLIC UNIV. OF AMERICA, WASHINGTON, DC.
A study of space-rated connectors using a robot end-effector
[NASA-CR-199116] p 3121 N95-32675
Trajectory planning and control of kinematically redundant robotic manipulators p 3194 N95-34807
CENTRAL RESEARCH AND DEVELOPMENT INST. ELEKTROPRIBOR, SAINT PETERSBURG (RUSSIA).
Navigational technology of dual usage
p 3048 N95-33131
CENTRAL RESEARCH INST. OF ELECTRIC POWER INDUSTRY, TOKYO (JAPAN).
Solar cell array design method for preventing power reduction due to module output fluctuation
[DE95-769745] p 3148 N95-32402
CENTRAL RESEARCH INST. OF TECHNOLOGY AND MACHINE BUILDING, KALININGRAD, MOSCOW (RUSSIA).
The concept of the space system based on the Rocket launch vehicle of light-weight class for direct sounding of large-scale natural hazards p 3057 N95-33128
CENTRE D'ETUDES ET DE RECHERCHES, TOULOUSE (FRANCE).
Low-level data fusion for landing runways detection
p 3048 N95-33136
CENTRO DI CULTURA SCIENTIFICA A. VOLTO, COMO (ITALY).
Atoms in strong fields
[AD-A294589] p 3209 N95-34423
CHAMPLAIN TECHNOLOGY, INC., WEST PALM BEACH, FL.
Structure and dynamics of excited atoms
[AD-A294997] p 3209 N95-34819
CIVIL AVIATION ADMINISTRATION (SWEDEN).
Presentation of a Swedish study program concerning recruitment, selection and training of student air traffic controllers: The MRU project phase 1
p 3167 N95-34775
CIVIL AVIATION AUTHORITY, FARNBOROUGH (ENGLAND).
Human factors certification in the development of future air traffic control systems p 3048 N95-34770
CKW NUCLEAR CONSULTING, LOS ALAMOS, NM.
Technical support in the area of theoretical support of nuclear preequilibrium
[DE95-011617] p 3212 N95-32960
CHINA NUCLEAR INFORMATION CENTRE, BEIJING (CHINA).
Study of impurity concentrations by VUV spectroscopy on HL-1
[DE95-614186] p 3221 N95-32562
The effects of H(+) implants on YBa2Cu3O7 superconducting materials
[DE95-614466] p 3227 N95-32698
CINCINNATI UNIV., OH.
Genetic algorithms as global random search methods
[NASA-CR-199088] p 3188 N95-32767
Genetic algorithm based input selection for a neural network function approximator with applications to SSME health monitoring
[NASA-CR-199089] p 3188 N95-32768
Identification of flexible structures under closed loop control p 3192 N95-33713
A robust control system for exact trajectory tracking
p 3192 N95-33714
Interfacial reactions during the liquid infiltration of titanium matrix composites p 3081 N95-34252
CLARK UNIV., WORCESTER, MA.
Mathematical modelling in plasma physics
[AD-A294972] p 3224 N95-34586
CLEVELAND STATE UNIV., OH.
Self-organizing neural network and its applications to vision-guided robot motion coordination
p 3191 N95-33324
Numerical thermal analyses of heat exchangers for the stirling engine application
[NASA-CR-199120] p 3110 N95-33398
COAST GUARD RESEARCH AND DEVELOPMENT CENTER, GROTON, CT.
The effect of sample holder material on ion mobility spectrometry reproducibility p 3071 N95-33282
A novel approach to increasing cocaine detection confidence utilizing ion mobility spectrometry
p 3072 N95-33283
COLORADO STATE UNIV., FORT COLLINS, CO.
Impact of cloud microphysics on cloud-radiation interactions in the CSU general circulation model
[DE95-008979] p 3153 N95-33205
Optimization problems in multitarget/multisensor tracking
[AD-A294978] p 3100 N95-34590
COLORADO UNIV., BOULDER, CO.
A three-dimensional nonlinear Timoshenko beam based on the core-congruential formulation
[NASA-CR-199042] p 3180 N95-32765
A survey of parametrized variational principles and applications to computational mechanics
[NASA-CR-199041] p 3180 N95-32766
Effects of gravity and light on plant growth and performance in normal and reduced gravity
p 3163 N95-32901
Zeolite membranes for gas separations
[DE95-012984] p 3068 N95-33224
Quantitative remote sensing of ammonium minerals, Cedar Mountains, Esmeralda County, Nevada
p 3128 N95-33734
Using dark current data to estimate AVIRIS noise covariance and improve spectral analyses
p 3129 N95-33736
Integration of AIRSAR and AVIRIS data for Trail Canyon alluvial fan, Death Valley, California
p 3134 N95-33760
Applied Information Systems Research Program (AISRP) Workshop 3 meeting proceedings
[NASA-CR-199103] p 3239 N95-34218
A land-surface testbed for EOSDIS
p 3158 N95-34223
Optical properties of lithium niobate waveguides, and prism coupling for optimizing waveguide fabrication
[AD-A294111] p 3218 N95-34498
COLUMBIA UNIV., NEW YORK, NY.
Abstracts of oral and poster sessions
[DE95-011951] p 3154 N95-33413
GRO: Studies of high energy pulsars with EGRET
[NASA-CR-199130] p 3248 N95-33499
COMMONWEALTH SCIENTIFIC AND INDUSTRIAL RESEARCH ORGANIZATION, HIGHETT, VICTORIA (AUSTRALIA).
Expert systems and artificial intelligence applications in engineering design and inspection p 3190 N95-33008
COMPTROLLER GENERAL OF THE UNITED STATES, WASHINGTON, DC.
Annual report to the Chairman, House and Senate Committees on Appropriations. Status of open recommendations: Improving operations of federal departments and agencies
[GAO/OP-94-1] p 3236 N95-32887
COMPUTER SCIENCES CORP., CALVERTON, MD.
Compton Observatory observations of clusters of galaxies and extragalactic radio sources
[NASA-CR-189431] p 3246 N95-33261
Beryllium and Boron abundances in population II stars
[NASA-CR-189434] p 3247 N95-33262
CONDUCTUS, INC., SUNNYVALE, CA.
Properties of high-T(sub c) Josephson junctions with Y(0.7)Ca(0.3)Ba2Cu3O(7-delta) barrier layers
[AD-A294852] p 3231 N95-34568
CONNECTICUT UNIV., STORRS, CT.
Synchrotron radiation studies of local structure and bonding in transition metal aluminides and rare earth transition metal magnetic nitrides
[DE95-011579] p 3079 N95-33065
CONSIGLIO NAZIONALE DELLE RICERCHE, ROME (ITALY).
CNR LARA project, Italy: Airborne laboratory for environmental research p 3129 N95-33735
CORNELL UNIV., ITHACA, NY.
Nucleation, propagation, electronic levels and elimination of misfit dislocations in 3-5 semiconductor interfaces
[DE95-011595] p 3231 N95-34485
Geochemical, genetic, and physiological control of pollutant biodegradation
[AD-A294902] p 3155 N95-34591
CRAY RESEARCH JAPAN, TOKYO (JAPAN).
Program developing environment and a CFD application on the Cray T3D p 3038 N95-34535

D

DAIKO LTD. (JAPAN).
Parallel computation of transonic flows about an aircraft configuration using multi-block structured grids
p 3039 N95-34537
DALIAN INST. OF TECH. (CHINA).
The method of model-based reasoning and application of an intelligent adaptive observer on the integrated process p 3190 N95-33005
DAVID SARNOFF RESEARCH CENTER, PRINCETON, NJ.
Hybrid pyramid/neural network vision system
[AD-A294919] p 3193 N95-34593
DAYTON UNIV., OH.
Experimental and numerical analysis of controlled impinging liquid jets p 3109 N95-33257
Human piloting factors in the design of control laws for precision landing p 3167 N95-33605
Perceptual dimensions of simulated scenes relevant for visual low-altitude flight
[AD-A294385] p 3056 N95-34344
Altitude cuing effectiveness of terrain texture characteristics in simulated low-altitude flight
[AD-A294369] p 3056 N95-34362
DE MONTFORT UNIV., MILTON KEYNES (ENGLAND).
Conceptual, causal and numerical modelling and analysis of physical systems p 3190 N95-33006
DEFENCE AND CIVIL INST. OF ENVIRONMENTAL MEDICINE, NORTH YORK (ONTARIO).
Methods for measuring physiological responses and protection in man exposed to high +G(z)
p 3166 N95-34058
DEFENCE RESEARCH AGENCY, BEDFORD (ENGLAND).
The Anglo-French Compact Laser Radar demonstrator programme p 3045 N95-32501
DEFENCE RESEARCH AGENCY, FARNBOROUGH, HAMPSHIRE (ENGLAND).
The application of helicopter mission simulation to Nap-of-the-Earth operations p 3044 N95-32496
Covert Night/Day Operations for Rotorcraft (CONDOR) programme p 3046 N95-32505
DEFENCE RESEARCH ESTABLISHMENT SUFFIELD, RALSTON (ALBERTA).
High resolution electrospray mass spectrometry with a magnetic sector instrument: Accurate mass measurement and peptide sequencing
[AD-A293564] p 3076 N95-34611
DEFENCE SCIENCE AND TECHNOLOGY ORGANISATION, MELBOURNE (AUSTRALIA).
The tensile fracture behavior of the weld metal of BIS 812 EMA and Q1N naval construction steels
[DSTO-RR-0021] p 3078 N95-32926
Operations manual for a compact electromechanical fatigue testing machine
[DSTO-GD-0036] p 3115 N95-32927
Industrial and Engineering Applications of Artificial Intelligence and Expert Systems: Invited and additional papers
[DSTO-GD-0051] p 3188 N95-32995
Water model tests on the Allison T56 series 3 combustion system
[DSTO-TR-0139] p 3054 N95-33250
DELPHIN CENTRAL RESEARCH INST., MOSCOW (RUSSIA).
Commercial usage of Navy components developed and manufactured by CRI Delfin p 3092 N95-33129
DEPARTMENT OF ENERGY, PITTSBURGH, PA.
High-tech controls for energy and environment
[DE95-004011] p 3191 N95-33060
DEPARTMENT OF ENERGY, WASHINGTON, DC.
Annual report to Congress 1994: Energy Information Administration
[DE95-011240] p 3237 N95-32482
Materials sciences programs: Fiscal year 1994
[DE95-011248] p 3211 N95-32483
DEPARTMENT OF THE AIR FORCE, BROOKS AFB, TX.
New advances in physiological measurements during high-G: Technology p 3165 N95-34057
G-protection capabilities and current G-protection issues p 3169 N95-34060

DEPARTMENT OF THE AIR FORCE, WRIGHT-PATTERSON AFB, OH.
Sum frequency generation of dual-wavelength Nd: YAP laser in LiIO3 crystal
| AD-A293094 | p 3117 N95-32472
Study of liquid crystal spatial light modulator application to Hadamard transform spectrometer: A fast and accurate decoding method
| AD-A293087 | p 3215 N95-32660
High-resolution TeO2 acousto-optical deflector for millimeter-wave spectrometer
| AD-A293054 | p 3215 N95-32701
New advances in 1341.4 nm Nd:YAP lasers
| AD-A293070 | p 3118 N95-32702
DEPARTMENT OF THE NAVY, WASHINGTON, DC.
A fiber-optic connector
| AD-D017424 | p 3215 N95-32923
Split gasket attachment method statement of government interest
| AD-D017443 | p 3123 N95-32924
Arbitrary waveform generator
| AD-D017451 | p 3097 N95-32925
Encapsulated dry electrolyte composition for time release into a solute
| AD-D017485 | p 3075 N95-34287
Method for making fiber-optic bundle collimator assembly
| AD-D017486 | p 3216 N95-34288
Acoustic-optic sound velocity profiler
| AD-D017487 | p 3201 N95-34289
Vertical velocity ambiguity resolution method
| AD-D017481 | p 3201 N95-34424
Crosspoint analog data selector
| AD-D017482 | p 3104 N95-34425
Fluid dynamometer having fluid characteristic power absorption adjustment capability
| AD-D017489 | p 3116 N95-34426
Device for dampening vibratory motion
| AD-D017490 | p 3127 N95-34427
Acoustic attenuation and vibration damping materials
| AD-D017465 | p 3201 N95-34444
Diamond multilayer multichip module substrate
| AD-D017468 | p 3104 N95-34445
Channel equalized DC squid flux-locked loop
| AD-D017469 | p 3104 N95-34446
Method of forming thin films on substrates at low temperatures
| AD-D017470 | p 3086 N95-34447
Apparatus for injection molding high-viscosity materials
| AD-D017471 | p 3065 N95-34448
Energy absorption device for shock loading
| AD-D017476 | p 3124 N95-34449
Conforming tuning coupler for flextensional transducers
| AD-D017285 | p 3105 N95-34617
Operational amplifier using bipolar junction transistors in silicon-on-sapphire
| AD-D017421 | p 3105 N95-34618
Method and apparatus for locking laser wavelength to an atomic transition
| AD-D017425 | p 3120 N95-34619
Method of installing a metallic threaded insert in a composite/rubber panel
| AD-D017522 | p 3065 N95-34620
DEUTSCHE FORSCHUNGSANSTALT FUER LUFT- UND RAUMFAHRT, BRUNSWICK (GERMANY).
The DLR research programme on an integrated multi sensor system for surface movement guidance and control p 3048 N95-33135
DEUTSCHE FORSCHUNGSANSTALT FUER LUFT- UND RAUMFAHRT, COLOGNE (GERMANY).
Dosimetry of heavy ions by use of CCD detectors p 3161 N95-32721
Inactivation, DNA double strand break induction and their rejoining in bacterial cells irradiated with heavy ions p 3161 N95-32724
Mutation induction in bacteria after heavy ion irradiation p 3162 N95-32727
Cosmic heavy ion tracks in mesoscopic biological test objects p 3163 N95-32730
DEUTSCHE FORSCHUNGSANSTALT FUER LUFT- UND RAUMFAHRT, GOETTINGEN (GERMANY).
A nonlinear vortex lattice method for unsteady flow with separated vortex
| DLR-FB-94-32 | p 3106 N95-32787
DIRECTION GENERALE DE L'AVIATION CIVILE, PARIS (FRANCE).
Advanced automated glass cockpit certification: Being wary of human factors p 3176 N95-34786
DRAPER (CHARLES STARK) LAB., INC., CAMBRIDGE, MA.
Dual-use micromechanical inertial sensors p 3092 N95-33132
DRUG ENFORCEMENT ADMINISTRATION, NATIONAL CITY, CA.
Application of the ionscan for the detection of methamphetamine and ephedrine in abondoned clandestine laboratories p 3072 N95-33284
DUKE UNIV., DURHAM, NC.
Design and analysis of lossless and lossy data compression methods with applications to communication and caching
| AD-A295025 | p 3101 N95-34790

E

EARTH SEARCH SCIENCES, INC., SALT LAKE CITY, UT.
A layered approach to technology transfer of AVIRIS between Earth Search Sciences, Inc. and the Idaho National Engineering Laboratory p 3117 N95-33746
EATON CORP., WILLOUGHBY HILLS, OH.
High-speed, low-damage grinding of advanced ceramics, phase 1
| DE95-011241 | p 3085 N95-33425
ECOLE POLYTECHNIQUE, MONTREAL (QUEBEC).
Low velocity impact damage in carbon fiber/PEEK composite laminates
| ISBN-0-315-86546-6 | p 3065 N95-33710
EDGEWOOD RESEARCH DEVELOPMENT AND ENGINEERING CENTER, ABERDEEN PROVING GROUND, MD.
Proton affinity determinations and proton-bound dimer structure indications in C2 to C15, (alpha),(omega)-alkyldiamines p 3069 N95-33266
Hand-portable gas chromatography-ion mobility spectrometer for the determination of the freshness of fish p 3071 N95-33277
Data collection in IMS: It's not as easy as it looks p 3072 N95-33286
EG AND G MOUND APPLIED TECHNOLOGIES, MIAMISBURG, OH.
Operational equations for three-dimensional data
| DE95-011332 | p 3196 N95-33248
EIC, INC., NORWOOD, MA.
Field Raman spectrograph for environmental analysis
| DE95-007969 | p 3153 N95-32316
ELMER, ROME (ITALY).
Helicopter HF communications using the NVIS mode p 3043 N95-32491
ELTRO G.M.B.H., HEIDELBERG (GERMANY).
Laser based obstacle warning sensors for helicopters p 3045 N95-32499
EMBRY-RIDDLE AERONAUTICAL UNIV., DAYTONA BEACH, FL.
Human Factors Certification of Advanced Aviation Technologies
| NASA-CR-199009 | p 3171 N95-34764
On the use of the systems approach to certify advanced aviation technologies p 3171 N95-34765
Certification of training p 3166 N95-34774
ENVIRONMENTAL TECHNOLOGIES GROUP, INC., BALTIMORE, MD.
The effects of CO2 on the negative reactant ions of IMS p 3069 N95-33267
The pinhole interface for IMS/MS p 3070 N95-33275
EROS DATA CENTER, SIOUX FALLS, SD.
Aircraft scanner data availability via the version 0 Information Management System p 3134 N95-33762
EUROCONTROL EXPERIMENTAL CENTRE, BRETIGNY (FRANCE).
Certification of tactics and strategies in aviation p 3172 N95-34768
Human factors certification: A useful concept? p 3173 N95-34769
EUROCOPTER DEUTSCHLAND G.M.B.H., MUNICH (GERMANY).
HeliRadar: A rotating antenna synthetic aperture radar for helicopter allweather operations p 3093 N95-33137
EUROPEAN SPACE AGENCY, PARIS (FRANCE).
ESA Bulletin, Number 82 p 3252 N95-32538
European Space Agency 1994 annual report p 3252 N95-32805
EUROPEAN SPACE AGENCY. EUROPEAN SPACE RESEARCH AND TECHNOLOGY CENTER, ESTEC, NOORDWIJK (NETHERLANDS).
OPEX: Second Workshop of the OLYMPUS propagation experimenters. Volume 1: Reference book on attenuation measurement and prediction
| ESA-WPP-083-VOL-1 | p 3096 N95-32747
OPEX Second Workshop of the OLYMPUS Propagation Experimenters. Volume 2: Reference book on depolarisation
| ESA-WPP-083-VOL-2 | p 3096 N95-32748
OPEX Second Workshop of the OLYMPUS Propagation Experimenters. Volume 3: Reference book on radiometry and meteorological measurements
| ESA-WPP-083-VOL-3 | p 3096 N95-32749
OPEX Second Workshop of the OLYMPUS Propagation Experimenters. Volume 4: Reference book on radar
| ESA-WPP-083-VOL-4 | p 3096 N95-32750
OPEX Second Workshop of the OLYMPUS Propagation Experimenters. Volume 5: Reference book on data processing
| ESA-WPP-083-VOL-5 | p 3096 N95-32751
EVKO PRODUCTIONS, INC., ALEXANDRIA, VA.
The Space Shuttle: America's team reaching for the future
| NASA-CR-199222 | p 3058 N95-33726

F

FABRICA ITALIANA APPARECCHIATURE RADIOELETTRICHE S.P.A., MILAN (ITALY).
An approach to sensor data fusion for flying and landing aid purpose p 3043 N95-32488
SIRPH: Steerable infrared picture on helmet mounted display p 3045 N95-32504
FEDERAL AVIATION ADMINISTRATION, ATLANTIC CITY, NJ.
Gas chromatography/ion mobility spectrometry as a hyphenated technique for improved explosives detection and analysis p 3071 N95-33278
FEDERAL AVIATION ADMINISTRATION, WASHINGTON, DC.
A psychologist's view of validating aviation systems p 3172 N95-34767
FEDERAL BUREAU OF INVESTIGATION, WASHINGTON, DC.
The use of ion mobility spectrometry and gas chromatography/mass spectrometry for the detection of illicit drugs on clandestine records p 3070 N95-33276
FERMI NATIONAL ACCELERATOR LAB., BATAVIA, IL.
Production asymmetries in x(sub f) and P(sup 2)(sub t) for D(sup + /-) mesons
| DE95-007207 | p 3201 N95-32379
Coating power RF components with TiN
| DE95-010357 | p 3082 N95-32541
CDF results on Z(gamma) production
| DE95-011500 | p 3213 N95-33406
Collaborating over the Web: Libraries and laboratories or the Librarian and the Webmaster
| DE95-010572 | p 3186 N95-33639
FLORIDA UNIV., GAINESVILLE, FL.
Solvent effects on the electronic spectrum of R hardt's dye
| AD-A293667 | p 3067 N95-32804
FUJITSU LTD., TOKYO (JAPAN).
Highly parallel computer AP1000: Architecture and basic software p 3038 N95-34534
Numerical analysis around the whole SST configuration p 3039 N95-34541
Computations of low speed flow about space-plane p 3040 N95-34544

G

GALAXY SCIENTIFIC CORP., PLEASANTVILLE, NJ.
Corrosion of fire-damaged aircraft
| AD-A294968 | p 3049 N95-34583
GEC-MARCONI AVIONICS LTD., ROCHESTER (ENGLAND).
A tactical navigation and routeing system for low-level flight p 3044 N95-32494
GENERAL ACCOUNTING OFFICE, WASHINGTON, DC.
Report to the Chairman, Subcommittee on Aviation, Committee on Commerce, Science, and Transportation, US Senate. Aviation safety: Data problems threaten FAA strides on safety analysis system
| GAO/AIMD-95-27 | p 3046 N95-32705
Aerospace Guidance and Metrology Center: Cost growth and other factors affect closure and privatization. Report to Congressional requesters
| GAO/NSIAD-95-60 | p 3235 N95-32706
Report to the Chairman, Committee on Science, House of Representatives. NASA's Earth Observing System: Estimated funding requirements
| GAO/NSIAD-95-175 | p 3142 N95-32707
Report to Congressional Committees. B-1B bomber: Evaluation of Air Force report on B-1B operational readiness assessment
| GAO/NSIAD-95-151 | p 3197 N95-32758
Fact sheet for Congressional requesters. Airport competition: Essential air service slots at O'Hare International Airport
| GAO/RCED-94-118FS | p 3055 N95-32759

Weather Forecasting: Systems architecture needed for National Weather Service modernization. Report to Congressional requesters
[GAO/AIMD-94-28] p 3157 N95-32760
Report to Congressional Committees. B-2 bomber: Cost to complete 20 aircraft is uncertain
[GAO/NSIAD-94-217] p 3033 N95-32782
Army aviation: Modernization strategy needs to be reassessed. Report to Congressional requestors
[GAO/NSIAD-95-9] p 3033 N95-32783
Report to the Chairman, Subcommittee on Aviation, Committee on Commerce, Science, and Transportation, US Senate. Aviation Safety: FAA can better prepare general aviation pilots for mountain flying risks
[GAO/RCED-94-15] p 3046 N95-32784
Metric conversion: Future progress depends upon private sector and public support. Report to Congressional requesters
[GAO/RCED-94-23] p 3089 N95-32785
Report to the Chairman, Subcommittee on Transportation and Related Agencies, Committee on Appropriations, US Senate. Airport Improvement Program: Reliever airport set-aside funds could be redirected
[GAO/RCED-94-226] p 3055 N95-32786
Report to Congressional Committees. Air Force fighters: More reliance on reserves increases the need to know their capabilities
[GAO/NSIAD-94-86] p 3197 N95-32807
Space Station: Estimated total US funding requirements. Report to Congressional Requesters
[GAO/NSIAD-95-163] p 3058 N95-32884
Aviation security: Development of new security technology has not met expectations. Report to Congressional requesters
[GAO/RCED-94-142] p 3046 N95-32885
Report to the Honorable William V. Roth, Jr., US Senate. Naval aviation: F/A-18 E/F acquisition strategy
[GAO/NSIAD-94-194] p 3197 N95-32886
Report to the Chairman, Subcommittee on Transportation and Related Agencies, Committee on Appropriations, US Senate. Airport Improvement Program: The Military Airport Program has not achieved intended impact
[GAO/RCED-94-209] p 3056 N95-32888
Report to the Chairman, Committee on Armed Services, US Senate. Strategic Bomber: Issues relating to the B-1B's availability and ability to perform conventional missions
[GAO/NSIAD-94-81] p 3198 N95-33263
Report to the Ranking Minority Member, Committee on Government Operations, House of Representatives. Paperwork reduction: Reported burden hour increases reflect new estimates, not actual changes
[GAO/PEMD-94-3] p 3236 N95-33907
Comanche helicopter: Testing needs to be completed prior to production decisions
[AD-A294408] p 3049 N95-34422

GENERAL ATOMICS CO., SAN DIEGO, CA.
Recent results from the D3-D tokamak and implications for future devices
[DE95-009605] p 3222 N95-32592
D3-D power supply, design, and development
[DE95-009603] p 3222 N95-32656
Optimized profiles for improved confinement and stability in the DIII-D tokamak
[DE95-009606] p 3222 N95-32756
Inertial confinement fusion target component fabrication and technology development support
[DE95-011655] p 3224 N95-34436

GENERAL ELECTRIC CO., SCHENECTADY, NY.
Solubility behavior of quartz and corundum in supercritical water: A quantitative thermodynamic interpretation
[DE95-012294] p 3234 N95-34211

GEOLOGICAL SURVEY, DENVER, CO.
Initial vegetation species and senescience/stress indicator mapping in the San Luis Valley, Colorado using imaging spectrometer data p 3130 N95-33741
Mapping minerals, amorphous materials, environmental materials, vegetation, water, ice and snow, and other materials: The USGS tricorder algorithm p 3130 N95-33742
Remote mineral mapping using AVIRIS data at Summitville, Colorado and the adjacent San Juan Mountains p 3134 N95-33761
Spectral identification of minerals using imaging spectrometry data: Evaluating the effects of signal to noise and spectral resolution using the tricorder algorithm p 3136 N95-33772

GEOLOGICAL SURVEY OF BRITAIN, KEYWORTH (ENGLAND).
United Kingdom minerals yearbook, 1994. Statistical data to 1993
[PB95-207841] p 3155 N95-32599
World mineral statistics, 1988-92. Production: Exports: Imports
[PB95-208096] p 3155 N95-32601
World mineral production, 1989-93. Preliminary statistics
[PB95-208104] p 3156 N95-32603

GEORGE MASON UNIV., FAIRFAX, VA.
Modeling and inference with fractional Brownian motion and fractional Gaussian noise p 3199 N95-33415
Time correlations between low and high energy gamma rays from discrete sources
[NASA-CR-199214] p 3248 N95-33916

GEORGIA INST. OF TECH., ATLANTA, GA.
Airborne passive polarimetric measurements of sea surface anisotropy at 92 GHz
[NASA-CR-197288] p 3143 N95-32823
Actively controlled shaft seals for aerospace applications
[NASA-CR-4678] p 3061 N95-33156
Stochastic network processes
[AD-A294939] p 3187 N95-34603

GEORGIA STATE UNIV., ATLANTA, GA.
Light particle emission in heavy ion reactions
[DE95-010727] p 3206 N95-32965

GERMAN AIR FORCE, KOENIGSBRUECK (GERMANY).
Selection and training of MiG-29 and future fighter pilots p 3166 N95-34059

GESELLSCHAFT FUER SCHWERIONENFORSCHUNG M.B.H., DARMSTADT (GERMANY).
DNA-DSB in CHO-K1 cells induced by heavy-ions: Break rejoining and residual damage (GSI) p 3162 N95-32725
Chromosomal damage observed in first postirradiation metaphases of repair-proficient and -deficient cell lines p 3162 N95-32726

GLASGOW UNIV. (SCOTLAND).
Track finding and fitting in the H1 forward track detector
[PB95-234985] p 3214 N95-34651

GOSUDARSTVENNYI KOMITET PO ISPOLZOVANIYU ATOMNOI ENERGII, LENINGRAD (USSR).
Search for N(sub (phi))(1960) baryon
[DE95-619290] p 3205 N95-32703
The (pi)(yields)e(nu)(gamma) decay in chiral perturbation theory
[DE95-619269] p 3206 N95-32806
Study of the p + N yields (Sigma(0)K(+)) + N reaction at E(sub p) 70 GeV
[DE95-619273] p 3207 N95-33171

GOSUDARSTVENNYI KOMITET PO ISPOLZOVANIYU ATOMNOI ENERGII, PROTVINO (USSR).
Scaling law for the Upsilon(4S) yields bar-BB and psi(3770) yields bar-DD decay constants from effective sum rules
[DE95-620538] p 3203 N95-32554

GOSUDARSTVENNYI KOMITET PO ISPOLZOVANIYU ATOMNOI ENERGII, SERPUKHOV (USSR).
Four heavy quark and bound state production in the e(+)e(-) yields Q + (bar-Q' + Q' + bar-Q and e(+)e(-) yields (Q(bar-Q')) + Q' + bar-Q processes in Z(sup 0)-boson pole
[DE95-620533] p 3205 N95-32704

GRAMBLING STATE UNIV., LA.
NQR-NMR studies of higher alcohol synthesis Cu-Co catalysts
[DE95-010524] p 3066 N95-32557

GRASEBY DYNAMICS LTD., WATFORD (ENGLAND)
An ammonia monitor for the water industry p 3071 N95-33281
Signal processing for ION mobility spectrometers p 3073 N95-33289

H

HARTFORD UNIV., CT.
Locus of control and coping style as stress moderators in achievement oriented individuals
[AD-A294275] p 3166 N95-34463

HARVARD UNIV., CAMBRIDGE, MA.
X-ray standing wave interferometry-optics at 1 angstrom with applications to surface and material sciences
[DE95-009688] p 3215 N95-32662
Micromechanics of fiber-reinforced ceramic composites p 3063 N95-32775
Cosmological consequences of topological and geometric phenomena in field theories p 3234 N95-33313

HELSINKI UNIV. OF TECHNOLOGY, ESPOO (FINLAND).
Optimization of a melting layer model in the radar backscatter, attenuation, and phase shift calculations at centimeter and millimeter wavelengths
[PB95-207189] p 3155 N95-32455
Polymerization of epsilon-caprolactone in the presence of Oh- or COOh-groups containing initiators. Copolymers of lactide with epsilon-caprolactone: Synthesis, characterization and processing
[PB95-208211] p 3084 N95-33227
DMTA studies of branching distribution in polyethylene
[PB95-208237] p 3084 N95-33228
Testing of a carpet catalyst
[PB95-208492] p 3068 N95-33242

HOLOPLEX, INC., PASADENA, CA.
Read/write module for high capacity memory disk
[AD-A294946] p 3178 N95-34745

HONEYWELL TECHNOLOGY CENTER, MINNEAPOLIS, MN.
Dual use: Opportunities, payoffs, and challenges p 3091 N95-33127

HONG KONG POLYTECHNIC, KOWLOON (HONG KONG).
Training and recognition of Cantonese phonemes by backpropagation through time p 3188 N95-32996

HOPITAL A. BECLERE, CLAMART (FRANCE).
Noninvasive determination of Cardiac Output
[PB95-208310] p 3164 N95-32611

HOUSTON UNIV., TX.
The background and theory of integrated risk management p 3236 N95-32431
Scanners, optical character readers, Cyrillic alphabet and Russian translations p 3194 N95-32433

HOUSTON UNIV.-CLEAR LAKE, HOUSTON, TX.
Image analysis used to count and measure etched tracks from ionizing radiation p 3210 N95-32424

HOWARD UNIV., WASHINGTON, DC.
Sub-pixel localization of highways in AVIRIS images p 3135 N95-33767
On the nonlinear stability of a nearby parallel and a non-unidirectional flow p 3112 N95-34284

HSS, INC., BEDFORD, MA.
A tactical present weather sensor for Air Force applications
[AD-A294900] p 3158 N95-34575

HUGHES AIRCRAFT CO., CULVER CITY, CA.
Advanced data visualization and sensor fusion: Conversion of techniques from medical imaging to Earth science p 3242 N95-34236

HUGHES AIRCRAFT CO., TORRANCE, CA.
A 75 watt, 59 to 64 GHz space TWT
[NASA-CR-195450] p 3104 N95-33915

HUGHES AIRCRAFT CO., TUCSON, AZ.
Zero discharge organic coatings: Powder paint - UV curable paint - E-coat
[AD-A293573] p 3087 N95-34614

HUGHES DANBURY OPTICAL SYSTEMS, INC., CT.
Characteristics of the HYDICE sensor p 3116 N95-33733

I

IBIS ASSOCIATES, INC., WELLESLEY, MA.
CVD diamond cost analysis update
[AD-A289990] p 3227 N95-32695

IDAHO NATIONAL ENGINEERING LAB., IDAHO FALLS, ID.
Fusion Safety Program annual report, fiscal year 1994
[DE95-008872] p 3221 N95-32588
A layered approach to technology transfer of AVIRIS between Earth Search Sciences, Inc. and the Idaho National Engineering Laboratory p 3117 N95-33746
Spray coating of metals. Proof of concept: Phase 2
[AD-A294393] p 3081 N95-34348

ILLINOIS UNIV., CHICAGO, IL.
Baseline experimental investigation of an electrohydrodynamically assisted heat pipe p 3113 N95-32427
Flow and heat transfer behavior of non-Newtonian fluids in rectangular ducts p 3107 N95-32907

ILLINOIS UNIV., URBANA, IL.
Investigation on deflagration to detonation transition in porous energetic materials
[DE95-011638] p 3088 N95-32605
Reducing cache misses in numerical applications using data relocation and prefetching
[AD-A293978] p 3182 N95-34455

ILLINOIS UNIV., URBANA-CHAMPAIGN, IL.
Design and analysis of transient nonlinear coupled systems p 3199 N95-33292
The linear elastic biaxial response of plain-woven meshes p 3064 N95-33468
A quantum Monte Carlo study of the high-pressure phases of solid hydrogen p 3074 N95-33469
Very large eddy simulations of spatially evolving supersonic turbulent shear layers p 3110 N95-33606

ILLINOIS UNIV. AT URBANA-CHAMPAIGN, SAVOY, IL.
Recoverable distributed shared memory under sequential and relaxed consistency
[AD-A293966] p 3178 N95-34453

INDIANA UNIV., BLOOMINGTON, IN.
Stability of steady state solutions for forced Navier-Stokes equations p 3112 N95-34286

INSTITUT FUER SPECTROCHEMIE UND ANGEWANDTE SPECTROSKOPIE, DORTMUND (GERMANY).
Determination of Benzene, Toluene, and Xylene by means of an ion mobility spectrometer device using photoionization p 3069 N95-33269
Exchange, interpretation, and database-search of ion mobility spectra supported by data format JCAMP-DX p 3070 N95-33274
FTP-Server for exchange, interpretation, and database-search of ion mobility spectra, literature, preprints and software p 3073 N95-33291

INSTITUTE FOR COMPUTER APPLICATIONS IN SCIENCE AND ENGINEERING, HAMPTON, VA.
Tracking a turbulent spot in an immersive environment [NASA-CR-198179] p 3180 N95-32834
A unified multigrid solver for the Navier-Stokes equations on mixed element meshes [NASA-CR-198183] p 3196 N95-33500
Krylov methods for compressible flows [NASA-CR-198176] p 3196 N95-33727

INSTITUTE FOR PRECISION INSTRUMENTATION, MOSCOW (RUSSIA).
Identification of terrain imagery with unstable reflectivity p 3093 N95-33138

INSTITUTE OF FORENSIC MEDICINE, BERNE (SWITZERLAND).
Application of Ion Mobility Spectrometry (IMS) in forensic chemistry and toxicology with focus on biological matrices p 3072 N95-33285

INSTITUTE OF GAS TECHNOLOGY, DES PLAINES, IL.
Gasoline from natural gas by sulfur processing [DE95-010651] p 3087 N95-32563

INSTITUTET FOER VATTEN-OCH LUFTVAARDSFORSKNING, STOCKHOLM (SWEDEN).
Environmental evaluation of lactates as cleaning agents [PB95-214854] p 3067 N95-32615

INSTITUTO NACIONAL DE PESACIAIS ESPACIAIS, SAO JOSE DOS CAMPOS (BRAZIL).
An algorithm for chlorophyll using first difference transformations of AVIRIS reflectance spectra p 3134 N95-33763
Tokamak ETE circuits: Analysis and specifications [INPE-5573-PRP/182] p 3224 N95-33873

INSTITUTO TECHNOLOGICO Y DE ESTUDIOS SUPERIORES DE MONTERREY, (MEXICO).
Induction of dependency structures from data and its application to ozone prediction p 3190 N95-33003

INSTITUUT TNO VOOR WERKTUIGKUNDIGE CONSTRUCTIES, DELFT (NETHERLANDS).
Design of deepwater pipelines [PB95-215109] p 3095 N95-33244

INTERNATIONAL CENTRE FOR THEORETICAL PHYSICS, TRIESTE (ITALY).
Maximum principle for subsolutions of degenerate elliptic operators [DE95-613373] p 3195 N95-32523
A study of luminescence and absorption spectra of GaP [DE95-614122] p 3202 N95-32524
Probe transparency in a two-level medium embedded by a squeezed vacuum [DE95-614123] p 3198 N95-32525
Tracing a planar algebraic curve [DE95-613375] p 3195 N95-33058

INTERNATIONAL CIVIL AVIATION ORGANIZATION, MONTREAL (QUEBEC).
Integrating human factors knowledge into certification: The point of view of the Internatioanal Civil Aviation Organization (ICAO) p 3175 N95-34782

IOWA STATE UNIV. OF SCIENCE AND TECHNOLOGY, AMES, IA.
Structural wave propagation and sound radiation study through time and spatial processing p 3200 N95-33251
Optical anisotropy of (110) surfaces of Ag and Cu [DE95-010130] p 3229 N95-33637
Nonlinear stability of unsteady viscous flow [AD-A294931] p 3113 N95-34597

IOWA UNIV., IOWA CITY, IA.
Multiscale characteristics and modeling of atmospheric methane p 3154 N95-33339

ISHIKAWAJIMA-HARIMA HEAVY INDUSTRIES CO. LTD., TOKYO (JAPAN).
Design of secondary flow control cascade using numerical simulation p 3034 N95-34507
A study of supersonic mixing flow field with ramp injector p 3035 N95-34512

J

JAPAN ATOMIC ENERGY RESEARCH INST., TOKYO (JAPAN).
Development and trial manufacturing of 1/2-scale partial mock-up of blanket box structure for fusion experimental reactor [DE95-737184] p 3219 N95-32408
Design concept of a cryogenic distillation column cascade for a ITER scale fusion reactor [DE95-737185] p 3220 N95-32409
Stability analysis of external kink mode for ITER L-mode profile plasmas [DE95-737207] p 3220 N95-32410
Transport studies of tokamak plasmas in JT-60 device [DE95-737227] p 3220 N95-32417
Hydrogen formation in metals and alloys during fusion reactor operation [DE95-737224] p 3202 N95-32529
Irradiation experiments of low copper A533B steels for reactor pressure vessel tested in JMTR [DE95-737266] p 3077 N95-32531
Irradiation tests of critical components for remote handling in gamma radiation environment [DE95-737223] p 3221 N95-32565
Evaluation of strength properties of developed SiC/C compositionally gradient graphite materials [DE95-737271] p 3063 N95-32711
Low-energy Ion-Beam Deposition apparatus equipped with surface analysis system [DE95-737272] p 3212 N95-32712

JET PROPULSION LAB., CALIFORNIA INST. OF TECH., PASADENA, CA.
A decade of neural networks: Practical applications and prospects [NASA-CR-198867] p 3188 N95-32659
Thermoelectric material development [DE95-007890] p 3149 N95-32811
Summaries of the Fifth Annual JPL Airborne Earth Science Workshop. Volume 1: AVIRIS Workshop [NASA-CR-198922] p 3128 N95-33730
Mapping target signatures via partial unmixing of AVIRIS data p 3129 N95-33737
Airborne Visible/Infrared Imaging Spectrometer (AVIRIS) onboard calibration system p 3116 N95-33739
New calibration techniques for the Airborne Visible/Infrared Imaging Spectrometer (AVIRIS) p 3116 N95-33740
Calibration to surface reflectance of terrestrial imaging spectrometry data: Comparison of methods p 3130 N95-33743
Evaluation of the photochemical reflectance index in AVIRIS imagery p 3131 N95-33747
High accuracy in-flight wavelength calibration of imaging spectrometry data p 3132 N95-33750
Determination of the in-flight spectral calibration of AVIRIS using atmospheric absorption features p 3117 N95-33751
An improved spectral calibration requirement for AVIRIS p 3117 N95-33752
Movement of water vapor in the atmosphere measured by an imaging spectrometer at Rogers Dry Lake, CA p 3132 N95-33753
In-flight radiometric calibration of AVIRIS in 1994 p 3117 N95-33754
Measurement of atmospheric water vapor, leaf liquid water and reflectance with AVIRIS in the Boreal Ecosystem-Atmosphere Study: Initial results p 3133 N95-33755
Measurement of the spectral absorption of liquid water in melting snow with an imaging spectrometer p 3133 N95-33756
Vegetation species composition and canopy architecture information expressed in leaf water absorption measured in the 1000 nm and 2200 spectral region by an imaging spectrometer p 3133 N95-33757
AVIRIS user's guide p 3117 N95-33759
Improving alpine-region spectral unmixing with optimal-fit snow endmembers p 3135 N95-33764
Airborne Visible/Infrared Imaging Spectrometer (AVIRIS): Sensor improvements for 1994 and 1995 p 3117 N95-33769
Summaries of the Fifth Annual JPL Airborne Earth Science Workshop. Volume 2: TIMS Workshop [NASA-CR-198923] p 3136 N95-33789
Analyses of TIMS and AVIRIS data, integrated with field and laboratory spectra, for lithological and mineralogical interpretation of Vulcano Island, Italy p 3137 N95-33790
The JPL Field Emission Spectrometer p 3117 N95-33794
The 1994 laboratory calibration of TIMS p 3117 N95-33796
The 1994 TIMS airborne calibration experiment: Castaic Lake, California p 3117 N95-33797
TIMS observations of surface emissivity in HAPEX-Sahel p 3139 N95-33799
Summaries of the Fifth Annual JPL Airborne Earth Science Workshop. Volume 3: AIRSAR Workshop [NASA-CR-198924] p 3139 N95-33801
Measuring soil moisture with imaging radars p 3139 N95-33803
Use of TOPSAR digital elevation data to determine the 3-dimensional shape of an alluvial fan p 3139 N95-33804
Accurate estimation of sigma(exp 0) using AIRSAR data p 3139 N95-33805
Bayes classification of interferometric TOPSAR data p 3140 N95-33808
The unique radar scattering properties of silicic lava flows and domes p 3141 N95-33811
On the potential of long wavelength imaging radars for mapping vegetation types and woody biomass in tropical rain forests p 3141 N95-33812
Estimation of penetration of forest canopies by Interferometric SAR measurements p 3141 N95-33814
Regional mapping of forest canopy water content and biomass using AIRSAR images over BOREAS study area p 3142 N95-33815
Geographic information system for fusion and analysis of high-resolution remote sensing and ground data p 3240 N95-34224
Knowledge-based assistance for science visualization and analysis using large distributed databases p 3241 N95-34227
A distributed system for visualizing and analyzing multivariate and multidisciplinary data p 3241 N95-34230
Planetary data analysis and display system: A version of PC-McIDAS p 3241 N95-34232
Multi-layer holographic bifurcative neural network system for real-time adaptive EOS data analysis p 3148 N95-34233
DataHub: Science data management in support of interactive exploratory analysis p 3243 N95-34241
DataHub sponsored analysis p 3243 N95-34242

JOINT INST. FOR NUCLEAR RESEARCH, DUBNA (USSR).
NJL Model with nonperturbative dependence on gluon condensate [DE95-623677] p 3233 N95-32405
The Q(2)-dependence of the Gross-Llewellyn Smith sum rule and of the parton distributions [DE95-623678] p 3202 N95-32406
Isgur-Wise function and polarization characteristics of Lambda(sub b)-baryon [DE95-623696] p 3202 N95-32407
A choice of input variables for a multilayer perceptron [DE95-623573] p 3187 N95-32476
Physics of the CEM92M Code [DE95-623579] p 3202 N95-32477
General-covariant Quantum Mechanics of Dirac particle in curved space-times [DE95-623600] p 3233 N95-32478
The method of integration of the nonlinear Schroedinger equation with a source [DE95-623601] p 3195 N95-32479
Transparent potential perturbations on lattices and in the periodical structures. Elements of the Qualitative Theory of Wave Motion Over the Channels [DE95-623602] p 3225 N95-32480
Campbell-Hausdorff formula and algebras with operator [DE95-623635] p 3195 N95-32609
Damage formation in silicon irradiated by heavy ions with energy more than 1 MeV/a.m.u. [DE95-623968] p 3204 N95-32610
Bogolyubov lectures [DE95-620495] p 3197 N95-32624
The structure of ion track in Solids produced by ions with high level inelastic energy losses [DE95-620942] p 3205 N95-32625
About the mechanism of heavy ion radiation influence on the metals at high temperature [DE95-620943] p 3078 N95-32626
Application of deformable templates for recognizing tracks detected with High Pressure Drift Tubes [DE95-621870] p 3188 N95-32627
Cathode readout with stripped resistive drift tubes [DE95-621871] p 3102 N95-32628
Analysis of radiation damages of electronic circuits by separate irradiation of their components with a collimated charged particle beam [DE95-621946] p 3102 N95-32629
On application of wavelet analysis to separation of secondary particles from nucleus-nucleus interactions [DE95-623572] p 3205 N95-32630

The interrelation of a Z(3) gauge theory on flat lattices and a spin-1 BEG model
[DE95-623634] p 3227 N95-32631
A novel approach to the problem of highly-sensitive regular analysis for man-made plutonium in environment and human body
[DE95-620764] p 3164 N95-32666
Zero modes of Gauss constraint in gaugeless reduction of Yang-Mills theory
[DE95-623676] p 3234 N95-32667
A Study of the A dependence of the deep inelastic scattering of leptons and implications for understanding of the EMC effect
[DE95-613711] p 3206 N95-32796
Spin effects in high energy photon-hadron scattering in QCD
[DE95-623679] p 3234 N95-32961
The Problem 4/3 as a consequence of contracted length non-covariance
[DE95-623628] p 3207 N95-33226

JUSTUS LIEBIG-UNIV., GIESSEN (GERMANY).
Estimation of spatially restricted LET using track structure models p 3161 N95-32722
Heavy ion induced DNA-DSB in yeast and mammalian cells p 3161 N95-32723
Heavy ion induced mutations in mammalian cells: Cross sections and molecular analysis p 3162 N95-32728
Heavy ion action on single cells: Cellular inactivation capability of single accelerated heavy ions p 3162 N95-32729
X-ray-provoked non-Mendelian transgenerational oncodeterminants p 3163 N95-32731

K

KANSAS STATE UNIV., MANHATTAN, KS.
Low energy collisions involving multiply charged ions
[DE95-010911] p 3203 N95-32564
High energy collisions involving multiply charged ions
[DE95-010912] p 3206 N95-32763
The mean lifetimes of the 2p(sigma) lowest bound state of HeH(2+) and its isotopes
[DE95-010812] p 3206 N95-32966
CDW-EIS calculation of longitudinal momentum distribution in single ionization of helium by Ni(24+) ions
[DE95-010816] p 3207 N95-33241
Velocity dependence of ionization and excitation of hydrogen molecules by fast proton impact
[DE95-010818] p 3207 N95-33370
State-selective single electron capture cross sections in He(exp 2+) + Li(2s) and Li(*)(2p) collisions
[DE95-010819] p 3207 N95-33371
An ion-ion collisions system at KSU
[DE95-010820] p 3208 N95-33372
Impact-parameter dependent L-K vacancy-transfer in collisions of Ni(23+) with Ge solid targets
[DE95-010821] p 3228 N95-33373
Electron-electron interaction in the ionization of hydrogenlike projectiles by He
[DE95-010822] p 3208 N95-33374
Mean lifetime measurements of (3)He(4)He2+
[DE95-010813] p 3209 N95-34355

KANSAS UNIV. CENTER FOR RESEARCH, INC., LAWRENCE, KS.
Development of an L-, C-, and X-band radar for backscattering studies over vegetation
[NASA-CR-199112] p 3097 N95-33033
Studies of microwave scattering and canopy architecture for boreal forests
[NASA-CR-199113] p 3099 N95-33497
Studies of microwave scattering and canopy architecture for boreal forests
[NASA-CR-199114] p 3099 N95-33726

KAWASAKI HEAVY INDUSTRIES LTD., TOKYO (JAPAN).
A large scale 3D Navier-Stokes analysis using NAL-NWT p 3039 N95-34539
Role of computational fluid dynamics in aeronautical engineering. Number 12: Formulation and verification of uni-particle upwind schemes for the Euler equations p 3039 N95-34540

KENTUCKY UNIV., LEXINGTON, KY.
Advanced boundary element methods in aeroacoustics and elastodynamics p 3200 N95-33694

KESTREL INST., PALO ALTO, CA.
Automated support for software engineering
[AD-A294965] p 3182 N95-34582

KOREA CANCER CENTER HOSPITAL, SEOUL (REPUBLIC OF KOREA).
Development of ultrasensitive spectroscopic analysis technology. Development of atomic spectroscopy technology
[DE95-614352] p 3066 N95-32566
Development of tokamak experiment technology: A study on the nuclear fusion reactor
[DE95-614255] p 3223 N95-33619

KYUSHU UNIV., KASUGA (JAPAN)
Numerical simulations of dynamic stall phenomena in low speed flows p 3040 N95-34546
Numerical simulation of unsteady viscous flow around an airfoil with oscillating spoiler p 3040 N95-34547

KYOTO INST. OF TECH. (JAPAN).
Parallel computation for two dimensional incompressible flow on array of transputers p 3042 N95-34558

KYOTO UNIV. (JAPAN).
Adaptive grid method using elliptic equation for compressible flows p 3035 N95-34515
Structure of weak shock waves in bubbly liquid p 3037 N95-34527
Direct numerical simulation of incompressible homogeneous isotropic turbulence using compressible Navier-Stokes equations p 3037 N95-34529

L

LABORATOIRE DE MEDECINE AEROSPATIALE, BRETIGNY-SUR-ORGE (FRANCE).
Anti-G suits p 3168 N95-34054

LANCASTER UNIV. (ENGLAND).
Track finding and fitting in the H1 forward track detector
[PB95-234985] p 3214 N95-34651

LAWRENCE LIVERMORE NATIONAL LAB., LIVERMORE, CA.
Visualization methods for high-resolution, transient, 3-D, finite element situations
[DE95-009479] p 3179 N95-32390
Metallic laminates for engine applications
[DE95-010259] p 3062 N95-32399
The future of finite element applications on massively parallel supercomputers
[DE95-011659] p 3184 N95-32415
Functional requirements analysis and human machine interface specifications for handheld metal detector wands
[DE95-009845] p 3167 N95-32535
Experimental study of the processes in the expander of the axisymmetric mirror device
[DE95-009846] p 3221 N95-32536
Differencing the diffusion equation on unstructured meshes in 2-D
[DE95-010410] p 3195 N95-32559
Ricor K506B cryocooler performance during the Clementine mission and ground testing
[DE95-010683] p 3089 N95-32568
Three-dimensional ground penetrating radar imaging using synthetic aperture time-domain focusing
[DE95-010731] p 3095 N95-32569
General limits on the performance of high power radiators
[DE95-010732] p 3095 N95-32570
Predicted operating conditions for maintaining mode purity in the 1MW 200 GHz FOM Free Electron Maser
[DE95-010795] p 3117 N95-32571
Single event and TREE latchup mitigation for a star tracker sensor: An innovative approach to system level latchup mitigation
[DE95-010331] p 3059 N95-32593
Status of the large-scale dark-matter axion search
[DE95-008828] p 3246 N95-32597
Fracture toughness and tensile behavior of multi-layer laminated metal composite of Al 6090-25 vol % SiCp and Al 5182
[DE95-011421] p 3062 N95-32602
Large-eddy simulation of the development of stably-stratified atmospheric boundary layers over cool flat surfaces
[DE95-009574] p 3156 N95-32697
A dual, parallel cavity Fabry-Perot interferometer
[DE95-010796] p 3115 N95-32900
Copper-diamond composite substrates for electronic components
[DE95-011520] p 3079 N95-33063
The uses of Electron Beam Ion Traps in the study of highly charged ions
[DE95-011537] p 3212 N95-33064
Energy and Technology Review
[DE95-011686] p 3223 N95-33066
A study of the effect of grain size on the ballistic performance of silicon carbide
[DE95-011724] p 3126 N95-33068
Background meeting and technology demonstration: Chromium electroplating of superconductor strand
[DE95-011736] p 3068 N95-33070
Quench antenna and fast-motion investigations during training of a 7T dipole magnet
[DE95-012371] p 3103 N95-33080
Observation of KLM dielectronic recombination resonances in highly charged uranium ions
[DE95-010266] p 3207 N95-33219
A comparison of risk assessment techniques from qualitative to quantitative
[DE95-011430] p 3197 N95-33220
Absolute wavefront measurements of high-energy laser beams in the Beamlet Demonstration Project for the National Ignition Facility
[DE95-012224] p 3118 N95-33378
Bicriteria network design problems
[DE95-012052] p 3099 N95-33387
Cost-effective data-parallel load balancing
[DE95-010985] p 3186 N95-33403
Lithogenic and cosmogenic tracers in catchment hydrology
[DE95-011523] p 3143 N95-33407
Machinability study of Aermet 100
[DE95-011532] p 3084 N95-33408
Feasibility of fullerene thin films for high-speed all-optical switching
[DE95-011735] p 3085 N95-33409
A low diffraction beam technique for scanning in the shallow ocean
[DE95-011742] p 3159 N95-33410
Phase control and measurement of ultrashort optical pulses
[DE95-011746] p 3216 N95-33411
Optical pulse generation using fiber lasers and integrated optics
[DE95-011517] p 3216 N95-33506
Gasdynamic model of turbulent combustion in an explosion
[DE95-010267] p 3074 N95-33627
Unitized Regenerative Fuel Cells for solar rechargeable aircraft and zero emission vehicles
[DE95-010684] p 3150 N95-33642
Proceedings: High performance functional computing
[DE95-010736] p 3186 N95-33643
Low-energy response of superconducting tunnel junction x-ray spectrometers
[DE95-011733] p 3230 N95-33650
Multiple-beam pulse shaping and preamplification
[DE95-011738] p 3216 N95-33651
Rigid bodies for metal forming analysis with NIKE3D
[DE95-011740] p 3182 N95-33652
The 3D metal forming applications of ALE techniques
[DE95-011745] p 3080 N95-33653
Plasma mediated ablation of biological tissues with ultrashort laser pulses
[DE95-011748] p 3164 N95-33654
Temporal dynamics of the multi-frequency spectrum generated by self-phase modulation of two frequencies in single-mode fiber
[DE95-010920] p 3119 N95-33703
Discrete modeling of optical pulse propagation in nonlinear media
[DE95-011515] p 3216 N95-34020
Consistent finite-volume discretization of hydrodynamic conservation laws for unstructured grids
[DE95-011730] p 3112 N95-34437
Measurements of cross sections and resonance structures following electron-impact excitation/ionization of Na-like Kr and Xe
[DE95-011731] p 3230 N95-34438
Multilayer thermoelectric films: A strategy for the enhancement of ZT
[DE95-011535] p 3081 N95-34482
The development of a distributed computing environment for the design and modeling of plasma spectroscopy experiments
[DE95-011725] p 3183 N95-34813

LEHIGH UNIV., BETHLEHEM, PA.
The effect of labyrinth seals on the dynamics of turbomachinery p 3122 N95-32752
Asymptotic structure of supersonic turbulent boundary layers p 3107 N95-32898
The effect of interaction on boundary-layer separation and breakdown p 3109 N95-33310
Microstructural studies of hydrogen damage in metastable stainless steels p 3080 N95-33774
Selective methane oxidation over promoted oxide catalysts
[DE95-012319] p 3075 N95-34021

LIEGE UNIV. (BELGIUM).
Beware of agents when flying aircraft: Basic principles behind a generic methodology for the evaluation and certification of advanced aviation systems p 3176 N95-34787

LIVERPOOL UNIV. (ENGLAND).
Track finding and fitting in the H1 forward track detector
[PB95-234985] p 3214 N95-34651

LOCKHEED-FORT WORTH CO., FORT WORTH, TX.
Application of advanced safety technique to ring laser gyro inertial navigation system integration
p 3048 N95-33140

LOS ALAMOS NATIONAL LAB., NM.
Off-training-set error for the Gibbs and the Bayes optimal generalizers
[DE95-006344] p 3187 N95-32375
Bolt preload selection for pulsed-loaded vessel closures
[DE95-006346] p 3121 N95-32376
Ductile damage model with void coalescence
[DE95-007855] p 3125 N95-32385
Training neural networks using sequential extended Kalman filtering
[DE95-007874] p 3187 N95-32386
Approaches to implementing deterministic models in a probabilistic framework
[DE95-009483] p 3197 N95-32391
Unexpected matching insensitivity in DTL of GTA accelerator
[DE95-011984] p 3211 N95-32416
TEM investigation on the low temperature phase of HfV2
[DE95-009500] p 3225 N95-32532
Intervals in evolutionary algorithms for global optimization
[DE95-010866] p 3179 N95-32572
A methodology for evaluating air pollution strategies to improve the air quality in Mexico City
[DE95-010874] p 3152 N95-32573
Semi-analytic computation of the driven fields in right circular cylindrical microwave applicators
[DE95-010875] p 3203 N95-32574
Design and testing criteria for bipolar plate materials for PEM fuel cell applications
[DE95-010878] p 3148 N95-32575
Behavior of structural and target materials irradiated in spallation neutron environments
[DE95-010879] p 3203 N95-32576
In situ ion-beam analysis and modification of sol-gel zirconia thin films
[DE95-010994] p 3203 N95-32577
Faddeev calculations of p(mu)+p collisions: Effect of hyperfine splitting on the cross sections
[DE95-007838] p 3203 N95-32583
Progress towards antihydrogen production by the reaction of cold antiprotons with positronium atoms
[DE95-007850] p 3204 N95-32584
Numerical analysis of the ultraprecision machining of copper
[DE95-007857] p 3089 N95-32585
Investigation on deflagration to detonation transition in porous energetic materials
[DE95-011638] p 3088 N95-32605
Message based event specification for debugging nondeterministic parallel programs
[DE95-006169] p 3179 N95-32669
Development of a composite satellite structure for FORTE
[DE95-009416] p 3058 N95-32713
Analysis of a HTSC current lead under nonlinear heat transfer conditions
[DE95-009420] p 3102 N95-32714
The RDB: A parallel, spatial database for the IES/BTI system
[DE95-009425] p 3179 N95-32715
On the Minimum Weight Steiner Triangular Tiling Problem
[DE95-009482] p 3180 N95-32716
High performance systems
[DE95-009523] p 3185 N95-32771
Open architecture CNC system
[DE95-009485] p 3177 N95-32955
Technical support in the area of theoretical support of nuclear preequilibrium
[DE95-011617] p 3212 N95-32960
Automatic script identification from images using cluster-based templates
[DE95-006339] p 3181 N95-33154
Historical detection of atmospheric impacts by large bolides using acoustic-gravity waves
[DE95-010864] p 3246 N95-33211
Function approximation using adaptive and overlapping intervals
[DE95-010865] p 3191 N95-33212
Magnetostriction and thermal expansion of the Kondo semiconductor Ce3Bi4Pt3
[DE95-011975] p 3229 N95-33386
Nonequilibrium problems in Quantum Field Theory and Schwinger's closed time path formalism
[DE95-012056] p 3234 N95-33388
Crystalline-as-deposited CaGa2S4: Ce via low-temperature metal-organic chemical vapor deposition
[DE95-010883] p 3229 N95-33401
Indirect measurements of hydrogen: The deficit method for a many-component system
[DE95-010993] p 3208 N95-33623
A comparison of interface tracking methods
[DE95-009481] p 3111 N95-33698
The oxidation of energetic materials in supercritical water
[DE95-010888] p 3088 N95-33702
Stress relaxation in discontinuously reinforced composites
[DE95-010928] p 3064 N95-33704
Lattice Polymer Automata
[DE95-011980] p 3062 N95-33848
Cooling tower and plume modeling for satellite remote sensing applications
[DE95-012000] p 3143 N95-33849
Development of local shear bands and orientation gradients in fcc polycrystals
[DE95-012072] p 3231 N95-34450

LOUISIANA TECH UNIV., RUSTON, LA.
Application of impact dampers in vibration control of flexible structures p 3127 N95-32420
Modeling of DC spacecraft power systems
p 3062 N95-32423

LUCAS ELECTRONICS, BIRMINGHAM (ENGLAND).
The application of Ada and formal methods to a safety critical engine control system p 3094 N95-33142

M

MACDONALD, DETTWILER AND ASSOCIATES LTD., RICHMOND (BRITISH COLUMBIA).
Combined hyperspatial and hyperspectral imaging spectrometer concept p 3129 N95-33738

MARYLAND UNIV., BALTIMORE, MD.
Toxin-mediated transfer and expression of genes in nerve cells
[AD-A290501] p 3164 N95-33200

MARYLAND UNIV., COLLEGE PARK, MD.
Application of vorticity transport analysis to the development of physically accurate turbulence models
p 3107 N95-32905
The Grid Analysis and Display System (GRADS): A practical tool for Earth science visualization
p 3241 N95-34231
VIEWCACHE: An incremental pointer-based access method for autonomous interoperable databases
p 3242 N95-34235

MASSACHUSETTS INST. OF TECH., CAMBRIDGE, MA.
Topography from shading and stereo
p 3241 N95-34229
Current issues in the design and information content of instrument approach charts
[AD-A294752] p 3047 N95-34562
Fabrication technology and measurement of coupled quantum dot devices
[AD-A294853] p 3231 N95-34569
The virtual sailor: Synthetic humans for virtual environments
[AD-A293560] p 3166 N95-34610
Numerical and symbolic algorithms for application specific signal processing
[AD-A294125] p 3100 N95-34749

MASSACHUSETTS INST. OF TECH., LEXINGTON, MA.
RASSP benchmark 1 technical description. Revision 1
[AD-A293030] p 3096 N95-32773
Space-time adaptive processing for airborne radar
[AD-A293032] p 3098 N95-33152
GPS-Squitter interference analysis
[AD-A293690] p 3047 N95-33480
The development of the automatic target recognition system for the UGV/RSTA LADAR
[AD-A294090] p 3100 N95-34474

MASSACHUSETTS UNIV., LOWELL, MA.
Mid-latitude ionospheric plasma drift: A comparison of digital ionosonde and incoherent scatter radar measurements at Millstone Hill p 3222 N95-32838

MATRA MARCONI SPACE, TOULOUSE (FRANCE).
GPS-based navigation for space applications
p 3058 N95-33144

MCAT INST., MOFFETT FIELD, CA.
Boundary layer transition studies
[NASA-CR-198983] p 3106 N95-32454

MCDONNELL-DOUGLAS AEROSPACE, LONG BEACH, CA.
Fan noise prediction assessment
[NASA-CR-195051] p 3200 N95-33831

MCDONNELL-DOUGLAS CORP., SAINT LOUIS, MO.
PSC algorithm description p 3051 N95-33013
PSC implementation and integration
p 3051 N95-33014
Propulsion Controlled Aircraft design and development
p 3053 N95-33022

MCMASTER UNIV., HAMILTON (ONTARIO).
Low strain behaviour of a particulate reinforced aluminum alloy
[ISBN-0-315-84906-1] p 3078 N95-32935
Dividing annular/two-phase flow in horizontal T-junctions
[ISBN-0-315-84910-X] p 3057 N95-33030

MELBOURNE UNIV., PARKVILLE (AUSTRALIA).
Doppleron resonances in the diffraction of atoms by an evanescent field
[DE95-619190] p 3204 N95-32622
Inversion of electron-water elastic scattering data
[DE95-619323] p 3204 N95-32623
The non-relativistic charged Bose gas in a magnetic field. Part 1: Formalism
[DE95-619698] p 3205 N95-32632
Comparison of lead zirconate titanate thin films on ruthenium oxide and platinum electrodes
[DE95-617597] p 3082 N95-32710
A declarative debugger for a logical-functional language p 3183 N95-33007

METEOROLOGICAL OFFICE, BRACKNELL (ENGLAND).
Enhanced shortwave cloud radiative forcing due to anthropogenic aerosols
[DE95-013319] p 3156 N95-34214

MIAMI UNIV., CORAL GABLES, FL.
Ocean observations with EOS/MODIS: Algorithm development and post launch studies
[NASA-CR-198928] p 3143 N95-32914

MICHIGAN UNIV., ANN ARBOR, MI.
Simulation of patch and slot antennas using FEM with prismatic elements and investigations of artificial absorber mesh termination schemes
[NASA-CR-198974] p 3097 N95-32822
Near-limit drop deformation and secondary breakup
p 3107 N95-32902
Transport phenomena in subsonic and supersonic flows in a duct with mass injection p 3108 N95-32934
Ignition and combustion of cellulosic dust particles
p 3073 N95-33308
A new approach to fracture of layered fibrous composites: Experiments and analysis
p 3063 N95-33309
Response and failure of thick composite rings subjected to uniform external hydrostatic pressure or radial contraction p 3064 N95-33326

MILITARY ACADEMY, WEST POINT, NY.
Implementation of a Single-Stage-To-Orbit (SSTO) model for stability and control analysis
p 3059 N95-32432

MILLITECH CORP., SOUTH DEERFIELD, MA.
Monolithic diode arrays for quasioptical millimeter wave beam steering
[AD-A294256] p 3100 N95-34460

MINNESOTA UNIV., MINNEAPOLIS, MN.
Parallel solution of large-scale nonlinear optimization
[AD-A294372] p 3186 N95-34340
Ultrafast near-field scanning optical microscopy (NSOM) of emerging display technology media: Solid state electronic structure and dynamics
[AD-A294879] p 3218 N95-34571
Si-device-related interface research
[AD-A293587] p 3076 N95-34615
The growth of ultrathin epitaxial intermetallic films
[AD-A295037] p 3232 N95-34795

MITRE CORP., MCLEAN, VA.
SAR
[AD-A295020] p 3101 N95-34788
Security and privacy in the NII
[AD-A293475] p 3244 N95-34816

MITSUBISHI ELECTRIC CORP., TOKYO (JAPAN).
Numerical simulation of film cooling effect around axisymmetric body in hypersonic flow field
p 3037 N95-34526

MITSUBISHI HEAVY INDUSTRIES LTD., TOKYO (JAPAN).
Verification of turbine cascade flow with tip clearance
p 3035 N95-34511
Calculation of supersonic combustion in SCRAMJET engines p 3035 N95-34513
Numerical simulation of two-dimensional compressible inviscid flow on unstructured grid system
p 3041 N95-34557

MONTANA STATE UNIV., BOZEMAN, MT.
Fundamental studies of gas phase ionic reactions by ion mobility spectrometry p 3069 N95-33268

MOSCOW INST. OF AVIATION TECHNOLOGY (USSR).
Development and application of the methods for pilot-aircraft system research to the manual control tasks of modern vehicles p 3094 N95-33139

MOUNT HOLYOKE COLL., SOUTH HADLEY, MA.
The role of the vestibular system in manual target localization p 3166 N95-32422

N

NAGOYA UNIV., NAGOYA (JAPAN).
A variation of the Riemann Problem solution and its application to implicit Godunov's scheme
p 3036 N95-34516
A simulation of damping process of pendulum motion due to aerodynamic forces p 3041 N95-34551

NATIONAL AERONAUTICS AND SPACE ADMINISTRATION, WASHINGTON, DC.
Budget estimates: Fiscal year 1994. Volume 1: Agency summary
[NASA-TM-110815] p 3244 N95-33069
Budget estimates: Fiscal year 1994. Volume 2: Construction of facilities
[NASA-TM-110816] p 3245 N95-33081
Budget estimates: Fiscal year 1994. Volume 3: Research and program management
[NASA-TM-110817] p 3245 N95-33082
Shuttle to Space Station. Heart assist implant. Hubble update. X-30 mock-up
[NASA-TM-110837] p 3056 N95-33167
NASA directives master list and index
[NHB-1410.13D] p 3238 N95-33249
Issues in NASA program and project management
[NASA-SP-6101(09)] p 3236 N95-34354

NATIONAL AERONAUTICS AND SPACE ADMINISTRATION. AMES RESEARCH CENTER, MOFFETT FIELD, CA.
Flight test of a low-altitude helicopter guidance system with obstacle avoidance capability p 3043 N95-32490
SOFIA: Aft cavities wind tunnel test
[NASA-TM-110673] p 3033 N95-32682
Full-scale hingeless rotor performance and loads
[NASA-TM-110356] p 3048 N95-32699
Reduction and analysis of seasons 15 and 16 (1991 - 1992) Pioneer Venus radio occulation data and correlative studies with observations of the near infrared emission of Venus
[NASA-CR-199071] p 3247 N95-32700
Minutes of the 12th Joint NASA/DARA-DLR Life Sciences Program Working Group Meeting
[NASA-TM-110655] p 3161 N95-32719
SOFIA 2 model telescope wind tunnel test report
[NASA-TM-110668] p 3033 N95-32764
The mini-CIDEX GC/IMS: Analysis of cometary ice and dust p 3069 N95-33270
A relational metric, its application to domain analysis, and an example analysis and model of a remote sensing domain
[NASA-TM-110358] p 3198 N95-33875
Construction of an advanced software tool for planetary atmospheric modeling p 3184 N95-34225

NATIONAL AERONAUTICS AND SPACE ADMINISTRATION. GODDARD SPACE FLIGHT CENTER, GREENBELT, MD.
SeaWiFS technical report series. Volume 15: The simulated SeaWiFS data set, version 2
[NASA-TM-104566-VOL-15] p 3158 N95-32545
SeaWiFS technical report series. Volume 22: Prelaunch acceptance report for the SeaWFS radiometer
[NASA-TM-104566-VOL-22] p 3159 N95-32672
SeaWiFS technical report series. Volume 31: Stray light in the SeaWiFS radiometer
[NASA-TM-104566-VOL-31] p 3159 N95-32833
NASA wide electronic publishing system: Electronic printing and duplicating. Stage 3 evaluation report
[NASA-TM-104620] p 3237 N95-32922
Correction of thin cirrus effects in AVIRIS images using the sensitive 1.375-micron cirrus detecting channel
p 3131 N95-33748
Remote sensing of smoke, clouds, and radiation using AVIRIS during SCAR experiments p 3132 N95-33749
AVIRIS spectral trajectories for forested areas of the Gifford Pinchot National Forest p 3135 N95-33766
Remotely sensed indicators of habitat heterogeneity and biological diversity: A preliminary report
p 3140 N95-33806
Application of IEM model on soil moisture and surface roughness estimation p 3142 N95-33816
Experimenter's laboratory for visualized interactive science p 3184 N95-34228
A Spatial Analysis and Modeling System (SAMS) for environment management p 3243 N95-34239
A distributed analysis and visualization system for model and observational data p 3243 N95-34240

NATIONAL AERONAUTICS AND SPACE ADMINISTRATION. HUGH L. DRYDEN FLIGHT RESEARCH CENTER, EDWARDS, CA.
An Electronic Workshop on the Performance Seeking Control and Propulsion Controlled Aircraft Results of the F-15 Highly Integrated Digital Electronic Control Flight Research Program
[NASA-TM-104278] p 3050 N95-33009
An overview of integrated flight-propulsion controls flight research on the NASA F-15 research airplane
p 3051 N95-33010
Performance seeking control program overview
p 3051 N95-33011
Minimum fuel mode evaluation p 3051 N95-33015
Minimum fan turbine inlet temperature mode evaluation p 3052 N95-33016
Maximum thrust mode evaluation
p 3052 N95-33017
Rapid deceleration mode evaluation
p 3052 N95-33018
Performance seeking control excitation mode
p 3052 N95-33019
Performance seeking control (PSC) for the F-15 highly integrated digital electronic control (HIDEC) aircraft
p 3053 N95-33020
Background and principles of throttles-only flight control p 3053 N95-33021
Flight test of a propulsion controlled aircraft system on the NASA F-15 airplane p 3049 N95-33023
Design challenges encountered in the F-15 PCA flight test program p 3049 N95-33025
FORTRAN program for analyzing ground-based radar data: Usage and derivations, version 6.2
[NASA-TP-3430] p 3181 N95-33193

NATIONAL AERONAUTICS AND SPACE ADMINISTRATION. JOHN F. KENNEDY SPACE CENTER, COCOA BEACH, FL.
Logistics Operations Management Center: Maintenance Support Baseline (LOMC-MSB)
[NASA-TM-110624] p 3245 N95-33489

NATIONAL AERONAUTICS AND SPACE ADMINISTRATION. LYNDON B. JOHNSON SPACE CENTER, HOUSTON, TX.
National Aeronautics and Space Administration (NASA)/American Society for Engineering Education (ASEE) Summer Faculty Fellowship Program, 1994, volume 1
[NASA-CR-188410] p 3248 N95-32418
Characterization of microgravity effects on bone structure and strength using fractal analysis
p 3165 N95-32419
Liftoff to learning: Assignment space
[NASA-TM-110820] p 3057 N95-32539
Third International Workshop on Ion Mobility Spectrometry
[NASA-CP-3301] p 3069 N95-33265
Twenty-five years of progress. Part 1: Birth of NASA. Part 2: The Moon-a goal
[NASA-TM-110819] p 3253 N95-33384
STS-42 mission highlights resource tape. Part 1 of 2
[NASA-TM-110838] p 3058 N95-34280
STS-42 mission highlights resource tape. Part 2 of 2
[NASA-TM-110840] p 3058 N95-34281
Certification for civil flight decks and the human-computer interface p 3176 N95-34784

NATIONAL AERONAUTICS AND SPACE ADMINISTRATION. LANGLEY RESEARCH CENTER, HAMPTON, VA.
A highly reliable, high performance open avionics architecture for real time Nap-of-the-Earth operations
p 3044 N95-32497
Drag measurements of an axisymmetric nacelle mounted on a flat plate at supersonic speeds
[NASA-TM-4660] p 3034 N95-32821
NASA/DOD Aerospace Knowledge Diffusion Research Project. Paper 50: From student to entry-level professional: Examining the role of language and written communications in the reacculturation of aerospace engineering students
[NASA-TM-110834] p 3237 N95-32883
NASA/DOD Aerospace Knowledge Diffusion Research Project. Report 33: The technical communications practices of US aerospace engineers and scientists: Results of the phase 1 AIAA mail survey
[NASA-TM-110180] p 3239 N95-34217

NATIONAL AERONAUTICS AND SPACE ADMINISTRATION. LEWIS RESEARCH CENTER, CLEVELAND, OH.
Steady-state dynamic behavior of an auxiliary bearing supported rotor system p 3121 N95-32690
Numerical simulation of heat and mass transport during space crystal growth with MEPHISTO
[NASA-TM-107015] p 3089 N95-32718
Investigation of water droplet trajectories within the NASA icing research tunnel
[NASA-TM-107023] p 3034 N95-32769
Low-order nonlinear dynamic model of IC engine-variable pitch propeller system for general aviation aircraft
[NASA-TM-107006] p 3050 N95-32916
Advanced propulsion for geostationary orbit insertion and north-south station keeping
[NASA-TM-107018] p 3060 N95-32917
The effects of ion implantation on the tribology of perfluoropolyether-lubricated 440C stainless steel couples
[NASA-TM-106965] p 3083 N95-32918
Spontaneous dewetting of a perfluoropolyether
[NASA-TM-106964] p 3083 N95-32919
Review of combustion-acoustic instabilities
[NASA-TM-107020] p 3108 N95-32930
Combustion-acoustic stability analysis for premixed gas turbine combustors
[NASA-TM-107024] p 3050 N95-32931
Experimental and analytical assessment of the thermal behavior of spiral bevel gears
[NASA-TM-107009] p 3123 N95-33179
Thermographic imaging for high-temperature composite materials: A defect detection study
[NASA-TM-106950] p 3125 N95-33209
Micromechanics of composites with shape memory alloy fibers in uniform thermal fields
[NASA-TM-107011] p 3063 N95-33210
Low Reynolds number kappa-epsilon and empirical transition models for oscillatory pipe flow and heat transfer
[NASA-TM-109785] p 3110 N95-33496
Metallized gelled propellants: Oxygen/RP-1/aluminum rocket combustion experiments
[NASA-TM-107025] p 3088 N95-33876
Bending strength model for internal spur gear teeth
[NASA-TM-107012] p 3124 N95-33908
A flux splitting scheme with high-resolution and robustness for discontinuities p 3036 N95-34518

NATIONAL AERONAUTICS AND SPACE ADMINISTRATION. MARSHALL SPACE FLIGHT CENTER, HUNTSVILLE, AL.
Research and technology 1994: Annual report of the Marshall Space Flight Center
[NASA-TM-108470] p 3252 N95-33042
NASA-Wide Fastener Technical Interchange Meeting
[NASA-CP-3308] p 3123 N95-33199

NATIONAL AEROSPACE LAB., KAKUDA (JAPAN).
Pop tests of storable biopropellant liquid apogee engine
[NAL-TR-1253] p 3060 N95-32755

NATIONAL AEROSPACE LAB., TOKYO (JAPAN).
Special publication of National Aerospace Laboratory
[NAL-SP-27] p 3034 N95-34505
Numerical simulation of high enthalpy shock tunnel
p 3035 N95-34514
Construction and analysis of difference approximation for scalar conservation laws and its consistency with entropy condition using Boltzmann-like approach
p 3036 N95-34519
Hypersonic CFD analysis for the aerothermodynamic design of HOPE p 3036 N95-34520
Direct numerical simulation of compressible isotropic turbulence p 3037 N95-34523
The effect of buoyancy on flow and heat transfer in curved pipes p 3037 N95-34528
Direct numerical simulation of incompressible homogeneous isotropic turbulence using NWT
p 3038 N95-34530
Elementary benchmarks of the NWT computer system and program performance p 3038 N95-34532
Performance evaluation of the NWT with incompressible NS code p 3038 N95-34533
An unsteady simulation of a centrifugal compressor stage using the NWT p 3038 N95-34536
Application of CFD techique for HYFLEX aerodynamic design p 3039 N95-34542
Flow and heat transfer in rotating curved pipes
p 3040 N95-34545
Direct analysis of transonic rotor noise with CFD technique p 3040 N95-34549
Dependency of a boundary layer flow on computational grids p 3040 N95-34550
Formation of high density cores in molecular cloud
p 3041 N95-34553
Upwind schemes for the two-dimensional Euler equations p 3042 N95-34559

NATIONAL CENTER FOR ATMOSPHERIC RESEARCH, BOULDER, CO.
Interactive interface for National Center for Atmospheric Research (NCAR) graphics p 3239 N95-34220

NATIONAL CHEMICALS INSPECTORATE, SOLNA (SWEDEN).
Chemical substances lists: A guide to the lists used in the Swedish Sunset Project. Supplement to report 13/94. Selecting multiproblem chemicals for risk reduction. A presentation of the Swedish Sunset Project
[PB95-211272] p 3073 N95-33328
Phthalic acid esters used as plastic additives. Volume 1: Ecotoxicological risk assessment. Volume 2: Comparisons of toxicological effects
[PB95-211280] p 3084 N95-33329
Risk assessment of polybrominated diphenyl ethers
[PB95-211306] p 3073 N95-33330

Sensitizing substances
[PB95-211256] p 3074 N95-33634

NATIONAL DEFENCE RESEARCH ESTABLISHMENT, LINKOEPING (SWEDEN).
Activities of the Division of Microwave Technology
[PB95-214524] p 3095 N95-32613
FH and DS spread-spectrum systems in interference-limited HF channels: A comparison
[PB95-211439] p 3098 N95-33230
DETVAg-90: Use of GTD for wave propagation over earth
[PB95-211447] p 3098 N95-33231
CADIR: A model for generating infrarad images
[PB95-222956] p 3215 N95-33239

NATIONAL DEFENCE RESEARCH ESTABLISHMENT, STOCKHOLM (SWEDEN).
Fatigue properties for the Al-Li alloy 2090, part 3
[PB95-214532] p 3078 N95-32614
Stimulus-response compatibility
[PB95-214722] p 3167 N95-33237

NATIONAL GEOPHYSICAL DATA CENTER, BOULDER, CO.
Solar-geophysical data number 607, March 1995. Part 1 (prompt reports). Data for January, February 1995 and late data
[PB95-216388] p 3248 N95-32963
Solar-geophysical data number 607, March 1995: Part 2 (comprehensive reports). Data for September 1994 and miscellaneous
[PB95-216800] p 3248 N95-32964

NATIONAL INST. FOR FUSION SCIENCE, NAGOYA (JAPAN).
Application of grating polarizer to 106.4GHz ECH system on Heliotron-E
[NIFS-334] p 3225 N95-34624

NATIONAL PHYSICAL LAB., TEDDINGTON (ENGLAND).
First NPL Calorimetry Workshop
[PB95-236063] p 3235 N95-34654

NATIONAL RENEWABLE ENERGY LAB., GOLDEN, CO.
Wind turbine trailing edge aerodynamic brakes
[DE95-004061] p 3033 N95-32548
HYBRID2: A versatile model of the performance of hybrid power systems
[DE95-004062] p 3148 N95-32551
Solving widespread low-concentration VOC air pollution problems: Gas-phase photocatalytic oxidation answers the needs of many small businesses
[DE95-004059] p 3152 N95-32668
Techniques for the determination of local dynamic pressure and angle of attack on a horizontal axis wind turbine
[DE95-009204] p 3149 N95-32685
Environmental chamber studies of atmospheric reactivities of volatile organic compounds: Effects of varying chamber and light source
[DE95-009225] p 3152 N95-32686
A comparison of modeled and measured energy use in hybrid electric vehicles
[DE95-000297] p 3102 N95-32808
The next generation of automobile emissions reduction: Innovative control of off-cycle emissions
[DE95-004057] p 3153 N95-32809
Device physics of thin-film polycrystalline cells and modules
[DE95-009209] p 3149 N95-32817
Photovoltaic Manufacturing Technology (PVMaT)
[DE95-004093] p 3149 N95-33153
The 17th Symposium on Biotechnology for Fuels and Chemicals
[DE95-004054] p 3150 N95-33225
Tomorrow's energy today for cities and countries
[DE95-012464] p 3150 N95-33383
Fatigue damage estimate comparisons for northern European and US wind farm loading environments
[DE95-011061] p 3150 N95-33706

NAVAL AIR WARFARE CENTER, CHINA LAKE, CA.
Multispectral image correlation for air-to-ground targeting p 3043 N95-32489
An investigation of the chemistry of citric acid in military soldering applications
[AD-A295042] p 3105 N95-34796

NAVAL AIR WARFARE CENTER, PATUXENT RIVER, MD.
The ANVIS head-up display: An analysis of its application to naval helicopters
[AD-A294342] p 3170 N95-34358

NAVAL MEDICAL RESEARCH INST., BETHESDA, MD.
Density, heat capacity, viscosity, and thermal conductivity of mixtures of CO2, He, H2, H2O, N2, and O2
[AD-A288731] p 3076 N95-34814

NAVAL POSTGRADUATE SCHOOL, MONTEREY, CA.
Speaker identification using the two-dimensional cepstrum transform
[AD-A294204] p 3099 N95-34304
Branch and bound methods for search problems
[AD-A294522] p 3182 N95-34349
An experimental study of collective sea state modes of deep water surface gravity waves
[AD-A294007] p 3160 N95-34372
Animation within a multimedia training system for night vision goggles
[AD-A294095] p 3170 N95-34475
Developing multimedia instructional systems: An example application for training in night vision goggles
[AD-A294521] p 3235 N95-34479
A real-time single-camera, stereoscopic video device
[AD-A294105] p 3116 N95-34496
The 11th Annual Review of Progress in Applied Computational Electromagnetics, volume 1
[AD-A294850] p 3100 N95-34566
The 11th Annual Review of Progress in Applied Computational Electromagnetics, volume 2
[AD-A294851] p 3100 N95-34567
Managing technological change in a military treatment facility: A case study of medical diagnostic imaging support (MDIS) system
[AD-A294894] p 3165 N95-34573
Image compression scheme for network transmission
[AD-A294959] p 3182 N95-34580
An LDV investigation of support structure influence on the flow field near the wingtip of a STOVL configuration in hover
[AD-A294126] p 3042 N95-34750
Turbulent heat flux measurements over the Greenland, Norwegian and Barents seas
[AD-A294129] p 3157 N95-34751

NAVAL RESEARCH LAB., BAY SAINT LOUIS, MS.
Proceedings of the ONR/NRL workshop on modeling the dispersion of nuclear contaminants in the arctic seas
[AD-A294373] p 3159 N95-34341

NAVAL RESEARCH LAB., WASHINGTON, DC.
Polarization and wavelength diversities of Gulf Stream fronts imaged by AIRSAR p 3140 N95-33807
On the virtues of parameterized uniform crossover
[AD-A293985] p 3182 N95-34456
Towards friendlier user interfaces for expert systems
[AD-A294056] p 3192 N95-34467
Adaptive strategy selection for concept learning
[AD-A294086] p 3193 N95-34473
Extreme broadening of stimulated Raman scattered light from high intensity laser plasma interactions
[AD-A294165] p 3120 N95-34761

NAVAL UNDERSEA WARFARE CENTER, NEW LONDON, CT.
A molecular dynamics investigation of the structural characteristics of amorphous and annealed poly (Vinylidene fluoride) and vinylidene fluoride - trifluoroethylene copolymers
[AD-A294116] p 3086 N95-34502

NAVY CENTER FOR APPLIED RESEARCH IN ARTIFICIAL INTELLIGENCE, WASHINGTON, DC.
Improving the comprehensibility, accuracy, and generality of reactive plans
[AD-A294104] p 3193 N95-34495
Conditions for implicit parallelism
[AD-A294110] p 3193 N95-34497
Is the genetic algorithm a cooperative learner?
[AD-A294112] p 3193 N95-34499
Explanations of empirically derived reactive plans
[AD-A294114] p 3193 N95-34501

NAVY PERSONNEL RESEARCH AND DEVELOPMENT CENTER, SAN DIEGO, CA.
Event-related potentials and electroencephalograms in adaptive operator training: Rationale and annotated bibliography
[AD-A294337] p 3166 N95-34356

NETHERLANDS ENERGY RESEARCH FOUNDATION, PETTEN (NETHERLANDS).
Corrosion of separator plate constituents in molten carbonate
[PB95-214490] p 3149 N95-32813

NEVADA UNIV., LAS VEGAS, NV.
A preliminary evaluation of histogram-based binarization algorithms
[DE95-009886] p 3179 N95-32470
Prediction of OCR accuracy using simple image features
[DE95-009887] p 3236 N95-32471

NEW ENERGY AND INDUSTRIAL TECHNOLOGY DEVELOPMENT ORGANIZATION, TOKYO (JAPAN).
Investigation research on introducing new energy technology, promoting its practical application, and providing its instruction
[DE95-769801] p 3148 N95-32403
Feasibility survey on international cooperation for high efficiency energy conversion technology in fiscal 1993
[DE95-769804] p 3148 N95-32546
Technical innovation for reducing emissions of greenhouse effect gas and survey of effects of changes of industrial structures
[DE95-769808] p 3151 N95-32547

NEW HAMPSHIRE UNIV., DURHAM, NH.
Modeling soil climate controls on the exchange of trace gases between the terrestrial biosphere and the atmosphere p 3153 N95-33337
High spectral resolution remote sensing of canopy chemistry p 3128 N95-33731

NEW MEXICO UNIV., ALBUQUERQUE, NM.
Use of AIRSAR to identify woody shrub invasion and other indicators of desertification in the Jornada LTER p 3141 N95-33810
High efficiency vacuum and plasma filled backward wave oscillators: A critical evaluation
[AD-A294963] p 3105 N95-34581

NEW YORK UNIV. MEDICAL CENTER, NEW YORK, NY.
Measurement and regulation of central noradrenergic receptors
[AD-A294065] p 3165 N95-34472

NEWCASTLE-UPON-TYNE UNIV., NEWCASTLE (ENGLAND).
Sleep sets method for partial order verification of concurrent systems
[PB95-236121] p 3183 N95-34655
Analysis of safety requirements in the context of system faults and human errors
[PB95-236105] p 3171 N95-34658

NONDESTRUCTIVE TESTING INFORMATION ANALYSIS CENTER, SAN ANTONIO, TX.
Microwave nondestructive evaluation: State-of-the-Art review
[AD-A294388] p 3125 N95-34346

NORTH CAROLINA AGRICULTURAL AND TECHNICAL STATE UNIV., GREENSBORO, NC.
A general solution to object matching problems by using the multiresolution approximation p 3189 N95-33002

NORTH CAROLINA STATE UNIV., RALEIGH, NC.
Thermo-chemical ablation of heat shields under Earth reentry conditions p 3059 N95-32903
Ice-ocean four dimensional structure and dynamics
[AD-A294017] p 3160 N95-34375

NORTH DAKOTA STATE UNIV. OF AGRICULTURE AND APPLIED SCIENCE, FARGO, ND.
Performance analysis of combined concurrency control and commit protocols in distributed database systems p 3238 N95-33711

NORTHROP GRUMMAN CORP., PRINCETON, NJ.
High beta and second stability region transport and stability analysis
[DE95-011298] p 3225 N95-34812

NORTHWESTERN UNIV., CHICAGO, IL.
Transverse acoustic properties of the B-phase of superfluid helium three p 3074 N95-33414
Enhanced stress projections for error estimation and a singular floating node element for static and dynamic fracture p 3064 N95-33463
Laser-based ultrasonics by dual-probe interferometer detection and narrow-band ultrasound generation p 3118 N95-33464
Bifurcation analysis of multimode instabilities in class B lasers p 3119 N95-33470
Inclusion models of tensile fracture in fiber-reinforced brittle-matrix composites p 3065 N95-33721

NORTHWESTERN UNIV., EVANSTON, IL.
Metal-ceramic interfaces: Overlayer-induced reconstruction and magnetism of 4d transition-metal monolayers
[DE95-011543] p 3075 N95-34483

NORWEGIAN DEFENCE RESEARCH ESTABLISHMENT, KJELLER (NORWAY).
Basis Image Processor Pr5210: Correlator technical description
[PB95-222485] p 3185 N95-32815
Analysis of samples for the first (1994) OPCW round robin interlaboratory comparison test
[PB95-210324] p 3068 N95-33243

NOTRE DAME UNIV., IN.
Quantum transport
[AD-A294977] p 3235 N95-34589

NOTTINGHAM UNIV. (ENGLAND).
A rose by any other name: Certification seen as process rather than content p 3047 N95-34766

NYMA, INC., BROOK PARK, OH.
Performance of partially fluorinated polyimide insulation for aerospace applications
[NASA-CR-198372] p 3060 N95-32673
Compression mass gauge testing in a liquid hydrogen dewar
[NASA-CR-198366] p 3115 N95-32687
Computation of noise radiation from turbofans: A parametric study
[NASA-CR-198359] p 3200 N95-32836

Numerical simulation of supersonic flow using a new analytical bleed boundary condition
[NASA-CR-198368] p 3054 N95-33208
Improved L-C resonant decay technique for Q measurement of quasilinear power inductors: New results for MPP and ferrite powdered cores
[NASA-CR-198373] p 3103 N95-33874
Life test of a xenon hollow cathode for a space plasma contractor
[NASA-CR-195403] p 3061 N95-33926

O

OAK RIDGE INST. FOR SCIENCE AND EDUCATION, TN.
A background subtraction routine for enhancing energy-filtered plasmon images of MgAl2O4 implanted with Al(+) and Mg(+) ions
[DE95-012850] p 3074 N95-33629
OAK RIDGE NATIONAL LAB., TN.
Magnetic excitations in a random exchange system Fe(x)Mn(1-x)TiO3
[DE95-006626] p 3225 N95-32377
A posterion pointwise error estimates for the boundary element method
[DE95-008099] p 3194 N95-32388
Strength, ductility, and fracture mode of ternary FeAl alloys
[DE95-010281] p 3077 N95-32400
Effect of heat treatment at 1,150 C on creep rupture properties of a Fe3Al-based alloy
[DE95-010295] p 3077 N95-32527
The fully correlated two-electron problem on a numerical lattice
[DE95-010280] p 3205 N95-32650
Fracture behavior of shallow cracks in full-thickness clad beams from an RPV wall section
[DE95-009175] p 3126 N95-32684
An instrument for gravimetric calibration of flow devices with corrosive gases
[DE95-009700] p 3116 N95-33206
Effect of phase transformations on the mechanical properties of a multiphase alloy based on NiAl+Fe
[DE95-010119] p 3079 N95-33217
On the expansion for surface displacement in the neighborhood of a crack tip
[DE95-012890] p 3126 N95-33222
Combining the QMR method with first principles electronic structure codes
[DE95-009927] p 3228 N95-33240
Laser ablation plume thermalization dynamics in background gases studied by time-resolved imaging, spectroscopic, and ion probe diagnostics
[DE95-010277] p 3118 N95-33246
High-speed, low-damage grinding of advanced ceramics, phase 1
[DE95-011241] p 3085 N95-33425
A background subtraction routine for enhancing energy-filtered plasmon images of MgAl2O4 implanted with Al(+) and Mg(+) ions
[DE95-012850] p 3074 N95-33629
Interfacial composition analysis of silicon nitride whisker reinforced oxynitride glass systems
[DE95-012895] p 3085 N95-33635
Carbon Dioxide Information Analysis Center and World Data Center: A for Atmospheric trace gases
[DE95-011769] p 3154 N95-33655
Thin-film rechargeable lithium batteries
[DE95-008975] p 3103 N95-33697
Effect of the colony microstructure on transport critical current of high-J(c) Tl-1223 thick films
[DE95-013049] p 3230 N95-34213
Patterns and perspectives in applied fracture mechanics
[DE95-012844] p 3127 N95-34442
Laser induced diffusion of ion-implanted bismuth in fused silica
[DE95-012869] p 3230 N95-34443
Formation of artificially-layered high-temperature superconductors using pulsed-laser deposition
[DE95-012884] p 3231 N95-34465
Modeling and simulation of pulsed laser annealing and ablation of solid materials
[DE95-012888] p 3119 N95-34466
Fabrication of optical channel waveguides in the GaAs/AlGaAs system by MeV ion beam bombardment
[DE95-008973] p 3218 N95-34480
R-curve behavior of whisker-reinforced ceramic composites
[DE95-012873] p 3087 N95-34798
Highly doped p-ZnTe films and quantum well structures grown by nonequilibrium pulsed laser ablation
[DE95-012885] p 3232 N95-34799
QMR methods in computational fluid dynamics
[DE95-012889] p 3113 N95-34800
The design of scalable software libraries for distributed memory concurrent computers
[DE95-012891] p 3244 N95-34801
Static displacements of atoms in crystalline metallic solid solutions
[DE95-012893] p 3233 N95-34802
OFFICE NATIONAL D'ETUDES ET DE RECHERCHES AEROSPATIALES, CHATILLON (FRANCE).
An original numerical method for autonomous navigation p 3044 N95-32495
OHIO STATE UNIV., COLUMBUS, OH.
X-Antenna: A graphical interface for antenna analysis codes
[NASA-CR-199212] p 3095 N95-32674
Turbulence and spatio-temporal chaos
[DE95-012912] p 3068 N95-33223
Protocol engineering for broadband networks
[AD-A294969] p 3186 N95-34584
OHIO UNIV., ATHENS, OH.
Quantitative analysis of volatile organic compounds using ion mobility spectra and cascade correlation neural networks p 3073 N95-33290
OKLAHOMA BAPTIST UNIV., SHAWNEE, OK.
Characterizing the fragmentation ring on witness plates p 3056 N95-32426
OKLAHOMA UNIV., NORMAN, OK.
Experimental investigation of the separation of texture and residual stress induced anisotropy via oblique incidence acoustoelasticity p 3126 N95-33253
OLD DOMINION UNIV., NORFOLK, VA.
Three-dimensional aerodynamic shape optimization using discrete sensitivity analysis p 3048 N95-32904
OREGON GRADUATE INST. OF SCIENCE AND TECHNOLOGY, BEAVERTON, OR.
An experimental and numerical analysis of hydrogen assisted cracking and weldability test methodology p 3079 N95-32936
OREGON STATE UNIV., CORVALLIS, OR.
Nonlinear adaptive control of highly maneuverable high performance aircraft p 3192 N95-33712
Comparison of theoretical predictions with field observations for a simple forward scattering sensor
[AD-A294948] p 3219 N95-34576
OREGON UNIV., EUGENE, OR.
High speed variability in x-ray binary systems
[AD-A294634] p 3247 N95-34561
OSAKA UNIV., OSAKA (JAPAN).
Technology Reports of the Osaka University, vol. 45, nos. 2205-2216 p 3090 N95-32984
Calculations of spatial higher modes without deflation procedure
[REPT-2205] p 3090 N95-32985
Practical improvement of MS-X alpha molecular orbital calculation as applied to dissociation process of CO molecule
[REPT-2206] p 3090 N95-32986
Analysis of evaporation in laser welding
[REPT-2207] p 3090 N95-32987
Measurement of laser wavefront using Shack Hartmann method with new lens array
[REPT-2208] p 3090 N95-32988
Control of the laser beam irradiation intensity distribution using aspherical multi lens array and edge-shaped plates
[REPT-2209] p 3090 N95-32989
Measurement of gain saturation on Nd: Doped phosphate laser glasses
[REPT-2210] p 3090 N95-32990
Enhancement of pool boiling heat transfer to lithium bromide aqueous solution
[REPT-2211] p 3091 N95-32991
Seismic response analysis of soil-structure interaction systems in the time domain
[REPT-2212] p 3091 N95-32992
Inelastic response spectra of a system with bilinear restoring characteristics: Effect of plastic-stiffness ratio
[REPT-2213] p 3091 N95-32993
A note on separation prediction of two-dimensional turbulent boundary layer
[REPT-2216] p 3091 N95-32994
OXFORD UNIV., OXFORD (ENGLAND).
Remarks on the KARMEN anomaly
[PB95-234977] p 3209 N95-34650

P

PACIFIC NORTHWEST LAB., RICHLAND, WA.
An electronic design guideline for incorporating pollution prevention into US Department of Energy design projects
[DE95-008935] p 3151 N95-32475
Irradiation-assisted stress corrosion cracking considerations at temperatures below 288 C
[DE95-006940] p 3077 N95-32555
Visualization of parallel molecular dynamics simulation on a remote visualization platform
[DE95-007806] p 3185 N95-32582
CRADA with United Solar Technologies and Pacific Northwest Laboratory (PNL-021): Thin film materialsfor low-cost high performance solar concentrators
[DE95-010423] p 3150 N95-33400
Influence of processing variables on the structure and properties of ZnO films
[DE95-011494] p 3084 N95-33405
Balloon-borne radiometer profiler: Field observations
[DE95-011493] p 3158 N95-33505
The development of a large-area chemical sensor: A new platform for selective coatings
[DE95-011489] p 3075 N95-33832
Implications of early stages in the growth of stress corrosion cracking on component reliability
[DE95-011498] p 3127 N95-33833
Multimedia Environmental Pollutant Assessment System (MEPAS(trademark)): Exposure pathway and human health impact assessment models
[DE95-012763] p 3155 N95-34441
PCP, INC., WEST PALM BEACH, FL.
A digital boxcar integrator for IMS spectra p 3072 N95-33288
PENNSYLVANIA STATE UNIV., UNIVERSITY PARK, PA.
Fundamental phenomena on fuel decomposition and boundary-layer combustion processes with applications to hybrid rocket motors
[NASA-CR-199126] p 3061 N95-32932
Observations of surface structure and regression behavior of solid propellant strands burning under narrow gap conditions p 3088 N95-33254
Cubic-B-spline boundary elements for two-dimensional and axisymmetric elastostatics p 3127 N95-33695
Development of thin film diamond based integrated circuit technology
[AD-A294519] p 3231 N95-34478
Molecular motion of phosphazene-bound NLO chromophores
[AD-A293526] p 3087 N95-34649
PENNSYLVANIA UNIV., PHILADELPHIA, PA.
Off-line programming using commerical CAD systems, and design criteria for manipulators with inherent accuracy p 3180 N95-32937
Radiative interactions with micromachined surfaces: Spectral polarized emittance
[DE95-011455] p 3097 N95-33061
The computation of electron transfer rates: The nonadiabatic instanton solution
[AD-A294523] p 3209 N95-34350
PHILLIPS LAB., HANSCOM AFB, MA.
Shuttle Potential and Return Electron Experiment (SPREE) electrostatic analyzer (ESA) calibration report
[AD-A293026] p 3057 N95-32772
MODTRAN3: An update and recent validations against airborne high resolution interferometer measurements p 3128 N95-33732
PHILLIPS LAB., KIRTLAND AFB, NM.
ABLEX: High altitude laser propagation experiment
[AD-A294914] p 3120 N95-34592
PHYSICAL OPTICS CORP., TORRANCE, CA.
Photonic band gap structures on polymer materials for microstructure waveguides and high-speed interconnects
[AD-A294119] p 3218 N95-34504
PITTSBURGH UNIV., PITTSBURGH, PA.
A model of long term learning: Integration of knowledge acquisition and knowledge compilation
[AD-A294123] p 3235 N95-34743
Surface chemistry of diamond single crystals
[AD-A294150] p 3232 N95-34755
PLANNING RESEARCH CORP., EDWARDS, CA.
Dynamic ground effects flight test of the NASA F-15 aircraft p 3049 N95-33024
POLISH ACADEMY OF SCIENCES, WARSAW (POLAND).
Propagation of spatial solitons generated by Gaussian beams in a non-linear Kerr medium
[IFTR-9/1995] p 3206 N95-32921
PRATT AND WHITNEY AIRCRAFT, WEST PALM BEACH, FL.
F-15 propulsion system p 3051 N95-33012
PRINCETON UNIV., NJ.
Requirements and trends of computational aerodynamics as a tool for aircraft design p 3034 N95-34506
Electronic processes in heterostructures, strained-layer materials, and laterally patterned structures
[AD-A294970] p 3235 N95-34585
Studies of hypersonic boundary layer behavior
[AD-A294137] p 3113 N95-34752
PUERTO RICO UNIV., MAYAGUEZ.
Charm decays and high energy photoproduction
[DE95-010165] p 3201 N95-32393

PURDUE UNIV., WEST LAFAYETTE, IN.
Active noise control in finite length waveguides
p 3098 N95-33322
Modeling liquid jet atomization processes
[AD-A294888] p 3112 N95-34572

R

RADEX, INC., BEDFORD, MA.
An improved algorithm for computing altitude dependent Corrected GeoMagnetic coordinates
[AD-A293967] p 3144 N95-34454
RAILWAY TECHNICAL RESEARCH INST., TOKYO (JAPAN).
Numerical simulation of aerodynamic problems in high speed railways, part 2 p 3041 N95-34554
RANGE COMMANDERS COUNCIL, WHITE SANDS MISSILE RANGE, NM.
Range graphics benchmark
[AD-A293541] p 3057 N95-34606
RENSSELAER POLYTECHNIC INST., TROY, NY.
A procedural framework for designing linear orienting devices p 3181 N95-33325
REVENUE CANADA, OTTAWA (ONTARIO).
IMS R and D program at Canada customs
p 3070 N95-33273
RICE UNIV., HOUSTON, TX.
Numerical solution of differential equations by artificial neural networks p 3194 N95-32434
High-resolution magnetic imaging and investigations of thin-film magnetism with spin-polarized electron, ion and atom probes
[DE95-012190] p 3074 N95-33392
Some issues in nonlinear programming algorithms for problems with simulation constraints
[AD-A294932] p 3182 N95-34598
RMS TECHNOLOGIES, INC., LANDOVER, MD.
Space probe data processing
[AD-A294124] p 3058 N95-34744
ROCHESTER UNIV., NY.
Distributed shared memory for new generation networks
[AD-A293722] p 3185 N95-32580
Three-dimensional recognition via two-stage associative memory
[AD-A293567] p 3183 N95-34612
Adaptive differential visual feedback for uncalibrated hand-eye coordination and motor control
[AD-A293607] p 3171 N95-34616
ROCKWELL INTERNATIONAL CORP., THOUSAND OAKS, CA.
Efficient time domain solutions of Maxwell's equations for aerospace systems
[AD-A294019] p 3196 N95-34377
ROME LAB., GRIFFISS AFB, NY.
Optical interconnects for 3D computer architectures
[AD-A294118] p 3178 N95-34503
ROSE ENGINEERING AND RESEARCH, INC., INCLINE VILLAGE, NV.
SOFIA: Aft cavities wind tunnel test
[NASA-TM-110673] p 3033 N95-32682
ROYAL AIR FORCE INST. OF AVIATION MEDICINE, FARNBOROUGH (ENGLAND).
Negative to positive Gz acceleration transition
p 3165 N95-34052
Positive pressure breathing for G protection (PBG)
p 3168 N95-34055
Quality assurance and risk management: Perspectives on Human Factors Certification of Advanced Aviation Systems p 3048 N95-34771
ROYAL INST. OF TECH., STOCKHOLM (SWEDEN).
Associative integral formulas and deformations of Yangians
[PB95-212189] p 3195 N95-32889
Counterexample to the lieb-thirring conjecture concerning the moments of the eigenvalues of the Schroedinger operator
[PB95-212197] p 3195 N95-32890
Turbulence models in the Navier-Stokes simulation of airfoil stall
[TRITA-NA-9312] p 3108 N95-33059
Mathematical methods applied to biotechnical processes
[PB95-212114] p 3163 N95-33232
Boundary and lens rigidity of Lorentzian surfaces
[PB95-212163] p 3196 N95-33233
Lieb-thirring constants L(sub gamma,1) for gamma greater than or equal to 1/2
[PB95-212171] p 3196 N95-33234
RUTGERS - THE STATE UNIV., NEW BRUNSWICK, NJ.
Modal identification and its applications to damage detection in vibrating structures p 3126 N95-32920
Vorticity in shock-accelerated density-stratified interfaces: An analytical and computational study
p 3111 N95-33607
RUTHERFORD APPLETON LAB., CHILTON (ENGLAND).
ENGIN mini-manual. Version 1.5
[PB95-218095] p 3206 N95-32814
Review of the research activities of the Energy Research Unit in 1994
[PB95-235008] p 3151 N95-34656
International Meeting on Muon Science
[PB95-236014] p 3209 N95-34657
RUTHERFORD APPLETON LAB., OXFORD (ENGLAND).
Remarks on the KARMEN anomaly
[PB95-234977] p 3209 N95-34650
Track finding and fitting in the H1 forward track detector
[PB95-234985] p 3214 N95-34651
Proceedings of the School for Young High Energy Physicists
[PB95-234993] p 3235 N95-34652
Analytic approach to small x structure functions
[PB95-236030] p 3214 N95-34653

S

SAINT PETERSBURG INST. OF AEROSPACE INSTRUMENTATION, SAINT PETERSBURG (RUSSIA).
Sea wave parameters, small altitudes and distances measurers design for movement control systems of ships, wing-in-surface effect crafts and seaplanes
p 3094 N95-33141
SAINT PETERSBURG STATE ELECTROTECHNICAL UNIV., SAINT PETERSBURG (RUSSIA).
Some results of international cooperation in military to commercial conversion of laser gyro technology
p 3092 N95-33130
SAITAMA UNIV., URAWA (JAPAN).
Numerical study on stabilization of a diffusion flame over a flat plate p 3035 N95-34510
Numerical simulation of interaction between shock wave and density interface p 3039 N95-34543
SAN DIEGO STATE UNIV., SAN DIEGO, CA.
Canopy reflectance modelling of semiarid vegetation
[NASA-CR-199117] p 3142 N95-32676
SANDIA NATIONAL LABS., ALBUQUERQUE, NM.
The development and application of massively parallel solid mechanics codes
[DE95-006307] p 3184 N95-32374
Application of fuzzy technology to risk-based design and decision problems
[DE95-006815] p 3178 N95-32378
Shock properties of high-strength ceramics
[DE95-007731] p 3082 N95-32380
The role of dynamic experimentation for computation analysis
[DE95-007733] p 3125 N95-32381
Models for predicting damage evolution in metal matrix composites subjected to cyclic loading
[DE95-007734] p 3077 N95-32382
Simulation of hypervelocity impact on massively parallel supercomputer
[DE95-007735] p 3184 N95-32383
Three-dimensional natural convection of a fluid with temperature-dependent viscosity in an enclosure with localized heating
[DE95-002606] p 3106 N95-32387
On bootstrapping local search with trail-markers
[DE95-009835] p 3187 N95-32533
Users' manual for LEHGC: A Lagrangian-Eulerian finite-element model of HydroGeoChemical transport through saturated-unsaturated media. Version 1.0
[DE95-010513] p 3179 N95-32543
Winter season air pollution in El Paso-Ciudad Juarez. A review of air pollution studies in an international airshed
[DE95-009083] p 3152 N95-32556
Congestion control over ATM local area networks
[DE95-010343] p 3184 N95-32558
COBRA accelerator for Sandia ICF diode research at Cornell University
[DE95-011018] p 3101 N95-32578
Smoothing during ion-assisted growth by transient ion beam-induced defects
[DE95-011021] p 3225 N95-32579
On the feasibility of using smoothed particle hydrodynamics for underwater explosion calculations
[DE95-008799] p 3106 N95-32587
Frequency response of a TeO2 slow shear wave acousto-optic cell exposed to radiation
[DE95-009588] p 3226 N95-32589
Mechanism(s) for the suppression of the switchable polarization in PZT and BaTiO3
[DE95-009589] p 3226 N95-32590
Intermetallic compound layer growth kinetics in non-lead bearing solders
[DE95-009595] p 3078 N95-32591
High resistivity InAlN by nitrogen or oxygen implantation
[DE95-011023] p 3226 N95-32594
The growth and optimization of InPSb/InGaAs/InAsSb strained-layer superlattice emitters by metal organic chemical vapor deposition
[DE95-011057] p 3226 N95-32595
Integration of diffractive lenses with addressable vertical-cavity laser arrays
[DE95-009850] p 3118 N95-32663
Evaluation of a bridge using simplified element modeling
[DE95-006281] p 3126 N95-32670
The effect of travel speed on thermal response in CO2 laser welding of small electronic components
[DE95-006314] p 3118 N95-32683
N-15 hydrogen profiling of IC metallizations
[DE95-011052] p 3102 N95-32708
Solving stiff chemistry problems with FIDAP
[DE95-011053] p 3067 N95-32709
PINCA: A scalable parallel program for compressible gas dynamics with nonequilibrium chemistry
[DE95-010581] p 3106 N95-32818
Growth and characterization of heterostructures and infrared emitters with compressed InAsSb layers
[DE95-009828] p 3226 N95-33213
Globally stable feedback laws for near-minimum-fuel and near-minimum-time pointing maneuvers for a landmark-tracking spacecraft
[DE95-009867] p 3191 N95-33214
Printability of substrate and absorber defects on extreme ultraviolet lithographic masks
[DE95-010916] p 3084 N95-33247
High rate dry etching of GaN, AlN and InN in ECR Cl2/CH4/H2/Ar plasmas
[DE95-011872] p 3223 N95-33412
xdamp: An IDL(R)-based Data Manipulation Program
[DE95-011242] p 3181 N95-33624
Design rules and reality check for carbon-based ultracapacitors
[DE95-010575] p 3103 N95-33640
Fatigue damage estimate comparisons for northern European and US wind farm loading environments
[DE95-011061] p 3150 N95-33706
Characterization of microenvironment polarity and solvent accessibility of polysilsesquioxane xerogels by the fluorescent probe technique
[DE95-011874] p 3062 N95-33835
An application of mechanical leverage to microactuation
[DE95-011883] p 3124 N95-33836
Evaluation of conductive, radiative, chemical, and convective heat transfer in complex systems using a fast-running, implicit, lumped-capacitance formulation
[DE95-011889] p 3111 N95-33837
A reconfigurable optoelectronic interconnect technology for multi-processor networks
[DE95-011895] p 3186 N95-33838
Unified model of the RF plasma sheath
[DE95-012114] p 3224 N95-33851
Electron beam joining of structural ceramics
[DE95-012521] p 3085 N95-34022
Fundamental surface chemistry of GaAs OMVPE
[DE95-011606] p 3231 N95-34486
Laser beaming demonstrations at the Starfire Optical Range
[DE95-007747] p 3120 N95-34811
SANDIA NATIONAL LABS., LIVERMORE, CA.
Ignition and early soot formation in a DI diesel engine using multiple 2-D imaging diagnostics
[DE95-010692] p 3122 N95-32863
The effects of high ambient density on diesel spray penetration and spread
[DE95-010761] p 3124 N95-33701
SCIENCE APPLICATIONS INTERNATIONAL CORP., MCLEAN, VA.
Mineralogic variations in fluvial sediments contaminated by mine tailings as determined from AVIRIS data, Coeur D'Alene River Valley, Idaho p 3131 N95-33745
SAVS: A Space Analysis and Visualization System
p 3242 N95-34238
SCIENCE UNIV. OF TOKYO (JAPAN).
Calculation for aerodynamic characteristics on delta wing with leading-edge separated vortex effect using boundary element method p 3037 N95-34524
Grid generation around airfoil with a flap using boundary element method p 3041 N95-34552
SCIENTIFIC RESEARCH ASSOCIATES, INC., GLASTONBURY, CT.
Design of ETO propulsion turbine using CFD analyses
[NASA-CR-199085] p 3123 N95-32915
SCIENTIFIC RESEARCH INST. OF MECHANICAL PROBLEMS, KIEV (UKRAINE).
Laser gyroscopy tendencies and their analysis of development in Ukraine p 3092 N95-33133

SCITRAN, INC., SANTA BARBARA, CA.
Study of liquid crystal spatial light modulator application to Hadamard transform spectrometer: A fast and accurate decoding method
[AD-A293087] p 3215 N95-32660
SEARCH TECHNOLOGY, INC., NORCROSS, GA.
Certify for success: A methodology for human-centered certification of advanced aviation systems
p 3173 N95-34773
SEXTANT AVIONIQUE, SAINT MEDARD EN JALLES (FRANCE).
A helmet mounted display for night missions at low altitude p 3045 N95-32503
SHELL DEVELOPMENT CO., HOUSTON, TX.
Design of deepwater pipelines
[PB95-215109] p 3095 N95-33244
SHIP RESEARCH INST., TOKYO (JAPAN).
A multigrid incompressible NS solver
p 3036 N95-34517
Numerical simulation of two-dimensional PAR-WIG
p 3040 N95-34548
SIEGEN UNIV., (GERMANY).
Proton-induced fragmentation of carbon at energies below 100 MeV p 3161 N95-32720
SOFTEK SYSTEMS, INC., TOKYO (JAPAN).
Large scale computing and volume visualization
p 3041 N95-34556
SOUTH CAROLINA UNIV., COLUMBIA, SC.
Boundary and lens rigidity of Lorentzian surfaces
[PB95-212163] p 3196 N95-33233
SOUTHAMPTON UNIV. (ENGLAND).
Causal correlation of foliar biochemical concentrations with AVIRIS spectra using forced entry linear regression
p 3130 N95-33744
Efficient pockel's modulators in optical fibers
[AD-A294009] p 3217 N95-34374
SOUTHERN METHODIST UNIV., DALLAS, TX.
The composite classification problem in optical information processing p 3244 N95-32430
SOUTHWEST RESEARCH INST., SAN ANTONIO, TX.
Evaluation of high-temperature lubricant under cyclic operating conditions
[AD-A294444] p 3086 N95-34494
SPACE TELESCOPE SCIENCE INST., BALTIMORE, MD.
Development of an expert data reduction assistant
p 3242 N95-34234
SPEEL LTD., PRAGUE (CZECHOSLOVAKIA).
Solid-state data recorder, next development and use
p 3094 N95-33143
SRI INTERNATIONAL CORP., MENLO PARK, CA.
Formal verification of an avionics microprocessor
[NASA-CR-4682] p 3181 N95-33396
STANFORD LINEAR ACCELERATOR CENTER, MENLO PARK, CA.
Study of the trapped modes at the vacuum ports
[DE95-010570] p 3203 N95-32544
Summary of the impedance working group
[DE95-012095] p 3211 N95-32606
Transverse multibunch instabilities for non-rigid bunches
[DE95-012098] p 3211 N95-32607
Fast feedback for linear colliders
[DE95-012099] p 3211 N95-32608
Minimum wakefield achievable by waveguide damped cavity
[DE95-012100] p 3095 N95-32616
Beam-based magnetic alignment of the final focus test beam
[DE95-012096] p 3212 N95-32657
Beam-based optical tuning of the Final Focus Test Beam
[DE95-012097] p 3215 N95-32658
Probing new physics in B Penguins
[DE95-012494] p 3208 N95-33375
STANFORD LINEAR ACCELERATOR CENTER, STANFORD, CA.
Impedance study for the PEP-2 B-factory
[DE95-010569] p 3203 N95-32567
Proceedings of the REXX symposium for developers and users
[DE95-010668] p 3185 N95-32820
Virtual effects of physics beyond the standard model
[DE95-012499] p 3207 N95-33201
Searching for new physics with charm
[DE95-012498] p 3207 N95-33245
The PEP-2 project-wide database
[DE95-012512] p 3213 N95-33333
Nonlinear analyses of storage ring lattices using one-turn maps
[DE95-012515] p 3213 N95-33335
A code to compute the action-angle transformation for a particle in an abritrary potential well
[DE95-012554] p 3098 N95-33336
Emittance and energy control in the NLC main linacs
[DE95-012556] p 3213 N95-33338
Emittance growth due to decoherence and wakefields
[DE95-012495] p 3213 N95-33376
Injection envelope matching in storage rings
[DE95-012496] p 3213 N95-33377
A map for the thick beam-beam interaction
[DE95-012561] p 3213 N95-33385
The effect of phase advance errors between interaction points on beam halos
[DE95-012559] p 3214 N95-34023
Studies of halo distributions under beam-beam interaction
[DE95-012560] p 3214 N95-34024
STATE POLLUTION CONTROL AUTHORITY, OSLO (NORWAY).
Pollution in Norway
[PB95-214565] p 3153 N95-33331
STATE UNIV. OF NEW YORK, BUFFALO, NY.
Synthesis and characterization of a series of organoindium-phosphides including molecular structures of ((Me3CCH2)2InPEt2)2 and ((Me3CCH2)2InP(H)(C6H11))3
[AD-A293965] p 3086 N95-34452
STATE UNIV. OF NEW YORK, STONY BROOK, NY.
Fifth International Conference on Hyperbolic Problems, Theory, Numerics, Applications: Abstracts
[DE95-008173] p 3194 N95-32389
Chiral restoration in hot and/or dense matter
[DE95-012176] p 3204 N95-32621
A document analysis system p 3244 N95-34804
STERLING SOFTWARE, INC., DALLAS, TX.
Evaluation in context: ATC automation in the field
p 3175 N95-34781
STOCKHOLM ENVIRONMENT INST., STOCKHOLM (SWEDEN).
Clearing-house mechanism to promote and facilitate technical and scientific cooperation under the UN Convention on Biological Diversity
[PB95-214557] p 3163 N95-33236
STOCKHOLM UNIV. (SWEDEN).
Turbulence models in the Navier-Stokes simulation of airfoil stall
[TRITA-NA-9312] p 3108 N95-33059
SUN CO., INC., MARCUS HOOK, PA.
Catalytic conversion of light alkanes: Proof of concept stage
[DE95-012318] p 3076 N95-34810
SUPERCONDUCTING SUPER COLLIDER LAB., DALLAS, TX.
Quench propagation velocity for highly stabilized conductors
[DE95-011040] p 3103 N95-33404
Ramp-rate sensitivity of SSC dipole magnet prototypes
[DE95-011162] p 3214 N95-33720
SVERDRUP TECHNOLOGY, INC., BROOK PARK, OH.
Genetic algorithm based input selection for a neural network function approximator with applications to SSME health monitoring
[NASA-CR-199089] p 3188 N95-32768
SWEDISH INST. FOR METALS RESEARCH, STOCKHOLM (SWEDEN).
Phase equilibria and phase diagrams in carbide systems
[PB95-211348] p 3068 N95-33229
SWEDISH NATIONAL TESTING AND RESEARCH INST., BORAS (SWEDEN).
Test method to measure resistance towards fragmentation by studded tires
[PB95-211017] p 3121 N95-32612
Foam spread experiments on a water surface
[PB95-211025] p 3083 N95-32962
SWEDISH NATURAL SCIENCE RESEARCH COUNCIL, STOCKHOLM (SWEDEN).
Boundary and lens rigidity of Lorentzian surfaces
[PB95-212163] p 3196 N95-33233
SWEDISH TRANSPORT AND COMMUNICATIONS RESEARCH BOARD, STOCKHOLM (SWEDEN).
Introductions of FFV
[PB95-214656] p 3088 N95-33332
SYRACUSE UNIV., NY.
Quantum cylinder fiber light amplifier
[AD-A294197] p 3217 N95-34300
SYSTEMS TECHNOLOGY, INC., HAWTHORNE, CA.
Proposed incorporation of mission-oriented flying qualities into MIL-STD-1797A
[AD-A294211] p 3055 N95-34306

T

TECHNICAL UNIV. OF BUDAPEST (HUNGARY).
Monitoring of the cutting operations using fuzzy logic
p 3189 N95-32999
TECHNISCHE UNIV., BRUNSWICK (GERMANY).
Effects of the specific military aspects of satellite navigation on the civil use of GPS/GLONASS
p 3048 N95-33134
TECHNISCHE UNIV., DELFT (NETHERLANDS).
Study on turbulent fluctuations in diffusion flames using laser induced fluorescence
[PB95-214425] p 3068 N95-32812
Raingauge network optimization and GIS: A case study of the Mananga basin. Communications of the Sanitary Engineering and Water Management Division
[PB95-214284] p 3157 N95-32891
Sum of fractional derivatives and m-accretive operators
[PB95-215307] p 3195 N95-32893
Supercritical crystallization: The RESs-process and the GAS-process
[PB95-214482] p 3228 N95-33235
Popov theory based approach to digital H(infinity)-control with measurement-feedback for Pritchard-Salamon systems
[PB95-218111] p 3192 N95-33399
TECHNISCHE UNIV., TWENTE (NETHERLANDS).
Simulation of a connectionless server for b-ISDN
[PB95-215091] p 3097 N95-32892
Formalization and representation of a product-driven approach to method assembly for situational systems development
[PB95-215190] p 3237 N95-33238
TELSTRA RESEARCH LABS., CLAYTON (AUSTRALIA).
An efficient inference engine for interactive fault diagnosis in a helpdesk application
p 3189 N95-33000
TEXAS A&M UNIV., COLLEGE STATION, TX.
An interactive environment for the analysis of large Earth observation and model data sets p 3239 N95-34219
Hardware implementation of a desktop supercomputer for high performance image processing
[AD-A294272] p 3178 N95-34462
TEXAS A&M UNIV., GALVESTON, TX.
Unified approach for incompressible flows
p 3113 N95-32425
Direct analysis of organic priority pollutants by IMS
p 3071 N95-33280
TEXAS TECHNOLOGICAL UNIV., LUBBOCK, TX.
Certification of a hybrid parameter model of the fully flexible Shuttle Remote Manipulator System
p 3125 N95-32421
Accuracy enhancement in optical computing
[AD-A294958] p 3219 N95-34579
TEXAS UNIV., AUSTIN, TX.
Parallel finite element methods and iterative solution techniques for viscous incompressible flows
p 3108 N95-33031
Top quark signatures in extended color theories
[DE95-007099] p 3234 N95-33202
Nonlinear symmetric stability of planetary atmospheres
[DE95-012133] p 3248 N95-33390
Studies of impurity mode and ITG mode in toroidal plasmas
[DE95-012134] p 3223 N95-33391
More on core-localized toroidal Alfven eigenmodes
[DE95-010857] p 3224 N95-33696
High-order Taylor-Galerkin and adaptive hp-methods for hyperbolic systems with application to structural acoustics p 3200 N95-33719
An object-oriented decomposition of the adaptive-hp finite element method
[DE95-012142] p 3186 N95-33852
Single Langmuir probe characteristic in a magnetized plasma at the TEXT tokamak
[DE95-012144] p 3224 N95-33853
Sinuous oscillations and steady warps of polytropic disks
[DE95-013473] p 3247 N95-34216
Low temperature growth of thin films by high kinetic energy supersonic molecular beams
[AD-A294516] p 3086 N95-34476
Elemental fluorine based syntheses of pentafluoro phenyl and other aromatic perfluoropolyether polymers
[AD-A294930] p 3087 N95-34596
TEXAS UNIV., EL PASO, TX.
Towards a formalism for program generation 1995
[AD-A294941] p 3183 N95-34604
TOKAI UNIV., TOKYO (JAPAN).
Numerical solutions of inviscid and viscous flows about airfoils by TVD method p 3036 N95-34521
TOKYO KOKO UNIV. (JAPAN).
Effect of schemes on numerical simulations of shock wave reflection p 3038 N95-34531
Vector-parallel simulations of transonic wind tunnel flows about a fully configured model of aircraft
p 3039 N95-34538

TOKYO UNIV. (JAPAN).
A study on the convergence of a 3-D Euler code for cascade flow calculations p 3034 N95-34508
DSMC method applied for reacting gas flows p 3035 N95-34509
Sidewall-effect of the wind tunnel on the estimation of the aerodynamic characteristics of a delta wing p 3037 N95-34525
Static pressure drop by swirling flow of an internal cooling air system through a turbine shaft p 3042 N95-34560
TOKYO UNIV., TANASHI (JAPAN).
Double-strangeness five-body system [DE95-737277] p 3202 N95-32404
VHS-tape system for general purpose computer. For next generation mass storage system [DE95-737268] p 3177 N95-32757
TORONTO UNIV. (ONTARIO).
Motion and force control of coordinated robots [ISBN-0-315-86323-4] p 3191 N95-33307
An empirical investigation of the semantic warrants exercised in thesaurus construction [ISBN-0-315-86393-5] p 3238 N95-33334
TSUKUBA UNIV. (JAPAN).
Solitary wave solution for mixing-layer turbulence p 3036 N95-34522
Turbulent solitary wave propagating through wall Boundary Layer p 3041 N95-34555
TULANE UNIV., NEW ORLEANS, LA.
Bicycle ergometer instrumentation to determine muscle and bone forces during exercise p 3176 N95-32428

U

UNIAX CORP., SANTA BARBARA, CA.
Industrial products based upon processible conductive polyaniline [AD-A294985] p 3087 N95-34817
UNIFORMED SERVICES UNIV. OF THE HEALTH SCIENCES, BETHESDA, MD.
Toxin-mediated transfer and expression of genes in nerve cells [AD-A290501] p 3164 N95-33200
UNIVERSITY OF CENTRAL FLORIDA, ORLANDO, FL.
User type certification for advanced flight control systems p 3055 N95-34772
UNIVERSITY OF EASTERN MICHIGAN, YPSILANTI, MI.
Is there a role for a test controller in the development of new ATC equipment? p 3174 N95-34778
UNIVERSITY OF SOUTHERN CALIFORNIA, LOS ANGELES, CA.
Photobiology and optical properties of planktonic and sea ice microalgae in the high arctic [AD-A294002] p 3160 N95-34457
UNIVERSITY OF SOUTHERN CALIFORNIA, MARINA DEL REY, CA.
Self stressing test structure cells [AD-A294386] p 3104 N95-34345
UNIVERSITY OF SOUTHERN ILLINOIS, SPRINGFIELD, IL.
Conceptual understanding and stability, and knowledge shields for fending off conceptual change [AD-A293555] p 3166 N95-34609
UNIVERSITY OF TECHNOLOGY, VICTORIA (AUSTRALIA).
Incorporating distributed problem solving technique into a case-based system p 3188 N95-32997
An alternative reasoning method p 3189 N95-33001
UNIVERSITY OF WESTERN WASHINGTON, BELLINGHAM, WA.
A thermophotovoltaic generator for use in a lightweight electric car: Year 1 progress report [DE95-011355] p 3102 N95-32968
UTAH UNIV., SALT LAKE CITY, UT.
Analyses and forecasts with LAWS winds [NASA-CR-199134] p 3157 N95-32933
Natural convection at microelectrodes [AD-A294338] p 3075 N95-34357
Use of D2 to elucidate OMVPE growth mechanisms [AD-A294999] p 3233 N95-34820

V

VANDERBILT UNIV., NASHVILLE, TN.
Representing incomplete knowledge in relational databases p 3238 N95-33722
VIRGINIA POLYTECHNIC INST. AND STATE UNIV., BLACKSBURG, VA.
Interlaminar stress analysis of dropped-ply laminated plates and shells by a mixed method p 3064 N95-33327
Large eddy simulation of turbulent vortices and mixing layers p 3109 N95-33340
Adhesion of novel high-performance polymers to carbon fibers: Fiber surface treatment, characterization, and microbond single fiber pull-out test p 3085 N95-34282
Analysis and finite element approximation of an optimal shape control problem for the steady-state Navier-Stokes equations p 3112 N95-34285
Theory and application of homotopy techniques in nonlinear programming and control systems [AD-A294934] p 3193 N95-34600
VIRGINIA UNIV., CHARLOTTESVILLE, VA.
The preservation of human surrogates for biomechanical studies p 3167 N95-33312
Control of initialization bias in queueing simulations using queueing approximations [AD-A294121] p 3194 N95-34742
Electron and hole transport in compound semiconductors [AD-A295003] p 3233 N95-34822

W

WALES UNIV. INST. OF SCIENCE AND TECHNOLOGY, CARDIFF (UNITED KINGDOM).
Practical guidelines for workload assessment p 3174 N95-34777
WASHINGTON UNIV., SAINT LOUIS, MO.
Analysis of LDEF experiment AO187-2 chemical and isotopic measurements of micrometeoroids by secondary ion mass spectrometry [NASA-CR-198849] p 3246 N95-32913
WASHINGTON UNIV., SEATTLE, WA.
Intrinsic charm contribution to double quarkonium hadroproduction [DE95-012170] p 3204 N95-32617
QCD mechanisms for double quarkonium and open heavy meson hadroproduction [DE95-012171] p 3204 N95-32619
Chiral restoration in hot and/or dense matter [DE95-012176] p 3204 N95-32621
TRAP: Tokamak Refueling by Accelerated Plasmoids [DE95-009925] p 3223 N95-33216
Wee partons in large nuclei: From virtual dream to hard reality [DE95-012168] p 3208 N95-33854
QCD and hadron structure [DE95-012173] p 3209 N95-33855
Indium mono-ion oscillator [AD-A293736] p 3104 N95-34451
Underwater acoustic field extrapolation: Theory and sensitivity analysis [AD-A294925] p 3201 N95-34595
Uncertainty analysis using stochastic finite elements p 3196 N95-34803
Investigation of starting and ignition transients in the thermally choked ram accelerator p 3054 N95-34805
WAYNE STATE UNIV., DETROIT, MI.
Design and implementation of a two-axis micromanipulator to enhance the gripper positional accuracy of a single flexible link p 3123 N95-33252
WESTINGHOUSE ELECTRIC CORP., WEST MIFFLIN, PA.
Design and operation of a thermionic converter in air [DE95-010151] p 3149 N95-32645
Integral cesium reservoir: Design and transient operation [DE95-010152] p 3211 N95-32647
WESTINGHOUSE HANFORD CO., RICHLAND, WA.
Glass science tutorial: Lecture no. 4, commercial glass melting and associated air emission issues [DE95-007818] p 3082 N95-32384
Nitrate stress corrosion crack growth rate in plain carbon steels [DE95-011689] p 3079 N95-32958
Glass science tutorial lecture no. 6: The melting of silicate glasses, a review of selected topics [DE95-010199] p 3084 N95-33218
ABCASH plotting program users guide [DE95-011652] p 3155 N95-34435
Certification of MCNP Version 4A for WHC computer platforms, revision 7 [DE95-011546] p 3178 N95-34484
WESTINGHOUSE SAVANNAH RIVER CO., AIKEN, SC.
Analytical modeling of the effect of crack depth, specimen size, and biaxial stress on the fracture toughness of reactor vessel steels [DE95-005886] p 3125 N95-32373
Incorporating bibliographic information into a spatial data query system for the Savannah River Site [DE95-010965] p 3238 N95-33402
WIEN UNIV. (AUSTRIA).
The 8th Winterschool on New Developments in Solid State Physics [AD-A290163] p 3227 N95-32677
WISCONSIN UNIV., MADISON, WI.
The effect of collisionality and diamagnetism on the plasma dynamo [DE95-012409] p 3223 N95-33221
Development of High Spectral Resolution Lidar (HSRL) technology [DE95-011906] p 3099 N95-33839
Remarks on the KARMEN anomaly [PB95-234977] p 3209 N95-34650
WOLLONGONG UNIV. (AUSTRALIA).
Knowledge-based system for metallurgical grade design p 3189 N95-32998
HOTQUA: An expert system prototype for quality monitoring in a rolling mill p 3190 N95-33004
WOODS HOLE RESEARCH CENTER, MA.
Completing below-ground carbon budgets for pastures, recovering forests, and mature forests of Amazonia [NASA-CR-199129] p 3143 N95-33498
WYOMING UNIV., LARAMIE, WY.
Validation of space/ground antenna control algorithms using a computer-aided design tool p 3183 N95-32429
Modeling seismic wave propagation in heterogeneous materials using finite elements p 3156 N95-34283

Y

YORK UNIV. (ENGLAND).
Analysis of safety requirements in the context of system faults and human errors [PB95-236105] p 3171 N95-34658

Z

ZURICH UNIV. (SWITZERLAND).
Extraction of ozone and chlorophyll-A distribution from AVIRIS data p 3136 N95-33770

Typical Contract Number Index Listing

AF- AFOSR-0090-93 ..... p 173 N95-10612

CONTRACT NUMBER | PAGE NUMBER | ACCESSION NUMBER

Listings in this index are arranged alphanumerically by contract number. Under each contract number the accession numbers denoting documents that have been produced as a result of research done under that contract are arranged in ascending order. The page number helps to locate the citation in the abstract section. The accession number denotes the number by which the citation is identified.

AF-AFOSR-0018-92 ..... p 3217 N95-34374
AF-AFOSR-0036-90 ..... p 3209 N95-34819
AF-AFOSR-0059-91 ..... p 3233 N95-34820
AF-AFOSR-0093-91 ..... p 3187 N95-34603
AF-AFOSR-0147-91 ..... p 3186 N95-34340
AF-AFOSR-0192-91 ..... p 3219 N95-34579
AF-AFOSR-0211-91 ..... p 3235 N95-34589
AF-AFOSR-0220-91 ..... p 3232 N95-34792
AF-AFOSR-0233-91 ..... p 3224 N95-34586
AF-AFOSR-0365-91 ..... p 3235 N95-34585
AF-AFOSR-0436-91 ..... p 3155 N95-34591
AF-AFOSR-0494-89 ..... p 3232 N95-34795
ARO-MIPR-122-93 ..... p 3164 N95-33200
ARPA ORDER A418 ..... p 3193 N95-34593
ARPA ORDER 5916 ..... p 3100 N95-34460
ARPA ORDER 8930 ..... p 3185 N95-32580
ARPA ORDER 9328 ..... p 3087 N95-34614
DA PROJ. 1L1-62211-A-47-A ..... p 3124 N95-33908
DA PROJ. 1L1-62211-A4-7A ..... p 3123 N95-33179
DA PROJ. 301-62787-A-878 ..... p 3170 N95-34378
p 3170 N95-34489
DA PROJ. 301-6287-A-878 ..... p 3170 N95-34492
DAAH01-94-C-R263 ..... p 3100 N95-34460
DAAH04-94-C-00021 ..... p 3199 N95-34477
DAAK70-92-C-0059 ..... p 3086 N95-34494
DAAL03-91-G-0093 ..... p 3186 N95-34584
DAAL03-92-G-0289 ..... p 3218 N95-34498
DAMD17-93-C-3159 ..... p 3165 N95-34754
DE-AC02-76CH-00016 ..... p 3125 N95-32392
p 3210 N95-32411
p 3236 N95-32412
p 3210 N95-32413
p 3210 N95-32414
p 3202 N95-32484
p 3211 N95-32485
p 3203 N95-32542
p 3205 N95-32651
p 3205 N95-32652
p 3205 N95-32654
p 3212 N95-33067
p 3153 N95-33192
p 3207 N95-33203
p 3213 N95-33204
p 3208 N95-33850
p 3156 N95-34214
DE-AC02-76CH-03000 ..... p 3201 N95-32379
p 3082 N95-32541
p 3246 N95-32597
p 3186 N95-33639
DE-AC02-91ER-40651 ..... p 3205 N95-32651
DE-AC03-76SF-00098 ..... p 3210 N95-32411
p 3101 N95-32596
p 3246 N95-32597
p 3227 N95-32600
p 3204 N95-32617
p 3204 N95-32619
p 3185 N95-32967
p 3103 N95-33080
p 3208 N95-33380
p 3215 N95-33381
p 3214 N95-33504
p 3247 N95-33625
p 3080 N95-33626
p 3229 N95-33628
p 3230 N95-33865
p 3230 N95-33880
p 3075 N95-34268
p 3199 N95-34269
p 3214 N95-34439
p 3151 N95-34481
DE-AC03-76SF-00515 ..... p 3203 N95-32544
p 3203 N95-32567
p 3211 N95-32606
p 3211 N95-32607
p 3211 N95-32608
p 3095 N95-32616
p 3204 N95-32617
p 3212 N95-32657
p 3215 N95-32658
p 3185 N95-32820
p 3207 N95-33201
p 3207 N95-33245
p 3213 N95-33333
p 3213 N95-33335
p 3098 N95-33336
p 3213 N95-33338
p 3208 N95-33375
p 3213 N95-33376
p 3213 N95-33377
p 3213 N95-33385
p 3214 N95-34023
p 3214 N95-34024
DE-AC03-89ER-51114 ..... p 3222 N95-32592
p 3222 N95-32656
p 3222 N95-32756
DE-AC03-91SF-18601 ..... p 3224 N95-34436
DE-AC04-76DP-00613 ..... p 3154 N95-33638
p 3103 N95-33864
DE-AC04-76DP-00789 ..... p 3222 N95-32592
p 3124 N95-33701
DE-AC04-94AL-85000 ..... p 3184 N95-32374
p 3178 N95-32378
p 3082 N95-32380
p 3125 N95-32381
p 3077 N95-32382
p 3184 N95-32383
p 3106 N95-32387
p 3187 N95-32533
p 3179 N95-32543
p 3152 N95-32556
p 3184 N95-32558
p 3101 N95-32578
p 3225 N95-32579
p 3106 N95-32587
p 3226 N95-32589
p 3226 N95-32590
p 3078 N95-32591
p 3226 N95-32594
p 3226 N95-32595
p 3118 N95-32663
p 3118 N95-32683
p 3102 N95-32708
p 3067 N95-32709
p 3106 N95-32818
p 3122 N95-32863
p 3228 N95-33213
p 3191 N95-33214
p 3084 N95-33247
p 3223 N95-33412
p 3181 N95-33624
p 3229 N95-33636
p 3103 N95-33640
p 3124 N95-33701
p 3150 N95-33706
p 3062 N95-33835
p 3124 N95-33836
p 3111 N95-33837
p 3186 N95-33838
p 3224 N95-33851
p 3085 N95-34022
p 3231 N95-34486
p 3120 N95-34811
DE-AC05-76OR-00033 ..... p 3074 N95-33629
DE-AC05-84OR-21400 ..... p 3225 N95-32377
p 3194 N95-32388
p 3077 N95-32400
p 3077 N95-32527
p 3222 N95-32592
p 3205 N95-32650
p 3126 N95-32684
p 3222 N95-32756
p 3116 N95-33206
p 3079 N95-33217
p 3126 N95-33222
p 3228 N95-33240
p 3118 N95-33246
p 3085 N95-33425
p 3074 N95-33629
p 3085 N95-33635
p 3154 N95-33655
p 3103 N95-33697
p 3230 N95-34213
p 3127 N95-34442
p 3230 N95-34443
p 3231 N95-34465
p 3119 N95-34466
p 3218 N95-34480
p 3087 N95-34798
p 3232 N95-34799
p 3113 N95-34800
p 3244 N95-34801
p 3233 N95-34802
DE-AC06-76RL-01830 ..... p 3151 N95-32475
p 3077 N95-32555
p 3185 N95-32582
p 3150 N95-33400
p 3084 N95-33405
p 3158 N95-33505
p 3075 N95-33832
p 3127 N95-33833
p 3155 N95-34441
DE-AC06-87RL-10930 ..... p 3082 N95-32384
p 3079 N95-32958
p 3084 N95-33218
p 3155 N95-34435
p 3178 N95-34484
DE-AC07-761D-01570 ..... p 3081 N95-34348
DE-AC07-94ID-13223 ..... p 3221 N95-32588
DE-AC09-89SR-18035 ..... p 3125 N95-32373
p 3238 N95-33402
DE-AC11-93PN-38195 ..... p 3149 N95-32645
p 3211 N95-32647
DE-AC12-76SN-00052 ..... p 3234 N95-34211
DE-AC21-92MC-29108 ..... p 3153 N95-32816
DE-AC21-93MC-29257 ..... p 3050 N95-32636
DE-AC22-93PC-92114 ..... p 3087 N95-32563
DE-AC24-88DP-43495 ..... p 3196 N95-33248
DE-AC35-89ER-40486 ..... p 3103 N95-33404
p 3214 N95-33720
DE-AC36-83CH-10093 ..... p 3033 N95-32548
p 3148 N95-32551
p 3152 N95-32668
p 3149 N95-32685
p 3152 N95-32686
p 3102 N95-32808
p 3153 N95-32809
p 3149 N95-32817
p 3149 N95-33153
p 3150 N95-33225
p 3150 N95-33383
DE-AI03-89SF-17905 ..... p 3149 N95-32811
DE-FC02-94ER-40818 ..... p 3246 N95-32597
DE-FC05-90CE-40905 ..... p 3074 N95-33705
DE-FC07-89ID-12903 ..... p 3083 N95-33079
DE-FC07-93ID-13230 ..... p 3095 N95-33393
DE-FC08-90NV-10872 ..... p 3179 N95-32470
p 3236 N95-32471
DE-FC21-90MC-26029 ..... p 3076 N95-34810
DE-FC36-86CH-10311 ..... p 3150 N95-33706
DE-FG01-94CE-15613 ..... p 3063 N95-33062
DE-FG02-85ER-53198 ..... p 3223 N95-33221
DE-FG02-86ER-13491 ..... p 3203 N95-32564
p 3206 N95-32763
p 3206 N95-32966
p 3207 N95-33241
p 3207 N95-33370
p 3207 N95-33371

	p 3208	N95-33372
	p 3226	N95-33373
	p 3208	N95-33374
	p 3209	N95-34355
DE-FG02-86ER-45278	p 3231	N95-34485
DE-FG02-88ER-13916	p 3068	N95-33223
DE-FG02-88ER-13964	p 3097	N95-33061
DE-FG02-88ER-40388	p 3204	N95-32621
DE-FG02-88ER-45372	p 3075	N95-34483
DE-FG02-89ER-45399	p 3215	N95-32662
DE-FG02-89ER-51124	p 3225	N95-34812
DE-FG02-90ER-40560	p 3246	N95-32597
DE-FG02-90ER-45424	p 3079	N95-33065
DE-FG02-90ER-61058	p 3099	N95-33839
DE-FG02-91CE-23810	p 3233	N95-32661
DE-FG02-91ER-61218	p 3153	N95-33205
DE-FG02-92ER-61477	p 3154	N95-33413
DE-FG02-93ER-40768	p 3205	N95-32651
DE-FG02-94ER-25195	p 3194	N95-32389
DE-FG02-94ER-40852	p 3234	N95-33202
DE-FG02-95ER-40896	p 3209	N95-34650
DE-FG03-93ER-40757	p 3234	N95-33202
DE-FG03-93ER-40759	p 3095	N95-32616
DE-FG03-93ER-45488	p 3083	N95-32819
	p 3229	N95-33641
DE-FG03-94ER-54241	p 3224	N95-33853
DE-FG03-95ER-45531	p 3074	N95-33392
DE-FG05-80ET-53088	p 3248	N95-33390
	p 3223	N95-33391
	p 3224	N95-33696
	p 3247	N95-34216
DE-FG05-84ER-40162	p 3206	N95-32965
DE-FG05-86ER-40272	p 3246	N95-32597
DE-FG05-88ER-53266	p 3186	N95-33852
DE-FG05-94ER-40842	p 3201	N95-32393
DE-FG06-90ER-40561	p 3204	N95-32617
	p 3204	N95-32619
	p 3204	N95-32621
	p 3208	N95-33854
	p 3209	N95-33855
DE-FG06-92ER-54176	p 3223	N95-33216
DE-FG06-94ER-12149	p 3102	N95-32968
DE-FG21-90MC-27115	p 3068	N95-33224
DE-FG21-92MC-29228	p 3075	N95-34021
DE-FG22-89PC-89761	p 3066	N95-32557
DLA900-90-D-0123	p 3125	N95-34346
DRET-91-1215-A	p 3164	N95-32611
DTFA01-93-Z-02012	p 3047	N95-33480
DTFA03-89-C-0043	p 3049	N95-34583
DTRS57-88-C-00078	p 3047	N95-34562
FAA-93-G-012	p 3189	N95-33002
F04701-93-C-0094	p 3157	N95-34613
F19628-90-C-0193	p 3058	N95-34744
F19628-92-C-0100	p 3158	N95-34575
F19628-93-C-0023	p 3144	N95-34454
F19628-95-C-0002	p 3096	N95-32773
	p 3098	N95-33152
	p 3047	N95-33480
	p 3100	N95-34474
F30602-91-D-0001	p 3104	N95-34345
F30602-93-C-0019	p 3217	N95-34300
F30602-94-C-0193	p 3218	N95-34504
F33615-90-C-0005	p 3056	N95-34344
	p 3056	N95-34362
F33615-92-C-0017	p 3164	N95-34789
F33615-92-C-3604	p 3055	N95-34306
F33615-93-1-1330	p 3105	N95-34565
	p 3193	N95-34602
F33657-84-D-0165	p 3217	N95-34459
F33657-88-D-2188	p 3117	N95-32472
	p 3118	N95-32702
	p 3215	N95-32957
	p 3059	N95-34493
F49620-87-C-0074	p 3180	N95-32765
F49620-91-C-0073	p 3182	N95-34582
F49620-92-J-0052	p 3104	N95-34451
F49620-92-J-0064	p 3231	N95-34569
F49620-92-J-0084	p 3165	N95-34472
F49620-92-J-0097	p 3113	N95-34597
F49620-92-J-0104	p 3087	N95-34596
F49620-92-J-0192	p 3232	N95-34755
F49620-92-J-0236	p 3193	N95-34600
F49620-92-J-0390	p 3112	N95-34572
F49620-92-J-0393	p 3233	N95-34822
F49620-92-J-0480	p 3217	N95-34374
F49620-92-J-0515	p 3101	N95-34790
F49620-93-C-0011	p 3087	N95-34817
F49620-93-C-0058	p 3231	N95-34568
F49620-93-C-0066	p 3196	N95-34377
F49620-93-1-0064	p 3113	N95-34752
F49620-93-1-0090	p 3042	N95-34763
F49620-93-1-0133	p 3100	N95-34590
F49620-93-1-0152	p 3183	N95-34604
F49620-93-1-0165	p 3183	N95-34605
F49620-93-1-0201	p 3219	N95-34791
F49620-93-1-0212	p 3182	N95-34598
F49620-94-C-0033	p 3081	N95-34821
F49620-94-C-0067	p 3232	N95-34588
F49620-94-C-0089	p 3178	N95-34745
F49620-94-1-0034	p 3187	N95-34603
F49620-94-1-0087	p 3105	N95-34581
F49620-95-I-0005	p 3100	N95-34601
MDA972-92-J-1012	p 3183	N95-34612
MDA972-93-C-0020	p 3087	N95-34614
NAGW-2031	p 3142	N95-32676
NAGW-3748	p 3143	N95-33498
NAGW-955	p 3110	N95-33496
NAG1-1058	p 3095	N95-32674
NAG1-1174	p 3246	N95-32913
NAG1-1478	p 3097	N95-32822
NAG1-1593	p 3171	N95-34764
NAG1-756	p 3180	N95-32765
	p 3180	N95-32766
NAG2-822	p 3167	N95-32688
NAG2-908	p 3048	N95-32928
NAG3-1507	p 3121	N95-32689
NAG3-443	p 3089	N95-32929
NAG3-955	p 3110	N95-33398
NAG3-974	p 3061	N95-33156
NAG5-1415	p 3121	N95-32675
NAG5-1490	p 3143	N95-32823
NAG5-1567	p 3248	N95-33916
NAG5-1580	p 3245	N95-32835
NAG5-2016	p 3248	N95-33499
NAG5-2344	p 3097	N95-33033
	p 3099	N95-33497
	p 3099	N95-33726
NASA ORDER S-93074-E	p 3246	N95-33261
NASA ORDER S-97228-E	p 3247	N95-33262
NASW-17605	p 3247	N95-33625
NAS1-18224	p 3059	N95-33264
	p 3059	N95-33890
NAS1-18580	p 3060	N95-32673
NAS1-18969	p 3181	N95-33396
NAS1-19247	p 3059	N95-33264
	p 3059	N95-33890
NAS1-19480	p 3180	N95-32834
	p 3196	N95-33500
	p 3196	N95-33727
NAS1-20103	p 3200	N95-33831
NAS3-25090	p 3104	N95-33915
NAS3-25365	p 3115	N95-32687
NAS3-25883	p 3061	N95-34625
NAS3-27186	p 3060	N95-32673
	p 3115	N95-32687
	p 3200	N95-32836
	p 3060	N95-32917
	p 3108	N95-32930
	p 3050	N95-32931
	p 3054	N95-33208
	p 3103	N95-33874
	p 3088	N95-33876
	p 3061	N95-33926
NAS3-27571	p 3108	N95-32930
	p 3050	N95-32931
NAS5-31363	p 3143	N95-32914
NAS5-31370	p 3142	N95-32717
NAS7-1260	p 3188	N95-32659
	p 3128	N95-33730
	p 3136	N95-33789
	p 3139	N95-33801
NAS8-38609	p 3066	N95-32581
NAS8-38865	p 3123	N95-32915
NAS8-39945	p 3061	N95-32932
NCC2-698	p 3106	N95-32454
NCC2-753	p 3247	N95-32700
NCC3-306	p 3188	N95-32767
	p 3188	N95-32768
NGT-44-001-800	p 3248	N95-32418
NGT-44-005-308	p 3194	N95-32433
NGT-44-005-803	p 3127	N95-32420
	p 3125	N95-32421
	p 3166	N95-32422
	p 3062	N95-32423
	p 3113	N95-32425
	p 3113	N95-32427
	p 3183	N95-32429
	p 3244	N95-32430
	p 3236	N95-32431
	p 3059	N95-32432
	p 3194	N95-32434
NGT-44-055-803	p 3176	N95-32428
NGT-50728	p 3134	N95-33760
NGT-51021	p 3097	N95-33033
NGT-70312	p 3122	N95-32693
NMRDC PROJ. MR0-4101	p 3076	N95-34814
NSF ATM-91-20072	p 3158	N95-33259
NSF CCR-94-10116	p 3187	N95-34587
NSF CDA-88-22724	p 3185	N95-32580
NSF DMR-91-20000	p 3228	N95-32810
	p 3110	N95-33389
NSF DMR-91-2497	p 3227	N95-32677
NSF DMR-95-36533	p 3226	N95-32594
NSF 87-17773	p 3180	N95-32765
N00014-88-K-0077	p 3166	N95-34609
N00014-88-K-0187	p 3160	N95-34457
N00014-89-J-1217	p 3160	N95-34594
N00014-89-J-1745	p 3218	N95-34571
N00014-89-J-1828	p 3082	N95-32552
	p 3086	N95-34361
N00014-90-C-0039	p 3112	N95-34343
N00014-90-J-1270	p 3178	N95-34453
N00014-90-J-1530	p 3086	N95-34452
N00014-90-J-1608	p 3067	N95-32804
N00014-90-J-4128	p 3160	N95-34375
N00014-91-J-1194	p 3087	N95-34649
N00014-91-J-1353	p 3064	N95-33704
N00014-92-C-6015	p 3219	N95-34576
N00014-92-J-1190	p 3218	N95-34498
N00014-92-J-1243	p 3209	N95-34350
N00014-92-J-1342	p 3086	N95-34476
N00014-92-J-1421	p 3231	N95-34478
N00014-92-J-1492	p 3076	N95-34615
N00014-92-J-1617	p 3177	N95-34301
N00014-92-J-1801	p 3185	N95-32580
N00014-92-J-1945	p 3235	N95-34743
N00014-92-J-4005	p 3166	N95-34610
N00014-93-C-0202	p 3193	N95-34593
N00014-93-C-2044	p 3227	N95-32695
N00014-93-C-2054	p 3231	N95-34568
N00014-93-1-0026	p 3077	N95-32474
N00014-93-1-0221	p 3183	N95-34612
	p 3171	N95-34616
N00014-93-1-0686	p 3100	N95-34749
N00014-93-1-6014	p 3234	N95-34464
N00014-94-C-0260	p 3105	N95-34458
N00014-94-G-0012	p 3247	N95-34561
N00014-94-I-0323	p 3075	N95-34357
N00014-94-WR-20019	p 3160	N95-34372
N00014-94-1-0516	p 3178	N95-34462
N00600-93-K-2051	p 3189	N95-33002
N68171-94-M-5310	p 3209	N95-34423
N68171-94-M-6429	p 3097	N95-32797
N68171-94-M-6700	p 3150	N95-34359
	p 3150	N95-34360
PROJ. FFI/566-E/139	p 3185	N95-32815
PROJ. FFITOX/625/138	p 3068	N95-33243
PROJ. SOFIA	p 3033	N95-32682
	p 3033	N95-32764
PROJ. 547352	p 3215	N95-33239
RTOP 198-36-60	p 3115	N95-32687
RTOP 199-06-30	p 3198	N95-33875
RTOP 232-01-00	p 3088	N95-33876
RTOP 233-01-0C	p 3103	N95-33874
RTOP 233-03-02-02	p 3059	N95-33264
	p 3059	N95-33890
RTOP 242-70-04	p 3061	N95-33156
RTOP 297-50-00	p 3060	N95-32673
RTOP 478-43-00	p 3061	N95-33926
RTOP 505-59-20-01	p 3034	N95-32821
RTOP 505-62-20	p 3054	N95-33208
RTOP 505-62-36	p 3123	N95-33179
	p 3124	N95-33908
RTOP 505-62-50	p 3050	N95-32916
RTOP 505-63-12	p 3125	N95-33209
RTOP 505-63-5B	p 3063	N95-33210
RTOP 505-64-10-13	p 3181	N95-33396
RTOP 505-68-50	p 3181	N95-33193
RTOP 505-90-00	p 3239	N95-34217
RTOP 505-90-52-01	p 3180	N95-32834
	p 3196	N95-33727
RTOP 505-90-52	p 3196	N95-33500
RTOP 506-72-00	p 3104	N95-33915
RTOP 508-68-10	p 3034	N95-32769
RTOP 537-02-21	p 3108	N95-32930
	p 3050	N95-32931
RTOP 538-03-11-01	p 3200	N95-33831
RTOP 538-03-11	p 3200	N95-32836
RTOP 564-09-20	p 3060	N95-32917
RTOP 584-03-11	p 3061	N95-34625
RTOP 616-00-00	p 3083	N95-32918
	p 3083	N95-32919
RTOP 655-81-00	p 3128	N95-33730
RTOP 665-81-00	p 3136	N95-33789
	p 3139	N95-33801
RTOP 674-21-05	p 3089	N95-32718
RTOP 888-00-01-00-01	p 3188	N95-32659
W-31-109-ENG-38	p 3219	N95-32401
	p 3152	N95-32553
	p 3225	N95-32586
	p 3226	N95-32598
	p 3082	N95-32664
	p 3212	N95-32665
	p 3067	N95-32671
	p 3228	N95-32810
	p 3102	N95-32956
	p 3079	N95-33215
	p 3228	N95-33382

W-7405-ENG-36 .....
p 3110 N95-33389
p 3154 N95-33394
p 3088 N95-33395
p 3213 N95-33406
p 3229 N95-33636
p 3124 N95-33834
p 3156 N95-33847
p 3209 N95-34212
p 3230 N95-34215
p 3075 N95-34440
p 3187 N95-32375
p 3121 N95-32376
p 3125 N95-32385
p 3187 N95-32386
p 3197 N95-32391
p 3211 N95-32416
p 3225 N95-32532
p 3179 N95-32572
p 3152 N95-32573
p 3203 N95-32574
p 3148 N95-32575
p 3203 N95-32576
p 3203 N95-32577
p 3203 N95-32583
p 3204 N95-32584
p 3089 N95-32585
p 3088 N95-32605
p 3179 N95-32669
p 3126 N95-32670
p 3058 N95-32713
p 3102 N95-32714
p 3179 N95-32715
p 3180 N95-32716
p 3185 N95-32771
p 3177 N95-32955
p 3212 N95-32960
p 3181 N95-33154
p 3246 N95-33211
p 3191 N95-33212
p 3229 N95-33386
p 3099 N95-33387
p 3234 N95-33388
p 3229 N95-33401
p 3186 N95-33403
p 3208 N95-33623
p 3111 N95-33698
p 3088 N95-33702
p 3064 N95-33704
p 3062 N95-33848
p 3143 N95-33849
p 3216 N95-34020
p 3231 N95-34450

W-7405-ENG-48 .....
p 3179 N95-32390
p 3062 N95-32395
p 3062 N95-32399
p 3184 N95-32415
p 3167 N95-32535
p 3221 N95-32536
p 3195 N95-32559
p 3089 N95-32568
p 3095 N95-32569
p 3095 N95-32570
p 3117 N95-32571
p 3222 N95-32592
p 3059 N95-32593
p 3246 N95-32597
p 3062 N95-32602
p 3156 N95-32697
p 3115 N95-32900
p 3079 N95-33063
p 3212 N95-33064
p 3223 N95-33066
p 3126 N95-33068
p 3068 N95-33070
p 3207 N95-33219
p 3197 N95-33220
p 3213 N95-33333
p 3118 N95-33378
p 3143 N95-33407
p 3084 N95-33408
p 3085 N95-33409
p 3159 N95-33410
p 3216 N95-33411
p 3216 N95-33506
p 3074 N95-33627
p 3150 N95-33642
p 3186 N95-33643
p 3230 N95-33650
p 3216 N95-33651
p 3182 N95-33652
p 3080 N95-33653
p 3164 N95-33654
p 3119 N95-33703
p 3112 N95-34437
p 3230 N95-34438
p 3081 N95-34482

W-7405-ENG-82 .....
p 3183 N95-34813
p 3066 N95-32394
p 3060 N95-32396
p 3198 N95-32397
p 3177 N95-32398
p 3066 N95-32540
p 3078 N95-32638
p 3227 N95-32640
p 3067 N95-32641
p 3227 N95-32643
p 3078 N95-32648
p 3228 N95-32959
p 3229 N95-33637
p 3080 N95-33699
p 3080 N95-33700

Typical Report Number Index Listing

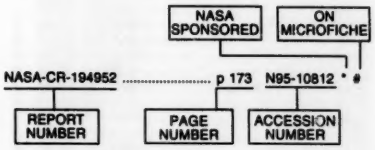

Listings in this index are arranged alphanumerically by report number. The accession number denotes the number by which the citation is identified. The page number helps to locate the citation in the abstract section. An asterisk (*) indicates that the item is a NASA report. A pound sign (#) indicates that the item is available on microfiche.

A-950069 ..... p 3048 N95-32699 * #
A-950075 ..... p 3198 N95-33875 * #

AD-A288731 ..... p 3076 N95-34814 #
AD-A289985 ..... p 3082 N95-32694 #
AD-A289990 ..... p 3227 N95-32695 #
AD-A290163 ..... p 3227 N95-32677 #
AD-A290501 ..... p 3164 N95-33200 #
AD-A291165 ..... p 3097 N95-32797 #
AD-A293026 ..... p 3057 N95-32772 #
AD-A293030 ..... p 3096 N95-32773 #
AD-A293032 ..... p 3098 N95-33152 #
AD-A293054 ..... p 3215 N95-32701 #
AD-A293070 ..... p 3118 N95-32702 #
AD-A293087 ..... p 3215 N95-32660 #
AD-A293088 ..... p 3215 N95-32957 #
AD-A293094 ..... p 3117 N95-32472 #
AD-A293115 ..... p 3082 N95-32552 #
AD-A293401 ..... p 3252 N95-32473 #
AD-A293455 ..... p 3057 N95-34815 #
AD-A293475 ..... p 3244 N95-34816 #
AD-A293526 ..... p 3087 N95-34649 #
AD-A293541 ..... p 3057 N95-34606 #
AD-A293544 ..... p 3232 N95-34607 #
AD-A293549 ..... p 3232 N95-34608 #
AD-A293555 ..... p 3166 N95-34609 #
AD-A293560 ..... p 3166 N95-34610 #
AD-A293564 ..... p 3076 N95-34611 #
AD-A293567 ..... p 3183 N95-34612 #
AD-A293568 ..... p 3157 N95-34613 #
AD-A293573 ..... p 3087 N95-34614 #
AD-A293587 ..... p 3076 N95-34615 #
AD-A293607 ..... p 3171 N95-34616 #
AD-A293622 ..... p 3077 N95-32474 #
AD-A293667 ..... p 3067 N95-32804 #
AD-A293690 ..... p 3047 N95-33480 #
AD-A293722 ..... p 3185 N95-32580
AD-A293736 ..... p 3104 N95-34451 #
AD-A293965 ..... p 3086 N95-34452 #
AD-A293966 ..... p 3178 N95-34453 #
AD-A293967 ..... p 3144 N95-34454 #
AD-A293978 ..... p 3182 N95-34455 #
AD-A293985 ..... p 3182 N95-34456 #
AD-A293988 ..... p 3243 N95-34420 #
AD-A293993 ..... p 3243 N95-34421 #
AD-A294002 ..... p 3160 N95-34457 #
AD-A294005 ..... p 3170 N95-34370 #
AD-A294006 ..... p 3182 N95-34371 #
AD-A294007 ..... p 3160 N95-34372 #
AD-A294008 ..... p 3081 N95-34373 #
AD-A294009 ..... p 3217 N95-34374 #
AD-A294017 ..... p 3160 N95-34375 #
AD-A294018 ..... p 3170 N95-34376 #
AD-A294019 ..... p 3196 N95-34377 #
AD-A294037 ..... p 3236 N95-34487 #
AD-A294038 ..... p 3105 N95-34488 #
AD-A294041 ..... p 3170 N95-34489 #
AD-A294042 ..... p 3218 N95-34490 #
AD-A294043 ..... p 3158 N95-34491 #
AD-A294047 ..... p 3170 N95-34492 #
AD-A294049 ..... p 3170 N95-34378 #
AD-A294056 ..... p 3192 N95-34467 #
AD-A294058 ..... p 3151 N95-34468 #
AD-A294060 ..... p 3120 N95-34469 #
AD-A294061 ..... p 3120 N95-34470 #
AD-A294064 ..... p 3218 N95-34471 #
AD-A294065 ..... p 3165 N95-34472 #
AD-A294067 ..... p 3104 N95-34379 #
AD-A294068 ..... p 3119 N95-34380 #
AD-A294086 ..... p 3193 N95-34473 #
AD-A294090 ..... p 3100 N95-34474 #
AD-A294095 ..... p 3170 N95-34475 #
AD-A294104 ..... p 3193 N95-34495 #
AD-A294105 ..... p 3116 N95-34496 #
AD-A294110 ..... p 3193 N95-34497 #
AD-A294111 ..... p 3218 N95-34498 #
AD-A294112 ..... p 3193 N95-34499 #
AD-A294113 ..... p 3059 N95-34500 #
AD-A294114 ..... p 3193 N95-34501 #
AD-A294116 ..... p 3086 N95-34502 #
AD-A294118 ..... p 3178 N95-34503 #
AD-A294119 ..... p 3218 N95-34504 #
AD-A294121 ..... p 3194 N95-34742 #
AD-A294123 ..... p 3235 N95-34743 #
AD-A294124 ..... p 3058 N95-34744 #
AD-A294125 ..... p 3100 N95-34749 #
AD-A294126 ..... p 3042 N95-34750 #
AD-A294129 ..... p 3157 N95-34751 #
AD-A294137 ..... p 3113 N95-34752 #
AD-A294138 ..... p 3246 N95-34753 #
AD-A294146 ..... p 3165 N95-34754 #
AD-A294150 ..... p 3232 N95-34755 #
AD-A294152 ..... p 3219 N95-34756 #
AD-A294156 ..... p 3158 N95-34757 #
AD-A294160 ..... p 3105 N95-34758 #
AD-A294161 ..... p 3219 N95-34759 #
AD-A294163 ..... p 3100 N95-34760 #
AD-A294165 ..... p 3120 N95-34761 #
AD-A294166 ..... p 3100 N95-34762 #
AD-A294167 ..... p 3042 N95-34763 #
AD-A294190 ..... p 3217 N95-34297 #
AD-A294192 ..... p 3217 N95-34298 #
AD-A294195 ..... p 3157 N95-34299 #
AD-A294197 ..... p 3217 N95-34300 #
AD-A294198 ..... p 3177 N95-34301 #
AD-A294199 ..... p 3061 N95-34302 #
AD-A294203 ..... p 3217 N95-34303 #
AD-A294204 ..... p 3099 N95-34304 #
AD-A294206 ..... p 3217 N95-34305 #
AD-A294211 ..... p 3055 N95-34306 #
AD-A294215 ..... p 3217 N95-34307 #
AD-A294217 ..... p 3119 N95-34308 #
AD-A294219 ..... p 3217 N95-34309 #
AD-A294221 ..... p 3105 N95-34458 #
AD-A294249 ..... p 3059 N95-34493 #
AD-A294253 ..... p 3217 N95-34459 #
AD-A294256 ..... p 3100 N95-34460 #
AD-A294258 ..... p 3160 N95-34461 #
AD-A294272 ..... p 3178 N95-34462 #
AD-A294275 ..... p 3166 N95-34463 #
AD-A294276 ..... p 3234 N95-34464 #
AD-A294337 ..... p 3166 N95-34356 #
AD-A294338 ..... p 3075 N95-34357 #
AD-A294342 ..... p 3170 N95-34358 #
AD-A294343 ..... p 3150 N95-34359 #
AD-A294347 ..... p 3150 N95-34360 #
AD-A294359 ..... p 3086 N95-34361 #
AD-A294369 ..... p 3056 N95-34362 #
AD-A294372 ..... p 3186 N95-34340 #
AD-A294373 ..... p 3159 N95-34341 #
AD-A294375 ..... p 3056 N95-34342 #
AD-A294377 ..... p 3112 N95-34343 #
AD-A294385 ..... p 3056 N95-34344 #
AD-A294386 ..... p 3104 N95-34345 #
AD-A294388 ..... p 3125 N95-34346 #
AD-A294390 ..... p 3104 N95-34347 #
AD-A294393 ..... p 3081 N95-34348 #
AD-A294408 ..... p 3049 N95-34422 #
AD-A294444 ..... p 3086 N95-34494 #
AD-A294516 ..... p 3086 N95-34476 #
AD-A294517 ..... p 3199 N95-34477
AD-A294519 ..... p 3231 N95-34478 #
AD-A294521 ..... p 3235 N95-34479 #
AD-A294522 ..... p 3182 N95-34349 #
AD-A294523 ..... p 3209 N95-34350 #
AD-A294589 ..... p 3209 N95-34423
AD-A294634 ..... p 3247 N95-34561 #
AD-A294752 ..... p 3047 N95-34562 #
AD-A294759 ..... p 3086 N95-34563 #
AD-A294839 ..... p 3165 N95-34564 #
AD-A294842 ..... p 3105 N95-34565 #
AD-A294850 ..... p 3100 N95-34566 #
AD-A294851 ..... p 3100 N95-34567 #
AD-A294852 ..... p 3231 N95-34568 #
AD-A294853 ..... p 3231 N95-34569 #
AD-A294878 ..... p 3047 N95-34570 #
AD-A294879 ..... p 3218 N95-34571 #
AD-A294888 ..... p 3112 N95-34572 #
AD-A294894 ..... p 3165 N95-34573 #
AD-A294895 ..... p 3171 N95-34574 #
AD-A294900 ..... p 3158 N95-34575 #
AD-A294902 ..... p 3155 N95-34591 #
AD-A294914 ..... p 3120 N95-34592 #
AD-A294919 ..... p 3193 N95-34593 #
AD-A294920 ..... p 3160 N95-34594 #
AD-A294925 ..... p 3201 N95-34595 #
AD-A294930 ..... p 3087 N95-34596 #
AD-A294931 ..... p 3113 N95-34597 #
AD-A294932 ..... p 3182 N95-34598 #
AD-A294933 ..... p 3076 N95-34599 #
AD-A294934 ..... p 3193 N95-34600 #
AD-A294936 ..... p 3100 N95-34601 #
AD-A294938 ..... p 3193 N95-34602 #
AD-A294939 ..... p 3187 N95-34603 #
AD-A294941 ..... p 3183 N95-34604 #
AD-A294944 ..... p 3183 N95-34605 #
AD-A294946 ..... p 3178 N95-34745
AD-A294948 ..... p 3219 N95-34576 #
AD-A294953 ..... p 3171 N95-34577 #
AD-A294956 ..... p 3100 N95-34578 #
AD-A294958 ..... p 3219 N95-34579 #
AD-A294959 ..... p 3182 N95-34580 #
AD-A294963 ..... p 3105 N95-34581 #
AD-A294965 ..... p 3182 N95-34582 #
AD-A294968 ..... p 3049 N95-34583 #
AD-A294969 ..... p 3186 N95-34584 #
AD-A294970 ..... p 3235 N95-34585 #
AD-A294972 ..... p 3224 N95-34586 #
AD-A294973 ..... p 3187 N95-34587
AD-A294976 ..... p 3232 N95-34588 #
AD-A294977 ..... p 3235 N95-34589 #
AD-A294978 ..... p 3100 N95-34590 #
AD-A294985 ..... p 3087 N95-34817 #
AD-A294993 ..... p 3113 N95-34818 #
AD-A294997 ..... p 3209 N95-34819 #
AD-A294999 ..... p 3233 N95-34820 #
AD-A295000 ..... p 3081 N95-34821 #
AD-A295003 ..... p 3233 N95-34822 #
AD-A295020 ..... p 3101 N95-34788 #
AD-A295024 ..... p 3164 N95-34789 #
AD-A295025 ..... p 3101 N95-34790
AD-A295030 ..... p 3219 N95-34791 #
AD-A295033 ..... p 3232 N95-34792 #
AD-A295035 ..... p 3049 N95-34793 #
AD-A295036 ..... p 3244 N95-34794 #
AD-A295037 ..... p 3232 N95-34795 #
AD-A295042 ..... p 3105 N95-34796 #
AD-A295108 ..... p 3047 N95-34797 #

AD-D017285 ..... p 3105 N95-34617
AD-D017421 ..... p 3105 N95-34618
AD-D017424 ..... p 3215 N95-32923 #
AD-D017425 ..... p 3120 N95-34619
AD-D017443 ..... p 3123 N95-32924 #
AD-D017451 ..... p 3097 N95-32925 #
AD-D017465 ..... p 3201 N95-34444
AD-D017468 ..... p 3104 N95-34445
AD-D017469 ..... p 3104 N95-34446
AD-D017470 ..... p 3086 N95-34447
AD-D017471 ..... p 3065 N95-34448
AD-D017476 ..... p 3124 N95-34449

AD-D017481 ..... p 3201 N95-34424
AD-D017482 ..... p 3104 N95-34425
AD-D017485 ..... p 3075 N95-34287
AD-D017486 ..... p 3216 N95-34288
AD-D017487 ..... p 3201 N95-34289
AD-D017489 ..... p 3116 N95-34426
AD-D017490 ..... p 3127 N95-34427
AD-D017522 ..... p 3065 N95-34620

AEDC-TR-95-5 ..... p 3113 N95-34818 #

AFIT/CI-95-028 ..... p 3047 N95-34570 #

AFIT/CI/CIA-95-002D ..... p 3246 N95-34753 #

AFOSR-TR-95-0257 ..... p 3252 N95-32473 #

AFOSR-95-0267TR ..... p 3081 N95-34821 #
AFOSR-95-0269TR ..... p 3182 N95-34582 #
AFOSR-95-0272TR ..... p 3178 N95-34745
AFOSR-95-0278TR ..... p 3233 N95-34820 #
AFOSR-95-0280TR ..... p 3235 N95-34589 #
AFOSR-95-0281TR ..... p 3235 N95-34585 #
AFOSR-95-0284TR ..... p 3232 N95-34792 #
AFOSR-95-0285TR ..... p 3219 N95-34579 #
AFOSR-95-0288TR ..... p 3224 N95-34586 #
AFOSR-95-0289TR ..... p 3209 N95-34819 #
AFOSR-95-0300TR ..... p 3100 N95-34590 #
AFOSR-95-0303TR ..... p 3101 N95-34790
AFOSR-95-0308TR ..... p 3233 N95-34822 #
AFOSR-95-0312TR ..... p 3232 N95-34795 #
AFOSR-95-0315TR ..... p 3219 N95-34791 #
AFOSR-95-0320TR ..... p 3104 N95-34451 #
AFOSR-95-0333TR ..... p 3232 N95-34755 #
AFOSR-95-0338TR ..... p 3165 N95-34472 #
AFOSR-95-0340TR ..... p 3113 N95-34752 #
AFOSR-95-0341TR ..... p 3196 N95-34377 #
AFOSR-95-0344TR ..... p 3042 N95-34763 #
AFOSR-95-0382TR ..... p 3113 N95-34597 #
AFOSR-95-0384TR ..... p 3183 N95-34605 #
AFOSR-95-0386TR ..... p 3182 N95-34598 #
AFOSR-95-0387TR ..... p 3193 N95-34600 #
AFOSR-95-0388TR ..... p 3100 N95-34601 #
AFOSR-95-0397TR ..... p 3112 N95-34572 #
AFOSR-95-0398TR ..... p 3231 N95-34569 #
AFOSR-95-0409TR ..... p 3105 N95-34581 #
AFOSR-95-0411TR ..... p 3232 N95-34588 #
AFOSR-95-0415TR ..... p 3187 N95-34603 #
AFOSR-95-0416TR ..... p 3183 N95-34604 #
AFOSR-95-0418TR ..... p 3087 N95-34817 #
AFOSR-95-0422TR ..... p 3087 N95-34596 #
AFOSR-95-0424TR ..... p 3155 N95-34591 #

AFPT-90-4M0-028 ..... p 3165 N95-34564 #

AFR-529025 ..... p 3199 N95-34477

AGARD-CP-556 ..... p 3091 N95-33126 #
AGARD-CP-563 ..... p 3042 N95-32486 #

AGARD-INDEX-92-94 ..... p 3237 N95-33198 #

AGARD-LS-202 ..... p 3168 N95-34050 #

AIAA PAPER 95-1210 ..... p 3063 N95-33210 * #
AIAA PAPER 95-2435 ..... p 3088 N95-33876 * #
AIAA PAPER 95-2469 ..... p 3108 N95-32930 * #
AIAA PAPER 95-2470 ..... p 3050 N95-32931 * #
AIAA PAPER 95-2513 ..... p 3060 N95-32917 * #

AL/EQ-TR-1994-52 ..... p 3081 N95-34348 #

AL/HR-TR-1994-0168 ..... p 3056 N95-34362 #
AL/HR-TR-1994-0170 ..... p 3056 N95-34344 #

AL/OE-TR-1994-0141 ..... p 3164 N95-34789 #

ANL-HEP-CP-95-20 ..... p 3213 N95-33406 #

ANL-HEP-TR-94-86 ..... p 3082 N95-32664 #
ANL-HEP-TR-95-11 ..... p 3212 N95-32665 #

ANL/CHM/CP-83703 ..... p 3228 N95-33382 #
ANL/CHM/CP-84094 ..... p 3225 N95-32586 #
ANL/CHM/CP-85037 ..... p 3230 N95-34215 #
ANL/CHM/CP-85859 ..... p 3154 N95-33394 #

ANL/CMT-ACL/CP-83198 ..... p 3067 N95-32671 #

ANL/CMT/CP-83389 ..... p 3102 N95-32956 #

ANL/ER/CP-84929 ..... p 3156 N95-33847 #

ANL/ES/CP-85765 ..... p 3088 N95-33395 #

ANL/ET/CP-83802 ..... p 3079 N95-33215 #

ANL/ET/CP-85237 ..... p 3152 N95-32553 #

ANL/FE/CP-83609 ..... p 3075 N95-34440 #

ANL/FPP/TM-280 ..... p 3219 N95-32401

ANL/MCS/CP-84761 ..... p 3209 N95-34212 #
ANL/MCS/CP-85304 ..... p 3099 N95-33379 #

ANL/MSD/CP-82574 ..... p 3228 N95-32810 #
ANL/MSD/CP-83373 ..... p 3229 N95-33636 #
ANL/MSD/CP-83776 ..... p 3226 N95-32598 #
ANL/MSD/CP-85925 ..... p 3110 N95-33389 #

ANL/TD/CP-85711 ..... p 3124 N95-33834 #

APL-UW-TR-9501 ..... p 3201 N95-34595 #

AR-007-138 ..... p 3054 N95-33250
AR-009-179 ..... p 3078 N95-32926
AR-009-182 ..... p 3115 N95-32927
AR-009-257 ..... p 3188 N95-32995

ARAED-TR-95009 ..... p 3056 N95-34342 #

ARC-R93-210 ..... p 3245 N95-32835 * #

ARCCB-TR-95007 ..... p 3081 N95-34373 #

ARI-RR-1117 ..... p 3081 N95-34821 #

ARL-TN-46 ..... p 3057 N95-34815 #

ARL-TR-421 ..... p 3104 N95-34347 #
ARL-TR-423 ..... p 3232 N95-34607 #
ARL-TR-425 ..... p 3232 N95-34608 #
ARL-TR-653 ..... p 3082 N95-32694 #
ARL-TR-745 ..... p 3076 N95-34599 #
ARL-TR-747 ..... p 3170 N95-34376 #
ARL-TR-838 ..... p 3124 N95-33908 * #
ARL-TR-852 ..... p 3123 N95-33179 * #

ARO-27890.1-LS ..... p 3164 N95-33200 #
ARO-28467.27-EL ..... p 3186 N95-34584 #

ARTI-660-50800 ..... p 3233 N95-32661 #

ATC-229 ..... p 3047 N95-33480 #

ATR-94(7270)-1 ..... p 3158 N95-33259 #

B-205879 ..... p 3236 N95-32887 #
B-233451.5 ..... p 3236 N95-33907 #
B-238858 ..... p 3089 N95-32785 #
B-248882 ..... p 3197 N95-32886 #
B-254704 ..... p 3046 N95-32784 #
B-255498 ..... p 3157 N95-32760 #
B-255905 ..... p 3197 N95-32807 #
B-256001 ..... p 3056 N95-32888 #
B-256104 ..... p 3198 N95-33263 #
B-256330 ..... p 3055 N95-32759 #
B-256584 ..... p 3046 N95-32885 #
B-257609 ..... p 3055 N95-32786 #
B-257642 ..... p 3033 N95-32782 #
B-257915 ..... p 3033 N95-32783 #
B-259097 ..... p 3046 N95-32705 #
B-259135 ..... p 3235 N95-32706 #
B-261347 ..... p 3197 N95-32758 #
B-261547 ..... p 3058 N95-32884 #
B-261656 ..... p 3142 N95-32707 #

BER-611-162 ..... p 3234 N95-34464 #

BNL-60197 ..... p 3153 N95-33192 #
BNL-60875 ..... p 3202 N95-32484 #
BNL-61158 ..... p 3210 N95-32411 #
BNL-61162 ..... p 3236 N95-32412 #
BNL-61165 ..... p 3210 N95-32413 #
BNL-61170 ..... p 3210 N95-32414 #
BNL-61173 ..... p 3211 N95-32485 #
BNL-61518 ..... p 3207 N95-33203 #
BNL-61527 ..... p 3213 N95-33204 #
BNL-61540 ..... p 3125 N95-32392 #
BNL-61575 ..... p 3205 N95-32652 #
BNL-61577 ..... p 3205 N95-32654 #
BNL-61578 ..... p 3203 N95-32542 #
BNL-61583 ..... p 3205 N95-32651 #
BNL-61755 ..... p 3212 N95-33067
BNL-61775 ..... p 3208 N95-33850 #
BNL-61815 ..... p 3156 N95-34214 #

BUDKERINP-93-64 ..... p 3202 N95-32481 #
BUDKERINP-93-96 ..... p 3221 N95-32560 #
BUDKERINP-94-1 ..... p 3221 N95-32561 #

CMP-178-0045B ..... p 3253 N95-33384 *

CMU-CS-95-117 ..... p 3187 N95-34587
CMU-CS-95-133 ..... p 3193 N95-34602 #
CMU-CS-95-140 ..... p 3105 N95-34565 #

CNIC-00779 ..... p 3227 N95-32698 #
CNIC-00784 ..... p 3221 N95-32562 #

CONF-8411210-7 ..... p 3203 N95-32542 #
CONF-9308260 ..... p 3197 N95-32624 #
CONF-9401114-1 ..... p 3179 N95-32390 #
CONF-940115-33 ..... p 3153 N95-33205 #
CONF-9402136-1 ..... p 3246 N95-32597 #
CONF-9404121-4 ..... p 3186 N95-33852 #
CONF-9404252 ..... p 3185 N95-32771 #
CONF-9404261-1 ..... p 3062 N95-33848 #
CONF-940451-2 ..... p 3244 N95-34801 #
CONF-9405161 ..... p 3185 N95-32820
CONF-940582-8 ..... p 3085 N95-33409 #
CONF-940616-91 ..... p 3201 N95-32379 #
CONF-9406241-2 ..... p 3159 N95-33410 #
CONF-9406270-8 ..... p 3222 N95-32756 #
CONF-9406279-ABSTS ..... p 3194 N95-32389 #
CONF-940632-28 ..... p 3152 N95-32573 #
CONF-9406335-1 ..... p 3127 N95-34442 #
CONF-940641-2 ..... p 3062 N95-32399 #
CONF-940665-2 ..... p 3089 N95-32568 #
CONF-9407166-2 ..... p 3212 N95-33064 #
CONF-9407181-ABSTS ..... p 3154 N95-33413 #
CONF-9407184-1 ..... p 3230 N95-34443 #
CONF-940723-40 ..... p 3095 N95-32569 #
CONF-940813-41 ..... p 3154 N95-33394 #
CONF-9408146-20 ..... p 3117 N95-32571 #
CONF-9408148-2 ..... p 3115 N95-32900 #
CONF-940829-3 ..... p 3083 N95-32819
CONF-940829-4 ..... p 3229 N95-33641 #
CONF-940830-3 ..... p 3066 N95-32394 #
CONF-9408[illegible]3-18 ..... p 3222 N95-32592 #
CONF-940922-8 ..... p 3207 N95-33219 #
CONF-9409264-2 ..... p 3204 N95-32584 #
CONF-9409278-4 ..... p 3185 N95-32582 #
CONF-9409331-1 ..... p 3074 N95-33627 #
CONF-9409347-1 ..... p 3228 N95-33382 #
CONF-9409351-1 ..... p 3113 N95-34800 #
CONF-941006-6 ..... p 3119 N95-33703 #
CONF-941013-36 ..... p 3228 N95-32810 #
CONF-941013-37 ..... p 3230 N95-33650 #
CONF-941013-41 ..... p 3214 N95-33504 #
CONF-941013-42 ..... p 3103 N95-33080
CONF-941013-43 ..... p 3215 N95-33381 #
CONF-941016-6 ..... p 3079 N95-33217 #
CONF-9410165-13 ..... p 3225 N95-32377 #
CONF-9410198-2 ..... p 3203 N95-32564 #
CONF-9410198-3 ..... p 3206 N95-32763 #
CONF-9410201 ..... p 3191 N95-33060 #
CONF-9410248-3 ..... p 3208 N95-33375 #
CONF-9410254-6 ..... p 3112 N95-34437 #
CONF-9410256-4 ..... p 3152 N95-32553 #
CONF-9410285-3 ..... p 3208 N95-33850 #
CONF-9410309-4 ..... p 3103 N95-33697 #
CONF-9410314-3 ..... p 3183 N95-34813 #
CONF-9410315-2 ..... p 3211 N95-32606 #
CONF-9410315-3 ..... p 3213 N95-33204 #
CONF-9410341-1 ..... p 3095 N95-32570 #
CONF-941109-3 ..... p 3150 N95-33642 #
CONF-9411149-28 ..... p 3153 N95-32816 #
CONF-9411152-4 ..... p 3216 N95-33651 #
CONF-9411210-5 ..... p 3205 N95-32652 #
CONF-9411210-6 ..... p 3205 N95-32654 #
CONF-941129-25 ..... p 3230 N95-34438 #
CONF-941144-121 ..... p 3226 N95-32590 #
CONF-941144-123 ..... p 3062 N95-32395 #
CONF-941144-124 ..... p 3198 N95-32397 #
CONF-941144-125 ..... p 3077 N95-32400 #
CONF-941144-142 ..... p 3077 N95-32527 #
CONF-941144-146 ..... p 3151 N95-34481 #
CONF-941144-148 ..... p 3229 N95 33636 #
CONF-941144-156 ..... p 3218 N95-34480 #
CONF-941144-157 ..... p 3229 N95-33628 #
CONF-941144-158 ..... p 3233 N95-34802 #
CONF-941221-3 ..... p 3102 N95-32956 #
CONF-941251-4 ..... p 3207 N95-33201 #
CONF-941268-1 ..... p 3205 N95-32650 #
CONF-950001-1 ..... p 3156 N95-34214 #
CONF-950110-20 ..... p 3060 N95-32396 #
CONF-950127-10 ..... p 3207 N95-33203 #
CONF-950127-7 ..... p 3208 N95-33854 #
CONF-950172-2 ..... p 3205 N95-32651 #
CONF-950172-3 ..... p 3208 N95-33380 #
CONF-950201-14 ..... p 3079 N95-33215 #
CONF-950209-7 ..... p 3067 N95-32671 #
CONF-9502101-2 ..... p 3209 N95-34212 #
CONF-950212-8 ..... p 3099 N95-33379 #
CONF-950220-7 ..... p 3203 N95-32577 #
CONF-950220-8 ..... p 3208 N95-33623 #
CONF-950220-9 ..... p 3102 N95-32708 #
CONF-950226-34 ..... p 3236 N95-32471 #

CONF-950226-35 ..... p 3179 N95-32470 #
CONF-950226-37 ..... p 3118 N95-33246 #
CONF-950226-38 ..... p 3118 N95-32663 #
CONF-950226-39 ..... p 3164 N95-33654 #
CONF-950226-40 ..... p 3216 N95-33411 #
CONF-950226-43 ..... p 3120 N95-34811
CONF-950226-47 ..... p 3084 N95-33247 #
CONF-950226-50 ..... p 3075 N95-34440 #
CONF-950228-6 ..... p 3226 N95-32598 #
CONF-950241-3 ..... p 3225 N95-32586 #
CONF-950256-4 ..... p 3102 N95-32808 #
CONF-950256-5 ..... p 3122 N95-32863 #
CONF-950256-6 ..... p 3088 N95-33395 #
CONF-950266 ..... p 3068 N95-33070 #
CONF-950285-2 ..... p 3207 N95-33245 #
CONF-950287-3 ..... p 3213 N95-33406 #
CONF-950292-1 ..... p 3110 N95-33389 #
CONF-950297-1 ..... p 3062 N95-33835 #
CONF-950299-1 ..... p 3234 N95-33388 #
CONF-950304-14 ..... p 3077 N95-32555 #
CONF-950309-1 ..... p 3148 N95-32551 #
CONF-950309-2 ..... p 3033 N95-32548 #
CONF-950309-6 ..... p 3150 N95-33706 #
CONF-9503113-2 ..... p 3124 N95-33834 #
CONF-9503119-2 ..... p 3078 N95-32591 #
CONF-9503128-1 ..... p 3151 N95-32475 #
CONF-9503135-1 ..... p 3179 N95-32572 #
CONF-9503135-2 ..... p 3191 N95-33212 #
CONF-9503140-1 ..... p 3153 N95-33192 #
CONF-9503140-3 ..... p 3158 N95-33505 #
CONF-9503141-1 ..... p 3238 N95-33402 #
CONF-9503146-1 ..... p 3230 N95-33880 #
CONF-950381-2 ..... p 3156 N95-32697 #
CONF-950381-4 ..... p 3156 N95-33847 #
CONF-950412-12 ..... p 3223 N95-33412 #
CONF-950412-14 ..... p 3119 N95-34466
CONF-950412-1 ..... p 3226 N95-32595 #
CONF-950412-2 ..... p 3148 N95-32575 #
CONF-950412-5 ..... p 3226 N95-32594 #
CONF-950412-7 ..... p 3225 N95-32579 #
CONF-9504126 ..... p 3186 N95-33643
CONF-9504138-1 ..... p 3222 N95-32656 #
CONF-9504144-1 ..... p 3186 N95-33639 #
CONF-9504145-1 ..... p 3067 N95-32709 #
CONF-9504147-1 ..... p 3246 N95-33211 #
CONF-9504156-1 ..... p 3127 N95-33833 #
CONF-9504163-1 ..... p 3124 N95-33701 #
CONF-950454-2 ..... p 3084 N95-33405 #
CONF-950463-1 ..... p 3050 N95-32636 #
CONF-950472-5 ..... p 3226 N95-32589 #
CONF-950494-12 ..... p 3075 N95-34021 #
CONF-950494-14 ..... p 3076 N95-34810 #
CONF-950494-20 ..... p 3068 N95-33224 #
CONF-950512-116 ..... p 3212 N95-33067
CONF-950512-31 ..... p 3095 N95-32616 #
CONF-950512-32 ..... p 3211 N95-32608 #
CONF-950512-33 ..... p 3212 N95-32657 #
CONF-950512-34 ..... p 3215 N95-32658 #
CONF-950512-35 ..... p 3211 N95-32607 #
CONF-950512-38 ..... p 3101 N95-32578 #
CONF-950512-48 ..... p 3210 N95-32411 #
CONF-950512-52 ..... p 3211 N95-32485 #
CONF-950512-55 ..... p 3236 N95-32412 #
CONF-950512-58 ..... p 3210 N95-32413 #
CONF-950512-63 ..... p 3210 N95-32414 #
CONF-950512-65 ..... p 3211 N95-32416 #
CONF-950512-68 ..... p 3213 N95-33338 #
CONF-950512-70 ..... p 3098 N95-33336 #
CONF-950512-72 ..... p 3213 N95-33335 #
CONF-950512-75 ..... p 3213 N95-33333 #
CONF-950512-90 ..... p 3213 N95-33377 #
CONF-950512-91 ..... p 3213 N95-33376 #
CONF-950512-94 ..... p 3214 N95-34023 #
CONF-950512-95 ..... p 3214 N95-34024 #
CONF-950512-96 ..... p 3213 N95-33385 #
CONF-9505121-2 ..... p 3079 N95-33063 #
CONF-9505121-3 ..... p 3186 N95-33838 #
CONF-9505157-2 ..... p 3229 N95-33401 #
CONF-9505186-1 ..... p 3229 N95-33386 #
CONF-9505192-2 ..... p 3230 N95-34215 #
CONF-9505201-2 ..... p 3116 N95-33206 #
CONF-9505203-1 ..... p 3089 N95-32585 #
CONF-9505216-1 ..... p 3231 N95-34486 #
CONF-9505219-1 ..... p 3231 N95-34465 #
CONF-950537-5 ..... p 3126 N95-33068
CONF-950540-10 ..... p 3118 N95-33378 #
CONF-950540-8 ..... p 3101 N95-32596 #
CONF-950540-9 ..... p 3227 N95-32600 #
CONF-950563-1 ..... p 3202 N95-32484 #
CONF-950587-ABSTS ..... p 3150 N95-33225 #
CONF-9506144-3 ..... p 3080 N95-33653 #
CONF-9506144-4 ..... p 3182 N95-33652 #
CONF-9506144-6 ..... p 3231 N95-34450 #
CONF-9506169-1 ..... p 3177 N95-32955 #
CONF-9506179-1 ..... p 3216 N95-33506 #
CONF-9506181-1 ..... p 3064 N95-33704 #
CONF-9506188-1 ..... p 3099 N95-33387 #
CONF-950634-1 ..... p 3111 N95-33698 #
CONF-950637-2 ..... p 3230 N95-34213 #
CONF-950646-16 ..... p 3152 N95-32668 #
CONF-950646-8 ..... p 3153 N95-32809 #
CONF-950650-1 ..... p 3124 N95-33836 #
CONF-950706-11 ..... p 3208 N95-33374 #
CONF-950706-12 ..... p 3228 N95-33373 #
CONF-950706-13 ..... p 3208 N95-33372 #
CONF-950706-14 ..... p 3207 N95-33371 #
CONF-950706-15 ..... p 3207 N95-33370 #
CONF-950706-17 ..... p 3207 N95-33241 #
CONF-950706-1 ..... p 3203 N95-32583 #
CONF-950706-4 ..... p 3209 N95-34355 #
CONF-950706-5 ..... p 3206 N95-32966 #
CONF-9507100-2 ..... p 3125 N95-32385 #
CONF-9507121-1 ..... p 3203 N95-32574 #
CONF-9507126-1 ..... p 3209 N95-33855 #
CONF-9507128-1 ..... p 3126 N95-33222 #
CONF-950729-1 ..... p 3211 N95-32647 #
CONF-950729-2 ..... p 3149 N95-32645 #
CONF-950729-3 ..... p 3081 N95-34482 #
CONF-950740-11 ..... p 3178 N95-32378 #
CONF-950740-21 ..... p 3197 N95-32391 #
CONF-950740-25 ..... p 3125 N95-32392 #
CONF-950740-36 ..... p 3197 N95-33220 #
CONF-950740-5 ..... p 3125 N95-32373 #
CONF-950740-9 ..... p 3121 N95-32376 #
CONF-950777-3 ..... p 3203 N95-32576 #
CONF-950778-1 ..... p 3187 N95-32375 #
CONF-950788-1 ..... p 3184 N95-32374 #
CONF-950788-3 ..... p 3125 N95-32381 #
CONF-950788-5 ..... p 3082 N95-32380 #
CONF-950788-6 ..... p 3077 N95-32382 #
CONF-950788-7 ..... p 3184 N95-32383 #
CONF-950789-1 ..... p 3187 N95-32386 #
CONF-950804-2 ..... p 3126 N95-32684 #
CONF-9508109-1 ..... p 3191 N95-33214 #
CONF-9508112-1 ..... p 3186 N95-33403 #
CONF-9508118-1 ..... p 3185 N95-32967
CONF-9508127-1 ..... p 3087 N95-34798 #
CONF-950820-1 ..... p 3232 N95-34799 #
CONF-950828-1 ..... p 3106 N95-32387 #
CONF-950828-5 ..... p 3118 N95-32683 #
CONF-950828-9 ..... p 3111 N95-33837
CONF-950833-1 ..... p 3058 N95-32713 #
CONF-950834-1 ..... p 3187 N95-32533 #
CONF-950863-1 ..... p 3179 N95-32669 #
CONF-950865-2 ..... p 3074 N95-33629 #
CONF-950869-1 ..... p 3181 N95-33154 #
CONF-950878-1 ..... p 3126 N95-32670 #
CONF-950889-1 ..... p 3179 N95-32715 #
CONF-950890-1 ..... p 3102 N95-32714 #
CONF-950891-1 ..... p 3180 N95-32716 #
CONF-950892-1 ..... p 3225 N95-32532 #
CONF-950892-5 ..... p 3085 N95-33635

CRAD-9310-TR-0128 ..... p 3200 N95-33831 * #

CRHC-95-03 ..... p 3182 N95-34455 #
CRHC-95-10 ..... p 3178 N95-34453 #

CRIE-T-93073 ..... p 3148 N95-32402 #

CSD-95-98140 ..... p 3106 N95-32787 #

CU-CSSC-92-05 ..... p 3180 N95-32765 * #
CU-CSSC-92-11 ..... p 3180 N95-32766 * #

DE95-000297 ..... p 3102 N95-32808 #
DE95-002606 ..... p 3106 N95-32387 #
DE95-004011 ..... p 3191 N95-33060 #
DE95-004054 ..... p 3150 N95-33225 #
DE95-004057 ..... p 3153 N95-32809 #
DE95-004059 ..... p 3152 N95-32668 #
DE95-004061 ..... p 3033 N95-32548 #
DE95-004062 ..... p 3148 N95-32551 #
DE95-004093 ..... p 3149 N95-33153 #
DE95-005826 ..... p 3228 N95-32810 #
DE95-005886 ..... p 3125 N95-32373 #
DE95-006169 ..... p 3179 N95-32669 #
DE95-006281 ..... p 3126 N95-32670 #
DE95-006307 ..... p 3184 N95-32374 #
DE95-006314 ..... p 3118 N95-32683 #
DE95-006339 ..... p 3181 N95-33154 #
DE95-006344 ..... p 3187 N95-32375 #
DE95-006346 ..... p 3121 N95-32376 #
DE95-006626 ..... p 3225 N95-32377 #
DE95-006815 ..... p 3178 N95-32378 #
DE95-007099 ..... p 3234 N95-33202 #
DE95-007138 ..... p 3152 N95-32553 #
DE95-007146 ..... p 3229 N95-33636 #
DE95-007207 ..... p 3201 N95-32379 #
DE95-007731 ..... p 3082 N95-32380 #
DE95-007733 ..... p 3125 N95-32381 #
DE95-007734 ..... p 3077 N95-32382 #
DE95-007735 ..... p 3184 N95-32383 #
DE95-007747 ..... p 3120 N95-34811
DE95-007806 ..... p 3185 N95-32582 #
DE95-007818 ..... p 3082 N95-32384 #
DE95-007838 ..... p 3203 N95-32583 #
DE95-007850 ..... p 3204 N95-32584 #
DE95-007855 ..... p 3125 N95-32385 #
DE95-007857 ..... p 3089 N95-32585 #
DE95-007874 ..... p 3187 N95-32386 #
DE95-007890 ..... p 3149 N95-32811 #
DE95-007969 ..... p 3153 N95-32816 #
DE95-008099 ..... p 3194 N95-32388 #
DE95-008173 ..... p 3194 N95-32389 #
DE95-008282 ..... p 3225 N95-32586 #
DE95-008288 ..... p 3226 N95-32598 #
DE95-008799 ..... p 3106 N95-32587 #
DE95-008828 ..... p 3246 N95-32597 #
DE95-008861 ..... p 3207 N95-33203 #
DE95-008865 ..... p 3213 N95-33204 #
DE95-008872 ..... p 3221 N95-32588 #
DE95-008935 ..... p 3151 N95-32475 #
DE95-008940 ..... p 3077 N95-32555 #
DE95-008973 ..... p 3218 N95-34480 #
DE95-008975 ..... p 3103 N95-33697 #
DE95-008979 ..... p 3153 N95-33205 #
DE95-009083 ..... p 3152 N95-32556 #
DE95-009175 ..... p 3126 N95-32684 #
DE95-009204 ..... p 3149 N95-32685 #
DE95-009209 ..... p 3149 N95-32817 #
DE95-009225 ..... p 3152 N95-32686 #
DE95-009416 ..... p 3058 N95-32713 #
DE95-009420 ..... p 3102 N95-32714 #
DE95-009425 ..... p 3179 N95-32715 #
DE95-009479 ..... p 3179 N95-32390 #
DE95-009481 ..... p 3111 N95-33698 #
DE95-009482 ..... p 3180 N95-32716 #
DE95-009483 ..... p 3197 N95-32391 #
DE95-009485 ..... p 3177 N95-32955 #
DE95-009500 ..... p 3225 N95-32532 #
DE95-009523 ..... p 3185 N95-32771 #
DE95-009545 ..... p 3125 N95-32392 #
DE95-009574 ..... p 3156 N95-32697 #
DE95-009588 ..... p 3226 N95-32589 #
DE95-009589 ..... p 3226 N95-32590 #
DE95-009595 ..... p 3078 N95-32591 #
DE95-009603 ..... p 3222 N95-32656 #
DE95-009605 ..... p 3222 N95-32592 #
DE95-009606 ..... p 3222 N95-32756 #
DE95-009635 ..... p 3233 N95-32661 #
DE95-009688 ..... p 3215 N95-32662 #
DE95-009700 ..... p 3116 N95-33206 #
DE95-009828 ..... p 3228 N95-33213 #
DE95-009835 ..... p 3187 N95-32533 #
DE95-009845 ..... p 3167 N95-32535 #
DE95-009846 ..... p 3221 N95-32536
DE95-009850 ..... p 3118 N95-32663 #
DE95-009867 ..... p 3191 N95-33214 #
DE95-009886 ..... p 3179 N95-32470 #
DE95-009897 ..... p 3236 N95-32471 #
DE95-009889 ..... p 3079 N95-33215 #
DE95-009908 ..... p 3102 N95-32956 #
DE95-009917 ..... p 3082 N95-32664 #
DE95-009918 ..... p 3212 N95-32665 #
DE95-009920 ..... p 3067 N95-32671 #
DE95-009925 ..... p 3223 N95-33216 #
DE95-009927 ..... p 3228 N95-33240 #
DE95-010119 ..... p 3079 N95-33217 #
DE95-010122 ..... p 3079 N95-32638 #
DE95-010123 ..... p 3227 N95-32640 #
DE95-010124 ..... p 3067 N95-32641 #
DE95-010125 ..... p 3227 N95-32643 #
DE95-010126 ..... p 3228 N95-32959
DE95-010128 ..... p 3080 N95-33699 #
DE95-010129 ..... p 3080 N95-33700
DE95-010130 ..... p 3229 N95-33637 #
DE95-010151 ..... p 3149 N95-32645 #
DE95-010152 ..... p 3211 N95-32647 #
DE95-010165 ..... p 3201 N95-32393 #
DE95-010186 ..... p 3154 N95-33638 #
DE95-010189 ..... p 3078 N95-32648 #
DE95-010199 ..... p 3084 N95-33218 #
DE95-010230 ..... p 3066 N95-32394 #
DE95-010236 ..... p 3062 N95-32395 #
DE95-010238 ..... p 3060 N95-32396 #
DE95-010239 ..... p 3198 N95-32397 #
DE95-010245 ..... p 3177 N95-32398 #
DE95-010246 ..... p 3066 N95-32540 #
DE95-010259 ..... p 3062 N95-32399 #
DE95-010266 ..... p 3207 N95-33219 #
DE95-010267 ..... p 3074 N95-33627 #
DE95-010277 ..... p 3118 N95-33246 #
DE95-010280 ..... p 3205 N95-32650 #
DE95-010281 ..... p 3077 N95-32400 #
DE95-010295 ..... p 3077 N95-32527 #
DE95-010308 ..... p 3050 N95-32636 #
DE95-010311 ..... p 3205 N95-32651 #

DE95-010316 ..... p 3205 N95-32652 #
DE95-010317 ..... p 3205 N95-32654 #
DE95-010331 ..... p 3059 N95-32593 #
DE95-010343 ..... p 3184 N95-32558 #
DE95-010357 ..... p 3062 N95-32541 #
DE95-010402 ..... p 3219 N95-32401
DE95-010410 ..... p 3195 N95-32559 #
DE95-010417 ..... p 3203 N95-32542 #
DE95-010423 ..... p 3150 N95-33400 #
DE95-010513 ..... p 3179 N95-32543 #
DE95-010524 ..... p 3068 N95-32557 #
DE95-010569 ..... p 3203 N95-32567 #
DE95-010570 ..... p 3203 N95-32544 #
DE95-010572 ..... p 3186 N95-33639 #
DE95-010575 ..... p 3103 N95-33640 #
DE95-010581 ..... p 3106 N95-32818 #
DE95-010611 ..... p 3083 N95-32819
DE95-010612 ..... p 3229 N95-33641 #
DE95-010651 ..... p 3087 N95-32563 #
DE95-010666 ..... p 3185 N95-32820
DE95-010683 ..... p 3089 N95-32568 #
DE95-010684 ..... p 3150 N95-33642 #
DE95-010692 ..... p 3122 N95-32863 #
DE95-010727 ..... p 3206 N95-32965 #
DE95-010731 ..... p 3095 N95-32569 #
DE95-010732 ..... p 3095 N95-32570 #
DE95-010736 ..... p 3186 N95-33643
DE95-010761 ..... p 3124 N95-33701 #
DE95-010795 ..... p 3117 N95-32571 #
DE95-010796 ..... p 3115 N95-32900 #
DE95-010812 ..... p 3206 N95-32966 #
DE95-010813 ..... p 3209 N95-34355 #
DE95-010816 ..... p 3207 N95-33241 #
DE95-010818 ..... p 3207 N95-33370 #
DE95-010819 ..... p 3207 N95-33371 #
DE95-010820 ..... p 3208 N95-33372 #
DE95-010821 ..... p 3228 N95-33373 #
DE95-010822 ..... p 3208 N95-33374 #
DE95-010857 ..... p 3224 N95-33696 #
DE95-010864 ..... p 3246 N95-33211 #
DE95-010865 ..... p 3191 N95-33212 #
DE95-010866 ..... p 3179 N95-32572 #
DE95-010874 ..... p 3152 N95-32573 #
DE95-010875 ..... p 3203 N95-32574 #
DE95-010878 ..... p 3148 N95-32575 #
DE95-010879 ..... p 3203 N95-32576 #
DE95-010883 ..... p 3229 N95-33401 #
DE95-010888 ..... p 3088 N95-33702 #
DE95-010896 ..... p 3153 N95-33192 #
DE95-010911 ..... p 3203 N95-32564 #
DE95-010912 ..... p 3206 N95-32763 #
DE95-010916 ..... p 3084 N95-33247 #
DE95-010920 ..... p 3119 N95-33703 #
DE95-010928 ..... p 3064 N95-33704 #
DE95-010951 ..... p 3074 N95-33705 #
DE95-010965 ..... p 3238 N95-33402 #
DE95-010985 ..... p 3186 N95-33403 #
DE95-010993 ..... p 3208 N95-33623 #
DE95-010994 ..... p 3203 N95-32577 #
DE95-011018 ..... p 3101 N95-32578 #
DE95-011021 ..... p 3225 N95-32579 #
DE95-011023 ..... p 3226 N95-32594 #
DE95-011040 ..... p 3103 N95-33404 #
DE95-011052 ..... p 3102 N95-32708 #
DE95-011053 ..... p 3067 N95-32709 #
DE95-011057 ..... p 3226 N95-32595 #
DE95-011061 ..... p 3150 N95-33706 #
DE95-011162 ..... p 3214 N95-33720
DE95-011239 ..... p 3103 N95-33884 #
DE95-011240 ..... p 3237 N95-32482 #
DE95-011241 ..... p 3085 N95-33425 #
DE95-011242 ..... p 3181 N95-33624
DE95-011248 ..... p 3211 N95-32483 #
DE95-011261 ..... p 3247 N95-33625 #
DE95-011262 ..... p 3080 N95-33626 #
DE95-011268 ..... p 3230 N95-33885 #
DE95-011271 ..... p 3185 N95-32967
DE95-011272 ..... p 3230 N95-33880 #
DE95-011273 ..... p 3151 N95-34481 #
DE95-011274 ..... p 3101 N95-32596 #
DE95-011281 ..... p 3227 N95-32800 #
DE95-011298 ..... p 3225 N95-34812 #
DE95-011332 ..... p 3196 N95-33248 #
DE95-011343 ..... p 3202 N95-32484 #
DE95-011347 ..... p 3211 N95-32485 #
DE95-011355 ..... p 3102 N95-32968 #
DE95-011421 ..... p 3062 N95-32602 #
DE95-011430 ..... p 3197 N95-33220 #
DE95-011455 ..... p 3097 N95-33061 #
DE95-011463 ..... p 3063 N95-33062 #
DE95-011469 ..... p 3075 N95-33832 #
DE95-011493 ..... p 3158 N95-33505 #
DE95-011494 ..... p 3084 N95-33405 #
DE95-011498 ..... p 3127 N95-33833 #
DE95-011500 ..... p 3213 N95-33406 #
DE95-011515 ..... p 3216 N95-34020 #
DE95-011517 ..... p 3216 N95-33506 #
DE95-011520 ..... p 3079 N95-33063 #
DE95-011523 ..... p 3143 N95-33407 #
DE95-011532 ..... p 3084 N95-33408 #
DE95-011535 ..... p 3081 N95-34482 #
DE95-011537 ..... p 3212 N95-33064 #
DE95-011543 ..... p 3075 N95-34483 #
DE95-011546 ..... p 3178 N95-34484 #
DE95-011557 ..... p 3210 N95-32411 #
DE95-011560 ..... p 3236 N95-32412 #
DE95-011562 ..... p 3210 N95-32413 #
DE95-011567 ..... p 3210 N95-32414 #
DE95-011579 ..... p 3079 N95-33065 #
DE95-011595 ..... p 3231 N95-34485 #
DE95-011606 ..... p 3231 N95-34486 #
DE95-011617 ..... p 3212 N95-32960 #
DE95-011638 ..... p 3088 N95-32605 #
DE95-011652 ..... p 3155 N95-34435 #
DE95-011655 ..... p 3224 N95-34436 #
DE95-011659 ..... p 3184 N95-32415 #
DE95-011686 ..... p 3223 N95-33066 #
DE95-011689 ..... p 3079 N95-32958 #
DE95-011703 ..... p 3212 N95-33067
DE95-011724 ..... p 3126 N95-33068
DE95-011725 ..... p 3183 N95-34813 #
DE95-011730 ..... p 3112 N95-34437 #
DE95-011731 ..... p 3230 N95-34438 #
DE95-011733 ..... p 3230 N95-33650 #
DE95-011735 ..... p 3085 N95-33400 #
DE95-011736 ..... p 3068 N95-33070 #
DE95-011738 ..... p 3216 N95-33651 #
DE95-011740 ..... p 3182 N95-33652 #
DE95-011742 ..... p 3159 N95-33410 #
DE95-011745 ..... p 3080 N95-33653 #
DE95-011746 ..... p 3216 N95-33411 #
DE95-011748 ..... p 3164 N95-33654 #
DE95-011769 ..... p 3154 N95-33655 #
DE95-011825 ..... p 3124 N95-33834 #
DE95-011872 ..... p 3223 N95-33412 #
DE95-011874 ..... p 3062 N95-33835 #
DE95-011883 ..... p 3124 N95-33836 #
DE95-011889 ..... p 3111 N95-33837
DE95-011895 ..... p 3186 N95-33838 #
DE95-011906 ..... p 3099 N95-33839 #
DE95-011951 ..... p 3154 N95-33413 #
DE95-011955 ..... p 3156 N95-33847 #
DE95-011975 ..... p 3229 N95-33366 #
DE95-011980 ..... p 3062 N95-33848 #
DE95-011984 ..... p 3211 N95-32416 #
DE95-012000 ..... p 3143 N95-33849 #
DE95-012052 ..... p 3099 N95-33387 #
DE95-012056 ..... p 3234 N95-33388 #
DE95-012072 ..... p 3231 N95-34450 #
DE95-012079 ..... p 3110 N95-33389 #
DE95-012081 ..... p 3208 N95-33850 #
DE95-012095 ..... p 3211 N95-32606 #
DE95-012096 ..... p 3212 N95-32657 #
DE95-012097 ..... p 3215 N95-32658 #
DE95-012098 ..... p 3211 N95-32607 #
DE95-012099 ..... p 3211 N95-32608 #
DE95-012100 ..... p 3095 N95-32616 #
DE95-012114 ..... p 3224 N95-33851 #
DE95-012133 ..... p 3248 N95-33390 #
DE95-012134 ..... p 3223 N95-33391
DE95-012142 ..... p 3186 N95-33852 #
DE95-012144 ..... p 3224 N95-33853 #
DE95-012154 ..... p 3083 N95-33079
DE95-012168 ..... p 3208 N95-33854 #
DE95-012170 ..... p 3204 N95-32617 #
DE95-012171 ..... p 3204 N95-32619 #
DE95-012173 ..... p 3209 N95-33855 #
DE95-012176 ..... p 3204 N95-32621 #
DE95-012190 ..... p 3074 N95-33392 #
DE95-012200 ..... p 3095 N95-33393 #
DE95-012212 ..... p 3154 N95-33394 #
DE95-012216 ..... p 3088 N95-33395 #
DE95-012224 ..... p 3118 N95-33378 #
DE95-012286 ..... p 3099 N95-33379 #
DE95-012294 ..... p 3234 N95-34211 #
DE95-012318 ..... p 3076 N95-34810 #
DE95-012319 ..... p 3075 N95-34021 #
DE95-012322 ..... p 3229 N95-33628 #
DE95-012368 ..... p 3208 N95-33380 #
DE95-012370 ..... p 3215 N95-33381 #
DE95-012371 ..... p 3103 N95-33080
DE95-012372 ..... p 3214 N95-33504 #
DE95-012409 ..... p 3223 N95-33221 #
DE95-012439 ..... p 3214 N95-34439 #
DE95-012461 ..... p 3228 N95-33382 #
DE95-012464 ..... p 3150 N95-33383 #
DE95-012485 ..... p 3075 N95-34440 #
DE95-012494 ..... p 3208 N95-33375 #
DE95-012495 ..... p 3213 N95-33376 #
DE95-012496 ..... p 3213 N95-33377 #
DE95-012496 ..... p 3207 N95-33245 #
DE95-012499 ..... p 3207 N95-33201 #
DE95-012512 ..... p 3213 N95-33333 #
DE95-012515 ..... p 3213 N95-33335 #
DE95-012521 ..... p 3085 N95-34022 #
DE95-012554 ..... p 3096 N95-33336 #
DE95-012556 ..... p 3213 N95-33338 #
DE95-012559 ..... p 3214 N95-34023 #
DE95-012560 ..... p 3214 N95-34024 #
DE95-012561 ..... p 3213 N95-33385 #
DE95-012759 ..... p 3075 N95-34268
DE95-012761 ..... p 3199 N95-34269 #
DE95-012763 ..... p 3155 N95-34441 #
DE95-012844 ..... p 3127 N95-34442 #
DE95-012850 ..... p 3074 N95-33629 #
DE95-012869 ..... p 3230 N95-34443 #
DE95-012873 ..... p 3087 N95-34798 #
DE95-012884 ..... p 3231 N95-34465 #
DE95-012885 ..... p 3232 N95-34799 #
DE95-012888 ..... p 3119 N95-34466
DE95-012889 ..... p 3113 N95-34800 #
DE95-012890 ..... p 3126 N95-33222 #
DE95-012891 ..... p 3244 N95-34801 #
DE95-012893 ..... p 3233 N95-34802 #
DE95-012895 ..... p 3085 N95-33635
DE95-012912 ..... p 3068 N95-33223 #
DE95-012948 ..... p 3209 N95-34212 #
DE95-012984 ..... p 3068 N95-33224 #
DE95-013049 ..... p 3230 N95-34213 #
DE95-013319 ..... p 3156 N95-34214 #
DE95-013411 ..... p 3230 N95-34215 #
DE95-013473 ..... p 3247 N95-34216 #
DE95-613373 ..... p 3195 N95-32523 #
DE95-613375 ..... p 3195 N95-33058 #
DE95-613711 ..... p 3206 N95-32796 #
DE95-614122 ..... p 3202 N95-32524 #
DE95-614123 ..... p 3198 N95-32525 #
DE95-614164 ..... p 3202 N95-32481 #
DE95-614170 ..... p 3221 N95-32560 #
DE95-614176 ..... p 3221 N95-32561 #
DE95-614186 ..... p 3221 N95-32562 #
DE95-614202 ..... p 3220 N95-32507 #
DE95-614203 ..... p 3220 N95-32508 #
DE95-614205 ..... p 3221 N95-32509 #
DE95-614206 ..... p 3221 N95-32510 #
DE95-614207 ..... p 3222 N95-32770 #
DE95-614255 ..... p 3223 N95-33619 #
DE95-614352 ..... p 3066 N95-32566 #
DE95-614466 ..... p 3227 N95-32698 #
DE95-617597 ..... p 3082 N95-32710 #
DE95-619190 ..... p 3204 N95-32622 #
DE95-619269 ..... p 3206 N95-32806 #
DE95-619273 ..... p 3207 N95-33171 #
DE95-619290 ..... p 3205 N95-32703 #
DE95-619323 ..... p 3204 N95-32623 #
DE95-619698 ..... p 3205 N95-32632 #
DE95-620495 ..... p 3197 N95-32624 #
DE95-620533 ..... p 3205 N95-32704 #
DE95-620538 ..... p 3203 N95-32554 #
DE95-620764 ..... p 3164 N95-32668 #
DE95-620942 ..... p 3205 N95-32625 #
DE95-620943 ..... p 3078 N95-32626 #
DE95-621870 ..... p 3188 N95-32627 #
DE95-621871 ..... p 3102 N95-32628 #
DE95-621946 ..... p 3102 N95-32629 #
DE95-623572 ..... p 3205 N95-32630 #
DE95-623573 ..... p 3187 N95-32476 #
DE95-623579 ..... p 3202 N95-32477 #
DE95-623600 ..... p 3233 N95-32478 #
DE95-623601 ..... p 3195 N95-32479 #
DE95-623602 ..... p 3225 N95-32480 #
DE95-623628 ..... p 3207 N95-33226 #
DE95-623634 ..... p 3227 N95-32631 #
DE95-623635 ..... p 3195 N95-32609 #
DE95-623676 ..... p 3234 N95-32667 #
DE95-623677 ..... p 3233 N95-32405 #
DE95-623678 ..... p 3202 N95-32406 #
DE95-623679 ..... p 3234 N95-32961 #
DE95-623696 ..... p 3202 N95-32407 #
DE95-623968 ..... p 3204 N95-32610 #
DE95-737184 ..... p 3219 N95-32408 #
DE95-737185 ..... p 3220 N95-32409 #
DE95-737207 ..... p 3220 N95-32410 #
DE95-737223 ..... p 3221 N95-32565 #
DE95-737224 ..... p 3202 N95-32529 #
DE95-737227 ..... p 3220 N95-32417 #
DE95-737266 ..... p 3077 N95-32531 #
DE95-737268 ..... p 3177 N95-32757 #
DE95-737271 ..... p 3063 N95-32711 #
DE95-737272 ..... p 3212 N95-32712 #
DE95-737277 ..... p 3202 N95-32404 #
DE95-769745 ..... p 3148 N95-32402 #
DE95-769801 ..... p 3148 N95-32403 #
DE95-769804 ..... p 3148 N95-32546 #
DE95-769808 ..... p 3151 N95-32547 #

DLR-FB-94-32 ..... p 3108 N95-32787 #

DOE/CE-15613/T4 ..... p 3063 N95-33062 #
DOE/CE-23810/51A ..... p 3233 N95-32661 #
DOE/CE-40905/57 ..... p 3074 N95-33705 #

DOE/EIA-0173(94) ..... p 3237 N95-32482 #

DOE/ER-0648 ..... p 3211 N95-32483 #
DOE/ER-12149/T1 ..... p 3102 N95-32988 #
DOE/ER-13491/741 ..... p 3206 N95-32763 #
DOE/ER-13491/742 ..... p 3203 N95-32564 #
DOE/ER-13491/765 ..... p 3208 N95-33374 #
DOE/ER-13491/766 ..... p 3228 N95-33373 #
DOE/ER-13491/768 ..... p 3208 N95-33372 #
DOE/ER-13491/769 ..... p 3207 N95-33371 #
DOE/ER-13491/770 ..... p 3207 N95-33370 #
DOE/ER-13491/772 ..... p 3206 N95-32966 #
DOE/ER-13491/773 ..... p 3209 N95-34355 #
DOE/ER-13491/776 ..... p 3207 N95-33241 #
DOE/ER-13916/T3 ..... p 3068 N95-33223 #
DOE/ER-13964/T1 ..... p 3097 N95-33061 #
DOE/ER-40162/T8 ..... p 3206 N95-32965 #
DOE/ER-40561/176 ..... p 3209 N95-33855 #
DOE/ER-40561/188 ..... p 3208 N95-33854 #
DOE/ER-40561/190 ..... p 3204 N95-32617 #
DOE/ER-40561/191 ..... p 3204 N95-32619 #
DOE/ER-40561/195 ..... p 3204 N95-32621 #
DOE/ER-40757/059 ..... p 3234 N95-33202 #
DOE/ER-40842/T1 ..... p 3201 N95-32393 #
DOE/ER-45278/T2 ..... p 3231 N95-34485 #
DOE/ER-45372-8 ..... p 3075 N95-34483 #
DOE/ER-45399/T1 ..... p 3215 N95-32662 #
DOE/ER-45424/2 ..... p 3079 N95-33065 #
DOE/ER-45488/4 ..... p 3083 N95-32819
DOE/ER-45488/5 ..... p 3229 N95-33641 #
DOE/ER-45531/1 ..... p 3074 N95-33392 #
DOE/ER-51124/20 ..... p 3225 N95-34812 #
DOE/ER-53198/259 ..... p 3223 N95-33221 #
DOE/ER-53266/50 ..... p 3186 N95-33852 #
DOE/ER-54176/T1 ..... p 3223 N95-33216 #
DOE/ER-54241/138 ..... p 3224 N95-33853 #
DOE/ER-61058/3 ..... p 3099 N95-33839 #

DOE/ET-53088/669 ..... p 3248 N95-33390 #
DOE/ET-53088/695 ..... p 3224 N95-33696 #
DOE/ET-53088/703 ..... p 3223 N95-33391
DOE/ET-53088/706 ..... p 3247 N95-34216 #

DOE/GO-10095-086 ..... p 3150 N95-33383 #

DOE/ID-12903/2 ..... p 3083 N95-33079
DOE/ID-13230/T1 ..... p 3095 N95-33393 #

DOE/MC-26029-95-C0461 ..... p 3076 N95-34810 #
DOE/MC-27115/95/C0478 ..... p 3068 N95-33224 #
DOE/MC-29108/95/C0417 ..... p 3153 N95-32816 #
DOE/MC-29228/95/C0462 ..... p 3075 N95-34021 #
DOE/MC-29257/95/C0452 ..... p 3050 N95-32636 #

DOE/PC-89761/T13 ..... p 3066 N95-32557 #
DOE/PC-92114/T6 ..... p 3087 N95-32563 #

DOE/SF-17905/T8 ..... p 3149 N95-32811 #

DOT-VNTSC-FAA-95-9 ..... p 3047 N95-34797 #

DOT/FAA/AAR-95/1 ..... p 3047 N95-34562 #

DOT/FAA/CT-94/89 ..... p 3049 N95-34583 #

DOT/FAA/RD-95/2 ..... p 3047 N95-34797 #

DRES-SR-622 ..... p 3076 N95-34611 #

DSTO-GD-0036 ..... p 3115 N95-32927
DSTO-GD-0051 ..... p 3188 N95-32995

DSTO-RR-0021 ..... p 3078 N95-32926

DSTO-TR-0139 ..... p 3054 N95-33250

E-9247 ..... p 3061 N95-33926 * #
E-9529 ..... p 3104 N95-33915 * #
E-9688 ..... p 3125 N95-33209 * #
E-9720 ..... p 3083 N95-32919 * #
E-9721 ..... p 3083 N95-32918 * #
E-9742 ..... p 3061 N95-33156 * #
E-9747 ..... p 3200 N95-32836 * #
E-9781 ..... p 3115 N95-32687 * #
E-9789 ..... p 3050 N95-32916 * #
E-9793 ..... p 3123 N95-33179 * #
E-9795 ..... p 3063 N95-33210 * #
E-9797 ..... p 3124 N95-33908 * #
E-9800 ..... p 3089 N95-32718 * #
E-9807 ..... p 3054 N95-33208 * #
E-9818 ..... p 3060 N95-32917 * #
E-9820 ..... p 3060 N95-32673 * #
E-9823 ..... p 3103 N95-33874 * #
E-9825 ..... p 3108 N95-32930 * #
E-9826 ..... p 3034 N95-32769 * #
E-9829 ..... p 3061 N95-34625 * #
E-9834 ..... p 3050 N95-32931 * #
E-9838 ..... p 3088 N95-33876 * #

ECE/GWOL/68 ..... p 3218 N95-34498 #

ECU-8200-270 ..... p 3181 N95-33396 * #

ERP-1155 ..... p 3057 N95-32772 #

ESA-WPP-083-VOL-1 ..... p 3096 N95-32747
ESA-WPP-083-VOL-2 ..... p 3096 N95-32748
ESA-WPP-083-VOL-3 ..... p 3096 N95-32749
ESA-WPP-083-VOL-4 ..... p 3096 N95-32750
ESA-WPP-083-VOL-5 ..... p 3096 N95-32751

ESC-TR-94-109 ..... p 3098 N95-33152 #
ESC-TR-94-111 ..... p 3100 N95-34474 #
ESC-TR-95-001 ..... p 3096 N95-32773 #

FFI/RAPPORT-94/03544 ..... p 3185 N95-32815 #

FNAL-TM-1926 ..... p 3082 N95-32541 #

FNAL/C-94/383 ..... p 3201 N95-32379 #
FNAL/C-95/056 ..... p 3186 N95-33639 #
FNAL/C-95/062-E ..... p 3213 N95-33406 #

FOA-R-94-00059-3.6-SE ..... p 3215 N95-33239 #
FOA-R-94-00077-5.2-SE ..... p 3167 N95-33237 #
FOA-R-95-00078-3.2-SE ..... p 3095 N95-32613

FRCR-454 ..... p 3186 N95-33852 #
FRCR-456 ..... p 3224 N95-33853 #

F0A-R-94-00003-3.5-SE ..... p 3098 N95-33231
F0A-R-94-00052-2.5-SE-PT-3 ..... p 3078 N95-32614
F0A-R-94-00067-3.5-SE ..... p 3098 N95-33230 #

GA-A-21757 ..... p 3222 N95-32756 #
GA-A-21814 ..... p 3222 N95-32592 #
GA-A-21957 ..... p 3222 N95-32656 #

GA-A21966 ..... p 3224 N95-34436 #

GAO/AIMD-94-28 ..... p 3157 N95-32760 #
GAO/AIMD-95-27 ..... p 3046 N95-32705 #

GAO/NSIAD-94-194 ..... p 3197 N95-32886 #
GAO/NSIAD-94-217 ..... p 3033 N95-32782 #
GAO/NSIAD-94-81 ..... p 3198 N95-33263 #
GAO/NSIAD-94-86 ..... p 3197 N95-32807 #
GAO/NSIAD-95-112 ..... p 3049 N95-34422 #
GAO/NSIAD-95-151 ..... p 3197 N95-32758 #
GAO/NSIAD-95-163 ..... p 3058 N95-32884 #
GAO/NSIAD-95-175 ..... p 3142 N95-32707 #
GAO/NSIAD-95-60 ..... p 3235 N95-32706 #
GAO/NSIAD-95-9 ..... p 3033 N95-32783 #

GAO/OP-94-1 ..... p 3236 N95-32887 #

GAO/PEMD-94-3 ..... p 3236 N95-33907 #

GAO/RCED-94-118FS ..... p 3055 N95-32759 #
GAO/RCED-94-142 ..... p 3046 N95-32885 #
GAO/RCED-94-15 ..... p 3046 N95-32784 #
GAO/RCED-94-209 ..... p 3056 N95-32888 #
GAO/RCED-94-226 ..... p 3055 N95-32786 #
GAO/RCED-94-23 ..... p 3089 N95-32785 #

H-1892 ..... p 3181 N95-33193 * #
H-2020 ..... p 3050 N95-33009 * #

IC-94/221 ..... p 3202 N95-32524 #
IC-94/243 ..... p 3198 N95-32525 #
IC-94/266 ..... p 3195 N95-32523 #
IC-94/279 ..... p 3195 N95-33058 #

ICASE-95-48 ..... p 3196 N95-33727 * #
ICASE-95-50 ..... p 3180 N95-32834 * #
ICASE-95-53 ..... p 3196 N95-33500 * #

IFSR-669 ..... p 3248 N95-33390 #
IFSR-695 ..... p 3224 N95-33696 #
IFSR-703 ..... p 3223 N95-33391
IFSR-706 ..... p 3247 N95-34216 #

IFTR-9/1995 ..... p 3206 N95-32921 #

IFVE-OEF-94-6 ..... p 3207 N95-33171 #

IHEP-OEF-93-97 ..... p 3205 N95-32703 #
IHEP-94-10 ..... p 3205 N95-32704 #
IHEP-94-15 ..... p 3206 N95-32806 #
IHEP-94-3 ..... p 3203 N95-32564 #

IM-3058 ..... p 3068 N95-33229 #

INEL-95/0002 ..... p 3221 N95-32588 #

INPE-5573-PRP/182 ..... p 3224 N95-33873 #

INS-T-529 ..... p 3177 N95-32757 #

INS-1055 ..... p 3202 N95-32404 #

IS-M-811 ..... p 3066 N95-32394 #
IS-M-813 ..... p 3060 N95-32396 #
IS-M-815 ..... p 3062 N95-32395 #
IS-M-816 ..... p 3196 N95-32397 #

IS-T-1598 ..... p 3066 N95-32540 #
IS-T-1633 ..... p 3078 N95-32648 #
IS-T-1695 ..... p 3227 N95-32643 #
IS-T-1697 ..... p 3080 N95-33700
IS-T-1702 ..... p 3228 N95-32959
IS-T-1714 ..... p 3229 N95-33637 #
IS-T-1721 ..... p 3067 N95-32641 #
IS-T-1725 ..... p 3078 N95-32638 #
IS-T-1727 ..... p 3227 N95-32640 #
IS-T-1732 ..... p 3080 N95-33699 #

IS-5109 ..... p 3177 N95-32398 #

ISBN-0-315-84906-1 ..... p 3078 N95-32935
ISBN-0-315-84910-X ..... p 3057 N95-33030
ISBN-0-315-86323-4 ..... p 3191 N95-33307
ISBN-0-315-86393-5 ..... p 3238 N95-33334
ISBN-0-315-86546-6 ..... p 3085 N95-33710
ISBN-0-85272-240-0 ..... p 3155 N95-32601 #
ISBN-0-85272-241-9 ..... p 3156 N95-32603 #
ISBN-1-884099-03-3 ..... p 3171 N95-34764 * #
ISBN-90-9007-495-3 ..... p 3228 N95-33235 #
ISBN-91-7848-475-8 ..... p 3083 N95-32962 #
ISBN-91-88370-70-4 ..... p 3088 N95-33332 #
ISBN-91-88714-05-5 ..... p 3163 N95-33236 #
ISBN-92-836-0009-6 ..... p 3042 N95-32486 #
ISBN-92-836-0016-9 ..... p 3168 N95-34050 #
ISBN-92-836-1016-4 ..... p 3091 N95-33126 #
ISBN-92-836-1019-9 ..... p 3237 N95-33198 #
ISBN-951-22-2228-0 ..... p 3155 N95-32455 #
ISBN-951-22-2237-X ..... p 3084 N95-33228 #
ISBN-951-22-2262-0 ..... p 3084 N95-33227 #
ISBN-951-22-2343-0 ..... p 3068 N95-33242 #

IVL-B-1160 ..... p 3067 N95-32615

IYAF-93-64 ..... p 3202 N95-32481 #
IYAF-93-96 ..... p 3221 N95-32560 #
IYAF-94-1 ..... p 3221 N95-32561 #

IYF-93-98 ..... p 3220 N95-32507 #
IYF-94-48 ..... p 3220 N95-32508 #
IYF-94-50 ..... p 3221 N95-32509 #
IYF-94-51 ..... p 3221 N95-32510 #
IYF-94-66 ..... p 3222 N95-32770 #

JAERI-RESEARCH-94-001 ..... p 3220 N95-32417 #
JAERI-RESEARCH-94-013 ..... p 3220 N95-32410 #
JAERI-RESEARCH-94-015 ..... p 3077 N95-32531 #
JAERI-RESEARCH-94-016 ..... p 3063 N95-32711 #
JAERI-RESEARCH-94-018 ..... p 3212 N95-32712 #

JAERI-TECH-94-003 ..... p 3221 N95-32565 #
JAERI-TECH-94-009 ..... p 3219 N95-32408 #
JAERI-TECH-94-011 ..... p 3220 N95-32409 #
JAERI-TECH-94-013 ..... p 3202 N95-32529 #

JINR-D-1-94-278 ..... p 3206 N95-32796 #
JINR-D-2-94-331 ..... p 3207 N95-33226 #

JINR-E-10-94-328 ..... p 3188 N95-32627 #
JINR-E-13-94-351 ..... p 3102 N95-32628 #
JINR-E-14-94-334 ..... p 3204 N95-32610 #
JINR-E-14-94-365 ..... p 3205 N95-32625 #
JINR-E-2-94-306 ..... p 3227 N95-32631 #
JINR-E-2-94-323 ..... p 3233 N95-32478 #
JINR-E-2-94-332 ..... p 3234 N95-32667 #
JINR-E-2-94-337 ..... p 3205 N95-32630 #
JINR-E-2-94-339 ..... p 3233 N95-32405 #
JINR-E-2-94-344 ..... p 3202 N95-32406 #
JINR-E-2-94-348 ..... p 3234 N95-32961 #
JINR-E-2-94-352 ..... p 3202 N95-32477 #
JINR-E-2-94-356 ..... p 3195 N95-32609 #
JINR-E-6-94-357 ..... p 3164 N95-32666 #

JINR-R-10-94-353 ..... p 3187 N95-32476 #
JINR-R-14-94-333 ..... p 3078 N95-32626 #

SC-MAG-457 ..... p 3214 N95-33504 #
SC-MAG-458 ..... p 3103 N95-33080
SC-MAG-462 ..... p 3215 N95-33381 #

SER-PK-001 ..... p 3033 N95-32764 * #

SGD-607-PT-1 ..... p 3248 N95-32963
SGD-607-PT-2 ..... p 3248 N95-32964 #

SIP-0066 ..... p 3221 N95-32562 #

SLAC-PUB-95-6821 ..... p 3207 N95-33245 #
SLAC-PUB-95-6822 ..... p 3207 N95-33201 #

SMC-TR-95-12 ..... p 3157 N95-34613 #

K-SS-12.12-REV-A ..... p 3245 N95-33489 * #

KAERI/RR-1329/94 ..... p 3066 N95-32566 #
KAERI/RR-1363/93 ..... p 3223 N95-33619 #

KAPL-4790 ..... p 3234 N95-34211 #

KCP-613-5537 ..... p 3103 N95-33864 #
KCP-613-5556 ..... p 3154 N95-33638 #

KEMI-10-94 ..... p 3073 N95-33328 #
KEMI-12-94 ..... p 3084 N95-33329 #
KEMI-3-93 ..... p 3074 N95-33634 #
KEMI-9-94 ..... p 3073 N95-33330 #

KFB-1994:11 ..... p 3088 N95-33332 #

L-17416 ..... p 3034 N95-32821 * #

LA-SUB-94-172 ..... p 3088 N95-32605 #
LA-SUB-95-22 ..... p 3212 N95-32960 #

LA-UR-95-1016 ..... p 3058 N95-32713 #
LA-UR-95-1027 ..... p 3225 N95-32532 #
LA-UR-95-1117 ..... p 3197 N95-32391 #
LA-UR-95-1130 ..... p 3177 N95-32955 #
LA-UR-95-1145 ..... p 3111 N95-33698 #
LA-UR-95-1155 ..... p 3180 N95-32716 #
LA-UR-95-1164 ..... p 3088 N95-33702 #
LA-UR-95-1168 ..... p 3064 N95-33704 #
LA-UR-95-1181 ..... p 3229 N95-33401 #
LA-UR-95-1196 ..... p 3179 N95-32572 #
LA-UR-95-1224 ..... p 3191 N95-33212 #
LA-UR-95-1263 ..... p 3246 N95-33211 #
LA-UR-95-1287 ..... p 3152 N95-32573 #
LA-UR-95-1288 ..... p 3203 N95-32574 #
LA-UR-95-1303 ..... p 3148 N95-32575 #
LA-UR-95-1312 ..... p 3203 N95-32576 #
LA-UR-95-1319 ..... p 3231 N95-34450 #
LA-UR-95-1375 ..... p 3234 N95-33388 #
LA-UR-95-1411 ..... p 3099 N95-33387 #
LA-UR-95-1417 ..... p 3143 N95-33849 #
LA-UR-95-1436 ..... p 3203 N95-32577 #
LA-UR-95-1437 ..... p 3208 N95-33623 #
LA-UR-95-1462 ..... p 3186 N95-33403 #
LA-UR-95-1524 ..... p 3211 N95-32416 #
LA-UR-95-1543 ..... p 3062 N95-33848 #
LA-UR-95-1555 ..... p 3229 N95-33386 #
LA-UR-95-21 ..... p 3181 N95-33154 #
LA-UR-95-320 ..... p 3126 N95-32670 #
LA-UR-95-38 ..... p 3187 N95-32375 #
LA-UR-95-423 ..... p 3187 N95-32386 #
LA-UR-95-433 ..... p 3179 N95-32669 #
LA-UR-95-47 ..... p 3121 N95-32376 #
LA-UR-95-619 ..... p 3125 N95-32385 #
LA-UR-95-626 ..... p 3089 N95-32585 #
LA-UR-95-728 ..... p 3204 N95-32584 #
LA-UR-95-790 ..... p 3203 N95-32583 #
LA-UR-95-910 ..... p 3179 N95-32715 #
LA-UR-95-987 ..... p 3102 N95-32714 #

LA-12930-C ..... p 3185 N95-32771 #

LBL-35421 ..... p 3214 N95-33504 #
LBL-35422 ..... p 3103 N95-33080
LBL-35426 ..... p 3215 N95-33381 #
LBL-36547 ..... p 3080 N95-33626 #
LBL-36585 ..... p 3101 N95-32596 #
LBL-36586 ..... p 3227 N95-32600 #
LBL-36619 ..... p 3247 N95-33625 #
LBL-36696 ..... p 3230 N95-33865 #
LBL-36750 ..... p 3185 N95-32967
LBL-36813 ..... p 3151 N95-34481 #
LBL-36842 ..... p 3214 N95-34439 #
LBL-36845 ..... p 3230 N95-33880 #
LBL-36908 ..... p 3208 N95-33380 #
LBL-36909 ..... p 3229 N95-33628 #
LBL-37027 ..... p 3075 N95-34268
LBL-37050 ..... p 3199 N95-34269 #

LC-79-640375 ..... p 3248 N95-32963

LC-79-640375 ..... p 3248 N95-32964 #

M-788 ..... p 3123 N95-33199 * #

MCAT-95-12 ..... p 3106 N95-32454 * #

MEMO-INF-94-75 ..... p 3237 N95-33238 #
MEMO-INF-95-06 ..... p 3097 N95-32892

MLM-3810 ..... p 3196 N95-33248 #

NAIC-ID (RS) T-0404-94 ..... p 3215 N95-32660 #

NAIC-ID(RS)T-0092-93 ..... p 3158 N95-34491 #
NAIC-ID(RS)T-0094-93 ..... p 3158 N95-34757 #
NAIC-ID(RS)T-0372-94 ..... p 3217 N95-34307 #
NAIC-ID(RS)T-0388-94 ..... p 3219 N95-34756 #
NAIC-ID(RS)T-0392-94 ..... p 3217 N95-34459 #
NAIC-ID(RS)T-0398-94 ..... p 3217 N95-34309 #
NAIC-ID(RS)T-0402-94 ..... p 3105 N95-34488 #
NAIC-ID(RS)T-0405-94 ..... p 3105 N95-34758 #
NAIC-ID(RS)T-0407-94 ..... p 3215 N95-32957 #
NAIC-ID(RS)T-0412-94 ..... p 3215 N95-32701 #
NAIC-ID(RS)T-0415-94 ..... p 3104 N95-34379 #
NAIC-ID(RS)T-0416-94 ..... p 3100 N95-34760 #
NAIC-ID(RS)T-0443-93 ..... p 3157 N95-34299 #
NAIC-ID(RS)T-0444-93 ..... p 3120 N95-34470 #
NAIC-ID(RS)T-0497-94 ..... p 3118 N95-32702 #
NAIC-ID(RS)T-0499-94 ..... p 3117 N95-32472 #
NAIC-ID(RS)T-0500-94 ..... p 3100 N95-34762 #
NAIC-ID(RS)T-0558-93 ..... p 3059 N95-34500 #
NAIC-ID(RS)T-0562-93 ..... p 3059 N95-34493 #
NAIC-ID(RS)T-0563-93 ..... p 3151 N95-34468 #
NAIC-ID(RS)T-0641-93 ..... p 3217 N95-34298 #
NAIC-ID(RS)T-0646-93 ..... p 3219 N95-34759 #
NAIC-ID(RS)T-0648-93 ..... p 3217 N95-34297 #
NAIC-ID(RS)T-0650-93 ..... p 3120 N95-34469 #
NAIC-ID(RS)T-0652-93 ..... p 3119 N95-34380 #
NAIC-ID(RS)T-0742-94 ..... p 3218 N95-34490 #
NAIC-ID(RS)T-0753-94 ..... p 3217 N95-34303 #
NAIC-ID(RS)T-0758-94 ..... p 3086 N95-34563 #
NAIC-ID(RS)T-0760-94 ..... p 3119 N95-34308 #
NAIC-ID(RS)T-0761-94 ..... p 3218 N95-34471 #
NAIC-ID(RS)T-0819-94 ..... p 3061 N95-34302 #
NAIC-ID(RS)T-0836-94 ..... p 3217 N95-34305 #

NAL-SP-27 ..... p 3034 N95-34505 #

NAL-TR-1253 ..... p 3060 N95-32755 #

NAS 1.15:104278 ..... p 3050 N95-33009 * #
NAS 1.15:104566-VOL-15 ..... p 3158 N95-32545 * #
NAS 1.15:104566-VOL-22 ..... p 3159 N95-32672 * #
NAS 1.15:104566-VOL-31 ..... p 3159 N95-32833 * #
NAS 1.15:104620 ..... p 3237 N95-32922 * #
NAS 1.15:106950 ..... p 3125 N95-33209 * #
NAS 1.15:106964 ..... p 3083 N95-32919 * #
NAS 1.15:106965 ..... p 3083 N95-32918 * #
NAS 1.15:107006 ..... p 3050 N95-32916 * #
NAS 1.15:107009 ..... p 3123 N95-33179 * #
NAS 1.15:107011 ..... p 3063 N95-33210 * #
NAS 1.15:107012 ..... p 3124 N95-33908 * #
NAS 1.15:107015 ..... p 3089 N95-32718 * #
NAS 1.15:107018 ..... p 3060 N95-32917 * #
NAS 1.15:107020 ..... p 3108 N95-32930 * #
NAS 1.15:107023 ..... p 3034 N95-32769 * #
NAS 1.15:107024 ..... p 3050 N95-32931 * #
NAS 1.15:107025 ..... p 3088 N95-33876 * #
NAS 1.15:108470 ..... p 3252 N95-33042 * #
NAS 1.15:109785 ..... p 3110 N95-33496 * #
NAS 1.15:110180 ..... p 3239 N95-34217 * #
NAS 1.15:110356 ..... p 3048 N95-32699 * #
NAS 1.15:110358 ..... p 3198 N95-33875 * #
NAS 1.15:110624 ..... p 3245 N95-33489 * #
NAS 1.15:110655 ..... p 3161 N95-32719 * #
NAS 1.15:110668 ..... p 3033 N95-32764 * #
NAS 1.15:110673 ..... p 3033 N95-32682 * #
NAS 1.15:110815 ..... p 3244 N95-33069 * #
NAS 1.15:110816 ..... p 3245 N95-33081 * #
NAS 1.15:110817 ..... p 3245 N95-33082 * #
NAS 1.15:110819 ..... p 3253 N95-33384 *
NAS 1.15:110820 ..... p 3057 N95-32539 *
NAS 1.15:110834 ..... p 3237 N95-32883 * #
NAS 1.15:4660 ..... p 3034 N95-32821 * #
NAS 1.18:1410.13O ..... p 3238 N95-33249 * #
NAS 1.21:6101(09) ..... p 3236 N95-34354 * #
NAS 1.26:188410 ..... p 3248 N95-32418 * #
NAS 1.26:189431 ..... p 3246 N95-33261 * #
NAS 1.26:189434 ..... p 3247 N95-33262 * #
NAS 1.26:195051 ..... p 3200 N95-33831 * #
NAS 1.26:195403 ..... p 3061 N95-33926 * #
NAS 1.26:195450 ..... p 3104 N95-33915 * #
NAS 1.26:197288 ..... p 3143 N95-32823 * #
NAS 1.26:198176 ..... p 3196 N95-33727 * #
NAS 1.26:198179 ..... p 3180 N95-32834 * #
NAS 1.26:198183 ..... p 3196 N95-33500 * #

NAS 1.26:198189 ..... p 3059 N95-33890 * #
NAS 1.26:198190 ..... p 3059 N95-33264 * #
NAS 1.26:198359 ..... p 3200 N95-32836 * #
NAS 1.26:198366 ..... p 3115 N95-32687 * #
NAS 1.26:198368 ..... p 3054 N95-33208 * #
NAS 1.26:198372 ..... p 3060 N95-32673 * #
NAS 1.26:198373 ..... p 3103 N95-33874 * #
NAS 1.26:198375 ..... p 3061 N95-34625 * #
NAS 1.26:198378 ..... p 3089 N95-32929 * #
NAS 1.26:198849 ..... p 3246 N95-32913 * #
NAS 1.26:198867 ..... p 3188 N95-32659 * #
NAS 1.26:198922 ..... p 3128 N95-33730 * #
NAS 1.26:198923 ..... p 3136 N95-33789 * #
NAS 1.26:198924 ..... p 3139 N95-33801 * #
NAS 1.26:198928 ..... p 3143 N95-32914 * #
NAS 1.26:198974 ..... p 3097 N95-32822 * #
NAS 1.26:198983 ..... p 3106 N95-32454 * #
NAS 1.26:199009 ..... p 3171 N95-34764 * #
NAS 1.26:199041 ..... p 3180 N95-32766 * #
NAS 1.26:199042 ..... p 3180 N95-32765 * #
NAS 1.26:199071 ..... p 3247 N95-32700 * #
NAS 1.26:199080 ..... p 3121 N95-32689 * #
NAS 1.26:199081 ..... p 3048 N95-32928 * #
NAS 1.26:199082 ..... p 3142 N95-32717 * #
NAS 1.26:199085 ..... p 3123 N95-32915 * #
NAS 1.26:199086 ..... p 3245 N95-32835 * #
NAS 1.26:199088 ..... p 3188 N95-32767 * #
NAS 1.26:199089 ..... p 3188 N95-32768 * #
NAS 1.26:199090 ..... p 3066 N95-32581 * #
NAS 1.26:199103 ..... p 3239 N95-34218 * #
NAS 1.26:199112 ..... p 3097 N95-33033 * #
NAS 1.26:199113 ..... p 3099 N95-33497 * #
NAS 1.26:199114 ..... p 3099 N95-33726 * #
NAS 1.26:199116 ..... p 3121 N95-32675 * #
NAS 1.26:199117 ..... p 3142 N95-32676 * #
NAS 1.26:199120 ..... p 3110 N95-33398 * #
NAS 1.26:199125 ..... p 3167 N95-32688 * #
NAS 1.26:199126 ..... p 3061 N95-32932 * #
NAS 1.26:199129 ..... p 3143 N95-33498 * #
NAS 1.26:199130 ..... p 3248 N95-33499 * #
NAS 1.26:199134 ..... p 3157 N95-32933 * #
NAS 1.26:199212 ..... p 3095 N95-32674 * #
NAS 1.26:199214 ..... p 3248 N95-33916 * #
NAS 1.26:4678 ..... p 3061 N95-33156 * #
NAS 1.26:4662 ..... p 3181 N95-33396 * #
NAS 1.55:3301 ..... p 3069 N95-33265 * #
NAS 1.55:3308 ..... p 3123 N95-33199 * #
NAS 1.60:3430 ..... p 3181 N95-33193 * #

NASA-CP-3301 ..... p 3069 N95-33265 * #
NASA-CP-3308 ..... p 3123 N95-33199 * #

NASA-CR-188410 ..... p 3248 N95-32418 * #
NASA-CR-189431 ..... p 3246 N95-33261 * #
NASA-CR-189434 ..... p 3247 N95-33262 * #
NASA-CR-195051 ..... p 3200 N95-33831 * #
NASA-CR-195403 ..... p 3061 N95-33926 * #
NASA-CR-195450 ..... p 3104 N95-33915 * #
NASA-CR-197288 ..... p 3143 N95-32823 * #
NASA-CR-198176 ..... p 3196 N95-33727 * #
NASA-CR-198179 ..... p 3180 N95-32834 * #
NASA-CR-198183 ..... p 3196 N95-33500 * #
NASA-CR-198189 ..... p 3059 N95-33890 * #
NASA-CR-198190 ..... p 3059 N95-33264 * #
NASA-CR-198359 ..... p 3200 N95-32836 * #
NASA-CR-198366 ..... p 3115 N95-32687 * #
NASA-CR-198368 ..... p 3054 N95-33208 * #
NASA-CR-198372 ..... p 3060 N95-32673 * #
NASA-CR-198373 ..... p 3103 N95-33874 * #
NASA-CR-198375 ..... p 3061 N95-34625 * #
NASA-CR-198378 ..... p 3089 N95-32929 * #
NASA-CR-198849 ..... p 3246 N95-32913 * #
NASA-CR-198867 ..... p 3188 N95-32659 * #
NASA-CR-198922 ..... p 3128 N95-33730 * #
NASA-CR-198923 ..... p 3136 N95-33789 * #
NASA-CR-198924 ..... p 3139 N95-33801 * #
NASA-CR-198928 ..... p 3143 N95-32914 * #
NASA-CR-198974 ..... p 3097 N95-32822 * #
NASA-CR-198983 ..... p 3106 N95-32454 * #
NASA-CR-199009 ..... p 3171 N95-34764 * #
NASA-CR-199041 ..... p 3180 N95-32766 * #
NASA-CR-199042 ..... p 3180 N95-32765 * #
NASA-CR-199071 ..... p 3247 N95-32700 * #
NASA-CR-199080 ..... p 3121 N95-32689 * #
NASA-CR-199081 ..... p 3048 N95-32928 * #
NASA-CR-199082 ..... p 3142 N95-32717 * #
NASA-CR-199085 ..... p 3123 N95-32915 * #
NASA-CR-199086 ..... p 3245 N95-32835 * #
NASA-CR-199088 ..... p 3188 N95-32767 * #
NASA-CR-199089 ..... p 3188 N95-32768 * #
NASA-CR-199090 ..... p 3066 N95-32581 * #
NASA-CR-199103 ..... p 3239 N95-34218 * #
NASA-CR-199112 ..... p 3097 N95-33033 * #
NASA-CR-199113 ..... p 3099 N95-33497 * #
NASA-CR-199114 ..... p 3099 N95-33726 * #
NASA-CR-199116 ..... p 3121 N95-32675 * #

NASA-CR-199117 ..... p 3142 N95-32676 * #
NASA-CR-199120 ..... p 3110 N95-33398 * #
NASA-CR-199125 ..... p 3167 N95-32688 * #
NASA-CR-199126 ..... p 3061 N95-32932 * #
NASA-CR-199129 ..... p 3143 N95-33498 * #
NASA-CR-199130 ..... p 3248 N95-33499 * #
NASA-CR-199134 ..... p 3157 N95-32933 * #
NASA-CR-199212 ..... p 3095 N95-32674 * #
NASA-CR-199214 ..... p 3248 N95-33916 * #
NASA-CR-199222 ..... p 3058 N95-33728 *
NASA-CR-4678 ..... p 3061 N95-33156 * #
NASA-CR-4682 ..... p 3181 N95-33396 * #

NASA-SP-6101(09) ..... p 3236 N95-34354 * #

NASA-TM-104278 ..... p 3050 N95-33009 * #
NASA-TM-104566-VOL-15 ..... p 3158 N95-32545 * #
NASA-TM-104566-VOL-22 ..... p 3159 N95-32672 * #
NASA-TM-104566-VOL-31 ..... p 3159 N95-32833 * #
NASA-TM-104620 ..... p 3237 N95-32922 * #
NASA-TM-106950 ..... p 3125 N95-33209 * #
NASA-TM-106964 ..... p 3083 N95-32919 * #
NASA-TM-106965 ..... p 3083 N95-32918 * #
NASA-TM-107006 ..... p 3050 N95-32916 * #
NASA-TM-107009 ..... p 3123 N95-33179 * #
NASA-TM-107011 ..... p 3063 N95-33210 * #
NASA-TM-107012 ..... p 3124 N95-33908 * #
NASA-TM-107015 ..... p 3089 N95-32718 * #
NASA-TM-107018 ..... p 3060 N95-32917 * #
NASA-TM-107020 ..... p 3108 N95-32930 * #
NASA-TM-107023 ..... p 3034 N95-32769 * #
NASA-TM-107024 ..... p 3050 N95-32931 * #
NASA-TM-107025 ..... p 3088 N95-33876 * #
NASA-TM-108470 ..... p 3252 N95-33042 * #
NASA-TM-109785 ..... p 3110 N95-33496 * #
NASA-TM-110180 ..... p 3239 N95-34217 * #
NASA-TM-110356 ..... p 3048 N95-32699 * #
NASA-TM-110358 ..... p 3198 N95-33875 * #
NASA-TM-110624 ..... p 3245 N95-33489 * #
NASA-TM-110655 ..... p 3161 N95-32719 * #
NASA-TM-110668 ..... p 3033 N95-32764 * #
NASA-TM-110673 ..... p 3033 N95-32682 * #
NASA-TM-110815 ..... p 3244 N95-33069 * #
NASA-TM-110816 ..... p 3245 N95-33081 * #
NASA-TM-110817 ..... p 3245 N95-33082 * #
NASA-TM-110819 ..... p 3253 N95-33384 *
NASA-TM-110820 ..... p 3057 N95-32539 *
NASA-TM-110834 ..... p 3237 N95-32883 * #
NASA-TM-110837 ..... p 3056 N95-33167 *
NASA-TM-110838 ..... p 3058 N95-34280 *
NASA-TM-110840 ..... p 3058 N95-34281 *
NASA-TM-4660 ..... p 3034 N95-32821 * #

NASA-TP-3430 ..... p 3181 N95-33193 * #

NAWCWPNS-TP-8199 ..... p 3105 N95-34796 #

NEDO-GET-9308 ..... p 3151 N95-32547 #

NEDO-NP-9322 ..... p 3148 N95-32403 #

NEDO-P-93-57 ..... p 3148 N95-32546 #

NHB-1410.13O ..... p 3238 N95-33249 * #

NIFS-334 ..... p 3225 N95-34624 #

NMRI-94-51 ..... p 3076 N95-34814 #

NNU-0001 ..... p 3227 N95-32698 #

NONP-NASA-VT-95-61007 ..... p 3253 N95-33384 *
NONP-NASA-VT-95-63905 ..... p 3058 N95-34280 *
NONP-NASA-VT-95-63906 ..... p 3058 N95-33728 *
NONP-NASA-VT-95-63907 ..... p 3056 N95-33167 *
NONP-NASA-VT-95-64175 ..... p 3058 N95-34281 *

NPRDC-TN-95-3 ..... p 3166 N95-34356 #

NPS-OR-95-003 ..... p 3182 N95-34349 #

NREL/SP-420-7849 ..... p 3150 N95-33225 #

NREL/TP-411-7693 ..... p 3149 N95-33153 #
NREL/TP-425-7621 ..... p 3152 N95-32686 #
NREL/TP-441-7805 ..... p 3033 N95-32548 #
NREL/TP-441-7807 ..... p 3148 N95-32551 #
NREL/TP-442-7393 ..... p 3149 N95-32685 #
NREL/TP-451-7709 ..... p 3149 N95-32817 #
NREL/TP-473-7444 ..... p 3102 N95-32808 #
NREL/TP-473-7569 ..... p 3152 N95-32668 #
NREL/TP-473-7570 ..... p 3153 N95-32809 #

NRL-CR/7181-94-0008 ..... p 3234 N95-34464 #

NRL/CR/7410-94-0028 ..... p 3219 N95-34576 #

NRL/MR/6790-95-7667 ..... p 3120 N95-34761 #
NRL/MR/7322-95-7584 ..... p 3159 N95-34341 #

NTIAC-95-01 ..... p 3125 N95-34346 #

NUWC-NL-TR-10857 ..... p 3086 N95-34502 #

ORNL/CDIAC-76 ..... p 3154 N95-33655 #

ORNL/SUB-92-SL807/1 ..... p 3085 N95-33425 #

ORNL/TM-12820 ..... p 3194 N95-32388 #
ORNL/TM-12873 ..... p 3228 N95-33240 #

PB95-207189 ..... p 3155 N95-32455 #
PB95-207841 ..... p 3155 N95-32599 #
PB95-208096 ..... p 3155 N95-32601 #
PB95-208104 ..... p 3156 N95-32603 #
PB95-208211 ..... p 3084 N95-33227 #
PB95-208237 ..... p 3084 N95-33228 #
PB95-208310 ..... p 3164 N95-32611
PB95-208492 ..... p 3068 N95-33242 #
PB95-210324 ..... p 3068 N95-33243 #
PB95-211017 ..... p 3121 N95-32612
PB95-211025 ..... p 3083 N95-32962 #
PB95-211256 ..... p 3074 N95-33634 #
PB95-211272 ..... p 3073 N95-33328 #
PB95-211280 ..... p 3084 N95-33329 #
PB95-211306 ..... p 3073 N95-33330 #
PB95-211348 ..... p 3068 N95-33229 #
PB95-211439 ..... p 3098 N95-33230 #
PB95-211447 ..... p 3098 N95-33231
PB95-212114 ..... p 3163 N95-33232 #
PB95-212163 ..... p 3196 N95-33233 #
PB95-212171 ..... p 3196 N95-33234 #
PB95-212189 ..... p 3195 N95-32889 #
PB95-212197 ..... p 3195 N95-32890 #
PB95-214284 ..... p 3157 N95-32891 #
PB95-214425 ..... p 3068 N95-32812 #
PB95-214482 ..... p 3228 N95-33235 #
PB95-214490 ..... p 3149 N95-32813
PB95-214524 ..... p 3095 N95-32613
PB95-214532 ..... p 3078 N95-32614
PB95-214557 ..... p 3163 N95-33236 #
PB95-214565 ..... p 3153 N95-33331 #
PB95-214656 ..... p 3088 N95-33332 #
PB95-214722 ..... p 3167 N95-33237 #
PB95-214854 ..... p 3067 N95-32615
PB95-215091 ..... p 3097 N95-32892
PB95-215109 ..... p 3095 N95-33244 #
PB95-215190 ..... p 3237 N95-33238 #
PB95-215307 ..... p 3195 N95-32893
PB95-216388 ..... p 3248 N95-32963
PB95-216800 ..... p 3248 N95-32964 #
PB95-218095 ..... p 3206 N95-32814
PB95-218111 ..... p 3192 N95-33399 #
PB95-222485 ..... p 3185 N95-32815 #
PB95-222956 ..... p 3215 N95-33239 #
PB95-234977 ..... p 3209 N95-34650
PB95-234985 ..... p 3214 N95-34651
PB95-234993 ..... p 3235 N95-34652
PB95-235008 ..... p 3151 N95-34656
PB95-236014 ..... p 3209 N95-34657
PB95-236030 ..... p 3214 N95-34653
PB95-236063 ..... p 3235 N95-34654
PB95-236105 ..... p 3171 N95-34658
PB95-236121 ..... p 3183 N95-34655

PL-LI-94-27 ..... p 3120 N95-34592 #

PL-TR-94-2210 ..... p 3057 N95-32772 #
PL-TR-94-2287 ..... p 3158 N95-34575 #
PL-TR-94-2310 ..... p 3144 N95-34454 #
PL-TR-95-2020 ..... p 3058 N95-34744 #

PNL-SA-24897 ..... p 3185 N95-32582 #
PNL-SA-25315 ..... p 3084 N95-33405 #
PNL-SA-25506 ..... p 3077 N95-32555 #
PNL-SA-25590 ..... p 3151 N95-32475 #
PNL-SA-26034 ..... p 3158 N95-33505 #
PNL-SA-26120 ..... p 3127 N95-33833 #
PNL-SA-26144 ..... p 3075 N95-33832 #

PNL-10416 ..... p 3150 N95-33400 #
PNL-10523 ..... p 3155 N95-34441 #

R/D-7184-MA-01/ENV ..... p 3209 N95-34423
R/D-7539-CH-02 ..... p 3150 N95-34360 #
R/D-7564-EE-02 ..... p 3097 N95-32797 #

RAL-95-004 ..... p 3151 N95-34656
RAL-95-017 ..... p 3206 N95-32814
RAL-95-023 ..... p 3209 N95-34657
RAL-95-026 ..... p 3209 N95-34650
RAL-95-033 ..... p 3235 N95-34652
RAL-95-035 ..... p 3214 N95-34653

RAL-95-037 ..... p 3214 N95-34651

RASSP-1-REV-1 ..... p 3096 N95-32773 #

RCC-166-95 ..... p 3057 N95-34606 #

REPT-A5017 ..... p 3100 N95-34460 #

REPT-030601-5-T ..... p 3097 N95-32822 * #
REPT-06-94-27 ..... p 3083 N95-33079
REPT-2205 ..... p 3090 N95-32985 #
REPT-2206 ..... p 3090 N95-32986 #
REPT-2207 ..... p 3090 N95-32987 #
REPT-2208 ..... p 3090 N95-32988 #
REPT-2209 ..... p 3090 N95-32989 #
REPT-2210 ..... p 3090 N95-32990 #
REPT-2211 ..... p 3091 N95-32991 #
REPT-2212 ..... p 3091 N95-32992 #
REPT-2213 ..... p 3091 N95-32993 #
REPT-2216 ..... p 3091 N95-32994 #
REPT-24 ..... p 3068 N95-33242 #
REPT-442427-22525 ..... p 3183 N95-34605 #
REPT-58 ..... p 3157 N95-32891 #
REPT-6 ..... p 3086 N95-34361 #
REPT-722792-8 ..... p 3095 N95-32674 * #
REPT-93-549/5 ..... p 3178 N95-34462 #
REPT-94-12 ..... p 3192 N95-33399 #
REPT-94-68 ..... p 3195 N95-32893
REPT-94B00041-VOL-15 ..... p 3158 N95-32545 * #
REPT-94B00126-VOL-22 ..... p 3159 N95-32672 * #
REPT-95-B00108-VOL-31 ..... p 3159 N95-32833 * #
REPT-95B00094 ..... p 3237 N95-32922 * #

RHPU-0429 ..... p 3247 N95-33262 * #
RHPU-0474 ..... p 3246 N95-33261 * #

RL-TR-94-227 ..... p 3178 N95-34503 #
RL-TR-95-18 ..... p 3104 N95-34345 #
RL-TR-95-20 ..... p 3217 N95-34300 #

RSL-10290-1 ..... p 3097 N95-33033 * #
RSL-10480-1 ..... p 3099 N95-33497 * #
RSL-10480-2 ..... p 3097 N95-33033 * #
RSL-10480-3 ..... p 3099 N95-33726 * #

RXR-94112 ..... p 3144 N95-34454 #

R95-9084-F ..... p 3123 N95-32915 * #

S-12871-F ..... p 3157 N95-32933 * #
S-799 ..... p 3069 N95-33265 * #

SA-51595 ..... p 3105 N95-34458 #

SAND-93-7081 ..... p 3179 N95-32543 #
SAND-94-2002C ..... p 3120 N95-34811
SAND-94-2294C ..... p 3178 N95-32378 #
SAND-94-2391 ..... p 3181 N95-33624
SAND-94-2436 ..... p 3106 N95-32818 #
SAND-94-2516C ..... p 3106 N95-32387 #
SAND-94-2519C ..... p 3226 N95-32589 #
SAND-94-2550C ..... p 3150 N95-33706 #
SAND-94-2637C ..... p 3184 N95-32383 #
SAND-94-2758C ..... p 3226 N95-32595 #
SAND-94-2795C ..... p 3226 N95-32594 #
SAND-94-2869C ..... p 3082 N95-32380 #
SAND-94-2966C ..... p 3101 N95-32578 #
SAND-94-3205C ..... p 3124 N95-33836 #
SAND-94-3231C ..... p 3118 N95-32683 #
SAND-95-0095C ..... p 3184 N95-32374 #
SAND-95-0197C ..... p 3067 N95-32709 #
SAND-95-0273 ..... p 3152 N95-32556 #
SAND-95-0284C ..... p 3125 N95-32381 #
SAND-95-0311 ..... p 3106 N95-32587 #
SAND-95-0351C ..... p 3077 N95-32382 #
SAND-95-0360C ..... p 3118 N95-32663 #
SAND-95-0560 ..... p 3228 N95-33213 #
SAND-95-0567C ..... p 3226 N95-32590 #
SAND-95-0573C ..... p 3078 N95-32591 #
SAND-95-0595 ..... p 3085 N95-34022 #
SAND-95-0671 ..... p 3103 N95-33640 #
SAND-95-0673C ..... p 3187 N95-32533 #
SAND-95-0720C ..... p 3191 N95-33214 #
SAND-95-0750C ..... p 3111 N95-33837
SAND-95-0753C ..... p 3186 N95-33838 #
SAND-95-0762C ..... p 3102 N95-32708 #
SAND-95-0775 ..... p 3224 N95-33851 #
SAND-95-0848C ..... p 3231 N95-34486 #
SAND-95-0850C ..... p 3225 N95-32579 #
SAND-95-0932C ..... p 3062 N95-33835 #
SAND-95-0936C ..... p 3223 N95-33412 #
SAND-95-1145C ..... p 3229 N95-33636 #
SAND-95-8218 ..... p 3184 N95-32558 #
SAND-95-8521-C ..... p 3122 N95-32863 #
SAND-95-8554C ..... p 3084 N95-33247 #
SAND-95-8563C ..... p 3124 N95-33701 #

SC-MAG-457 ..... p 3214 N95-33504 #
SC-MAG-458 ..... p 3103 N95-33080
SC-MAG-462 ..... p 3215 N95-33381 #

SER-PK-001 ..... p 3033 N95-32764 * #

SGD-607-PT-1 ..... p 3248 N95-32963
SGD-607-PT-2 ..... p 3248 N95-32964 #

SIP-0066 ..... p 3221 N95-32562 #

SLAC-PUB-95-6821 ..... p 3207 N95-33245 #
SLAC-PUB-95-6822 ..... p 3207 N95-33201 #

SMC-TR-95-12 ..... p 3157 N95-34613 #

SP-RAPP-1994:16 ..... p 3083 N95-32962 #
SP-RAPP-1994:21 ..... p 3121 N95-32612

SSCL-PREPRINT-37 ..... p 3103 N95-33404 #
SSCL-PREPRINT-568 ..... p 3214 N95-33720

SU-SLAC-PUB-95-6732 ..... p 3211 N95-32606 #
SU-SLAC-PUB-95-6769 ..... p 3212 N95-32657 #
SU-SLAC-PUB-95-6770 ..... p 3215 N95-32658 #
SU-SLAC-PUB-95-6782 ..... p 3208 N95-33375 #
SU-SLAC-PUB-95-6815 ..... p 3213 N95-33376 #
SU-SLAC-PUB-95-6816 ..... p 3213 N95-33377 #
SU-SLAC-PUB-95-6830 ..... p 3211 N95-32607 #
SU-SLAC-PUB-95-6839 ..... p 3098 N95-33336 #
SU-SLAC-PUB-95-6845 ..... p 3213 N95-33338 #
SU-SLAC-PUB-95-6861 ..... p 3211 N95-32608 #
SU-SLAC-PUB-95-6863 ..... p 3095 N95-32616 #
SU-SLAC-PUB-95-6886 ..... p 3214 N95-34023 #
SU-SLAC-PUB-95-6887 ..... p 3214 N95-34024 #
SU-SLAC-PUB-95-6888 ..... p 3213 N95-33385 #
SU-SLAC-PUB-95-6896 ..... p 3213 N95-33333 #
SU-SLAC-PUB-95-6903 ..... p 3213 N95-33335 #

SU-SLAC-447 ..... p 3185 N95-32820

SU-SLAC/AP-98 ..... p 3203 N95-32544 #
SU-SLAC/AP-99 ..... p 3203 N95-32567 #

SWOE-94-8 ..... p 3100 N95-34578 #

TA-995/1993 ..... p 3153 N95-33331 #

TFLRF-301 ..... p 3086 N95-34494 #

TIOS-95/04 ..... p 3097 N95-32892

TR-1006 ..... p 3100 N95-34474 #
TR-1015 ..... p 3098 N95-33152 #
TR-11 ..... p 3209 N95-34350 #
TR-1291-1 ..... p 3055 N95-34306 #
TR-25 ..... p 3067 N95-32804 #
TR-26 ..... p 3087 N95-34649 #
TR-41 ..... p 3086 N95-34452 #
TR-565 ..... p 3183 N95-34612 #
TR-578 ..... p 3185 N95-32580
TR-597 ..... p 3171 N95-34616 #
TR-5 ..... p 3075 N95-34357 #
TR-7 ..... p 3166 N95-34609 #
TR-94(4925)-1 ..... p 3157 N95-34613 #

TRITA-MAT-1994-0042 ..... p 3195 N95-32889 #
TRITA-MAT-1994-0045 ..... p 3196 N95-33233 #
TRITA-MAT-1995-0004 ..... p 3195 N95-32890 #
TRITA-MAT-1995-0005 ..... p 3196 N95-33234 #
TRITA-MAT-94-43 ..... p 3163 N95-33232 #

TRITA-NA-9312 ..... p 3108 N95-33059 #

TRS-495 ..... p 3183 N95-34655
TRS-504 ..... p 3171 N95-34658

UC-109 ..... p 3075 N95-34268
UC-400 ..... p 3230 N95-33880 #
UC-404 ..... p 3247 N95-33625 #
UC-404 ..... p 3080 N95-33626 #
UC-404 ..... p 3230 N95-33865 #
UC-405 ..... p 3185 N95-32820
UC-414 ..... p 3208 N95-33380 #
UC-414 ..... p 3214 N95-33504 #
UC-414 ..... p 3199 N95-34269 #
UC-414 ..... p 3214 N95-34439 #
UC-630 ..... p 3155 N95-34441 #
UC-704 ..... p 3085 N95-34022 #

UCRL-CR-112910-2 ..... p 3216 N95-34020 #
UCRL-CR-118994 ..... p 3221 N95-32536
UCRL-CR-119401 ..... p 3167 N95-32535 #

UCRL-ID-114325 ..... p 3059 N95-32593 #
UCRL-ID-116354 ..... p 3184 N95-32415 #
UCRL-ID-119045 ..... p 3195 N95-32559 #
UCRL-ID-119659 ..... p 3143 N95-33407 #
UCRL-ID-119964 ..... p 3084 N95-33408 #
UCRL-ID-119966 ..... p 3062 N95-32602 #

UCRL-JC-112929 ..... p 3230 N95-34438 #
UCRL-JC-115700 ..... p 3062 N95-32399 #
UCRL-JC-116341 ..... p 3095 N95-32569 #
UCRL-JC-116856 ..... p 3115 N95-32900 #
UCRL-JC-116858 ..... p 3085 N95-33409 #
UCRL-JC-117130 ..... p 3150 N95-33642 #
UCRL-JC-117133 ..... p 3095 N95-32570 #
UCRL-JC-117360 ..... p 3119 N95-33703 #
UCRL-JC-117491 ..... p 3216 N95-33651 #
UCRL-JC-117773 ..... p 3080 N95-33653 #
UCRL-JC-118333 ..... p 3074 N95-33627 #
UCRL-JC-118345 ..... p 3089 N95-32568 #
UCRL-JC-118357 ..... p 3246 N95-32597 #
UCRL-JC-118397 ..... p 3117 N95-32571 #
UCRL-JC-118405 ..... p 3156 N95-32697 #
UCRL-JC-118421 ..... p 3126 N95-33068
UCRL-JC-118724 ..... p 3207 N95-33219 #
UCRL-JC-118788 ..... p 3112 N95-34437 #
UCRL-JC-118794 ..... p 3197 N95-33220 #
UCRL-JC-118992 ..... p 3079 N95-33063 #
UCRL-JC-119004 ..... p 3118 N95-33378 #
UCRL-JC-119193 ..... p 3212 N95-33064 #
UCRL-JC-119287 ..... p 3159 N95-33410 #
UCRL-JC-119291 ..... p 3230 N95-33650 #
UCRL-JC-119826 ..... p 3183 N95-34813 #
UCRL-JC-119862 ..... p 3182 N95-33652 #
UCRL-JC-119879 ..... p 3179 N95-32390 #
UCRL-JC-120006 ..... p 3216 N95-33411 #
UCRL-JC-120215 ..... p 3164 N95-33654 #
UCRL-JC-120255 ..... p 3081 N95-34482 #
UCRL-JC-120517 ..... p 3216 N95-33506 #

UCRL-52000-95-3 ..... p 3223 N95-33066 #

UILU-ENG-95-2208 ..... p 3182 N95-34455 #
UILU-ENG-95-2211 ..... p 3178 N95-34453 #

UM-P-93/101 ..... p 3204 N95-32623 #
UM-P-93/74 ..... p 3082 N95-32710 #
UM-P-93/78 ..... p 3205 N95-32632 #
UM-P-93/85 ..... p 3204 N95-32622 #

US-PATENT-APPL-SN-037880 ..... p 3116 N95-34426
US-PATENT-APPL-SN-043706 ..... p 3065 N95-34448
US-PATENT-APPL-SN-065321 ..... p 3105 N95-34618
US-PATENT-APPL-SN-083602 ..... p 3124 N95-34449
US-PATENT-APPL-SN-095557 ..... p 3104 N95-34446
US-PATENT-APPL-SN-129728 ..... p 3075 N95-34287
US-PATENT-APPL-SN-134191 ..... p 3127 N95-34427
US-PATENT-APPL-SN-143893 ..... p 3105 N95-34617
US-PATENT-APPL-SN-169923 ..... p 3104 N95-34425
US-PATENT-APPL-SN-186058 ..... p 3201 N95-34444
US-PATENT-APPL-SN-191454 ..... p 3201 N95-34424
US-PATENT-APPL-SN-199927 ..... p 3065 N95-34620
US-PATENT-APPL-SN-207312 ..... p 3086 N95-34447
US-PATENT-APPL-SN-215799 ..... p 3104 N95-34445
US-PATENT-APPL-SN-217816 ..... p 3201 N95-34289
US-PATENT-APPL-SN-263206 ..... p 3120 N95-34619
US-PATENT-APPL-SN-287028 ..... p 3216 N95-34288
US-PATENT-APPL-SN-345957 ..... p 3215 N95-32923 #
US-PATENT-APPL-SN-375335 ..... p 3123 N95-32924 #
US-PATENT-APPL-SN-382708 ..... p 3097 N95-32925 #

US-PATENT-CLASS-156-91 ..... p 3065 N95-34620
US-PATENT-CLASS-188-267 ..... p 3127 N95-34427
US-PATENT-CLASS-244-138 ..... p 3124 N95-34449
US-PATENT-CLASS-257-635 ..... p 3104 N95-34445
US-PATENT-CLASS-324-248 ..... p 3104 N95-34446
US-PATENT-CLASS-367-128 ..... p 3201 N95-34289
US-PATENT-CLASS-367-163 ..... p 3105 N95-34617
US-PATENT-CLASS-367-1 ..... p 3201 N95-34444
US-PATENT-CLASS-367-89 ..... p 3201 N95-34424
US-PATENT-CLASS-370-58 ..... p 3104 N95-34425
US-PATENT-CLASS-372-29 ..... p 3120 N95-34619
US-PATENT-CLASS-385-147 ..... p 3216 N95-34288
US-PATENT-CLASS-425-145 ..... p 3065 N95-34448
US-PATENT-CLASS-427-575 ..... p 3086 N95-34447
US-PATENT-CLASS-429-70 ..... p 3075 N95-34287
US-PATENT-CLASS-437-31 ..... p 3105 N95-34618
US-PATENT-CLASS-73-862 ..... p 3116 N95-34426

US-PATENT-5,363,346 ..... p 3105 N95-34617
US-PATENT-5,374,567 ..... p 3105 N95-34618
US-PATENT-5,379,270 ..... p 3201 N95-34289
US-PATENT-5,380,382 ..... p 3065 N95-34620
US-PATENT-5,381,384 ..... p 3201 N95-34424
US-PATENT-5,387,095 ..... p 3065 N95-34448
US-PATENT-5,387,864 ..... p 3104 N95-34446
US-PATENT-5,390,203 ..... p 3120 N95-34619
US-PATENT-5,391,914 ..... p 3104 N95-34445
US-PATENT-5,392,881 ..... p 3127 N95-34427
US-PATENT-5,393,016 ..... p 3124 N95-34449
US-PATENT-5,396,811 ..... p 3116 N95-34426
US-PATENT-5,398,239 ..... p 3104 N95-34425
US-PATENT-5,399,388 ..... p 3086 N95-34447
US-PATENT-5,399,444 ..... p 3075 N95-34287
US-PATENT-5,400,296 ..... p 3201 N95-34444
US-PATENT-5,400,429 ..... p 3216 N95-34288

USAARL-95-10 ..... p 3170 N95-34378 #
USAARL-95-17 ..... p 3170 N95-34492 #
USAARL-95-19 ..... p 3049 N95-34793 #
USAARL-95-20 ..... p 3170 N95-34489 #
USAARL-95-9 ..... p 3171 N95-34574 #

USAMRMC-T95-10 ..... p 3170 N95-34370 #

USARIEM-TN-95-5 ..... p 3171 N95-34577 #

VJSC-1246-PT-1 ..... p 3058 N95-34280 *
VJSC-1246-PT-2 ..... p 3058 N95-34281 *

WAPD-T-3062 ..... p 3149 N95-32645 #
WAPD-T-3066 ..... p 3211 N95-32647 #

WES/TR/EL-95-15 ..... p 3160 N95-34461 #

WHC-MR-0489 ..... p 3082 N95-32384 #
WHC-MR-0494 ..... p 3084 N95-33218 #

WHC-SD-EN-CSUD-002 ..... p 3155 N95-34435 #

WHC-SD-MP-SWD-30001-REV-7 . p 3178 N95-34484 #

WHC-SD-WM-ES-349 ..... p 3079 N95-32958 #

WL-TR-94-3162 ..... p 3055 N95-34306 #

WSRC-MS-94-0463 ..... p 3125 N95-32373 #
WSRC-MS-95-0031 ..... p 3238 N95-33402 #

ZDOC/9501 ..... p 3087 N95-34614 #

APPENDIX

NASA SCIENTIFIC AND TECHNICAL INFORMATION OFFICE PRODUCTS AND SERVICES

The NASA Scientific and Technical Information (STI) Office provides for the collection and announcement of aerospace-related reports and literature obtained worldwide through agreements and exchanges. The result of the collection is the comprehensive NASA STI Database that covers aeronautics, space, and supporting disciplines.

The STI Database, documents generated or obtained by NASA, and products and services derived from or supporting the database are made available to the NASA research community and to the public. Descriptions and sources of these items are presented in the following pages.

Scientific and Technical Aerospace Reports (STAR) is an abstract journal, listing citations with abstracts for aerospace-related reports obtained from worldwide sources. *STAR* is issued on the first of each month, and announces current documents that have been entered into the NASA STI Database during the previous month. The reports are of the following types:

- NASA, NASA contractor, and NASA grantee reports;
- Reports issued by other U.S. Government agencies, domestic and foreign institutions, universities, and private firms;
- Translations in report form;
- NASA-owned patents and patent applications
- Other U.S. Government agency and foreign patents and patent applications
- Domestic and foreign dissertations and theses.

Journal, book, and conference literature, journal translations, and certain foreign dissertations having the same subject scope as *STAR* are announced in a companion journal, *NASA Open Volumes on Aerospace (NOVA). NOVA* is issued on the 15th of each month and is available from the NASA Center for AeroSpace Information, at the address below.

ELIGIBILITY AND REGISTRATION FOR NASA STI PRODUCTS AND SERVICES

Organizations of the type listed below that have registered with NASA can receive products and services.

- NASA offices and installations, contractors, subcontractors, grantees, and consultants;
- Other U.S. Government agencies and their contractors;
- Libraries in the United States that have arrangements with NASA to maintain collections of NASA documents for public reference;
- Other organizations in the United States having a need for NASA documents in work related to aeronautics and space research;
- Organizations abroad that have established reciprocal documents exchange arrangements with NASA.

The central service points—central points of document acquisition and control within qualified organizations—or individuals are eligible to register for NASA STI products and services. Domestic organizations or individuals may be eligible to receive various classes of NASA publications and services and should address their requests for registration or further information to:

ATTN: Registration Services
NASA Center for AeroSpace Information
800 Elkridge Landing Road
Linthicum Heights, MD 21090-2934
301-621-0390

Organizations abroad should direct requests to:

National Aeronautics and Space Administration
Scientific and Technical Information Office (JT)
International STI Office
Washington, DC 20546-0001
USA
703-271-5640

SUBJECT SCOPE

The subject scope of *STAR* and *NOVA* includes all aspects of aeronautics and space research and development, supporting basic and applied research, and applications. Aerospace aspects of Earth resources, energy development, conservation, oceanography, environmental protection, urban transportation, and other topics of high national priority are also covered.

HOW TO USE *STAR* SUBJECT CATEGORIES

Abstracts in *STAR* are categorized by 10 major subject divisions that are divided further into 76 specific subject categories. The subject divisions and categories are listed in the Table of Contents together with a note for each that defines its scope and provides any cross-references. For example:

16 SPACE TRANSPORTATION

Includes passenger and cargo space transportation, e.g., shuttle operations; and space rescue techniques. For related information see also *03 Air Transportation and Safety* and *18 Spacecraft Design, Testing and Performance*. For space suits see *54 Man/System Technology and Life Support*.

CROSS-REFERENCES

Individual *STAR* abstracts are not ordinarily cross-referenced, except for certain conference reports or book translations that have had separate abstracts written for their component papers or chapters. Citations and abstracts of the components follow immediately after those of the parent document. When the subject content of a component differs sufficiently from the general content of the parent, a cross-reference citation also is printed at the end of the category to which it normally would have been assigned if it were independent.

DOCUMENTS ON MICROFICHE

Documents available on microfiche are designated by a pound sign (#) following the accession number.

LIMITED REPRODUCIBILITY

A note of limited reproducibility appears in the citation, if there are factors affecting the reproducibility of more than 20% of the document. These factors include faint or broken type, color photographs, black and white photographs, foldouts, dot matrix print, or some other factor that limits the reproducibility of the document. This notation also appears on the microfiche header.

NASA PATENTS AND PATENT APPLICATIONS

Patents and patent applications owned by NASA are announced in *STAR* under appropriate subject categories and are referenced in the *STAR* indexes. In the Report Number Index, patents are indexed by the NASA Case Number, and the U.S. Patent Class. Patent applications are indexed by the NASA Case Number and the U.S. Patent Application Serial Number.

Printed copies of patents (which are not microfiched) are available for purchase from the U.S. Patent and Trademark Office.

When ordering patents, the U.S. Patent Number should be used, and payment must be remitted in advance, by money order or check payable to the Commissioner of Patents and Trademarks. Prepaid purchase coupons for ordering are also available from the U.S. Patent and Trademark Office.

NASA patent application specifications are sold in both paper copy and microfiche by the NASA Center for AeroSpace Information (CASI). The N accession number should be used in ordering either paper copy or microfiche from CASI.

The patents and patent applications announced in *STAR* are owned by NASA and are available for royalty-free licensing. Requests for licensing terms and further information should be addressed to:

National Aeronautics and Space Administration
Associate General Counsel for Intellectual Property
Code GP
Washington, DC 20546-0001

SOURCES FOR DOCUMENTS

One or more sources from which a document announced in *STAR* is available to the public is ordinarily given on the last line of the citation. The most commonly indicated sources and their acronyms or abbreviations are listed below, and their addresses are listed on page A-6. If the publication is available from a source other than those listed, the publisher and his address will be displayed on the availability line or in combination with the corporate source line.

Avail: CASI. Sold by the NASA Center for AeroSpace Information. Prices for hard copy (HC) and microfiche (MF) are indicated by a price code following the letters HC or MF in the *STAR* citation. Current values for the price codes are given in the tables on page A-7.

NOTE ON ORDERING DOCUMENTS: When ordering publications from NASA CASI, use the N accession number or other report number. It is also advisable to cite the title and other bibliographic identification.

Avail: SOD (or GPO). Sold by the Superintendent of Documents, U.S. Government Printing Office, in hard copy.

Avail: BLL (formerly NLL): British Library Lending Division, Boston Spa, Wetherby, Yorkshire, England. Photocopies available from this organization at the price shown. (If none is given, inquiry should be addressed to the BLL.)

Avail: DOE Depository Libraries. Organizations in U.S. cities and abroad that maintain collections of Department of Energy reports, usually in microfiche form, are listed in *Energy Research Abstracts*. Services available from the DOE and its depositories are described in a booklet, *DOE Technical Information Center - Its Functions and Services* (TID-4660), which may be obtained without charge from the DOE Technical Information Center.

Avail: ESDU. Pricing information on specific data, computer programs, and details on Engineering Sciences Data Unit (ESDU) topic categories can be obtained from ESDU International Ltd. Requesters in North America should use the Virginia address while all other requesters should use the London address, both of which are on page A-6.

Avail: Fachinformationszentrum Karlsruhe. Gesellschaft für wissenschaftlich-technische Information mbH 76344 Eggenstein-Leopoldshafen, Germany.

Avail: HMSO. Publications of Her Majesty's Stationery Office are sold in the U.S. by Pendragon House, Inc. (PHI), Redwood City, CA. The U.S. price (including a service and mailing charge) is given, or a conversion table may be obtained from PHI.

Avail: Issuing Activity, or Corporate Author, or no indication of availability. Inquiries as to the availability of these documents should be addressed to the organization shown in the citation as the corporate author of the document.

Avail: NASA Public Document Rooms. Documents so indicated may be examined at or purchased from the National Aeronautics and Space Administration (JBD-4), Public Documents Room (Room 1H23), Washington, DC 20546-0001, or public document rooms located at NASA installations, and the NASA Pasadena Office at the Jet Propulsion Laboratory.

Avail: NTIS. Sold by the National Technical Information Service. Initially distributed microfiche under the NTIS SRIM (Selected Research in Microfiche) are available. For information concerning this service, consult the NTIS Subscription Section, Springfield, VA 22161.

Avail: Univ. Microfilms. Documents so indicated are dissertations selected from *Dissertation Abstracts* and are sold by University Microfilms as xerographic copy (HC) and microfilm. All requests should cite the author and the Order Number as they appear in the citation.

Avail: US Patent and Trademark Office. Sold by Commissioner of Patents and Trademarks, U.S. Patent and Trademark Office, at the standard price of $1.50 each, postage free. (See discussion of NASA patents and patent applications on page A-3.)

Avail: (US Sales Only). These foreign documents are available to users within the United States from the National Technical Information Service (NTIS). They are available to users outside the United States through the International Nuclear Information Service (INIS) representative in their country, or by applying directly to the issuing organization.

Avail: USGS. Originals of many reports from the U.S. Geological Survey, which may contain color illustrations, or otherwise may not have the quality of illustrations preserved in the microfiche or facsimile reproduction, may be examined by the public at the libraries of the USGS field offices whose addresses are listed on page A-6. The libraries may be queried concerning the availability of specific documents and the possible utilization of local copying services, such as color reproduction.

FEDERAL DEPOSITORY LIBRARY PROGRAM

In order to provide the general public with greater access to U.S. Government publications, Congress established the Federal Depository Library Program under the Government Printing Office (GPO), with 53 regional depositories responsible for permanent retention of material, inter-library loan, and reference services. At least one copy of nearly every NASA and NASA-sponsored publication, either in printed or microfiche format, is received and retained by the 53 regional depositories. A list of the regional GPO libraries, arranged alphabetically by state, appears on page A-8. These libraries are *not* sales outlets. A local library can contact a regional depository to help locate specific reports, or direct contact may be made by an individual.

PUBLIC COLLECTION OF NASA DOCUMENTS

An extensive collection of NASA and NASA-sponsored publications is maintained by the British Library Lending Division, Boston Spa, Wetherby, Yorkshire, England for public access. The British Library Lending Division also has available many of the non-NASA publications cited in *STAR*. European requesters may purchase facsimile copy or microfiche of NASA and NASA-sponsored documents, those identified by both the symbols # and * from FIZ—Fachinformation Karlsruhe—Bibliographic Service, D-76344 Eggenstein-Leopoldshafen, Germany and TIB—Technische Informationsbibliothek, P.O. Box 60 80, D-30080 Hannover, Germany.

SUBMITTING DOCUMENTS

All users of this abstract service are urged to forward reports to be considered for announcement in *STAR*. This will aid NASA in its efforts to provide the fullest possible coverage of all scientific and technical publications that might support aeronautics and space research and development. If you

have prepared relevant reports (other than those you will transmit to NASA, DOD, or DOE through the usual contract- or grant-reporting channels), please send them for consideration to the NASA Center for AeroSpace Information, 800 Elkridge Landing Road, Linthicum Heights, MD 21090-2934.

Reprints of journal articles, book chapters, and conference papers are also welcome. These will be considered for announcement in *STAR's* companion journal, *NOVA*.

You may specify a particular source to be included in a report announcement if you wish; otherwise the report will be placed on a public sale at the NASA Center for AeroSpace Information. Copyrighted publications will be announced but not distributed or sold.

PURCHASE OF *STAR*

STAR is publicly available on annual subscription from the NASA Center for AeroSpace Information (CASI). 1995 *STAR* subscription prices are $100.00/domestic and $125.00/foreign. Single copy prices: $33.00/domestic, $41.00/foreign.

An annual, cumulative *STAR Index* is also available at $70.00/domestic and foreign.

STAR is available to registered users on annual subscription from the NASA Center for AeroSpace Information, ATTN: Registration Services, 800 Elkridge Landing Road, Linthicum Heights, MD 21090-2934.

ADDRESSES OF ORGANIZATIONS

British Library Lending Division
Boston Spa, Wetherby, Yorkshire
England

Commissioner of Patents and Trademarks
U.S. Patent and Trademark Office
Washington, DC 20231

Department of Energy
Technical Information Center
P.O. Box 62
Oak Ridge, TN 37830

European Space Agency-
Information Retrieval Service ESRIN
Via Galileo Galilei
00044 Frascati (Rome) Italy

Engineering Sciences Data Unit International
P.O. Box 1633
Manassas, VA 22110

Engineering Sciences Data Unit
International, Ltd.
251-259 Regent Street
London, W1R 7AD, England

Fachinformationszentrum Karlsruhe
Gesellschaft für wissenschaftlich-technische
Information mbH
76344 Eggenstein-Leopoldshafen, Germany

Her Majesty's Stationery Office
P.O. Box 569, S.E. 1
London, England

NASA Center for AeroSpace Information
800 Elkridge Landing Road
Linthicum Heights, MD 21090-2934

National Aeronautics and Space Administration
Scientific and Technical Information Office (JT)
Washington, DC 20546-0001

National Technical Information Service
5285 Port Royal Road
Springfield, VA 22161

Pendragon House, Inc.
899 Broadway Avenue
Redwood City, CA 94063

Superintendent of Documents
U.S. Government Printing Office
Washington, DC 20402

University Microfilms
A Xerox Company
300 North Zeeb Road
Ann Arbor, MI 48106

University Microfilms, Ltd.
Tylers Green
London, England

U.S. Geological Survey Library National Center
MS 950
12201 Sunrise Valley Drive
Reston, VA 22092

U.S. Geological Survey Library
2255 North Gemini Drive
Flagstaff, AZ 86001

U.S. Geological Survey
345 Middlefield Road
Menlo Park, CA 94025

U.S. Geological Survey Library
Box 25046
Denver Federal Center, MS914
Denver, CO 80225

NASA CASI PRICE CODE TABLE

(Effective January 1, 1995)

CASI PRICE CODE	NORTH AMERICAN PRICE	FOREIGN PRICE
A01	$ 6.00	$ 12.00
A02	9.00	18.00
A03	17.50	35.00
A04-A05	19.50	39.00
A06-A09	27.00	54.00
A10-A13	36.50	73.00
A14-A17	44.50	89.00
A18-A21	52.00	104.00
A22-A25	61.00	122.00
A99	Call For Price	Call For Price

IMPORTANT NOTICE

For users not registered at the NASA CASI, prepayment is required. Additionally, a shipping and handling fee of $1.00 per document for delivery within the United States and $9.00 per document for delivery outside the United States is charged.

For users registered at the NASA CASI, document orders may be invoiced at the end of the month, charged against a deposit account, or paid by check or credit card. NASA CASI accepts American Express, Diners' Club, MasterCard, and VISA credit cards. There are no shipping and handling charges. To register at the NASA CASI, please request a registration form through the NASA Access Help Desk at the numbers or addresses below.

RETURN POLICY

Effective June 1, 1995, the NASA Center for AeroSpace Information will gladly replace or make full refund on items you have requested if we have made an error in your order, if the item is defective, or if it was received in damaged condition and you contact us within 30 days of your original request. Just contact our NASA Access Help Desk at the numbers or addresses listed below.

NASA Center for AeroSpace Information
800 Elkridge Landing Road
Linthicum Heights, MD 21090-2934
Telephone: (301) 621-0390
E-mail: help@sti.nasa.gov
Fax: (301) 621-0134

FEDERAL REGIONAL DEPOSITORY LIBRARIES

ALABAMA

AUBURN UNIV. AT MONTGOMERY LIBRARY
Documents Dept.
7300 University Dr.
Montgomery, AL 36117-3596
(205) 244-3650 Fax: (205) 244-0678

UNIV. OF ALABAMA
Amelia Gayle Gorgas Library
Govt. Documents
P.O. Box 870266
Tuscaloosa, AL 35487-0266
(205) 348-6046 Fax: (205) 348-0760

ARIZONA

DEPT. OF LIBRARY, ARCHIVES, AND PUBLIC RECORDS
Research Division
Third Floor, State Capitol
1700 West Washington
Phoenix, AZ 85007
(602) 542-3701 Fax: (602) 542-4400

ARKANSAS

ARKANSAS STATE LIBRARY
State Library Service Section
Documents Service Section
One Capitol Mall
Little Rock, AR 72201-1014
(501) 682-2053 Fax: (501) 682-1529

CALIFORNIA

CALIFORNIA STATE LIBRARY
Govt. Publications Section
P.O. Box 942837 - 914 Capitol Mall
Sacramento, CA 94337-0091
(916) 654-0069 Fax: (916) 654-0241

COLORADO

UNIV. OF COLORADO - BOULDER
Libraries - Govt. Publications
Campus Box 184
Boulder, CO 80309-0184
(303) 492-8834 Fax: (303) 492-1881

DENVER PUBLIC LIBRARY
Govt. Publications Dept. BSG
1357 Broadway
Denver, CO 80203-2165
(303) 640-8846 Fax: (303) 640-8817

CONNECTICUT

CONNECTICUT STATE LIBRARY
231 Capitol Avenue
Hartford, CT 06106
(203) 566-4971 Fax: (203) 566-3322

FLORIDA

UNIV. OF FLORIDA LIBRARIES
Documents Dept.
240 Library West
Gainesville, FL 32611-2048
(904) 392-0366 Fax: (904) 392-7251

GEORGIA

UNIV. OF GEORGIA LIBRARIES
Govt. Documents Dept.
Jackson Street
Athens, GA 30602-1645
(706) 542-8949 Fax: (706) 542-4144

HAWAII

UNIV. OF HAWAII
Hamilton Library
Govt. Documents Collection
2550 The Mall
Honolulu, HI 96822
(808) 948-8230 Fax: (808) 956-5968

IDAHO

UNIV. OF IDAHO LIBRARY
Documents Section
Rayburn Street
Moscow, ID 83844-2353
(208) 885-6344 Fax: (208) 885-6817

ILLINOIS

ILLINOIS STATE LIBRARY
Federal Documents Dept.
300 South Second Street
Springfield, IL 62701-1796
(217) 782-7596 Fax: (217) 782-6437

INDIANA

INDIANA STATE LIBRARY
Serials/Documents Section
140 North Senate Avenue
Indianapolis, IN 46204-2296
(317) 232-3679 Fax: (317) 232-3728

IOWA

UNIV. OF IOWA LIBRARIES
Govt. Publications
Washington & Madison Streets
Iowa City, IA 52242-1166
(319) 335-5926 Fax: (319) 335-5900

KANSAS

UNIV. OF KANSAS
Govt. Documents & Maps Library
5001 Malott Hall
Lawrence, KS 66045-2800
(913) 864-4660 Fax: (913) 864-3855

KENTUCKY

UNIV. OF KENTUCKY
King Library South
Govt. Publications/Maps Dept.
Patterson Drive
Lexington, KY 40506-0039
(606) 257-3139 Fax: (606) 257-3139

LOUISIANA

LOUISIANA STATE UNIV.
Middleton Library
Govt. Documents Dept.
Baton Rouge, LA 70803-3312
(504) 388-2570 Fax: (504) 388-6992

LOUISIANA TECHNICAL UNIV.
Prescott Memorial Library
Govt. Documents Dept.
Ruston, LA 71272-0046
(318) 257-4962 Fax: (318) 257-2447

MAINE

UNIV. OF MAINE
Raymond H. Fogler Library
Govt. Documents Dept.
Orono, ME 04469-5729
(207) 581-1673 Fax: (207) 581-1653

MARYLAND

UNIV. OF MARYLAND - COLLEGE PARK
McKeldin Library
Govt. Documents/Maps Unit
College Park, MD 20742
(301) 405-9165 Fax: (301) 314-9416

MASSACHUSETTS

BOSTON PUBLIC LIBRARY
Govt. Documents
666 Boylston Street
Boston, MA 02117-0286
(617) 536-5400, ext. 226
Fax: (617) 536-7758

MICHIGAN

DETROIT PUBLIC LIBRARY
5201 Woodward Avenue
Detroit, MI 48202-4093
(313) 833-1025 Fax: (313) 833-0156

LIBRARY OF MICHIGAN
Govt. Documents Unit
P.O. Box 30007
717 West Allegan Street
Lansing, MI 48909
(517) 373-1300 Fax: (517) 373-3381

MINNESOTA

UNIV. OF MINNESOTA
Govt. Publications
409 Wilson Library
309 19th Avenue South
Minneapolis, MN 55455
(612) 624-5073 Fax: (612) 626-9353

MISSISSIPPI

UNIV. OF MISSISSIPPI
J.D. Williams Library
106 Old Gym Bldg.
University, MS 38677
(601) 232-5857 Fax: (601) 232-7465

MISSOURI

UNIV. OF MISSOURI - COLUMBIA
106B Ellis Library
Govt. Documents Sect.
Columbia, MO 65201-5149
(314) 882-6733 Fax: (314) 882-8044

MONTANA

UNIV. OF MONTANA
Mansfield Library
Documents Division
Missoula, MT 59812-1195
(406) 243-6700 Fax: (406) 243-2060

NEBRASKA

UNIV. OF NEBRASKA - LINCOLN
D.L. Love Memorial Library
Lincoln, NE 68588-0410
(402) 472-2562 Fax: (402) 472-5131

NEVADA

THE UNIV. OF NEVADA LIBRARIES
Business and Govt. Information Center
Reno, NV 89557-0044
(702) 784-6579 Fax: (702) 784-1751

NEW JERSEY

NEWARK PUBLIC LIBRARY
Science Div. - Public Access
P.O. Box 630
Five Washington Street
Newark, NJ 07101-7812
(201) 733-7782 Fax: (201) 733-5648

NEW MEXICO

UNIV. OF NEW MEXICO
General Library
Govt. Information Dept.
Albuquerque, NM 87131-1466
(505) 277-5441 Fax: (505) 277-6019

NEW MEXICO STATE LIBRARY
325 Don Gaspar Avenue
Santa Fe, NM 87503
(505) 827-3824 Fax: (505) 827-3888

NEW YORK

NEW YORK STATE LIBRARY
Cultural Education Center
Documents/Gift & Exchange Section
Empire State Plaza
Albany, NY 12230-0001
(518) 474-5355 Fax: (518) 474-5786

NORTH CAROLINA

UNIV. OF NORTH CAROLINA - CHAPEL HILL
Walter Royal Davis Library
CB 3912, Reference Dept.
Chapel Hill, NC 27514-8890
(919) 962-1151 Fax: (919) 962-4451

NORTH DAKOTA

NORTH DAKOTA STATE UNIV. LIB.
Documents
P.O. Box 5599
Fargo, ND 58105-5599
(701) 237-8886 Fax: (701) 237-7138

UNIV. OF NORTH DAKOTA
Chester Fritz Library
University Station
P.O. Box 9000 - Centennial and University Avenue
Grand Forks, ND 58202-9000
(701) 777-4632 Fax: (701) 777-3319

OHIO

STATE LIBRARY OF OHIO
Documents Dept.
65 South Front Street
Columbus, OH 43215-4163
(614) 644-7051 Fax: (614) 752-9178

OKLAHOMA

OKLAHOMA DEPT. OF LIBRARIES
U.S. Govt. Information Division
200 Northeast 18th Street
Oklahoma City, OK 73105-3298
(405) 521-2502, ext. 253
Fax: (405) 525-7804

OKLAHOMA STATE UNIV.
Edmon Low Library
Stillwater, OK 74078-0375
(405) 744-6546 Fax: (405) 744-5183

OREGON

PORTLAND STATE UNIV.
Branford P. Millar Library
934 Southwest Harrison
Portland, OR 97207-1151
(503) 725-4123 Fax: (503) 725-4524

PENNSYLVANIA

STATE LIBRARY OF PENN.
Govt. Publications Section
116 Walnut & Commonwealth Ave.
Harrisburg, PA 17105-1601
(717) 787-3752 Fax: (717) 783-2070

SOUTH CAROLINA

CLEMSON UNIV.
Robert Muldrow Cooper Library
Public Documents Unit
P.O. Box 343001
Clemson, SC 29634-3001
(803) 656-5174 Fax: (803) 656-3025

UNIV. OF SOUTH CAROLINA
Thomas Cooper Library
Green and Sumter Streets
Columbia, SC 29208
(803) 777-4841 Fax: (803) 777-9503

TENNESSEE

UNIV. OF MEMPHIS LIBRARIES
Govt. Publications Dept.
Memphis, TN 38152-0001
(901) 678-2206 Fax: (901) 678-2511

TEXAS

TEXAS STATE LIBRARY
United States Documents
P.O. Box 12927 - 1201 Brazos
Austin, TX 78701-0001
(512) 463-5455 Fax: (512) 463-5436

TEXAS TECH. UNIV. LIBRARIES
Documents Dept.
Lubbock, TX 79409-0002
(806) 742-2282 Fax: (806) 742-1920

UTAH

UTAH STATE UNIV.
Merrill Library Documents Dept.
Logan, UT 84322-3000
(801) 797-2678 Fax: (801) 797-2677

VIRGINIA

UNIV. OF VIRGINIA
Alderman Library
Govt. Documents
University Ave. & McCormick Rd.
Charlottesville, VA 22903-2498
(804) 824-3133 Fax: (804) 924-4337

WASHINGTON

WASHINGTON STATE LIBRARY
Govt. Publications
P.O. Box 42478
16th and Water Streets
Olympia, WA 98504-2478
(206) 753-4027 Fax: (206) 586-7575

WEST VIRGINIA

WEST VIRGINIA UNIV. LIBRARY
Govt. Documents Section
P.O. Box 6069 - 1549 University Ave.
Morgantown, WV 26506-6069
(304) 293-3051 Fax: (304) 293-6638

WISCONSIN

ST. HIST. SOC. OF WISCONSIN LIBRARY
Govt. Publication Section
816 State Street
Madison, WI 53706
(608) 264-6525 Fax: (608) 264-6520

MILWAUKEE PUBLIC LIBRARY
Documents Division
814 West Wisconsin Avenue
Milwaukee, WI 53233
(414) 286-3073 Fax: (414) 286-8074

*U.S. GOVERNMENT PRINTING OFFICE: 1995-405-129/20014

SCAN Goes Electronic!

If you have NASA Mail or if you can access the Internet, you can get biweekly issues of *SCAN* delivered to your desktop absolutely free!

Electronic SCAN takes advantage of computer technology to alert you to the latest aerospace-related, worldwide scientific and technical information that has been published.

No more waiting while the paper copy is printed and mailed to you. You can review *Electronic SCAN* the same day it is released—up to 191 topics to browse at your leisure. When you locate a publication of interest, you can print the announcement. You can also go back to the *Electronic SCAN* home page and follow the ordering instructions to quickly receive the full document.

Electronic SCAN
Timely
Flexible
Complete
Free!

Start your free access to *Electronic SCAN* today. Over 1,000 announcements of new reports, books, conference proceedings, journal articles . . . and more—delivered to your computer every two weeks.

For access to *E-SCAN* via the NASA STI home page:

http://www.sti.nasa.gov
ftp.sti.nasa.gov
gopher.sti.nasa.gov
listserv@sti.nasa.gov

To subscribe via e-mail, enter **scan@sti.nasa.gov** on the address line. Leave the subject and message areas blank and send. You will receive an automatic reply with instructions in minutes.

For additional information, e-mail a message to **help@sti.nasa.gov**

Phone: (301) 621-0390 Fax: (301) 621-0134

Write: NASA Access Help Desk
NASA Center for AeroSpace Information
800 Elkridge Landing Road
Linthicum Heights, MD 21090-2934

National Aeronautics and Space Administration

Scientific and Technical Information Office

10/95

National Aeronautics and
Space Administration
Code JT
Washington, DC 20546-0001

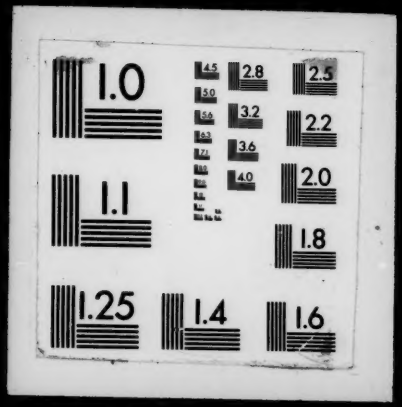
1.0
1.1
1.25
1.4
1.6
2.8
3.2
3.6
4.0
2.5
2.2
2.0
1.8